Solvent Extraction for the 21st Century

Proceedings of ISEC'99

volume one

edited by
Michael Cox
Manuela Hidalgo
Manuel Valiente





where science meets business

SOLVENT EXTRACTION FOR THE 21ST CENTURY

(Proceedings of ISEC '99)

Volume 1

Edited by

Michael Cox
Department of Physical Sciences, University of Hertfordshire, UK

Manuela Hidalgo
Departamento de Química, Universitat de Girona, Spain

and

Manuel Valiente
Departamento de Química, Universitat Autònoma de Barcelona, Spain

sci
where science meets business

ISEC'99

SOLVENT EXTRACTION FOR THE 21ST CENTURY
Proceedings of ISEC '99

© 2001 Society of Chemical Industry (SCI)
All rights reserved. No part of this publication may be reproduced, stored in a retrieval system, or transmitted in any form or by any means, electronic, mechanical, photocopying, recording, or otherwise, without the prior written permission of the copyright owners, Society of Chemical Industry.

Volume 1

ISBN: 0-901001-83-X

First published in 2001 by

Society of Chemical Industry (SCI)
14/15 Belgrave Square
London SW1X 8PS
UK
T: +44 (0)20 7598 1500
F: +44 (0)20 7235 0887
W: www.soci.org

British Library Cataloguing-in-Publication Data
A catalogue record for this book is available from the British Library.

Note. No responsibility is assumed by either the Society of Chemical Industry, ISEC or the Editors for any injury and/or damage to persons or property as a matter of products liability, negligence or otherwise, or from any use or operation of any methods, products, instructions or ideas contained in the material herein.

The material is produced from the authors' electronic manuscripts.

This book is only available as part of a two-volume set and is not available separately.
ISBN Volume 1: 0-901001-83-X
ISBN Volume 2: 0-901001-84-8

Orders should be sent to:
Accounts Department
SCI, 14/15 Belgrave Square
London SW1X 8PS, UK

Printed on acid-free paper in Great Britain by Page Bros Ltd (Norwich)

FOREWORD

The property of a chemical species to move between immiscible liquid phases has revolutionised the science of separations in the millennium that finishes soon. During the present century, the most significant event has been the growth and development of the field of Solvent Extraction. This technique has lead to hundreds of separation methods and thousands of systems that have been described, investigated and several of which have successfully been applied to solve, in a unique manner, complicated problems in the industrial fields of hydrometallurgy, petrochemical, food, pharmaceutical, environmental, waste treatment and analytical chemistry. Scientific and technologically the most important contribution of liquid-liquid distribution studies has been to the acquisition of basic knowledge in co-ordination chemistry, chemical thermodynamics, interfacial phenomena, hydrodynamics of two phases and mechanisms of chemical reactions, as well as process development, equipment design and process control. It must be emphasised that such knowledge has been applied not only to process separations but also to other important aspects of the areas mentioned above, i.e., development of chemical sensors, controlled release devices, etc.

Because of this record of achievement, Solvent Extraction can be considered as a mature technique and thus further innovation becomes more difficult. This is always a challenge to practitioners in the technique, but it never will be a final barrier in itself, unless we confuse the creation of scientific knowledge with the opportunity of obtaining funds for research. In addition, at this moment, when environmental concern has reached a significantly high social and scientific consideration, the name of Solvent Extraction is sometimes interpreted as a negative factor that has been reflected in some political decisions. We know well that again, this is a consequence of ignorance, but still, we must consider this fact and include it in the real scientific and technological challenges.

The area of Solvent Extraction has several well-identified areas and topics with specific demands for scientific and technological research. Some of these areas are related to the *chemistry* of Solvent Extraction and include: the need for speciation studies of the compounds formed both in the aqueous and organic phases during the operation of the process; understanding the interrelation between chemical thermodynamics vs. real operation; the role of the diluent in relation to its chemical nature; degradation of reagents as an important chemical factor that influences system performance. In addition, there are the new methods for Solvent Extraction which include: non-dispersed extraction; microemulsions; extraction chromatography; etc.

Yet another area is concerned with the engineering aspects of Solvent Extraction and here a proper understanding of modelling of both the chemistry and system design is important. Also here there is a lack of data on thermodynamics in concentrated solutions which is the typical situation in plant operations. Monitoring and control of the process is an area which needs specific attention. Monitoring of the two phase process is a system dependent problem which possesses several weak points that are key factors to the advance of the appropriate knowledge to predict the behaviour of solvent extraction systems. Therefore it is important that both specific on-line analytical equipment and robust monitoring techniques should be implemented in the Solvent Extraction process.

Concerning the environmental aspects, the real impact of the Solvent Extraction process must be characterised in several areas: the health effects of solvents and solutions; toxicity of new hazardous reagents; fire hazards; treatment of wastes. In addition design of equipment must also address safety i.e., minimising venting, use of columns, entrainment. These are all considered in an overall risk assessment analysis.

These are just a few aspects of the challenge to be faced by future practitioners in the subject.

So, the International Solvent Extraction Conference has come to Barcelona, the capital city of Catalunya (Spain), in July 1999. Most of the above mentioned areas in need of research and development have been the subject of excellent contributions from the participants and will be presented and discussed during the Conference sessions.

We understand that such an international meeting to discuss Solvent Extraction has to provide the facilities to make the transmission of knowledge easier, to stimulate the will to meet the exciting challenges we are now facing and to make Solvent Extraction attractive to newcomers. To accomplish this, we have organised the International Solvent Extraction School to take place simultaneously with the Conference, and invited international experts to provide tutorials in their fields of expertise and thus to increase our knowledge of Solvent Extraction.

During preparations for the Conference the idea presiding over all the discussions and plans was the question:

> *Will this way of thinking, studying, developing and applying the optimum give the answers to the actual needs and competitiveness that may arise in the next century?*

The Organising Committee has been working to try to answer this question, and we believe that ISEC'99 will be able to provide an appropriate answer. For all their work and dedication which has gone to make ISEC'99 possible, I would like to thank all members of the Organising Committee because without them this Conference would not have been possible.

The Organising Committee in turn wish to express their warm appreciation to all the authors for their contribution and to all those who will be attending ISEC'99 and thus contributing to a most exciting and enjoyable Conference. We thank you for accepting our invitation to meet on the Mediterranean and we hope you will have happy memories of this meeting.

These Proceedings have been compiled from electronic versions of papers submitted by the authors after refereeing and have not been submitted to full textual editing by the editors. We hope that they will provide a valuable resource for the future.

Manuel Valiente
Chairman, Organising Committee

TABLE OF CONTENTS

PLENARY AND KEYNOTE LECTURES 1

Molecular Dynamics of Liquid Surfaces and Interfaces 3
I Benjamin

Solvent Extraction and Materials Science 9
M Muhammed and AA Zagorodni

One Phase Micellar Extraction as a New Separation Technique 19
J Szymanowski

Physico-chemical Modelling of Liquid–Liquid Extraction Systems of Highly Concentrated Electrolytes 25
P Dannus

State of the Art and Future Directions in Solvent Extraction 37
GM Ritcey

ANALYTICAL CHEMISTRY 45

Liquid-supported Membranes as Sample Interfaces in a Flow Probe Optosensor for Chromium(VI) Analysis 47
E Castillo, M Granados, MD Prat, AM Sastre, A Kumar and JL Cortina

Recent Advances in the Development of Extraction Chromatographic Materials for the Isolation of Radionuclides from Biological and Environmental Samples 53
ML Dietz, EP Horwitz and R Chiarizia

Ion–paired Extraction of Copper into Chloroform and its Application in Practical Analyses 59
I Kojima, M Ito and T Mizuno

Determination of Arsenic in Biological Matrices by Anodic Stripping Voltammetry Coupled with a Two-step Extraction Process 65
J-M Lo, J-D Lee and C-M Tseng

Solvent Extraction Separation Studies of Some Metal Ions with 2-Ethylhexylphosphonic Acid Mono-2-Ethylhexyl Ester 71
SV Bandekar and PM Dhadke

Bis(ethanedithioamido)-2,4-dioxo-3-oxyminopentane as a New Analytical Reagent for the Extractive Radiochemical-spectrophotometric Determination of Selenium(IV) and its Separation from other Elements 77
A Varadarajan and SP Malve

BIOTECHNOLOGY 81

A Novel Protein Refolding Technique Utilizing Reversed Micellar Extraction 83
M Goto, S Furusaki and TA Hatton

Effect of Interaction between Protein and Surfactant in Aqueous Phase on Extraction Rate of Protein into Reversed Micellar Solution 89
T Kinugasa, K Sanagi, K Watanabe and H Takeuchi

Reverse Micellar Extraction of Proteins Using pH Responsible Mixed Micellar Systems 95
K Shiomori, T Honbu, Y Kawano, R Kuboi and I Komasawa

Extraction of Proteins using Reversed Micelles in a Graesser "Raining Bucket" Contactor 101
LH Poppenborg, S Jarudilokkul and DC Stuckey

Tailoring of Reverse Micellar System for Selective Separation of Proteins Using Protein–Protein Affinity Interactions 107
M Adachi, M Harada, A Shioi and S Katoh

Selective Separation of α-Amylase, Bovine Serum Albumin and Trypsin Inhibitor using Reverse Micelles 113
S Jarudilokkul, LH Poppenborg and DC Stuckey

Strategies for Extraction Methods in the Extractive Fermentation Process of Carboxylic Acid 119
W Qin and ST Yang

Recovery of Carboxylic Acids from Fermentation Broths using Reactive Sorption 125
M Traving and H-J Bart

Extraction and Interactions in Two-phase, Multi-acid, Multi-base Systems 131
N Cohn-Syzov and AM Eyal

Extractive Synthesis of Peptides with Catalytically Active Enzymes in Organic Media 137
Y Murakami, H Kawakita and A Hirata

Protease-catalyzed Synthesis of Peptides Utilizing an Extractive Reaction in an Aqueous/ Organic Biphasic System 143
Y Murakami, T Oda, A Takehara and A Hirata

Extractive Hydrolysis of Proteins with Enzymes in an Aqueous Two-phase System 149
Y Murakami and A Hirata

The Effect of Surfactants during Solvent Extraction of Erythromycin-A from Buffer and Filtered Fermentation Broth 155
MR Pursell, MA Mendes-Tatsis and DC Stuckey

Recovery of Ethanol from Aqueous Solution by Extraction with 1-Dodecanol 161
F Ruiz, V Gomis, N Boluda and H Bailador

ENVIRONMENTAL IMPACT 165

Soil Remediation by Supercritical Extraction with Solvent Recirculation under Quasiisobaric Operation Conditions. Application to Soil Polluted by Hydrocarbons 167
E Alonso, JJ Alonso and MJ Cocero

Organic Solvent-free Extraction of Phenol Through Liquid-Coacervate Systems 171
EL de Barros Neto, JP Canselier and C Gourdon

Removal of VOCs from Wastewater with Membrane Extraction 177
Y Wang, S Zhu and Y_Dai

Removal of Dyestuffs From Dilute Solution with Electro-extraction 183
GS Luo, YC Lu, WB Jiang and YY Dai

Recovery of Pickling Liquors from the Steel-making Industry 189
CE Da Silva, JS Benedetto and EB Tambourgi

The Chromium Recovery Process from Tanning Effluents by Microemulsion in the Morris Extractor 195
TN de C Dantas, AA Dantas Neto and MCPA Moura

A New Zinc Solvent Extraction Application: Spent Domestic Batteries Treatment Plant 201
D Martín, MA García, G Diaz and J Falgueras

Micellar Extraction versus Solvent Extraction: Advantages and Drawbacks 207
M Hebrant and C Tondre

Interaction of Thorium with Gray Humic Acid 213
A-A A Helal

Extractive Recovery of Boron in Wastewater from a Coal Thermal Power Plant 219
M Hirata, H Takanashi, S Kokubu, M Matsumoto, T Takada and T Hano

Reactive Liquid–Liquid Extraction of Heavy Metals from Landfill Leachate 225
W Mickler, A Reich and E Uhlemann

A Comparative Study of the Treatment of Chromium Electroplating Wastewater using Two Extractants, Alamine 336 and Aliquat 336 231
YKP Sze, CSW Lam, WK Long and JMY Ho

EXTRACTANTS AND DILUENTS 237

Tailor-made Aromatic Cage Compounds as Tools for Selective Solvent Extraction of Metal Ions 239
K Gloe, C Chartroux, T Rambusch, F Ahuis, S Ibach and F Vögtle

Solvent Extraction Separation of some Transition Elements with Hexaacetato-calix(6)arene 245
DD Malkhede, PM Dhadke and SM Khopkar

Lanthanide and Actinide Extraction with Calix[4]- and Calix[6]-arenes Bearing Amide Groups 249
NTK Dunga, K Kunogi, and R Ludwig

Coextraction of Various Metal Ions with Calix[4]arene Carboxylate Complexed with Sodium Ion 255
K Ohto, H Ishibashi, S Kuwata and K Inoue

Extraction of Europium(III) and Americium(III) with Diamide Compounds from Nitric Acid Solution 259
W-J Chen, L Zhu, S-D Ding, Z-Q Liu, S-J Chen, C Xia, Z Huang and Y-D Jing

Application of Diazapolyoxabicyclic Ligands to the Quantitative Extraction Separation of Alkali and Alkaline Earth Metal Ions as the Ion-size Selective Masking Reagents 265
S Tsuruboi, S Umetani and Y Komatsu

Solvent Extraction of Base Metal Cations such as Iron(III) from Hydrochloric Acid Solutions using N,N'-Substituted Malonamides 271
MC Costa, CE Fernandes, MJ Hudson and PB Iveson

Recent Advances in Structure–Reactivity Studies of Solvent Extractants in Metal Extraction 277
CY Yuan, SS Li, SG Yuan and HL Ma

Extraction Studies and *ab initio* Calculations of some Substituted Malonamides 281
L Spjuth, JO Liljenzin, MJ Hudson, MGB Drew, PB Iveson and C Madic

Photostability of Hydroxyoxime Commercial Copper Extractants: Acorga P5100 and SME529 287
E Krzyanowska and A Olszanowski

Photodegradation of Oximes of 2-hydroxy-5-*t*-octylbenzophenone, 2-Hydroxy-5-*t*-octyl-benzaldehyde as Models of Hydroxyoxime Extractants of Metals 293
E Krzyanowska and A Olszanowski

Synergistic Effects in the Extraction of Metal Ions by Mixtures of Dialkylphosphoric Acids and Substituted Crown Ethers 299
R Chiarizia, ML Dietz, AH Bond, VJ Huber, AW Herlinger and BP Hay

Solvent Extraction of Calcium and Some Divalent Transition Metals by Mixtures of Organophosphorus Acids and Bifunctional Phosphonates 305
JS Preston and AC du Preez

The Effect of Reagent Structure on the Extraction and Separation of Nickel and Cobalt by Mixtures of Carboxylic Acids and Pyridine Derivatives 311
JS Preston and AC du Preez

Synergistic Systems for the Selective Extraction of Trivalent Actinides from Mixtures of Trivalent Actinides and Lanthanides. 317
PY Cordier, N François, N Boubals, C Madic, MJ Hudson and JO Liljenzin

Separation of Trivalent Americium and Europium with some Substituted Oligopyridines and Triazines in Synergy with 2-Bromodecanoic Acid 323
Å Enarsson, L Spjuth, JO Liljenzin, G Källvenius, MJ Hudson, PB Iveson, ML Russell, C Madic and PY Cordier

Synergetic Solvent Effects in the Kinetics of the Extraction of Chromium(III) 329
C Mack and MJ Hampe

Micellar Extraction of Complexes of Lanthanides with Humic Acids 335
J Reitmeir, JI Kim and P Plucinski

Solvent Extraction of Transition Metals by an *in situ* Extractant Formation Method. VI. Utilization of an Easily-solidifying Solvent 341
K Fujinaga, Y Seike, and M Okumura

A New Hydroxamic Acid Derivative Extractant for the Extraction of Cobalt(II) and Uranium(VI) from Nitrate Medium 347
FA Shehata, S El-Afifi and HF Aly

Solvent Extraction of UO_2^{2+} and Th^{4+} with Petroleum Sulfoxide 353
S-N Yu, Z-P Fan, L Ma, Y-Z Yang and B-R Bao

Palladium(II) Extraction with Alkyl Derivatives of Nicotinamide 359
M Wiœniewski, I Szczepanska and A Borowiak-Resterna

Cloud Point Extraction of Gallium(III) with Nonionic Surfactants from Hydrochloric Acid Media 363
S Akita, N Hyodo, N Kobayashi, S Nii, K Takahashi and H Takeuchi

Additive Tailoring in Biphasic Systems for an Enzymatic Condensation Reaction 369
R Dunowicz and AM Eyal

LIX®-7800 Series: a New Reagent Family for Reversibly Extracting Anions from Alkaline Solutions 375
P Mattison and M Virnig

Advances in Gold(III)-Chloride Solvent Extraction Using Neutral Organo-phosphorous Derivatives. Estimation of $AuCl_4^-$–H^+ Interaction Coefficients 381
AM Sastre and FJ Alguacil

Solvent Extraction of Gallium(III) with Nonionic Surfactants from Hydrochloric Acid Media 387
N Kobayashi, N Hyodo, S Nii, K Takahashi, H Takeuchi and S Akita

Solvent Extraction of Gold from Hydrochloric Acid Solutions Using Bis(dialkylphosphonate)s 393
S Kamata, S Fukunaga and DA Chowdhury

Sulphur–Nitrogen Ligands in the Solvent Extraction of Silver from Chloride Solutions 399
AP Paiva

Foam Separation of Tributyl Phosphate from Aqueous Solution by Sodium Dodecylsulfate 405
Z-D Chang, H-H Liu, N Yao and J-Y Chen

Extraction Equilibria of Nicotinic Acid using Alamine 300/Diluent and Conventional Solvent Systems 411
A Senol

Separation of Phenol from Aqueous Solution by Predispersed Solvent Extraction 419
Y-D Wang, M Chen, L Xu and Y-Y Dai

EXTRACTION EQUIPMENT AND DESIGN 425

The AP Column – Development of a High Capacity Extraction Column 427
RW Cusack, DJ Glatz and TL Holmes

Development of a Multistage Mixer–Settler Column with a Novel Impeller 433
M Yamaguchi, H Yamashita, M Kaneda and H Noda

Drop Size and Phase Distribution in Extraction Columns 439
J Koch and A Vogelpohl

The Application of Electrical Capacitance Tomography to Liquid–Liquid Extraction Columns 445
GT Bolton, WJ Korchinsky, RC Waterfall and PD Martin

Study on Characteristics of Pulsed Packed Columns using Super-Mini-Rings (SMR) 451
J Yu and W Fei

Impacts of Packing on Mass Transfer of High Viscosity Solvents Drop Swarms 457
J Yu and W Fei

Flow Structure and Turbulent Flow Energy in Stagewise Extraction Columns: Influence of Stage Configuration 463
G Angelov and C Gourdon

Hydrodynamic and Mass Transfer Characteristics of Super-Mini-Ring (SMR), Raschig Ring and Pulsed Perforated Plate Columns 469
D Chen, W Fei, HRC Pratt and GW Stevens

Axial Mixing in a Large-scale Packed Extractor 475
O Becker, C Lewis, R Hardy and F Seibert

Performance of a Vibrating Perforated Plate Extractor – Hold-up and Characteristic Velocity 481
LMN Góis, EB Tambourgi, JAFR Pereira and JJ Marques

The Importance of Drop Coalescence in a Stirred Liquid–Liquid Extraction (Kühni) Column 487
MLACN Gomes, MML Guimarães, G Zamponi, J Stichlmair, PFR Regueiras and JJC Cruz-Pinto

Stage Efficiencies and Mass Transfer Coefficients in a Mixer–Settler Extraction Column 493
K Takahashi, T Ban, K Tani, S Nii and F Kawaizumi

Effect of Phase Entrainment on the Process in Centrifugal Extractors 499
GI Kuznetsov, AV Kosogorov, AA Pushkov and VS Skachkov

The Effect of Air Sparging on the Electrical Resolution of a Water-in-Oil Emulsion 503
PJ Bailes and PK Kuipa

Use of a Video Camera for the Development, Monitoring and Documentation of SX Processes 509
B Grinbaum

Multicomponent Kinetics in Liquid–Liquid Systems: an Experimental Study 513
MJ Brodkorb and MJ Slater

In-line Mixers for the Extraction of Uranium by a Tertiary Amine from Ore Leach Sulphuric Acid Solutions 519
GM Ritcey

Fast Pre-neutralisation and Extraction in a Tubular Reactor using an Acidic Extractant 525
E Jääskeläinen and E Paatero

Comparison between Different Extractors for a High Viscosity Extraction Application 531
D Kirschneck, H Schmitt and R Marr

Extraction Behavior of Pd(II) with Tri-*n*-octylamine in a Vibro-mixer Type Extractor 537
Y Kawano, K Shiomori, S Yamada, H Yoshizawa and Y Hatate

Comparison of Membrane-assisted Solvent Extraction Technologies for the Separation of Cd–Ni Mixtures 543
I Ortiz, F San Román, B Galán and AM Urtiaga

Reactive Extraction using a Karr Column for the Production of Dioxolane from an Aldehyde 549
B Grinbaum, M Adda and Ch Eidelman

FUNDAMENTAL STUDIES 553

Studies of the Extraction Thermodynamics of f-Elements 555
KL Nash

Synergistic Solvent Extraction of Aluminium(III), Gallium(III), and Indium(III) with 2-Thenoyltrifluoroacetone and TOPO 561
J Noro, A Hokura, I Tanaka, M Yamada and T Sekine

The Influence of 1-Octanol on Metal Extraction into HDEHP 567
OA Sinegribova, V Kim, NV Bukar, OV Sviridenkova and OO Olenicheva

Extracting Emulsions — Theoretical Review and Practical Usage 573
EV Yurtov and M Yu Koroleva

Gel-like DEHPA Salt Systems in Organic Solutions and on the Interface 579
EV Yurtov and NM Murashova

Extraction Behaviour of Alkali Metals under the Control of pH in Crown Ether–β-Diketone Extraction and Crown Ether–Substituted Phenol Extraction Systems 585
T Shimosato, N Hirayama and T Honjo

A Mechanistic Study on Ion Association Extraction with Quaternary Ammonium Ions 591
S Motomizu, T Takayanagi and E Wada

pH Dependence of Dicarboxylic Acid Extraction by a Strong Amine Based Extractant 597
R Canari and AM Eyal

A Spectral Study of the Relative Basicity of Long Chain Water-immiscible Organic Amines 603
L Poulad-Meyer and AM Eyal

A Study of the Motion of a Single Drop under the Influence of a Pulsed DC Electric Field 609
PJ Bailes, JGM Lee and AR Parsons

Single Drop Coalescence – Experiment and Simulation 615
A Eckstein and A Vogelpohl

Diffusivities for Multicomponent Mass Transfer Calculations 619
AR Uribe-Ramírez and WJ Korchinsky

Characterization of Polymeric Reversed Micelles 625
Y-D Wang, Z Li, H Huang and YY Dai

Membrane Coalescence as a Novel Phase Separation Stage for Extraction Processes 631
S Hoffmann and W Nitsch

Third Phase Formation: a New Predictive Approach 637
L Lefrancois, F Belnet, D Noel and Ch Tondre

Salt Effect in the Quaternary System Water + Ethanol + 1-Pentanol + Sodium Chloride at 25°C 643
MM Olaya, A Botella and A Marcilla

Study of Inclusion Complex Formation of Substituted Cyclodextrins with Xylene Isomers 651
I Uemasu

Modelling TBP/Diluent Mixtures and Water Extraction by these Mixtures Using the UNIQUAC Equation and Taking Account of Complex Formation 655
B Rat, B Dinh and C Poitrenaud

GUEST–HOST BINDING 661

A Novel Strategy for the Design of Organic Ligands of High Selectivity 663
S Umetani and QTH Le

The Ligand-thickness Effect Leads to Enhanced Preference for Large Anions in Alkali Metal Extraction by Crown Ethers 669
BA Moyer, TJ Haverlock and RA Sachleben

Liquid–Liquid Extraction of Metal Ions with a Monoazatetrathiacrown Ether and its Acyclic Analogues 675
K Chayama, C Kurihara, H Tsuji and E Sekido

Solvent Extraction of Rare Earth Nitrates by Phosphorylated Calix[4]arenes 681
M Burgard, B Ernst, MR Yaftian, CB Dieleman, C Wieser-Jeunesse and D Matt

QSPR of Extractability Trends of the Lanthanoid Series Using Novel Molecular Mechanics Calculations 687
K Yoshizuka, K Inoue, K Ohto, K Gloe, H Stephan, T Rambusch and P Comba

Extraction Behavior for Trivalent Lanthanides with Amides and EXAFS Study of their Complexes 693
H Narita, T Yaita and S Tachimori

Extraction of Uranium(VI) and Plutonium(IV) from Nitric Acid Solutions by Substituted Cyclic Amides 697
S Suzuki, K Tamura, S Tachimori and Y Usui

Oxidation of Cyanex 302 and Cyanex 301 by FT-Raman and UV-V Spectroscopy 703
A Almela, B Menoyo, MP Elizalde and F Mijangos

HYDROMETALLURGY 709

Indium Recovery from Industrial Zinc Residues 711
JS Benedetto, EB Tambourgi and RM Mingote

Indium Recovery by Solvent Extraction with D2EHPA using a Statistical Approach to the Experimental Design 717
MCB Fortes, AH Martins and JS Benedetto

A Separation and Recovery Process of Gallium and Indium from Zinc Refinery Residue 723
S Nishihama, T Hirai and I Komasawa

A Highly Efficient Process to Strip Iron from a New Organophosphorus Extractant 729
F Delmas and CA Nogueira

Solvent Extraction Studies for Cobalt and Nickel Separation from the Processing of Ammonium Carbonate Mixed Sulfides 735
E Garcia Liranza, AM Moreno Daudinot, R Viera Martínez and B Rosales Barazaga

Application of Solvent Extraction in Metal Recovery from Spent Nickel-Metal Hydride Batteries 741
P Zhang, T Yokoyama, O Itabashi, Y Wakui, TM Suzuki and K Inoue

Hydrometallurgical Process for Ni and Cd Recovery from Batteries: Preliminary Data. 747
Loris Pietrelli, Gianni Ponzo and Laura Ranieri

Cation Separation in Sulphate Medium using Solvent Extraction 753
AM Moreno Daudinot and E García Liranza

Extraction of Copper Contained in Ammonia Solutions from the Electronics Industry with LIX84 759
JM Chimenos, MA Fernández, M Segarra, AI Fernández, A Esparducer and F Espiell

Recovery Process of Ni with EHO from a Waste Etching Solution of Lead Frame Material 765
J Shibata, S Matsumoto, M Sano and S Nishimura

Strategies for Platinum Group Metal (PGM) Separation using Impregnated Resins 771
M Rovira, JL Cortina and AM Sastre

Solvent Extraction of Gold from Chloride Copper Anode Slime Liquors 777
K Soldenhoff and D Wilkins

Study of a Microemulsion System for Application in the Extraction of Gold 783
TN de C Dantas, AA Dantas Neto and WF de La Salles

Production of High Purity Tantalum Oxide by Solvent Extraction 789
A Feather, P Clark and G Boshoff

Recovery and Purification of Cerium(IV) and Thorium(IV) from Bastnasite Ore 795
J Lu, D Li, J Tang and T Zheng

Precipitation Stripping of Samarium Hydroxide from Tri-*n*-Butyl Phosphate with Aqueous NaOH Solutions 801
K Koyama and M Tanaka

New Extraction Technologies for the Treatment of Rare Metal Raw Materials Using Mechanochemical Methods 805
SV Chizhevskaya, AM Chekmarev, MV Povetkina, VL Shafirov and M Cox

Author index I

Keyword index IX

VOLUME 2

KINETICS AND INTERFACIAL PHENOMENA 811

A Study of Metal Ion Extraction at the Oil/Water Interface Using Evanescent Wave Spectroscopy 813
P Deljouie, JM Perera, GW Stevens and F Grieser

External Reflection Spectra at the Liquid–Liquid Interface of Extraction Systems Containing Porphyrins 819
N Ogawa, Y Moriya and H Watarai

Some Ideas on the Nature of Interfacial Processes in HDEHPA Extraction of Metals 825
VV Tarasov, OA Sinegribova and OV Sviridenkova

Mechanism of Interfacial Reactions in the Extraction of Iron by D2EHPA 829
T Kanki, H Kim, A Tomita, T Asano and N Sano

Mass Transfer of Organic Acids at Charged Liquid Interfaces 835
C Czapla and H-J Bart

The Coupling of Diffusion Coefficients in Continuous Phases at Liquid–Liquid Interfaces 841
A Tokarz, M Millies and D Mewes

Mass Transfer and Fluorescence Tracer Technique in Solvent Extraction 847
M Mörters and H-J Bart

Kinetics of Mass Transfer and the Different Effects of Surfactants 853
M Weigl and W Nitsch

Mass Transfer Characterization in Forward and Back Extractions of an Amino Acid by Reverse Micelles across a Flat Liquid–Liquid Interface 859
T Nishiki, K Nakamura and D Kato

Effect of Applied Voltage on the Extractive Separation of Rare Earth Metals by D2EHPA in the Presence of an Oil-soluble Complexing Agent 865
M Yamaguchi, D Kojima, M Goto, F Nakashio and S Nagao

Effect of Global Salt Concentration on the Rate of Extraction of Copper(II) by Acorga® CLX-50 and Germanium(IV) by Kelex® 100S 871
G Cote and C Bouvier

A Rotating Membrane Cell Technique for the Study of LLX Kinetics. Application to the Study of Salt Effects 877
JP Simonin, H Hendrawan and J Weill

Kinetic Studies and Molecular Dynamics Simulations of Interfacial Complexation in Solvent Extraction Systems 883
H Watarai and Y Onoe

Mass Transfer Kinetics of Rare Earth Elements with Hollow Fibre Membrane Based Extraction 889
Yujie Wang and D Li

Solvent Extraction Kinetics through Hollow Fibre and Flat Membranes. Investigation with Nitroxide Radicals 893
NM Kocherginsky, AN Osipov and AB Grishchenko

Kinetics and Mechanism of Synergistic Extraction of Gallium(III) with an Acidic Organophosphorus Compound in the Presence of Oxine Derivatives 899
K Kondo, M Matsumoto, K Yano and T Okubo

Extraction Kinetics in the Er(III) 2-Ethylhexyl-2-ethylhexylphosphonic acid (HEH/EHP) Heptane System 905
J Lu, Z Zheng, D Li and G Ma

The Rule of Transition of Extraction Kinetic Behaviour of Rare Earth Elements with DMHMP 911
D Sun, S Le and D Li

Extraction of Iron(III) from Aqueous Sulphuric Acid Solution Using a Packed Column 915
M Rosinda, C Ismael and JMR Carvalho

A Mass Transfer Model for the Extraction of Te(IV) in the Presence of Se(IV) using Tri-*n*-Butylphosphate as Extractant 921
M Bandyopadhyay, S Datta and SK Sanyal

Extraction–Chromatography: Equilibria and Kinetics 927
A Schöneberger, H-J Bart, A Nanoti and A Wildberger

Computer Simulation of Interfacial Behaviour of N-8-Quinolylsulfonamide for the Extraction Kinetics of Copper 933
F Nakashio, A Sakoguchi, E Zushi, R Ueoka and K Yoshizuka

The *LAP*-Model – a New Approach for Modeling the Kinetics of Reactive Extraction 939
M Roos and H-J Bart

LIQUID MEMBRANES 945

Comparing Cyanex 301 with D2EHPA for the Extraction of Nickel through Emulsion Liquid Membranes 947
A Hoffmann, M Verhaege and RF De Ketelaere

Effects of some Parameters on Cobalt/Nickel Separation and on Cobalt Permeation by a Liquid Surfactant Membrane Process 953
A Salum, GL da Silva, MB Mansur, TLS Miranda and VST Ciminelli

Liquid Membrane Permeation of Zinc in a Continuous Countercurrent Column 959
MTA Reis, H-J Bart and JMR Carvalho

Purification of a Radioactive Liquid Effluent: Elimination of Caesium by Liquid Surfactant Membrane Extraction 965
D Pareau, P Kaplan, M Stambouli and G Durand

Mechanism of Transmembrane Water Transfer and Emulsion Swelling 971
MYu Koroleva, NV Bakastova and EV Yurtov

Recovery of 4-Hydroxybenzoic Acid from Aqueous Solutions by Emulsion Liquid Membranes 977
PFMM Correia and JMR Carvalho

Purification and Concentration of Lactic Acid by Emulsion Liquid Membrane Extraction 983
T Berrama, D Pareau, M Stambouli and G Durand

Preparation of Metal–Silicate Microballoons with Liquid Surfactant Membrane 989
T Hano, M Hirata, H Takanashi and Y Nakahara

Selective Recuperation of Copper by Supported Liquid Membrane (SLM) Extraction 995
RF De Ketelaere and J Van der Linden

Uphill Transport of Silver(I) from Nitric Acid Media using Binary Extractants as Potential Liquid Membrane Carriers 1001
A Kumar, PK Gautam, JP Shukla, RK Singh and AM Sastre

Chromium(VI) and Chromium(III) Separation by Supported Liquid Membranes and Polymeric Inclusion Membranes 1007
J Gega, C Kozlowski and W Walkowiak

Dispersion-free Membrane Based Extraction and Stripping of Pb(II) and Cd(II) with Kelex 100 as Carrier 1013
J de Gyves, JC Aguilar and E Rodríguez de San Miguel

Membrane-based Solvent Extraction for Indium(III)–Iron(III) Separation using a Hollow Fibre Contactor 1019
E Rodríguez de San Miguel and J de Gyves

Pertraction of Neodymium and Holmium in a Hollow Fibre Contactor 1023
G Cara, Š Schlosser, M Muñoz and M Valiente

Characterisation of the Stability and Efficiency of a Hollow Fibre Supported Liquid Membrane Containing Aliquat 336 as Carrier for Rhodium(III) Transport 1029
C Fontàs, C Palet, V Salvadó and M Hidalgo

Separation of Amine and Amino Acid Enantiomers Using Supported Liquid Membranes with Chiral Phosphoric and Phosphonic Acid Esters 1035
P Wieczorek, P Dzygiel and P Kafarski

Pertraction and Membrane Based Extraction of Carboxylic Acids in Hollow Fibre Contactors 1041
Š Schlosser, E Sabolová and J Marták

Transport Properties of Activated Composite Membranes Containing Di-(2-Ethylhexyl)-Dithiophosphoric Acid as a Carrier Towards Polyvalent Metal Ions 1047
M Oleinikova, J Macanas, M Muñoz and M Valiente

Use of a PVC-based Aliquat 336 Membrane to Extract Cd(II) and Cu(II) from Chloride Solutions 1053
L Wang, R Paimin, RW Cattrall and SD Kolev

Separation of Esters of Polyunsaturated Fatty Acids by Bulk Liquid Membrane with a Porous Partition 1059
S Nii, R Yokosawa and K Takahashi

Transport of Phenol through Bulk Liquid Membranes 1065
W Cichy, Š Schlosser and J Szymanowski

Recovery of Silver Traces from Electronic Wastes 1071
G Durand, D Pareau and K Ennassef

METAL AND NON-METAL EXTRACTION 1079

Rare Earths Separation Study 1081
D Li

Solvent Extraction Separations of Trivalent Lanthanide and Actinide Ions using an Aqueous Aminomethanediphosphonic Acid 1089
MP Jensen and KL Nash

Extraction and Separation of Lanthanides and Actinides in Aqueous Nitric Acid by 'CMPO-like' Calixarenes 1095
A García-Carrera, H Rouquette, JF Dozol, V Böhmer and AM Sastre

Solvent Extraction of Rare Earth Elements(III) with a Bifunctional Phosphinic acid 1103
Y Wakui, T Yokoyama and K Akiba

Solvent Extraction of Lanthanides and Yttrium from Nitrate Solutions with Cyanex 923 1109
D Chu, G Ma and D Li

Separation of Yttrium and Neodymium from Nitrate Solutions by Di-(2-Ethylhexyl)-phosphoric Acid Impregnated on Amberlite XAD-2 Resin 1115
M Iglesias, E Anticó and V Salvadó

Distribution of Neodymium(III) between Acidic Aqueous Nitrate Solutions and Organic Solutions of Di-(2-Ethylhexyl)phosphoric Acid in Kerosene at Low Metal Concentration 1121
JM Sánchez, M Hidalgo, M Valiente and V Salvadó

Solvent Extraction Studies of Erbium(III) by 2-Ethylhexylphosphonic Acid Mono-2-Ethylhexyl Ester (Ionquest 801) from Hydrochloric Acid Solutions 1127
IO Masson, PSM Soares, M Aguilar and JL Cortina

Synergistic and Antagonistic Behaviour in the Stripping of Heavy Rare Earth Elements from Solvent Mixtures Containing Phosphonic and Phosphinic Acids and Trialkylphosphine Oxides 1133
D Nucciarone, CD Pagnucco, B Jakovljevic and WA Rickelton

Extraction of Chloro Complex Acids of Platinum Group Metals with Binary Extractants 1139
VV Belova, AI Kholkin and TI Jidkova

Thermodynamic and Kinetic Studies of Palladium(II) Extraction by LIX 63–Aliquat 336 Mixtures 1143
C Foulon, S Pareau, M Stambouli and G Durand

Extraction Behaviour of Platinum(IV) in Chloroform with a Crown Ether from Acidic Media 1149
KZ Hossain and T Honjo

Comparative Studies of Solvent Extraction and Liquid Membrane Permeation of Gold(III) from Chloride Media 1155
R Haddad, A Kumar, FJ Alguacil and AM Sastre

Extraction of Pentachloroaquaosmate(IV) Ion from Sulphuric Acid Solutions 1161
AB Maiboroda, ID Troshkina and AM Chekmarev

Solvent Extraction of Ruthenium(III) as a Thiocyanate Complex 1167
B Tamhina, V Vojkovic and N Brajenovic

Extraction of Iron(III) from Hydrochloric Acid Solutions by an α-Hydroxyoxime 1173
T Sato, M Ito and M Hotta

Third Phase Appearance in Cobalt(II) and Nickel(II) Extraction with Mono-(2-Ethylhexyl)-phosphonic Acid 2-Ethylhexyl Ester (MOOP) 1177
Da Maljkovic, Z Lenhard and Du Maljkovic

Extraction Equilibria of Nickel with LIX860 and DEHPA 1181
T Sana, K Shiomori, Y Kawano and K Nagayoshi

Stoichiometry of the Extraction of Nickel with Organophosphorus Acids 1187
CC Bourget, M Cox and DS Flett

Copper Extraction from Ammoniacal Solutions with Commercial Chelating Extractants and their Mixtures 1193
G Kyuchoukov, MB Bogacki and J Szymanowski

Extraction of Copper from Chloride Media with a New Alkyl Derivatives of Pyridine-3,5-Dicarboxamide 1197
A Borowiak-Resterna, G Cote and J Szymanowski

Extraction of Copper and Zinc from Chloride Solutions by an Hydrophobic Alkyl Derivative of 8-Hydroxyquinoline 1203
G Kyuchoukov, A Jakubiak and J Szymanowski

Liquid–Liquid Extraction of Zinc(II) by Solvating Extractants from HCl/H_2SO_4 Mixed Media 1209
JA Barron Zambrano, M Avila-Rodríguez, TI Saucedo Medina, R Navarro Mendoza and AM Sastre

Solvent Extraction of Divalent Zinc and Cadmium from Hydrochloric Acid Solutions by Dihexylsulphoxide 1215
T Sato, I Ishikawa and K Sato

Solvent Extraction of Divalent Zinc and Lead from Sodium Hydroxide Solutions by an Alkylated Hydroxyquinoline 1221
T Sato, K Sato and F Tahiani

Extraction of Lead(II) by Cyanex 302 and Cyanex 301 from 2.19 mol/dm^3 Phosphoric Acid Medium 1227
B Menoyo and MP Elizalde

Solvent Extraction of Scandium(III) with Cyanex 302 and H[BTMPTP] 1233
D Li , C Wang and Z Wei

Solvent Extraction of Scandium(III) by Cyanex 272 and H[BTMPP] 1239
C Wang and D Li

Solvent Extraction of Tin(IV) from Hydrochloric Acid Solutions by High Molecular Weight Amines 1245
T Sato, K Sato and Y Noguchi

Separation of Cesium and Strontium from s-Block Metal Ions by Double and Triple Phase Systems 1249
Y Komatsu, S Umetani and S Tsurubou

The Stoichiometric Modelling of the Exchange Extraction of Mg, Ca and Na with Potassium Di-2-Ethylhexylphosphate from Concentrated Brines 1255
NM Rice and MA Tomlinson

Extraction of Arsenic(III) and Arsenic(V) from Sulphuric Acid Solutions with Trialkylphosphine Oxides and Hydroxamic Acids 1261
M Wisniewski, L Iberhan and J Szymanowski

New Developments in Solvent Impregnated Resins. An Overview 1267
A Warshawsky, JL Cortina, M Aguilar and K Jerabek

Influence of Polymeric Support on Selectivity of Extractant in Solvent Impregnated Resins 1273
A Gonzalo, D Muraviev and M Valiente

Extraction of Heavy Metal Ions using Encapsulated Extractant-impregnated Resin 1279
S Nii, M Masutani and H Takeuchi

Design of a Truly Continuous Fluidized Bed System for Metal Recovery using Impregnated Resins 1285
M Rovira, J Herranz, JL Cortina, N Miralles, J Arnaldos and AM Sastre

Extraction of Non-extractable Ionic Species in Aqua Impregnated Resin Systems 1291
D Muraviev, A Torrado and M Valiente

Extraction of Rare Earth Metals with PC-88A by a Hollow Fibre Membrane System 1297
F Kubota, M Goto, S Furusaki, K Yoshizuka, F Nakashio and T Hano

Hollow Fibre non-Dispersive Solvent Extraction: a Promising Approach to Environmental and Hydrometallurgical Applications 1303
A Kumar and AM Sastre

Hydration of Metal Perchlorates Extracted with Trioctylphosphine Oxide in Hexane 1309
S Kusakabe

Solvent and Solid Extraction of Metal Ions with 4-*n*-Dodecyl-6-(2-thiazolylazo)resorcinol 1313
H Matsunaga

The Separation of Phenol from Neutral Oils by Liquid–Liquid Extraction 1319
DL Venter and I Nieuwoudt

Extraction of Acetic and Propionic Acids from Aqueous NaCl Solutions by Trioctylphosphine Oxide 1325
HF Al-Mudhaf, AI Abu-Shady, SA Amer and MF Hegazi

NUCLEAR APPLICATIONS 1331

Extraction of Lanthanides(III) and Actinides(III) by N,N′-Substituted Malonamides: Thermodynamic and Kinetic Data 1333
MC Charbonnel, M Daldon, C Berthon, MT Presson, C Madic and C Moulin

The Solvent Extraction Behaviour of Tetravalent Actinides in the Presence of Simple Hydroxamic Acids 1339
RJ Taylor, I May and NJ Hill

Development of a Universal Cobalt Dicarbollide Solvent for the Removal of Actinides, Cesium and Strontium from Acidic Wastes 1345
TA Todd, KN Brewer, JD Law, RS Herbst, DJ Wood, VN Romanovskiy, V Esimantovskiy, IV Smirnov, VA Babain and B Zaitsev

Extraction of Tetravalent Uranium from Phosphate Medium by HDEHP and OPAP 1351
JA Daoud, MM Zeid and HF Aly

Synergistic Extraction of U(VI) and Th(IV) from Nitric Acid with HBMPPT and TOPO in Toluene 1357
S-N Yu, L Ma and B-R Bao

Study on the Solvent Extraction of U(VI) and Th(IV) from Nitric Acid with HBMPPT 1361
S-N Yu, T-J Wang and B-R Bao

Solvent Extraction of Tc and Cs from Alkaline Nitrate Wastes 1365
BA Moyer, PV Bonnesen, LH Delmau, TJ Haverlock, RA Sachleben, RA Leonard, C Conner and GJ Lumetta

Extraction of Strontium and Cesium Using a Synergistic Solvent Mixture 1371
TA Todd, DJ Wood, MA Afonin and VV Romanovski

Use of Binary Extractants for Recovery of Silver(I) from Waste: a Novel Concept in Solvent Extraction 1375
A Kumar, PK Gautam, JP Shukla, RK Singh and AM Sastre

New Reducing Agents for Neptunium(VI) and Plutonium(IV) 1381
RJ Taylor, I May, IS Denniss, VS Koltunov, SM Baranov, VI Marchenko, EA Mezhov, VG Pastuschak, GI Zhuravleva and OA Savilova

Thermodynamics of Extraction Behavior of Eu(III) And Tm(III) by Thenoyl-trifluoroacetone and Crown Ethers in Organic Solvents from Nitrate Medium 1387
FA Shehata, N El-Hefny and HF Aly

PETROLEUM APPLICATIONS 1395

A Deep Desulfurization Process for Light Oil by Photochemical Reaction in an Organic Two–Phase Liquid–Liquid Extraction System 1397
Y Shiraishi, T Hirai and I Komasawa

Hydrogen Sulfide Removal from Hydrocarbon C_3–C_4 Fraction 1403
S Costic, F Oprea and F Enachescu

PHARMACEUTICAL APPLICATIONS 1409

Extraction of Citric Acid in Hollow Fibre Modules 1411
I Miesiac, P Kirschling and J Szymanowski

Solvent Extraction of Phthalic Acid with Basic Extractants, and the Structure of the Complexes Formed 1417
S Rambocus, N Kelly, BG Reuben and A Drake

Specific Inhibitory Effects of Hybrid Membranes on the Growth of Tumors *in vitro* and *in vivo* 1423
R Ueoka, Y Matsumoto, T Kato, A Kanno, M Tsuchiya, K Tsuzaki and Y Murakami

PLANT EXPERIENCE 1429

The Thermal Oxide Reprocessing Plant at Sellafield: Four Years of Active Operation of the Solvent Extraction Plant 1431
C Phillips

Mini-plant Trials on the Recovery of Nickel by Solvent Extraction 1437
VM Nagel, BM Davies and PM Cole

Pilot-plant Evaluation of Manganese Removal and Cobalt Purification by Solvent Extraction 1443
A Feather, KC Sole, and DB Dreisinger

Updated Available Solvent Extraction Technologies 1449
G Díaz, D Martín, C Frías and O Pérez

Comparison of the Performance of Full Scale Pulsed Columns *vs* Mixer–Settlers for Uranium Solvent Extraction 1455
RL Movsowitz, R Kleinberger, EM Buchalier, B Grinbaum and S Hall

PROCESS DEVELOPMENT 1461

The Development of Chemical Flowsheets for an Advanced Purex Process 1463
AL Wallwork, P Bothwell, JE Birkett, IS Denniss, RJ Taylor and I May

Distribution behaviour of Uranium, Plutonium, Neptunium and Technetium in an Advanced PUREX Process (PARC process) 1469
G Uchiyama, T Kihara, H Mineo, T Asakura, S Hotoku, M Watanabe, K Kamei, Y Nakano, S Kimura, M Goto and S Fujine

Development of Fission Product (artificial) Palladium Liquid–Liquid Extractive Recovery and Refining Operations 1475
Ed V Renard, VG Torgov, VV Tatarchuk, TM Korda and IA Druzhinina

A New Process Producing Phosphoric Acid from Phosphate Rock and Hydrochloric Acid via Ferric Phosphate 1481
J Mizrahi

Selection of Extractants for the Removal of Cadmium from Industrial Grade Phosphoric Acid 1487
I Ortiz, S Zamacona and AM Urtiaga

Production of WO_3 from Scheelite Concentrates by Extraction Technology 1493
SI Stepanov, VG Giganov, GP Giganov and AM Chekmarev

Separation and Concentration of l-Phenylalanine in Hollow Fibre Modules: Decrease of the Extraction Rate 1499
H Escalante and A Irabien

Process Development, Design and Scale-up Using a Large Scheibel Extraction Column 1503
TC Lo

SIMULATION AND MODELLING 1509

Modelling of the Separation of Cadmium from Phosphoric Acid using Emulsion Liquid Membranes 1511
T Gallego Lizon and ES Pérez de Ortiz

Hollow Fibre Modules as Novel Phase Contactors for the Separation of Multi-cation Mixtures by Chemical Extraction 1517
A Geist, JI Kim, P Plucinski and W Nitsch

Modelling of Continuous Reactive Extraction and Stripping of Zinc in Hollow Fibre Modules 1523
P Schöner, W Nitsch, P Plucinski and A Fedorov

Mathematical Modelling of Metal Permeation across Supported Liquid Membranes Considering Membrane Rate Controlling Parameters 1529
G Benzal, A Kumar, A Delshams and AM Sastre

Modelling Phase Equilibria in the Industrial Caprolactam Recovery from Aqueous Ammonium Sulphate Solutions with Benzene 1537
AB de Haan and SH Niemann

Modelling and Optimization of Sulfolane Extraction: a Neural Network Approach 1543
G Su, X Wen, and W Fei

A New Method for the Simulation of Multistage Metal Extraction Processes Based on the Steady-State Local Linearization 1549
M Tanaka, K Koyama and J Shibata

DISTREC: a New Computer Program for Solvent Extraction Equilibrium Calculations, Modelling and Simulation 1555
M Aguilar, JL Beltran and JL Cortina

Soft Modelling Techniques: a Tool for Studying Solvent Extraction Processes 1561
JL Cortina, M Aguilar, M El-Gharbi and R Tauler

Co-current Extraction: Design of Industrial Equipment by Scaling-up Laboratory Tests 1567
V Alessi, A Franzoni, C Gradella, R Penzo and MJ Slater

Influence of Continuous Phase Flow Field and Compartment Geometry on Droplet Breakage in Rotating Disc Contactors 1573
G Modes and H-J Bart

Mass Transfer Performance in a Pulsed Sieve Plate Extraction Column 1579
GS Luo, HB Li, W Fei and JD Wang

Prediction of Flooding in Random and Structured Packed Columns using a Drift Flux Methodology 1585
LS Hutahaean, DM Schaefer, JS Kanel and V Van Brunt

Supercritical Extraction 1593

A Mechanically Agitated Supercritical Extraction Column 1595
A Laitinen and J Kaunisto

Separation of Enantiomeric Acids and Bases by Supercritical Fluid Extraction 1601
B Simándi, S Keszei, E Fogassy, E Székely, A Prechl, V Varga, S Kemény and J Sawinsky

Supercritical Fluid Extraction of Tocopherols from Olive Tree Leaves 1607
A de Lucas, E Martínez de la Ossa, J Rincón, MA Blanco and I Gracia

Supercritical Fluid Extraction of Borage Oil 1611
A Delgado, A Molero and E Martínez de la Ossa

Supercritical Fluid Extraction of Anthocyanins from Grape Pomace 1615
C Mantell, E Martínez de la Ossa and M Rodríguez

Acetic Acid Extraction by Supercritical Carbon Dioxide: Pressure Effect 1619
C Pereyra, G Di Giacomo and E Martínez de la Ossa

Regeneration of ß-Cyclodextrin with Supercritical Carbon Dioxide 1623
G Del Re, G Di Giacomo and M Cinti

Tocopherol Extraction by Liquid and Supercritical Carbon Dioxide 1629
MA Blanco, A Molero and E Martínez de la Ossa

Extraction of Wheat Germ Oil by Liquid and Supercritical Carbon Dioxide 1633
A Molero and E Martínez de la Ossa

Extraction of the Antibiotic Pleuromutilin from Fermentation Broth using Compressed Carbon Dioxide 1639
T Walford, T Lu, R Santos, MB King, AJ Biddlestone and A Stefanska

Direct Supercritical Fluid Extraction of Organic Compounds from Aqueous Solutions 1645
Yu A Zolotov, IA Revelsky and IN Glazkov

Supercritical Fluid Extraction of PCBs from Real World St. Lawrence River Sediments 1651
Z Wu and LL Tavlarides

Ligand-assisted Supercritical Fluid Extraction and Environmental Management needs for Removal of Metals 1657
RV Fox, RD McMurtrey and JD Navratil

Supercritical Fluid Extraction in Gold Hydrometallurgy 1663
EO Otu

Modelling of Supercritical Fluid Extraction from Natural Materials with Interaction between Solutes and Solid 1669
M Goto, A Kodama and T Hirose

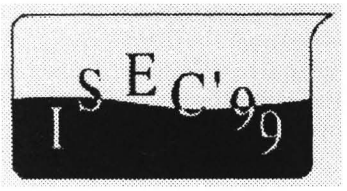
Modelling of the Fluid–Solid Equilibria of the Antibiotic Penicillin G in Supercritical Carbon Dioxide 1675
MD Gordillo, A Molero and E Martínez de la Ossa

Author index I

Keyword index IX



Plenary and Keynote Lectures



MOLECULAR DYNAMICS OF LIQUID SURFACES AND INTERFACES

Ilan Benjamin
Department of Chemistry and Biochemistry, University of California, Santa Cruz, California 95064, USA

ABSTRACT
Molecular dynamics computer simulations have been used in recent years to gain important insight into the structure, dynamics and the thermodynamic of the interface between two immiscible liquids. This insight makes it possible to study some of the fundamental processes involve in the liquid extraction process. This include the adsorption of solute molecules, and the processes of solute transfer across the interface. Recent progress in this area is reviewed. It is demonstrated that an account of the molecular molecular structure of the interface is important for understanding fundamental chemical processes at the interface.

Keywords: molecular dynamics, modelling, interfacial adsorption, solvation

INTRODUCTION

Understanding fundamental processes such as adsorption, solvation and solute transfer at the interface between two immiscible liquids is of fundamental importance for liquid extraction processes as well as for other interfacial phenomena in chemistry and biology. In recent years, the traditional techniques for studying the structure of the neat interface (such as measurements of surface tension and surface potential)[1,2] have been complemented by new approaches that have the ability to provide a detailed understanding of the system at the microscopic level . For example, using non-linear optical techniques[3-6] and light and neutron scattering[7,8] new insight into the structure of liquid interfaces and into several phenomena at liquid interfaces has been achieved.

In parallel to this progress, molecular dynamics computer simulations have provided new insight into the structure and dynamics of the neat liquid/liquid interface and into processes such as solvation and reactions that take place at the interface.[9-11] In this paper we provide a brief account of the application of the method of molecular dynamics computer simulations to studying the neat liquid/liquid interface and the process of solvation and solute transfer at the interface. The results of the molecular simulations underscores the unique properties of the interfacial region between two immiscible liquids. This is significant because the thermodynamics and kinetics of chemical reactions in liquids are known to be significantly influenced by the solvent. Thus, it is expected that the transition from the bulk to the interface region will give rise to major affects on chemical reactivity.

METHODS

The application of molecular dynamics computer simulations to study structure and dynamics at liquid interfaces has been reviewed recently[12] and only brief account will be given here. There are also several excellent books on the general techniques of molecular dynamics simulation[13,14] and the reader is referred to them for additional information. The fundamental basis of (classical) molecular dynamics computer simulations is the numerical solution of the Newton equations of motion:

$$m_i \frac{d^2 r_i}{dt^2} = -\nabla_i U(r_1, r_2, ..., r_N) \qquad (1)$$

for a system of up to a few thousand particles where $U(r_1, r_2, ...r_N)$ is the potential energy of the system.. In principle, this potential energy function can be determined by solving the Schrödinger equation for the ground state energy. Unfortunately, this is not practical for a system made of several thousands of atoms.

© 2000 Society of Chemical Industry

As a result one uses an empirically determined potential energy function which is selected to reproduce certain experimental data.
A simple, commonly used form for this function is based on representing the total system potential energy as a sum of interactions between pairs of atoms. Each atom is characterised by a set of Lennard Jones parameters and point charges:

$$U = \sum_{i<j}^{N} \left\{ 4\varepsilon \left[\left(\frac{\sigma}{r} \right)^{12} - \left(\frac{\sigma}{r} \right)^{6} \right] + \sum_{k,l}^{S} \frac{q_{ik} q_{jl}}{r_{kl}} \right\} \qquad (2)$$

where r is the distance between molecules i and j, r_{kl} is the distance between two point charges in two different molecules. For example, in the Simple Point Charge (SPC) model of water, one charge is fixed at the location of the oxygen ($q = -0.82$ au) and two charges at the location of the two hydrogens ($q = +0.41$). The OH bond distance is taken to be 0.1 nm, and the HOH angle is 109.47 degrees. For the SPC model, $\sigma = 0.316\,\text{nm}, \varepsilon = 0.650\,\text{kJ/mol}$. Despite the simplicity of this model, many structural and dynamical properties of water calculated using it are in reasonable agreement with experimental results.[15]
Simulations of bulk liquids involve enclosing a certain number of molecules in a box of a fixed volume. The integration of the equation of motion is done in such away as to satisfy conditions of fixed temperature. Fluctuations in the system volume can be introduced in order to satisfy constant pressure conditions. In simulations of the interface between two liquids, one try to create the typical experimental geometry of a planar interface by employing normal periodic boundary conditions in the two directions perpendicular to the interface normal. Along the direction normal to the interface, the system composition changes. Proper choice of the system's potential energy function is necessary to avoid complete mixing of the two liquids. In practice, one starts from two separate rectangular boxes containing the two liquids. The two boxes have the same cross sections, but different lengths depending on the number of molecules used and the density of the liquids. The two boxes are brought together face to face to form the simulation box.
An important aspect of computer simulations at liquid interfaces is the calculation of adsorption free energy of small solute molecules. A discussion of this topic will be given below.

RESULTS

The neat interface

Proper account of the structure and dynamics of the neat interface between two immiscible liquids is of prime importance for the interpretation of experimental data and for the development of simple models of the interface and of processes that takes place at the interface. In general we expect that the asymmetry in the intermolecular forces experienced by molecules in the liquid interface region gives rise to unique structural and dynamical properties of the interface, but direct experimental observation of these properties is difficult because of the relatively small size of the region and the buried nature of the interface. As a result, most of our detailed knowledge about the neat liquid/liquid interface has been obtained from molecular dynamics computer simulations. This include simple model liquids[16-18] (hard spheres or Lennard-Jones potentials), and the interface between water and benzene[19], hexanol,[20] hexane,[21] 1,2-dichloroethane,[22] decane,[23] nonane,[24] octanol,[25] carbon tetrachloride[26] and nitrobenzene.[27] The reader is referred to these original papers for details about the systems potentials and other simulations details. Below we summarise the main general results.

The most basic question about the interface between two immiscible liquids that is quite difficult to obtain experimentally but has been relatively straightforward to answer by computer simulations is how big the interfacial region is. A related issue is the degree of the inter-penetration of the two liquids at the interface. Although in principle one can use light and neutron scattering to gain information about the liquid/liquid interface structure, in practice these techniques have mainly been applied to the free liquid surface.[7,28-33]

Molecular dynamics simulations provide direct information about the density profile of the two liquids. In most cases the density of each liquid varies smoothly in the interface region, whose total thickness is on the order of few nm. Although the monotonic change in the densities is common to many liquids there is evidence from molecular dynamics simulations[18,22-24] for some oscillations in the densities on the bulk side of the liquid/liquid interfacial region. It is not clear that these oscillations are a real physical aspect of the system or an artifact due to the small system size and/or short simulation time.

Other important structural properties obtained by molecular dynamics computer simulations are the microscopic (molecular) structure of molecules at the interface. These properties can be directly compared with the corresponding properties in the bulk liquid phase. Because of the asymmetry in the forces experienced by molecules at the interface, in a number of liquid/liquid systems these molecules have a preferential orientation. For example water molecules tend to have their dipole parallel to the interface which is consistent with the relatively small potential drop across the interface. The organic molecules can have very little orientational ordering (as in the case of 1,2-dichloroethane[22] and CCl_4)[26], can lie parallel to the interface (as in the case of nonane[24] and decane[23]) or lie perpendicular to the interface (as in the case of octanol).[25]

Another important microscopic property about which a wealth of information has become available in recent years is the degree of hydrogen bonding of interfacial water molecules. A unified picture has emerged from several molecular dynamics simulations of water/organic liquid interfaces:[19-22,24,26] The number of hydrogen bonds per water molecule decreases from about 3.6 to 2 as one moves from the bulk to the interface. However, when one takes into account the reduced density of water at the interface by dividing the number of hydrogen bonds per water molecule by the co-ordination number of water, one finds that the probability that any hydrogen bond exists goes up from about 0.8 in bulk water to 0.9 at the interface. This means that although at the interface there are less water molecules to hydrogen bonds, the existing hydrogen bonds are more stable.

In addition to structural information the molecular dynamics calculations provide informations about the dynamics of the interface. This include the dynamics of variables such as the average location of the interface and its width, as well as single molecule reorientation time and diffusion rates. This has been discussed for the water/DCE interface[22] and also, to some degree, for the water/CCl_4 interface[26] and the water/nitrobenzene interface.[27] The dynamics of surface width and location fluctuations for these interfaces are on the tens of picoseconds time scale and can be described in terms of water and organic molecule "fingers" that protrude into the other phase. The motion of the water "fingers" involves the diffusion of water molecules as well as the breaking and forming of hydrogen bonds in interfacial water molecules. Molecular dynamics computer simulations generally find that the water molecules' reorientation at the liquid/liquid interface is quite similar to the dynamics in bulk water.[22]

Adsorption and solvation at liquid/liquid interfaces

Adsorption of solute molecules at the interface between two immiscible liquids is a fundamental factor in the discussion of any chemical process that takes place at the interface. This is because any interfacial reaction must begin with the adsorption of the reactants at the interface or the transfer of solute across the interface. For the purpose of a quantitative study of adsorption at the interface, one define the interface region as the region where the density of the two liquids is smaller than their bulk density. Another important concept is the Gibbs dividing surface. This is the plane $z = Z_{Gibbs}$ such that the excess of molecules of one of the components on one side of the interface is exactly balanced by the depletion on the other side. Although a different location would be defined with respect to each of the two liquids, the difference is quite small and of no fundamental importance.[34]

Adsorption at the liquid/liquid interface is different from that at a solid/liquid interface by one important factor: the solute can cross the liquid/liquid interface. Thus studies of adsorption is directly related to solute transfer. The main theoretical effort has been concentrated on deriving an adsorption isotherm, calculating the surface tension, and on determining the density and orientational profile of the solute. Some details are given in a recent review by Markin and Volkov.[35] Unfortunately, the main limitation of most of the existing theoretical tools is that information about the microscopic structure of the

solvent and the solvated solute are not included. The molecular dynamics and Monte Carlo computer simulations allows one to gain important microscopic insight while computing experimentally accessible thermodynamic properties such as adsorption free energy.

Solute transfer across the interface between two immiscible liquids is one of the most basic processes that is part of many other chemical processes of importance in electrochemistry, extraction science and pharmacology. Although it has been the focus of a significant number of experimental[36-39] and theoretical studies,[11] there are still open fundamental questions regarding the transfer mechanism. One of the problems is that the rate of transfer is difficult interpret because of the need to disentangle the contribution due to the diffusion through the bulk region and because of an incomplete knowledge about the interface structure.

Some of the outstanding problems are:

1. Is the solute transfer process an activated process? If so, what is the molecular nature of the activation barrier? Is there a structurally well-defined transition state?
2. Is the process of switching the solvation shell an activated process?
3. Does the process of ion transfer from one phase to the other involve significant dragging of the solvation shell? Is there a significant perturbation of the neat liquid/liquid interface structure?

Partial answer to the above questions can be obtained by using molecular dynamics computer simulations . In particular, one of the important ingredients of any model of solute transfer, the free energy profile of the solute across the interface, can be easily computed by molecular dynamics simulations. For technical details see.[12] The free energy profile has been calculated for a large number of interfacial systems,[11] and has been determined for several neutral solutes[40] and ions[41-43] across the liquid/liquid interface. Examples of these free energy profile and their utility in helping clarify the mechanism for ion transfer will be discussed in the lecture.

Additional insight into the mechanism of solute transfer across the liquid/liquid interface may be gained by non-equilibrium molecular dynamics simulations. Typically, a solute molecule is placed in one of the phases and it is allowed to diffuse to the other phase under the free energy driving force. Extensive non-equilibrium calculations[41] of an ion transfer across liquid/liquid interfaces have been performed and will be discussed as well.

One of the main results of the above calculations that will also be discussed is that surface roughness plays an important role in the transfer mechanism. For example, the transfer of an ion from 1,2-dichloroetahne to water is initiated by water molecules that are only weakly hydrogen-bonded to other interfacial water molecules, and which typically extend out into the organic phase as "water fingers". These fingers can extended to more than 10Å into the organic phase and interact with the ion. Although they are a normal property of the interface, they are also induced by the presence of the ion. As soon as a few water molecules begin to interact with the ion, the build-up of the water co-ordination shell, which occurs at the interfacial region, is quite rapid. The opposite transfer of the ion from the water to organic phase under the influence of an external electric field is characterised by the fact that the ion keeps a water co-ordination shell nearly intact through its motion in the interfacial region, which results in increased roughness and "fingering" at the interface.

REFERENCES

1 Bard AJ and Faulkner LR. *Electrochemical methods: fundamentals and applications,* Wiley, New York, (1980).

2 Adamson AW. *Physical Chemistry of Surfaces*, Fifth ed., Wiley, New York, (1990).

3 Shen YR. *The Principles of Nonlinear Optics,* Wiley, New York, (1984).

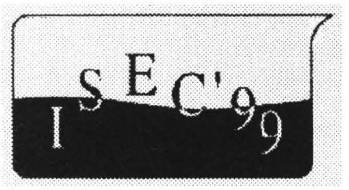
4 Corn RM and Higgins DA. *Chem. Rev.* **94,** 107 (1994).

5 Brevet PF and Girault HH, in *Liquid-Liquid Interfaces*, edited by Volkov AG and Deamer DW, CRC press, Boca Raton, 103, (1996).

6 Eisenthal KB. *Chem. Rev.* **96,** 1343 (1996).

7 Pershan S. *Faraday Discuss. Chem. Soc.* **89,** 231 (1990).

8 Lee LT, Langevin D, Mann EK and Farnoux B. *Physica B* **198,** 83 (1994).
9 Pohorille A and Wilson MA. *J. Mol. Struct. (Theochem)*, **284,** 271 (1993).
10 Zhu S-B, Singh S and Robinson GW. *Adv. Chem. Phys.* **85,** 627 (1994).
11 Benjamin I. *Chem. Rev.* **96,** 1449 (1996).
12 Benjamin I. in *Modern Methods for Multidimensional Dynamics Computations in Chemistry*, edited by D. L. Thompson, World Scientific, Singapore, 101, (1998).
13 Allen MP and Tildesley DJ. *Computer Simulation of Liquids,* Clarendon, Oxford, (1987).
14 *Computer Simulations in Chemical Physics*, Vol. 397, edited by M. P. Allen and D. J. Tildesley, Kluwer, Dordrecht, (1993).
15 Berendsen HJC, Postma JPM, Gunsteren WFV and Hermans J. in *Intermolecular Forces*, edited by B. Pullman, D. Reidel, Dordrecht, 331, (1981).
16 Meyer M, Mareschal M and Hayoun M, *J. Chem. Phys.* **89,** 1067 (1988).
17 Smit B, *Phys. Rev. A.* **37,** 3431 (1988).
18 Toxvaerd S and Stecki J. *J. Chem. Phys.* **102,** 7163 (1995).
19 Linse P. *J. Chem. Phys.* **86,** 4177 (1987).
20 Gao J and Jorgensen WL. *J. Phys. Chem.* **92,** 5813 (1988).
21 Carpenter IL and Hehre WJ. *J. Phys. Chem.* **94,** 531 (1990).
22 Benjamin I. *J. Chem. Phys.* **97,** 1432 (1992).
23 Vanbuuren AR, Marrink SJ and Berendsen HJC. *J. Phys. Chem.* **97,** 9206 (1993).
24 Michael D and Benjamin I. *J. Phys. Chem.* **99,** 1530 (1995).
25 Michael D and Benjamin I. *J. Phys. Chem.* **99,** 16810 (1995).
26 Chang TM and Dang LX. *J. Chem. Phys.* **104,** 6772 (1996).
27 Michael D and Benjamin I. *J. Electroanal. Chem.* **450,** 335 (1998).
28 Als-Nielsen J. *Physica* **140A,** 376 (1986).
29 Beaglehole D. in *Fluid Interfacial Phenomena*, edited by C. A. Croxton, Wiley, New York, 523, (1986).
30 Penfold J and Thomas RK. *J. Phys. A Condens. Matter* **2,** 1369 (1990).
31 Meunier J. in *Liquids at Interfaces*, edited by J. Charvolin, J. F. Joanny, and J. Zinn-Justin, North-Holland, Amsterdam, (1990).
32 Cowley RA. in *Equilibrium Structure and Properties of Surfaces and Interfaces*, edited by A. Gonis and G. M. Stocks, Plenum, New York, 1, (1992).
33 Wegdam GH and Bonn D. *J. Phys. I. France*, **2,** 1755 (1992).
34 Rowlinson JS and Widom B. *Molecular Theory of Capillarity,* Clarendon, Oxford, (1982).
35 Markin VS and Volkov AG. in *Liquid-Liquid Interfaces*, edited by A. G. Volkov and D. W. Deamer, CRC Press, Boca Raton, 63, (1996).
36 Hanna GJ and Noble RD. *Chem. Rev.* **85,** 583 (1985).
37 Girault HH. in *Modern Aspects of Electrochemistry*, Vol. 25, edited by J. O. M. Bockris, B. E. Conway, and R. E. White, Plenum Press, New York, 1, (1993).
38 Samec Z. in *Liquid-Liquid Interfaces*, edited by A. G. Volkov and D. W. Deamer, CRC press, Boca Raton, 155, (1996).
39 Kakiuchi T. in *Liquid-Liquid Interfaces*, edited by A. G. Volkov and D. W. Deamer, CRC Press, Boca Raton, 1, (1996).
40 Pohorille A, Cieplak P and Wilson MA. *Chem. Phys.* **204,** 337 (1996).
41 Benjamin I. *J. Chem. Phys.* **96,** 577 (1992).
42 Benjamin I. *Science,* **261,** 1558 (1993).
43 Schweighofer KJ and Benjamin I. *J. Phys. Chem.* **99,** 9974 (1995).



SOLVENT EXTRACTION AND MATERIALS SCIENCE

Mamoun Muhammed and Andrei A Zagorodni
Materials Chemistry Division, Royal Institute of Technology,
SE-100 44 Stockholm, Sweden.

ABSTRACT
Solvent extraction is a mature science that has shown to be a versatile technique both as an analytical laboratory method as well as efficient industrial selective separation process. There is a need for extending the use of solvent extraction into new areas of application. In this presentation, two such new areas are presented. A solvent impregnated resin extends the use of the selective extraction reagents for the treatment industrial streams of high volume with low metal content. The use of templating increases the stability of the resin. The use of solvent extraction process for the fabrication of functional materials is also presented. Precipitation stripping can be used for the fabrication of a wide range of metal oxides.

Keywords: impregnated resin, templating, synthesis of materials, precipitation stripping

INTRODUCTION

Our fundamental knowledge of the basic phenomena in solvent extraction as a science and technology has increased tremendously during the past few decades. Albeit such high degree of maturity of the field of solvent extraction, there are vast world-wide on-going research activities on the different aspects of solvent extraction. This includes studies on liquid-liquid distribution equilibria and kinetics as well as different technological applications.

Solvent extraction has been used for decades as an analytical technique.[1] However, the first application of solvent extraction as technological process has originated from its use in the purification of uranium in Manhattan project.[2] Numerous studies were then reported on the extraction and separation of different isotopes and transuranium elements. The breakthrough for solvent extraction as a competitive separation technology was first demonstrated in the 60's, where solvent extraction was used for the recovery of copper from waste flotation tailings. Since then, numerous reports were published for the different processes where solvent extraction has been used as a key separation technique. There is a rich literature data on solvent extraction as can be seen from the Proceedings of the International Conference on Solvent Extraction ISEC,[3] demonstrating a wide variety of innovative applications of solvent extraction. Interesting enough, there is a significant number of papers dealing with the basic solvent extraction phenomena. This covers both studies of the distribution equilibrium as well as kinetic studies aiming at the understanding of extraction reaction mechanisms. There are as well several important studies developing approaches for the prediction of extraction equilibria.

The basic bi-phasic solvent extraction process is associated with several other reactions taking place in both phases. Figure 1 demonstrates the complexity of the solvent extraction systems. The extraction reaction results in a mass-transfer between the aqueous and the organic phases. The extraction reaction can also be used to determine the different interactions taking place in either phase. As example, micelle formation of tertiary amines in organic solvents has been investigated by studying the distribution of the amines between aqueous and organic phases.[4] Similarly, several reactions in aqueous solutions; some metal ions hydrolysis or complex formation have been determined by the extraction of metal ions into different organic solvents.[5] A wide variety of highly selective extraction reagents have also been developed during the past decades, which extends the application of solvent extraction to new areas, e.g. pollution abatement. There are over 1000 studies on the investigation of novel extraction reagents published every year in top scientific journals. However, there is limitation on the use of solvent extraction for the treatment of different streams as shown in Figure 2. The use of solvent extraction reagents in the form of membranes; e.g. liquid surfactant membranes and solid

© 2000 Society of Chemical Industry

supported liquid membrane, represent a further extension of the application of solvent extraction to new area, thus allowing the treatment of different waste effluents and process streams.

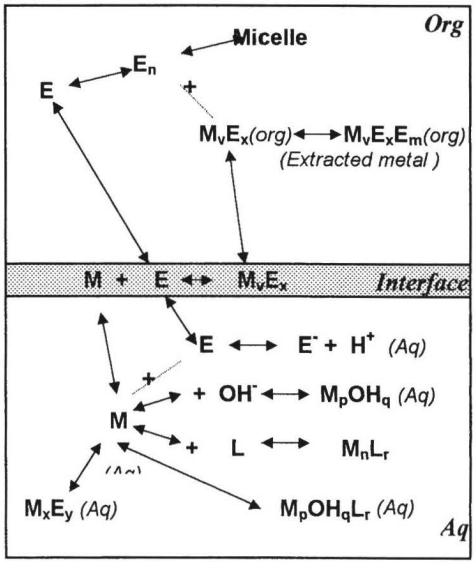


Figure 1. A schematic representation of different reactions associated with the biphasic extraction reaction

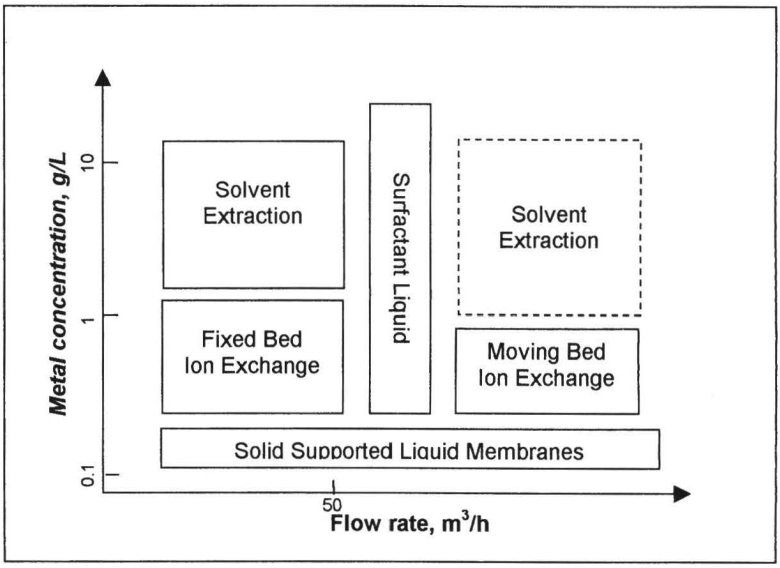


Figure 2. The suitability of selective separation techniques for the treatment of process or waste streams as a function of concentration of metal ions and discharge rate.

The significantly high number of solvent extraction studies suggests that the field is far from being stagnant. However, there is need for looking for new areas where the gained knowledge and know-how can be utilised. Materials science is such promising area where solvent extraction can make a significant contribution.

Materials science and engineering is a relatively new area, which combines expertise from chemistry, physics as well as engineering. While the discipline of materials science involves investigating the relationship between structure and properties of the materials, materials engineering in contrast, deals with the design or the engineering of the materials structure to produce the desired set of properties. In the following we present some prospective on novel areas of application where solvent extraction community can profit. Specifically we give two examples; the first is concerning the development of new materials for selective separation, which extend the use of solvent extraction technology into new areas. The second is the use of solvent extraction processes for the preparation of functional materials.

SOLVENT IMPREGNATED RESINS

Solid ion exchange resins play a significant role in separation technologies. Advantages of the ion exchange separation are the ease of phase separation and possibility to incorporate them into column-based processes, with the benefit of both selective ion exchange interaction and chromatographic separation. However, there is a limited number of selective ion exchange resins which are commercially available (e.g. iminodiacetic, phospho-organic, thiourea, as functional groups). Few more resins were prepared on a laboratory scale. The complexity of their production process, relatively high cost, and in some cases, the low stability cause significant limitations on the use of chelating resins. There is therefore a high demand for the development of inexpensive solid extractants with high selectivity towards different ions under wide variety of conditions.

Solvent Impregnated Resins, SIR, is a relatively new concept based on physical incorporation of the ligands into polymeric network. The idea was initially suggested by Small [6] at beginning of 60's. However, a significant research activity in this area can be found only in mid-70's, when several essential studies were published by Warshawsky,[7-9] and a significant increase in the research in this area is noted in the 90's. There has been an increasing demand for the treatment of industrial streams with highly selective methods. The limited available chelating resins have a serious limitation as being expensive and have a poor selectivity. It is thus obvious that the wide variety of solvent extraction reagents that are commercially available offer good substitutes for the chelating resins. Moreover, design and production of new reagents are relatively simple and non-expensive. Solvent impregnated resins can be used in column-based processes in the separation, which is significantly advantageous compared to liquid-liquid contacting.

Comparing with Solvent Extraction	Comparing with Ion Exchange
Advantages	
• Possibility for Column-based operation process. • Possibility to treat very dilute solutions	• Highly selective ion exchangers can be obtained by incorporating a wide variety of chelating reagents into the resin matrix
• High contact surface area without any mixing	• Lower production costs
• Less reagent loss at cyclic operations	• Faster mass transfer (in some cases)
Disadvantages	
• Less percentage of the reagent efficient use and less capacity	• Low capacity
• Relatively higher cost	• Relatively unstable under cyclic use

Table 1 Comparison of SIR with Solvent Extraction and Ion Exchange

Table 1 shows a comparison of SIR with both solvent extraction and conventional ion exchange technique. It is interesting to note that attempts to increase capacity of the sorbents lead to reduction of their stability (the reagent emission increase).[10,11]

Despite the fact that the first idea of resins solvent impregnation was targeted to the needs of chromatography,[6] their main use can be found in selective separation of transition metals, with many examples available. Macroporous sorbents were impregnated on different commercial and specially designed phosphorous-organic compounds to extract and separate copper, zinc, cadmium.[12-25] Another target for SIR is the extraction of noble metals,[26,27] which is often requested in hydrometallurgy and waste recycle. There is also a need for the extraction of organic substances or waste and process streams, e.g. citric acid.[28,29] Also complicated tasks such as the purification of biologically produced substances can be performed as well.[30]

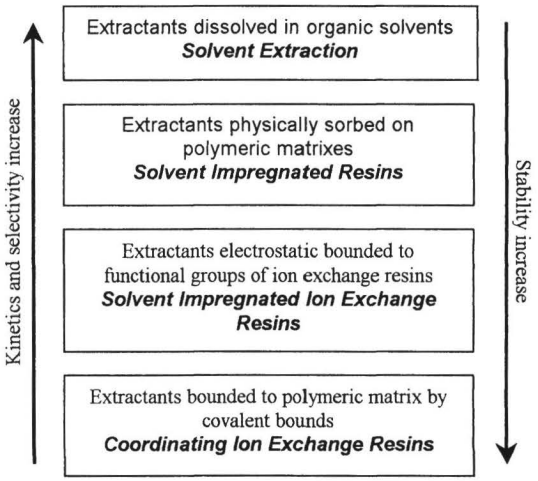


Figure 3. A representation of the stability of the resins, ranging from solvent impregnated to grafted functional groups, and the effect on selectivity and kinetics

MATERIALS ASPECTS FOR 'SIR' FABRICATION

The way by which the solvent extraction reagent is attached to the polymer matrix affects the extraction equilibria and kinetics. Figure 3 shows in a qualitative way the effect of different methods of binding. Non-functionalised polymers are usually used for the preparation of solvent impregnated resins. A very convenient matrix is the styrene-divinylbenzene copolymer Amberlite XAD-2 that is often used.[12-21,31-34] The stability of the resin is a problem, as the reagent is leached out from the organic polymer during the operation. Conventional ion exchange resins can be used as the polymeric support as well. Their functionality can be useful to provide stronger incorporation of the impregnating reagent into the polymer network. For example, in a study of the extraction of gold by a thiourea derivative reagents [26,35-37] the rate of the extraction for the same reagents in different forms war compared. The $t_{½}$ (half reaction time) was measured for the "free" reagent dissolved in chloroform and as solvent impregnated resins (the chloroform solution is absorbed on a non-functionalised polystyrene polymer) and as covalently bonded to a polymer matrix. Figure 4, shows that the "free" solvent extraction reagent has a faster kinetics and the SIR reagent is slightly slower. However, covalently bound reagent has dramatically slower extraction kinetics, which affected by the structure of the resin, spacer length (i.e. length of aliphatic chain connecting the functional group to the polymer matrix).

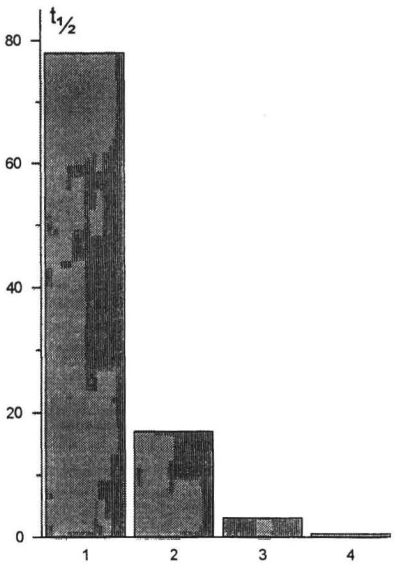


Figure 4. Reaction half-time ($t_{½}$) for extraction of Au^{3+} with a thiourea derivative reagent:
1 – reagent is covalently bounded to a polystyrene matrix;
2 - reagent is bounded to the matrix via a long spacer;
3 - solvent impregnated resin;
4 – "free" extraction reagent.

MOLECULAR IMPRINTING AND TEMPLATING

Molecular imprinting is a technique for the preparation of solid extractant based on a shape memory templating of the polymer matrix. Molecular imprinting is illustrated in the Figure 5a.[38] Functional monomers dissolved in a suitable solvent are assembled on a substrate molecule to be used as a template. The polymerisation is then initiated e.g. using free radical polymerisation. The structure obtained is used to maintain the functional groups positioning after polymerisation. Finally, the substrate is extracted from the formed binding sites. The resulting network polymers can in favourable cases rebind the substrate molecule with a high order of selectivity.[39,40] These materials have shown to be successfully used in the field of chemical separations, chiral technologies and in catalysis. Similarly, the method can be adopted to imprint the shape of a suitable side chain of the extraction reagent. In this manner, the reagent with the side chain will be fitted into the cavity and thus increase the reagent stability due to the decrease of the loss or reagent (Figure 5b).

ADJUSTED CHELATING RESINS

These are prepared by a similar method to the imprinting approach and can be used by templating the reacting species. This method is called adjusted resins. The selectivity of all traditional ion exchange sorbents is based on the chemical nature of the reagents and functional groups used. The basic principle (called "adjustment") of the chelating polymers preparation was first proposed by Efendiev.[41] The

method is based on a pre-templating of the soluble polymer's functional groups prior to cross-linking. This results in preserving the optimal location of the functional groups. Therefore, the sorption process does not encounter a counter-action from the elastic force of the distorted polymer chains. This results in thermodynamically favourable sorption of ions having a certain co-ordination structure.

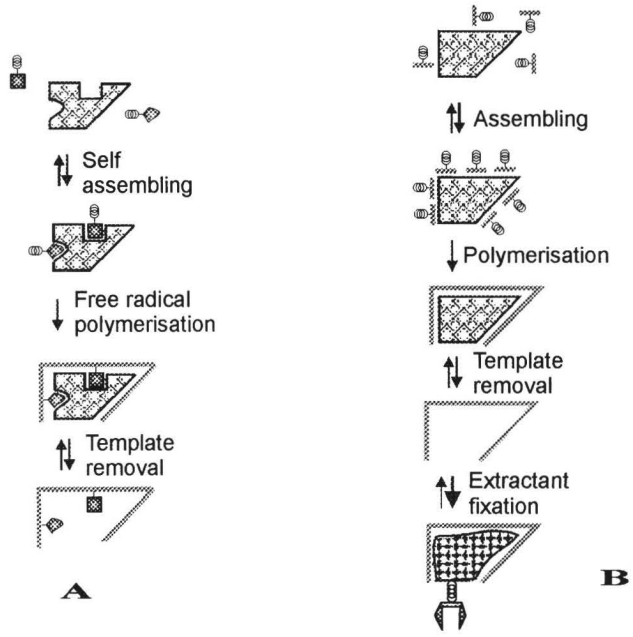


Figure 5. A schematic representation of molecular imprinting method (A) and suggested polymer templating (B) for enhancing reagent stability

FABRICATION OF FUNCTIONAL MATERIALS USING SOLVENT EXTRACTION

Functional materials, e.g., ceramics, have been a very active research area in recent years, since they can be designed to exhibit a specific functionality. Functional materials can be tailored with respect to composition and microstructure in order to achieve an intelligent performance. The intrinsic properties of such materials make them sensitive to a specific aspect of the environment such as temperature, electric field, magnetic field optical wavelength or adsorbed molecules. Several new types of functional materials have been recently developed. The newly discovered high temperature superconducting ceramics with a critical temperature (T_c) above that of liquid nitrogen temperature is a good example for functional materials. The synthesis of such materials is a major challenge since the superconductivity is extremely sensitive to the variation of the chemical composition. In conventional method of synthesis, the different metal oxides are thoroughly mixed and heated for several tens of hours to form the superconducting perovskite structure. Mixing of different components should be extremely uniform in order to allow the solid state reactions to proceed towards the formation of the required phase. Small particle size is advantageous for the formation of high phase purity and also shortens reaction time.

Chemical methods offer several distinct advantages over solid state reactions for the preparation of functional materials. Sol-gel and precipitation are most common chemical methods for the synthesis of functional materials. Different metal ions can be precipitated from solution with the required

composition and with controlled particle size. The precipitation can also be carried out through a biphasic reaction, using suitable solvent extraction system.

Solvent extraction system resembles the sol-gel processing, however, it is much more cost efficient and easily scalable synthesis route. It can be advantageously used for the fabrication of sub-micron, monosized particles. For a solvent extraction system, metal extraction (e.g. by an acidic extraction reagent HR) and back extraction (stripping) reactions can be represented by equations 1 and 2 respectively.

$$M^{z+}_{(aq)} + HR_{(org)} \rightarrow RM_{z(org)} + zH^{+}_{(Aq)} \quad (1)$$

$$RM_{z(org)} + L^{y-}_{(aq)} \rightarrow M_yL_{z(aq)} + R_{(org)} \quad (2)$$

where L is a water-soluble complexing reagent, present in the strip solution. The metal ions can be precipitated from the organic phase by selecting a suitable reagent that forms an insoluble complex in the aqueous phase. The advantage of the direct precipitation is that the diffusion of the reacting species from the two phases across the interface can be controlled in order to vary the morphology and size of the solid particle formed.

Few researchers have studied precipitation-stripping routes for the fabrication of functional materials. Doyle et al.[42-47] have studied the precipitation of a wide range of oxide powders by direct hydrolysis of metal-loaded organic solutions, at elevated temperatures, using carboxylic acid and di-2-etheyhexyl phosphoric acid (D2EHPA) extractants. Valiente et al.[48] have studied the precipitation stripping of $Y_2(C_2O_4)_3$ from D2EHPA solutions. As seen in Figure 6, different particle morphology and size can be obtained.

This approach can be further extended to fabricate multi-component powders with controlled composition and particle size. Sub-micron size, and nano-sized particles have very interesting properties, and can be prepared by this technique. The use of solvent extraction for the preparation of powder allows the fabrication of high quality powder using inexpensive raw materials.



Figure 6. SEM micrograph of yttrium oxalate precipitated by stripping the organic phase by oxalate solution.

CONCLUDING REMARKS

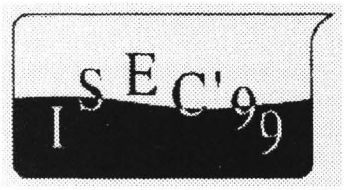
Solvent extraction has reached a high degree of maturity, where the basic phenomena are fairly understood. This paper attempts to shed light on new venues for a valued added solvent extraction

operation. The first is the solvent impregnated resin (SIR) where the selective solvent extraction reagent can physically adhere the polymer surface. Polymer templating or imprint can be used for the development of physically novel reagents that can extend the area for solvent extraction. Such reagents make it possible to treat solutions with higher metal concentration at high flow rates.

REFERENCES:

1. Frieser H. *Anal. Chem.* **38**,131R-154R, (1966)
2. Handbook of Solvent Extraction, Edited by Lo TC, Baird MHI, and Hanson C, John Wiley & Sons, N.Y., 1983.
3. Proceedings of ISEC'96, Edited by Shallcross D, Paimin R and Prvcic LM, The University of Melbourne, Australia, 1996.
4. Högfeldt E. in ICSEC Jerusalem. Jerusalem, Wiley-Interscience, 157. T405 (1968).
5. Sekine T and Hasegawa Y, Solvent Extraction Chemistry, Marcel Dekker Inc., N.Y., 1977.
6. Small H, J. *Inorg. Nucl. Chem.* **18**, 232 (1961).
7. Warshawsky A, *Talanta*, **21**, 624 (1974).
8. Warshawsky A, *Talanta*, **21**, 963 (1974).
9. Warshawsky A, *Trans. Inst. Min. Metall.*, **83**, C101 (1974).
10. Muraviev DN and Hogfeldt E, *Reactive Polymers*, **8**, 97 (1988).
11. Muraviev DN, *Chemica Scripta*, **29**, 9 (1989).
12. Ruey-Shin J and Jenn-Yih S, *Ind. Eng. Chem. Res.*, **31**, 2774 (1992).
13. Ruey-Shin J and Jenn-Yih S, *Ind. Eng. Chem. Res.*, **31**, 2779 (1992).
14. Cortina JL, Miralles N, Sastre A, Aguilar M, Profumo A and Pesavento M, *Reactive Polymers*, **18**, 67 (1992).
15. Cortina JL, Miralles N, Sastre A, Aguilar M, Profumo A and Pesavento, M, *Reactive Polymers*, **21**, 89 (1993).
16. Cortina JL, Miralles N, Aguilar M and Warshawsky A, *Reactive & Functional Polymers*, **27**, 61 (1995).
17. Cortina JL, Miralles N, Sastre A and Aguilar M, *Hydromet.* **37**, 301 (1995).
18. Strikovsky AG, Jerabek , Cortina JL, Sastre AM and Warshawsky A., *Reactive & Functional Polymers*, **28**, 149 (1996).
19. Cortina JL, Miralles N, Sastre A and Aguilar M, *Reactive & Functional Polymers*, **32**, 221 (1997).
20. Cortina JL, AradYellin R, Miralles N, Sastre AM and Warshawsky A, *Reactive & Functional Polymers*, **38**, 269 (1998).
21. Kabay N, Demircioglu M, Ekinci H, Yuksel M, Saglam M and Streat M, *Reactive & Functional Polymers*, **38**, 219 (1998).
22. Cortina JL, Miralles N, Sastre A, Aguilar M, Profumo A and Pesavento M, *Reactive Polymers*, **21**, 103 (1993).
23. Akita S, Maeda T and Takeuchi, H., *J. Chem. Eng. Japan*, **27**, 126 (1994).
24. Juang RS and Lee SH, *Reactive & Functional Polymers*, **29**, 175 (1996).
25. Juang RS and Chen MLA, *Reactive & Functional Polymers*, **34**, 93 (1997).
26. Zuo G and Muhammed M, *Solv. Ext. and Ion Exch.* **13**, 879 (1995).
27. Villaescusa I, Salvado V, De PJ, Valiente M and Aguilar M, *Reactive Polymers*, **17**, 69 (1992).
28. Juang RS and Chang HL, *Ind. Eng. Chem. Res.*, **34**, 1294 (1995).
29. Juang RS and Chou TC, *Sep. Sci. Technol.*, **31**, 1409 (1996).
30. Kitazaki H, Ishimaru M, Inoue K and Yoshida K, *Kagaku Kogaku Ronbunshu*, **22**, 287 (1996).
31. Villaescusa I, Salvado V and de Pablo J, *Hydromet.*, **41**, 303 (1996).
32. Villaescusa I, Salvado V and de Pablo J, *Reactive & Functional Polymers*, **32**, 125 (1997).
33. Rovira M, Hurtado L, Cortina JL, Arnaldos J and Sastre AM, *Reactive & Functional Polymers*, **38**, 279 (1998).
34. Rovira M, Cortina JL, Arnaldos J and Sastre AM, *Solv. Ext. and Ion Exch.*, **16**, 1279 (1998).
35. Zuo G and Muhammed M, *Solv. Ext. and Ion Exch.*, **13**, 855 (1995).
36. Zuo G and Muhammed M, *Reactive Polymers*, **24**, 165 (1995).
37. Zuo G and Muhammed M, *Solv. Ext. and Ion Exch.*, **27**, 187 (1995).
38. Sellergren B, *Amer. Lab.*, **29**, 14 (1997).

39. Mosbach K and Ramstrom O, *Bio-Technology*, **14**, 163-170 (1996).
40. Sellergren B, http://www.uni-mainz.de/FB/Chemie/AKUnger/Boerje/Welcome.html
41. Efendiev AA, *Macromol. Symp.*, **131**, 29-38 (1998).
42. Doyle FM, *Hydromet.*, **29**, 527 (1992).
43. Konishi Y and Doyle FM, *Hydromet.*, **35**, 203 (1994).
44. Konishi Y and Doyle FM, *Hydromet.*, **35**, 233 (1994).
45. Doyle FM and Monhemius AJ, *Hydromet.*, **35**, 251 (1994).
46. Doyle FM, *Hydromet.*, **20**, 65 (1988).
47. Yoon JH and Doyle FM, *J.Metals*, **40**, 88 (1988).
48. Iglesias M, Anticó E, Salvado V, Masana A and Valiente M, *Solv. Ext. and Ion Exch.* **17**(2) 277-300 (1999).



ONE PHASE MICELLAR EXTRACTION AS A NEW SEPARATION TECHNIQUE

Jan Szymanowski
Poznan University of Technology, Institute of Chemical Technology and Engineering, Pl. Sklodowskiej-Curie 2, 60-965 Poznan, Poland

ABSTRACT
Surfactant enhanced extractions are presented and discussed. They include micellar enhanced ultrafiltration and cloud point extraction. The ideas of the processes are given and the main features are presented and compared to classical solvent extraction.

Keywords: micellar enhanced ultrafiltration, cloud point extraction.

INTRODUCTION

Solvent extraction is broadly used to recover inorganic and organic substances from various aqueous media, including technological solutions and liquid waste streams. Various extractants are used. Atypical processes carried out in the presence of surfactants have been proposed and some of them have found practical applications. They include reversed micelle and microemulsion extraction of biochemicals. Reversed micelles and microemulsions are also used to accelerate the extraction of several metal ions or even to make the process feasible as in the case of germanium and gallium extraction. The use of liquid emulsion membranes to recover various chemicals has been broadly described. An organic diluent, usually containing low aromatic high boiling aliphatic hydrocarbons is used in each of these methods. Such systems, especially those containing surfactants, are very inconvenient from the environmental point of view and the possible formation of stable emulsions.

New ideas and processes ecologically attractive have been recently proposed. They include the use of atypical one phase surfactant enhanced "extraction", i.e., surfactant enhanced ultrafiltration and cloud point extraction.

SURFACTANT ENHANCED UTRAFILTRATION

Surfactants form aggregates in the aqueous or in the organic solutions with various structures that depend on the geometry of surfactant molecules, which may be described by the ratio $v/a_o l$, where v is the volume of the hydrocarbon chain, a_o is the optimal cross-sectional area per polar head group in a planar interface and l is approximately 80 to 99% of the fully extended length of surfactant chain. A smaller cross-sectional area of tail (hydrocarbon chain) compared to the head group favours aggregation in the aqueous phase. Spherical micelles, cylindrical micelles and lamellas (or vesicles) are formed for $v/a_o l < 1/3$, $1/3 < v/a_o l < 1/2$ and $½ < v/a_o l < 1$, respectively. Reversed micelles in the organic phase are formed when the cross-sectional area of tail is greater than that of the head, i.e., $v/a_o l > 1$. The latter case is used in reversed micelle and microemulsion extraction discussed previously. Now the use of aqueous micellar systems for separation of various substances will be discussed.

Depending on type of surfactant, micelles can be negatively charged (anionic surfactants), positively charged (cationic surfactants) or can be neutral (non-ionic surfactants). Ionic micelles usually contain 50-100 surfactant ions. In diluted solutions and at ambient temperatures they are spheroid with the polar groups on the surface and the hydrophobic chains at the centre. The ionic head groups and some counter-ions form a compact Stern layer, in which about 60 - 70% of the micellar charge is neutralised. The remaining counter-ions form a Gouy-Chapman layer extending radially into the aqueous phase. The micelles also contain a considerable quantity of water, e.g., 33 - 46% in the case of sodium dodecylsulphate. Water molecules are located not only in the surface layer but also in the

© 2000 Society of Chemical Industry

hydrophobic core of the micelles, the content decreasing with the distance from the polar head group into the interior of the micelle.

The charged micelles bind ions of opposite charge. The binding is controlled primarily by electrostatic interactions. This means that multiple charged ions are easily bound by ionic micelles, e.g., toxic Cd(II) cations by anionic micelles and toxic CrO_4^{2-} by cationic micelles. Steric and hydrophobic effects enhance such sorption of ionic species.

The hydrocarbon core of a micelle is similar to a liquid hydrocarbon although it is more ordered, e.g., microviscosity is considerably higher in micelles than in hydrocarbons. As a result, micelles can solubilize various organic substances that are sparingly soluble in water. Depending on the solute hydrophilicity, solute molecules can be located in various parts of micelles: at the micelle surface; at a particular depth within the surface layer, or in the micelle core. Solubilisation phenomenon permits the binding of various organic pollutants, including toxic phenols and their derivatives, various pesticides, etc. The solubilisation capacity depends on the surfactant concentration and is small in dilute isotropic solutions below the critical micelle concentration (cmc). A sharp increase of solubilisation is observed at the cmc. With a further increase in surfactant concentration the solubility increases proportionally, mainly because of the increase in the total number of micelles in the unit volume. It means that the binding of various substances by micelles is limited by the following factors: number of micelles, and size and charge of the micelles. As a result, the use of micelle enhanced processes tends to be limited to dilute solutions and different diluted liquid waste streams.

Such micro-heterogeneous media, having a micro-interfacial area, may be considered as two pseudophase systems consisting of the aqueous and micellar pseudo-phases in which micelles are in dynamic equilibrium with individual molecules with a resistance time (i.e. the exchange of one surfactant molecule between the micelle and the aqueous pseudophase) and a micelle lifetime (micelle breakdown) of the order of microseconds and milliseconds respectively. In reality these characteristic times depend significantly upon the surfactant and alkyl chain length and it is impossible to give general values. Thus, the interface is continuously renewed in a micellar system. As a result, the distribution of solutes between aqueous and micellar pseudo-phases is always at equilibrium, and does not depend on any reaction occurring in the system.

Both pseudo-phases can be separated by ultrafiltration using a membrane having pores smaller than the size of micelle. As a result, solutes sorbed on the micelle interface by electrostatic forces or solubilised in the hydrophobic micellar interior are separated from the aqueous pseudo-phase containing the surfactant below the cmc, mainly in the form of monomers. Polyelectrolytes can be also used instead of surfactants. The molecular weight cut-off amounts to 500 Dalton. This method is particularly effective for multicharged ions, but the sorption is not selective.

Micellar solutions can be considered as solvents for reagents which can complex ions present in solution. However typical extractants cannot be used. They are too hydrophobic and too bulky to obtain enough high solubilisation in the micelles. Thus, low molecular analogues must be used instead of the typical hydrophobic extractants, e.g., salicylaldoxime instead of commercial LIX and ACORGA hydroxyoxime reagents for copper removal, 8-hydroxyquinoline instead of KELEX (LIX) reagents, etc. Moreover, micelles must be neutral or have the same charge as the extracted ionic species. The separations may be based on thermodynamic or kinetic reasons as demonstrated by Tondre et al.[1,2] In the first case the effect of the acidity of the aqueous phase is considered as in the typical extraction process. The shape of the curves, % extracted vs pH, bears a close similarity to that observed in the classical extraction. Thus Ni(II) and Co(II) can be separated with 8-hydroxyquinoline and with KELEX 100 at pH values below 4. Better separations are obtained with the hydrophobic KELEX 100. Co(II) is strongly bound to the chelating agent and solubilized in the micelle, while Ni(II) remains in the aqueous pseudo-phase. It is interesting that the separation of these two species in the micellar systems are significantly better than in the traditional extraction, since there is a separation of about 0.5 pH units between the % extracted vs pH curves in micellar separations, whereas the corresponding curves in classical extraction are almost indistinguishable. The complexation of both Ni(II) and Co(II) can be carried out at a higher pH and then the micellar solution can be acidified to pH 3 and filtered through an

ultrafiltration membrane. Ni(II) ions appear then in the permeate (filtrate) and complexed Co(II) remains in the retentate (micellar phase).

The comparison of micellar enhanced ultrafiltration of copper(II) with the traditional extraction using hydroxyoxime extractants demonstrates that the separation curves in utrafiltration are shifted towards higher pH values in comparison to the extraction process. The magnitude of the shift depends on the surfactant and is stronger for cationic hexadecyltrimethylammonium chloride (CTAB) in comparison to the system containing non-ionic alcohol ethoxylate and amounts to 2 and 1 pH unit, respectively.[3]

Reactions between ionic species occur rapidly in homogenous solutions. The rate can be even increased in micellar systems as a result of micellar catalysis. The complexation of metal cations with different low-molecular weight chelating agents carried out in the presence of an anionic surfactant is a classical example. A sharp acceleration of the complexation rate occurs in the region of critical micelle concentration. At the cmc, the metal cations are strongly sorbed by the micelles and their concentration in the Stern layer achieves a maximum. Then the concentration of metal ions at the micelle interface falls with increasing surfactant concentration and the rate of complexation decreases.

An opposite kinetic effect is observed in micellar solutions containing cationic and non-ionic surfactants caused by electrostatic repulsion between ions of the same charge, i.e., metal cations and positively charged micelles, and additional diffusion of metal ions and/or reagent (extractant) molecules through the dense layers occupied in the micelles by long polyoxyethylene chains. The effect depends additionally on extractant hydrophobicity and is stronger for more hydrophobic reagents.[4,5] The time needed for complexation increases from microseconds to minutes and even hours, e.g., Co(II) is complexed in micellar CTAB solutions with KELEX 100 in 1-2 minutes while Ni(II) needs 1-2 hr. Thus, if ultrafiltration is carried out between these limiting times separation can be achieved with non-complexed Ni(II) appearing in the permeate and complexed Co(II) remaining in the micellar medium

In micellar solutions the following kinetic model can be considered for acidic and chelating reagents:

$$HL_W = HL_M \quad (1)$$

$$HL_{W,M} = H^+_{W,M} + L^-_{W,M} \quad (2)$$

$$M^{2+}_{W,M} + L^-_{W,M} = ML^+_{W,M} \quad (3)$$

$$ML^+_{W,M} + L^-_{W,M} = ML_{2\,W,M} \quad (4)$$

$$ML_{2\,W} = ML_{2\,M} \quad (5)$$

where HL denotes the extractant and subscripts *W* and *M* the aqueous and micellar pseudo-phase, respectively. The double subscript (*W,M*) means that the reaction can occur in any of the pseudo-phases. In some specific cases additional equilibria, such as the complexation with the neutral reagent, protonation of reagent and reaction with the protonated extractant, must be considered.

The model shows great similarities to that discussed in classical extraction. The main important simplification is connected with the rapid formation and breaking of micelles. As a result, the effects of diffusion can be neglected and only the chemical steps considered. The second difference is connected with the limiting chemical step. The formation of the intermediate complex ML^+ (eq. 3) is the slowest step. The other equilibria (eqs 1, 2, 4 and 5) are rapid. Complexation can occur in the micelles or in the aqueous pseudo-phase or in both pseudo-phases. It depends on two factors: the charge of the micelles in comparison to the charge of extracted species and the hydrophobicity of the extracting reagent. Electrostatic attraction between metal cations and negatively charged micelles (anionic surfactants) favours reaction in the micelles. Electrostatic repulsion between metal cations and positively charged micelles (cationic surfactants) decreases the rate of complexation and gives the possibility of different complexation sites: in the micellar or aqueous pseudo-phase for a hydrophobic and a hydrophilic extractant, respectively. The rate of extraction decreases when the hydrophobicity of extractants increases. The same effect of hydrophobicity is observed in micellar systems containing non-ionic surfactants.

The surfactant enhanced separations presented above seem to be an interesting new method for specific separations of toxic contaminants, both inorganic and organic, present in small quantities in various aqueous waste streams. The method permits the concentration of the separated species to a level acceptable for other separation methods. The main drawback of the method is connected with the presence of surfactants that must be further removed or biodegraded.

CLOUD POINT EXTRACTION

Cloud point extraction technique, initially reported by Watanabe[6] stems from the phase phenomenon exhibited by non-ionic and zwitterionic surfactant micelle systems. Upon appropriate variation of conditions, i.e. temperature, addition of salt or other additives, the separation of an aqueous surfactant micellar solution into a concentrated phase containing most of the surfactant (termed surfactant-rich, micellar or coacervate phase) and a dilute aqueous phase containing a low concentration of surfactant is observed. Any component(s) originally present that bind to the micellar aggregate can be extracted from the original solution and concentrated in the small volume of the surfactant-rich phase. The phases can then be separated by centrifugation to speed up the separation.

Non-ionic surfactants, e.g., $RX(OCH_2CH_2)_nOH$, where R is an alkyl group and X stands for an intermediate fragment: phenyl ring, oxygen atom and carbonyl group in oxyethylated alkylphenols, alcohols and carboxylic acids, respectively and zwitterionic surfactants, e.g., $R(CH_3)_2N^+(CH_2)_nOSO_3^-$, are appropriate surface active agents for which micellar solutions undergo temperature dependent phase separation. When the temperature is raised, solutions of non-ionic surfactants become turbid in a narrow temperature range referred to as the cloud point. Above the cloud point the system separates into two isotropic phases. This phase separation is reversible and on cooling, the two separated phases form a clear micellar solution once again. Considering the phase diagrams, areas of different isotropic micellar solutions are observed at ambient temperatures depending on surfactant concentration. They are as follows: the typical isotropic phases L_1 L_2 and L_3 and the isotropic liquid crystalline phases L_a, H_1 and V_1. A heating of a diluted isotropic solution decreases the hydration of the hydrophilic oligooxyethylene chain and as a result a change of the micelles from spherical to cylindrical ones is observed. At appropriate temperature the clouding occurs. The two phase system may not be, however, suitable for separations because the surfactant-rich phase may be enough concentrated. A further heating may give the crystalline phase with lamellar micelles L_a which quickly is transferred into the isotropic phase L_3. A further heating may give two phase system suitable for separations in which the surfactant-rich phase L_2 is in the equilibrium with almost pure water.

Depending on surfactant a different phase diagram is obtained. Some conclusions can be, however, given. For oxyethylated non-ionic surfactants, the cloud point increases with decreasing length of the hydrocarbon chain and increasing length of the oligooxyethylene chain. The cloud point is lowered by the branching of the alkyl group, the replacement of the terminal hydroxyl group by a short alkyl group, e.g., methyl group and by a broad distribution of the hydrophilic oxyethylene chain in industrial surfactants. The cloud point can be altered by various additives including electrolytes, polar organic compounds and other surfactants. As a result, the system can be modified in such a way that the phase separation can occur at a convenient temperature.

Zwitterionic surfactant solutions behave in the opposite way and the phase separation occurs on solution cooling. Again, as in the case of non-ionic surfactants, the cloud point can be modified by the presence of various additives.

The cloud point phenomena have been applied for the preconcentration of various inorganic and organic molecules present in low concentrations in various aqueous media. The physical extraction works only for organic substances which are dissolved in the surfactant-rich phase. Metal ions must be, however, first converted into some less hydrophilic substances by reaction with sparingly water-soluble complexing agents. The surfactant-rich phase acts as an organic solvent with the extracted substance partitioned between this phase and the aqueous solution containing only very small amounts of the dissolved surfactant. The cloud point phenomenon permits to eliminate the use of ultrafiltration and the

cloud point separation technique can be considered as an separation technique alternative to the surfactant enhanced ultrafiltration.

The volume of the separated surfactant-rich phase and thus the concentration factor depends on the nature of surfactant, its concentration and temperature of separation. Typically, the surfactant concentration is kept in the range of 0.2-2.0% with a corresponding volume of surfactant-rich phase being between 2 and 10% of the initial solution volume. Thus, the concentration factor assumes the values of 10-50. Partitioning coefficients both of complexing agents and extracted complexes are lower than in the typical solvent extraction but enough high to achieve almost quantitative separations.

As in the case of the micellar enhanced ultrafiltration, the cloud point extraction found numerous applications for separation of biochemicals and clinical species, including antibiotics, enzymes, proteins, etc. The separation of toxic organic substances such as aromatic hydrocarbons, including pyrene and its derivatives, phenols and its derivatives, acids, e.g., 2,4-D acid and 2,4,5-T acid, etc., is one of main interest in environmental science. A great number of various examples can be found in the reviews of Pramauro[7,8] and in few hundreds original works.

The main disadvantage of the cloud point extraction arises from small solubility of complexing agents in aqueous surfactant solutions. This imposes a limit on the amount of ligand available in such systems. Moreover, due to the presence of surfactants, the recovery and purification of the separated metal ions is more difficult compared to the classical liquid-liquid extraction.

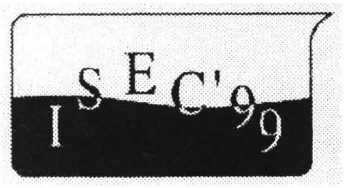
Another interesting separation technique include polyoxyethylene glycol/salt systems which separate into two phases, e.g.[9-11].

ACKNOWLEDGEMENT

The work was supported by Polish KBN donation for Institute activity DS No. 32/221.

REFERENCES

1 Kim KS and Tondre C. *Sep. Sci. Technol.* **24**, 485, (1989).
2 Ismael M and Tondre C. *J. Colloid Interface Sci.*, **160**, 252, (1993).
3 Richmond W, Tondre C, Krzy ſanowska E and Szymanowski J. *J. Chem. Soc. Faraday Trans.* **91**, 657, (1995).
4 Tondre C, Claude-Montigny B, Ismael M, Scrimin P and Tecilla P. *Polyhedron*, **10**, 1791, (1991).
5 Cierpiszewski R, Hebrant M, Szymanowski J and Tondre C. *J. Chem. Soc., Faraday Trans.* **92**, 249, (1996).
6 Watanabe H. in *Solution Behavior of Surfactants*, Mittal KL and Fendler EJ. Eds., Plenum Press, New York, 1305, (1982).
7 Hinze WL and Pramauro E. *Crit. Rev. Anal. Chem.* **24**, 133, (1993).
8 Pramauro E. *Pure Appl. Chem.* **67**, 551, (1995).
9 Shkinev VM, Molochnikova NP, Zvarova TI, Ya B, Spivakov, Myasoedov BF and Zolotov YA. *J. Radioanal. Nucl. Chem.*, **88**, 115, (1985).
10 Rogers RD, Bond AH and Bauer CB. *Sep. Sci. Technol.*, **28**, 1091, (1993).
11 Rogers RD, Bauer CB and Bond AH. *Sep. Sci. Technol.*, **30**, 1217, (1995).



PHYSICO-CHEMICAL MODELLING OF LIQUID-LIQUID EXTRACTION SYSTEMS OF HIGHLY CONCENTRATED ELECTROLYTES

P Dannus
Institut National des Sciences et Techniques Nucléaires. Commissariat à l'Energie Atomique,

ABSTRACT
A review of the studies conducted in our laboratories over the last fifteen years in the field of solution chemistry applied to concentrated ionic media is presented. A new representation of stability constants in aqueous solutions is developed along with a method for handling the salting-out effect in liquid-liquid extraction operations. Finally a methodology for completed physico-chemical modelling of complex liquid-liquid extraction systems is presented.

Keywords: Modelling; Concentrated Solutions; Extraction; Electrolytes.

INTRODUCTION

The same thermodynamic laws as diluted media chemistry of course, govern solution chemistry dealing with concentrated ionic media. However, the simplifying assumption permitted in diluted media is no longer acceptable and it thus becomes necessary to quantify or **control** solution non-ideality, i.e., the activity coefficients of species involved in chemical equilibria, so as to eliminate the effect of the medium on the phenomenon being studied.

Our studies show that it is more often the control of the effect of the medium rather than its quantification that allows a good perception of the chemical phenomenon, thus giving access to new fields that are usually difficult to explore. As examples, the determination of low stability constants in aqueous solutions and the controlling of the salting-out effect in liquid-liquid extraction operations are described.
In the approach that we implement, the activity coefficient depends on only two physico-chemical variables: the water activity of the solution and the total concentration of dissolved species, for which other methods require the ionic strength, the species concentration and a more or less large number of empirically determined "interaction parameters".

This approach also allows, to some extent, the calculation of the stoichiometric activity coefficient of an electrolyte present in a mixture, if again we know the water activity and the total concentration of all the components of this solution. That possibility again opens up new horizons, especially in the field of liquid-liquid extraction.

For instance, the most favourable medium for the extraction of a metallic element can be predicted, which is particularly useful in the field of analysis. Complex systems modelling can be completed, which prompts us to propose organic complex stoichiometries and their associated constants. Such modelling allows us to understand the effect of the variations in the *feed* composition (acid, salt concentrations) on hydrometallurgical processes by making predictive calculations.
This physico-chemical model also allows understanding and prediction in such sophisticated fields as rare-earth metals separation.

NON-IDEALITY TREATMENT IN AQUEOUS SOLUTIONS: FUNDAMENTALS

In 1936, the Russian physical chemist Zdanovskii[1] published the following empirical rule based on experimental observations:
"When binary electrolytic solutions of the same water activity (isopiestic solutions) are mixed, the resulting mixture has the same water activity as the initial solutions, provided there is no new chemical interaction between the electrolytes within the mixture".
This behaviour can be mathematically represented by:

© 2000 Society of Chemical Industry

$$\sum_i \frac{m_i}{m_i^{bi}} = 1 \qquad (1)$$

m_i = concentration of the electrolyte i in the mixture,

m_i^{bi} = concentration of the electrolyte i in the binary solution of the same water activity as that of the mixture.

The same type of behaviour was also observed by Stockes and Robinson in 1966[2] for the case of sugar mixtures. The ZDANOVSKI-STOCKES-ROBINSON (ZSR) law therefore applies to electrolytic and neutral molecular mixtures.

Ryazanov and Vdovenko[3] showed that when equation (1) is introduced into the McKAY-PERRING[4] thermodynamic relation, a simple expression for the stoichiometric activity coefficient could be obtained for a component MX_i present in a mixture;

$$\gamma_{MX_i} = \frac{\nu_{MX_i} . m_{MX_i}^{bi} . \gamma_{MX_i}^{bi}}{\sum_k \nu_{MX_k} . m_{MX_k}} \qquad (2)$$

γ_{MX_i} = activity coefficient for i in the mixture,

$\gamma_{MX_i}^{bi}$ = activity coefficient for i in the binary solution of the same water activity as the mixture,

ν_{MX_i} and ν_{MX_k} = number of ions liberated after the assumed total dissociation of i and k,

m_{MX_k} = molality of electrolyte k in the mixture,

$m_{MX_i}^{bi}$ = molality of i in the binary solution of the same water activity as the mixture.

Equation (2), later widely used by Mikulin,[5] is known under the name of this Russian physical chemist.

Equations (1) and (2) show that it is possible to calculate the water activity of a mixture and the activity coefficient of the components if the composition of the mixture and the binary data ($a_{H2O}, m_{MX_i}^{bi}, \gamma_{MX_i}^{bi}$) associated with each of the components are known. These binary data are available for a large number of electrolyte.[6] We have access to a database and associated software which allows automatic calculation of a_{H2O} and γ_{MX_i}.

The term in the numerator of Equation (2) depends solely on the water activity of the solution and the nature of the electrolyte MX_i. The denominator represents the sum of the mixture's components. Equation (2) may therefore be represented as follows:

$$\gamma_{MX_i} = \frac{F_{MX_i}(a_{H2O})}{\sum} \qquad (3)$$

Where F_{MX_i} is a characteristic function of the electrolyte MXi which depends solely on the water activity, and $\sum = \sum_k \nu_{MX_k} . m_{MX_k}$

Strictly speaking, Mikulin's law is applicable only if the special ZSR behaviour is confirmed. In 1968, Ryazanov and Vdovenko [7] generalised Equation (3) to include chemical species. If new interactions exist in the mixture, leading to the formation of new chemical species, the mixture of binary isopiestic solutions of all these chemical species (of course, a hypothetical solution) must comply with the ZSR law. The activity coefficient of any chemical species x would itself depend solely on the mixture's water activity and the sum of the concentrations of all the chemical species present in the mixture, according to the RYAZANOV-VDOVENKO (RV) relation;

$$\gamma_x = \frac{f_x(a_{H2O})}{\sigma} \quad (4)$$

where f_x is a characteristic function of the species x depending solely on the water activity, and σ is the sum of the concentrations of all chemical species in the mixture.
Unlike the water activity function F_{MX_i}, the function f_x cannot be calculated. In the case of a chemical species, this approach does not allow an activity coefficient value to be calculated. However, as in the case of a component, we can see that only two physico-chemical parameters control the influence of the medium on species reactivity.

CONTRIBUTION OF THE RYAZANOV-VDOVENKO RELATION TO CONTROL OF SALTING-OUT EFFECTS

The RV relation allows widely varying problems to be solved. In particular, by controlling the variables a_{H2O} and σ (easily fixed by the addition of background salts), it allows salting-out phenomenon to be held at a constant level for the study of liquid-liquid extraction systems.
It also leads to a new representation of chemical equilibrium constants data.

New representation of equilibrium constants

For example, the complexation reaction of Fe^{3+} by SCN^- thiocyanate ions can be written as follows:

$$Fe^{3+} + SCN^- \leftrightarrow Fe(SCN)^{2+}$$

The mass action law applied to this equilibrium gives:

$$\beta_1 = \frac{[Fe(SCN)^{2+}]}{[Fe^{3+}][SCN^-]} = \beta_1^0 \cdot \frac{\gamma_{Fe^{3+}} \cdot \gamma_{SCN^-}}{\gamma_{Fe(SCN)^{2+}}}$$

where β_1 is the apparent constant of equilibrium, and β_1^0 is the thermodynamic constant of equilibrium.
If the activity coefficients γ_i of the species participating in the equilibrium are developed by applying the RV expression, the mass action law may be written in the form:

$$G_1(a_{H2O}) = \beta_1 . \sigma$$

where G_1 is the water activity function which characterises the equilibrium.
If the activity coefficient quantification according to the RV approach is valid, the representation of the product $(\beta_1 . \sigma)$ should depend solely on the solution's water activity, irrespective of the nature of the background salts used for determining the values of β_1.

Based on values from the literature,[8] we have represented (Figure 1) the variation of the apparent constant β_1 as a function of the ionic strength I. It can be easily seen that, for the same ionic strength, the value of the apparent constant depends on the nature of the background salt used.

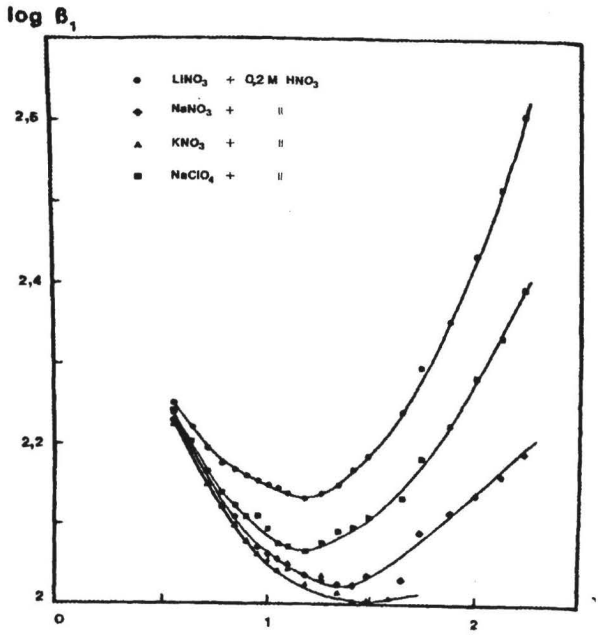


Figure 1. Effect of the ionic strength and the nature of background salts on the complexation of Fe^{3+} by SCN^- anions to form $FeSCN^{2+}$. Data from reference 8.

In contrast (Figure 2), the product $(\beta_1.\sigma)$ is now solely dependent on the variable a_{H2O}.
On the basis of such a representation, it is thus possible to determine the value of the apparent constant β_1 for any medium, provided its composition (and therefore its water activity) is known.
The accuracy and utility of this new representation for equilibrium constants have been verified for a large number of chemical equilibria. [9-11]

Salting-out control in liquid-liquid extraction operations

Two liquid-liquid extraction studies have made use of the RV relation. The systems contained aqueous solutions of copper (II)[12] or zinc (II)[13] with high chloride concentrations, and neutral extractants. The extraction equilibrium is of the type:

$$Zn^{2+} (\text{or } Cu^{2+}) + 2Cl^- + \overline{E} \leftrightarrow \overline{ZnCl_2E}$$

In such a system, interpretation of experimental results is particularly tricky. When Cl^- ion concentration increases, three antagonistic phenomena occur:
1. The formation of a complex containing Zn (or Cu), the extractant and Cl^- ions, which allows the extraction of Zn or Cu with positive influence of both extractant and Cl^- ion concentrations,
2. The formation of Zn (II) (or Cu (II)) chloro-complexes in the aqueous phase, which tends to depress the extraction,
3. The salting-out effect, which favours zinc extraction.

At constant a_{H2O} and σ, the salting-out effect has a constant influence within the whole range of chloride ion concentrations investigated and thus the depressing effect of the complexes formation can be clearly observed as Cl^- ion concentration is increased. Conversely, at non-constant a_{H2O} and σ, any increase in chloride ion concentration has both the tendency to depress the extraction, as a result of the chloro-complexes formation, and also to favour the extraction, as a result of an increase in the salting-out effect and, of course, a mass effect on the extraction equilibrium. Control of the salting-out effect thus

allowed determination of the extraction constants and the chloro-complexes stability constants in aqueous solution without ambiguity. [13]

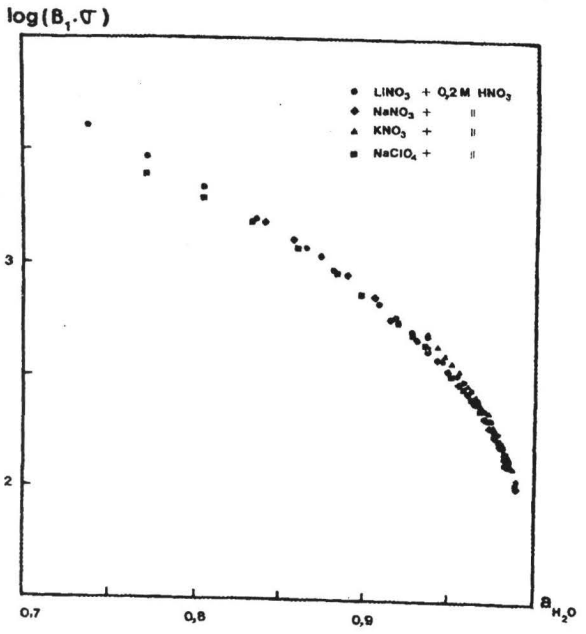


Figure 2. Effect of the water activity and the total concentration of species on the complexation of Fe^{3+} by SCN^- anions to form $FeSCN^{2+}$. Data from reference 8.

CONTRIBUTION OF THE MIKULIN RELATION TO MODELLING OF EXTRACTION SYSTEMS

Here, the non-ideality of the aqueous phase is treated in an overall manner, without attempting to distinguish between chemical and physical phenomena. This approach is particularly useful when the aqueous chemistry of the metallic elements to be extracted is not well known or subject to caution. In the case of extraction systems using a neutral extractant, this approach allows the application of an analytical method to the organic phase by searching, in particular, for the number and stoichiometry of formed complexes.

Selection of most favourable aqueous medium for extraction

The possibility of quantifying non-ideality of aqueous phases using the MIKULIN (2) relation allows, in certain cases, the prediction simply by calculation of the medium best suited to performing an extraction operation.

A recent study[14] examined the extraction of U(VI) using an acid extractant reagent of the type "Calixarene" governed by the equilibrium:

$$UO_2^{2+} + \overline{LH_3} \leftrightarrow \overline{LUO_2H} + 2H^+$$

The application of this study concerned the definition of an analysis protocol. The goal was to determine the aqueous medium most suitable for uranium recovery.

It should be noted that, for such a system, the value of the effective extraction constant K is "constant" (for a fixed extractant concentration) irrespective of the medium under consideration.

The effective extraction constant, K, can be represented by:

$$K = \frac{\left[\overline{LHUO_2}\right]\left[H^+\right]^2}{\left[\overline{LH_3}\right]\left[UO_2^{2+}\right]} \frac{\gamma_{H+}^2}{\gamma_{UO_2^{2+}}}$$

where $\left[H^+\right]$, $\left[UO_2^{2+}\right]$ are the concentrations of the species H^+ and UO_2^{2+},

γ_{H^+}, $\gamma_{UO_2^{2+}}$ are the activity coefficients of the species H^+ and UO_2^{2+}.

By introducing the stoichiometric activity coefficients, and taking as an example a chloride medium, we obtain,

$$K = \frac{\left[\overline{LHUO_2}\right]\left[C_H\right]^2}{\left[\overline{LH_3}\right]\left[U(VI)\right]} \frac{\gamma_{HCl}^4}{\gamma_{UO2Cl2}^3}$$

where $\left[C_H\right]$ is the concentration of the acid component (normality),

$\left[U(VI)\right]$ is the concentration of the component $UO_2(Cl)_2$,

γ_{HCl}, γ_{UO2Cl2} are the stoichiometric activity coefficients for the components HCl and $UO_2(Cl)_2$.

$$\text{i.e., } \log D_U = \log K + \log\left[\overline{LH_3}\right] - 2\log C_H + 3\log(\gamma_{UO2Cl2}) - 4\log(\gamma_{HCl})$$

In chloride medium, the medium effect on extraction performance is therefore quantified by the expression:

$$\mathbf{M.E = 3\log(\gamma_{UO2Cl2}) - 4\log(\gamma_{HCl})}$$

In nitrate medium, it becomes,]: $\mathbf{M.E = 3\log(\gamma_{UO2(NO3)2}) - 4\log(\gamma_{HNO3})}$

In perchlorate medium, it becomes: $\mathbf{M.E = 3\log(\gamma_{UO2ClO4}) - 4\log(\gamma_{HClO4})}$

This medium-related effect quantifies all the interactions undergone by the U(VI) and acid components in the aqueous phase. It therefore concerns both physical and chemical interactions (i.e. formation of complexes between UO_2^{2+} and the medium's counter-anion, proton association).

Calculation of the term (**M.E**), which quantifies the **global** medium effect, makes it possible to determine the medium that provides best performance, i.e.; that giving the highest **M.E** value. The values of the stoichiometric activity coefficients were calculated using the MIKULIN relation and the binary data relating to the electrolytes in question.[6]

For a given value of water activity, the nitrate medium gives the highest **M.E** values. Predicted extraction performance, as a function of medium nature was then experimentally confirmed.[14]

Advanced physico-chemical modelling of neutral extractant systems

Software has been developed (EXTRACTION software) to model as completely as possible the extraction system corresponding to the general extraction equilibrium,

$$i\overline{E} + jH^+ + kM^+ + (j+k)NO_3^- + hH_2O + d\overline{Dil} \leftrightarrow \overline{(E)_i(H)_j(M)_k(NO_3)_{k+j}(H_2O)_h(Dil)_d}$$

Depending on the value of the stoichiometric coefficients (i, j, k, h, d), it is possible to take into account various types of equilibria:

- polymerisation of the extractant and/or diluent molecule,
- hydration of the extractant and/or diluent molecule,
- distribution of the acid or salt between the aqueous and diluent phases,
- extraction of the acid or salt, with or without hydration, by the extractant or diluent,
- mixed extraction (acid + salt), with or without hydration, by the extractant or diluent.

The hydration water molecules given in the extraction equilibrium have "strong" interactions with the organic complex. However, many studies[15,16] have shown that water interacting "weakly" with the

organic species (whether hydrated or not) participated in the general phenomenon of hydration of the organic phases of these systems. To distinguish them from the hydration water molecules without ambiguity, we refer to them as water molecules solubilized by the organic species. Those physical interactions with the organic species can be removed from the corresponding activity coefficients by using the **SERGIEVSKI** [17] relation, with the applications of some modifications.[15] For an organic species i this relation is given by:

$$\overline{\gamma_i} = \overline{\gamma_i^{\oplus}} . \exp\left[s_i^{\oplus}(1 - a_{H2O})\right]$$

where $\overline{\gamma_i^{\oplus}}$ denotes the activity coefficient of species i in the same organic phase (i.e., same diluent and same concentration), but in equilibrium with pure water (i.e., $a_{H2O} = 1$),

$s_i^{\oplus}$ is the number of water molecules solubilized by species i., for $a_{H2O} = 1$.

For the specific case of extraction equilibrium which corresponds to:

$$i\overline{E} + M^+ + NO_3^- + hH_2O \leftrightarrow \overline{(E)_i(MNO_3)(H_2O)_h}$$

the associated thermodynamic extraction constant can be written:

$$K^0 = \frac{\left[\overline{m_{ih}}\right]}{\left[\overline{m_E}\right]^i . a_{MNO3} . a_{H2O}^h} \cdot \frac{\overline{\gamma_{ih}^{\oplus}}}{(\overline{\gamma_E^{\oplus}})^i} \frac{\exp\left[s_{ih}^{\oplus}(1 - a_{H2O})\right]}{\exp\left[i.s_E^{\oplus}(1 - a_{H2O}\right]}$$

At this stage, only non-ideality caused by physical interactions between the organic species and the diluent are contained in the terms $\overline{\gamma^{\oplus}}$.

If we assume, for a constant extractant/diluent ratio, that the relationship between activity coefficients $\overline{\gamma^{\oplus}}$ is constant along an extraction isotherm, it is then possible to write an "effective" extraction constant:

$$K = \frac{\left[\overline{m_{ih}}\right]}{\left[\overline{m_E}\right]^i . a_{MNO3} . a_{H2O}^h} . \exp\left[(s_{ih}^{\oplus} - is_E^{\oplus})(1 - a_{H2O})\right]$$

where $a_{MNO_3} = m_M . m_{NO3} . \gamma_{MNO3}^2$

Calculation of the thermodynamic activities of the components H_2O and MNO_3 is carried out by using, respectively, the ZSR relation (1) and the MIKULIN relation (2). Of course, these calculations are possible only if the binary data relating to the aqueous solution components are known.

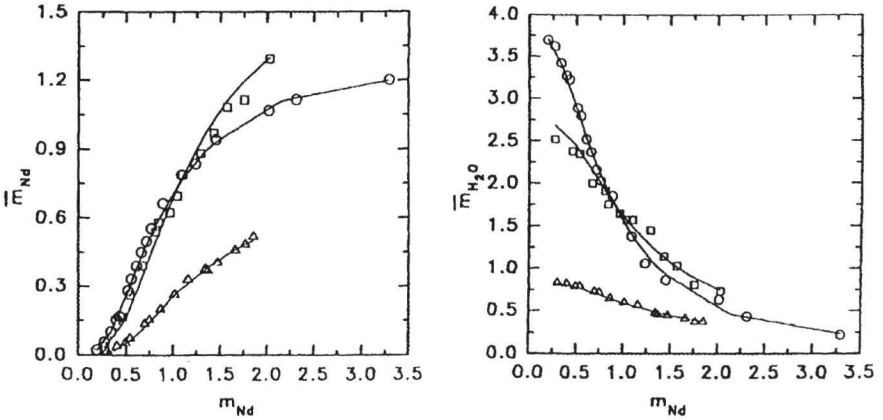
In these studies, modelling consists of testing the validity of a set of organic species with respect to the experimental extraction isotherms. If this set constitutes a convincing image of the organic phase, there should be a good agreement between the calculated and experimental values for both acid or salt extraction isotherms and those for water. This phase of the calculation consists of an adjustment of the parameters $(K, s^{\oplus})$ with respect to each of the proposed species. This is referred to as the **adjustment step**. The adjustment step is generally only applied to systems containing one component (in addition to water).

To confirm whether or not the proposed species and their associated parameters are convincing, the system of equations is then used in a second stage in predictive mode. The quantities of acid, salt and water present in the organic phases equilibrated with the multicomponent aqueous phases are calculated (acid, extractable salt, non-extractable salt). This is referred to as the **predictive step**. If non-ideality has been correctly accounted for based on the sub-systems, there should be a good agreement between calculated and experimental values.

This model was first applied to the extraction of nitric acid HNO_3 alone, or in the presence of salting-out agents, by TBP (pure and diluted at 30% by weight in hydrogenated tetrapropylene (HTP), and at 10%, 30%, 50% in dodecane) [15,18] and by a monoamide (DOPA), pure or diluted in HTP (10%, 30%,

60%).[15] The acid and water extraction isotherms have been perfectly modelled over a very wide concentration range (0-14 M) using a limited number of organic complexes.

We then studied the modelling of metallic elements; uranyl nitrate by a monoamide (DOPA) (diluted at 30% in HTP),[15] and lanthanide nitrates (Ln = Nd, Pr) by TBP (pure and diluted at 30, 50 in dodecane).[19] In the case of U(VI), to correctly represent the extraction isotherms for U(VI) and water over the full concentration range, it was necessary to take into account two non hydrated complexes $(UO_2(NO_3)_2)(DOPA)_2$ and $(UO_2(NO_3)_2)_2(DOPA)_3$. In the case of $Ln(NO_3)_3$/TBP-dodecane systems, modelling leads to two complexes; $(TBP)_3Ln(NO_3)_3$ and $(TBP)_4Ln(NO_3)_3$, irrespective of the TBP concentration. In Figures 3 are represented the calculated extraction isotherms for neodymium (on the left) and water (on the right), along with the experimental points.



Figures 3. Experimental (points) and calculated (lines) extraction isotherms (Nd, on the left, and water, on the right) as a function of neodymium nitrate concentration in the aqueous phase. Extraction system: $Nd(NO_3)_3$ - H_2O / TBP (Δ = 30, □ = 50, O = 100 vol%)-dodecane.

This modelling has also permitted an accurate prediction of lanthanide and water concentrations present in the organic phases in equilibrium with the aqueous phases containing a salting-out agent (NH_4NO_3, non-extracted salt).[19] Finally, the predictive calculations relating to systems containing lanthanide and nitric acid,[19] slightly disagree with the experimental values for domains of high acidity. The formation of a mixed acid complex $(TBP)_3HLn(NO_3)_4$ was then considered, for which the parameters $(K, s^{\oplus})$ were adjusted based on the experimental points corresponding to the $Ln(NO_3)_3$-HNO_3/TBP-dodecane system.

A more recent study[20,21] investigates an even more complex system; $CsNO_3$-$NaNO_3$-HNO_3/ Calixarene(10^{-2}M)-nitrophenyloctylether (NPOE). In effect, three additional difficulties exist here.

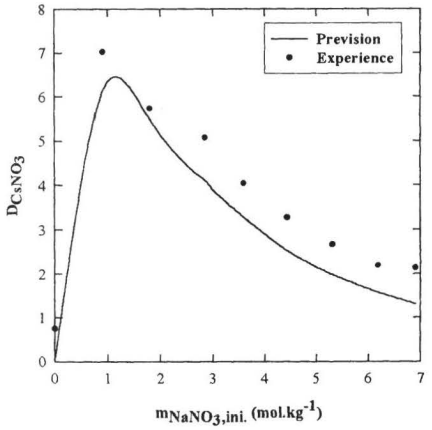
Firstly, three components (as opposed to two previously) are extracted by calixarene: HNO_3, $CsNO_3$ and $NaNO_3$.

Secondly, the diluent (NPOE) extracts a non-negligible quantity of nitric acid.

Finally, caesium, for the calixarene used in this study displays a strong affinity, is present as traces in a matrix containing high concentrations of $NaNO_3$ and HNO_3. In the previous work, all the components were present in macro-concentrations.

For conditions under which calixarene is saturated by caesium, the study reveals a non-negligible extraction of nitric acid by the Calix-Caesium complex. On the basis of these experimental results, modelling leads to the suggestion of two mixed complexes of the formula $(Calix)HCs(NO_3)_2$ and. $(Calix)H_2Cs(NO_3)_3$.[21] Finally, predictive calculations of the distribution ratio values for trace caesium (10^{-5}M) in matrixes of high $NaNO_3$ and/or HNO_3 concentrations were carried out by considering eleven

complexes whose parameters ($K, s^{\oplus}$) had first been adjusted on the simpler systems (HNO_3/NPOE, HNO_3/calix-NPOE, $CsNO_3$/calix-NPOE, $NaNO_3$/calix-NPOE). Figures 4 and 5 present these predictive calculations. Good agreement between experimental and calculated values can be seen. The improved performance of the extraction system in acid medium can therefore be explained by the formation of acid-caesium complexes.



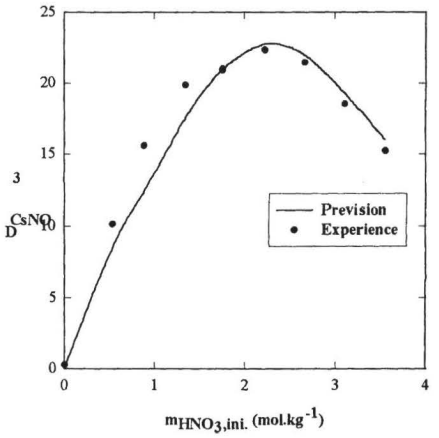


Figure 4 (on the left), **Figure 5** (on the right): Predicted and experimental distribution ratio of nitrate caesium at tracer level concentration (10^{-5}M) in concentrated $NaNO_3$ (fig.4) or HNO_3 (fig.5) solutions. Extraction system: $CsNO_3$ - MNO_3(M = Na or H) - H_2O / 0.0076mol / kgNPOE

Prediction of separation selectivity

The Mikulin-Sergievskii model allows determination of the values of the parameters ($K, s^{\oplus}$) with respect to the extracted species. Knowledge of these values should allow prediction of the separation selectivity between two elements of similar properties.

We thus took an interest in selectivity for lanthanide nitrate-/TBP-dodecane extraction systems.[22,23] In these systems, the principal extraction equilibrium can be written:

$$Ln^{3+} + 3NO_3^- + 3\overline{E} \leftrightarrow \overline{(E)_3 Ln(NO_3)_3}$$

By expanding the expression of the effective extraction constant and by using the MIKULIN relation under form (3), it is possible to write an expanded expression of the separation selectivity factor ($SF_{A/B}$) between two lanthanides A and B (organic lanthanide complexes formed with TBP have identical stoichiometries):

$$SF_{A/B} = \frac{D_A}{D_B} = \frac{K_A}{K_B} \cdot \exp\left[\left(s_B^{\oplus} - s_A^{\oplus}\right)\left(1 - a_{H2O}\right)\right] \cdot \left[\frac{F_A(a_{H2O})}{F_B(a_{H2O})}\right]^4$$

In this expression, the term K_A/K_B, ratio of effective extraction constants, depends solely (apart from temperature and pressure) on the lanthanide pair A-B and the extractant/diluent proportion. Depending on the pair considered, it might be greater than 1 or less than 1 (Figure 6).

The exponential term depends on the pair considered and the system's water activity. For increasing lanthanide atomic number, we have observed (in previous studies mentioned earlier [22] that the number of water molecules solubilized by the organic complex, $s^{\oplus}$, decreases. In this way, if we let $Z_A > Z_B$, then $s_A^{\oplus} < s_B^{\oplus}$ and the exponential term increases when water activity decreases, i.e., when salt concentration increases (lanthanide, nitric acid or non-extractable salt concentration).

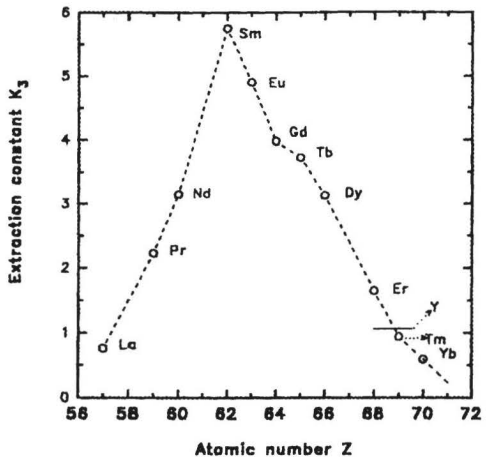
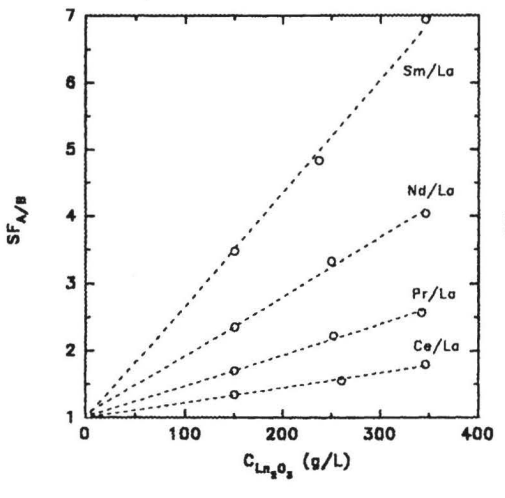


Figure 6. Effective extraction constant of the trisolvate $(TBP)_3.Ln(NO_3)_3$ versus lanthanide atomic number Z. Extraction system: $Ln(NO_3)_3$ - H_2O - TBP 100 vol%. Data from reference 24.

Finally, the term F_A/F_B is also solely dependent on the pair considered and water activity. The values of $F_{Ln}(a_{H2O}) = 4m^{bi}_{Ln}.\gamma^{bi}_{Ln}$ can be calculated for each lanthanide nitrate since the binary data relating to these electrolytes are available in the literature. We can observe [23] that the functions F_{Ln} are strictly increasing as water activity decreases and the values of F_{Ln} increase proportionally with the lanthanide atomic number.

Hence, for $Z_A > Z_B$, $F_A/F_B \geq 1$. The power of four, typical of lanthanide salt stoichiometry, of course increases the weight of this third term.



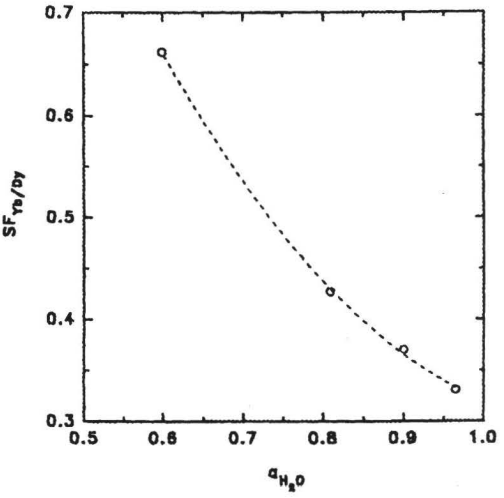


Figure 7 (on the left). Separation factors of selected lanthanide pairs versus lanthanide nitrate concentration (a_{H2O} decreases when C(g/l) increases). Data from reference 25.

Figure 8 (on the right). Yb/Dy separation factor versus water activity. Data from reference 26.

To summarise the various arguments, we may write the expression:

$$SF_{A/B} = SF_1 . SF_2 . SF_3$$

For $Z_A > Z_B$, SF_2 and $SF_3 \geq 1$

If $K_A > K_B$, then $SF_1 > 1$ and $SF_{A/B}$ increases when a_{H2O} decreases; selectivity is improved (Fig. 7).
If $K_A < K_B$, then $SF_1 < 1$ and $SF_{A/B}$ is less than 1 in a diluted solution and tends to 1 when a_{H2O} decreases; selectivity is diminished (Fig. 8).
This formalism has made it possible to explain a large number of experimental observations reported in the literature. [22]

CONCLUSIONS

The Mikulin-Sergievskii model as we have expanded it (and the EXTRACTION application software that we have computed) appears to be a very useful working tool for the solution chemists, as it offers them a very accurate image of the organic phase. In this respect, it can be considered as a further information along with other tools such as spectroscopic methods.

It also concerns industrial processes. The pronounced physico-chemical character it has got, allows predictive calculations of isotherms, efficiency and selectivity relative to extraction in conditions that deviate from those the optimisation of parameters have been achieved for.

This model takes the non-ideality of the aqueous phase into account according to a global approach, and therefore allows to free oneself from the lack of data or complexity concerning the aqueous solution chemistry of certain chemical elements. That is why it particularly concerns the actinide elements. However, as all models, it has got its own limits. The global approach we develop here shows itself very convenient, but can only be considered if the binary data of the studied components are available. On the other hand, the optimised values of the extraction constants related to each organic species depend on (apart from T and P) the extractant/diluent proportion, which of course limits predictions.

To finish with, we will underline the important - either theoretical or practical - breakthrough allowed by the expression of the species activity coefficient according to Ryazanov-Vdovenko (4). The *constant water activity and total concentration of species* method should be favoured in the place of the *constant ionic strength* method, if we aim at maintaining a medium effect that's constant and non-dependent on the nature of background salts.

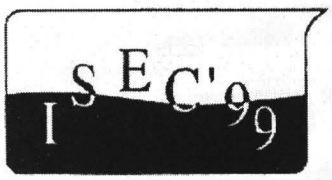
ACKNOWLEDGEMENTS

The author would like to acknowledge the support of Pr.C.POITRENAUD (Commissariat à l'Energie Atomique/INSTN).

REFERENCES

1 Zdanovskii AB. *Trudy Solyanoî Lab. Akad. Nauk.SSSR*, **6**, 1, (1936).
2 Stockes RH and Robinson RA. *J.Phys.Chem.*, **70**, 2126-2130, (1966).
3 Vdovenko VM and Ryazanov MA. *Radiokhimiya*, **7**, 39, (1965).
4 McKay HAC and Perring JK. *Trans.Faraday Soc.*, **49**, 163-165, (1953).
5 Mikulin GI. "Voprozy Fizicheskoï Khimii Rastvorov Electrolitov", Izd. *Khimiya*, Leningrad, (1968)
6 Lobo VMM. *Handbook of electrolyte solutions, Part A and B*, Elsevier, (1989)
7 Vdovenko VM and Ryazanov MA. *Russ. J. Phys. Chem.*, **42**, (1968) and *Russ. J. Phys. Chem.*, **44**, 175-178, (1970).
8 Vasil'ev VP. *Russ.J.Inorg.Chem*, **7**, 924, (1962).
9 Ly FJ. *Thèse de Doctorat d'Etat*, Université P.et M.Curie, Paris, (1984).
10 Pitsch H. *Thèse de Doctorat de l'Univ. P.et M.Curie*, Paris, (1986).
11 Camacho Frias E, Pitsch H, Ly J and Poitrenaud C. *Talanta*, **42**, 1675-1683.
12 Cote G, Jakubiak A, Bauer D, Szymanovski J, Mokili B and Poitrenaud C. *Solv. Extr. Ion Exch.*, **12**, 99-120, (1994).

13 Cote G and Jakubiak A. *Hydrometallurgy*, **43**, 277-286, (1996).
14 Dinse C. *Thèse de Doctorat de l'Univ. Louis Pasteur*, Strasbourg, (1999).
15 Dannus P. *Thèse de Doctorat de l'Univ. P.et M.Curie*. Paris, (1991).
16 Schulz WW, Navratil JD and Kertes AS. *Science and Technology of TBP—Vol.IV*. CRC Press, (1991).
17 Frolov Y, Sergievskii VV and Zuev AP. *Sov.Atom.Energ.*, **35**, 731-739 (1973).
18 Mokili B and Poitrenaud C *Solvent Extr. and Ion Exch.* **13**, 731-754, (1995).
19 Mokili B and Poitrenaud C. *Solvent Extr. and Ion Exch.* **14**, 617-634, (1996).
20 Dannus P, Sorel C, Dozol JF and Poitrenaud C. *Proceedings of ISEC'96*, Ed.Shalcross et al, University of Melbourne, 1367-1372, (1996).
21 Sorel C. *Thèse de Doctorat de l'Univ. P.et M.Curie*. Paris, (1996).
22 Mokili B. *Thèse de Doctorat de l'Univ. P.et M.Curie*. Paris, (1992).
23 Mokili B and Poitrenaud C. *Solvent Extr. and Ion Exch.*, **15**, 455-481, (1997).
24 Yagodin GA, Sergievskii VV, Evdokimova LV and Bambeko LM. *Dok.Phys.Chem.*, **258**, 695, (1981).
25 Korpusov GV. *Proceedings of ISEC'88*, vol.IV, 120, Moscow-Nauka, (1988).
26 Knapp LL, Smutz M and Spedding FH. *U.S.Atomic Energy Commission Report ISC-766*, (1956).



STATE OF THE ART AND FUTURE DIRECTIONS IN SOLVENT EXTRACTION. SUMMARY OF THE 1ST INTERNATIONAL SOLVENT EXTRACTION WORKSHOP, 5–8TH OCTOBER 1997, BANFF, ALBERTA, CANADA

Gordon M Ritcey
G M Ritcey & Associates Inc., Nepean, Ontario, Canada, K2H8A9

ABSTRACT
The plan to hold a "small meeting of Solvent Extraction specialists" sometime between the Melbourne 1996 meeting and the next ISEC'99 in Barcelona in 1999 was formulated early in 1996. The purpose would be to bring together many of the experts in solvent extraction to identify and to discuss the various problem areas in this unit process. The recommendations should provide the many researchers throughout the world with valid project ideas that could ultimately result in process improvements and therefore significant reductions in capital and operating costs of solvent extraction plants. If the Workshop was to be successful, the total attendees would be limited to about 75. Invitees included those from all aspects of chemistry, chemical engineering, process design, engineering contractors, and operating plants. These "experts" would:

1) critically review the individual areas of concern --from R&D to industrial scale-up;
2) improve interaction between chemistry-engineering-process development-plant design and construction, to optimise the design of future solvent extraction operations;
3) provide some guidance to future R&D and plant design; and,
4) provide a document for wide circulation amongst practitioners.

The Solvent Extraction Workshop'97 that was held October 5-8, 1997 in Banff, Alberta, Canada, was probably the first of its kind covering all aspects of the Solvent Extraction process, and was by invitation. The meetings took place over a 4-day period. The format comprised an informal technical session in the morning, followed by lunch and then breaks in the afternoon. This permitted the attendees to visit the area for sightseeing, or participate in sporting activities of their choice. Following dinner, the evening sessions commenced. The objectives of the Workshop were:

to address and critique the various areas of the solvent extraction process, including:

A) Fundamental research in chemistry and chemical engineering
B) Flowsheet development through to piloting
C) Engineering design, control, plant design and plant construction
D) Plant operation (problems and solutions)

INVITED PRESENTATIONS

A number of invited keynote presentations took place on the first day of the Workshop. The object of these short presentations was to provide an "overview" or state-of-the-art" of a particular area in the solvent extraction process. These presentations therefore were helpful in setting the stage for the subsequent in-depth discussions that subsequently took place.

CONCERNS IDENTIFIED FOR DISCUSSION IN THE WORKSHOPS

An open discussion by all the participants identified the following areas of concern that would subsequently, where time permitted, be discussed in more detail in the smaller workshop groups. It was left to each separate working group to select from the list of concerns below those that they could discuss in the time available for the Workshop. It should be noted that some items were addressed by more than one group, and often with similar statements of concern.

Chemistry:

* What are the restrictions on reagents imposed by the mineralogy and plant operations;
* Need a reagent for Co extraction at about pH 1.5;
* Research is required on reagent degradation, the causes and mechanisms occurring;
* Speciation studies are required on all solutions throughout the process;

© 2000 Society of Chemical Industry

* Understanding the process as regards the fundamental chemistry vs. real operation because of changes in the kinetics, viscosity and physical aspects as loading occurs.
* Sampling/analyses frequency a) on-line vs. off-line; b) modern instruments vs. "wet"
* Is there a better way to treat fouled organics other than by clay treatment?

Chemical Engineering

* Requirement for more sophisticated design models of equipment, e.g., columns
* Modelling/simulation: a) can it help in the SX plant design? b) in the total plant?
* There is a lack of data on the thermodynamics in concentrated (typical plant) solutions
* Application of columns to metals such as copper--will depend on the kinetics.

Design

* Use typical plant solutions for design as soon as possible in the investigation;
* SX process operation in dynamic and changing continually in physically and chemical compositions, (including surfactants)--not a simple static system.
* Dependence of design on the aqueous media, e.g. SO_4^{2-}, Cl^-, NH_4^+ as regards reagent degradation, contactor choice, physical dynamics, final product, economics etc.
* Fundamentals of chloride systems, or other novel systems could be considered.
* Relate pilot contactors to eventual plant design; mixer settlers have been the most common; very little interest has been on other possible contactors, such as columns.
* Piloting should be considered in the context of the total (metallurgical) flowsheet;
* Interface the upstream/downstream compatibility with economics and environmental.

Operation

* Information required by the operator to operate the process most efficiently..
* Amount and type of data necessary for design engineers, and duration of a pilot plant.
* Guidelines are required on entrainment (mechanical and chemical), the causes and the effect of tip speed, shear, etc., on entrainment.
* There is a need for sensors that are robust to the process.
* Good partnerships between the engineering company and operators are necessary.
* Effects of possible additives to the diluent due to possible changes in the legislation (limit addition of aromatics); no reliable analytical methods exist;
* Determine the major parameters for optimum process operation;
* Organic removal/recovery/regeneration: equipment and processes are required.

General

* SX-EW is considered as "known technology" by many operators, but not by all the industry, nor the financial institutions. Better communication is required.
* Solvent extraction is often perceived as an environmental risk because of the general public understanding, and the "green process technology" which would eliminate the use of solvents the removal of the word "solvents" from processing;
* Biodegradability and toxicity must be addressed.
* There is a requirement for a book for operators of pilot plants and plants.
* Funding for pilot plants often is difficult to obtain, while research funding is usually easier to attain. Funding agencies for generic R&D should be identified.
* Considerable information and data are available in the literature, mostly from academia, which needs to be "translated to the plants" so as to be more useful.

WORKSHOP SUMMARY RECOMMENDATIONS

The smaller Workshop groups identified specific items of concern, from the original above list of general

concerns, pertinent to their technical/scientific area. Those items were discussed in depth where possible, and the summaries are given below. There was not sufficient time for all items.

Chemistry

1) Reagents

* The chemistry in the organic phase is often different from that in the aqueous phase,.
* Hydration of organic species is related to the nature of entrainment.
* "Chemistry" research - mostly on dilute solutions, while "process" operation is in the region where micelles exist; thus work on more concentrated solutions.
* Work on "real solutions", and don't exclude stripping.
* Acidity depends on the H^+ activity which varies with ionic concentration.
* Speciation of mass transfer complexes will differ with conditions. (e.g. pH effect).

2) Degradation

* Degradation is system dependent
* Plants should be encouraged to put solvent treatment stages into the circuits.
* Degradation may affect the chemistry as well as the physical operation.
* Solvent regeneration process requires some investigations

3) Diluents

Role of the diluent is least understood; more basic work on the aromatic content vs. performance required. The problem of environmental impact plus a bad image of organic compounds exists.

4) Analysis/Monitoring (in-line; on-line; off-line)

In-line systems are required for continuous analyses inside the stream, although on-line are acceptable. Off-line is where the sample is sent to a lab for determination and is thus not desirable for process control. Some examples of on-line are: a) entrainment, b) solution composition, and c) organic phase analysis. Techniques include: XRF/AA/Spectroscopy/Density/Viscosity

5) Novel Systems

These include: microemulsions; non-dispersed solvent extraction (membranes and barrier between organic and aqueous); liquid membranes (supported membranes, emulsion membranes); extraction chromatography.

Conclusions: these would be useful in the future in niche applications, but do not see these systems replacing solvent extraction. They also still need considerable R&D.

6) Environmental Aspects/Image

The word "solvent" has a bad image and there is a need to sell the positive aspect; development of a "solvent-less" technology, although this is probably not possible; alternatives to solvent extraction should be costed on a full life cycle analysis (often the alternatives are worse as regards environmental aspects); competition from distillation in organic chemistry.

Chemical Engineering

1) Mass Transfer/Kinetics for Multi-Component Systems

* Models of multi-component real systems are required, with mass transfer and kinetics.
* Acquisition of pilot plant data
* Prediction of rates for design for mixer settler and columns
* Diffusivity data and models for diffusivity coefficients for multi-component systems.
* Methods of interpreting effects of contaminants at interfaces
* Phase continuity effects must be established in the system.
* Laboratory scale test equipment for generating engineering data.
* Effect of degradation products on the chemical engineering and mass transfer

2) Equilibrium/Thermodynamics

* Data collection and better prediction methods are required for real systems.
* Research is encouraged to define the computer codes to enable optimum design.
* Species identification necessary.
* Fluid structures, such as micelles and interfaces
* Systems containing water

3) Design Models

* Prediction is required for first-level design of columns and mixers based on drops.
* More data are required on coalescence and breakage coefficient; for pilot plant data.
* Rate of sedimentation of drops in swarms at high phase fraction for a range of physical properties and energy input to be determined.
* Computational fluid dynamic models (CFD) at present are not promising for column design in hydrometallurgy. Problems to answer include: a) couple effect of energy dissipation; b) inclusion of drop population equation to describe drop dynamics; and, c) incorporate interface mass transfer with reactions in the continuous phase.
* Encourage the design of computer codes that are user-friendly for the design engineer.
* Verify computer-aided calculation procedures.
* Laboratory scale data acquisition
* Financial support is required for research.
* Education/collaboration with industry

4) Process Dynamics/Control Start-Up

* Control of processes with drift in chemical properties of both solutions over time.
* Classical control principals are useful on a day-to-day basis.
* Models are available on drop population balances for multi-variable control.
* Tailored solutions are required for small batch processing of exotic separations.
* Option to use small continuous extraction columns

5) Scale-Up

* Collaboration between academia and industry desirable.
* Validation of computer models require information from column designers and the manufacturer to provide large scale-up data.
* Provision of a data bank of useful, non-proprietary data for scale-up required.
* All types of solvent extraction contactors should be considered in the design.
* Drop coalescence and break-up phenomena; flow patterns can change with scale-up.

6) Monitoring

* Sample integrity and obtaining relevant data
* Principal component analyses are useful for complex systems.
* Use of models are helpful, and the understanding of basic principles are necessary.
* Robust monitoring techniques are required and should be implemented in the process
* On-line analytical equipment desirable.

7) Entrainment/Crud/Solvent Maintenance

* Must determine the minimum drop size generated by various impellers over a range of physical properties and energy input.
* Micelles may be the cause of producing stable emulsions and cruds.
* Flow patterns in vessels that could lead to entrainment need to be modelled.
* Study required to define physical characteristics of emulsions (L-S) leading to crud.
* Studies are required on crud formation and de-stabilisation.
* Use of CFD to understand entrainment problems
* Large scale equipment studies where possible

8) Novel Systems

* Supported membranes
* Equipment for systems operating at extreme phase ratios (e.g. 10/1).
* Supercritical extraction is a possibility, but economics may be a deterrent.
* Active adsorbent as particles or in membrane form
* Application to 3-phase systems (L-L-S)

9) General Comments

* Education and challenging projects.
* Communication with industry and engineer/researcher/politician interface.
* High turnover of personnel throughout industry, and greater pressure on the universities; really a post-graduate rather than an undergraduate activity at the universities. Continuing education courses, major conferences and Workshops.
* "Liquid-liquid extraction " instead of solvent extraction if "solvent" a problem.
* Incorporate knowledge into software and expert systems to transfer to industry.
* There is a need for a text for the industry that has the practical applications.
* A general lack of funds often makes research difficult.

Process design, plant design and operations

1) Models

More sophisticated models required:

a) equipment (design and operation methodology for system performance optimisation);
b) process (operating variables and scale-up);
c) fundamental.

Shortfalls of existing models:

a) practicality of using academic models;
b) physical aspects (e.g. dispersion/coalescence) to be considered in the models;
c) engineering application (use);
d) better definition of requirements of the model by the engineers;
e) lack of settler models;
f) limits of the models;
g) lack of fundamental data for the model optimisation; and
h) validation of the model.

2) Contacting Equipment And Operation

Equipment selection:

a) consider the chemical aspects (mass transfer, kinetics) and the physical operation (dispersion/ coalescence, emulsions), e.g. pump-mix vs. pumping and mixing; in-line mixers, or other contactors.

3) Piloting to Scale-Up

* Feed characteristics (composition, flow)
* Process chemistry, equilibrium data
* Use kinetics in the design (discrimination, reduce mixing time and stable emulsions).
* Introduction of purification (scrub) stages where possible.
* Contactor choice based on chemical equilibria, kinetics, and dispersion/coalescence.
* Phase separation and settling tests, if possible in a special unit such as a deep settler.
* Continuous testing and piloting are required for each specific plant.
* Objectives of continuous testing need clarification to obtain the most information.
* The size of a pilot plant will depend on the company objectives.
* Duration of pilot testing depends on the objectives (chemistry, physical, bankers, etc).
* Sound scale-up methods are required.
* Materials of construction in the pilot plant differ compared to the plant.

* Consider economics relevant to the capital and the operating costs.
* Process guarantees--many plants been designed based on what has been done before.

4) Start-Up Problems

Need more sharing of experience; very little has been published on the problems experienced.

5) Operational Information Required to Operate the Process

* What are the actual operating parameters limits
* Entrainment measurements (on-line) for the specific stream
* Reliable sampling and analyses (on-line, off-line).
* Solution composition characteristics regarding possible emulsion or precipitation.
* EMF analyses
* More information at "upstream and downstream" of the SX circuit
* Phase continuities and the effect on the chemistry as well as the physical aspects
* O/A ratios dependent on the (changing) feed composition, and the recycle phase
* More organic monitoring and analyses for performance (loss, poisoning, degradation)
* Crud characterisation, and analyses

6) Entrainment Reduction (mechanical/chemical)

* What is good operating practice (Cu circuit 10-50 ppm; U circuit 20-200 ppm);
* Aqueous entrainment in organic affected by phase continuity
* Inventory is a guide to the amount lost. GC for organic entrainment in aqueous
* Some releases monitored and tested by toxicity tests prior to release.
* Equipment sizing, selection and operation (columns, mixer settlers/mixer type)
* After-settlers, coalescence media; flotation columns; dual media filters
* Specific flowrates across the settler
* Organic operating depth in the settler
* Having a loaded organic tank and barren organic tank (entrainment removal)
* Extractant/diluent can affect mass transfer and the amount of entrainment.
* Operating philosophy on losses that may be tolerated varies with country and process.
* Influence of air on entrainment, due to the design and the operation of the contactor.
* Phase continuity control a problem in most mixer settlers, but in most columns.

7) Organic Removal from Aqueous

Need to achieve lower levels of entrainment through present and new equipment designs.

8) Reagent Degradation

The type of degradation is system-dependent.
The extractant is destroyed:

a) UV- cover the settlers or use columns if kinetics favourable);
b) high oxidant levels (e.g. metal oxidants, reagent oxidants such as nitrates, chlorine);
c) temperature;
d) conc. acid addition to organic phase produces degradation products and surfactant which cause phase separation and entrainment problems;
e) inappropriate storage and/or long storage, e.g. tertiary amines stored in the protonated form causes degradation to secondary amines; and
f) bacteria.

* Degradation of components and formation of "surfactants";
* Design for inert gas atmosphere may be required; columns and in-line mixers .
* Poisoning of organic phase (active sites) may appear as "degradation".
* Reversible degradation (regeneration) can affect:
    a) loading capacity;
    b) scrubbing - stripping efficiency;

c) phase separation;
d) selectivity;
e) reaction kinetics;
f) crud;
g) contamination in sequential circuits;
h) analytical error.

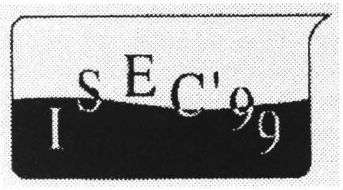
* Methods of regeneration/prevention (removal of surfactant):
  a) sodium carbonate regeneration;
  b) distillation of organic phase;
  c) removal of degradation products (clay treatment used in Cu circuits);
  d) change of aqueous ionic strength;
  e) addition of anti-oxidants to decrease degradation.

Environmental concerns

* Soil, water, air
* Metals, organics:
  a) health effects of the solutions, and identifying the toxicity of the potential new hazardous chemicals; acute toxicity data available on most commercial reagents;
  b) fire hazard (some plants automatic discharge to an external sump).
* Safe containment of wastes:
  a) within the plant;
  b) containment of organics and crud.
* Waste disposal:
  a) cruds;
  b) incineration;
  c) landfill or leach pad
* Risk assessment analysis
* Environmental impact data
* Decommissioning protocols
* Safety design in plant equipment:
  a) remote sampling/operation;
  b) ventilation - negative pressure;
  c) minimise venting as much as possible, e.g. cover mixer settlers, or use of columns where applicable. Also keep sampling and viewing hatches closed;
  d) selection of the reagent-equipment-operation to reduce the environmental impact
* Waste reduction:
  a) to reduce the amount of entrainment and the amount of crud. The optimisation of equipment choice and its operation and control are required.
* Oxidation of wastes (dissolved and entrained organics):
  a) organic wastes/aqueous wastes;
  b) achieved by: $O_3/O_2/H_2O_2/UV/TiO_2$, supercritical water as an oxidisingagent; use of reverse osmosis to concentrate organics prior to oxidation
* SX plants in communities vs. "green fields" --amounts of solvent, as well as the facilities for treatment/ disposal differ
* Hazard planning:
  a) containment for diluent storage;
  b) iso-containers for extractants;
  c) portable units for treatment for organic recovery and re-use
* Biodegradability vs. performance
* Life Cycle Analysis (cradle to grave):
  a) "green technology"; and
  b) zero discharge



Analytical Chemistry



LIQUID-SUPPORTED MEMBRANES AS SAMPLE INTERFACES IN A FLOW PROBE OPTOSENSOR FOR CHROMIUM(VI) ANALYSIS

E Castillo[2], M Granados[2], MD Prat[2], AM Sastre[1], A Kumar[1] and JL Cortina[1]

[1]Chemical Engineering Department, ETSEIB.Universitat Politècnica de Catalunya, Diagonal 647, E-08028-Barcelona, Spain.
[2]Analytical Chemistry Department. Universitat de Barcelona, Martí i Franqués 1, E-08028- Barcelona, Spain.

ABSTRACT

A flow probe optosensor for chromium(VI) has been developed using flat sheet liquid supported membranes (FSLSM). The membrane acts as the interface of the optosensor between the sample and the sensor head, which contains diphenylcarbazide as spectrophotometric reagent for chromium. Changes in the absorption of light as a function of time results from the formation of the reaction product between chromate ion and the reagent inside the sensor head, are monitored in situ.

Keywords: analysis, chromium(VI), optosensor, supported liquid membrane, diphenylsemicarbazide

INTRODUCTION

FlowProbe optosensors[1,2] are chemical analyzers incorporating three main aspects of chemical analysis: 1) sampling by a membrane interface, 2) chemical transduction by formation of an optically detectable complex of the target analyte with a selective reagent in the sensor head, and 3) optical analyte detection. These fiber optic based sensors can be adapted to many different types of analytes, depending on the reagent used within the sensor head, and the type of membrane sampling interface chosen. Multiple analyses can be performed with a single probe head with the unique feature that the sensing mechanism is regenerated in-situ[3].

The membrane plays a very important role in FlowProbe sensors, since it should allow an effective transport of the analyte from the sample to the sensor head in a reasonable time. Moreover the membrane should be impermeable to potentially interfering species. In fact the proper selection of the membrane together with the choice of the chromogenic reagent, are the key points for the success of the sensing system.

The determination of chromium (VI) in aqueous solutions is an application of special interest. The use of anionic exchange membranes in the analysis of anionic chromium (VI) has been shown not suitable due to the slow transport of Cr(VI) anions through the membranes and the irreversible Cr(VI) retention in the membrane. This work presents a new strategy to promote selective transport of Cr(VI) based in the use of Flat Sheet Liquid Supported Membranes (FSLSM)[4] as the interface of the FlowProbe sensor. Diffusion-limited transport of the target analytes across FSLSM represents a powerful novel tool and excels most of the conventional approaches, since it combines the steps of extraction, stripping and regeneration into a single step. In this study the combination of the transport of anionic chromium species through FSLSM and the subsequent reaction between Cr(VI) and diphenylcarbazide (DPC) in a sulphuric acid medium has been evaluated.

Analyte transport enhancement through the membrane was achieved by addition of a non-volatile complexing agent ("carrier") to the organic solvent. Complexing agents based on alkylated tertiary amines and quaternary ammonium salts were used as ionophore carriers to increase the diffusing ability of the liquid membrane to chromium species. The use of these carriers led to an improvement of diffusion in several orders of magnitude, due to the selective and reversible reaction with the target species[5]. Furthermore, the transport of Cr(VI) through the FSLSM was facilitated by the complexation of Cr(VI) and DPC inside the sensor head, producing a coloured Cr(III)-DPC complex[6].

© Society of Chemical Industry

The facilitated transport of Cr(VI) through FSSLM was investigated as a function of hydrodynamic conditions, concentration of chromium, pH in the sample solution, structure of carrier, carrier concentration in the membrane, and strippant characteristics[7].

Preliminary experiments pointed out that, among the different polymeric supports and organic solvents assayed to prepare the FSLSM, Durapore support and kerosene were the ones that provided better results. Thus, membranes prepared with this combination were used through the study here reported, owing to its best performance.

EXPERIMENTAL

Reagents and solutions

Analytical grade kerosene (Fluka) was used as received. 1g.dm^{-3} chromium(VI) standard solution was prepared by dissolving sodium chromate (Merck) in water. 0.4 % (w/v) 1,5-diphenylcarbazide (DPC) solutions were prepared by dissolving 0.25 g of DPC (Merck) in 10 cm^3 of acetone and diluting to 100 cm^3 with water. Working DPC solutions were prepared by appropriate dilution of 0.4% solutions with sulphuric acid solutions.

Aliquat 336, a quaternary ammonium chloride ($(CH_3)R_3N^+Cl^-$), from Merck, and Alamine 336, a C_8-C_{10} tertiary amine (R_3N), from Henkel were used as received. Other chemicals used were analytical reagent grade.

Apparatus

A 640 Varian Atomic Absorption Spectrophotometer was used for chromium measurements in the source phase. An optical fiber based transmittance probe (Photonetics) coupled to a diode array absorption spectrophotometer (Hewlett Packard HP8453) was used to follow *in line* the formation of the Cr(III)-DFC complex in the receiving phase.

Membrane Support

The organic membrane phase was prepared by dissolving a weighted amount of Aliquat 336 or Alamine 336 in kerosene to obtain carrier solutions of various concentrations. Durapore support was impregnated with the carrier solutions by immersion for 24 hours, and then leaving it to drip for a few seconds before being placed in the permeation cell.

Table 1. Polymeric support characteristics: Durapore (GVHP) from Millipore

Appearance:	white colour, smooth surface and hydrophobic
Chemical composition:	Polyvinylidenedifluoride
Tortuosity :	1.67
Porosity (%):	75
Thickness (μm):	125

FSSLM Preparation and Measurements

Single stage FSSLM measurements were carried out with a simple two compartments permeation cell, which consisted of a source phase (200 cm^3) and a receiving phase chamber (200 cm^3), separated by a liquid membrane having an effective membrane area of 11.33 cm^2. Thus, the source phase simulated the sample solution, whereas the receiving phase simulated the reagent solution inside the sensor head of the FlowProbe.

Both source and receiving phases were mechanically stirred at about 1200 rpm at room temperature (25 ± 1°C) to avoid concentration polarisation conditions at the membrane interfaces and in the bulk of the

solutions.
Membrane permeabilities were determined by monitoring chromium concentration as a function of time in both the source phase (by atomic absorption spectrophotometry) and the receiving solution (by molecular absorption spectrophotometry). The sum of Cr content in both phases was found to be reproducible within ±5%.
Permeation coefficient (P_{Cr}) was computed by the following equation :

$$\ln(C/C_0) = -(A/V)P_{Cr} \times t$$

where V is the volume of the source phase solution (cm^3), A the effective membrane area (cm^2), C_o and C are concentrations of metal ion ($mol.L^{-1}$) in source phase at time zero and at time t, respectively, and t the elapsed time (s).

RESULTS AND DISCUSSION

Cr(VI) membrane transport evaluation

The first step of permeation is the partition of the Cr(VI) anions into the anion-exchange liquid supported membrane. This is a spontaneous process based on the reaction of $HCrO_4^-$ with the ionophores (Aliquat 336 or Alamine 336) present in the liquid membrane. Thus, once in the membrane, $HCrO_4^-$ reacts with the ionophore to form Cr(VI)-amine complex.

On the other hand, the stripping of Cr(VI) from the membrane to the receiving solution includes a reduction process to Cr(III). The combination of the reduction step of the metal anion ($HCrO_4^-$) by DFC (DFC_{red}) to produce Cr(III), and the specific complexation of Cr(III) with the oxidized form of DFC (DFC_{ox}), leads to an increase of both the membrane-phase diffusivities and the concentration gradients of the targeted Cr(VI) anions.

The sensor transduction mechanism of the analyte could be described by the following transport and chemical reactions steps:

Transport step 1:

$$Cr(VI)\ (sample) \Rightarrow Cr(VI)\ (membrane)$$

Accomplished by the extraction reaction between the amine carrier and $HCrO_4^-$:

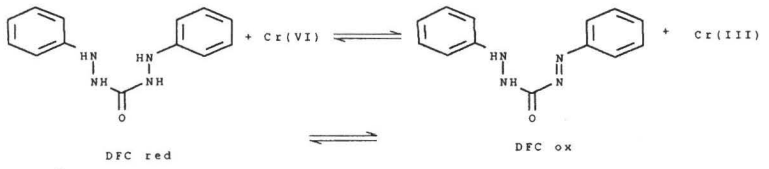
i) Aliquat 336: $HCrO_4^- + R_4N^+ X^- \leftrightarrow R_4N^+ HCrO4^- + X^-$
ii) Alamine 336: $HCrO_4^- + R_3NH^+ X^- \leftrightarrow R_3NH^+HCrO_4^- + X^-$

Transport step 2:

$$Cr(VI)\ (membrane) \Rightarrow Cr(III)\ (sensor\ head)$$

Accomplished by the combination of Cr(VI) stripping and the following reactions:

a) Cr(VI) reduction step: $HCrO_4^- + DFC_{red} \Rightarrow Cr(III) + DFC_{ox}$



b) Complexation step: $Cr^{3+} + 3\ DFC_{ox} \Leftrightarrow Cr(DFC_{ox})_3$

The Cr(III) complex is not retained by the supported extractants of the liquid membrane, resulting in the increased diffusivities of $HCrO_4^-$. Moreover the concentration gradient of the targeted

ions is kept high, because the number of free ions capable of back-diffusion is dramatically reduced by complexation. On the other hand other transition metal ions, considered the interfering metal ions here, are not favorable either in transport through the membrane or in complexation with DFC.

Data for Cr(VI) transport of two liquid supported membranes based on Aliquat 336 and Alamine 336 are displayed in figure 2. As can be seen the higher efficiency is obtained with Aliquat 336 membrane, which was selected for further experiments.

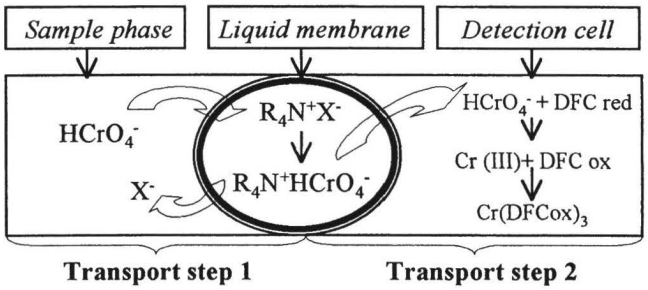


Figure 1. Scheme of the transport process of analytes from the sample to the probe cavity of the sensor head.

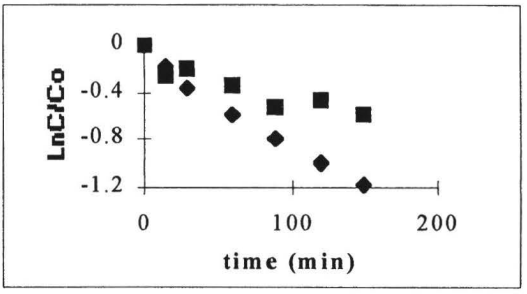


Figure 2. Permeability behaviour of Cr(VI) with anion exchange liquid supported membranes: ◆ 0.2 mol/dm^3 Aliquat 336,■ 0.2 mol/dm^3 Alamine 336. Solvent: Kerosene. Source phace:1,6X10^{-4} mol/dm^3 Chromium (VI) in H_2SO_4 medium, pH=3. Receiving phase: 4,1X10^{-5} mol/dm^3 Diphenylcarbazide, pH= 1 in H_2SO_4 medium.

Spectrophotometric detection of Cr(VI) with DFC

The optical sensor is based on the absorbance measurements of the Cr(III)-DFC_{ox} complex. Figure 3 shows chromium complex spectra collected *in situ* at several elapsed times by using the optical fiber transmission probe, for a 10 ppm Cr(VI) sample solution.

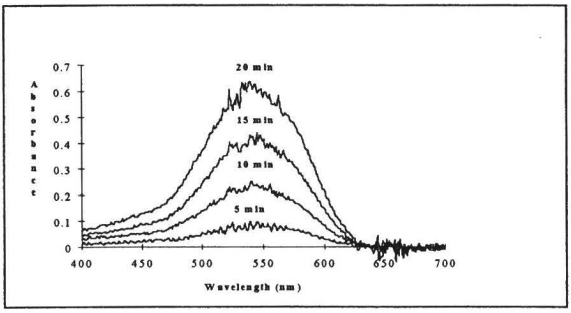


Figure 3. Cr(III)-DFC_{ox} complex spectra at several elapsed times. Sample:$1.6x10^{-4}$ mol/dm^3 Cr(VI).

Light intensity is modulated by absorption changes in the visible range that occur when chromium anions diffuse across the liquid supported membrane.

Like any analytical instrument the sensor simple provides a signal in response to the sample it is exposed to. It is up to the calibration model to convert the measured response signal into relevant information about the concentration of the analytes in the sample. In order to develop the calibration model it is necessary to collect the response to samples of known concentrations. Typical sensor responses to a series of concentrations of Cr(VI) as a function of time are shown in Figure 4.

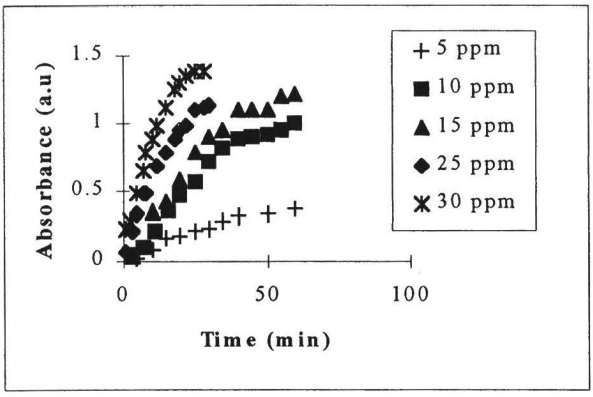


Figure 4. Sensor response at 543 nm vs. time as a function of Cr(VI) concn. in the aqueous sample.

Figure 5 shows the sensor signal at 543 nm for a dialysis time of 35min, which corresponds to a steady state. The absorbance variation was linearly dependent on metal concentration in the aqueous sample and a correlation factor of 0.999 was obtained.

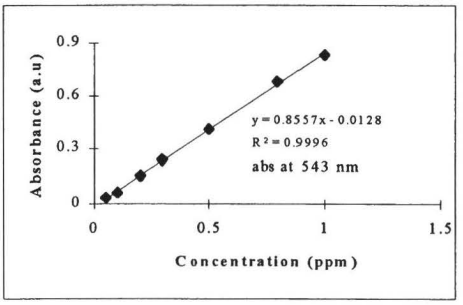


Figure 5. Sensor response as a function of Cr(VI) concentration in the sample.

CONCLUSIONS

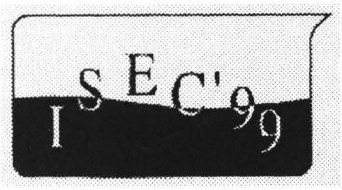
Liquid Supported Membranes have shown a high potential as interfaces in FlowProbe sensor configurations for Cr(VI) analysis. This type of membranes opens the possibilities of designing a highly selective interface, according to the analyte and interfering species characteristics. Moreover the sensor operational concentration range can be adjusted by adjusting the membrane parameters.

ACKNOWLEDGEMENTS

This work was supported by the Universitat Politècnica de Catalunya through Project PRE95-02, and by CICYT projects AMB98-0327 and QUI 96-1025-CO3 (Ministry of Science and Culture of Spain). Finally, authors want to acknowledge, L.K. Moore and L.W. Burgess at Center for Process Analytical Chemistry for suggestions.

REFERENCES

1. Berman RJ, Christian GD and Burgess LW, *Anal. Chem.*, **62**, 2066, (1990).
2. Lin Z and Burgess LW, *Anal. Chem.*, **66**, 2544, (1994).
3. Moore LK, Veltkamp DJ, Cortina JL, Lin Z and Burgess LW, *Sensors and Actuators B.*, **38-39**, 130, (1997).
4. Danesi PR, in *Developments in Solvent Extraction*, Ed. S. Alegret, Ellis Horwood Series, (1988).
5. Salazar E, Ortiz MI , Urtiaga AM and Irabien JA, *Ind. Eng. Chem. Res.*, **31**,1523, (1992).
6. Cheng KL, Ueno K and Imamura T, *Handbook of Organic Analytical Reagents*, CRC Press, Boca Raton, FL, (1982).
7. Castillo E, Granados M, Prat MD and Cortina JL, *Journal of Membrane Science* (submitted).



RECENT ADVANCES IN THE DEVELOPMENT OF EXTRACTION CHROMATOGRAPHIC MATERIALS FOR THE ISOLATION OF RADIONUCLIDES FROM BIOLOGICAL AND ENVIRONMENTAL SAMPLES

ML Dietz, EP Horwitz and R Chiarizia
Chemistry Division, Argonne National Laboratory, Argonne, IL 60439, USA

ABSTRACT
The determination of low levels of radionuclides in environmental and biological samples is often hampered by the complex and variable nature of the samples. One approach to circumventing this problem is to incorporate into the analytical scheme a separation and preconcentration step by which the species of interest can be isolated from the major constituents of the sample. Extraction chromatography (EXC), a form of liquid chromatography in which the stationary phase comprises an extractant or a solution of an extractant in an appropriate diluent coated onto an inert support, provides a simple and efficient means of performing a wide variety of metal ion separations. Recent advances in extractant design, in particular the development of extractants capable of metal ion recognition or of strong complex formation even in acidic media, have substantially improved the utility of the method. For the preconcentration of actinides, for example, an EXC resin consisting of a liquid diphosphonic acid supported on a polymeric substrate has been shown to exhibit extraordinarily strong retention of these elements from acidic chloride media. This resin, together with other related materials, can provide the basis of a number of efficient and flexible schemes for the separation and preconcentration of radionuclides form a variety of samples for subsequent determination.

Keywords: radionuclide, preconcentration, extraction chromatography, diphosphinic acid

INTRODUCTION

Extraction chromatography (EXC) is a type of liquid-liquid chromatography in which the stationary phase consists of an extractant or a solution of an extractant in an appropriate diluent supported on an inert substrate. The technique thus couples the selectivity of solvent extraction with the multi-stage character of a chromatographic process and the ease of handling of an ion-exchange resin.[1] Since its introduction by Siekierski in 1959,[2] extraction chromatography has been extensively studied,[1] and it is now widely recognized that it provides a simple and effective means by which the separation and preconcentration of any of a variety of metal ions can be accomplished. In the determination of radionuclides in environmental or biological samples, for example, the low levels of the nuclides typically encountered and the complexity of the sample matrix often preclude a direct determination of the species of interest. Rather, a preliminary separation and preconcentration step is a prerequisite to quantitation. Although numerous approaches have been described by which this can be accomplished e.g., solvent extraction, ion exchange, none is entirely satisfactory. Solvent extraction, for example, is unsuitable for routine use on large numbers of samples, since it is cumbersome and generates large volumes of organic waste. Similarly, ion-exchange methods are frequently complicated by the lack of specificity of conventional ion-exchange resins. Extraction chromatography overcomes all of these shortcomings, and provides a selective and facile separation of the radionuclide of interest from complex sample matrices.

In an earlier report,[3] we described the development of several new EXC resins based on TRUEX and SREX Process chemistries and related extractant design studies, and outlined the application of these materials in the separation and preconcentration of actinides and/or radiostrontium for subsequent determination. Since this time, certain limitations of these materials and thus, the need for improved EXC materials, have become evident. For example, although one of these materials, referred to as TRU•resin, has been found to be useful in the selective recovery of actinides from complex sample matrices, actinide retention on it has been found to be not particularly strong when high concentrations of complexing anions (e.g., fluoride, phosphate, or oxalate) are present in the sample.[4] This poses a significant problem in attempts to isolate actinides from soil samples, as hydrofluoric acid is generally added to dissolve any silica present. In addition, americium retention on the TRU•resin, while better than that seen with many previous

© 2000 Society of Chemical Industry

EXC materials, has been found to be inadequate for certain applications, e.g., large volume natural water samples, where acidification of the sample to ≥ 1 M nitric acid is not feasible.

Earlier work in this laboratory on the design of improved water-soluble complexants for use as masking or stripping agents has led to the development of a series of substituted methanediphosphonic acid derivatives capable of forming highly stable complexes in acidic media with a variety of metal ions in the tri-, tetra- and hexavalent oxidation states.[5] It has since been shown that by replacing two of the four hydrogen atoms with an alkyl group, lipophilic dialkyl-substituted diphosphonic acids can be prepared that are powerful actinide extractants from highly acidic solutions.[6] Recently, we have demonstrated that if an inert polymeric support is impregnated with one such compound, di-(2-ethylhexyl)methanediphosphonic acid (H_2DEH[MDP]), an extraction chromatographic resin (referred to hereafter as "Actinide Resin") capable of extremely strong retention of actinides is obtained.[7] In this report, we summarize our recent work with this material, and describe our preliminary investigations of a new configuration for EXC, the resin disc format, which promises to significantly improve sample throughput.

EXPERIMENTAL

The sources of all reagents and methods for the preparation and characterization of the EXC resins have been given previously.[7-9] Determination of the metal ion uptake properties of the EXC resins was performed as previously described.[7-9]

RESULTS AND DISCUSSION

Characterization of the Actinide Resin.

Figure 1A depicts the acid dependency of the uptake of several representative actinides from 0.01 to 10 M HCl, while Figure 1B presents analogous results for various non-actinide metal ions commonly encountered in analytical procedures involving environmental or bioassay samples. (Bi(III) and Ti(IV), for example, are common and troublesome constituents of fecal and soil samples.) As can be seen, retention of actinides by the resin is extraordinarily high, a result anticipated from prior studies of the extraction behavior of H_2DEH[MDP] in o-xylene.[6] Especially noteworthy is the strong retention of Am(III). Its k' values, in fact, exceed those of the other actinides up to 0.5 M HCl. Although k'_{Am} falls off rapidly at higher acidity, it nonetheless remains above 1000 over nearly the entire range of acidities examined. Of the non-actinides, Eu(III) and Fe(III) exhibit the highest k' values, as expected from the known affinity of the diphosphonic acid ligand for trivalent lanthanides and iron. (Note, however, that if Fe(III) is reduced to Fe(II), its k' values become much smaller.) The behavior of alkaline earth cations on the Dipex resin is consistent with the results of solvent extraction studies using o-xylene solutions of the extractant. Specifically, little selectivity is observed among the various alkaline earths.

The kinetics of metal ion uptake by the Actinide Resin are somewhat slower than those previously observed for U/TEVA or TRU resins, with the time required to achieve equilibrium uptake of a metal ion approaching 20 minutes (vs. 10 minutes for the U/TEVA or TRU resins). This is not unexpected given the greater viscosity of the H_2DEH[MDP] stationary phase. One aspect of the resin behavior that is not readily predictable from the properties of the extractant is that the experimental capacity for metal ion uptake is typically much smaller than that calculated on the basis of the metal:extractant stoichiometric ratios required for charge neutralization, a possible consequence of extractant aggregation, polymerization of the complex at high metal ion loadings, or slow diffusion of metal ions in the viscous extractant film. Note, however, that the capacity values are sufficiently high to permit efficient actinide uptake by the resin.

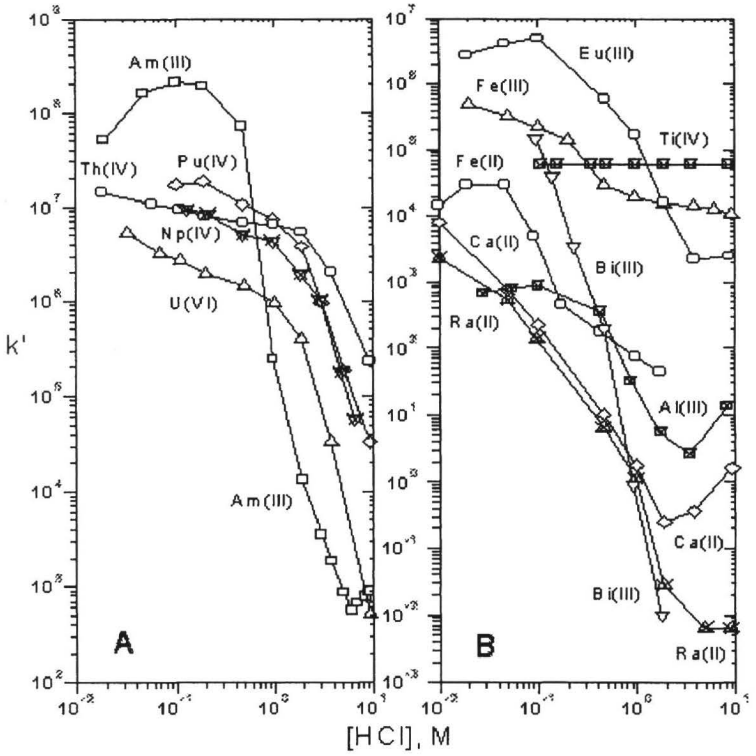


Figure 1. Hydrochloric acid dependency of k' for selected ions on the Actinide Resin.

Figure 2 shows the effect of HF on the retention of representative actinides in the tri-, tetra-, and hexavalent oxidation states on the Actinide Resin. Although the k' values for U(VI) and Np(IV) fall rapidly at the highest acid concentrations, up to ~2M HF can be tolerated without serious adverse impact on actinide retention. This is significant for two reasons. First, several potential interfering cations, among them Ti(IV), Zr(IV), and Al(III), form strong anionic fluoride complexes; as a result, their sorption on the actinide resin is significantly reduced (and thus, their intereference minimized) by addition of fluoride. In addition, these results, taken together with those of similar studies with other complexing anions (e.g., PO_4^{3-}) and common cations (e.g., Ca^{2+}), illustrate the relative insensitivity of actinide uptake to matrix composition, a property that considerably simplifies the application of the resin in the analysis of environmental and biological samples, and that represents a significant advantage of the Actinide Resin over previously described EXC materials.

Applications of the Actinide Resin.

Analysis of large-volume water samples.

The properties of the Actinide Resin that have been described here, in particular its extremely strong retention of actinides even in the presence of high concentrations of a variety of matrix constituents, make it well-suited to the preconcentration of actinides from soils or large-volume water samples for subsequent determination. In a simple experiment that nicely illustrates the potential usefulness of the resin in such applications, aliquots of acidified (HNO_3) river water were spiked with Am-241 and contacted with various amounts of the Actinide Resin in a batch mode. After a fixed time, the supernatant solution was counted to determine the extent of Am sorption by the resin. The results indicate that a single gram of the

resin can sorb Am quantitatively from as much as 3.5 L of water. Under the same conditions, approximately 90% recovery of tetra- and hexavalent actinides is observed.

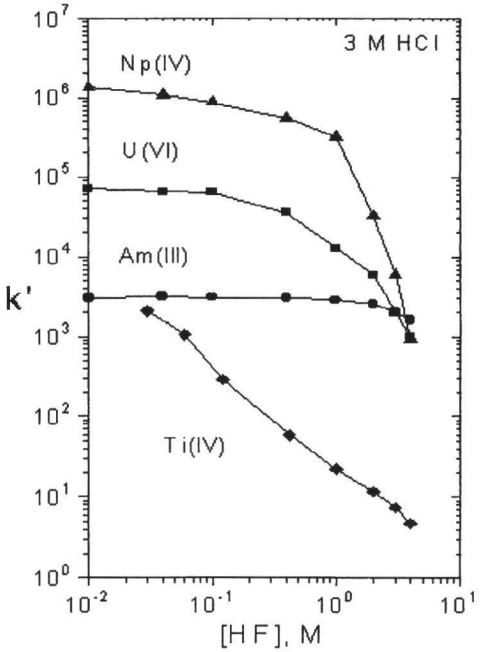


Figure 2. Effect of HF on the retention of selected metal ions on the Actinide Resin.

Soil analysis.

The Actinide Resin provides a means of simplifying complex sample matrices, thereby facilitating subsequent actinide determinations. For the determination of actinides in soils, for example, dissolution of the sample via NaOH fusion is followed by washing and dissolution of the iron hydroxide residue in HCl, removal or sequestration of the silica, and addition of ascorbic acid to reduce iron to the divalent state. At this point, the sample solution can be loaded onto a column of the Actinide Resin, where at 2 M HCl, actinides will be strongly sorbed. Following column rinsing to remove, for example, Ti(IV) and residual Si, the actinides can be eluted from the column with a small volume of isopropanol. This treatment, which also removes the stationary phase (i.e., extractant) from the resin, yields a small quantity of actinide-DPA complexes, which must be oxidized to convert the actinides to a form suitable for chemical separations. The oxidation product of this extractant is phosphoric acid, which upon addition of Ca^{2+}, can be made to precipitate basic calcium phosphate. At this point, a complex soil matrix has been converted to a much simpler form ($CaHPO_4$), thereby making subsequent separation schemes simpler and more predictable. A scheme consisting of columns of the U/TEVA and TRU resins operated in tandem have, for example, been shown to provide an effective method for the isolation of U and Th (U/TEVA•resin) or Am and Pu (TRU•resin) for subsequent quantitation.

Gross alpha activity.

One of the most frequently requested radioanalytical analyses in environmental monitoring involves the determination of "gross alpha" activity. In standard protocols for this analysis,[10] aqueous samples are evaporated onto a stainless steel planchet followed by counting in a gas flow proportional counter (GPC) after a prescribed period. This method suffers from a number of limitations, among them low counting efficiency, long counting times, large counting errors, and self-absorption problems (making coprecipitation necessary for radionuclide isolation from samples containing high levels of solids). These problems can be

avoided by taking advantage of the nearly quantitative sorption of actinides and the very high (~80%) sorption of Ra-226 from acidified (pH 2) water samples. Specificially, the water sample is reacted in a batch mode with the Actinide Resin, after which the sample is filtered and the collected resin transferred to a scintillation vial containing liquid scintillation (LS) cocktail. The cocktail dissolves the extractant (and radionuclide-extractant complexes) from the support, leaving the inert, translucent beads at the bottom of the vial. Samples are then counted on an LS counter. Application of this technique to the analysis of ten natural water samples has demonstrated that it yields results that agree well with those obtained by the conventional GPC method. At the same time, counting efficiency, precision, sample throughput, and detection limits are significantly improved. Average recoveries from groundwater simulants range from 76.2% for Th-232 to 95.9% for U-234/238.[11]

Disc-format EXC.

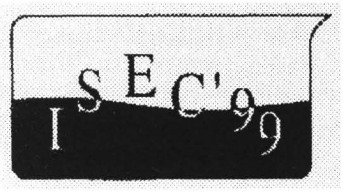
For the determination of the concentration of individual actinides in various samples, tandem EXC column arrangements, in which the effluent from one column becomes the influent for another (e.g., an Actinide Resin column followed by U/TEVA and TRU columns) have been suggested.[9,12] Passing large volume samples through multiple EXC columns, however, can be time-consuming. For this reason, there has been considerable recent interest in the development of new physical configurations for EXC by which the speed of a separation might be increased. Recently, an EXC resin consisting of Aliquat 336™ sorbed on silica has been incorporated into a glass fiber filter to yield an EXC disc.[13] This "TEVA (for tetravalent actinide specific) Disc" can be positioned in a standard filtering funnel and the sample solution passed through it without applied pressure. Following appropriate rinsing, sorbed radionuclides (e.g., Tc-99) can be counted. This format has been found to permit flow rates of up to ~33 mL/min; thus, a 1 L water sample requires only 30 minutes for treatment. In tests of the TEVA Disc in the determination of Tc-99 in groundwater simulants, recoveries averaging 95.9% have been obtained. Higher volume samples (3-6 L) yield slightly lower recoveries (85-90%), but provide improved limits of detection (0.30 pCi/L for a 6 L sample). These results compare favorably with those of traditional TBP extraction methods, and suggest that the disc format offers many possibilities for the improvement of EXC methods.

ACKNOWLEDGEMENTS

This work was performed under the auspisces of the Office of Basic Energy Sciences, U.S. Department of Energy, under Contract No. W-31-109-ENG-38.

REFERENCES

1. Braun T and Ghersini G, *"Extraction Chromatography"*, Elsevier, New York, 1975.
2. Siekierski S and Kotlinska B, *At. Energiya* **7**, 160, (1959).
3. Dietz ML, Horwitz EP, Chiarizia R and Diamond H in *"Solvent Extraction in the Process Industries"*, eds. Logsdail DH and Slater MJ, Elsevier, London, **3**, 1805, (1993).
4. Horwitz EP, Chiarizia R, Dietz ML, Diamond H and Nelson DM, *Anal. Chim. Acta* **281**, 361, (1993).
5. Horwitz EP, Diamond H, Gatrone RC, Nash KL and Rickert PG in *"Solvent Extraction 1990"*, ed Sekine T, Elsevier, New York, 357, (1992).
6. Chiarizia R, Horwitz EP, Rickert PG,and Herlinger AW, *Solv. Extr. Ion Exch.* **14**, 773, (1996).
7. Horwitz EP, Chiarizia R and Dietz ML, *React. Funct. Polym.* **33**, 25, (1997).
8. Burnett WC, Corbett DR, Schultz M, Horwitz EP, Chiarizia R, Dietz M, Thakkar A and Fern M, J. *Radioanal. Nucl. Chem.* **226**, 121, (1997).
9. Horwitz EP, Dietz ML, Nelson DM, LaRosa JJ, and Fairman WD, *Anal. Chim. Acta* **238**, 263, (1990).
10. Franson MAH, ed., *"Standard Methods for the Examination of Water and Wastewater"*, 15th ed., American Public Health Association, Washington, DC, 1981.
11. Analytical Procedure ACW11, EIChroM Industries, Inc., Oct. 1996.
12. Horwitz EP, Dietz ML, Chiarizia R, Diamond H,. Maxwell III SL and Nelson MR, *Anal. Chim. Acta* **310**, 63, (1995).
13. Analytical Procedure TCW02, EiChroM Industries Inc., May 1998.



ION-PAIRED EXTRACTION OF COPPER INTO CHLOROFORM AND ITS APPLICATION IN PRACTICAL ANALYSES

Isao Kojima, Mamoru Ito and Tomoyuki Mizuno
Laboratory of Analytical Chemistry, Department of Applied Chemistry, Nagoya Institute of Technology, Gokiso-cho, Showa-ku, Nagoya 466-8555, Japan

ABSTRACT
Inorganic and organic univalent anions were tested as a counter anion for the ion-paired extraction of cationic copper-3,6-dithiaoctane complex into chloroform. Of these 15 anions studied here, bromothymol blue, bromocresol green, picric acid, ethylorange, cobalt(III)-dihydroxy-azobenzene and -5-Br-PAPS complexes were found to be very effective anions for the extraction of ternary copper complex. For the determination of copper with one-drop flame atomic absorption spectrometry using 50 uL volume of the chloroform extract, 6 anions were very effective and only 2 anions were effective with spectrophotometry. The present method was well applied to the determination of copper in three geological standard rocks from Geological Survey of Japan (GSJ) and United States Geological Survey (USGS).

Keywords: Copper(I), ion-pair extraction, 3,6-dithiaoctane, flame AAS, geological standard rocks

INTRODUCTION

Many organic reagents for the extraction-separation and/or the spectrophotometric determination of copper have been reported.[1] Recently, many cyclic and acyclic organic reagents containing sulfur atoms as a coordinating atom were also used for the selective extraction and highly effective ion-selective electrode membranes of softer metal ions, like silver(I), copper(I) and mercury.[2-4] These reagents react with these softer metal ions to make a cationic complex and the cationic complex formed is selectively extracted into organic solvents in the presence of a univalent counter anion. In previous papers, we studied the selective extraction of the ternary silver complex into a small volume of chloroform in the presence of picrate or perchlorate anion and applied to the determination of silver in the practical samples.[5,6]

This paper deals with the extraction of the ternary copper(I) complex with 3,6-dithiaoctane into chloroform in the presence of 15 kinds of univalent anion and the possibility for the determination of copper by the one-drop flame atomic absorption specrometry and spectrophotometry.

EXPERIMENTAL

Apparatus

An atomic absorption spectrometer equipped with a 100 mm burner head and deuterium background corrector (Seiko Model SAS-727) was used for copper measurements with a one-drop technique using a fuel-lean air-acetylene flame under the optimum operating conditions: flow-rate of acetylene, 3.5 L/min (49 kPa); flow-rate of air, 17 L/min (245 kPa); observation height, 13.5 mm above the burner head and wavelength for copper, 324.8 nm.[7] The sample solution of 50 μL was injected with a micropipette (Gilson P-200) into the PTFE funnel coupled directly to the nebulizer needle. Signal intensity was recorded on a strip-chart recorder (Nippon Denshi Kagaku, Unicorder U-228). The pH of the aqueous solutions was measured with a Radiometer Type PHM-22 pH meter (Copenhagen Denmark) with a combined electrode. The spectrophotometric measurements were carried out on a Shimadzu UV-2100 recording spectrophotometer using 10 mm silica cell with the sample volume of 650 μL.

Chemicals

Copper stock solution, 2 mg/g in 0.5 mol/dm^3 nitric acid was prepared by dissolving copper metal of 99.999 % purity (Mitsuwa Chemicals, Osaka) in nitric acid directly in a PTFE bottle of 120 cm^3 capacity,

© 2000 Society of Chemical Industry

followed by dilution by mass with water. Working standard copper solutions of chloroform extract were prepared by extracting the copper-APDC complex or ternary copper complex into chloroform. Chloroform of analytical reagent grade was used without further purification. Commercially available 3,6-dithiaoctane (8-2S, Wako Chemicals, Osaka) of analytical reagent grade was used by dissolving in chloroform (0.05 mol/dm^3). Aqueous ammonium pyrrolidin-1-yldithio-carbamate (APDC, Nacalai Tesque, Osaka) solution (1 %) was prepared by dissolving in water. To test the percentage extraction of copper, working chloroform solutions containing Cu-APDC complex were prepared by extracting the mixed solution containing 1 cm^3 of copper (1 μg), 0.5 cm^3 of 1 % APDC solution and 3.5 cm^3 of water with 1 cm^3 of chloroform. The anion-forming substances (Fig. 1) were dissolved in water or in a appropriate volume of 0.1 mol/dm^3 sodium hydroxide solution. The acids, sodium acetate and disodium hydrogen phosphate of analytical reagent grade (Wako Chemicals, Osaka) were used to control the extraction pH. De-ionized Milli-Q water was used throughout.

Procedure

Into a 10 cm^3 stoppered glass test-tube were placed 1 cm^3 of sample solution (weighed), 0.5 cm^3 of 0.2 mol/dm^3 sodium acetate, 0.5 cm^3 of anion solution, 3 cm^3 of water and 0.5 (or 1.0) cm^3 of 8-2S chloroform solution (weighed). After shaking for 10 seconds (three times) by hand, the phase separation was carried out by centrifuging at 3000 rpm. An aliquot of the chloroform extract was used for copper measurements.

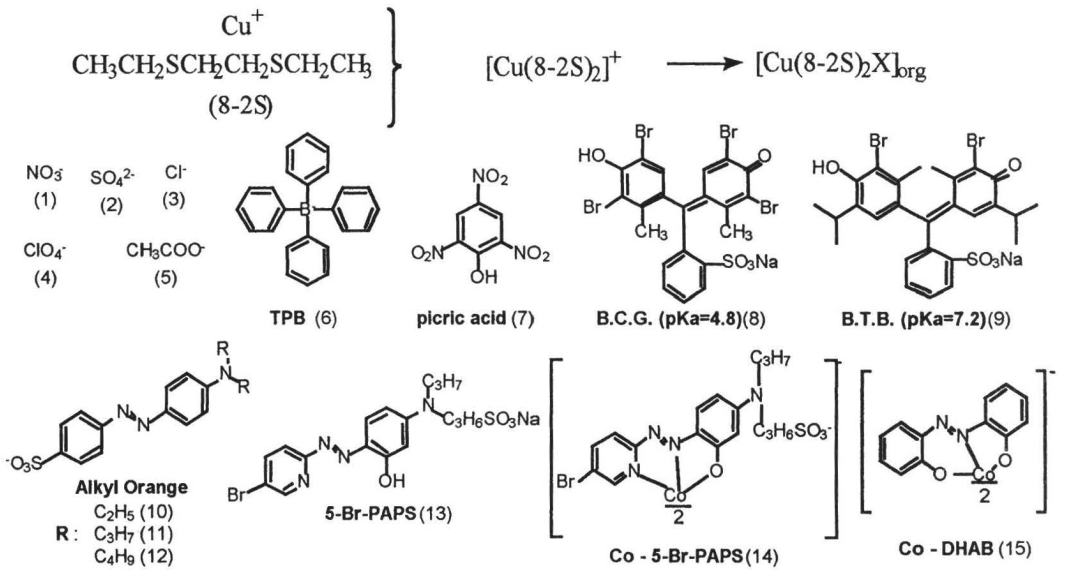


Figure 1 3,6-Dithiaoctane (8-2S) and counter anions used

Calibration Graph

To a 10 cm^3 stoppered glass test-tube were added, aliquots (0 - 1.0 cm^3, weighed) of a standard aqueous copper solution, 0.5 cm^3 of anion solution, 1 cm^3 of buffer solution and 3.5-2.5 cm^3 of water. After shaking for 10 s (three times) by hand with 0.5-1.0 cm^3 (weighed) of 8-2S chloroform solution, the test-tube was centrifuged at 3000 rpm. A 50 μL of the chloroform extracts are directly nebulized into the flame for AAS measurement and 650 μL was used for spectrophotometry.

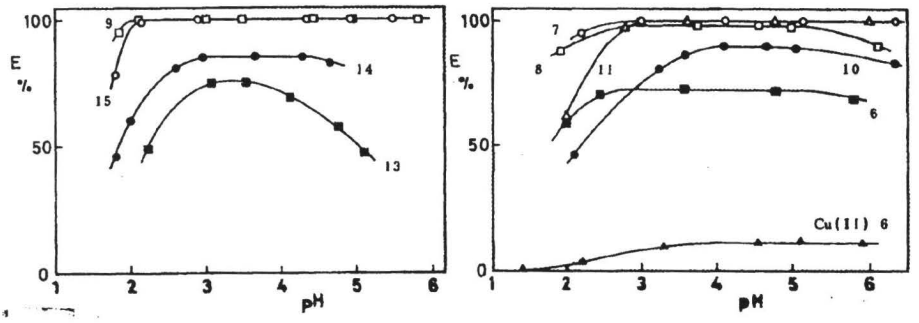
Sample Composition

A sample of 200 mg was taken in a PTFE vessel of 15 cm^3 capacity with 4 cm^3 of nitric acid and 4 cm^3 of hydrofluoric acid. After sealing by hand, the vessel was stood overnight at room temperature and then evaporated to dryness on a hot-plate and again with 2 cm^3 of nitric acid. Finally the residue was dissolved in 10 cm^3 of 0.02 mol/dm^3 perchloric acid and the mass of sample solution was weighed. An aliquot of the solution thus prepared was used for the determination of copper.

RESULTS AND DISCUSSION

Extraction behaviour of copper with 8-2S

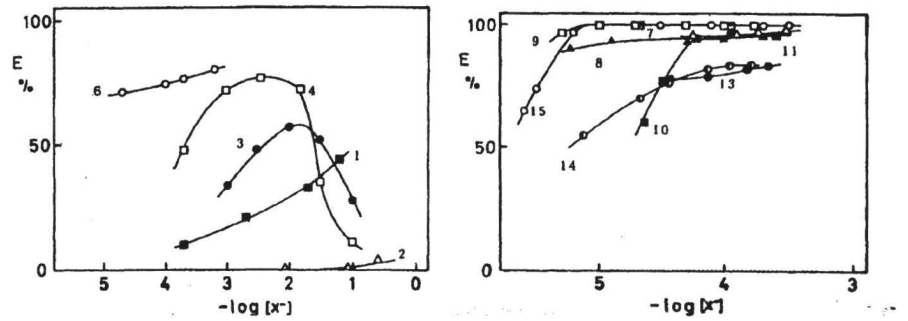
The extraction behavior of copper from the aqueous solution, in the presence of each anion, into 0.05 mol/dm^3 chloroform solution of 8-2S was examined in the pH range < 7. Percent extraction of copper (I) against the aqueous pH is shown in Figures 2 and 3. Rather good and steady extraction greater than 85 % was obtained in the presence of picrate (100 %, pH 3-6), BCG (95 %, pH3-4.5), BTB (100 %, pH 2-7), Co-5-Br-PAPS (85 %, pH 3-4.5), Co-DHAB (100 %, pH 3-4.5), EO (90 %, pH 4-5), PO (95 %, pH 3-6), BO (98 %, pH 3-6, omitted in Figure 3 for simplicity) and TPB (70 %, pH 3-5). For 5-Br-PAPS, percent extraction was poor (70 %) and the pH range was very narrow (pH 3-3.5). An increase in the carbon number in alkylorange gave a good extractability, as is expected from the regular solution theory but phase separation was getting worse. And also, about 20 % of copper (II) was extracted in the presence of TPB. The reason why this occurs comes from the reduction of copper (II) to (I) with TPB.



Figures 2 & 3 Effect of pH on the extraction of copper (Numbers are given in Figure 1)

Effect of anion concentration on extraction of copper

The extraction of the ternary copper complex depends on the kind of anion and their concentration. The relationships between the percent extraction of copper and anion concentration are shown in Figures 4 and 5. These data were obtained by keeping the extraction pH of aqueous solution constant, i.e., around 4.3, except for the inorganic anions. As is evident from the figures, the constant and larger percentage extraction was obtained with organic anions but extraction with inorganic anions was very poor. With organic anion concentration of (4-20) x 10^{-5} mol/dm^3, the steady and good extraction was attained at pH around 4-4.5. Picrate, BTB and Co-DHAB are good extracting anions for copper. The molar ratio method showed that the anion number incorporated in the extracted species was one in the case of BTB and Co-DHAB.



Figures 4 & 5 Effect of anion concentration on the percent extraction of copper (Numbers are given in Figure 1).

Absorption spectra of ternary copper complexes

The absorption spectra of the ternary copper complexes extracted with the colored anions are shown in Figure 6 and their characteristics in chloroform extracts are given in Table 1, with the analytical working range of copper by flame AAS and spectrophotometry. The working range by AAS is the same irrespective of the anions used, while by spectrophotometry it depends on the molar absorptivity of the complex, i.e., anion. Judging from the molar absorptivity, the Co-5-Br-PAPS seems to be a sensitive anion for determining copper but the extractability is not very good and is affected by the presence of the coexisting other anion. The Co-DHAB complex seems to be a good anion but owing to the extraction of the Co-DHAB complex without a counter anion at pH less than 3, this is not suitable for the spectrophotometry of copper. Of these colored anions used here, ethylorange seems to be a most sensitive but the phase separation was very bad. At the moment, we do not know why a higher molar absorptivity of the ternary copper complex with ethylorange as a counter anion is obtained. The details on this phenomenon will be described elsewhere after more detailed experiments.

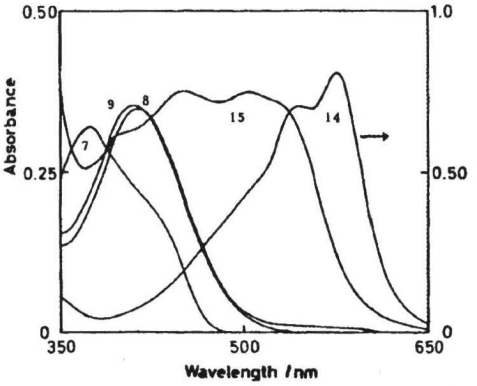


Figure 6 Absorption spectra of ternary copper complexes in chloroform
Cu : 1 μg/cm^3 in chloroform ; 8-2S : 0.05 mol/dm^3
Anion : (4-10) x 10^{-5} mol/dm^3 in aqueous solution
(Numbers are given in Table 1)

Table 1 Characteristics of The Ternary Copper Complexes in Chloroform

Anion	Extraction		10^5x[X^-]	max	10^4	Working range
	pH range	%	mol/dm^3	nm		μg/g in $CHCL_3$
						AAS SP
Picrate	3 - 6	100	10	370	1.9	0 - 2 0 - 2
BCG	3 - 4.5	95	10	416	2.6	0 - 2 0 - 2
BTB	2 - 7	100	5	411	2.6	0 - 2 0 - 2
Co-5-Br-PAPS	3 - 4.5	85	4	580	7.4	0 - 2 0 - 1
Co-DHAB	3 - 4.5	100	8	485	2.5	0 - 2 0 - 2
EO	4 - 6	90	30	430	14.5	0 - 2 0 - 0.5
PO	3.6	95	4	420	--	0 - 2 --

Vaq : Vorg = 5 mL : 1 mL

Determination of copper in standard geological samples

The currrent method was applied to the determination of copper in standard rock samples from Geological Survey of Japan and United State Geological Survey by FAAS and spectrophotometry. The results obtained by both methods are shown in Table 2. The results obtained with BTB and BCG by both methods were acceptable but those using Co-DHAB and picrate as anions by spectophotometry were very bad. One reason of this phenomenon comes from coloration of the extract without 8-2S. The reason why this occurs is not known at the moment.

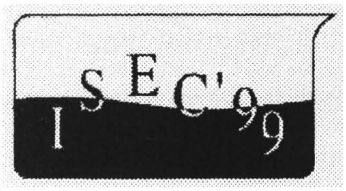
Finally, the spectrophotometric determination of copper by the present method was strongly affected in the presence of silver and mercury. However, the determination of copper in practical samples could be carried out without problem, because the content of these two metals in samples selected is very low, comparing with the content of copper.

Table 2 Analytical Results for Copper in Standard Rock Samples

Anion	Content/ μg/g						
	GSJ-JA-1		GSJ-JB-1		USGS-GSP-1		n
	AAS	SP	AAS	SP	AAS	SP	
BTB	41	42	53	54	30	30	5
BCG	41	42	52	53	30	29	5
Co-DHAB	41	70	52	76	--	--	4
Picrate	41	51	52	67	--	--	4
Certified [8]	41.7		56.3		33		

REFERENCES

1. Ohnishi H, "Photometric Determination of Traces of Metals", John Wiley & Sons, 3, Part IIA, (1986).
2. Saito K, Murakami S, Muromatsu A and Sekido E, *Anal. Chim. Acta*, **237**, 245, (1990) and papers cited therein
3. Heitzsh O, Gloe K, Stephan H and Weber E, *Solv. Extn. and Ion Exch.*, **12**, 475, (1994).
4. Oue M, Kimura K, Akama K, Tanaka M and Shono T, *Chem. Lett.*, 409, (1988).
5. Kojima I and Takayanagi A, *J. Anal. At. Spectrom.*, **11**, 607, (1996).
6. Kojima I and Katsuzaki M, *Anal. Sci.*, **13**, 1021, (1997).
7. Kojima I, Inagaki K and Kondo S, *J. Anal. At. Spectrom.*, **9**, 1161, (1994).
8. Gladney ES, O'Malley BT, Roelandts I and Gills TE, "*Compilation of Elemental Concentration Data for NBS Clinical, Biological, Geological and Environmental Standard Reference Materials*", NBS Special Publication 260-111, (1987)



DETERMINATION OF ARSENIC IN BIOLOGICAL MATRICES BY ANODIC STRIPPING VOLTAMMETRY COUPLED WITH A TWO-STEP EXTRACTION PROCESS

Jem-Mau Lo[1], Jun-Der Lee[1], and Chi-Ming Tseng[2]
[1]Department of Nuclear Science, National Tsing Hua University, Hsinchu 300, Taiwan, China
[2]Department of Chemistry, National Chung Hsin University, Taichung 400, Taiwan, China

ABSTRACT
A novel method employed for determining trace arsenic in biological samples was developed in the study. The arsenic rendered as the form of As(III) ion was pre-concentrated from the digested biological samples through means of tetramethylene dithiocarbamate extraction in conjunction with Au^{3+} back extraction. The pre-concentrated solution, which contained the enriched arsenic ion with the possible transition metal ions and non-reacted Au^{3+}, was next transferred to an electrochemical cell for detecting arsenic via differential pulse anodic stripping voltammetry (DPASV) through the usage of a gold film carbon electrode. Au^{3+} was selected as a back-extracting agent in light of its standing as of highest extraction constant with tetramethylene dithiocarbamate, being much greater than that of As(V). Besides, the excess non-reacted Au^{3+} in the pre-concentrated solution could be used in situ as the source of generating the gold film of the working electrode in the DPASV. Reliability and accuracy of this method were confirmed from the NBS biological standard reference material analyses.

Keywords: analysis, arsenic, tetramethylene dithiocarbamate, voltammetry

INTRODUCTION

Detection of arsenic in environmental and biological samples in the nanogram to subnanogram range needs sensitive analytical methods. Hydride generation atomic absorption spectrometry[1-6] and neutron activation analysis [7-13] have long been recognized to be most suitable for the purpose. In addition, electrochemical techniques have recently been developed in advanced instrumentation complying with its inherent sensitivity in arsenic determinations. The use of anodic stripping voltammetry (ASV) to determine very low concentrations of arsenic has been reported.[14] Differential pulse anodic stripping voltammetry (DPASV) achieves considerable improvements in sensitivity and accuracy for arsenic detection.[15-23] Pretreatment of the sample is generally required for the electrochemical methods for the dual purposes of conditioning the sample solution for electrochemical analysis as well as removing the matrix interferences. The present paper is a report on the determination of arsenic by DPASV. The previously reported method employed for determining mercury in water and biological samples by DPASV was simulated.[24] The arsenic was pre-concentrated from the digested biological samples by a two-step extraction process. The pre-concentration procedure was coupled with DPASV where an *in situ* gold film carbon electrode was employed as the working electrode. The optimal conditions for the two-step extraction / DPASV for sensitive arsenic detection were investigated.

EXPERIMENTAL

Reagents and Samples

Stock solutions (100mg/dm^3) of arsenic(III) and arsenic(V) were prepared by dissolving reagent grade As_2O_3 and Na_3AsO_4 in deionized water with the required amount of NaOH then acidifying with HCl. Standard solutions were prepared from the stock solutions by appropriate dilution with deionized water and by certain pH adjustment. Ammonium tetramethylene dithiocarbamate (APDC), 1g, of analytical reagent grade (E. Merck Co.) was dissolved in 100 cm^3 of deionized water, stirred well, and

© 2000 Society of Chemical Industry

then shaken twice with 10 cm^3 of chloroform. The organic phase was discarded, removing any possible impurity of the metals, As, Hg, Zn, Cd, Pb, Cu, etc., already present in the reagent. This aqueous phase is referred to as the purified extracting agent used in the work. Gold metal (99.99%) was purchased from Koch-Light Co, Colnbrook, England. An appropriate amount of the gold metal was weighed and dissolved in *aqua regia*. The solution was repeatedly evaporated on a water bath to near dryness to remove hydrochloric acid (adding water to avoid drying out). This solution was finally diluted with pure water and adjusted to pH 0.63 with 65% HNO_3. A 300 mg/dm^3 Au(III) solution was prepared as the back-extraction reagent with a pH adjustment before use. The standard reference materials were purchased from the National Bureau of Standards of U.S.A. including Citrus Leaves (SRM1572), Tomato Leaves (SRM1573) and Pine Needles (SRM1575). The biological materials were digested in a microwave digester (MDS – 81 D, CEM Co.). The samples were weighed, 0.5g, and placed in a 120 cm^3 Teflon PFA bottle in which 10mL concentrated HNO_3 and 5 cm^3 concentrated HCl had been placed. Immersion of the samples in the strong acids was maintained for at least 1 hour. Thereafter the microwave digestion was conducted by adjusting the power to 50% and maintaining for 8 minutes, which was followed by 100% power for 4 minutes. The digested solution was then cooled to ambient temperature. Finally the solutions were filtered by filter paper and adjusted to the required pH.

Two-Step Extraction Process

The digested biological samples adjusted to pH 4 by 1.0 mol/dm^3 NaOH was placed in a 250 cm^3 Pyrex separatory funnels. 25% $Na_2S_2O_3$, 2 cm^3 was added to reduce any As(V) in the samples to the As(III) ion. 12% Na_2EDTA, 2 cm^3 was subsequently added as the masking agent to complex with the metallic ions, e.g., Cu^{2+}, in the samples by vigorously shaking for 20 minutes. A 4 cm^3 portion of the purified extracting agent was then added. Precisely 20 cm^3 of chloroform was added into the funnels and the mixture was shaken vigorously by an up-and-down motion shaking machine for 20 minutes. After a 5 minute wait to allow the phases to separate, the organic phase was transferred to a flask. The organic solution was washed with 10 cm^3 0.02 mol/dm^3 NaOH by shaking for 10 minutes to remove excess retained HPDC. Five milliliters of a 300 mg/dm^3 Au^{3+} solution was then added for back extraction. The separated aqueous phase was adjusted to the required pH and added with 0.20 cm^3 6.0 mol/dm^3 HCl. This finally accumulated to 10 cm^3 with the deionized water. The solution was immediately transferred to the electrochemical cell for DPASV.

Differential Pulse Anodic Stripping Voltammetry (DPASV)

Voltammetric measurement was taken in an electrochemical cell, i.e., a 20 cm^3 covered beaker with the three electrodes (i.e., working, reference, and auxiliary) being immersed in the electrolyte solution. A glassy carbon electrode was employed as the working electrode and a silver/silver chloride electrode as the reference electrode. The auxiliary electrode consisted of a platinum wire which was well separated from the analyte solution by a porous Vycor frit inserted into a piece of glass tube. The tube was filled with 0.1 mol/dm^3 $N_2H_4 \cdot 2HCl$. The three electrodes, as well as the tube used for N_2 purging, were inserted through the four holes via an O-ring on the cell cover. The multipurpose microprocessor-based voltammetric analyzer used was purchased from Bioanalytical Systems, Inc. (Model BAS-100B).

The pre-concentrated solution mentioned above was purged with N_2 and stirred for at least 5 minutes prior to analysis by DPASV. The glassy carbon electrode was polished with a very fine paper (wet and dry), alumina, and finally diamond paste before use. Analysis of As(III) in the pre-concentrated solution was started by electrochemical formation of a gold film on the glassy carbon electrode by applying a deposition potential at –600 mV for 150 seconds. Simultaneously, the As(III) ion was reduced to form As^0 on the gold film during the deposition step. After deposition was terminated, the solution was purged with N_2 to drive off any bubbles adhered on the gold film, and the arsenic was then stripped from the gold film back into the solution. Differential pulse anodic stripping voltammery was employed for the measurement of the arsenic under the following conditions : stripping potential from -600 to 400 mV, scan rate 20 mV/s, pulse amplitude 17 mV, sample width 50

ms, pulse width 50 mV, pulse period 200 ms, and stirring rate 20 rpm. The arsenic was identified by the stripping potential at 60mV and quantified by the corresponding oxidation peak current.

RESULTS AND DISCUSSION

The electrolytic solution for DPASV was controlled at 0.12 mol/dm^3 HCl containing 60-150 mg/dm^3 Au(III). A suitable concentration of Au(III) was required to generate in situ an ideal gold film on glassy carbon electrode working for the arsenic analysis. The relationship of anodic stripping peak current of arsenic with the concentration of Au(III) is shown in Figure 1. Sufficient concentration of Au(III), i.e., 330 mg/dm^3, was required to form an uniform gold film working out a maximal arsenic stripping peak. In practical analytical work, 10 cm^3 of 60~150 mg/dm^3 Au(III) was used as the back extracting solution, which would be supra-stoichiometric and even much higher than the arsenic transferred from the sample and present as the As(PDC)$_3$ complex in the organic phase. Free PDC might be present in a considerable amount in the organic solution which would consume an appreciable quantity of Au(III) by formation of Au(PDC)$_3$. This problem, however, had been circumvented by eliminating the free PDC in the organic solution with 0.02 mol/dm^3 NaOH. Therefore only a small fraction of Au(III) was lost and the remaining Au(III) in the pre-concentrated solution would match the required concentration range for DPASV as elucidated above. A clear and sharp oxidation peak of arsenic could usually be obtained under the electrolyte 0.12 mol/dm^3 HCl as shown in a typical voltammogram in Figure 2.

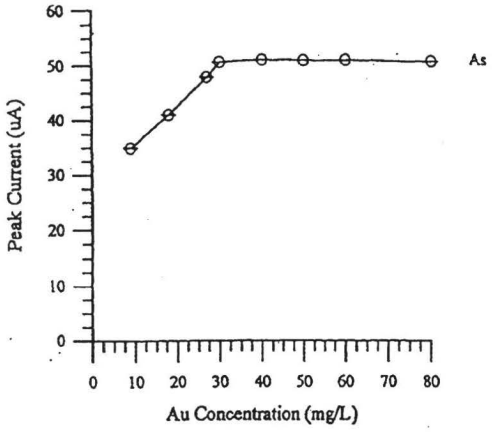


Figure 1. Relationship between peak current of arsenic and Au(III) concentration

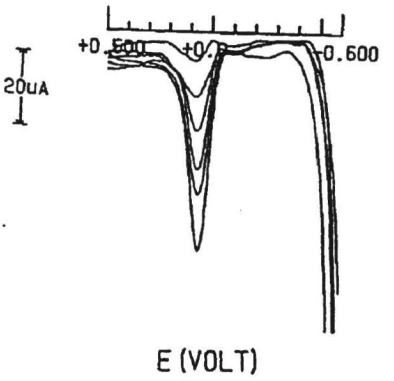


Figure 2. DPASV voltammograms of increasing concentration (from 5 to 50 μg/dm^3)

It should be noted that Pt auxiliary electrode used was designed to be well separated from the analyte solution by a porous Vycor frit inserted into a piece of glass tubing. The counter electrode compartment was filled with aqueous 0.1 mol/dm^3 N_2H_4·2HCl. This additional set-up for the Pt auxiliary electrode was found to be necessary in the analysis of As(III) in media of Cl^- content such as 0.12 mol/dm^3 HCl. Without the separation, the stripping peak would gradually decrease in magnitude through a series of replicate DPASV measurements, possibly due to the oxidation of As(III) analyte to electro-inactive As(V) by Cl_2 which was generated at the counter electrode in the deposition stage. The As(III) → As(V) oxidation process should have been terminated in the above mentioned proposed design in light of elimination of Cl_2 by N_2H_4·2HCl. The stripping peak of arsenic was thus found to become very stable. The relationship between the stripping peak current of arsenic and the deposition

time is illustrated in Figure 3. The result was obtained in the DPASV of As(III) in 0.12 mol/dm^3 HCl containing 60.00 mg/dm^3 Au(III). Increases in deposition time could produce corresponding increases in peak current for electrolysis periods ranging from 60 seconds up to at least 210 seconds. A stripping peak in all of these periods of deposition time appeared only at 60 mV. The deposition time period during practical analytical procedure was chosen at 150 seconds, i.e., sufficient enough for generating a prominent peak current.

The deposition potential was set at -600 mV and the deposition time was at 150 seconds. The same family of metals as As include Sb and Bi in their trivalent oxidation states which may be the major interferences in the determination of As(III) by DPASV. The oxidation potentials of Sb(III) and Bi(III) were found at 70 mV and 200 mV respectively under the electrolyte, 0.12 mol/dm^3 HCl and with the deposition potential, -600 mV. Both may cause interference with the arsenic detection due to the superimposition or overlapping of oxidation potentials. Hamilton et al.[22] reported that the interference of Sb and Bi could be technically estimated and deducted. Allowing the DPASV to be carried out with the deposition potential at -100 mV instead of -600 mV, the stripping peaks of Sb and Bi will remain on the voltammogram while arsenic does not appear. Therefore the magnitudes of Sb and Bi peaks can be estimated and their contributions to the As peak deducted when -600 mV is used for the DPASV for arsenic detection. Aside from Sb(III) and Bi(III), Cu^{2+} might also be considered to interfere with the arsenic analysis according to the literature.[16,20,23,25,26] However, this is not a problem in the present study employing the *in situ* gold film carbon electrode and running under 0.12 mol/dm^3 HCl. The oxidation potential of Cu was found at 300 mV which was far from that of As at 60 mV.

A calibration method was used for the quantitative measurement of arsenic in the pre-concentrated solution by DPASV. The calibration of arsenic in the electrolyte of 0.12 M HCl containing 150 mg/dm^3 Au(III) with a deposition of 150 seconds at –600 mV is indicated in Figure 4. A strictly linear relationship is maintained between the peak current and the arsenic concentration over the range from 0.01 μg/dm^3 to at least 60.00 μg/^{3}. The correlation coefficient of linearity is 0.9989.

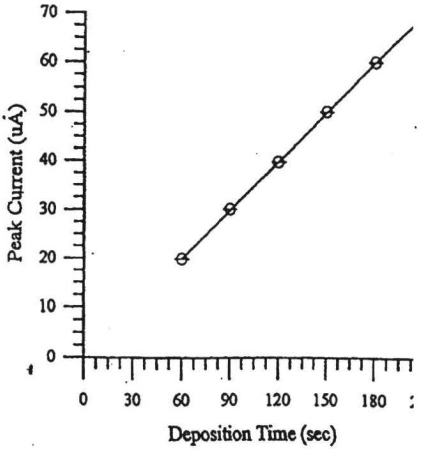


Figure 3. Relationship between peak current and deposition time

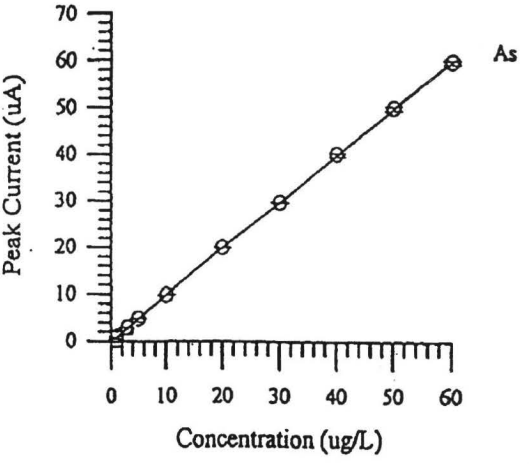


Figure 4. Calibration curve for DPASV of As(III)

Table 1 Analytical Results by the Proposed Method for Determining Arsenic in the Biological Samples of NBS Standard Reference Materials (SRM)

Biological Sample	Concentration of As (mg/kg)	
	Average and Standard Deviation	Certified
Cirtrus Leaves (SRM 1572)	3.22±0.05	3.1±0.3
Tomato Leaves (SRM 1573)	0.30±0.02	0.27±0.05
Pine Needles (SRM 1575)	0.21±0.04	0.21±0.04
Bovine Liver (SRM 1577a)	0.051±0.003	0.047±0.006
Oyster Tissue (SRM 1566a)	14.32±0.16	14.0±1.2

The feasibility and reliability of the DPASV coupled with the two-step extraction in practical analysis of biological samples for arsenic were investigated as follows. The NBS standard biological samples including Citrus Leaves (SRM 1572), and Bovine Leaves (SRM 1573), Pine Needles (SRM 1575), and Bovine Leaves (SRM 1577a) were analyzed. All of the samples were microwave digested and run through the proposed pre-concentration procedure prior to DPASV. Voltammograms for the biological samples are all with clear arsenic peaks. The analytical results are listed in Table 1. The concentrations of As found in the various biological samples sufficiently correlate with the certified values (also indicated in Table 1). The reliability and accuracy of the proposed method was also confirmed in the biological analyses.

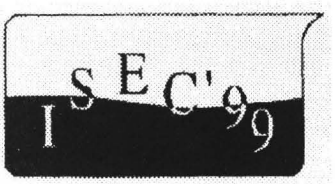
ACKNOWLEDGEMENTS

This work was supported by the National Science Council of R.O.C.(project NSC 87-2113-M-007-031).

REFERENCES

1. Heumann KG, Kastenmayer P and Zeiniiger H. *Fresenius Z. Anal. Chem.* **306**, 173-177, (1981).
2. Douglas DJ and French JB. *Anal. Chem.* **53**, 37-41, (1981).
3. Maher WT. *Talanta*, **1978** ,311-316.
4. Terashima S. *Anal. Chem. Acta*, **86**, 43-51, (1976)
5. Fiorino JA, Jones JW and Caper SG. *Anal. Chem.* **48**, 120-125, (1976).
6. Stoeppler M, Burow M, Backhaus F, Schramm W and Nurnberg HW. *Marine Chem*, **18**, 321-334, (1986).
7. Mok WM, Shah NK and Wai CM. *Anal. Chem.* **58**, 110-113, (1986).
8. Mok WM and Wai CM. *Anal. Chem* **59**, 233-236, (1987).
9. Mok WM and Wai CM. *Talanta* **35**, 183-186, (1988).
10. Wu CY, Chen PY and Yang MHJ. *Radioanal. Nucl Chem-Articles* **112**, 133-140, (1987).
11. Milkinson RE and Hardcastle WS. *Weed Sci.* **17**, 536-537, (1969).
12. Golanski A. *J. Radioanal. Chem.* **3**, 161-173, (1969).
13. Gohda S. *Bull. Chem. Soc. Jpn.* **45**, 1704-1708, (1972).
14. Trushina LF and Kaplan AA. *Zh. Anal. Chem.* **25**, 1616, (1970).
15. Siergerman H and O'Dom G. *Amer. Lab.* **4**, 59, (1972).
16. Myers DJ and Osteryoung J. *Anal. Chem.* **45**, 267-271, (1973).
17. Forsberg G, O'Laughlin JW and Megargle RG. *Anal. Chem.* **47**, 1586-1592, (1975).
18. Bodewig FG, Valenta P and Nurnberg HW. *Fresenius Z. Anal. Chem.* **311**, 187-191,(1982).
19. Leug PC, Subramania KS and Meranger JC. *Talanta* **29**, 515-518, (1982).

20. Davis PH, Dulude GR, Griffin RM, Matson WR and Zink EW. *Anal. Chem.* **50**, 137-143, (1978).
21. Lee SW and Meranger JC. *Anal. Chem.*, **53**, 130-131, (1981).
22. Hamilton TW, Ellis J and Florence TM. *Anal. Chim. Acta.* **119**, 225-233, (1980).
23. Jagner D, Josefson M and Westerlund S. *Anal. Chem.*, **53**, 2144-2146, (1981).
24. Lo JM and Lee JD. *Anal. Chem.*, **66**, 1242-1248, (1994)
25. Sadana RS. *Anal.Chem.* **55**, 304-307, (1983).
26. Holak W. *Anal. Chem.* **52**, 2189-2192, (1980).



SOLVENT EXTRACTION SEPARATION STUDIES OF SOME METAL IONS WITH 2-ETHYLHEXYL PHOSPHONIC ACID MONO-2-ETHYLHEXYL ESTER

Sunita V Bandekar and PM Dhadke
Inorganic Chemistry Laboratory, Department of Chemical Technology, University of Mumbai, Matunga, Mumbai - 400 019, India.

ABSTRACT
PC-88A (2-ethylhexylphosphonic acid mono-2-ethylhexyl ester) has been effectively employed as a reagent for solvent extraction and separation of platinum(IV), palladium(II), rhodium(III), bismuth(III), tin(IV), antimony(III) and thallium(III) at trace level. Various parameters affecting the extraction of metals were studied systematically.
Rh was extracted from 1.0-2.0 M HCl while Sb and Tl were extracted from 0.1 mol/dm^3 HCl and 4.25 mol/dm^3 H_2SO_4 respectively. These metals were stripped out from the organic phase using different stripping agents and determined spectrophotometrically. The methods were further extended for the separation of the metal ions from the commonly associated metal ions. The proposed methods were applied for analysis of these metals in various real samples.

Keywords: 2-ethylhexylphosphonic acid mono-2-ethylhexyl ester, PC-88A, platinum, palladium, rhodium, bismuth, tin, antimony, thallium

INTRODUCTION

The introduction of commercial extractants has increased the interest in the use of various organophosphorus extractants in the hydrometallurgical metal processing. Since last decade, organophosphorus reagents have been extensively used for solvent extraction of various metal ions [1-3] and are found to have very good extractability and high separation efficiency of the metals. Monoesters of phosphonic acids have also been known to possess higher separation factors for chemically similar elements.[4]

The acidic organophosphorus extractant, PC-88A was used for the extraction of various rare earth metals,[5,6] transition and some of the main group metals [7] but not employed for the separation of noble metals like platinum, palladium and rhodium and main group metals like bismuth, antimony, tin, thallium. Many organophosphorus reagents have been reported for the extraction of noble metals and main group metals. The extraction of platinum group metals such as platinum, palladium, rhodium was carried out with triphenylphosphine (TPP) but heating of the aqueous phase prior to the extraction was required and these metals could not be separated from each other.[8] Bismuth(III) and antimony(III) were completely extracted with triphenylphosphine oxide (TPPO) but by multistep extraction.[9] Recently, tributyl phosphate (TBP) was used as an extractant for the recovery of tin(IV) from other associated metal ions. But the method was tedious due to multistep stripping with varying concentrations of hydrochloric acid.[10] Thallium(III) was extracted with trioctylphosphine oxide (TOPO) from chloride media but the method suffered from the drawback of coextraction of commonly associated metals.[11]

In the present study, PC-88A has been employed as an extractant for the separation of metals such as rhodium, antimony and thallium. The detailed study of extraction behaviour of these metals with PC-88A was carried out and on the basis of various results obtained they were separated from other commonly associated metals. Further, the validity of these methods was tested by determining the metal ions in various real samples.

© 2000 Society of Chemical Industry

EXPERIMENTAL

A digital pH meter (Elico Pvt. Ltd., India, model LI-120) was used to measure H^+ ion concentration and uv-visible spectrophotometer (GBC Scientific Equipments Pvt. Ltd., Australia, model GBC 911A) was used for absorbance measurements.

The extractant 2-ethylhexylphosphonic acid mono-2-ethylhexyl ester (PC-88A) kindly supplied by Daihachi Chemical Industries Ltd., Japan was used without further purification. The stock solutions of metal ions were prepared using AR grade salts and standardised.[12]

The aqueous phase (10 ml) containing metal ion was adjusted to required acidity/pH and transferred to a separating funnel. Then 10 ml of PC-88A in toluene was added to it, shaken for 5 min. and allowed the two phases to settle and separate. The metal ions from the organic phase were stripped out with stripping agents and determined by suitable spectrophotometric methods [13] (Table 1).

Table 1 Extraction of Metals with PC-88[a]

Metal Ion	Conc µg	Aqueous Phase	Reagent Conc. (mol/dm^3)	Stripping Agent	Spectrophotometric Reagent (λ_{max} nm)
Pt(IV)[14]	100	0.5-2.25 mol/dm^3 HCl, 4×10^{-3} mol/dm^3 $SnCl_2$	5.0×10^{-3}	4 mol/dm^3 HCl	Stannous chloride (403)
Pd(II)[14]	100	0.75-2.25 mol/dm^3 ($HCl+HClO_4$), 2.5×10^{-2} mol/dm^3 $SnCl_2$	6.0×10^{-4}	-	Direct spectro-photometry (486)
Rh(III)	200	1.0-2.0 mol/dm^3 HCl, 1×10^{-1} mol/dm^3 $SnCl_2$	2.0×10^{-2}	6 mol/dm^3 HCl	Stannous chloride (470)
Bi(III)[15]	150	0.1 mol/dm^3 NH_4NO_3 at pH = 1.5-2.75	6.0×10^{-3}	2 mol/dm^3 HNO_3	Thiourea (470)
Sn(IV)[16]	60	0.1-0.3 mol/dm^3 HCl	2.5×10^{-2}	4 mol/dm^3 HCl	Pyrocatechol violet (555), Morin (430)
Sb(III)	60	0.1 mol/dm^3 HCl	1.5×10^{-1}	8.5 mol/dm^3 H_2SO_4	Iodide (425)
Tl(III)	50	4.25 mol/dm^3 H_2SO_4	1.0×10^{-2}	0.1 mol/dm^3 H_2SO_4	PAR (530)

RESULTS AND DISCUSSION

The extraction of Rh(III) was carried out in the range of 1.0-5.0 mol/dm^3 HCl and was found to be quantitative with 1.0-2.0 mol/dm^3 HCl. The concentration of stannous chloride in the aqueous phase was varied from 0.004 - 0.4 mol/dm^3 and the minimum concentration of stannous chloride required for complete extraction was found to be 0.1 mol/dm^3. Rh(III) was extracted with varying concentration of PC-88A (5×10^{-4} - 5×10^{-2} mol/dm^3) and the optimum concentration required for quantitative extraction was 2×10^{-2} mol/dm^3.

The HCl concentration of the aqueous phase containing Sb(III) was varied from 0.05-2.0 mol/dm^3 and the extraction was found to be quantitative with 0.1 mol/dm^3 HCl. Sb(III) was extracted with varying concentrations of PC-88A ranging from 1×10^{-3} - 2×10^{-1} mol/dm^3 dissolved in toluene and the minimum concentration required for quantitative extraction was 1.5×10^{-1} mol/dm^3.

The extraction of Tl(III) was carried out with 1×10^{-2} mol/dm^3 PC-88A in toluene at different sulphuric acid concentrations ranging from 0.1-6.0 mol/dm^3 H_2SO_4. It was observed that with increase in sulphuric acid concentration the percentage extraction of Tl(III) increased and it was quantitative at

4.25 mol/dm^3 sulphuric acid but decreased thereafter with increase in acid concentration. The extraction of Tl(III) was studied for different concentrations of PC-88A in toluene ranging from 5×10^{-4}-1×10^{-1} mol/dm^3 and optimum concentration required was found to be 1×10^{-2} mol/dm^3 of PC-88A in toluene.

Various diluents like benzene, toluene, xylene, chloroform, carbon tetrachloride, hexane, cyclohexane were tested. Toluene was found to be the best diluent for all the metal ions due to quantitative extraction and better phase separation.

The metal ions loaded in the organic phase were stripped out using different concentrations of various acids (Table 2).

Table 2 Effect of Stripping Agents

Metal Ion	% Recovery in Acids									
	Acid Conc. (mol/dm^3)									
	HCl						$HClO_4$		HNO_3	
	1.0	2.0	4.0	6.0	8.0	10.0	1.0	2.0	1.0	2.0
Rh(III)	17.8	54.3	75.2	**99.2**	**99.2**	98.4	7.9	17.8		
Sb(III)	-	12.8	29.2	29.2	36.4	-	-	-		
Tl(III)	52.0	38.0	-	-	-	-	39.7	16.5	16.5	13.2
	H_2SO_4									
	0.05	0.1	1.0	2.0	4.0	6.0	8.0	8.5	10.0	
Rh(III)	-	-	10.3	23.7	-	-	-	-	-	
Sb(III)	-	-	-	17.1	41.0	56.7	75.0	**99.2**	**99.2**	
Tl(III)	43.8	**99.2**	63.6	29.75	-	-	-	-	-	

The aqueous phase containing these metal ions was shaken with PC-88A in toluene for a period ranging from 30 seconds to 20 minutes and the minimum period of equilibration required for complete extraction of these metal ions was as: Rh - 5 min., Sb - 1 min. and Tl - 3 min. There was no decrease in extraction of these metal ions even when equilibrated for longer time periods.

Table 3 Separation of metal ions from some important multi-component mixtures

Metal Ion	Conc. µg	Aqueous Phase	[PC-88A] (mol/dm^3)	Stripping Agent	% Found
Au(III)	200	1.0 M HCl	5×10^{-2}	-	98.5
Rh(III)	100	1.0 M HCl + 1×10^{-1} M $SnCl_2$	2×10^{-2}	6 M HCl	99.1
Ru(III)	100		unextracted	-	98.3
Au(III)	100	1.0 M HCl	5×10^{-2}	-	99.2
Pd(II)	100	(1.0 M HCl + 1.0 M $HClO_4$ +	6×10^{-4}	-	100
Pt(IV)	100	2.5×10^{-2} M $SnCl_2$)	5×10^{-3}	4 M HCl	99.2
Rh(III)	100		unextracted	-	99.1
Sn(IV)	100	0.2 M HCl	2.5×10^{-2}	4.0 M HCl	99.2
Bi(III)	100	pH 1.5, 0.1 M NH_4NO_3	6×10^{-3}	2.0 M HNO_3	99.8
Pb(II)	50	pH 1.5, 0.1 M NH_4NO_3	unextracted	-	98.5
Sb(III)	100	0.1 M HCl	1.5×10^{-1}	8.5 M	99.1
Sn(IV)	50	0.1 M HCl	1.5×10^{-1}	H_2SO_4	99.2
Bi(III)	150	pH 1.5, 0.1 M NH_4NO_3	6×10^{-3}	4.0 M HCl	99.6
Tl(I)	50	pH 1.5, 0.1 M NH_4NO_3	unextracted	2.0 M HNO_3	98.5
				-	

Separation of the metals from multi-component mixtures:

The metal ions were separated by taking advantage of difference in their extraction and stripping conditions with PC-88A. Tl(III) was separated from In(III), Ga(III), Cu(II) and Ni(II) as they remained unextracted with 1.0×10^{-2} mol/dm^3 PC-88A in toluene from 4.25 mol/dm^3 H_2SO_4. The separation of other important selective multi-component mixtures is given in Table 3.

Analysis of real samples

Analyzing these metals in various real samples tested the validity of the methods. The experimental results were found to be in good agreement with the theoretical values (Table 4).

Table 4 Analysis of real samples

Sample	Metal	Present	Found	% recovery
Cisplatin (Biochem Pharmaceuticals Industries, Mumbai)	Pt	65.0 %	64.9 %	99.8
Platinum wire (Ravidra Hindustan Platinum Pvt. Ltd.)	Pt	99.9 %	99.7 %	99.8
Pd on calcium carbonate (s. d. Fine Chemicals Ltd.)	Pd	5 .0 %	4.98 %	99.6
Pd on charcoal (s. d. Fine Chemicals Ltd.)	Pd	5.0 %	4.96 %	99.2
Wood's alloy (Indalloy158) Indium Corp. of America	Bi	50.0 %	49.7 %	99.4
Trymo(Raptakos Brett Ltd., India)	Bi	107.64 mg	106.9 mg	99.3
Denol (Elder Pharmaceuticals Ltd., India)	Bi	107.64 mg	107.11 mg	99.5
Leaded gun metal (BCS -183/4)	Sn	7.27 %	7.22 %	99.3
Leaded gun metal (ITA-LAB- 4382)	Sn	4.86 %	4.85 %	99.8
Pineapple slices	Sn	123.6 μg/g	122.85 μg/g	99.4
Orange pulp	Sn	98.3 μg/g	97.65 μg/g	99.2
Tin base white-metal (BCS 178/2)	Sb	9.45 %	9.40 %	99.5
Sodium stibogluconate (Albert David, Ltd. Calcutta, India)	Sb	100 mg	99.45 mg	99.4

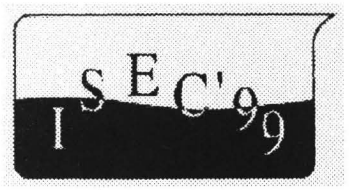
CONCLUSIONS

2-ethylhexylphosphonic acid mono-2-ethylhexyl ester (PC88A) was effectively employed as an extractant for the separation of Pt, Pd, Rh, Bi, Sn, Sb and Tl from commonly associated metals and was found to be quite suitable for the separation and determination of these metals in various real samples The methods are readily combined with suitable spectrophotometric methods for determination of these metals after their extraction and separation. The methods are simple, rapid, selective and sensitive. The

extractions were achieved in a short period of equilibration with very low reagent concentration for each of these metal ions. The extractant, PC-88A is found to be advantageous over several earlier reported extractants including many organophosphorus extractants like TPP, TPPO, TBP, TOPO, etc.

REFERENCES

1. Binghua Y and Nagaosa Y. *Solv. Extr. Ion Exch.*, **14,** 849, (1996).
2. Sole KC, Ferguson TL and Hiskey JB *Solv. Extr. Ion Exch.*, **11,** 1033, (1993).
3. Zhao J, Wu Z and Chen J. *Hydrometallurgy*, **46,** 363, (1997).
4. Otu E and Westland A *Solv. Extr. Ion Exch.*, **8,** 759, (1990).
5. Sato T *Hydrometallurgy*, **22,** 121, (1989).
6. Kubota F, Goto M and Nakashio F. *Solv. Extr. Ion Exch.*, **11,** 437, (1993).
7. Jayachadran J. *Ph. D. Thesis* , University of Mumbai, Dec. 1997.
8. Mohski M. *Talanta*, **27,** 7, (1980).
9. Mehrotra A, Rajan M and Shinde VM. *Indian. J. Chem.*, **35A,** 530, (1996).
10. Fuerstenau MC and Wang G. *Hydrometallurgy*, **46,** 229, (1997).
11. Mitchell JW and Riley JE *Radiochem. Radioanalyt. Lett.*, **21,** 41, (1975).
12. Vogel AI *Textbook of Quantitative Inorganic Analysis*, Longmans Green and Co. Ltd., London, (1978).
13. Snell FD. *Photometric and Fluorimetric Methods of Analysis*, Wiley, New York, (1978).
14. Bandekar SV and Dhadke PM. *Sep. Purif. Technol.*, **13,** 129, (1998).
15. Bandekar SV and Dhadke PM. *Chem. Anal.(Warsaw)*, **43,** 417, (1998).
16. Bandekar SV and Dhadke PM. *Talanta*, **46,** 1181, (1998).



BIS(ETHANEDITHIOAMIDO)-2,4-DIOXO-3-OXYMINO-PENTANE AS A NEW ANALYTICAL REAGENT FOR THE EXTRACTIVE RADIOCHEMICAL-SPECTROPHOTOMETRIC DETERMINATION OF SELENIUM(IV) AND ITS SEPARATION FROM OTHER ELEMENTS

A Varadarajan and SP Malve
Faculty of Chemistry, The Institute of Science, 15, Madam Cama Road Mumbai 400032, India

ABSTRACT
Bis(ethanedithioamido)-2,4-dioxo-3-oxyminopentane [bis(EDADOP)] is proposed as a new sensitive and selective analytical reagent for the extractive radiochemical-spectrophotometric determination of microgram amounts of selenium. The method is based on the formation of an insoluble yellow-orange complex, when heated at 50 ^{0}C for 2.0 min, which is extractable in 1-octanol from an acidic solution of 2-3 mol L^{-1} hydrochloric acid by shaking for 1.5 min. The absorbance of the extracted species was measured at 495 nm and its color in 1-octanol was found to remain stable for more than 24 hours. Under optimum conditions, the calibration graph was linear over the range 0.2-15.0 ppm selenium (IV) in 1-octanol, with a molar absorptivity of 1.268 x 10^{4} l mol^{-1} cm^{-1} in Ringbom's optimum working range of 4.36-12.02 ppm for effective spectrophotometric determination of Se (IV) at 495 nm. The method has been satisfactorily applied to the determination of traces of selenium in various synthetic, environmental, biological, pharmaceutical, and food samples etc. in the presence of Cu (II), Ag (I), As (III), Te (IV) and Pb (II), usually associated with selenium in nature. The method offers advantages of high sensitivity, selectivity, stability, reproducibility and interference free determination of traces of selenium.

Keywords: Selenium(IV), bis(ethanedithioamido)-2,4-dioxo-3-oxyminopentane, radiochemical-spectrophotometry

INTRODUCTION

Selenium is one of the most widely distributed elements with considerable significance.[1,2] In appropriate amounts, it can enhance our ability to protect against certain cancer and heart diseases while on the other hand selenium deficiency syndromes have also been reported.[1,2] In more recent studies epidemiological investigations have indicated a decrease in human cancer deaths rates (age and sex adjusted) correlated with increasing selenium content of forage crops.[3] There is a range of selenium intake that is consistent with health and outside this range deficiency or toxicity effects can occur. Since it is the element with the narrowest difference between these two levels and because of several limitations of existing methods, with the need for a reagent with higher extraction ability and negligible interference problems, it was considered worthwhile to develop sensitive methods for determination of selenium traces with bis(EDADOP) and bis(TSKDOP) as potential extractants.

Bis(ethanedithioamido)-2,4-dioxo-3-oxyminopentane [bis(EDADOP)][4] forms a yellow-orange colored complex extractable in 1-octanol. The proposed method has been satisfactorily applied to the spectrophotometric determination of trace selenium in various samples, in the presence of Cu(II), Ag(I), As(III), Te(IV) and Pb(II), usually associated with selenium in nature.

The proposed method has been successfully compared with bis(thiosemicarbazone)-2,4-dioxo-3-oxyminopentane [Bis(TSKDOP)][5] and the universally accepted 3,3-diaminobenzidine (DAB)[6] methods by extractive radiochemical-spectrophotometry.

© 2000 Society of Chemical Industry

EXPERIMENTAL

Instrumentation

A Shimadzu-140-02 UV-visible spectrophotometer with 1.00 cm light path quartz cells was used for all absorbance measurements. The pH measurements were made with a digital Elico, Model LI-120, pH meter equipped with a combined glass electrode assembly. Radioactivity measurements were made with a calibrated gamma-ray spectrophotometer fitted with a single channel pulse height analyzer in conjunction with a 3.8 x 3.8 cm NaI(Tl) crystal detector.[7]

All chemicals were of analytical-reagent grade. ^{75}Se radioisotope was supplied by the Isotope Division, Bhabha Atomic Research Centre, Mumbai, India. Deionised, double-distilled water was used throughout the experiment.

A 0.05997 mol L^{-1} bis(EDADOP) solution was prepared in a methanol:DMF (2:1) mixture and used as required for further investigations. A 1 mg mL^{-1} stock solution of Se(IV) was prepared in water and standardized by a known method.[8]

Standard Procedure

An aliquot containing up to 100 μg Se(IV) (<100 μg carrier Se(IV) solution labelled with ^{75}Se tracer) was placed in a beaker well covered with watch glass and concentrated hydrochloric acid added so as to make the aqueous solution acidic with respect to 2-3 mol L^{-1} hydrochloric acid. Bis(EDADOP) solution, 1.0 ml of 0.05997 mol L^{-1} was then added and the contents heated on a water bath for 2.0 min at 50 ^{0}C, after diluting to 20 ml with distilled water. The mixture was cooled for 5 min and transferred carefully to a 125 ml separatory funnel. The solution was equilibrated once with 20 ml 1-octanol for 1.5 minutes. A 2.5 ml aliquot of the organic phase was diluted to 20 ml and the absorbance of the yellow-orange complex measured at 495 nm against pure solvent. In a separate experiment a 2 ml aliquot of each phase was evaporated to dryness in a planchet under an IR lamp and taken for counting on a gamma-ray spectrophotometer.

RESULTS AND DISCUSSION

A comparative chart of the results obtained with bis(EDADOP), bis(TSKDOP) and DAB are shown in Table 1.

The absorption spectra of bis(EDADOP) and bis(TSKDOP) and their Se(IV) complexes in 1-octanol and toluene respectively are shown in Figure 1.

The described methods are superior to most of the existing methods of selenium analyses for both spectrophotometric and extractive spectrophotometric determination, exceeding even the universally accepted DAB reagent. The developed methods are free from limitations and offer advantages such as sensitivity, better selectivity, excellent stability and interference-free analysis of traces of selenium in the presence of its associated elements, in various synthetic and real samples.

TABLE 1 Comparative Analytical Data of Bis(EDADOP), Bis(TSKDOP) and DAB for the Spectrophotometric Determination of Selenium(IV)

Parameter	Bis(EDADOP)	Bis(TSKDOP)	DAB
1	2	3	4
Wavelength	495 nm	420 nm	420 nm
pH/Acidity	2.0-3.0 mol l^{-1} HCl	1.7-2.5 mol l^{-1} HCl	7.0-8.0
Total Color Development & Heating Time	35.0/2.0 min	45.0 min	60.0/5.0 min
Temperature	45-70 ^{0}C	50-70 ^{0}C	100 ^{0}C
Shaking Time	1.5 min	5.0 min	30.0 s
Solvent	1-Octanol	Toluene	Toluene
Stability	>24 h	>24 h	>24 h
Beer's Range (ppm)	0.2-15.0	0.1-2.1	0.5-2.5
Molar Absorptivity ($l\ mol^{-1}\ cm^{-1}$)	12,680	37,190	6,268
Sandell Sensitivity ($ng\ cm^{-2}$)	2.210	2.125	12.730
Stoichiometry (M : HR)	1 : 2	1 : 2	2 : 1
Preconcentration	9.0 times	11.0 times	15.0 times
Interference	Interference due to Cu(II) masked with sodium cyanide	Interference due to As(III) and Ni(II) masked with hydrogen peroxide and EDTA respectively	Interference due to oxidising and reducing agents

1	2	3	4
Applications (RSD)			
Synthetic Mixtures	1.59%	1.27%	1.86%
Environmental Samples	1.58%	1.59%	2.03%
Biological Samples	1.58%	1.68%	2.15%
Pharmaceutical Samples	1.76%	1.33%	1.94%
Food Samples	1.62%	1.51%	2.04%

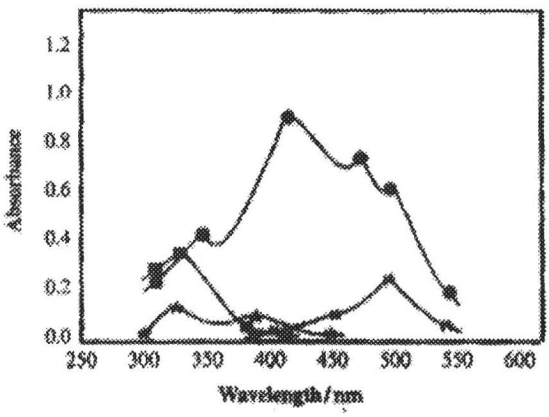


Figure 1. Absorption Spectra of Bis(EDADOP) (-•-) and Bis(TSKDOP) (-•-) and their Selenium Complex in 1-Octanol (-•-) and Toluene (-•-) respectively

ACKNOWLEDGEMENT

The authors wish to express their deep sense of gratitude to the Director, The Institute of Science, and Professor Zarin R. Turel, Nuclear Chemistry Department for extending facilities of their laboratory to carry out this work. The authors are also grateful to the University of Mumbai for the financial assistance (Scholarship No 5937/97) and Mr. S. Varadarajan for typing of this manuscript.

REFERENCES

1. Shapira J R, Klayman DL and Gunther WH, '*Organic Selenium Compounds, their Chemistry and Biology*', Wiley Interscience, New York, 701, (1971).
2. Patty FA, '*Industrial Hygiene and Toxicology*', Wiley Interscience, New York, **2**, 886, (1962).
3. Carpentor H and Robertson IM, *Metals*, **2**, 445, (1939).
4. Varadarajan A, Utekar SS and Malve SP, *Acta Polon. Pharm.-Drug Res.*, **55(2)**, 137, (1998).
5. Varadarajan A, Kulkarni AJ, Jadhav SB, Utekar SS and Malve SP, *Analyst* (in press), (1998).
6. Cheng KL, *Anal. Chem.*, **28**, 1738, (1956).
7. Talwar UB and Haldar BC, *Anal. Chim. Acta*, **57**, 53, (1970).
8. Vogel AI, '*Textbook of Quantitative Chemical Analysis*', 5th Ed., ELBS, London, 465, (1991).



Biotechnology

A NOVEL PROTEIN REFOLDING TECHNIQUE UTILIZING REVERSED MICELLAR EXTRACTION

Masahiro Goto[1], Shintaro Furusaki[1] and T Alan Hatton[2]
[1]Department of Chemical Systems and Engineering, Graduate School of Engineering, Kyushu University, Fukuoka 812-8581, Japan
[2]Department of Chemical Engineering, Massachusetts Institute of Technology, Cambridge MA 02139, USA

ABSTRACT
Protein refolding was performed by reversed micelles formulated with sodium di-2-ethylhexyl sulfosuccinate (AOT) in isooctane. In the novel refolding technique, a solid-liquid extraction was utilized as an alternative to the ordinary protein extraction by reversed micelles based on a liquid-liquid extraction. The effects of operational parameters such as concentration of AOT, water content and pH were examined on the extraction of denatured proteins. A high AOT concentration and a high water content in reversed micelles facilitated the extraction efficiency. A complete renaturation of denatured RNase A was accomplished by adding redox reagents. In the final step, the renatured RNase A was effectively recovered from the reversed micellar solution without the loss of the enzymatic activity.

Key-words: Protein extraction, Surfactant, Reverse micelle, Enzyme, AOT

INTRODUCTION

A large number of proteins from eukaryotic genes cultivated in a bacterial system by recombinant DNA technology are often produced inactive misfolded or aggregated proteins, which actually consist only a small portion of native and active conformation.[1] These insoluble aggregates in an aqueous solution are misfolded protein molecules. In order to obtain biologically active proteins, these insoluble proteins must first be extracted from the inclusion bodies and solubilized using strong denaturants such as guanidine hydrochloride or urea under reducing conditions. On the removal of the denaturant by dialysis or dilution with an appropriate buffer, the proteins are allowed to refold up to the native and active conformation. However, a high refolding yield may not be obtained at high protein concentration due to the formation of irreversible aggregates by the excess inactive protein molecules.

Recently, a novel preparation method aimed at improving the efficiency of refolding at higher protein concentration has been reported.[2,3] Hagen et al. has suggested that isolating protein molecules in a reversed micellar matrix reduces intramolecular interaction which causes formation of irreversible aggregates. Reversed micelles provide nano-structural aqueous droplets constituting water pools in an organic solvent, so that proteins solubilized in the water pool can maintain their high-structural conformation and activity.[4] These features are favorable for protein refolding, because protein molecules can be isolated from each other during the refolding process. However, in a liquid-liquid extraction system, protein transfer into a reversed micellar solution was considerably inhibited by the denaturants contained in the aqueous solution.

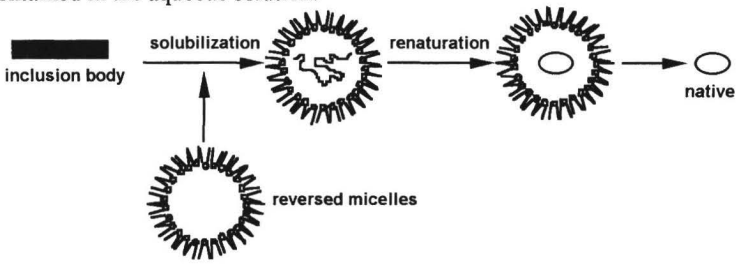


Figure 1. Schematic illustration of protein refolding by reversed micellar solution utilizing solid-liquid extraction technique

© 2000 Society of Chemical Industry

In the present study, we demonstrate that the reversed micellar system utilizing solid-liquid extraction is a promising and attractive technique for refolding proteins. Some key operational parameters were investigated on the efficiency of refolding denatured proteins. This novel refolding process is schematically shown in Figure 1. Furthermore the optimal conditions for the protein refolding are discussed in this paper.

EXPERIMENTAL

Materials.

Bovine pancreatic RNase A (EC 3.1.27.5) as a model protein and cytidine 2':3'-cyclic monophosphate as a substrate for the activity test were obtained from Sigma Chemicals Co. (USA). AOT (Sodium bis-2-ethylhexyl sulfosuccinate), urea and β-mercaptoethanol were purchased from Kishida Chemicals Co. (Japan). Reduced and oxidized glutathione (GSH, GSSG) were purchased from Wako Pure Chemical Industries, Ltd. (Japan). Other chemicals were of the highest grade commercially available.

Extraction of Solid Denatured RNase A into Reversed Micelles.

A reversed micellar solution was prepared by injecting a 0.1 M Tris-HCl buffer into a 50-400 mM AOT-isooctane solution. The solid denatured RNase A was dissolved into the reversed micellar solution under ultrasonic irradiation for approximately 1 hour. The concentration of RNase solubilized in the reversed micellar solution was determined by measuring its absorbance at 278 nm with a UV-VIS spectrophotometer (U-best 570 JASCO). The average diameter of reversed micelles containing proteins was analyzed by a DLS-7000 system (75mW Ar- or He-laser, Otsuka Electric Co. Ltd., Japan).

Renaturation of RNase A in Reversed Micelles.

Renaturation was initiated by adding 1 ml of reversed micellar solution containing glutathione into the 2 ml reversed micellar solution containing solubilized RNase A. The specific activity of RNase A in the reversed micelles was measured against time progress, considering the time when glutathione solution was added as the initial time. The renaturation yields of denatured RNase A was evaluated by comparing the enzymatic activity of denatured RNase A to that of native RNase A which was solubilized in the reversed micelles as a control experiment.

Recovery of Renatured RNase A from Reversed Micelles

One volume of reversed micellar solution containing the renatured RNase A was added into 5-40 volumes of cold acetone and stirred in a magnetic stirrer for 20 minutes. The reprecipitated RNase A was collected by centrifugation and washed several times with cold acetone to remove AOT molecules that may be adsorbed to the collected RNase A. Furthermore, the precipitates were dried under vacuum condition. The obtained precipitates were solubilized in a 0.025 M phosphate buffer (pH 7.5). The amounts of recovered RNase A were determined by measuring the absorbance in the buffer solution at 278 nm with the UV-VIS spectrophotometer.

RESULTS AND DISCUSSION

Solubilization of Solid Denatured RNase A into Reversed Micellar Solution by Solid-Liquid Extraction Technique

In the previous study[2] protein refolding utilizing reversed micelles showed that solubilization of denatured RNase A into reversed micelles was difficult owing to a huge amount of denaturant (6M

GuHCl or 8M urea) in aqueous solution, which interrupts the mass transfer of proteins. The denaturant reduces the electric interaction between surfactants and the surface of proteins, which is considered to be one of the main driving forces in protein extraction by reversed micelles. Therefore, the denaturant concentration ought to have been reduced to an appropriate concentration which would have facilitated denatured RNase A to be transferred efficiently into reversed micelles in the unfolded state. In order to improve the overall yield in the protein refolding process, we have introduced solid-liquid extraction technique to enhance the solubilization of unfolded proteins directly into reversed micelles.[5]

In the present study, the effects of some important parameters in preparing the reversed micellar solution were examined on the solubilization of solid denatured RNase A. The degree of solubilization of the solid denatured protein was significantly influenced by surfactant concentration. Figure 2 shows the effect of AOT concentration in isooctane on the solubilization of the solid denatured RNase A into the reversed micellar solution along with the average diameter of reversed micelles formed after the solubilization of protein. A high concentration of AOT in isooctane facilitates the solubilization of the denatured proteins. Furthermore, increasing the concentration significantly decreased the size of reversed micelles.

When the surfactant-protein interaction is stronger than the protein-protein interaction in the denatured proteins, the protein solubilization into the reversed micelles proceeds well.

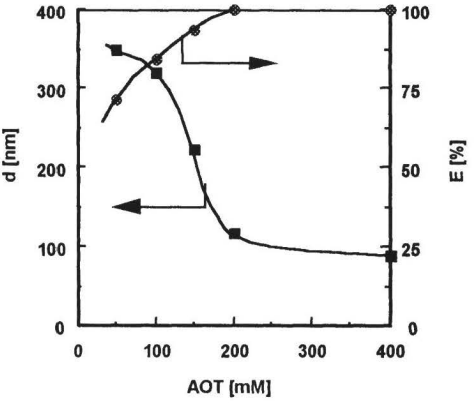


Figure 2. Effect of AOT concentration in isooctane on both solubilization (E) and average diameter (d) of reversed micelles after solubilization: 2.3 mg/ml RNase A, Wo=20, pH 8.7.

From the result of DLS measurement, it was found that the average diameter of the stable reversed micelles containing denatured RNase A in the organic solvent was approximately 100 nm. On the other hand, under the same experimental condition the average diameter of reversed micelles which contain native RNase A was only about 10nm. This result means that the solubilization state of the denatured proteins is different from that of native proteins. The denatured proteins are considered to form a small cluster in reversed micelles.

The effect of water content of the reversed micelles on the solubilization of solid denatured RNase A is shown in Figure 3. The degree of solubilization of denatured RNase A into reversed micelles increases along with the increase of water content. These results suggest that water molecules in organic media play an important role for solubilization and dispersion of denatured protein aggregates. Moreover, it is considered that hydration of proteins is essential for dissociation of nonspecific interactions among aggregated protein molecules. Later it became clear that the dependence of Wo on the diameter of reversed micelles supports this idea since the size of reversed micelles containing denatured proteins decreases with increasing Wo in the reversed micelles.

Later it became clear that the dependence of Wo on the diameter of reversed micelles supports this idea since the size of reversed micelles containing denatured proteins decreases with increasing Wo in the reversed micellar system.

Enzymatic activity of RNase A was recovered by addition of reversed micellar solution containing glutathione to the reversed micellar solution containing denatured proteins. Associated activity is recovered completely within 30 hours. Using reversed micellar media at higher protein concentration enhanced the efficiency of refolding. On the basis of the result, it is clear that the denatured protein molecules were isolated from each other in the reversed micelles and efficiently refolded without formation of protein aggregations.

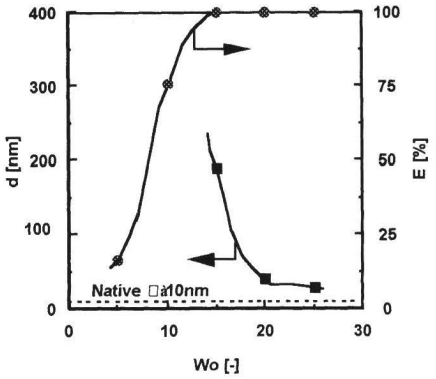


Figure 3. Effect of Wo (=[H2O]/[AOT]) on solubilization (E) and average diameter (d) of reversed micelles after solubilization of denatured protein: 2.3 mg/ml RNase A, 400 mM AOT, pH 8.7.

. According to circular dichroism (CD) spectra, it is obvious that the conformation of denatured RNase A entrapped in reversed micelles remained in denatured states (data not shown) and the activity was almost zero. This implies that reoxidation of reduced thiols is essential to obtain native conformation and to recover the enzymatic activity. Hence we used reduced and oxidized glutathione (GSH and GSSG, respectively) which are the most widely used compound as thiol/disulfide reagents. We investigated the effect of redox reagents on the refolding yield.

Figure 5 shows the effect of GSH/GSSG ratio on the renaturation of RNase A in reversed micelles. The total glutathione concentration in the reversed micellar system was kept constant at 0.61 mM based on the organic phase.

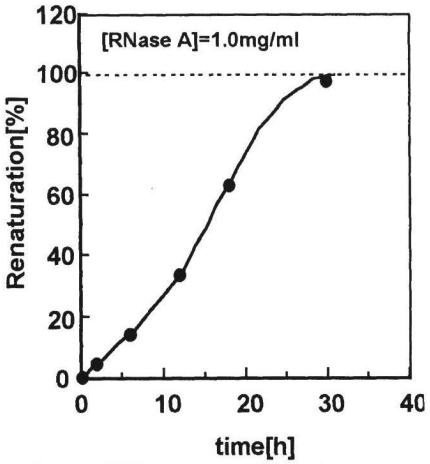


Figure 4 Time course of protein refolding in reversed micellar solutions

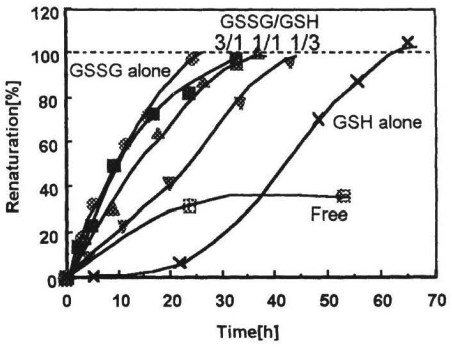


Figure 5 Effect of redox reagents on refolding efficiency

This concentration offered a maximum reactivation rate. RNase A in reversed micelles recovered its enzymatic activity up to about 36 % even without the addition of the redox reagent glutathione. Result shows that the reactivation rate was influenced by the ratio of GSH/GSSG, however, the renaturation yields were almost 100 % in all cases expect for the glutathione free system. The ratio was found to affect the refolding rate of proteins in reversed micelles.

In addition, the visible protein aggregates were not observed during refolding operations under the present experimental conditions.

We are convinced that it is possible to improve the renaturation yield and time at high protein concentration by optimizing factors such as the (GSH/GSSG) ratio, concentration of a redox reagent, Wo, pH of water pools, reversed micellar system, and renaturation temperature, etc.

Recovery of Renatured RNase A from Reversed Micelles

Denatured RNase A has now been successfully reactivated in reversed micellar media. The final step is to recover the active proteins from the reversed micellar solution. The recovery of proteins solubilized in reversed micelles has been performed by "back extraction" operation, in which the reversed micellar solution contacts with a fresh aqueous solution with a high ionic strength and a pH value that facilitates electrostatic repulsion between the encapsulated protein and the head group of surfactant molecules. However this method often provides a low extraction yield due to the formation of irreversible precipitates which involve surfactant molecules at the organic-aqueous interface. Furthermore, the activity of recovered proteins is often reduced during the back-extraction operation. In order to overcome this problem, we introduced a different approach to recover the proteins from the reversed micellar solution more effectively. This approach is the precipitation method in which a solid protein was recovered by the addition of a polar organic solvent. In the present study, acetone was used as the polar organic solvent. The effect of the amount of the added acetone on the recovery and activity yields of renatured RNase A from the reversed micellar solution is summarized in Table 1.

Table 1 Recovery and activity of renaturated protein from reversed micellar solution

Vacetone / Vrm	Recovery [%]	Activity [%]
5	88.4	>100 [a]
10	87.4	>100 [a]
20	92.0	>100 [a]
40	94.2	>100 a

a: The activity of recovered RNase A was more than that of material one.

The addition of 5-40 times volume of acetone to the reversed micellar solution provided 84-94 % recovery yields. Furthermore, the recovered RNase A retained a high enzymatic activity. The addition of acetone induces destabilization of reversed micelles. The resulting proteins can be released from the reversed micellar solution as a solid.

The overall yield of the novel process was found more favorable in comparison with the conventional dilution method. Thus, this reversed micellar system utilizing the solid-liquid extraction technique was demonstrated to be effective for protein refolding even at high dosage of proteins. Our next objective is to extend the scope of this study to the direct refolding of inclusion bodies by utilizing the solid-liquid extraction technique.

CONCLUSION

A solid-liquid extraction process utilizing reversed micelles was introduced as a novel protein refolding technique. Solid denatured RNase A was completely solubilized into the AOT reversed micellar solution and was reactivated by the addition of the redox reagent glutathione. The novel refolding process is mainly devided into three steps: solubilization, renaturation and recovery step. The renatured RNase A in reversed micelles was completely recovered by the addition of acetone.
The benefits of the novel process are that a high concentration of proteins can be dealt with and that the amount of an expensive redox reagent can be reduced due to the small water content in reversed micelles. However, the most advantage of this novel reversed micellar refolding process compared to the conventional dilution method is that the novel process does not require denaturants such as guanidine chloride or urea. It is hoped that this solid-liquid extraction technique will be found useful for application in the biochemical industry.

ACKNOWLEDGMENTS

This work was partially supported by a Grant-in-Aid for Scientific Research (No. 10555284) from the Ministry of Education, Science, Sports and Culture of Japan, and Chemical Materials Research & Development Foundation.

REFERENCES

1. Marston FAO. *Biochem. J.*, **240,** 1, (1986).
2. Hagen AJ, Hatton TA and Wang DIC. *Biotechnol. Bioeng.* **35**, 955, (1990).
3. Batas B and Chaundhuri JB. *Biotechnol. Bioeng.* **50**, 16, (1996).
4. Goto M, Ishikawa Y, Ono T, Nakashio F and Hatton TA, *Biotechnol. Prog.*, **14**(5), 729, (1998).
5. Wolf R and Luisi PL. *Biochem. Biophys. Res. Commun..*, **89**(1), 209, (1979).
6. Hashimoto Y, Ono T, Goto M, Hatton TA, *Biotechnol. Bioeng.* **57**, 620, (1998).

EFFECT OF INTERACTION BETWEEN PROTEIN AND SURFACTANT IN AQUEOUS PHASE ON EXTRACTION RATE OF PROTEIN INTO REVERSED MICELLAR SOLUTION.

Takumi Kinugasa[1], Kimiko Sanagi[1], Kunio Watanabe[1] and Hiroshi Takeuchi[2]

[1] Department of Applied Chemistry and Biotechnology, Niihama National College of Technology, Niihama 792, Japan

[2] Department of Chemical Engineering, Nagoya University, Nagoya 464-01, Japan

ABSTRACT

The relationship between the extraction rate of proteins and the formation of the complex in aqueous salt solution was investigated. The extraction rate of lysozyme was measured from the aqueous phase presaturated with an organic surfactant AOT solution in advance. In NaCl aqueous system, the rate from aqueous solution containing the surfactant was similar to that from the unsaturated organic solution, whereas in KCl media, the faster extraction was observed in the surfactant containing solution in the range of lower salt concentration. The solubilization rate of AOT from organic to aqueous KCl phase was lower than that to NaCl solution. We can conclude that the complex formation of protein and surfactant promoted the protein extraction.

Keywords : Reverse Micelle, Protein, Extraction Rate, Mechanism of Extraction

INTRODUCTION

Reversed micellar extraction technique is attractive methods for separation and purification of proteins. For a practical application, it is important to elucidate the characteristics of the mass transfer of protein from aqueous to reversed micellar phase. In the previous study,[1] we examined the effect of pH, salt species, and its concentration on the extraction rate of protein and proposed the interfacial distortion model for protein extraction.

Recently, some investigators have represented the new extraction model via the formation of a surfactant-protein complex. Adachi and Harada[2] reported that the hydrophobic cytochrome c adsorbing the surfactant molecules would be entrapped in the reverse micelles. Paradoker and Dordick[3] found that α-chymotrypsin is easily extracted into isooctane at very low surfactant concentration as a hydrophobic ion-pair with surfactants. Goto *et al.*[4] investigated the behavior of protein extraction into the organic solutions containing some synthesized surfactants, and then suggested that hemoglobin would be extracted into organic phase when the hydrophobicity of interfacial complex formed by protein and surfactants is sufficiently high. The protein-surfactant complex might be formed in aqueous phase during the protein extraction, because the amphiphilic surfactant would be distributed from organic to aqueous phase.

In the present study, we examined the effect of such complex formation in aqueous solution on the extraction rate of protein. Furthermore, the interfacial distortion model of the protein extraction would be improved considering the complex formation.

EXPERIMENTAL

Sodium bis(2-ethylhexyl)sulfosuccinate (AOT) as an anionic surfactant was obtained from Nacalai Tesque and used without further purification. Protein used in this study was lysozyme from chicken egg white obtained from Sigma. All other chemicals were of reagent grade. An aqueous solution was prepared by dissolving lysozyme in distilled water containing salt and buffer for the adjustment of ionic strength and pH, respectively. In all experiments, the feed concentration of lysozyme in the aqueous phase was 0.5 kg/m^3. A reversed micellar solution was prepared by dissolving AOT in 2,2,4-

© 2000 Society of Chemical Industry

trimethylpentane (isooctane) as an organic solvent. In some experiments, the aqueous solution was presaturated with the reversed micellar solution before dissolving lysozyme, where the aqueous solution contains AOT at the equilibrium concentration.

The kinetic studies were carried out at 298 K using a stirred cell made of glass, fitted with four baffles, shown in Figure 1. Equal volumes (50 cm^3) of the organic and aqueous solutions were located in the upper and lower section of the cell, respectively, and then agitation for each phase was started by four-blades disk-turbine impeller, driven in opposite directions at 150 r.p.m.

All experiments were performed in batch operation. The organic samples were taken out at regular intervals from a sampling port by a syringe. The concentration of lysozyme in organic phase was determined on an UV spectrophotometer (Shimadzu, UV-1200) at 280 nm.

Concentration change of the solubilized protein in the organic phase is given by the following equation:

$$(V_O/A)(dC_{P,O}/dt) = K_P(C_{P,W} - C_{P,O}/m) \quad (1)$$

where K_P is the overall mass-transfer coefficient of protein, $C_{P,W}$ and $C_{P,O}$ are the protein concentrations in the aqueous and organic phases, respectively, and m is the distribution ratio of protein. Equation (1) can be integrated to yield

$$\ln[1 - (1 + 1/m)C_{P,O}/C_{P,W}{}^0] = -(1 + 1/m)K_P t \quad (2)$$

which makes possible the evaluation of the overall mass-transfer coefficient, K_P, from the time-course of protein concentration in the organic phase.

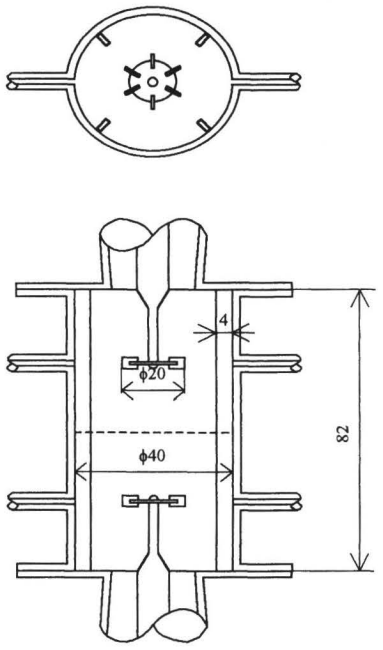


Figure 1 Details of Stirred Cell.

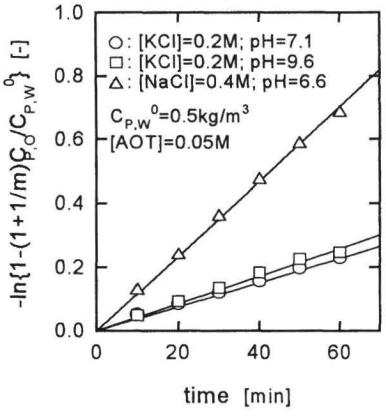


Figure 2 Time course of protein concentration in organic phase.

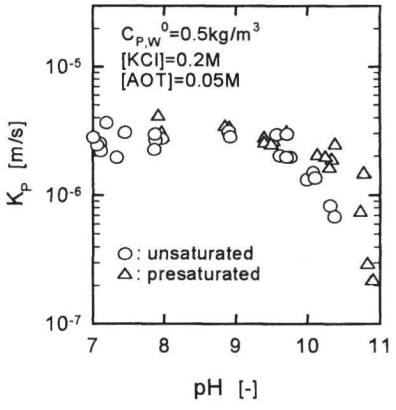


Figure 3 Effect of pH on K_P.

In the distribution and kinetic experiments of AOT between the aqueous and organic phases, AOT concentration in an aqueous phase was determined from the measurement of sulfur atom with an ICP-atomic emission spectroscope (Nippon Jarrell-Ash, IRIS).

RESULTS AND DISCUSSION

Typical data for protein extraction is shown in Figure 2 plotted according to Equation (2) and then we can determine the overall mass-transfer coefficient, K_P, from the slopes of each line.

Figure 3 shows the effect of solution pH on the overall mass-transfer coefficient, K_P, of lysozyme from aqueous KCl media which is unsaturated and presaturated with an organic AOT solution. In the lower pH region, the K_P values were constant in the both cases. From the previous report[1], it is considered that the protein extraction is controlled by a diffusion process through the aqueous boundary film. Above pH 9.5, the K_P value is decreased with increasing pH due to the reduction in the electrostatic attraction between the protein and surfactant head-groups.
Figure 3 also shows the K_P value for presaturated system is higher than that for unsaturated in the higher pH region. This suggests that the formation of protein-surfactant complex in the presaturated aqueous phase would promote the protein extraction.

Figures 4 and 5 show the effects of the respective concentration of KCl and NaCl in the aqueous feed on the overall mass-transfer coefficient, K_P. In the both systems, the K_P values were decreased with increasing the salt concentration. This will be attributable to an electrostatic screening effect. In the NaCl system, the K_P value from aqueous presaturated solution was similar to that from unsaturated solution, whereas for KCl media, the faster extraction was observed in the presaturated solution in the range of lower salt concentration. Such difference in the extraction behavior between the two systems would be caused by the distribution properties of surfactant AOT into the aqueous salt solution.

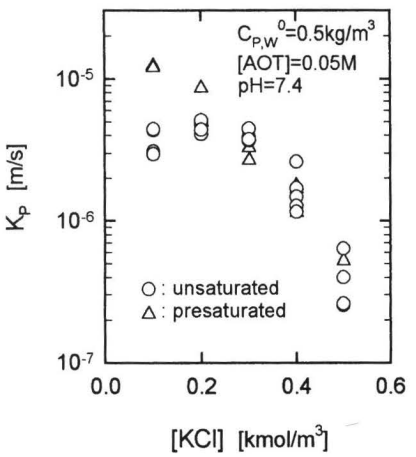


Figure 4 Effect of KCl concentration on K_P.

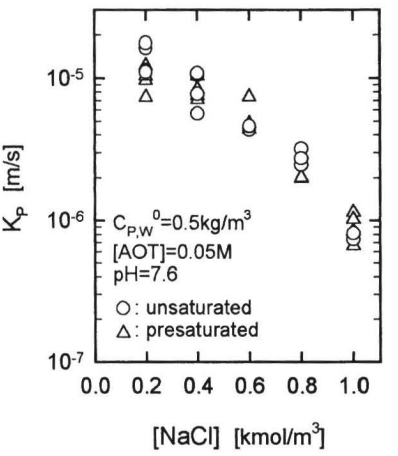


Figure 5 Effect of NaCl concentration on K_P.

The distribution ratio, m_S, of AOT between isooctane and aqueous salt solution is plotted against the salt concentration in Figure 6. The m_S value was decreased with increasing the salt concentration due to salting effect, although there is no difference of the m_S value between the KCl and NaCl systems.

Figure 7 shows the change in the concentration of AOT solubilized from the organic to aqueous salt solutions. The solubilization rate of AOT to the aqueous NaCl phase was higher than that to the KCl solution. In the NaCl system, it would be easy to form the complex even in the case using the unsaturated solution because the solubilization rate of AOT was higher. Thus, both K_P values between the unsaturated and presaturated systems were similar each other. On the other hand, thedifference in AOT concentration between in the unsaturated and presaturated solution was not negligible in the KCl system because of the lower solubilization rate of AOT, and this leads to the higher K_P value in the presaturated system. The electrostatic interaction between the protein and surfactants is reduced with increasing the salt concentration due to the electrostatic screening effect, and then it would be difficult to form the protein-surfactant complex. Therefore, there is no significant difference in the K_P value between the unsaturated and presaturated systems in the higher concentration region of KCl.

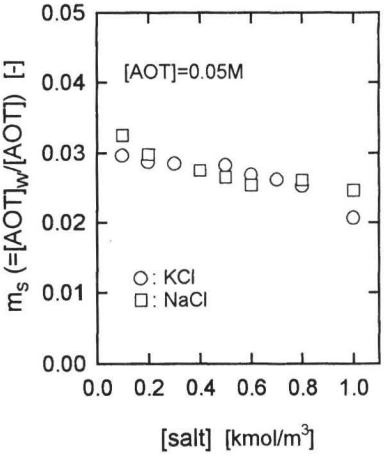


Figure 6 Distribution ratio of AOT between organic and aqueous phases.

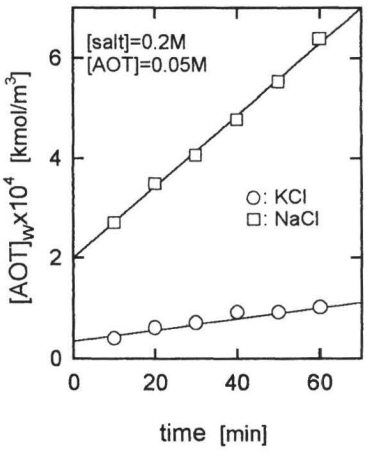


Figure 7 Solubilization rate of AOT from organic to aqueous phase.

From these results, we would improve our interfacial distortion model[1] for protein extraction into reverse micelle at oil-water interface. A protein will adsorb a few surfactants in the aqueous phase to form the protein-surfactant complex. The surfactants could be adsorbed at the protein surface by the electrostatic interaction rather than the hydrophobic interaction. This complex diffuses through the aqueous boundary film and then approached the oil-water interface according to the concentration gradient. The interface is distorted so as to surround the complex with more surfactants, forming the interfacial complex. When the hydrophobicity of this complex is sufficiently high, the complex can be solubilized in the organic phase and the surfactants will be rearranged to make the protein filled reverse micelle.

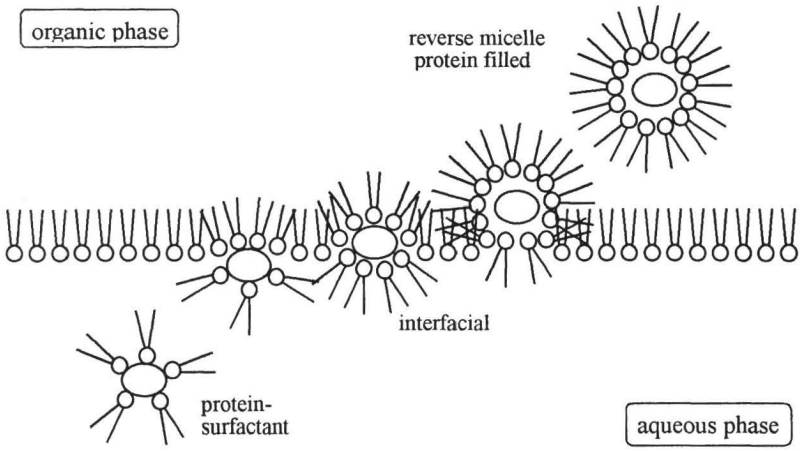


Figure 8 Schematic model for protein extraction from aqueous to organic phase via protein-surfactant complex.

CONCLUSIONS

The extraction kinetics of lysozyme from aqueous salt media to organic reversed micellar solution was studied to elucidate an entrapping mechanism of protein into reverse micelles at the oil-water interface. In conclusion, the following results were obtained.

1) The K_P value of lysozyme from the aqueous KCl solution presaturated with AOT organic solution is higher than that obtained for the unsaturated system in the higher pH region.

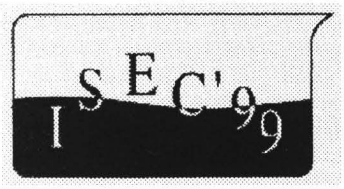
2) The K_P value from aqueous NaCl presaturated solution was similar to that from unsaturated solution, whereas the higher extraction rate was observed in the presaturated system in the lower KCl concentration.

3) The solubilization rate of AOT to the aqueous NaCl phase was higher than that to the KCl solution. This will affect the formation of protein-surfactant complex in the aqueous phase and thus cause the difference in the extraction rate of protein between the unsaturated and presaturated system.

4) The interfacial distortion model via formation of protein-surfactant complex in the aqueous phase was proposed. We can conclude that the complex formation of protein and surfactant promote the protein extraction.

REFERENCES

1. Kinugasa T, Okuda Y, Koishi N, Kawajiri K, Nishioka K, Watanabe K and Takeuchi H, *"Value Adding Through Solvent Extraction"*, ed Shallcross DC et al, Proc ISEC'96 University of Melbourne, **2**, 1414, (1996)
2. Adachi M and Harada M, *J.Phys.Chem.*, **97**, 3631, (1993)
3. Paradokar VMand Dordick JS, *Biotechnol.Bioeng.*, **93**, 994, (1994)
4. Goto M, Ono T, Nakashio F and Hatton TA, *Biotechnol.Bioeng.*, **54**, 26, (1997)



REVERSE MICELLAR EXTRACTION OF PROTEINS USING pH RESPONSIBLE MIXED MICELLAR SYSTEMS

K Shiomori[1], T Honbu[1], Y Kawano[1], R Kuboi[2] and I Komasawa[2]

[1]Dept. Materials Sci., Miyazaki Univ., Miyazaki, Japan

[2]Dept. Chem. Sci. & Eng., Osaka Univ., Toyonaka, Osaka, Japan

ABSTRACT

In mixed micellar systems of sodium bis(2-ethylhexyl)sulfosuccinate and long chain alkyl amines, such as tri-*n*-octylamine and bis(2-ethylhexyl)amine, di-*n*-octylamine, and *n*-octylamine, the extraction characteristics of proteins and water were investigated. Extraction of water into the mixed micellar systems, which would affect protein extraction, was controlled by the pH value in the aqueous phase. The pH dependence of the water extraction was affected by the basicity of the amines added. Reverse micelles do not form from the mixture of AOT and cationic species of long chain alkyl amines at acidic pH range. Extraction of lysozyme was controlled by the formation of the reverse micelles. The formation of aggregates of proteins triggered by the electrostatic interaction with AOT was suppressed in the mixed micellar systems. The proteins extracted into the mixed micellar systems could be fully back-extracted by destruction of the micelles at acidic pH values.

Keywords: Reverse micelles, Protein extraction, Amines, AOT.

INTRODUCTION

Reverse micelles have been extensively investigated as a media for extraction of proteins and enzymes[2,5,6,8]. Most previous studies were carried out in the system using sodium bis(2-ethylhexyl) sulfosuccinate (AOT) as surfactants. Extraction of proteins with the AOT reverse micellar system can be carried out by control of the electrostatic interaction. Thus forward extraction can be carried out at a pH lower than the isoelectric point (pI) of protein, where proteins have a positive charge, and back extraction at pH higher than the pI, where proteins have a negative charge. The electrostatic interaction can be most effective for the extraction of protein. However, at the same time, the electrostatic interaction often causes a structural change and inactivation of proteins.

Some studies have been reported on the control of the formation of reverse micelles by pH,[3,4] pressure[7] and temperature[1] for the purpose of developing novel and effective extraction processes of protein.

In this paper, the mixed systems of AOT and long chain alkyl amines, such as tri-*n*-octylamine (TOA), bis(2-ethylhexyl)amine (DEHA), di-n-octylamine (DOA), n-octylamine (OA) were used as a reverse micellar solution. The effect of pH on the extraction characteristics of lysozyme and water in the mixed micellar systems was investigated.

EXPERIMENTAL

The surfactant used to construct reverse micelles was sodium bis(2-ethylhexyl)sulfosuccinate (AOT) from Nacalai Tesque Co. The long chain alkyl amines used as additives for the modification of the reverse micellar system, are shown in figure 1. AOT was dissolved in isooctane, and then the amine was solubilized in the solution. A buffer solution containing NaCl (0.1 - 1.0 M) was used as the aqueous phase. Acetic acid-sodium acetate (pH 3-6), dimethyl glutamate-NaOH (pH 5-8), glycine-NaOH (pH 9-11) and Na_2HPO_4-NaOH (pH 11-12) were used as a buffer at 50 mM in all experiments. Egg white lysozyme was purchased from Wako Pure Chemical Co. Protein was dissolved in the buffer solution containing salt

Extractions of water and proteins were carried out by the following method. The same volume (5 ml) of the organic and the aqueous solutions were placed in the screw capped sample tube. The two phases were dispersed completely by a magnetic stirrer for 30 minutes at 298 K. After mixing, the

© 2000 Society of Chemical Industry

solution was separated into two phases by centrifugation at 3,500 rpm for 30 minutes. Back-extraction of proteins from the micellar phase was carried out by contacting the organic phase containing the extracted protein with a new aqueous phase in the same manner as for the forward extraction. The water concentration in the micellar organic phase after extraction was determined by Karl-Fisher titration with Kyoto Electronics MKS-1s. The concentration of protein in the aqueous and the organic phases was measured by the adsorption at 280 nm. using Hitachi UV 3200.

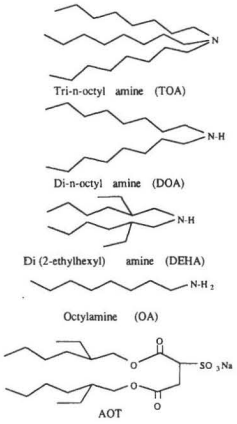


Figure 1 Structures of the amine added and AOT.

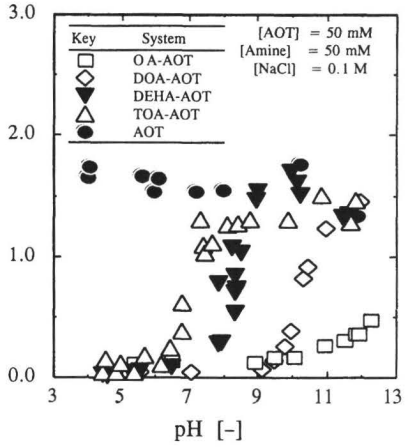


Fig. 2 Effects of pH on the water extraction in the AOT, the mixed systems.

RESULTS AND DISCUSSION

Extraction of water

The extraction of water by the AOT reverse micellar system and the mixed system of AOT and long chain alkylamine was carried out at 0.1 M NaCl and various pH values. The effects of pH on the water extraction in the AOT, the mixed systems are shown in figure 2. Extraction of water in the AOT system was not influenced by the pH values. In the mixed micellar systems with long chain alkyl amines, the water extracted into the organic phase decreased with a decrease in pH at pH range lower than a specific pH value and was negligibly small at further lower pH range. The pH values at which water extraction begins to decrease are dependent on the kind of amine. On the other hand, water extraction of both mixed systems at high pH range was not affected by pH and was the same degree with that of the AOT system.

The effect of the concentration of long chain alkylamines added to the system was examined. The mixed solutions were contacted with the aqueous phase containing 0.1 M NaCl at various pH values. The results in the TOA-AOT and the DEHA-AOT systems are shown in figure 3. The water extraction at all concentrations of the amines decreased with pH. In the low pH range, the concentration of water in the organic phase increased with decreasing in the amine concentration and was negligibly small at the amine concentration almost equal to or higher than the concentration of AOT.

Model of the control of micellar formation

In the mixed micellar systems containing both AOT and long chain alkylamines, the water

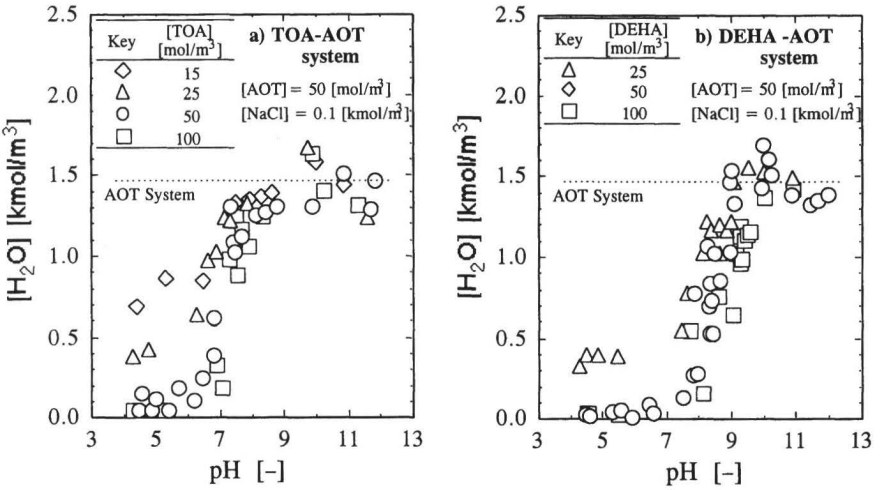


Figure 3 Effect of the concentration of long chain alkyl amines on the pH dependence of the water extraction in the mixed micellar systems. a) TOA-AOT system, b) DEHA-AOT system

extraction is controlled by pH in the aqueous phase. This shows that the formation of the micelles can be controlled by pH. The control mechanism of the micellar formation in the mixed micellar systems of AOT and the amines is illustrated in figure 4.

The amines, B, undergo protonation and form a cationic ammonium ion in acidic pH range as follows:

$$B + H^+ \longrightarrow BH^+ \qquad (1)$$

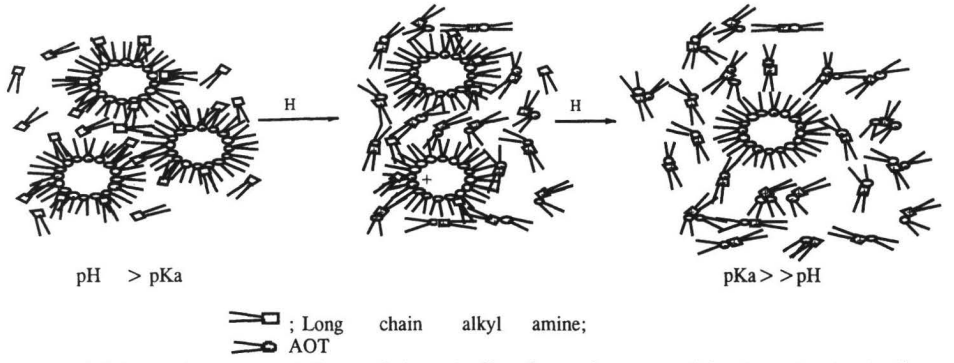


Figure 4 Schematic representations of the micellar formation control in the mixed micellar systems of AOT and the long chain alkylamines.

This reaction will be affected by the basicities of the amine added. The ammonium ion formed reacts with AOT by electrostatic interaction and the intermolecular ion complex is formed as follows:

$$AOT + BH^+ \longrightarrow AOT\text{-}BH \qquad (2)$$

It is considered that the complex has less surface activities and no ability to form reverse micelles, and consequently water is not extracted into the organic phase. A large decrease in water extraction in the

acidic pH range and a concentration of the amines lower than that of AOT is inexplicable by only the reaction presented by Equation (2). Hence, the complex, AOT–BH, is considered to further react with AOT as follows:

$$\text{AOT–BH} + (n\text{-}1)\text{AOT} \longrightarrow (\text{AOT})_n\text{–BH} \quad (3)$$

The decrease in the water extraction is considered to be due to the consumption of AOT, which forms reverse micelles and extracts water, by these complexation reactions.

Extraction of lysozyme by the mixed micellar systems

Since in the mixed micellar systems consisting of both AOT and long chain alkyl amine, it is able to control the micellar formation by pH change, it is expected to control the protein extraction based on the micellar formation. The extraction of lysozyme was carried out using the mixed micellar systems.

Forward extraction

Extraction of lysozyme was carried out at 0.1 mol/dm^3 NaCl by the AOT, TOA-AOT and DEHA-AOT systems. Effect of pH on the extraction of lysozyme is shown in figure 5. The extracted fraction into the micellar phase, E_f, and the removed fraction from the aqueous phase, R_f, are plotted against pH. In the AOT system, lysozyme extraction effectively occurred at wide pH range around neutral pH. In the pH range lower than 5, E_f was decreased, however, R_f is very high and a large amount of aggregates was observed at the interface and in the aqueous phase. Lysozyme is considered to be denatured by strong electrostatic interaction with AOT.

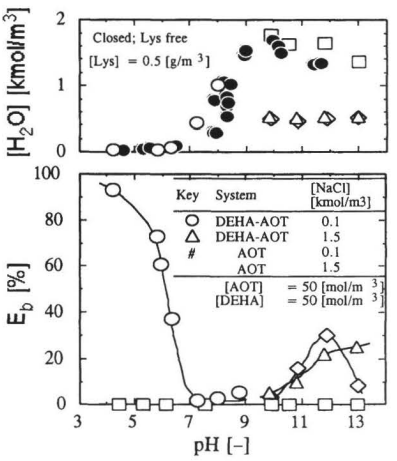


Figure 5 Effect of pH on the extraction of lysozyme at 0.1 mol/dm^2 NaCl in the AOT, TOA-AOT and DEHA-AOT systems.

E_f in the TOA-AOT and DEHA-AOT mixed micellar systems also decreased with an increase in pH values lower than a certain pH, which is, however, higher than that in the AOT system. In this time, R_f decreased with pH and the aggregations were not formed. The decrease in both E_f and R_f almost corresponded to the decrease in the water extraction. Because the reverse micelles does not form at acidic pH,as shown in earlier section, it is considered that lysozyme extraction does not occur.

Back-extraction of proteins from the micellar phase.

Back-extraction of lysozyme extracted into the micellar phase at pH 9 and 0.1 mol/dm^3 NaCl was carried out using a new aqueous phase at various conditions. The effect of pH on the back-extracted fraction, E_b, into the aqueous phase is shown in figure 6 together with that in the AOT system. In the AOT system, lysozyme could not be back-extracted using the aqueous phase containing 0.1 mol/dm^3 NaCl regardless of the pH values. By increasing NaCl concentration up to 1.5 mol/dm^3, lysozyme could be back-extracted at pH values higher than the pI.

Since lysozyme is basic protein and has very high pI (pI = 11.1), back-extraction of lysozyme in the AOT system requires the aqueous phase at very high pH range and high salt concentration. The extraction process in such a condition is likely to cause denaturation and inactivation of proteins. Further, a desalting process is needed in the following process. In the DEHA-AOT mixed micellar system, lysozyme was effectively back-extracted at more acidic pH range than the extraction where the water extraction is very low and the reverse micelles are not formed. This efficiency of the lysozyme back-extraction in the DEHA-AOT system is considered to be due to the destruction of the reverse micelles resulting from the complex formation between AOT and cationic ammonium ion formed at acidic pH range. The back-extraction characteristics of lysozyme at pH range higher than

the pI was almost the same with that in the AOT system. The mixed micellar systems can control the extraction of proteins by only pH change.

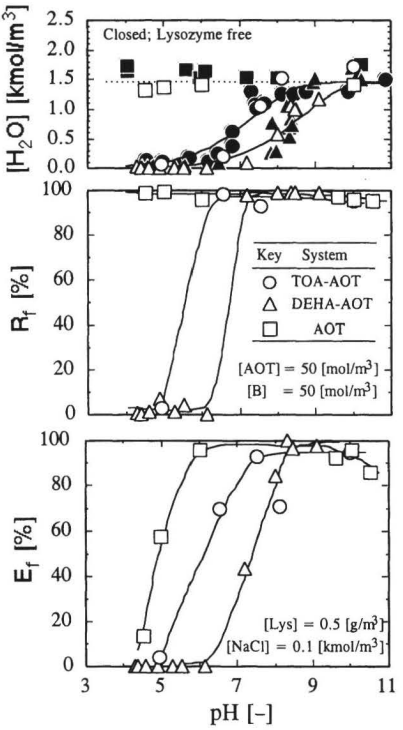


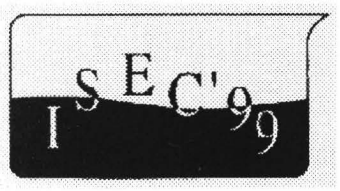
Figure 6 Effect of pH on the back-extraction of lysozyme in the DEHA-AOT and the AOT systems

NOMENCLATURE

E_f = extracted fraction of protein into organic phase [%]
E_b = back extracted fraction of protein into aqueous phase [%]
R_f = removed fraction of protein from aqueous phase [%]
Wo = molar ration of water to AOT [-]

REFERENCES

1. Dekker M, van't Riet K, van Der Pol JJ, Baltussen JWA, Hilhorst R and Bijsterbosch BH, *Chem. Eng. J.*, **46**, B69, (1991).
2. Fletcher PDI and Parrott D,*'Structure and Reactivity in Reverse Micelles'*, p.303, Elsevier, Amsterdam, (1989).
3. Goto M, Kondo K and Nakashio F, *J. Chem. Eng.,Japan*, **23**, 513, (1990).
4. Kinugasa T, Hisamatsu A, Watanabe K and Takeuchi H, *J. Chem. Eng.,Japan*, **27**, 557, (1994).
5. Leodidis EB and Hatton TA,*'Structure and Reactivity in Reverse Micelles'*, p.270, Elsevier, Amsterdam, (1989).
6. Leser ME and Luisi PL, *Chimia*, **44**, 270, (1990).
7. Philips JB, Nguyen H and John VT, *Biotechnol Prog.*, **7**, 43, (1991).



EXTRACTION OF PROTEINS USING REVERSED MICELLES IN A GRAESSER "RAINING BUCKET" CONTACTOR

Ludger H Poppenborg, Somnuk Jarudilokkul and David C Stuckey

Department of Chemical Engineering and Chemical Technology
Imperial College of Science, Technology and Medicine, London SW7 2BY, UK

ABSTRACT

The partitioning of proteins between an aqueous and a reversed micellar phase represents a potentially useful method for large-scale protein extraction due to the established traditions of solvent extraction in biotechnology, and its ease of scale up. There is considerable interest in developing this method for general applications because proteins can be separated efficiently by partitioning into these reversed micellar two-phase systems. Ionic surfactants interact with proteins of opposite charge, and the equilibrium transfer of proteins into a reversed micellar phase is governed by their size, their charge, the operating pH, and surfactant concentration. Nevertheless, at present reverse micelle phases are not selective for target proteins. Hence, the aim of this work was to investigate the effect of system parameters on protein selectivity.

In this paper, we present equilibrium and kinetic data of protein partitioning between an aqueous solution and a reversed micellar phase consisting of an anionic surfactant, AOT, in 2,2,4-trimethylpentane. The aqueous solution consisted either of ribonuclease A, cytochrome c and lysozyme dissolved in buffer, or diluted hen egg white spiked with Cytochrome c. Experiments were carried out in a two-phase stirred cell with a flat interface (Lewis cell), and a Graesser raining bucket contactor, a design which is of interest in biotechnology due to its low shear and relatively large interfacial transfer area. The influence of pH, ionic strength, temperature, co-extracted proteins and mixing speed on the forward extraction of each of the proteins was examined. The formation of emulsions during mixing was also investigated.

Keywords: Reverse micelles, extraction kinetics, protein extraction, Lewis cell, Graesser contactor, AOT.

INTRODUCTION

Recent advances in genetic engineering have made it possible to produce a wide variety of proteins using recombinant microorganisms, or more traditional animal cell cultures. Therefore, cost effective methods that can separate, concentrate and purify proteins continuously, and can be easily scaled-up are of great commercial interest. One such method which has this potential is liquid-liquid extraction utilizing reverse micelles.[3] Reverse micelles are thermodynamically stable nanometer-sized water droplets within an organic solvent stabilized by a monolayer of surfactant molecules. Their inner cores contain an aqueous microphase which is able to solubilize bioproducts such as amino acids, and proteins. The protein is still active inside the core,[4] and can be re-extractacted into an aqueous phase under certain conditions. However, a number of key questions need to be answered in order for this technique to be scaled up to a commercial process. These questions revolve around issues such as selectivity, protein activity recovery, phase separation, emulsification and contactor design.

The effect of system parameters on both forward and backward transfer of proteins using reverse micelles needs to be studied in more depth in order to improve the selectivity of the system for specific proteins. In forward transfer, the major system parameters have been defined as pH and salt concentration in the aqueous phase,[3] and surfactant and solvent type and structure in the organic phase.[5] Hence, selective extraction can be achieved by adjusting the optimum pH and ionic strength. More recently, coupling of liquid-liquid extraction with tailor-made affinity interaction has been developed to selectively purify and separate specific proteins.[6,7] Interestingly, while the kinetics of reverse micellar extraction of proteins have been studied in a stirred cell with a flat interface,[8] these findings have not yet been used for the kinetic separation of proteins.

Most work on reverse micelles has been done in small scale experiments in which the aqueous and organic phase are thoroughly mixed in test tubes and then centrifuged to achieve phase separation.

© 2000 Society of Chemical Industry

This usually gives two clear phases, but often a gel-like precipitate containing valuable protein occurs at the interface. Very high shear forces during the mixing might be partly responsible for this. In large scale reverse micellar extraction intense mixing leads to emulsification and makes phase separation difficult. Therefore, a contactor design that reduces or eliminates emulsion formation without markedly reducing the rate of extraction is needed. A Graesser "raining bucket" contactor[2] is a design that enables mixing with low shear and a relatively large interfacial transfer area.

The objective of this work was to investigate the kinetics of protein partitioning in a Lewis cell, and to examine the possibility of kinetically separating proteins in a Graesser contactor. In addition, the formation of emulsions during reverse micellar extraction was also investigated.

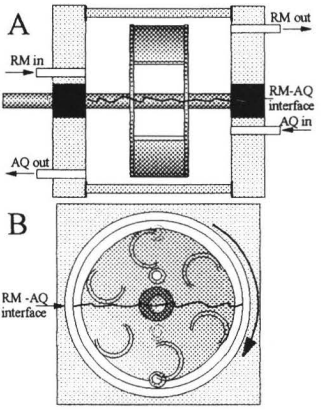


Figure 1. Diagram of a single compartment Graesser contactor; side view (A) and front view (B).

EXPERIMENTAL

Bis(2-ethylhexyl)sulfosuccinate sodium salt (AOT) and 2,2,4-trimethylpentane (isooctane) were obtained from Sigma (Poole, UK). KCl, KH_2PO_4, K_2HPO_4, K_2CO_3 and $KHCO_3$ were Anal-R grade from Merck (Dorset, UK). Trioctyl-methylammonium chloride (TOMAC), lysozyme (hen egg white; pI 11; 14300 Da), ribonuclease A type IIA (bovine pancreas; pI 7.8; 13700 Da) and cytochrome c (horse heart; pI 10.6; 12348 Da) were purchased from Sigma. Hen egg white was separated from egg yolk from fresh eggs bought at a local supermarket. All other chemicals were purchased from Sigma and were of analytical grade.

Forward extraction procedure

The reverse micellar phase consisted of 50 mM AOT in isooctane. Aqueous solutions for forward transfer consisted of 50 mM KCl and 50 mM K-phosphate or K-carbonate buffer made up to the required pH, containing 1.0 g/L cytochrome c, 1.5 g/L lysozyme or 2.1 g/l ribonuclease A. Hen egg white was diluted fifteen-fold in the same buffer adjusted to pH 9, and 1 g/L cytochrome c was added. Forward extraction was performed by contacting equal volumes of aqueous phase and reverse micellar phase in a Lewis cell (total volume 128 mL) or a Graesser contactor (total volume 450 mL, Figure 1). After half filling these contactors with aqueous solution they were then filled carefully with reverse micellar solution. The solutions were adjusted to the desired temperature prior to contacting.

Protein assay

The concentration of each protein in the aqueous phase was determined using an HPLC system (Shimadzu, UK) fitted with a Zorbax 300SB C8 reversed phase chromatography column (Jones, UK). The peak areas of the absorbance at 280 nm were used to calculate the protein concentrations. Protein concentrations in reverse micellar phases were measured after back-extraction by adding 500 µL of 60 mM TOMAC in isooctane and 500 µL aqueous solution consisting of 50 mM KCl and 50 mM potassium phosphate buffer pH 8 to 500 µL of organic phase sample in a 1.5 mL test tube.[9] The test tubes were then rotary inverted at 50 rpm for 10 min. Phase separation was achieved by centrifuging the tubes for 2 min at 12000 rpm. It was assumed that 100% of the protein in the reverse micellar phase sample had been back-extracted into the aqueous phase. The coefficient of variation for the entire back-extraction process was ±2%.

Determination of overall mass transfer coefficients in a Lewis cell

Experiments were conducted in a temperature controlled Lewis cell. The impeller speeds were set to result in laminar flow (*Re*=1000) in both phases. 500 µL samples were taken from the aqueous as well as the reverse micellar phase at certain times. Y in Equation 1 (with initial protein concentration in the aqueous phase c_{aq}°, protein concentration in the reverse micellar phase c_{rm}, surface area A, phase volume V, phase distribution coefficient m_{ft}) was plotted against the extraction time. Only the protein concentration values of samples which gave a straight line in this plot were used for further calculations (usually the first five to eight samples). After linear fitting, the slope of the regression line gave the overall mass transfer coefficient (k_0). All experiments were done in duplicate, and the coefficient of variation for k_0 was ±8%.

$$\ln[\{c_{aq}^{\circ} - (1 + 1 / m_{ft})\, c_{rm}\} / c_{aq}^{\circ}] / (A / V) / (1 + 1 / m_{ft}) = Y \qquad (1)$$

RESULTS AND DISCUSSION

Equilibrium experiments in 1.5 mL test tubes showed that the optimum conditions for reverse micellar extraction were pH 5-10.5 and 50-500 mM KCl for lysozyme, pH 5-10 and 50-250 mM KCl for cytochrome c, and pH 4.5-6.5 and 25-100 mM KCl for ribonuclease A, respectively. Therefore it is possible to separate each of these proteins from the others with one or two reverse micellar extraction steps simply by choosing the right pH and ionic strength.[3] The pI of the target protein is of particular importance in reverse micellar extraction using ionic surfactants, since the higher the net (opposite) charge of the protein, the stronger will be the driving force for extraction.[10] This electrostatic driving force also influences the mass transfer kinetics of reverse micellar extraction.[11] Our measurements of the individual overall mass transfer coefficients, k_0, of lysozyme, cytochrome c and ribonuclease A in a Lewis cell (Table 1) showed that at pH 5.5 - a pH at which the equilibrium distribution of the three proteins is very similar - cytochrome c was extracted fastest, followed by ribonuclease A and lysozyme, but with all k_0 values in the same range.

Table 1
Overall mass transfer coefficient, k_0, for lysozyme, cytochrome c and ribonuclease A obtained in a Lewis cell. All experiments were carried out at 4°C. Numbers in brackets are the k_0 values based on protein appearance in the reverse micellar phase. The standard deviation of the measurements was ±8%. n.d.: not detected.

pH	lysozyme	cytochrome c	ribonuclease A
		$k_0 \times 10^{-6}$ [m sec^{-1}]	
10	1.23 (0.75)	0.04 (0.01)	n.d.
5.5	2.74 (0.56)	5.25 (4.08)	3.23 (2.69)

It appears from this data that other factors besides electrostatic interactions have an effect on the extraction kinetics, because one would expect a much lower k_0 value for ribonuclease A since it has a much lower pI than the other two proteins. Wolbert et al.[12] showed that the symmetry of charge distribution had an effect on extraction equilibrium, and the less symmetrically the charge was distributed on the protein surface the higher the amount of protein extracted. The charge distribution of cytochrome is less symetrical compared to lysozyme, which might explain its faster extraction.

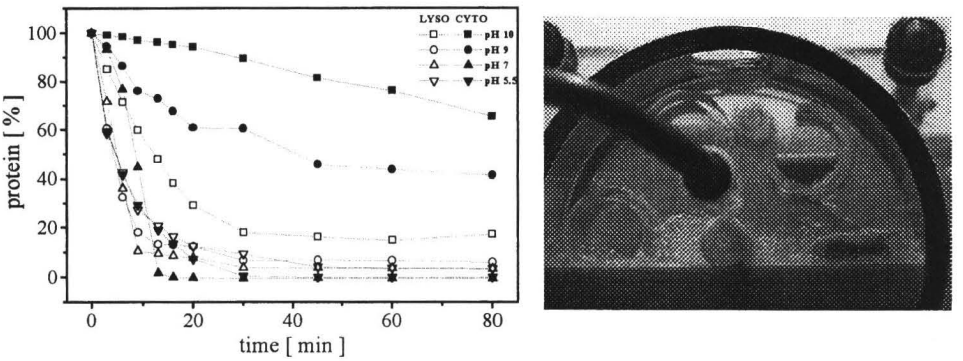


Figure 2. A) Disappearance of cytochrome c (cyto) and lysozyme (lyso) during extraction in a single compartment Graesser contactor at different pH. The extractions were carried out at 4°C and 3 rpm. B) Side view of a single compartment Graesser contactor during the extraction of cytochrome c and lysozyme.

A different situation occured at pH 10, where ribonuclease A was not extracted, but where both lysozyme and cytochrome c were extracted almost completely (~95%). Here, the k_0 of lysozyme was considerably higher than that of cytochrome c. Electrostatic attraction is low at this pH, which is close to both proteins pI, and hydrophobic interaction seem to have a greater effect on the extraction kinetics. It has been reported[13] that both cytochrome c and lysozyme were solubilised in the interfacial zone of reverse micelles, and our results sugest that lysozyme interacts more strongly with this interface than cytochrome c.

Experiments with a single compartment Graesser contactor (Figure 2) confirmed the findings from the Lewis cell. At a pH close to the pI of cytochrome c and lysozyme, the latter was transferred to the reverse micellar phase much faster. This difference between the two proteins became much less pronounced at more acidic pHs, and at pH 5.5 cytochrome c was extracted slightly faster than lysozyme. At pH 10 the two proteins could be separated kinetically if the extraction in the Grasser was stopped after 30 minutes, with more than 83% of the lysozyme already extracted into the reverse micellar phase, and only 11% of the cytochrome c. This separation can be improved if the rotor speed is set to only 2 rpm (data not shown). Not surprisingly, higher rotor speeds lead to faster extraction, mainly as an effect of an increased surface area. Higher temperatures also increased the extraction rate due to higher diffusion and coalescence rates. However, higher rotor speeds also caused an increase in emulsion formation.

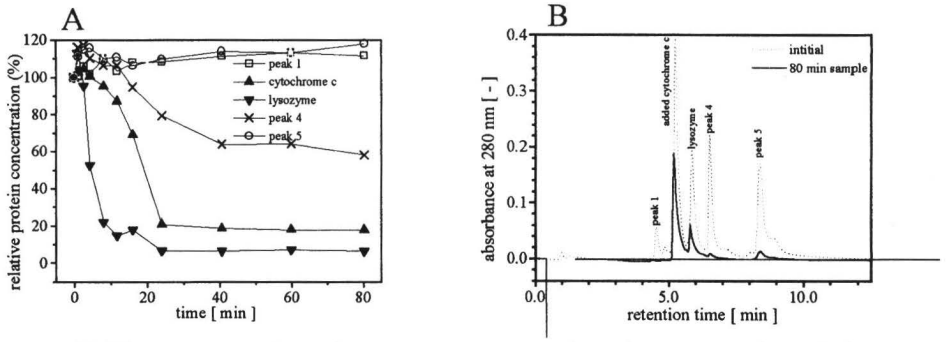


Figure 3. A) Disappearance of cytochrome c and lysozyme from the aqueous phase during extraction with a single compartment Graesser contactor at pH 10, 4°C, and 3 rpm. B) HPLC

chromatograms of the initial fifteen-fold diluted hen egg white with 1 g/L cytochrome c added, and the proteins found in the organic phase after 80 min extraction in the Graesser.

We also investigated the performance of the Graesser contactor for the reverse micellar extraction of hen egg white as a protein source.[14] Figure 3A shows that the extraction of lysozyme from egg white was very similar to the extraction from pure buffer under the same conditions of temperature, rotor speed and pH. Somewhat surprising is the much faster extraction of added cytochrome. This might have been caused by the higher viscosity of the egg white solution. Also, a very different phase behaviour was observed during the extraction. After 80 min the Graesser contactor was almost totally filled with an emulsion, with only a little clear top phase left. Only after the contactor was left on the bench for ~ 2 days did the emulsion brake completely. In experiments with buffer both phases stayed fairly clear throughout the 80 min of extraction (see Figure 2B). Figure 3B shows that the added cytochrome c and lysozyme were extracted to high purity, despite the emulsion. Only a few low strength impurities were found in the reverse micellar phase.

CONCLUSIONS

Kinetic data obtained from experiments with a stirred cell with a flat interface (Lewis cell) showed that the pH not only influenced the phase distribution equilibrium of reverse micellar extraction, but also the extraction kinetics. This is because the pH determines the net surface charge of a protein, and consequently the electrostatic attraction to a charged surfactant. At pHs close to the pI of a protein other factors became important such as hydrophobic interactions.

These phenomena can be used to kinetically separate proteins, and this was demonstrated with lysozyme and cytochrome c in a single compartment Graesser contactor. In such a contactor a simple protein solution and a reverse micellar solution can be mixed gently with little emulsion formation or precipitation. For more complex solutions like diluted egg white, even the slow mixing in a Graesser leads to the formation of an emulsion at the interface, and this can eventually occupy the whole reactor. For the continuous operation of such a contactor clear phases are required in order to avoid additional centrifugation or settlements. Hence, further investigations into the reasons for emulsification are necessary.

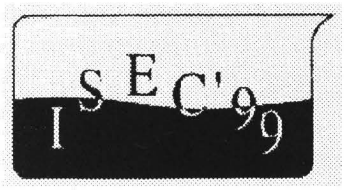
ACKNOWLEDGEMENT

The authors wish to thank the Biotechnology and Biological Sciences Research Council for their support of this project.

REFERENCES

1. Lewis JB. *Chem. Eng. Sci.* **3**, 260-278, (1954)
2. Sheikh AR Ingham J and Hanson C *Trans. Inst. Chem. Eng.* **50**, 199-207, (1972)
3. Göklen KE and Hatton TA *Sep. Sci. Tech.* **22**, 831-841, (1987)
4. Martinek K, Levashov AV, Klyachko N. Khemelnitski YL and Berzin IV *Eur. J. Biochem.* **155**, 453-468, (1986)
5. Mat HB, *Ph.D. thesis*, Imperial College of Science, Technology and Medicine, London, UK (1994).
6. Adachi M, Yamazaki M, Harada M, Shioi A and Katoh S. *Biotechnol. Bioeng* **53**, 406-408, (1997)
7. Paradkar VM and Dordick JS. *Biotechnol. Prog.* **7**, 330-4, (1991)
8. Lye GJ, Asenjo JA and Pyle DL. *Chem. Eng. Sci.* **49**, 3195-3204, (1994)
9. Jarudilokkul S, Poppenborg LH and Stuckey DC. *Biotechnol. Bioeng.* (1999), in press
10. Pires MJ, et al. Biotechnol. Bioeng., **44**, 773-780, (1994)

11. Dekker M, Van't Riet K, Bijsterbosch BH, Fijneman P and Hilhorst R. *Chem. Eng. Sci.*, **45**, 2949-2957, (1990)
12. Wolbert RB, et al. *Eur. J. Biochem.*, **184**, 627-33, (1989)
13. Naoe K, Tamai M, Kawagoe M, Imai M and Shimizu M *Trans IChemE*, **75C**, 143-147, (1997)
14. Naoe K, Shintaku Y, Mawatari Y and Kawagoe M *Biotechnol. Bioeng.*, **48**, 333-340, (1995)



TAILORING OF REVERSE MICELLAR SYSTEMS FOR SELECTIVE SEPARATION OF PROTEINS USING PROTEIN–PROTEIN AFFINITY INTERACTIONS

M Adachi, M Harada, A Shioi and S Katoh[1]
Institute of Advanced Energy, Kyoto University, Uji, Kyoto 611-0011, Japan
[1]Department of Chemical Science and Engineering, Kobe University, Rokko-dai, Kobe 657-8501, Japan

ABSTRACT
An ideal bioaffinity separation of proteins can be realized using reverse micellar systems composed of nonionic surfactants instead of ionic surfactants. Reverse micelles composed of ionic surfactants have essential disadvantages, i.e., denaturation and unsuitability for selective separations. Reverse micelles composed of nonionic surfactants interact with proteins mildly, resulting in low denaturation of proteins and are unable to extract water-soluble proteins. Thus, reverse micellar system composed of nonionic surfactants provides an ideal system when the affinity ligands are introduced to the system. We extended this method for protein-protein affinity interaction system. Tiny amount of trypsin in many contaminating proteins, i.e., trypsin in pancreatin could be recovered selectively without loss of activity using trypsin inhibitor immobilized in reverse micelles. Chymotrypsinogen could be separated selectively using antigen-antibody reaction system, which enables to extend this method to any kind of target proteins.

Keywords: Bioaffinity separation, pancreatin, trypsin, antigen-antibody interaction, reverse micelles, nonionic surfactant

INTRODUCTION

Selective separation of a target protein from a mixture containing many contaminating proteins is a central issue for bioaffinity separation. In recent years, separation of proteins using bioaffinity ligands has been investigated by several research groups in reverse micellar systems.[1-4] The selective separation, however, has not been sufficiently achieved in reverse micellar systems, because the reverse micelles composed of ionic surfactants have been mainly used for protein separation.

Ionic surfactant such as sodium bis(2-ethylhexyl)sulfosuccinate (AOT) interact strongly with the opposite charge residues on the protein surface by electrostatic interactions, causing denaturation of proteins. The adsorption of surfactant molecules by electrostatic interactions makes the protein surface hydrophobic, resulting in the solubilization of the protein into the reverse micellar phase.[5] By this mechanism, many kinds of proteins are extracted to the reverse micellar phase under usual operating conditions, preventing selective separation of a target protein.

Reverse micelles composed of nonionic surfactants interact mildly with proteins, resulting in low denaturation of proteins and have almost no capability to extract water-soluble proteins, because of no strong interactions between the reverse micelles and the proteins. The driving force of the extraction is originated from the entropic effect, i.e., the dispersion of proteins to the water pool of the micelles.[6] In fact, reverse micelles composed of tetra-oxyethylenemonodecylether (C10E4) hardly extract water-soluble proteins such as cytochrome c, lysozyme, chymotrypsinogen and concanavalin A.[7,8] Therefore, reverse micelles composed of nonionic surfactant provide an ideal system for selective separation of proteins if a protein-specific interaction is introduced into the system.

We reported that concanavalin A was extracted selectively from contaminating proteins by using alkyl-pyranoglucosides as affinity ligands.[7] We extended this method to a typical protein-protein interaction system, i.e., trypsin-trypsin inhibitor (TR-TRI) system. TR from bovine pancreas (B-TR) was selectively separated by the forward and backward extractions using TRI, which was immobilized in the reverse micelles composed of nonionic surfactant by covalently combining cholesteryl groups.[8]

In this paper, we present that tiny amount of trypsin in many contaminating proteins, i.e., trypsin in pancreatin can be recovered selectively without loss of activity by reverse micellar extraction operations using TRI immobilized in reverse micelles as an affinity ligand. We also

© 2000 Society of Chemical Industry

extended this method to the antigen-antibody interaction system in order to enable the selective separation of any kind of target proteins, using chymotrypsinogen-anti-chymotrypsinogen antibody system.

EXPERIMENTAL

Materials

Pancreatin from porcine pancreas, trypsin from porcine pancreas (P-TR) type IV, trypsin inhibitor (TRI) from soybean type I-S, chymotrypsinogen-A (CTN) from bovine pancreas type II-A, lysozyme (LYZ) from chicken egg white grade IV and rebonuclease (RNase) from bovine pancreas type II-A were purchased from Sigma Chemical Co. The antisera against chymotrypsinogen-A raised in rabbits. Specific antibodies were purified by affinity chromatography using antigen-Sepharose 4B. Tetra-oxyethylenemonodecylether (C10E4) was purchased from Nikkol, and was used as supplied. Cholesteryl-chloroformate (CC) and αN-benzoil-DL-arginine-p-nitroanilide (BAPA) were purchased from Aldrich Chemical Co. Inc. and Nacalai Tesque Inc., respectively. Distilled water, spectroscopic reagent-grade n-hexane, reagent grade tris(hydroxymethyl)aminomethane (Tris), sodium chloride and hydrogen chloride were used.

Immobilization of Trypsin Inhibitor or anti-CTN antibodies in Reverse Micelles

TRI was solubilized into the reverse micelles composed of C10E4 by the injection method. A typical procedure is as follows: TRI (20 mg) was dissolved in 0.35 cm^3 of 0.1 mol/dm^3 borate buffer (pH 12), and this TRI solution was mixed with 10 cm^3 of 0.2 mol/dm^3 C10E4 solution in n-hexane to solubilize in the reverse micelles. Then, 1 cm^3 of 0.1 mol/dm^3 of CC solution in n-hexane was added to the reverse micellar solution of C10E4. Cholesteryl groups were introduced to amino groups of lysine residues of TRI at 298 K for 20 hours. Finally, the reverse micellar phase was washed with 0.05 mol/dm^3 Tris-HCl buffer solution containing 0.2 mol/dm^3 NaCl (pH 8) to remove water-soluble components.

Anti-CTN antibodies were immobilized in reverse micelles as follows: 0.6 cm^3 of 0.01 mol/dm^3 borate buffer solution containing antibodies (1.64×10^{-5} mol/dm^3, pH 9) was injected in 22 cm^3 of 0.2 mol/dm^3 C10E4/n-hexane solution. Then, 0.1 cm^3 of 1.66×10^{-4} mol/dm^3 CTN aqueous solution was added to the C10E4 solution to protect the biding sites of antibodies. After several hours, 0.1 cm^3 of 0.05 mol/dm^3 of CC solution in n-hexane was added to the reverse micellar solution of C10E4, and the solution was kept at 298 K for 20 hours. Thereafter, the reverse micellar phase was washed with 0.03 mol/dm^3 HCl solution containing 0.2 mol/dm^3 NaCl.

The amount of immobilized TRI or antibodies was determined from that remained in the reverse micellar phase after washing.

Forward and Backward Extractions

The forward extraction procedure for P-TR from pancreatin is as follows. Pancreatin (100 mg) was dissolved in 10 cm^3 of 0.05 mol/dm^3 Tris-HCl buffer (pH 8) containing 0.2 mol/dm^3 NaCl. Since the aqueous solution was slightly turbid, the solution was centrifuged, because P-TR dissolved in the solution completely. After centrifugation, the supernatant solution was contacted with the same volume of reverse micellar phase containing immobilized TRI (the feed concentration ratio [P-TR]/[TRI] was mostly 2), and P-TR was extracted. Before back-extraction, the reverse micellar phase was washed by 0.05 mol/dm^3 Tris-HCl (pH 8) buffer containing 0.2 mol/dm^3 NaCl. Backward extraction of P-TR from the reverse micellar phase was performed successfully using an 0.015 mol/dm^3 hydrochloric acid aqueous solution containing 0.2 mol/dm^3 NaCl. The experimental temperature was 298 K.

The extraction procedure of CTN by anti-CTN antibodies from contaminating proteins is as follows: a mixture of four types of protein (CTN, LYZ, TRI, RNase) in 0.05 mol/dm^3 Tris-HCl

buffer (pH 8) containing 0.2 mol/dm^3 NaCl was contacted with reverse micellar phase containing antibodies and CTN was extracted. Back extraction of CTN from the reverse micellar phase was performed successfully using 0.05 mol/dm^3 borate buffer solution (pH 11) containing 0.2 mol/dm^3 NaCl and 5 vol.% of ethanol. Temperature was kept at 308 K.

Measurements of Concentration of P-TR or CTN and Activity of P-TR

The concentrations of P-TR or CTN were measured by the optical density at 280 nm (the molecular absorption coefficient was 3200 and 5133 m^2/mol, respectively) when it existed without contaminating proteins. The concentration of P-TR in the aqueous solution of pancreatin or CTN in the mixture solution was determined by hydrophobic-interaction liquid chromatography with Shodex HICPH-815 column (length 7.5 cm, diameter 8 mm) at 1.0 cm^3/min by a linear gradient from 1.7 mol/dm^3 ammonium sulfate to 10 mmol/dm^3 borate buffer solution (pH 7.5) for 30 minutes.

The activity of TR was measured from the hydrolysis rate of BAPA as a function of TR concentration.[9] The sample solution containing TR (300□l) was added to 3cm^3 of 0.001 mol/dm^3 BAPA solution in 0.05 mol/dm^3 Tris-HCl buffer (pH 8), and the time course of the absorbance at 410 nm was measured.

RESULTS AND DISCUSSION

Extraction of P-TR from Pancreatin

The extraction of P-TR from pancreatin is characterized by co-existence of large amounts of various contaminating proteins. The reverse micelles composed of nonionic surfactants have no specific interactions with water-soluble proteins. Thus, the driving force of the extraction is only the entropic effect, i.e., dispersion of protein molecules to the water pools of the micelles. The amounts of proteins extracted by the entropic effect are usually very small. However, when the amounts of contaminating proteins are over several tens of a target protein, the contaminating proteins cannot be neglected.

Since the target protein P-TR is bound tightly with the immobilized affinity ligand TRI, simple washing procedure are expected to remove the contaminating proteins easily from the reverse micellar phase. Thus, we tried the separation procedure shown in figure 1. The immobilized TRI was prepared as mentioned above. The resultant liquid chromatograms for the washing aqueous solutions and for the final product after back-extraction are shown in figure 2.

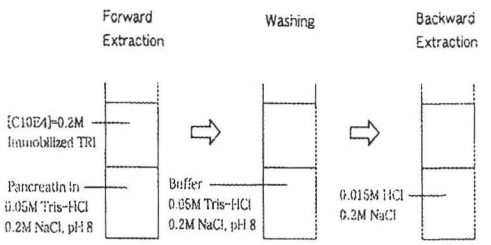


Figure1. Procedure of selective separation of trypsin for pancreatin from porcine pancreas

The original solution of pancreatin included a large amount of contaminating proteins with the retention time less than 10 minutes and also a small amount of those with the retention time from 25 to 45 minutes. The aqueous solution of pancreatin was contacted with the micellar phase. At this stage, negligible amounts of the proteins with retention time 25 to 45 minutes were extracted to the micellar phase. However, appreciable amount of the components with the retention time less than 10 minutes was extracted, because the aqueous phase after first washing did not contain the contaminating proteins with the retention time from 25 min to 45 minutes, but contained those with the retention time less than 10 min. After second washing, no contaminating proteins were detected, indicating that the contaminating proteins were washed out completely by the first wash. No loss of the extracted P-TR was detected through the washing process. Finally, the P-TR in the reverse micellar phase was backextracted by HCl solutions.

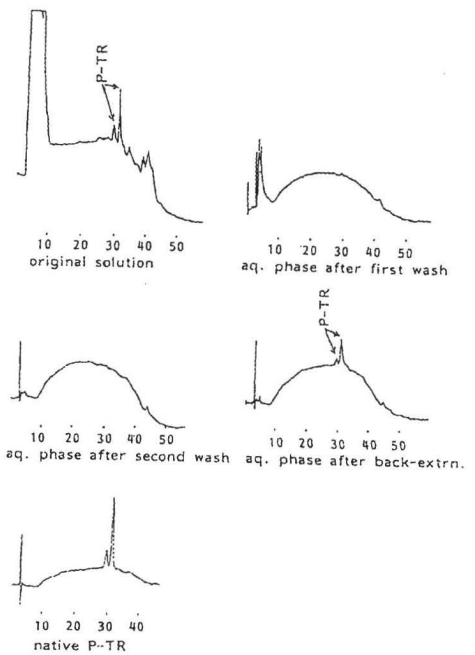


Figure2. Liquid chromatograms in selective separation of TR from pancreatin. Liquid chromatogram of the native P-TR is also shown.

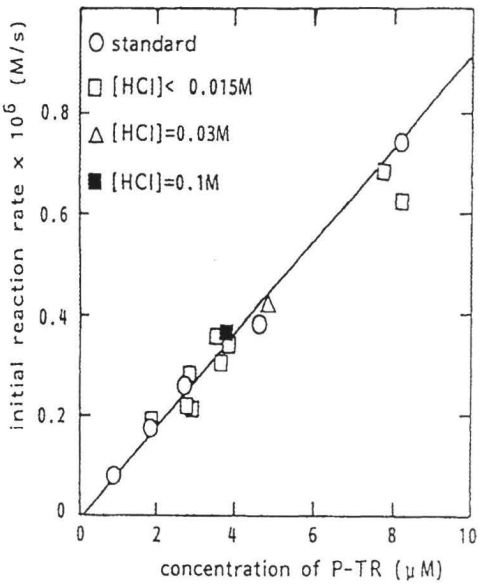


Figure 3. Activity of recovered TR from pancreatin.

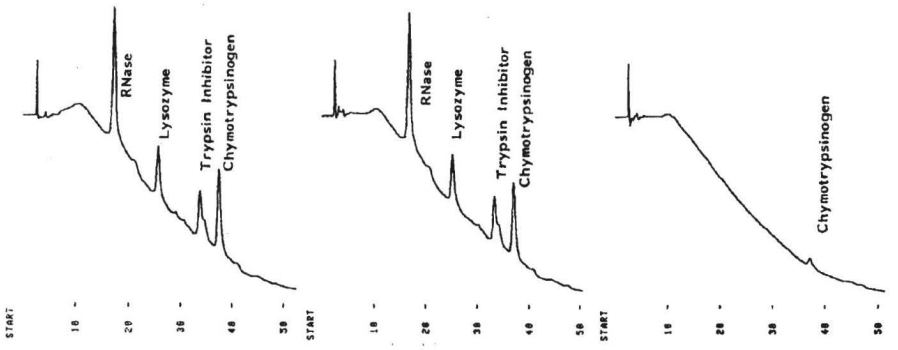
The aqueous solution after the backward extraction contained only P-TR, because the chromatogram after the backward extraction agreed with that of native P-TR. Thus, the selective separation of P-TR from many contaminating proteins was realized by the present method. The overall recovery of P-TR was around 35 % to 50 % at present.

The enzymatic activity of the recovered P-TR was measured from the hydrolysis rate of BAPA as a function of P-TR concentration. As shown in Figure 3, the activity agreed with that obtained using standard P-TR, indicating that the P-TR in the product retains its enzymatic activity. Self-digestion for P-TR was not observed for the recovered P-TR. This is very advantageous for the separation of proteases. Both TRI in the forward extraction process and the acidic condition in the backward extraction process prevent the self-digestion of P-TR.

Extraction of CTN Using Immobilized Anti-CTN Antibodies

The extraction of CTN by the immobilized anti-CTN antibodies was not observed when antibodies were immobilized by CC without protection of binding sites with antigen. The immobilized antibodies became active when the binding sites of them were protected with antigen, and the concentration of CC for immobilization was decreased. The immobilized fraction of antibodies to the feed was about 55% under this condition described in the experimental section.

The selective separation of CTN using antibodies immobilized in a C10E4 reverse micelles was examined by extracting CTN from a mixture of four proteins, i.e., RNase (4.22×10^{-6} mol/dm^3), LYZ (7.24×10^{-7} mol/dm^3), TRI (1.24×10^{-6} mol/dm^3) and CTN (8.91×10^{-7} mol/dm^3) in Tris-HCl buffer (pH 8). The backward extraction was carried out using a 0.05 mol/dm^3 borate buffer solution (pH 11) containing 0.2 mol/dm^3 NaCl. Figure 4 shows chromatograms of this experiment. It is clearly shown that CTN was selectively extracted from the aqueous feed solution, because the aqueous solution after the backward extraction contained only CTN. The concentrations of RNase, LYZ and TRI in the aqueous phase after the forward extraction were the same as those in the aqueous feed solution, whereas, only CTN concentration decreased. The recovered CTN concentration was 9.6×10^{-8} mol/dm^3, and the active fraction of binding sites of antibodies was 21% for this experiment.



original solution | aq. Phase in forward extraction | aq. Phase in backward extraction

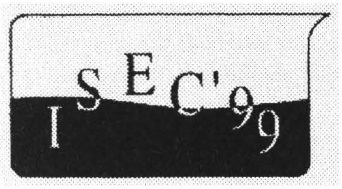
Figure 4 Liquid chromatograms in selective separation of CTN using anti-CTN antibodies.

CONCLUSION

Selective separation of porcine trypsin from pancreatin was achieved without loss of activity of the recovered trypsin using trypsin inhibitor immobilized in reverse micelles composed of a nonionic surfactant. Chymotrypsinogen was selectively separated from a protein mixture using anti-chymotrypsinogen antibodies immobilized in reverse micelles composed of the same nonionic surfactant tetra-oxyethylenemonodecylether.

REFERENCES

1. Woll JM, Hatton TA and Yarmush ML, *Biotechnol. Prog.*, **5**, 57, (1989).
2. Coughlin RW and Baclaski JB, *Biotechnol. Bioeng.*, **6**, 307, (1990).
3. Paradkar VM and Dordick JS, *Biotechnol. Prog.*, **9**, 199, (1993).
4. Kelley BD, Wang DIC and Hatton TA, *Biotechnol. Bioeng.*, **42**, 1199, (1993).
5. Adachi M and Harada M, *J.Phys.Chem.*, **97**, 3631, (1993).
6. Shioi A, Harada M, Takahashi H and Adachi M, *Langumuir*, **13**, 609, (1997).
7. Adachi M, Harada M, Shioi A, Takahashi H and Katoh S, *J.Chem.Eng.Japan*, **29**, 982, (1996).
8. Adachi M, Yamazaki M, Harada M, Shioi A and Katoh S, *Biotechnol. Bioeng*, **53**, 406, (1997).
9. Erlanger BF, Kokowsky N and Cohen W, *Arch. Biochem. Biophys.*, **95**, 271, (1961).



SELECTIVE SEPARATION OF α-AMYLASE, BOVINE SERUM ALBUMIN AND TRYPSIN INHIBITOR USING REVERSE MICELLES

Somnuk Jarudilokkul, Ludger H Poppenborg and David C Stuckey

Department of Chemical Engineering and Chemical Technology, Imperial College of Science, Technology and Medicine, Prince Consort Road, London SW7 2BY, UK

ABSTRACT

Protein mixtures consisting of ∝-amylase, bovine serum albumin and trypsin inhibitor, all of which have similar pIs but different molecular weights, were used as a model mixtures. Parameters examined in the forward extraction from buffer solution were pH and surfactant concentration. It was found that a minimum surfactant concentration exists for extracting 90% individual proteins, and this parameter together with pH can be used to selectively extract specific proteins from buffer solution.

Keywords: Reverse micelles, Protein extraction selectivity

INTRODUCTION

Liquid-liquid extraction is a traditional chemical engineering unit operation for which the design and scale up of both batch and continuous processes is relatively easy, and the use of such an established system for bioseparation is attractive. However, the low solubility of most commercially interesting solutes in solvents has traditionally precluded its widespread application to the separation of many polar biological products. Reverse micellar solutions are an attractive organic solvent system for use in the liquid-liquid extraction of biological products because many biochemicals, including amino acids, proteins, and nucleic acids, can be solubilised within and recovered from such solutions without loss of native function.[1] A reverse micelle is a nanometer-sized droplet of an aqueous solution stabilised in an apolar environment by the presence of surfactant at the interface. The potential application of reverse micelles in biotechnology is: as a media for hosting enzymatic reactions, and as an extractant for hydrophilic bioproducts. The ability of reverse micelle systems to selectively extract a target protein from a mixture is known to be influenced by a number of factors, particularly pH, salt type and concentration, solvent type, temperature, surfactant type and concentration, and the incorporation of bioaffinity ligands.[2,3] However, the question of controlling the selective solubilization of proteins into a reverse micellar phase has only been addressed by a few researchers. It has been demonstrated that the separation of a single protein from a simple synthetic protein mixture can be accomplished relatively easily.[2] Woll and Hatton[4] separated ribonuclease A from concanavalin A, while Aires-Barros and Cabral [5] were able to separate a crude mixture of two lipases in buffer solution. Furthermore, it was shown that a reverse micellar phase can selective extract alkaline protease from whole fermentation broth.[6] Recently, Krei and Hustedt[7] extracted α-amylase from a complex fermentation medium. However, there were many problems encountered in these studies, in particular low extraction yields and severe emulsion formation, and a number of key system variables have not been investigated in much depth. Therefore, to improve protein selectivity, a number of important system parameters such as surfactant concentration and temperature, still need to be studied.

The objective of this study was to examine the specific effects of surfactant concentration and pH on the selective solubilization of proteins in a reverse micellar phase. In particular, altering the minimum surfactant concentration required for the complete forward extraction of a single protein (cytochrome c and lysozyme)[8,9] has shown the potential of this parameter to selective separate a

© 2000 Society of Chemical Industry

target protein from a protein mixture. A protein mixture of α-amylase, bovine serum albumin and trypsin inhibitor was used as a model system because while the molecular weight of the proteins are different, the pIs are quite similar. This mixture represents a realistic challenge to this separation technique.

MATERIALS AND METHODS

Bovine serum albumin (BSA, pI 4.6; 65000 Da), trypsin inhibitor (TryI, pI 4.5; 24500 Da), α-amylase (pI 4.6; 55000 Da) and 2,2,4-trimethylpentane (isooctane), were purchased from Sigma (Poole, UK). Cetyltrimethylammonium bromide (CTAB) was obtained from Aldrich (Dorset, UK). All other chemicals were purchased from Sigma and were of analytical grade.

Forward extraction

All forward extractions were performed in duplicates by contacting the aqueous and reverse micelle phases (hexanol:isooctane (1:9)) in a 1.5 ml test tube at room temperature. The salt concentration in the aqueous phase was kept constant at 0.1 M NaCl. The organic phase consisted of 3.13-50 mM cationic surfactant CTAB in hexanol:isooctane. The proteins, 1g/l α-amylase, 1 g/l bovine serum albumin, 1 g/l trypsin inhibitor, were dissolved in an 80% 0.1M NaCl and 20% 0.1 M phosphate buffer at pH 4-11. The ternary protein mixture consisted of 1g/l α-amylase, 1 g/l bovine serum albumin and 1 g/l trypsin inhibitor which were dissolved in the same phosphate buffer at pH 4-11. Extraction equilibrium was achieved by rotary inversion at 50 rpm for 30 min. Samples were then centrifuged at 3000 rpm for 5 minutes to separate the phases, and the aqueous phase was then analysed by HPLC.

Protein assay

The concentration of protein in the aqueous phase was determined by HPLC. A Zorbax 300 SB C8 reversed phase column was fitted to a Shimadzu A-6 chromatography system, and UV detection was used at 280 nm. The protein was eluted from the column with a mobile phase consisting of 0.1% trifluoroacetic acid and acetonitrile (gradient 0 -70%v/v) at a flow rate of 1.5 ml/min. The coefficient of variation was ±2%.

RESULTS AND DISCUSSION

Single protein extraction

The extraction yield of the three proteins, α-amylase, bovine serum albumin and trypsin inhibitor were studied as a function of pH and CTAB concentration, and this data is shown in figure 1. The CTAB concentration at which 90% extraction was attained was defined as the minimal CTAB concentration, and from experimental data this was found to be 6.25, 6.25 and 25 mM for α-amylase, bovine serum albumin and trypsin inhibitor, respectively.

These concentrations were found to depend on the pH, and the minimal concentration given is the one measured at the optimum pH for extraction of each protein, which was pH 10, pH 6 and pH 11 for α-amylase, bovine serum albumin and trypsin inhibitor, respectively and this variation can be explained by the hydrophilicity of each protein. The order of elution from a hydrophobic HPLC column showed that trypsin inhibitor was more hydrophilic than bovine serum albumin and α-amylase (figure 5). Hence for more hydrophilic proteins there is a greater amount of water surrounding them, and hence higher minimal surfactant concentrations and greater pH driving force are required for substantial protein solubilization.

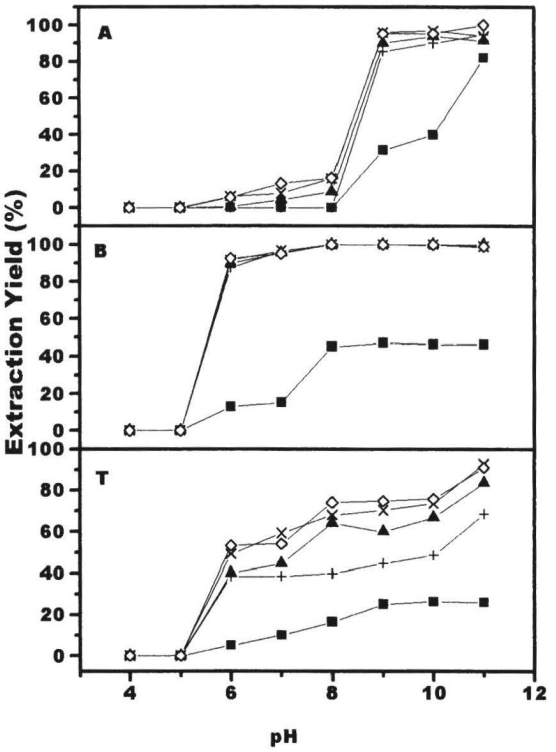


Figure 1 Effect of pH and surfactant concentration on the extraction yield of : α-amylase (A), bovine serum albumin (B), and trypsin inhibitor (T) at ◊ 50 mM CTAB, × 25 mM CTAB, ▲ 12.5 mM CTAB, + 6.25 mM CTAB, and ■ 3.13 mM CTAB.

Ternary protein extraction

Figures 2-3 show the effect of surfactant concentration and pH on the extraction of the three proteins with reverse micelles. Under the optimum conditions (6.25 mM CTAB and pH 7) bovine serum albumin can be separated (95 versus 15 and 5%) from the mixture as shown in figure 3. Finally, trypsin inhibitor can be separated from α-amylase using the conditions, 50 mM CTAB and pH 7, as shown in figure 4. Wolbert *et al.*,[10] reported that the higher the molecular weight of the protein, the greater the shift of extraction pH (pH_{ext}) from the isoelectric point. Therefore, the pH_{ext} of the three proteins should be in the order of BSA pH_{ext} > α-amylase pH_{ext} > TryI pH_{ext}, and this occurs with the separation behaviour of α-amylase and trypsin-inhibitor. However, the separation of bovine serum albumin indicates that the transfer of the protein is due not only to the effect of electrostatic interactions, but also to hydrophobic interactions. This result has also been reported by Lu Quing *et al.*[11] This observation was confirmed by HPLC data (figure 5) which shows that the hydrophobicity of α-amylase and bovine serum albumin are both greater than trypsin inhibitor.

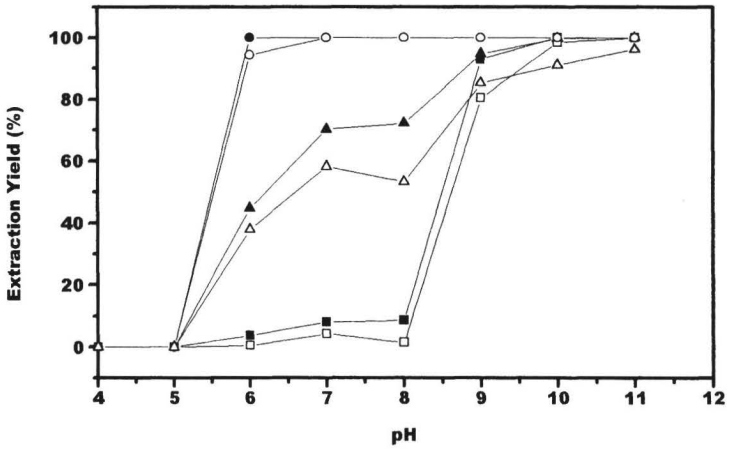


Figure 2 Effect of pH and surfactant concentration on the extraction of the three proteins: ■α-amylase 50 mM CTAB, □ α-amylase 25 mM CTAB, ● BSA 50 mM CTAB, * BSA25mM CTAB,4 TryI 50 mM CTAB, 6 TryI 25 mM CTAB.

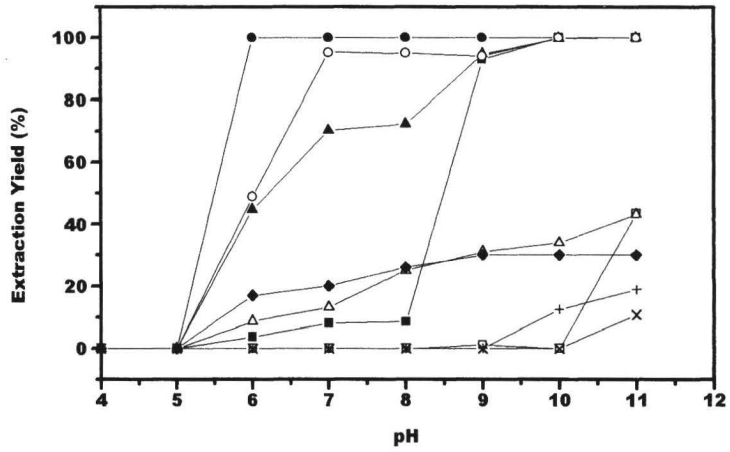


Figure 3 Effect of pH and surfactant concentration on the extraction of the three proteins: ■ α-amylase 12.5 mM CTAB, □ α-amylase 6.25 mM CTAB, × α-amylase 3.13 mM CTAB, ● BSA 12.5 mM CTAB, * BSA 6.25 mM CTAB, ♦ BSA 3.13 mM CTAB, 4 TryI 12.5 mM CTAB, 6 TryI 6.25 mM CTAB, + TryI 3.13 mM CTAB

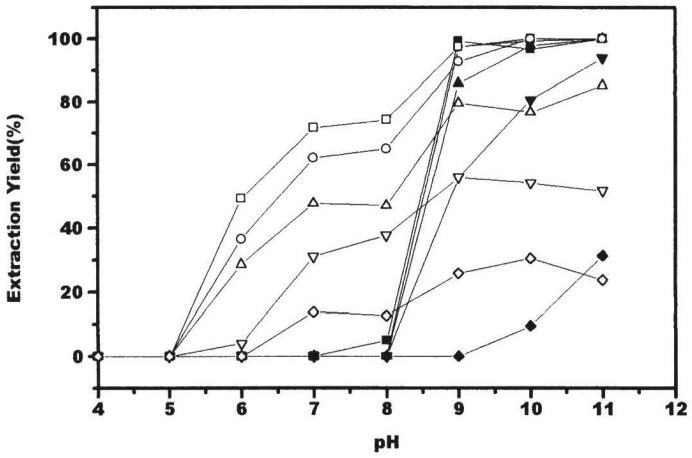


Figure 4 Effect of pH and surfactant concentration on the extraction of the two proteins: ■ α-amylase 50 mM CTAB, ● α-amylase 25 mM CTAB, 4 α-amylase 12.5 mM CTAB, 5 α-amylase 6.25 mM CTAB, ɜ α-amylase 3.13 mM CTAB, □ TryI 50 mM CTAB, * TryI 25 mM CTAB, 6 TryI 12.5 mM CTAB, 7 TryI 6.25 mM CTAB, (TryI 3.13 mM CTAB.

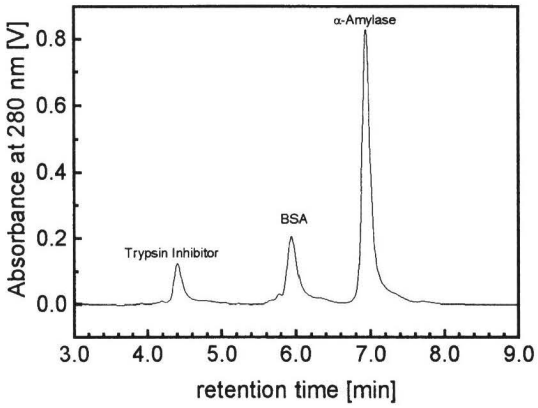


Figure 5 HLPC chromatogram of α-amylase, BSA and trypsin inhibitor

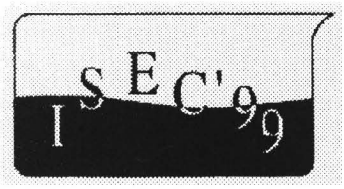
CONCLUSIONS

- A minimal AOT concentration exists, defined as the surfactant concentration required for ≥ 90% protein extraction, which is dependent on both solution pH and the hydrophobicity of the protein. For α-amylase, bovine serum albumin and trypsin inhibitor these values were 6.25, 6.25, and 25 mM CTAB at pH 10, 6, and 11 respectively.

- Selective separation of a protein mixture which all have the same pIs, but different molecular weights, can be achieved by using variations in the optimum surfactant concentrations and pH
- The main driving force involved in the transfer of α-amylase and trypsin-inhibitor is electrostatic interaction, whereas hydrophobic interactions between protein and surfactant play an important role in the case of bovine serum albumin.

REFERENCES:

1. Martinek K, Levashov AV, Klyachko N, Khmelnitski YL and Berzin IV *Eur. J. Biochem.* **155**, 453, (1986).
2. Göklen KE and Hatton TA *Sep. Sci. Technol.* **22**, 831, (1987).
3. Kelly BD, Wang DIC and Hatton TA *Biotechnol. Bioeng.* **42**, 1199, (1993).
4. Woll JM and Hatton TA *Bioprocess Eng.* **4**, 193, (1989).
5. Aires-Barros MR and Cabral JMS *Biotechnol. Bioeng.* **38,** 1302, (1991).
6. Rahaman RS, Chee JY, Cabral JMS and Hatton TA *Biotechnol. Prog.* **4**, 218, (1988).
7. Krei GA and Hustedt H *Chem. Eng. Sci.* **47**, 99, (1992).
8. Noe K, Imai M and Shimizu M *Trans IChemE.* **74**, 163, (1992).
9. Ichikawa S, Imai M and Shimizu M *Biotechnol. Bioeng.* **39**, 20, (1992).
10. Wolbert RBG, Hilhorst R, Voskuilen G, Nachtegaal H, Dekker M, van't Riet K and Bijsterbosch BH *Eur. J. Biochem.* **184**, 627, (1989).
11. Lu Q, Li K and Shi Y *Chinese J. Chem. Eng.* **1**, 184, (1993).



STRATEGIES FOR EXTRACTION METHODS IN THE EXTRACTIVE FERMENTATION PROCESS OF CARBOXYLIC ACID

Wei Qin[1] and Shang Tian Yang[2]

[1]Department of Chemical Engineering, Tsinghua University, Beijing 100084, China

[2]Department of Chemical Engineering, The Ohio State University, Columbus, Ohio, 43210, USA

ABSTRACT

Extractive fermentation affords a means of avoiding product inhibition by the removal of product during the fermentation process. The fermentation broth of the carboxylic acid is a solution with low concentration, multiple components and high pH. The lower content of solvent can be used, that is also good for reducing the toxic to bacteria. Higher concentration ratio of product to the other component is benefit for obtaining higher purity of the product. The extractive fermentation can be carried out by attaching the extractor to the homolactic fermentor, even the homoacetic fermentation process run at higher pH. 94% purity of acetic acid can be obtained by controlling the concentration ratio in the extractive fermentation. The concentration ratio at inlet of extractor is constant for parallel fermentation process. The higher purity of the product still can be obtained by using the fractional extractor.

Keywords: Extractive Fermentation, Carboxylic acids.

INTRODUCTION

Extractive fermentation is a typical combination process of separation method with reaction. *In-situ* extractive fermentation of carboxylic acid resulted in reducing end-product inhibition during fermentation and obtained higher cell density, product yield and productivity.[1-7] Product in fermentation process can be removed by extraction attached with the fermentation that makes it possible to carry out a continuous fermentation process. According to the extraction method, aqueous two-phase extraction,[6,8] adsorption to solid sorbents [3,4,9] and reactive extraction with organic solvent [1,2,7,10-14] were mainly used in extractive fermentation process.

Liquid-liquid extraction is a typical technique used commonly in the biotechnology industry for product recovery. The use of organic solvent for extraction products during fermentation often limited by the incompatibility of the solvent, or the toxicity to the cell. Long-chain alcohol served well for the extraction compatibility since they are less toxic to micro-organism.[7] The toxic solvent affected the cells through two mechanisms: the water-soluble portion and the immiscible portion. While immobilization significantly protected the cells from immiscible solvent phase, adding soybean oil to the *k*-carrageenan matrix could trap the diffusing solvent molecules, and therefore reduce the toxic effect of the water-soluble solvent [11]. There has been increasing interest in using membrane in such extractive modes as a means of increasing transfer area, reducing emulsification and reducing the toxic effects of the solvents on the micro-organism.[14]

The research of removal and recovery of carboxylic acid from dilute aqueous solutions have shown that extraction by reversible chemical complexation were effective. Amine-based extractants could remove carboxylic acid from solutions at pH of the fermentation broth, where the acid exists mostly as the carboxylate anion.[1,10,15-19]

This article presents the feature of fermentation process, the mechanism and characteristics of extraction process for two component system of carboxylic acid. Two typical fermentation process, serial fermentation and parallel fermentation with products of the same functional were selected as the systems. The samples of the fermentation systems were acetic acid fermentation and propionic acid fermentation respectively. The extraction with organic solvent was selected as the extractive method. The organic solvent was selected according to the polarity and the acidity of the products and by-

© 2000 Society of Chemical Industry

products in the fermentation broth. The extraction style and the flow diagram were proposed for each fermentation process.

PROCESS ANALYSES

The Feature of Fermentation Process of Carboxylic Acid

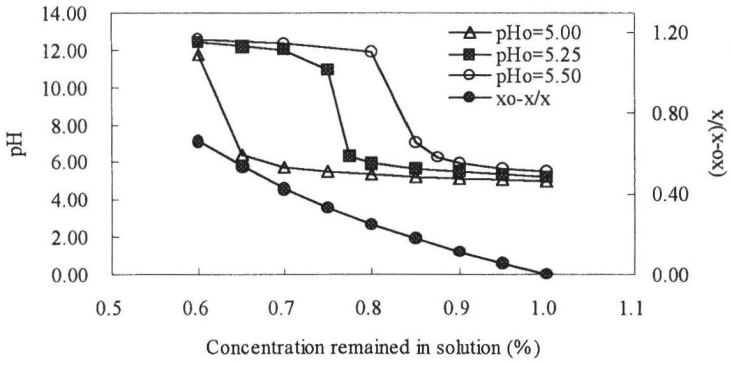
The fermentation broth of carboxylic acid is a complicated system with low concentration, multiple components and high pH. In a fermentation process, a successful fermentation results in an aqueous suspension, which contains the desired product, the cell as well as by-products and remainders from the nutrient solution, and the desired product and by-product are two main components. The pH of the growth medium is an important parameter to many fermentation processes. Usually the growth rates of micro-organisms are maximum at pH values around neutrality and fall quickly at high and low pH values. The undissociated acid was found to be more inhibitory than the dissociated acid for many carboxylic acid fermentation processes.[20,21] The medium pH influenced the dissociation of weak acid in the solution. In general, a higher final product concentration can be obtained by fermentation conducted at a higher pH value when the undissociated acid is the major inhibitor. However, some bacteria for acid product are usually limited by the low acid concentration attained in the final fermentation broth. This is due to the strong product inhibition caused by the acid.

The Behavior of Extraction Process for Fermentation Broth of Carboxylic Acid

The fermentation broth for carboxylic acid is the polar organic solutes of dilute solution. Chemical extraction is selected to remove the solutes due to decreasing distribution coefficient with the concentration. Tertiary amines seem to be more suitable extractants for carboxylic acid removal compared to the primary and secondary amines.[11] In general, the extraction power for a solvent is dictated by the difference between basicity of the amine and acidity of the acid [22] and increase with acidity of the acid.[17]

The solutions with the pH above their own values are formed by adding the base, it is obvious that the pH of the solution will increase with removal of the acid. The pH values can be calculated based on the dissociation equation (Figure 1). The results showed that the higher the initial pH, the more sensitive the solution pH to removal of the acid. It can be deduced that the recovery of the acid is lower and can not be improved by using more equilibrium stages for the fermentation process with pH above pK_a of the acid.

Figure 1.



Generally speaking, the distribution coefficient (K_d) increases with the content of solvent. Most of the content of solvent in the mixture extractant are 5%~30% for the extraction of carboxylic acid. The K_d decreases with increasing pH. The difference of K_d among the content of solvent reduces with the pH, and will be close to zero at pH about 7.00 for all of the content of solvent [23] for the extraction by hydrogen bonding. There is a big difference of the K_d between normal pH and the pH about pK_a. The lower content of solvent can be used at pH about pK_a, that is also good for reducing the toxicity to bacteria.

The extraction process of carboxylic acids consist of physical extraction and complexation extraction using solvent + diluent as the organic solvent. The equilibrium constant of physical extraction based on the hydrophobicity of the diluent is much less than that of complexation extraction, and can be neglected at pH above pK_a of the acid and the higher content of solvent. The equilibrium constant of physical extraction of the weak acid is larger than that of the strong acid. On the contrary, the equilibrium constant of complexation extraction of the strong acid is larger [17].

The extraction mechanism in mixture system is competitive extraction. One acid competes for the organic solvent with the other. The influence of the content of solvent and the pH on the K_d in the multiple component system is similar to the results in the single component. The separation factor, determined mainly by the ratio of the equilibrium constants of complexation extraction, increased with the pH and not affected by the concentration ratio and the content of solvent except for lower content significantly. The higher concentration ratio is beneficial to obtain a higher purity of the product.

Pure diluent can provide a larger separation factor, but the K_d is smaller. There is an optimum content of solvent for larger K_d and separation factor. The separation factor of the strong acid to the weak acid will be from <1 to >1 for different solvents, for instance, the separation factor for acetic acid to lactic acid is <1 for Adogen 283 as the solvent, and >1 for the Alamine 336 [24].

According to the behavior of extraction process for the fermentation broth above, it is good for higher purity of the product to operate the extraction process at higher concentration ratio of product to the other component. The lower content of solvent can be used, that is also good for reducing the toxicity to bacteria. Lower fermentation pH will provide more chance to carry out extractive fermentation.

RESULTS AND DISCUSSION

Serial Fermentation – Homoacetic and Homolactic Fermentation.

In the conversion of lactose to acetate in anaerobic fermentation, *S.lactis* and *C. Formicoaceticum* sequentially convert lactose to lactate and then to acetate. The pH should be above 5 for the first step[25], and 6.5 for the second [26]. A product concentration of 40g/l is the better result due to the inhibition of product[25].

In this system, the pK_a of acetic acid (4.76) is larger than that of lactic acid (3.86), but the weak acid is the product. It is obvious according to the literature [24] that the separation factor for tertiary amine is less than 1. A unique solvent or the physical extraction should be used to get a higher separation factor. 5% Adogen283 + 95% octanol was suggested as the solvent.

For this fermentation process, there are two types of *in-situ* extractive fermentation, extraction attached to the homolactic fermentor and the homoacetic fermentor. The pH of the extraction process is determined by the fermentation pH. The second style is not feasible due to the higher pH of the fermentation process.

The concentration ratio of the product to the other component, i.e. acetic acid to lactic acid, can be adjusted based on the material balance and pH conditions of the fermentation process. Homolactic fermentation provided not only the suitable pH for extraction process but also enough lactic acid to convert acetic acid in the next fermentation process. The homoacetate fermentation must produce the

same acetic acid from lactic acid as the removal in the extraction process at the fermentative pH. The ratio of the acetic acid to lactic acid for the first type is limited.

An immobilized column was use as the fermentor and hollow fiber membrane extractor was used for extraction process considering the toxicity of the solvent. The feasible conditions for the first type of extractive fermentation was obtained based on the fermentation mechanism and extraction equilibrium. One of the feasible conditions examined had the pH of homolactic fermentation (6.5~6.25), the pH of extractor (6.25~6.8), the pH of homoacetic fermentation (6.8~6.5). The purity of the product was about 94%, while the ratio of acetic acid to lactic acid at inlet of extractor was controlled around 10 under the above conditions.

The first type is feasible because of the suitable pH, but the purity is limited by the concentration ratio at the inlet of extractor, if the simple extraction is used. In the second type, the majority component in the fermentation broth entering the extractor is acetic acid if the fermentation process is well controlled. It is easy to obtain high purity of the product and larger extraction rate by increasing the mass transfer coefficient using increasing the flow rate of two phases. If the fermentation process can be operate at lower pH, for example, 5.5~6.0, the second style will replace the first one.

Parallel Fermentation – Propionic Fermentation.

In the conversion of glucose to propionic acid, *P. acidipropionici* is used as the bacterium, acetic acid is produced as by-product, and the product ratio of propionic acid to acetic acid is around 3:2 [14]. The operating pH values should be above 5.0. In this system, the pK_a of the propionic acid (4.87) is close to that of acetic acid (4.76). The acidity of acetic acid is little stronger than that of propionic acid. The equilibrium constant of complexation extraction is similar for those acids. However, the polarity of propionic acid is less due to the longer carbon-chain, the equilibrium constant of physical extraction is larger, propionic acid is (1.778~2.138) and acetic acid is (0.490~0.677) [28]. The separation factor should be great than 1 for normal solvent. 20% TOA+80%hexane was suggested to be the solvent[27]. The separation factor is about 4 [14]. The maximum purity of the propionic is about 85% in the conventional extractor for *in-situ* extractive fermentation. The larger separation factor is good for obtaining higher purity of the product. However, the purity can be improved by modifying the extractor. Fractional extraction is commonly used in hydrometallurgy and petroleum chemical engineering, the stripping stage back-extracts the non-product component to improve the concentration ratio in the solvent, then increases the purity of product. The other advantage of fractional extraction used in the extractive fermentation process is that the pH at the inlet of the extractor will be lower duo to joining the stripping solution with acids. Part of the stripping solution entered the extractor to keep the total volume balance.

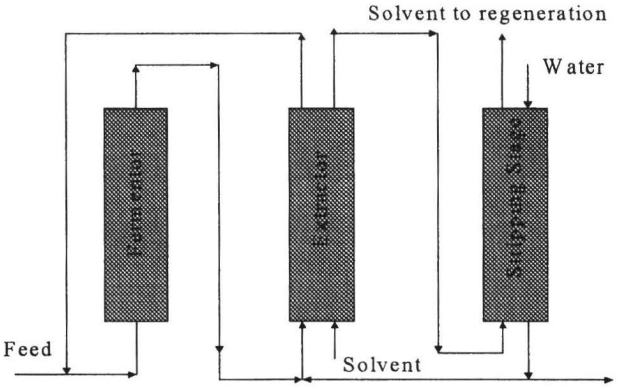


Figure 2. The Diagram of Propionic Extractive Fermentation

Figure 2 is the diagram of the propionic extractive fermentation with the fractional extraction process. Water was use as the stripping solution in the stripping stage. The hollow fiber membrane extractors were used as extraction equipment. Unlike the extraction part, the equilibrium stage numbers of the stripping extractor can be added by the requirement of the purity of product under the condition of normal pH.

CONCLUSIONS

The fermentation broth of the carboxylic acid is a solution with low concentration, multiple components and high pH. The lower content of solvent can be used, that is also good for reducing the toxicity to bacteria. Higher concentration ratio of product to the other component is benefit for obtaining higher purity of the product. Lower fermentation pH will provide more chance to carry out extractive fermentation.

Attaching the extractor to the fermentor with lower pH it is possible to carry out the extractive fermentation for serial fermentation even the product fermentation process run at higher pH. For the homolactic and homoacetic fermentation, 94% purity of acetic acid can be obtained by controlling the concentration ratio in the extractive fermentation.

The concentration ratio at inlet of extractor is constant for parallel fermentation process. The higher purity of the product still can be obtained by using the fractional extractor. The requirement for the purity of product can be obtained by adding the equilibrium stage numbers of the stripping extractor as the conventional extraction.

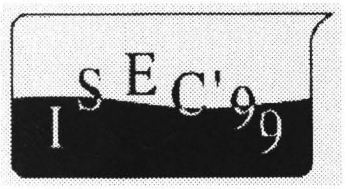
ACKNOWLEDGMENTS

Some literature in this paper was obtained when the author worked in the Ohio State University.

REFERENCES

1. Yabannavar VM and Wang DIC, *Biotechnol. Bioeng.*, **37**, 1095, (1991).
2. Lewis VP and Yang ST, *Biotechnol. Prog.*, **8**, 104, (1992).
3. Srivastava A, Roychoudhury PK and Sahai V, *Biotechnol. Bioeng.*, **39**, 607, (1992).
4. Wang J-L, Liu P and Zhou D, *Biotechnol. Techniq.*, **8**, 905, (1994).
5. Honda H, Toyama Y, Takahashi H, Nakazeko T and Kobayashi T, *J Ferment. Bioeng.*, **79**, 589, (1995).
6. Kwon YJ, Kaul R and Mattiasson B, *Biotechnol. Bioeng.*, **50**, 280, (1996).
7. Chen R and Lee YY, *Appl. Biochem. & Biotechnol.*, **63-65**, 435, (1997).
8. Planas J, Radstrom P, Tjerneld F and Hahn HB, *Appl. Microbiol. & Biotechnol.* **45**, 737, (1996).
9. Wang Z-H and Zhao K-F, *Biotechnol. Bioeng.*, **47**, 1, (1995).
10. Yabannavar VM and Wang DIC, *Ann. NY Acad. Sci.*, **506**,523, (1987).
11. Yabannavar VM and Wang DIC, *Biotechnol. Bioeng.*, **37**, 716, (1991).
12. Mueller U, Traeger M and Onken U, *Berichte der Bunsengesellschaft fuer Physikalische Chemie*, **93**, 1001, (1989).
13. Evans PJ and Wang HY, *Appl. Microbiol. & Biotechnol.*, **32**, 393, (1990).
14. Solichien MS, O'Brien D, Hammond EG and Glatz CE, *Enzyme Microb. Technol.*, **17**, 23, (1995).
15. Kertes AS and King CJ, *Biotechnol. Bioeng.*, **28**, 269, (1986).
16. Tamada JA, Kertes AS and King CJ, *Ind. Eng. Chem. Res.*, **29**,1319, (1990).
17. Tamada JA and King CJ, *Ind. Eng. Chem. Res.*, **29**,1327, (1990).
18. Tamada JA and King CJ, *Ind. Eng. Chem. Res.*, **29**,1334, (1990).
19. Yang ST and Okos MR, *J Chin. I.Ch.E.*, **22**, 410, (1991).
20. Wang G and Wang DIC, *Appl. Environ. Microbiol.*, **47**, 294, (1984).
21. Monot F, Engasser JM and Petitdemange H, *Appl. Microbiol. Biotechnol.*, **19**, 442, (1984).
22. Eyal AM and Canari R, *Ind. Eng. Chem. Res.*, **34**,1789, (1995).

23. Yang ST, White SA and Hsu ST, *Ind. Eng. Chem. Res.* **30**, 1335, (1991).
24. Qin W and Yang ST, *AIChE 1997 Ann. Meeting,* Los Angeles, California, (1997).
25. San Nicolas E, Qin W and Yang ST, *AIChE 1997 Ann. Meeting,* Los Angeles, California, (1997).
26. Tang IC, Okos MR and Yang ST, *Biotechnol. Bioeng.* **34**, 1063, (1989).
27. Fahin MA, *Sep. Sci. & Tech.*, **27**,1809, (1992).
28. Leo A, Hansch C and Elkins D, *Chemical Reviews*, **71**, 525, (1971).



RECOVERY OF CARBOXYLIC ACIDS FROM FERMENTATION BROTHS USING REACTIVE SORPTION

M Traving and H-J Bart
Universität Kaiserslautern, Lehrstuhl für Thermische Verfahrenstechnik, 67653 Kaiserslautern, Germany,

ABSTRACT
The recovery of highly diluted organic substance from viscous fermentation broths by liquid-liquid extraction is difficult. Reactive sorption can achieve very high distribution coefficients and it can be applied in fixed beds and fluidized beds, in order to handle entrained solids or high viscosity. The reactive sorption is investigated in different systems (tartaric acid / tri-n-octylamine and citric acid / tri-n-octylamine) using the macroporous resins XAD 4 and XAD 16. The equilibria are described using a modified Langmuir-isotherm, taking into account the fraction of the ion exchanger on the resin. The mass transfer in a fixed bed is calculated with a dispersion model, describing diffusion and reaction kinetics. For determination of the necessary parameters, experiments in different laboratory units are carried out. In a stirred cell the kinetics are measured to investigate the effective pore diffusion. The experimental breakthrough curves are well predicted by the model.

Keywords: reactive sorption, fermentation broth, dispersion model, citric acid, tartaric acid, extraction chromatography, XAD-4 and XAD-16 resins

INTRODUCTION

Reactive sorption is a combination of reactive extraction and adsorption.[2,3] For this unit operation a liquid ion exchanger (e.g. tri-n-octylamine) is adsorbed onto a macroporous resin (e.g. Amberlite resin XAD 16). It is possible to adsorb high concentrations of the reactive component on the surface of the resin, which enables the separation of extremely diluted feed components.[5] The result is a product adsorbed directly on the extractant-impregnated resin (EIR). One advantage of this operation is that biomolecules should not denature as in organic solvents used for the reactive extraction[1] since the surface of the ion exchanger always provides a contact with water. The EIR's are thus an alternative for recycling or separating organic substances from dilute or highly viscous aqueous solutions or fermentation broths, even in the presence of solid cell material.

EXPERIMENTAL

Reagents

Citric acid (CA, Riedel de Haen, > 99 %), tartaric acid (TA, Merk, > 99 %) and sodium acetate (NaOH, Mallinckrodt Baker, >95 %) was used in various concentrations. N-hexane (Mallinckrodt Baker, technical quality, >96 %) and tri-n-octylamine (TOA, Henkel, >95 %) was used for impregnation. For purification, n-hexane was distilled and tri-n-octylamine was washed with a 0.1 M caustic soda solution. The Amberlite resins XAD 4 and XAD 16 (Rohm & Haas) were washed with distilled water.

Impregnation

The impregnation method is based on the impregnation method published by Juang.[2] First a mixture of the selected ion exchanger (TOA) and an organic solvent (n-hexane) was produced. In the next step the macroporous resin (XAD 4 or XAD 16) was contacted with the impregnation solution. After a swelling time of 48 h the impregnation solution was deducted and the wet resin was dried at 350 K and 24 mbar. The result is a macroporous resin with a loading of ion exchanger on the surface. The

© 2000 Society of Chemical Industry

loading of ion exchanger can be determined by titration. For the titration analyses the EIR's were crushed in methanol and then titrated with a 0.05 NaOH solution. The resulting effective surface was determined by BET-surface-analysis. The results show a rapid decrease of the effective surface (figure 1). This effect is caused by filling the pore space gradually from the smallest up to the larger pores.[4]

Equilibria

The equilibrium of the reactive sorption can be described with a Langmuir-isotherm. This model gives the equilibrium for an EIR with a specific loading of ion exchanger on the surface of the macroporous resin. Whereas the traditional Langmuir-isotherm is insufficient to describe all effects occurring, a modified Langmuir-isotherm was used to describe the equilibria for a system with different loadings of ion exchanger. The dissociation constant of the isotherm can be estimated as a power function depending on the loading of ion exchanger. The number of binding sites for the organic substances is calculated with a linear function of the ion exchanger loading, which takes the inactive TOA in the sealed pores into account.

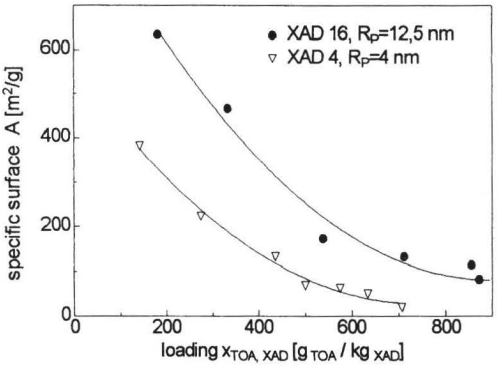


Figure 1: Influence of the ion exchanger loading on the specific surface

$$x_{org,EIR} = \frac{x_{TOA,xad}^{C_1} \cdot (x_{TOA,xad} \cdot c_2 + c_3) \cdot x_{org,aq}}{1 + x_{TOA,xad}^{C_1} \cdot x_{org,aq}} \qquad [1]$$

This modified isotherm is able to describe the equilibria in the system citric acid / TOA / XAD 16 (Fig.2) as well as in the system tartaric acid / TOA / XAD 16 (figure 3).

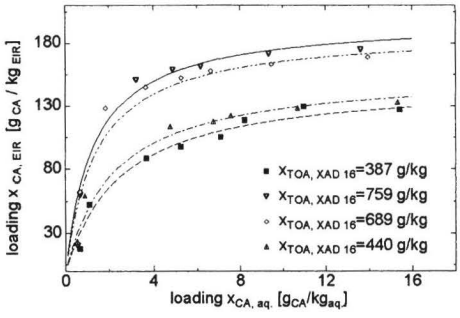


Figure 2 : Equilibria in the system citric acid / TOA / Amberlite resin XAD 16 at 25°C

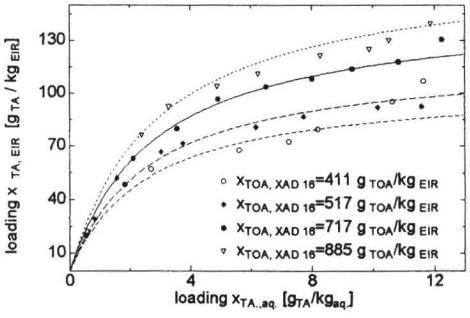


Figure 3 : Equilibria in the system tartaric acid / TOA / Amberlite resin XAD 16 at 25°C

Mass transfer

The inner mass transfer in the resin was investigated in a thermostated stirred cell. In a well mixed aqueous phase, the diffusion film surrounding the particle is negligible. In this case, the changes in the aqueous phase can be attributed to the mass transfer in the particle. The cell has a volume of 1

litre. Analysis was by an online UV- detector and HPLC. Assuming that the reaction between the organic acid and the ion exchanger is instantaneous, the effective diffusion coefficient in the pores of the particle can be determined. In a bench scale fixed bed equipment the mass transfer coefficient k_f and the axial dispersion coefficient D_{ax} were estimated. The fixed bed was equipped with an online UV-detector and a fraction collector. The column was 300 mm high and had a diameter of 30 mm and was controlled by a computer. The miniplant was able to run without any user interference for five days. In this time five sorption and desorption cycles can be freely programmed by the user (figure 4).

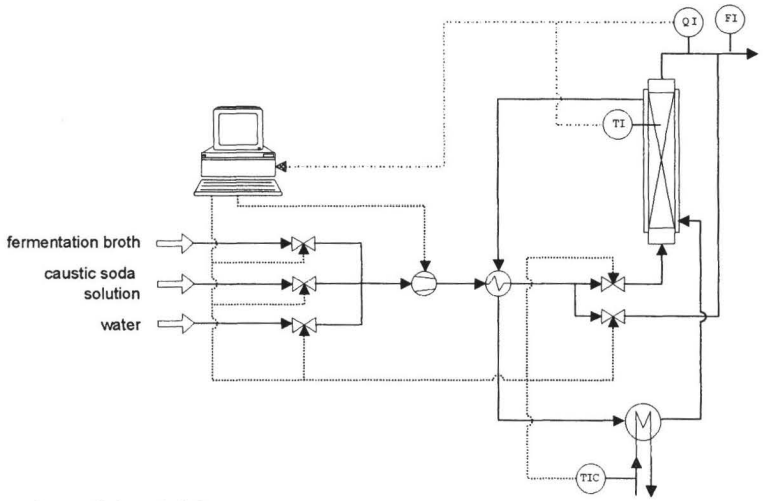


Figure 4: Flowsheet of the miniplant

RESULTS AND DISCUSSION

The mass transfer of the reactive sorption can be divided in four transport processes: convective mass transport through the fixed bed, film diffusion, diffusion through the pore system and reaction with the applied ion exchanger. The kinetics are influenced by the selected porous material. The breakthrough curve of the fixed bed using EIRs is distributed using resin with small pore diameter. This fact lead to the conclusion, that the reactive sorption is a pore diffusion limited process. Further investigations showed that the temperature has a strong effect on the kinetics. For liquid acid concentrations lower than 2 g_{ca}/kg_{aq} the corresponding EIR loading becomes extremely low with increasing temperature. This leads to a shoulder in the breakthrough curve at a concentration at about 2 g_{ca}/kg_{aq} which is confirmed in fixed bed experiments (figure 5).

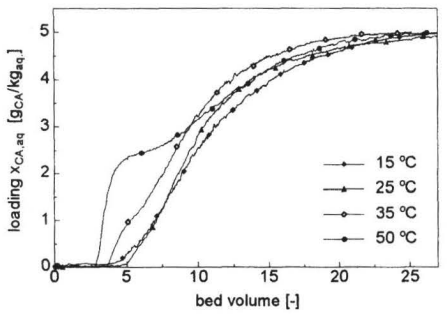


Figure 5 : Influence of the temperature on the shape of the breakthrough curve (XAD 16, F=0.5 kg/h, $x_{TOA,XAD16}$=535 g/kg)

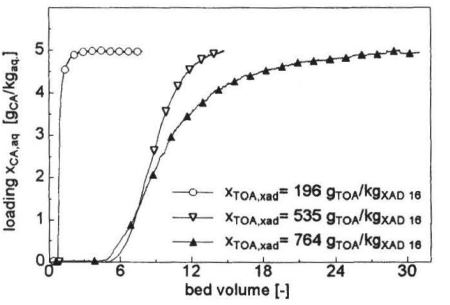


Figure 6 : Influence of the TOA loading on the resin on the shape of the breakthrough curve (XAD 16, T= 25°C, F=0.43 g/h)

The capacity of the EIR's increased with increasing loading of ion exchanger on the porous media. By increasing the loading the breakthrough curve will broaden (figure 6). At a high loading of ion exchanger at the surface of the resin the distribution coefficient will decrease. This effect can be explained with the sealing of wide pores. The pore system behind this sealed pore is shielded and cannot react with the organic substances in the aqueous phase. The recovery of the adsorbed organic substance can be realized in different ways. The first way is to increase the pH value. This causes a decrease of the equilibrium and the organic substance will be back extracted into the aqueous phase at high concentrations. For this process NaOH is used and sodium will be found in the product. Another way to recover the adsorbed organic substance is to increase the temperature. This process gives an aqueous solution, in which only the adsorbed organic acid is gained at high purity and concentration.

Bleeding

The loss of ion exchanger is extremely low. Only when the fixed bed, packed with fresh impregnated resin, is used for the first time an ion exchanger peak is detected (figure 7). After three bed volumes the ion exchanger concentration in the aqueous phase is negligible. Due to the sorption process the bleeding values are always less than the physical solubility (7.5 mg tri-n-octylamine).

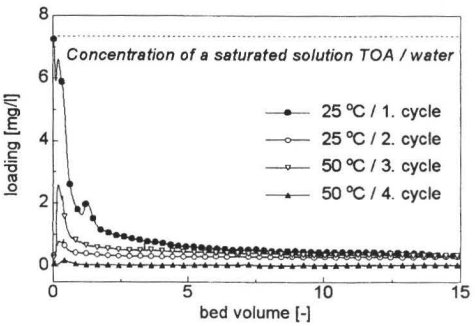


Figure 7 : Bleeding

SIMULATION

In order to describe the mass transfer of the reactive sorption in a fixed bed, a dispersion model is used.

$$\frac{\partial x(z,t)_{aq}}{\partial t} = D_{ax}\frac{\partial^2 x(z,t)_{aq}}{\partial z^2} - \frac{u_0}{\varepsilon}\frac{\partial x(z,t)_{aq}}{\partial z} - \frac{3}{R_p}\frac{1-\varepsilon}{\varepsilon}k_f(x(z,t)_{aq} - x(R,t)_p) \qquad [2]$$

$$\frac{\partial x(r,t)_P}{\partial t} = D_p\left(\frac{\partial^2 x(r,t)_{org,aq}}{\partial r^2}\right) - \frac{\varepsilon_p}{1-\varepsilon_p}\frac{\partial x(r,t)_{org,EIR}}{dt} \qquad [3]$$

$$\frac{\partial x(r,t)_{org,EIR}}{\partial t} = k_A\, x(r,t)_{org,aq}\,(x^*_{org,EIR} - x(r,t)_{org,EIR}) - k_D\, x(r,t)_{org,EIR} \qquad [4]$$

The mass transfer into a single particle can be described with a mass balance (Equation. 3). Assuming that the reaction between ion exchanger and organic acid is instantaneous, the adsorption rate can be described as the difference between adsorption and desorption of the organic acid on the ion exchanger (Eqn. 4). The kinetic constants k_A and k_D result from the dissociation coefficient of the modified Langmuir-isotherm (Equation 1). The mass transfer coefficient k_f and the axial dispersion coefficient D_{ax} can be determined by experiments in a fixed bed (Equation 2).

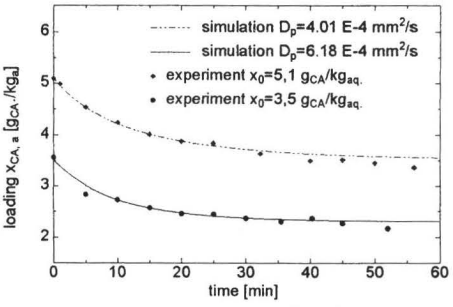


Figure 8 : Simulation results for the mass transfer of XAD 16 ($x_{TOA/XAD16}$=767 g/kg) in the stirred cell at 25°C

The simulation of the reactive sorption was carried out using the NAG® numerical library. The diffusion coefficient D_p is estimated from experiments in the stirred cell. The required equilibrium data were calculated with the modified Langmuir-isotherm. The following simplifications have been assumed: the pore diffusion coefficient, the pore diameter in the particle and the ion exchanger loading on the resin are constant and the diffusion film surrounding the particle can been neglected. The results are depicted in figure 8. The value of the intra-particle diffusion coefficient is in the range between 6E-5 and 6E-4 mm²/s depending on the temperature and the used resin. On the basis of this, even when neglecting D_{ax} in equation 2 and using a common Sh correlation for k_f a rather good prediction of the fixed bed behaviour is possible.

CONCLUSIONS

The EIR equilibrium data can be calculated with a modified Langmuir-isotherm taking the loading of ion exchanger on the resin into account. The effective diffusion coefficient in the pore system can be estimated from single particle experiments. The experimental data leads to the conclusion, that the mass transfer in a single particle is limited by pore diffusion. With increasing temperature the equilibrium loading of the EIR decreases and causes a double s shape in the breakthrough curve. The recovery of the adsorbed substance can be realized by either a temperature swing or pH swing process. The mass transfer of the reactive sorption was investigated and it was found, that a dispersion model could predict the breakthrough curve of a fixed. The reactive sorption was tested on a fermentation broth of a *aspergillus niger* (DSM 63263) fermentation. The citric acid from the aqueous phase was separated und recovered in high concentration.

ACKNOWLEDGEMENT

This work was supported by the DFG under Grant No.DFG-GRK123/3-96, which is greatly appreciated.

REFERENCES

1 Hartmann R, Anspach FB, Papamichael N and Deckwer WD, GVC-Vortrags- und Diskussionstagung 5./6. Mai 97, Goslar, , (1997).
2 Juang R.S and Chou TC, *Sep. Sci. Technol*, **31(10)**,.1409-1425 (1996).
3 Tavlarides LL, Bae JH and Lee CK, *Sep. Sci. Technol.* **22(2&3)**, pp. 581-617 (1987).
4 Jerabek K, Hankoa L, Stribovsky AG and Warshawsky A, *React. Funct. Polymers*, **28**, 201-207 (1996).
5 Bart HJ and Traving M, *Chemie Ingenieur Technik*, **(9)**, 1152 (1998).
6 Hartl J and Marr R, *Sep.Sci. Technol.* **28(1-3)**, 805-819, (1993).
7 Kertes AS and King CJ, *Biotech. Bioeng.* **28**, 269-282 (1986).

NOMENCLATURE

Symbols

D_{ax}	axial dispersion coefficient	[m²/s]
D_P	diffusion coefficient in the pores	[m²/s]
ε	porosity	[-]
k_A	kinetics constant of the adsorption	[kg/g s]
k_D	kinetics constant of the desorption	[l/s]
k_f	mass transfer coefficient	[m/s]
c_1,c_2,c_3	Langmuir parameter	[-]
r	radius [mm]	
R	radius of a particle	[mm]
t	time	[min]
u_0	velocity	[m³/s]

Subscripts

aq	aqueous phase	
CA	citric acid	
EIR	extractant impregnated resin	
org	organic acid	
P	particle	
TA	tartaric acid	
TOA	tri-n-octylamine	
x	loading	[g/kg]
z	axial coordinate	[m]
XAD	Amberlite resin	



EXTRACTION AND INTERACTIONS IN TWO-PHASE, MULTI-ACID, MULTI-BASE SYSTEMS

Nadia Cohn-Syzov and Aharon M Eyal
Casali Institute for Applied Chemistry, The Hebrew University of Jerusalem, Jerusalem 91904, Israel

ABSTRACT
Acid-base interactions are used for analysis of extraction systems comprising up to three acid and three base functions. The most complex systems tested here are those of amino acids extraction by acid-base couple extractants. These extractants were found to extract quite efficiently amino acids in their zwitterionic form and allow for back-extraction without using mineral acid and/or base. Reagents' consumption and by-product salt formation are avoided. Analysis of the extraction mechanism explains the effects of parameters such as acid-base properties of extractant components, pH and the properties of the extracted acid.

Keywords: Amino acid, acid base couple extractants, zwitterion, ion-pair extraction

INTRODUCTION

Extraction of mineral, carboxylic, amino acids and their salts are examples of the complexity of multi-acid, multi-base systems. The extraction of mineral acids and carboxylic acids by amines (systems comprising one acidic and one basic component) has already been studied.[1] More complicated systems, containing two acidic and one basic groups are represented by the two phase system of acid extraction by acid base couple (ABC) extractants (composed of an amine, an organic acid and a diluent, all of which are water-immiscible). A comprehansive study[2,3,4] found that these extractants extract acids and their mineral salts with high selectivity, efficiency and reversibility according to:

$$H^+X^-_{aq} + B^+A^-_{org} = B^+X^-_{org} + HA^-_{org} \quad (1)$$

$$M^+X^-_{aq} + B^+A^-_{org} = B^+X^-_{org} + MA^-_{org} \quad (2)$$

where H^+X^-, B, A and M denote the extracted mineral/carboxylic acid, the amine, the anion of the water-immiscible acid and the water-miscible cation, and aq. and org. refer to aqueous and organic phase, respectively.

One aim of the present research was to explore even more complex multi-component two phase systems, comprising of up to three acidic and three basic groups in order to build the full picture of such systems. Another aim is to study the possibility of using ABC extractants for recovery of amino acids from fermentation liquors, while in zwitterionic form.

Previous studies show that amino acids are extracted in their anionic or cationic form, using liquid anion exchangers or liquid cation exchangers as extractants. The choice of extractants for this mechanism is limited, as only strong amines or strong organic acids are charged at pH ranges required for charging the amino acids. In addition, acids or bases are used in the extraction or stripping steps resulting in the formation of by-product salts. A way to avoid these drawbacks, by extraction of the amino acids in their zwitterionic form, was conceived. By analogy to extraction of salts, protonated amine of the ABC extractant would form an ion-pair with the carboxylic function, while dissociated organic acid there would form similar interaction with the amino group. In that case, again by analogy to extraction of salt, the extraction would be reversible, allowing for extraction and back-extraction using no acid-base reagents, and forming no by-product salts. In order to extract amino acid according to this mechanism the components of the ABC extractant need to be charged in equilibrium with the extracted aqueous phase.

This article presents the results of extracting several amino acids with some ABC extractants, and analyzes the results according to the acid-base interactions in the system.

© 2000 Society of Chemical Industry

METHODS AND MATERIALS

The following organic amines and acids were used as the extractant components: tris(2-ethylhexyl)amine (TEHA), Hoechst; Alamine 336 (A336), tricaprylylamine, Henkel; Primene JM-T (JMT), a mixture of primary aliphatic amines (C_{18}-C_{22}), Rohm & Haas, Aliquat 336 (Alqt336), methyl tricaprylyl ammonium chloride, Henkel; lauric acid (LA), Fluka; di(2-ethylhexyl)phosphoric acid (D2EHPA), Sigma and di-nonylnaphthalene sulfonic acid (DNNSA), King Industries. Isopar K (Exxon) was used as the diluent.

The concentrations of both amine and organic acid in the ABC extractants were 0.5 mol/kg. In the preparation of Aliqt336 containing ABC extractants, the chloride ion was washed out to concentrations of < 0.025 mol/kg. Solutions of the carboxylic acids, amino acids and their salts were prepared and equilibrated with the extractants at 1:1 phase ratio. Equilibrium organic phases containing carboxylic acids or acidic amino acids were analyzed by direct acid/base titration using phenolphthalein as an indicator. Other organic phases were washed with water and the washings were analyzed by HPLC.

RESULTS AND DISCUSSION.

The mechanisms of extraction, in two phase multi-component systems, are affected by many factors, including the acid base properties of extractant components and their hydrophilic/hydrophobic properties, steric and diluent effects, pH of the aqueous phase, inter-molecular interactions and water co-extraction.

One acidic and one basic group systems

Extraction of mineral and carboxylic acids by amine-based extractants

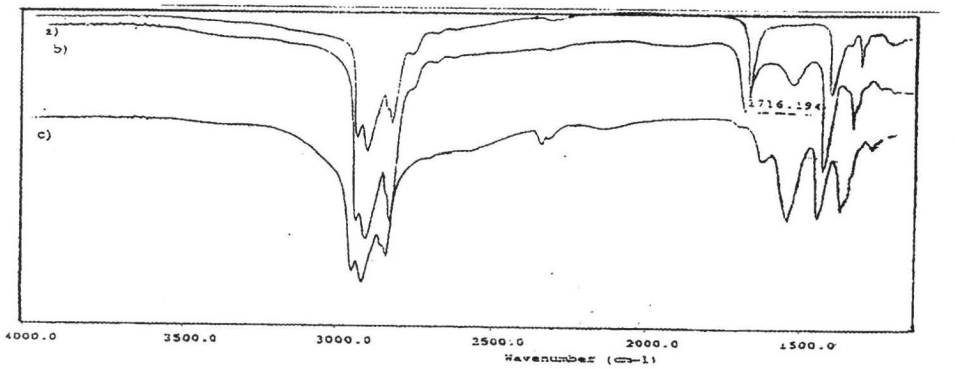
For most mineral acids the amine is a much stronger base than the anion of the acid. On interaction, it is protonated to form an ammonium cation, which binds the anion of the acid to form an ion-pair.

This is the case also for extraction of carboxylic acids, if their anion is a weaker base than the extractant amine. Some examples are, extraction of most carboxylic acids by primary aliphatic amines (apparent pK_a of 6-7) and extraction of relatively strong carboxylic acids (pK_a <2.5) by tertiary aliphatic amines. However, when the basicity of the anion is similar to that of the amine, or higher, the interaction is more of the nature of H-bonding or solvation. These bonds are weaker than those in ion-pairs and are, therefore, more sensitive to solvent and steric effects.

Interactions between the components of acid-base couple extractants

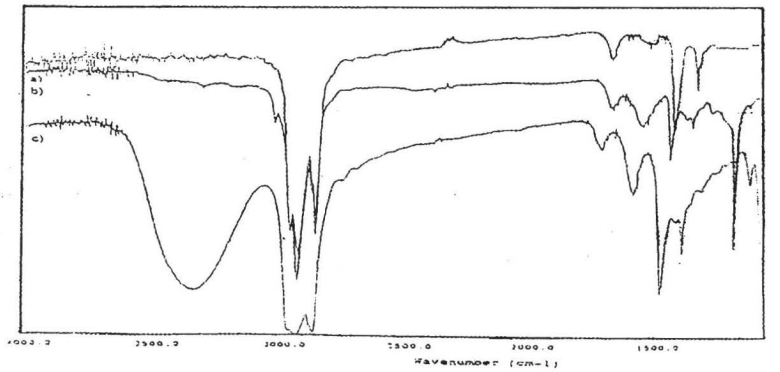
The organic acid component of ABC extractants is water immiscible and does not distribute between the phases as the carboxylic acids of above. Yet, their interactions with the amines are similar. The nature of the bond formed is expected to be determined mainly by the relative basicity of the amines and the anion of the acid. Direct determination of those basicities for water-immiscible components is problematic. Using pH of half neutralization (pHhn) method of Grinstead,[5] the apparent pK_a values for TEHA, A336, JMT and Alqt336 were found to be respectively, 1.4, 3.4, 7 and 12. These figures could serve just as an indication for the interaction in ABC extractants.

ABC extractants composed of lauric acid and TEHA, A336 or JMT were prepared. IR spectroscopy was used to study the interaction between the amine and the carboxylic acid through the degree of dissociation of the acid (comparison of the ratio between the COOH and COO^- peaks at 1630 and 1716 cm^{-1} respectively).



IR spectra of acid-base coupls dissolved in parasol with amines of different strengths:
a) 0,5 M TEHA+0,5 M LA
b) 0,5 M A336 + 0,5 M LA
c) 0,5 M JMT + 0,5 M LA

Figure 1 Infrared spectra



. IR spectra of (0,5 M A336 + 0,5 M LA) in different diluents
a) in parasol b) in $CHCl_3$ c) IN OCTANOL

Figure 2 Infrared spectra

No dissociation is seen in the case of the weakest amine, TEHA, (figure 1), indicating no ion-pair formation in the TEHA-LA, ABC extractant. The interaction here has some form of H-bonding. In case of the strong base, JMT, on the other hand, LA seems to be nearly fully converted into its dissociated form, indicating the formation of the ion-pair B^+A^- . (B and B^+ denote the amine in free and protonated/charged form, respectively, while HA and A^- denote the water immiscible acid component of the ABC extractant in protonated and dissociated form, respectively.) The A336-LA ABC extractant presents an intermediate case.

Studies of carboxylic acid extraction show that polar diluents enhance the extraction through stabilization of the ion-pair. The IR spectra of the couple extractants (figure 2) show that polar diluents enhance the amine protonation in the extractant, probably for the same reason. For the A336:LA system the degree of LA dissociation (resulting in COO^- formation and amine protonation) significantly grows according to the sequence: parasol < chloroform < octanol.

One basic and two acidic groups as in the case of extracting mineral and carboxylic acids by ABC extractants

Strong mineral acids are extracted by couple extractants through the displacement mechanism:

$$H^+X^-_{aq} + B^+A^-_{org} = B^+X^-_{org} + HA^-_{org} \qquad (3)$$

The mineral acid replaces the weaker organic acid in its interaction with the organic amine. The selectivity of the mineral acids' extraction is based on this phenomenon, where the stronger acid is preferred.

The data about extraction of the carboxylic acids by ABC extractants are much more limited. Based on the above analysis, in cases where the extracted carboxylic acid is stronger than HA, the displacement mechanism will take place, as for mineral acids. Yet, in most cases, the carboxylic acid is the weaker one and H-bonding/solvation mechanisms play the major role.

An ABC extractant, composed of A336 and DEHPA, was used to extract pyruvic, propionic and lactic acid (with pK_a values of 2.6, 4.9 and 3.8, respectively). The distribution curves are presented in figure 3. Propionic acid is too weak to displace DEHPA, but is lypophilic enough to allow efficient extraction by solvation mechanism. Lactic acid and pyruvic acid are much more hydrophilic, however strong enough to have some degree of DEHPA displacement. By analogy to the extraction of mineral acids, the stronger acid, pyruvic, is better extracted.

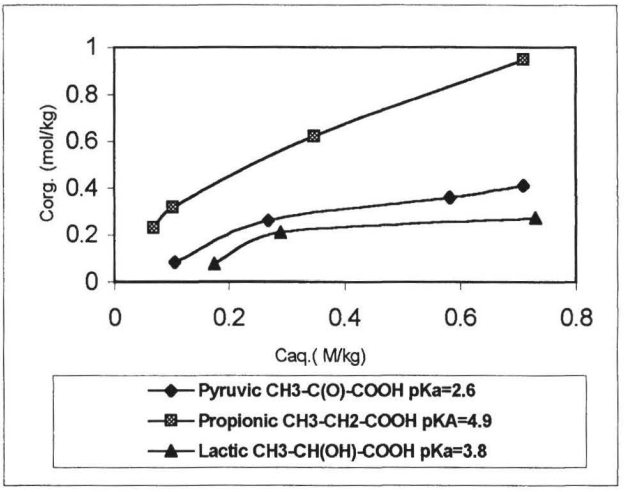


Figure 3 Distribution curves for carboxylic acids extraction by 0.5mol/kg A336+DEHPA.

Extraction of amino acids by ABC extractants, a system with up to three acidic and three basic groups

As suggested above, extraction of amino acids, in their zwitterionic form, requires charged pairs of the extractant components. Extraction efficiency is, thus, determined by factors such as: the acid / base strengths of the water immiscible amine and organic acid, the pH of the equilibrated aqueous phase and the pK_a values of the amino acids.

In neutral solutions, typical neutral amino acids are present in their zwitterionic form and the organic acids of the extractant are dissociated (at least to some extent). The degree of protonation of the amine component depends on its basicity. The concentration of charged extractant components is, therefore, higher in extractants containing JMT compared with those containing A336, resulting in better extraction of neutral amino acids (Table 1).

Amino acid	A336+DEHPA $D(C_{org}/C_{aq})$	JMT+DEHPA $D(C_{org}/C_{aq})$
Aspartic	0.046	0.057
Glutamic	0.038	0.038
Valine		0.007
Threonine		0.005
Proline	0.266	0.538
Betaine	0.316	0.429

Table 1: Extraction of the amino acids by ABC couple extractants

Basic amino acids exist in their zwitterionic form at basic pH (about 11). In equilibrium, the acids of the organic phase are dissociated/charged, but water-immiscible tertiary, secondary and primary amines are too weak to be protonated. Based on this analysis, extraction of basic amino acids would be possible only by quaternary amine containing extractants, as those amines are charged at any pH. For similar reasons, the latter are expected to be efficient in extraction of most amino acids (Table 2).

Typically, acidic amino acids are present in their zwitterionic form at pH of 3-4. In equilibrium, couple extractants composed of amines with $pK_a > 3$ (most straight chain ones) and relatively weak organic acids are partially charged. Such extractants show some extraction of acidic amino acids (Tables 1 and 2).

		Alqt336+DEHPA	
Asp	Caq.mol/kg	Corgmol/kg	D(Corg/Caq)
Glu	0.033	0.004	0.121
Val	0.056	0.004	0.071
Thr	0.41	0.15	0.366
Pro	0.6	0.4	0.667
Betaine	0.65	0.35	0.538

Table 2: Extraction of the amino acids by ABC couple extractant (Alqt336+DEHPA)

The results show that proline is extracted better than valine and threonine (Tables 1 and 2). Being cyclic and carrying a secondary amine group rather than a primary one makes it somewhat less polar. Yet, betaine carries a quaternary amine and is highly hydrophilic, but still extracts well. Our suggestion is that, in the case of neutral amino acids that carry primary amines, the strong H-bond between the carboxylic group and the amino group (forming a kind of an inner ring) hinders the interaction with the charged components of the extractant. Such a strong interaction is less feasible for proline and betaine (secondary and quaternary amine groups, respectively), so that their charged functions are more accessible for forming ion-pairs with the components of the ABC extractant.

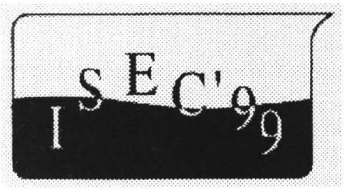
In order to confirm this analysis, we have tested the extraction of amino acids with amino group distanced from the carboxylic group, where such strong H-bond (inner ring) is hindered. The results of extracting γ– and δ-amino acids (see Table 3) confirm with our expectation. Approximately a 10 fold increase in distribution coefficients was found compared with extraction of α-amino acids.

Amino acid	Caq M/kg	Corg M/kg	D= Corg/Caq
2-amino butyric acid	0.92	0.03	0.033
3-amino butyric acid	0.66	0.3	0.455
4-amino-n-valeric acid	0.745	0.24	0.322

Table 3: Extraction of 2-, 3-, and 4-amino acids by Aliquat336 + DEHPA

REFERENCES

1. Eyal AM and Riki C, *Ind. Eng. Chem. Res.*, **34,** 1789, (1995).
2. Eyal AM, *Ind. Eng. Chem. Res.*, **33**, 5, 1076-85, (1994).
3. Eyal AM, Bloch R and Hazan B, *Ind. Eng. Chem. Res.*, **33**, 5, 1067-75, (1994).
4. Eyal AM and Baniel A, *Ind. Eng. Chem. Process Des. Dev.*, **21**, 334-337, (1982).
5. Grinstead RR, *Proceedings of International Solvent Extraction Conference. (ISEC)* 426, (1967).



EXTRACTIVE SYNTHESIS OF PEPTIDES WITH CATALYTICALLY ACTIVE ENZYMES IN ORGANIC MEDIA

Y Murakami, H Kawakita and A Hirata
Department of Chemical Engineering, Waseda University
3-4-1 Ohkubo, Shinjuku-ku, Tokyo, 169-8555 Japan

ABSTRACT
A new process for enzymatic synthesis of biologically active peptides with enzyme catalytically active in organic media was proposed, and applied to the protease-catalyzed synthesis of kyotorphin (TyrArg, anodyne peptide) derivatives. In this method, aqueous substrate solution was fed to a stirred reactor that contained the organic solvent where surfactant-coated enzyme are retained. The peptide synthesized was extracted to aqueous phase continuously. *N*-Benzyloxycarbonyl TyrArg alkyl ester was synthesized in *ca.* 30% of yield, which was 2-fold higher than that in an aqueous medium.

Keywords: Enzymatic peptide synthesis, kyotorphin synthesis, surfactant-coated enzyme, non-aqueous enzymology, aqueous/organic biphasic system

INTRODUCTION

Enzymes generally possess extremely high catalytic activity and unique substrate specificity, and therefore select substrates strictly, which bound to their active center due to their higher-order structure. This conformationality had made us believe that enzymes function effectively only in a water-rich medium. On the other hand, there are many processes where substrates or products are hydrophobic, and it is difficult to perform these reactions in an aqueous medium. However, the interactions between the organic solvent molecules and aminoacid residues in the enzyme molecules had been thought to denature and inactivate enzymes in organic media. This consensus had hindered a wide application of biocatalysis in biotechnological. Recent advances in non-aqueous enzymology, however, have greatly reversed this established consensus[1-4] since the pioneer works by Klibanov *et al.* in 1980's.[5-8]

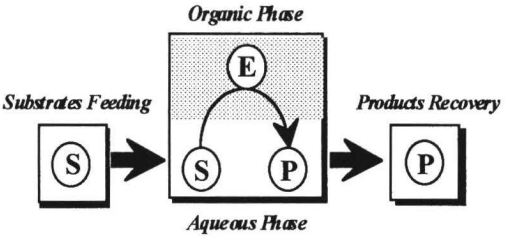


Figure 1 Scheme for the prptease-synthesis of biologically active peptides with enzyme catalytically active in organic media utilizing an extractive reaction in an aqueous/organic biphasic medium (E: enzyme, P: product, S: substrate).

In this study, we propose a novel method to synthesize biologically active peptides with enzymes catalytically active in organic media utilizing an extractive reaction in an aqueous/organic biphasic system. Figure 1 shows the simplified concept for the extractive synthesis of peptides in an aqueous/organic biphasic system. The substrate is first dissolved in an aqueous solution, and fed to a reactor. It is extracted into the organic phase, and catalyzed with modified enzyme only in the organic medium. The synthesized product is extracted selectively into aqueous phase due to its hydrophilicity. We used here surfactant-coated enzymes retained in an organic phase to enhance the hydrophobicity

© 2000 Society of Chemical Industry

of hydrophilic enzymes. Surfactant-coated enzymes have been recently used as a biocatalyst in an organic-solvent rich medium.[9-11]

We applied this method to the protease-catalyzed synthesis of kyotorphin. Kyotorphin, L-tyrosyl-L-arginine (TyrArg), is one of the best-known peptides. This peptide has an anodynic effect by releasing enkephalin that has an important role in the control of pain to combine with enkephalin receptors in the brain.[12] Kyotorphin is attracted attention because of its non-narcotization, which differs from traditional anodyne morphine. To date, no process has been proposed to synthesize a kyotorphin precursor effectively.

EXPERIMENTAL

Materials

α-chymotrypsin was purchased from Sigma and used without further purification. *N*-(Benzyloxycarbonyl)-L-tyrosine (Z-L-Tyr) and L-arginine methyl and ethyl ester dihydrochloride salts (L-ArgOMe·2HCl and L-ArgOEt·2HCl) were purchased from Kokusan Chemical Works (Tokyo, Japan). Nonionic surfactant Span60 (Kanto Chemical, Tokyo) was used to coat the enzyme. 3-(2-Furylacryloyl)-glycyl-L-leucine amide (FAGLA, Sigma) was used as a substrate for the hydrolysis to determine the activity of surfactant-coated enzyme. All other reagents were of analytical grade and purchased from Kokusan Chemical Works.

Synthesis of kyotorphin precursor in an aqueous monophasic medium

Kyotorphin precursors (Z-TyrArgOMe and Z-TyrArgOEt) were synthesized at 40°C in 100 mM MES/NaOH buffer. The initial concentrations of the substrates, Z-L-Tyr and L-Arg alkyl esters, were 55 and 100 mM, respectively. The concentrations of substrates and products were measured by High Performance Liquid Chromatography (HPLC).

Determination of distribution ratio of substrates and product in an aqueous/organic biphasic medium

The pH-dependency of the distribution ratios of substrates and kyotorphin precursors were determined in an aqueous/organic biphasic system at 40°C. Each component was dissolved in an aqueous/organic solution, and its concentrations in both phases was determined by HPLC. Butyl formate, ethyl acetate, butyl acetate, propyl acetate, *n*-amyl alcohol, *t*-amyl alcohol, 1-butanol, 2-methyl-1-propanol, toluene, methylisobutylketone and methylethylketone were used as phase-forming organic solvents.

Preparation of surfactant-coated enzyme

The surfactant-coated enzyme was prepared by the method proposed by Goto *et al.*.[13] An aqueous enzyme solution (phosphate buffer adjusted to pH 7.0) and isooctane containing 10mM of surfactant were mixed with a homogenizer (PH-91 (SMT, Japan)) at 10000min^{-1} for 2 minutes. Stable w/o emulsion was formed which was dried at room temperature for 4 days. The activity of surfactant-coated enzyme was determined by hydrolyzing FAGLA in isooctane dried by molecular sieve, and was compared with that of the native enzyme.

Synthesis of kyotorphin precursor in an aqueous/organic biphasic medium

Kyotorphin precursors were synthesized with an extractive operation in an aqueous/organic biphasic media. Initial concentrations of carboxyl, and amine substrates were 18 and 220mM, respectively. The concentration of enzyme in an organic phase was 0.4g/l with a native enzyme base. The temperature was constant at 40°C.

Analysis

The HPLC system was used to measure the concentrations of substrate and product. This

system was consisted of a UV8020 detector and a CCPS solvent delivery system (Tosoh Co., Japan). The 3.0 x $10^{-6}m^3$ aliquots of aqueous and organic phases were taken and the concentrations of the substrates and product were measured with an HPLC system on columns, G2000SW (Tosoh Co.) at 259nm and ODS-3 (GL Science, Japan) 220nm. A mixture of acetonitrile/water (70/30, v/v) adjusted to pH 6.1 containing acetic acid and methanol/water (40/60, v/v) adjusted to pH 7.5 containing phosphoric acid were used as an elution buffer for above HPLC systems with the flow rate of 1ml/min.

RESULTS AND DISCUSSION

Synthesis of kyotorphin precursors in an aqueous monophasic medium

Z-TyrArgOMe and Z-TyrArgOEt were synthesized enzymatically in an aqueous monophasic medium. Figure 2 shows a typical time-course of the batch synthesis of Z-TyrArgOEt in an aqueous medium. The concentration of product increased early in the reaction, reached the saturation concentration, and then decreased gradually. This is because one of the substrates, alginine alkyl ester, was decomposed non-enzymatically, which is a general phenomenon when peptides are synthesized with a proteolytically active enzymes.[14-16] The maximum initial synthetic rate was obtained at pH 7.0, where the peptide yield was *ca.* 15% in the synthesis of Z-TyrArgOMe and Z-TyrArgOEt.

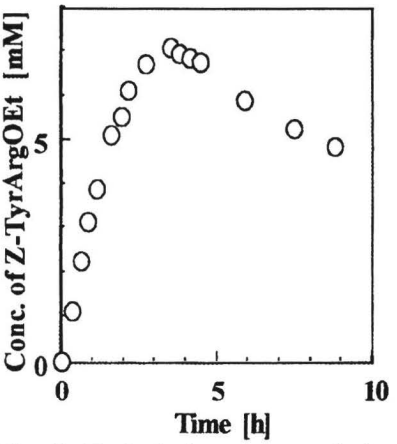


Fig. 2 Typical time-course of the batch synthesis of kyotorphin precursor in an aqueous monophasic medium.

Determination of distribution ratios of substrates and product in an aqueous/organic biphasic medium.

Figure 3 shows the pH-dependency of distribution ratios of substrates in an aqueous/alcohols biphasic medium.

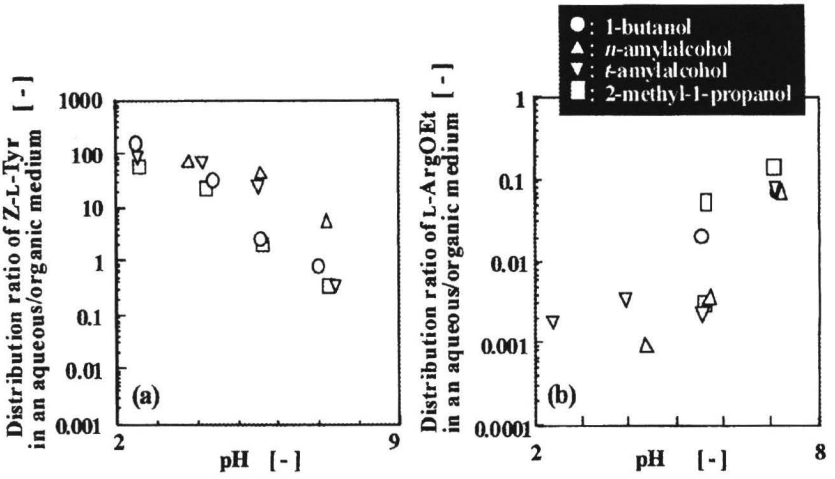


Fig.3 pH-dependency of distribution ratios of (a) Z-L-Tyr and (b) L-ArgOMe in an aqueous/organic biphasic medium. 1-butanol, *n*-amylalcohol, *t*-amylalcohol and 2-methyl-1-propanol were used as organic solvent.

The distribution ratio is defined here as a concentration of components in an organic phase divided by that in an aqueous phase. The nonionic component selectively distributes to an organic phase in a aqueous/organic biphasic medium.[17] Since Z-L-Tyr and L-ArgOR (R: Me or Et) have carboxyl and amine groups in their molecules, the nonionic components increase at acid and alkaline pH, respectively.

Therefore as pH increases, Z-L-Tyr and L-ArgOR distributed more to an aqueous and an organic phase, respectively. Since L-ArgOMe was hydrophilic, acetates have little ability to extract it in a biphasic medium. No difference was observed between the distribution behaviors of L-ArgOMe and L-ArgOEt in a biphasic medium (data not shown).

Figure 4 shows the pH-dependency of the kyotorphin precursor (Z-TyrArgOEt) in an aqueous/1-butanol biphasic medium. Since the kyotorphin precursor has a carboxyl and amine groups in its molecule, it charges positively at low pH, negatively at high pH and nonionic at moderate pH. Therefore it distributed more to aqueous phase at low and high pH, and more to an organic phase at moderate pH.

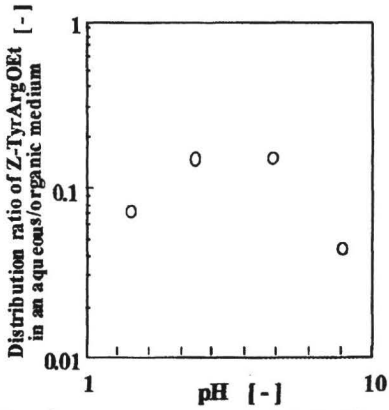


Fig.4 pH-dependency of distribution ratios of kyotorphin precursor in an aqueous/1-butanol biphasic medium.

Activity of surfactant coated enzyme in organic medium.

FAGLA,3-(2-furylacryloyl)-glycyl-L-leucine amide, was hydrolyzed in organic medium with native and surfactant-coated α-chymotrypsins. We could confirmed that surfactant-coated enzyme showed a *ca.* 11-fold higher activity in organic media than the native one. It is because the hydrophobic part of surfactant increases the solubility of surfactant-coated enzyme in organic media. We recently examined the use of other surfactants to coat enzyme, however insufficient data has been obtained to be shown here.

Synthesis of kyotorphin precursor in an aqueous/organic biphasic medium

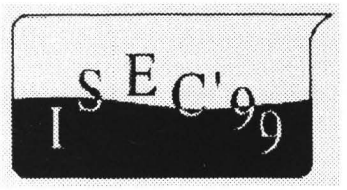
Kyotorphin precursor was synthesized in an aqueous/organic biphasic medium with Span60-coated α-chymotrypsin dissolved in 1-butanol as the organic solvent. Figure 5 shows a typical time-course of the concentration of substrates and kyotorphin precursor. The peptide has anion and cation dissociated groups, and is hydrophilic. As shown in figure 5 we could confirm that almost all peptides synthesized are selectively extracted to an aqueous phase. The native enzyme, surfactant-coated enzyme and surfactant were not detected in an aqueous phase with HPLC. Therefore the surfactant-coated enzyme was retained only in an organic phase without its conformational destruction. We could achieve 30% of peptide yield, which was 2-fold higher than that in an aqueous monophasic medium.

CONCLUSION

We propose here a novel method to synthesize biologically active peptides with enzyme catalytically active in organic media utilizing an extractive reaction in an aqueous/organic biphasic system. In this method, the peptide is synthesized only in an organic phase, and distributes selectively to an aqueous phase due to its hydrophilicity. We applied this method to the α-chymotripsin-catalyzed synthesis of precursor of hydrophilic anodyne peptide, kyotorphin. We could achieve 30% of peptide yield, which was 2-fold higher than that in an aqueous monophasic medium.

REFERENCES

1. Khmelnitsky YuL, Levashov AV, Klyachko NL and Martinek K, *Enzyme Microb. Technol.*, **10**, 710-724, (1988).
2. Klibanov AM, *Trends Biochem. Sci.*, **14**, 141-144, (1989).
3. Gupta MN, *Eur. J. Biochem.*, **203**, 25-32, (1992).
4. Klibanov AM, *Trends Biotechnol.*, **15**, 97-101, (1997).
5. Zaks A and and Klibanov AM, *Proc. Natl. Acad. Sci. USA*, **82**, 3192-3196, (1985).
6. Russell AJ and Klibanov AM, *J. Biol. Chem.*, **263**, 11264-11626, (1988).
7. Zaks A and Klibanov AM, *J. Biol. Chem.*, **263**, 3194-3201, (1988).
8. Zaks A and Klibanov AM, *J. Biol. Chem.*, **263**, 8017-8021, (1988).
9. Okahata Y, Fujimoto Y and Ijiro K, *J. Org. Chem.*, **60**, 2244-2250, (1995).
10. Okazaki S, Kamiya N, Goto M and Nakashio F, *Biotechnol. Lett.*, **19**, 541-543, (1997).
11. Isono Y, Nakajima M and Nabetani H, *J. Ferment. Bioeng.*, **86**, 138-140, (1998).
12. Takagi H, Shiomi H, Ueda H and Amano H, *Nature*, **282**, 410-412, (1979).
13. Goto M, Sumura H, Abe K and Nakashio F, *Biotechnol. Tech.*, **9**, 101-104, (1995).
14. Murakami Y, Hirata M and Hirata A, *J. Ferment. Bioeng.*, **82**, 246-252, (1996).
15. Murakami Y and Hirata A, *J. Ferment. Bioeng.*, **83**, 38-42, (1997).
16. Murakami Y, Yoshida T and Hirata A, *Biotechnol. Lett.*, **20**, 767-769, (1998).
17. Martinek K, Semenov AN and Berezin, *Biochim. Biophys. Acta*, **658**, 76-89, (1981).



PROTEASE-CATALYZED SYNTHESIS OF PEPTIDES UTILIZING AN EXTRACTIVE REACTION IN AN AQUEOUS/ORGANIC BIPHASIC SYSTEM

Y Murakami, T Oda, A Takehara and A Hirata
Department of Chemical Engineering, Waseda University
3-4-1 Ohkubo, Shinjuku-ku, Tokyo, 169-8555 Japan

ABSTRACT
A new method has been developed to synthesize peptides in an aqueous/organic biphasic system with simultaneous operation of an enzymatic reaction and a product separation, and has been applied to the protease-catalyzed synthesis of Z-GlyPheOMe, a precursor of Z-GlyPhe which acylates lysosomotropic detergent, a useful anticancer drug, and masks its introduction into normal cells. The extremely high yield *ca.* 100% was obtained continuously.

Keywords: Enzymatic peptide synthesis, thermolysin catalysed synthesis, extractive reaction, aqueous/organic biphasic system, glycylphenylalanine

INTRODUCTION

Enzymes as biocatalysts differ from chemical catalysts because of their exceeding high catalytic activity in mild conditions and substrate specificity. The mild reaction conditions of the enzyme-catalyzed reactions guarantee racemization-free syntheses, and chirally homogeneous products are obtained even when racemic aminoacid derivatives are used as starting materials owing to the stereospecificity of enzymes. These properties should have provided enzymes a wide application in biotechnological catalytic processes. Recently much attention has been paid to the protease-catalyzed synthesis of oligopeptides.[1-3] However, the product yield is extremely low in conventional aqueous media. To date, several attempts have been performed to enhance the efficiency of enzymatic reactions. The authors propose an effective method to synthesize peptides continuously in an aqueous/organic biphasic medium, and have applied it to the thermolysin-catalyzed synthesis of the aspartame precursors (Z-AspPheOMe and F-AspPheOMe). The yield of these peptides in an aqueous medium is less than 10%,[4, 5] however, an extremely high yield, *ca.* 100%, was obtained using the extractive method in a biphasic medium.[6-8]

In this study, we applied this method to the thermolysin-catalyzed synthesis of *N*-benzyloxycarbonyl-L-glycyl-L-phenylalanine (Z-GlyPhe) derivative, a precursor of Z-GlyPhe acylating lysosomotropic detergents. Lysosomotropic detergent is an useful anticancer drug and destroys lysosomes to release lysosomonal enzymes which attack target cancer cells.[9] The detergent also attacks normal cells causing side effects, which is a serious problem to be addressed. Z-GlyPhe (called as a masking into cells) derivatives acylates lysosomonal detergents, and mask their introduction into normal cells to prevent side effects.[10] To date, Z-GlyPhe and its derivatives have been synthesized as an intermediate product in the enzymatic synthesis of a tripeptide[11] and Leu-enkephalin,[12] however, no effective method was proposed to synthesize them. In this study, we examined the effective synthesis of the Z-GlyPhe precursor, *N*-benzyloxycarbonyl-L-glycyl-L-phenylalanine methyl ester (Z-GlyPheOMe) from *N*-benzyloxycarbonyl-L-glycine (Z-L-Gly) and L-phenylalanine methyl ester (L-PheOMe) in an aqueous/organic biphasic medium, because Z-GlyPheOMe, nonionic peptide, was expected to be selectively extracted to an organic phase due to its hydrophobicity.

EXPERIMENTAL

Materials

N-Benzyloxycarbonyl-L-glycine (Z-L-Gly) was purchased from Kokusan Chemical Works (Tokyo). L-Phenylalanine methyl ester hydrochloride salt (L-PheOMe.HCl) for batch experiments was purchased from Kokusan Chemical Works, while that for continuous experiments was prepared from

© 2000 Society of Chemical Industry

L-phenylalanine (L-Phe) purchased from Kokusan Chemical Works with methyl esterification. *N*-Benzyloxycarbonyl-L-glycyl-L-phenylalanine methyl ester (Z-GlyPheOMe) was synthesized enzymatically and purified. Thermolysin was used as an enzyme for batch experiments due to its strict selectivity for L-Phe. Crude thermolysin, thermoase PS-160, was purchased from Daiwa Kasei K.K. (Osaka, Japan) and used for continuous experiments without further purification.

Batch synthesis of Z-GlyPheOMe in an aqueous monophasic medium

Z-GlyPheOMe was synthesized at 40°C in 100 mM MES/NaOH buffer. The initial concentrations of the substrates, Z-L-Gly and L-PheOMe, were 50 and 100 mM, respectively. The concentrations of substrates and products were measured by High Performance Liquid Chromatography (HPLC).

Determination of distribution ratios of substrates and product in an aqueous/organic biphasic medium

The pH-dependency of the distribution ratios of substrates and product were determined in an aqueous/organic biphasic system at 40°C. Each component was dissolved in an aqueous/organic solution, and its concentration in both phases was determined by HPLC.

Batch synthesis of Z-GlyPheOMe in an aqueous/organic biphasic medium

Z-GlyPheOMe was synthesized in an aqueous/organic biphasic media. Initial concentrations of carboxyl, and amine substrates were 50 and 400mM, respectively. The concentration of enzyme in an organic phase was 0.8g/l with a native enzyme base. The temperature was constant at 40°C.

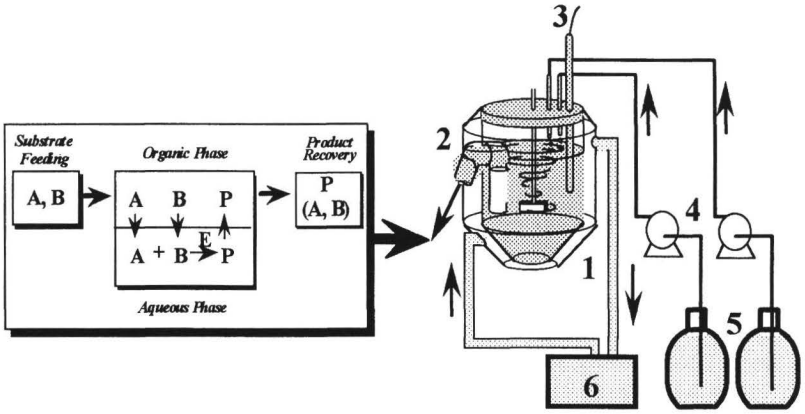


Figure 1 Scheme and experimental apparatus for the continuous protease-catalyzed synthesis of Z-GlyPheOMe (A: Z-L-Gly, B: L-PheOMe, E: enzyme, P: Z-GlyPheOMe). The apparatus consisted of: 1, a stirred reactor; 2, a settler; 3, a pH electrode; 4, feed pumps; 5, feed organic solution containing substrate and 6, a thermostat.

Continuous synthesis of Z-GlyPheOMe in an aqueous/organic biphasic medium

Figure 1 shows the scheme and experimental apparatus for the continuous synthesis of thermoase-catalyzed synthesis of Z-GlyPheOMe in an aqueous/organic biphasic medium. The organic solvent containing the substrates was fed to a stirred bioreactor. The substrates were extracted to the aqueous phase where the enzyme was dissolved. Z-GlyPheOMe, which was synthesized enzymatically in an aqueous phase, was extracted to the organic phase from the aqueous phase. The low concentration of Z-GlyPheOMe in an aqueous phase enhanced a peptide synthesis and extremely high yield could be obtained. Since enzyme was retained in the reactor because of the immiscibility of

organic solvent to water, Z-GlyPheOMe could be synthesized continuously. The initial concentrations of Z-L-Gly, L-PheOMe, thermoase were 5mM, 80mM, 20g/l, respectively. n-Butyl acetate was used as an organic solvent. The hold-up of organic phase was kept at 0.1, the stirring rate was 450 rpm and the pH was varied from 5.0 to 6.5.

Analysis

The HPLC system was used to measure the concentrations of substrate and product consisted of a UV8020 detector and a CCPS solvent delivery system (Tosoh Co., Japan). The concentrations of the substrates and product were measured with HPLC system on columns, $G2000_{SW}$ (Tosoh Co.) at 259nm. A mixture of acetonitrile/water (70/30, v/v) adjusted to pH 6.1 containing acetic acid was used as an elution buffer with the flow rate of 1ml/min.

RESULTS AND DISCUSSION

Batch synthesis of Z-GlyPheOMe in an aqueous monophasic medium

Figure 2 shows the typical time-course of the batch synthesis of Z-GlyPheOMe in an aqueous monophasic medium. The concentration of peptides increased early in the reaction, reached the saturation concentration, and then decreased gradually, because the amine substrate was non-enzymatically decomposed, a general phenomena when peptides are synthesized with proteolytically active enzymes.[4, 5, 8] The substrate conversions were less than 10% at any pH. The optimal pH was pH 6.5.

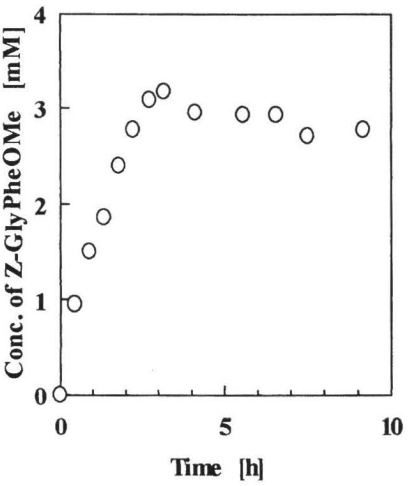


Figure 2 Typical time-course of the batch synthesis of Z-GlyPheOMe in an aqueous monophasic medium.

Determination of distribution ratios of substrates and product in an aqueous/organic biphasic medium

Figure 3 shows the pH-dependency of distribution ratios of substrate and product in an aqueous/organic biphasic medium (distribution behavior of L-PheOMe in a biphasic system was previously reported[13]). The distribution ratio is defined as the concentration of components in an organic phase divided by that in an aqueous phase. The nonionic component selectively distributes to an organic phase in a aqueous/organic biphasic medium.[14]

Since Z-L-Gly has carboxyl groups in its molecules, the concentration of nonionic Z-L-Gly increases at acidic pH. Therefore Z-L-Gly distributed more to an organic phase as pH decreases, and distributed to more to aqueous phase at the optimal pH for the enzymatic synthesis of Z-GlyPheOMe. Distribution behaviour of Z-L-Gly was almost the same even when we used various organic solvents. It distributed, however, more to an organic phase in aqueous/ethyl acetate, propyl acetate, tributyl phosphate (TBP) media. The organic solvents which have a high extract ability of Z-L-Gly have a high dielectric constant (ethyl acetate: 6.05, propyl acetate: 6.00, TBP: 8.91[15]). Dielectric constant is an indicator to express the electric characteristics of organic solvents. We can conclude that components distributed more to an organic phase in an aqueous/organic medium when we use organic solvents whose dielectric constants are high (hydrophilic organic solvents).

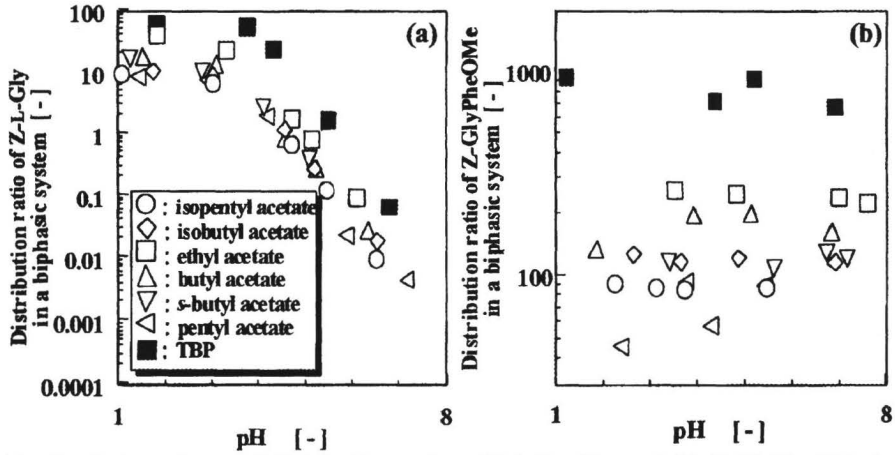


Fig. 3 pH-dependency of distribution ratios of (a) Z-L-Gly and (b) Z-GlyPheOMe in an aqueous/organic biphasic medium.

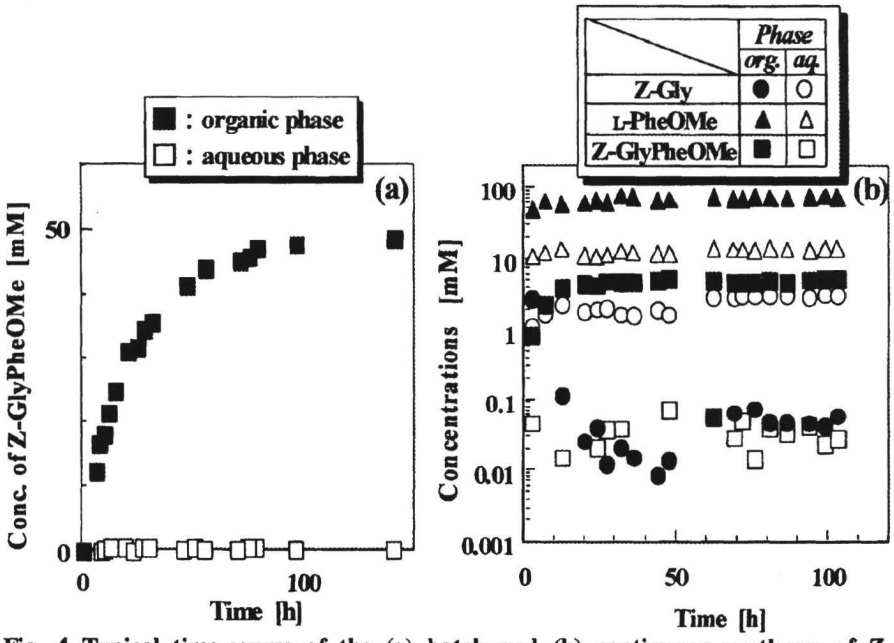


Fig. 4 Typical time-course of the (a) batch and (b) continuous syntheses of Z-GlyPheOMe in an aqueous/organic biphasic medium.

The above arguments for the Z-L-Gly distribution behavior could be applied to the Z-GlyPheOMe distribution behavior in a biphasic system. Z-GlyPheOMe distributed more to an organic phase when we use organic solvents whose dielectic constants are high (hydrophilic organic solvents). Since this peptide is nonionic without any dissociation groups in its molecule, the distribution behavior of Z-GlyPheOMe has no pH-dependency. It is therefore selectively extracted to an organic phase in an aqueous/organic biphasic medium.

Batch and continuous syntheses of Z-GlyPheOMe in an aqueous/organic biphasic medium

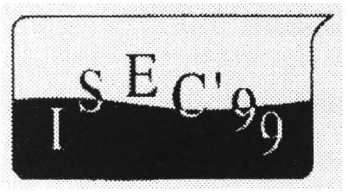
Figure 4 shows a typical time-course of the batch and continuous syntheses of Z-GlyPheOMe in an aqueous/organic biphasic medium. Butyl acetate was used as an organic solvent. The initial concentration of Z-L-Gly in an aqueous phase was 50mM in the batch synthesis of Z-GlyPheOMe. Finally, however, the concentration of the peptide was *ca.* 50mM in an organic phase, while it was less than 0.1mM in an aqueous phase, because the peptide was selectively extracted to the organic phase due to its hydrophobicity. The peptide yield was *ca.* 98%. In the continuous synthesis of Z-GlyPheOMe, the concentration of Z-L-Gly in an organic phase was kept to be very low, while the concentration of Z-L-Gly in an aqueous phase is very high enough for the enzymatic reaction. It is because the distribution ratio of Z-L-Gly is very low, namely, Z-L-Gly distributes more to an aqueous phase in an aqueous/organic biphasic medium. We obtained over 98% of peptide yield continuously.

CONCLUSION

A continuous extractive method has been developed to synthesize peptides in an aqueous/organic biphasic medium, and applied to the protease-catalyzed synthesis of Z-GlyPheOMe. To achieve a high peptide yield with this method, nonionic peptides are preferable to be selectively extracted to an organic phase in a biphasic medium. Organic solvents such as butyl acetate, ethyl acetate, TBP, which have a high dielectric constants are hydrophilic, and have a great ability to extract compounds. When butyl acetate was used as an organic solvent, a high yield, *ca.* 98% could be achieved continuously for Z-GlyPheOMe synthesis.

REFERENCES

1. Sears P and Wong CH, *Biotechnol. Prog.*, **12**, 423-433, (1996).
2. Gill I, Lopez-Fandino R, Jorba X and Vulfson EN, *Enzyme Microbial. Technol.*, **18**, 162-183, (1996).
3. Murakami Y and Hirata A, *Seibutsu-kogaku*, **76**, 238-254, (1998).
4. Murakami Y, Hirata M and Hirata A, *J. Ferment. Bioeng.*, **82**, 246-252, (1996).
5. Murakami Y and Hirata A, *J. Ferment. Bioeng.*, **83**, 38-42, (1997).
6. Hirata M, Ishimine T and Hirata A, *J. Chem. Eng. Jpn*, **30**, 467-477, (1997).
7. Murakami Y and Hirata A, *J. Ferment. Bioeng.*, **84**, 264-267, (1997).
8. Murakami Y, Yoshida T and Hirata A, *Biotechnol. Lett.*, **20**, 767-769, (1998).
9. Firestone RA, Pisano JM and Bonney RJ, *J. Med. Chem.*, **22**, 1130-1133, (1979).
10. Firestone RA, Pisano JM, Bailey PJ, Sturm A, Bonney RJ, Wightman P, Devlin R, Lin CS, Keller DL and Tway PC, *J. Med. Chem.*, **25**, 539-544, (1982).
11. Kimura Y, Yoshida T, Muraya K, Nakanishi K and Matsuno R, *Agric. Biol. Chem.*, **54**, 1433-1440, (1990).
12. Klein JU and Cerovsky V, *Int. J. Pepetide Protein Res.*, **47**, 348-352, (1996).
13. Hirata A and Hirata M, *Kagaku Kogaku Ronbunsyu*, **17**, 511-517, (1991).
14. Martinek K, Semenov AN and Berezin, *Biochim. Biophys. Acta*, **658**, 76-89, (1981).
15. Riddick JA, Bunger WB and Sakano TK, *"Organic Solvents. Physical Properties and Methods of Purification,"* John Wiley & Sons, New York, United States, (1986).



EXTRACTIVE HYDROLYSIS OF PROTEINS WITH ENZYMES IN AN AQUEOUS TWO-PHASE SYSTEM

Y Murakami and A Hirata
Department of Chemical Engineering, Waseda University
3-4-1 Ohkubo, Shinjuku-ku, Tokyo, 169-8555 Japan

ABSTRACT
We proposed a novel method to synthesize biologically active peptides utilizing an extractive hydrolysis of proteins in an aqueous two-phase system, and applied it to the thermolysin-catalyzed hydrolysis of zein (corn protein, *Zea mays L.*) to synthesize angiotensin converting enzyme (ACE) inhibitory peptides. Zein and its enzymatic hydrolysates (angiotensin converting enzyme inhibitory peptides) distributed to poly(ethyleneglycol) (PEG) and dextran (DEX) rich phases, respectively, in an aqueous PEG/DEX two-phase system. The ACE inhibitory peptides are selectively distributed in a DEX rich phase.

Keywords: Aqueous two-phase system, zein, thermolysin-catalyzed hydrolysis, biologically active peptides, ACE inhibitory peptides

INTRODUCTION

Proteins from natural resources have played important roles in supplying energy and nutrients, which were defined as primary functions of proteins. Proteins also have many tertiary functions relating to physiological regulations. To date, a number of functional peptides have been identified. One of the most interesting functions is a reduction of blood pressure.

Angiotensin-converting enzyme (dipeptidyl carboxypetidase, EC3.4.15.1(ACE)) is a dipeptide-liberating exopeptidase which plays an important physiological role in the regulation of blood pressure in renin-angiotensin and kallikrein-kinin systems.[1] ACE catalyses two different reactions; the conversion of inactive angiotensin to a powerfully vasoconstrictive angiotensin, and the inactivation of bradykinin (the vasodilator and natriuretic nonapeptide). Specific inhibitors of ACE are thus useful as antihypertensive drugs. [2, 3]

Enzymes as biocatalysts differ from chemical catalysts in their exceedingly high catalytic activity under mild conditions and a substrate specificity.[4] The mild reaction conditions of the enzyme-catalyzed reactions guarantee racemization-free syntheses, and chirally homogeneous products are obtained even when racemic aminoacid derivatives are used as starting material owing to the stereospecificity of enzymes.[5] These properties should ensure a wide application of enzymes in catalytic processes. Peptides have been synthesized enzymatically using aminoacid derivatives as starting materials,[6-8] however, lowering of cost must be addressed since aminoacid derivatives and enzymes are still expensive. Recently much attention has been paid to the enzymatic hydrolysis of food proteins to synthesize peptides, because it can be an attractive alternative to a traditional peptide synthesis due to the low cost of starting material. A number of angiotensin converting enzyme inhibitory peptides are isolated and identified from food proteins such as sardines,[9-12] tuna,[13] bonitos,[14-16] milk (casein)[17] and corn protein (zein).[18-20] To date, however, no processes to control the production of biologically active peptides utilizing enzymatic hydrolysis of proteins has been developed, even though many investigators focused on the separation and purification of peptides from enzymatic hydrolysates of proteins and the evaluation of their biological activities.

In this study, we propose a novel method to synthesize angiotensin converting enzyme inhibiory peptides from zein (corn protein, *Zea mays L.*) in an aqueous two-phase system (figure 1). In this method, an aqueous dextran (DEX) rich solution with a maize protein was fed to a stirred reactor which contained the aqueous polythyleneglycol (PEG) rich solution where a native enzyme is retained. The peptide produced was extracted to a DEX rich phase.

© 2000 Society of Chemical Industry

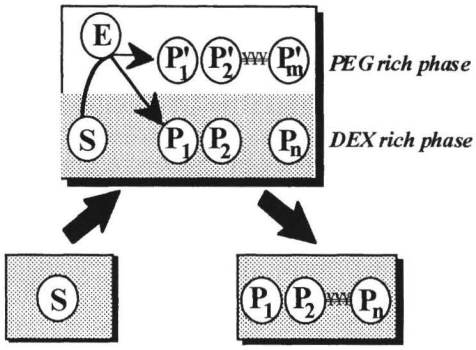


Figure 1 Scheme of an extractive enzymatic hydrolysis of zein in an aqueous two-phase system (E: thermolysin, P: enzymatic hydrolysates, S: zein).

EXPERIMENTAL

Materials

Thermolysin (8360 U/mg) was purchased from Daiwa Kasei Co. Ltd. (Osaka, Japan). Zein was separated from maize endosperm meal by the method proposed by Esen.[21] Polyethyleneglycol 1540 (of molecular weight (MW) 1500) and dextran 100000-200000 (of MW 100000-200000) were obtained from Wako Pure Chemical Ind. (Osaka, Japan). All other reagents were of analytical grade and purchased from Kokusan Chemical Works (Tokyo, Japan).

Batch enzymatic hydrolysis of zein in an aqueous, an aqueous-organic and an aqueous two-phase systems

Zein was hydrolyzed at pH7.0 and 40.0°C in an aqueous, an aqueous-organic and an aqueous two-phase system. Zein (1g) and thermolysin (0.03g) were added to 20ml of a Tris-buffer, an aqueous isopropyl alcohol solution (isopropyl alcohol: water = 9:1) and a PEG/DEX solution (total concentration of each polymers is 12 w/w %, with or without an addition of isopropyl alcohol). The concentrations of zein and enzymatic hydrolysates were measured by High Performance Liquid Chromatography (HPLC).

Assay for ACE inhibitory activity

The ACE inhibitory activity of enzymatic hydrolysates was assayed by the method of Maruyama *et al.*[22] HipHisLeu (5mM) and ACE inhibitors were dissolved in a 100mM of sodium borate buffer (pH8.3) containing 300mM NaCl. The solution was incubated for 30 minutes with 8 milliunits of ACE at 37.0°C. The concentration of ACE inhibitors required to inhibit 50% of the ACE activity under the above conditions was defined as IC_{50}.

Analysis

The HPLC system was used to measure the concentrations of zein, enzymatic hydrolysates and polymers, and to evaluate a molecular weight distribution of enzymatic hydrolysates. For the measurement of the concentration of zein and enzymatic hydrolysates, a UV-8020 detector and a DP-8020 solvent delivery system (Tosoh Co., Japan) on a column $G2000SW_{XL}$ (Tosoh Co., Japan) at 220nm was used. A mixture of acetonitrile/water (63/37, v/v) adjusted to pH 2.5 containing 0.5% phosphoric acid was used as an elution buffer with the flow rate of 1ml/min. For the evaluation of a molecular weight distribution of enzymatic hydrolysates, the same system was used except that a high purity water adjusted to pH 2.5 containing 0.5% phosphoric acid was used as an elution buffer. For the measurement of the concentration of polymers, a RI-8020 (Tosoh Co., Japan) detector and a column

$G4000PW_{XL}$ (Tosoh Co., Japan) were used with a high purity water as an elution. The $3.0 \times 10^{-6} m^3$ of sample solutions was taken and the concentrations of each component were measured with the above HPLC system.

RESULTS AND DISCUSSION

Batch enzymatic hydrolysis of zein in an aqueous and an aqueous-organic system

First, zein was hydrolyzed in a Tris-buffer, an aqueous isopropyl alcohol solution (isopropyl alcohol : water = 9 : 1). The enzymatic hydrolysates were separated and evaluated by their retention time (R. T. [min]) on a gel filtration chromatography.

Figure 2 shows a typical time-course of the batch hydrolysis of zein in an aqueous and an aqueous-organic media. Since the solubility of zein in a pure aqueous medium is less than 1 w/w%, the hydrolysis of zein in an aqueous medium is heterogeneous. The hydrolysis ratio was *ca.* 2% that was calculated with the concentration of a recovered zein. Some enzymatic hydrolysates were detected with HPLC (figure 2(a)). On the other hand, the hydrolysis ratio of zein in an isopropyl alcohol aqueous solution was *ca.* 20% (figure 2(b)). The hydrolysis of zein in an aqueous-organic medium is homogeneous because zein is completely soluble in a 90% isopropyl alcohol solution.[21] The addition of water-soluble alcohol led to a water stripping phenomena (which could be explained by the stripping of water bound to enzymes by organic solvents[23]). The concentration of zein gradually decreased early in the reaction and reached the saturation concentration due to the decrease of an enzyme activity.

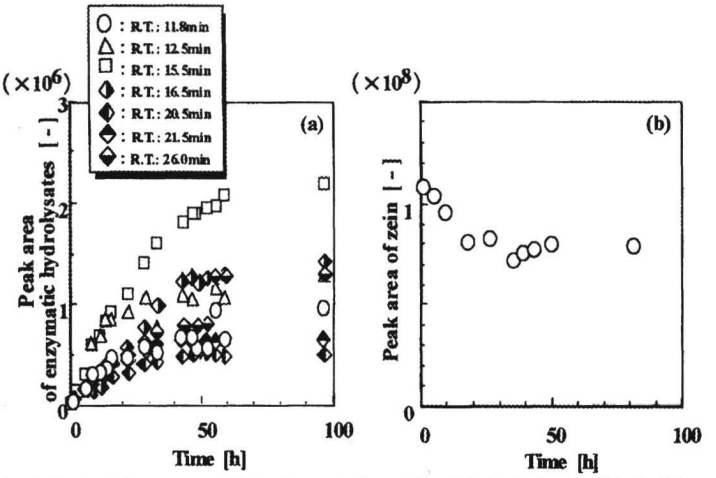


Fig. 2 Typical time-course of the thermolysin-catalysed hydrolysis of Zein in (a) a Tris-buffer and (b) an aqueous isopropyl alcohol solution (isopropyl alcohol : water = 9 : 1).

Batch enzymatic hydrolysis of zein in an aqueous two-phase systems

Figure 3 shows the typical time-course of the concentration ratio of zein and its enzymatic hydrolysates in an aqueous PEG/DEX two-phase system. The concentration ratio was defined as the concentration of each component in a PEG rich phase divided by that in a DEX rich phase. Since the aqueous two-phase system is consisted of water, the hydrolysis of zein there is heterogeneous. The hydrolysis ratio was thus very low, *ca.* 4%. The ratio was, however, *ca.* 30% in an aqueous PEG/DEX two-phase system by adding 2 v/v% of isopropyl alcohol due to the enhancement of the solubility of zein (figure 4 shows the comparison of the hydrolysis ratios of zein in various reaction media at 100

hours).

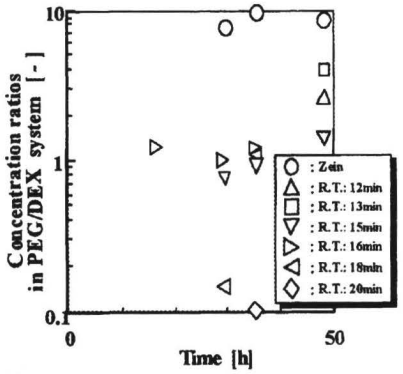


Fig. 3 Typical time-course of the concentration ratios of zein and its enzymatic hydrolysates in a PEG/DEX system, defined as the concentration of each component in PEG rich phase divided by that in DEX rich phase.

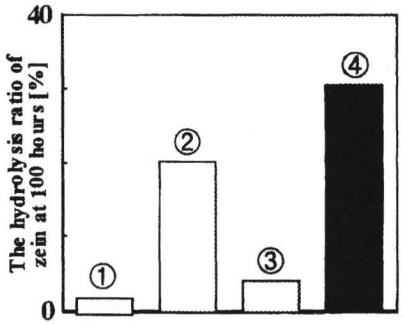


Fig. 4 The hydrolysis ratios of zein in (1) an aqueous, (2) an aqueous-organic and an aqueous two-phase systems (3) without and (4) with the addition of 2v/v% isopropyl alcohol at 100 hours.

Zein distributed to a PEG-rich phase in a PEG/DEX two-phase system as shown in figure 3 due to the high hydrophobicity of zein. The molecular weights of enzymatic hydrolysates (R.T.: 12-16 minutes) which distributed to both phases were *ca.* 1000-10000, while that (R.T: 18-20 minutes) which distributed to a DEX rich phase was less than 1000. Therefore we can conclude here that the enzymatic hydrolysates of low molecular weights selectively distributed to the bottom phase. The distribution ratio of thermolysin in above PEG/DEX system was 2.1 (unpublished data). The retention of enzyme in a PEG-rich phase was thus addressed in the future by some method such as a chemical or physical modification of an enzyme to enhance its hydrophobicity.

Assay for ACE inhibitory activity

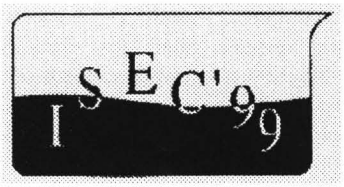
The ACE inhibitory activity of zein and its enzymatic hydrolysates (recovered in a DEX rich phase) was evaluated with an ACE-catalyzed hydrolysis of HipHisLeu. The concentration of ACE inhibitors required to inhibit 50% of the ACE activity was defined as IC_{50}. The compounds with low IC_{50} values are strong inhibitors because even small amount of them can inhibit ACE. IC_{50} for native zein was more than 1000μL/mL (the accurate determination of IC_{50} values for zein was difficult due to its high hydrophobicity). IC_{50}s for enzymatic hydrolysates were less than 200μL/mL. In particular, IC_{50} for enzymatic hydrolysate with retention time of 18 minutes (MW: less than 1000) was 70.3μL/mL. It was therefore confirmed that the enzymatic hydrolysates that selectively distributed to a DEX rich phase have a high ACE inhibitory activity.

CONCLUSION

We propose a novel method to synthesize biologically active peptides utilizing an extractive hydrolysis of proteins in an aqueous two-phase system, and apply it to the thermolysin-catalyzed hydrolysis of zein (corn protein) to synthesize angiotensin converting enzyme (ACE) inhibitory peptides. The hydrolysis ratio of zein in an aqueous medium is generally very low due to a high hydrophobicity of zein. We can improve the hydrolysis ratio by adding water-miscible organic solvent to the reaction medium. Zein distributed to a PEG-rich top phase, while the enzymatic hydrolysates with a high ACE inhibitory activity selectively distributed to a DEX-rich bottom phase.

REFERENCES

1. Oishi S, Kato H and Miyake Y, "*Kinin and angiotensin*", Koudansya Scientific, Tokyo, Japan, (1994).
2. Lucas BD Jr. and Hilleman DE, *Pharmacy Times*, **59**, 29-41, (1993).
3. Moser M, *J. Am. Col. Cardiol.*, **29**, 1414-1421, (1997).
4. Tramper J, *Biotechnol. Bioeng.*, **52**, 290-295, (1996).
5. Schellenberger V and Jakubke HD, *Angew. Chem. Int. Ed. Engl.*, **30**, 1437-1449, (1991).
6. Sears P and Wong CH, *Biotechnol. Prog.*, **12**, 423-433, (1996).
7. Gill I, Lopez-Fandino R, Jorba X and Vulfson EV, *Enzyme Microb. Technol.*, **18**, 162-183, (1996).
8. Murakami Y and Hirata A, *Seibutsu-kogaku*, **76**, 238-254, (1998).
9. Sugiyama K, Takada K, Egawa M, Yamamoto I, Onzuka H and Oba K, *Nippon Nogeikagaku Kaishi*, **65**, 35-43, (1991).
10. Ukeda H, Matsuda H, Osajima K, Matsufuji H, Matsui T and Osajima Y, *Nippon Nogeikagaku Kaishi,* **66**, 25-29, (1992).
11. Matsufuji H, Matsui T, Seki E, Osajima K, Nakajima M and Osajima Y, *Biosci. Biotech. Biochem.*, **58**, 2244-2245, (1994).
12. Seki E, Osajima K, Matsufuji H, Matsui T and Osajima Y, *Nippon Nogeikagaku Kaishi*, **69**, 1013-1020, (1995).
13. Kohama Y, Matsumoto S, Oka H, Teramoto T, Okabe M and Mimura T, *Biochem. Biophys. Res. Commun.*, **155**, 332-337, (1988).
14. Yokoyama K, Chiba H and Yoshikawa M, *Biosci. Biotech. Biochem.*, **56**, 1541-1545, (1992).
15. Matsumura N, Fujii M, Takeda Y and Shimizu T, *Biosci. Biotech. Biochem.*, **57**, 1743-1744, (1993).
16. Astawan M, Wahyuni M, Yasuhara T, Yamada K, Tadokoro T and Maekawa A, *Biosci. Biotech. Biochem.*, **59**, 425-429, (1995).
17. Kohmura M, Nio N, Kubo K, Minoshima Y, Munekata E and Ariyoshi Y, *Agric. Biol. Chem.*, **53**, 2107-2114, (1989).
18. Miyoshi S, Ishikawa H, Kaneko T, Fukui F, Tanaka H and Maruyama S, *Agric. Biol. Chem.*, **55**, 1313-1318, (1991).
19. Miyoshi S, Kaneko T, Yoshizawa Y, Fukui F, Tanaka H and Maruyama S, *Agric. Biol. Chem.*, **55**, 1407-1408, (1991).
20. Miyoshi S, Kaneko T, Ishikawa H, Tanaka H and Maruyama S, *Ann. N. Y. Acad. Sci.*, **750**, 429-431, (1995).
21. Esen A, *J. Cereal Sci.*, **5**, 117-128, (1987).
22. Maruyama S, Nakagomi K, Tomizuka N and Suzuki H, *Agric. Biol. Chem.*, **49**, 1405-1409, (1985).
23. Gorman LAS. and Dordick JS, *Biotechnol. Bioeng.*, **39**, 392-397, (1992).



THE EFFECT OF SURFACTANTS DURING SOLVENT EXTRACTION OF ERYTHROMYCIN-A FROM BUFFER AND FILTERED FERMENTATION BROTH

MR Pursell, MA Mendes-Tatsis and DC Stuckey
Department of Chemical Engineering & Chemical Technology, Imperial College of Science, Technology and Medicine, London, SW7 2BY, U.K.

ABSTRACT
Solvent extraction of the antibiotic erythromycin-A from buffer and filtered fermentation broth into 1-decanol was investigated. The presence of the soluble surface active compounds (SAC) in the filtered broth led to a 45% reduction in mass transfer rates. The addition of Softanol 120 and Softanol 30 reduced extraction rates from the buffer, but had no effect on the broth extraction. Interfacial turbulence enhanced mass transfer by up to 55% for extraction from both buffer and filtered broth when SDS and LDS where present.

Keywords: fermentation broth, surfactants, interfacial convection, Lewis cell, erythromycin, 1-decanol.

INTRODUCTION

Solvent extraction in the biotechnological industries is often more complicated than in traditional chemical industries. Microbial cells and surface active compounds (SAC) produced during fermentation can lead to the formation of stable emulsions and cause significant reductions in the extraction rate. The addition of anti-foaming agents and de-emulsifiers can further complicate the situation. It has been found[1] that whole and filtered broth created very stable emulsions, while a <10 Dalton molecular weight fraction of the broth had no greater effect than distilled water. This led to the conclusion that macromolecules such as proteins caused emulsion stabilisation. The effect of yeast cells on ethanol extraction from distilled water has been investigated,[2] and the authors report that an 86% decrease in the mass transfer coefficient occurred at a cell concentration of 0.1 kg/m^3. This decrease was related to the reduction in the interfacial area caused by the close packing of the adsorbed yeast cells. It is well established that SAC can affect mass transfer rates both positively and negatively, a number of different mechanisms have been identified: interfacial rigidification[3] by a surfactant layer preventing turbulence occurring at the interface; altered partition coefficients[4] which would lead to changes in concentrations and thus affect the driving force for mass transfer and an interfacial barrier[5] which would affect the solutes ability to cross the liquid-liquid interface. However, SAC may also cause interfacial turbulence[6] which can dramatically increase the rate of mass transfer by replacing the stagnant diffusional layers either side of the interface with turbulent fluid flows. Recently,[7] an increase in mass transfer of erythromycin was identified which could not be explained through interfacial turbulence; it was postulated that this was caused by an interaction/aggregation between the surfactant and the solute at the interface. Literature on the effects of microbial SAC tends to concentrate mainly on their effects during microbial growth on hydrocarbons and applications in enhanced oil recovery. The types of SAC found in broths has been reviewed;[8] the main classes of compounds reported are glycolipids, phospholipids, lipopeptides, fatty acids and particulates (cells). Hence, the aim of this work was to investigate the effect of soluble broth constituents and added surfactants on the mass transfer rate of a macrolide antibiotic.

EXPERIMENTAL

The extraction of erythromycin-A was examined from a 50 mM carbonate buffer and a filtered fermentation broth into 1-decanol (Aldrich). Erythromycin is a macrolide antibiotic which is a weak base with a pK_a of 8.6; in solutions above pH 8.6 erythromycin will exist in its non-polar unprotonated form and will readily partition into 1-decanol. The partition coefficient, $K_P = C_{org}/C_{aq}$, is 99 at pH 10,[7]

© 2000 Society of Chemical Industry

with dissociation higher than 96%. Fermentation broth of the erythromycin producing bacteria *Streptomyces Erythreus* was obtained and filtered using a 0.2μm ceramic filter; the residual concentration of erythromycin in the broth was only 0.05 g/dm^3; to enable the concentration in the broth to be analysed this was increased to 1 g/l by the addition of commercially purchased erythromycin-A (Sigma). The broth was adjusted to pH 10 using NaOH; the pH 10 buffered phases also had an initial concentration of 1 g/dm^3 erythromycin.

The effect of four surfactants, two anionic and two non-ionic, on the extraction process was also examined. The anionic surfactants were sodium dodecylsulphate (SDS) and lithium dodecylsulphate (LDS) (Sigma). Both surfactants are soluble in the aqueous phase and were used at a concentration of 2 g/dm^3. The non-ionic surfactants were Softanol 120 (S120) and Softanol 30 (S30) (Honeywill & Stein Ltd.), which are soluble in the organic phase, and the concentration was also 2g/dm3.

The surface tension of the filtered broth was measured at 25°C using a Kruss K10 digital tensiometer fitted with a platinum Du-Nouy ring, and measurements were reproducible to ± 0.1mN/m.

A modified Lewis cell,[7] which is a non-dispersive, fixed interfacial area contactor, was used to measure dynamic mass transfer. The modified Lewis cell consists of a jacketed cylindrical glass vessel, which contains two counter rotating propellers positioned equidistant from the interface. The total liquid volume was 630 cm^3 (315 cm^3 per phase) and sampling was achieved via a re-sealable Teflon septum fixed in the end plates. All experiments were performed at 25°C and with stirrer speeds of 120 rpm on the aqueous side and 200 rpm on the organic side, which maintained a flat unperturbed interface. Samples of 0.5 cm^3 were taken from the aqueous phase for analysis with equal organic volumes removed to maintain the phase volume ratio. The erythromycin concentration in the buffer and in the filtered broth was assayed based on a spectrophotometric technique,[9] the detection limit of the assay was 2 to 0.1 g/dm^3 erythromycin. The error in the overall mass transfer coefficients determined in the Lewis cell was ± 6%.

A Schlieren optical apparatus[6] was used to qualitatively examine the presence of interfacial turbulence. The method uses a Ne-He laser (25mW and λ = 532.8nm) as a monochromatic light source. The beam of light was collimated and then passed through the test space that consisted of a PTFE cell, internal dimensions (50x75x18 mm) with quartz glass windows. The test space was filled with 1-decanol and a drop of the buffer/broth phase was formed at the end of a capillary positioned in the path of the light beam. The beam of light leaving the test cell was focused on a knife edge. When a refractive index change occurs in the test cell, as would be caused by changes in concentration, the light is deflected differently and passes by the knife edge to be projected onto a screen. The images were recorded using a Sony DVD1000 digital video camera for later analysis.

RESULTS AND DISCUSSION

The concentration vs. time plots for the extraction of erythromycin from buffer and filtered broth are presented in Figures 1 and 2, respectively. The anionic surfactants (SDS and LDS) caused a substantial increase in the extraction rate with 49% and 55% more erythromycin extracted from the buffer and broth systems respectively. The presence of the anionic surfactants increased broth extraction to the levels found for extraction from the surfactant free buffer. Table 1 presents values for the overall mass transfer coefficient, K_{oc}, for the "clean" systems and for the Softanol systems as determined by the "two film" theory.

Results show that the mass transfer rates for extraction from the filtered broth were significantly lower than those from the buffer. For the case of surfactant free broth a 45% reduction in the overall mass transfer coefficient, K_{oc}, was measured. The presence of Softanol 120 and 30 in the buffer system reduced the extraction rate, with S120 showing a greater decrease; in the broth systems the presence of either Softanol 120 or 30 had no effect on the mass transfer rate.

In the cases involving the anionic surfactants SDS and LDS it was not possible to obtain values of K_{oc} because the data did not fit the two film theory.

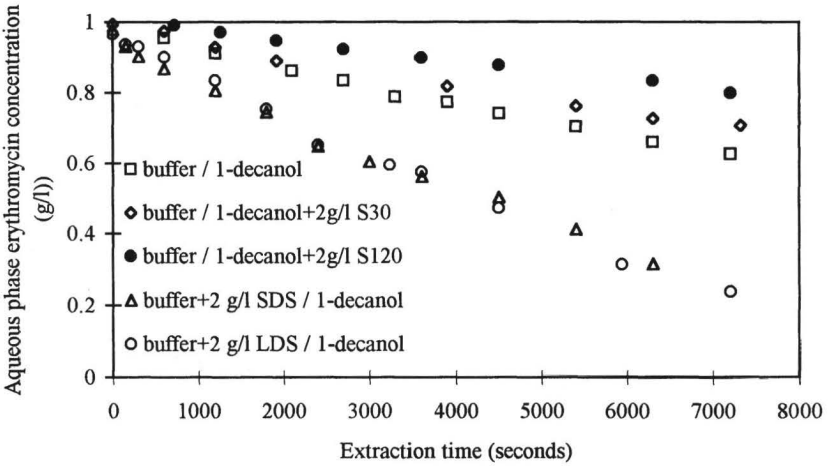


Figure 1 The effect of added surfactants on the extraction of erythromycin from buffer.

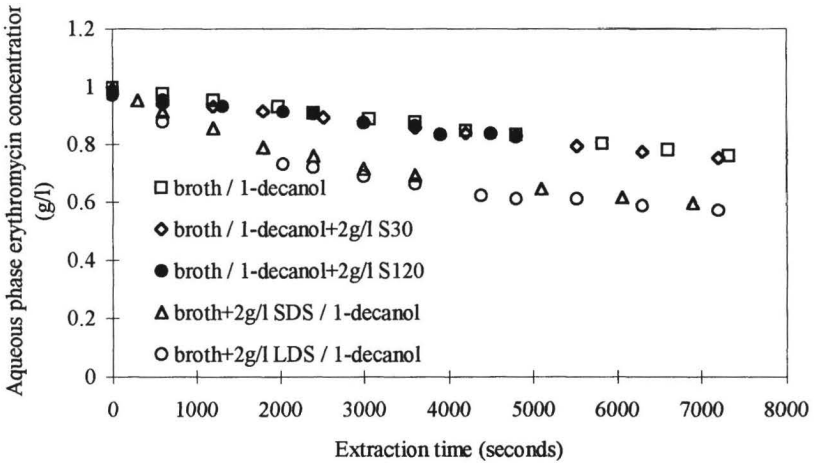


Figure 2 The effect of added surfactants on the extraction of erythromycin from filtered broth.

	Organic Phase		
Aqueous Phase	1-Decanol	1-Decanol + 2g/l S30	1-Decanol + 2g/l S120
Buffer	4.5	3.3	2.2
Broth	2.4	2.5	2.4

Table 1 The effect of changes of aqueous phase and with the addition of Softanol 30 and 120 (S30/120) on the overall mass transfer coefficients, K_{oc}, ($x10^6$ m/s).

In Figure 4a, Schlieren images at selected times of the transfer of erythromycin from the broth drop to the continuous 1-decanol phase are shown. It may be observed that the aqueous/organic interface is

quiescent and therefore transfer is diffusional. However, in Figures 4b and 4c, which show the transfer of erythromycin from drops containing broth plus SDS and broth plus LDS, into 1-decanol, interfacial convection is observed. Schlieren images have also been taken for the cases of erythromycin transfer from buffer with and without the addition of SDS and LDS, and similar interfacial behaviour was observed. However, in the cases of the systems involving Softanol 120 and 30 interfacial convection was not observed. These findings explain why the two-film theory could not be applied to the systems where SDS and LDS were present. The main assumption of the two-film theory is that stagnant layers exist on both sides of the interface through which mass transfer occurs by diffusion only. The Schlieren images for the SDS and LDS cases show that mass transfer does not occur by diffusion alone but is aided by interfacial convection. The interfacial convection observed also explains the higher transfer rates obtained for those systems, as shown in Figures 1 and 2.

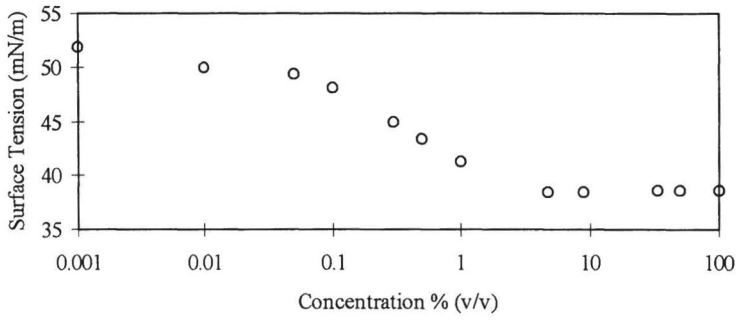
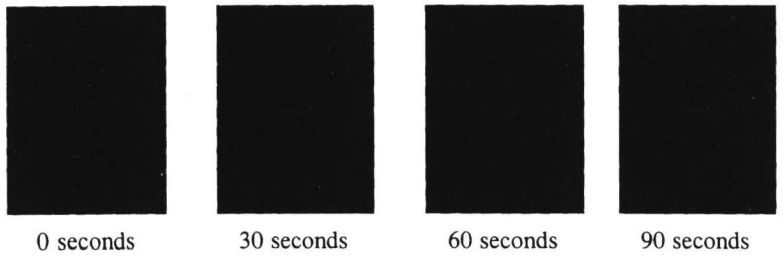
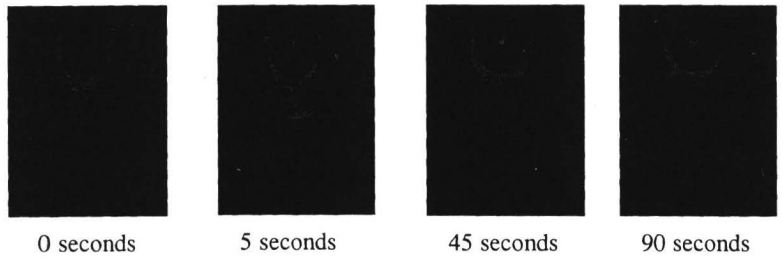


Figure 3 The change in surface tension with dilution of the filtered broth.

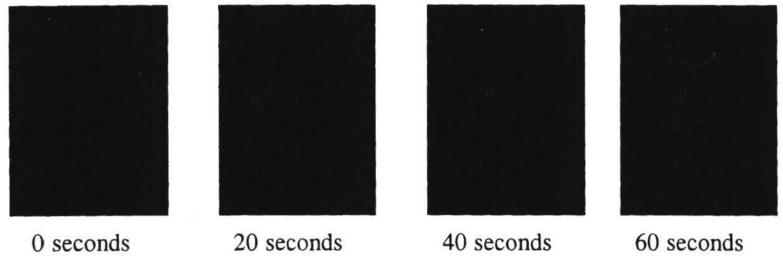
The addition of surfactants to the phases reduced the interfacial tension in all cases, the most significant reductions being with SDS and LDS. This would explain the occurrence of interfacial convection that arises as a result of localised variations in the interfacial tension. The surfactants are themselves also solutes and the transfer of surface-active material through the interface may cause the interfacial tension gradients required to create the interfacial fluid flows which can lead to the destabilisation of the interface.

The nature and quantity of the SAC present in the broth is unknown. However, an indication of their effect on the physical properties of the broth can be seen in Figure 3 which shows the change in surface tension for increasing concentrations of the broth. (The variation in broth concentration was obtained by dilution with distilled water.) At very high dilutions (0.001% v/v) there is a significant reduction in the surface tension to 51.8 mN/m compared to the value for distilled water of 72 mN/m. The value of the surface tension continues to decrease with increasing concentrations up to 5% v/v after which the surface tension remains constant at 38.6 mN/m, indicating that the surface is saturated with SAC and the formation of micelles has occurred. An interface laden with SAC, which in biological systems are typically quite large molecules, may lead to an interfacial resistance through the formation of a energy barrier to mass transfer which would explain the reduction in all the extraction rates from broth relative to the buffer. The organic soluble Softanols had little effect on the mass transfer rate from the filtered broth. This may be due to the SAC present in the aqueous broth having a greater influence on the mass transfer process, in comparison to the buffer system where the Softanols do reduce the mass transfer rate. Similarly, the enhancing affect of the aqueous soluble surfactants SDS and LDS is not as evident in the broth system as it is in the buffer systems and again this may be due to effects caused by the presence of microbial SAC, however turbulence is still present which discounts the possibility of a rigid layer damping turbulent transfer.





(a)



(b)

(c)

Figure 4 Schlieren images of the extraction of erythromycin from filtered broth.
a) broth / 1-decanol.; b) broth + 2g/l SDS / 1-decanol.; c) broth + 2g/l LDS / 1-decanol.

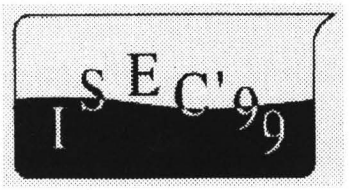
CONCLUSIONS AND FUTURE WORK

It was found that the presence of soluble SAC in the filtered broth considerably reduced mass transfer. The presence of non-ionic surfactants had little effect but the anionic surfactants (SDS and LDS) were found to cause interfacial turbulence which increased the extraction rate by up to 55%. Future work will include characterising the broth to establish which groups of compounds primarily influence the extraction process and the effect that these compounds and added surfactants have on solute diffusion rates close to the interface.

REFERENCES

1. Lennie S, Halling PJ and Bell G, *Biotechnol. Bioeng.*, **35**, 948, (1990)

2. Crabbe PG, Tse CW and Munro PA, *Biotechnol. Bioeng.*, **28**, 939, (1986)
3. Lewis JB, *Chem. Eng. Sci.*, **3**, 248, (1954)
4. Garner FH and Hale AR, *Chem. Eng. Sci.* , **2**, 157, (1953)
5. Mudge LK and Heideger WJ, *AIChE J.*, **16**, 602, (1970)
6. Agble DK, *PhD Thesis,* University of London, 1998
7. Lye GJ, Pursell MR and Stuckey DC, submitted to Chem. Eng. Sci., 1998
8. Desai JD and Banat IM, *Microbiol. Mol. Biol. Rev.*, **61**, 47, (1997)
9. Gallagher PA and Danielson ND, *Talanta*, **42**, 1425, (1995)



RECOVERY OF ETHANOL FROM AQUEOUS SOLUTION BY EXTRACTION WITH 1-DODECANOL

F Ruiz , V Gomis, N Boluda and H Bailador
Departamento de Ingeniería Química. Universidad de Alicante, Aptdo. 99, E-03080 Alicante, Spain.

ABSTRACT
The process of recovery by liquid-liquid extraction of ethanol manufactured in a fermentation process could be improved by using solvents such as 1-dodecanol which have a good separation factor. In this work, liquid-liquid equilibrium data for the ternary system water - ethanol - 1-dodecanol have been determined experimentally at 5, 15 and 30° C. The results obtained make it possible to carry out the design calculation of a proposed suitable extraction process for separating ethanol and water using fatty alcohol.

Keywords: ethanol extraction, 1-dodecanol, fatty alcohols

INTRODUCTION

Fermentation ethanol from carbohydrates and other renewable raw materials is a potential large-scale fuel of the future. However, ethanol produced by using the conventional process of batch fermentation of sugars with yeast, followed by distillation to recover the ethanol, is uneconomic compared to fossil fuels.[1] However new technologies for separating alcohol from water solutions may soon significantly lower the cost of producing ethyl alcohol by fermentation.

Liquid-liquid extraction is one possible means of accomplishing this separation. Several investigators have obtained experimental data of distribution coefficients and separation factors at high dilution of ethanol for a wide range of solvents,[2,3,4] although the design calculations cannot be done using only these data because they depend of the ethanol concentration. Along these same lines, in three previous works [5,6,7] different processes for the extraction of ethanol were studied. The design calculations of each process were carried out, and the properties that the solvent should offer to decrease the energetic requirements of the extraction process were studied.

Also along the same lines, Gyamerah and Glover[8] constructed a pilot plant for fermentation production of ethanol using liquid-liquid extraction with 1-dodecanol to remove the product and with recycling of the fermented broth raffinate. However the flow rate of the solvent had to be fixed without knowing the liquid-liquid equilibrium of the system water-ethanol-1-dodecanol.

In this work, equilibrium data for this system have been determined experimentally at 5, 15 and 30 °C. 1-dodecanol is the fatty alcohol of the longest carbon chain that is liquid at 25° C. The combination of liquid-liquid and liquid-solid equilibria at the temperature range of 5-30°C could improve the economical aspects of the extraction process.

EXPERIMENTAL

All chemicals (Merck) contained negligible amounts of impurities and were used as supplied. Firstly the binodal curve of the liquid-liquid equilibrium was obtained by titration [9] using the cloud point method. After reaching the end point of the titration, the refractive index of the homogeneous mixtures obtained was measured with an automatic refractometer (Leica AR600). A refractive index versus ethanol concentration curve was prepared for each temperature of study.

Once the binodal curve was known, equilibrium data were obtained by preparing mixtures of known overall mass composition, stirring vigorously and settling at a constant temperature for at least 72 hours to ensure equilibrium was reached. Then the measurement of the refractive index in each phase and its interpolation in the refractive index versus ethanol concentration curve for each temperature provides sufficient information to determine a tie line.

© 2000 Society of Chemical Industry

RESULT AND DISCUSSION

Figures 1, 2 and 3 show the equilibrium diagrams in weight percentage at the different temperatures. As can be seen, at 5° C the ternary system does not present any region with two liquid phases in equilibrium. At higher temperatures (15° C) regions with two liquid phases and with three phases solid+liquid+liquid appear. Finally, when the temperature increases (30° C) the equilibrium diagram presents only a heterogeneous region that contains two liquid phases. These changes in the shape of the equilibrium diagram can be used to improve the process of extraction and recovery of the ethanol.

In this respect, figure 4 shows the conceptual flow sheet of a process to produce anhydrous alcohol when a solvent less volatile than ethanol such as 1-dodecanol is used. Stream 1 containing for example 20 mol % ethanol and coming from the beer still of a typical fermentation plant is fed to the extraction column P. An extractive distillation column Q dehydrates the extract producing a bottom stream without water. The bottom stream only contains ethanol and the solvent and it is transferred to a second distillation column R where it is separated into an overhead stream containing only ethanol and a bottom stream containing the solvent, which is recycled.

The improvements in the process are based on the easy separation of 1-dodecanol via crystallization (C) in the streams where it is the predominant component. Thus, the 1-dodecanol could be separated from stream 2 and used as entrainer in column Q. Moreover, the previous separation of 1-dodecanol in stream 6 would decrease notably the cost of operation of column R. Both separations would produce important saving in the cost of the process.

In this way, the melting and solidification of the solvent could be an excellent method to improve the economy of the process of recovery of ethanol from aqueous solutions. The results can be extrapolated to other heavier fatty alcohols although other ranges of temperatures should be used.

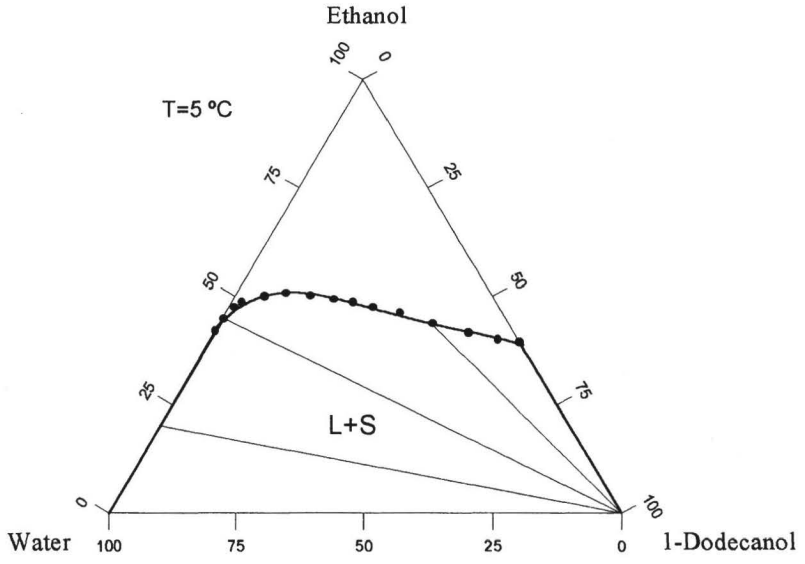


Figure 1. Representation of the equilibrium data (weight percent) for the ternary system 1-Dodecanol - Ethanol - Water at 5 °C

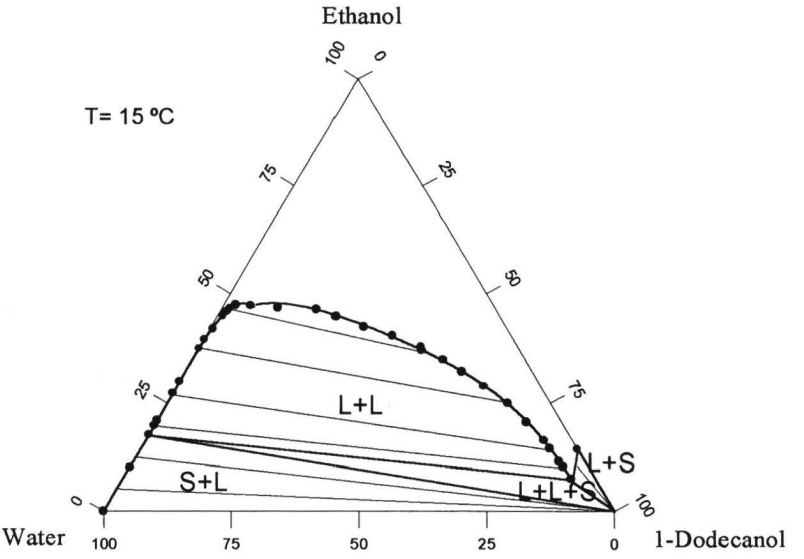


Figure 2. Representation of the equilibrium data (weight percent) for the ternary system 1-Dodecanol - Ethanol – Water at 15 °C

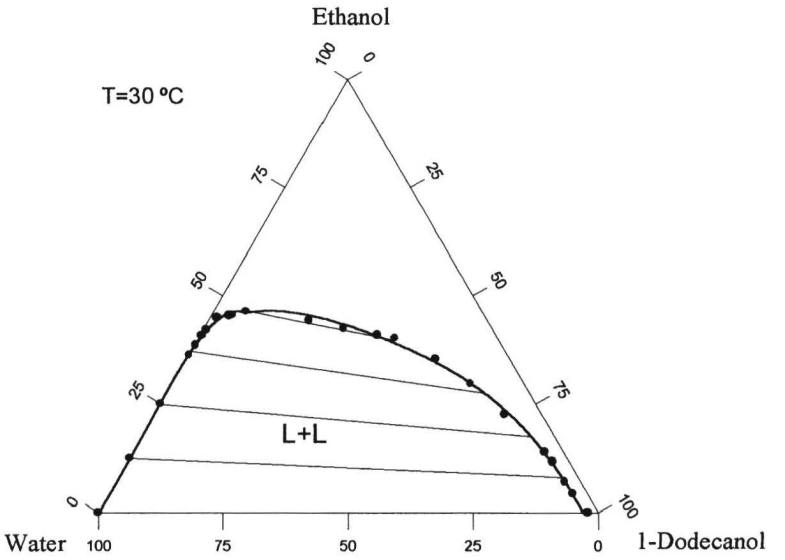


Figure 3. Representation of the equilibrium data (weight percent) for the ternary system 1-Dodecanol – Ethanol – Water at 30 °C.

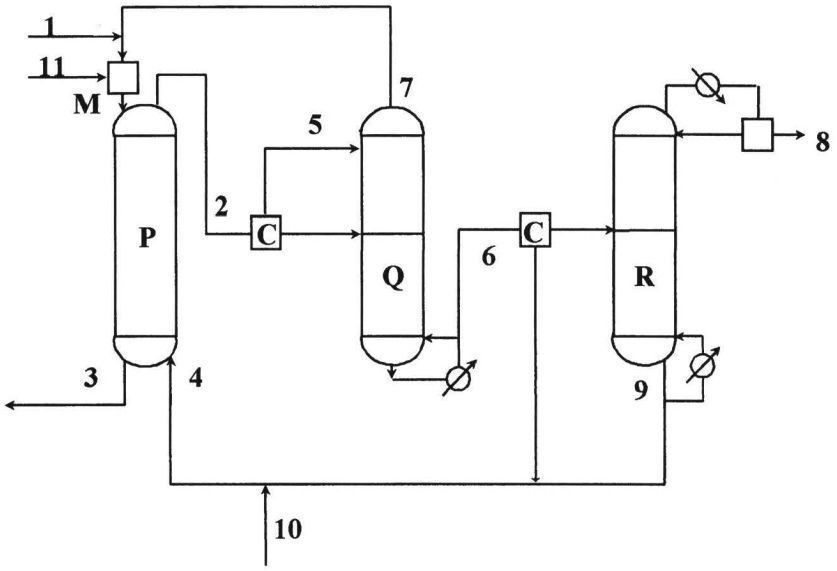


Figure 4. Conceptual flow sheet of a process to produce anhydrous alcohol when 1-dodecanol is used.

ACKNOWLEDGEMENTS

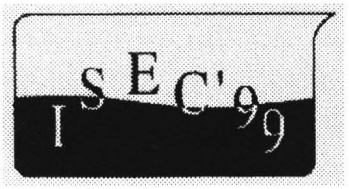
The authors wish to thank the DGES for the financial aid of project PB96-0338.

REFERENCES

1. Barnard GW '*Biotechnology*', ed. H.Dellweg. Verlag Chemie GmbH, Weinheim, **3**, (1983).
2. Roddy JW, *Ind. Eng. Chem. Process Des. Dev.*, **20**, 104, (1981).
3. Roddy JW and Coleman CF, *Ind. Eng. Chem. Fundam.*, **20**, 250, (1981).
4. Munson CL and King CJ, *Ind. Eng. Chem. Process Des. Dev.*, **23**, 109, (1984).
5. Ruiz F, Gomis V and Botella R, *Ind. Eng. Chem. Res.*, **26**, 696, (1987).
6. Ruiz F, Gomis V and Botella R, *Ind. Eng. Chem. Res.*, **27**, 648, (1987).
7. Gomis V, Ruiz F, Boluda N and Saquete MD, *Ind. Eng. Chem. Res.*, **37**, 599, (1998).
8. Gyamerah M and Glover JJ, *Chem. Tech. Biotechnol.*, **66**, 145, (1996).
9. Alders L, *Liquid-liquid Extraction*. Elsevier, Amsterdam, (1959)



Environmental Impact



SOIL REMEDIATION BY SUPERCRITICAL EXTRACTION WITH SOLVENT RECIRCULATION UNDER QUASIISOBARIC OPERATION CONDITIONS. APPLICATION TO SOIL POLLUTED BY HYDROCARBONS

E Alonso, JJ Alonso and MJ Cocero.
Dept. Ingeniería Química. Universidad de Valladolid, 47006 Valladolid. Spain

ABSTRACT
Soil regeneration using CO_2 supercritical extraction processes is one innovative technique available nowadays. This technology has been successfully applied on a pilot plant scale basis to a variety of soil pollutants, for example, hydrocarbons, pesticides, phenols, i.e. persistent pollutants difficult to treat. Conclusions obtained from such studies indicate, that though this technology is highly valuable for treating specific types of soil, it is associated with a high cost of treatment. This is mainly the cost of re-compressing the supercritical fluid (usually CO_2), since it is necessary to de-pressurize to gaseous CO_2 to recirculate it free of contaminants and to operate under most favourable conditions. In the present work a novel alternative approach is presented. This relies upon solute-supercritical fluid separation by adsorption onto activated carbon. Under these conditions the plant would be operating in a quasi-isobaric state and, therefore, the de-pressurization-re-pressurization cycle is avoided and energy costs minimized. The pilot plant used in this work has been designed and built at the Chemical Engineering Department of Valladolid University. Normal operating conditions include 7-30 MPa and 30-70°C for a soil load of around 1 Kg. Results show that for a regeneration time of 60 minutes, pollutant concentration was reduced to below 25 mg/kg.

Keywords: supercritical extraction, isobaric process, organic extraction, soil remediation, carbon dioxide

INTRODUCTION

Today pollution is mainly a direct consequence of inadequate urban, traffic and industrial practices. As such, there is a great dead of concern about their improvement to reduce pollution. But, in some cases, such as polluted soil, not only it is necessary to stop the ingress of new pollutants but it is also compulsory to eliminate the existing pollutants because of their threat to the environment. The Spanish National Inventory of Polluted Soils 95 detail 4902 registered sites. Five hundred million dollars have been allocated for the period 1995-2005 for studies and remediation treatment.

Depending on the type of the pollutant to be eliminated, several conventional processes, including solvent extraction, biodegradation and incineration, have been proposed for soil regeneration. Though successful for some applications, in many cases they possess several drawbacks,[1] with generally poor efficiencies but even the production of more toxic by-products.

Recently, solvent extraction using supercritical fluids has been postulated to overcome these drawbacks.[2] It is claimed that supercritical fluid extraction (SFE) applied to soil regeneration renders a solvent-free soil at high efficiencies. Most of the literature cited supercritical carbon dioxide (SC-CO_2) as the solvent of choice.[3] Though technically viable, poor pollutant solubility in SC-CO_2 makes the process costly in terms of CO_2 expenditure. To reduce it, recent developments are pointing to increasing pollutant solubility by using co-solvents.[4] This approach would not be a straight forward solution, since it would produce a soil impregnated with co-solvent, that would require re-treatment to eliminate it. Also CO_2 re-circulation has to be carefully designed to balance pollutant recovery efficacy and CO_2 recompressions costs, which determine the overall energetic cost of the process.

Bearing is mind the objective of CO_2 re-compression is cost minimization, acting on pressure and/or temperature in the separation step, so that the pollutant is recovered and CO_2 re-circulated, should be discarded, since to obtain CO_2 pollutant-free would imply a drastic reduction of pressure. Recently some authors have proposed isobaric CO_2-solute separations to reduce energy cost.[5,6] In this paper the feasibly of pollutant adsorption on active carbon under isobaric conditions is considered.

© 2000 Society of Chemical Industry

In order to accomplish this objective, a pilot plant for soil regeneration has been designed and built. It consists of a two-step integrated plant: pollutant CO_2 supercritical extraction and pollutant adsorption on active carbon. The pilot plant would operate under quasi-isobaric conditions, and CO_2-SC re-circulation. It was designed to operate at $P < 0$ MPa, $T < 80°C$ and CO_2 total flow of 1 to 10 kg/h.

EXPERIMENTAL

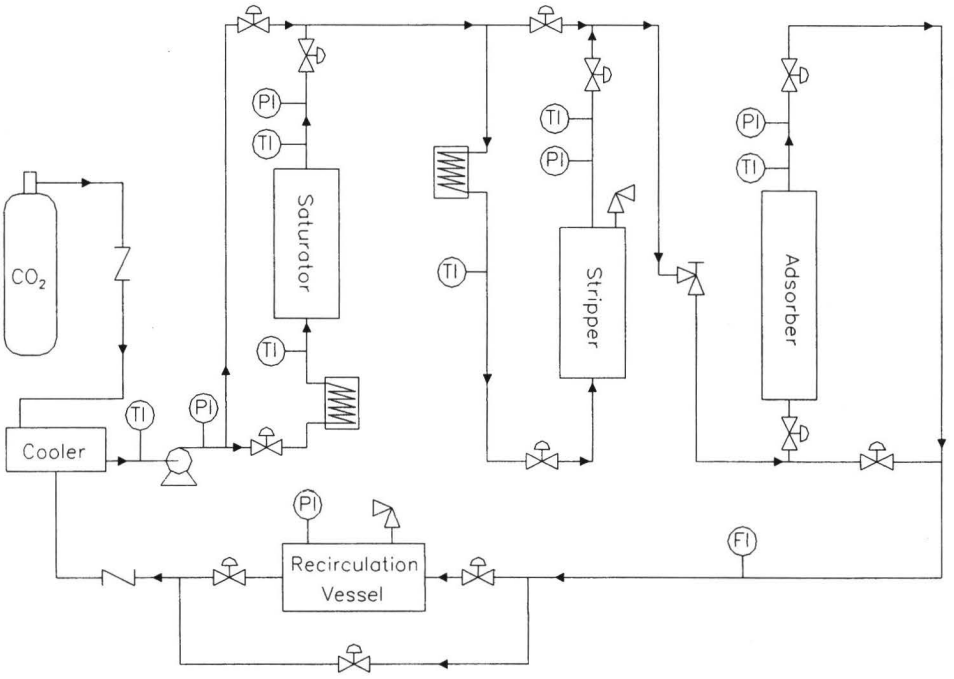
The flow diagram of the pilot plant is schematically presented in Figure 1. It was based on an initial pressurized vessel acting as stripper (where the soil to be regenerated was placed), a second pressurized vessel acting as adsorber (where active carbon was placed), a pump for solvent supply and auxiliary equipment heat exchangers, pressure, temperature and flow meters.

Both pressurized vessels were made of jacketed stainless steel tube end capped at the bottom and screws and flange at the upper end. Soil was placed inside a basket that was fitted to the walls by gaskets to avoid by-pass of the solvent. A diffuser at the bottom of the chamber achieved uniform distribution of solvent. When it was needed, a second desorber was placed in series.

To prepare synthetic soils of the desired pollutant and/or specific concentration, a third pressurized vessel, similar to the ones cited above, was used as CO_2-saturator, so that CO_2 saturated with pollutant was desorbed over a standard soil. It was assumed that pollutant was uniformly distributed over the standard soil.

A LEWA, diaphragm pump head type EH1, LEWA Herbert Leomberg (Germany) was used the admission valve of this pump will withstand 27.5 Mpa. In this way, direct pumping from the CO_2 bottle (3-4 Mpa) and re-compression of the CO_2-recirculated was achieved with the same pump.

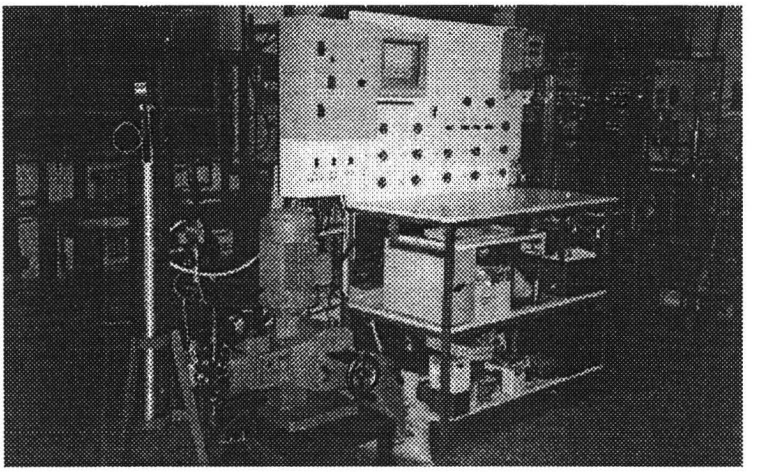
Figure 1. Flow diagram of pilot plant for supercritical extraction under isobaric operation conditions.



Auxiliary equipment

Heat exchangers were made of coils immersed in stirred temperature-controlled baths. Mass flow meters were RHEONIK RHM 01 GNT provided with an electronic unit RHE 08. Tubing (1/4 inch) and valves were from commercial pressure equipment and junctions were made using commercial tube fittings.
Acquisition data systems, pressure and temperature meters were from Desin Instruments Barcelona (Spain). A whole plant view is presented in Figure 2.

Figure 2: View of pilot plant.



Operating procedure

The pilot plant was used to study soil regeneration of industrial soil polluted by hydrocarbons from "El Fangal" Murcia Spain. Soil pollution in this works was typically around 2000-5000 mg/kg as measured by infrared method.[7] It may be considered an aged-type material since it is recorded as being polluted for the last 20 years.[8] Industrial granular active carbon used was Chemviron F 300 which is claimed to be useful for separation of organic pollutants in water.

Because of the lack of European and Spanish legal limits for a soil to be considered polluted by organic compounds the Dutch legal limit of 50 mg/kg was selected as an upper limit for the soil to be considered as "no risk" and for multifunctional use, that is, de-contaminated.[9]

Pilot plant operation was started by loading the soil in the basket and placing it into the stripper. Previously, active carbon was placed in the adsorber, then the operation variables: pressure, flow, stripper and adsorber temperatures were set. Once selected temperatures were reached, the CO_2 circulation was initiated.

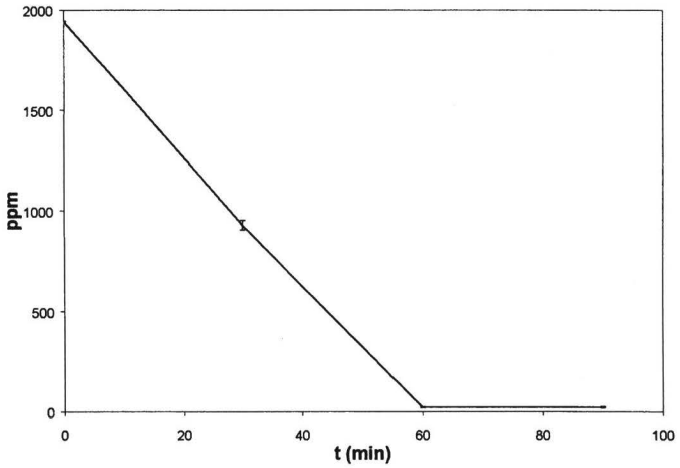
Evolution of total hydrocarbon concentration from the soil at times 0, 30, 60 and 90 minutes was studied. Each experiment was repeated three times by using three soil loads.

RESULTS

Mineralogical or chemical analysis of the soil was out of place since it was made of little stones, pieces of bricks, etc., a typical land filling dump. When portions of this material were loaded into the pilot plant and treated, soil regeneration was not achieved. Typical total hydrocarbon concentration of around 500 mg/kg was achieved after 90 minutes and longer. When the size was reduced, soil

regeneration was achieved. It was concluded that diffusion in the particle was the limiting process for regeneration.
Figure 3 shows the total hydrocarbon concentration versus time for a 2000 mg/kg polluted soil, particle size < 212 mm, at a pressure of 25 Mpa, stripper temperature 45°C, adsorber temperature 35°C and 4.5 kg/h flow of carbon dioxide. After 60 minutes pollutant concentration was under 25 mg/kg, so that soil regeneration process would be finished.

Figure 3: Total hydrocarbon concentration versus time.

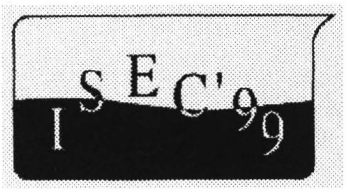


ACKNOWLEDGMENTS

Financial support of this work by CICYT project QUI96-0560 Spain, and EMGRISA (Spain) for providing technical information about the soil are gratefully acknowledged.

REFERENCES

1. Bellandi B, *"Innovative Engineering Technologies for Hazardous Waste Remediation"* Inter Thomson Publishing EEUU (1994)
2. Tomasko DL, Macnaughton SJ, Foster RR and Eckert CA, *Separation Science and Technology* **30 (7-9)** 1901, (1995).
3. Laitinen A, Michaux A and Aaltonen O, *Environmental Technology* **15**, 715, (1994)
4. Dooley KM , Ghonasgi D and Knopf C, *Environmental Progress* **9(4)**, 197, (1990)
5. Brunner G, NATO ASI. *Supercritical fluids* (in press) 1998.
6. Madras G, Erkey C and Akgerman A, *Environmental Progress* **13(1)**, 45, (1994)
7. *Standard Methods.* (Method 5520 c) 19th edition 1995
8. González Aurioles JM, *Ingeniería Química.* Sept 29, 242, (1996)
9. Informe técnico *"Recuperación de suelo contaminado en Boecillo"*. Junta de Castilla y León. Valladolid (1997).



ORGANIC SOLVENT-FREE EXTRACTION OF PHENOL THROUGH LIQUID-COACERVATE SYSTEMS

E Lins de Barros Neto, JP Canselier and C Gourdon
Laboratoire de Génie Chimique (UMR CNRS 5503 INPT-UPS) Ecole Nationale Supérieure d'Ingénieurs de Génie Chimique, 18, chemin de la Loge, F31078 Toulouse Cedex 4, France

ABSTRACT
Two-aqueous phase extraction processes appear as an answer to the restricted use of organic solvents on a large scale. The cloud-point property of polyethoxylated nonionic surfactants is turned to account in liquid-coacervate extraction of phenol. The phase diagrams of a few H_2O/nonionic/C_6H_5OH systems are investigated. Isoresponse curves regarding the efficiency of phenol extraction, the volume fraction of coacervate and the residual concentrations of phenol and surfactant in the dilute phase are presented. High yields in phenol extraction can be achieved. The feasibility of a stripping procedure for coacervate recovery using calcium hydroxide has been checked. The pseudophase model for microemulsions is able to predict the percentage of phenol extracted.

Keywords: liquid-coacervate extraction, nonionic surfactant, cloud point, phenol, pseudophase model, aqueous two-phase extraction

INTRODUCTION : OVERVIEW, AIM OF THE STUDY

Adsorption of surfactants at interfaces, reducing the surface free energy of liquid-liquid systems, makes them useful in liquid-membrane, reverse micelle or microemulsion extraction processes.[1-4] However, nowadays, the restricted use of volatile organic compounds, often toxic, is a difficult challenge. Water/polyethoxylated nonionic surfactant (EONIS) systems offer an interesting opportunity in the field of extraction processes with no need for organic solvent, thanks to the existence of a lower consolute point curve. The origin of this phase separation with a temperature rise lies in a delicate balance between repulsive and attractive solute-solute and solute-water interactions, associated with entropy increase.[5,6] A huge amount of experimental studies on such cloud point phenomena has been so far accumulated,[7,8] including the influence of surfactant molecular structure and additive effects.[9-12] A temperature rise above the cloud point of the solution will allow solubilization and concentration of a hydrophobic or amphiphilic substance into the so-called coacervate (surfactant-rich phase), thus removal of the said substance (with possible recovery) from the original aqueous solution. This operation has been known for years as liquid-coacervate or cloud-point extraction.[13-15]

EXPERIMENTAL

Choice of systems

As model systems, aqueous phenolic solutions of alkylphenol or alcohol ethoxylates will be considered.[16-18] Phenol is chosen as a model pollutant as its physical removal and chemical destruction have been very often considered by means of various techniques.[19] The EONIS, belonging to the octylphenol ethoxylate (TRITON X100 and X114 with 9-10 of 7-8 EO units), nonylphenol ethoxylate (NONAROX 575 and TRITON N101 with 5 or 9-10 EO units) or terminated alcohol ethoxylate (TRITON DF12 and DF16) families, show cloud point values ranging from below room temperature to 66°C. They were kindly provided by SEPPIC or Rohm & Haas and used as received. The phenol sample was of analytical grade. Distilled water was used throughout. Coacervate and dilute phases were analyzed by reversed phase HPLC.

© 2000 Society of Chemical Industry

RESULTS AND DISCUSSION

Phase diagrams

Partial phase diagrams of H_2O/EONIS systems were constructed (figure 1a). As already noticed with a DF16 sample,[20] the cloud curve of terminated alcohol ethoxylates (TAE) shows an unusual shape.

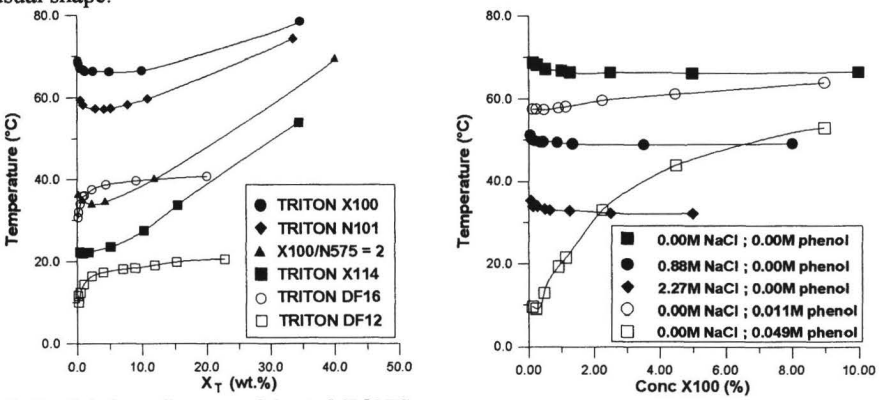


Figure 1. Partial phase diagrams of the H_2O/EONIS systems:
a) EONIS: alkylphenol ethoxylates and terminated alcohol ethoxylates;
b) Effect of NaCl and phenol on the cloud-point of Triton X100

The location of the phase separation curve and the cloud point coordinates are often very sensitive to the effect of an additive. As with a lot of strong electrolytes (lyotropic solutes), NaCl lowers the cloud point (figure 1b), both ions being considered as structure-makers.[10] Besides, the cloud-point lowering due to an amphiphilic solute, such as phenol (aqueous solubility: 8.0 wt. % at 25 °C, log P = 1.5), is more noticeable at low surfactant concentrations and the curve looks like those of TAE (figure 1a). It is likely that micellarsolubilization opposes the salting-out effect to a certain extent. It is likely that micellar solubilization opposes the salting-out effect to a certain extent. On the other hand, the addition of a second nonionic surfactant to a binary system leads to a phase separation curve intermediate between those of pure components.[21]

The ternary phase diagrams of some H_2O/EONIS/C_6H_5OH systems (EONIS: TRITON X100, X114 and NONAROX575 at t = 45 °C; TRITON X114 at 29.2 °C) are represented in figure 2. In these phase diagrams, two two-phase regions are observed visually. However, except for TRITON X114 at 29.2 °C, only one of these appears in the above schemes: the second one, close to the water corner and the water-surfactant side is quite narrow and its delimitation would require a much larger scale. This would still be more difficult for the three-phase domain, located in-betweeen. In figure 2d, the tie-lines of the upper two-phase region join a very dilute, nonmicellar aqueous phase and the coacervate, whereas in the lower one the dilute phase contains micelles. The strongly ascending slope of the tie-lines in the upper two-phase region gives information on the high extracting power of the coacervate.

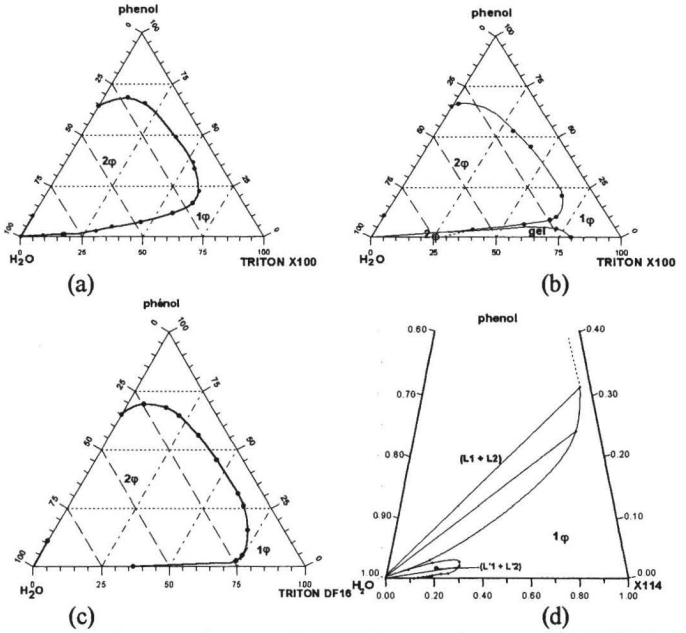


Figure 2. Partial phase diagrams of systems H_2O/EONIS/C_6H_5OH: a) TRITON X100, 45°C; b) NONAROX 575, 45 °C; c) TRITON DF16, 45 °C; d) TRITON X114, 29.2 °C

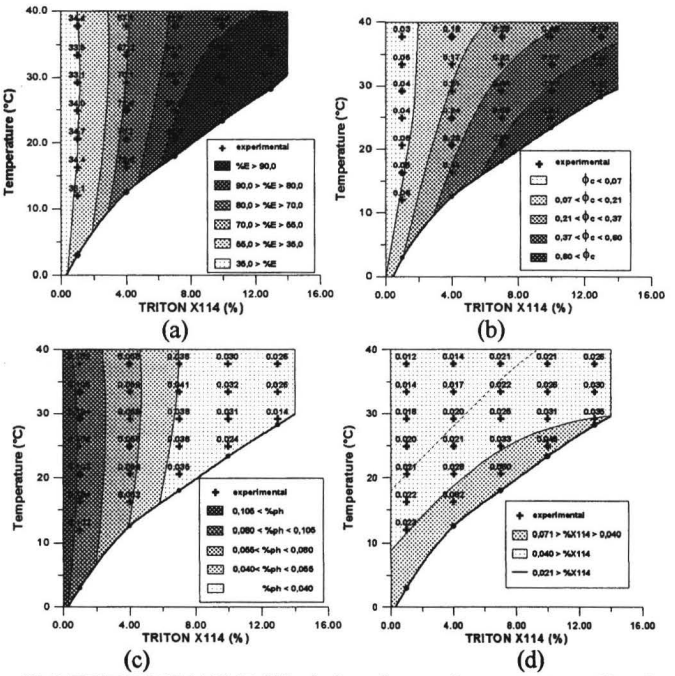


Figure 3. System H_2O/TRITON X114/C_6H_5OH: a) phenol extraction percentage; b) volume fraction of coacervate; c) residual concentration of phenol in dilute phase; d) residual concentration of surfactant in dilute phase

Phenol extraction

The results of the extraction experiments are expressed as: percentage of phenol extraction, volume fraction of coacervate and residual concentrations (phenol and surfactant) in dilute phase as functions of overall surfactant concentration (weight percentage, X_T) and temperature (T). Initial phenol concentration was kept constant (0.15 wt. %).
Each series of data (response Y), fitted to a quadratic model:

$$Y = C_0 + C_1X_T + C_2T + C_{12}X_TT + C_{11}X_T^2 + C_{22}T^2$$

which allows the drawing of iso-response curves (figure 3) from a set of six equations yielding six coefficients. With the systems studied, the extraction yields of phenol proved to be fairly high. As expected, the yield is an increasing function of the overall surfactant concentration and a slow decreasing function of temperature. In the optimum conditions, this yield amounts to 90% or more. For instance, it reaches 93.6% for an overall concentration of 13 wt.% of a mixture of TRITON X100/NONAROX575 (2/1 weight ratio) at 42.5 °C, that is 5 °C above the cloud point. The residual surfactant concentration in the dilute phase (0.01%) is only 0.08% of the initial amount. On the whole, the volume fraction of coacervate decreases with a temperature rise and with a higher surfactant dilution. The dilute phase contains less phenol and less surfactant for higher overall surfactant concentrations, and less surfactant at higher temperature.

Thermodynamic model

The present approach consists of an adaptation of the pseudophase model for microemulsions[22-27] to water/surfactant/solute systems. In a ternary system, the solute is distributed between the true phases (dilute and coacervate) and between the pseudophases (aqueous" and "membrane") as well. The distribution constant of the surfactant between the pseudophases, K_T, is easily derived from the expressions the chemical potentials of the surfactant, and the true phase compositions are determined through simple mass balance calculations.[21] If a solute is present, its effect on the cmc must be considered; the distribution constant, K_S, of the solute between the two pseudophases and additional terms in the mass balance equations are also involved. This model is applied to the extraction of phenol by X114 coacervate ($K_T = 3.45*10^5$; $K_S = 269$).[21] Predicted phenol concentrations ($x_{S,W}$ and $x_{S,C}$) in both true phases agree with experimental ones (dilute phase: slope, $x_{S,W}(cal) = 1.05\ x_{S,W}(exp)$, $\rho^2 = 0.988$; coacervate: slope, $x_{S,C}(cal) = 0.994x_{S,C}(exp)$, $\rho^2 = 0.9999$).

Continuous process

First of all, consider the kinetics of phase separation after a 1 minute stirring at 300 rpm. From figure 4a, it is quite noticeable that the equilibrium volume fraction of coacervate is reached from higher or lower values according to the overall surfactant concentration. For higher surfactant concentrations, the dilute phase separates immediately from the coacervate (continuous phase) with its equilibrium composition. On the contrary, in the lower surfactant concentration range, both phases exchange their role and the coacervate composition does not change with time. Around 6% surfactant, volume fractions remain constant, but the separation of the two turbid layers is much longer. On the hand, as shown in figure 4b, phase separation through heating of the homogeneous medium is quite straightforward. It always takes place along with a decreasing volume of coacervate. The aqueous phase is transparent and in the equilibrium state.

The principle of a two-stage cross-currrent process for phenol extraction is summarized in figure 5. Starting from adequate amounts of aqueous solutions containing 0.365 wt.% phenol (point F) and 14 wt.% TRITON X114 (point S), respectively, leads to point M1, represented by equilibrium phases of respective compositions R1 and E1. Further addition of "solvent" gives point M2, corresponding to equilibrium phases of compositions R2 and E2. Finally, between

the feed and the second raffinate a 140-fold reduction of the initial phenol concentration is achieved.

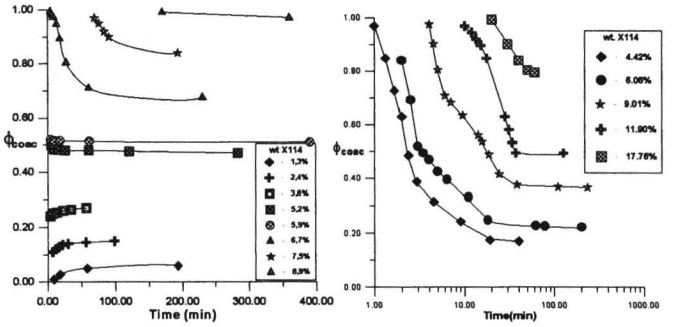


Figure 4. System H_2O/Triton X114/C_6H_5OH (0.15 %): Phase separation as a function of time: a) contact by stirring, t = 26 °C; b) phase separation through heating of the homogeneous medium, t = 40°C. Symbols in the box refer to initial surfactant mass percentages

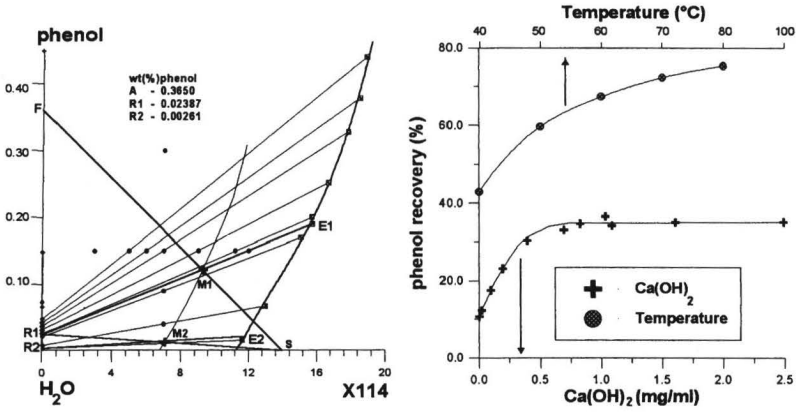


Figure 5(left). Multistep extraction of phenol with TRITON X114; t = 29.2 °C

Figure 6(right). Percentage of phenol recovery vs. $Ca(OH)_2$(mg/ml), C_6H_5OH: 0.20 wt. %, t=38°C; and vs. temperature (°C), C_6H_5OH: 0.24 wt. %, $Ca(OH)_2$ = 0.159 wt. %.

TRITON X114: 10.5wt.% in both cases

Back extraction and coacervate recovery

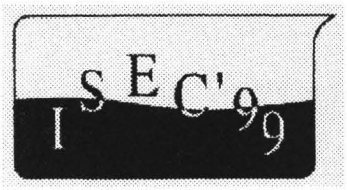
The weakly acidic properties of phenol (pK_a = 9.8) makes it possible to recover the coacervate through addition of a strong base, such as sodium or calcium hydroxide, followed by heating and phase separation. In fact, the surfactant does not interact anymore with the strongly hydrophilic phenolate ion. The introduction of solid $Ca(OH)_2$ is especially suitable, since i) calcium phenolate is water-soluble and concentrates in the new aqueous phase, ii) no dilution water is added and iii) coacervate may be further purified, e.g. by adding oxalic acid (going back to neutral pH and precipitation of calcium oxalate). The results presented in figure 6 are related to experiments performed with TRITON X114. These experiments show that a high amount of phenol is removed from the coacervate.

CONCLUSION

Liquid-coacervate extraction, using aqueous solutions of polyethoxylated nonionic surfactants, is a powerful operation for the purification of liquid effluents. High yields can be achieved in phenol extraction and "chemical" stripping ensures concentration of the polluting solute and recycling of the surfactant solution. To describe and predict the behaviour of such systems, a thermodynamic model, based on the pseudophase approximation, has been developed. A continuous process, currently under study, already shows good performances.

REFERENCES

1. Wasan DT, Ginn ME and Shah DO (eds.), *"Surfactants in Chemical/Process Engineering"*, Surfactant Science Series, Marcel Dekker, New York, **28**,(1988).
2. Scamehorn JF and Harwell JH (eds.), *"Surfactant-based Separation Processes"*, Surfactant Science Series, Marcel Dekker, New York, **33**, (1989)
3. Canselier JP, *Jorn. Com. Esp. Deterg.*, **22,** Palma de Mallorca, March 13-15, pp. 1, (1991)
4. Canselier JP, Mans C and Llorens J, *Ingenieria Quimica,* 149, (1995)
5. Ravey JC, *J. Colloid Interface Sci.*, **94**, 289, (1983)
6. Lindman B and Karlström G, *Zeitschr. Phys. Chem. Neue Folge*, **155**, 199, (1987)
7. Degiorgio V, in *"Physics of amphiphiles: micelles, vesicles and microemulsions"*, Corti M and Degiorgio V eds., North-Holland, Amsterdam, 303-335, (1985)
8. Mitchell DJ, Tiddy GJT, Waring L, Bostock T and McDonald MP, *J.Chem. Soc. Faraday Trans. I*, **79**, 975, (1983).
9. Ward AJI, *J. Pharm. Pharmacol.*, **34**, 612, (1982).
10. Schott H and Royce AE, *J. Pharm. Sci.*, **73**, 793, (1984).
11. Attwood D and Florence AT, *" Surfactant systems"*, Chapman & Hall, London, 280, (1983).
12. Sharma KD, Sudha Gupta, Suri SK and Randhawa HS, *J. Am. Oil Chem. Soc.*, **66**, 1015, (1989).
13. Gullickson ND, Scamehorn JF and Harwell JH, in ref. 1, 139, (1989).
14. Hinze WL and Pramauro E, *CRC Crit. Rev. Anal. Chem.*, **24**, 133, (1993).
15. Rogers RD and Eiteman MA (eds.), *"Aqueous Biphasic Separations: Biomolecules to Metal Ions"*, Plenum Press, New York , (1995).
16. Hinze WL, *Water Resour. Res.* Inst. Univ. N. C., 269,(1992).
17. Frankewich RP and Hinze WL, *Anal. Chem.*, **66**, 944, (1994).
18. Akita S and Takeuchi H, *Sep. Sci. Technol.*, **30**, 833, (1995).
19. Trabelsi F, Aït-Lyazidi H, Ratsimba B, Wilhelm AM, Delmas H, Fabre PL and Berlan J, *Chem. Eng. Sci.*, **51**(10), 1857, (1996).
20. Canselier JP, Chemat F, Petrissans M and Gauthier F, *Tenside*, **34**, 272, (1997).
21. Lins de Barros Neto E and Canselier JP, *Jorn. Com. Esp. Deterg.*, **28**, Barcelone, May 6-8, 433 (1998).
22. Biais J, Bothorel P, Clin B and Lalanne P, *J. Disp. Sci. Technol.*, **2**, 67, (1981).
23. Lalanne P, Clin B and Biais J, *Chem. Eng. Comm.*, **27**, 193, (1984).
24. Ovejero-Escudero FJ, Casamatta G and Angelino H, *J. Disp. Sci. Technol.*, **8**, 89, (1987).
25. Voca BR, Canselier JP, Noïk C and Bavière M, *Progr. Colloid Polym. Sci.*, **76**, 144, (1988).
26. Canselier JP, Pellegatta JL and Monfort JP, *Progr. Colloid Polym. Sci.*, **81**, 253, (1990).
27. Lins de Barros Neto E, *Mestrado*, Univ. Federal do Rio Grande do Norte, Natal, (1996).



REMOVAL OF VOCS FROM WASTEWATER WITH MEMBRANE EXTRACTION

Yujun Wang , Shenlin Zhu and Youyuan Dai
Chemical Engineering Department, Tsinghua University, Beijing 100084, China

ABSTRACT
Removal of VOCs with membrane extraction from waste-water has attracted many researchers. In this paper, Kerosene-Chloroform-Water is used as experimental system. In hydrophobic polypropylene hollow fibre module the mass transfer characteristics of membrane extraction process have been studied. The overall mass transfer coefficient based on aqueous phase K_w is calculated and the reasons for deviation between the experimental value and the calculated one have been studied. The results indicate that the resistance of mass transfer is mainly from the diffusion in aqueous phase, but the non-ideality of the shell-side is the major factor causing the deviation. By the calculation of HTU, the high performance of MHF is proved. It is also shown that MHF is highly efficient for removal of the COD value of chloroform solution.

Keywords: hollow fibre membrane extraction, VOCs, wastewater treatment, chloroform

INTRODUCTION

Contamination of water supply by volatile organic compounds is an established problem.[1] These contaminants are highly toxic to human beings and animals. Such water is formed in so many industrial processes that removal of VOCs is necessary before the water can be used. Current technology for removal of volatile contaminants includes active carbon adsorption, packed-tower aeration and oxidation method. Each method has significant strengths as well as considerable weakness.

A new approach to this problem is studied here. Volatile organic compounds are removed from water into a stripping oil in dispersion-free extraction across a microporous membrane. Membrane based non-dispersive extraction is characterized by the stabilization of the organic-aqueous interface at a porous material, avoiding the dispersion of the organic phase into the aqueous phase or vice versa and thus eliminating emulsion formation or phase entrainment.[2,3] Additional advantages have been widely mentioned in the literature.[4,5] These specific characteristics of the non-dispersive extraction make it an interesting technology for its use in the removal of VOCs from waste-water. Membrane extractors for this experiment consist of hydrophobic polypropylene hollow fibres. Water containing chloroform is pumped through the interior of the fibres and an oil with high affinity for the organic compounds studied is pumped counter-currently to the water on the exterior of the fibres. The chloroform are stripped from the water phase across the membrane and concentrated in the oil in response to a chemical potential gradient. The contaminant concentrated in the stripping oil may be removed by distillation and the oil and solutes may be reused if desired.

EXPERIMENTAL

The characteristics of experimental systems and parameters of modules are presented in the follow tables.(table 1 and table 2)

Table 1 Structural Parameters of Modules

Parameters	l ($\times 10^{-3}$m)	D_i($\times 10^{-3}$m)	n	τ_m	d_o($\times 10^{-6}$m)	t_m($\times 10^{-6}$m)	φ	ε_m
Module A	300	32	3600	2	400	30	0.563	>0.3
Module B	600	32	3200	2	450	45	0.633	>0.3

© 2000 Society of Chemical Industry

Table 2 Characteristics of the Experimental Systems

Experimental Systems	m	υ_o (m^2/s)	D_w (m^2/s)	D_o(m^2/s)
Kerosene-chroloform-water	118.2	$2.5¡Á10^{-8}$	$0.99¡Á10^{-9}$	$0.50¡Á10^{-9}$

The initial and final water phase concentrations were analyzed by gas chromatograph equipped with a capillary column and a hydrogen flame detector. Samples were directly analyzed by GC without pretreatment. The chemical oxidation demand value of water phase was measured by standard potassium dichromate oxidation method. In addition, the distribution coefficient of this experiment system was found to be 118.2.

RESULTS AND DISCUSSION

Assume both phases are plug flow and solute distribution coefficient m is constant over the concentration range, the overall mass transfer coefficient based on the aqueous phase K_w can be obtained:[6]

$$K_w = \frac{L_w}{A} \frac{1}{1-\frac{L_w}{mL_o}} \ln \frac{x_0 - x_0^*}{x_1 - x_1^*} \qquad (1)$$

where L_w¡¢L_o represents the aqueous phase flow rate and oil phase flow rate, respectively. x_0 ¡¢x_1 are the inlet concentration and outlet concentration of aqueous phase, respectively.

According to the binary film theory, for hydrophobic membrane, the correlation between K_w and individual mass transfer coefficient is obtained:

$$\frac{1}{K_w} = \frac{1}{k_w} + \frac{1}{mk_m} + \frac{1}{mk_o} \qquad (2)$$

Many workers have studied mass transfer characteristics of membrane extraction and obtained many individual mass transfer coefficient correlations for prediction. The typical correlations are:[7]

$$k_w = 1.62 \frac{D_w}{d_i} \left(\frac{d_i^2 u_w}{lD_w}\right)^{\frac{1}{3}} \qquad (3)$$

$$k_o = 8.58 \frac{D_o}{d_e} \left(\frac{d_e^2 u_o}{l\upsilon_o}\right)\left(\frac{\upsilon_o}{D_o}\right)^{\frac{1}{3}} \qquad (4)$$

$$k_m = \frac{D_o \varepsilon_m}{\tau_m t_m}, \quad \tau_m = 2.0 \qquad (5)$$

where u_w¡¢u_o presented the superficial velocity of the water phase and oil phase. d_e is the equivalent diameter of shell side $d_e = \frac{D_i^2 - nd_i^2}{nd_i}$

The quantity HTU (Height of transfer unit) is defined by :

$$(HTU)_w = \frac{L_w}{K_w \cdot a \cdot s} = \frac{U_w \cdot S_w}{K_w \cdot a \cdot s} \qquad (6)$$

where $a = 4nd_i / D_i^2, S = \frac{\pi}{4} D_i^2, S_w = \frac{\pi}{4} nd_i^2$

Mass transfer

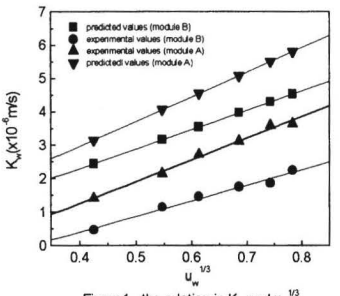


Figure1. the relation in K_w and $u_w^{1/3}$

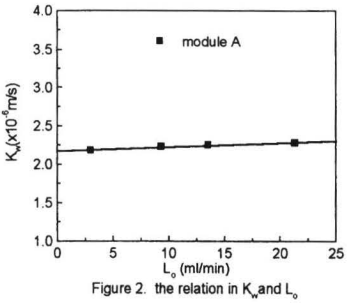


Figure 2. the relation in K_w and L_o

For the experimental system with m>>1, the second term and the third term in the right of Equation (2) can be neglected. Consider the distribution coefficient of this system is 118.2, then $K_w \approx k_w$. From Equation(3), $K_w \approx k_w \propto u^{1/3}$. The results indicate that the mass transfer coefficient increases with the increasing water flow rate. And there is a rapid increase of K_w in low u_w, while slow increase of K_w in high u_w. It is shown that K_w varies linearly with u to the power of 1/3 (Figure 1). Other results show that no significant change in mass transfer coefficient accompanies a change in oil flow rate at a constant water flow rate (Figure 2). All of these illustrate that using a membrane extractor the overall mass transfer coefficient for this experimental system with a high distribution coefficient is mainly controlled by the aqueous phase film transfer coefficient.

For module A and B, the predicted value of K_w can be calculated from Equation (2) to Equation (5) at the given operation conditions. K_w as a function of $u^{1/3}$ is also plotted in Figure 1. It is obvious that the predicted K_w is much higher than the experimental one. The differences in the predicted value and experimental value can be due to the high packing density of hollow fibre membrane extractor. For module A, packing density φ is 0.5625; for module B, φ=0.633. The fluid flow of oil phase in shell side is not ideal plug flow because of swelling deform of hollow fibres. 'Dead zone '-regions where fibres are close or touch can leads to the reduction of mass transfer area and channeling also exists in shell side. These cause the increasing of resistance of mass transfer and decreasing of mass transfer coefficient.

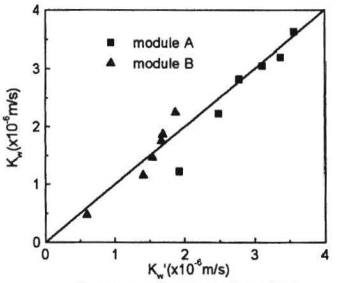


Figure 3. the relation in K_w and K_w'

The method similar to that in literature[6] is used to modify the predicted mass transfer coefficient, assume:

$$K_w' = (-0.27 + a\varphi - b\varphi^2) K_w'' \qquad (7)$$

where K_w' is the modified predicted value, K_w'' is the initial predicted value obtained from Equation (2)to Equation (5). The experimental data are put in the Eq(7). The fitting result is a=7.86,b=9.93.

Comparison in the modified predicted K_w' and the experimental value is shown (Figure 3). Obviously, the modified correlation is satisfying.

Separation Efficiency

The extraction percentage declines with the decreasing the ratio of L_o/L_w at a constant oil flow rate (Figure 4). But even though L_o/L_w is very low, the extraction percentage is still high.

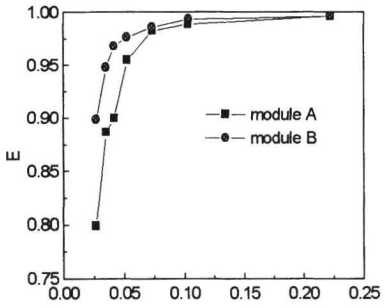


Figure 4. the relation in E and L_o/L_w

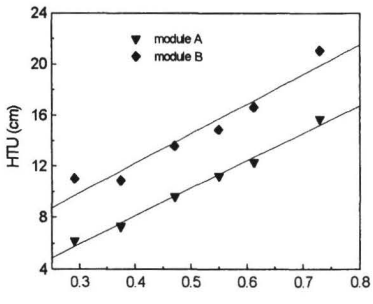


Figure 5. the relation in HTU and $u_w^{2/3}$

Additionally, the extraction percentage of module B are higher than that of module A. This is due to the length of module B is as twice times as module A and mass transfer area of module B is larger.
The HTU value can be obtained from the Equation (3) and the Equation (6):

$$(HTU)_w \propto u_w^{2/3} \cdot L^{1/3} \cdot d_i^{4/3}$$

the HTU values achieved with membrane contactor are very low (Figure 5). This proves that mass transfer efficiency of hollow fibre membrane extraction is very high. Moreover, the HTU values increase with the increasing of water superficial velocity. The HTU values are linear with $u^{2/3}$.

Removal of COD

As we now know, the efficiency of removal of chloroform using membrane extraction is very high. Though the concentration of chloroform in water phase and its chemical oxidation demand value have no certain mathematical correlation, the trend of their changes is similar. The result of removal of COD for module A and module B are shown in the follow tables.(table 4 and table 5)

Table 4 Removal of COD (module A) (the inlet concentration of aqueous solution is about 1600mg/L)

$L_o(cm^3/min)$	$L_w(cm^3/min)$	L_o/L_w	The COD values of raffinate(mg/dm^3)
3.47	45.3	0.077	83.3
3.45	63.9	0.055	81.8
3.48	80.1	0.043	108.5
3.46	94.5	0.037	146.9
3.47	123.0	0.027	123.7

Table 5 Removal of COD(module B) (the inlet concentration of aquous solution is about 2400mg/dm^3)

L_o(cm^3/min)	L_w(cm^3/min)	L_o/L_w	The COD value of raffinate(mg/dm^3)
2.99	32.2	0.093	63.9
3.02	45.1	0.067	50.0
3.05	63.8	0.048	65.4
2.97	80.4	0.037	69.1
3.02	94.7	0.032	88.3
3.00	123.0	0.024	86.3

CONCLUSIONS

Through experiments, it is proved that hollow fibre membrane/oil stripping is an efficient method for the removal of volatile organic compounds from water. The research illustrates that mass transfer increases with the increasing water flow rate at a constant oil flow rate for two different types of modules. No significant change in mass transfer coefficient accompanies a change in oil flow rate at a given water flow rate. These indicate that the diffusion of the solute from the bulk water phase to the membrane surface is dominated. The non-ideal flow in shell side causes the difference between the experimental overall mass transfer coefficient and the predicted one. The HTU values achieved with membrane extraction are low and the relation in the HTU values and $u^{2/3}$ is linear. Many data show that even though the ratio of two phases flow rate is very low, the percentage of removal of volatile organic compounds achieves high. The COD values of raffinate are satisfying.

NOTATION

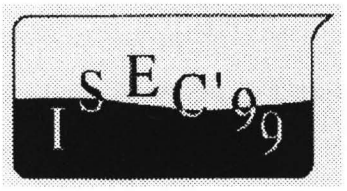
The following symbols are used in this paper:

A= surface area of mass transfer(m^2);
D= module diameter (m);
D_i= D_w,D_o diffusivity of solute in water,oil phases,respectively(m^2/s);
d_o= fibre outer diameter (μm);
K_W= overall mass transfer coefficient based on water phase.(m/t);
K_w,k_m,k_o=individual mass transfer coefficient in water, membrane, oil phases, respectively(m/s);
l = fibre length (m);
L_w,L_o = aqueous phase flow rate and oil phase flow rate (cm^3/min);
n= number of fibres
t_m= membrane thickness(μm);
x_0,x_1= the inlet concentration and outlet concentration of aqueous phase respectively (kg/m^3);
τ_m=membrane tortuosity;
ν_o= kinematic viscosity(m^2/s);
ε_m= membrane porosity;
φ= packed fraction of module.

REFERENCES

1. Clark RM,*et al, J.Envir.Engrg., ASCE*, **112**(4) ,729, (1984)
2. Li Yunfeng , Qin Wei, Dai Youyuan , *J. Memb. Sci. and Technol.* **14**(3), 36, (1994) (in Chinese),.
3. Zhang Weidong, Zhu Shenlin, Luo Guangsheng *et al*, Water Treatment Technology, **24**(1),39, (1998).
4. D'elia H, Dahuron L and Cussler EL, *J. Memb. Sci.*, **29**, 309, (1990).
5. Prasad R and Sirkar KK, *J. Memb. Sci.*, **50**, 153, (1990).

6. Dai Youyuan, *J.Memb Sci and Technol* **12**(1),1, (1992) (in Chinese).
7. Dai Youyuan, Wang Xiuli and Wang Jiading, *J.Chem Eng of High Institute*), **5**(2),87, (1991), (in Chinese).



REMOVAL OF DYESTUFFS FROM DILUTE SOLUTION WITH ELECTRO-EXTRACTION

GS Luo, YC Lu, WB Jiang and YY Dai
Department of Chemical Engineering, Tsinghua University, Beijing 100084, China

ABSTRACT
Electro-extraction, a coupled separation technique of solvent extraction with electrophoresis, was used to remove dyestuffs from their stream. A study of the characteristics of the separation technique was carried out with n-butanol / acid-chrome blue K / water, and n-butanol / methyl red / water as working systems. A continuous separation equipment was designed and used in this work. The influences of two-phase flow, field strength, and concentration of the feed on the recovery of solute were studied. The results showed that very higher recovery of solute with less solvent consumption could be achieved by using this technique to remove dyes from their streams, especially for the separation of the dilute solution. With the field strength increasing, the recovery and mass flux increase. When the feed flow rate and the initial solute concentration increase, the recovery decreases and the mass flux increases.

Keywords: dyestuffs, electro-extraction, butanol

INTRODUCTION

With the development of biotechnology and environmental science, many new separation tasks required by industry are separation of solutes from dilute solutions. Normally it is very difficult to achieve high recovery by using conventional separation technologies. Dyestuffs removal from their dilute solution is one of such examples.[1-5]

Two-phase electrophoresis is a coupled separation technique of solvent extraction with electrophoresis. The new separation technique was first developed by J. Stichlmair, et al.[6,7] The convention mixing effect caused by difference of temperature and concentration of solute in the separation solution in electrophoresis separation can be nullified or controlled by the stable liquid-liquid interface. Some reported results [6-11] on the use of the technique have shown the new technique is a promising separation process. The aim of this work is to use the new technique to separate dyestuffs from dilute solution.

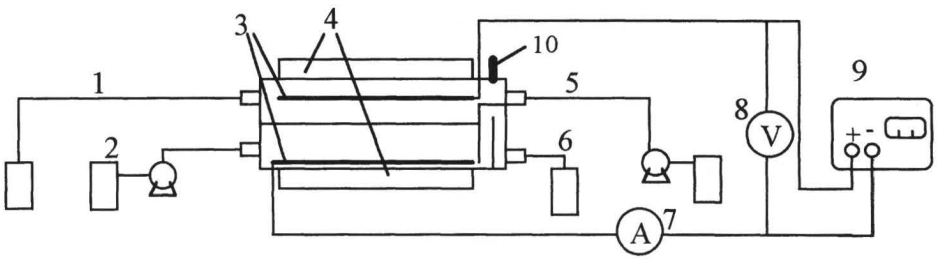
EXPERIMENTAL

Materials and Equipment

Acid-chrome blue K, and methyl red were purchased from Beijing Chemical Products Company, and n-butanol was obtained from the Chemical Solvent Products Factory of Beijing. The dyestuffs concentration was analysed with a PC 801 colorimeter at the wavelength of 520nm. The setup of experimental apparatus is shown as figure 1. Water jackets were designed to control the experimental temperature at room temperature. The anode electrode was inserted in the organic phase and the cathode electrode in the water phase. The size of the electro-extraction equipment was length 8 cm, width 5 cm and height 2 cm. The distance between the two electrodes was 1.7 cm.

In this work, conventional liquid-liquid extraction experiments have been carried out with n-butanol as solvent. Almost no acid-chrome blue K was extracted by n-butanol, conversely, almost all the methyl red was extracted by the organic phase. So, in electro-extraction process, n-butanol was used to extract acid-chrome blue K and methyl blue from their aqueous solutions, and water was used to extract methyl red from its organic solution.

© 2000 Society of Chemical Industry



1. Light phase outlet 2. Feed inlet 3. Electrodes 4. Water jackets 5. Light phase inlet
6. Heavy phase outlet 7. Amperemeter 8. Voltmeter 9. Electropherosis apparatu
10. Gas hole

Figure 1 The Configuration of the Experimental Apparatus

RESULTS AND DISCUSSION

Influence of Electric Field Strength on recovery (R)

Figures 2 and 3 show the influence of field strength (U) on the recovery ratio of acid-chrome blue K, and methyl red respectively. It can be seen that the recovery ratio (R) increases with an increase of the field strength (U) while all other experimental conditions are unchanged. This is because when the other experimental conditions are not changed, the velocity (v) of a solute migrating to the phase interface will increase with increasing field strength. Therefore, for the same flow rate more solute will pass through the interface to be recovered and a much higher recovery will be reached. If the field strength is increased high enough, as much as 100% recovery will be achieved. As to methyl red, it can be seen that n-butanol will be re-generate very well by the technique, although the solubility of methyl red in n-butanol is very high.

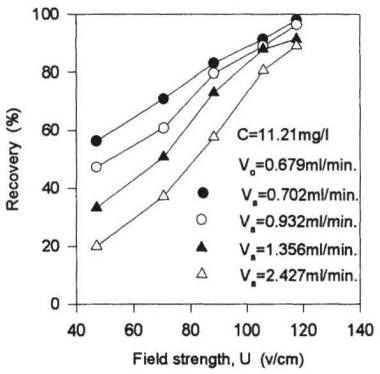


Figure 2 Influence of Field Strength on Recovery of Acid-chrome Blue K

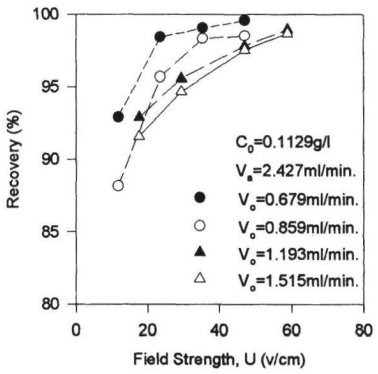


Figure 3 Influence of Field Strength on Recovery of Methyl Red

Influence of Feed Flow Rate on Mass Flux and Recovery

The mass flux, defined as the amount of solute passing through the interface per second, is plotted vs. the flow rate of the feed in figures 4 and 5.

One can see that the mass flux increases with increasing the flow rate of the feed when the other experimental conditions are the same. These results also mean that the mass transfer coefficients of the solutes are increased with increasing feed flow rate. As is well known, the mass flux strongly depended on the driving force for a solute. The driving force is decided not only by the field strength, but also by the flow conditions and the solute concentration. The mass transfer here will include electrically driven migration, diffusion, and conventional driving forces. In the case of transport across a stable interface, the effect of convection may be negligible. In this separation process, the contact time of the two phases will be decreased with the increase of the flow rate. Under the same experimental conditions, the solute concentration in feed stream for the high flow rate is decreased much more slowly than that for the low flow rate. This means that there are much more charge solutes moving to the other phase under the same field strength per second for the high flow rate, which causes the mass flux to be increased. Meanwhile when the equilibrium concentration of the dyes in the butanol phase is very low, or very high, the back diffusion will influence the mass transfer. The higher flow rate will make the solute concentration in the feed phase larger, therefore, the rate of back diffusion at high flow rate will be less than that at low flow rate. Moreover, the boundary layer at the interface may decrease due to the higher flow rate, which causes the mass transfer coefficients to be increased. All these factors may cause the mass flux to increase with increasing flow rate. Of course the charges passing through the interface are not the same as that in the bulk phase, and as there are few research works on the movement of charges in the organic phase, so that, the mechanism of this phenomenon needs further study.

As shown in figures 2 and 3, the recovery decreases with increasing flow rate. This is because with increasing flow rate, the total solute in the feed increases, consequently the recovery ratio decreases.

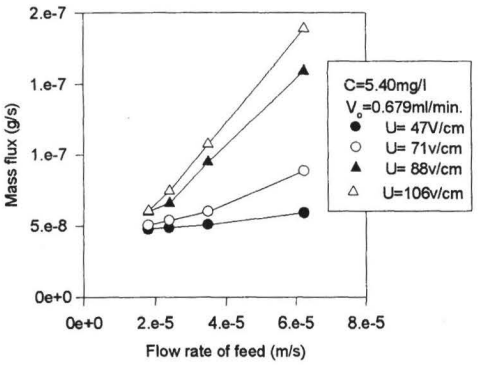


Figure 4 Influence of Feed Flow Rate on Mass Flux of Acid-chrome Blue K

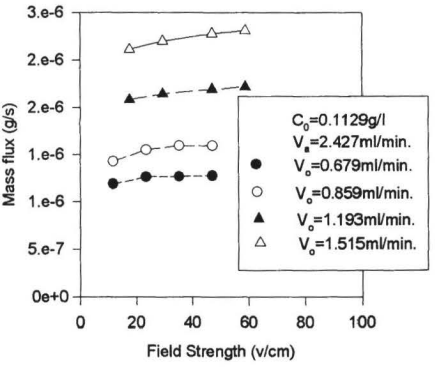


Figure 5 Influence of Feed Flow Rate on Mass Flux of Methyl Red

Influence of Solute Concentration on Mass Flux and recovery

Figures 6 shows the influence of initial solute concentration on the mass flux for acid-chrome blue K. When the other experimental conditions are the same, the mass flux will increase with increasing solute concentration. This is because much more solute passes through the interface under the same field strength when the initial solute concentration increases. But with the initial solute concentration increasing, the total solute concentration also increases, consequently, as shown in figure 7 the recovery ratios decrease.

A Mixed Process of Extraction and Electro-extraction

Based on the experimental results, a mixed process of extraction and electro-extraction for the recovery of dyestuffs may be suggested. As is well known, most dyestuffs are charged compounds, and can be divided into two kinds according to their solubility in organic solvents, i.e. high solubility and low solubility compounds. For dyestuffs with a high solubility in organic solvents, they can be recovered by solvent extraction from their dilute solution, then the loaded organic solvent can be regenerated by electro-extraction. While for the dyestuffs with low solubility in organic solvents, they can be separated from their dilute solution by electro-extraction, then the solutes could be back extracted by water from the loaded solvent.

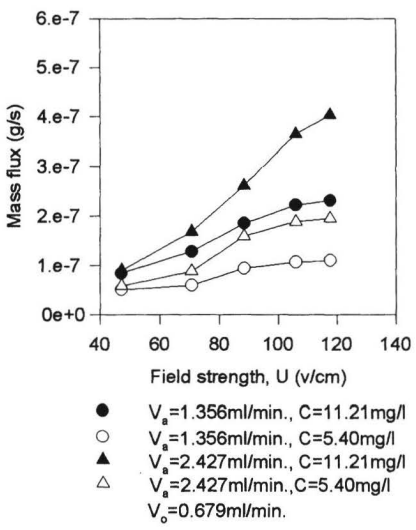


Figure 6 Influence of Solute Concentration on Mass Flux of Acid-chrome Blue K

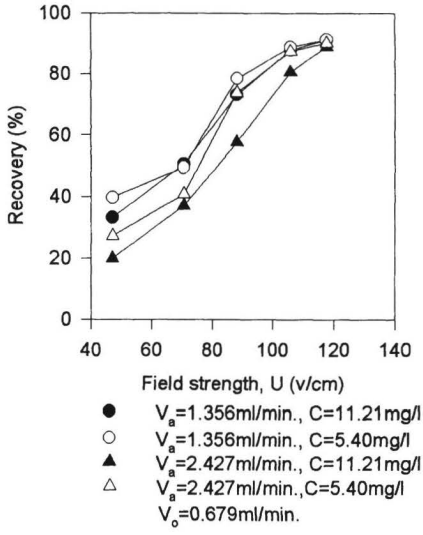


Figure 7 Influence of Solute Concentration on Recovery of Acid-chrome Blue K

CONCLUSION

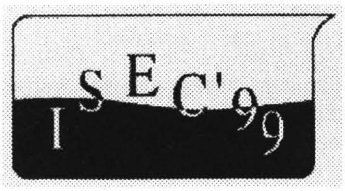
The results showed the coupled separation technique of solvent extraction with electrophoresis is an example of a very useful technique for recovering dyestuffs from their dilute solution. With increasing field strength, the recovery and mass flux increase. When the feed flow rate and the initial solute concentration increases, the recovery decreases and the mass flux increases. A much higher recovery ratio of solute with less solvent consumption can be achieved by using this technique, especially for separation from dilute solutions. If the field strength and flow rates of the two phases are well controlled, almost 100% recovery can be reached. Thus a mixed separation process of solvent extraction and two-phase electrophoresis could be a highly efficiency process for the separation of dyestuffs.

ACKNOWLEDGMENT

We acknowledge the support of the National Science Foundation of China on this work.

REFERENCES

1 McKay G. *J Chem. Tech. Biotechnol.*, **32**, 759, (1982).
2 McKay G, Prasad GR and Mowli PR *Water Air Soil Pollut.*, **29**, 273, (1986).
3 Gupta GS, Prasad G and Singh VN *Fly Ash and Coal. Wat. Res.*, **24(1)**, 45, (1990).
4 Juang RS and Swei SL *Sep. Sci. Technol.*, **31(5)**, 2143, (1996).
5 Zollinger H (Ed.) *Color Chemistry*, VCH, New York, 255, (1987).
6 Stichlmair J, Schmidt J and Proplesch R. *Chem. Eng. Sci.*, **47(12)**, 3015, (1992).
7 Stichlmair J. *DBP 3742292*, 14 December (1987).
8 Raghava Rao KSMS, Stewart RM and Todd P. *Sep. Sci. and Technol.*, **25**, 985, (1990).
9 Marando MA and Clark WM *Sep. Sci. Technol*, **28(8)**, 1561, (1993).
10 Luo GS, Zhu SL, Fei WY and Wang JD. *Solv. Extract. Res. & Develop.*, Japan, **4**, 135, (1997).
11 Luo GS, Yu MJ, Jiang WB, Zhu SL and Dai YY In: *Advances in Enviromental Engineering and Chemical Engineering*, Qian Y and Chen HQ (eds.). Guangzhou, P.R. China, 153, (1997).



RECOVERY OF PICKLING LIQUORS FROM THE STEEL-MAKING INDUSTRY

CE Da Silva[1], JS Benedetto[1] and EB Tambourgi[2]
[1]Centro de Desenvolvimento da Tecnologia Nuclear - CDTN/CNEN, Rua Prof. Mário Werneck, s/no. - C.P. 941 - Cidade Universitária, 30123-970 - Belo Horizonte - MG - Brazil
[2]Universidade Estadual de Campinas - UNICAMP/FEQ/DESQ, Cidade Universitária Zeferino Vaz - CP 6066 - Barão Geraldo, 13081-970 - Campinas - SP – Brazil

ABSTRACT
This paper presents a study of the recovery of a mixture of nitric and hydrofluoric acids, as well as iron, nickel and chromium present in industrial wastes from stainless steel pickling processes. Two process routes have been investigated. Acids are recovery by solvent extraction using tributylphosphate as extractant and a pure aqueous phase in the stripping step. Continuous tests were carried out in a pulsed column with an effective height of 185 cm and an internal diameter of 26 mm. Hydrodynamic parameters were investigated for simulation propose. Iron and nickel are recovered by solvent extraction using a mixer-settler cascade, while chromium is recovered by precipitation. This study lead to the definition of the process parameters for both of the proposed routes, with a high acids and metals recovery rate.

Keywords: pickling liquor, acid, pulsed column, TBP, D2EHPA

INTRODUCTION

Over 2 million tons of stainless steel are produced annually in the world, 10% of which comes from Brazil. Stainless steel is pickled in the final steps of the production line in acid bath to remove the oxides layer that is formed on the its surface. The pickling solution is a mixture of nitric and hydrofluoric acids. Due to this pollution potential and corrosiveness this waste is considered hazardous from the environmental legislation viewpoint[1].

In general, neutralization is carried out before the discharge of this pickling bath, resulting in the precipitation of the metals and anions present in the solution. The re-utilization of both acids and metals, which represents large savings potential, is thus made impossible. In other countries process development studies for the recovery of valuable acids and metals present in these industrial waste have been devised, leading to commercial applications aiming at the reduction of the environmental impact, while keeping a favorable economic balance.[1,2,3]

The technique of solvent extraction, by its selectivity, has been broadly applied to the recovery of elements present in aqueous solutions with a high degree of purity.[4]

This paper presents a study of the recovery of acids and metals present in the industrial pickling waste liquor, through two process routes. In the first, the acids are recovered by solvent extraction in a pulsed column, followed by metals precipitation. The second and more complex route, includes the separate recovery of the metals. Iron and nickel are recovered by solvent extraction using a mixer-settler cascade, while chromium is recovered by precipitation.

EXPERIMENTAL

Materials

The aqueous phase used in this work was waste liquor from stainless steel pickling processes. The composition of the waste is shown in table 1.

Tributylphosphate (TBP) diluted in iso-paraffin was used as extractant for the acids extraction and water as stripping agent. Di-2-ethylhexyl phosphoric acid (D2EHPA) was used for the recovery of iron and nickel in the extraction step, and hydrochloric acid in the stripping step.

© 2000 Society of Chemical Industry

Apparatus and Measurement Techniques

Acid extraction and stripping were tested in a pulsed column as shown on figure 1. The main section (1) consisted of a 185 cm glass tube with internal diameter of 26 mm enclosing a stack with 37 perforated plates. The distance between the plates was 50 mm. The diameter of the holes in the plates was 3 mm and the hole area 23 % of the column area. The diameter of the top (3) and bottom (2) settlers of the column was 75mm. The aqueous and organic phases were fed in counter current flux through peristaltic pumps (4) which permit constant flows, essential to maintain a stable operation. The pulse was generated with a diaphragm pump (5). The amplitude could be varied between 0 to 15 mm and the frequency between 0 to 120 cycles per minute. Metals extraction and stripping were tested in a mixer-settler cascades of capacity of 0.15 L/h and 3.3 L/h.

Hydrodynamic parameters were investigated to determinate the operating conditions of the pulsed column. Flooding point was measured by two different methods. The first one consists on visual observation of accumulations of dispersed phase at individual points in the column that block the counter-current flow, and sometimes a phase reversal can also be observed. Measurement of the rates of the phases running out is another method. In steady state, the mass flow of raffinate and extract are constant. If, however, the counter-current flow is disturbed by flooding, the dispersed phase running out is reduced and the continuous phase rise, until finally the dispersed phase is discharged together with the continuous phase.

Dispersed phase hold-up was determined by drainage method. The column was allowed to operate at the desired conditions until steady state was reached, at which time all inlet and outlet flow rates were simultaneously stopped, and the droplets allowed to settle. The dispersed phase was then drained into a measuring cylinder, and the volume determined.

Mass transfer performance was investigated by measuring the inlet and outlet concentration flow and used a simulation program to determine the performance parameters.

In all experiments the metals Fe, Cr and Ni were analyzed by atomic absorption. Fluoride and nitrate were measured with a selective ion electrode and acidity was determined by potentiometric titration with sodium hydroxide.

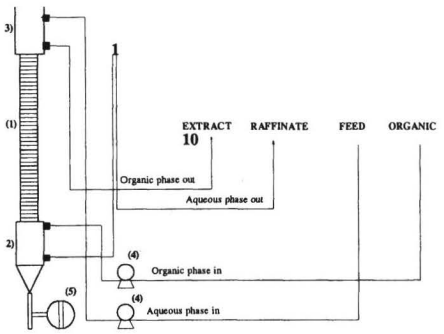


Figure 1 - Diagrammatic arrangement of pulsed column.

Table 1 - Chemical characterization of the waste solution.

species	Concentration
H^+	1.80 mol/L
NO_3^-	110 g/L
F^-	45.3 g/L
Fe^{3+}	30.2 g/L
Ni^{2+}	5.9 g/L
Cr^{3+}	3.5 g/L

RESULTS

Process Routes

Preliminarily studies in laboratory scale permitted the definition of two different process routes, which are shown in figures 2 and 3. The first idea for the process (route 1) encompasses the recovery of nitric and hydrofluoric acids after pre-conditioning the waste solution with sulfuric acid, followed by joint precipitation of the metals, through neutralization of the leached liquors. In route 2, initially

the iron is extracted with D2EHPA. The high acidity of the liquor allows a selective extraction of the iron in relation to other metals present, which gives an additional advantage to this process. The acid extraction occurs after the iron recovery stage, with the liquor conditioning being accomplished by hydrochloric acid. The aqueous industrial waste, almost without any acid (nitric and hydrofluoric acids) and iron, feeds a solvent extraction step where the separation of the nickel and chromium metals are carried out.

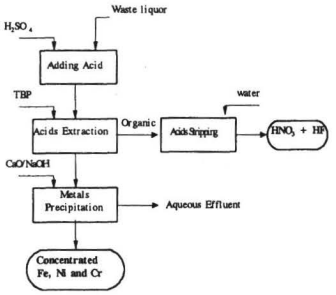


Figure 2 - Route 1 flowsheet

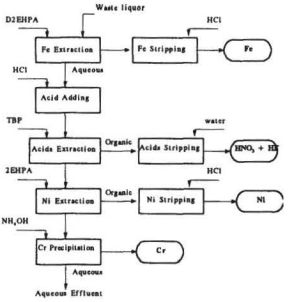


Figure 3 - Route 2 flowsheet

Hydrodynamics of the Column

The pulsed column was operated with a aqueous dispersed phase and an organic continuous phase. Results for operating characteristics in emulsion regime indicated an amplitude of 8 mm and a frequency range of 20-100 cycles/minute.

For a given separation problem, the column diameter is dictated by the flooding throughput. The sum of dispersed and continuous phase flow rates is plotted against frequency, figure 4. The amplitude was kept constant at 8 mm. The measured flooding curves exhibit the well-known behavior as function of frequency. The total throughput decreases with increasing frequency. There is a very pronounced influence of the phase ratio, R, on flooding. When the phase ratio is reduced from 0.70 to 0.40, the total throughput is doubled. For design propose, assumes an operating load equal 50 - 80 % of the flooding load.

Holdup and drop size of dispersed phase were determined under operating conditions of the column and used for simulation propose.

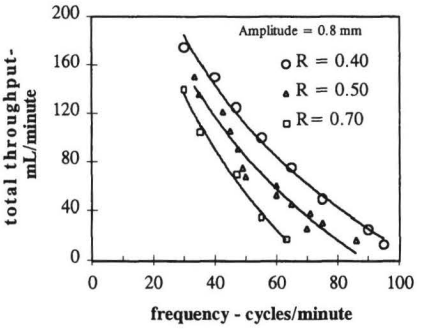


Figure 4 – Flooding curves of pulsed column

Nitric and hydrofluoric acids recovery

By adding HCl, the metal complexes with nitrates and fluorides in the Fe-free waste are converted into chlorides, and HNO_3 and HF are set free. Next nitric-hydrofluoric acids are extracted using TBP as extractant. Table 2 shows the composition of the liquor after the extraction of iron.

The extraction of HNO_3 and HF increases almost linearly with the TBP concentration in the organic phase. To obtain satisfactorily high distribution ratios for these acids, the TBP concentration was chosen to be 75 % (by volume). Although higher TBP concentration produces higher distribution ratios, the physical properties of the higher concentration are not recommended. In these conditions two phase systems make handling them difficult under practical extraction conditions.

Figure 5 shows the distribution of acids between aqueous and organic phases. The McCabe-Thiele diagram indicates seven theoretical stages for extraction of 95 % of the acids in a ratio R = 0.45, as shown by the operation line. Operational conditions for experimental runs in a pulsed column are presented in table 3. These conditions were based on hydrodynamic studies of the column.

The HNO_3 and HF in the aqueous phase were then contacted with a counter-current flow of the organic solvent, as the continuous phase, containing 75 % (by volume) of TBP in iso-paraffin. The interface was kept at a constant level by adjusting the height of a flexible aqueous take-off leg. Steady-state operation was achieved after a throughput of 4-6 continuous phase volumes. Samples were collected for analysis from aqueous and organic extract. The tests SX-2 and SX-3 presented similar mass transfer performance and better performance than test SX-1. Typical results from the extraction are shown in table 4. Results of simulations indicated a pulsed column with effective height of 245 cm for total extraction of HNO_3 and 84 % of HF, under operating conditions of the test SX-2.

Table 2 - Composition of the waste liquor after the extraction of iron

species	Concentration
H^+	1.92 mol/L
NO_3^-	80 g/L
F^-	34.0 g/L
Fe^{3+}	0.2 g/L
Ni^{2+}	5.8 g/L
Cr^{3+}	3.1 g/L

Figure 5 - McCabe-Thiele diagram for extraction of acids.

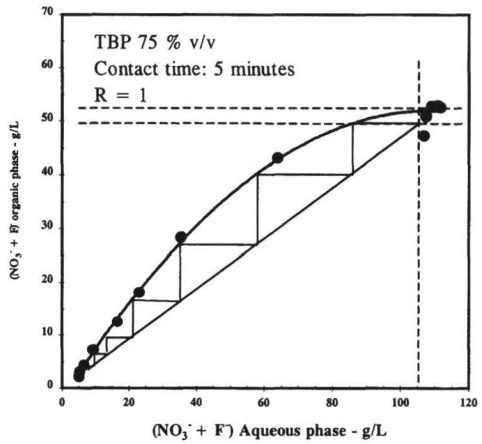


Table 3 - Operational conditions of the pulsed column for acid extraction

Parameters	Tests		
	SX-1	SX-2	SX-3
A_p (mm)	8	8	8
f (cycles/minute)	70	40	55
F_a (mL/min)	9	24	14
F_o (mL/min)	18	60	35
t (minutes)	75	25	40

Table 4 - Nitric and Hydrofluoric acids extraction results

Parameters	Inlet		Outlet	
	Aqueous	Organic	Raffinate	Extract
F (mL/min)	24.3 Ý 0.1	60.0 Ý 0.2	22.5 Ý 0.1	63.5 Ý 0.2
NO_3^- (g/L)	76.0	0.0	2.3	28.0
F^- (g/L)	31.0	0.0	6.0	9.3
	Distribution (%)			
NO_3^-	100	0	3	97
F^-	100	0	19	81

CONCLUSIONS

This study allowed the definition of the process parameters for the two proposed alternatives. The main conclusions drawn from this research were:

It was possible to obtain an aqueous solution of high purity containing nitric and hydrofluoric acids that may return to the steel pickling process after adjusting for the required concentration it. For the removal of these acids it is necessary adding to the liquor other acids of lower cost, sulfuric or hydrochloric, depending on the selected alternative. The yield of the extraction of these acids was 97% corresponded to nitric acid and 81% corresponded to the hydrofluoric acid.

The extraction of iron with D2EHPA in chloride medium was highly selective, considering that no other metals were identified in the iron concentrate. The yield of the separation of this element was of approximately 99%.

In the laboratory tests of nickel extraction, also using D2EHPA, it was possible to obtain a high purity concentrate of this metal. The confirmation of this stage of the process must be obtained through continuous assays on a mixer-settler unit, keeping a very effective pH control.

In the adjusted conditions for the extraction of iron and nickel later on, chromium was kept in solution from which it may be separated through precipitation.

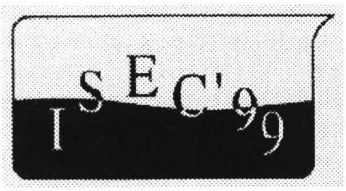
The work carried out provided the necessary information to subsidize a study of economic pre-feasibility and market analysis, what will allow for the selection of one of the alternatives for proving the process in a pilot unit to be installed next to the stainless steel pickling unit.

ACKNOWLEDGEMENTS

The authors thank the FAPEMIG (Fundação de Amparo à Pesquisa do Estado de Minas Gerais), and CNPq (Conselho Nacional de Desenvolvimento Científico e Tecnológico) for financial support to this work..

REFERENCES

1. Rydberg J, Reinhardt H, Lunden B and Haglund R, *International Symposium on Hydrometallurgy*. 589 (1973).
2. Negro C, Latorre R, Dufor J, Formoso A and Mateos FL, *J. Environ. Sci. Health*, **A29(9),** 1899 (1994).
3. Saracco G and Onofrio M, *Resources, Conservation and Recycling*, **9**, 141 (1993).
4. Ritcey GM and Ashbrook AW, *'Solvent Extraction- Principles and Applications to Process Metallurgy"*, Elsevier, New York, (1984).



CHROMIUM RECOVERY PROCESS FROM TANNING EFFLUENTS BY MICROEMULSION IN THE MORRIS EXTRACTOR

Tereza Neuma de C Dantas, Afonso A Dantas Neto and Maria Carlenise PA Moura
Universidade Federal do Rio Grande do Norte UFRN/ PPGEQ-Campus Universitário -59.072-970 - Natal/RN, Brazil

ABSTRACT
The recovery of chromium from tannery effluents using microemulsion extraction in a Morris extractor is described. The microemulsion is formed using saponified cocoanut oil with n-butanol as co-surfactant. The process was studied using a factorial experimental design and using the optimised process the effluent was successfully treated in 5 stages giving a treated effluent containing 39 mg/L chromium

Keywords: microemulsion extraction, Morris extractor, saponified coconut oil, chromium, tannery effluent

INTRODUCTION

The tanning industries, due to the complexity of the animal's hide (or skin) transformation into leather, are industries that use a great number of chemical agents and produce an enormous volume of residual waters and solid effluents. The industry is interested in efficient effluents treatment processes to reach the patterns established by the norms of environmental preservation. One of the problems that has not been totally solved is the removal of heavy metals, mainly chromium, of its residual waters and of the receiving waters.

Now forty million cubic meters of chromium-containing tannery waste water are discharged each year in waterways in the whole world. The modern tanneries have satisfactory treatment processes, but the effluents of several small or/and old leather industries do not receive the convenient treatment for the reduction of the chromium content to the levels established by the legislation.[1]

In the world, the most usual technology for the treatment of the liquid residues generated by the leather industries is a physico-chemical treatment, involving precipitation of the chromium and sulfide oxidation, followed by biological treatment, usually activated sludge or aerated lagoons systems, a overall process that represents high capital and/or operacional costs.[2]

The development of new techniques applicable to the Brazilian situation led to research in this area using a non-conventional process, new to Brazil, of liquid-liquid extraction using a microemulsion as solvent. Previous works[3,4,5,6] demonstrated that microemulsions are quite efficient in recovery of metallic ions in laboratory scale. In this work the optimization of chromium recovery process of tannery effluents in the Morris extractor[7] is described.

EXPERIMENTAL METHODOLOGY

The reagents used during the development of the experimental phase was of quality P.A., except the coconut oil (indiano) and the kerosene (Petrobrás).

The concentration of chromium present in aqueous phases in the extraction process was measured in aqueous samples by flame atomic absorption spectroscopy (FAAS) using a VARIAN SpectrAA - 10 PLUS in an air-acetylene flame.

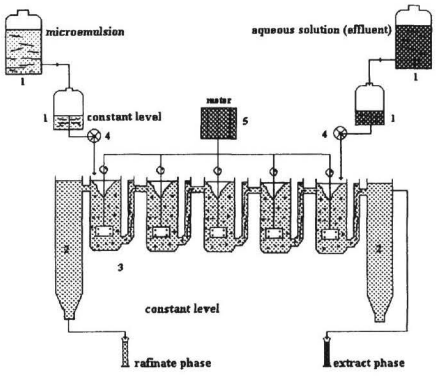
Chromium extraction of the industrial effluent

The system of extraction used was composed basically by a microemulsion phase in equilibrium with an aqueous phase in excess (Winsor's II). The composition of the microemulsion was: 3.3 wt.%

© 2000 Society of Chemical Industry

surfactant (saponified coconut oil); 13.2 wt.% co-surfactant (n-butanol); 57 wt.% aqueous phase (effluent); 26.5 wt.% oil phase (kerosene).

The MORRIS extractor[7] was used in the extraction process with the effluent of the tannery industry. The equipment as used in the process is shown in the Figure 1. At each end of the extractor there are two large settler tanks. The tank close to the microemulsion feed has an opening in the lower part where the depleted chromium aqueous phase is removed (raffinate phase), while the other, close to the effluent feed, has an opening in the upper part where the microemulsion phase loaded with chromium is removed (extract phase). In this countercurrent extraction, the two phase streams flow from stage to stage in opposite directions. The effluent was the continuous phase and the microemulsion, passing as liquid droplets, was the dispersed phase. To operate the extractor the effluent feed was started, with the flow rate adjusted to the required value. As soon as the extractor operation level was reached the microemulsion feed was introduced at the desired flow rate.



1 - mariote flask
2 - decanter vessel
3 - mixer-settlers vessels
4 - flow control
5 - electric motor 380V - 1 CV with rotation control through frequency converter

Figure 1 System used in the extraction process with the MORRIS extractor.

RESULTS AND DISCUSSION

Model of the chromium extraction process.

The optimization process seeks to evaluate in a quantitative form, the important variables of an experimental design, their influences on the results of interest, as well as any possible interactions. To obtain important information with a minimum of experiments, thus reducing the operational costs, the researcher can use a complete factorial design that will give a global answer about the behavior of the process under study.

The experiments in the MORRIS extractor were accomplished according to a 2^3 factorial design, in 5 stages, with extent of variation of the selected factors as follows: agitation speed: high level 490 rpm and low level 365 rpm; total flow rate of the effluent and the microemulsion phases: high level 2.0 L/h and low level 0.7 L/h; and the solvent rate: high level 0.5 and low level 0.25. Each experiment took approximately 2 hours to obtain a working flow rate in the extractor. To analyse the evolution of the extraction process, samples were collected at each 0.5h up to 5.5 hours of operating at a controlled flow rate. The collected aqueous phases were analyzed in FAAS.

Table 1 shows us the levels of variation of each factor and the medium responses (Y) obtained for each experiment. The two last extraction percentages obtained for each experiment were taken for the calculation of this medium response.

To calculate the main and interaction effects a statistical software (Quatro-Pro 5.0 for Windows) was used.

The main effects A, B and C and the two and three-factor interaction effects were calculated through equations, and included at a confidence level of 95%, where all the factors were considered in the statistical significance test.

EXPERIMENT	MAIN FACTORS			Y1	Y2	Y
	A	B	C	(%)	(%)	(%)
1	-	-	-	86.88	85.12	86.00
2	+	-	-	98.43	98.47	98.45
3	-	+	-	98.61	98.17	98.39
4	+	+	-	98.07	97.45	97.76
5	-	-	+	95.21	96.67	95.94
6	+	-	+	57.05	58.10	57.57
7	-	+	+	99.31	98.94	99.12
8	+	+	+	99.36	99.34	99.35
A = agitation speed (rpm) (+) 490 (-) 365						
B = solvent rate (+) 0.50 (-) 0.25						
C = total flow rate (l/h) (+) 2.0 (-) 0.70						

Table 1. Data from a 2^3 factorial design to chromium extraction process.

The empirical model obtained i.e. the model that describes the behavior of the chromium extraction process based on experimental conditions is given by the following equation, where Y represents the response function.

$$Y = 91.57375 - 3.29\,A + 7.0825\,B - 3.57625\,C + 3.18875\,AB - 6.245\,AC + 4.1575\,BC + 6.45875\,ABC$$

with an estimated standard error of 0.1659.

Based on the results obtained, some important points stand out:

The agitation speed (A) exerted a negative effect (-3.29) in the chromium extraction process, causing little influence in the extraction percentage obtained.

The solvent rate (B) produced a very significant positive effect (7.0825) in the chromium extraction process

The total flow rate (C) exerted a not very important negative effect (-3.57625) in the result obtained in the extraction process.

The contribution of the main and interaction effects on the extraction percentage obtained can be easily understood and visualized through the interaction diagrams. For the construction of these diagrams two factors were taken and all the possible level combinations included, i.e., (+,+), (-, -), (- ,+) and (+, -). Each quadrant of the diagram represents the average of the results obtained by the two factors in the prestablished levels, Figure 2.

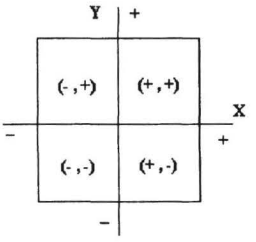


Figure 2 Two-factor interaction diagram in a 2^n factorial design.

Figure 3 shows the two-factor interaction diagrams related to the responses in the chromium extraction percentage (Y).

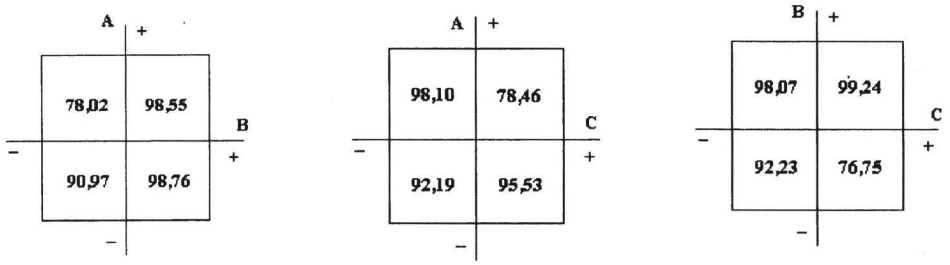


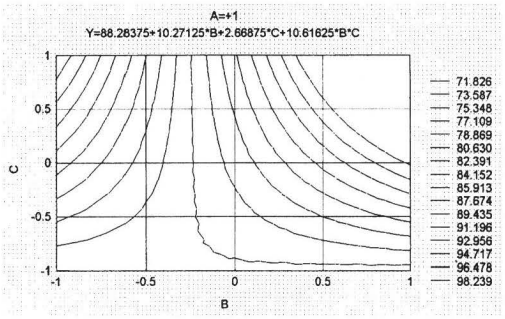
Figure 3 Interaction diagram for the chromium extraction process(%):
(a) The solvent rate (B) - agitation speed (A)
(b) The total flow rate (C) - agitation speed (A)
(c) The total flow rate (C) - solvent rate (B)

Analysis of Figure 3 indicates that the best results were obtained in the high level of the solvent rate (B= 0.5) with the low level of agitation speed (A = 375 rpm) and high level of total flow rate (C = 2L/h), corresponding the following combinations: A (-) B (+) = 98.76%, A (+) C (-) = 98.10% and B (+) C (+) = 99.24%.

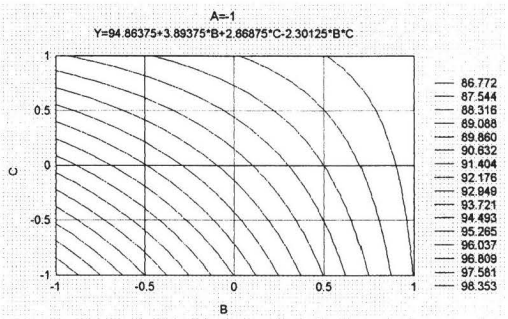
Analysis of the iso-response surfaces graphs generated from the obtained model.

The iso-response graph is the representation, in the two-dimensional space, of the studied variables, and they clearly indicate a tendency in the response that should be analyzed in detail. After the determination of the region where the relevant aspects of the situation of interest was obtained, the experimenter can study this particular area to obtain the conditions where the yield of the process will be better.

For the chromium extraction process the search of the region of high yield can be made through the interpretation of the surfaces presented in the Figure 4. These curves allow the knowledge and optimisation of the extraction process in all the domain points of the variables studied.



(a)



(c)

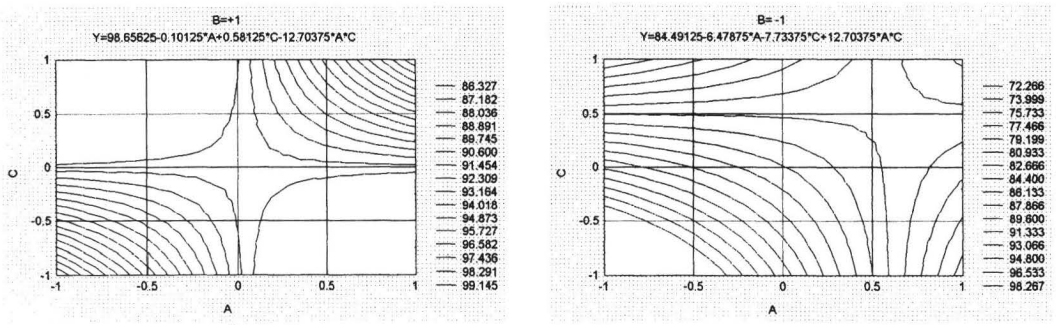


Figure 4 Iso-response Surfaces representing the relationship between:
(a) high level of A+ and C and B
(b) low level of A- and C and B
(b) high level of B+ and C and A
(d) low level of B- and C and A

From figures 4(a to d) it can be seen that the model allow the construction of two different response surfaces for each variable in study, that is, one for the high level and another for the low level, totalling six curves. A fact justified by the statistical analysis where it was verified that all the variables influenced the chromium extraction process in a significant way.

The variable A was chosen among the studied variables as presenting the smallest individual effect (-3.29) and B for presenting the greater statistical significance (7.0825).

The analysis of these results shows that: for the same value of the total flow rate, an increase in the solvent rate leads to the growth of the percentage chromium extraction; however in the low level of the agitation speed (365 rpm) maximum values in the extraction percentage (98.35%) can be reached even when the high level of the solvent rate (0.375) is reduced by 25% (figures 4a and 4b).

For the medium values of the total flow rate and agitation speed (figure 4c) their variation among the high and low levels does not interfere in the chromium extraction process, 99.14% extraction being obtained.

Through analysis of figure 4d it can be observed that for the low level of the solvent rate the results obtained for the extraction percentage (72.26%), when the total flow rate was maximum, were not very good.

The conclusions obtained in these analyses are in complete agreement with those obtained in the study of the two-factor interaction diagrams.

CONCLUSIONS

The results of the present study allowed the understanding and improvement of the chromium extraction process using microemulsions in a semi-pilot scale.

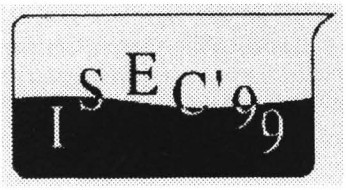
During its development, the researches were studied in stages, which allowed the following conclusions about the several aspects studied to be obtained:

- The chromium extraction process with the effluent from the chrome stream of a local tannery industry was carried out in a MORRIS extractor with the best results obtained under the following operational conditions: agitation speed: 365.0 rpm, solvent rate: 0.5, total flow rate: 2.0 L/h and with the MORRIS extractor working with 5 stages.
- The application of a statistical treatment to optimise the process showed that a 25% reduction in the higher level of the solvent rate would not modify the chromium extraction percentage obtained.

- The analysis of the parameters studied regarding the effluent before and after chromium extraction, showed that the treated effluent contained a very small amount of chromium (39 mg/l), demonstrating the efficiency of the extraction process used.

REFERENCES

1. Walsh AR and O'Halloran J, *Wat. Res.*, **30 (10)**, 2401, (1996).
2. Cherniccharo CAL, and von Sperling M, Anais do Seminário Internacional - Tendências no Tratamento Simplificado de Águas Residuárias Domésticas e Industriais, Belo Horizonte, Brazil, pp. 158, (1996).
3. Leite RHL, *Master of Science Thesis*, UFRN-PPGEQ, Natal, Brazil, (1994).
4. Barros Neeto EL, *Master of Science Thesis*, UFRN-PPGEQ, Natal, Brazil, (1996).
5. Ramos AC, *Master of Science Thesis*, UFRN-PPGEQ, Natal, Brazil, (1996).
6. Moura MCPA, *Master of Science Thesis*, UFRN-PPGEQ, Natal, Brazil, (1997)
7. Morris W, *British Patent No 885503*, London, England, (1961)



A NEW ZINC SOLVENT EXTRACTION APPLICATION: SPENT DOMESTIC BATTERIES TREATMENT PLANT

Daniel Martín,[1] MA García,[1] G Diaz[1] and J Falgueras[2]

[1] Técnicas Reunidas, S.A., Research and Development Division, Sierra Nevada 16, 28830 San Fernando de Henares, Madrid, Spain

[2] R.F. Procés, S.A., Mallorca 245, 4-1, 08008 Barcelona, Spain

ABSTRACT

A new industrial plant located in Catalonia near Barcelona was started in December 1997 for the treatment of 2000 t/y of spent domestic batteries. This is a new application of the MODIFIED ZINCEX Process (MZP) developed by Técnicas Reunidas, S.A. together with PROCES, S.A to resolve this kind of environmental problems.

After battery classification, trituration and removal of paper, plastics and iron components by physical procedures, a zinc-manganese impure dust material is produced. This solid is treated by sulphuric acid leaching and the pregnant liquor is purified by solvent extraction. The MZP allows the recovery of the metallic components: zinc as an extremely pure zinc sulphate solution completely suitable to produce SHG Zn, Mn as manganese sulphate from the raffinate bleed, and the other minor metals (Cu, Cd, Ni, Hg, etc.) as a metallic cement.

The solvent extraction operation conditions, using D_2EHPA for the MZP, allow the best Zn/impurities separation coefficients and, consequently, an extremely pure product. Besides, most of the acid consumption is saved by means of raffinate recycling to leaching containing the acidity equivalent to the Zn extracted. The Solvent Extraction (SX) stages used are the following: one depletion stage, three extraction stages, three washing stages and two stripping stages.

Some relevant characteristics of leaching, solid-liquid separation, cementation and solvent extraction processes are:

-starting-up at full capacity in a very short time
-Zn recovery higher than 98%
-high quality Zn product
-smooth plant operation
-all the products have a potential economic value
-no solid, liquid or gas effluents are produced.

Keywords: batteries, zinc, D2EHPA, modified ZINCEX Process

INTRODUCTION

General

The problem caused by the spent domestic batteries is widely known because of its environmental repercussion. This results from the presence of soluble heavy metals (Zn, Mn, Cd, Ni and Hg) and is increased in that batteries are frequently used today, as well as by their short life cycle and the low efficiency of their recovery and recycling processes. Among them, there are two types of batteries that have more impact in the market: Leclanché (55%) and Alkalines (45%), the latter having a progressive increase in use.

Several recovery processes have been developed almost exclusively at laboratory and pilot plant level. These processes are based on two concepts: pyrometallurgical calcination and/or metal volatilisation, followed by recovery. Some disadvantages encountered in these processes are the frequent operation problems, and a mixture of products difficult to commercialise and/or recycle. Moreover, hydrometallurgical or pyro-hydrometallurgical processes have neither obtained acceptable results or a relevant industrial implementation. The success of these processes has been made difficult by several problems encountered during recovery of the wide variety of components, low plant capacities and low quality of products.

Application of solvent extraction (SX) for the spent batteries dust treatment

Applications of SX technology to purify and concentrate one of the main components, i.e. zinc, is an alternative for eliminating the above mentioned difficulties. The Modified Zincex Process (MZP) is

© 2000 Society of Chemical Industry

applicable to hydrometallurgical treatment of other secondary zinc materials and was developed at a commercial level more than ten years ago, and was a feasible option for this use. The Spanish Company Técnicas Reunidas, S.A. (TR), proprietary of this technology, has been a pioneer in SX use for the industrial production of Zn SHG,[1] from other secondary materials[2-7] and together with the 'Spanish Company PROCES, S.A., developed this application.

PLANT AND PROCESS DESCRIPTION

The use of MZP for the recovery and recycling of metallic elements contained in trituration dust from spent domestic batteries is an industrial reality today. In December 1997, a Spent Batteries Treatment Plant of 2000 t/y, operating 5 days/week and having a capacity of processing of 2800 t/y of batteries in continuous operation was started in Catalonia. Thus, this was an effective and clean process to obtain the following products:

Zinc, obtained in a pure and concentrated solution by applying Solvent Extraction, which is suitable for directly producing electrolytic SHG Zn.

Manganese, in impure powder sulphate form having various uses, i.e., in agriculture as an additive and soil conditioner for some cultivation.

Manganese, as dioxide, mixed largely with graphite, for its use in special steel plants.

The rest of metallic elements, obtained as cement, can be also recycled.

To obtain these products, first batteries have to be classified, then triturated under cryogenic conditions, and finally their components are separated into plastics, papers, iron scraps and spent batteries dust, (see figure 1).

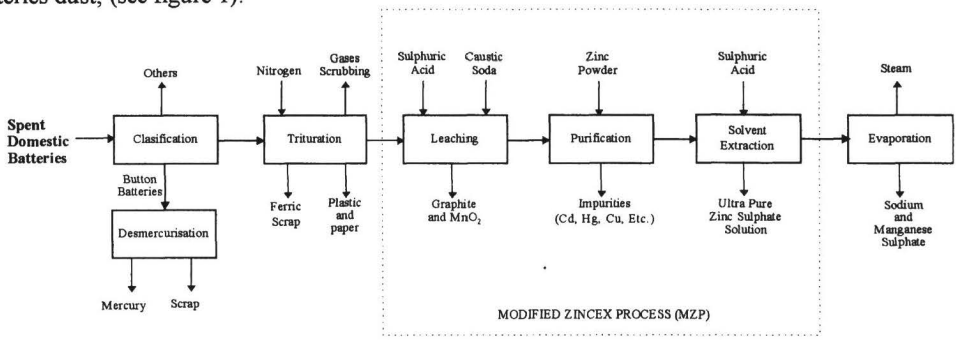


Figure 1 Scheme of a spent domestic battery treatment plant

Spent battery dust, which is a mixture of graphite and metallic oxides, are then treated as described in the following sections of MZP:

Leaching-neutralisation: to leach Zn and to produce a residue mainly composed of MnO_2 and graphite.

Zinc Dust Cementation: to produce a metallic cement with some impurities like Hg, Ni, Co, Cd, etc., and a Pregnant Liquor, which is fed to a solvent extraction.

Solvent Extraction: from the above mentioned PLS, this produces a high quality loaded zinc electrolyte suitable to produce Zn metal SHG or a highly pure Zn sulphate by evaporation, and a raffinate with the remainder Mn as a sulphate solution. The acidified SX raffinate is recycled for leaching in order to take advantage of the contained acidity. A bleed (10% of the flowrate) which contains soluble Mn and alkaline impurities is sent to the evaporation unit after neutralisation with caustic soda.

Mercury found in spent batteries does not create any problem for this process. A second leaching step with hot acidic ferric chloride solution removes the mercury from the solid MnO_2 by-

product. Mercury leach solution is combined with the main circuit from which results in mercury fixation in the impurity cement.

Table 1 shows the composition of the main streams of PZM.

In bleed evaporation, which is done with a spray dryer, $MnSO_4$ crystals are produced eliminating water and thus, maintaining liquid balance. There are no effluents but only products and by-products that can be recycled through existing processes and applications.

Concept	*Battery Dust %*	*Leaching Residue %*	*Metals Cement %*	*Pregnant Liquor g/L*	*Neutralised Bleed g/L*	*Aqueous Extract g/L*
Zn	21	0.36	22	22	-	140
Mn	26	32	-	53	51	0.3
Ni	1.3	0.02	36	-	-	<0.0001
Cd	1.4	0.01	39	0.002	-	<0.0001
Cu	0.04	0.01	0.5	0.001	-	<0.001
Hg	0.1	0.01	1.7	<0.05	-	ND
Fe	1.0	3.0	-	0.001	-	<0.01
H^+	-	-	-	pH=4	-	1.4
$SO_4^=$	0.4	1.2	-	112	108	275
Cl^-	3.8	0.4	-	31	30	<0.1
Graphite and others	45	63	-	-	-	-
Humidity	10	40	10	-	-	-

Table 1 Spent Batteries Treatment - Approximate composition of the main PZM streams

ZINC SX STAGE. MZP ADVANTAGES

General

The pregnant liquor solution fed to SX section is a Zn sulphate solution with a very high content of Mn^{2+} and Cl^- among other impurities.

For this MZP application, D_2EHPA reagent diluted in Escaid 100 was used and the distribution of stages is as follows:

Three extraction stages with free acidity generation equivalent to the extracted Zn
One depletion stage of the raffinate bleed, adjusted to pH=2
Two washing stages in special conditions using water and a bleed of the aqueous extract to assure a perfect physical and chemical washing
Two stripping stages with 5.7N sulphuric acid solution
A small regeneration stage with 6M HCl for removing the co-extracted Fe.

TR contribution to this project was the following:

Head-Tail Engineering,
Detail Engineering of the hydrometallurgical section of the plant
Training of people involved in operation of MZP
Starting up and subsequent assistance of the hydrometallurgical section.

The main equipment of the SX section, incorporated chiefly mixers-settlers and active carbon columns which have afforded excellent results. Several improvements in design were made in the TR R&D Division: degree of agitation , type of mixture, flow distributors, internal recycling, overflow system, interface control, etc. All of these, complemented with a careful selection of the instrumentation

and control system, resulted in the production of an extremely pure Zn solution (aqueous extract or Zn electrolyte) (see table 1).

The raffinate contains all impurities fed to SX and an acidity equivalent to the extracted Zn that is further utilised in the leaching steps. The residual zinc contained in a small bleed of this raffinate is depleted in a pH-controlled step. The depleted raffinate bleed is then sent to neutralisation and evaporation.

Extraction and stripping sections

Figure 2 shows a qualitative scheme of McCabe-Thiele Diagrams for extraction and stripping.
In the extraction section, two isotherms are shown, one for free acidity evolution (three stages) and one for depletion at constant pH to treat the bleed. The stripping isotherm shows the loading of the sulphuric solution to 140 g/l of zinc in only two stages.

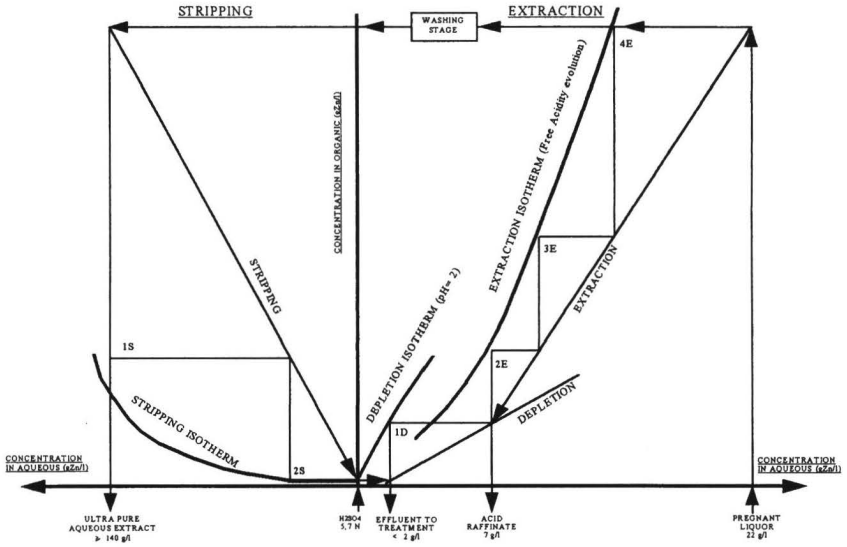


Figure 2 McCabe-Tiele diagram for D2EHPA (Isotherms)
Modified ZINCEX process applied to spent domestic battery treatment

Selectivity

Extraction operating conditions suggests good selectivity for zinc against impurities for Zn-D2EHPA system. Previous to the washing stage, some of the major pregnant liquid impurities, such as Mn^{2+} and Cl^- were present in the organic stage due to physical and chemical co-extraction. However, impurities are totally eliminated during this washing stage as can be seen in table 2. The only impurity that is co-extracted by the organic phase, is Fe^{3+}. Its concentration in PLS is <5ppm and this quantity is finally eliminated by the HCl regeneration stage. Selectivity against other impurities is so high that, as it is indicated in the electrolyte composition in table 1, final co-extraction or entrainment is negligible.

Impurity	Mn^{2+}	Cl^-
Previous to the washing stage	>50	>400
After the washing stage	>400	>1500

Table 2 Main impurities co-extracted - Zn/Impurity ratio in the organic phase.

Aqueous Zn Extract quality

The plant produces an extremely pure acidic zinc solution, as seen in Table 1. Presently, it is being supplied to an electrolytic zinc production plant. The small zinc production in one year does not justify the installation of an electrowinning unit in the spent battery treatment plant.

Other SX advantages

From a designing and operational point of view, other additional advantages have been gained and demonstrated:

Clean and easy operation, practically without maintenance.
Optimisation of operating conditions.
Optimised design of mixers-settlers.
Automatic control that practically eliminates labour requirement in this section.
Installation of a safety system that avoids both operational and accidental organic losses (the former by means of an adequate adsorption system on active carbon columns).
Flexibility in the operation with respect to Aqueous Extract, as well as the Acid and Depleted Raffinates.
Operation with possibility of interruption (for example during the weekend) without any disturbance in the equilibrium system.

ECONOMICAL ASPECTS

This plant was designed firstly considering a pure and complete environmental solution to the domestic spent batteries problem, and secondly, to avoid the creation of new residues or effluents. That was the reason for using, for example, caustic soda reagents instead of other cheaper ones such as lime and limestone, which would again produce a potential solid residue (gypsum).

In spite of the limited plant capacity, minimisation of possible operation costs has been attempted, and all products and by-products have been valued. The economic viability requires a compensatory canon for the treatment process, through direct consumers, or through official organisations. The first of these alternatives has been successfully established in some countries, for example, Switzerland.

CONCLUSIONS

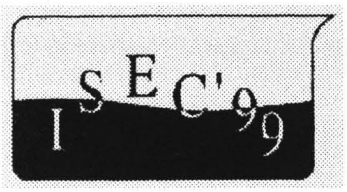
The Spent Batteries Treatment Plant was started in December 1997. This plant has been demonstrated as a MZP industrial application, and an environmentally clean option. Considering the advantages of Zn SX applications, one can get high efficiency and selectivity. Thus products such as an ultra pure Aqueous Extract suitable for obtaining Zn SHG ingots and a solution for producing Mn sulphate salt are obtained and, in addition, there is a saving of more than the half of the total necessary acid to leach the battery dust.

The SX application for this kind of residues allows flexibility in operation. The best products and by-products quality, easy operational control and other advantages make SX a pioneer and advanced environmental technology for the treatment of secondary materials in general and spent domestic batteries in particular.

REFERENCES

1 Nogueira ED, Regife JM and Viegas MP. *Design Features and Operating Experience of the Quimigal Zincex plant*, (Paper presented at the 111th Annual Meeting, Dallas, Texas, 59, (1982).

2 Martín D et al. *Process for the Production of Electrolytic Zinc or High Purity Salt from Secondary Zinc Raw Materials, US Patent No. 4401531.* 1983.
3 Nogueira ED et al. *Using Zinc Secondaries to Feed and Electrowinning Plant". Zinc'85,* (Paper presented at the International Symposium on Extractive Metallurgy of Zinc, Tokyo, (Japan), 763, (1985).
4 Díaz G and Martín D. *The Modified Zincex Process: The Clean, Safe and Profitable Solution to the Zinc Secondaries Treatment,* (Paper presented at the 3rd European East-West Conference on Materials. Symposium E: Recycling of Materials in Industry. Strasbourg (France), (1992).
5 Díaz G and Martín D. *The Modified Zincex Process: The Clean, Safe and Profitable Solution to the Zinc Secondaries Treatment,* (Paper presented at the International Solvent Extraction Conference (ISEC), London, (UK) 1993).
6 Díaz G and Martín D. *Resources, Conservation and Recycling*, **10**, 43, (1994).
7 Díaz G, Martín D and Lombera C. *Zinc Recycling through The Modified Zincex Process,* (Paper presented at the 3rd International Symposium on Recycling of Metals and Engineering Materials, Alabama (USA), (1995).



MICELLAR EXTRACTION VERSUS SOLVENT EXTRACTION: ADVANTAGES AND DRAWBACKS

Marc Hebrant and Christian Tondre

Laboratoire de Chimie Physique Organique et Colloïdale, Unité Mixte de Recherche CNRS-UHP (UMR 7565), Université Henri Poincaré-Nancy I, B.P. 239, 54506 Nancy Vandoeuvre Cedex, France

ABSTRACT

Here new results are compared relative to the removal of nickel ions from aqueous solutions either by standard solvent extraction or by micellar extraction coupled with ultrafiltration. For this purpose the extractant 7-(4-ethyl-1-methyloctyl)-8-hydroxyquinoline (C_{11}-HQ) was either solubilized in an organic solvent (iso-octane or chloroform) or in nonionic micelles (Triton X-100). The effects of the extractant to metal ratio (L/M) and of the pH on the extraction yields have been investigated in relation to the stoichiometries of the extracted complexes. For L/M ratios up to 5, the extraction yields at a fixed pH were found to be almost identical in both processes, provided that the extractant concentrations (measured in the organic phase or in the micellar pseudophase, respectively) are similar. When the L/M ratio is much larger, the micellar extraction is shifted to lower pH's compared to standard solvent extraction. Based on these results in addition to previously reported ones, the advantages and drawbacks of micellar extraction will be discussed.

Keywords: micellar extraction, ultrafiltration, Triton X-100, Kelex 100, surfactants, nickel

INTRODUCTION

During the past few years a significant amount of work has been devoted to the application of micellar systems (and more generally of surfactant-based systems) for the removal of metal ions from aqueous solutions.[1] Among these studies those concerning the complexation and extraction of metal ions by micelle-solubilized long chain extractants has been given special attention.[2-4] Provided that the metal/extractant complex is strongly partitioned in favour of the micellar pseudo-phase, a simple ultrafiltration can allow to remove the metal ions at the same time as the colloid particles. Although such processes are in principle restricted to the treatment of dilute solutions they show large similarities with standard solvent extraction. They are attractive from the environmental point of view since they completely avoid the use of organic solvents. The recent technological advances in the field of ultrafiltration (new ultrafiltration modules and new membranes) constitute another favourable factor for the development of these almost totally aqueous processes. Previous works have shown that many parameters have to be taken into consideration to optimize the yield of metal extraction.

To the best of our knowledge only two papers have so far reported systematic comparisons between micellar-enhanced ultrafiltration and conventional solvent extraction.[5,6] Both papers were concerned with copper removal. In the present paper some new results are reported on the removal of nickel ions using the extractant 7-(4-ethyl-1-methyloctyl)-8-hydroxyquinoline (C_{11}-HQ), either solubilized in nonionic micelles (Triton X-100) or in an organic solvent. Special attention will be given to the stoichiometries of the extracted complexes depending on the experimental conditions. On the basis of the previous data, in addition to the new results reported here, the advantages and drawbacks of micellar extraction coupled with ultrafiltration compared to standard solvent extraction will be critically examined.

Let us first recall that micelles are organized assemblies which form generally in aqueous solutions (reverse micelles may form in organic solvents), when the concentration of a surfactant molecule becomes higher than the critical micellar concentration (cmc). These entities are usually more or less spherical with diameters in the order of 25-50 Å (they may exhibit elongated structures in specific condition). They consist of a hydrophobic core surrounded by a layer of polar heads exposed to the aqueous phase. Micellar solutions have thus a micro-heterogeneous nature and the

© 2000 Society of Chemical Industry

micro-domains constituted of the alkyl chains of the surfactant molecules are hydrocarbon-like. Many similarities between solvent extraction and micellar extraction can be found, as indicated in Table 1:

Solvent extraction	Micellar extraction
➢ biphasic systems (two macroscopic phases)	➢ pseudo-biphasic systems (two microscopic phases)
➢ organic solvent	➢ hydrophobic core of micelles
➢ organic/aqueous interface	➢ micelles/aqueous phase microscopic interfaces
➢ solvent-solubilized lipophilic extractants	➢ micelle-solubilized lipophilic extractants

Table 1 Similarities between solvent extraction and micellar extraction

These strong similarities have some limitations. For instance the solubilization of extractant molecules in the micelles is restricted and it will never be as high as in an organic solvent. On the other hand, even though the nature of the organic/aqueous interface can be modified to some extent by certain additives, the properties of the micellar surface can be infinitely varied due to the diversity of surfactant molecules (chemical structure, electric charge, etc.).

EXPERIMENTAL

8-Hydroxyquinoline (HQ) was obtained from Fluka (puriss.). The extractant 7-(4-ethyl-1-methyloctyl)-8-hydroxyquinoline (C_{11}-HQ), an hydrophobic analog of HQ, was prepared by chromatographic purification of Kelex 100 (Schering, Germany). The quality of the separation was checked by GC-MS (Fisons, Mega 2/Trio 1000), indicating a purity of 96%. Triton X-100, $NiCl_2$-$6H_2O$ (purum), and isooctane (puriss) were purchased from Fluka; chloroform (puriss) was from SDS. The pH of the solutions was usually adjusted with drops of diluted HCl or NaOH (Merck Titrisol). Due to the slow rate of complexation of Ni^{2+} ions an equilibration time of several hours under agitation was allotted for all the extraction experiments before phase (or pseudophase) separation. For the solvent extraction experiments at fixed pH a triethanolamine buffer (TEA, Fluka puriss., $5x10^{-2}$ mol/dm^3) was added to avoid the uncertainty in the final pH. The ultrafiltration experiments were performed at room temperature with a stirred cell of 10 cm^3 (Amicon 8010), equipped with cellulose disk membranes (Millipore, molecular weight cut-off 10,000 Da). The applied pressure was 4 bar. The permeate (subscript "per") was analysed after 50% of the initial solution had been filtered. The yield of nickel extraction was defined as

$$Y(\%)=100x([Ni^{2+}]_{init}-[Ni^{2+}]_{per})/[Ni^{2+}]_{init}.$$

For solvent extraction the aqueous phase concentration $[Ni^{2+}]_{aq}$ remaining after phase separation replaced $[Ni^{2+}]_{per}$ in the preceding equation. The Ni^{2+} concentrations were obtained from atomic absorption measurements (Varian AA-1275). The apparatus was calibrated with standard solutions, which included a surfactant concentration equal to the cmc in the case of micellar extraction.

RESULTS AND DISCUSSIONS

The heterogeneous extraction constant K_{ex} of Ni^{2+} ions by HQ in chloroform/water systems was previously shown to be smaller than that of Cu^{2+} ions by almost four orders of magnitude (log K_{ex} were –2.18 and +1.77, respectively, for the $Me(HQ)_2$ complexes).[7] For this reason, in a first series of experiments, a large excess of complexing agents relatively to the concentration of Ni^{2+} have been used. For the results reported in figure 1 the extractant/metal ratio L/M was equal to 50. The metal ion concentration was 10^{-4} mol/dm^3. The extractant concentration ($5x10^{-3}$ mol/dm^3) refers to

either the organic solvent or the micellar aqueous solution. In this figure the yields of extraction (as defined in Experimental) have been plotted as a function of pH, for different situations. Solvent extraction experiments were performed either in iso-octane (for the sake of comparison with the previous work [6] concerning Cu^{2+} or in chloroform (for comparison with the work of J. Stary,[7] with in both cases the same volumes of aqueous phase and organic phase. Micellar extraction (after ultrafiltration of the micellar solution) was determined in aqueous solutions of Triton X-100 $2x10^{-2}$ mol/dm^3 (i.e. a surfactant concentration 83 times larger than the cmc usually reported for the pure surfactant). In this figure three types of data relative to C_{11}-HQ fall in the pH range from 5 to 8: (i) liquid-liquid extraction with chloroform in the absence of buffer; (ii) liquid-liquid extraction in iso-octane with a TEA buffer and (iii) the same without TEA buffer. All these data are consistent with a single extraction curve (curve ① in the figure 1) within the experimental uncertainties due to the pH adjustments and to the accuracy of the atomic absorption measurements.

In the same figure, a second series of extraction data falls in the pH range from 2 to 5: (i) micellar extraction with C_{11}-HQ; (ii) liquid-liquid extraction involving HQ in chloroform. Again all the data in this second series of experiments can be considered consistent with a single extraction curve (curve ② in the Figure 1), which is shifted by about 2.4 pH units in the direction of the low pHs compared to the previous curve. Note however that, as will be seen below, two different K_{ex} values are associated with this curve, depending on the true extractant concentration to be considered.

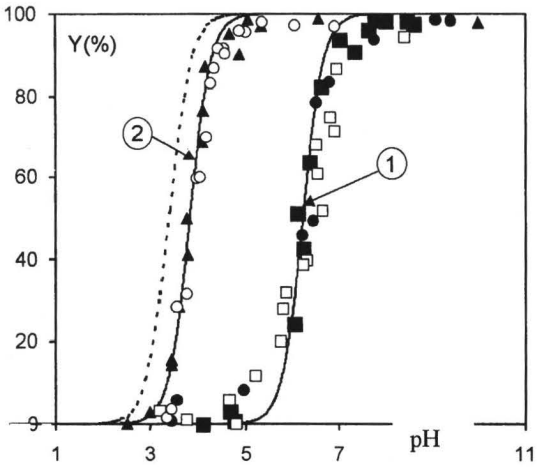


Figure 1 : Yields of extraction of Ni^{2+} ions versus pH with different systems : (□) HQ or (●) C_{11}HQ in $CHCl_3$; (▲) : C_{11}HQ in Triton X-100 micelles ; (■) and (□) : C_{11}HQ in isooctane with buffered and non-buffered aqueous phase respectively. Experimental conditions and theoretical curves : see text.

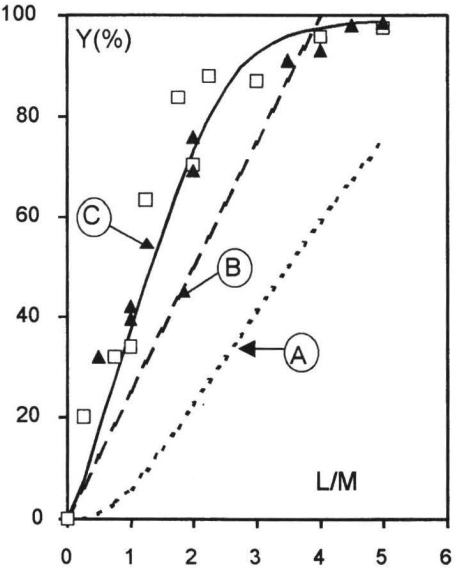


Figure 2 : Yields of extraction of Ni^{2+} ions versus L/M ratios in Triton X-100 micelles (▲) or in the isooctane/buffered aqueous phase system (□) with v_{org}/v_{aq}=1/100. Experimental conditions and theoretical curves : see text.

Using the theoretical treatment and the mathematical method described in detail in a previous publication,[6] the best fit of the experimental data has been calculated when the stoichiometry of the extractant/metal complex is varied, K_{ex} being an adjustable parameter. The best simulations (see curves shown in Figure 1) were obtained for the stoichiometries 2:1 (L_2Ni) or 4:1 ($(LH)_2L_2Ni$),

which lead to identical curves because of the displacement of two protons in both cases (simulations obtained for complexes of the types (LH)LNi or LNi gave higher sums of squared deviations). The values obtained for K_{ex} were the following:

Triton X-100 micelles (curve ② in figure 1)

(Values calculated with a volume fraction of the micellar pseudo-phase, φm=0.012)

L_2Ni $K_{ex}=1.2x10^{-5}$

$(LH)_2L_2Ni$ $K_{ex}=8.4x10^{-5}$

Solvent extraction (curve ① in figure 1), in iso-octane/water (TEA buffer)

L_2Ni $K_{ex}=1.5x10^{-8}$

$(LH)_2L_2Ni$ $K_{ex}=7.2x10^{-4}$

Remembering that in the previous work on copper extraction[6] the results indicated the same (or at least a very close) value for the extraction constants measured with micelles or with an organic solvent, the shift of the extraction curve being explained by the true concentration of extractant in the micellar pseudo-phase, a critical examination of the above values of K_{ex} can be done on the same basis. This suggests that the L_2Ni complex is very unlikely because three orders of magnitude separate the values measured in micelles and in an organic solvent respectively. The values of K_{ex} are much closer for the $(LH)_2L_2Ni$ complex. If in this case the K_{ex} value measured in solvent extraction with a 1/1 organic/aqueous phase volume is applied to an organic phase volume comparable to that of the micellar pseudo-phase, the extraction curve is shifted by 0.4 pH unit compared to the micellar case (see curve in dashed line in figure 1). This difference originates from small variations in the solvation properties when comparing the oily core of the Triton X-100 micelles and iso-octane. It can also be attributed to the fact that a single type of complex was considered in the simulations, neglecting the possible coexistence of another minor complex.

The large excess of extractant used in this series of experiments explains by itself that a 4:1 stoichiometry is strongly favoured here. It can also be noticed that the large difference in the K_{ex} values found respectively for the extraction of Cu^{2+} ([6]) or Ni^{2+} by C_{11}-HQ is consistent with the observation made by Stary[7] in the case of HQ (see above). The fact that the curves (but not the K_{ex} values) obtained for the micellar extraction of Ni^{2+} by C_{11}-HQ and for the solvent extraction (chloroform) of Ni^{2+} by HQ are practically superimposable is probably fortuitous. However the stronger complexing ability of HQ compared to C_{11}-HQ has been already reported by Ismael and Tondre.[8] The similitarity of the three types of data fitted by curve ① in figure 1 indicates a negligible solvent effect when going from chloroform to iso-octane and it also proves that the effect of the TEA buffer is minor (in fact, this could be expected from the weak value of the stability constant reported for the TEA-Ni^{2+} complex, logK=-5.0).[9]

In another set of experiments the effect of the extractant to metal ratio on the extraction yield, when the pH was fixed at 7.4 has been studied. In this case L/M was kept below 5, which is very low compared to the previous set of data in which L/M was fixed equal to 50. The results of micellar extraction (Triton X-100) are compared in figure 2 with those of solvent extraction (iso-octane/water (TEA buffer)). The latter were obtained with an organic/aqueous volume ratio of 1/100, i.e. very close to the volume fraction of the micellar pseudophase in the micellar case. The experimental results shown in figure 2 appear to be very similar for the two types of processes considered, which further substantiates the strong analogy already noticed. Unfortunately the theoretical curve which can be calculated from the value of K_{ex} previously determined assuming a 4:1 stoichiometry ($K_{ex}=7.2x10^{-4}$) is in no means consistent with the experimental data (see curve A in figure 2). Curve B which has been drawn in the same figure indicates the largest extraction yields that can be obtained when a 4:1 complex is formed (assuming an infinite extraction constant).

The fact that most of the experimental data show higher values is a firm indication that such a complex cannot exist in the present experimental conditions. Curve C represents the predicted curve for the 2:1 complex (L_2Ni), which is in quite satisfactory agreement with the results. Thus it can be concluded that the stoichiometry of the complex is not unique: the 4:1 complex is largely

favoured when the L/M ratio is very large, but this is no longer true for the low values of the L/M ratio, where the 2:1 complex is more likely. The important thing is that, in the latter case, the extraction yield appears to be almost unchanged whether the complex is formed in micelles or in an organic solvent, provided that the extractant concentrations are similar in both cases.

Having given here new evidence of the strong analogy existing between the micellar and solvent processes, it is interesting to examine the advantages and drawbacks of micellar extraction compared to solvent extraction. The essential features are summarised in Table 2.

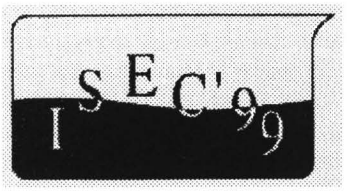
Advantages	Drawbacks
• no organic solvent (extraction in 99% aqueous media) • extraction takes place at lower pH • membrane process easy to implement (continuous flow treatment) • counterions of the micelles can contribute to the formation of a neutral metal complex (case of cationic surfactants)[6] • in favourable cases selective separations can be achieved on kinetic criteria[10]	• restricted to low metal content (up to the order of millimolar concentrations) • leakage of monomeric surfactant (cmc)[11] • ion expulsion effects may have to be considered[6] (they may also be taken as an advantage[12]) • problem of recycling of the micellar phase not completely solved[13]

Table 2 Advantages and drawbacks of micellar extraction compared to solvent extraction

Finally it should be added that, considering the previous observations, micellar ultrafiltration will be clearly more appropriate to solve environmental problems (low level metal ion pollution) or problems of recovery of precious metals at high dilution than to solve industrial problems associated, for instance, with hydrometallurgy.

REFERENCES

1. Scamehorn JF, Christian SD and Ellington RT in *Surfactant-Based Separation Processes, Surfactant Science Series,* ed. Scamehorn JF, Harwell, Marcel Dekker, New York, **33**, 29, (1989)
2. Tondre C,. Son S-G, Hebrant M, Scrimin P and Tecilla P, *Langmuir* **9**, 950, (1993)
3. Fillipi BR, Scamehorn JF, Taylor RW and Christian SD; *Sep.Sci.Technol.* **32**, 2401 (1997)
4. Pramauro E, Bianco-Prevot A, Pelizzetti E, Marchelli R, Dossena A, Biancardi A, *Anal. Chim. Acta,* **264**, 303, (1992)
5. Fillipi BR, Scamehorn JF, Christian SD and Taylor RW, *J. Membr. Sci.* **145**, 27, (1998)
6. Hebrant M, Francois N and Tondre C, *Colloids Surfaces A* **143**, 77, (1998)
7. Stary J, *Anal. Chim. Acta,* **28**, 132, (1963)
8. Ismael M and Tondre C; *Sep. Sci. Technol.* **29**, 651, (1994)
9. Smith RM, Martell AE and Motekaitis QJ, *NIST Critically Selected Stability Constants of Metal Complexes Database, Version 3.0, Database 46* (1997)
10. Ismael M and Tondre C, *J. Colloid Interface Sci.* **160**, 252, (1993)
11. Tounissou P, Hebrant M, Rodehuser L and Tondre C, *J. Colloid Interface Sci.* **183**, 484, (1996); Tounissou P, Hebrant M, and Tondre C, *idem* **183**, 491, (1996)
12. Christian SD, Tucker EE, Scamehorn JF, Lee B-H, Sasaki KJ, *Langmuir* **5**, 876, (1989)
13. Tondre C, Hebrant M, Perdicakis M and Bessiere J, *Langmuir* **13,** 1446, (1997)



INTERACTION OF THORIUM WITH GRAY HUMIC ACID

Abd-Allah A Helal
Hot Laboratories Center, Atomic Energy Authority,
Cairo - 13759, Egypt

ABSTRACT
A humic acid sample was separated from the bottom sediments of Lake Quarun, in Egypt. The sample was purified and characterized by: elemental analysis, potentiometric titration, IR, UV-visible and C-13 NMR spectroscopies. The product of humic acid was very low (0.009%), gray in colour and has low carboxylate capacity (2.4 meq/g). The first derivative of the titration curve indicated only one maximum, which implies one kind of carboxylate group.
The binding constant of Th-234 with Lake Quarun humic acid was determined using solvent extraction. One parameter, β_1, was required to fit the binding as a function of carboxylate concentration: the Th^{4+} bound to the carboxylate sites in the gray humic acid only forming 1:1 complex. The binding constant increased with the degree of ionization of the humic acid.

Keywords: humic acid, thorium

INTRODUCTION

The environmental contamination of air, water, soils and food have become a threat to many plant and animal communities of the ecosystem including the human race. The nuclear energy industry during the past several decades has added significant amount of radioactive materials to the environment. Soil, oceans, seas, rivers and streams represent a major part of man's environment which receive most of contaminants either accidentally or on purpose. The most widely distributed materials on the earth's surface, occurring in soils, lakes, rivers and seas, are humic substances. These materials are naturally occurring, high molecular weight, polymers containing a variety of functional groups such as -COOH, -OH, -C=O, ... etc. According to their solubilities in aqueous solutions, humic substances are classified in three fractions of different acidities: *fulvic acid*, soluble at all pH's; *humic acid (HA)*, soluble at high pH, insoluble at low pH; *humin*, insoluble at all pH values.[1]

As natural polyelectrolytes, humic substances are strong complexing agents toward metal ions and they participate in controlling many reactions that occur in the environment. The binding of some metal ions with humic materials have been reported.[2-7] However, further investigations are needed since little is known about the binding of gray HA with metal ions. Moreover, humic acids are complex mixtures of molecules of various sizes and shapes and their properties vary with location, season, etc. In this work, the binding constant of the radiotoxic ion Th^{4+} with gray HA isolated from the Egyptian Lake Quarun was measured.

EXPERIMENTAL

Chemicals and Materials

Unless otherwise stated, the chemicals used were of analytical purity. Di(2-ethylhexyl)phosphoric acid, HDEHP, used in the solvent extraction experiments was obtained from Union Carbide, and purified according to Peppard et al.[8]

Humic acid (HA) was isolated from the bottom sediments of Lake Quarun (LQ), an old lake of area 235 Km^2, located at Fayoum, Egypt. The method of isolation and purification of HA is described elsewhere.[9]

Tracer

The radioactive tracer Th-234 was separated from natural uranium by solvent extraction using 30% tributylphosphate (TBP), diluted in benzene. Thus uranyl nitrate $UO_2(NO_3)_2.6H_2O$ (10 g) were

© 2000 Society of Chemical Industry

dissolved in 6 mol/dm^3 HCl (20 cm^3) and placed in a separating funnel together with 30% TBP (20cm^3) pre-saturated with 6mol/dm^3 HCl. The mixture was shaken and the yellow coloured organic phase was separated. This step was repeated three times with fresh TBP until the yellow colour of the aqueous phase, which contains the Th-234 disappeared. The pH was then adjusted with dilute NH_3 solution to the desired value. The radiochemical purity of Th-234 was checked by measuring the respective γ-spectrum with Ge(Li) detector using a multi-channel analyzer. The γ-emissions of Th-234 were counted with a NaI(Tl) well-counter of ORTEC type.

Procedures

The humic acid sample was characterized by elemental analysis, potentiometric titration, CP/MAS C-13 NMR, IR and visible spectroscopies.

The acid-base behaviour of the HA was determined at an ionic strength (μ) of 0.1mol/dm^3 by direct titration.[9] The C-13 NMR spectrum was determined using the cross polarization technique with magic angle spinning on an IBM/BRUKER WP200 SY NMR spectrometer. The infrared spectroscopic measurements were made with Perkin Elmer 1650 FT-IR spectrometer. The absorption in the visible region was measured using a Shimadzu recording spectrometer 160A.

For the solvent extraction (SX) experiments, the organic phases consisted of the desired concentration of HDEHP diluted with toluene. Because of the precipitation problems encountered when contacting humic acid (HA) solutions with organic phases, the later were pre-equilibrated against equal volumes of the corresponding buffer solutions before use.[5] This pre-equilibration was continued with fresh aqueous solutions until no pH change was observed in the fresh aqueous phase. The aqueous phases were prepared by using the suitable buffer solutions for the desired pH values.[5] These buffer solutions also contained the necessary quantity of $NaClO_4$ to make the total ionic strength 0.1 [including contributions from free acid ($HClO_4$ used for adjusting HA to the desired pH) and ionized buffer species].

A working solution of HA was prepared by dissolving ca. 0.1g in 10cm^3 of 0.1mol/dm^3 NaOH with overnight stirring under nitrogen gas. The solution was titrated to the desired pH with 0.1mol/dm^3 $HClO_4$, and diluted to 100 cm^3 in a measuring flask with the suitable buffer solution of the same pH. Aliquots of this working solution were diluted in measuring flasks with the buffer to obtain solutions of varying HA concentrations. The free humate concentration (in eq/dm^3) was determined by multiplying the concentration (g/dm^3) by the total capacity (eq/g) and by the degree of ionization corresponding to the final pH of the investigation. After removing aliquots for the SE investigations, the reminder of each solution was used to establish a calibration curve for measuring the different HA concentrations.

A sample of each phase (5 cm^3) and tracer (10μl) were added to a glass scintillation vials (coated with silicon compounds[10] to minimize the loss of activity by wall adsorption) and sealed with polyethylene caps. The buffer solution (5 cm^3), without HA, was used as a blank for each investigation. The vials were vigorously shaken in a thermostated shaker at 25±1°C for 6 hours, then they were centrifuged and the phases separated into glass test tubes and centrifuged before removing aliquots for counting. The reminder of the aqueous phases was used to measure the final HA concentrations and the final pH values.

RESULTS AND DISCUSSION

The yield of HA isolated from LQ was found 0.009%. This yield is very low, as compared with that obtained from other lakes, such as Lake Bradford, USA, which yielded 1%.[11] The small concentration of HA in LQ sediments is related to the nature and components of water in this lake which receives 390 million m^3/year of drain water containing remains of fertilizers and pesticides.[12] The mineral salts added to this lake were estimated to be 350 tons/year.[12]

It was reported that humic materials bind to N-containing fertilisers[13] and pesticides.[1] This binding prevents the precipitation of HA and decreases its amount in the bottom sediments. In addition, the pH of the lake water is 8.3, which causes solubilization of the HA.

The HA obtained was gray in colour. It was pointed out by Stevenson[1] that the gray fraction of HA can be separated from the original HA by adding electrolyte. This means that the LQ HA is a fraction coagulated by the mineral salts abundant in the lake.

The elemental analysis of the HA sample indicated that it contains C: 57.13%, O: 33.01%, H: 5.04%, N: 3.30% and S: 1.52%. The data show that these values agree with those previously published.[1] The relative high contents of H and N are related to the aliphatic nature of the compounds which characterise the lake humic materials.[14]

Figure 1 shows the potentiometric titration curve and the first derivative of the HA sample. Two inflections can be observed in the titration curve and its general behaviour is similar to titration curves for weak acids. The single maximum of the first derivative indicates one type of ionic functional group. The maximum occurs at pH 8.44, which is low for ionisation of phenolic groups, so the ionizing functional groups are probably carboxylate. The carboxylate capacity was calculated from this maximum and was found to be 2.4 meq/g. This value is smaller than those reported for soil HA, but it agrees with that for lake HA.[15] A generalized form of the Henderson-Hasselbalch equation[9] was applied to evaluate the pK_a of the HA sample :

$$pH = pK_a + n \log [\alpha /(1-\alpha)]$$

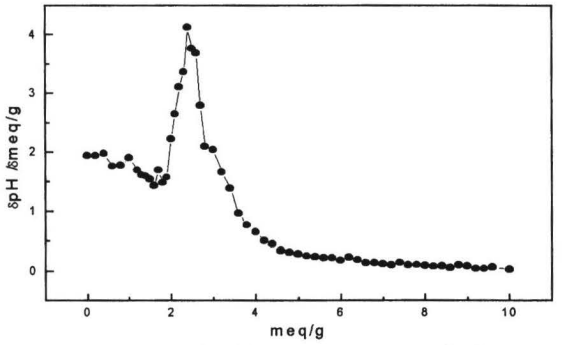


Fig.(1): The Potentiometric Titration Curve and the First Derivative of Lake Quarun Humic Acid

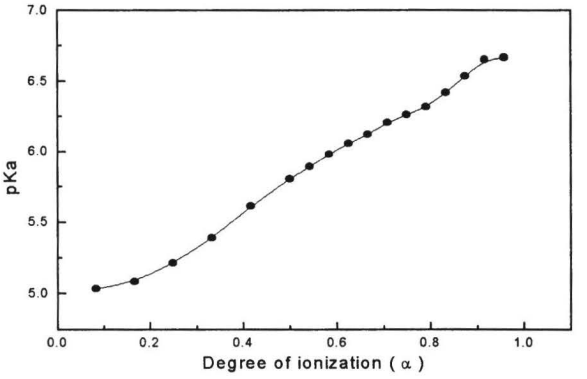


Fig.(2): Variation of pKa with the Degree of Ionization of Lake Quarun Humic Acid

Figure 2 represents the plot of pK_a vs the degree of ionization (α). The sample displayed typical characteristics of polyelectrolyte, i.e. the pK_a increased with increasing degree of ionisation of the carboxylate groups. The pK_a value at 50% ionisation ($\alpha = 0.5$) is found to be 5.80.

The C-13 NMR spectrum is shown in figure 3. It exhibits fairly distinct peaks in the aliphatic (ca. 30ppm), aromatic (ca. 130ppm) and carboxyl (ca.175ppm) regions. It is clear from the figure that the peak of the aliphatic region is stronger than the aromatic one.

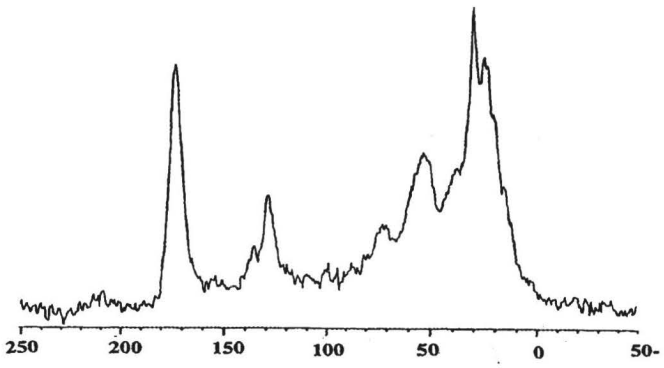


Figure 3 C-13 NMR Spectrum of Lake Quarun Humic Acid

The IR spectrum is illustrated in figure 4. Main absorption bands are in the regions of 3300 cm^{-1} (H-bonded OH groups), 2920 cm^{-1} (aliphatic C-H stretching), 1650 cm^{-1} (C=O stretching of amide groups), 1540 cm^{-1} (COO^- symmetric stretching), 1460 cm^{-1} (aliphatic C-H), 1390 cm^{-1} (COO^- antisymmetric stretching), 1230 cm^{-1} (C-O stretching and OH deformation of COOH) and 1040 cm^{-1} (C-O stretching of polysaccharide or Si-O of silicate impurities). The spectrum is similar to that of Lake Mud HA, Florida.[16] It is characterized by weak absorption near 1720 cm^{-1} which implies the low carboxylate capacity.

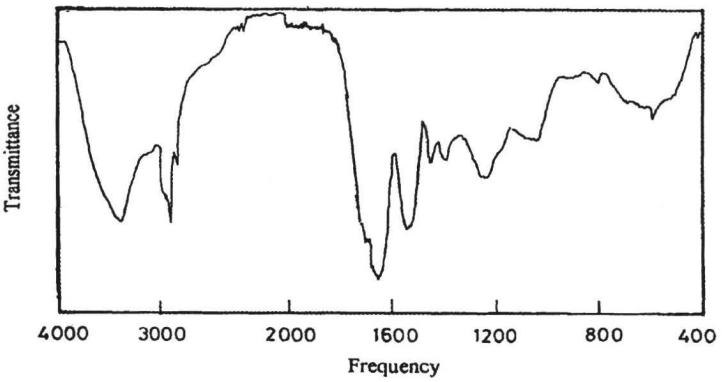


Figure 4 The Infrared Spectrum of Lake Quarun Humic Acid

The ratio of the absorbances of dilute aqueous HA solution at 465 and 665 nm, E_4/E_6 ratio, was found 1.93. It is lower than that of brown HA,[9] but it is close to that of gray HA.[17] The low E_4/E_6 ratio show that the investigated HA had high mean residence time. It was pointed out by Stevenson[1] that E_4/E_6 ratio above 1.3 indicate that much of the material is aliphatic in nature.

The SX technique involves measuring the extent that the presence of HA inhibits the extraction of the cation of interest into the organic phase. For a SE system of a cation M^{n+}, the following equations are defined[5] (for simplicity the charge on the cation is omitted). When no complexing agent is present in

the aqueous phase, the partition of the cation between the aqueous (a) and organic (o) phases follow the relation :

$$D_o = [M]_o / [M]_a \quad (1)$$

Hydrolysis and/or complexation by a ligand B interferes with the extraction so the partition is then represented by :

$$D_1 = [M]_o / \{ [M]_a + \Sigma [M(OH)_i]_a + \Sigma [MB_j]_a \} \quad (2)$$

Thus, when the aqueous phase includes complexation by a second ligand (L) :

$$D_2 = [M]_o / \{ [M]_a + \Sigma [M(OH)_i]_a + \Sigma [MB_j]_a + \Sigma [ML_k]_a \} \quad (3)$$

In the current system B is the buffer anion and L is the carboxylate group of HA. For a ligand (L), the binding constant for a particular complex in a solution of constant ionic strength is defined by :

$$\beta_i = [M(L)_i] / \{ [M] [L]^i \} \quad (4)$$

The concentration of each complex with any ligand can be replaced by the binding constant; the free ligand concentration and the free metal concentration. Replacing the total concentration of each complexed species in terms of the free ligand concentration, the free metal concentration and the respective binding constant allow equations (1), (2) and (3) to be solved. If the investigations are carried out at constant pH and buffer concentration, equations (1) - (4) can be combined to give the relation :

$$1/D_2 - 1/D_1 = 1/D_o \Sigma \beta_i [L]^I \quad (5a)$$

or

$$1/D_2 - 1/D_1 = (1/D_o) \{ \beta_1[L] + \beta_2[L]^2 + \ldots\ldots \} \quad (5b)$$

upon rearrangement, this leads to :

$$(D_o/[L]) (1/D_2 - 1/D_1) = \beta_1 + \beta_2[L] + \ldots\ldots \quad (6)$$

Therefore, if the ligand (L) is the concentration of carboxylate groups from the HA, a plot of $(D_o/[HA])$ $(1/D_2 - 1/D_1)$ vs free carboxylate concentration [HA] should give a straight line with an intercept equal to β_1 and a slope of zero if only a 1:1 complex is formed, or a straight line of intercept equals β_1 and a slope of β_2 if a 1:2 complex is formed.

The D_o values for Th^{4+} was calculated from the equation:[18]:

$$\log D_o = 4.00\ pH + 3.00 \log [HDEHP] + 1.55 \quad (7)$$

where pH is the negative logarithm of H^+ molarity.

The plots of $\{D_o/[HA]\}\{(1/D_2)-(1/D_1)\}$ vs the free humate concentration [HA], equation (6), for Th^{4+} with the gray HA was linear with zero or negative slopes, (figure 5). Thus, the binding function required analysis with one constant β_1 implying formation of only a 1:1 complex .

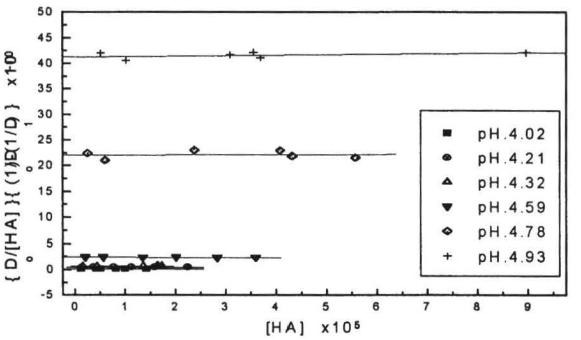


Fig.(5): Variation of $\{ D_o/[HA] \} \{ (1/D_2)-(1/D_1) \}$ with the Free HA Concentration

This result agrees with the potentiometric titration of the HA where one maximum is observed in the first derivative curve, figure 1, which implies one type of ionic functional group. The variation of the binding constants obtained at different pH values with the degree of ionization (α) of the humate

polyelectrolyte is shown in figure 6. The strength of the binding of Th^{4+} to the HA sample increases with the degree of ionization, which is a function of pH. Increasing the solution pH increases the ionisation of the HA acidic groups, and increases the binding constant. From figure 6, equation 8 could be derived for the value of the binding constant as a function of the degree of ionization of HA :

$$\log \beta_1 = 7.93 + 12.50\ \alpha \qquad (8)$$

Thus, the value of the binding constant at 50% ionisation ($\alpha = 0.5$) is equal to 14.18 . This value lies in the range of the reported values[11,19] for the binding of Th^{4+} with soil and lake humic acids. By comparing the values of $\log\beta_1$ and pK_a obtained in this work with previous studies, it is noted that the binding constant of Th^{4+} at any value of (α) increases with increasing pK_a of the HA.

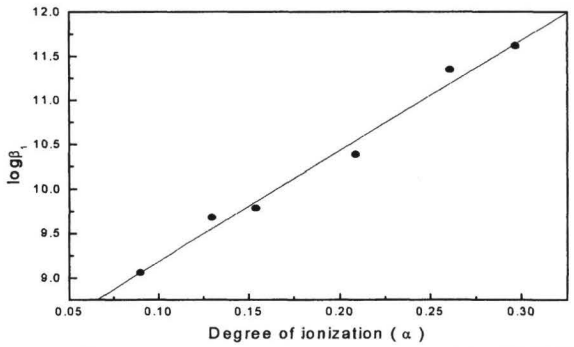


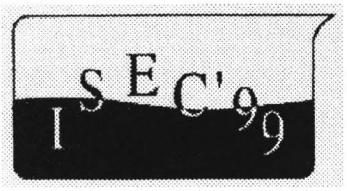
Fig.(6): Variation of the Binding Constant with the Degree of Ionization

ACKNOWLEDGMENTS

The author is grateful to Prof. H. F. Aly and Prof. S. M. Khalifa for their encouragement, and to Mr. Aly A. Helal for performing part of the experiments.

REFERENCES

1. Stevenson FJ, *"Humus Chemistry (Genesis, Composition, Reactions)"*, 2nd edition, John Wiley and Sons, New York, (1994).
2. Helal AA, Aly HF, Imam DM and Khalifa SM, *J. Radioanal. Nucl. Chem.*, **227**(1-2), 49, (1998).
3. Pinheiro JP, Mota AM and Simoes Goncalves ML, *J. Analytica Chimica Acta*, **284**, 525, (1994).
4. Hargitai L, *J. Sc. Total Environ.*, **81/82**, 643, (1989).
5. Torres RA and Choppin GR, *J. Radiochemica Acta*, **35**, 143, (1984).
6. Shanbhag PM and Choppin GR, *J. Inorg. Nucl. Chem.*, **43**, 3369, (1981).
7. Helal AA, Imam DM andAly HF, *J. Radioanal. Nucl. Chem.*, **237** (1-2), (1998).
8. Peppard DF, Mason GW, Maier JL and Driscoll WJ, *J. Inorg. Nucl. Chem.*, **4**, 334, (1957).
9. Helal AA, Imam DM and Aly HF, *Egypt. J. Anal. Chem.*, **5**, 79, (1996).
10. Caceci MS and Choppin GR, *J. Radiochemica Acta*, **33**, 113, (1983).
11. Nash NL and Choppin GR, *J. Inorg. Nucl. Chem.*, **42**, 1045, (1980).
12. Tolba NA, *Proc. 1st. symp. Lake Quarun, Fayoum* 8 April, (1995).
13. Helal AA, Imam DM, Khalifa SM and Aly HF, *J. Radioanal. Nucl. Chem.*, **232** (1-2), 159, (1998).
14. Steinberg C and Muenster U; *Geochemistry and Ecological Role of Humic Substances in Lake Water*, in: " *Humic Substances in Soil, Sediment and Water"*, John Wiley & Sons, New York, 166, (1985).
15. Ishiwatari R, *J. Soil Sci.*, **107**, 53, (1969).
16. Stevenson FJ and Goh KM, *J. Geochim. Acta*, **35**, 417, (1971).
17. Schnitzer M and Khan SU, *"Humic Substances in the Environment"*, Marcel Dekker, New York, 59, (1972).
18. Torres RA, Ph. D. Thesis, Florida State University, USA, (1982).
19. Helal AA, Ph. D. Thesis, Ain Shams University, Egypt, (1989).



EXTRACTIVE RECOVERY OF BORON IN WASTEWATER FROM A COAL THERMAL POWER PLANT

M Hirata[1], H Takanashi[1], S Kokubu[1], M Matsumoto[2], T Takada[3] and T Hano

[1]Department of Applied Chemistry, Oita University, Oita 870-1192, Japan

[2]Department of Chemical Engineering and Materials Science, Doshisha University, Kyoto 610-0394, Japan

[3]Organo Corporation, Tokyo 113-0033, Japan

ABSTRACT

Extractive recovery of boron in wastewater was examined by using 2-butyl-2-ethyl-1,3-propandiol (BEPD) as an extractant and 2-ethylhexanol (EHA) as a diluent. Boron is well extracted in this system and extracted boron was completely recovered by alkaline solution. In the continuous operations of extraction and stripping, equilibrium separations can be carried out at low specific velocity though there was the lowering of efficiency by increasing the specific velocity. Since it was considered that this is based as extraction rate was comparatively low, the measurement of extraction rate was also carried out.

Keywords: boron, wastewater, diol derivatives, mixer-settler, 2-ethylhexanol, 2-butyl-2-ethyl-1,3-propandiol

INTRODUCTION

The acidic wastewater from desulfurization plant of a thermal power plant using coal as a fuel contains boron in relatively high level. It is known that though boron of a small amount is essential for the growth of plants, the growth is inhibited in the concentration of more than 5 mg/l [1]. At present, boron is not a regulation object, however, it is an inspected item with the index value of 0.2 mg/l and it will be regulated in the near future, in Japan.

Boron exists as boric acid or borate in water and it can be practically recovered by using the chelating resin having *N*-methyl (polyhydroxyhexyl) amino group and this method is used for ultrapurification of water in semiconductor manufacturing industry [2]. Solvent extraction method may be more advantageous for wastewater treatment since it can be treat a large quantity easily [3]. Though boron can be extracted physically, from the viewpoint of extractability, chemical extraction using extractant may be more preferable for practical use [4].

In this study, the process for the extractive recovery of boron in acidic wastewater was studied. The extraction and stripping of boric acid was examined using 2-butyl-2-ethyl-1,3-propandiol (BEPD) as an extractant and 2-ethylhexanol (EHA) as a diluent by considering extractability, selectivity and stability [5]. Based on the data of extraction and stripping, mixer-settler type extraction system was equipped and continuous operation was carried out. Furthermore, the extraction rate of boron was measured by using a flat interface contactor.

EXPERIMENTAL

Desulfurization waste water.

In this study desulfurization wastewater from coal thermal power plant with fluorine, metals and calcium removed was used. The actual composition analysis of this wastewater is shown in Table 1. As the concentrations of components except B, Na, Mg, Cl and SO_4 were very low an aqueous solution of boric acid was used as a model wastewater in this study.

Extraction and Stripping of Boric Acid.

For the measurement of the extent of extraction, aqueous solution of boric acid and organic solvent of EHA containing BEPD of the same volume were taken into a Erlenmeyer flask and shaken

© 2000 Society of Chemical Industry

at 25 °C. After extraction equilibrium was reached, the concentration of boric acid was measured. For the stripping, boron in the organic solvent was back-extracted into aqueous alkaline solution in a similar manner.

TABLE 1
Composition of Desulfurization Wastewater

Item	Concentration [kmol/m^3]
B	0.012
Na	0.26
Mg	0.11
Ca	8.0×10^{-3}
NH_4	5.8×10^{-4}
K	6.6×10^{-4}
Ni	2.2×10^{-5}
Cu	3.3×10^{-7}
Li	4.0×10^{-7}
Zn	1.7×10^{-5}
P	n. d.
V	4.0×10^{-7}
Cr	1.6×10^{-7}
Mn	4.9×10^{-5}
Fe	2.7×10^{-3}
Mo	3.9×10^{-7}
W	3.3×10^{-7}
Al	3.2×10^{-5}
Si	4.1×10^{-4}
Cl	0.096
SO_4	0.09

Continuous Operation Using Mixer-Settler.

Continuous operations were carried out using a mixer-settler (mixer, 0.185×10^{-3} m^3; settler, 0.545×10^{-3} m^3) at room temperature. For extraction, the model wastewater (C_{ai} = 0.030 kmol/m^3) and the organic solvent, 1.0 kmol/m^3 BEPD/EHA, were fed at the same flow rate into the mixer in the one-pass. For one-pass recovery, the organic solvent containing borate (C_{oi} = 0.030 kmol/m^3) and 0.5 kmol/m^3 aqueous alkaline solution were fed at the same flow rate (Sv = 0.41 h^{-1}). For concentrating recovery, the alkaline solution was circulated from settler to mixer at the same flow rate of the organic solvent feeding (C_{oi} = 0.0235 kmol/m^3; Sv = 0.41 h^{-1}), and pH of the aqueous solution was kept at pH 11 by pH controller.

Extraction Rate of Boron.

Extraction rate of boron was measured by using a flat interface contactor with interface area of 4.30×10^{-3} m^2. To obtain the initial rate of the extraction, 0.200 kmol/m^3 boric acid solution was contacted with the same volume of BEPD/EHA at 25 °C. Each phase was stirred by reverse rotation of two six-blade turbine impellers at 30 min^{-1}.

Analysis.

The concentration of boron was obtained spectrophotometrically by azomethine H coloration method [6]. The absorbance of sample was measured by UV/VIS Spectrophotometer Ubest-35, JASCO Corp., Japan.

RESULTS AND DISCUSSION

Extraction and Stripping of Boric Acid

The extraction equilibrium was examined in batch experiments of extraction and stripping. Figure 1 shows the effect of BEPD concentration in organic phase on the extent of extraction in initial boron concentration of 0.030 kmol/m^3 in aqueous phase. The value of the y-intercept was not zero, and it is because diluting solvent, EHA, could extract boron [7]. The extent was saturated at more than 2 kmol/m^3 BEPD, but phase separation was not easy at this range. From the viewpoints of extractability and stability, 1 kmol/m^3 BEPD/EHA was considered to be suitable. The effect of initial boron concentration on the extraction with 1 kmol/m^3 BEPD/EHA is shown in Figure 2. The values were roughly constant under the experimental condition except the case of that initial boron concentration was extremely low as 0.001 intercept was not zero, and it is because diluting solvent, EHA, could extract boron [7]. The extent was saturated at more than 2 kmol/m^3 BEPD, but phase separation was not

easy at this range. From the viewpoints of extractability and stability, 1 kmol/m^3 BEPD/EHA was considered to be suitable. The effect of initial boron concentration on the extraction with 1 kmol/m^3 BEPD/EHA is shown in Figure 2.

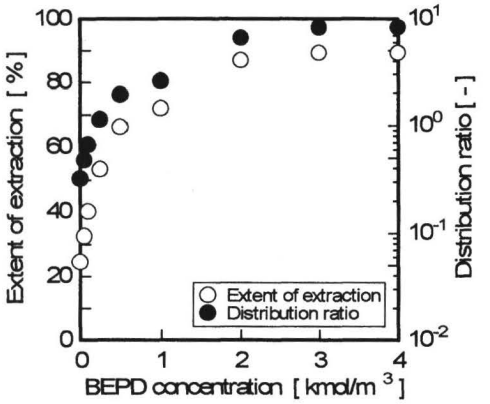


Figure 1. Effect of extractant concentration on extraction

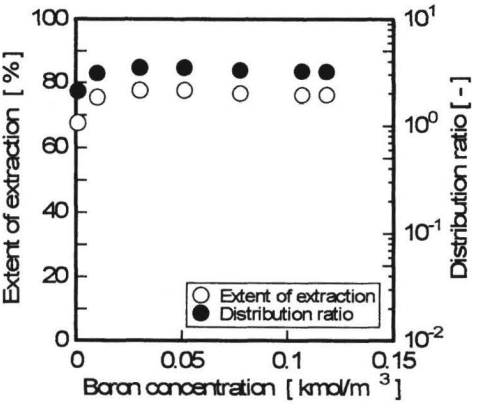


Figure 2. Effect of boron concentration on extraction

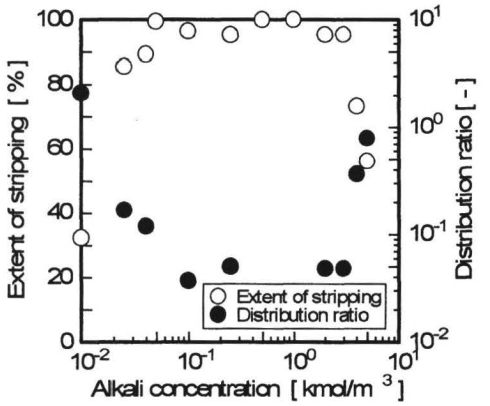


Figure 3. Effect of alkali concentration on stripping

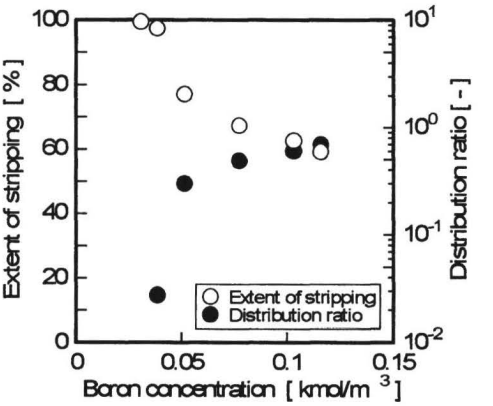


Figure 4. Effect of boron concentration on stripping

The values were roughly constant under the experimental condition except the case of that initial boron concentration was extremely low as 0.001 kmol/m^3, and 75% of boron was extracted even if the boron concentration was low as 0.01 kmol/m^3. The extraction from actual waste-water was also attempted and there was no remarkable effect of coexistence components since the same results were obtained. Figure 3 shows the effect of alkali concentration in stripping phase on the stripping in initial boron concentration of 0.023 kmol/m^3 in 1.0 kmol/m^3 BEPD/EHA. Though the extent increased with alkali concentration up to 0.05 kmol/m^3 and approximately 100% strippings were achieved up to 3 kmol/m^3, the extent decreased above this concentration. Since the similar behavior was observed by the addition of sodium chloride, it was considered that the extent decrease was caused by the increase of salt concentration. Figure 4 shows the effect of initial boron concentration in 1.0 kmol/m^3

BEPD/EHA on the stripping by 0.5 kmol/m^3 alkaline solution. The extent of stripping was decreased with increasing the boron concentration in organic phase. This was caused by pH decrease with the increase of boron concentration in aqueous phase and more than 80% of boron could be stripped by adjusting pH to 11.

Continuous Operation Using Mixer-Settler

A mixer-settler type extraction system was equipped for extraction and stripping, and continuous operation was carried out. The effect of specific velocity of feed on the extraction in one-pass extraction is shown in Figure 5.

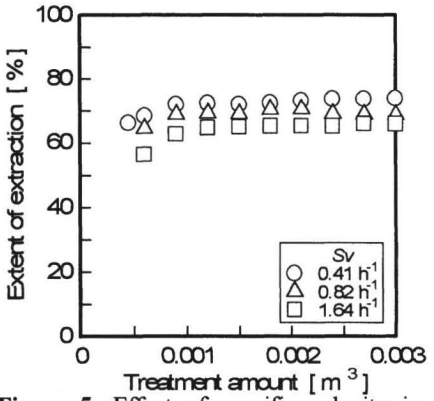


Figure 5. Effect of specific velocity in one-pass extraction

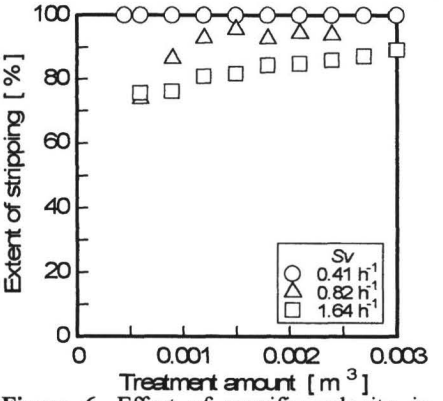


Figure 6. Effect of specific velocity in one-pass recovery

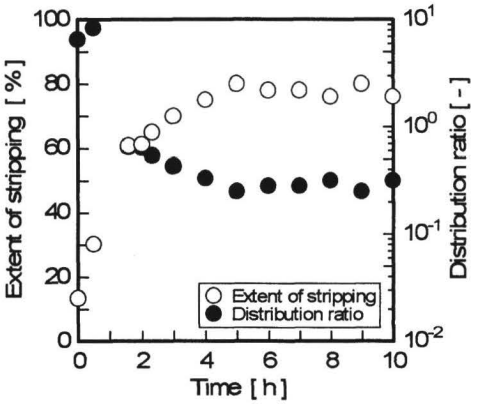


Figure 7. Time course of extent of stripping in concentrating recovery

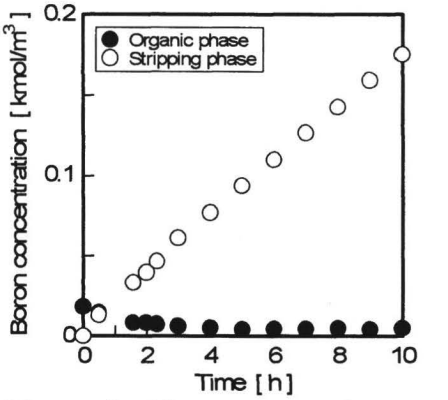


Figure 8. Time course of boron concentration in concentrating recovery

At the time when 4 times volume of the mixer-settler was fed, the extents of the extraction were 74, 69 and 66% at Sv = 0.41, 0.82 and 1.64 h^{-1}, respectively. Though a value near to the equilibrium was obtained at Sv = 0.41 h^{-1}, the value lowered with increasing Sv. The effect of specific velocity of feed on the stripping in one-pass recovery is shown in Figure 6. Though a result that was not in steady state completely was contained, more than 80% of the extents of stripping were obtained and complete stripping was achieved at Sv = 0.41 h^{-1}. From these results of one-pass experiment, it was considered

that the extraction and stripping rates was comparatively low since though equilibrium separations were achieved in the case of low specific velocity, the extents were lowered with increasing the feed rate. Figures 7 and 8 shows the results of a concentrating recovery. In this run, stripping phase was circulated with pH control. The extent of stripping that stabilized after 5 hours was only about 80%, though specific velocity was low as $Sv = 0.41\ h^{-1}$ (Figure 6). However, boron was concentrated well as boron concentration in the circulating stripping phase increased linearly and it in the effluent organic solvent could be kept low (Figure 7).

Extraction Rate of Boron

Because there was the effect of space velocity, initial extraction rate was examined by using a flat interface contactor. The effect of BEPD concentration on the flux of boron extraction is shown in Figure 9. The flux was increased according to the first order against BEPD concentration. The rate of extraction only with EHA was very low and it was improved by addition of BEPD. The extraction rate was low after all, and it was proven from this result that to extract boron effectively was important in this system.

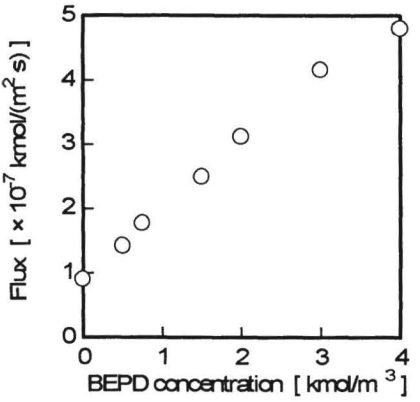


Figure 9. Effect of extractant concentration on extraction rate

NOMENCLATURE

C_{ai}:	inlet concentration of boron in aqueous solution	[kmol/m^3]
C_{oi}:	inlet concentration of boron in organic solvent	[kmol/m^3]
Sv:	specific velocity based on the total working volume of mixer-settler	[h^{-1}]

REFERENCES

1. Poslu Kand Dudeney AWL, *Hydrometallurgy*, **10**, 47, (1983).
2. Kunin R and Preuss AF, *Ind. Eng. Chem. Res. Dev.*, **3**, 304, (1964).
3. Tsuboi I, Kunugita E and Komasawa I, *J. Chem. Eng. Japan*, **23**, 480, (1990).
4. Brown CG and Sanderson BR, *Chem. Ind*, 68, (1980).
5. Matsumoto M, Kondo K, Hirata M, Kokubu S, Hano T and Takada T, *Sep. Sci. Technol.*, **32**, 983, (1997).
6. Ozawa T, *Bunseki Kagaku*, **35**, 709, (1986), (*in Japanese*)
7. Vinogradov EE and Tarasova GN, *Russian J. Inorg. Chem.*, **39**, 1401, (1994).

REACTIVE LIQUID–LIQUID EXTRACTION OF HEAVY METALS FROM LANDFILL LEACHATE

W Mickler, A Reich and E Uhlemann†
Universität Potsdam, Institut für Anorganische Chemie und Didaktik der Chemie, PF 60 15 53, D-14415 Potsdam, Germany

ABSTRACT
Toxic heavy metals can be extracted simultaneously by reactive liquid-liquid extraction from a model landfill leachate.
Commercial alkylphosphoric acids (D2EHPA, D2EHTPA), ß-diketones (LIX 54®) and a novel alkylmethylphosphonic acid (ironex®) were used as extractants and compared with 4-acyl-5-pyrazolones. According to their ligand strength, the presence of complexing agents in the aqueous phase (tartrate, ammonia, cyanide, chloride and humic acid) hinders the extraction.
The composition of the extracted species with the phosphoric acids were found as $ML_2(HL)$ or $ML(HL)_2$ respectively. The ß-diketones form 1:2 complexes.
The influence of the aromatic or chloric solvents on the extraction behaviour is not advantageous in contrast to the non-toxic aliphatic hydrocarbons.
All tested compounds extract the toxic heavy metals quantitatively but only LIX 54 is able to perform the separation from alkaline earth metals.

Keywords: landfill leachate, D2EHPA, D2EHTPA, pyrazolone derivatives, ß-diketones, reactive extraction.

INTRODUCTION

About 2.4 kg of heavy metals are released in Germany per hectare landfill and year by landfill leachate. Their recovery represents an extensive reduction of the environmental pollution.[1] As landfill leachate consists of a multi-component mixture, precipitation connected with the landfill is especially used to its decontamination. In general, hydrometallurgical processes focus on the selective separation of some single components.[2] The advantage of the reactive liquid extraction consists in the possibility of separating selectively the dangerous components from an unproblematic matrix.

Within the large number of potential extractants, alkylphosphoric acids are of crucial importance[3] whereas ß-diketones or 4-acyl-5-pyrazolones respectively play a limited role in spite of their favourable qualities such as co-ordination ability, stability or acidic strength.[4,5,6,7] In contrast to the alkylphosphoric acids these compounds allow additionally the specific and selective extraction of heavy metals.[8,9] The reported experiments will also include studies of the influence of secondary contents of the aqueous phase on the extraction equilibrium.

For comparison, a new extractant, an alkylsubstituted aminomethylphosphone acid (Ironex®, BASF), was used because of its excellent parameters for the iron (III) extraction[10,11].
Generally, the aim of the experiments is the simultaneous separation of heavy metals from a model landfill leachate by reactive liquid-liquid extraction to form an unproblematic matrix.

EXPERIMENTAL

Extraction parameters

The experimental conditions of the liquid-liquid extraction were the following:

$c_{Me}n+$	10^{-5} ... 10^{-4} mol/dm^3 (I= 0.1 mol/dm^3 KNO_3)
c_{HL}	10^{-3} ... 10^{-2} mol/dm^3 (solvent : kerosene), n-octanol as modifier
phase ratio	1+1 (20 cm^3, separation funnels)
temperature	25^0 C
extraction cycle	10 minutes (mechanical shaker)

† deceased

© 2000 Society of Chemical Industry

The pH-adjustment was carried out by adding HNO_3 or NaOH respectively. For the measurements a pH-meter MV 86 (praecitronic, Germany) with glass electrode (Schott, Germany) was used. The metal concentration was determined by AAS (AAS 1100 B, Perkin Elmer) after re-extraction from the organic phase. The metal stock solutions were prepared by dilution of a Merck-standard solution with bidistilled water. All chemicals were of p.a.-quality.

Assuming the general equation:

$$M^{n+}_{(aq)} + n\ HL_{(org)} = ML_{(org)} + n\ H^{+}_{(aq)},$$

$$D = c_M n+_{(org)} / c_M n+_{(aq)}$$

the distribution coefficient (D) was calculated from the metal concentration in the aqueous phase before extraction and from the organic phase after re-extraction with sulphuric acid.

The extraction yield (E/%) can be calculated using the relation R = (D / D+1) 100%. For the extraction constant K_{ex}, the equation: $-\log K_{ex} / n = pH_{0.5} + \log c_{HL}$ is valid.

The distribution coefficient and extraction constant are connected by the relation:

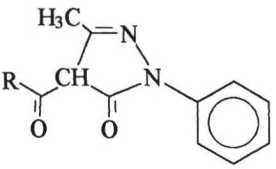
$$\log D = n\ pH + \log K_{ex} + n \log c_{HL}.$$

The slope n of the functions log D = f (pH) and log D = f (c_L) corresponds to the number of coordinated ligands.

Extractants

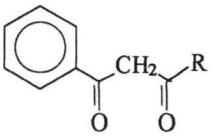
4-Acyl-5-pyrazolones

The syntheses of 1-phenyl-3-methyl-4-(2-ethylhexanoyl)-5-pyrazolone were performed following the method of Jensen[12] by the reaction of 1-phenyl-3-methyl-5-pyrazolone with the corresponding acid chloride. The compounds were purified by distillation in vacuum. Some analytical data have already been published.[13] (R=alkyl)



ß-Diketones

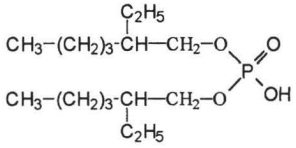
The syntheses were performed following a Claisen condensation of acetophenone with the corresponding phenyl- or ethyl esters in the presence of sodium amide.[14] The compounds were purified by distillation in vacuum. Some of their analytical data are given elsewhere. LIX 54 was purified by distillation. (R= i-octanoyl / alkyl)



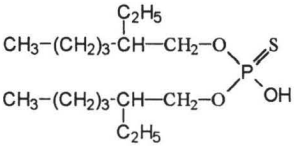
Alkylphosphoric acids

The commercial extractants were used as received (Bayer AG) .

Di-(2-ethylhexyl)-phosphoric acid (D2EHPA)

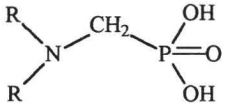


Di-(2-ethylhexyl-monothio)-phosphoric acid (D2EHTPA)



Aminomethylphosphonic acid® (AMPS)

The compound were used as received (BASF) after several washing operations to the neutral state. The syntheses are described.[11]



R= 2-ethylhexyl

RESULTS AND DISCUSSION

The contents of the used model landfill leachate compared with the German legal values are given in table 1.

Element	Concentration in µg/dm³	legal limiting values in µg/dm³
Calcium	100000	--
Magnesium	20000	--
Iron	10000	--
Cadmium	100	100
Lead	1000	500
Chromium	10000	500
Copper	2000	500
Nickel	1000	500
Zinc	10000	2000

Table 1 Typical contents of the (model) landfill leachate (pH: 4.75 - 7.10)

With the help of the function E% = f (t), for the most systems it was found that extraction equilibrium was reached after 5 minutes. Only in the case of Cr(III) the ligand exchange was hindered and the extraction time increased by about 4 times.

The suitability of different solvents for the extraction processes was examined by the function log D= f (pH). Comparably, the best results were obtained for aliphatic hydrocarbons.

Table 2 summarises the results for the extraction of typical contents of landfill leachate with different commercial extractants. It can be seen that the thiophilic soft cations are better separated by the extractant D2EHTPA than by D2EHPA. The results for AMPS could be found in the same region. Generally, the ß-diketones show better separation factors than the phosphoric acids.

	$pH_{0.5}$				lg K_{ex}			
Extractant	Cu	Zn	Cd	Ni	Cu	Zn	Cd	Ni
Di-(2-ethylhexanoyl)-								
-5-pyrazolone	2.05	5.80	8.20	6.70	-0.10	-5.90	-10.4	-7.40
D2EHPA®	5.18	4.80	5.18	5.48	-4.14	-3.39	-4.30	-4.81
D2EHTPA®	3.50	4.95	3.85	5.78	-0.79	-3.67	-0.99	-5.41
LIX 54®	3.90	6.55	*	6.40	-3.80	-7.10	*	-7.86
AMPS®	3.35	6.57	7.25	7.85	-1.35	-3.45	-2.08	-3.38

* Extraction less than 50 %

Table 2 Extraction data of 4-Acyl-5-pyrazolones, ß-Diketones, Alkylphosphoric acid

Figure 1 represents the log D/pH-function of a substituted 4-acyl-5-pyrazolone. In the neutral pH region copper, iron and zinc are extracted quantitatively whereas the alkaline earth metals are not included. Nickel and cadmium are extracted only incompletely and a significant separation of the heavy metals from the alkaline earth metals could not be observed.

In the case of LIX 54 it can be shown that the heavy metals are extracted simultaneously in a good yield whereas the extractability of calcium (6%) and magnesium (23%) is only small. The phase transfer of the cadmium complex with LIX 54 is hindered since it should be realised that the octahedral complex can be co-ordinated with two water molecules. The results of the extraction experiments are put together in figure 3. Especially in the case of AMPS the excellent separation of iron is obvious.

In figure 2, using copper extraction as an example, the loading capacities of different commercial extractants are compared with that of a substituted 4-acyl-5-pyrazolone. Generally, the extractants show similar results, especially LIX 54 permits the extraction of 11.8 g/L.

In the case of the alkylphosphoric acids, the composition of the extracted compounds could be found as $ML(HL)_2$ or $ML_2(HL)$ respectively. The ß diketones form a 1:2 complex.

The influence of some typical contents of an aqueous leaching liquor were tested by the function log D = f (c_{anion}). Corresponding to the increasing complex stability of the anions, the metal extraction is hindered. The sequence cyanide > tartrate > ammonia >chloride was observed. In the case of humic acids that can be regarded as representatives of a metal-soil-interaction, the stability relations are similar to tartrate.

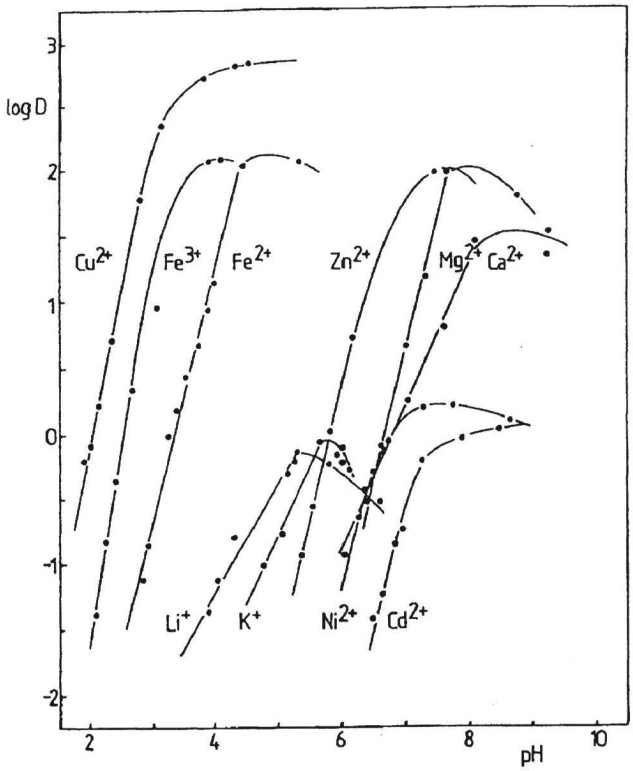


Figure 1 Separation of different metals with 1-phenyl-3-methyl-4-(2-ethylhexanoyl)-5-pyrazolone
log D = f (pH)

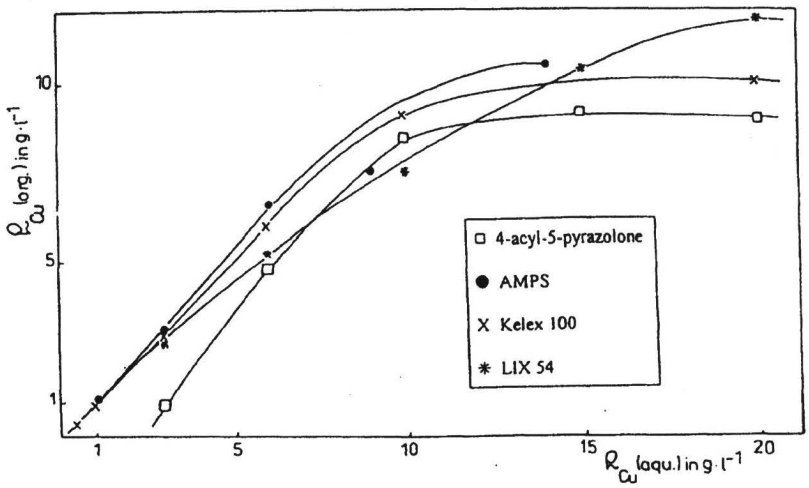


Figure 2 Extraction isotherm of copper with different extractant pH = 4.4 w_{HL} = 10 %

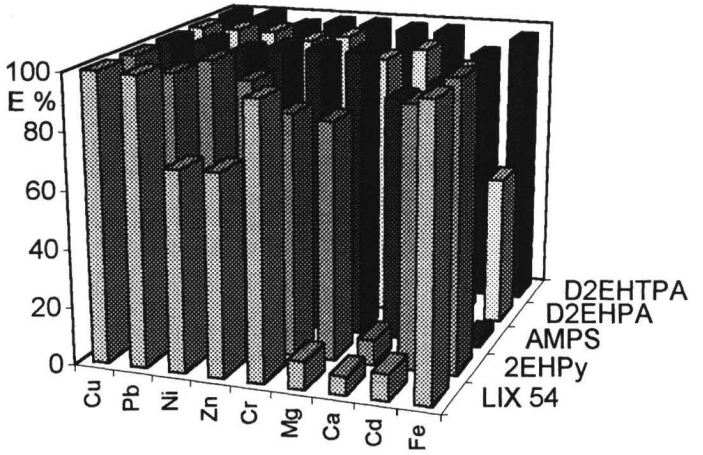


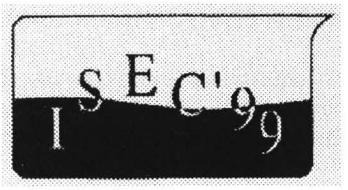
Figure 3 Simultaneous extraction from landfill leachate
pH = 4.9 c_{HL} = 10 % in kerosene

ACKNOWLEDGEMENT

The authors wish to thank the Henkel KGaA, Bayer AG and BASF AG for kindly providing the commercial extractants.

REFERENCES

1. BMFT - report, 02-WA 8721/0, Witten, (1990).
2. *Handbook of Extractive Metallurgy*, ed. Habashi F, Wiley-VCH, Weinheim, (1997).
3. *Value Adding through Solvent Extraction, Proc. ISEC'96,* eds Shallcross DC, Paimin R, Prvcic LM, Melbourne Univ. Press, (1996).
4. Akama Y, Iwadate T, Tong A, Takahashi Y and Tanaka S, J. Chromatogr. A, **789**, 479, (1997).
5. Dukov IL and Jordanov VM, Hydrometallurgy, **48(2)**, 145, (1998).
6. Umetani S, Kawase Y, Le QTH and Matsui M, *Inorg. Chim. Acta*, **267**, 201, (1998).
7. Sigit, Goetz-Grandmont GJ, Brunette JP, *Monats. Chemie*, **129**, 787, (1998).
8. Szymanowski J, *Hydroxyoximes and Copper Hydrometallurgy*, CRC Press, Boca Raton, (1993).
9. Mickler W, Reich A and Uhlemann E, *Value Adding through Solvent Extraction, Proc. ISEC'96,* eds Shallcross DC, Paimin R, Prvcic LM, Melbourne Univ. Press, 415, (1996).
10. Ehle M and Oppenländer K, (BASF) *Ger. Patent, DE 4421932*, (1996).
11. Delmas F, Ehle M, Koch RO, Nogueira C, Oppenländer K, Placenat C, Ujma KH and Weigel V, *Value Adding through Solvent Extraction, Proc. ISEC'96,* eds Shallcross DC, Paimin R, Prvcic LM, Melbourne Univ. Press, 293, (1996).
12. Jensen BS, *Acta Chem. Scand.*, **13**, 1668, (1959).
13. Mickler W, Uhlemann E, *Proc. Inter. Solv. Extract. Conf. ISEC'93*, SCI, London, 1369, (1993).
14. Man, E. H.; Swamer, W.; Hauser, C. R., J. Am. Chem. Soc., **73**, 901, (1951).



A COMPARATIVE STUDY OF THE TREATMENT OF CHROMIUM ELECTROPLATING WASTEWATER USING TWO EXTRACTANTS, ALAMINE 336 AND ALIQUAT 336

YK Peter Sze, Cliff SW Lam, WK Long and JMY Ho
Department of Biology and Chemistry, City University of Hong Kong, Hong Kong, China

ABSTRACT
At a molar ratio of extractant to hexavalent chromium, Cr(VI), of 4 to 1, Aliquat 336 can effectively extract Cr(VI) with a percentage of extraction greater than 90% over a wide pH range (1.5 to 7). Fairly high concentrations of stripping agents, e.g. 0.5 mol/dm^3 NaOH, are required for effective stripping. At the same molar ratio, Alamine 336 can extract more than 90% of Cr(VI) over a much narrower pH range (1.5 to 2.5). Cr(VI) loaded Alamine 336 solutions can be effectively stripped with NaOH at low concentrations, e.g. 0.1 mol/dm^3. The stoichiometries of the Cr(VI) species in the organic solutions in equilibrium with simulated rinse-waters at different pH values are examined.

Keywords: chromium(VI), waste-water treatment, Aliquat 336, Alamine 336

INTRODUCTION

Hexavalent chromium, Cr(VI), is an extremely toxic metal.[1,2] Very stringent discharge standards have been set by environmental authorities to limit its discharge.[3,4] The removal of Cr(VI) from waste-water by solvent extraction has been the subject of extensive studies.[5-11] Some of these studies were aimed at the development of processes for the treatment of Cr(VI)-containing waste-water and the development of mathematical models for the processes.[5-7] Some focused on a more fundamental understanding of the extraction chemistry.[8-11] Recently, we reported the results of treatment of simulated chromium electroplating rinse-water with mixer-settlers using Aliquat 336 as the extractant and NaOH as the stripping agent for Cr(VI) recovery.[12] We were able to reduce the concentration of Cr(VI) in the simulated rinse-water from 130 ppm (2.5 x 10^{-3} mol/dm^3) to a level below detection limit, estimated to be 0.04 ppm, meeting very stringent discharge standards. In this paper, we present more up-to-date results that we have obtained with Aliquat 336. Another extractant, Alamine 336, was included in this study for comparison.

EXPERIMENTAL

The experimental procedures and the chemicals used were essentially the same as those described previously.[12] Briefly, simulated rinse-water was prepared by diluting 1000-fold a simulated chromium plating bath containing 248 g/dm^3 CrO_3 (Reag. ACS, RDH) and 2.5 g/dm^3 H_2SO_4. The Cr(VI) concentration of the simulated rinse-water was 2.5 x 10^{-3} mol/dm^3 with a pH at 2.6. A 2 mol/dm^3 NaOH or 2 mol/dm^3 H_2SO_4 solution was used for pH adjustment for study at other pH values. A solvent containing 0.01 mol/dm^3 Aliquat 336 (Henkel Corporation, Tucson, Arizona, USA) and 5% v/v n-decanol (98%, Aldrich Chemical) in Isopar M (Exxon Chemical International, Hong Kong) was used to extract Cr(VI).[12] In the present study, Alamine 336 (Henkel Corporation) at 0.01 mol/dm^3 in 5% v/v n-decanol and Isopar M was also used. Aqueous solutions were similarly prepared from CrO_3. In addition, a solution prepared from $K_2Cr_2O_7$ (Reag. ACS, RDH) was also used.

RESULTS AND DISCUSSION

The percentages of extraction of chromium by the two solvents at different equilibrium pH values of the aqueous solutions are shown in Figure 1. The results for the Aliquat 336 extractant are in good agreement

© 2000 Society of Chemical Industry

with those reported previously,[12] but in the present study, we have extended the pH range to 1. An increase in Cr(VI) extraction is observed when the pH increases from 1 to 2. The percentage of Cr(VI) extraction remains almost 100% between pH at 2 and 6, and then declines.

The pH dependence of Cr(VI) extraction by Alamine 336 is very much different from that by Aliquat 336 (Figure 1). After the maximum extraction which occurs at an equilibrium pH of 2, Cr(VI) extraction by Alamine 336 decreases rapidly with increasing pH. This decrease can be attributed to a conversion of R_3NH^+(org) to R_3N(org), which cannot extract Cr(VI).

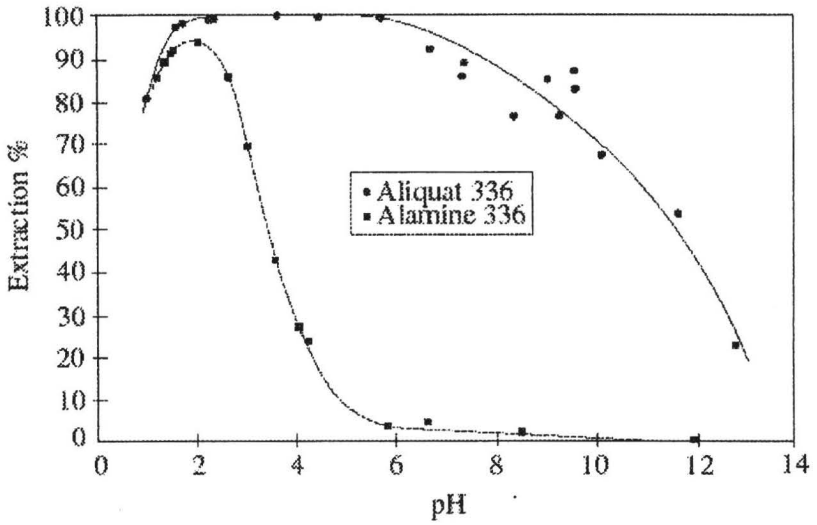


Figure 1. Extraction percentages of Cr(VI) by Aliquat 336 and Alamine 336 solvents as a function of the equilibrium pH of the aqueous phase. The two solvents contained 0.01 mol/dm^3 of Aliquat 336 and Alamine 336, respectively. The initial concentration of Cr(VI) in all aqueous solutions ($[Cr(VI)(aq)]_{init}$) was 2.5 x 10^{-3} mol/dm^3.

The results in Figure 1 suggest that it should be much easier to strip Cr(VI) with alkalis from Alamine 336 solutions than from Aliquat 336 solutions. The results of stripping with NaOH solutions are shown in Figure 2. While NaOH at fairly high concentrations is required for effective stripping of Cr(VI) from the Aliquat 336 solution, NaOH at 0.01 mol/dm^3 can strip almost 90% of the Cr(VI) from the Alamine 336 solution. This property is an advantage for Alamine 336 when considering which extractant to be used for the treatment of Cr(VI)-containing wastewater. An overall consideration will also have to take into account properties such as the degree of Cr(VI) decontamination required for the wastewater, stability towards oxidation in the organic phase, etc.

In aqueous solutions of Cr(VI), the following equilibrium processes occur:[13,14]

$$H_2CrO_4 \equiv H^+ + HCrO_4^- \qquad K_1 = 0.16$$

$$HCrO_4^- \equiv H^+ + CrO_4^{2-} \qquad K_2 = 3.2 \times 10^{-7}$$

$$2HCrO_4^- \equiv Cr_2O_7^{2-} + H_2O \qquad K_3 = 33.0$$

Using the equilibrium constants, K_1, K_2 and K_3, we calculated the concentrations of the species, H_2CrO_4, $HCrO_4^-$, CrO_4^{2-} and $Cr_2O_7^{2-}$, in the aqueous solutions. At the Cr(VI) concentration that we used, 2.5 x 10^{-3} mol/dm^3, the dimer, $Cr_2O_7^{2-}$, was present as a minor species, amounting to less than 12.5% at maximum. The concentration of $HCrO_4^-$ increased with pH up to pH 3.5 at the expense of H_2CrO_4. It then decreased as CrO_4^{2-} gradually increased in concentration and became the predominant species at pH ≥ 7.

In our previous work,[12] we obtained the UV and visible spectra for the organic solutions in equilibrium with the aqueous solutions at different equilibrium pH's from 2 to 12.5 with the initial Cr(VI) concentration being 2.5 x 10^{-3} M for all the aqueous solutions. We found in the pH range between 2 and 4, the spectra were almost identical and as the pH increased between 4 and 9, there was a gradual transition of the spectral contour. Between 9 and 12.5, the spectral contours were unchanged except that the intensity decreased with increasing pH in accord with the decrease in the percentage of extraction. We proposed that there were mainly two extracted species in the organic phase, one prevailing at equilibrium aqueous pH between 2 and 4, and the other prevailing at equilibrium aqueous pH between 9 and 12.5.[12] In the transition between the two pH ranges, the predominance of the species shifted from one to the other.

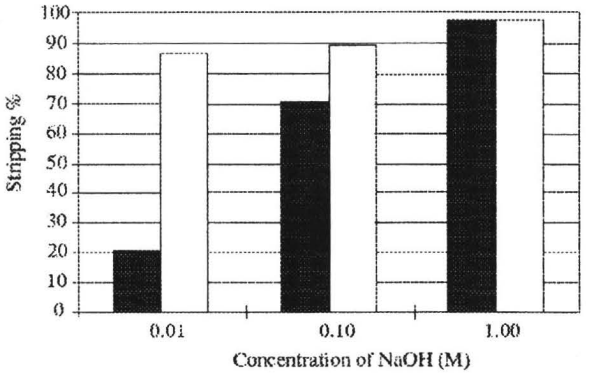


Figure 2. Stripping percentage of Cr(VI) from the Aliquat 336 (black columns) and Alamine 336 (white columns) organic solutions at three concentrations of NaOH. The Aliquat 336 and Alamine 336 organic solutions contained 2.5 x 10^{-3} mol/dm^3 and 2.0 x 10^{-3} mol/dm^3 Cr(VI), respectively, before stripping.

The species in the organic phase in equilibrium with aqueous solution in the pH range of 9 to 12.5 can easily be identified as $(R_3N^+CH_3)_2.CrO_4^{2-}$ because of the close resemblance between the spectra of the organic phase and of aqueous solutions in which CrO_4^{2-} is the only important species (see Figures 3d and 3e). The species in the organic phase in equilibrium with aqueous solutions in the pH range of 2 to 4 was assigned to $R_3N^+CH_3.HCrO_4^-$ in view of the fact that $HCrO_4^-$ is the predominant species in the equilibrium aqueous phase.[12]. This assignment needs a closer examination because of the possibility of a higher degree of dimerization in the organic phase.

There have been several studies on Cr(VI) speciation in organic solutions of tertiary amines or quaternary ammonium salts. Deptula [11] studied Cr(VI) extraction by tri-n-octylamine from sulphuric acid solutions containing up to 10 g l^{-1} (0.19 M) using the dilution and maximum saturation methods, and proposed that the following extraction mechanism took place in dilute sulphuric acid:

$$Cr_2O_7^{2-}(aq) + 2R_3N^+H(org) \rightleftharpoons (R_3N^+H)_2.Cr_2O_7^{2-}(org)$$

The maximum distribution method in the study of Cr(VI) extraction is not conclusive as it is unable to distinguish between the $R_3N^+H.HCrO_4^-$(org) and the $(R_3N^+H)_2.Cr_2O_7^{2-}$(org) species since the extractant to Cr(VI) molar ratio is equal to 1 in both cases. Our own data obtained at equilibrium pH 3 also shows that the ratio of the extractant to Cr(VI) is close to 1 (Figure 4). Huang et al.[10] studied the extraction of Cr(VI) by triisooctylamine in o-xylene from hydrochloric acid solutions containing about 1 g/dm^3 of Cr(VI) (0.019 mol/dm^3). They concluded that $R_3N^+H.HCrO_4^-$ was the dominant form in the organic phase. Lo and Shiue[8] used a concentration of 1 x 10^{-3} mol/dm^3 Cr(VI) in a study of the solvent extraction system of Aliquat 336 dissolved in a mixture of kerosene and xylene. They proposed that $R_3N^+CH_3.HCrO_4^-$ was the major form in

the organic phase. However, their data could almost equally well fit a model in which, the dimer, $(R_3N^+CH_3)_2.Cr_2O_7^{2-}$, was the only extracted species. Yamada and Sekine[9] studied the solvent extraction of Cr(VI) from acidic aqueous nitrate solutions into chloroform by ion-pairing with tetrabutylammonium ions. Their numerical method takes into account both $R_4N^+.HCrO_4^-$(org) and $(R_4N^+)_2.Cr_2O_7^{2-}$(org) in the distribution expression and allows calculation of the apparent dimerization constant defined as follows:

$$K_{dimer,org} = [(R_4N^+)_2.Cr_2O_7^{2-}(org)] / [R_4N^+.HCrO_4^-(org)]^2$$

The value for $K_{dimer,org}$ was found to be $10^{4.7}$, which is about three orders of magnitude larger than that for aqueous solutions. In Yamada and Sekine's system,[9] it can be calculated that at a total concentration of 2.5 x 10^{-3} mol/dm^3 of Cr(VI) in the organic phase, about 94% of the Cr(VI) exists as the dimer.

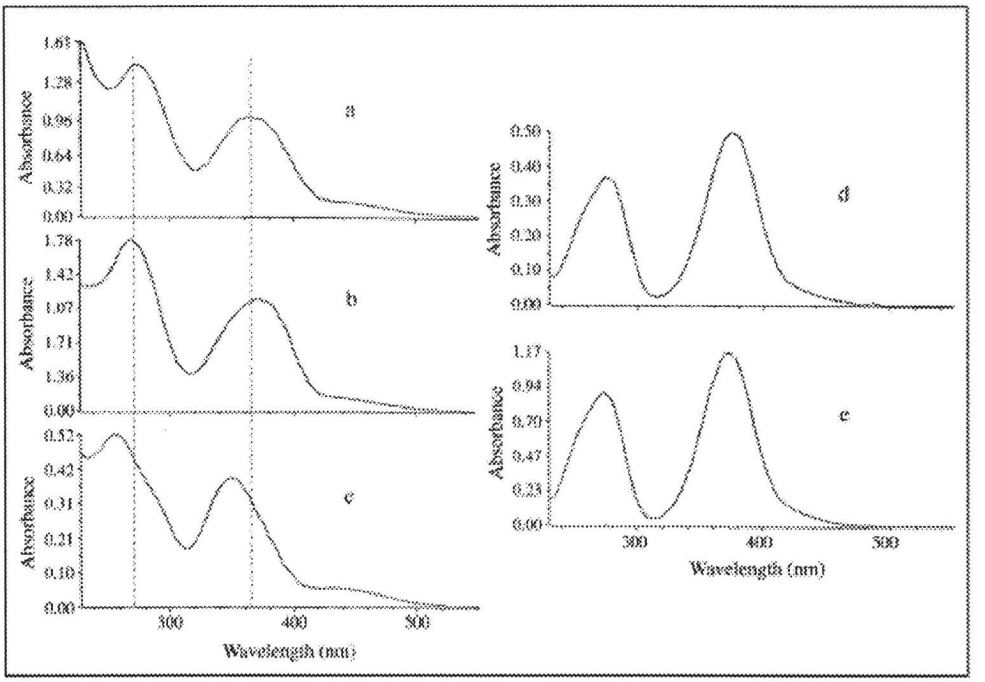


Figure 3. UV-visible spectra of (a) organic solution (0.01 mol/dm^3 Aliquat 336) containing Cr(VI) extracted from an aqueous solution ($[Cr(VI)(aq)]_{init}$ = 2.5 x 10^{-3} mol/dm^3) at equilibrium pH 3; 2 mm pathlength, (b) aqueous solution of 0.65 mol/dm^3 $K_2Cr_2O_7$ at pH 4; Cr(VI) exists mainly as $Cr_2O_7^{2-}$ (86%, calculated) and 14% as $HCrO_4^-$, ca. 0.01 mm pathlength, (c) aqueous solution of 2.5 x 10^{-4} mol/dm^3 Cr(VI) at pH 4; Cr(VI) mainly exists as $HCrO_4^-$ (98%, calculated) and 2% as $Cr_2O_7^{2-}$; 10 mm pathlength, (d) organic solution (0.01 mol/dm^3 Aliquat 336) containing Cr(VI) extracted from an aqueous solution ($[Cr(VI)(aq)]_{init}$ = 2.5 x 10^{-3} mol/dm^3) at equilibrium pH 12; 2 mm pathlength, and (e) aqueous solution of 2.5 x 10^{-4} mol/dm^3 Cr(VI) at pH 12; Cr(VI) exists as 100% CrO_4^{2-}; 10 mm pathlength.

The spectrum of a solution containing 2.5 x 10^{-3} mol/dm^3 Cr(VI) in our Aliquat 336 solution is shown in Figure 3a. This solution was obtained by equilibrating the organic solvent with an aqueous solution of Cr(VI) ($[Cr(VI)_{init}$ = 2.5 x 10^{-3} mol/dm^3) at an equilibrium pH of 3. The spectra of aqueous solutions of Cr(VI) in which the predominant species are $Cr_2O_7^{2-}$ and $HCrO_4^-$, respectively, are shown in Figures 3b and

3c. The close resemblance between Figure 3a and Figure 3b suggests that there should be a significant concentration of the dichromate species, $CH_3N^+R_3)_2.Cr_2O_7^{2-}$, in the organic phase.

The spectra of Cr(VI) extracted into the Alamine 336 solvent at equilibrium pH values of up to 4.3 are similar to the spectrum shown in Figure 3a, with different intensities reflecting the different concentrations of Cr(VI) extracted. The dichromate species, $(R_3NH^+)_2.Cr_2O_7^{2-}$ is again expected to be present in significant concentration in the Alamine 336 organic phase. We were unable to obtain spectra at higher equilibrium pH's (5.8-11.9 studied) because of the low concentrations of Cr(VI) extracted.

The presence of dimeric Cr(VI) species in significant concentration in Alamine 336 and Aliquat 336 solutions is of great interest and deserves further attention.

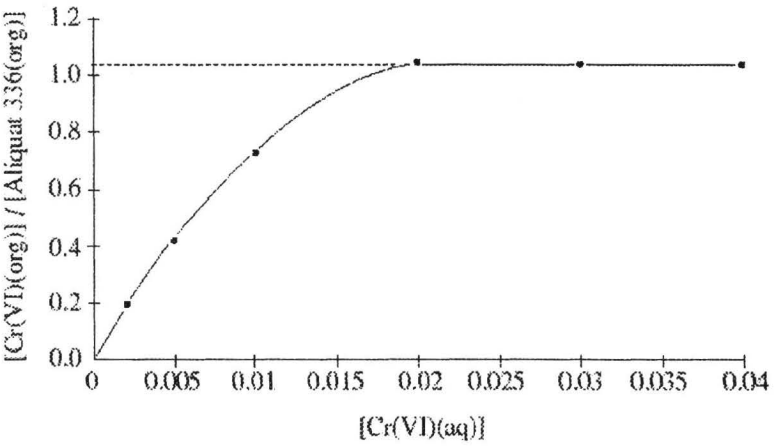


Figure 4. Molar ratio of [Cr(VI)(org)] to [Aliquat 336(org)] as a function of initial [Cr(VI)(aq)]. [Aliquat 336(org)] was 0.010 mol/dm^3 and the equilibrium pH of the aqueous phase was 3.0.

ACKNOWLEDGEMENTS

This work was supported by a Hong Kong RGC (Research Grant Council) Earmarked Grant, which is deeply appreciated. Thanks are also due to Henkel Corporation for supplies of Aliquat 336 and Alamine 336.

REFERENCES

1. Rai D, Eary LE and Zachara JM, *Sci. Total Environ.*, **86**, 15, (1989).
2. von Burg R and Liu D, *J. Appl. Toxicol.*, **13**, 225, (1991).
3. Groshart E, *Metal Finish.*, **86**, 63, (1988).
4. Marvin CG, *Amer. Ceram. Soc. Bull.*, **72**, 66, (1993).
5. Alonso AI and Pantelides CC, *J. Membrane Sci.*, **110**, 151, (1996).
6. Alonso AI, Urtiaga AM, Irabien A and Ortiz MI, *Chem. Eng. Sci.*, **49**, 901, (1994).
7. Fraser BG, Pitzker MG and Legge RL, *Sep. Sci. Technol.*, **29**, 2097, (1994).
8. Lo SL and Shiue SF, *Wat. Res.*, **32**, 174, (1998).
9. Yamada Y and Sekine T, *Solvent Extr. Res. Dev, Jpn.*, **3**, 99, (1996).
10 Huang YH, Chen CY and Kuo JF, *Hydrometallurgy*. **28**, 297, (1992).
11. Deptula C, *J. Inorg. Nucl. Chem.*, **30**, 1309, (1968).
12. Sze YKP and Lam CSW, *Environ. Technol.*, **18**, 987, (1997).
13. Sengupta A, Subramonian S and Clifford D, *J. Environ. Eng.*, **114**, 137, (1988).
14. Vinter E, in *Standards in Absorption Spectrometry*, Chapman and Hall, London, pp. 48, (1981).



Extractants and Diluents

TAILOR-MADE AROMATIC CAGE COMPOUNDS AS TOOLS FOR SELECTIVE SOLVENT EXTRACTION OF METAL IONS

K Gloe, C Chartroux, T Rambusch[1], F Ahuis, S Ibach and F Vögtle[2]

[1]Institut für Anorganische Chemie. Technische Universität Dresden, D-01062 Dresden, Germany.

[2]Kekulé-Institut für Organische Chemie und Biochemie. Universität Bonn, D-53121 Bonn, Germany.

ABSTRACT

Differently functionalized aromatic cage compounds were synthesized and investigated in view of their extraction properties toward metal ions. The compounds show a pronounced selectivity for Ag(I) over various hard and soft metal ions. The extraction efficiency of Ag(I) strongly depends on the extractant structure and is controlled by different coordination patterns. Molecular modeling calculations of the complex structures allow the interpretation of the experimental results.

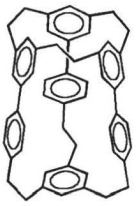
Keywords: cage compounds, silver, molecular modeling.

INTRODUCTION

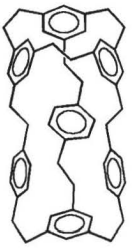
Selective binding and effective removal of metal ions from solution by solvent extraction require a perfect conformity between metal and extractant combined with a high lipophilicity of the formed complex. Supramolecular chemistry offers interesting possibilities [1] in designing tailor-made molecular architectures with different nature, arrangement and number of donor sites and thus, in controlling metal extraction selectivity. In this connection, a cage-like framework with aromatic coordination centers linked by functionalized spacer units represents an interesting concept [2].



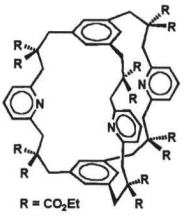
1



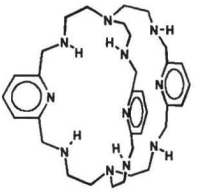
2



3



4



5

The aim of this work is the design of selective extractants, especially for silver. For this purpose, the novel aromatic cage compounds **2-5**, which differ in shape, size and donor functionalities, have been synthesized.[3] The extraction behavior of these compounds was investigated in the system metal salt-picric acid-H_2O/ligand-$CHCl_3$ or CH_2Cl_2. For comparison, the [2.2.2]paracyclophane **1**, which forms stable 1:1 complexes with Ag(I), [4] was also tested in the extraction experiments. The results obtained are interpreted on the basis of molecular modeling calculations for the ligands and their silver complexes.

© 2000 Society of Chemical Industry

EXPERIMENTAL

Liquid-liquid extraction

The extraction experiments were performed in micro reaction tubes (2 cm^3) at 25 ± 1°C by means of mechanical shaking. The phase ratio $V_{(aq)}:V_{(org)}$ was 1:1 (0.5 cm^3 of each phase). A shaking time of 30 minutes was sufficient to achieve equilibrium. After extraction the phases were separated and centrifuged. The metal concentrations in both phases were determined by γ-radiation measurement of the radioisotopes ^{22}Na, ^{60}Co, ^{64}Cu, ^{65}Zn, ^{109}Pd, ^{110m}Ag, ^{203}Hg with a NaI(Tl)scintillation counter (Cobra II; Canberra-Packard) and β-radiation measurement of the radioisotopes ^{45}Ca, ^{204}Tl with a liquid scintillation counter (Tricarb 2500; Canberra-Packard). The radioisotopes were supplied by Medgenix Diagnostics GmbH (Ratingen, Germany).

The stoichiometries of the extracted species were determined by multiple regression analysis of the experimental data with a modified Marquardt procedure[5] on the basis of the following extraction equilibrium:

$$M^{n+}_{(aq)} + n\,Pic^-_{(aq)} + s\,L_{(org)} \Leftrightarrow ML_s(Pic)_{n\,(org)}$$

Molecular modeling

The molecular modeling studies have been performed at a semi-empirical level using PM3 (extractants) and ZINDO/1 (Ag(I) complexes). The molecules under study were completely geometry optimized until a gradient norm less than 0.001 $kcal \cdot mol^{-1} \cdot Å^{-1}$. All calculations were done on a Pentium II/400 MHz computer. HyperChem 5.02 (Hypercube) and CERIUS[2] 1.6.2 (Molecular Simulations Inc.) were used for computer graphics and the initial building of the molecular models. The usefulness of the methods was proven by calculation of different ligand and complex structures and comparison with the related X-ray structures [6].

RESULTS AND DISCUSSION

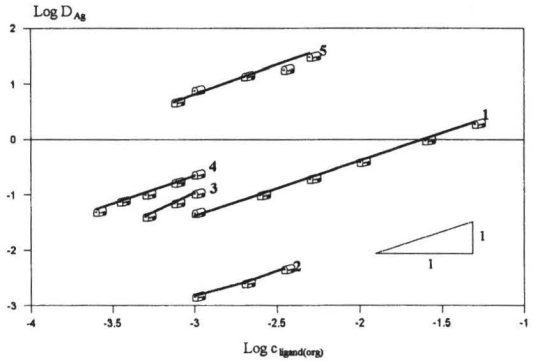
The extraction behavior of the extractants **1-5** toward various metal ions has been investigated under comparable experimental conditions. The results are summarized for Ag(I), Tl(I), Co(II) and Hg(II) in Table 1. The metal ions Na(I), Ca(II), Cu(I), Cu(II), Zn(II) and Pd(II) are not extracted; the D_M values are always lower than 10^{-3}. As it is shown in Table 1, the extraction efficiency for Ag(I) very strongly depends on the ligand structure. For example, **2** gives a very low silver extractability, indicating only weak metal-ligand interactions. The distribution ratio is more than one order of magnitude lower than with the simple [2.2.2]paracyclophane **1**. In contrast to this, compound **3**, which differs from **2** only by the two central aromatic bridges (**2**: biphenyl; **3**: diphenyl ethane), shows a significant improvement of silver extraction and provides some support for the idea of using weak silver-π interactions to control the extraction selectivity.

As expected, **4** and especially **5** lead to improved extractability for silver, obviously caused by the introduction of the strongly complexing pyridine units into the molecule [7]. In addition to the pyridine functions, **5** possesses a tris(2-aminoethyl)amine unit on the top and on the bottom of the molecule. This unit is well known as the complexing agent "tren" for transition metal ions [8]. In spite of this, the silver selectivity over Tl(I), Hg(II), Zn(II) and Cu(II) is surprisingly high. Furthermore, in the case of **5**, a pronounced extraction of Co(II) over Hg(II), Zn(II) and Cu(II) was observed. This result is contrary to the stability order of metal binding by "tren" [9] and points to a sharp change of complexation behavior going from the simple chelate to the cage compound. One disadvantage of this compound is the protonation of amine nitrogen at pH < 5 and the accompanying change of solubility properties.

Table 1. Distribution ratios for Tl^{I}, Ag^{I}, Co^{II}, Hg^{II} with extractants **1-5**

	D_{Tl}	D_{Ag}	D_{Co}	D_{Hg}
1	$< 10^{-3}$	$4.2 \cdot 10^{-2}$	/	$< 10^{-3}$
2	$< 10^{-3}$	$4.0 \cdot 10^{-3}$	/	$< 10^{-3}$
3	$8 \cdot 10^{-3}$	$1.1 \cdot 10^{-1}$	/	$5.0 \cdot 10^{-2}$
4	$< 10^{-3}$	$2.4 \cdot 10^{-1}$	/	$< 10^{-3}$
5	$< 10^{-3}$	19	$1.1 \cdot 10^{-1}$	$< 10^{-3}$

1-4: $[MeCl_n]$ or $[Me(NO_3)_n] = 1 \cdot 10^{-4}$ mol/dm^3; [picric acid] = $1 \cdot 10^{-2}$ mol/dm^3; [ligand] = $1 \cdot 10^{-3}$ mol/dm^3 in $CHCl_3$.
5: $[MeCl_n]$ or $[Me(NO_3)_n] = 1 \cdot 10^{-4}$ mol/dm^3; $[KNO_3] = 1 \cdot 10^{-2}$ mol/dm^3 pH = 6 (MES/NaOH-buffer); [ligand] = $1 \cdot 10^{-3}$ mol/dm^3 in CH_2Cl_2.



1-4:$[AgNO_3] = 1 \cdot 10^{-4}$ mol/dm^3; [picric acid] = $1 \cdot 10^{-2}$ mol/dm^3; [ligand] = $5 \cdot 10^{-4}$ ... $1 \cdot 10^{-2}$ mol/dm^3 in $CHCl_3$.
5: $[AgNO_3] = 1 \cdot 10^{-4}$ mol/dm^3; $[KNO_3] = 1 \cdot 10^{-2}$ mol/dm^3; pH = 6 (MES/NaOH-buffer); [**5**] = $5 \cdot 10^{-4}$ ... $5 \cdot 10^{-3}$ mol/dm^3 in CH_2Cl_2.

Figure 1. Extraction of Ag(I) with **1-5** at varying ligand concentrations

Extraction experiments for silver(I) at varying ligand concentrations shown in Figure 1 demonstrate that in all cases, 1:1 complexes $[AgL]^+$ predominate in organic solution. Semiempirical molecular modeling calculations for the ligand-silver interactions in the extracted 1:1 complexes allow the interpretation of the extraction results. Generally, the results point to a clear improvement of the Ag(I) coordination by the ligands in going from extractant **2** to **5**. In the first structure $[Ag \cdot \mathbf{2}]^+$ (Figure 2), the silver ion is fixed outside the cavity and coordinates at the molecule surface only with one π-arene system. The Ag ... π-arene distance (2.95 Å) is relatively long compared with the [2.2.2]paracyclophane **1** (2.55 – 2.67 Å)[4]. In the case of the hydrocarbon **3**, in contrast, the silver ion is enclosed within the cavity (Figure 2), and as for the [2.2.2]paracyclophane complex, silver interactions with three π-systems are possible. The Ag ... π-arene distances are shorter (2.60 – 2.68 Å) than for **2** and similar to **1**. This result supports the observed increase in the silver extractability in comparison with compound **2**.

Molecular modeling studies were also performed to estimate the activation energies [10] for the complexation and decomplexation processes of Ag(I) with the compounds **2** and **3**. Significant differences were found, which support the experimental finding. As expected from the extraction results, the energy barrier for **3** is much lower (12.1 kcal/mol) than that for **2**. Compound **3** possesses a larger entrance on its surface, which facilitates the transfer of the silver ion into the cavity. The binding of the silver ion inside the cavity of **3** leads to a gain in stabilization of about 7 kcal/mol versus **2**.

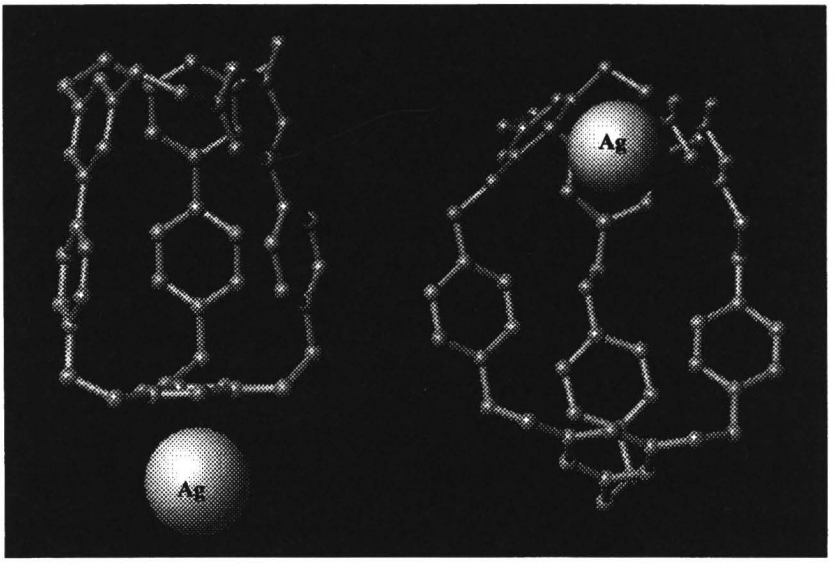


Figure 2. Calculated structures of $[Ag{\cdot}\mathbf{2}]^+$ (left) and $[Ag{\cdot}\mathbf{3}]^+$ (right).

The calculated structure of $[Ag{\cdot}\mathbf{4}]^+$ (Figure 3) shows that, in analogy to **3**, the silver cation is included within the cavity. In this case, the silver ion can interact with the lone electron pairs of two pyridine nitrogen atoms. An interaction with the third nitrogen atom is not possible for sterical reasons, caused by the rigid bridging aromatic rings at the top of the molecule. Therefore Ag(I) adopts a favorable linear arrangement between two pyridine units (Ag ... N(1), N(2) 2.51 Å; Ag ... N(3) 7.09 Å). Because the binding Ag ... N-pyridine is stronger than a cation-π interaction, an enhancement of silver extraction results.

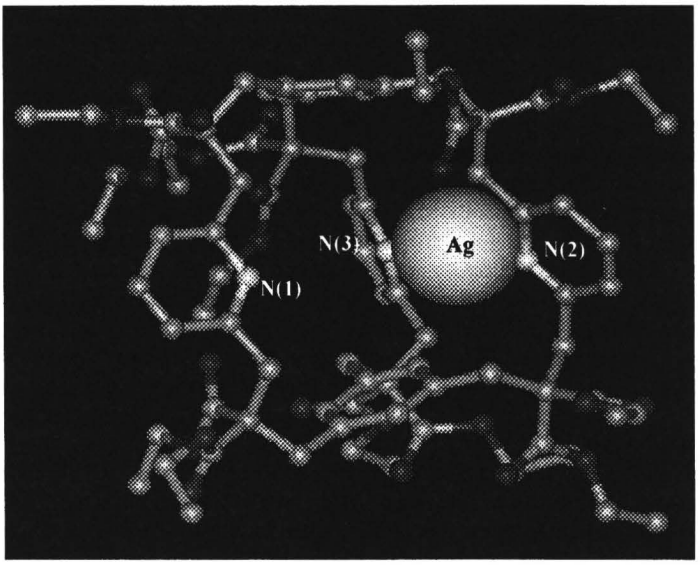


Figure 3. Calculated structure of $[Ag{\cdot}\mathbf{4}]^+$

The calculated structure of $[Ag\cdot\mathbf{5}]^+$ (Figure 4) shows that all three pyridine nitrogen atoms bind the silver ion in the cavity. As a result of the significant flexibility of **5**, the pyridine units can turn (from the free ligand to the complex) toward the central cavity of the molecule and interact with Ag(I) (Ag ... N(1), N(2) 2.50 Å; Ag ... N(3) 2.51 Å) . The consequence of this observation with respect to solvent extraction is that **5** yields the highest extractability for silver obtained during these studies.

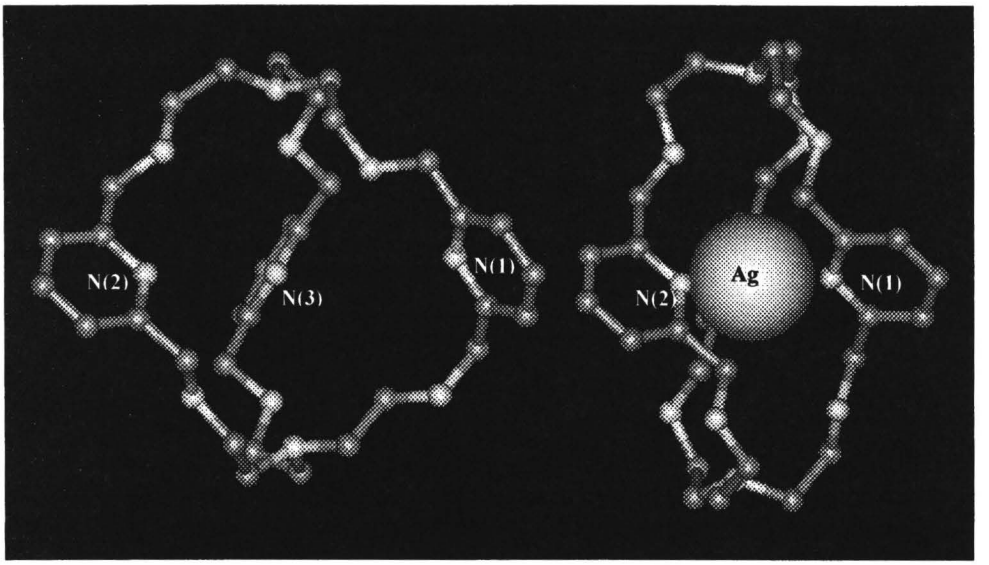


Figure 4. Calculated structures of ligand **5** and its $[Ag\cdot\mathbf{5}]^+$ complex

In contrast to the silver complex structure, preliminary calculations of the Co(II) complex with **5** give some evidence for the metal arrangement near one "tren" group inside the molecule. Therefore the manipulation of "tren" by introduction in the rigid cavity of **5** should be the reason for the observed binding changes in comparison with the free chelate ligand [8,9].

CONCLUSIONS

Extractants with a preorganized spherical architecture based on aromatic subunits are appropriate to assure the selective transfer of silver ions from an aqueous into an organic phase. Shape, size, flexibility of the ligands, type and number of donor sites play an important role in selectivity control. It has been shown that cation-π interactions can provide an useful basis for the design of selective extractants for silver. Remarkable selectivity, together with a high extractability, have been obtained using cage ligands with pyridine subunits. Molecular modeling calculations of ligand and complex structures have been shown to give important information for the understanding and the interpretation of the host-guest interactions in these systems.

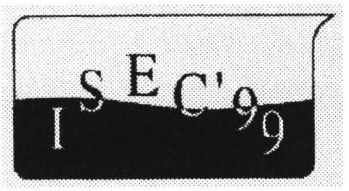
ACKNOWLEDGEMENTS

We thank the Deutsche Forschungsgemeinschaft for support of this work.

REFERENCES

1. Moyer BA, in *Comprehensive Supramolecular Chemistry*, J. L. Atwood, J. E. Davies, D. D. MacNicol, F. Vögtle, Eds., Pergamon, Oxford, **1**, 377, (1996).
2. Seel C and Vögtle F, in *Perspectives in Coordination Chemistry*, A. F. Williams, C. Floriani, A. E. Merbach, Eds., VCH, Weinheim, 31, (1992).

3. Gross J, Harder G, Siepen A, Harren J, Vögtle F, Stephan H, Gloe K, Ahlers B, Cammann K, Rissanen K, *Chem. Eur. J.* **2**, 1585, (1996); Vögtle F, Ibach S, Nieger M, Chartroux C, Krüger T, Stephan H, Gloe K, *Chem. Commun.*, 1809, (1997); Jazwinski V, Lehn JM, Lilienbaum D, Ziessel R, Guilhem J, Pascard C, *J. Chem. Soc., Chem. Commun.* **1987**, 1691.
4. Cohen-Addad C, Baret P and Chautemps P, J.-L. Pierre, *Acta Crystallogr.* **C 39**, 1346, (1983).
5. Petrich M, Beyer L, Gloe K, Mühl P, *Anal. Chim. Acta*, **228**, 229, (1990).
6. Krüger T, Gloe K, Habermann B, Mühlstädt M and Hollmann K, *Z. anorg. allg. Chem.*, **623**, 340, (1997); Gloe K, Krüger T, Stephan H, Wagner M, Drutkowski U, Olk R-M, Leckelt U, Richter R and Hoyer E, *Z. anorg. allg. Chem.*, **624**, 152, (1998)
7. Stephan H, Krüger T, Gloe K, Hasse W, Ahlers B, Cammann K, Rissanen K, Brodesser G and Vögtle F, *Chem. Eur. J.* **4**, 430, (1998).
8. Prue JE and Schwarzenbach G, *Helv. Chim. Acta*, **33**, 963, (1950)
9. Anderegg G and Wenk F, *Helv. Chim. Acta* **54**, 216, (1971).
10. Sheu C and Houk KN, *J. Am. Chem. Soc.* **118**, 8056, (1996)



SOLVENT EXTRACTION SEPARATION OF SOME TRANSITION ELEMENTS WITH HEXAACETATO-CALIX(6)ARENE

DD Malkhede, PM Dhadke and SM Khopkar[1]
Department of Chemical Technology, University of Mumbai, Mumbai, 400 019, India.
[1]Department of Chemistry, Indian Institute of Technology, Bombay-400 076, India

ABSTRACT
Solvent extraction separation of thorium (IV), chromium (III), manganese (II), bismuth (III) and lead(II) was carried out with $1x\ 10^{-4}$ mol/dm^3 of hexaacetato-calix(6)arene in toluene at pH 6.0 – 7.5 The elements from the organic phase were stripped with 2 – 4 mol/dm^3 of mineral acid excepting thorium which was stripped with 0.05 mol/dm^3 nitric acid. Elements from the aqueous phase were determined spectrophotometrically with suitable chromogenic ligands. They were separated from several multicomponent mixtures. The methods were extended for analysis of these elements from the real samples.

Keywords: thorium, chromium(III), manganese, bismuth, lead, calixarene, analysis

INTRODUCTION

The supramolecular compounds are promising extractants for transition and main group metals. They have flexible structures with the possibility of enlarging annular space by synthesizing higher homologues. Their selectivity can be enhanced by the effective substitution of the upper or lower rim with hydrophillic substituents like acetate. These compounds are relatively inexpensive. They can be easily synthesized by the base catalysed reaction of tertiary butyl phenol and formaldehyde.[1] The substitution of hydroxyl group by acetyl group leads to formation of hexaacetato-calix(n)arene. This ligand has proved to be promising extractant for cobalt,[2] palladium[3] and iron.[4] By extending these studies it was observed that thorium, chromium, manganese, bismuth and lead could also be quantitatively extracted. The hydroxamic acid derivative of this ligand was used for extractions of chromium[5] and manganese[6] while the sulphonyl carbamide[7] derivative was used for extraction of lead. This paper presents a systematic investigation of the solvent extraction of some transition elements with hexaacetato-calix(6)arene.

EXPERIMENTAL

Apparatus and reagent

A Jasco V-530 UV-visible spectrophotometer with matched quartz cuvettes and a digital pH meter with combined electrode assembly were used in these studies.

The hexaacetato-calix(6)arene was synthesised by the base catalysed reaction of p-t-butyl phenol and formaldehyde and acetylated by usual procedure.[1, 2] The compound was purified and characterised by various spectral methods.[2] A solution of $1x10^{-4}$ mol/dm^3 reagent concentration in toluene was used for the extractions. Solutions of thorium, chromium, manganese, bismuth and lead were prepared and standardised colorimetrically with suitable chromogenic ligands such as Thoron (0.1% aq)(thorium), Xylenol orange (10^{-3} mol/dm^3)(chromium), periodate (0.4%)(manganese), 4-2-(pyridylazo) resorcinol (0.1 %)(lead) and thiourea(12%)(bismuth).

General procedure

An aliquot of solution containing about 3–10 μg/cm^3 of the element (thorium/chromium/ manganese/bismuth/lead) was taken. The pH of the solution was adjusted to between pH 6.0 -7 by the addition of dilute mineral acid.(with the exception of bismuth). The resulting solution was transferred to a separating funnel. Then 10 cm^3 of $1x10^{-4}$ mol/dm^3 hexaacetato-calix(6)arene in toluene was added to it. The solution was then vigorously shaken for 2-3 minutes. The two phases were allowed to settle and separate. The metals were stripped from the organic phase with suitable mineral acid and

© 2000 Society of Chemical Industry

was determined spectrophotometrically with the appropriate chromogenic ligand. The amount of metal was calculated from the calibration curve.

RESULTS AND DISCUSSION

Effect of pH

The extraction was carried out in the pH range of 1.0 – 7.5 (figure 2). Quantitative extraction for thorium was possible at pH 7.5, chromium at pH 6.0, manganese at pH 5.7 – 6.7, lead at pH 6.0 and bismuth in 0.1M hydrochloric acid. The extraction usually commenced at pH 1.0 increased to >60% at pH 3.0, was quantitative between pH 6.0 – 7.5 and declined above pH 8.0. The extraction occurred by bond formation through acetyl group. The extractant was stable in aqueous acidic medium and it was possible to use the same organic phase after metal stripping several times to obtain the same extraction performance.

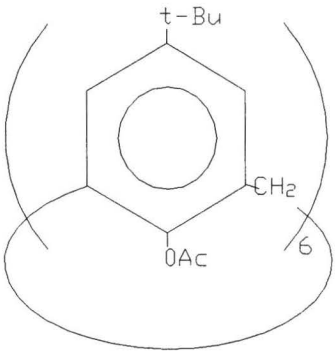


Figure 1

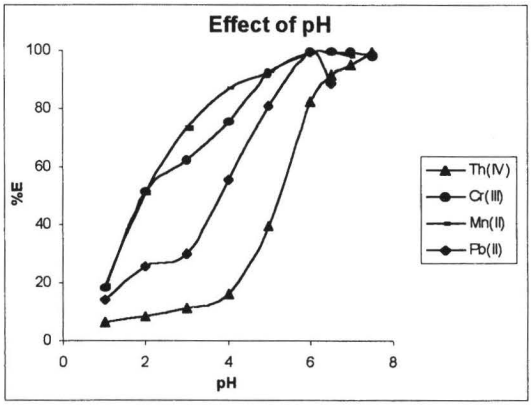


Figure 2

Effect of reagent concentration

The reagent concentration was varied from $1x10^{-4}$ to $1x10^{-6}$ mol/dm^3 with the optimum reagent concentration being $1x10^{-4}$ M for all metals. Extraction of the metals commenced at 0.75×10^{-4} mol/dm^3 increased to >75% with $1x10^{-4}$ mol/dm^3 reagent and was quantitative at 5×10^{-4} mol/dm^3 of hexaaceto-calixarene. The use of higher reagent concentration did not improve the extent of extraction.

Effect of diluent

Various non-polar and polar solvents e.g. benzene, toluene, xylene, hexane, carbon tetrachloride, chloroform, dichloromethane and dichloroethane were tested as diluents. Toluene proved to be best for thorium, chromium and bismuth, while for manganese hexane was best and for lead xylene was ideal. All extractions were however carried with a common diluent namely toluene as it was less toxic and offered clear-cut phase separations.

Effect of stripping agent

Mineral acids like hydrochloric, nitric sulphuric, perchloric and acetic acids were studied as stripping agents in the concentration range of 0.01 – 4.0 mol/dm^3. In all the cases quantitative stripping was observed for the acids listed in Table1.

Nature of extracted species

The composition of the extracted species for each metal was ascertained by plotting graph of log distribution ratio against log reagent concentration
at fixed pH of quantitative extraction. The corresponding slopes for the elements are given: thorium(3.73), chromium(2.74), manganese(2.3), lead(1.8), bismuth(2.87). Hence thorium was

extracted in the ratio of 1:4 for metal to ligand, chromium and bismuth were extracted in a ratio of 1:3 and manganese and lead were extracted in ratio of metal to ligand of 1:2.

Table 1 Quantitative stripping with various acids.(molar concentrations)

Metals	HCl	HNO_3	H_2SO_4	$HClO_4$	CH_3COOH
Th	0.05	0.05	-	-	0.5
Cr	4.0	-	2.0	3.0	-
Mn	3.0	3.0	2.0	-	-
Bi	2.0	2.0	2.0	-	4.0
Pb	4.0	4.0	0.1	-	-

Extraction time

The period of equilibration was varied from 2 – 10 minutes. It was observed that quantitative extraction was possible within an equilibration time of 3 minutes.

Separation from binary mixtures

All these metals were extracted under the optimum conditions of extraction in the presence of various diverse ions. The tolerance limit was calculated as the error of $\pm$1.2% in recovery of the metal. Transition metals were tolerated at a ratio of 1:15 while main group elements were tolerated at a ratio of 1:10 but anions were tolerated at a higher ratio of 1:20. It was significant that alkali and alkaline earths were tolerated in the ratio of 1:25

Table 2 : Separation from multicomponent mixtures.

No.	Metal	Conc. $\mu g/cm^3$	pH	Stripping Agents (mol/dm^3)	Recovery(%)
1	Cr (III)	3	7.0	4.0 HCl	99.3
	Th(IV)	5	7.5	0.005 H_2SO_4	98.6
	Fe(III)	10	7.0	1.0 HCl	99.7
2	Th(IV)	5	7.5	0.005 H_2SO_4	98.6
	Co(II)	3	7.5	1.5 NH_4SCN	99.9
	Cr(III)	3	6.0	4.0 HCl	99.5
	Pb(II)	5	6.0	4.0 HNO_3	99.5
3	Th(IV)	5	7.5	0.005 H_2SO_4	98.6
	Pb(II)	3	6.0	4 HCl	98.5
	Fe(III)	4	7.0	1 HCl	99.7
4	Th(IV)	5	7.5	0.005 H_2SO_4	98.6
	Mn(II)	10	6.0	0.1 CH_3COOH	96.4
	Cr(III)	5	6.0	4.0 HCl	99.5
	Fe(III)	4	7.0	1.0 HNO_3	99.0
5	Th(IV)	5	7.5	0.005 H_2SO_4	98.6
	Tl (III)	5	3.0	2M $HClO_4$	99.5
	Bi(III)	10	1.0	2 M HNO_3	99.6

Separation from multicomponent mixtures

The metals were separated from multicomponent mixtures containing 3-4 elements. A representative separation is illustrated from Table 2 for each metal in tertiary mixtures of chromium, thorium and iron, chromium was stripped with 4mol/dm^3 hydrochloric acid, thorium with 0.005 mol/dm^3 sulphuric acid and iron with 1mol/dm^3 hydrochloric acid.

In a quaternary mixture of thorium, cobalt, chromium and lead, thorium was stripped with dilute sulphuric acid, cobalt with 1.5 mol/dm^3 amonium thiocyanate, chromium with 4mol/dm^3 hydrochloric acid and lead with 4 mol/dm^3 nitric acid.

In another quaternary mixture of thorium, manganese, chromium, iron, thorium was stripped with dilute sulphuric acid, manganese with 0.1 mol/dm^3 acetic acid, chromium with 4 mol/dm^3 hydrochloric and iron with 1 mol/dm^3 nitric acid. Using the same methodology separations of other mixtures were carried out.

Application to real samples

The proposed method was extended for analysis of chromium and manganese from steel sample and analysis of bismuth and lead from pharmaceutical samples.

Advantages of calixarene as an extractant

There are several methods for extraction of these metals however their separation with hexaacetato-calix(6)arene had several advantages. It is possible to substitute the lower or upper rim of the calixarene to suit complexation. The cavity for intercalation can also be modified by using higher homologues to accommodate any metal with varying coordination number. Calixarenes have adequate flexibility to suit the stereochemistry of a particular metal. The substitution of the litigating group can improve its solubility in solvents and provide better selectivity. Non-centrosymmetric structures are attractive for complexation.

The proposed methods are simple, rapid, selective and reproducible. The total time required for separation and determination is less than 30 minutes. The relative standard deviation is $\pm$1.2% with as little as 3.5 μg of metal can be analysed by the proposed method.

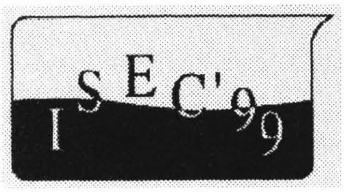
The method also permits separation of elements from matrix containing commonly associated metals. The proposed methods are applicable for these metals from real samples.

ACKNOWLEDGEMENT

Thanks are due to Dept. of Science and Technology, Govt. of India for sponsoring this project and to the Director UDCT Bombay for providing all laboratory facilities.

REFERENCES

1. Gutsche CD, Calixarenes, Monographs on Supramolecular Chemistry, Royal Society of Chemistry, (1989).
2. Gupta A, Khopkar SM, *Talanta*, **42**, 1493, (1995).
3. Mathew VJ, Khopkar SM, *Talanta*, **45**, 1699, (1997).
4. Khandwe RM, Khopkar SM, *Talanta*, **46**, 521, (1998).
5. Deligoz H, Yilmaz M, *Solvent Extr. Ion. Exch.*, **13**, 19, (1995).
6. Subramanian S, Zawrotkar MJ, *J. Am. Chem. Soc.*, **29**, 8719, (1992).
7. Talanova GG, Hawana HS, Talanova S, Bartch RA, *J. Chem. Soc. Chem.Commun*, 419, (1998).



LANTHANIDE AND ACTINIDE EXTRACTION WITH CALIX[4]- AND CALIX[6]ARENES BEARING AMIDE GROUPS

Nguyen TK Dunga[1], Kenji Kunogi[2] and Rainer Ludwig
FU Berlin, Institute fur Inorganic and Analytical Chemistry, Fabeckstr. 34-36, 14195 Berlin, Germany
[1]visitor from: VINATOM, Centre for Analytic Chemistry and Environment, 59. Ly Thuong Kiet, Hanoi, Vietnam.
[2]Saga University, Dept. of Chemistry, 1-Honjo machi, Saga 840, Japan

ABSTRACT
The solvent extraction of trivalent Am, Nd, Eu, Tb, Dy, Er and Yb by newly synthesized macrocyclic compounds was investigated. The compounds are calix[n]arenes (n=4, 6) substituted with carboxylic acid and amide groups, differing in cavity size and arrangement of the ligating groups. The influence of the molecular structure on the extractability and selectivity towards f-element ions is discussed in terms of extraction constants.

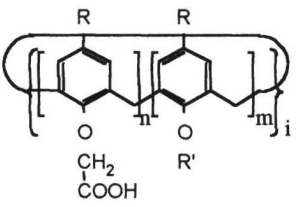
Keywords: lanthanides, actinides, macrocyclic compounds, calixarenes

INTRODUCTION

Macrocyclic extractants, which offer the possibility to selectively recognize metal ions, are of interest for improving separation processes. Calixarenes[1] of different ring size combine a cyclophane backbone with hydrophobic as well as ionophilic groups and allow the selective inclusion[2] and extraction[3] of ions, ranging from alkaline and alkaline earth to heavy metal ions.

In this work, we report on extractability, extraction equilibria and extraction constants of lanthanide and actinide ions, which were subjected to solvent extraction by the ligands according to Scheme 1. The ligands differ in the number and position of carboxylic acid and amide groups. Cooperative binding of the acid and amide groups in calix[6]arenes was observed in the extraction of Am^{3+}.[4,5] The extractability of metal ions with high coordination numbers (Ln^{3+}) by calix[4]arenes is significantly lower than the extractability of metal ions with low coordination numbers such as Au^{3+} and Pd^{2+}.[6,7] The results of loading tests are reported. The calculated extraction constants are compared with reference systems.

L	R	R'	n	m	i
1	*t*-bu	$-CH_2-C(O)-NH(n-C_4H_9)$	3	1	1
2	*t*-oct	$-CH_2-C(O)-N(i-C_4H_9)_2$	3	1	1
3	*t*-bu	$-CH_3$	5	1	1
4	*t*-bu	$-CH_2-C(O)-N(C_2H_5)_2$	3	3	1
5	*t*-bu	$--CH_3$	3	3	1
6	*t*-oct	$-CH_2-C(O)-N(C_2H_5)_2$	1	1	3
7	*t*-bu	$-CH_2-COOH$	1	1	3
8	*t*-oct	$-CH_2-COOH$	1	1	3



Scheme 1: Investigated ligands

© 2000 Society of Chemical Industry

EXPERIMENTAL

Materials

The parent calix[n]arenes (n = 4,6) were synthesized and products complied with NMR-, mass spectral-, mp-, IR- and elemental analytical data.[1] Air-sensitive reactions were done under N_2-atmosphere using transfer techniques. NMR-spectra were recorded at 250 MHz (^1H) and 63 MHz (^{13}C) if not stated otherwise at room temperature with $CDCl_3$ as solvent. TLC was carried out on Merck Silica gel $60F_{254}$. All solvents were distilled and chemicals were of p.a. grade. The terms 'lower' and 'upper' rim refers to the ionophilic and hydrophobic side of the macrocycle, respectively.

The synthesis of compounds **1**, **2**, **4**, **5**, **6**, **7** and **8** was reported previously.[4,5,8] Ligand **3** was synthesized from parent *tert*-butylcalix[6]arene in three steps via the intermediates **3a**, and **3b** as follows:

Synthesis of 5,11,17,23,29,35-Hexa-*tert*-butyl-37,38,39,40,41-pentahydroxy-42-methoxy-calix[6] arene **3a**: p-*tert*-Butylcalix[6]arene (1 equiv.) is refluxed with 3 equiv. BaO and 9.8 equiv. MeI in acetone until TLC (CH_2Cl_2) shows a maximum at R_f = 0.47 (ca. 5 hours). The product mixture is cooled, quenched, filtrated, and the filtrate is dried. After dissolving in CH_2Cl_2 it is washed with HCl/H_2O and dried again. Removal of the impurities, which in TLC show lower R_f-values, is achieved by Soxhlet-extraction using n-hexane. The separation of **3a** from the main by-product 5,11,17,23,29,35-hexa-*tert*-butyl-37,38,40,41-tetrahydroxy-39,42-dimethoxycalix[6]arene **3c** was easy after derivatization to the corresponding esters **3b** and **3d** by fractionated crystallization from ethanol. Identification of **3a** and **3c** was done by comparison of the NMR-spectra with reference[9].

Synthesis of **3b**: 1.5 g of the hexane-insoluble fraction is refluxed with 0.35 g NaH in THF for 4hours. After cooling and addition of 2.2 ml ethylbromoacetate reflux is continued for 20 hours. After cooling, residual NaH is decomposed with ethanol, the suspension filtrated and evaporated. The residue is dissolved in $CHCl_3$, washed with 0.5 M HCl and dried. From ethanol, first 0.5 g of **3d** crystallize, followed by 1 g of the desired product **3b**. The symmetric tetraester **3d** as well as its hydrolyzed product, the tetraacid **3e** are insoluble in most solvents.

5,11,17,23,29,35-Hexa-*tert*-butyl-37,38,39,40,41-penta[(ethoxycarbonyl)methoxy]-42-methoxy-calix [6]arene **3b**. MS(EI): 1417 (L), 1371 (Frakt. -O-C_2H_5); NMR (^1H, $CDCl_3$): 1.01 (s, 18H), 1.07 (s) and 1.09 (s) (27H), 1.24 (m, 15H), 1.36 (s, 9H), 2.17 (bs, 2H), 4.17 (bm, 29H), 4.43 (bs, 4H), 6.71 (s, 2H), 6.84 (s, 2H), 6.92 (s, 2H), 7.14 (s, 2H), 7.19 (s, 2H); (^{13}C): 14.02, 14.12, 30.60, 31.12, 31.23, 31.37, 31.52, 33.96, 33.99, 34.08, 60.29, 60.66, 69.42, 69.84, 124.61-126.57 (6s), 127.64, 132.23, 132.70, 133.19, 133.40, 145.44, 146.03, 146.11, 146.21, 152.31, 152.51, 155.27, 168.85, 169.16; Calc. C 73.7, H 8.25, found C 73.33, H 8.09%, mp 195-196°C.

5,11,17,23,29,35-Hexa-*tert*-butyl-37,38,39,40,41-penta(carboxymethoxy)-42-methoxy-calix[6]aren **3**. By refluxing **3b** with 25 eq. tetramethylammonium hydroxyde in THF/water for 12 hours. NMR (^1H, $CDCl_3$): 1.0 (s, 27H), 1.15 (s, 27H), 3.32-3.43 (m, 9H), 3.95-4.08 (m, 6H), 4.21 (s, 4H), 4.45 (t, 6H), 6.83 (s, 6H), 7.00 (s, 6H), 7.60 (bs, -OH and H_2O); (^{13}C): 29.55, 30.27, 31.23, 31.33, 34.05, 34.15, 60.91, 69.37, 69.64, 71.71, 123.88, 125.39, 126.41, 132.56-133.03 (5s), 146.12, 146.55, 146.72, 150.98-151.74 (4s), 153.25, 156.52, 172.16; IR 1744 ν_{CO}; Calc. C 72.39, H 7.57, found C 70.08, H 7.56%.

5,11,17,23,29,35-Hexa-*tert*-butyl-37,38,40,41-tetrakis[(ethoxycarbonyl)methoxy]-39,42-dimethoxy-calix[6]arene **3d**. MS (EI): 1345 (L); NMR (^1H, $CDCl_3$): 1.06 (s, 9H), 1.11 (s, 27H), 1.32 (m, 12H), 1.39 (s, 18H), 3.44 (bm, 4H), 4.01 (s) and 4.28-4.56 (m) (30H), 6.61 (s, 6H), 7.18 (s, 6H); (^{13}C): 14.00, 14.14, 30.11,31.18, 31.49, 34.10, 58.87, 60.84, 69.90, 123.65, 126.72, 127.77, 132.41, 132.77, 133.69, 145.67, 146.41, 151.87, 154.73, 169.09.

5,11,17,23,29,35-Hexa-*tert*-butyl-37,38,40,41-tetrakis(carboxymethoxy)-39,42-dimethoxy-calix[6] aren **3e**. As described for **3**. NMR (^1H, $CDCl_3$): 1.12 (s, 54H), 3.24 (s, 12H), 3.38 (s, 6H), 3.97 (s, 8H), 6.93 (s, 12H).

Two-Phase Solvent Extraction Procedure

Extraction of ^{241}Am at tracer levels from diluted HNO_3 was carried out at 296 K with phase volumes of 3 ml each on a magnetic stirring plate in a glove box for 4 h at 400 rpm, followed by liquid scintillation counting (model LSC 6500, Beckmann Instr.) of the aqueous phase. The specific activity was 1 kBq/cm^3 ($3.3 \cdot 10^{-8}$ mol/dm^3) before extraction. The oxides (>99.9%) of Nd, Eu, Tb, Dy, Yb and Er were converted to perchlorate stock solutions (pH 2.5). The extraction experiments were carried out at 298 K for 4 hours at 100 rpm using an overhead shaker in a thermostatted box. The aqueous phase for lanthanide extraction contained either $1 \cdot 10^{-4}$ mol/dm^3 of Nd(III) (single element extraction) or 6 lanthanides (Nd + Eu + Tb + Dy + Yb + Er, $1 \cdot 10^{-4}$ mol/dm^{3}M each, competitive extraction). The pH-values given in the figures are equilibrium values, measured with an Ross combination electrode. Equal phase volumes were used for extraction and for stripping. The solvent was chloroform (p.a.), washed and saturated with water before use. Complete stripping of the lanthanides from the organic phases was achieved with 10 mmol/dm^3 DTPA at pH 5 (mass balance 100%). Lanthanide concentrations in the aqueous and stripping solutions were analyzed by ICP-AES (model IRIS/AP,TJA). The data are averages of at least 3 measurements. No extraction took place by chloroform in the absence of calixarenes. Extraction equilibria were attained within 30 min. of magnetic stirring, as tested with ligand **1**.

Data Treatment

The distribution ratio D, defined as the ratio between the metal concentration in the organic and in the aqueous phase at equilibrium, serves as a measure of extractability and of the stability of the complexes, which formed between ligand and metal. As the solubility of the extractants in aqueous solutions is very low (*e.g.* less than 2.10^{-5} mol/dm^3 ligand **1** dissolves in pure water) and their distribution constant between chloroform and water are high (*e.g.* log K = 3.15 for **1** at pH 6), the complex formation occurs at the liquid-liquid interface and the complexation in the aqueous phase can be neglected in the data treatment.

Extraction constants K_{ex} were calculated according to the equations (I) and (II) (vide infra) where a solid line denotes the species in the organic phase.

Due to the low ionic strength in the investigated solutions, activity coefficients were not taken into account in the calculations. The concentration of uncomplexed ligand in the organic phase c_L was calculated from the initial ligand concentration and the measured concentration of complexed Ln(III) in the organic phase. In case of Am(III) extraction, the initial ligand concentration can be regarded as the equilibrium concentration due to the trace concentration of Am(III).

RESULTS AND DISCUSSION

Figure 1 shows the plot of log D *vs.* the pH in the extraction of Am(III) into chloroform by calixarenes of various ring size and with different functional groups (Scheme 1). Despite the ring size, the following molecular features are different: the number of -O-CH_2-COOH groups ranging from 6 (ligands **7**, **8**) over 5 (ligand **3**) to 3 (ligands **4**, **5**, **6** and **1**, **2**). In the calix[6]arenes the -COOH groups are more flexible than in calix[4]arenes due to the rotational freedom of the phenyl rings. The compounds **1**, **2**, **4** and **6** are bearing amide groups; **7** and **8** differ in the hydrophobicity, while **1** and **2** differ in both hydrophobicity and the kind of amide group.

In the range of pH below 3.5, a slope of 3.0 was obtained from the plot for the calix[6]arenes **4**, **6**, **7**, and **8** and for calix[4]arene **2**, in accordance with the ionic charge. A slope less than 3 was obtained for ligands **1** and **5**.[5]

From the order of extractability being **1** < **2** = **5** < **4** < **6** < **3** = **7** < **8**, it is concluded that:

(i) a high number of ligating groups calix[n]arenes promotes the extractability, with a maximum being around n = 6±1, which is similar to the extraction of Ln(III)[8,10,11];

(ii) monoalkyl amide-substituted calix[4]arene **1** shows the lowest extractability, possibly due to intramolecular hydrogen bonding between NH and CO;
(iii) three flexible -COOH groups in a larger open cavity (ligand **5**) result in an extractability comparable with a rigid narrow cavity (ligand **2**).
(iv) the difference in extraction of Am(III) and Ln(III) by calix[6]arenes increases when the number of -COOH groups decreases from 6 to 3.[4,5]

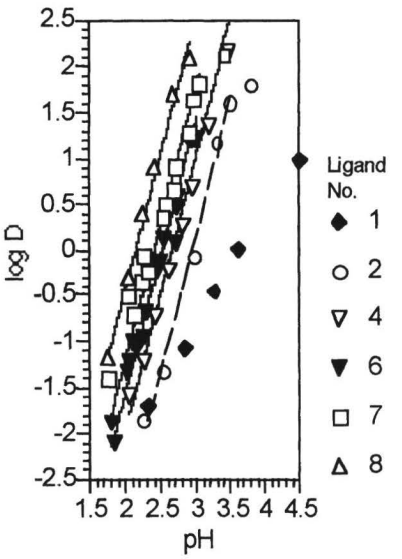


Figure1. Extraction of Am(III) at 293K by various calixarenes
Aq. Phase: ^{241}Am(III), activity 1kBq/ml ($3.3*10^{-8}$M) in 0.0002 to 0.03M HNO_3, Org. Phase: chloroform containing 3mM ligand

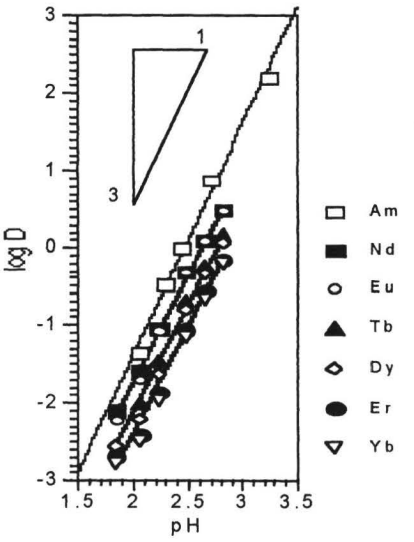


Figure 2. Extraction of Am(III) and Ln(III) by ligand 3.
Aq.Phase: Am-series: see Fig.1; Ln series: 0.6mM $Ln(ClO_4)_3$ (various concentrations), Org.Phase: chloroform ocntaining 3mM ligand

The extraction constants (Table 1) for the calix[6]arenes **4**, **6**, **7** and **8**, which were determined from the plot of log D - 3pH *vs.* log c_L according to Eq. (I) or (II) as indicated, were used to calculate the solid lines in Figure 1, fitting well the experimental data.

The extraction of Ln(III) and Am(III) by the recently synthesized ligand **3** is shown in Figure 2. A slope of 3.0 was obtained in this plot for Am(III) and all six lanthanides(III). The order of extractability showed as: Am > Nd > Eu > Tb> Dy > Er > Yb, following the order of the ionic radii in the series of Ln(III).

The extraction data for trivalent Nd and Am at various ligand concentrations are plotted in Figure 3. Although the experimental conditions for Nd in single element and in competitive extraction were different, an excellent agreement was found between these data as seen in Figure 3. The stoichiometry of the extracted complexes is different for Am(III) (1:1) and Nd(III) (1:2 metal to ligand). The values of K_{ex} for all six Lanthanide(III) were obtained from the plot logD-3pH *vs.* $\log c_L$ in Figure 4, which were used to draw the solid lines in Figure 2. These lines fit well the extraction data and it proved the stoichiometry as above-mentioned.

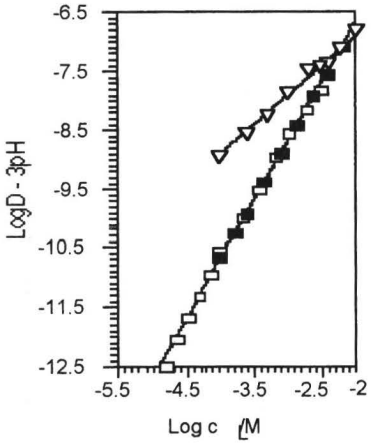


Figure 3. Comparison of the extraction of trivalent Am(▽) and Nd (□■) at various concentrations of ligand. Aq.phase; Am-series: see Fig.1, Nd. series: 0.1mM Nd(III)(□), or 0.1mM each of 6 Ln(III)(■) in $HClO_4$. Org.phase: $CHCl_3$ containing vairous amounts

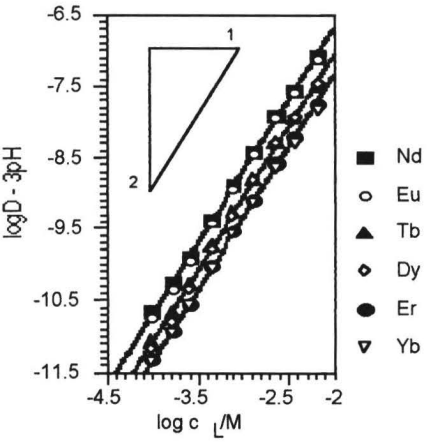


Figure 4. Competitive Extraction of 6 Ln(III) with Ligand 3 as function of ligand concentration Aq.phase: dilute $HClO_4$ containing 0.1mM each of 6 Ln(III). Org phase: $CHCl_3$ containing various amounts of ligand

The loading test for Nd was carried out in order to learn the influence of metal ion concentration in the aqueous phase to the extraction of Ligand **3**. The results was given in Figure 5. It is seen that the stoichiometry of the extracted Nd(III)-complex remains 1:2 at high loading.

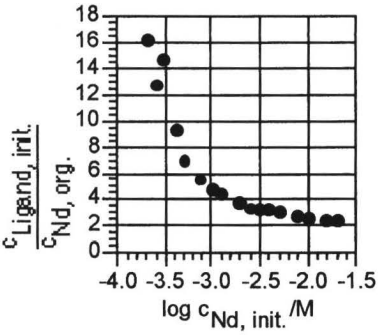


Figure 5. Loading test for Nd(III) extracted by Ligand 3. Aq.phase: dilute $HClO_4$ containing various amounts of $Nd(ClO_4)_3$. Org.phase: $CHCl_3$ containing 3mM of 3

Extraction Equilibria

$$M^{3+} + \overline{H_iL} = \overline{MH_{i-3}L} + 3H^+$$

$$\log K_{ex} = \log D - \log c_L - 3pH \qquad (I)$$

$$M^{3+} + 2\,\overline{H_jL} = \overline{ML{\cdot}H_{j-3}L} + 3H^+$$

$$\log K_{ex} = \log D - 2 \cdot \log c_L - 3 \cdot pH \qquad (II)$$

Table 1 Values of $\log(K_{ex}/dm^3 \cdot mol^{-1})$ for the extraction from water to chloroform

Metal	Am[c]	Nd[d]	Nd[c]	Eu[d]	Tb[d]	Dy[d]	Er[d]	Yb[d]	Eq.
Ligand **3**	-4.90								(I)
Ligand **3**		-2.66	-2.66	-2.71	-3.04	-3.09	-3.32	-3.37	(II)
Ligand **4**	-2.92	-4.12	-4.11	-4.29	-4.53	-4.65	-4.87	-4.94	(II)[e]
Ligand **5**		-5.48		-5.47	-5.84	-5.88	-6.10	-6.19	(II)[e]
Ligand **6**	-2.52	-4.31	-4.55	-4.56	-4.77	-4.96	-5.24	-5.18	(II)[e]
Ligand **7**	-4.9								(I)
Ligand **8**	-4.14								(I)

[c] from single element extraction; [d] from competitive extraction of 6 lanthanides; [e] from ref.[5]

CONCLUSIONS

The order of extractability of Ln(III) and Am(III) by the investigated calixarenes is: **1** < **2** = **5** < **4** < **6** < **3** = **7** < **8**. It shows, that the number of ligating groups as well as the size of the cavity which is formed by them determine the extraction efficiency. Stepwise removal of -COOH groups from ligands **7** or **8** reslts in decreasing extraction; the decrease is stronger for Ln(III) than for Am(III) and can be partly compensated by amide groups.

ACKNOWLEDGEMENT

Financial support by Alexander von Humboldt-Foundation and by Deutsche Forschungsgemeinschaft (DFG) is highly appreciated.

REFERENCES

1 Gutsche CD, *"Calixarenes"*. Cambridge, UK, The Royal Society of Chemistry, (1989); and Gutsche CD, *"Calixarenes Revisited"* Cambridge, UK, The Royal Society of Chemistry, (1998).
2 Vicens J, Böhmer V, *"Calixarenes. A Versatile Class of Macrocyclic Compounds"* Dortrecht/Boston/London, Kluwer Acad. Publ., (1990).
3 Ludwig R, *Review on Calixarene-Type Macrocycles and Metal Extraction Data,* JAERI-Review 95-022, Japan Atomic Energy Research Institute, (1995).
4 Ludwig R, Kunogi K, Nguyen TKD, and Tachimori S, *Chem. Comm.*, 1985, (1997).
5 Nguyen TKD, Kunogi K and Ludwig R (submitted)
6 Ludwig R and Tachimori S, *Solv. Extr. Res. and Develop., Jpn.*, **3**, 244, (1996).
7 Ludwig R, Nguyen TKD, Kunogi K and Tachimori S, *NUCEF'98,* JAERI-Report Conf. (in press)
8 Ludwig R, Tachimori S and Yamato T, *Nukleonika*, **43**(2), 161, (1998).
9 Otsuka H, Araki K and Shinkai S, *J. Org. Chem*, **59**(6), 1542, (1994).
10 Ohto K, Yano M, Inoue K, Yamamoto T, Goto M, Nakashio F, Shinkai S and Nagasaki T, Analyt. Sci., **11**, 893, (1995).
11 Ohto K, Yano M, Inoue K, Nagasaki T, Goto M, Nakashio F and Shinkai S, *Polyhedron*,**16**(10), 1655, (1997).

COEXTRACTION OF VARIOUS METAL IONS WITH CALIX[4]ARENE CARBOXYLATE COMPLEXED WITH SODIUM ION

Keisuke Ohto, Hideaki Ishibashi, Shigemasa Kuwata and Katsutoshi Inoue

Department of Applied Chemistry, Faculty of Science and Engineering, Saga University, 1-Honjo, Saga 840-8502, Japan

ABSTRACT

Solvent extraction of sodium ion with p-t-octylcalix[4]arene tetracarboxylate was investigated to elucidate coextraction mechanism of sodium and other metals. The result suggested that two sodium ions are simultaneously extracted by a single molecule of calix[4]arene derivative under the present experimental conditions. The first sodium ion was found to be complexed at the inside of the calix[4]arene cavity. It was found that the complexation with the first sodium facilitates the extraction of the second sodium ion, which was complexed at the outside of the cavity; that is, the extraction of sodium ion may be concluded as coextraction of sodium ion itself. Most of metal ions were also coextracted together with sodium by calix[4]arene tetracarboxylate.

Keywords: calix[4]arene carboxylate, coextraction, sodium.

INTRODUCTION

Calixarenes are phenolic cyclic oligomers. A number of studies have been conducted on the recognition properties of calixarenes such as ionic recognition and molecular recognition.[1-4] In particular, calix[4]arene compounds have been found to show high sodium selectivity due to their rigid structures. Ludwig et al.[5] and we[6] have reported that the extraction and the separation abilities of calix[4]arene carboxylate for rare earth metal ions were significantly enhanced in the presence of sodium ion. Although both authors have proposed that these are attributable to the co-extraction of sodium together with other metal ions, the extraction mechanism have not been elucidated in detail yet.

In the present paper, we report for the extraction of sodium ion with calix[4]arene carboxylate to elucidate the coextraction mechanism of sodium and another metal ion. Furthermore, the extraction of another metal ions with the sodium-complexed extractant was investigated to determine the extraction mechanism of the metals.

EXPERIMENTAL

Reagents.

25,26,27,28-Tetrakis(carboxymethoxy)-5,11,17,23-tetrakis-(1,1,3,3-tetramethylbutyl)calix[4]arene (cone conformation) was synthesised in a similar manner to that described in the previous paper.[7] The chemical structure of the extractant was shown in Figure 1.

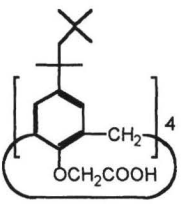


Figure 1. Chemical structure of the extractant.

Extraction of sodium ion.

The extraction of sodium ion with calix[4]arene carboxylate was carried out in a similar manner to that described in the previous paper.[8]

Determination of extraction mechanism for various metal ions.

The extraction of metal ions with sodium-loaded calix[4]arene carboxylate was carried out in a similar manner to that described in the previous paper.[9]

© 2000 Society of Chemical Industry

RESULTS and DISCUSSION

Extraction of sodium ion.

Figure 2 shows aryl peak of the extractant in ^{1}H-NMR at some pH values. Arduini et al. and Arimura et al. reported that the chemical shifts of *p*-t-butylcalix[4]arene tetraester was observed in the complexation with sodium ion due to the structural change caused by surrounding the sodium ion by phenoxy oxygens and carbonyl groups.[10] The aryl peak of the sodium loaded extractant molecule appears at 7.05 ppm apart from the original peak at 6.90 ppm. Although the extent of the shift increased with the increase of pH, the further second shift was not observed. That is, the change of the chemical shift was observed only once from 6.90 ppm to 7.05 ppm. Since the ratio of the integral ratios between the original and shifted peaks may be related to loading percentage of sodium ion with the extractant, the relationship between the loading percentage and the shifted percentage was examined.

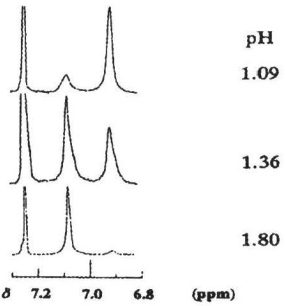


Figure 2. ^{1}H-NMR spectra of aryl peak of the extractant at various pH.

Figure 3 shows the effect of pH on loading percentage of sodium ion, % L, and on percentage of the chemically shifted extractant, % S. The % L was calculated from the amount of the extracted sodium ion measured by AAS. The % S was evaluated in terms of the integral ratio of the shifted peak of the aryl protons recorded by using ^{1}H-NMR spectrometer. At around pH 2, the % L attains to 200 %, which means that the stoichiometry of the extractant and sodium ion is 1:2. On the other hand, since only one chemical shift was observed, the % S attains to only 100 %. Furthermore, the shape of both plots are analogous and at pH 1 - 2 the observed value of % L appears to be nearly twice of that of % S. If the plotted value of % S completely coincide with those of % L at low loading region (at pH 1.0 - 1.6), the complexation should take place only for the first sodium ion, until the vacant cavity of calix[4]arene is saturated with the first sodium ion, where chemical shift is observed. However, the observed % S appears to be nearly half of % L over whole pH under the present condition, which seems to suggest the following two conclusions. The first is that both of two sodium ions are not complexed at the inside of the cavity, but that the first sodium ion is complexed at the inside of the cavity causing chemical shift and the second one is complexed at the outside of the cavity causing no chemical shift. The second is that two sodium ions are simultaneously extracted with a single molecule of the extractant, which means that the complexation with the first sodium facilitates the extraction of the second. This conclusion was further strongly supported by the result of the competitive extraction of four kinds of alkali metal ions. That is, potassium was extracted as the second ion even at pH 1.4 in the presence of sodium ion, while it was not extracted at pH lower than 3.0 in the absence of sodium ion. This result also suggests that even alkali metal ion is coextracted with sodium ion by calix[4]arene carboxylate.

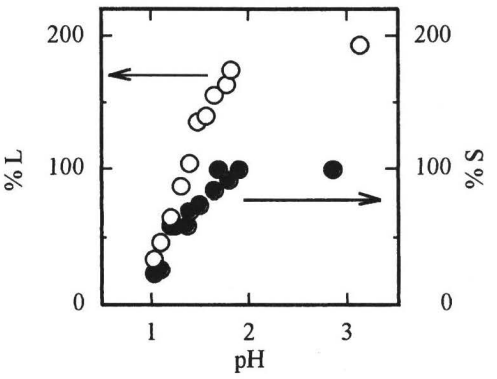


Figure 3. Effect of pH on %Loading of sodium ion (%L) and on % Shifted of the extractant (%S). O% Loading of sodium ion, ●: % Shifted of extractant, $[Na^+]$=0.1 mmol dm^{-3}, [Extractant] = 5 mmol dm^{-3}

As shown in Fig. 4, we can propose the model of the simultaneous extraction of two sodium ions with a single extractant molecule under the present condition. Since the complexation with the first sodium ion enhances the extraction ability of the extractant and the sodium concentration is kept

at as high as 0.1 mol dm^{-3} under the present condition, the second sodium ion was easily complexed with the extractant preorganised by first sodium ion causing simultaneous extraction of two sodium ions. The enhancement of the extraction of the second sodium ion induced by that of the first ion may be attributable not only to the enhancement of the dissociation of the second carboxyl group but also to the breakdown of intramolecular hydrogen bonding. As mentioned above, p-t-octylcalix[4]arene tetracarboxylate derivative complexed with sodium ion coextracts not only other kinds of metal ions but also sodium ion itself. This result strongly supports the coextraction behaviour of various metal ions with the sodium-loaded p-t-octylcalix[4]arene tetra-carboxylate. Since the interaction between the extractant and the second sodium ion is not so strong, because it is extracted just by one carboxyl group, it is preferably substituted by other metal ions with higher affinity than sodium ion with carboxyl groups.

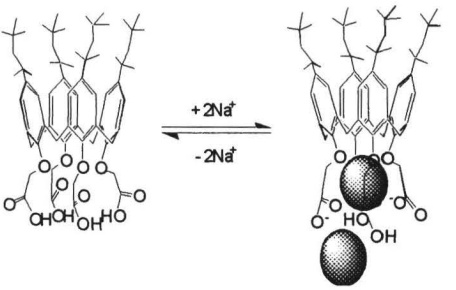


Figure 4. Model of the simultaneous extraction of two sodium ions with the extractant under the present conditions

Determination of the extraction mechanism for various metal ions.

In our previous work, rare earth metal[6] and copper[9] ions were suggested to be coextracted together with sodium ion by calix[4]arene carboxylate. However, it has not been confirmed whether other metal ions are coextracted with the sodium-loaded extractant or not. Since two sodium ions are extracted with a single molecule of the extractant, three extraction mechanisms can be proposed as shown in Figure 5, where the stoichiometry of another metal ion and the extractant is assumed to be 1:1. The first is that two sodium ions are still kept to be complexed with the extractant even after the extraction and another metal ion is further extracted. The second is that only first sodium is kept to be complexed, while the second sodium ion is released and substituted by another metal ion at the extraction. The third is that both of two sodium ions are substituted by another metal ion. The former two mechanisms are named as the "coextraction" mechanism, while the third one as the "ion-exchange" mechanism. In order to determine the extraction mechanism for all metal ions, the extraction of various metal ions was carried out with the sodium-loaded calix[4]arene. Table 1 lists the relation between the eluted sodium concentration and the extracted nickel ion as typical result. The concentration of extracted nickel ion corresponds with that of released sodium ion. Therefore, the extraction of nickel ion comes under the "co-extraction" mechanism. The extraction mechanism of other various metal ions was also inferred in the similar manner as shown in Figure 6 in a periodic table. Majority of metal ions except for lead ion were found to be extracted by either of the two "coextraction" mechanisms. The extraction mechanism for some metal ions was not able to be inferred due to the formation of precipitate or because they were not extracted under the present condition. That is, all metal ions the extraction mechanism of which were inferred are extracted by the "coextraction" mechanism with

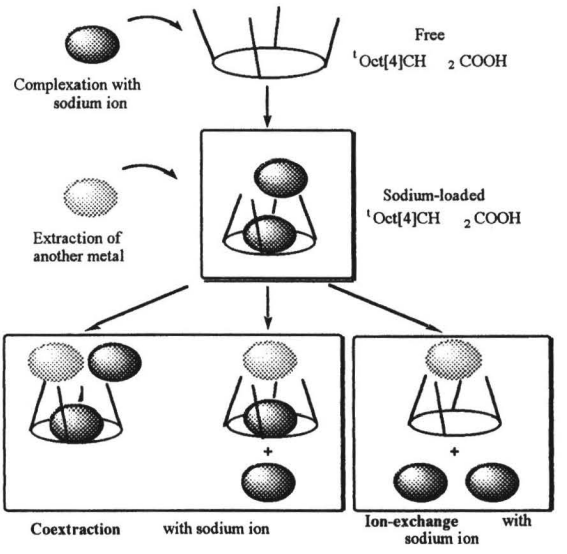


Figure 5. Three proposed extraction mechanisms.

calix[4]arene carboxylate in the presence of sodium ion. This result supports the fact that the extraction ability of calix[4] arene carboxylate is enhanced by the complexation with the first sodium ion and even the second sodium ion can be extracted by exchanged with proton.

pH_{eq}	$[Ni]_i$	$[Ni]_{eq}$	$[Ni]_{org}$	$[Ni]_{elu}$
4.80	1.479	0.920	0.559	0.529
4.80	1.224	0.683	0.541	0.473
4.81	0.773	0.328	0.445	0.432
4.86	0.465	0.123	0.342	0.367
4.91	0.248	0.025	0.223	0.272

Table 1 Relation between the eluted sodium concentration and the extracted nickel concentration

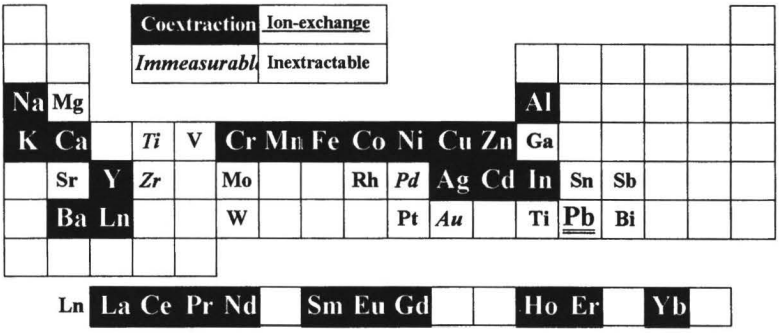


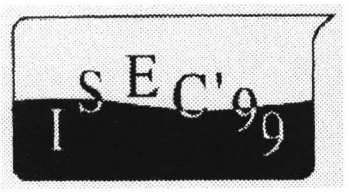
Figure 6. Extraction mechanism of various metal ions.

ACKNOWLEDGEMENT

This work was financially supported in part by a Grant-in-Aid for Scientific Research (No.09450293 and 09750843) from Ministry of Education, Science and Culture of Japan.

REFERENCES

1 Gutsche CD. *Calixarenes*, Royal Society of Chemistry, Cambridge, (1989).
2 Vicens J and Boehmer V. *Calixarenes: A Versatile Class of Macrocyclic Compounds*, Kluwer Academic Publishers, Netherlands, (1992).
3 Ikeda A and Shinkai S. *Chem.Rev.*, **97**, 1713, (1997).
4 Ludwig R. *JAERI-Review*, 95-022, 1, (1995).
5 (a) Ludwig R, Inoue K and Yamato T. *Solv.Extr.Ion Exch.*, **11**, 311, (1991).
(b) Ludwig R, Inoue K, Shinkai S and Gloe K. *Solvent Extraction in the Process Industries Proc. ISEC'93*, York, pp.273, (1993).
(c) Ludwig R and Gauglitz R. *Value Adding Through Solvent Extraction, Proc.ISEC'96*, Melbourne, pp.365, (1996).
(d) Ludwig R, Kunogi K, Dung N and Tachimori S. *Chem.Commun.* 1985, (1997).
6 Ohto K, Yano M, Inoue K, Nagasaki T, Goto M, Nakashio F and Shinkai S. *Polyhedron*, **16**, 1655, (1997).
7 Ohto K, Yano M, Inoue K, Yamamoto T, Goto M, Nakashio F, Shinkai S and Nagasaki T. *Anal.Sci.* **11**, 893, (1995).
8 Ohto K, Ishibashi H and Inoue K. *Chem.Lett.*, 631, (1998).
9 Ohto K, Shiratsuchi K, Inoue K, Goto M, Nakashio F, Shinkai S and Nagasaki T. *Solv. Extr. Ion Exch.* **14**, 459, (1996).
10 (a) Arduini A, Pochini A, Reverberi S and Ungaro R. *Tetrahedron*, **42**, 2089, (1986).
(b) Arimura T, Kubota M, Matsuda T, Manabe O and Shinkai S. *Bull.Chem.Soc.Jpn.* **62**, 1674, (1989).



EXTRACTION OF EUROPIUM(III) AND AMERICIUM(III) WITH DIAMIDE COMPOUNDS FROM NITRIC ACID SOLUTION

Wen-Jun Chen, Lin Zhu, Song-Dong Ding, Zhong-Qun Liu, Sao-Jin Chen, Chuanjin Xia, Zhongliang Huang and Yong-Dong Jing

Department of Chemistry, Siochuan University, Chengdu 610064, China

ABSTRACT

The solvent extraction properties of the diamides, $(R^1\ R^2NC(O))_2R^3$ for Eu^{3+} and Am^{3+} have been examined. The primary factor effecting their extractive properties is the bridged radical linking up two terminal amide groups. The extractive ability of the diamides for Eu^{3+} and Am^{3+} is in the order of R^3= -(-CH_2OCH_2-)->-(-CH_2OCH_2-)$_2$>>-(-CH_2-)$_n$. Using diamides with R^3= -(-CH_2OCH_2-)$_n$ as extractants, the Eu(III) and Am(III) can be extracted effectively from nitric acid solution, and the extractive ability of the diamides with n=1 is remarkably larger than that of n=2. The effect of R^1 and R^2 on the extractive is exhibited to a less extent. With the extractive systems developed in this paper, the amido podands might be utilised in separation/recovery of trivalent actinides and lanthanides from the reprocessing wastes in nuclear industry or the hydrometallurgy of rare earth elements.

Keywords: diamide extractants, europium(III), americium(III)

INTRODUCTION

Trivalent actinide and lanthanide ions can be extracted effectively with some selected diamide compounds, $[R^1R^2NC(O)]_2R^3$, if the substitute groups R^1, R^2 and R^3 have suitable structures. As the diamide compounds contain no phosphorus atoms they are fully incinerateable and show good prospects for applications in the nuclear industry.[1-5] In the case of R^3 = -(-CH_2-)$_n$, their extractive ability for trivalent actinide and lanthanide ions was very poor. Cuillerdier et al.[3] reported that some pentaalkyl malonamides, $[(R^1\ R^2NC(O)]_2\ CHR^4$ (especially for R^4 = alkyl or oxyalkyl) have good extractive power for trivalent actinide and lanthanide ions. It is reported that a special kind of diamide compounds of R^3 = -(-CH_2OCH_2-)$_n$, called amido-podands, have selective co-ordination properties similar to crown ethers, with the advantage of being easy to synthesise, and lower toxicity. Compared to the pentaalkyl malonamides, the amido-podands display the following advantages: much higher extractive ability for lathanides and actinides; very easy synthesis and high yield. Some articles[6-8] reported the extraction of lanthanides with amido-podands in the presence of a large anion such as picrate. It follows that these extractive systems are difficult to apply on a plant scale.

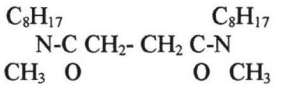
This paper reports our recent investigation on the extraction of Eu(III) and Am(III) with some amido-podands from nitric acid solutions without the presence of a large anion. It appears that the primary factor effecting their extractive properties is the bridged radical linking two terminal amide groups. Using suitable diluents, the lanthanide and actinide cations can be extracted effectively without a large anion by amido-podands. So, these extractants could be used in separation / recovery of trivalent actinides and lathanides from reprocessing wastes in the nuclear industry or hydrometallurgy of rare earths from wide range of nitric acid concentrations.

EXPERIMENTAL

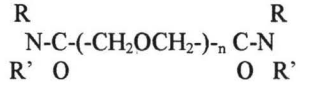
Reagent

The extractants shown in figure 1 were synthesised in our laboratory, and characterised by I.R., M.S., H^1NMR and elemental analysis. Purity of the products was >98%. ^{152,154}Eu and ^{241}Am were provided by the China Institute of Atomic Energy with radiochemical purity >99%. All other chemicals used in this work were reagent grades.

© 2000 Society of Chemical Industry



N,N'-dimethyl-N,N'-dioctylsuccinoamide (MDOSA ,I)



R = CH_3, R' = C_8H_{17}, n = 1: N,N'-dimethyl-N,N'-3-oxy-dioctylglularamide(.DMDOGA ,II)
R = R'= C_4H_9, n =1: N,N,N',N'-tetrabutyl3-oxy-glularamide(TBGA ,III)
R = R'= C_4H_9, n = 2: N,N,N',N'--tetrabutyl3,6-dioxy--octandiamide(TBODA ,IV)

Figure 1. Extractants investigated in this work

Procedures

Equal volume of aqueous and organic phases were pipetted to a ground tube, and shaken for 20-30 minutes with a mechanical shaker at 200.5 rpm, temperature 12C. The equilibrium concentrations of Eu^{3+} and Am^{3+} in each phase were determined by means of counting radioactivities of $^{152,154}Eu$ and ^{241}Am in a NaI(Tl) scintillation counter respectively. The distribution ratio D_M was calculated from the quotient of the radioactivities in organic and aqueous phase.
FTIR spectra were recorded on a 170X Nicolet Fourier Transform Spectrometer for all samples.

RESULTS AND DISCUSSION

Effect of the structure of diamides

The results of the extraction of Eu^{3+} and Am^{3+} from nitric acid solutions with extractants I to IV as a function of the nitric acid concentration in the aqueous phase, C_H, are shown in figure 2. The distribution ratios of Eu^{3+} and Am^{3+}, D_{Eu} and D_{Am}, increase with the HNO_3 concentrations in the aqueous phase. The amido-podands with bridged radical R^3 = $-CH_2OCH_2-$, DMDOGA and TBGA, exhibit good extractive power for both Eu^{3+} and Am^{3+}, and the D_{Eu} values are about an order of magnitude higher than those for D_{Am}. For DBODA, an amido-podand with the R^3 = $-(-CH_2OCH_2-)-$, the distribution ratios of Eu^{3+} and Am^{3+} ,D_{Eu} and D_{Am} are remarkably lower than that of both diamides mentioned above, and the D_{Eu} values lie close to D_{Am}. In the case of R^3 = $-CH_2CH_2-$, DMDOSA, the D_{Eu} and D_{Am} are much lower than that of DMDOGA, TBGA, and TBODA, and reach a maximum at C_H= 2.5 mol/l.

Compared to the results reported, [3] shown in table 1 and figure 2, the extractive power of the amido-podands DNDOGA, TBGA for Eu^{3+} and Am^{3+} is remarkably higher than that of extractants I, V and VII. This shows that the effect of the bridged radical R^3 on the extractive power of diamide compounds is more important than that of substitute radicals R^1 and R^2. Meanwhile, it denotes that the selectivity between the metal ion and the chain length of bridged radical linking up two terminal amide groups is emerging in these extractants. The existence of oxygen atom(s) in R^3 is favourable for the formation of the cyclic structure of the extractive chelate complexes between metal ion and ligand. For the case of R^3 = $-(-CH_2OCH_2-)-$, enlargement of cyclic chelate causes decrement in the stability of the extractive chelate complexes.

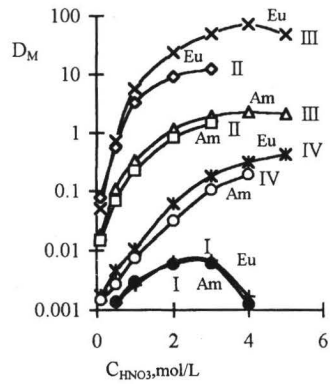


Figure 2. Extraction of Eu(III) and Am(III) with Diamides (Organic Phase: 0.01mol/l diamides, 20%(v/v) n-Octanol-kerosene; aqueous phase: C_{Eu}=5x10^{-4} mol/L, C_{Am}=trace amounts (using 50μg/mL as carrier))

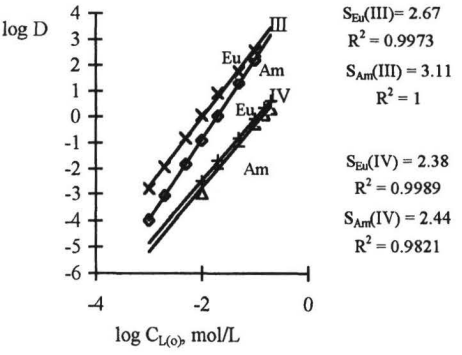


Figure 3. Dependence of D_{Am} and D_{Eu} on the Extractant Concentrations (Organic Phase: diamides, 20%(v/v) n-Octanol, kerosene; aqueous phase: C_{Eu}=5x10^{-4} mol/L, C_{Am}=trace amounts (using 50μg/mL as carrier))

Table 1. Extractive properties of some diamide compounds (C_{Am}= tracer, C_{Eu} = 510^{-4} mol/L, $C_{L(o)}$= extractant concentrations, t: 20±1°C)

N°	R^1	R^2	R^3	diluent	$C_{L(o)}$ M	D_{max} Am	D_{max} Eu	D_{max} conditions
I	CH_3	C_8H_{17}	CH_2CH_2	20%-octnol-kerosene	0.05	0.01	0.02	2-3MHNO$_3$
II	CH_3	C_8H_{17}	CH_2OCH_2		0.01	1.7	15	4-5MHNO$_3$
III	C_4H_9	C_4H_9	CH_2OCH_2		0.01	2.5	73.1	
IV	C_4H_9	C_4H_9	$(CH_2OCH_2)_2$		0.01	0.22	0.44	
V[1]	CH_3	C_4H_9	CH_2	benzene	0.5	0.55	--	2-3MHNO$_3$
VI[1]	CH_3	C_4H_9	CHR^4	*t*-butylbenzene	0.5	7.55	--	5 MHNO$_3$
VII[2]	C_4H_9	C_4H_9	$(CH_2)_3$	toluene	0.5	<0.01	<0.01	2-3MHNO$_3$

$R^4 = C_2H_4\text{-}O\text{-}C_6H_{13}$

Effect of nitric acid concentration in aqueous phase

The values of D_{Eu} and D_{Am} increased with increasing nitric acid concentration in aqueous phase C_H, see figure 2. In the case of DNDOGA, TBGA and TBODA, the maxima of D_{Eu} and D_{Am} appear near C_H = 4--5 mol/L. For the other extractants, the maxima emerge near C_H = 2--3 mol/L. Reduction of D_{Eu} and D_{Am} at higher acidity is induced by the competition of nitric acid.

Effect of extractant concentration in organic phase

The values of D_{Eu} and D_{Am} increased with increasing extractant concentration in organic phase $C_{L(o)}$, shown in figure 3. Plots of log D_{Eu} and log D_{Am} vs. log $C_{L(o)}$ are straight lines. Slopes of the straight lines are not integers and further study on the complexation ratios of Eu^{3+} and Am^{3+} with extractants remains to be done. From Stephan et al,[8] we may assume that the complexation ratio of Eu^{3+} or Am^{3+} to the extractant equals 2.

Extraction of nitric acid

The extraction of nitric acid with increasing extractant concentration in the organic phase $C_{L(o)}$ is shown in figure 4. For TBGA , the slope of the plot log D_H vs. log $C_{L(o)}$ varies from S = 0.67 at $C_{L(o)}$ < 0.25mol/L to S = 1.37 at $C_{L(o)}$ >0.25mol/L .For TBODA, S = 1.30. It appears that the complexation ratio of nitric acid to extractant varies with the structure of extractant and the ratio of nitric acid to extractant in organic phase.

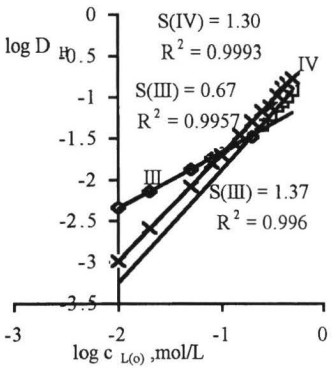


Figure 4. Extraction of Nitric Acid with Diamides (Organic Phase: diamides, 20%(v/v) n-Octanol-kerosene; aqueous phase: $1.5x10^{-3}$ mol/L $Fe(NO_3)_3$, HNO_3

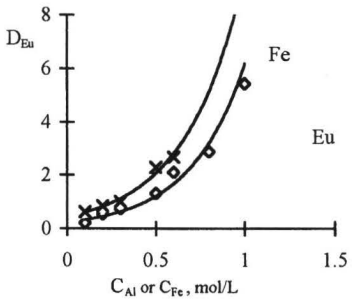


Figure 5. Effect of $Fe(NO_3)_3$ or $Al(NO_3)_3$ Concentrations in Aqueous Phase on D_{Eu} (Organic Phase: $5x10^{-3}$ mol/L DMDOGA, 20%(v/v) n-Octanol- kerosene; aqueous phase: 1 mol/L HNO_3, $C_{Eu}=5x10^{-4}$ mol/L

Effect of $Fe(NO_3)_3$ and $Al(NO_3)_3$ on the D_{Eu}

The dependences of the value of D_{Eu} upon the concentration of $Fe(NO_3)_3$ and $Al(NO_3)_3$ in aqueous phases are shown in figure 5. $Fe(NO_3)_3$ and $Al(NO_3)_3$ are used as salting-out agents for the extraction of Eu^{3+}. The extraction of $Fe(NO_3)_3$ was checked with 0.1 mol/L TBGA--20(v/v)% n-Octanol-Kerosene from 0.1-- 5 mol/L HNO_3. The distribution ratios of Fe(III), D_{Fe}, were in the range of 0.1--0.2, with a maximum about 0.196 at C_H = 1 mol/L.

$Al(NO_3)_3$ cannot be extracted. Therefore, the selectivity of DMDOGA to Eu^{3+} against Fe^{3+} was better than that of the pentaalkylpropanamides reported by Cuillerdier et al.[3]

Infrared spectroscopy investigation

The infrared absorption spectrum of pure TBGA and the extractants equilibrated with aqueous phases containing HNO_3 - $NaNO_3$ and $Eu(NO_3)_3$ - HNO_3 - $NaNO_3$ are shown in table 2 and figures 6 - 7. As a hydrogen bond is formed with the nitric acid, the OH stretching frequency decreased remarkably. This result agrees with that of the DMDBTDMA reported by Nigond et al.[4] In addition the N-C=O stretching band is shifted to 1615 cm^{-1}. The band of 1380 cm^{-1} comes from the stretching band of nitric acid and CH_3. In figure 7, the formation of complex of Eu^{3+} with TBGA induces the splitting of the N-C=O stretching band to two bands: 1645 cm^{-1} and 1620 cm^{-1}, and the shifting of the stretching band of C-O-C to 1139 cm^{-1}. Based on the experimental results, we suppose that C=O of the amide radicals and the C-O-C of the bridged radical all take part in the formation of the extractive complex of Eu^{3+} with TBGA.

Table 2 Infrared absorption spectrum

	Directions	IR absorption bands, cm^{-1}			
		-OH	-N-C=O	$-CH_2OCH_2-$	HNO_3 ,etc.
TBGA	Pure	3664-3246(m)	1653	1120	--
extractant equil. with HNO_3	equilibrated with 5.0 M HNO_3 --1 M $NaNO_3$	---	1615	1148	1380 1512
extractant equil. with $Eu^{3+}$and HNO_3	equilibrated with 7E-3 M Eu^{3+}, 5.6 M HNO_3, 1 M $NaNO_3$	---	1642(Eu) 1617(HNO_3)	1169	1378 1514

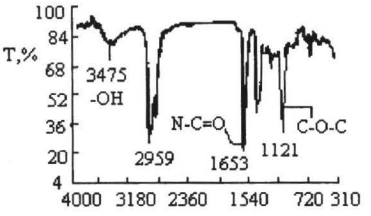


Figure 6. IR spectrum of pure TBGA

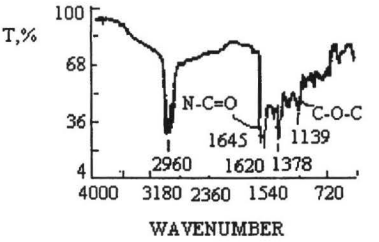


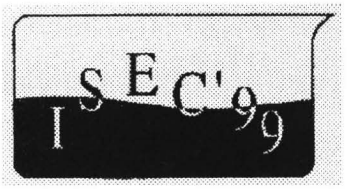
Figure 7. IR spectrum of TBGA equilibrated with an aqueous phase containing $7x10^{-3}$ mol/L $Eu(NO_3)_3$, 0.5 mol/L HNO_3, 1 mol/L $NaNO_3$

CONCLUSIONS

The primary factor effecting the extractive properties of diamide compounds is the bridged radical linking up two terminal amide groups, R^3. The effect of R^1 and R^2 on the extractive ability exhibited to a less extent. With suitable organic solvents as the diluent, the Eu(III) and Am(III) can be extracted effectively with the amido-podands from nitric acid solution without external large anions. These systems could be utilised in separation /recovery of trivalent actinides and lanthanides from the reprocessing wastes in nuclear industry or the hydrometallurgy of rare earth elements.

REFERENCES

1 Thiollert G and Musikas C. *Solv Extn. Ion Exch.* **7**, 813, (1989).
2 Charbonnel MC and Musiokas C. *Solv Extn. Ion Exch.* **7**, 1007, (1989).
3 Cuillerdier C, Musiokas C et al. *Sep. Sci. Technol.* **26**, 1229, (1991).
4 Nigond L and Musiokas C. *Solv Extn. Ion Exch.* **12**, 261, (1994).
5 Spjuth L et al. in *Value Adding Solvent Extraction (Proc. ISEC'96)*, Shallcross DC, Paimin R and Prvcic LM. (Eds) University of Melboune, **2**, 1309, (1996).
6 Yang Y-S et al. *He Huaxue Yu Fangshe Huaxue* (Chinese), **6**, 196, (1984).
7 Ding Y-Z et al. *Huaxue Shiji* (Chinese), **8**, 201, (1986).
8 Stephan H et al. *Solv Extn. Ion Exch.*, **9**, 459, (1991).



APPLICATION OF DIAZAPOLYOXABICYCLIC LIGANDS TO THE QUANTITATIVE EXTRACTION SEPARATION OF ALKALI AND ALKALINE EARTH METAL IONS AS THE ION-SIZE SELECTIVE MASKING REAGENTS

Shigekazu Tsurubou,[1] Shigeo Umetani[2] and Yu Komatsu[3]

[1]Department of Chemistry, Asahi University, Hozumi-cho, Gifu 501-0296, Japan

[2]Institute for Chemical Research, Kyoto University, Uji, Kyoto 611-0011, Japan

[3]National Institute for Research in Inorganic Materials, Tsukuba, Ibaraki 305-0044, Japan

ABSTRACT

Quantitative extraction separations of alkali and alkaline earths have been achieved by adding the macrocyclic ionophores as the masking reagents to the aqueous phase. Diazapolyoxabicyclic ligands (cryptands) were applied as the ion-size selective masking reagents to the synergistic solvent extraction system with benzoyltrifluoroacetone (BFA) and tri-n-butylphosphate (TBP) or tri-n-octylphosphine oxide (TOPO) into cyclohexane. Quantitative extraction separations between magnesium and calcium and between lithium and sodium were achieved with BFA and TBP or TOPO in the presence of cryptand [2.2.1]. Calcium could be also quantitatively separated from strontium in the synergistic extraction with BFA and TBP in the presence of cryptand[2.2.2].

Keywords: macrocyclic compounds, ion-size selective masking reagent, cryptands, alkali metal, alkaline earth metal

INTRODUCTION

One of the most important aims for the development in the solvent extraction is designing the more selective or quantitative extraction separation system. It is known that the selectivity in the solvent extraction of metal ions can be improved by adding the appropriate masking reagents to the aqueous phase. Generally, the extractability of metal ions with open chain chelating reagents such as β-diketones is governed by the stability of the metal complexes. In the solvent extraction of alkali, alkaline earth and lanthanide metal ions with β-diketones, metal ions having smaller ionic radii exhibit higher extractability. On the other hand, the stability of the complex formation between the macrocyclic ionophores, such as crown ethers and cryptands, and the above mentioned metal ions exhibits a quiet different tendency. Thus, combining the chelating reagents and the macrocyclic ionophores could possibly develop the more selective or quantitative extraction separation system. We have already reported the synergistic solvent extraction systems of higher selectivity among alkaline earths and lanthanides by the combination of chelating reagents and macrocyclic compounds as ion-size selective masking reagents.[1-5] Especially, in the synergistic extraction of alkaline earths with 1-phenyl-3-methyl-4-benzoyl-5-pyrazolone (HPMBP) and tri-n-octylphosphine oxide (TOPO) in the presence of cryptand[2.2.2], we could attain the quantitative separation between calcium and strontium.[6]

Diazapolyoxabicyclic ligands (cryptands) exhibit a prominent selectivity for alkali and alkaline earth metals. They are soluble in water and their stability in complexation is large enough for use as practical masking reagents. Their selectivity for metal ions depends largely on the ring size, and therefore, one can choose an appropriate cryptand according to the purpose. However, the masking effect of cryptands depends on the pH unlike crown ethers, because they incorporate nitrogen as an element constituting the ring structure. Accordingly, in order to utilize the masking effect of cryptands more effectively, it is desirable to employ them in the alkaline region.

In the present work, both cryptand[2.2.1] and [2.2.2] were applied to the synergistic extraction of alkali and alkaline earths into cyclohexane with benzoyltrifluoroacetone (BFA) and tri-n-butylphosphate (TBP) or TOPO. BFA, whose acidity is lower than HPMBP, was employed in order to

© 2000 Society of Chemical Industry

shift the extraction pH to more alkaline region than in the case of HPMBP. .

EXPERIMENTAL

Materials.

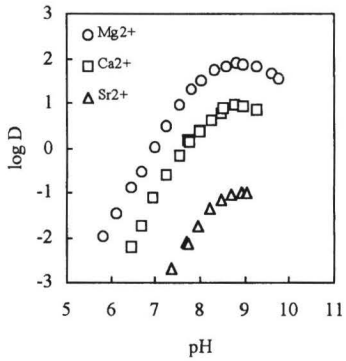
Cryptand[2.2.1] and cryptand[2.2.2] were purchased commercially from Merck, BFA and TOPO from Dojindo, TBP from Nacalai Tesque, and they were used without further purification. Other chemicals were of reagent-grade materials. Water was demineralized and distilled.

Procedure.

A 10 cm^3 portion of an aqueous phase containing the required amount of metal ion, cryptand and 0.02 M Good's buffer such as tris(hydroxymethyl)aminomethane was adjusted to the desired pH with hydrochloric acid and tetramethylammonium hydroxide. The aqueous phase was shaken for 2-20 hours until the reaction reached equilibrium with an equal volume of an organic phase (cyclohexane) containing the required amount of BFA and TBP or TOPO at 25±1°C. After centrifugation of the mixture, the pH in the aqueous phase was measured. The metal concentrations in the aqueous phase was determined by atomic absorption spectophotometry and in the organic phase after back-extraction with a hydrochloric acid solution.

RESULTS AND DISCUSSION

The results for the extraction of magnesium, calcium and strontium with 2.5×10^{-3} M BFA and TBP into cyclohexane are shown in Figure1. Logarithm of the distribution ratio of metal ions between the cyclohexane and the aqueous phase, log D, is plotted against the pH. Alkaline earths were extracted in the order Mg>Ca>Sr, which is the same order in which their ionic radii decrease. The slopes of the straight portion of the plots are two, indicating that two protons are released through the extraction reaction.



Fiure 1. Extraction ofalkaline earths into cyclohexane with BFA and TBP. [BFA]o=[TBP]o=2.5X10^{-3}M.

The stability constants of cryptates inclusion complexes between several kinds of cryptands and alkali, alkaline earth metal cations have been reported by JM Lehn et.al. in 1975.[7] Some stability constants of alkali and alkaline earths with cryptand[2.2.1] and [2.2.2] are shown in Table 1. These stability constants show the considerable differences between neighboring two metals, for example between Mg and Ca, and Li and Na with cryptand [2.2.1] and also between Ca and Sr with

cryptand[2.2.2]. The quantitative extraction separation method between Mg and Ca, Li and Na and also Ca and Sr have been examined using cryptand[2.2.1] and [2.2.2] as ion-size selective masking reagents.

Table 1 Stability constants (β)*

	Mg	Ca	Sr	Ba	Li	Na
[2.2.1]	<2	6.95	7.35	6.30	2.50	5.40
[2.2.2]	<2	4.4	8.0	9.5	<2	3.9

* taken from ref.7.

Synergistic extraction of alkaline earths with BFA and TBP in the presence of cryptand [2.2.1] or [2.2.2]

Figure 2 shows the results for the extraction of Mg and Ca into cyclohexane with 2.5 x 10^{-3} M BFA and TBP in the presence of 0.01 M cryptand[2.2.1]. The distribution ratio of Ca decreases rapidly over pH 7.5, while that of Mg are quite similar to those in the absence of cryptand[2.2.1] as shown in Figure 1. Mg can be separated from Ca quantitatively at the pH range 8.5 - 9.5 where more than 98% of Mg (log D*>1.80) is extracted into cyclohexane with slope of +2, while more than 99% of Ca (log D*<-2) remains in the aqueous phase at the same time. On the other hand, the distribution of Sr was very low (log D*<-3) in the pH range 7.0 – 9.5.

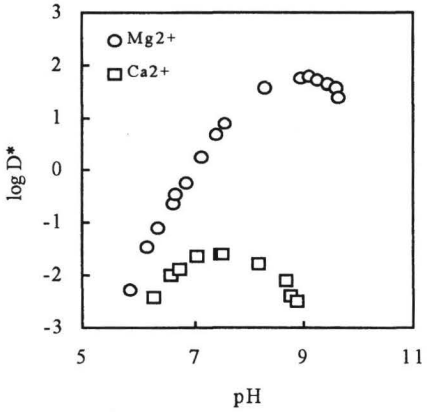


Figure 2. Extraction of Mg and Ca into cyclohexane with BFA and TBP in the presence of cryptand[2.2.1]. [BFA]o=[TBP]o=2.5X10^{-3} M, [L]=0.01 M.

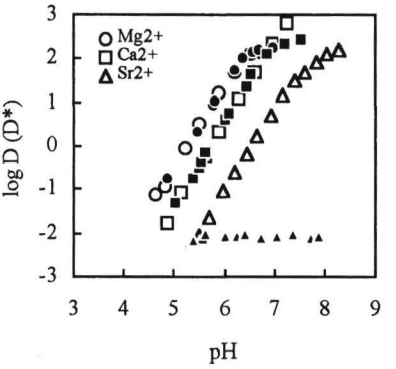


Figure 3. Extraction of Mg, Ca and Sr into cyclohexane with BFA and TBP in the absence (blank symbols) and presence (solid symbols) of cryptand[2.2.2]. [BFA]o=[TBP]o=0.015 M, [L]=0.01 M.

The application of cryptand[2.2.2] to the synergistic extraction of alkaline earths with BFA and TBP has been also examined. Figure 3 shows the results for the extraction of Mg, Ca and Sr into cyclohexane with 0.015 M BFA and TBP in the absence (blank symbols) and presence (solid symbols) of 0.01 M cryptand[2.2.2]. Very low and constant (about log D*?-2.0) extraction of Sr was observed over pH 5.2, while that of Mg and Ca are quite similar to those in the absence of cryptand[2.2.2]. By controlling the concentration of BFA and TBP, Sr can be separated quantitatively from Mg and Ca in the pH range 6.7 – 8.0, where more than 99% (log D*>2) of Ca and Mg are extracted into cyclohexane with slopes of +2, while more than 99% (log D*<-2) of Sr remains in the aqueous phase at the same time.

time.

Synergistic extraction of alkali metals with BFA and TOPO in the absence and presence of cryptand[2.2.1]

Cryptand[2.2.1] has been also applied to the synergistic extraction of alkali metals with BFA and TOPO. Because of the low synergistic effect of TBP for alkali metals, TOPO has been used as a synergistic reagent instead of TBP. Figure 4 shows the results for the extraction of Li and Na into cyclohexane with 0.1 M BFA and 0.03 M TOPO in the absence (blank symbols) and presence (solid symbols) of 0.01 M cryptand[2.2.1]. As shown in Figure 4, the distribution ratio of Na decreases rapidly over pH 7.5, while that of Li is quite similar to those in the absence of cryptand[2.2.1]. From this results, Na can be separated quantitatively from Li over pH 8, where more than 99% (log D*>2) of Li is extracted into cyclohexane with slope of +1, while more than 99% (log D*<-2) of Na remains in the aqueous phase at the same time.

Extraction species

The effect of BFA (HA) and TBP concentrations in the synergistic extraction of alkaline earths (M^{2+}) has been examined in order to clarify the extraction species. The effect of BFA and TOPO concentrations in the synergistic extraction of alkali metals (M^{+}) has also examined. From these results, the extraction species of alkaline earths were confirmed to be $MA_2(TBP)_2$, and that of alkali metals to be MA(TOPO).

Extraction parameters

In the synergistic extraction of alkaline earths (M^{2+}) with BFA (HA) and TBP, the extraction constant, $K_{ex,s}$, can be written as follows:

$$\text{Log } K_{ex,s} = \log D - 2pH - 2\log[HA]_o - 2\log[TBP]_o \quad (1)$$

where subscript o denotes the organic phase and D, $[MA_2(TBP)_2]_o / [M^{2+}]$, is the distribution ratio of alkaline earths.

The distribution ratios of alkaline earths in the presence of cryptand[2.2.1] or [2.2.2] (L), D*, can be expressed as follows:

$$D^* = K_{ex,s}[HA]_o^2[TBP]_o^2 / [H^+]^2\{1 + \beta[L]\} \quad (2)$$

where β is the complex formation constant of cryptand[2.2.1] or [2.2.2] with alkaline earths in the aqueous phase, defined as $[ML^{2+}]/[M^{2+}][L]$.
Dividing D by D* gives:

$$D/D^* = 1 + \beta[L] \quad (3)$$

The values of logβ were obtained from the straight portion of the plots in Figure 5 on the basis of Equation (3). The concentration of the neutral form of cryptands [L] is obtained by the first and the second acid dissociation constants, K_1 and K_2, and the initial concentration of cryptands,$[L]_{ini}$, as follows:

$$[L] = [L]_{ini}K_1K_2/ (K_1K_2 + K_1[H^+] + [H^+]^2) \quad (4)$$

On the other hand, in the synergistic extraction of alkali metals (M^+) with BFA (HA) and TOPO, the extraction constant, $K_{ex,s}$, and the distribution ratios of alkali metals in the presence of cryptand[2.2.1] (L), D*, can be expressed as follows:

$$\text{Log } K_{ex,s} = \log D - pH - \log[HA]_o - \log[TOPO]_o \quad (5)$$

$$D^* = K_{ex,s}[HA]_o[TOPO]_o/[H^+]\{1 + \beta[L]\} \quad (6)$$

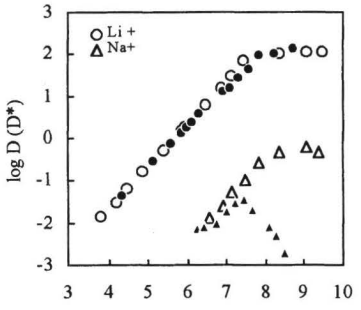


Figure 4. Extraction ofLi and Na into cyclohexane with BFA and TOPO in the absence (blank symbols) and presence (solid symbols) ofcryptand[2.2.1]. [BFA]o=0.1 M, [TOPO]o=0.03 M, [L]=0.01 M.

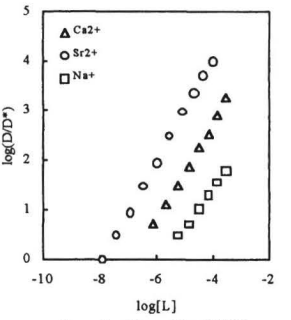


Figure 5. Plots of log(D/D*) vs. log[L] for Ca, Sr and Na.

The values of log $K_{ex,s}$ for alkali and alkaline earths calculated from Equations (1) and (2), and the values of logβ obtained from Equation (3) are summarized in Table 2. These values are in good agreement with those in Table 1.

Combining the chelating reagents and the macrocyclic ionophores, such as cryptand [2.2.1] and cryptand[2.2.2], having an opposite complexation tendency has been proved to be a powerful means to separate alkali and alkaline earths. This concept is universal and is of particular interest because it generates many opportunities for analytical and separation chemistry.

Table 2 Extraction parameters for alkali and alkaline earth metals

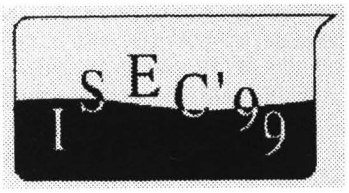
	$K_{ex,s}$	log β	log β*
(A) Mg	-3.50	---	<2.0
Ca	-4.60	6.85	6.95
(B) Ca	-4.24	---	4.4
Sr	-5.78	7.93	8.0
(C) Li	-3.50	---	2.50
Na	-5.60	5.40	5.40

* taken from ref.7.

REFERENCES

1 Umetani S, Matsui M and Tsurubou S, *J. Chem. Soc., Chem. Comm.*, 914, (1993)
2 Tsurubou S, Mizutani M, Kadota Y, Yamamoto T, Umetani S, Sasaki T, Le QTH and Matsui M Anal. Chem., **67**, 1465, (1995),
3 Sasaki T, Umetani S, Le QTH, Matsui M and Tsurubou S, *Analyst*, **121**, 1051, (1996)
4 Tsurubou S, Sasaki T, Umetani S and Matsui M, *Anal. Sci.*, **13**, 127, (1997)

6 Sasaki T, Umetani S, Matsui M and Tsurubou S, *Chem. Lett.*, 1195, (1994)
7 Lehn JM and Sauvage JP, *J. Am. Chem. Soc.*, **97**, 6700, (1975)



SOLVENT EXTRACTION OF BASE METAL CATIONS SUCH AS IRON(III) FROM HYDROCHLORIC ACID SOLUTIONS USING N,N'-SUBSTITUTED MALONAMIDES

MC Costa,[1] CE Fernandes,[2] MJ Hudson[3] and PB Iveson[3]

[1] UCTA, Universidade do Algarve, Campus de Gambelas, 8000 Faro, Portugal.

[2]Departamento de Química, Universidade da Madeira, Complexo científico pedagógico da Penteada, 9000 Funchal, Madeira, Portugal.

[3]Department of Chemistry, University of Reading, Box 224, Whiteknights, Reading RG66AD, UK.

ABSTRACT

The possibility of using new malonamides such as N,N'-dimethyl-N,N'-diphenyltetradecyl malonamide (DMDPHTDMA) for the extraction of base metals from hydrochloric acid solutions has been evaluated. It has been shown that Fe(III) may be selectively separated from other base metals such as Cu(II), Zn(II), Ni(II) from hydrochloric acid solutions of concentration greater than 4 M. Iron(III) is extracted as the tetrachloroferrate (III) anion $[FeCl_4]^-$. Spectroscopic data - IR, UV, NMR - suggest an ion-pair mechanism for HCl concentration equal or greater than 10 M in which the DMDPHTDMA is mono or diprotonated, while a solvation mechanism should be considered for lower acid concentrations. The effect of variables including acidity and chloride concentration are discussed in relation to the extraction data. Comparisons are made with extraction data from nitric acid media.

Overall DMDPHTDMA acts as a very weak base or ligand operating through an ion-pair or solvation mechanism, depending on the hydrochloric acid concentration.

Keywords: malonamides, ion-pair extraction, solvation, iron(III), hydrochloric acid.

INTRODUCTION

Recognising the need of alternative and efficient extractants to be used for hydrometallurgical purposes, our group decided to investigate the possibility of using newly synthesised malonamides, to recover base metals from acid chloride solutions. The increasing interest in extraction from this medium and the environmental advantages presented by diamides,[1-4] justified the present investigation. The studies developed until now have mainly considered the applicability of malonamides to the treatment of effluents from the nuclear industry.[3-8]

The ability of malonamides (RR`NCOCHR``CONRR`) to extract polyvalent metals can be explained by the weakly basic nature of the amide carbonyl group.[9] The selection of R, R` and R`` groups should follow two criteria: to allow the solubility of the diamide and its metallic complexes in the organic phase, and to facilitate the formation of metal complexes in the aqueous solution. To achieve these objectives R and R' must have different sizes. If R is a small group (typically CH_3), the steric hindrance around the carbonyl oxygen atoms is kept to a minimum and both oxygen's can co-ordinate to a metal ion.[4,5] The lipophilicity of the ligands is increased by the presence of alkyl or aryl groups at R` and R``. The non-substituted amides (for which R``=H) generally present a maximum of extraction that depends on the acid concentration, while substituted amides show a constant increase of the quantity of extracted solute. The low basicity of the amide carbonyl groups reduces the competition between HNO_3 and the metal when bonding to the extractant molecules.[10,11]

DMDPHTDMA, a substituted malonamide with the following structure (figure 1), was the object of the present investigation. In this molecule the above criteria are satisfied: R=CH_3; R`=C_6H_5 (phenyl); R``=$C_{14}H_{29}$. Previous studies with this compound [4,6,11] showed that DMDPHTDMA has less basic character than most of malonamides owing to the presence of the phenyl groups, which are bonded to the nitrogen atoms. This feature influences its extractive properties for the extraction of metallic nitrates from highly concentrated nitric media. DMDPHTDMA was found to be a good extractant of lanthanide(III) and actinide(III) ions from nitric acid solutions.[4,12] In a comparative study

© 2000 Society of Chemical Industry

it was found that DMDBTDMA (N,N'-dimethyl-N,N'-dibutyltetradecyl malonamide) and DMDCHTDMA (N,N'-dimethyl-N,N'-dicyclohexyltetradecyl malonamide) have a maximum of metal extraction (U(IV), Th(IV) and trivalent actinides) for HNO_3 concentrations between 7 M and 8 M, while for DMDPHTDMA the extraction increases continuously with the acid concentration.[6] The extraction of metal cations from nitric acid solutions is also enhanced when the extractant concentration increases. The dependence of extraction is almost linear with exception for HNO_3 concentrations lower than 1 M and low diamide concentrations. This can be explained by a change of mechanism. For low HNO_3 concentrations a solvation mechanism prevails while for higher concentrations the ion-pair is predominant.

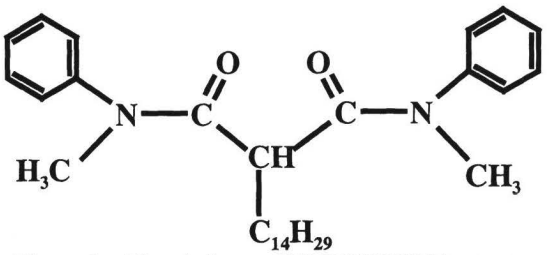


Figure 1 - The cis form of DMDPHTDMA structure

Crystallographic studies have been carried out on DMDPHMA (N,N`-dimethyl-N,N`-diphenyl malonamide) a similar ligand to DMDPHTDMA but without the long alkyl chain.[4] The structural studies of the lanthanide complexes indicated that both carbonyl groups were in the cis conformation and both were co-ordinated to the metal ions.

EXPERIMENTAL

The unalkylated malonamide was prepared by reaction of methylaniline and dimethylmalonate. Alkylation on the central carbon atom was achieved by reaction with sodium hydride and then with bromotetradecane. The synthesised compound (20% overall yield) was characterised by melting point, elemental analysis and by spectroscopic techniques (^{1}H NMR and IR) and the data obtained were in accordance with previously reported results.[4,13,14]

Extraction experiments were generally carried out by shaking the two phases for 15 minutes at a temperature of 25°C, with a ratio between aqueous and organic phases equal to 1. Solutions of DMDPHTDMA in CCl_4 (0.1 M and 0.5 M) were used as the organic phases. Hydrochloric acid solutions (1, 4, 5, 6, 8, 10 and 12 M) and metal feed solutions with 0.1 M iron(III), copper(II), zinc(II) or nickel(II) in HCl were used as aqueous phases. In all metal solutions the chloride concentration was maintained at 12 M by adding LiCl. In the HCl extraction studies the acid remaining in the aqueous phase was analysed by potentiometric titration with NaOH. The organic phases were analysed by IR and proton NMR spectroscopy. Analysis of the metal content before and after extraction was carried out in the aqueous phases by atomic absorption spectroscopy (Shimatzu AA 680). The charged organic phases were analysed by UV-visible spectroscopy (Shimatzu UV160).

RESULTS AND DISCUSSION

Hydrochloric acid extraction

With the present work our group tried, as a first approach, to establish parallels between the extractive behaviour of DMDPHTDMA in both nitric and chloride acid media.
An ion-pair mechanism for c_{HCl} ° 10 M and [DMDPHTDMA]=0.5 M, generically represented by:

$$DMDPHTDMA + HCl \text{ Ü } DMDPHTDMAH^{+}.Cl^{-} \quad (1)$$

and a solvation mechanism, for c_{HCl} È 10 M and [DMDPHTDMA] = 0.5 M:

$$DMDPHTDMA + HCl \text{ Ü } DMDPHTDMA.HCl \quad (2)$$

were suggested, since no evidence of diamide protonation was obtained in the latter case. This conclusion is supported by proton NMR and IR spectra presented in figures 2 and 3.

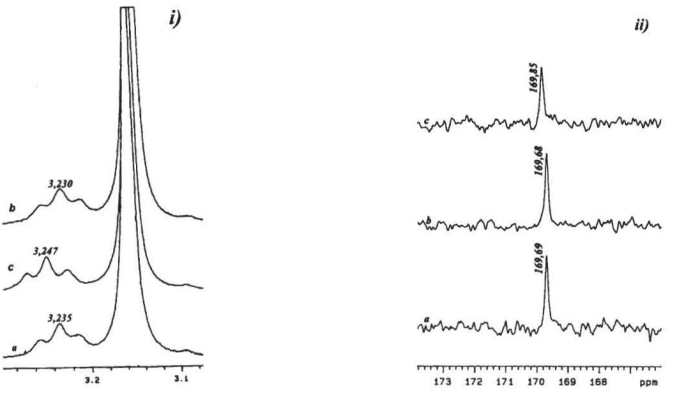


Figure 2 – A regions of ^{1H}NMR spectrum of DMDPHTDMA in CCl_4
i) - d_H values of the CH proton
ii) - d_C values of the carbonyl carbon
(a) - before contact
(b) - after contact with HCl 4 M
(c) - after contact with HNO_3 4 M

The occurrence of protonation, already proved in previous studies for HNO_3 medium (c_{HNO3} > 1 M),[6] causes a shift in the marked bands of spectra 2c that is not observed in the spectra after HCl 4 M contact (spectra 2b).[4] The IR spectra of the organic phase (figure 3) confirm these conclusions. The peaks at 1658cm^{-1} and 1678cm^{-1} can be attributed, respectively, to the vibrations of the aromatic ring and to the stretching of the carbonyl group.[4,13,14] The peak of a symmetrical stretch of the carbonyl group of the diamide -1678cm^{-1}- shows a decrease in the transmittance, T, in comparison with the same band of the free amide (figure 3a) after contact with HCl solutions of 10M (figure 3c) and 12M. This feature is consistent with the expected protonation, which is reported to cause a decrease in the intensity of the carbonyl peak and the appearance of bands corresponding to the hydroxyl group.[5] In fact, the increase in the dielectric constant of the organic phase, since more acid is extracted, favours the proton transfer to the diamide.[15] For c_{HCl} < 10M there is no difference in the spectra, as could be seen in figure 3b[+]. In those cases the amount of acid extracted is low which favours the solvation over the ion-pair mechanism and causes no difference in the IR and NMR spectra. The following species $(MA)_2HCl$, (MA).HCl, $(HMA)^{+}Cl^{-}$ $(HMA)^{+}Cl^{-}$.HCl and $(H_2MA)^{2+}(Cl^{-})_2$, similar to those already identified in previous studies for nitric acid media, are suggested.[4,11] Studies of the distribution coefficient, D, with respect to HCl extraction will be done to confirm this hypothesis and will be reported.

[+] Spectra after contact with HCl of all concentrations from 4 M and 12 M were obtained.

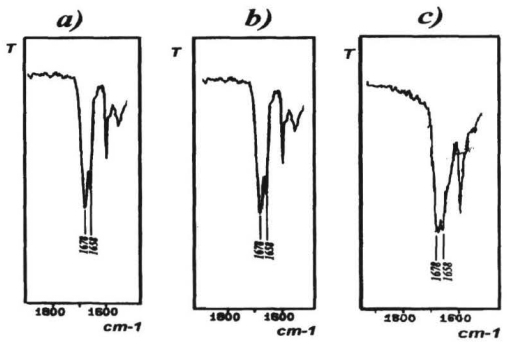


Figure 3 - A region of IR spectra of DMDPHTDMA in CCl_4 (a) and after contact with HCl 4 M (b) and 10 M (c).

In the solvation mechanism there is probably the formation of hydrogen bonds between the oxygen of the carbonyl group and the HCl molecules, as it was previously suggested for HNO_3 medium.[4,11] No acid extraction was detected for $c_{HCl} < 4$ M, even after several hours of contact between the two phases.

Extraction of metals

The efficiency and selectivity of DMDPHTDMA for the extraction of some basic metals - Fe(III), Cu(II), Zn(II), Ni(II) - usually present in pregnant leaching solutions was studied.
The analysis of the aqueous solution after contact with the organic phase showed that iron(III) was extracted from HCl solutions - with 12 M total chloride concentration - with an acid concentration higher than 4 M (figure 4). For $c_{HCl} > 4$ M iron(III) ion is completely removed while no extraction occurs for $c_{HCl} \leq 4$ M. This behaviour is similar to that previously observed for other malonamides: DMDCHTDMA, DEDCHTDMA (N,N`-diethyl-N,N`-dicyclohexyltetradecyl malonamide) and DIPDCHTDMA (N,N`-diisopropyl-N,N`-dicyclohexyltetradecyl malonamide).[16] No extraction was detected for the other basic metals (Cu(II), Zn(II) and Ni(II)). The same results were obtained when no other chloride than the acid was added to the solution. The selectivity for Fe(III) over the other mentioned ions is very promising considering that in some hydrometallurgical processes, zinc and copper are co-extracted together with iron.[17,18] Moreover, taking into account that iron is frequently used as a leaching agent, as $FeCl_3$, the selective extraction of this metal makes possible its recovery and eventual reutilization.

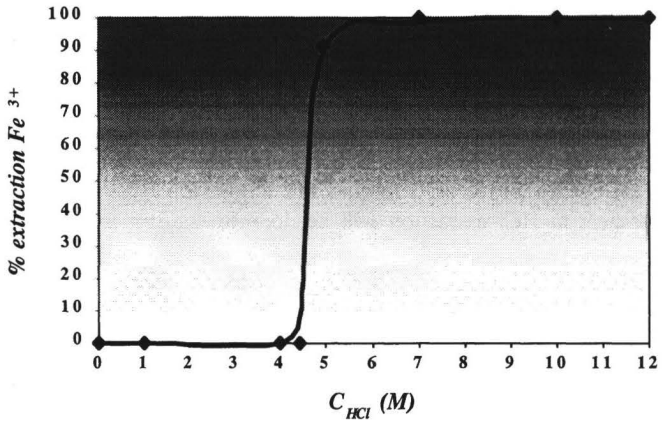


Figure 4 - Extraction of Fe^{3+} from HCl solutions by DMDPHTDMA

UV-visible spectroscopy was used to identify the $[FeCl_4]^-$ species in the organic phases after extraction (figure 5). $[Fe(H_2O)_6]^{3+}$ was identified as the predominant species in HCl solutions with acid and total chloride concentrations lower than 4 M. This explains why no extraction was observed from these solutions. For acid solutions with $c_{HCl} > 4$ M the $[FeCl_4]^-$ species prevails and, therefore, the extraction is possible.

The extraction mechanism involves the transfer of the iron complex to the organic phase in the form of the following structures $DMDPHTDMA.H^+FeCl_4^-$ (solvation mechanism) and $DMDPHTDMAH^+.FeCl_4^-$ or $DMDPHTDMAH_2^{2+}.(FeCl_4^-)_2$ (ion-pair mechanism). There is other evidence confirming this hypothesis:

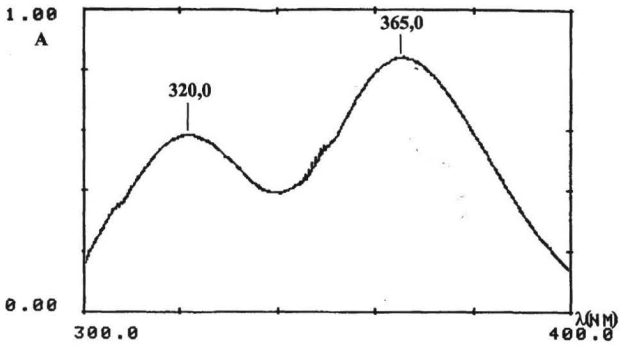


Figure 5 - UV-vis spectrum of DMDPHTDMA 0.1M after contact with iron (III) (0.01M) in HCl 12M solution*.

1) when HCl was replaced by LiCl, for a total chloride concentration of 8 M, iron is still extracted. However, when NaCl replaced the acid, no extraction was observed. Lithium is small and thus can possibly act in a similar way to a proton, giving a mechanism similar to protonation:

$$DMDPHTDMALi^+Cl^-_{(org)} + Li^+FeCl_4^-_{(aq)} \text{ Ü } DMDPHTDMALi^+.FeCl_4^-_{(org)} + Li^+Cl^-_{(aq)} \quad (3)$$

In any case the co-ordination mechanism should also be considered:

$$DMDPHTDMA_{(org)} + Li^+FeCl_4^-_{(aq)} \text{ Ü } DMDPHTDMA.Li^+FeCl_4^-_{(org)} \quad (4)$$

The larger radius of sodium does not allow this phenomenon to occur and so no extraction was observed.

2) when HCl was substituted for HNO_3, for a total chloride concentration of 10 M, the percentage of metal extracted was much lower (33%). This behaviour can be explained by the lack of formation of anionic nitrocomplexes for $c_{HNO3} < 9$ M.[16]

Preliminary stripping assays

Stripping of iron(III) from the organic phase was accomplished with contact with water or diluted HCl solution allowing complete iron removal. The stripping reaction can be represented by equations (5) or (6), depending on the mechanism formerly verified for metal extraction:

$$DMDPHTDMAH^+.FeCl_4^-_{(org)} + 6H_2O \text{ Ü } DMDPHTDMA_{(org)} + [Fe(H_2O)_6]^{3+}(Cl)_{3(aq)} + HCl_{(aq)} \quad (5)$$

$$DMDPHTDMA.H^+FeCl_4^-_{(org)} + 6H_2O \text{ Ü } DMDPHTDMA_{(org)} + [Fe(H_2O)_6]^{3+}(Cl)_{3(aq)} + HCl_{(aq)} \quad (6)$$

* Similar spectra were obtained after contact with Fe^{3+} in HCl solutions from 5M to 12M.

CONCLUSIONS AND PERSPECTIVES

The results obtained for HCl extraction, supported by proton NMR and IR spectroscopy, suggest two extraction mechanisms: an ion-pair mechanism for $c_{HCl} > 10M$ and a solvation mechanism (probable formation of hydrogen bonds between the acid and the carbonyl oxygen) for lower acid concentrations, as have already been proposed for HNO_3 medium.

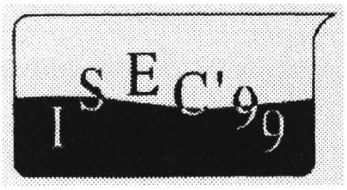
Among the base metals studied (iron, copper, zinc and nickel) only iron(III) was completely extracted from HCl solutions at concentrations higher than 4M.

UV-visible spectroscopy proved that iron was extracted in the form of a chloro anion complex, $[FeCl_4]^-$, which is in agreement with the two mechanisms previously suggested.

Further work should be done to clarify the occurrence of these two mechanisms, the structure of the adducts and the selectivity of the extractant over other trivalent ions. A measure of the dielectric constant of the organic phases after acid contact and the determination of distribution coefficients will be a valuable contribution to this investigation.

REFERENCES

1. Dalton RF, Diaz G, Price R, Zunckel AD, *J. Metals*, **8**, 16, (1991).
2. Abe Y, *Proceedings of ISEC`90*, Japan eds. T. Sekine, S. Kusakabe, 1127, (1990).
3. Musikas C, Hubert H, *Solv. Extr. Ion Exch.*, **5**, 877, (1987).
4. Spjuth L, Liljenzin JO, Skalberg M, Hudson MJ, Chan GYS, Drew MGB, Iveson PB, Madic C, *J. Chem. Soc. Dalton Trans.*, 649, (1997).
5. Byers P, *PhD Thesis*, University of Reading, 1996.
6. Spjuth L, Liljenzin JO, Skalberg M, Hudson MJ, Chan GYS, Drew MGB, Feaviour M, Iveson PB, Madic C, *Radiochimica Acta*, **78**, 39, (1997).
7. Musikas C, *Sep. Sci. Technol.*, **23**, 1211, (1988).
8. Siddall TH, *J. Inorg. Nucl. Chem.*, **25**, 883, (1963).
9. Tian Q, Hughes MA, *Hydrometallurgy*, **36**, 79, (1994).
10. Cuillerdier C, Musikas C, Hoel P, Nogond L, Vitart X, *Sep. Sci. Technol.*, **26**, 1229, (1991).
11. Tian Q, Hughes MA, *Hydrometallurgy*, **36**, 315, (1994).
12. Nigond L, Musikas C, CuillerdierC, *Solv. Extr. Ion. Exch.*, **12**(2), 297, (1994).
13. Silverstein RM, Bassler GC, Morril TC, *Spectrometric Identification of Organic Compounds*, 5th ed., John Wiley and Sons, New York, 1991.
14. Bellamy LJ, *The IR Spectra of Complex Molecules*, 2nd ed., Chapman and Hall, 1980.
15. Thiollet G, Musikas C, *Solv. Extr. Ion Exch.*, **7**, 813, (1989).
16. Chalmers PD, *MSc Dissertation*, University of Reading, 1995.
17. Monhemius J, *Chem. Ind.*, 410, 20th June 1981.
18. Nogueira ED, Regife JM, Blythe PM, *Chem. Ind.*, 63, 19th January 1980.



RECENT ADVANCES IN STRUCTURE–REACTIVITY STUDIES OF SOLVENT EXTRACTANTS IN METAL EXTRACTION

CY Yuan, SS Li, SG Yuan and HL Ma
Shanghai Institute of Organic Chemistry, Chinese Academy of Sciences, Shanghai, China

ABSTRACT
Various approaches including HSAB principle, computational chemistry, involving cluster analysis and factor analysis, theoretical chemistry, consisting quantum mechanics calculation and molecular mechanics as well as QSAR are applied to the structure-reactivity studies of organic extractants in metal extraction. Several new synergistic extraction systems are also reported.

Keywords: extractants, HSAB principle, computational chemistry, molecular mechanics, QSAR studies, synergism

INTRODUCTION

Quantitative molecular design of organic extractants, in very practical term, contributes both to discovery of new selective extractants and to the progress of extraction chemistry in general. One understandable objective in the application of the progress of solvent extraction to the separation of metal is to obtain a maximum selectivity for a given metal. Development of such new extractants, up to now, is usually studied by the screening method, which requires a large amount of investment and labour. A much more effective way should be available if one follows the quantitatively relationship between chemical structure and the extraction properties of organic extractants. This is the basis for quantitative molecular design. Recent progress in computational and theoretical chemistry provides powerful tools in such studies.

RESULTS AND DISCUSSIONS

HSAB Principle and structure modification

Metal extraction may be considered simply as the replacement reaction of water molecule in the hydration shells of metallic ions in aqueous solution by an organic ligand (extractant), Both metal ions (acceptor) and coordinating atoms (donors) are classified as hard, soft and borderline acids and bases according to the Pearson scale. Oxygen containing ligands (ether, alcohol, carboxylate, phosphate and phosphonate) are referred to as hard bases, which prefer to coordinate with hard acids such as lanthanides, actinides, niobium, tantalum, zirconium and hafnium. As soft bases, sulfur-containing ligands (thioether, thiourea, thio-carboxylate or dithiophosphate) prefer to combine with soft acids such as copper, gold, silver, platinum, palladium or mercury. A nitrogen-containing ligand e.g. aniline or pyridine, being a borderline base, reacts smoothly with a borderline acid such as iron, cobalt, nickel, ruthenium and rhodium.

The hardness of donor atoms can be modified by the inductive or conjugation effect of the neighboring atom or group. An aliphatic hydroxyoxime, being a hard base, possesses poor ability for extracting Cu (borderline acid) at pH 2. An aromatic hydroxy-oxime, on the other hand, owing to the presence of a conjugated system, especially in the presence of an electron withdrawing group on the benzene ring, the hardness of the base is decreased dramatically and the extraction ability of Cu will be enhanced accordingly. It is evident that the HSAB principle is helpful for the prediction and design of effective solvent extractant in an empirical way.[1]

Computational chemistry in solvent extraction

Since metal extraction is based on the formation of complex by organic ligands with metal ions or corresponding ionic species, may be regarded as a multi-component coordination process

© 2000 Society of Chemical Industry

between heterogeneous phases, it is therefore reasonable to understand the limitation of structure-reactivity studies based on universal analysis. To overcome this imperfection, the application of pattern recognition gave however some promising results. Meanwhile, various methods of multivariate analysis were developed rapidly in recent years as an effective way to extract valuable information from multi-dimensional data and has been applied extensively to chemistry. As one of the new approaches to the molecular design of extractants we have reported the application of cluster analysis and factor analysis to structure-reactivity studies of acidic phosphorus esters in extraction of neodymium, samarium, ytterbium and yttrium as representatives of light, medium and heavy rare earths.[2]

In our study, two of the most common methods of cluster analysis, i.e. Hierarchical Cluster and Minimal Spanning Tree were used. Bin the Hierarchical Cluster method, it is necessary to calculate first the Euclidean distances between all possible pairs of points from the original data. These distances are usually arranged in a matrix with which a connection dendrogram, which is a hierarchy of points ordered by the relative distance between points, may be generated. The vertical axis is labeled the similarily value and the more similar the compounds, the higher and nearer to a unit is their similarily value. Large jumps in similarily value indicate the difference in the type of compounds. It is reasonable to make the boundary of the clusters.

This resulted in four clusters and the first cluster was clearly divided into two sub-clusters. The Minimal Spanning Tree method is an imaginative diagrammatic method, by which all points are connected together in a single "tree", where the sum of the lengths of "branches" is minimal. Therefore, the longest branches of this tree correspond to the linkage between different clusters. The selection of there longest branches is, however, made by pruning as few branches as possible, and allowing the length of any branch in the same group to be less than double the mean length of the cluster. In the case of the seventeen acidic phosphorus esters studied, four clusters were obtained by this method. This result is coincident with that obtained by the Hierachical Cluster method.

Cluster analysis helps to classify these compounds in hyperspace, however, it can hardly display clearly their relationship. At the present time, several available methods, including Eigenvector Projections and Nonlinear Mapping, can be used to project the multidimensional space into a two- or three-dimensioned space with the maintenance of the original spatial relationships.

Eigenvector projection reflects the relationship in the hyperspace with less distortion, and eigenvector analysis of the hyperspace results in a new coordinate system where the axes are eigenvectors. The result of analysis showed that the first two eigenvectors contain 99.88% of the total variance. Consequently, the result of the Minimal Spanning Tree methods displays concisely and visually the relationship between structure and behaviour of the compounds investigated.

On the basis of the above studies further investigation was made by factor analysis. The extraction equilibrium constants of compounds investigated can be calculated by the following equations:

$(\log K_{ex})_{Nd,i} = -3.80f_{1,i} + 0.28f_{2,I}$ $\quad$ $(\log K_{ex})_{Sm,i} = -2.92f_{1,i} + 1.49f_{2,i}$

$(\log K_{ex})_{Y,I} = -1.01f_{1,i} + 3.65f_{2,I}$ $\quad$ $(\log K_{ex})_{Yb,i} = -0.24f_{1,i} + 5.08f_{2,i}$

Theoretical chemistry in solvent extraction

The reactivity of coordinating atom or group can be represented by charge density or bond order calculated by quantum chemical methods. In some cases, the PMO method is helpful in evaluating the relationship between ionization constant and distribution of π-electrons of aromatic base and acid.[3] Our laboratory is the first research group working on the structure-reactivity studies of solvent extractants based on Huckel molecular orbital method including EMO, EHMO, CNDO and MNDO.[4,5] As shown by charge density calculation, as expected qOH is very important for acidic phosphorus esters in rare earth extraction. However, the contribution of qO cannot be neglected. In transition metal extraction by hydroxyoxime type chelating agents, besides qOH, the contribution of qN in the oximido group is also important. With the aid of MNDO method, Rozen investigated the structure-reactivity relationship of extractants,[6] but he was unable to get distinct results as his work was not based on the most stable configuration. However, by molecular mechanics calculation we

studied the structure-reactivity relationship based on the most stable configuration of extractants under investigation.[7,8] In general, various molecular orbital calculation methods provide data related to charge density of atoms in functional group. On the other hand, molecular mechanic calculation is a powerful tool to evaluate the contribution of steric effects of the molecule based on energy calculation.

Table 1 $E_{s,ex}$ Values of alkyl and alkoxyl groups calculated by molecular mechanics (kcal mol^{-1})

R	R			RO		
	ΔE_{LSE}	$\Delta\Delta E_{LSE}$	$E_{s,ex}$	ΔE_{LSE}	$\Delta\Delta E_{LSE}$	$E_{s,ex}$
CH_3	4.5890	-0.0737	-0.037	2.9348	0.0	0.0
C_2H_5	4.6627	0.0	0.0	2.9410	0.006	0.003
C_3H_7	4.6764	0.0137	0.007	1.9406	0.006	0.003
i-C_3H_7	5.1053	0.4326	0.216	2.9757	0.041	0.021
n-C_4H_9	4.6834	0.0207	0.010	2.9405	0.006	0.003
i-C_4H_9	4.7682	0.1055	0.053	2.9638	0.029	0.015
s-C_4H_9	5.1546	0.4919	0.246	3.1395	0.204	0.102
t-C_4H_9	5.7516	1.0889	0.545	--	--	--
n-C_5H_{11}	4.6825	0.0198	0.010	0.9478	0.013	0.007
n-C_6H_{13}	4.6833	0.0196	0.010	2.9515	0.017	0.008
cycl-C_6H_{11}	5.0981	0.4359	0.218	--	--	--
n-C_7H_{15}	4.6825	0.0205	0.0	2.9556	0.021	0.010
n-C_8H_{17}	4.6845	0.0218	0.011	2.9596	0.025	0.012
i-C_8H_{17}*	4.8347	0.1720	0.086	2.9810	0.046	0.023
s-C_8H_{17}	5.2162	0.5535	0.277	3.2732	0.338	0.169
n-$C_{12}H_{25}$	--	--	--	2.9763	0.042	0.021

* i-C_8H_{17} is $C_4H_9CHEtCH_2$-

The molecular mechanics calculations (Allingers MM2 Program) were successfully used in our laboratory to study the steric effect of substituents (R and Ro) on extraction of metals (Ni, Co, RE) by acidic phosphorus ethers. Some parameters for phosphorus that were not included in MM2 were estimated and used to reproduce the known structure of some phosphorus compounds with satisfactory results.

For the evaluation of the steric effect of substituents, dialkyl t-butylphosphate or phosphinate was proposed as model structure for the simulation of the steric enviroment of complexes. The optimum geometry of these compounds was determined by molecular mechanics program. It was found that the difference of the local steric energy of hydroxyl oxygen in these two structures is closely correlated with the degree of the size of substituents and can thus be used as a measurement of the steric effect of the substituents($E_{s,ex}$) (Table 1).[9]

QSAR in solvent extraction

For quantitative structure--reactive relationship (QSAR) study, as the result of our systematic investigations, an equation for regression analysis was introduced by us.[10]

$$\log K_{ex,M} = \rho\Sigma\sigma + \delta\Sigma Es + \varepsilon \log P + c$$

where σ is the polar parameter, as shown by us, the polar substituent effect in organophosphorus compounds parallels that of carbon compounds;[11] Es is the parameter that is related to the configuration of the complex formed during extraction process. P is the partition constant of the ligand. Based on numerous experimental data we introduced specific Es parameters for R and RO groups of extractant molecule in extractive separation of rare earths,[12] cobalt and nickel [13,14] that are successfully used in QSAR study in solvent extraction.

For the illustration of such QSAR studies, the results of multiple regression of metal extraction by acidic phosphorus compounds is shown in Table 2.

Table 2 Multiple regression of metal extraction reaction by acidic phosphorus compounds
$\log K_{ex,M} = \rho\Sigma\sigma + \delta\Sigma Es + \varepsilon \log P + c$

M	ρ	-δ	-ε	c	RMS	r^2	T_ρ	$-T_\delta$	$-T_\varepsilon$	n
Co^{2+}	0.341	1.012	0.159	4.498	0.106	0.915	3.314	4.970	4.464	19
Ni^{2+}	1.984	2.696	0.259	2.607	0.494	0.913	3.850	2.376	1.561	19
Nd^{3+}	3.601	4.327	1.543	7.291	0.532	0.939	4.573	1.778	3.224	8
Sm^{3+}	3.036	4.972	1.757	9.096	0.607	0.928	3.973	1.792	3.216	8
Y^{3+}	2.982	6.244	1.743	11.282	0.603	0.928	3.927	2.263	3.211	8
Yb^{3+}	2.766	5.707	1.754	11.691	0.547	0.935	4.056	2.302	3.598	8

RMS = root mean square error: r = correlation coeffecient: $T_\rho, T_\delta, T_\varepsilon$ = T-test for terms of ρ,δ and ε respectively.

Synergism in solvent extraction

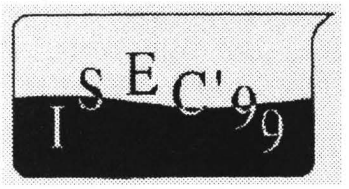
The synergistic effect of extraction of uranium by D2EHPA and TBP was reported in the early 60's. The mechanism of such effect was explained by ligand exchange or ligand substitution of metal complexes. In recent years, significant progress was achieved by binary extraction systems.[15,16] As found by us a mixture consisting Cyanex 272 [bis(2,4,4-trimethylpentyl)phosphinic acid,Cytec Industries] and C-274 (an organic monobasic acid bearing stereospecific alkyl chains) provides excellent extraction performance in heavy rare earth separation in particular thulium, ytterrbium and lutetium.[17] Preliminary investigation indicated that this system possesses characteristics of synergistic extraction. The mechanistic study of this system is under investigation. A new type synergistic binary extraction system involving dialkyl(aryl)sulfide and an acidic component as kinetic catalysts for selective extraction of gold and palladium from precious metals mixture was also reported.[18]

ACKNOWLEDGEMENT

This project was supported by the National Natural Science Foundation of China.

REFERENCES

1 Yuan CY *Proceedings ISEC'80,* Liege-Belgium, Paper No.80-81, (1980).
2 Yuan SG and Yuan CY *Kexue TongBao* (Eng.ed.) **33**,1182, (1988).
3 Li SS and Yuan CY *Acta Chimica Sinica*, **40**, 97, (1982).
4 Yuan CY, Zhou CM and Chen KC *Acta Chimica Sinica*, **39**, 699, (1981).
5 Yuan CY *J.Chin. Rare Earth Society,* **1**, 78, (1983).
6 Rozen AM and Krupnov BV *Russian Chem.Rev.* **65**, 973, (1996).
7 Li SS and Yuan CY *Acta Physico Chemica Sinica*, **5**, 56, (1989).
8 Li SS and Yuan CY *Nuclear Science and Technology*, **23**, 38, (1989)
9 Yuan CY, Li SS, Yuan SG *Solvent Extraction, Proc. ISEC'90* (Ed.T.Sekine) Elsevier Sci. 321, (1992).
10 Yuan CY and Hu SS *Scientia Sinica,* (B) **31**,137, (1988).
11 Yuan CY, Li SS, Hu WX and Feng HZ *Heteroatom Chem.* **4**,23, (1993).
12 Yuan CY, *J. Chin. Rare Earth Society*, **1**,13, (1983).
13 Yuan CY, Yuan SG, Hu SS. *Acta Chimica Sinica* **45**, 625, (1987).
14 Yuan CY, Xu QR, Yuan SG, Long HY and Shen DZ *Solv.Extr.and Ion Exch.* **6**, 393, (1988).
15 Yuan CY and Ma HL *U.S. Patent 5,622,679* (Apr.22,1997).
16 Yuan CY and Ma HL *U.S. Patent 5,639,433* (Jun.17,1997).
17 Yuan CY, Ma HL, Pan C and Rickelton WA *Value Adding through Solvent Extraction, Proc ISEC'96* (Ed D.C.Smallcross) University of Melbourne, Australia **1**, 733, (1996).
18 Ma HL, Yuan CY and Li SS *Chinese Patent CN 1039135C* (July 15, 1998).



EXTRACTION STUDIES AND *AB INITIO* CALCULATIONS OF SOME SUBSTITUTED MALONAMIDES

L Spjuth[1], JO Liljenzin[1], MJ Hudson[2], MGB Drew[2], PB Iveson[2] and C Madic[3]

[1] Department of Nuclear Chemistry, Chalmers University of Technology, S-41296 Göteborg, Sweden.

[2] Department of Chemistry, University of Reading, Box 224, Whiteknights, Berkshire, RG6 6AD, UK.

[3] CEA-Valrhô, Marcoule, BP171, 30207 Bagnols-sur-Cèze, France

ABSTRACT

The extraction ability for Am(III) and nitric acid with four different malonamides is presented together with experimentally determined basicities and calculated gas-phase basicities. The highest metal extraction was achieved with the ligands of lowest basicity. The relative order of calculated basicities, using *ab initio* methods, showed to be in good agreement with experimentally determined basicities.

Keywords: malonamides, *ab initio* calculations, americium(III)

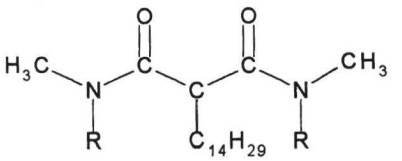
INTRODUCTION

Malonamides have been suggested as suitable co-extractants for the minor actinides and lanthanides in advanced reprocessing of spent nuclear fuel [1,2]. The long-lived minor actinides are then to be separated from the lanthanides and transmuted to short-lived nuclides in a reactor or an accelerator-driven sub-critical system. It is therefore important to study the chemistry and extraction behaviour of the malonamides. The extraction efficiency of the malonamides is considered to be related to both electroinductive effects and to steric hindrances around the binding site[1]. The influence of the different malonamide structures on both metal and nitric acid extraction has therefore been studied and the extraction is related to the basicity of the malonamide. Gas-phase basicities have been calculated using *ab initio* methods (Gaussian 94 software).

EXPERIMENTAL

Reagents

The different malonamides that have been studied experimentally all have the same general structure, but differ in the nitrogen substituent, R.



R	Abbreviation
phenyl	DMDPHTDMA
cyclohexyl	DMDCHTDMA
4-chlorophenyl	DMD(pClPH)TDMA
butyl	DMDBTDMA

Table 1. The different malonamides investigated.

© 2000 Society of Chemical Industry

All the malonamides, except DMDBTDMA, were synthesised at the University of Reading and their purity checked by ^{1}H-NMR, elemental analysis and melting point[3]. DMDBTDMA, 99% purity, was purchased from Panchim, France. *Tert*-butylbenzene (TBB), 99% purity, was used as the diluent in all experiments and was purchased from Acros.

Experimental Procedure

The metal extractions were carried out in 3.5 mL test-tubes by contacting equal volumes of organic and aqueous phase for 5 minutes. The aqueous solutions contained different nitric acid concentrations and 0.1M solutions of the malonamides dissolved in *tert*-butylbenzene (TBB) were used as the organic phase in the extractions. After centrifugation, samples of each phase were withdrawn for analysis. γ-Spectrometry with a HPGe-detector (EG&G ORTEC) was used to determine the ratio of the radioactivity in the two phases (D-value) when metal extraction was considered. For the nitric acid extractions, samples from each phase after extraction equilibrium were titrated with 0.1M NaOH. The organic phase was titrated in ethanolic media.

The basicities of the malonamides were determined by titrations in acetic anhydride media, using 0.1M $HClO_4$ in anhydrous acetic acid as the titrand. The outer salt-bridge in a double junction Ag/AgCl reference electrode was changed to 0.1M $LiClO_4$ in acetic anhydride.

RESULTS AND DISCUSSION

The protonation of the malonamide is an important issue when considering the metal extraction from relatively high nitric acid concentrations. During the extraction, the proton and the metal ion are competing for the same binding sites in the malonamide, the carbonyl oxygen atoms. Previous studies have shown that protonation occurs on the carbonyl oxygens rather than on the nitrogen atoms[4]. *Ab initio* calculations performed on protonated malonamides supports these results.

Structure	C=O-H^+ (hydrogen bonded)	C=O-H^+	N-H^+ (hydrogen bonded)
DMDPHMA H^+	-913.296 a.u.	-913.287	-913.262
DMDPHMA $2H^+$	-913.519	-913.526	-913.476
DMDCHMA H^+	-920.293	-920.280	-920.270
DMDCHMA $2H^+$	-920.513	-920.520	not calculated

Table 2 Calculated energies (a.u.) for different protonation conformations with Gaussian 94 HF/6-31G*.

Model structures were built from the molecular conformations found in crystal structures of related compounds and then geometry-optimised with the Gaussian software. As seen in table 2, protonation on the nitrogen results in the highest energy for each species, which is the least stable conformation. The energetically most favourable conformation is when the malonamide is monoprotonated on a carbonyl oxygen atom and hydrogen bonded to the other carbonyl oxygen. The diprotonated forms are in their most stable conformations when they are not hydrogen-bonded.

Metal extraction and nitric acid extraction are assumed to be related to the basicity of the molecule. Low basicity of the ligand is considered to give good metal extraction since the competition between proton and metal ion is less severe than with a more basic ligand. The basicity of a few malonamides has therefore been determined experimentally by titrations in acetic anhydride media. The potential at the half-neutralisation volume (HNP) was taken as a measure for basicity. Figure 1 shows the titration curves for four different malonamides and the HNP's are listed in table 3. The higher the potential at the HNP the less basic the molecule. The 4-chlorophenyl substituted malonamide is thus the least basic malonamide and the cyclohexyl- and butyl- substituted

malonamides are the most basic ones.

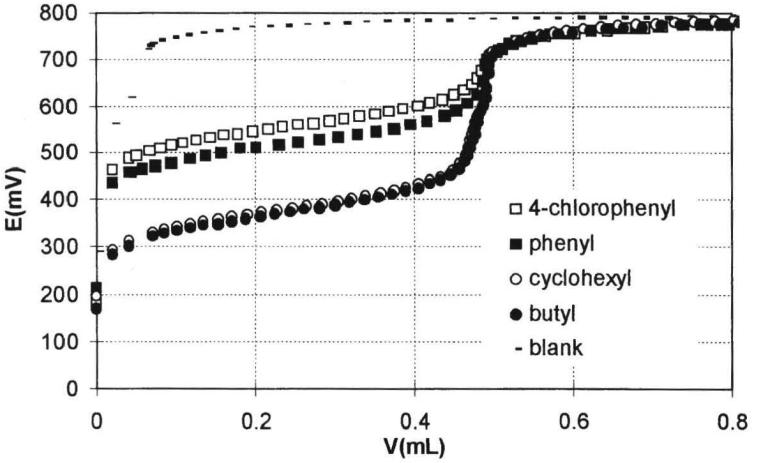


Figure 1 Titration with 0.1M $HClO_4$ in acetic acid, acetic anhydride media of four malonamides, $(CH_3\text{-}NR\text{-}C{=}O)_2\text{-}CH\text{-}C_{14}H_{29}$, with different nitrogen substituents (R).

R	HNP (mV)
4-chlorophenyl	557±0.5
phenyl	520±2
cyclohexyl	372±6
butyl	369±5

Table 3 HNP for the different malonamides studied. The potential is adjusted with an external reference (butaneamide).

These basicity data are consistent with earlier extraction studies[3]. The metal extraction shows a decrease in extraction for the cyclohexy- and butyl- substituted malonamides at high nitric acid concentration, figure 2. This could be due to the higher basicity for these ligands and thus the competition between protons and metal for the binding site is more severe than for the less basic molecules. The 4-chlorophenyl and phenyl- derivatives are less basic and do not show this decrease in extraction at high nitric acid concentration. The nitric acid extraction, figure 3, also shows the same tendency; that is the highest nitric acid extraction for the cyclohexyl- substituted malonamide and lowest for the least basic ligand, the 4-chlorophenyl derivative.

Some *ab initio* calculations were carried out to investigate if calculated gas-phase basicities could be related to the experimentally determined basicities. Gas-phase basicity is defined as the negative of the Gibbs free energy of the protonation reaction: $L + H^+ \leftrightarrow LH^+$, where L is the ligand. The more negative the ΔG the more basic the molecule. The method for calculating the free energies for the protonation reaction at 25°C is well established [5-7]:

$$\Delta G_R = \Delta H_R - T\Delta S_R$$

$$-T\Delta S_R = -298.15[S(LH^+) - S(L) - S(H^+)]$$

$$\Delta H_R = E(LH^+) - E(L) - E(H^+) + \Delta(PV)$$

$$E = E_{elec} + E_{ZPE} + (E - E_0)$$

E_{elec} is the energy of the geometrically optimised structure at 0K, E_{ZPE} is the zero-point energy and (E - E_0) is the energy difference between 0 and 298.15K. The zero-point energies are adjusted by the correction factor of 0.91 [5-7]. The electronic energy for the proton is zero and the only energy term that contributes to $E(H^+)$ is the translational energy which is equal to 3/2RT. Since one mole of gas disappears in the reaction the Δ(PV) term is equal to -RT and the entropy term of a free proton is equal to 7.76 kcal/mol [5-7].

$$\Delta H_R = E(LH^+) - E(L) - 3/2\ RT - RT = E(LH^+) - E(L) - 0.889\ \text{kcal/mol}$$

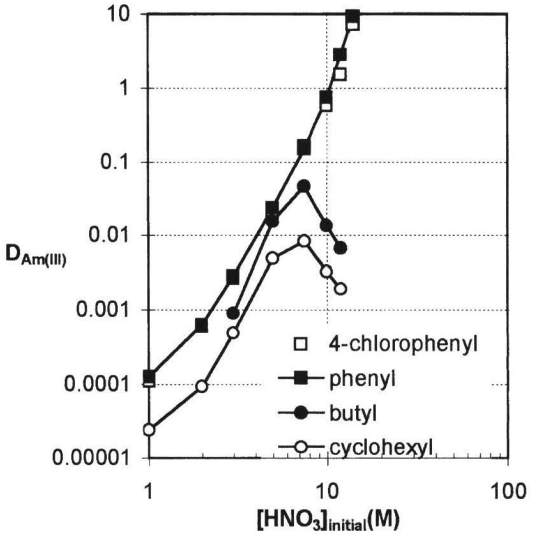


Figure 2 Extraction of Am(III) by 0.1M of the four different malonamides studied in TBB (room temperature).

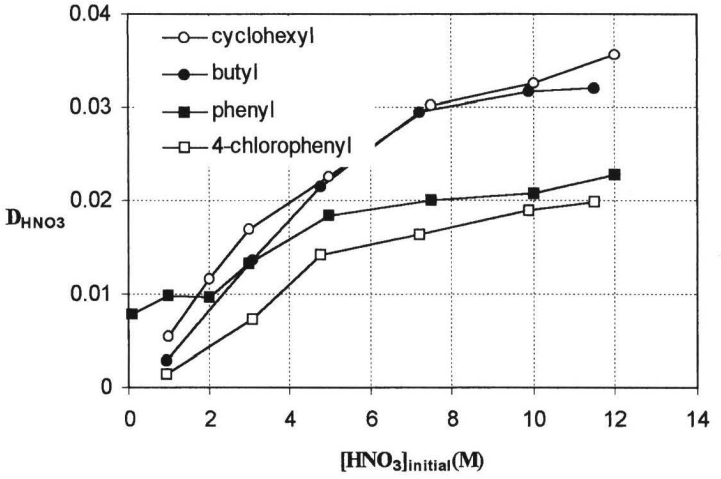


Figure 3 Nitric acid extraction with 0.1M of the four different malonamides studied in TBB (room temperature).

The energies and entropies for the unprotonated (L) and protonated (LH^+) malonamides were obtained from frequency calculations preceded by a full geometric optimisation, using the Gaussian 94

software. The 3-21G basis set was used in the geometry calculations and 6-31G* was used for the frequency calculations. All computations were carried out on Silicon Graphics Origin 2000 at Reading University.

The calculated ΔG values in table 4 are ordered from the least basic, -215.30 kcal/mol, to the most basic structure, -230.71 kcal/mol. The long carbon chain at the central carbon ($-C_{14}H_{29}$), which is needed to achieve enough lipophilicity in the extractions, was replaced by a hydrogen atom to minimise the computation time. These calculated basicity data show the same relative order of basicity as the experimentally determined basicities.

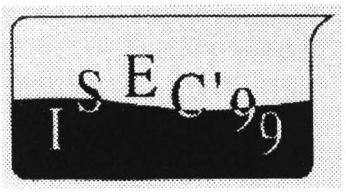
R	R_2	ΔG_R(kcal/mol)
4-chlorophenyl	H	-215.30
phenyl	H	-228.56
2,6-dichlorophenyl	H	-229.35
cyclohexyl	H	-230.71

Table 4 The difference free Gibbs energy for the protonation reaction of some different substituted malonamides (Gaussian94, full geometry optimisation).

The position of the chlorine atoms on the phenyl groups seems to have a great influence on the basicity. The calculated basicity for the 2,6-dichlorophenyl derivative was shown to be considerably higher than the 4-chlorophenyl substituent but there are, so far, no experimental data for the 2,6-dichlorophenyl ligand to verify this. More calculations and measurements on new malonamides, e.g. with alkoxy groups on the central carbon, are in progress and are needed to verify the relation between calculated and experimental basicity and the correlation between basicity and extraction. If a property, like basicity, which seems to be related to the metal extraction, could be calculated accurately it might simplify the design of optimal extractants.

REFERENCES

1 Nigond L, Thèse de Doctorat D'Université de Clermont-Ferrand II, *CEA-R-5610*, (1992)
2 Madic C, Hudson MJ, *EUR 18038 EN*, (1998)
3 Chan GYS, Drew MGB, Hudson MJ, Iveson PB, Liljenzin JO, Skålberg M, Spjuth L and Madic, C., *J. Chem. Soc., Dalton Trans.*, 649, (1997).
4 Nigond L, Musikas C and Cuillerdier C, *Solv. Extr. Ion Exch.* **12**(2), 261, (1994)
5 Zhang K, Zimmerman DM, Chung-Phillips A, and Cassady CJ, *J. Amer. Chem. Soc.*, **115**, 10812, (1993)
6 Jebber KA, Zhang K, Cassady CJ, and Chung-Phillips A, *J. Amer. Chem. Soc.* **118**, 10515, (1996)
7 Zhang K, Cassady CJ and Chung-Phillips A, *J. Amer. Chem. Soc.*, **116**, 11512, (1994)



PHOTOSTABILITY OF HYDROXYOXIME COMMERCIAL COPPER EXTRACTANTS: ACORGA P5100 AND SME529

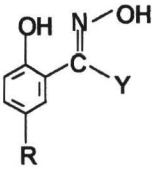
Ewa Krzyanowska and Andrzej Olszanowski
Institute of Chemical Technology and Engineering, Poznan University of Technology, Pl.Skodowskiej-Curie 2, 60-965 Poznan, Poland.

ABSTRACT
The photostability of hydroxyoxime commercial copper extractants, Acorga P5100 and SME529 are studied under exposure to UV light. Extractant samples in a mixture of octane:toluene (4:1 v/v) are exposed to a temperature below 22°C in a Heraeus photoreactor. The influence of water and sulphuric acid on the photo-degradation of oximes is also studied.
2-Hydroxy-5-nonylbenzaldehyde and 2-hydroxy-5-nonylacetophenone, respectively, are the main products of the photo-degradation of both extractants. 2-hydroxy-5-nonylbenzaldehyde oxime is less stable than 2-hydroxy-5-nonylacetophenone oxime in both dry and wet solvents. The opposite order of stability is observed in the presence of sulphuric acid. The rate of photo-degradation is enhanced by the bubbling of water and sulphuric acid through the hydrocarbon phase. However, the high loading of hydroxyoxime depresses the photo-degradation and protects extractants against light, including sunlight.

Keywords: Acorga P5100, SME 529, 2-hydroxy-5-nonylbenzaldehyde oxime, 2-hydroxy-5-nonylacetophenone oxime, degradation.

INTRODUCTION

Hydroxyoximes of the general formula:



$Y = H, CH_3, C_6H_5;$

$R = C_9H_{19}, C_{12}H_{25};$

are active substances in commercial copper extractants such as LIX and ACORGA, produced by Henkel and Zeneca. According to the literature hydroxyoxime degradation under the conditions of copper extraction from acid sulphate solutions is less than the losses induced by incomplete phase disengagement.[1] The stability of metal extractants is, however, an important parameters which needs to be considered in the industrial extraction of metals.

Degradation of hydroxyoxime extractants is promoted by elevated temperature, high concentration of sulphuric acid and light, and involves mainly the hydrolysis of the oximino group. Oximes of aromatic hydroxyketoximes are more resistant to hydrolysis than oximes of aliphatic α-hydroxyketones, e.g. LIX 63, and the hydrolytic resistance increases in the following order: 2-hydroxy-5-alkylbenzaldehyde oxime, e.g. ACORGA P 50, P 5100, < 2-hydroxy-5-alkylacetophenone oxime, e.g. SME 529 and LIX 84, < 2-hydroxy-5-alkylbenzophenone oxime, e.g. LIX 65N.

The resistance of the extractant to light is important during extraction and stripping, especially in kinetic studies with diluted solutions, and in industry in older extraction installations having open mixers and settlers in those countries where exposure to light is unavoidable (e.g. Africa, South America and Australia). This problem was not considered for a long period of time.

The photostability of the commercial hydroxyoxime copper extractants, ACORGA P5100 and SME 529 under exposure to UV light are studied in this paper together with the influence of water and sulphuric acid on the photo-degradation.

EXPERIMENTAL

Samples of commercial extractants: ACORGA P5100, (ZENECA) and an archive sample of

© 2000 Society of Chemical Industry

SME 529, produced earlier by Shell were used. Photo-degradation was carried out as reported for the case of individual model hydroxyoximes containing the short methyl group instead of the branched alkyl group.[2-4]

RESULTS AND DISCUSSION

With these commercial extractants the analysis of the photodegradation products is more complicated, compared to the individual models, because, a) the nonyl group consists of several branched isomers, b) ACORGA 5100 contains free nonylphenol added as a modifier, and c) the presence of other components present in the nonylphenol used in surfactant industry cannot be excluded (Figure 1).

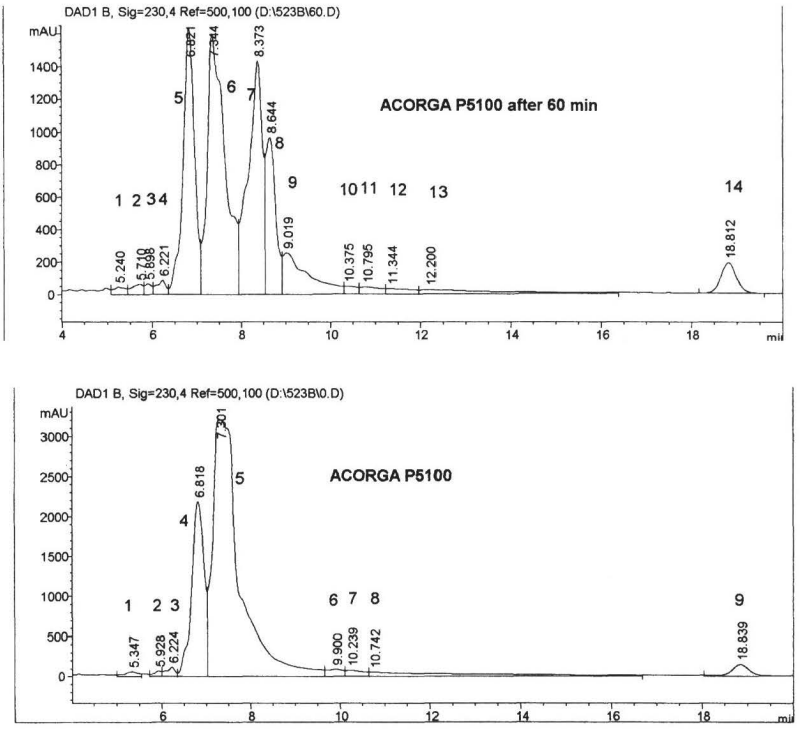


Figure 1. Chromatograms of ACORGA P5100 before (4, p-nonylphenol; 5, 2-hydroxy-5-nonylbenzaldehyde oxime) and after 60 min of photodegradation (5, p-nonylphenol; 6, 2-hydroxy-5-nonylbenzaldehyde oxime and 7 and 8, hydroxyaldehydes.).

The main product of ACORGA P5100 degradation is 2-hydroxy-5-nonylbenzaldehyde (peak 6 Figure 1) which can be recycled after oximation (Figure 2). However, after longer exposure to light the aldehyde undergoes further photodegradation to non-recycleable products. Rapid destruction of the extractant was observed between 10 and 30 minutes. The effect of the presence of water on the photo-degradation is small and almost negligible. The fastest degradation was noted when the medium contained sulphuric acid (Figure 3). These conclusions are also valid for the degradation of SME 529 (Figure 4). Total disappearance of the initial hydroxyaldehyde oxime in ACORGA P5100 was observed after 80 minutes.

During photoreaction a gradual decomposition of p-nonylphenol is observed yielding alkylphenols of lower molecular masses, which exhibit higher solubility in aqueous solutions. Such degradation was not observed with individual models containing normal alkyl groups.

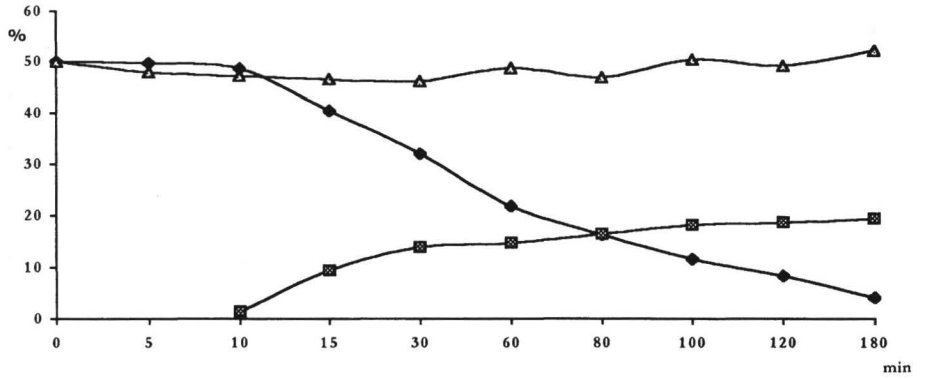
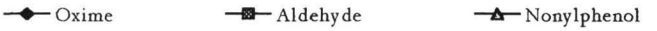


Figure 2. Composition of ACORGA P 5100 after photo-degradation in a mixture of octane and toluene:



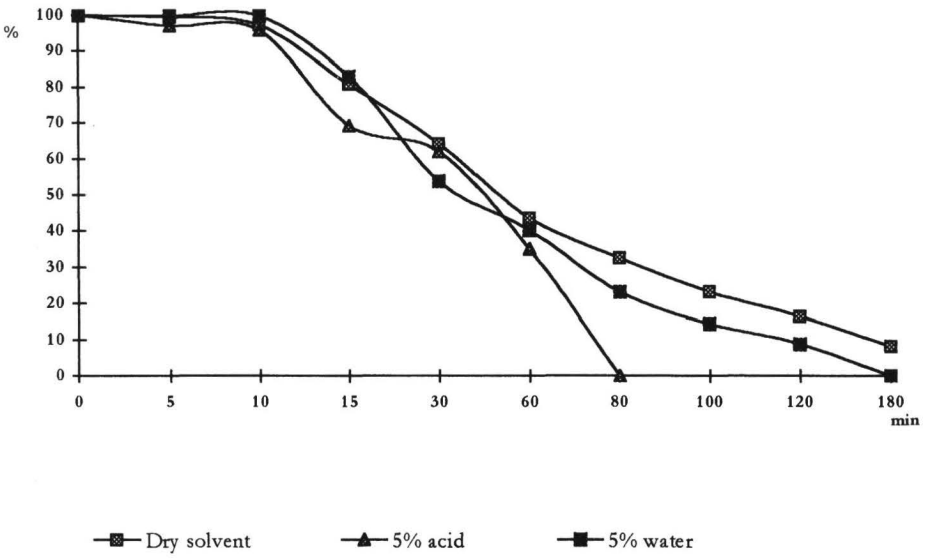


Figure 3. Relative content of non-degraded 2-hydroxy-5-nonylbenzaldehyde oxime in ACORGA P5100 dissolved in octane:toluene (4:1 v/v) :

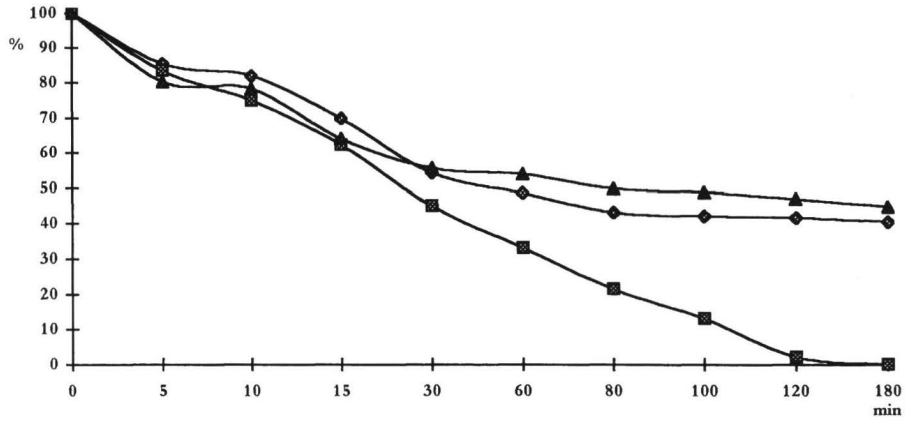


Figure 4. Relative content of non-degraded 2-hydroxy-5-nonylacetophenone oxime in SME529 dissolved in octane:toluene (4:1 v/v):

Table 1. Extent of total photo-degradation to recycled products for ACORGA P5100 and SME 529.

Reagent	System	Total degradation / degradation to recycled products* (% / %)					
		10 min	15 min	30 min	60 min	80 min	100 min
ACORGA P5100	Dry solvent	2.8 2.8	19.2 18.8	35.8 27.8	56.4 29.4	67.4 32.8	76.8 33.2
ACORGA P5100	Water (5%)	0.2 0	17.0 4.7	46.2 20.8	59.2 28.4	76.8 31.8	85.6 33.8
ACORGA P5100	Acid (5%)	4.2 0	30.8 9.8	38.0 13.8	65.0 19.8	100 14.7	100 13.8
SME 529	Dry solvent	18.0 16.0	30.2 25.1	45.6 33.5	51.3 38.5	57.0 42.9	57.8 43.7
SME 529	Water (5%)	21.8 19.2	36.0 27.0	44.3 40.3	46.1 41.8	50.1 42.2	51.1 43.1
SME 529	Acid (5%)	25.1 21.4	37.3 28.5	55.0 42.3	66.9 51.9	78.5 62.3	86.1 70.8

- the first value denotes the total degradation, while the second one the degradation towards the products which can be oximated and then recycled. The values are given in per cents in relation the initial content of the active substance.

The results of the photodegradation of both extractants are similar, thus 2-hydroxy-5-nonyl-acetophenone and 2-hydroxy-5-nonylbenzaldehyde are respectively the main products of the photo-degradation. A comparison of the stability of both extractants shows that SME 529 (which contains 2-hydroxy-5-nonylacetophenone oxime) is more stable than ACORGA P5100 (with 2-hydroxy-5-nonylbenzaldehyde oxime) in dry and wet solvents. The opposite order of stability was observed in the presence of sulphuric acid.

The data given in table 1 indicate that in each system the degradation of SME 529 yields a higher percentage of products which can be recycled following an additional regeneration step; i.e.

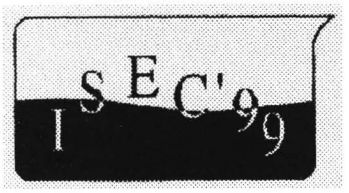
oximation of the hydroxyketone produced during degradation. The degradation of 2-hydroxy-5-nonylbenzaldehyde oxime yields mainly 2-hydroxy-5-benzaldehyde in the first step (up to 30 minutes reaction), which however undergoes further degradation to non-recyclable products. This means that degradation should be monitored in order that regeneration can be carriedut the before the undesired degradation of intermediate 2-hydroxy-5-nonylbenzaldehyde.

ACKNOWLEDGEMENTS

The work was supported by grant BW 32/287.

REFERENCES

1 Szymanowski J *Hydroxyoximes and Copper Hydrometallurgy*, CRC Press, Boca, Raton, USA, 1993.
2 Olszanowski A and Krzyzanowska E, *Hydrometallurgy*, **35**, 79 (1994).
3 E Krzyzanowska and A Olszanowski, *Hydrometallurgy*, **37**, 375 (1994).
4 Olszanowski A, Krzyzanowska E and Alejski J, *J. Chem. Tech. Biotechnol.*, **68**, 236 (1997).



PHOTODEGRADATION OF OXIMES OF 2-HYDROXY-5-t-OCTYLBENZOPHENONE, 2-HYDROXY-5-t-OCTYLBENZALDEHYDE AS MODELS OF HYDROXYOXIME EXTRACTANTS OF METALS

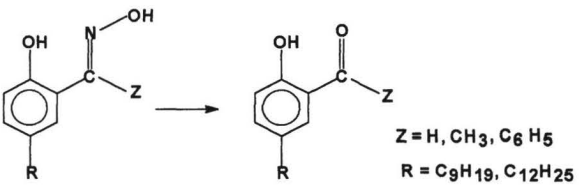
Ewa Krzyanowska and Andrzej Olszanowski
Institute of Chemical Technology and Engineering, Poznan University of Technology, Pl.Skodowskiej-Curie 2, 60-965 Poznan, Poland.

ABSTRACT
2-Hydroxy-5-t-octylbenzophenone oxime (I), 2-hydroxy-5-t-octylacetophenone oxime (II) and 2-hydroxy-5-t-octylbenzaldehyde oxime (III) and their copper complexes are used to study their photo-stability under UV light in a mixture of octane:toluene (4:1 v/v). The influence of water as well as sulphuric acid on the photo-degradation of oximes is also studied. Degradation products are identified. Photo-degradation of I yields different products compared with II and III. 2-Hydroxy-5-t-octylbenzophenone or 2-phenyl-5-t-octylbenzoxazole is the main degradation product of I depending on reaction conditions (diluent, water or sulphuric acid content). The former can be oximated to the oxime and recycled. The latter becomes a ballast substance. A photo-isomerization of (E)-isomer into non-active (Z)-isomer is also observed. II and III yields mainly 2-hydroxy-5-t-octylacetophenone and 2-hydroxy-5-t-octylbenzaldehyde, respectively, which may be oximated and the reagent recycled.
Copper complexes increase the stability of hydroxyoximes and may be considered as natural stabilizers.

Keywords: 2-hydroxy-5-t-octylbenzophenone oximes, 2-hydroxy-5-t-octylacetophenone oxime, 2-hydroxy-5-t-octylbenzaldehyde oxime, degradation, isomerization.

INTRODUCTION

Degradation of hydroxyoxime extractants is promoted by elevated temperature, high concentration of sulphuric acid and light. Hence, it mainly takes place in the stripping section but does so to a lower extent than one would expect, considering the hydroxyoxime structure.[1,2] Degradation of hydroxyoxime extractants involves mainly the hydrolysis of the oximino group, e.g.



In our previous papers[3-5] the photo-isomerization and photo-degradation of 2-hydroxy-5-methylbenzophenone (E)-and (Z)-oxime in ethanol, octane, toluene and a mixture of octane and toluene under exposure to UV light were studied. The main path of photo-degradation of (E)-oxime led via (Z)-oxime to 3-phenyl-5-methylbenzisoxazole, 2- phenyl-5-methylbenzoxazole and 2-hydroxy-5-methylbenzophenone. Photo-isomerization and photo-degradation kinetic models were developed for both oximes.[5]

Hydroxyoxime extractants are complex mixtures having various structures of the nonyl or dodecyl group (propylene trimer or tetramer).[6] Hydroxyoximes having the 1,1,3,3-tetramethylbutyl group (isobutylene dimer), abbreviated as t-octyl, can be considered as appropriate models of commercial reagents. Such hydroxyoximes exhibit similar hydrophobicity and as a result possess similar partition and solubility data and extraction properties as analogs having 9 and 12 carbon atoms in the alkyl group.

2-Hydroxy-5-t-octylbenzophenone oxime (I), 2-hydroxy-5-t-octylacetophenone oxime (II) and 2-hydroxy-5-t-octylbenzaldehyde oxime (III) and their copper complexes were used to study their

© 2000 Society of Chemical Industry

photostability under UV light in a mixture of octane:toluene (4:1 v/v). The influence of water as well as sulphuric acid on the photo-degradation of oximes was also studied.

EXPERIMENTAL

Oxime samples, 4.056 $x10^{-3}$ M in a mixture of octane : toluene (4:1 v/v) were exposed in a Heraeus photoreactor of 120 cm^3 volume. To the solution of octane : toluene in some experiments, water or sulphuric acid (150 g/dm^3) was also added up to 5% of volume. The photo-degradation was carried in the same way as in the case of individual model hydroxyoximes containing the short methyl group instead of the branched alkyl.[3,4] Analyses of oxime solutions were carried out using a Hewlett-Packard HPLC series 11000 with a diode array detector.

RESULTS AND DISCUSSION

2-Hydroxy-5-t-octylbenzophenone, 2-phenyl-5-t-octylbenzoxazole, 3-phenyl-5-t-octyl-benzisoxazole were detected as products of the photo-degradation of I. Also photo-isomerization of (E)-oxime to (Z)-oxime was observed. N-(2-hydroxy-5-octylphenyl)-benzamide and N-phenyl-2-hydroxy-5-octylbenzamide were not detected as products of the photo-degradation, as opposed to the photo-reaction of 2-hydroxy-5-methylbenzo-phenone (E)- and (Z)-oxime (Figure 1).

When water or sulphuric acid (150 g/dm^3) was added to the reaction medium, differences in the conversion rate, the amount of photo-degradation products and the content of the products of the photo-degradation of 2-hydroxy-5-t-octylbenzophenone oximes were observed. For all systems rapid reduction of (E)-oxime was observed between 30 and 60 minutes of light exposure. The yields of 2-hydroxy-5-t-octylbenzophenone and 2-phenyl-5-t-octylbenzoxazole differed and depended on the photoreaction conditions. The highest and lowest amounts of 2-hydroxy-5-t-octylbenzophenone were formed in those systems containing water and dry solvents, respectively (Figure 2).

The formation of ketone was observed only after 80 minutes of photo-reaction in the octane-toluene mixture. This could be explained by other competing reactions, mainly those that lead to benzisoxasole and benzoxazole derivatives.

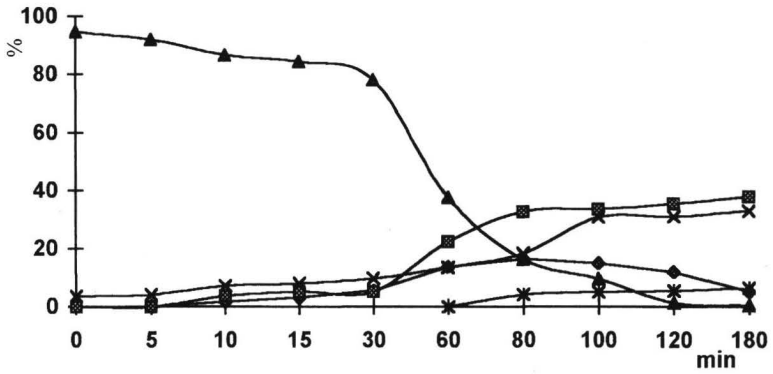


Figure 1. Photo-degradation of 2-hydroxy-5-t-octylbenzophenone oximes in a mixture of octane and toluene.

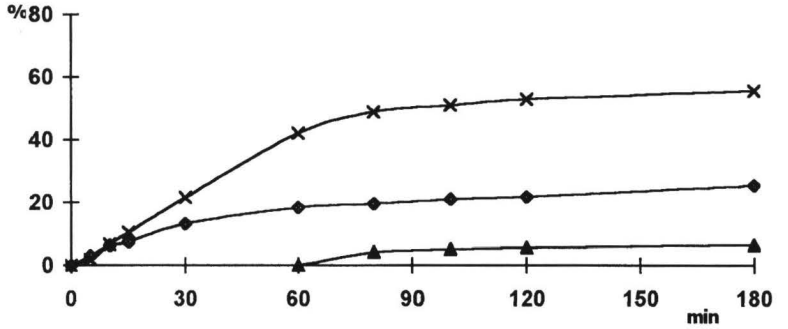


Figure 2. Comparison of the content of 2-hydroxy-5-t-octylbenzophenone formed during photo-degradation of 2-hydroxy-5-t-octylbenzophenone oximes in an octane-toluene solution:

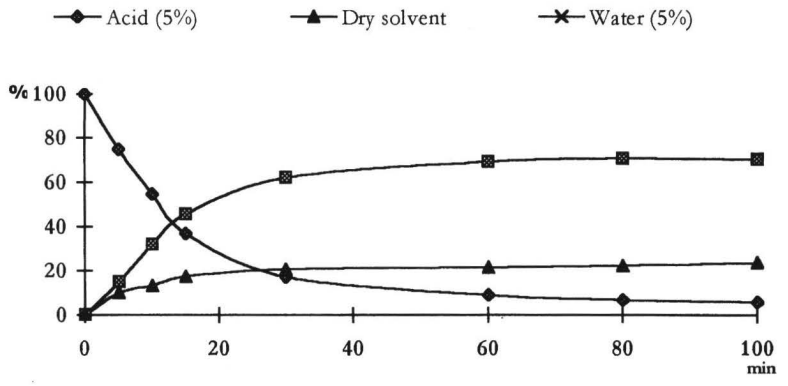
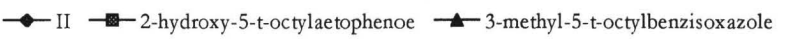


Figure 3. Photo-degradation of 2-hydroxy-5-t-octylacetophenone oxime (II) in a mixture of octane and toluene:



The main path of the photo-degradation of II led to 2-hydroxy-5-t-octyl-acetophenone and 3-methyl-5-t-octylbenzisoxazole. The degradation of this oxime was faster in comparison to I, with the ketone as the main product of photo-degradation; the content of 3-methyl-5-t-octylbenzisoxazole as a by-product of degradation was much lower than during the same process of I (Figure 3).

The results obtained of the photo-degradation of III indicated that the main product of degradation is 2-hydroxy-5-t-octylabenzaldehyde. A small amount of 5-t-octylbenz-oxazole and a minimal amount of N-(2-hydroxy-5-t-octylphenyl)formamide were observed as by-products of degradation. The effect of water and sulphuric acid on the photo-degradation of III was similar to that of I.

An important factor in the progress of photo-degradation is the concentration of oxime. With an increase in a concentration of oxime, degradation decreased (Figure 4).

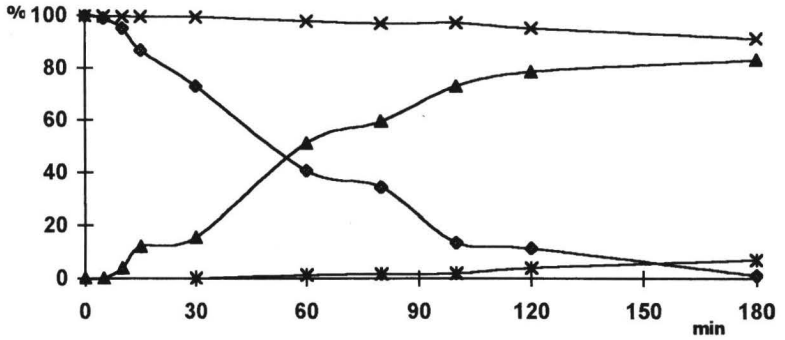


Figure 4. Photo-degradation of 2-hydroxy-5-t-octylbenzaldehyde oxime in octane toluene 4:1 v/v, initial concentration of III; 10^{-2}mole (conc.) and 10^{-4}mole (dil.).

Oxime dil. Aldehyde dil. Oxime conc. Aldehyde conc.

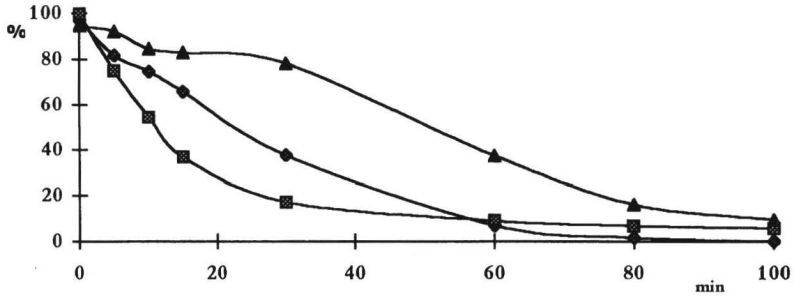


Figure 5. Comparison of the photo-degradation of hydroxyoximes in an octane-toluene solution.

III II I

A comparison of the photo-degradation of all analysed oximes under the same conditions indicated that I is the most stable in light, with III more easily degraded under the same experimental conditions (Figure 5).

Analysis of the main products formed during photo-degradation shows that the processes of photo-degradation are different. In the case of the photo-reaction of II and III, the main products are appropriate ketone or aldehyde, which are formed at the initial step of the reaction, and their volume is large. 2-Hydroxy-5-t-octylbenzophenone is not formed in the initial stage of reaction, and its content is not high (Table 1, Figure 6). These data are very important if the regeneration of an extractant through its supplementary oximation with hydroxyloamine, in the presence of an alkaline substance is being considered. The results obtained show that such regeneration can only be carried out for the acetophenone and benzaldehyde derivatives.

Table 1. Extent of total photo-degradation and degradation to recycled products.

Reagent	System	Total degradation/degradation to recycled products (% / %)					
		10 min	15 min	30 min	60 min	80 min	100 min
I	Dry	8.4	10.9	17.5	52.0	82.8	89.8
	solvent	0	0	0	0	4.2	5.1
I	Water	12.3	20.0	42.9	73.4	90.1	93.8
	(5%)	7.0	10.9	22.6	44.4	51.7	53.9
I	Acid	13.0	17.1	42.3	78.6	94.9	97.1
	(5%)	6.6	7.8	13.8	19.4	20.6	22.2
II	Dry	45.4	63.1	82.7	90.9	93.1	94.1
	solvent	32.0	45.6	62.0	69.3	70.3	70.7
III	Dry	23.2	32.2	61.2	81.4	98.2	99.8
	solvent	20.4	29.2	56.3	78.4	82.4	86.1
III	Water	14.3	20.1	90.2	96.9	98.7	99.9
	(5%)	13.4	18.5	77.1	80.4	83.9	86.7
III	Acid	19.0	22.3	27.4	85.1	98.0	99.2
	(5%)	15.1	18.9	23.3	72.3	80.9	86.4

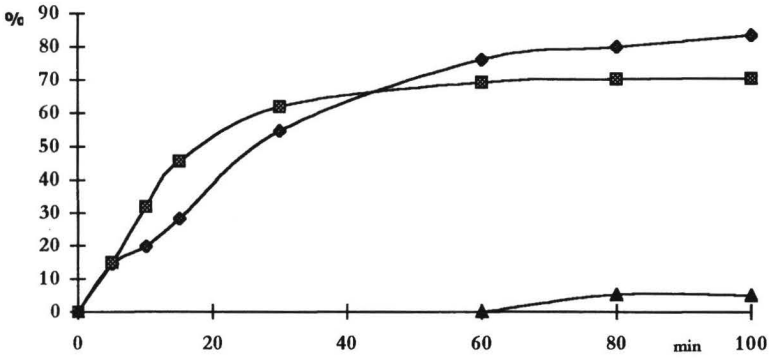


Figure 6. Comparison of the content of hydroxyketones and hydroxyaldehydes formed during the photo-degradation of oximes I, II and III in an octane-toluene solution:

2-hydroxy-5-t-octylbenzaldehyde
2-hydroxy-5-t-octylacetophenone
2-hydroxy-5-t-octylbenzophenone

The photo-stability of the oxime complexes of copper(II) was much greater than the oxime alone (Figure 7). Thus the complex of oxime with copper substantially protected the oxime against light.

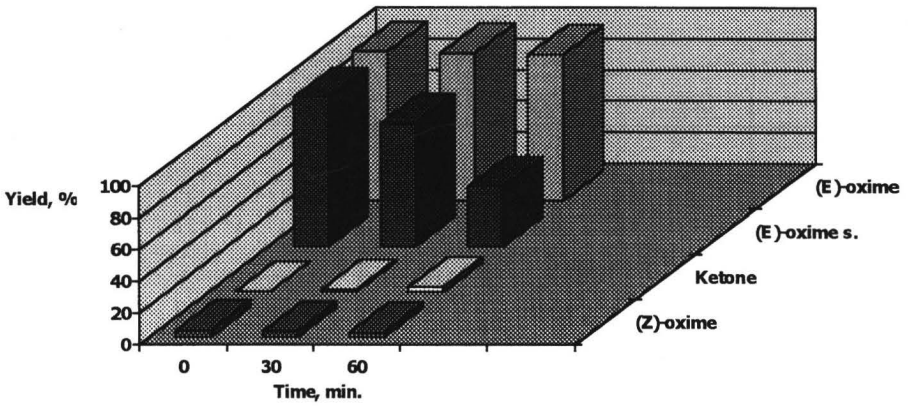


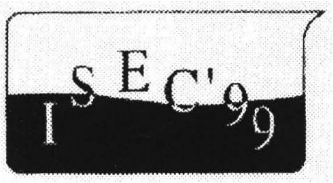
Figure 7. Photo-degradation of the copper complex of 2-hydroxy-5-t-octylbenzophenone oximes in a mixture of octane and toluene

ACKNOWLEDGEMENTS

The work was supported by grant BW 32/287.

REFERENCES

1 Szymanowski J, *Hydroxyoximes and Copper Hydrometallurgy*, CRC Press, Boca, Raton, USA, 1993.
2 Szymanowski J, *Crit. Rev. Anal. Chem.*, **95**, 143, (1995)
3 Olszanowski A and Krzyzanowska E, *Hydrometallurgy*, **35**, 79, (1994).
4 Krzyzanowska E and Olszanowski A, *Hydrometallurgy*, **37**, 375, (1994
5 Olszanowski A, Krzyzanowska E and Alejski K, *J. Chem. Tech. Biotechnol.*, **68**, 236, (1997)
6 Szymanowski J, Szewczyk H and Hetper J, *Tenside Deterg.*, **18**, 333, (1981)



SYNERGISTIC EFFECTS IN THE EXTRACTION OF METAL IONS BY MIXTURES OF DIALKYL-PHOSPHORIC ACIDS AND SUBSTITUTED CROWN ETHERS

R Chiarizia[1], ML Dietz[1], AH Bond[1], VJ Huber[1], AW Herlinger[2] and BP Hay[3]

[1] Chemistry Division, Argonne National Laboratory, Argonne, IL 60439, USA

[2] Department of Chemistry, Loyola University Chicago, Chicago, IL 60626, USA

[3]Pacific Northwest National Laboratory, Richland, WA 99352, USA

ABSTRACT

The extraction of alkaline earth cations from weakly acidic solutions by three dialkylphosphoric acids and various isomers of dicyclohexano-18-crown-6, both alone and in combination in toluene solutions, has been examined to determine the effect of both the crown ether stereochemistry and the structure of the organophilic anion on the magnitude of the synergistic effects. The synergistic effects have been found to differ considerably among the crown ether isomers and to vary with the extent of alkyl chain branching in the dialkylphosphoric acid. Attempts to correlate the synergistic effects with ligand strain energies from molecular mechanics calculations are described.

Keywords: synergism, alkaline earths, crown ether stereoisomers, dialkylphosphoric acids

INTRODUCTION

In an effort to develop guidelines for the rational design of synergistic extraction systems for metal ions using macrocyclic polyethers, we have examined the extraction of Ca^{+2}, Sr^{+2} and Ba^{+2} into toluene by various organophosphorus acids and crown ether isomers, both alone and in combination. Although synergistic effects involving mixtures of crown ethers and organophosphorus acid anions are well known, [1-7] few of the previously described studies have taken a systematic approach to the elucidation of the factors responsible for the observed synergism. By contrast, the present work employs structurally well-defined macrocycles and organophilic anions, thereby providing a means of determining the influence of the crown ether stereochemistry and anion structure on the observed synergistic effects.

The series of dicyclohexano-18-crown-6 (DCH18C6) isomers shown in Figure 1 and the dialkylphosphoric acids of increasing steric bulk shown in Figure 2 were used. The extraction data were then used to determine if a correlation exists between macrocyclic ligand strain energies (calculated by molecular mechanics) and the synergistic effects.

EXPERIMENTAL

The preparation and purification of the materials used in this work can be found in reference 8. The distribution ratios, D, of ^{45}Ca, ^{85}Sr and ^{133}Ba were determined at 23±1°C as reported in reference 9. For the pH dependencies of the metal distribution ratios, the procedure described in reference 2 was followed. The details of the calculations of the crown ether ligands reorganization energy, ΔU_{reorg}, are reported in reference 10.

© 2000 Society of Chemical Industry

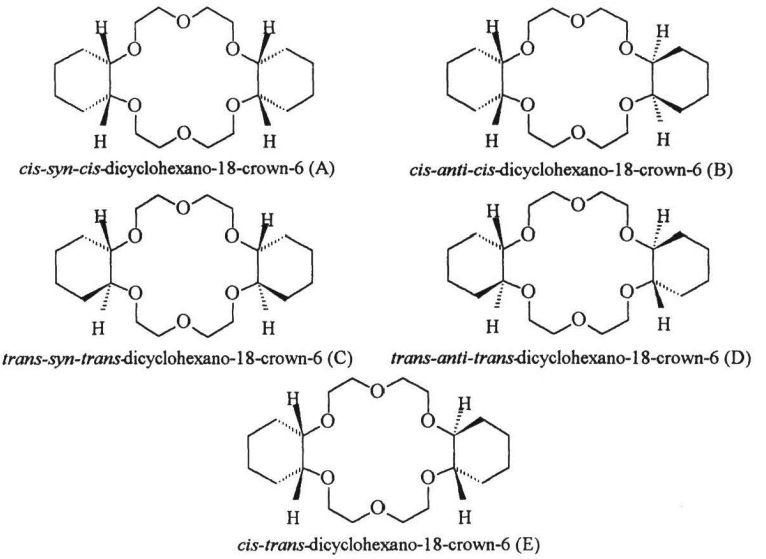


Figure 1. DCH18C6 isomers used in this work

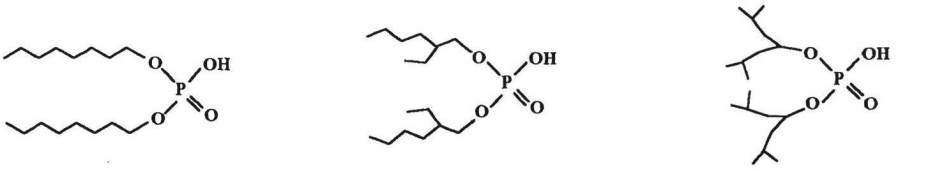


Figure 2. Dialkylphosphoric acids used in this work

RESULTS AND DISCUSSION

Figure 3 shows the results of a continuous variation study of the distribution ratios of Ca^{+2}, Sr^{+2} and Ba^{+2} as a function of the crown ether (CE) mole fraction in HDOP-CE mixtures at constant HNO_3 and metal ion concentrations. Similar results have been obtained for the other dialkylphosphoric acids used in this study.

These data illustrate a number of features of the investigated systems. First, the extraction of the metal cations by the CE alone is negligible, which allows us to define a synergistic factor, SF, simply as the ratio of the *D* values in the presence and in the absence of crown ether under each set of experimental conditions. Next, no significant synergism is observed for Ca^{+2}, probably due to the poor ability of DCH18C6 to complex this cation. [7,11] In contrast, a strong synergistic effect is observed with Sr^{+2} and Ba^{+2}, both of which are strongly complexed by 18-membered crown ethers. [7,11] For these two cations, the various stereoisomers of DCH18C6 yield remarkably different SF values, in the order A>B>E>C≥D (*vide infra*). Finally, the maximum *D* values generally occur at a CE mole fraction of 0.2, indicating that the synergistic complexes of Sr^{+2} and Ba^{+2} contain four molecules of dialkylphosphorc acid for each CE molecule.

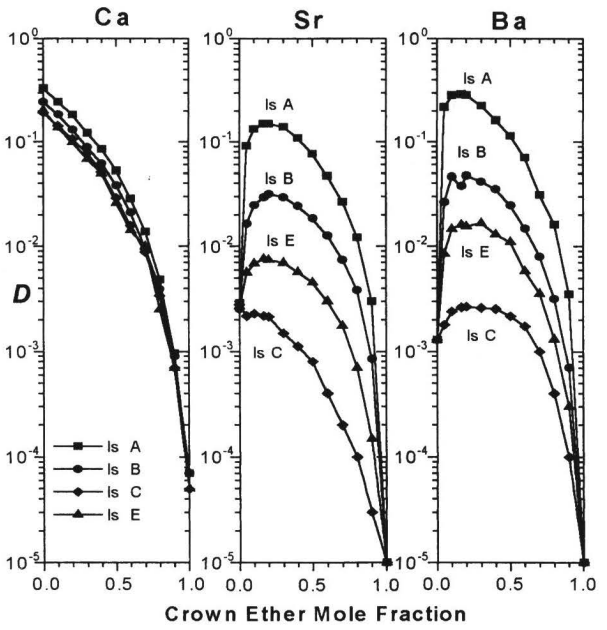


Figure 3. Continuous variation plots for the HDOP-CE system. [HDOP]+[CE] = 0.1 M in toluene; $[HNO_3]$ = 0.01 M; $[M(NO_3)_2]$ = 0.001 M

Figure 4 shows the pH dependencies of the metal distribution ratios at constant ionic strength and temperature measured with 0.1 M HDOP either alone or in the presence of 0.025 M CE (various isomers), that is, under conditions corresponding to the maxima in the continuous variation plots in Figure 3. Similar data, not shown here, were obtained for HDEHP and HD(DiBM)P. The data in Figure 4 confirm both the lack of synergism for Ca^{+2} and the order of effectiveness of the various isomers of DCH18C6 in enhancing Sr^{+2} and Ba^{+2} extraction by HDOP (*vide supra*). The same order was verified with the other two dialkylphosphoric acids with one exception, the HD(DiBM)P- Sr^{+2} system, in which isomer B was slightly more effective than isomer A.

Error! Not a valid link.

Figure 4. pH dependencies with 0.1 M HDOP alone or with 0.025 M DCH18C6 in toluene; $[M(NO_3)_2]$ = 0.001 M

In all cases, the slope value of the pH dependencies is +2, indicating that when the cations are extracted by HDOP, HDEHP or HD[DiBM]P, either alone or in combination with the various isomers of DCH18C6, two H^+ ions are liberated during extraction.

The extractant dependencies of the *D* values were also measured and slope analysis of the logarithmic plots of *D* vs. extractant concentration obtained at a constant aqueous phase pH (between 2 to 3) and at very low organic phase loading was performed. With the dialkylphosphoric acids alone, slopes of the dependencies were 2.5 for Ca^{+2} and 3.0 for Sr^{+2} and Ba^{+2}, although some deviation from these values was observed with HD(DiBM)P. Overall, our results agree with previous literature information concerning extraction of alkaline earth cations by dialkylphosphoric acids. [12]

Extractant dependencies were also determined for synergistic systems (not shown for the sake of brevity). In all cases, the slope of the logarithmic plots of D vs. the dialkylphosphoric acid concentration (at constant DCH18C6 concentration) was +2. When the DCH18C6 concentration was varied, keeping the dialkylphosphoric acid concentration constant, slope values of +1 were obtained. In several cases, however, slopes less than unity were observed at the highest CE concentrations, in agreement with previous studies.[2] Using these results, together with the dimeric state of aggregation of organophosphorus acids in toluene [13] and the absence of interaction between the two extractants in the organic phase (confirmed by vapor pressure osmometry and infrared spectroscopy measurements[14]), the equilibria describing the extraction of alkaline earth cations by mixtures of dialkylphosphoric acids and DCH18C6 can be written as follows, where HA and B represent the two extractants in the organic phase:

$$M^{+2} + (2+n/2)(HA)_2 \Leftrightarrow M(HA_2)_2 \cdot nHA + 2H^+ \qquad K_{ex}$$

in the absence of crown ether, with n = 1 for Ca^{+2} and n =2 for Sr^{+2} and Ba^{+2}. For Sr^{+2} and Ba^{+2} in the presence of DCH18C6, this becomes:

$$M^{+2} + 2(HA)_2 + B \Leftrightarrow MB(HA_2)_2 + 2H^+ \qquad K_{ex,s}$$

The synergistic constant K_s, defined as the $K_{ex,s}/K_{ex}$ ratio,[13] corresponds to the organic phase reaction that leads to the formation of the final Sr^{+2} and Ba^{+2} complexes:

$$M(HA_2)_2 \cdot 2HA + B \Leftrightarrow MB(HA_2)_2 + 2HA \qquad K_s$$

The K_s values listed in Table 1 have been used to quantitatively describe the synergism in the investigated systems. Because of the low reagent concentrations in both phases, these values can be considered to be nearly thermodynamic constants.

Table 1: Values of the synergistic equilibrium constants, K_s

DCH18C6 isomer	HDOP		HDEHP		HD(DiBM)P	
	Sr	Ba	Sr	Ba	Sr	Ba
A	(1.07±0.09) x10^2	(5.32±0.64) x10^3	(1.96±0.24) x10^3	(5.26±0.69) x10^3	(4.19±0.57) x10^2	(7.25±1.45) x10^3
B	(3.17±0.31) x10^1	(1.27±0.17) x10^3	(3.49±0.52) x10^2	(1.84±0.20) x10^3	(5.48±0.55) x10^2	(8.01±1.44) x10^2
E	(9.43±0.44) x10^0	(4.09±0.49) x10^2	(8.08±1.00) x10^1	(3.62±0.40) x10^2	(6.54±0.95) x10^1	(1.95±0.33) x10^2
C	(3.36±0.18) x10^0	(3.58±0.94) x10^1	(1.03±0.13) x10^1	–	(1.45±0.29) x10^1	–
D	(2.60±0.23) x10^0	(1.58±0.32) x10^1	–	–	–	–

Figure 5 shows the relationship between the log K_s (Table 1) and the ligand reorganization energy (ΔU_{reorg}) calculated through molecular mechanics for the metal complexes of the various stereoisomers of DCH18C6. These reorganization energies represent the degree to which complex formation between a crown ether and a given metal ion induces steric strain in the crown ether. Ligands highly organized for binding exhibit small ΔU_{reorg} values, down to the limiting value of $\Delta U_{reorg} = 0$ for ligands that are perfectly organized for binding. Extrapolation to $\Delta U_{reorg} = 0$ of the linear correlation between the logarithm of the binding constant and ΔU_{reorg} allows an estimation of the binding constant for ligands with an optimum configuration.

The results shown in Figure 5, which represent the first report of a correlation between synergistic constants and ligand strain energies, seem to indicate that the primary factor determining the magnitude of the observed synergistic effects is the reorganization energy of the various DCH18C6

isomers. It also appears that the steric hindrance due to the branching of the alkyl groups of the dialkylphosphoric acids also plays a role, although a more limited one.

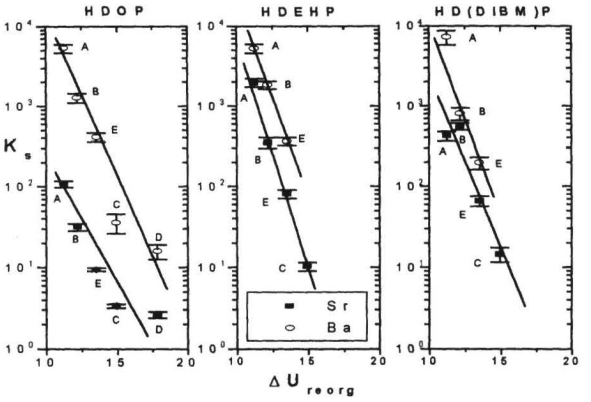


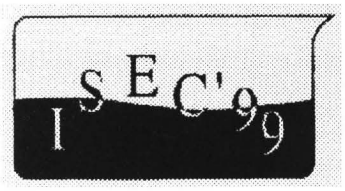
Figure 5. Relationship between log K_s values and DCH18C6 isomers reorganization energy

ACKNOWLEDGMENTS

Work performed under the auspices of the Office of Basic Energy Sciences, Division of Chemical Sciences (crown ether synthesis), and the Environmental Management Sciences Program of the Offices of Energy Research and Environmental Management, United States Department of Energy, under Contract No. W-31-109-ENG-38.

REFERENCES

1 Kinard WF, McDowell WJ and Shoun RR, *Sep. Sci. Technol.*, **15**, 1013 (1980).
2 Kinard WF and McDowell WJ, *J. Inorg. Nucl. Chem.*, **43**, 2947 (1981).
3 McDowell WJ, Case GN and Aldrup DW, *Sep. Sci. Technol.*, **18**, 1483 (1983).
4 McDowell WJ, Moyer BA, Case GN and Case FI, *Solv. Extr. Ion Exch.*, **4**, 217 (1986).
5 Gloe K, Muehl P, Beyer L, Muehlstaedt M and Hoyer E, *Solv. Extr. Ion Exch.*, **4**, 907 (1986).
6 Izatt RM, Clark GA and Christensen JJ, *Sep. Sci. Technol.*, **21**, 865 (1986).
7 Dietz ML, Chiarizia R, Horwitz EP, Bartsch RA and Talanov V, *Anal. Chem.*, **69**, 3028 (1997).
8 Bond AH, Chiarizia R, Huber VJ, Dietz ML, Herlinger AW and Hay BP, *Synergistic Solvent Extraction of Alkaline Earth Cations by Individual Isomers of Dicyclohexano-18-crown-6 and Di-n-octylphosphoric Acid*, *Anal. Chem.*, submitted (1998).
9 Chiarizia R, Horwitz EP, Rickert PG and Herlinger AW, *Solv. Extr. Ion Exch.*, **14**, 773 (1996).
10 Hay BP, *A Molecular Mechanics Method for Predicting the Influence of Ligand Structure on Metal Ion Binding Affinity*, in *Metal Ion Separation and Preconcentration: Progress and Opportunities*, A.H.Bond, M.L.Dietz and R.D.Rogers, Eds., ACS Symposium Series 716, ACS, Washington, DC, (1998), in press.
11 Izatt RM, Pawlak K, Bradshaw JS and Bruening RL, *Chem. Rev.*, **95**, 2529 (1995).
12 Šístková NV, Kolarík Z, Bárta K and Pánková H, *J. Inorg. Nucl. Chem.*, **30**, 1595 (1968), and references therein.
13 Marcus Y and Kertes AS, *Ion Exchange and Solvent Extraction of Metal Complexes*, Wiley-Interscience, J.Wiley and Sons, London, UK, 1969.
14 Herlinger AW, Ferraro JR, Chiarizia R, Bond AH and Dietz ML, to be published.



SOLVENT EXTRACTION OF CALCIUM AND SOME DIVALENT TRANSITION METALS BY MIXTURES OF ORGANOPHOSPHORUS ACIDS AND BIFUNCTIONAL PHOSPHONATES

JS Preston and AC du Preez
Process Chemistry Division, Mintek, Private Bag X3015, Randburg 2125, South Africa

ABSTRACT
In this work we describe the extraction of some alkaline-earth metals (principally calcium) and divalent transition metals (Mn, Co, Ni and Cu) by selected organophosphorus acids in admixture with monofunctional or bifunctional neutral oxygen-donor compounds containing P=O groups. It was found that the extraction of the alkaline-earth metals from nitrate media (0.40 M $NaNO_3$) by organophosphorus acids (0.20 M in toluene) is appreciably enhanced by the addition of the bifunctional P=O donor compound, tetraisopropyl methylenediphosphonate (TIPMDP, 0.10 M) to the organic phase. The synergistic shifts in the pH_{50} values lie in the order: Mg < Ca > Sr > Ba. For calcium, the synergistic shifts obtained with the different types of organophosphorus acid decrease in the order: $(RO)_2POOH$ > (RO)RPOOH > R_2POOH, where R = 2-ethylhexyl. The corresponding ethylenediphosphonate (TIPEDP) and analogous monofunctional compounds, such as diisopropyl *n*-hexylphosphonate, give rise to much smaller shifts. The synergistic shifts with TIPMDP are greater for calcium than for manganese, cobalt, nickel and copper, thus permitting the selective removal of calcium impurities from solutions of the transition metals in some cases. In a batch-countercurrent experiment, 99% of the calcium was removed from a gypsum-saturated simulated cobalt electrolyte (30 gL^{-1} Co as sulphate) in 3 stages at pH 3.0, with only 0.3% extraction of cobalt.

Keywords: calcium, phosphorus acids, bifunctional phosphonates, synergism.

INTRODUCTION

Recently, we observed that the extraction of the trivalent rare-earth metals by alkylsalicylic acids was considerably enhanced by the addition of certain diphosphonate esters, $(RO)_2PO.(CH_2)_n.PO(OR)_2$, such as tetraisopropyl methylenediphosphonate (R = isopropyl, n = 1) to the organic phase.[1] This enhancement was quantified in terms of the synergistic shift in the pH_{50} value produced by adding the neutral diphosphonate (L) to the acidic extractant (HA):

$$\Delta pH_{50} = pH_{50}^{HA} - pH_{50}^{HA+L}$$

where pH_{50} represents the pH value for 50% metal extraction at unit phase ratio in the system identified by the superscript. The synergistic shifts were particularly marked in the case of the light rare-earth metals lanthanum, cerium, praseodymium and neodymium (up to 1.65 pH units), which was taken as an indication of the probable coordination of the diphosphonate in a bidentate mode. In contrast, the heaviest rare earths showed considerably smaller shifts, similar to those produced by monofunctional phosphonates (about 1.0 pH unit), which suggests that the smaller radii of these cations might be insufficient to permit bidentate coordination of the diphosphonate ligand.

Since the light rare-earth metals have trivalent cationic radii in the range 100-106 pm, similar to the radius of divalent calcium (99 pm), the possibility exists that the steric requirements for the coordination of the diphosphonate to the latter cation might also be favourable and, consequently, marked synergistic effects might be produced. In contrast, valuable transition metals such as cobalt, nickel, manganese and zinc, the hydrometallurgical sources of which are almost invariably contaminated with calcium, have much smaller cationic radii (69-80 pm) than the latter metal. Since calcium is partially extracted by the reagents commonly used in the recovery of these transition metals, organophosphorus and carboxylic acids, it can build up to saturation level in the recycled strip liquor and cause problems associated with the precipitation of gypsum.

Accordingly, we considered that it would be interesting to examine the extraction of calcium and some transition metals by alkylsalicylic and organophosphorus acids in the presence of suitable

© 2000 Society of Chemical Industry

diphosphonate esters, with the aim of developing a synergistic system suitable for the selective removal of the alkaline-earth metal from base metal solutions.

EXPERIMENTAL

The experimental methods and the sources of the reagents used have been described previously. [1,2] All organic phases were made up in toluene of analytical reagent grade.

RESULTS AND DISCUSSION

Extraction from nitrate media

As expected according to the argument outlined in the introduction, appreciable synergistic effects were obtained when tetraisopropyl methylenediphosphonate (TIPMDP) was used as an additive in the extraction of calcium by alkylsalicylic acids such as 3,5-diisopropylsalicylic acid (DIPSA). Thus, for example, the addition of 0.10 M TIPMDP to 0.25 M DIPSA produced a synergistic shift (ΔpH_{50}) of 1.54 pH units in the extraction of calcium (0.02 M) from 0.40 M $NaNO_3$, compared with somewhat smaller shifts for divalent transition metals such as manganese 1.26, nickel 0.80, and zinc 0.69 pH units, under the same conditions.

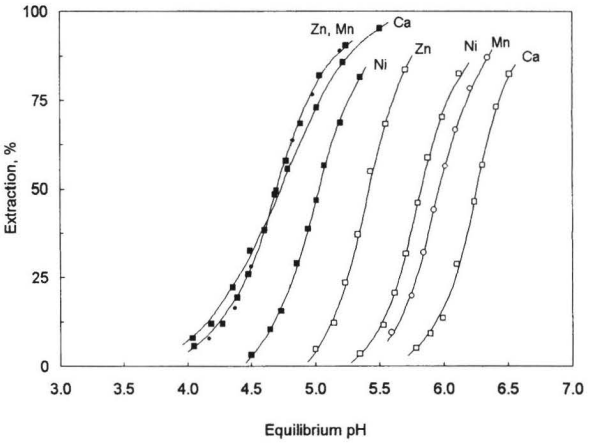


Figure 1 Extraction of divalent metals (0.02 M as nitrates) from 0.40 M sodium nitrate by 0.25 M DIPSA alone (open symbols) and in admixture with 0.10 M TIPMDP (closed symbols) in toluene at 20°C.

Unfortunately, however, owing to the weak extraction of calcium by DIPSA itself, the relative positions of the shifted extraction curves do not allow any useful separations to be made, as is evident in Figure 1.

Attention was therefore turned to analogous mixed extractant systems based on organophosphoric acids, some of which are themselves known to show a high affinity towards calcium.[2] Table 1 shows the effect of some phosphonate additives on the extraction of calcium and other alkaline-earth metals by di(2-ethylhexyl) phosphoric acid (D2EHPA). It can be seen that significant synergistic shifts are obtained only for the methylenediphosphonate (TIPMDP), and that the shifts lie in the order Mg < Ca > Sr > Ba, that is, with a maximum at calcium. The same order is obtained with the ethylenediphosphonate (TIPEDP), but the shifts are considerably smaller. The shifts are smaller still with the monophosphonate (DIPHP), and no maximum is observed in the series.

Table 1 Values of pH_{50} and ΔpH_{50} for the extraction of the alkaline-earth metals by mixtures of D2EHPA (0.20 M) and additives (0.10 M) in toluene at 20°C

Additive	Mg		Ca		Sr		Ba	
	pH_{50}	ΔpH_{50}	pH_{50}	ΔpH_{50}	pH_{50}	ΔpH_{50}	pH_{50}	ΔpH_{50}
None	4.13	--	3.17	--	4.22	--	4.47	--
TIPMDP	3.72	0.41	2.41	0.76	3.61	0.61	4.04	0.43
TIPEDP	3.98	0.15	2.92	0.25	4.03	0.19	4.38	0.09
DIPHP	3.99	0.14	3.05	0.12	4.09	0.13	4.50	-0.03

TIPMDP = tetraisopropyl methylenediphosphonate.
TIPEDP = tetraisopropyl ethylenediphosphonate.
DIPHP = diisopropyl *n*-hexylphosphonate.

Table 2 Values of pH_{50} and ΔpH_{50} for the extraction of divalent transition metals by mixtures of D2EHPA (0.20 M) and additives (0.10 M) in toluene at 20°C

Additive	Mn		Co		Ni		Cu	
	pH_{50}	ΔpH_{50}	pH_{50}	ΔpH_{50}	pH_{50}	ΔpH_{50}	pH_{50}	ΔpH_{50}
None	3.19	--	3.99	--	4.52	--	3.27	--
TIPMDP	2.85	0.34	3.88	0.11	4.25	0.27	3.21	0.06
TIPEDP	3.14	0.05	3.99	0.00	4.30	0.22	3.28	-0.01
DIPHP	3.09	0.10	4.04	-0.05	4.51	0.01	3.30	-0.03

The effects of the addition of the same series of bifunctional compounds on the extraction of some divalent transition metals by D2EHPA are shown in Table 2. The shifts are considerably smaller than the corresponding values for calcium, which results in good separations between calcium and the transition metals in some cases: $pH_{50}^{Me} - pH_{50}^{Ca} = 1.84$, 1.47, 0.80 and 0.44 pH units for Me = Ni, Co, Cu and Mn, respectively, as seen in Figure 2. These separations considerably exceed those obtainable using D2EHPA alone (1.35, 0.82, 0.10 and 0.02 pH units, respectively). Also, the Mn/Co separation increases from 0.80 pH units for D2EHPA alone to 1.03 for the mixed extractant.

Table 3 Values of pH_{50} and ΔpH_{50} for the extraction of calcium and manganese by mixtures of different organophosphorus acids (0.20 M) and tetraisopropyl methylenediphosphonate (0.10 M) in toluene at 20°C

Acid type	Alkyl group, R	Ca		Mn	
		pH_{50}	ΔpH_{50}	pH_{50}	ΔpH_{50}
$(RO)_2POOH$	*n*-Octyl	1.84	0.42	2.29	0.32
	2-Ethylhexyl	2.41	0.76	2.85	0.34
	2,6-Dimethyl-4-heptyl	5.12	0.59	4.47	0.00
(RO)RPOOH	2-Ethylhexyl	4.28	0.33	3.93	0.06
R_2POOH	2-Ethylhexyl	6.05	0.10	--	--

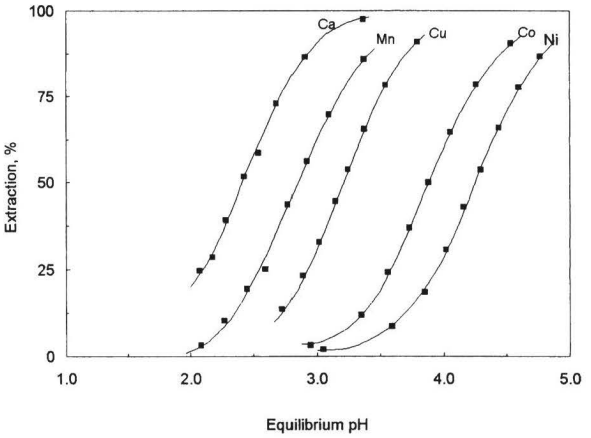


Figure 2 Extraction of divalent metals (0.02 M as nitrates) from 0.40 M sodium nitrate by a mixture of 0.20 M D2EHPA and 0.10 M TIPMDP in toluene at 20°C.

Table 3 shows the effect of the addition of 0.10 M TIPMDP on the extraction of calcium and manganese by different organophosphorus acid extractants (0.20 M in toluene). For the series of acids with a given substituent alkyl group (R = 2-ethylhexyl), the synergistic shifts for calcium (ΔpH_{50}^{Ca}) decrease in the order: $(RO)_2POOH > (RO)RPOOH > R_2POOH$, as do the separations between the extraction curves ($pH_{50}^{Mn} - pH_{50}^{Ca}$). For the organophosphoric acids $(RO)_2POOH$ with increasingly bulky alkyl groups R (*n*-octyl < 2-ethylhexyl < 2,6-dimethyl-4-heptyl), the synergistic shifts for both metals show a maximum value at the middle member of the series, but in no case can the efficient separation of these metals be effected (Table 3), the highest value of $pH_{50}^{Mn} - pH_{50}^{Ca}$ being only 0.45 pH units.

Extraction from sulphate media

It is well known that the effect of extraction from sulphate media is to increase the pH_{50} values relative to those in nitrate solutions, owing to ion pair formation between the metal cation and the SO_4^{2-} anion. [3] For the 0.20 M D2EHPA/0.10 M TIPMDP mixture, the pH_{50}^{Ca} value shifts from 2.41 to 2.72 in passing from 0.40 M $NaNO_3$ to 1.00 M Na_2SO_4. The corresponding pH_{50}^{Co} values are 3.88 and 4.48, giving a separation ($pH_{50}^{Co} - pH_{50}^{Ca}$) of 1.76 pH units in the sulphate system, as compared to 1.47 pH units in the nitrate system. Unsatisfactory values of $pH_{50}^{Mn} - pH_{50}^{Ca}$ were once again obtained, however, these being 0.53 and 0.44 pH units for the above-mentioned extractant mixture

Batch-countercurrent extraction experiments

The distribution isotherm for the extraction of calcium from 1.0 M sodium sulphate solutions by 0.20 M D2EHPA plus 0.10 M TIPMDP in toluene shows that efficient recovery (96-99%) can be obtained in 3-4 stages at pH 3.0 and an organic-to-aqueous phase ratio of 1:1, as shown in Figure 3. As an example of a possible practical application, a batch-countercurrent experiment with 3 extraction stages was carried out to remove calcium from a gypsum-saturated solution (600 mgL^{-1} Ca) containing 0.50 M cobalt sulphate and 0.50 M sodium sulphate. The above-mentioned organic phase was used at unit phase ratio, and each stage was adjusted to pH 3.0 using concentrated sodium hydroxide solution. After steady-state conditions had been reached, the raffinate was found to contain 6 mgL^{-1} of calcium (99% removal), whilst the calcium-loaded organic phase contained 90 mgL^{-1} of cobalt (0.3% loss).

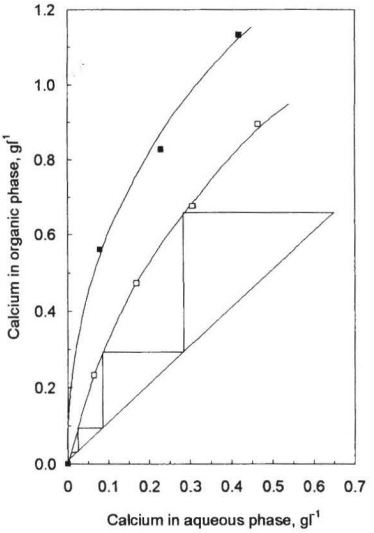
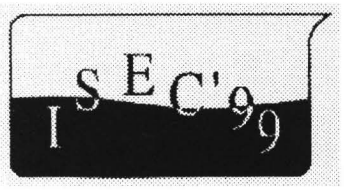


Figure 3 Distribution isotherms for the extraction of calcium from 1.0 M sodium sulphate by a mixture of 0.20 M D2EHPA and 0.10 M TIPMDP in toluene at 20°C. McCabe-Thiele construction drawn for an organic-to-aqueous phase ratio of unity.

REFERENCES

1. Preston JS and du Preez AC, *Solvent Extr. Ion Exch.*, **16**, 687, (1998).
2. Preston JS and du Preez AC, *Mintek Report, No.M378*, Randburg, 30pp, (1988).
3. Preston JS, *Hydrometallurgy*, **9**, 115, (1982).



THE EFFECT OF REAGENT STRUCTURE ON THE EXTRACTION AND SEPARATION OF NICKEL AND COBALT BY MIXTURES OF CARBOXYLIC ACIDS AND PYRIDINE DERIVATIVES

JS Preston and AC du Preez
Process Chemistry Division, Mintek, Private Bag X3015, Randburg 2125, South Africa

ABSTRACT
The effect of alkylpyridines and related compounds upon the extraction of divalent nickel and cobalt from nitrate media by solutions of some carboxylic acids in xylene was studied. Addition of the pyridine compounds caused substantial synergistic shifts in the pH_{50} values for the extraction of both metals, and these were greater for nickel than for cobalt in any given system. With regard to the influence of the nature of the individual extractants on the extent of the synergistic effects, the shifts in the pH_{50} values were found to increase with increasing pK_a and with increasing steric bulk of the carboxylic acid component. These observations can be rationalized in terms of the ease of replacement of solvating carboxylic acid ligands (HA) by the N-donor ligands (L). In contrast, the synergistic effects were somewhat less dependent on the structure of the pyridine derivative, and the shifts did not usually decrease significantly when L contained an electron-withdrawing group. However, the shifts were greatly decreased when the substituent group on the pyridine ring was located adjacent to the nitrogen atom (i.e., the metal-coordinating site), presumably for steric reasons. Batch countercurrent experiments were carried out with an aqueous feed solution containing 5 gL^{-1} nickel and 5 gL^{-1} cobalt, and an organic phase containing 0.50 M 4-(5-nonyl)pyridine and 0.25 M 4-*tert*-butylbenzoic acid. Four extraction stages at pH 4.9 and two scrubbing stages were used to obtain a 99.6% pure nickel product and a 98.7% pure cobalt product. Complete stripping of the loaded organic phase was readily achieved by contact with dilute mineral acid to give an equilibrium pH of 3.0.

Keywords: nickel, cobalt, carboxylic acids, pyridine derivatives, synergism.

INTRODUCTION

Over the past few years we have carried out a number of studies on the separation of divalent nickel and cobalt in dilute acid media by solvent extraction with synergistic mixtures of carboxylic acids and pyridinecarboxylate esters.[1-4] Most of the data pertain to systems based on alkylsalicylic acids, [2-4] since these were found to be especially conducive to large synergistic effects upon addition of the pyridine esters. However, it remains uncertain whether the synergistic shifts and nickel-cobalt separations obtained have been optimized with respect to their dependence upon the structure of either the acid or the N-donor component of the extractant mixture. Neither has it been established if the presence of the electron-withdrawing substituent (CO.OR) on the pyridine ring plays an important role in the development of substantial synergistic effects.

From a practical point of view, the likelihood of these systems being used commercially would be enhanced, for economic reasons, if the structures and syntheses of the reagents involved were the simplest possible. Accordingly, we now report on the use of simple alkyl-substituted pyridines as synergists for the extraction of nickel and cobalt by alkylsalicylic acids and some less complex carboxylic acids.

The carboxylic acids used were based upon notional modifications to the structure of 3,5-di-*tert*-butylsalicylic acid (1a in Figure 1; R = X = *tert*-C_4H_9), which was previously identified as giving the largest synergistic shifts amongst the salicylic acids examined in combination with pyridinecarboxylate esters.[3] The other acids investigated were (R = *tert*-C_4H_9 in all cases): 5-*tert*-butyl-3-methylsalicylic (1b; X = CH_3), 5-*tert*-butylsalicylic (1c; X = H), 3-bromo-5-*tert*-butylsalicylic (1d; X = Br), 4-*tert*-butylbenzoic (2), 4-*tert*-butylcyclohexane carboxylic (3), and 4-*tert*-butylphenoxyacetic acid (4).

The pyridine derivatives used included those of the 4-alkyl type (5 in Figure 1; R = 5-nonyl, *tert*-butyl, or benzyl), as well as the 3- and 2- isomers where R = benzyl (6 and 7, respectively), the 4-, 3-, and 2-benzoylpyridines (8, 9 and 10, respectively; R = phenyl) and the benzyl 3-pyridinecarboxylate (11; R = benzyl).

© 2000 Society of Chemical Industry

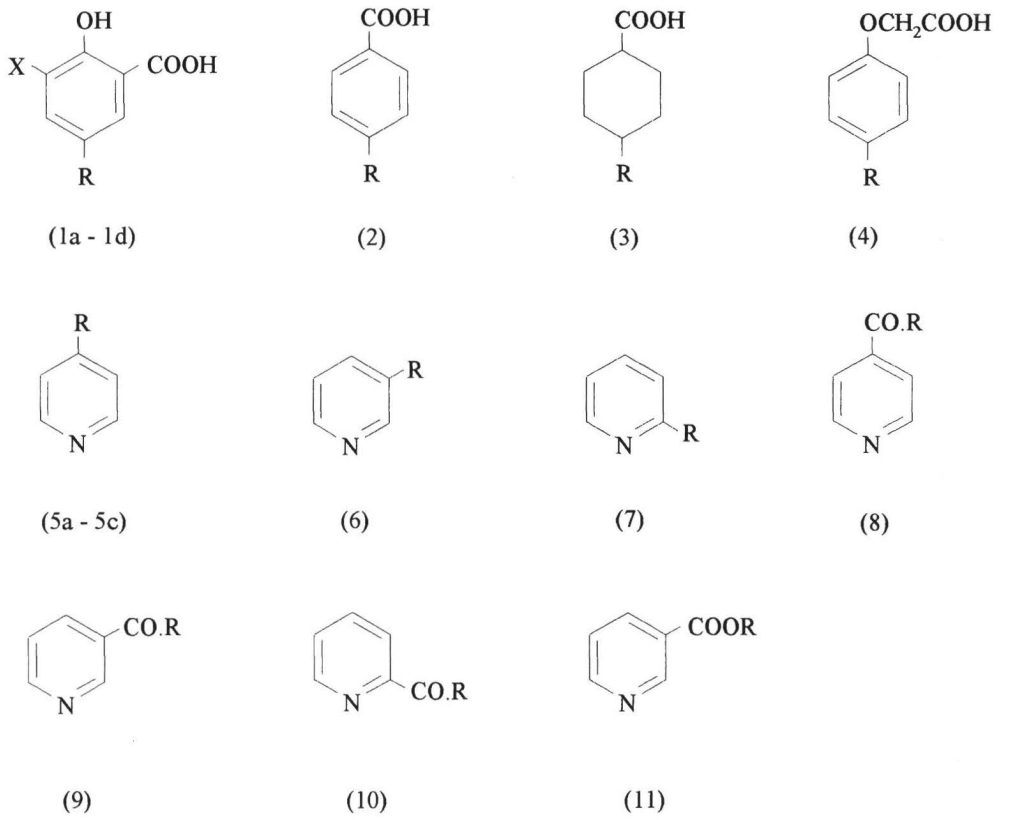


Figure 1. Structures of carboxylic acids and pyridine derivatives used (see introduction for individual identities of groups R and X).

EXPERIMENTAL

The carboxylic acids were synthesized and purified as reported previously,[3-5] whilst the pyridine derivatives were used as supplied by the Aldrich Chemical Company or Janssen Chimica (97-99% pure).

Distribution equilibria for nickel and cobalt were determined at 20°C, using the technique described previously.[2] The aqueous phases usually contained 0.02 M nickel or cobalt (as nitrates) in 0.40 M sodium nitrate. Unless stated otherwise, organic phases contained 0.25 M carboxylic acid together with 0.25 M pyridine derivative in xylene of AR grade.

RESULTS AND DISCUSSION

Effect of Structure of Carboxylic Acid on Metal Extraction

Figure 2 shows the extraction of nickel (0.02 M) from 0.40 M sodium nitrate by mixtures of 4-(5-nonyl)pyridine (0.25 M) and different carboxylic acids (0.25 M) in xylene at 20°C.

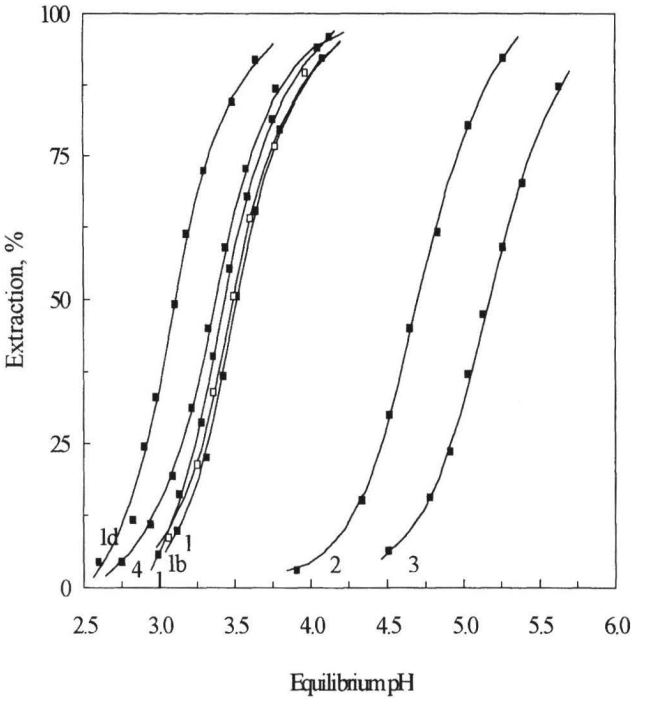


Figure 2. Extraction of nickel (0.02 M) from sodium nitrate solutions (0.40 M) by mixtures of 4-(5-nonyl)pyridine (0.25 M) and carboxylic acids (0.25 M) in xylene. Numbers on curves correspond to structures of acids shown in Fig. 1 and Table 1.

The values of pH_{50} (the pH value at 50% extraction) and ΔpH_{50} (pH_{50}^{acid} - $pH_{50}^{acid+pyridine}$) for the extraction of nickel and cobalt by these mixtures are given in Table 1. It can be seen that the order of the pH_{50} values follows that of the pK_a values of the acid component (determined as previously [5] in 50 vol.% 2-propanol containing 0.10 M sodium nitrate at 20°C), which are also shown in Table 1. However, the slopes of plots of pH_{50}^{Ni} and pH_{50}^{Co} against pK_a are considerably less than unity: the data for nickel fit the relationship:

$$pH_{50}^{Ni} = 0.313 + 0.716\ pK_a$$

with a correlation coefficient of 0.981, and those for cobalt fit the equation:

$$pH_{50}^{Co} = 0.971 + 0.712\ pK_a$$

with a correlation coefficient of 0.909.

The parallel nature of these plots confirms that separation between the two metals ($pH_{50}^{Co-Ni} = pH_{50}^{Co} - pH_{50}^{Ni}$) is almost independent of pK_a, and equal to an effectively constant value of about 0.7 pH units.

Notwithstanding the nearly constant values of pH_{50}^{Co-Ni}, there is considerable variation in the ΔpH_{50}^{Ni} and ΔpH_{50}^{Co} shifts shown in Table 1. However, it is apparent that the values for the prototype acid (1a) are not enhanced by any of the structural modifications investigated.

The particularly low shifts obtained with the phenoxyacetic acid (4) probably result from the low degree of steric hindrance in its own solvation of the metal complexes, together with the competing reaction of this relatively strong acid (HA) with the alkylpyridine (L) to form the ion-pair LH^+A^- in the organic phase.

Table 1 Values of pH_{50} and ΔpH_{50} for the Extraction of Nickel and Cobalt by Mixtures of 4-(5-Nonyl)pyridine (0.25 M) and Different Carboxylic Acids (0.25 M) in Xylene

Acid in Fig. 1 [a]		pK_a	pH_{50}			ΔpH_{50}	
No.	Group X	of acid	Ni	Co	Co-Ni	Ni	Co
1a	*t*-C_4H_9	4.82	3.51	4.29	0.78	2.29	1.60
1b	CH_3	4.55	3.49	4.26	0.77	2.11[b]	1.44[b]
1c	H	4.36	3.43	4.20	0.77	2.03	1.40
1d	Br	3.63	3.11	3.90	0.79	1.41[c]	0.85[c]
2	--	5.91	4.70	5.39	0.69	1.91	1.13
3	--	6.75	5.16	5.83	0.67	1.57	1.05
4	--	4.31	3.37	4.15	0.78	0.53	-0.13

[a] Group R is *tert*-C_4H_9 in all cases for compounds 1-4.

[b] Hypothetical pH_{50} values for acid 1b alone were estimated by means of the correlation established previously between the pH_{50} and pK_a values,[3] since it is insufficiently soluble in xylene in the absence of the alkylpyridine.

[c] Acid 1c is insufficiently soluble in xylene in the absence of the alkylpyridine, and its pK_a falls outside the range established for the correlation mentioned above. The pH_{50} values for this acid alone were therefore replaced by the corresponding values for the structurally similar 3-bromo-5-nonylsalicylic acid.

Effect of Structure and Concentration of Pyridine Derivative on Metal Extraction

Figure 3 shows the extraction of nickel (0.02 M) from 0.40 M sodium nitrate by mixtures of 4-*tert*-butylphenoxyacetic acid (0.25 M) with various pyridine derivatives (0.25 M) in xylene at 20°C.

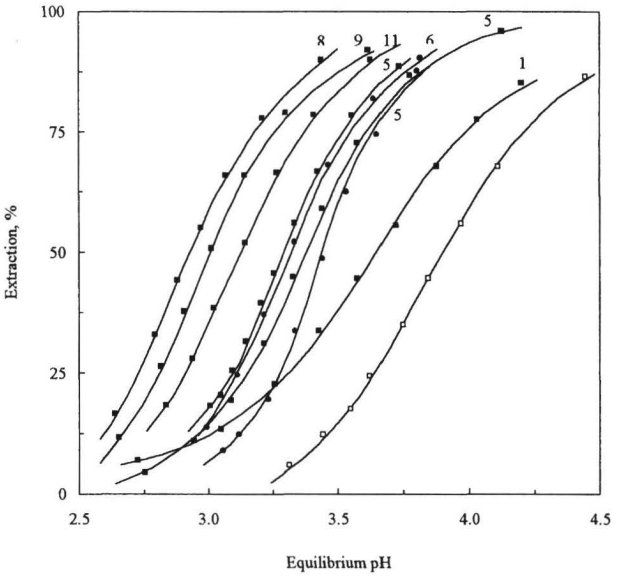


Figure 3. Extraction of nickel (0.02 M) from sodium nitrate solutions (0.40 M) by 4-*tert*-butylphenoxyacetic acid (0.25 M, open symbols) and its mixtures with pyridine derivatives (0.25 M, closed symbols) in xylene. Numbers on curves correspond to structures of pyridine derivatives shown in Figure 1 and Table 2. Open symbols show extraction by acid alone.

Table 2 shows the pH_{50} and ΔpH_{50} values for nickel and cobalt in these systems, as well as those for corresponding mixtures containing 4-*tert*-butylbenzoic acid as the acid component. It can be seen that, in most cases, nickel-cobalt separations in the range 0.64-0.78 were obtained, irrespective of the nature of the substituent group in the pyridine derivative. Similarly, the synergistic shifts for a given acid/metal combination covered a relatively small range (*e.g.*, 1.85-2.18 for nickel in systems based on 4-*tert*-butylbenzoic acid). The only exceptions to these generalizations concern systems in which the pyridine derivative contains a substituent in the 2-position (compounds 7 and 10), in which case steric effects clearly interfere with the coordination of these ligands to the metal.

Table 2 Values of pH_{50}^{Co-Ni} and ΔpH_{50} for the Extraction of Nickel and Cobalt by Mixtures of 4-*tert*-Butyl-phenoxyacetic or 4-*tert*-Butylbenzoic Acids (0.25 M) and Different Pyridine Derivatives (0.25 M) in Xylene

Pyridine deriv. in Fig. 1		4-*tert*-Butylphenoxyacetic[a]			4-*tert*-Butylbenzoic[b]		
No.	R	pH_{50}^{Co-Ni}	ΔpH_{50}^{Ni}	ΔpH_{50}^{Co}	pH_{50}^{Co-Ni}	$\Delta pH_{50}^{N}{}_{i}$	$\Delta pH_{50}^{C}{}_{o}$
5a	$(C_4H_9)_2CH$	0.78	0.53	-0.13	0.69	1.91	1.13
5b	$(CH_3)_3C$	0.65	0.45	-0.08	0.64	2.03	1.31
5c	$C_6H_5CH_2$	0.73	0.61	0.01	0.67	2.02	1.27
6	$C_6H_5CH_2$	0.77	0.59	-0.07	0.71	2.01	1.22
7	$C_6H_5CH_2$	--[c]	--[c]	--[c]	-0.12	-0.11	-0.08
8	C_6H_5	0.76	0.97	0.34	0.64	1.95	1.22
9	C_6H_5	0.75	0.89	0.27	0.69	2.18	1.40
10	C_6H_5	0.41	0.25	0.04	0.11	0.41	0.22
11	$C_6H_5CH_2$	0.77	0.78	0.12	0.68	1.85	1.10

[a] For acid alone, $pH_{50}^{Ni} = 3.90$ and $pH_{50}^{Co} = 4.02$.
[b] For acid alone, $pH_{50}^{Ni} = 6.61$ and $pH_{50}^{Co} = 6.53$.
[c] Precipitation of the extracted metal complex occurred.

For practical purposes, increasing the concentration of the pyridine dervative was found to increase the nickel-cobalt separation, as shown in Table 3 for mixtures of 4-(5-nonyl)pyridine with 0.25 M 4-*tert*-butylbenzoic acid.

Table 3 Values of pH_{50} and ΔpH_{50} for the Extraction of Nickel and Cobalt by Mixtures of 4-*tert*-Butylbenzoic Acid (0.25 M) and Different Concentrations of 4-(5-Nonyl)pyridine in Xylene

Pyridine	pH_{50}			ΔpH_{50}	
Concn. (M)	Ni	Co	Co-Ni	Ni	Co
0.00	6.61	6.53	-0.08	0.00	0.00
0.10	5.03	5.65	0.62	1.58	0.88
0.25	4.70	5.39	0.69	1.91	1.13
0.50	4.52	5.28	0.77	2.09	1.24
1.00	4.28	5.24	0.96	2.33	1.28

Batch Countercurrent Separation of Nickel from Cobalt

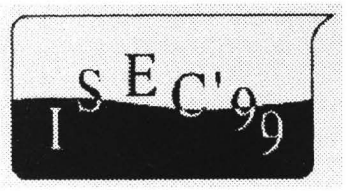
A batch countercurrent experiment [2] was carried out using a feed solution containing 5 gL^{-1} each of nickel and cobalt in 0.40 M sodium nitrate, and an organic phase comprising 0.25 M 4-*tert*-

butylbenzoic acid and 0.50 M 4-(5-nonyl)pyridine in xylene. In order to simulate more exactly an overall process, the organic phase had been previously loaded with nickel and then stripped with dilute nitric acid to pH 3.0.

On the basis of the distribution isotherm for nickel, 3 extraction stages were used at an organic-to-aqueous phase ratio of unity and an equilibrium pH of 4.9. After steady state was reached (6 full cycles), the raffinate was found to contain 95.9% pure cobalt, which was increased to 98.7% purity by the addition of a fourth extraction stage. The loaded organic phase was found to contain 94.0% pure nickel, which was increased to 99.6% purity by the addition of 2 scrubbing stages using a solution containing 25 gL^{-1} nickel at an organic-to-aqueous phase ratio of 25.

REFERENCES

1. Preston JS and du Preez AC, *J. Chem. Tech. Biotechnol.*, **61**, 159 (1994).
2. Preston JS and du Preez AC, *Solvent Extr. Ion Exch.*, **13**, 465 (1995).
3. Preston JS and du Preez AC, *Solvent Extr. Ion Exch.*, **14**, 179 (1996).
4. Preston JS and du Preez AC, *J. Chem. Tech. Biotechnol.*, **66**, 293 (1996).
5. Preston JS, *Hydrometallurgy*, **11**, 105 (1983).



SYNERGISTIC SYSTEMS FOR THE SELECTIVE EXTRACTION OF TRIVALENT ACTINIDES FROM MIXTURES OF TRIVALENT ACTINIDES AND LANTHANIDES

PY Cordier[1], N François[1], N Boubals[1], C Madic[1], MJ Hudson[2] and JO Liljenzin[3]

[1]CEA-Valrhô DCC/DRDD/SEMP, Marcoule, BP 171, 30207 Bagnols-sur-Cèze, Cédex, France

[2]Department of Chemistry, University of Reading, Box 224, Whiteknights, Berkshire RG6 2AD, UK

[3]Department of Nuclear Chemistry, Chalmers University of Technology, S-41296 Göteborg, Sweden

ABSTRACT

The extracting properties at low pH of synergistic systems composed of a soft donor ligand (Tpy or TPTZ) and a lipophilic carboxylic acid (α-bromodecanoïc acid) are summarised. The differences in the extraction performances can be explained by the difference in the basicity of the soft donor complexing ligands, in terms of competition for the complexation between the proton and the metallic cation. The extraction results can be directly linked to the properties of the ligands in the aqueous phase.

Keywords : synergism, actinides, lanthanides, carboxylic acid, triazines, terpyridine

INTRODUCTION

The separation of trivalent actinides, americium and curium, from actinides and lanthanides mixtures is an important step in an advanced partitioning process for wastes issued from the reprocessing of spent nuclear fuel. To achieve this separation, the use of soft donor complexants and/or extractants containing N or S atoms is a potential way.[1,2] In this paper, we investigate the potentialities of these systems along two complementary axes. First, we study in details the mechanism of extraction of M(III) (M = Am, Eu) by synergistic extraction systems composed either of 2,4,6-tri-2-pyridyl-1,3,5-triazine (TPTZ) or 2,2':6',6" terpyridine (Tpy) and of α-bromodecanoic acid (HαBrC10). Then, we study the complexation properties of some ligands, including TPTZ and Tpy. We try to link the extraction results with the complexation ones.

EXPERIMENTAL

Chemicals

α–Bromodecanoic acid (HαBrC10) was from Fluka (98 % purity). Nitrogen polydendate ligands (L): TPTZ and Tpy were provided by Aldrich (analytical grade reagents). Hydrogenated tetrapropene (TPH) was from Prochrom (Champignols, 54, France) and used as received as the organic diluent.

M(III) extraction procedure and determination of complexation constants.

Extraction of Am(III) and Eu(III) at tracer level was performed using ^{241}Am and ^{152}Eu (γ counting at 59.54 keV and 121.78 keV for ^{241}Am and ^{152}Eu respectively). Organic and aqueous phases were mixed for 30 minutes at 22°C. Distribution ratios D_M were calculated according to the equation $D_M = [Activity]_{org.}/[Activity]_{aq.}$; $[Activity]_{org.}$ and $[Activity]_{aq.}$ being the radioactivity (in counts/s) of

© 2000 Society of Chemical Industry

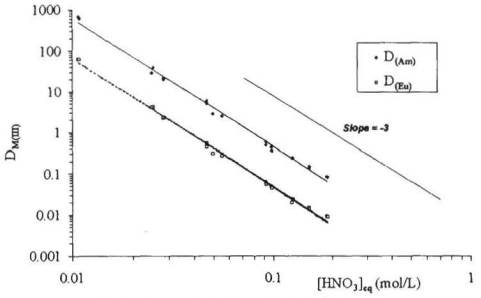
^{241}Am or ^{152}Eu at equilibrium for equal volumes of organic and aqueous phases respectively. Separation factors $SF_{Am/Eu}$ were calculated as D_{Am}/D_{Eu} ratios for the same experimental conditions.

Complexation constants were determined using UV visible spectrophotometry. Different solutions containing the same initial concentration of ligand and increasing concentrations of HCl (or MCl_3) were prepared. The ionic strength was maintained constant at I = 2, through addition of LiCl. The modifications of the ligand spectrum, namely the UV bands at 220 and 270 nm, were recorded. The experimental spectra were fitted with the theoretical ones, using a non-linear regression method (Partial Least Squares or PLS), over a wide range of wavelengths (usually 100 nm, including the two regions of interest (220 and 270 nm)). The fitting parameter was the protonation constant (or the complexation constant in case of M(III) complexation). The fitted theoretical spectra thus gave the values of these constants.

RESULTS AND DISCUSSION

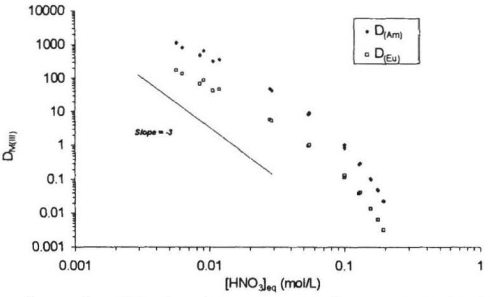
M(III) synergistic extraction system.

Figures 1 and 2 present some typical results obtained for M(III) extraction by these systems. These systems have been studied a lot recently,[3-6] for their potential ability to extract selectively Am(III) over Ln(III) from aqueous solutions of low pH.



Org. Ph.: [TPTZ] = 0.1 M, [HαBrC10] = 1 M, TPH
Aq. Phase : [HNO3] = variable, room temperature

Figure 1 : Extraction of Am(III) and Eu(III) by TPTZ in a synergistic system



Org. Ph. : [Tpy] = 0.1 M, [HαBrC10] = 1 M, TPH
Aq. Phase : [HNO3] = variable, room temperature

Figure 2 : Extraction of Am(III) and Eu(III) by Tpy in a synergistic system

The synergistic extraction of M(III) (= M^{3+}) by TPTZ or Tpy (= L) and $H\alpha BrC_{10}$ mixtures have been already studied, as mentioned before. The global formula for the extraction system was shown to be :

$$M^{3+} + z.L + (x+y).H\alpha BrC_{10} \leftrightarrow \overline{M(L)_z(\alpha BrC_{10})_x(H\alpha BrC_{10})_y^{3+}} + x.H^+ \qquad (1)$$

Such studies have outlined different phenomena for these extraction systems:

- at low pH (below pH = 1), TPTZ became soluble in aqueous phase, and there was a decrease in its extraction performance. This phenomenon was even more important in the case of Tpy;[4]
- for high $H\alpha BrC_{10}$ concentrations (above $[H\alpha BrC_{10}]$ = 0.5 mol/L), the acid dimerised in the diluent;[7]
- for high $H\alpha BrC_{10}$ and TPTZ concentrations, there was a strong interaction between TPTZ and $H\alpha BrC_{10}$, resulting in adduct formation. This was also the case with Tpy;[4]

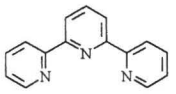
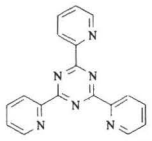
- increase in the lipohilicity of the system did not automatically lead to an increase in the M(III) extraction performances.[6]

All these results allowed us to understand the mechanisms of extraction, but no definite proof was obtained about the reason for the better M(III) extraction by TPTZ system than Tpy at low pH. For that reason we focused our interests in the determination of the protonation and M(III) complexation constants of these two ligands in similar media.

Complexation and protonation constants.

Some protonation constants of Tpy and TPTZ are already available in literature, but the media always differed. Table 1 below summarises the results available, and introduces the values found in this work.

Table 1 : Protonation constants of Tpy and TPTZ in different media

	References	Conditions	pKa_1	pKa_2
Terpyridine 	7		4.69	3.99
	8	H_2O (I = 0.001)		3.27
		H_2O (I = 0.01)	4.66	3.28
		H_2O (I = 0.05)	4.81	
	9	H_2O - I = 0.05	4.55	3.45
	This work	MeOH/H_2O (I = 2)	3.2 ± 0.2	2.9 ± 0.2
TPTZ 	3	H_2O (I = 1)	3.3 ± 0.2	1.8 ± 0.3
		H_2O (I = 1)	3.8 ± 0.2	2.7 ± 0.3
	This work	MeOH/H_2O (I = 2)	2.4 ± 0.2	0.9 ± 0.1

The values presented have a wide dispersion. Nonetheless, the values for high ionic strength media are in good accordance within each other. TPTZ appears less basic than the Tpy, which is in accordance with the extraction data concerning these two systems :

- TPTZ was a better extractant than Tpy at low pH;
- Tpy was more soluble in aqueous phase at low pH.

The next step was the determination of complexation constants with Eu(III) as explained in the experimental section.

The different equilibria in aqueous phase can be written as follows:

$$LH^+ \rightleftharpoons L + H^+ \qquad \text{with } K_{a1} = \frac{[L]\cdot[H^+]}{[LH^+]} \qquad (2)$$

$$LH_2^{2+} \rightleftharpoons LH^+ + H^+ \qquad \text{with } K_{a2} = \frac{[LH^+]\cdot[H^+]}{[LH_2^{2+}]} \qquad (3)$$

$$L + M^{3+} \rightleftharpoons ML^{3+} \qquad \text{with } \beta = \frac{[ML^{3+}]}{[L]\cdot[M^{3+}]} \tag{4}$$

By expressing the conservation of the species, M^0 being the initial concentration of the metal and L^0 the initial concentration of the ligand, we have :

$$L^0 = \alpha \cdot [L] + \beta \cdot [L] \cdot [M^{3+}] \qquad \text{with } \alpha = 1 - \frac{[H^+]}{K_{a1}} + \frac{[H^+]^2}{K_{a1} \cdot K_{a2}} \tag{5}$$

$$M^0 = [M^{3+}] + \beta \cdot [L] \cdot [M^{3+}] \tag{6}$$

By using Equations (2), (3) and (4) into Equations (5) and (6), it becomes :

$$\alpha \cdot \beta \cdot [L]^2 + (\beta \cdot (M^0 - L^0) + \alpha) \cdot [L] - L^0 = 0 \tag{7}$$

Equation (7) is a classical square equation, which can be resolved into:

$$[L] = \frac{-\beta \cdot (M^0 - L^0) - \alpha + \sqrt{\Delta}}{2 \cdot \alpha \cdot \beta} \quad \text{with } \Delta = (\beta \cdot (M^0 - L^0) + \alpha)^2 + 4 \cdot \alpha \cdot \beta \cdot L^0 \tag{8}$$

We thus have the expression of the ratio of the complexed species over the protonated ones:

$$\frac{[ML^{3+}]}{[LH^+] + [LH_2^{2+}]} = \frac{2 \cdot \alpha \cdot \beta \cdot M^0}{\alpha - 1} \cdot \frac{1}{\alpha - \beta \cdot (M^0 - L^0) + \sqrt{\Delta}} \tag{9}$$

This expression can be simplified, by taking into account the chemical properties of the system, and the different possible approximations:

K_{a1} and $K_{a2} << 1$; M^0 and $L^0 << 1$; $pH \leq 1$ (strong acidity)

Then we have:

$$\alpha \approx \frac{[H^+]^2}{K_{a1} \cdot K_{a2}}, \; \alpha >> \beta \cdot L^0, \text{ and } \alpha >> \beta \cdot (M^0 - L^0) \tag{10}$$

So the ratio of the complexed species over the protonated ones can be expressed as:

$$\frac{[ML^{3+}]}{[LH^+] + [LH_2^{2+}]} \approx \frac{\beta \cdot M^0 \cdot K_{a1} \cdot K_{a2}}{[H^+]^2} \tag{11}$$

Or in logarithmic presentation :

$$\log\left(\frac{[ML^{3+}]}{[LH^+] + [LH_2^{2+}]}\right) \approx \log\beta - pK_{a1} - pK_{a2} + 2 \cdot pH + \log M^0 \tag{12}$$

We used Equation (12) to present our results in table 2 below.

Table 2 : Complexation constants of Tpy and TPTZ with Eu(III)

	Acidity constants		Complexation constants with Eu^{3+}	Selectivity Eu^{3+}/H^+	
	pK_1	pK_2	log β_1(Eu)	pH = 0	pH = 1
Tpy	3.6	2.9	2.4	-4.1	-2.1
TPTZ	2.3	0.9	2.9	-0.3	1.7

Solvent medium CH_3OH/H_2O (76/24%$_{vol}$), I = 1 mol.L^{-1} (LiCl), 25°C

This table enabled us to deduce the speciation of the elements in an aqueous phase containing nitric acid and europium nitrate:

- in the case of Tpy, the data showed that for both pH values (0 and 1), the protonation reaction was the strongest, due to the high basicity of Tpy;
- in the case of TPTZ, at pH = 0, the protonation reaction was preponderant, but at pH = 1 it was the M(III) complexation reaction which was the strongest one, thus indicating a possible extraction of M(III) for this pH value.

These results explained the behaviour of the molecules in the extraction system, and allowed us to understand why TPTZ was a better extractant than Tpy from low pH aqueous solutions.

CONCLUSIONS

In this study, we were able to explain the differences in the behaviours of complicated synergistic systems, by the behaviour of one of their components in the aqueous phase (the nitrogen polydendate ligand). The importance of M(III)/H^+ competition was pointed out in our systems. In our search for the design of new extractants for the An(III)/Ln(III) separation from nitric acid solutions, this will enable us in the future to look for ligands with a very low pK_a. As was shown in this study this is the most important parameter to look for.

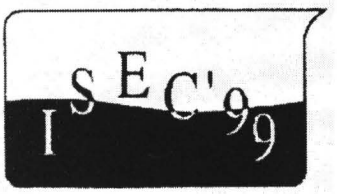
ACKNOWLEDGEMENTS

One of the author (PYC) wishes to thank Dr. Guillaneux for the mathematical treatment of the spectrophotometric data.

REFERENCES

1. Musikas C, *Proc. Int. Symp.*, Honolulu, 1984, Choppin, Navratil and Schulz Ed., World Scientific, Singapore.
2. Nash DL, *Solv. Extr. and Ion Exch.*, **11**, 729, (1993).
3. Vitorge P, PhD thesis, University Paris VI, (1983).
4. Hagstrom I, Spjuth L, Enarsson Å, Liljenzin JO, Skalberg M, Hudson MJ, Iveson PB, Madic C, Cordier PY and Hill C, *accepted for publication Sep. Sci. and Tech.(1999)*
5. Cordier PY, Hill C, Baron P, Madic C, Hudson MJ and Liljenzin JO, *J. All. and Comp.*, **271-273**, 738, (1998).
6. Cordier PY, Madic C, Liljenzin JO, Iveson PB and Hudson MJ, *Fifth international information exchange meeting on actinide and fission product partitioning and transmutation*, Mol (Belgium), OECD/NEA (1998).

7. Madic C, PhD thesis, University Paris VI, (1975).
8. James BR and Williams RJP, *J. Chem. Soc.*, 2007, (1961).
9. Offenhartz POD, George P and Haight GP, *J. Phys. Chem.*, **67**, 116, (1963).
10. Bullock JI and Simpson PWG, *J. Chem. Soc.*, Faraday Trans., **77**, 1991, (1981).



SEPARATION OF TRIVALENT AMERICIUM AND EUROPIUM WITH SOME SUBSTITUTED OLIGOPYRIDINES AND TRIAZINES IN SYNERGY WITH 2-BROMODECANOIC ACID

Å Enarsson[1], L Spjuth[1], JO Liljenzin[1], G Källvenius[1], MJ Hudson[2], PB Iveson[2], ML Russell[2], C Madic[3] and PY Cordier[3]

[1] Department of Nuclear Chemistry, Chalmers University of Technology, S-41296 Göteborg, Sweden.

[2] Department of Chemistry, University of Reading, Box 224, Whiteknights, Berkshire RG6 6AD, UK.

[3]CEA-Valrhô, Marcoule, BP 171, 30207 Bagnols-sur-Cèze, Cédex, France

ABSTRACT

The separation of trivalent americium and europium with some substituted oligopyridines and triazines in synergy with 2-bromodecanoic acid was studied. All ligands, except the quinolinyl-derivatives, showed high metal extraction and good separation factors for trivalent americium over europium. The substituted di-pyridyltriazines and the quaterpyridine showed the highest distribution ratios and quater- and quinquepyridine the highest separation factors, at low nitric acid concentration. The basicity of the different ligands was determined by titration in acetonitrile media and was related to the metal extraction. The substituted di-pyridyltriazines, which showed the highest metal extraction also showed the lowest basicity.

Keywords: americium, europium, non-aqueous titration, synergism, 2-bromodecanoic acid, oligopyridines, triazines

INTRODUCTION

In future reprocessing of spent nuclear fuel, transmutable actinides are considered to be selectively extracted from the fission products.[1] One of the major problems in this reprocessing is the separation of the trivalent actinides, mainly Am and Cm, from the trivalent lanthanides, because of their similar chemical properties in aqueous solution.[2] Previous studies on tri-pyridyltriazines (TPTZ) showed that these ligands had the potential to separate trivalent actinides from trivalent lanthanides.[3] Batch extraction experiments were performed to investigate the possibility of separating trivalent actinides from lanthanides by solvent extraction with a synergistic mixture of substituted oligopyridine or triazine, and 2-bromodecanoic acid. Both extraction and separation ability were studied and the basicity of the different ligands was also determined by titration in non-aqueous media. The extraction and separation performances were related to the basicity of the ligands.

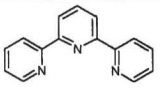
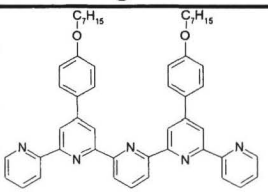
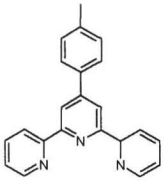
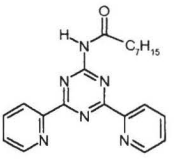
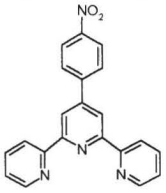
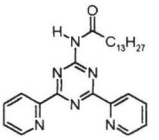
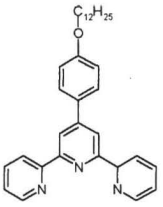
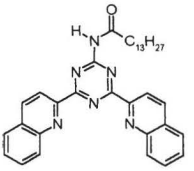
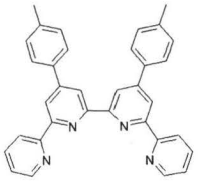
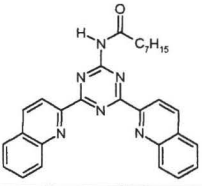
EXPERIMENTAL

Reagents

The oligopyridines and triazines listed in Table 1, were synthesised at the University of Reading except for Terpyridyl, 98% purity, which was purchased from Aldrich. The purity of the synthesised ligands was checked by ^{1}H-NMR, elemental analysis and melting point determination. *Tert*-butylbenzene (99%) from Acros, was used as the diluent in all experiments and 2-bromodecanoic acid (HA), 98% purity, was obtained from Fluka. HPLC-grade acetonitrile (Fischer Scientific), with less than 0.0040% water, was used in the non-aqueous titrations.

© 2000 Society of Chemical Industry

Table 1 Ligands studied in this work

Ligand	Name/Abbreviation	Ligand	Name/Abbreviation
	2,2′-6′,2′′-terpyridine **Terpy**		(4′,4′′′)-di-(4-heptyloxyphenyl)-2,2′:6′2′′:6′′2′′′:6′′′2′′′′-quinquepyridine **Quinque**
	4′-tolyl-2,2′:6′2′′-terpyridine **Tolpy**		4-octanoyl amino-2,6 di(2-pyridyl) 1,3,5 triazine **OADPTZ**
	4′-(4-nitrophenyl)-2,2′:6′2′′-terpyridine **Nitrotolpy**		4-tetradecanoyl amino-2,6 di(2-pyridyl) 1,3,5 triazine **TADPTZ**
	4′-(4-dodecyloxyphenyl)-2,2′:6′2′′-terpyridine **Dodoxy**		4-tetradecanoyl amino-2,6 di(2-quinolinyl) 1,3,5 triazine **TADQTZ**
	(4′,4′′)-ditolyl-2,2′:6′2′′:6′′2′′′-quaterpyridine **Quater**		4-octanoyl amino-2,6 di(2-quinolinyl) 1,3,5 triazine **OADQTZ**

Procedure

The solvent mixture of 1 M 2-bromodecanoic acid and 0.02 M of the extractant (oligopyridine or triazine) in TBB was vigorously shaken with the aqueous phase, containing tracer amounts of ^{241}Am and ^{152}Eu, for five minutes at room temperature. After phase disengagement by centrifugation, aliquots of each phase were withdrawn for radiometric analysis. The γ-activities at 59.6 keV and 122 keV, for ^{241}Am and ^{152}Eu respectively, were measured using a HPGe detector (EG&G ORTEC). The distribution ratio D_M was taken as the ratio of the measured radioactivity of aliquots of organic and aqueous phases, with equal volumes of each phase. The basicities were determined by titration in acetonitrile media, using 0.1M $HClO_4$ in anhydrous acetic acid as the titrand.[4] The half-neutralisation potential (HNP) was used as a value for the basicity. To facilitate dissolution of the ligands in the titration media, a constant amount of HA (0.25 mmol) was added to the solvent in each experiment.

For Quater and Quinque, which are even harder to dissolve, a modified titration media was used (60% acetonitrile, 40% chlorobenzene). A higher amount of HA (1 mmol) was also added to each experiment and the ligands were thereafter compared to Terpy in the same modified media.

RESULTS AND DISCUSSION

Metal Extraction

Extraction studies were carried out on a number of oligopyridines and triazines in synergy with 2-bromodecanoic acid (HA) in *tert*-butylbenzene.

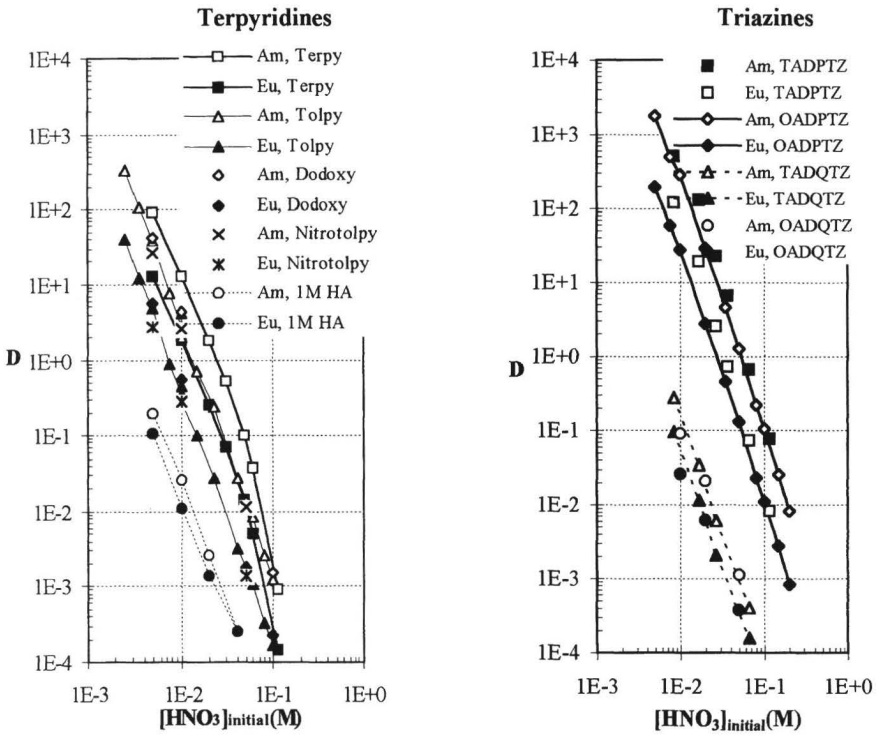


Figure 1 Extraction of americium and europium with 0.02M oligopyridine or triazine and 1M HA in *tert*-butylbenzene compared to extraction with only 1M HA.

Substitution on the terpyridine was expected to increase the distribution ratios due to an increase in lipophilicity of the ligand, but the distribution ratios for the substituted terpyridines are lower than for the unsubstituted Terpy. Other effects, like the basicity of the ligands, seem to be more important for the metal extraction than lipophilicity. The substituted terpyridines in figure 1, i.e. Tolpy, Dodoxy and Nitrotolpy, show similar nitric acid dependency, distribution ratios and separation factors for americium and europium. The different substituents on the central pyridyl groups do not seem to effect the extraction considerably. The substituted triazines, TADPTZ and OADPTZ, showed even better extraction than the oligopyridines, although the separation factor is similar to the oligopyridines, see figure 1 and table 2. On the other hand, the quinolinyl derivatives, OADQTZ and TADQTZ, showed almost no synergistic enhancement in metal extraction or separation compared to extraction with only HA, figure 1.

The oligopyridines with four and five pyridyl-groups respectively, Quater and Quinque, both showed larger selectivity for americium over europium than both the substituted terpyridines and the triazines at low nitric acid concentration, figure 2. The number of nitrogens that are coordinated to the

metal could be the important factor to achieve good separation of trivalent actinides from trivalent lanthanides. However, when the nitric acid concentration is increased the separation factor decreases to a value below the separation factor for the terpyridines, indicating that protonation at higher nitric acid concentration might hinder the coordination of the metallic cation.

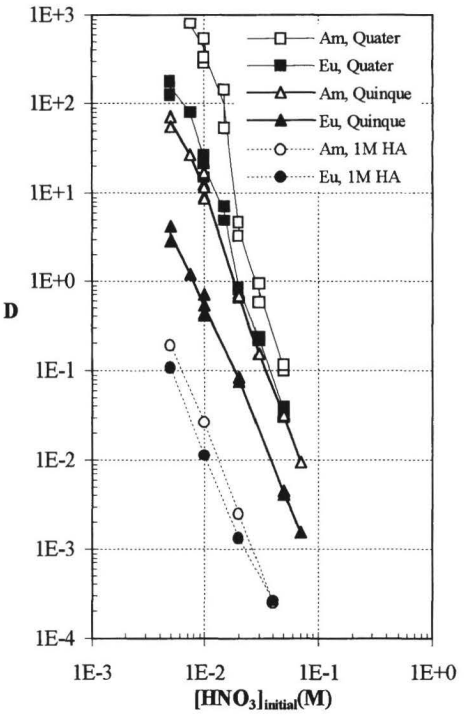


Figure 2 Extraction of americium and europium by 0.02M of Quater or Quinque and 1M HA in *tert*-butylbenzene from nitric acid.

Basicity

The basicity of the ligands is assumed to be related to the metal extraction due to the competition between protons and metal ions for the binding sites in the molecules, when extracted from acidic media. The basicity was therefore measured for the different ligands, by titration in acetonitrile media, where the potential at the half-neutralisation volume (HNP) was taken as a measure for the basicity.

The titrations of the different ligands showed lower basicity, higher HNP, for Terpy compared to the substituted terpyridines, Dodoxy and Tolpy, as seen in table 2. The metal extraction is highest for Terpy compared to the other terpyridines, which is consistent with the assumption that low basicity gives high metal extraction. However, Nitrotolpy showed the lowest basicity of the terpyridines but also the lowest metal extraction. Low solubility of this ligand in the organic phase might be the cause for this lower extraction.

The substituted triazines showed even lower basicity than the substituted oligopyridines, table 2. The di-pyridyltriazines, TADPTZ and OADPTZ, also showed better metal extraction than the substituted oligopyridines, but the quinolinyl derivatives, TADQTZ and OADQTZ, showed the lowest metal extraction of all studied ligands. The metal extraction with TADQTZ and OADQTZ seen in figure 1 is mainly due to HA in this system. Molecular modeling shows that there is sterical hindrance in the molecule and this might make coordination difficult and therefore decreases the extraction.

Table 2 Extraction data with 0.02M oligopyridine and 1M HA in *tert*-butylbenzene at 0.01M HNO_3 and average HNP measured in acetonitrile with addition of 0.25mmol HA.

Ligand	HNP(mV)	D_{Am}	SF (D_{Am}/D_{Eu})
Dodoxy	137	4.2	7.7
Tolpy	143	2.8	8.3
Terpy	157	13	7.2
Nitrotolpy	179	2.6	9.0
TADPTZ	195	359	7.5
OADPTZ	198	287	10
OADQTZ	233	0.09	3.5
TADQTZ	234	0.16	3.0

The separation factor does not seem to change much when basicity changes. The best separation factors were achieved with Quater and Quinque at low nitric acid concentration and their basicities were shown to be even higher than Terpy, table 3. The number of nitrogens that coordinate to the metal during the extraction might be more important for the separation, as mentioned earlier. Crystallography of a Y(III)-Quater complex showed that Quater is coordinating with its four nitrogen atoms to the metal and a Eu(III) complex with an oligopyridine with six pyridyl-groups showed coordination of six nitrogen atoms to the metal. [5,6] Both the separation factor and the high distribution ratios for Quater could be due to the large number of nitrogens that coordinate to the metal. If Quinque is assumed to coordinate to the metal with its five nitrogen atoms, it would be expected to be an even better extractant and show better selectivity. However, the metal-Quater complexes were shown to have more stable conformations than metal complexes with Quinque which results in the better metal extraction with Quater.

Table 3 Extraction data with 0.02M oligopyridine and 1M HA in *tert*-butylbenzene at 0.01M HNO_3. Average HNP measured in 60% acetonitrile/40% chlorobenzene with addition of 1mmol HA.

Name	HNP(mV)	D_{Am}	SF (D_{Am}/D_{Eu})
Quinque	167	12	22
Quater	175	390	19
Terpy	191	13	7.2

The relation between metal extraction and basicity is seen in figure 3 where $D_{Am(III)}$ at 0.01M HNO_3 is plotted versus the HNP for the different ligands. The quinolinyl derivatives were excluded from this graph since they do not contribute to the extraction compared to HA alone. Nitrotolpy is also a bit out of range, but, as discussed earlier, solubility problems with this ligand are probably affecting the metal extraction.

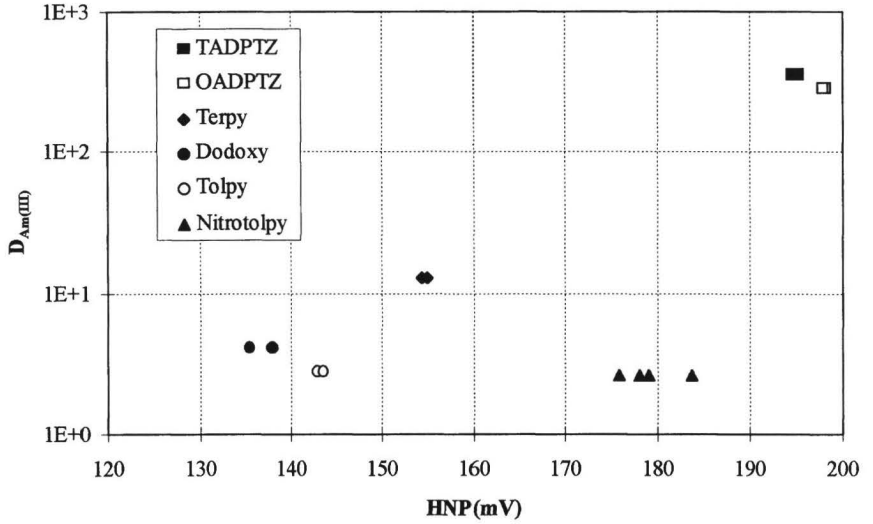
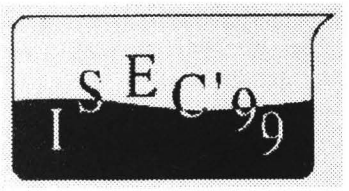


Figure 3 Extraction of Am(III) at 0.01M HNO_3 with 0.02M of the ligand, 1M HA in *tert*-butylbenzene plotted versus basicity (HNP) in acetonitrile.

REFERENCES

1 Madic C and Hudson MJ, *EUR 18038 EN*, 1998
2. Nash KL, *Solv. Extr. Ion Exch.*, **11**(4), 729-768, (1993)
3. Vitorge P, *CEA-R-5270*, (1984)
4. Fritz JS, *Anal. Chem.* **25**(3), 407, (1953)
5. Constable EC, Chotalia R, and Tocher D, *J. Chem. Soc. Chem Com.*, No.10, 771, (1992)
6. Constable EC, Elder SM, and Tocher DA, *Polyhedron*, **11**(20), 2599, (1992)



SYNERGETIC SOLVENT EFFECTS IN THE KINETICS OF THE EXTRACTION OF CHROMIUM(III)

C Mack and MJ Hampe
Institute of Chemical Process Engineering, Darmstadt University of Technology, Petersenstr. 30, D-64287 Darmstadt, Germany

ABSTRACT
Kinetics of extraction of chromium(III) by bis(2-ethylhexyl)phosphoric acid (D2EHPA) is studied experimentally. The influence of contact time and of type and concentration of the organic diluent is discussed. Single drop experiments have been carried out using a single drop and drop swarm cell, which allows to contact both phases for definite times. The structure of the organic diluent is of strong influence on both extraction kinetics and equilibrium.

Key-words: extraction kinetics, solvent effects, chromium(III), bis(2-ethylhexyl)phosphoric acid, synergism

INTRODUCTION

Chromium(III) is used as a catalyst for organic syntheses and for the tanning of leather.[4] In effluent streams chromium may give rise to environmental problems. Chromium as other heavy metals too, acts toxic on fishes (> 52 mg/l), plants (algae: >5 mg/l) and arthropodes (> 0,32 mg/l), so that a decontamination of industrial effluents containing these metals is necessary. Liquid-liquid extraction is one possibility in order to decrease the concentration of metal ions in aqueous solutions. Efficient process design is based on knowledge of the transport properties of the transfer component, its equilibrium and in this case also of the kinetics of the ion exchange reaction.

Extraction of chromium(III) from aqueous solutions by D2EHPA was studied by some authors before, but systematic and detailed observations of the influence of the diluents on kinetics and equilibrium are scarce. Pandey[4] studied the extraction of chromium(III) with combinations of D2EHPA, Cyanex and isodecanol in kerosene; slow kinetics of extraction is reported, which could be confirmed by our studies. The dependency of extraction equilibrium on acidity, concentration, temperature and kind of diluent has been discussed by Islam and Biswas.[2] The present work focuses on the difference of the extraction kinetics of chromium(III) and by bis(2-ethylhexyl)phosphoric acid (D2EHPA) with respect to different diluents. Results are compared to those of the extraction of zinc(II).

EXPERIMENTAL PROCEDURES

The aqueous solutions (0,01 M) were prepared by dissolving $CrCl_3 \cdot 6\ H_2O$ and $ZnCl_2$ in water. The reagent grade salts were commercially supplied by Merck KGaA (Darmstadt, Germany). Chromium(III) forms hexa-coordinated complexes with many inorganic species. After the salt is dissolved, the solution is coloured darkgreen. Because of the substitution of chloride ions by water molecules within the first co-ordination sphere, after some time the colour changes to violet.

$$\underset{\text{darkgreen}}{[CrCl_3\,(H_2O)_3]\cdot 3H_2O} \quad \leftrightarrow \quad \underset{\text{violet}}{Cr(H_2O)_6Cl_3}$$

The aqueous phases containing chromium(III) were stored for 24 hours, so that only violet solutions were used for the experiments. Organic solutions were made of D2EHPA (Merck KGaA and Bayer AG, Germany) dissolved in toluene (Merck KGaA), cyclohexane (Merck KGaA) and isododecane (Bayer AG). The aqueous phase was saturated with the diluent of the organic phase before the salts were dissolved. No modifiers were used. The starting pH-value in the aqueous phase was 3. All chemicals were used without further purification. Experiments were carried out at $25 \pm 0{,}1$ ° C. Metal concentrations were detected using a Perkin Elmer AAnalyst 300 atomic absorption spectrometer.

© 2000 Society of Chemical Industry

Equilibrium experiments were carried out in a glass vessel of 200 ml capacity by taking equal amounts (50 ml) of aqueous and organic phases. The contact times of the equilibrium experiments were up to 48 hours. Kinetics of extraction was observed using the experimental setup shown below.

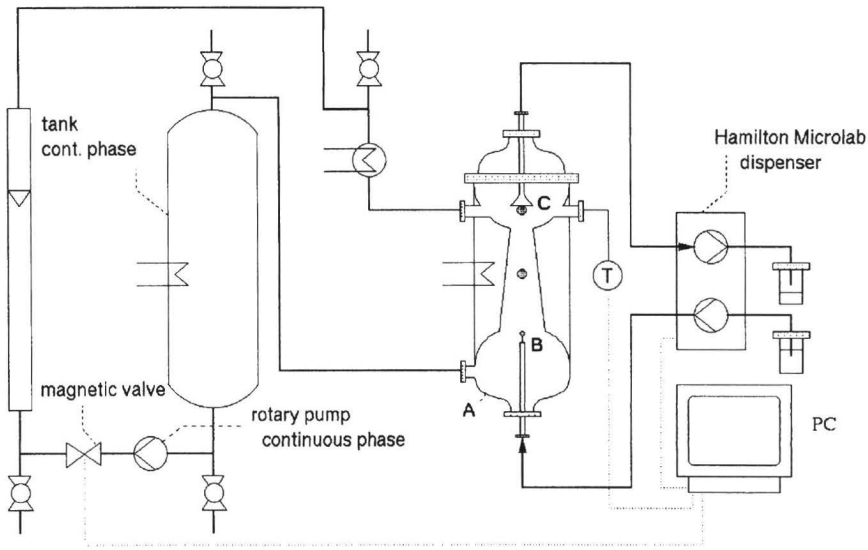


Figure 1: Experimental set-up used for kinetic experiments

The experimental set-up shown in figure 1 was developed and tested by Schröter et al.[5] Its main part is device A allowing to contact two fluid phases in countercurrent flow for a definite time. Single drops or swarms of drops of the dispersed phase are fixed at a velocity-dependent location in a cone by the continuous phase moving in the opposite direction. The flow of the continuous phase is sustained by a rotary pump. Drops of the disperse phase are generated at the orifice of a capillary (B) using one of two syringes of a Hamilton Microlab 541C dispenser. The drop size depends on the diameter of the orifice of the capillary, the ejecting velocity and the properties of the liquids used. The radius of the droplets varied between 2.5 mm and 2.7 mm depending in the nature of the diluent. The contact time between the two phases is controlled by a magnetic valve interrupting the flow of the continuous phase. The drops rise to a collecting capillary (C) and are sucked off automatically using the second syringe of the Hamilton dispenser. The circulating volume of the continuous (aqueous) phase is about two liters and can be increased up to about 4.5 liters using an accessory tank (not shown). Because of the large excess of the volume of the aqueous phase over the volume of the organic phase the concentrations of the aqueous phase do not change significantly during experiments.

RESULTS AND DISCUSSION

Equilibrium models

The basic reaction for the extraction of chromium(III) is (a bar indicates species in the organic phase)

$$CrCl_3 + 3\,\overline{RH} \leftrightarrow \overline{CrR}_3 + 3\,HCl \qquad (1)$$

D2EHPA is considered to be mainly monomeric in aromatic and dimerized in aliphatic diluents.

Dependency of extraction on contact time

The molar flux of a component i from the bulk to the interface is given by

$$\dot{n}_i = \beta_i (c_i - c_i^*) \qquad (2)$$

with β_i being the mass transfer coefficient, c_i the concentration in the bulk and c_i^* the concentration at the interface. If the mass transfer is at unsteady state, penetration theory can be used to describe the mass transfer between the interface and the bulk. Use of Fick's second law of diffusion

$$\frac{\partial c_i}{\partial t} = D_{ij} \frac{\partial^2 c_i}{\partial x^2} \qquad (3)$$

leads to the definition of β_i

$$\beta_i = \sqrt{\frac{D_{ij}}{\pi t}} \qquad (4)$$

in terms of the diffusion coefficient D_{ij} and the contact time t of the liquid elements at the liquid-liquid interface. β_i exhibits the characteristic dependency on the inverse square root of contact time. This characteristic could be found in all experiments. Figure 2 shows the mean concentration of chromium(III) in an organic droplet dependent on the contact time and the diluent. The time in seconds is represented as absciss and the concentration of Cr(III) in the organic phase as ordinate.

Mass transfer

To model the mass transfer, it is necessary to know whether the mass transfer is governed by chemical reaction or molecular transport. As D2EHPA is nearly insoluble in the aqueous phase, it is probable, that the liquid-liquid interface is the location where the chemical reaction takes place.

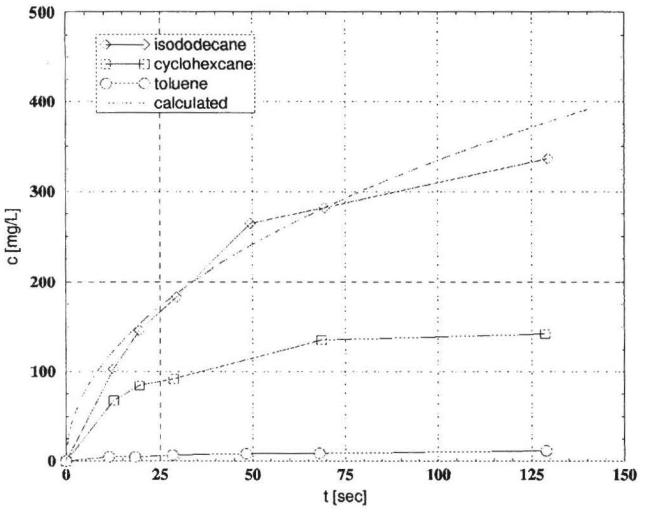


Figure 2: Mean concentration of Cr(III) in the organic phase; initial concentrations 0,01 M (520 mg/L) Cr(III) in the aqueous phase and 0,09 M D2EHPA in the organic phase; broken line given by equation (5)

To get a first impression, experimental results are compared with calculations based on the model of a rigid sphere where mass transfer takes place only by radial diffusion. Transformation of Fick's second law of diffusion to spherical co-ordinates and solving it under the assumption of a constant concentration at the interface leads to the time-dependent mean concentration in the sphere

$$c_i = c_o \left[1 - \frac{6}{\pi^2} \sum_{n=1}^{\infty} \frac{1}{n^2} \exp\left(- \frac{D_{ij} n^2 \pi^2 t}{R^2} \right) \right] \qquad (5)$$

with the radius of the sphere R and the equilibrium concentration at the interface c_0 . Calculations have been carried out for D2EHPA/isododecane. The diffusion coefficient D_{ij} was estimated as $3.25 \cdot 10^{-10}$ m²/sec (0.09 M D2EHPA) and $2.02 \cdot 10^{-10}$ m²/sec (0.9 M D2EHPA) by the method of Wilke and Chang using the molar mass of a complex containing one chromium(III) ion and three D2EHPA anions. Diffusion coefficents are going to be determined experimentally in the near future. The calculated concentrations as function of time are shown in figure 2 (0.09 M D2EHPA) and figure 3 (0.9 M D2EHPA) by the broken lines. The measured concentrations are in the same range as the ones calculated by equation (5). Similar results have been discovered for the other diluents used. The limiting case of purely diffusive transport and vanishing convection is reached for rigid drops. However, the droplets were not rigid but clearly exhibited the circulating regime. If mass transfer from the bulk of the continuous phase to the interface is supposed to be very fast and to offer no significant mass transfer resistance, the influence of the chemical reaction on the interfacial resistance can be estimated. Keeping in mind that the model used is for a rigid sphere without convection inside, the observed concentrations should be higher than the calculated ones. Taking into consideration the effect of convection (circulation inside the droplet) by using the model of Kronig and Brink,[3] calculated results would be even higher. This leads to the conclusion, that the mass transfer of chromium(III) is influenced by chemical reaction rates.

Dependency of the extraction on D2EHPA-concentration

Figure 3 compares the curves for D2EHPA-concentrations of 0,9 M and 0,09 M dissolved in the diluents isododecane and toluene.

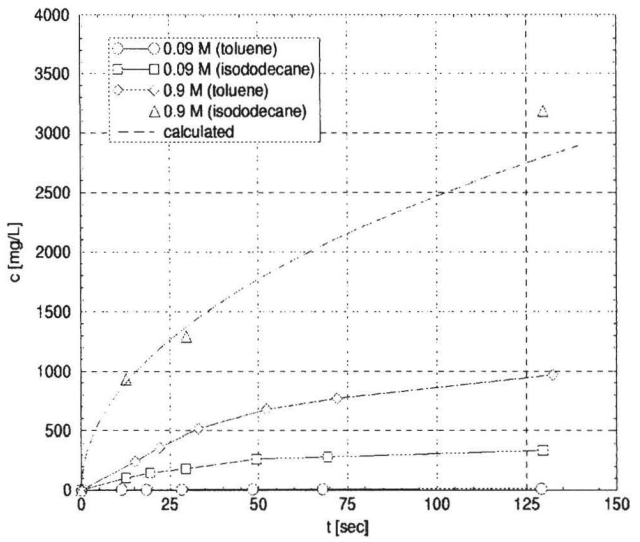


Figure 3: Mean concentration of Cr(III) in the organic phase; initial concentrations 0,01 M (520 mg/L) Cr(III) in the aqueous phase and 0,09 M and 0,9 M D2EHPA in the organic phase; broken line given by equation (5)

The ratio of the time-dependent concentration of chromium(III) in the droplet for higher D2EHPA contents is about ten times for isododecane, but about hundred times in the case of toluene. Further investigations dealing with this effect are necessary.

Dependency of extraction on the diluent

Figures 2 and 3 show, that an aliphatic diluent is more applicable to the extraction of chromium(III) with D2EHPA than diluents with cyclic structure and aromatic diluents. The rate of extraction increases in the order:

$$\text{toluene} < \text{cyclohexane} < \text{isododecane}$$

Similar results have been reported by Islam and Biswas.[2]

Comparison of the extraction of zinc(II) and chromium(III)

Figure 4 shows the mass transfer coefficient of zinc(II) and chromium(III) dependent on the time. The mass transfer coefficient of zinc is about six times as high as the one of chromium(III).

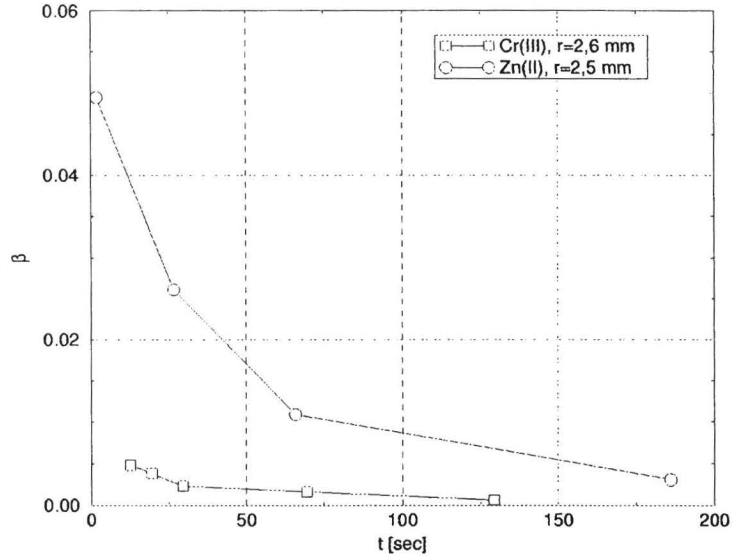
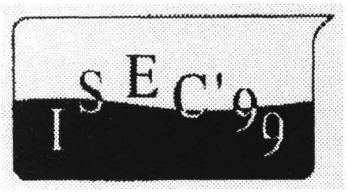


Figure 4: Mass transfer coefficient ß [mm/sec] for 0,09 M D2EHPA in isododecane dependent on contact time *t*; initial concentrations of chromium(III) and zinc(II) 0.01M.

REFERENCES

1. Godfrey JC and Slater MJ, *'Liquid-Liquid Extraction Equipment'*, John Wiley & Sons, Chichester, New York, (1994).
2. Islam MF and Biswas RK, *Canad. J. Chem.*, **57**(23), 3011, (1979).
3. Kronig R and Brink JC, *Applied Scientific Research*, **A2**(2), 142, (1950).
4. Pandey BD et al, *Hydrometallurgy*, **40**(3), 343, (1996).
5. Schröter J et al, *Chem.-Ing.-Technik* **1998** (70), 279.



MICELLAR EXTRACTION OF COMPLEXES OF LANTHANIDES WITH HUMIC ACIDS

J Reitmeir, JI Kim[1] and P Plucinski[2]
Technische Universität München, Institut für Technische Chemie, 85748 Garching, FRG
[1]Forschungszentrum Karlsruhe, Institut für Nukleare Entsorgungstechnik, 76021 Karlsruhe, FRG
[2] University of Bath, Department of Chemical Engineering, Bath BA2 7AY, UK

ABSTRACT
A new method has been proposed for the recovery of lanthanides from aqueous streams. Lanthanides, existing in the soil or in the groundwater, form stable, water soluble complexes with fulvic or humic acids. In this work, the application of microemulsions for the extraction of the lanthanide/humic acid complexes has been developed. The extraction of metal ions together with the polyelectrolytes (humic or fulvic acid) is accomplished by contacting an aqueous solution of the lanthanide complexes with a water-in-oil microemulsion stabilised by cationic surfactants. This process of recovery proceeds via interactions of cationic surfactants with carboxylic and phenolic groups of humic acid.

Keywords: lanthanides, humic acids, surfactants, reverse micelles

INTRODUCTION

In the past few years much effort has been directed towards the safe isolation, for a long time, from the biosphere of the radioactive wastes resulting from commercial power production. Since the standard method of managing reactor wastes is to assign them to shallow burial sites, the mounting waste volumes can be viewed as a potential source of contamination of groundwater systems[1]. There are documented examples in the literature of the leakage of radioactive compounds to the environment.[2] Such leakage of radioactive wastes releases these compounds to subsurface flow systems, where they can migrate and contaminate large areas. One of the most important reactions of free lanthanides and actinides in the groundwater/soil system is their complexation with humic substances.[3,4]

Humic acids (HA) are formed by the random condensation of breakdown products of terrestrial and aquatic plants and extracellular metabolites of phytoplankton. These substances are a mixture of polydispersed, heterogeneous polyelectrolytes, whose conformation is determined by the environmental conditions. They are predominantly negatively charged due to the presence of carboxylic acid and phenolic groups. Thus, they can interact with the heavy metals present in groundwaters. The interactions between humic substances and metal ions have been described as ion exchange, surface adsorption, chelation, coagulation and peptization reactions.[5,6]

In our earlier work[7] it was found that quaternized polyvinylpyridine derivatives (polycations) reacted with AOT (sodium bis(2-ethylhexyl)sulfosuccinate) to form insoluble (either in isooctane or in water) complexes whenever the surfactant/cation monomer concentration was less than 1.4. A surplus of AOT in the system led to quantitative transfer of the complex from aqueous to micellar phase. The same principle can be applied for the extraction of metal ions adsorbed at the surface of humic acid molecules.

The aim of this work is to apply micellar extraction to remove lanthanide/humic acid complexes from contaminated aqueous streams (groundwater). The surfactants present in the form of water-in-oil microemulsion interact with humic substances dissolved in the aqueous phase (the so-called Winsor II system: water-in-oil microemulsion in contact with an excess of aqueous phase) enabling their solubilization in the organic phase. In this way the lanthanides enter the organic phase as species adsorbed on the surface of humic acids. The humic acids naturally present in soil/groundwater systems can act as a benign chelating agent and carrier for the removal of lanthanides, utilising the enrichment effect due to strong electrostatic interactions between trivalent lanthanides and humic acids.

© 2000 Society of Chemical Industry

EXPERIMENTAL

The extractional equilibria were measured with the standard methods.[8] Equal volumes (usually 10 ml) of aqueous HA/La solution and the microemulsion phase were shaken at 175 strokes min^{-1} (SM 25, E. Bühler) for 12 hours. The dispersion was then left for phase separation for at least 24 hours. If the phase separation was not complete, the system was centrifuged at 3000 rpm for 15 minutes to obtain clear phases. The experiments were done at room temperature. The concentration of lanthanum in the aqueous phase was measured directly by inductive coupled plasma atomic emission spectroscopy (SPECTROFLAME, Spectro, Germany); the concentration of metal ions in the organic phase was measured after re-extraction with 1.0 kmol m^{-3} nitric acid. The water content of the micellar phase was determined by Karl Fischer titration (633 Karl-Fischer Automat, Metrohm, Switzerland). The concentration of humic acid in both phases was determined spectroscopically (Cary 1E, Varian). The pH of the aqueous phase was measured using a 746 Multi-Calimatic pH meter (Knick, Germany). All chemicals used were of analytical grade or better. The humic acid used was supplied by Aldrich. Various quaternary ammonium compounds (Merck, Fluka) were investigated as surfactants to prepare stable water-in-oil microemulsions and then, stable Winsor II systems.

RESULTS AND DISCUSSION

Humic acids can bind lanthanides due to the presence of negatively charged carboxylic and phenolic groups.[5,6] In the case of very dilute solution of radioactive elements, an excess of free negatively charged groups results at the surface of humic acid. These groups interact with cationic surfactants, enabling the solubilization of a La/HA complex in the micellar phase. The interactions, and therefore the partitioning of lanthanides between the phases, depend on the dissociation of carboxylic and phenolic groups of HA, i.e. on the pH of the aqueous phase.

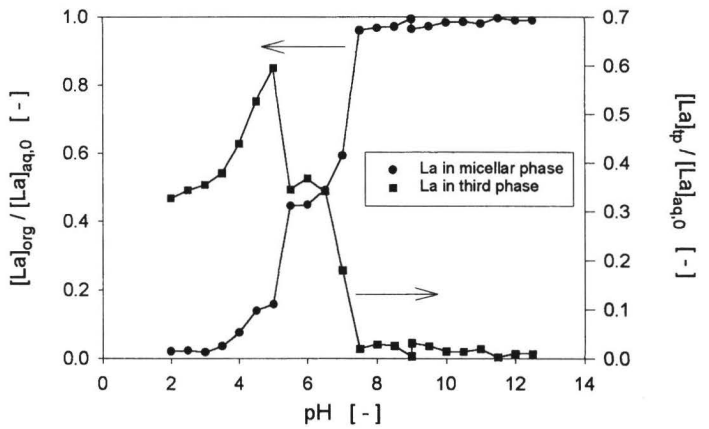


Figure 1 The dependence of the efficiency of lanthanum extraction on the pH of the aqueous phase.
org = organic phase, aq = aqueous phase, tp = third phase, 0 = initial
Aqueous phase: [NaCl] = 0.1 kmol m^{-3}, $[La^{3+}]_0$ = 10 ppm, [HS] = 0.4 kg m^{-3}, buffer conc. 0.02 kmol m^{-3};
Organic phase: [CTABr] = 0.1 kmol m^{-3}

Such dependence is shown in Figure 1 for lanthanum as a representative element. As the surfactant, hexadecyl-trimethylammonium bromide (CTABr) was used, while the organic solvent was a mixture of isooctane and n-hexanol (9:1 by vol.) containing 20 % (v/v) n-butanol. Such a solvent was applied for the extraction of enzymes by microemulsions in the work of Krei.[9]

With an increase in pH, an increase in the efficiency of lanthanum extraction was observed. For pH ≥ 7.0, it was possible to extract quantitatively (within the range of analytical error) lanthanum adsorbed on humic acid. This result opens a new field of application of microemulsion systems in the environmental sector. If the pH value of the aqueous phase was lower than 7, the extraction efficiency diminished considerably. Simultaneously, the formation of a dark brown third phase at the oil/water interface was observed. The amount of lanthanum in this phase was not measured directly; it was calculated from the mass balance of lanthanum in the aqueous and micellar phase. It is worth mentioning that no formation of a third phase was observed for pH ≥ 7.0. Probably, at low pH, most of the acidic groups of HA were protonated and their interactions with La^{3+} and CTA^{+} were thus strongly hindered. The application of amphoteric surfactants (dimethylalkylammoniumpropane sulfonate; alkyl = cetyl-, tetradecyl-, and dodecyl-) also led to the formation of a third phase. In addition it was necessary for the aqueous phase to be saline to stabilise the extraction system. Unfortunately, the organic solvent applied in this series of experiments (isooctane, n-butanol and hexanol) is ecologically harmful (for 1:1 phase ratio the equilibrium concentration of n-butanol in the aqueous phase was ca. 4 vol. % - Krei[9]). In addition, relatively strong salinity of the aqueous phase was necessary to obtain a stable Winsor II system. Thus, further research was directed on finding a surfactant and a mixture of organic solvents meeting the ecological demands.

In the next series of experiments, a tri-chain surfactant (trioctylmethylammonium chloride) was used together with aliphatic alcohols (n-hexanol, n-octanol and n-decanol) as co-solvents. No electrolyte was used in the aqueous phase to stabilise the two-phase surfactant system. The results of measurements of the efficiency of lanthanum extraction are shown in Figure 2.

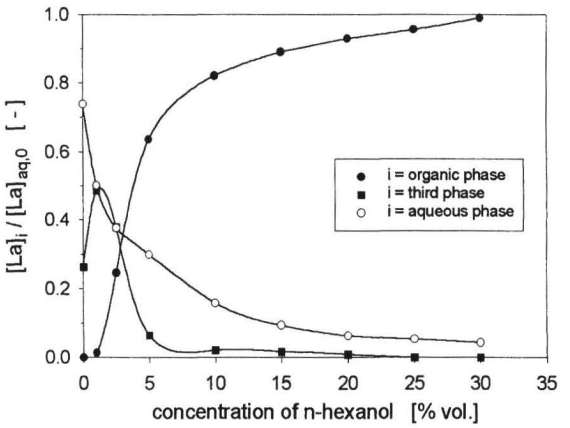


Figure 2 The influence of the concentration of n-hexanol on the efficiency of lanthanum extraction.
Aqueous phase: $[La^{3+}]$ = 10.4 ppm, [HA] = 0.4 kg m^{-3}, pH = 8.7;
Organic phase: [TOMAC] = 8.05 mol m^{-3}, isooctane.

Quantitative transfer of lanthanum took place at high concentration of hexanol in isooctane (30 % by vol.). At lower alcohol concentrations, the extraction efficiency was diminished and the formation of a third phase was observed. It is presently difficult to distinguish the action of alkanols on the lanthanum partitioning. Two options are possible: either the alkanols function as a co-solvent (change of the polarity of the organic phase) or as a co-surfactant (incorporation into the surfactant chains around the molecule of humic acid).

As was the case with CTABr, the distribution of lanthanum between the phases depends strongly on the pH value of the aqueous phase (Figure 3). By pH = 8.7 (resulting from dissolution of Aldrich humic acids present as sodium salt) lanthanum was efficiently (> 90%) extracted. Over the entire range of pH, no third phase formation was observed; the humic acid was extracted quantitatively

by the micellar phase. This indicates a different "strength" of the interactions of surfactant cations with humic acids than with La^{3+}.

From the pH dependence of the efficiency of lanthanum extraction, one can envisage a possible scenario for lanthanide recovery: the separation of lanthanides can be achieved at basic pH, whereas the stripping takes place in an acidic solution. For the recovery of humic acids from the micellar phase the additional separation step (e.g. thermal phase transition[10], precipitation of HA/TOMA complexes) is necessary.

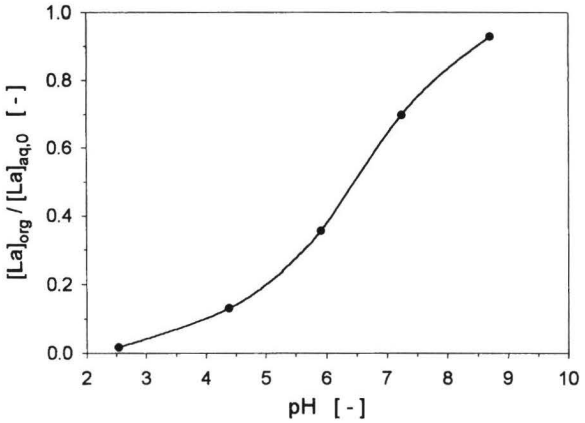


Figure 3 The influence of pH in the aqueous phase on the efficiency of lanthanum extraction.
Aqueous phase: $[La^{3+}]$ = 10.4 ppm, [HA] = 0.4 kg m^{-3}, pH adjusted by the addition of HCl or NaOH to the system;
Organic phase: [TOMAC] = 8.05 mol m^{-3}, isooctane/hexanol (8 : 2 by vol.).

The efficiency of lanthanum extraction depends strongly on the relationship between the amounts of lanthanum, humic acid and surfactant in the system (Figures 4 - 5).

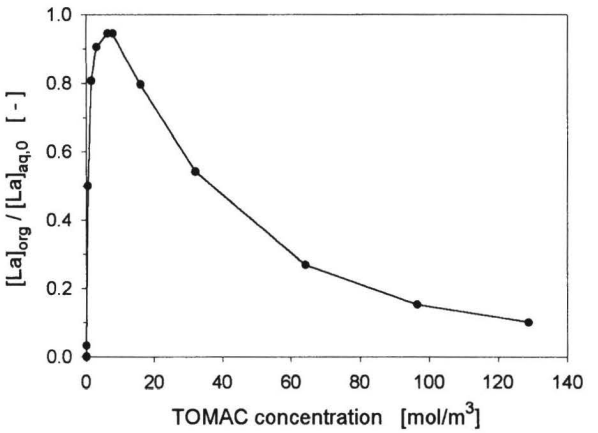


Figure 4 The influence of TOMAC concentration on the efficiency of lanthanum extraction.
Aqueous phase: $[La^{3+}]$ = 9.9 ppm, [HA] = 0.4 kg m^{-3}, pH =8.7;
Organic phase: isooctane/hexanol (8 : 2 by vol.).

The partitioning of lanthanum between the micellar and aqueous phases depends on the concentration of surfactant (Figure 4). The extraction efficiency passes through a maximum with increasing TOMAC concentration. Too high a concentration of TOMAC hinders the extraction of lanthanum.

With increasing initial lanthanum concentration in the aqueous phase the efficiency of extraction decreases and on the other hand the formation of the third phase increases (Figure 5).

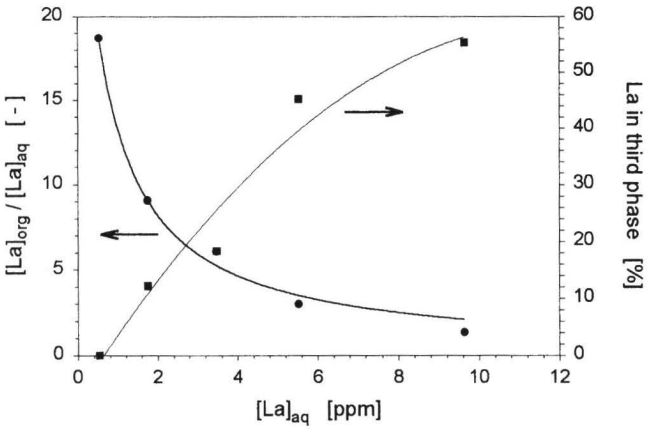
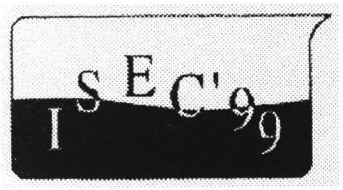


Figure 5 The influence of initial La concentration on the partitioning of lanthanum.
Aqueous phase: [HA] = 0.4 kg m^{-3}, pH =8.7;
Organic phase: [TOMAC] = 8.05 mol m^{-3}, isooctane/hexanol (8 : 2 by vol.).

All of these results indicate the importance of competitive chemisorption of La^{3+} and surfactant cations at the active sites of humic acid. An excess of surfactant leads to the quantitative transfer of lanthanum/humic acid complexes from the aqueous to the organic phase. These first results show the great potential of surfactant systems for the removal of toxic radioactive species from aquatic systems. Future work should be directed towards the thermodynamic modelling of the interaction of lanthanum, surfactant and humic acids in a two-phase system in order to derive the stability constants and optimise the solvent composition and surfactant concentration as well as towards the kinetics of the mass transfer. With this knowledge, it will be possible to evaluate the extraction efficiency and to determine the optimal choice of the phase contactor.

REFERENCES

1. Freeze RA and Cherry JA, *"Groundwater"*, Prentice-Hall, Inc., Englewood Cliffs, (1979).
2. Anon., *Ground Water Newsletter*, **5**, 3, (1976).
3. Kim JI, Buckau G, Bryant E and Klenze R, *Radiochim. Acta*, **48**, 135, (1989).
4. Kim JI, Rhee DS and Buckau G, *Radiochim. Acta*, **52/53**, 49, (1991).
5. Schnitzer M and Khan SU, *"Humic Substances in the Environment"*, Marcel Dekker, Inc., New York, (1972).
6. Stevenson FJ, *"Humus Chemistry, Genesis, Composition, Reactions"*, John Wiley & Sons, New York, (1982).
7. Nitsch W and Plucinski P, *J. Colloid Interface Sci.*, **136**, 338, (1990).
8. Plucinski P and Reitmeir J, *Colloids & Surfaces A*, **122**, 75, (1997).
9. Krei GA, *"Flüssig-Flüssig Extraktion von Enzymen mittels inverser Mizellen", PhD thesis*, TU Braunschweig, (1994).
10. Kahlweit M, *Tenside, Surfactants, Detergents*, **30**, 83, (1993)



SOLVENT EXTRACTION OF TRANSITION METALS BY AN *IN SITU* EXTRACTANT FORMATION METHOD. VI. UTILIZATION OF AN EASILY-SOLIDIFYING SOLVENT

Kaoru Fujinaga, Yasushi Seike and Minoru Okumura
Department of Material Science, Faculty of Science and Engineering, Shimane University, 1060 Nishikawatsu, Matsue 690-8504 Japan

ABSTRACT
It was found that a ternary mixed solvent containing carbon disulfide, pyrrolidine, and *p*-xylene formed pyrrolidinedithiocarbamic acid during the course of extraction and could successfully extract metal ions such as Fe^{3+}, Ni^{2+}, Pb^{2+}, and Mn^{2+} into the organic phase without using a chelate extractant at all. The present method is advantageous over the usual extraction methods since the organic phase could be solidified by cooling, thus centrifuge and the phase separation could be carried out by decantation simply and conveniently.

Keywords: *in situ* extractant formation, easily-solidifying extractant, pyrrolidinedithiocarbamic acid

INTRODUCTION

The *in situ* extractant formation method, which was originated by the present authors, is characterized by forming an extractant upon mixing solvents and by capability of metal extraction without using chelate extractants at all. Since the preparation of a chelate solution or the precautions for storing the unstable chelate solution are not required, the present method is simple, convenient, and not costly. So far, isoamylxanthic acid forming system[1,2] and diethyldithiocarbamic acid(DTC) forming system[3,4] have already reported that these methods could be successfully applied to the extraction of transition metals. The present study was undertaken to find out new extractant formation system and a mixture of carbon disulfide(CS_2) and pyrrolidine was observed to form pyrrolidine dithiocarbamic acid(PDC). However, if mixed CS_2 and pyrrolidine directly, the mixture produced a precipitate and solidified, so that the third solvent was required as a diluent.

While, in the solvent extraction, the most tedious step is the phase separation, and many studies to separate phases simply by solidifying the organic solvent have been carried out for a long time. The mixture of paraffin with different solvents,[5] benzophenone (m. p. 48°C), [6] and naphthalene (m. p. 80.2°C)[7] were purposely used as a solidifying solvent. But these solidifying solvents have a higher melting point than room temperature. Therefore, the methods using these solvents were not always simple since it was necessary to dissolve the solidified organic phase in other solvents for the determination of extracted species, although the methods were still advantageous with respect to kinetics due to the high temperature at equilibration. If the organic solvent with a melting point in the vicinity of room temperature (called an easily-solidifying solvent) is utilized as an organic phase and if phase separation is carried out at low temperature by a cooling centrifuge, the above-mentioned tedious procedure can be avoided. In this case, the organic phase is re-liquefied by being left at room temperature for a while, after decanting the aqueous phase. As a result of preliminary experiments observing the solidifying behavior of 11 different solvents, *p*-xylene was found to be the most suitable for this extraction method and was mainly used in this study as a diluent.

Consequently, the *p*-xylene-CS_2-pyrrolidine ternary mixed solvent system, which produced a well-known chelating reagent in the name of ammonium pyrrolidinedithiocarbamate(APDC), was examined for the simultaneous extraction of transition metals such as Ni(II), Pb(II), Fe(II), Mn(II), etc.

© 2000 Society of Chemical Industry

EXPERIMENTAL

Reagents and apparatus.

A Hitachi model Z-5000 atomic absorption spectrophotometer was used to measure the metal concentration with a flame atomizer, and a Nihonbunko V-560 double-beam spectrophotometer was used to obtain absorption spectra with 1.0 cm pathlength quartz cells. The metal solutions were stored in polyethylene bottles and were mixed in a volumetric flask so that the concentration of each metal was 0.2 mM, prior to use. The other reagents were of analytical grade.

Procedure.

A 10ml portion of the metal ion solution, which was masked and buffered with 0.033 M diammonium hydrogen citrate and 0.017 M citric acid and was maintained ionic strength of 1.0 M with potassium nitrate, was equilibrated with a 2 ml of the PDC-forming solvent having a composition of 1.0:1.0:98(v/v%) for CS_2:C_4H_8NH: p-$C_6H_4(CH_3)_2$ in a 30 ml extraction vial by shaking vigorously for 5 min. After phase separation by cooling centrifuge at −3°C at 3000 rpm for 30 min, the metal ion concentration in the aqueous phase was determined by atomic absorption spectrophotometry. The extraction ratio was obtained by subtracting the determined metal ion concentration from the known one in the aqueous phase.

RESULTS AND DISCUSSION

Selection of easily-solidifying solvent.

The 11 solvents: p-xylene (m.p. 13°), 1,2,4-trichlorobenzene (m.p. 17-18°), diphenylmethane (m.p. 26-27°), cyclohexanol (m.p. 25°), phenoxyethanol (m.p. 14°), dimethoxybenzene (m.p. 23°), acetophenone (m.p. 20°), propiophenone (m.p. 21°), benzylbenzoate (m.p. 19°), p-chlorotoluene (m.p. 8°), and phenylether (m.p. 27°), were examined for their solidifying behaviors using a cooling centrifuge after equilibration with an 0.1 M KNO_3 aqueous solution. p-Xylene was chosen as an easily-solidifying solvent since it gave the best result, but there was still a problem. p-Xylene solidified at the bottom of an extraction vial when an aqueous phase was water but solidified at the top covering the aqueous phase when 0.1 M KON_3 was used as an aqueous phase, and it was difficult to take out the aqueous phase by decantation. This problem was solved by setting the extraction vial upside-down in the rotor during a cooling centrifuge. The other solvents did not exactly solidify under the experimental conditions.

Formation of PDC.

A 0.1 M KNO_3 aqueous solutions adjusted at pH 9.0 were equilibrated with CS_2 and pyrrolidine-, CS_2-, and pyrrolidine-containing p-xylene solution, respectively, and were subjected to the measurement of UV absorption spectrum, followed by comparing with that of APDC aqueous solution. The absorption maxima (λ_{max}) of the spectrum for the aqueous phase equilibrated with CS_2 and pyrrolidine-containing p-xylene solution were 254 and 275 nm and that for the APDC solution were 253 and 277 nm, respectively. These two spectra coincide fairly well with each other, while other two solutions did not give any absorption maximum at these wavelengths. Therefore, it can be said that PDC is formed in the aqueous phase by shaking with the mixed solvent. The amount of formed PDC in the organic phase should be equal to the amount of added pyrrolidine by assuming that pyrrolidine was perfectly converted by CS_2 into PDC. Since PDC is considered to exist in the form of pyrrolidinium pyrrolidine dithiocarbamate (PPDC) in the organic phase by analogy with the results of DTC-forming system reported previously, $\{PPDC\}_{o,calcd.}$, which referred to the PPDC amount in the organic phase calculated from the added amount of pyrrolidine, is mainly used in this study to discuss quantitatively the metal extractability.

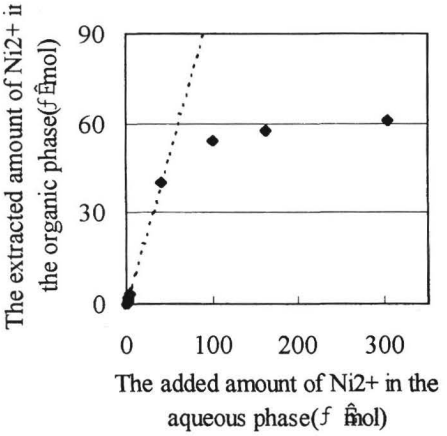


Fig. 1. Extraction capability of PDC-forming *p*-xylene solution.
: Curve for quantitative extraction. Shaking time: 5 min. pH.: 4.4.

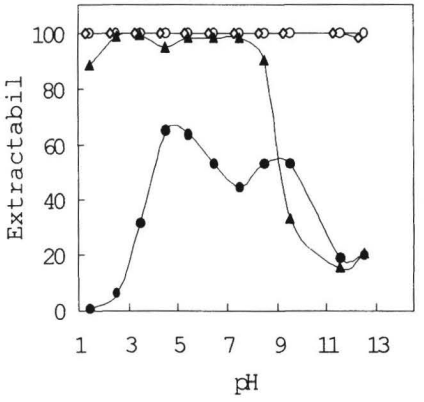


Fig. 2. The pH dependence of extractability of metal.
O: Pb^{2+}, ◊: Ni^{2+}, □: Fe^{3+}, •: Mn^{2+}.

Extractability of Ni^{2+} with the mixed solvent.

The extractability of Ni^{2+} with 2 ml of the PDC-forming solvent with the composition 1.0-1.0-98(v/v%) for CS_2-pyrrolidine-*p*-xylene ($\{PPDC\}_{o,calcd}$ = 120 μmol) was examined by changing the amount of Ni^{2+} in the aqueous phase from 0.2 μmol to 303μmol. Figure 1 demonstrates that the extracted amount of Ni^{2+} increased linearly till 40 μmol with the increment of Ni^{2+} in the aqueous phase and afterward became constant, 57.7±3.5 μmol. Taking into account the fact that Ni^{2+} is extracted in the form of dipyrrolidine-dithio-carbamate complex in the usual APDC extraction method, this experimental result proved the validity of above-mentioned assumptions, i.e., (1) CS_2 and pyrrolidine react quantitatively to form PPDC in the organic phase and (2) the formed amount of PPDC, $\{PPDC\}_{o,calcd}$, is exactly half of the added amount of pyrrolidine.

Extraction of metal ions.

The extraction curves for metal ions as a function of pH, are shown in Fig. 2. The pH ranges for the quantitative extraction of metals obtained by the present PDC-forming solvent are wider compared to those obtained by the usual APDC extraction method[8]. APDC is more stable against acid than DTC but is still labile in the acidic aqueous solution, the half-life value for PDC was reported as 18±5 minutes in 0.8 M HCl[9]. In the usual DTC extraction method, by dissolving diethylammonium diethyldithiocarbamate (DEDTC) in the organic phase, acidic decomposition is avoided. However, in the APDC extraction method, the equivalent compound to DEDTC, PPDC, is not commercially available.

As among the examined metals, Mn^{2+} gave the worst extractability the effect of the mixing ratio of CS_2 and pyrrolidine on the Mn^{2+} extraction was examined. Figure 3 clearly demonstrates that the extractability was remarkably improved by increasing the mixing ratios for CS_2 and pyrrolidine.

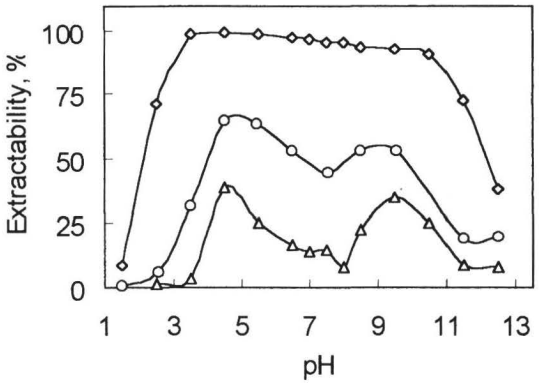


Figure 3. Effect of the mixing ratio on the extraction of Mn^{2+}. $[Mn^{2+}]_{aq}$ = 0.2mM, CS_2-pyrrolidine-p-xylene compositions (v/v%) are 0.5:0.5:99 for ♠, 1.0:1.0:98 for O and 2.0:2.0:96 for ◊, respectively.

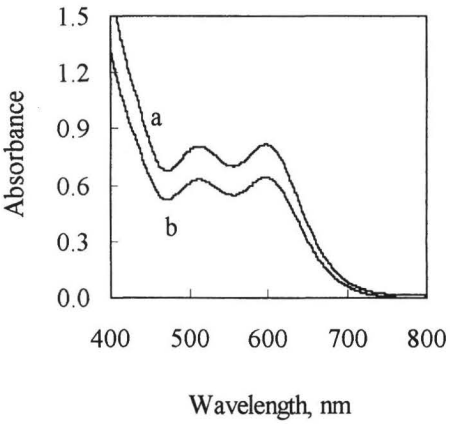


Figure 4. Absorption spectrum of *p*-xylene layer containing Fe^{3+} complex.
(b) Extracted with APDC and (b) extracted with the mixed solvent containing 1% of CS_2 and pyrrolidine. Aqueous phase 10 ml of 0.2 mM Fe^{3+} solution adjusted at pH 5.3, and both organic phase were 10 ml.

Extraction mechanism.

Ten milliliter aliquots of *p*-xylene and of the PDC-forming solvent with the composition 0.5-0.5-99(v/v%) for CS_2-pyrrolidine-*p*-xylene were equilibrated with the equal volume of 0.2 mM Fe^{3+} aqueous solution adjusted at pH 5.3, and visible absorption spectrum was measured.

Figure 4 clearly shows that the positions of λ_{max} and shapes for both spectrum agree fairly well. Therefore, it can be confirmed that Fe^{3+} was extracted with PDC-forming solvent in the form of pyrrolidine dithio-carbamate complex. Taking into account the above results, metal extraction is considered to proceed as shown in Figure5.

In conclusion, by associating the usage of an easily-solidifying solvent with cooling centrifuge method, phase separation in solvent extraction could be improved to simple and convenient method, since the aqueous phase can be removed by decantation. The superiority of this PDC-forming system in the metal extractability over the usual APDC extraction method was explicitly demonstrated in the extraction curve as a function of pH.

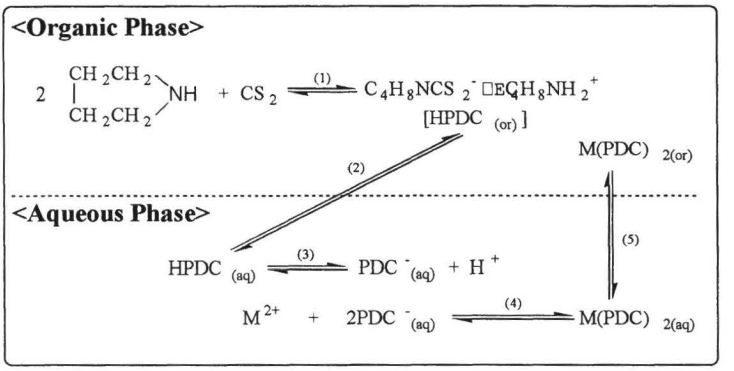
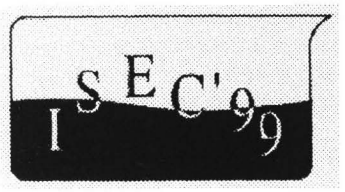


Figure 5. Extraction mechanism.
HPDC, pyrrolidine dithiocarbamic acid; (or), organic phase; (aq), aqueous phase; M, metal.

REFERENCES

1. Fujinaga K, *Anal. Sci.*, **7,** Supplement, 29 (1991).
2. Fujinaga K, *Anal. Chem. Acta*, **264**, 71 (1992).
3. Fujinaga K, Seike Y and Okumura M, *Proc. ISEC'96*, ed D. C. Shallcross, et. al., University of Melbourne, 93, (1996)
4. Fujinaga K, Seike Y and Okumura M, *Anal. Sci.*, **13,** 225 (1997).
5. Kuznetsov VI and Seryakova IV, *Zh. Anal. Khim.*, **14**, 161 (1959); *Chem. Abstr.*, **53,** 12925g, (1959).
6. Korenman IM, Sheyanova FR and Savelva MI, *Tr. po Khim. i Teknol.(Gor'kii)*, No.1, 66 (1959).
7. For example: Fujinaga T, Satake M and Shimidzu M, *Bunseki Kagaku*, **25**, 313 (1976). Their works fully reviewed by Puri BK, Jackson KW and Katyl M, *Microchem. J.*, **36**, 135 (1987).
8. Ueno K and K. L. Cheng KL, *"Handbook of Organic Analytical Reagents 2nd Edition"*, CRC Press, Boca Raton, 464, (1992).
9. Dellien I and Pearson L, *Talanta*, **26**, 1101 (1979).



A NEW HYDROXAMIC ACID DERIVATIVE EXTRACTANT FOR THE EXTRACTION OF COBALT(II) AND URANIUM(VI) FROM NITRATE MEDIUM

FA Shehata, S El-Afifi and HF Aly
Hot Laboratories Centre, Atomic Energy Authority, Cairo 13759 Egypt,

ABSTRACT
A new extractant of hydroxamic acid derivative, which is weak organic acid, was synthesised and used for Co(II) and U(VI) extraction from nitrate medium. The distribution ratio of Co(II) and U(VI) between chloroform and the aqueous phase was measured as functions of the pH and the extractant concentration at 291K at an ionic strength of 0.1M $NaNO_3$. The stoichiometry of the extracted complexes is 1:2 [metal:ligand]. Extraction of more than 99% U(VI) was achieved by the new extractant in chloroform. Extraction of U(VI) in the absence and presence of Nd(III) was evaluated.

Keywords: hydroxamic acid derivative, cobalt, uranium, nitrate

INTRODUCTION

Hydroxamic acids have received a considerable attention as reagents in analytical chemistry[1] for gravimetric analysis, for solvent extraction and spectrophotometric determination of metals.[2] Detailed information has been published on hydroxamic acid complexes with the first transition metal series.[3] In this respect, 0.1M tri-n-butylaceto-hydroxamic acid solution in diethylbenzene (and its isomers) in 10% octanol has been chosen as an organic solution to treat the alkaline wastes coming from regeneration of solvent utilised in a reprocessing plant using a Purex flow sheet.[4] Shal'gin and Konnik[5] studied the reaction of Cr(III), Fe(III) and Cu(II) nitrates with 2,4-dichloro- and 2-methyl-4-chlorophenoxyacetyl hydroxamic acid (H_2L). Formation of Cr(III) and Fe(III) hydroxamates of the composition $M(HL)_2.OH.nH_2O$ was detected but Cu(II) nitrate affords chelate-type compounds of CuL. Tait et al[6] investigated the extraction of Mn(II), Fe(III), Co(II), Ni(II), Cu(II), Zn(II) and Cd(II) from 1M sodium sulphate by LIX-1104 (hydroxamic acid) at various aqueous pH values. The extraction order was Fe>Cu>Zn>Ni ≅Co>Cd>Mn. The results showed that LIX-1104 form chelates of ML_2 with Mn, Co, Zn, Cd and ML.2HL with Ni and Cu.

In this work, a synthesised derivative of hydroxamic acid which has two functional groups as an acidic chelating organic ligand (HL), is evaluated as a new extractant for Co(II) and U(VI). The parameters affecting the extraction of Co(II) and U(VI) by HL in chloroform from an aqueous medium of constant ionic strength of 0.1M $NaNO_3$ and the appropriate pH for extraction have been investigated. The extraction of U(VI) in the absence and in the presence of Nd(III) has been also studied.

EXPERIMENTAL

Chemicals and reagents

All chemicals were of analytical grade and used without further purification. Radioactive tracer ^{60}Co was prepared by neutron irradiation of $CoCO_3$ in the ET-RR-1 Inshas reactor, Egypt.

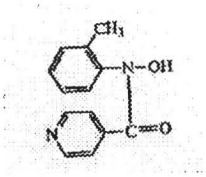
The hydroxamic acid derivative was prepared by condensation of the acid chloride of iso-nicotinic acid with o-tolylhydroxylamine.[1,7,8] Detailed synthetic procedure and structure characterisation by elemental analysis, IR and NMR spectroscopic analysis have been published[9] and the proposed structure is shown below.

Extraction procedure and apparatus

HNO_3 acid was used to buffer the aqueous solution at a concentration of 0.01M and the ionic

© 2000 Society of Chemical Industry

strength was adjusted to 0.1M with $NaNO_3$. The aqueous phase contained the tracer of radioactive Co(II) or a certain concentration of U(VI). The organic phase used was a chloroform solution of HL, as chloroform showed the highest solubility for the extractant of the tested diluents e.g. benzene, toluene, CCl_4, MIBK, xylene and kerosene. Pre-equilibration of the two phases was always carried out before the extraction.



N-isonicotinyl-N-(o)tolylhydroxylamine or
N-(o)tolylisonicotinohydroxamic acid

Equal volumes of organic and aqueous phases were equilibrated for 30 minutes, under vigorous shaking in a thermostat water bath (18±2°C). After phase separation, known aliquots of each phase were sampled for analysis. The distribution ratio D was determined from the ratio between the concentration of the respective species in the organic to the aqueous phase.

U(VI) was determined spectrophotometrically[10] using a Shimadzu, UV-visible spectrophotometer Model UV-160A. Uranium solutions were measured by the colour of the nitrate solution at λ_{max} of 417 ±2 nm. ^{60}Co was analysed radiometrically by γ-spectroscopy using a Bicon scintillation detector connected to a multichannel analyser coupled with a well-type NaI(Tl) detector.

RESULTS AND DISCUSSION

The extraction behaviour of the radioactive Co(II) and U(VI) ions was investigated with chloroform solutions containing hydroxamic acid reagent (HL) from nitrate medium. Slope analysis of the effect of $[H^+]$, [HL] and $[NO_3^-]$ on the extraction of the two cations are given in Figures 1-3. The effect of $[H^+]$ on the distribution as log-log plot gave a slope of –2 for the straight part for both Co(II) and U(VI) , Figure 1. This indicates that two protons are released into the aqueous phase.

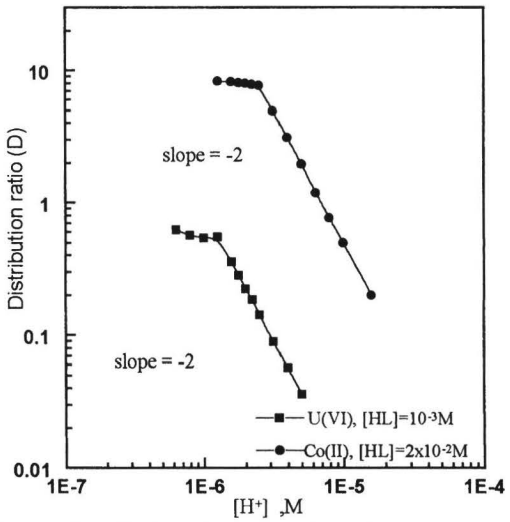


Figure 1. Effect of hydrogen ion concentration on the extraction of 10^{-1} M U(VI) and Co(II) extracted by HL in chloroform from 0.1 M $NaNO_3$

The relation between log D and log [HL] gave a straight line of slope equal 2, Figure 2, indicating that the extracted species of both Co(II) and U(VI) contain two chelated molecules. The effect of nitrate ion concentration on the distribution gave a straight lines having small fractional slopes of about 0.2 for both Co(II) and U(VI) cations, Figure 3, indicating a negligible contribution of nitrate ions in the extraction.

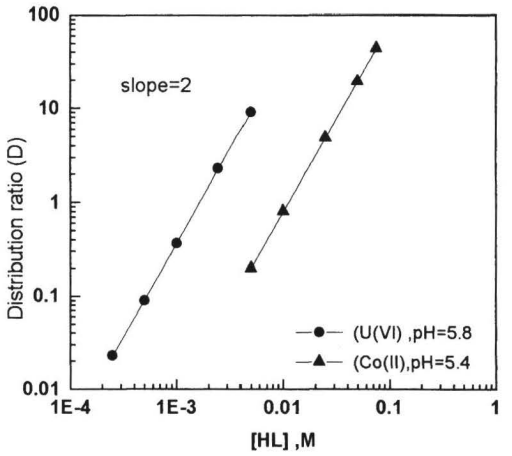


Figure 2. Effect of ligand concentration in chloroform on the extraction of 10^{-3}M U(VI) and Co(II) from 0.1M $NaNO_3$

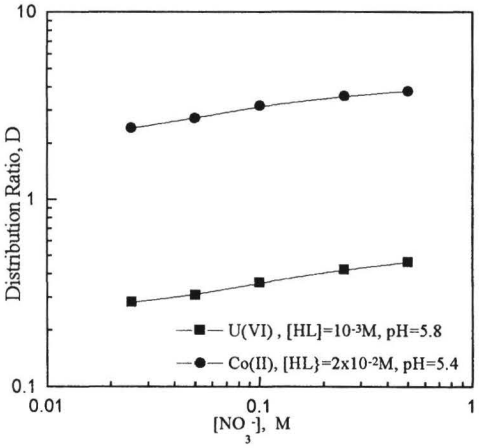


Figure 3. Effect of nitrate ion concentration on the extraction of 10^{-3}M U(VI) and Co(II) extracted by HL in chloroform

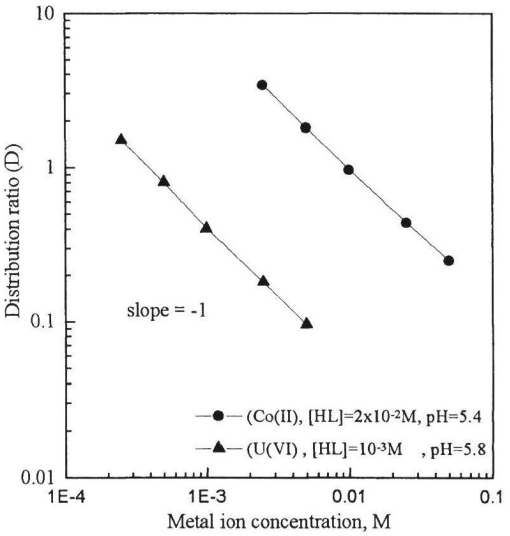


Figure 4. Effect of metal ion concentration on the extraction of Co(II) and U(VI) extracted by HL in chloroform from 0.1M $NaNO_3$

The effect of the Co(II) and U(VI) cations concentrations on the extraction of the organic chelating hydroxamic acid is shown in Figure 4. A log-log relation between the molar concentrations of Co(II) and U(VI) ions in aqueous phase against the distribution ratio, D, gave straight lines with a negative slopes of 1.

This result with those obtained from the studies of $[H^+]$ and [HL] effects, supported that, the organic phase extracted chelates are formed as a result of a combination of two anions of the hydroxamic acid as a ligand with only one metal ion of both Co(II) and U(VI).

Based on the results described above, it can be considered that, Co(II) and U(VI) extracted with HL according to the following extraction reaction at equilibrium:

$$M^{2+} + 2\overline{HL} \overset{E_x}{\longleftrightarrow} \overline{ML_2} + 2H^+ \qquad (1)$$

Where M^{2+} = Co(II) or U(VI) and bars refer to the organic phase species The extraction constant, E_x, is expressed by :

$$E_x = \overline{[ML_2]}\,[H^+]^2 \,/\, [M^{2+}]\,\overline{[HL]}^2 = D\,[H^+]^2 \,/\, \overline{[HL]}^2 \qquad (2)$$

E_x for Co(II) and U(VI) with HL were calculated using equation 2. The results obtained show that the extraction constants are $1.24 \pm 0.02 \times 10^{-7}$ and $8.96 \pm 0.13 \times 10^{-7}$ for Co(II) and U(VI), respectively. From these results, it is clear that the co-ordination of U(VI) as oxy-cation is more than the co-ordination of Co(II) which is reflected by its high extraction.

Use of extractant for determination of Uranium (VI)

It is found that the extracted uranium forms a coloured complex with HL in the organic phase, with a maximum absorbancy in UV-VIS spectrum at 385±2 nm. Based on this finding, the possible use of the

extractant for extractive determination of U(VI) from nitrate medium was assessed. Therefore, the effect of HL on the extraction of different amount of U(VI) was carried out with a three concentrations of uranyl ion (10^{-4}, 10^{-3} and 10^{-2}) with different concentrations of HL within the range 0.0001-0.5M, Figure 5. From the figure, it is found that when U(VI) concentration is 10^{-4} M, more than 99.9% of U(VI) is extracted using $5x10^{-2}$ M HL.

Based on this finding, the absorbancy of different concentrations of U(VI) ranging from 10^{-2}-10^{-5} M in

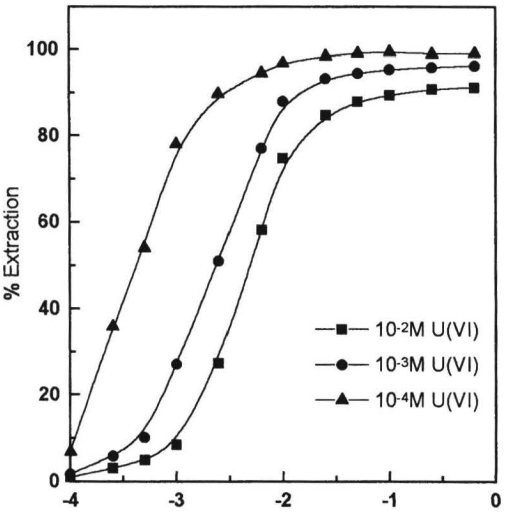


Figure 5. Effect of ligand concentration on the extraction of 10^{-2}, 10^{-3} and 10^{-4}M U(VI) from 0.1M $NaNO_3$ at pH=5.8.

0.1 M $NaNO_3$ and extracted by $5x10^{-2}$ M HL in chloroform was measured spectrophotometrically at λ_{max} =385±2 nm. A linear relation was obtained as the measured absorbancy and U(VI) concentration. From this relation, the molar absorptivity, ε, was calculated and was found equal to 310.

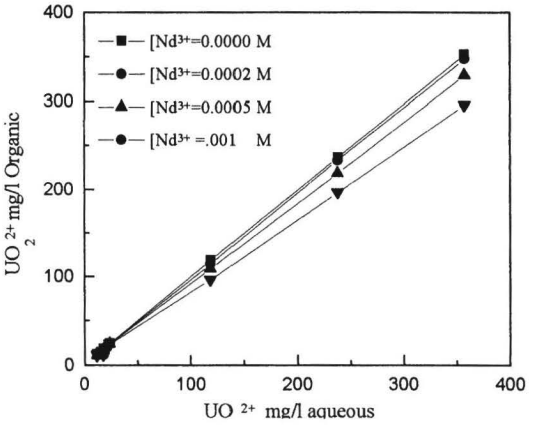


Figure 6. Effect of Nd^{3+} concentration on the extraction of U(VI)from $NaNO_3$ at pH=5.8 by 0.05M HL in chloroform

Based on the previous results, uranium was determined in presence of Nd(III) ions. In this concern, different concentrations of U(VI) ions ($5x\ 10^{-5}$ –$5x10^{-3}$) were extracted by constant 0.05M HL in presence of different concentrations of Nd(III) ions ($2x\ 10^{-4}$,$5x10^{-4}$ and $1x10^{-4}$M). Fig. (6) represents the results obtained, where linear relations are given. It is clear that, the presence of $2x10^{-4}$M Nd(III) ions does not affect the extraction of U(VI) in the range $5x\ 10^{-5}$ -$1.5x10^{-3}$ M, while the presence of $5x\ 10^{-4}$ and $1x10^{-3}$ start to affect the extraction of U(VI).

It was found that the extraction of 10^{-3}M Nd(III) alone by 0.05M HL in chloroform is negligible compared with U(VI) extraction, therefore, the effect of Nd(III) on the extraction of U(VI) is due to the salt effect.

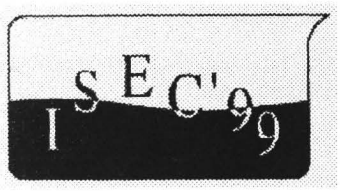
CONCLUSIONS

Studies on the extraction behaviour of Co(II) and U(VI) cations with the new synthesised hydroxamic acid reagent in chloroform from nitrate medium were conducted at 18± 1°C and the following can be concluded:

- the extracted species of Co(II) and U(VI) with the organic reagent (HL) were evaluated and found of the type ML_2 for both Co(II) and U(VI).
- quantitative extraction of U(VI) (≈99.9%) was achieved from 0.1M $NaNO_3$ solution containing 10^{-4} M of U(VI) by ~ 0.05M HL in chloroform
- the presence of $2x10^{-4}$M Nd(III) ions does not affect the extraction of U(VI), while higher concentrations of Nd(III) start to affect the extraction of U(VI) .

REFERENCES

1 Majumdar AK. *N-Benzoylphenylhydroxlamine and its Analogues*, Pergamon Press, Oxford, 31, (1972).
2 Agrawal YK and Patel SA. *Anal. Chem.*, **4**, 237, (1980).
3 Barbara K, Henryk K and Etelka F. *Coord. Chem. Rev.*, **114**,169, (1992).
4 Caarei M, Carlini D, Gasparini G, Grossi G and Torri G. *Dechema, West Germany*, **1**, 355, (1986).
5 Shul'gin VF and Konnik OV. *Ukr. Khim. Zh.*, **59**, 1246, (1993).
6 Tait BK, Mdlaose KE and Talijaard I. *Hydrometallurgy (S.Afr.)* **38**, 1, (1995).
7 Abdel Badei MM. *J Serb. Chem. Soc.* **57**, 739, (1991).
8 Vogel AI. *A Text Book of Practical Organic Chemistry* , Longman, London,4th ed. p.264, (1978).
9 El-Afifi El SM *M.Sc. Thesis*, Faculty of Science (Banha), Zagazig University, Egypt, (1997).
10 Marczenko Z. *Spectrophotometric Determination of Elements*, John Wiley and Sons Inc. N.Y. (1986).



SOLVENT EXTRACTION OF UO_2^{2+} AND Th^{4+} WITH PETROLEUM SULFOXIDE

Shao-Ning Yu, Zheng-Ping Fan, Li Ma, Yan-Zhao Yang and Bo-Rong Bao
Institute of Nuclear Research, Shanghai 201800, China

ABSTRACT
The influence of the concentration of nitric acid, hydrochloric acid, phosphoric acid, petroleum sulfoxides (PSO), salting-out agent, kind of diluent and temperature on the distribution ratio of U(VI) and Th(IV) has been systematically studied. It is found that the extraction regularity of PSO is similar to that of TBP. The distribution ratio in phosphoric acid is lower, but it increases with the increase of hydrochloric acid concentration and reaches a high value. The U(VI) exhibits the maximum distribution ratio at 3-4 mol/dm^3 HNO_3. The distribution ratio of U(VI) and Th(IV) increases rapidly at the presence of salting-out agent. The extracted compounds are determined to be $UO_2(NO_3)_2$2PSO and $Th(NO_3)_4$2PSO. The extraction enthalpies of U(VI) and Th(IV) with PSO are also calculated.

Keywords: U(VI), Th(IV), sulfoxide derivatives

INTRODUCTION

Petroleum sulfoxide (PSO) is a high efficient extraction agent. As a mixture of large amount of sulfoxide-like substances of similar qualities, PSO has such advantages as low cost, wide sources, no poisonousness, anti-radiation, less pollution and high efficiency in extraction, which have been studied in the extraction of precious metals.[1-4] The extraction of U(VI) with sulfoxides has been studied by some authors.[5] This paper makes use of the sulfoxide from Jiang Han oil field to perform a systematic study on the extraction behaviour of U(VI) and Th(IV) to provide some referential data for industrial use.

EXPERIMENTAL

Materials

Industrial PSO is offered by Jiang Han Petroleum Co. Its average molecular weight is 270 (260-290); the amount of contained sulphur is 9.3%; the purity is about 95%; its specific gravity is 0.95 g/cm^3 (25 °C); its boiling point is about 300 °C. Kerosene is offered by Shanghai Chemical Agent Co. Other chemical reagents are all analytical pure.

Measurement of PSO concentration

PSO concentration was measured with $HClO_4$ potentiometric titration in organic system.[6] We measured the contained amount of sulphur with the contained amount of =S=O. In the experiment, the DOSO($(C_8H_{17})_2SO$) was used as the standard (in $(CH_3CO)_2O$ solution).

Potentiometric titration method

This was used first to determine the concentration of $HClO_4$ in 1,4-dioxane solution:

$$R_2SO + HClO_4 \text{---} R_2SOH^+ + ClO_4^-$$

Then the PSO concentration was measured with $HClO_4$, whose concentration was already known. PSO concentration can be calculated as follows:

$$M_{PSO}V_{PSO}=M_{HClO4}V_{HClO4}$$

Measurement of Distribution Ratio

Certain volume of aqueous and organic phase (Vo : Vi = 3:3) was placed in centrifuge tubes which were shaken for 15 minutes, then the two phases were separated. The concentration of U(VI) and Th(IV) in aqueous were determined by Arsenazo III spectrophotometric method,[2] and the

© 2000 Society of Chemical Industry

distribution ratio was calculated.

RESULT AND DISCUSSION

Effect of diluent on distribution ratio

The distribution ratio of U(VI) is higher in benzene, toluene and kerosene, but lower in chloroform. Here is the order of distribution ratio of U(VI) in some diluents at 25°C, $[UO_2^{2+}]$= $5.48x10^{-4}$ mol/dm^3, [PSO]=0.32 mol/dm^3, $[HNO_3]$=3.0 mol/dm^3, $[NH_4NO_3]$=0.1mol/dm^3.

toluene(13.2) > benzene (11.8) > cyclohexane (7.2) > kerosene (7.1) > petroleum benzine (6.8) > dichloromethane (1.2) > chloroform (0.8)

Effect of acid concentration in solution on distribution ratio

In some kinds of acid media, the distribution ratio of U(VI) in phosphoric acid is lower, but it increases with the increase of hydrochloric acid concentration and reaches a high value. In nitric acid, the distribution ratio exhibits the maximum point at $[HNO_3]$ ~ 3-4mol/dm^3 (Figure 1).

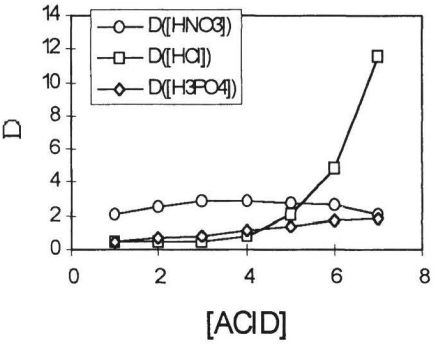


Figure 1 Distribution ratio of U(VI) as a function of aqueous acid concentration at 25°C; $[UO_2^{2+}]$ = 5.48 x 10^{-4} mol/dm^3; [PSO] = 0.32 mol/dm^3; $[NH_4NO_3]$ = 0.1mol/dm^3.

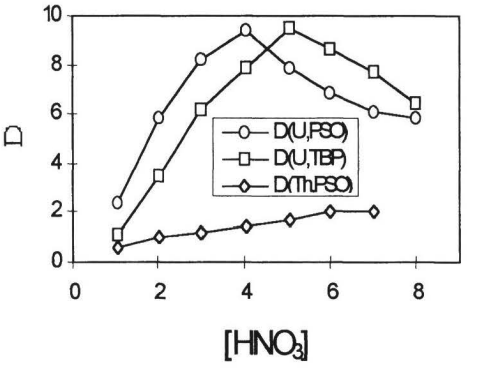


Figure 2. Distribution ratio of U(VI) and Th(IV) as a function of aqueous HNO_3 concentration at 25°C; $[UO_2^{2+}]$ = 5.48 x 10^{-4} mol/dm^3; $[Th^{4+}]$ = 5.68 x 10^{-4} mol/dm^3; [PSO] = 0.32 mol/dm^3 (or [TBP] = 0.32 mol/dm^3); $[NH_4NO_3]$ = 0.1mol/dm^3 .

The effect of nitric acid concentration in solution on distribution ratio is shown in Figure 2. The distribution ratio of U(VI) increases with the increase of nitric acid concentration, but begins to decrease when nitric acid concentration reaches certain level. This results from the competition between the nitric acid and uranium nitrate. On the other hand, when the nitric acid concentration is fairly high, the [UO2(NO3)]-, which is difficult to be extracted, is possible to be formed. The rule of extraction uranium by using TBP is the same as that by using PSO , but the extraction rule of Th(IV) is different (Figure 2).

Effect of PSO concentration on distribution ratio

The effect of PSO concentration on distribution ratio is shown in Figure 3. When the nitric acid concentration in solution is 3.0 mol/dm^3 , the distribution ratio of U(VI) and Th(IV) increases with the increase of PSO concentration. Log[D] and Log[PSO] are in linear relationship with the slope being 2. This shows that the extraction reaction formula is:

$$UO_2^{2+} + 2NO_3^- + 2PSO_{(o)} \xrightarrow{Ku} UO_2(NO_3)_2 2PSO_{(o)} \qquad \text{or}$$

$$Th^{4+} + 4NO_3^- + 2PSO_{(o)} \xrightarrow{KTh} Th(NO_3)_4 2PSO_{(o)}$$

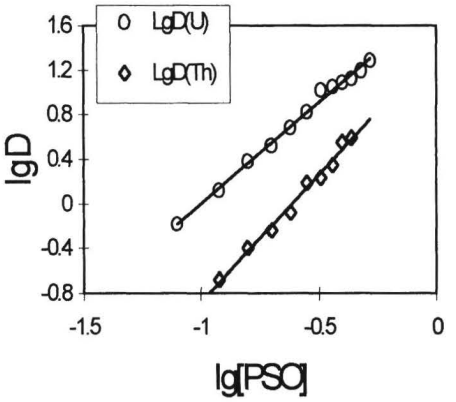


Figure 3. Distribution ratio of U(VI) and Th(IV) as a function of PSO concentration on distribution ratio at 25°C; [UO_2] = 5.48 x 10^{-4} mol/cm^3; [Th^{4+}] = 5.68 x 10^{-4} mol/dm^3; [HNO_3] = 3.0 mol/dm^3; [NH_4NO_3] = 0.1 mol/dm^3

Effect of salting-out agent concentration on distribution ratio

The effect of salting-out agent on distribution ratio is shown in Figure 4. When the nitric acid concentration in solution is 0.5 mol/dm^3 , the distribution ratio of U(VI) and Th(IV) rapidly increases with the increase of salting-out agent (NH_4NO_3) concentration.

Effect of U(VI) concentration on distribution ratio

The effect of U(VI) and Th(IV) concentration on distribution ratio is shown in Table 1. When the U(VI) or thorium concentration in solution is quite low, the distribution ratio changes little with the increase of the U(VI) or Th(IV) concentration. When the U(VI) or Th(IV) concentration in solution is high, the distribution ratio decreases with the increase of the U(VI)or Th(IV) concentration, which is mainly because of the increase of the saturation in organic phase.

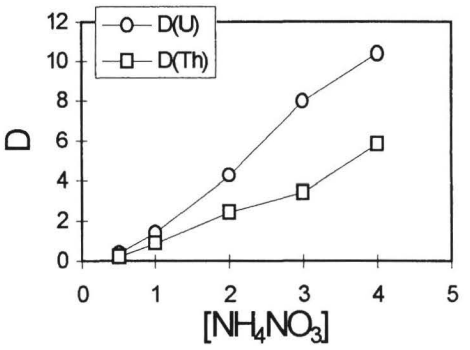


Figure 4. Distribution ratio of U(VI) and Th(IV) as a function of aqueous NH_4NO_3 concentration on distribution ratio at 25°C; [PSO] = 0.32 mol/dm^3; [UO_2^{2+}] = 5.48 x 10^{-4}mol/dm^3; [Th^{4+}] = 5.68 x 10^{-4} mol/dm^3; [HNO_3] = 0.5 mol/dm^3.

[U](*10^{-4} mol/ml)	2.74	5.48	11.0	21.9	43.8	109.6	274.0
D_U	8.25	8.08	7.97	7.84	6.69	5.52	4.69
D_{Th}	1.20	1.23	1.27	1.18	1.09	0.98	0.73

Table 1 Effect of U(VI) and Th(IV) concentration on distribution ratio at 25°C; [PSO] = 0.32 mol/dm^3; [HNO_3] = 3.0mol/dm^3; [NH_4NO_3] = 0.1mol/dm^3

Effect of temperature on distribution ratio

The effect of temperature on distribution ratio of U(VI) and Th(IV) is shown in Table 2 and Figure 5. The distribution ratio of U(VI) and Th(IV) decreases with the increase of temperature. Log[D] and 1/T are in linear relationship with the slope being 0.8 and 0.9 respectively. The extraction process is actually the exothermic process. The extraction enthalpies of U(VI) with PSO can be calculated:[7] ΔH_U=-14.2KJ/mol; ΔH_{Th}=-16.8KJ/mol.

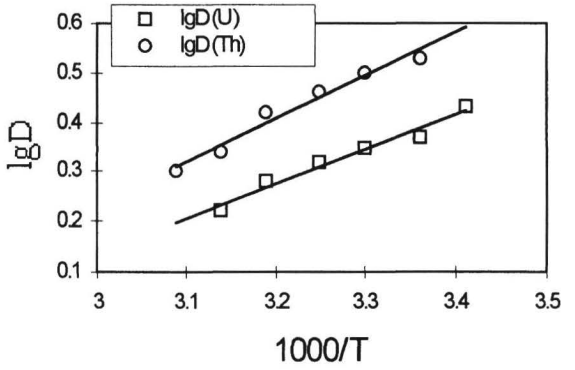


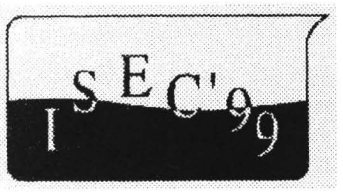
Figure 5. Effect of temperature on distribution ratio of U(VI) and Th(IV) at 25°C; [PSO] = 0.32 mol/dm^3 (for [UO_2^{2+}] = 5.48 x 10^{-4} mol/dm^3); [PSO] = 0.20 mol/dm^3 (for [Th^{4+}] = 5.68 x 10-4 mol/dm^3); [HNO_3] = 3.0 mol/dm^3; [NH_4NO_3] = 0.1mol/dm^3.

t(°C)	20	25	30	35	40	45	50
D_U([PSO] = 0.20 mol/dm^3)		3.29	3.23	2.95	2.66	2.19	2.05
D_{Th}([PSO] = 0.32 mol/dm^3)	3.30	3.29	3.23	2.95	2.66	2.19	

Table 2 Effect of temperature on distribution ratio of U(VI) and Th(IV) at $[UO_2^{2+}] = 5.48 \times 10^{-4}$ mol/dm^3;
$[Th^{4+}] = 5.68 \times 10^{-4}$ mol/dm^3; $[HNO_3] = 3.0$ mol/dm^3; $[NH_4NO_3] = 0.1$ mol/dm^3

REFERENCES

1 Cheng F and Long T. *Precious Metals (in Chinese)*, **10**, 10, (1991).
2 Ji J-G, Zhou Z-M and Mao J-J. *Precious Metals (in Chinese)*, **17**, 1, (1996).
3 Yan G-L, Long T-W and Zhang Z-M. *Engineering Chemistry and Metallurgy (in Chinese)*, **15**, 7, (1987).
4 Ma H-L- *Atomic Energy Science and Technology (in Chinese)*, **6**, 748, (1964).
5 Wang J-H, Zhou Z-M and Xu D-M. *Journal of Nuclear and Radiochemistry (in Chinese)*, **14**, 226, (1992).
6 Mao J-J, Fang M, Fu L et al. *Journal of Fudan University (Natural Science) (in Chinese)*, **31**, 221, (1992).
7 Wang Y-S, Sun G-X, Xie D-F et al. *J. Radional. Nucl. Chem. Letters*, **214,** 67.



PALLADIUM(II) EXTRACTION WITH ALKYL DERIVATIVES OF NICOTINAMIDE

M Wiœniewski, I Szczepanska, Aleksandra Borowiak-Resterna
Institute of Chemical Technology and Engineering, Poznan University of Technology, Poznan, Poland

ABSTRACT
Model individual N-alkyl- and N,N-dialkylnicotinamides were used for palladium(II) extraction from aqueous HCl solutions. The extraction is fast and equilibrium is obtained after 15 minutes. N-dodecylnicotinamide (DDNA) extracts palladium(II) the most rapidly and the equilibrium is obtained after 1 minute. The composition of formed complex was determined.

Keywords: palladium(II), nicotinamide derivatives, chloride media

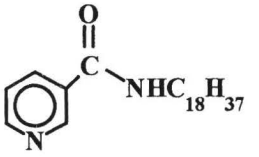
INTRODUCTION

The extraction of palladium(II) inspired a lot of interest in the last ten years and is used in industry. Various types of extractants have been proposed, e.g. derivatives of hydroxyquinoline, hydroxyoximes, dialkyl sulphides, aminoacids, pyridine carboxylates, 4-alkylphenylamines. Dialkyl sulphides, hydroxyoximes and aminoacids are well known as selective extractants of precious metals, which are used in several plants, including the Acton Precious Metal Refinery of INCO, Matthey Rustenberg, Lonhro Refiners. The extraction of palladium(II) is usually a slow process as a result of the symmetry of the palladium chlorocomplex $PdCl_4^{2-}$ and of the high hydrophobicity of extractants.[1] Recently ICI proposed using of ACORGA CLX-50 for palladium(II) extraction from its acidic solutions.[2-4] Two interesting features were reported; viz. an appropriate selectivity and good kinetics of extraction. The extractant contains hydrophobic pyridine carboxylates of unknown structure and concentration. One may suppose, that also other derivatives of pyridine carboxylic acids[5-8] can be used for palladium (II) extraction from chloride solutions.

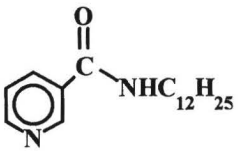
The aim of this work is the synthesis of some model individual N-alkyl- and N,N-dialkylnicotinamides and the studies of extraction equilibrium in systems containing palladium(II) ions in 3 mol/dm^3 HCl, 0.1 mol/dm^3 HCl and 0.1 mol/dm^3 HCl in the presence of 0.5 mol/dm^3 NaCl.

EXPERIMENTAL

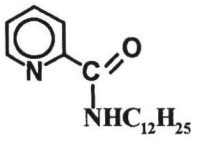
Materials



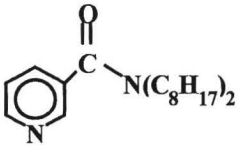
N-octadecylnicotinamide (ODNA)



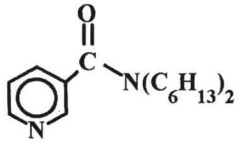
N-dodecylnicotinamide (DDNA)



N-dodecylpicolinamide (DDPA)



N,N-dioctylnicotinamide (DONA)



N,N-dihexylnicotinamide (DHNA)

© 2000 Society of Chemical Industry

Palladium(II) extraction

Extraction was carried out typically in a disperse system using equal volumes of the aqueous and the organic phases at ambient temperature. Aqueous phases contained $5x10^{-3}$ mol/dm^3 of palladium (II) in 3 mol/dm^3 HCl, 0.1 mol/dm^3 HCl and 0.1 mol/dm^3 HCl in the presence of 0.5 mol/dm^3 NaCl and organic phases were prepared by dissolution of extractants in toluene. The palladium (II) content was determined in the aqueous phase before and after extraction by using spectrophotometrically iodidation.[9] The composition of the formed complex was estimated. The UV-VIS spectra of analysed solutions have been measured in mixture of chloroform to methanol ratio equal 2:1. The solutions of N-dodecylnicotinamide (DDNA) in mixture chloroform and methanol was reference material.

RESULTS AND DISCUSSION

Figures 1 and 2 show the effect of the number and length of the alkyl group of alkyl derivatives of nicotinamide on equilibrium extraction of palladium(II) from 3 mol/dm^3 HCl and 0.1mol/dm^3 HCl in the presence of 0.5 mol/dm^3 NaCl. The equilibrium extraction of palladium (II) is obtained after 15 minutes. N-dodecylnicotinamide (DDNA) extracts palladium (II) the most rapidly and the equilibrium is obtained after 1 minute. The percentage extraction of palladium (II) increases as the length of the alkylamide group decreases, as a result of increased hydrophobicity of alkyl derivatives of nicotinamide. The rate of palladium (II) extraction with N,N-dioctylnicotinamide (DONA) and N,N-dihexylnicotinamide (DHNA) is less than the rate of palladium(II) extraction with N-octadecylnicotinamide (ODNA) and N-dodecylnicotinamide (DDNA).

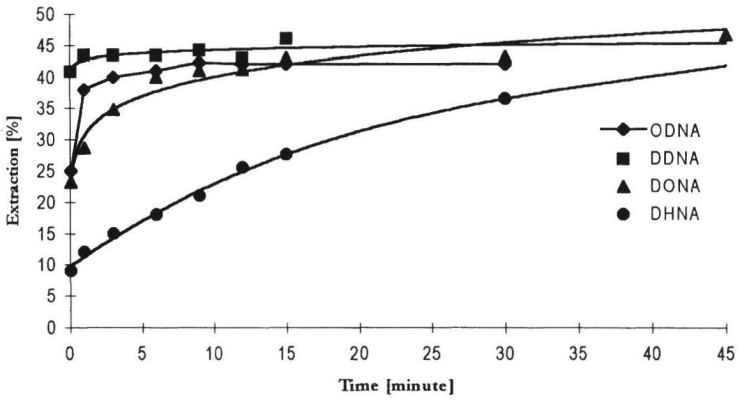


Figure 1. Extraction of palladium (II) from aqueous 3 mol/dm^3 HCl solution with alkyl derivatives of nicotinamide.

The percentage of extracted palladium (II) by means of alkyl derivatives of nicotinamide amounts about 50% what indicates that the maximum extraction capacity is 0.5 mol Pd(II)/mol amide. The addition of NaCl and decreasing of HCl concentration in initial solutions slightly results in percentage of extraction process. It also causes a better phase separation.

The composition of the complex is confirmed by the method of Vosburgh and Cooper (Table 1). The band characteristic for $PdCl_4^{2-}$ in chloroform-methanol solution is observed at 438 nm. The band is shifted towards shorter wavelengths as the ligand is added. Simultaneously, the absorbance decreases from 0.118 to 0.058, i. e. the half of the initial value. At molar ratio of the ligand to palladium (II) exceeding 2 both the wavelength and the absorbance at maximum are approximately constant. All this means that half of chloride ions is liberated from $PdCl_4^{2-}$ giving the complex $PdCl_2L_2$.

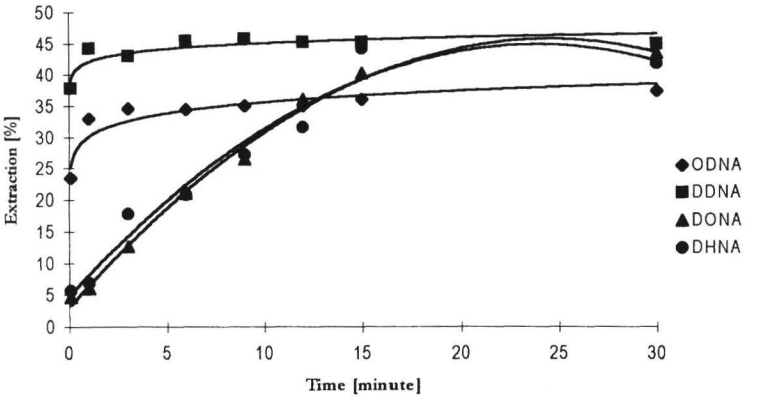


Figure 2. Extraction of palladium (II) from aqueous 0.1 mol/dm^3 HCl in presence of 0.5 mol/dm^3 NaCl solution with alkyl derivatives of nicotinamide.

Ligand to palladium (II) ratio	Wavelength [nm]	Absorbance
0.0 : 1	438	0.118
0.4 : 1	427	0.093
0.8 : 1	402	0.083
1.2 : 1	396	0.082
1.8 : 1	394	0.069
2.0 : 1	394	0.061
2.2 : 1	393	0.052
3.0 : 1	390	0.061
5.0 : 1	390	0.058

Table 1 The composition of analysed solution, wavelength of peak maximum and absorbance.

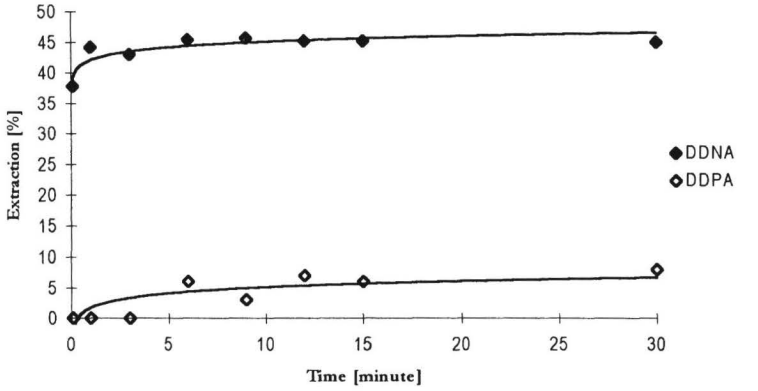


Figure 3. Extraction of palladium(II) from aqueous 0.1 M HCl in the presence of 0.5 M NaCl solution with N-dodecylnicotinamide (DDNA) and N-dodecylpicolinamide (DDPA).

Figure 3 shows the change of the position of the alkylamide group in the pyridine ring. Pyridine derivatives having an alkylamide group at the 2 position are weaker extractants than those with amide group in the position 3. It is probably caused by steric hindrance or/and formation of hydrogen bonds between nitrogen in pyridine ring and amide group. Figure 4 shows a spontaneous transfer of palladium(II) to the toluene phase without any phase mixing.

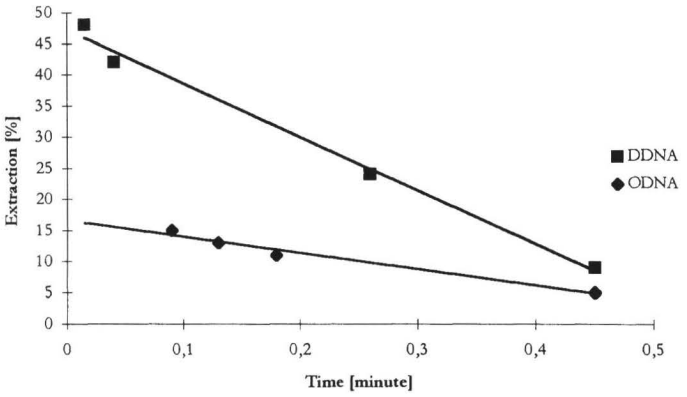


Figure 4. A spontaneous transfer of palladium(II) to the toluene phase from aqueous 3 M HCl solution with N-dodecylnicotinamide (DDNA) and octadecylnicotinamide (ODNA).

CONCLUSIONS

Extraction of palladium (II) monoalkyl pyridinecarboxamides increases when the length of the alkyl group decreases. A higher extraction is observed for the derivative with the alkylamide group at position 3 in comparison to the derivative having the group at position 2. A spontaneous transfer of palladium (II) to the organic phase is observed. A replacement of HCl with NaCl has only a small effect on the extraction of palladium (II)

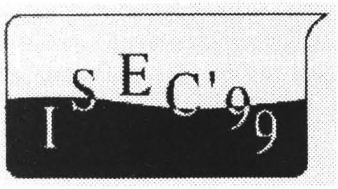
The complex with the molar ratio of extractant to palladium (II) equal to 2:1 is extracted.

ACKNOWLEDGEMENT

The work was supported by KBN donation for Institute activity. DC PP No. 32/221/98

REFERENCES

1 Wiœniewski M, Jakubiak A and Szymanowski J. *J. Chem.Tech. Biotechnol.* **63**, 209, (1995).
2 Burgess A and Dalton RF. *Proc. Int. Solvent Extraction Conf., ISEC'90*, 1087, (1992).
3 Dalton RF, Burgess A and Townson B. *Proc. Int. Solvent Extraction Conf ISEC'93*, 1341, (1993).
4 Dalton RF and Burgess A. *Eur. Pat. EP 322*, 314, (1989).
5 WiVniewski M and Szymanowski J. *Analytical Sciences*, **14**, 241, (1998).
6 Cote G, Jakubiak A, Bauer D, Szymanowski J, Mobil B and Poitrenaud C. *Solv.Extr.Ion Exch.*,**12**, 99, (1994).
7 Bogacki MB, Jakubiak A, Cote G and Szymanowski J. *Ind. Eng. Chem. Res.* **36**, 834, (1997).
8 Jakubiak A, Szymanowski J and Cote G. *Value Adding Through Solvent Extraction*, Shallcross DC, Paimin R and Prvcic LM. (Eds.), The University of Melbourne, **1**, 517, (1996).
9 Marczenko Z. *Spektrofotometryczne oznaczanie pierwiastków*, PWN, Warszawa, (1979).



CLOUD POINT EXTRACTION OF GALLIUM(III) WITH NONIONIC SURFACTANTS FROM HYDROCHLORIC ACID MEDIA

Shigendo Akita[1], Nobuhisa Hyodo[2], Norihiro Kobayashi[2], Susumu Nii[2], Katsuroku Takahashi[2] and Hiroshi Takeuchi[2]

[1]Nagoya Municipal Industrial Research Institute, Rokuban, Atsuta-ku, Nagoya 456-0058, Japan

[2]Dept. of Chem. Eng., Nagoya University, Chikusa-ku, Nagoya 464-8603, Japan

ABSTRACT

An aqueous solution of polyethylene glycol-type nonionic surfactants becomes turbid at a particular temperature referred to as the cloud point, and exhibits spontaneous phase separation at higher temperatures. Cloud point extraction makes use of this phenomenon to effect separations. In the present study, we have investigated the cloud point extraction of gallium(III) from hydrochloric acid media using polyoxyethylene-nonyl-phenyl ether having an average chain length of 7.5 ethylene oxide units (PONPE7.5). Phase separation of aqueous PONPE7.5 solutions occurs upon heating, and Ga(III) has been successfully extracted into the small surfactant-rich phase produced without any additives such as extractants. An increase in HCl concentration gives rise to an improvement in the extraction, and the maximum concentration of Ga(III) in the surfactant-rich phase is obtained at 4 M HCl. The selective separation of Ga(III) from some heavy metals has been achieved due to the poorer extractions of the other metals. Back extraction of Ga(III) from the loaded surfactant-rich phase can be effected with dilute HCl solutions.

Keywords: cloud point extraction, gallium(III), nonionic surfactant, polyoxyethylene- nonyl-phenyl ether

INTRODUCTION

Many separation methods take advantage of the transfer or partitioning of solutes between two immiscible phases. Two immiscible aqueous phases can be created by using water-soluble surfactants or polymers, and these systems have recently attracted special attention in separations since they need no toxic and flammable organic solvents. An aqueous two-phase system is formed when two water-soluble polymers such as polyethylene glycol (PEG) and dextran are mixed at appropriate concentrations. These systems have been investigated mainly for the separation of biomaterials[1,2]. Cloud point extraction is another water-based separation method, which makes use of the coacervation characteristics of PEG-type nonionic surfactants.

Nonionic surfactants containing ethylene oxide (EO) chains exhibit a change in water solubility upon temperature alteration; on heating, the aqueous surfactant solution becomes turbid at a well-defined temperature referred to as cloud point (CP). CP depends strongly on the hydrophilic-lipophilic balance (HLB) of the surfactant: the longer the surfactant EO unit, the higher the CP of its aqueous solution. Such a clouding phenomenon has been ascribed to the dehydration of EO chains at elevated temperatures. At a temperature above the CP, the aqueous solution spontaneously separates into a small surfactant-rich phase, which still contains a substantial amount of water, and a bulk aqueous phase. The two phases thus formed have distinct chemical and physical properties, and this phase separation provides the basis of CP extraction methods for the separation of organic and inorganic compounds from aqueous streams. Along with its intrinsic safety, CP extraction is considered to have several advantages, including cost saving resulting from a relatively small amount of surfactant required, the ability to concentrate a variety of solutes into the small surfactant-rich phase, and applicability to solvent-sensitive bioproducts.

To date, CP extraction has been applied for separating organic and inorganic compounds in the field of analytical chemistry [3-9] and biochemistry.[10-13] In our previous papers,[14,15] the CP extraction of aromatic compounds from aqueous media was investigated using polyoxyethylene nonyl phenyl ethers. We also found that gold(III) is effectively concentrated into the small surfactant-rich phase from hydrochloric acid solutions without any complexing agents[16,17] in the same way as the solvent

© 2000 Society of Chemical Industry

extraction with the same surfactants.[18] In the present study, the technique is applied to the recovery of gallium(III) from hydrochloric acid media, and the effects of operating parameters on the CP extraction are elucidated.

EXPERIMENTAL

Polyoxyethylene-nonyl-phenyl ethers (PONPE) having an average ethylene oxide (EO) number of 7.5 and 10 were obtained from Tokyo Kasei Kogyo Co., Ltd. and used with no further purification. The general formula of PONPEn is $HO(CH_2CH_2)nC_6H_4C_9H_{19}$, where n is the EO number. Metal stock solutions were prepared by dissolving an appropriate amount of each metal chloride in deionized water. All chemicals used were of reagent grade.

A prescribed amount of PONPE and/or NaCl was combined with appropriate volumes of standardized HCl and metal stock solution, and diluted with deionized water to a final volume of 20 cm^3. A well-mixed aqueous feed contained in a 25 cm^3 graduated glass tube was heated slowly in a thermostatted water bath, and the cloud point (CP) was recorded as a temperature at which the solution turned turbid. When the CP was lower than room temperature, the solution was first cooled to near the freezing point before heating. Subsequently, the solution was allowed to stand at a prescribed settling temperature (ST) for 12 hr to attain the phase separation, and the equilibrium volumes of the surfactant-rich and aqueous phases were determined. The metal concentration in the aqueous phase was measured by inductively coupled plasma spectroscopy (ICP), and that in the other phase was calculated on the basis of mass balance. The initial concentrations of the surfactant and metal were 2.5 wt% and 100 ppm, respectively, unless otherwise stated.

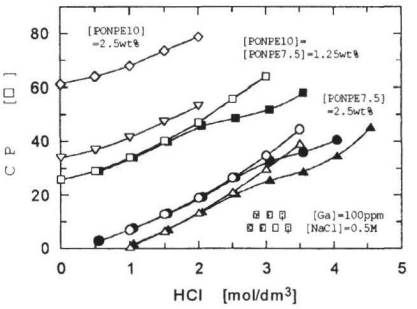


Fig.1 Effect of HCl concentration on cloud point of surfactant solutions with and without Ga(III).

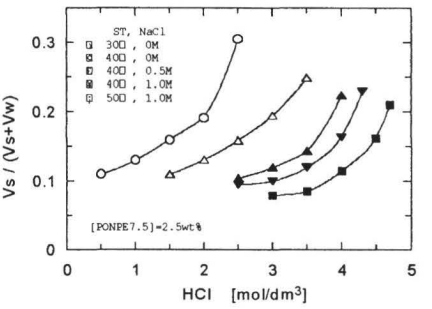


Fig.2 Effect of HCl concentration on volume ratio of surfactant-rich phase.

RESULTS AND DISCUSSION

Cloud Point and Phase Separation

Figure 1 shows the relationship between the CP of aqueous PONPE solutions and HCl concentration, with and without a small amount of Ga(III) present. The CP rises monotonously with an increase in HCl concentration, *viz.* salting-in of the surfactant, thus, requiring a higher ST for attaining phase separation. On the other hand, the addition of NaCl brings about a decrease in CP, *viz.* salting-out of the surfactant, due to competition for water of hydration between the electrolyte and the surfactant. Aqueous PONPE7.5 solutions yield much lower CP than those of PONPE10 since the former surfactant has lower aqueous solubility, resulting from its lesser hydrophilicity. Thus, the PONPE7.5 system allows the CP extraction to apply to a more highly acidic solution or a lower ST; in fact, phase separation could be obtained at ambient temperature at HCl concentrations less than 2.5 M. The mixed surfactant system of PONPE7.5 and PONEP10 yields a single intermediate CP between those of individual surfactants rather than two discrete CPs, indicating the formation of mixed

micelles of two surfactants.

In the presence of a small amount of Ga(III), a slight decrease in the CP is observed at HCl concentrations over 2.5 M. This decline in CP is more prominent for solutions with higher metal concentration, although the data are not shown here. It is thought that Ga(III) ion replaces the water associated with the surfactant EO chains at high acidities, and makes the surfactant micelles more hydrophobic.

Figure 2 represents the effect of HCl concentration on the equilibrium volume ratio of the surfactant-rich phase to the total volume, $Vs/(Vs+Vw)$, where V stands for the volume and the subscripts s and w correspond to the surfactant-rich and bulk aqueous phases, respectively. In the present study, the apparent phase separation was completed within 40 minutes for all runs, and the surfactant-rich phase was formed as a lower phase. When the prescribed ST was sufficiently higher than the CP, favorable phase separation could be obtained from aqueous PONPE7.5 solutions. The volume of the surfactant-rich phase formed is as little as 20 % of that of the aqueous feed; thus, significant enrichment of target solutes can be expected in CP extraction. The volume ratio, however,

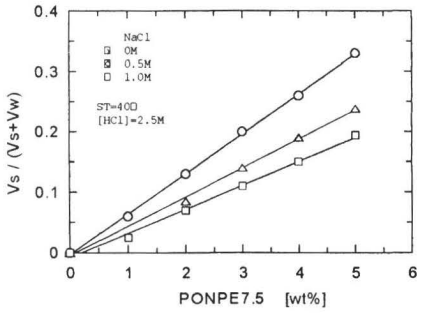


Fig.3 Effect of feed PONPE concentration on volume ratio of surfactant-rich phase.

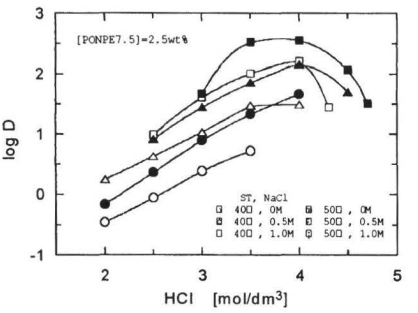


Fig.4 Effect of HCl concentration on distribution ratio of Ga(III).

increases with increasing HCl concentration. Also, increased acidity leads to poor phase separation due to a too small difference between the CP and ST. On the other hand, adding NaCl or raising ST not only decreases the volume ratio, but also permits the phase separation from solutions with higher HCl concentration.

Figure 3 shows the effect of feed PONPE7.5 concentration on the volume ratio of the surfactant-rich phase after the phase separation at 40°C, indicating a linear increase in the ratio with the feed concentration. The addition of NaCl and the rise in ST have the same effect on the volume ratio as seen in Fig. 2. The residual amount of surfactant in the bulk aqueous phase was found to be as small as its critical micelle concentration (CMC),[19] reagent loss is therefore not a serious problem in CP extraction.

Cloud Point Extraction of Gallium(III)

Nonionic surfactants posses a number of electron-donating oxygen atoms, and high affinity for Ga(III) might be expected in such the same manner as for Au(III).[16,17] Typical results for the CP extraction of Ga(III) using PONPE7.5 are shown in Figure 4 as a plot of the distribution ratio, D, against HCl concentration. The distribution ratio is defined as $D = Cs/Cw$, where C denotes the concentration of metal. Although the salt concentration and ST were varied depending on the solution acidity to be treated, the extraction can be seen to improve with increasing HCl concentration, and almost complete extraction can be achieved. The volume of the surfactant-rich phase is so small that high concentration of the metal can be attained; the logarithmic ratio of over 2.5 was obtained at around 4 M HCl. However, a further increase in HCl concentration reduces the distribution ratio due to the poor phase

separation resulting from the CP rise.

Thus, Ga(III) can be satisfactorily extracted into the surfactant-rich phase with no addition of any complexing agents into the system, and the surfactant-rich phase can function as a pseudo-organic phase for Ga(III), much like conventional solvent extraction using solvating extractants. Since the metal is known to exist in the form of $GaCl_4^-$ in solutions with high chloride concentrations, the extraction might take place through the coordination of the surfactant EO unit to hydrogen tetrachlorogallate, $HGaCl_4$.

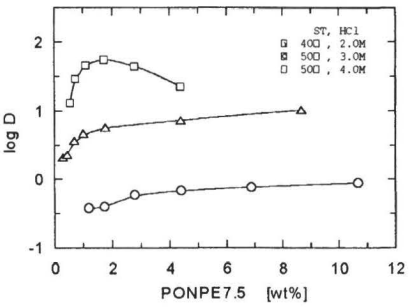


Fig.5 Effect of PONPE7.5 concentration on distribution ratio of Ga(III).

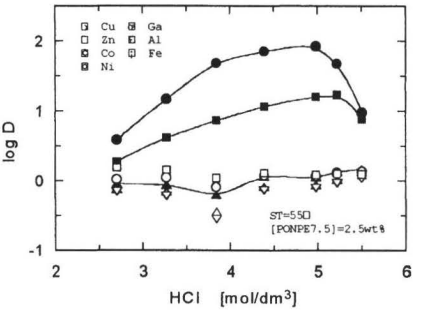


Fig.6 Metal separation via cloud point extraction using PONPE7.5.

Table 1 Back extraction of Ga(III) from metal-loaded surfactant-rich phase

Strippant	% extraction	% stripping	% recovery
H_2O	91	90	81
0.5M HCl	91	89	80

The effect of feed PONPE7.5 concentration on the distribution ratio of Ga(III) is shown in Figure 5. Although the distribution ratio (i.e. metal enrichment) does not improve much, the percent extraction increases with an increase in the surfactant concentration due to an increased volume of the surfactant-rich phase at high feed concentrations (see Figure 3). For extraction from 4 M HCl solution, there exists a maximum in the distribution ratio at about 2.0 wt% PONPE7.5. This indicates that an excess of the surfactant would lower the concentration of target solute in the surfactant-rich phase, unlike solvent extraction where the extractant concentration has no effect on the volume ratio of the two phases.

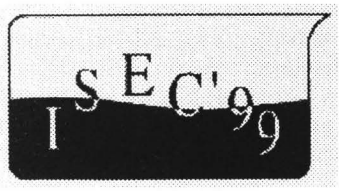
The back extraction of Ga(III) from the surfactant-rich phase was examined using deionized water and 0.5 M HCl solution as the stripping agent. The results are summarized in Table 1. After forward CP extraction at 50 °C from 4 M HCl, the metal-loaded, surfactant-rich phase was separated from the aqueous phase and combined with a stripping solution to bring the total volume to 20 cm^3. Then, after mixing the solution was phase separated again at 30 °C. As expected from Figure 4, at low acid concentration, the metal can be transferred into the newly formed bulk aqueous solution, and percent stripping values as high as 90% are obtained, with a total recovery of around 80%. This procedure of back extraction, however, leads to dilution of the concentrated metal according to the volume ratio of the two phases, and direct burning of the loaded surfactant-rich phase might be a more suitable option, especially for valuable metals.

Figure 6 shows the results for the separation of various metals from an aqueous multi-element solution via CP extraction with PONPE7.5 at 55°C. Values of log *D* for the other metals (Cu(II), Zn(II), Co(II), Ni(II) and Al(III)) are close to zero, regardless of HCl concentration, and the separation of Ga(III) from these metals improves with increasing HCl concentration up to 5 M. The extraction of Fe(III), however, is similar to that of Ga(III), and as a result, their separation is poor. These results

indicate that in CP extraction the unexpected metals are partitioned equally between the two phases, not excluded from the surfactant-rich phase. This suggests that the efficiency of separation strongly depends on the phase ratio; thus, it is crucial to select operation conditions so as to yield the smallest surfactant-rich phase possible. In conclusion, CP extraction is thought to be superior in the enrichment of a target solute, but inferior in the separation, compared with solvent extraction.

REFERENCES

1. Albertsson PA, *'Partitioning of Cell Particles and Macromolecules'*, John Wiley & Sons Inc., New York, (1971).
2. Zaslavsky BY, *'Aqueous Two-Phase Partitioning'*, Marcel Dekker Inc., (1995).
3. Fernandez AE, Ferrera ZS and Rodriguez JJS, *Anal. Chim. Acta*, **358**, 145, (1998).
4. Ferrer R, Beltran JL and Guitera J, *Anal. Chim. Acta*, **330**, 199, (1996).
5. Pinto CG, Pavon JLP and Cordero BM, *Anal. Chem.*, **67**, 2606, (1995).
6. Watanabe H and Tanaka H, *Talanta*, **25**, 585, (1978).
7. Igarashi S and Endo K, *Anal. Chim. Acta*, **320**, 133, (1996).
8. Silva MF, Fernandez L, Olsina RA and Stacchiola D, *Anal. Chim. Acta*, **342**, 229, (1997).
9. Justice JM, Murtagh JJ, Moss JJ and Vaughan M, *J. Biol. Chem.*, **270**, 1797, (1995).
10. Nikas YJ, Liu CL, Srivastave T, Abbott NL and Blankschtein D, *Macromolecules*, **25,** 4797, (1992).
11. Saitoh T and Hinze WL, *Talanta*, **42**, 119, (1995).
12. Tani H, Kamidate T and Watanabe H, *J Chromatogr.*, **A780**, 229, (1997).
13. Akita S and Takeuchi H, *Sep. Sci. Technol.*, **30**, 833, (1995).
14. Akita S and Takeuchi H, *Sep. Sci. Technol.*, **31**, 401, (1996).
15. Akita S and Takeuchi H, *'Value Adding Through Solvent Extraction (Proc. ISEC'96)'* **1**, 529, (1996).
16. Akita S, Rovira M, Sastre AM and Takeuchi H, *Sep. Sci. Technol.*, **33**, 2159, (1998).
17. Akita S, Yang L and Takeuchi H, *Hydrometallurgy*, **43**, 37, (1996).
18 Akita S, Rovira M, Sastre AM, Hyodo N and Takeuchi H, *'Liquid-Liquid Two Phase Flow and Transport Phenomena'*, Begell House Inc., New York, 371 (1997).



ADDITIVE TAILORING IN BIPHASIC SYSTEMS FOR AN ENZYMATIC CONDENSATION REACTION

Raanan Dunowicz and Aharon M Eyal
Casali Institute of Applied Chemistry. School of Applied Science and Technology. The Hebrew University of Jerusalem. Jerusalem 91904, Israel

ABSTRACT
The enzymatically catalysed reaction between dodecanol and glucose to form dodecylglucoside was studied. This reaction serves as a model for two phase reaction systems in which the reagents have very little mutual solubility. Typically, both the rate and the yield in such reactions are slow. Five solvents (additives) were tested for their effect on reaction equilibrium, butanone, butanedione, formamide, methylformamide and dimethylformamide. These additives were introduced in relatively small amounts, insufficient to combine the two phases into one. Butanone addition reduced the yield of the reaction, while the others increased it in the sequence: butanedione >> methylformamide > dimethylformamide >> formamide. Addition of butanedione to the reaction system, in an amount equal to about 15% of the total, resulted in 500% increase in the yield of dodecylglucoside formation. Analysing the effects of the various additives indicate that the most efficient ones are: a) lypophilic solvents of relatively high polarity, which increase the solubility of the product in the organic phase and b) hydrophilic solvents of relatively low polarity, which improve the solubility of dodecanol in the aqueous reaction medium.

Keywords: biphasic reactions, enzymatic condensation reaction, alkylglucoside

INTRODUCTION

Reactions between reagents of low mutual miscibility present a great challenge, particularly where large volumes of a co-solvent need to be avoided (e.g. for product dilution reasons) or when the only suitable co-solvents are toxic. That is the case in manufacture of esters or ethers composed of a long chain lypophilic reagent and a low molecular weight hydrophilic reagent. The present work studied the reaction of dodecanol and glucose to form dodecyl glucoside.

In the absence of catalyst, the reaction is very slow due to the low mutual solubilities of the reagents and due to the formation of by-product water, which tends to push the reaction backwards. A strong acid catalyst and elevated temperature increase the rate, but result in uncontrolled reactions in which colored and other undesired products are formed. Enzymatic catalysis was studied for such systems.

While accelerating the reaction, enzymes do not solve the problem of low yields, imposed mainly by low activity of reagents and high activity of the products in the equilibrium reaction phase. The yield of the reaction can be improved by transfer of the product to another phase.[1,2,3] Thus, in case of single phase reaction, adding an immiscible liquid, which is a good solvent for the product, results in better conversions. In two-phase systems, like the one tested in the present work, improvement might be achieved by increasing the volume of the phase, which is preferred by the product (provided that there is no interference with other parameters). The product concentration in that phase could still be low and recovery could be expensive.

The purpose of the present work is to study improvement in the yield of the two-phase reaction by affecting the equilibrium of the reaction. Several researchers studied addition of a co-solvent in amounts sufficient to combine the two phases into one.[4,5] In some cases this route was successful in increasing the yield, but diluted the product and complicated its recovery. We studied the addition of solvents (referred to in the following as additives) in relatively small amounts. The additives distribute between the two phases, but do not combine them into one. The additives used in the present phase of the study were butanone, butanedione, formamide, methylformamide and dimethylformamide. They were selected for their polarity and H-bond formation capability, which are in the range between those of the main solvents, water and dodecanol.

These additives may affect the kinetics of the reaction both through the activity of the reagents and the products and through the effect on enzyme activity. Yet, while most previous studies dealt with kinetics, the main focus of the present work is shifting the equilibrium in the direction of higher

© 2000 Society of Chemical Industry

conversion into dodecylglucoside (DoG). Equilibrium data is more easily obtained by working in the opposite direction, i.e. hydrolysis of DoG. The experiments were therefore conducted in systems comprising two phases, dodecanol and an aqueous solution containing buffer and glucose. Dodecylglucoside, additive (except for the blank trials) and enzyme were added. After equilibrium was reached, the two phases were analysed for their DoG content. As equilibrium does not depend on the direction of the reaction and in order to avoid confusion, dodecanol and glucose are termed reagents and water and DoG are termed products according to the intended manufacture.

EXPERIMENTAL

Materials

Dodecyl alcohol (DodOH) (99%), n-dodecyl β-D-glucopyranoside (DoG) (98%), 2,3-butanedione (BD), potassium dihydrogen phosphate (99%), di-sodium hydrogen phosphate and the enzyme, β-Glucosidase E.C. 3.2.1.21 were all obtained from Sigma. D(+)-Glucose anhydrous (Glc.) (99.9%) and N-methylformamide (MF) (99%) were from Merck, butanone (B) (Chem.Pure.) and N,N-dimethylformamide (DMF) 99% from Riedel-deHaën, formamide (F) 98.5% from BDH, water column deionized

Methods

348.6 mg DodOH, 1.4 mg DoG 1.4mg, 343.6 mg phosphate buffer (pH = 5 0.1 mol/dm^3), 42.23 mg Glc 43.23 additive and 40u ß-Glucosidase were introduced into microtube plastic vial of 2 cm^3 capacity, 3 glass beads were added to each microtube and shaken at 200 strokes per minute in a linear shaking bath (GFL) at 35°C. Several trials were made with different amounts of each additive added. Each experiment was repeated at least twice. In one of these vials the reaction was terminated approximately after 100 hours. 5-10u enzyme was added to the other vial, which was shaked for an additional 100 hours. In all the experiments the second addition of enzyme had less than 10% effect on the results, indicating that equilibrium was reached in the first 100 hours. Blank trials were conducted in a similar way except for no addition of an additive. These blank test were conducted with each additive and amount in order to avoid possible errors due to changes in parameters, such as the calibration of the analytical systems.

The vials were centrifuged and samples were taken for DoG analysis by HPLC: Column RP-18e Merck, MeOH:H_2O 85:15, 0.4 cm^3/min., 35°C, detector RI 71 (Merck). No DoG was found in the aqueous phase.

The vials used for the enzymatic reaction were too small to detect changes in phase amounts on addition of the tested additives. The change in the amount of the phases (containing most of the product) was determined for each trial by introducing into a test tube all the components (except for the enzyme) at ten times the above-listed amounts, equilibrating at 35°C, phase separation and weighing.

RESULTS AND DISCUSSION

Figure 1 presents the effect of butanone and butanedione content on the organic phase concentration of DoG in equilibrium. Comparison to the blank (percentage) is shown too. Equilibrium DoG concentrations in the case of butanone are lower than those in the blank. This trend increases slightly on further addition of butanone, indicating that that additve shifts the equilibrium towards formation of dodecanol and water – the products in the intended reaction. An opposite effect is found for butanedione addition. The concentration of DoG increases nearly linearly with the content of this additive reaching four times the blank concentrations on addition of modest amounts of additive.

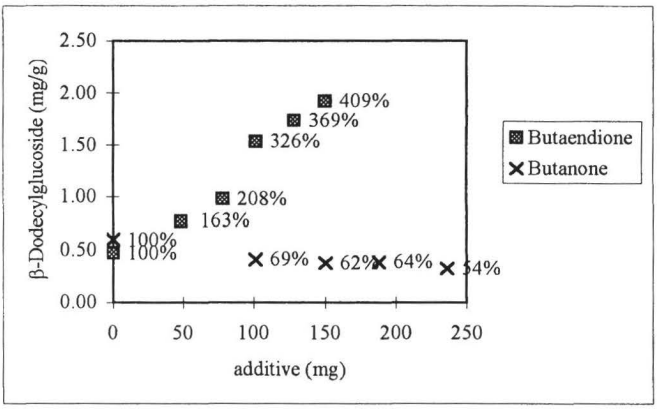


Figure 1 Additive effect on β-Dodecylglucoside concentration

Table 1 summarizes the data for the five additives in terms of DoG concentrations in the organic phase (additive trial, blank and the ratio between the two), changes in the amount of the organic phase and yield gain (taking into consideration changes in both concentration and volume of the organic phase).

Additive	mg	[DoG] mg/g	org phase change %	[DoG] blank mg/g	[DoG] ratio add / blank mg/mg	Yield gain %
Butanone	100	0.41	22.6	0.59	0.69	-15
Butanone	200	0.32	45.2	0.59	0.54	-21
2,3-Butanedione	50	0.77	16.0	0.47	1.64	90
2,3-Butanedione	150	1.92	48.0	0.47	4.09	505
Formamide	100	0.68	4	0.65	1.05	9
Formamide	300	1.6	4	0.65	2.46	156
Formamide	600	2.8	4	0.65	4.31	348
m-Formamide	100	0.83	5	0.65	1.28	34
m-Formamide	150	1.13	7	0.65	1.74	86
m-Formamide	200	2.5	9	0.65	3.85	319
DMF	100	0.87	6	0.67	1.30	38
DMF	150	1.08	12	0.67	1.61	81
DMF	200	1.8	18	0.67	2.69	217

Table 1 Effects of additive on equilibrium concentration of dodecylglucoside, on the amount of the organic phase concentration and on the overall yield.

Out of the five additives used here, one reduced the yield slightly, while the others increased it significantly. In cases of butanone (B) and butanedione (BD) there is a significant increase in the amount of the organic phase – the phase that the product prefers. In case of BD that increase contributed to the increase in the yield.

Yet, we are mainly interested in the effect on the equilibrium of the reaction, which is better seen by comparing the product concentration in the additive containing trial to its concentration in the blank. Based on this parameter for similar weight additions, the improvement related to the additives follows the sequence: BD >> methylformamide (MF) > dimethylformamide (DMF) >> formamide (F) >> B.

The effect of the additive is analyzed in the following based on their effects on the activity of the reagents and the products of the condensation reaction. Increasing the activity of the reagents (dodecanol and glucose) in the reaction medium and decreasing that of the products (water and dodecyl glucoside) is expected to shift equilibrium to the product side. The analysis uses the following observations and assumptions:

1. The non-enzymatic reaction is much slower than the enzymatically catalyzed one and is therefore negligable.
2. The enzymatically catalyzed reaction takes place in the aqueous phase.
3. Glucose (Glc) hardly transfers into the organic phase.
4. Dodecanol (DodOH) concentration in the aqueous phase is low.
5. Dodecylglucoside (DoG) strongly prefers the organic phase.
6. The data in Table 1 presents equilibrium concentrations.

Let us now analyze the effects of the additives on the activities of the reagents and products in the reaction medium:

a. Glc activity in the reaction phase (aqueous) is high and does not present a limiting factor. Our assumption is that it stays so with the tested additive and their tested amounts.
b. Additives that distribute mostly into the organic phase dilute the DodOH there, and decrease its activity in both phases. Additives that prefer the aqueous phase and reduce its polarity may increase the activity of DodOH there. Based on that consideration, shifting the reaction towards the product side would follow the sequence: DMF > MF > F >> B and BD.
c. Water activity in the reaction phase is not affected significantly by lypophilic additives that distribute mostly into the organic phase. Hydrophilic additives that dissolve in the aqueous phase, dilute it and interact with the water molecules, would reduce water activity there and shift the equilibrium to the product side. Based on that consideration, the sequence would be F > MF > DMF >>B and BD.
d. Assuming that DoG activity in the reaction phase is equivalent to that in the organic phase, additives which prefer the organic phase and increase its polarity are expected to shift the equilibrium to the product side. Based on that consideration, the sequence would be BD > B >> DMF, MF and F.

As suggested above, glucose activity does not seem to be a limiting parameter, but the thermodynamic data we have is not sufficient for determining the relative contribution of the other parameters. Some indication is obtained from the experimentally found sequence of additives contribution to shifting the equilibrium to the products side: BD >> methylformamide (MF) > dimethylformamide (DMF) >> formamide (F) >> B.

The fact that the greatest contribution comes from botanedione indicates that transfer of dodecyl glucoside to the organic phase was very important. The finding that formamide had less effect than methylformamide and dimethylformamide indicates that increasing the concentration of the dodecanol in the reaction phase was somewhat more important than reducing water activity there. This finding does not support the suggestions in most previous publications that water activity is the most important parameter.

Our results indicate that most efficient additives are either lypophilic enough to prefer the organic phase, but increase its polarity or hydrophilic enough to prefer the aqueous phase, but reduce its polarity.

Table 2 and Figure 2 present the additives tested here, as well as water, dodecanol and glucose, according to the H-bond and polarity elements of their solubility parameter. It shows that the additives which contributed most to shifting the equilibrium (BD, MF and DMF) have solubility parameters, which are about half the way between those of water and dodecanol. The contribution decreases on further increasing of the protic/polarity contribution (going from methylformamide to formamide) or on decreasing it from that of butanedione to that of butanone.

		δ_d	δ_p	δ_h	δ
1	Dodecanol	14.0	3.3	9.3	17.2
2	Water	15.6	16.0	42.3	47.8
3	Butanone	15.9	9.0	5.1	19.0
4	Butanedione	18.0	13.4	9.5	24.4
5	Formamide	27.2	21.3	19.4	39.7
6	m-Formamide	12.3	17.4	12.6	24.8
7	DMF	17.4	13.7	11.3	24.9
8	Glucose	13.2	13.5	21.2	28.3

Table 2 Solubility Parameter δ/MPa$^{1/2}$

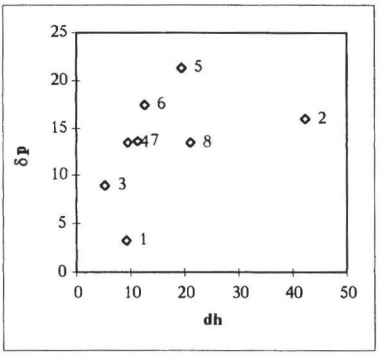


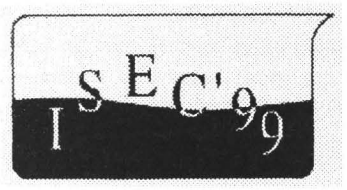
Figure 2 Solubility Parameter by Hansen[6]

As shown in Figure 2, the most efficient additives are quite similar in solubility parameter (and therefore probably have good mutual solubility), but are different enough to strongly prefer one of the phases. Is there a compound that would distribute more evenly between the phases, and play both the role of increasing the polarity of the organic phase and decreasing that of the aqueous one? This possibility should not be ruled out and such compound might be found among the other additives under study. One has, however to keep in mind that additive with good solubility in both phases would increase the mutual miscibility of the main solvents, water and dodecanol. This could have negative effects, e.g. increasing product (DoG) concentration in the reaction phase, which may shift he equilibrium backwards and interfer with its recovery

In summary, our work shows that relatively small amounts of suitable additives shift the reaction equilibrium to the product side. Thus, addition of butanedione to the reaction system, in an amount equal to about 15% of the total, resulted in 500% increase in the yield of dodecylglucoside formation. Analysis of the results pointer out the properties of desired additives. Further work is planned for optimization of additives selection.

REFERENCES

1. Martinek K, Semenov AN and Berezin IV, *Biochim et Biophys Acta*, **685**: 76, (1981).
2. Eggers DK, Blanch HW and Prausnitz JM, *Enzyme Microbiol Technol*, **11**, 84, (1989).
3. Halling JP, *Biotechnol Bioeng*, **35**, 691, (1990).
4. Gabin V, Biton J, Le Beller D, Michel J-M and Thomas D, *Biotechnol Bioeng*, **46**, 109, (1995).
5. Gabin V, Thomas D and Crout DHG, *Enzyme Microbiol Technol*, **20**, 597, (1997).
7. Barton F and Allan M. *Handbook of solubility parameters and other cohesion parameters*, second edition. CRC Press Boston London (1991).



LIX®-7800 SERIES: A NEW REAGENT FAMILY FOR REVERSIBLY EXTRACTING ANIONS FROM ALKALINE SOLUTIONS

Phillip Mattison, Henkel Corporation, 300 Brookside Ave, Ambler, PA, USA
Michael Virnig, Henkel Corporation, 2430 N. Huachuca Dr., Tucson, AZ, USA

ABSTRACT
The combination of a weak acid such as nonylphenol with a quaternary ammonium salt provides a new method for solvent extraction of anions from alkaline solutions, while allowing stripping with strong alkali.

Keywords: anion extraction (cyanides), alkaline solutions, nonyl phenol, quaternary ammonium salt,

INTRODUCTION

The reversible solvent extraction of anions from alkaline solutions has long been a difficult challenge. Quaternary amines are very capable of extracting anions from either acidic or alkaline solutions, but the anion cannot be stripped by varying the pH. The extracted anion must be displaced from the quaternary cation by another anion, either one which is preferred in the organic phase or which is at much higher concentration. In the area of aurocyanide extraction, this means that the preferred zinc tetracyanide anion is used to crowd off the gold, and then acid is used to decompose the zinc tetracyanide, capturing the liberated hydrogen cyanide with caustic scrubbing. The resulting quaternary salt is then returned to extraction. This process is not only cumbersome, but it raises concerns regarding process hazards.

Amines have low effectiveness because they are protonated under acidic conditions to give an extracting cation, but are deprotonated under even mildly alkaline conditions.

The development in recent years of the guanidine functionality as an extractant[1,2] has allowed the extraction of anions up to an aqueous pH of 12 or more, but the extraction was reversed with strongly basic solutions of pH 13.5 or higher. This is due to the high basicity of the guanidine functionality, which has a pK_b of 12 to 13. The first introduction of this functionality was as the AURIX™ 100 ion exchange resin, suited especially for extraction of gold from cyanide leach solutions. The second product was LIX® 79, a formulation of a tri-alkyl substituted guanidine in kerosene.[3]

RESULTS AND DISCUSSION

LIX®-7820, previously designated XI-78, now presents an alternative, less expensive solvent extraction system based on a formulation of a quaternary ammonium compound and an organic-soluble weak acid such as an alkylphenol. In this system, the alkylphenol is used to effectively render the quaternary ammonium cation pH-dependent. Under extraction conditions of around pH 12 or below, the alkylphenol is protonated and the quaternary ammonium compound extracts an anion from the aqueous phase. But under more highly alkaline strip conditions, the alkylphenol becomes anionic, forms an ion pair with the quaternary ammonium cation, and consequently expels the extracted anion to the aqueous phase. Thus if Q^+ is the quaternary ammonium cation, HP is the protonated form of the alkylphenol, and X^- is the extracted anion, the reaction can be described as follows:

$$(Q^+ X^-)_{org} + (HP)_{org} \leftrightarrow (Q^+ P^-)_{org} + (X^-)_{aq}$$

© 2000 Society of Chemical Industry

extraction stripping

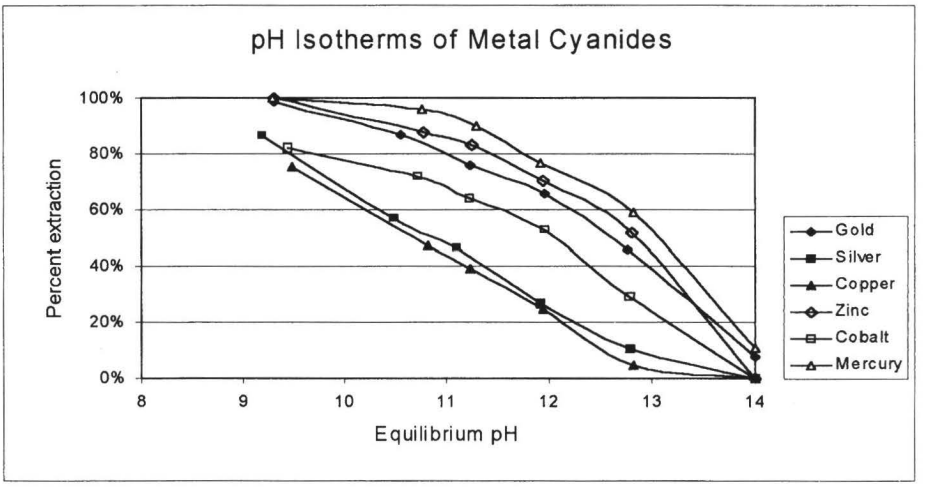
Other weakly acidic materials can be used in place of nonylphenol as long as they have high organic solubility and low water solubility. A number of such possibilities are described in Henkel's patent on the subject, US 5,158,603. In most applications, however, nonylphenol is a good match for the desired pH range.

Thus one is able to generate pH isotherms for various anions. In the following experiments, the organic phase was formulated to contain 0.05 molar Aliquat 336 (methyl-triC_{8-10}ammonium chloride) and 0.10M nonylphenol in Conoco 170E, a low-aromatic kerosene. Both of these components have very low water solubility. Organic phase was first washed with 0.5M sodium hydroxide solution to convert the nonylphenol to its phenoxide and displace chloride from the organic. The resulting organic was shaken with an aqueous solution containing a complex metal cyanide of interest, pre-adjusting the initial pH using either sodium hydroxide or sodium bicarbonate. The initial solutions contained an amount of metal related to the expected anionic charge, and added cyanide to give the indicated ratio of equivalents of total cyanide to equivalents of metal.

Metal	Au^+	Ag^+	Cu^+	Zn^{++}	Co^{++}	Hg^+
Metal conc., millimolar	2.5	2.5	2.5	1.25	1.25	1.25
Eq. CN^-/Eq. Metal	3.5	4.6	4.6	7.2	7.2	7.2

The equilibrium pH after extraction was determined, and the aqueous phase analyzed for remaining metal level. Results for several metals are shown in Figure 1.

Figure 1



Values for the $pH_{1/2}$ of each metal, i.e., the pH at which half of the metal is extracted, are given in Table 1 for both LIX® 7820 and for LIX® 79, a tri-alkylguanidine solvent extraction reagent.

Table 1. Values of $pH_{1/2}$ for LIX® 7820 and LIX®79

Metal	Au	Ag	Cu	Co	Hg	Zn
XI-78	12.6	10.8	10.7	12.8	12.9	12.3
LIX®79	12.0	10.7	10.4	11.8	**	11.5

The extraction behavior of these two reagents differs in two ways:

(1) LIX®7820 is a somewhat stronger extractant than LIX®79, requiring somewhat higher hydroxide concentrations for effective stripping.

(2) In most cases, the LIX®79 isotherms tend to be more "S" shaped, while the LIX® 7820 curves are more gradually sloped.

Figure 2a

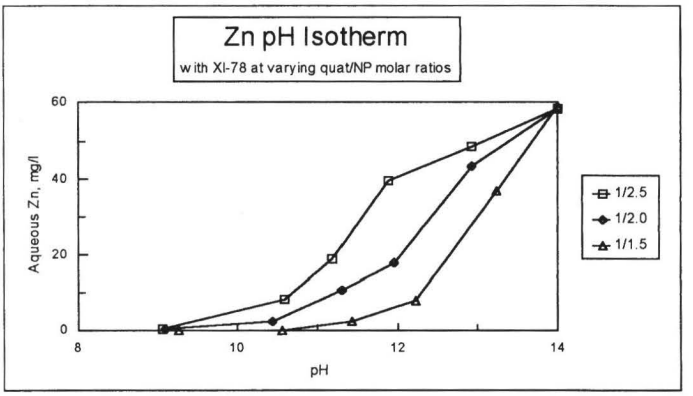
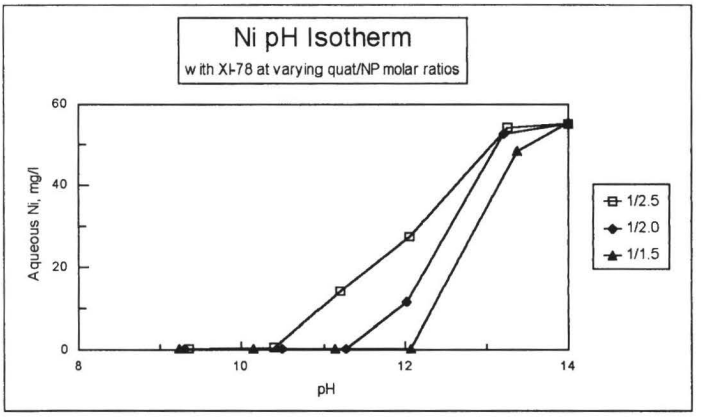


Figure 2b



Interestingly, the value of the $pH_{1/2}$ for a given anion is dependent on the ratio of quaternary ammonium compound to alkylphenol. Figures 2a and 2b show the effect of varying the ratio from 1/1.5 to 1/2.5 on the pH isotherms of zinc and nickel.

The pH isotherms of gold, silver and copper were determined at quaternary ammonium to alkylphenol ratios of 1/1.25 and 1/2.0; values are in Table 2.

Table 2. $pH_{1/2}$ Values for Gold, Silver and Copper

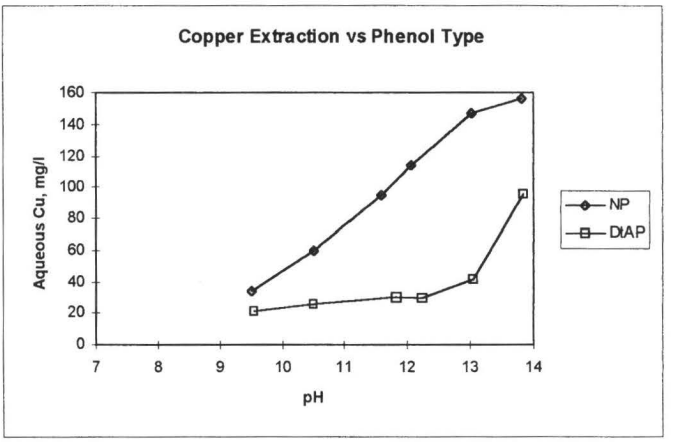
Quat/Phenol Ratio	1/1.25	1/2.0
Gold	13.5	12.1
Silver	12.3	11.5

Copper	11.5	11.1

This sensitivity of $pH_{1/2}$ to nonylphenol concentration suggests that there is a strong role for solvation of the quat-phenoxide ion pair, with phenolic concentrations above stoichiometric serving to stabilize the ionized phenoxide. Thus the extraction and stripping behavior can be fine-tuned by varying the ratio of nonylphenol to quaternary cation. Interestingly, the addition of tridecanol has virtually no effect on the $pH_{1/2}$. Apparently the solvating species must be acidic enough to share a proton with the phenoxide anion; simple hydrogen bonding is not sufficient. Consistent with this point is the observation that when phenols are solvent-extracted by a quaternary ammonium extractant, the ratio of phenol to quat rises to 3 to 1.

The alkylphenol component must not be so hindered that it cannot participate via solvation. Figure 3 shows the pH isotherms of organic phases containing 0.05M Aliquat 336 and 0.10M of either nonylphenol or 2,4-di-tert-amylphenol. The aqueous phase contained 0.0025M CuCN plus 0,006M additional CN^-.

Figure 3

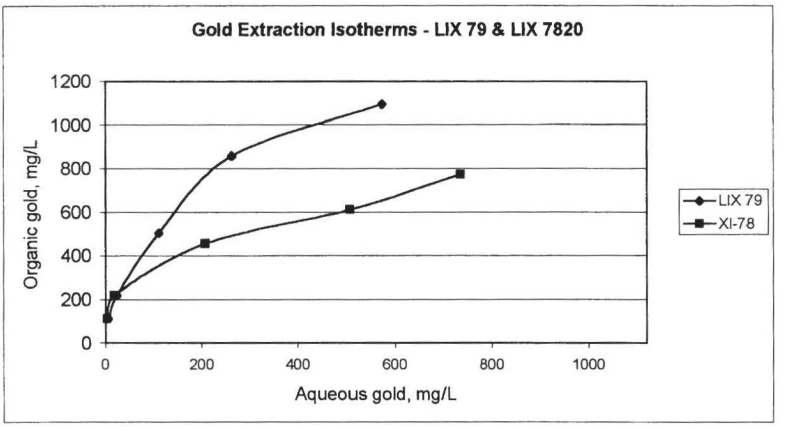


In this case, the hindered phenol is unable to approach a phenoxide ion close enough to provide solvation, so that deprotonation (and consequent anion displacement) does not begin to take place until very high pH values.

To predict extraction behavior in a continuous system, McCabe-Thiele isotherms were generated with gold for LIX® 79 and LIX® 7820. The starting aqueous feed solution contained 1120 mg/L of gold as aurocyanide at pH 9.8; the organic phases contained 0.005M Aliquat 336 and 0.010M nonylphenol, and LIX® 79 at 0.005M guanidine. Solutions were contacted at varying phase ratios, and the aqueous phases analyzed. The equilibrium pH values varied from 10.3 to 11.4. The isotherms are shown in Figure 4.

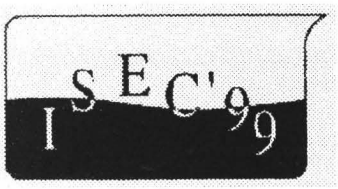
This implies that a LIX® 7820 operating circuit would have to run with a higher concentration of active reagent than a LIX® 79 circuit to obtain similar extraction results. A separate study of the extraction of copper from a gold cyanide leach raffinate indicates that a system for recovery of copper and its associated cyanide is feasible.[4]

Figure 4



REFERENCES

1. Hidden Wealth, Johannesburg, *S. African Inst. Min. & Metallurgy*, 151-6, (1996).
2. III Int'l Gold Symposium, Lima, Peru, in press, (1998).
3. *Proceedings of ISEC '96,* Univ. of Melbourne, **1**, 311, (1996).
4. Paper at *ALTA Copper Hydrometallurgical Forum*, Brisbane, Australia, Oct., 1998.



ADVANCES IN GOLD(III)-CHLORIDE SOLVENT EXTRACTION USING NEUTRAL ORGANO-PHOSPHOROUS DERIVATIVES. ESTIMATION OF $AuCl_4^-$–H^+ INTERACTION COEFFICIENTS

AM Sastre[1] and FJ Alguacil[2]

[1] Department of Chemical Engineering. Universitat Politècnica de Catalunya. ETSEIB, Diagonal 647. E-08028 Barcelona. Spain.

[2] Centro Nacional de Investigaciones Metalúrgicas (CSIC). Avda. Gregorio del Amo 8. Ciudad Universitaria. 28040 Madrid. Spain.

ABSTRACT

The extraction of gold(III) from hydrochloric acid media by a series of novel extractants dissolved in various diluents had been studied. The reagents are neutral organophosphorous extractants such as phosphine oxides (Cyanex 921, Cyanex 923 and Cyanex 925) and phospholene derivatives (DMPL, EHMPL and NMPL), whereas the diluents have different nature. The distribution of gold has been studied under different variables: equilibration time, temperature, ionic strength, metal and extractant concentrations, etc. The experimental data were treated numerically in order to define the extracted species for each system. The experimental and numerical data were also used to estimate the interaction coefficient in the aqueous solution between $AuCl_4^-$ and H^+ using the Specific Interaction Theory. Furthermore, experimental data on the extraction of HCl by these phosphorous derivatives were also presented.

Keywords: gold, chloride, Cyanex 921, Cyanex 923, Cyanex 925, phospholene derivatives.

INTRODUCTION

The traditional route for the extraction and separation of precious metals consists of a series of selective dissolution-conditioning and precipitation steps that are generally inefficient in terms of the degree of separation that can be achieved.[1] Solvent extraction is an alternative procedure for separation and purification of these metals and particularly gold(III). Since $AuCl_4^-$ is normally found in these aqueous solutions, either basic or neutral extractants seem to be suitable for its extraction.[2-4]

In the present study the application possibilities have been evaluated and compared for various solvation extractants such as phosphine oxides and phospholene derivatives in the extraction of gold(III) from tetrachloroaurate solutions; the extraction mechanism are also defined in order to increase the knowledge of these lesser known extraction systems. Results on HCl extraction were also presented.

EXPERIMENTAL

The extractants used were obtained from CYTEC Inc. (phosphine oxides) and Bayer Leverkusen (phospholene derivatives) and were used as obtained from the manufacturers The general characteristics of the reagents are summarized in Table 1.

Recently, it was stated[5] that the compositions of Cyanex 923 and Cyanex 925 are more complex than that reported in previous literature.[6] All other chemicals were of AR grade.

Extractions were accomplished by mechanical shaking of equal volumes of organic and aqueous solutions in separatory funnels thermostatted at the required temperature. Gold was determined by AAS, whereas hydrochloric acid concentration was determined by titration with standard sodium hydroxide solutions using Bromothymol Blue as indicator. Respective concentrations in the equilibrated organic (Au) and aqueous (HCl) phases was calculated by mass balance.

© 2000 Society of Chemical Industry

Table 1 General characteristics data for phosphines oxides and phospholene derivatives

Name	Type	Composition
Cyanex 921	phosphine oxide	tri-n-octyl phosphine oxide
Cyanex 923	phosphine oxide	mixture of phosphine oxides
Cyanex 925	phosphine oxide	mixture of phosphine oxides
DMPL	phospholene derivative	1-(dodecyloxy)-3-methyl-1-oxo-Δ^3-phospholen
EHMPL	phospholene derivative	1-(2-ethylhexyloxy)-3-methyl-1-oxo-Δ^3-phospholen
NMPL	phospholene derivative	1-(2,6-dimethylhept-4-yloxy)-3-methyl-1-oxo-Δ^3-phospholen

RESULTS AND DISCUSSION

Hydrochloric acid extraction

Neutral reagents extract HCl from aqueous solutions, the extraction can be represented by the general reaction:

$$HCl_{(aq)} + L_{(org)} \longrightarrow HClL_{(org)}$$

where L stands for the corresponding reagent. From the experimental data, the extraction constants (log ß) for the extraction of HCl using these solvation extractants were calculated using the program LETAGROP-DISTR (7), some of the results are summarized in Table 2

Table 2 Log ß values for the extraction of HCl

Reagent	$[HCl]_{init}$, mol/L	Diluent	log ß
Cyanex 925	1.0	xylene	-0.99
Cyanex 923	1.0	n-decane	-0.93
Cyanex 921	1.0	xylene	-0.89
DMPL	1.0	kerosene	-0.84
DMPL	1.0	cumene	-0.59
NMPL	1.0	cumene	-0.54

In the range of extractants concentrations from 0.01 to 0.8 mol/L the apparent extraction order for HCl is: Cyanex 921 > NMPL > EHMPL = DMPL > Cyanex 923 = Cyanex 925.

Gold extraction

To study the influence of equilibration time on gold extraction, experiments were carried out using different extractant (0.91 mM Cyanex 925 in xylene or 0.1 mol/L DMPL in cumene) and gold concentrations

(0.05 mM Au in 1 mol/L HCl media (Cyanex 925) or 0.14 mM Au in 1 mol/L HCl media (DMPL)); the agitation time was varied from 1 to 60 min. The results obtained show that, under the experimental conditions used, the extraction is slightly dependent upon the agitation time and extraction equilibrium is nearly achieved within 5 min (phospholene derivatives) or 1 min of contact (phosphine oxides).

The influence of temperature was also studied using organic phases of the phosphine oxides and gold solutions in 6 mol/L HCl media. The increase of temperature decreases gold extraction. Table 3 shows the values of the change of enthalpy for these systems. The reactions are exothermic.

Table 3 Values of ΔH° for the extraction of gold by phosphine oxides

Reagent	Diluent	Initial gold, mM	ΔH°, kJ/mol
Cyanex 921	xylene	0.25	-44.6
Cyanex 923	n-decane	0.25	-43.7
Cyanex 925	xylene	0.05	-45.9

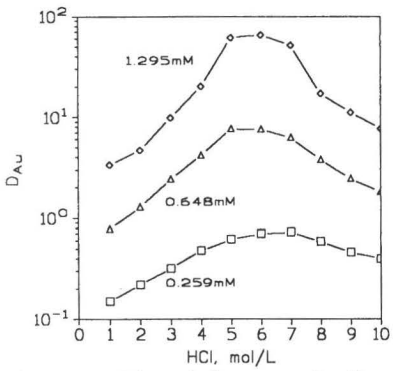


Figure 1.-The influence of Cyanex 921 concentration on gold extraction.

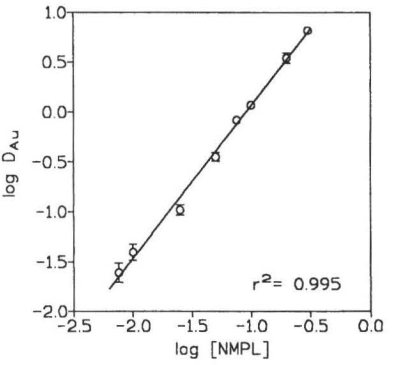


Figure 2.-The influence of metal concentration on gold extraction.

The effect of changing the extractant concentration on gold extraction was studied using aqueous solutions which contained 0.25 mM gold at various HCl concentrations and organic solutions of different Cyanex 921 concentrations in xylene. The results of these experiments (figure1) shows that at all acidic concentrations there is an increase in gold extraction as the initial extractant concentration is increased, maximum metal extraction is achieved in the range 5-7 mol/L HCl.

The effect of changing the initial metal concentration (0.06 to 0.24mM) on gold extraction was studied using organic phases of NMPL in cumene. Averaging results, obtained on three gold concentrations at 1.0 mol/L HCl, are shown in figure 2. The independence of log D_{Au} with metal concentration suggest that metal polynuclear species were not formed in the extraction reaction.

The extraction of gold from acidic tetrachloroaurate solutions by solvation extractants can be represented by the general equation:

$$pL_{(org)} + AuCl_4^- + H^+_{(aq)} \longrightarrow HAuCl_4L_{p(org)}$$

Experimental results were treated numerically, using the same program as mentioned above, in order to define the stoichiometry of the extracted species and their equilibrium constants. Table 4 summarizes the results obtained.

Table 4 Species for gold extraction by solvation extractants

Extractant	HCl, mol/L	p	log K_{ext}
Cyanex 921[1]	1.0	2	6.78
Cyanex 923	1.0	2	6.71
Cyanex 925	1.0	2	7.87
DMPL	1.0	1 2	1.11 MAX 1.32 3.06
EHMPL	1.0	1 2	1.28 2.74
NMPL	1.0	1 2	0.68 2.19

[1] Species with p=1 only is formed from HCl concentrations of 3 mol/L

Results obtained shows that the composition of extracted species are independent of I (HCl concentration), however, the value of the extraction constant depends on ionic strength. The variation in the extraction

$$\log \gamma_i = - z_i^2 D(I) + \Sigma \varepsilon_{(i,k)} m_k$$

constant with I can be correlated using the SIT.[8] In this approach the activity coefficient of an anion of charge z in a solution of strength I can be expressed as:
where D(I) is the Debye-Hückel term in the molality scale and ε is the interaction coefficient. It can be correlated the experimental results with the above expression, and the values of $\varepsilon_{(AuCl4-,H+)}$ can be estimated, results were summarized in Table 5.

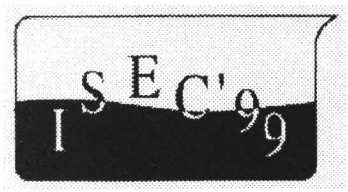
Table 5 Values of estimated interaction coefficients for ($AuCl_4^-$,H^+)

Extractant	Species	Interaction coefficient
Cyanex 921	$HAuCl_4L$ $HAuCl_4L_2$	0.23 0.25
Cyanex 923	$HAuCl_4L_2$	0.23
Cyanex 925	$HAuCl_4L_2$	0.28
DMPL	$HAuCl_4L$ $HAuCl_4L_2$	0.26 0.28
EHMPL	$HAuCl_4L$ $HAuCl_4L_2$	0.28 0.28
NMPL	$HAuCl_4L$ $HAuCl_4L_2$	0.28 0.28

From experimental data the extractability order for gold from HCl media can be deduced using these solvation extractants at reagent concentrations higher than 0.01 mol/L is: Cyanex 925 > Cyanex 923 > Cyanex 921 >> EHMPL = DMPL > NMPL.

REFERENCES

1. Cox M, *Principles and Practices of Solvent Extraction,* Rydberg J, Musikas C and Choppin GR (eds.), Marcel Dekker, New York (1992).
2. Villaecusa I, Miralles N, de Pablo J, Salvado V and Sastre AM, *Solv. Extr. and Ion Exch.*, **11**, 613 (1993).
3. Alguacil FJ and Caravaca C, *Hydrometallurgy*, **34**, 91, (1993).
4. Chowdhury DA and Kamata S, *Solv. Extr. and Ion Exch.*, **15**, 231, (1997).
5. Dziwinski E and Szymanowski J, *Solv. Extr. and Ion Exch.*, **16**, 1515, (1998).
6. American Cyanamid (now CYTEC Inc.), Cyanex Extractants Technical Data Sheet, Wayne (1991).
7. Liem DH, *Acta Chem. Scand.*, **25**, 1521, (1971).
8. Aguilar M, de Pablo J, Valiente M and Högfeldt E, *Chem. Scripta*, **26**, 635, (1986).



SOLVENT EXTRACTION OF GALLIUM(III) WITH NONIONIC SURFACTANTS FROM HYDROCHLORIC ACID MEDIA

Norihiro Kobayashi, Nobuhisa Hyodo, Susumu Nii, Katsuroku Takahashi, Hiroshi Takeuchi and Shigendo Akita[1]
Dept. of Chem. Eng., Nagoya University, Chikusa-ku, Nagoya 464-8603, Japan
[1]Nagoya Municipal Industrial Research Institute, Rokuban, Atsuta-ku, Nagoya 456-0058, Japan

ABSTRACT
The solvent extraction of Ga(III) from hydrochloric acid solutions using a nonionic surfactant having an average chain length of 10 ethylene oxide units (polyoxyethylene nonyl phenyl ether, PONPE10) as an extractant is described. Gallium(III) is successfully extracted into a chloroform solution of the surfactant; the extraction improves with an increase in HCl concentration and nearly complete extraction can be achieved from > 6M HCl solutions. The extraction efficiency increases with an increase in the ethylene oxide number of the surfactant, and varies with diluent in the order: chloroform < dichloromethane < dichloroethane. It has been found that the extraction takes place through the coordination of one surfactant molecule to one hydrogen tetrachlorogallate with all combinations of surfactant and diluent. The selective separation of Ga(III) from some heavy metals has been demonstrated, as has back extraction from the metal-loaded solvents with a dilute HCl solution.

Keywords: nonionic surfactant, polyoxyethylene nonyl phenyl ether, gallium(III), hydrochloric acid, mechanism of extraction

INTRODUCTION

A long-range strategy for securing a stable supply of gallium is a matter of great importance because of the increasing demand for the metal, especially in the field of electronics. Profitable gallium ores are very rare, and much attention has been paid to the recovery of gallium from secondary sources such as waste residues from the hydrometallurgical processing of aluminum or zinc. Solvent extraction is one of the most promising methods for recovering gallium from dilute streams, and has been investigated with various kinds of extractants, including high molecular weight amines,[1,2] organophosphorus compounds,[1,3] β-diketones[4] and ketones[5] for extraction from acid solutions, and hydroxyquinolines[6,7] for extraction from alkaline solutions.

Polyethylene glycol-type nonionic surfactants have a number of electron-donating oxygen atom in their ethylene oxide chains, and are thus expected to form complexes with various solutes including metal ions,[8] in the same manner as solvating extractants (e.g. methyl isobutyl ketone (MIBK) or macrocyclic polyethers, viz. crown ethers). Several studies have been described on the solvent extraction of alkaline earth metals[9-11] and heavy metals[12-13] using nonionic surfactants as the extractant. In a previous paper,[14] we demonstrated the solvent extraction of Au(III) from hydrochloric acid media using nonionic surfactants in chlorinated organic solvents. In the present study, the solvent extraction of gallium from hydrochloric acid solutions is investigated using the same nonionic surfactants in three chlorinated organic solvents, and the extraction mechanism is proposed.

EXPERIMENTAL

Nonionic surfactants, polyoxyethylene nonyl phenyl ethers (PONPE or P) with an average ethylene oxide (EO) unit of 7.5, 10 and 20, were obtained from Tokyo Kasei Kogyo Co., and used without further purification. The general formula of PONPEn is $HO(CH_2CH_2O)C_9H_{19}$, where n is the EO number. As a diluent for the surfactants, three chlorinated organic solvents, chloroform ($CHCl_3$), dichloromethane (CH_2Cl_2) and 1,2-dichloroethane ($ClCH_2CH_2Cl$) were selected. Aqueous stock

© 2000 Society of Chemical Industry

solutions of metal were prepared by dissolving an appropriate amount of each metal chloride in a hydrochloric acid solution. All chemicals used were of reagent grade.

In the equilibrium extraction study, equal volumes (10 cm^3) of aqueous and organic phases placed in a 50 cm^3 glass stoppered flask were shaken for 1 hr using a mechanical shaker. The initial concentrations of the surfactant and metal were set to be 0.05 M and 100 ppm, unless otherwise indicated. After equilibration, the metal concentration in the aqueous phase was assayed by inductively coupled plasma spectroscopy (ICP), and that in the organic phase was calculated from the mass balance. The amount of the dissolved surfactant in the aqueous phase from the organic phase were determined by UV spectrophotometry at 277 nm, while the water content of the organic phase was determined using Karl Fischer Reagent SS (Mitsubishi Chemicals Co.)

RESULTS AND DISCUSSION

Figure 1 shows typical results for the solvent extraction of Ga(III) with several combinations of surfactant and diluent, plotted as the percent extraction against the equilibrium HCl concentration. The percent extraction, E, is defined as:

$$E = 100\,(1 - [M] / [M]_0) \qquad (1)$$

where [M] and $[M]_0$ denote the equilibrium and initial concentrations of metal in the aqueous phase, respectively. It should be noted that all of the surfactants used in this study dissolved readily in the three chlorinated solvents, and phase separation from aqueous HCl solutions could be obtained with little foaming and emulsification. The extraction improves with increasing HCl concentration, and complete extraction can be achieved at high acidities for all systems. Low values of the percent extraction at low acidities indicate that back extraction of Ga(III) using dilute HCl solutions will be highly efficient.

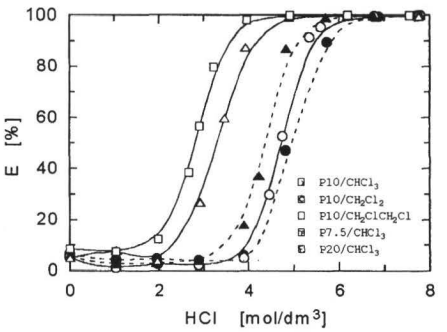


Figure 1 Effect of HCl concentration on percent extraction of Ga(III) with a variety of surfactant and diluent.

Figure 2 shows the effect of the initial PONPE concentration on the percent extraction of Ga(III). No increase in the solution viscosity was observed within the concentration range studied. As would be expected, the percent extraction increases as the surfactant concentration increases. The percent extraction also increases with an increase in the EO number of PONPE, i.e. the extractability of surfactant was found to be PONPE7.5 < PONPE10 < PONPE20. This implies that the interaction between the metal and electron-donating oxygen in the surfactant EO chains plays an important role in the extraction.

As the diluent for PONPEs, both dichloromethane and 1,2-dichloroethane not only yield much higher Ga(III) extraction, but also allow the extraction from lower acid concentrations than chloroform does. Thus, the extraction improves with increasing the dielectric constant of the diluents. The same sequence of extractability, $CHCl_3 < CH_2Cl_2 < CH_2ClCH_2Cl$, was observed previously in the extraction of Au(III) using the same nonionic surfactant.[14] Unfortunately, the use of other solvents

such as carbon tetrachloride and kerosene, however, resulted in incomplete phase separation.

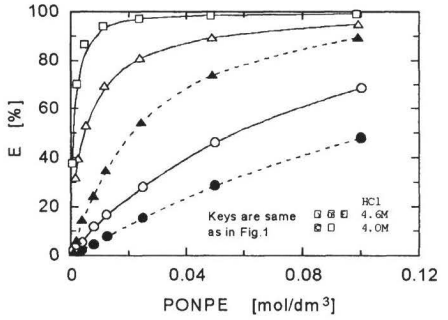


Figure 2 Effect of PONPE concentration on percent extraction of Ga(III) with a variety of surfactant and diluent.

Figure 3 shows the effect of hydrogen ion concentration on the distribution ratio of Ga(III), defined as:

$$D = [M]org / [M] \quad (2)$$

where the subscript "org" denotes the organic phase. The extraction was carried out from mixed solutions of hydrochloric acid and sodium chloride at a constant chloride ion concentration of 4.5 M. Straight lines of slope 1 are obtained for all combinations of surfactant and diluent. Given the existence of $GaCl_4^-$ in solutions at high chloride concentration,[15] the extraction probably takes place through the coordination of the neutral solvating extractant, PONPE, to hydrogen tetrachlorogallate, $HGaCl_4$, like that in the solvent extraction of Ga(III) with MIBK.[5]

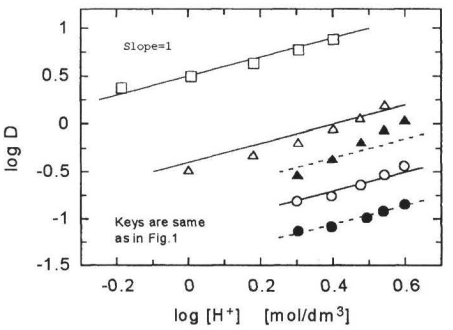


Figure 3 Relationship between hydrogen ion concentration and distribution ratio of Ga(III).

Figure 4 shows the relationship between the surfactant concentration in the organic phase and the distribution ratio of Ga(III) at a constant HCl concentration. The experimental data give straight lines with a slope of 1, indicating that the complex formation between one molecule of Ga(III) and one PONPE occurs in the organic phase. From the above results, we can derive the following stoichiometry for the extraction of Ga(III) from HCl solutions with PONPEs in the three chlorinated organic solvents, in the same manner as for Au(III) extraction.[14]

$$GaCl_4^- + H^+ + PONPE_{org} = HGaCl_4PONPE_{org} \quad (3)$$

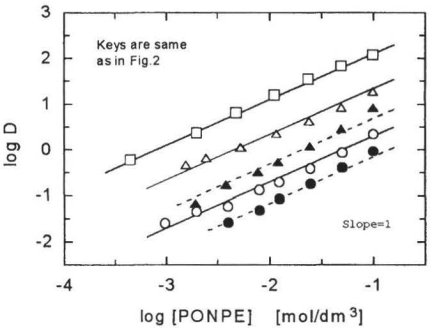


Figure 4 Relationship between PONPE concentration and distribution ratio of Ga(III).

An experiment on the extraction of heavy metals from HCl media with 0.05M PONPE10 in chloroform was conducted for an aqueous solution containing Cu(II), Zn(II), Co(II), Ni(II), Al(III) and Fe(III), as well as Ga(III). In Fig. 5 is plotted the percent extraction of each metal as a function of HCl concentration. The extraction of divalent metals is less than 10 % over the whole HCl concentration range studied. Thus, a selective extraction of Ga(III) can be achieved at > 4 M HCl. It should be noted that small amounts of the contaminating metals entrained in the organic phase might be removed by scrubbing with concentrated HCl solutions. Unfortunately, the extraction curve of Fe(III) is close to that of Ga(III), resulting in a lower separation factor between them.

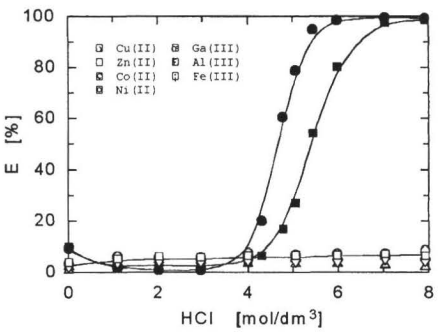


Figure 5 Metal separation via solvent extraction using PONPE10 in $CHCl_3$.

Table 1 summarizes results for the back extraction of Ga(III) using 0.1 M HCl solution as the stripping agent. The metal-loaded organic solvents were prepared by the forward extraction from 6 M HCl solutions with 0.05 M PONPE in the respective diluents, and the mixing time for the back extraction was set to be 40 min. High efficiency can be obtained both in the forward and back extractions under the experimental conditions selected, and the total recovery of Ga(III) reaches 97 % or more for all runs.

Following Ga(III) extraction from 6.3 M HCl with 0.05 M PONPE in the various diluents, the amount of dissolved surfactant in the aqueous phase and the water content of the organic phase were determined. The results are given in Table 2. With increasing EO number of PONPE, the residual surfactant concentration in the aqueous phase increases due to a rise in the surfactant hydrophilicity. However, even for PONPE20, the concentration is only 0.047 mM, and the loss of the surfactant might be negligible in the solvent extraction. A slight increase in the water content of the organic

phase is observed by using the surfactant with higher EO number or the diluent showing higher extractability for Ga(III), i.e. having a higher dielectric constant.

Table 1 Back extraction of Ga(III) from metal-loaded solvents with 0.1 M HCl

Surfactant	Solvent	% extraction	% stripping	% recovery
PONPE7.5	$CHCl_3$	97	100	97
PONPE10	$CHCl_3$	99	100	99
PONPE20	$CHCl_3$	100	100	100
PONPE7.5	CH_2Cl_2	98	99	98
PONPE7.5	CH_2ClCH_2Cl	98	99	97

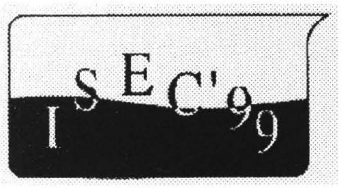
Table 2 Surfactant concentration in aqueous phase and water content of organic phase

Surfactant	Solvent	[PONPE]	$[H_2O]_{org}$
PONPE7.5	$CHCl_3$	$3.2x10^{-5}$ M	0.14 %
PONPE10	$CHCl_3$	$4.1x10^{-5}$ M	0.15 %
PONPE20	$CHCl_3$	$4.7x10^{-5}$ M	0.19%
PONPE10	CH_2Cl_2	$4.8x10^{-5}$ M	0.22 %
PONPE10	CH_2ClCH_2Cl	$4.1x10^{-4}$ M	0.25 %

In conclusion, all of the nonionic surfactants tested show a strong affinity for Ga(III), and in combination with the chlorinated organic solvents, provide an effective method for recovering the metal from hydrochloric acid streams. The expected advantages of using the nonionic surfactants over conventional extractants are non-toxicity, relative ease of chemical modification, and commercial availability of surfactant types with various EO numbers, which affect the extraction efficiency as well as the surfactant solubility in water.

REFERENCES

1. Sato T, Nakamura T and Ishikawa S, *Solv.Extr. Ion Exch.*, **2**, 201, (1984).
2. Abisheva ZS, Blaida IA, Ponomareva EI and Rozen AM, *Hydrometallurgy*, **37**, 393, (1995).
3. Jorger R and Kolarik Z, *Solv. Extr. Ion Exch.*, **11**, 33, (1993).
4. Gutierrez B, Pazos C and Coca J, *Solv. Extr. Ion Exch.*, **11**, 769, (1993).
5. Rafaleoff R, *Anal. Chem.*, **43**, 272, (1971).
6. Sato T and Oishi H, *Hydrometallurgy*, **16**, 315, (1986).
7. Cluzeau YP, Desbarres J and Bauer D, *Solv. Extr. Ion Exch.*, **4**, 301, (1986).
8. Yanagida S and Okahara M, *Hyomen*, **17**, 77, (1979).
9. Yanagida S, Takahashi K and Okahara M, *Bull. Chem. Soc. Jpn.*, **50**, 1386, (1977).
10. Sasaki Y, Nakamura H, Takagi M and Ueno K, *Bull. Chem. Soc. Jpn.*, **59**, 381, (1986).
11. Sasaki Y, Shimura M, Otsuka H and Takagi M, *Bull. Chem. Soc. Jpn.*, **60**, 545, (1987).
12. Sotobayashi T, Suzuki T and Yamada K, *Chem. Lett.*, 77, (1976).
13. Sotobayashi T, Suzuki T and Tonouchi S, *Chem. Lett.*, 585, (1976).
14. Akita S, Yang L and Takeuchi H, *Hydrometallurgy*, **43**, 37, (1996).
15. Baba Y, Nakamura H and Inoue I, *J. Chem. Eng. Jpn.*, **19**, 497, (1986).



SOLVENT EXTRACTION OF GOLD FROM HYDROCHLORIC ACID SOLUTIONS USING BIS(DIALKYLPHOSPHONATE)S

Satsuo Kamata[1], Seitaro Fukunaga[1] and Didarul A Chowdhury[2]
[1]Department of Applied Chemistry and Chemical Engineering, Faculty of Engineering, Kagoshima University, Japan
[2] Bangladesh Atomic Energy Commission, Dhaka, Bangladesh

ABSTRACT
The extraction of gold(III) from hydrochloric acid medium is studied by using newly synthesized extractants, the α,ω-alkane-diyl-bis(dialkylphosphonate)s (ABDAP),commonly known as the bis(dialkylphosphonate)s. Gold is most favorably extracted with these reagents at HCl concentrations above 5M and the extraction is not interfered by palladium(II), silver(I), copper(II) and lead(II) ions, when methylene bis(diiso-propylphosphonate) (MBDIPP) dissolved in 1,2-dichloroethane (DCE) is used as the extractant. In 5M HCl, the extraction of Au(III) by MBDIPP reaches equilibrium in 1 min. through formation of a 1:1 solvating complex, MBDIPP:$HAuCl_4$. For ABDAPs, the extractability is affected by the alkoxy substituent attached to the phosphorus atoms while the selectivity of gold(III) extraction is governed by the length of the hydrocarbon chain separating the two P=O sites in the diphosphonate molecule. Various extraction parameters are evaluated in relation to the recovery of the metal from acidic waste solutions and the data are compared with those of tri-n-butyl phosphate (TBP) and tri-n-octylphosphine oxide (TOPO).

Key-words: gold(III), hydrochloric acid media, bis(dialkylphosphonate) derivatives

INTRODUCTION

Solvent extraction of gold(III) from halide solutions is gaining increasing interest in relation to the recovery of gold from electronic scrap and other waste solutions of non-cyanide origin. Long-chain amines (basic ion-exchanger type)[1,2,3] and neutral organophosphorus esters (solvating type) [4,5,6] have so far been the most widely studied extractants for recovery of gold(III) from hydrochloric acid solutions. These mono-functional reagents are known to provide good extraction efficiency and kinetics for Au(III) but their selectivity data with respect to some important interfering species viz. Cu(II), Pd(II) are often missing in the literature. In the present work, the solvent extraction recovery of gold(III) from hydrochloric acid medium is studied by using a different class of reagents, namely, the bis(dialkylphosphonate)s. These compounds containing two P=O donor sites separated by a flexible alkylene chain are expected to offer better Au(III) extraction properties compared to those of mono-functional reagents. The results of the Au(III) extraction involving the new reagents are analyzed in terms of the equilibrium, kinetics and stoichiometry of the process. The effect of structural variants in the ligand molecule, the effect of aqueous phase composition, selectivity of Au(III) extraction etc. are also evaluated and are compared with those of TPB and TOPO

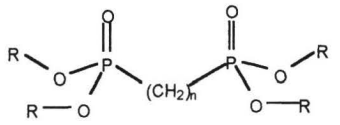
EXPERIMENTAL

Reagents

The bis(dialkylphosphonate)s: ethylene bis(diethylphosphonate)(EBDEP), methylene bis(di-iso-propylphosphonate)(MBDIPP), ethylene bis(di-iso-propylphosphonate) (EBDIPP), methylene bis(dibutylphosphonate) (MBDBP) were synthesized by a known method[7] as exemplified here by the preparation of MBDIPP. Di-iso-propylphosphite (0.15 mol) was allowed to react with metallic sodium (0.15 mol) kept under refluxing heptane (100 ml), the former being added in small aliquots over a period of 2 hours. After complete dissolution of sodium and attainment of clear solution of the mixture, a benzene solution (100 ml) of dibromomethane (0.075 mol) was added drop-wise under vigorous stirring condition. The reaction mixture was cooled and the white mass of NaBr was removed by filtration. The

© 2000 Society of Chemical Industry

solvent was evaporated and the product was purified by flush chromatography. The synthetic reagents used in this study are shown in Figure 1.



R	n	Ligand
CH_3CH_2-	2	EBDEP
$(CH_3)_2CH$-	1	MBDIPP
$(CH_3)_2CH$-	2	EBDIPP
$CH_3(CH_2)_2$-	1	MBDBP

Figure 1: Structure and composition of the synthetic bis(dialkylphosphonate)s

Reagent grade tri-n-butylphosphate and tri-n-octylphosphine oxide were obtained from Wako Pure Chemicals, Japan and were used without further purification.

Stock solutions (0.1 M) of Au(III) and other metal ions were prepared by dissolving their chloride salts in 1M HCl.

Solvent Extraction Studies

These were carried out in batch operations using 10 ml of the organic phase containing an extractant dissolved in the appropriate diluent was shaken with an equal volume of the metal ion solution in stoppered glass tubes (50 ml) with the help of a mechanical shaker. After a predetermined time, the two phases were allowed to settle and the concentration of the metal ion in the aqueous phase was measured by atomic absorption spectrometry. The per cent extraction (E) and the distribution ratio (D) of the concerned metal ion were calculated by equating mass balance between the two phases.

RESULTS AND DISCUSSION

The extraction of Au(III) with the presented reagents was studied under varying concentration of HCl (1-6 M) in the aqueous phase and in presence of potential interfering ions like Cu(II), Ag(I) and Pd(II), while keeping other conditions similar. Figure 2 shows the extraction isotherms obtained with MBDIPP and TOPO. With each of the reagents except TOPO, the extraction of Au(III) increased with increasing HCl concentration and reached a maximum and almost constant value around 5M HCl. For TOPO, the extraction was similar throughout the range of acidity. The optimum Au(III) extractability of the reagents was in the order: TOPO(93) > MBDIPP(92) > MBDBP(89) > EBDIPP(80) >EBDEP(77)>TBP(40), the number in the parentheses representing the percent extraction values for gold.

This order of extractability is more or less in accordance with the extent of basicity available at the active P=O site(s) in the respective extractants. It can be noticed that MBDIPP has higher extractability than EBDIPP, even though the later contains one more -CH_2- unit in the molecule. This means that the >P(O)-CH_2-(O)P< ligand cavity is more effective than the >P(O)-CH_2CH_2-(O)P< cavity to accommodate the Au(III) species. It was seen that TOPO provides somewhat better Au(III) extraction efficiency than MBDIPP. But with the former reagents TOPO, co-extraction of Ag(I) and Pd(II) is unavoidable at all acid concentrations. This may appear as a big disadvantage when the recovery of gold from industrial wastes and precious metal concentrates is considered.[8] The extraction of gold with MBDIPP is completely free of interference from Ag(I), Cu(II), and Pd(II) at HCl concentrations above 5 M. Comparison of the extraction behavior of MBDIPP and MBDBP reveals that strength and selectivity of gold extraction with neutral bi-functional phosponates improve with

branching in the attached alkoxy chain. In consideration of the experimental results, MBDIPP appears to be the most suitable reagent for extraction of gold from hydrochloric acid solutions.

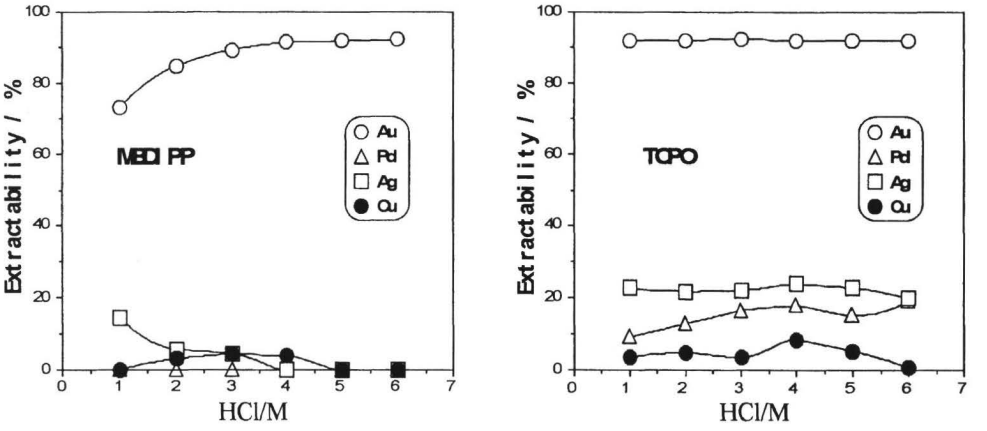


Figure 2. Solvent Extraction of Au(III) with MBDIPP and TOPO in presence of other metal cations at 25±1°C. Extraction conditions were: [Ligand] = 5.0×10^{-3} M in DCE, $[M^{n+}] = 1.0 \times 10^{-4}$ M, Shaking Time = 3 h.

The kinetics of any solvent extraction process is important for its commercial application. The equilibration time for the extraction of Au(III) using MBDIPP was measured in 1,2-dichloroethane and nitrobenzene and the results are produced in Figure 3. In both the diluents, the extraction of gold reaches equilibrium in less than 1 minute providing nearly 90% gold transferred to the organic phase.
Such a reaction may be suitable for adoption in a counter-current continuous process of gold recovery.

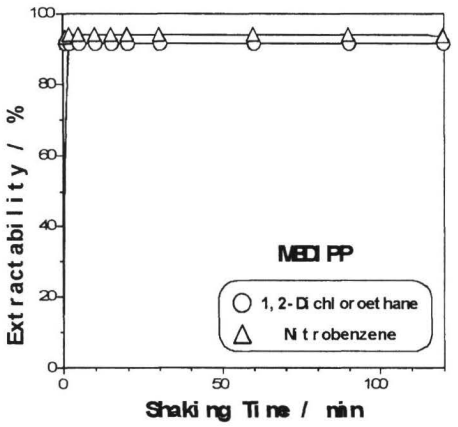


Figure 3: Effect of shaking time on the extraction of gold using MBDIPP at 25±1°C. [MBDIPP]=5.0×10^{-3} M, [Au(III)]=1.0×10^{-4} M, [HCl] = 5 M.

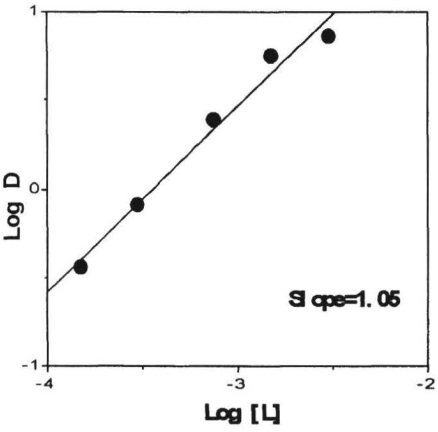


Figure 4: Log D vs. log [L] plots obtained in the extraction of Au(III) with MBDIPP at 25±1°C. [Au(III)]=1.0×10^{-4}M. [HCl]=5 M.

The composition of the Au(III)-MBDIPP complex, was determined by the Slope Ratio method as shown in Figure 4. The log D vs. log [L] plot for the extraction of Au(III) yields a slope nearly equal to unity, indicating the formation of a 1:1 Au(III)-MBDIPP complex during the transfer of the metal to the organic phase. At higher HCl concentrations (~5M) gold exists almost exclusively as the tetrachlorocomplex, $AuCl_4^-$.[9] By analogy with other phosphoryl reagents, the extraction of gold in the present case may be defined as the solvation of the $HAuCl_4$ species by the P=O groups in the MBDIPP molecule.[4] Figure 5 shows the influence of diluent on the extraction of $AuCl_4^-$.

The extraction order is: nitrobenzene > 1,2-dichloroethane > chlorobenzene. There was no extraction in carbon tetrachloride and chloroform. It is therefore understood that diluents with high dielectric constants are needed to solubilize the MBDIPP-$HAuCl_4$ complex.

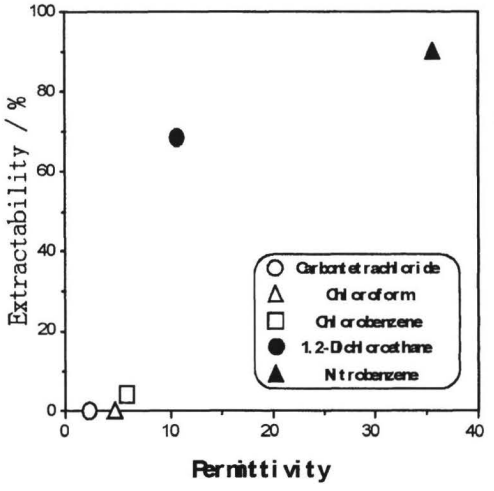


Figure 5: Effect of diluent on the extraction of Au(III) at 25±1°C. [MBDIPP] = 5.0 × 10^{-3} M in DCE, [Au(III)] =1.0 × 10^{-4} M, [HCl] = 0.5 M, Shaking Time = 1 h.

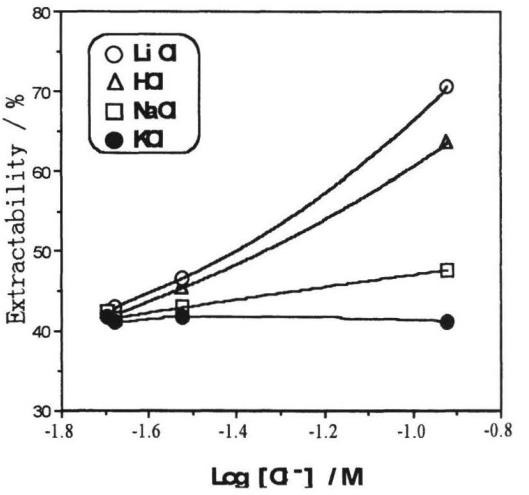


Figure 6: Effect of alkali metal ions on the extraction of Au(III) at 25±1°C. [MBDIPP]=1.0×10^{-2}M in DCE. [Au(?)] =1.0×10^{-4}M in 2.0×10^{-2}M HCl.

Solvent extraction processes based on solvating extractants are known to be highly dependent on the presence of counter-ions that ultimately affect the ionic strength of the aqueous feed solutions and also salting out effect. Figure 6 gives the effect of some alkali metal chlorides on the extraction of gold(III). It is seen that larger ions of small hydration degree like Na^+ and K^+ destabilizes the Au(III)-MBDIPP complex whereas the presence of Li^+ with large hydration degree greatly enhances the extractability.

Almost quantitative stripping of Au(III) from the Au(III)-MBDIPP complex loaded in DCE was possible in 1 minute contact time with 0.5M thiourea dissolved in 0.1M HCl

CONCLUSIONS

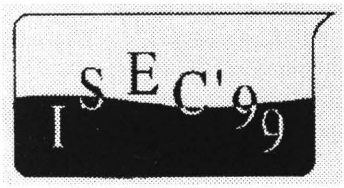
The bi-functional bis(dialkylphosphonate)s are better reagents for extraction of gold from hydrochloric acid medium than the monofunctional trialkylphosphates containing comparable number of carbon atoms in the structure.

In the bis(phosphonate) reagents, branching in the alkoxy groups favors selectivity of gold extraction.

A separation method based on extraction of gold(III) with MBDIPP could be tried for the recovery of the metal from industrial wastes dissolved in hydrochloric acid.

REFERENCES

1. Alguacil FJ and Caravaca C, *Hydrometallurgy* **34**, 91, (1993)
2. Villacescusa I, Miralles N, DePablo J, Salvado V and Sastre AM, *Solv Extr. Ion Exch.* **11**, 613, (1993) 123, (1996).
3. Argiropoulos G, Cattrall RW, Hamilton IC and Paimin R, *Proc. Int. Solv Extr.Conf., ISEC96,* Melbourn **1**, 123, (1996)
4. Madi A, Miralles N, Cortina JL, Arnaldos J and Sastre A, *Proc. Int. Solv. Extr. Conf., ISEC96*, Melbourn **1**, 463, (1996)
5. Martinez S, Sastre A, Miralles N and Alguacil FJ, *Hydrometallurgy*, **40**, 77, (1996)
6. Salvado V, Hidalgo M, Masana A, Munoz M, Valiente M and Muhammed M, *Solv. Extr. Ion Exch.* **8**, 491(1990)
7. Sliles A.R., Esters of Alkane Diphosphonic Acids, *U.S. Patent No.2,957,904.* (1960)
8. Mooiman MB, *Precious Metals* **17**, 411, (1993)
9. Edwards RI, te Reile WAM. in *Handbook of Solvent Extraction*, Lo, T.C., Baird, M.H., Hanson, C. (Eds.), John Wiley, New York, 725, (1983)



SULPHUR–NITROGEN LIGANDS IN THE SOLVENT EXTRACTION OF SILVER FROM CHLORIDE SOLUTIONS

AP Paiva

Departamento de Química e Bioquímica da Faculdade de Ciências da Universidade de Lisboa, Centro de Electroquímica e Cinética da Universidade de Lisboa *(CECUL)*, Rua Ernesto de Vasconcelos, C1, 5º Piso, 1749-016 Lisboa - Portugal

ABSTRACT

A concise review focusing on the solvent extraction of silver from concentrated chloride solutions is completed with new data for the metal extraction and stripping using the following N- and S- containing extractants: diphenylthiourea *(DPT)*, dibutylthiourea *(DBT)*, thiuram disulphide *(disulfiram, DSF)*, 5,5'-dithiobis-(1-phenyl-1-H-tetrazole) *(TPT)* and pyridine disulphide *(aldrithiol, ADT)*. The extraction abilities are interpreted in terms of extractant composition and influence of structural modifications. The selectivity of the above mentioned extractants for the precious metal, when it coexists with high contents of copper, iron and lead in the feed aqueous solution, is also evaluated and discussed. Analysis of equilibrium data collected for silver extraction by *DBT* and *DSF* allows the proposal of the most probable reaction pathways involved in the metal extraction process.

Keywords: silver, chloride, thiourea derivatives, nitrogen disulphides

INTRODUCTION

There has been an increasing interest in the development of chloride hydrometallurgy for the treatment of complex sulphide ores and concentrates during the past few years.[1,2] In addition, the leaching solutions resulting from the hydrometallurgical treatment of, e.g., pyrites and chalcopyrites, usually contain traces of silver.

For silver recovery, processes such as precipitation as silver chloride[3] or cementation[4] are well established. However, the solubility of silver chloride in water increases considerably when high chloride concentrations are involved, due to the formation of anionic chlorocomplexes of the type $AgCl_2^-$, $AgCl^{2-}$ and $AgCl_4^{3-}$.[5] Hence, it is interesting to investigate a profitable way to recover the significant quantities of silver remaining in highly concentrated chloride solutions, and this has motivated some recent research to promote solvent extraction alternatives for silver recovery from such media.[6,7]

Within the various types of organic compounds that were tested as extractants of silver from chloride media, some open chain thioethers and oxathioethers deserve a mention.[8] Other studies concerning silver recovery from chloride media involved the use of calixarene amide derivatives [7] and some neutral organophosphorous compounds, namely O,O-di-n-butyl-α-phenylamino-phenylmethane-thiophosphonate[9], triisobutylphosphine sulphide *(TIBPS)* and triphenylphosphine *(TPP)*[6,10] and triphenylphosphine sulphide *(TPPS)*.[11] For an identical set of experimental conditions, *TPP* proved to be the most efficient extractant, followed by *TIBPS*;[6,10] *TPPS* showed a very poor extraction ability, which can be considered a surprising result if the similarities of *TIBPS* and *TPPS* (replacement of isobutyl by phenyl groups) are taken into account.[11] In terms of selectivity for silver recovery, when the precious metal coexists with excess quantities of some base metals such as iron, copper and lead, *TIBPS* was largely the most suitable ligand.[6] In addition, the presence of iron in the aqueous feed solution caused a synergistic effect on silver extraction by *TIBPS* and *TPPS*, phenomenon which also happened when the four metals were involved.[6,10,11]

Equilibrium studies performed with *TIBPS* support a sort of "solvation" reaction pathway for silver extraction, which can be expressed by equation (1), if only the predominant chlorocomplex species for chloride concentrations between 1M and 5M is considered.[5]

$$AgCl_3^{2-}(aq) + 2TIBPS_{(org)} \Leftrightarrow AgCl.2TIBPS_{(org)} + 2\,Cl^-(aq) \qquad (1)$$

© 2000 Society of Chemical Industry

For stripping, a stabilised sodium thiosulphate solution showed an efficient behaviour, represented by equation (2).[6,12] Here also only the most stable anionic thiosulphate species is taken into account.

$$AgCl.2TIBPS_{(org)} + 2\ S_2O_3^{2-}(aq) \Leftrightarrow Ag(S_2O_3)_2^{3-}(aq) + Cl^-(aq) + 2TIBPS_{(org)} \quad (2)$$

In this work, to provide additional information concerning the solvent extraction of silver from concentrated chloride solutions, some commercial organic compounds containing nitrogen and sulphur atoms have been chosen and tested as extractants.

EXPERIMENTAL

Base-electrolytes were prepared using hydrochloric acid and sodium chloride, in which the total chloride concentration varied between 2.5 and 5 mol/dm^3; the strongly acidic electrolytes always had a 2M hydrochloric acid concentration. Silver feed solutions with concentrations between $5x10^{-4}$ and $3x10^{-3}$ mol/dm^3 in silver were obtained by dissolving the required amount of silver nitrate (Merck, 99.5% purity) in the base-electrolytes. Solutions containing copper, lead and iron were prepared from the respective chloride salts using the 2 mol/dm^3 HCl + 3 mol/dm^3 NaCl electrolyte. All chemicals were pro-analysis quality. For the stripping experiments, a stabilized sodium thiosulphate solution whose composition is referred to by Rickelton[13] was used; a 2 mol/dm^3 sulphuric acid solution and a 5 mol/dm^3 hydrochloric acid solution were also tested as stripping agents for some loaded solvents.

Organic phases were obtained by dissolution of the respective ligands in 1,2-dichloroethane *(1,2-DCE*, Riedel-de-Haen, 99.8%). The organic extractants were obtained from Aldrich and used without further purification.

Extraction and stripping experiments were performed by mixing equal volumes of the aqueous and organic phases (A/O=1) for 30 minutes, at a controlled temperature of 20±2°C and at a constant stirring speed of 1250 rpm, which was enough to guarantee a good emulsion. The same procedure was also applied for the evaluation of the selectivity of the organic extractants towards silver, as well as for the equilibrium studies with *DBT* and *DSF*.

Analysis of the metal contents was carried out in the aqueous phases, before and after extraction, by Atomic Absorption Spectrophotometry using a Unicam 929 model. For each sample, three aliquots were analysed and the values obtained were critically treated and only accepted if a reasonable relative standard deviation was obtained. Metal concentrations in organic phases were found by mass balance.

RESULTS AND DISCUSSION

Extraction and stripping

For the preliminary extraction experiments using the above mentioned organic ligands, a 2 mol/dm^3 HCl + 3 mol/dm^3 NaCl solution containing $2x10^{-3}$ mol/dm^3 of silver was used. The results obtained are presented in Table 1. Phenyl disulphide *(PDS)* was used for direct comparison with *ADT*.

Under the experimental conditions used, the thiourea derivatives exhibited similar extraction behaviour, being the most efficient ligands for silver extraction amongst those tested. Therefore, the presence of either phenyl or n-butyl groups on the thiourea moiety did not produce significant differences on the extraction performance of both thioureas (the replacement of isobutyl by phenyl groups on thiophosphines caused a marked decrease in silver extraction, e.g. for *TIBPS* and *TPPS* [11]).

Amongst the disulphides, *PDS* was the best and *DSF* the worst, although the extraction values obtained were quite close. The pyridine rings in *ADT*, when compared with the phenyl groups in *PDS*, were not beneficial for enhancing silver extraction; on the other hand, the simultaneous presence of a disulphide link on a sort of thiourea moiety markedly reduced the affinity of such a ligand *(DSF)* for

silver ion in a chloride media. *ADT* and *TPT* showed identical extraction behaviour, although some stereochemical hindrance affecting *TPT* performance could be expected.

Table 1 Percentage of silver extraction by the sulphur-nitrogen ligands.

Extractants	% of extraction
DPT	96
DBT	96
DSF	21
TPT	25
ADT	27
PDS	34

* 0.1 mol/dm^3 in 1,2-DCE, A/O=1, 30 minutes of shaking, 20°C, 1250 rpm

The silver loaded organic solvents resulting from the above extraction experiments were then equilibrated with a stabilised sodium thiosulphate solution.[13] The stripping results obtained and the total silver recovery for each extractant are displayed in Table 2.

Table 2 Percentage of silver stripping and total metal recovery.

Extractants	% of stripping	% total recovery
DPT	71	68
DBT	71	68
DSF	80	17
TPT	4	<1
ADT	<1	<1
PDS	1	<1

* A/O=1, 30 minutes shaking, 20°C, 1250 rpm

It can be seen from Table 2 that the stabilised sodium thiosulphate solution was effective for stripping silver from *DPT* and *DBT* (similar stripping efficiencies were achieved), and also from *DSF*. Silver contained in the other disulphides was not stripped under identical experimental conditions. Regarding the total silver recoveries using this stripping agent, only *DPT* and *DBT* can be considered as promising ligands for extracting the precious metal from chloride media, but the possibility of efficiently stripping silver from *DSF* using a thiosulphate solution can also be of interest.

Hydrochloric and sulphuric acid solutions were also tested as stripping agents for silver contained in *DBT* and *DSF* solvents, using the same experimental conditions for extraction and stripping as reported earlier. The latter did not work at all for stripping the precious metal from the solvents tested (percentages lesser than 2.5%), but an efficiency of 76% was achieved using HCl as a stripping agent for *DSF*, leading to a total silver recovery of 14%.

It is worthwhile mentioning that, for all cases, it was confirmed that the extraction and stripping equilibria were achieved within a 30 minute stirring time, and also that the rate of phase separation for both processes was always fast, about 2-3 minutes.

Selectivity and interference studies

It was decided to evaluate the behaviour of the extractants towards silver in the presence of relatively large concentrations of copper, iron and lead. Accordingly, synthetic feed solutions containing $3x10^{-2}$

mol/dm^3 of copper, 1x10^{-2} mol/dm^3 of lead and 9x10^{-2} mol/dm^3 of iron, added as Cu(II), Pb(II) and Fe(III) chlorides, together with 1x10^{-3} mol/dm^3 of silver in a 2 mol/dm^3 HCl + 3 mol/dm^3 NaCl solution, were prepared, and the selectivity towards the precious metal exhibited by the chosen set of ligands was analysed, Table 3.

A general survey of the contents of Table 3 reveals that the ligands studied are not generally selective towards the precious metal. In fact, *DPT* and *DBT*, always exhibiting a similar extraction behaviour as stressed earlier, decreased their affinity for silver and extracted high percentages of copper, but also significant quantities of iron and, to a lesser extent, lead. On the other hand, the last three disulphides on the table did not significantly extract silver; however, it is interesting to notice that, although having quite similar structures, *TPT* and *DPS* extracted lead selectively, whereas *ADT* showed a remarkable affinity towards iron. Regarding *DSF*, it revealed an identical extraction performance for the four metals as both thiourea derivatives, but an interesting phenomenon is that the silver extraction efficiency increased to 92%. A contribution to an explanation of this feature will be highlighted in the next section.

Table 3 Selectivity of the sulphur-nitrogen extractants towards silver.

Extractants	% of extraction			
	Ag	Cu	Pb	Fe
DPT	71	82	6	21
DBT	73	89	2	28
DSF	92	96	6	26
TPT	1	--	20	--
ADT	3	--	--	32
PDS	5	--	8	--

* 0.1mol/dm^3 in 1,2-DCE, A/O=1, 30 minutes shaking, 20°C, 1250 rpm

These general selectivity results suggest once more[6] that, under the adopted experimental conditions, copper is frequently co-extracted by ligands which efficiently extract silver and, inversely, it is not extracted when the organic compounds do not have a special affinity for the precious metal. Such a fact can be explained by the similarities between silver and copper, elements belonging to the same group in Periodic Table.

DPT, *DBT* and *DSF* revealed a quite poor affinity for lead. Therefore, it was decided to study their selectivity towards the precious metal in presence of lead only. Using similar experimental conditions (9x10^{-4} mol/dm^3 silver and 1x10^{-2} mol/dm^3 lead in a 2 mol/dm^3 HCl + 3 mol/dm^3 NaCl solution), it was found that none of the ligands extracted lead; *DPT* and *DBT* extracted all the silver but *DSF*, as expected, extracted only 24% of the precious metal.

Extraction pathways involving DBT and DSF

To clarify the reactions involved in silver extraction by some of the ligands studied in this work, *DBT* and *DSF* were chosen. *DSF* is the only ligand of those tested that showed a marked tendency to increase silver extraction when an excess of iron is present. This phenomenon was also found when *TIBPS* and *TPPS* were used for identical extraction systems and, based on the equilibrium data collected for the phosphorous extractants,[6] an identical type of reaction is to be expected for *DSF*. Indeed, the synergistic effect of iron on silver extraction suggests that there is some ability of ferric chloride to act over the anionic silver chlorocomplexes, shifting the equilibria to the formation of silver chloride in solution, which could justify the easier formation of species such as AgCl.nL in organic phase.[12] This assumption is supported by some research performed on leaching of silver using either ferric or cupric

chloride solutions,[14,15] which showed that the contribution of free chloride ions by a given concentration of cupric chloride always exceeds that of a similar concentration of ferric chloride, considering in both cases a constant total chloride concentration. However, taking into account that there still is an appreciable excess of free chloride ions in the polymetallic solution, further studies are needed to identify some other factors responsible for this synergism phenomenon.

Extraction experiments with *DBT* and *DSF* were carried out to evaluate the dependence of silver distribution coefficients on ligand and chloride concentrations. Figure 1 shows two plots of log D *vs.* log [L] for *DBT* and *DSF*, using an initial feed solution containing $5x10^{-4}$ mol/dm^3 of silver in a 2 mol/dm^3 HCl + 3 mol/dm^3 NaCl matrix, and other two plots of log D *vs.* log [Cl^-], using 0.01mol/dm^3 *DBT* and 0.06 mol/dm^3 *DSF*, for an initial solution containing $5x10^{-4}$ mol/dm^3 of silver and at least 2 mol/dm^3 HCl, the remaining chloride concentrations being made up with NaCl.

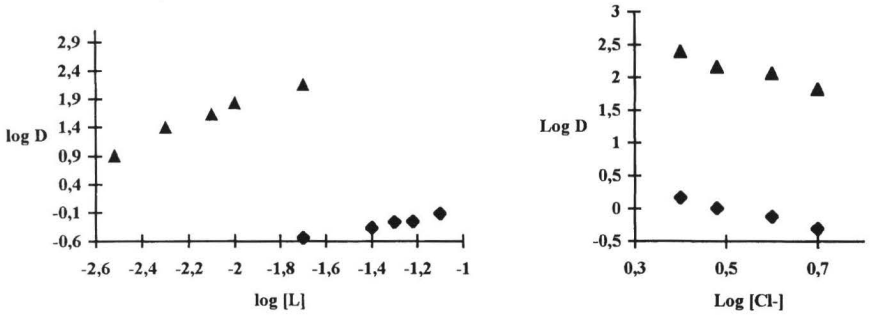


Figure 1. Dependence of silver distribution coefficient on ligand and chloride concentrations (Δ- DBT; ♦- DSF; L in 1,2-DCE, 20ºC, 1250 rpm, 30 minutes shaking, A/O=1)

The experimental ligand/silver and chloride/silver ratio, given by the slope of the straight lines which best fit the equilibrium data, have values of 0.7 and -1.5 for *DSF* and 1.5 and -1.7 for *DBT*, respectively. Accordingly, the results obtained for *DSF* and the synergistic effect of iron on silver extraction suggest a metal extraction reaction pathway as in equation (3), considering only the predominant chlorocomplex in solution.[5]

$$AgCl_3^{2-}(aq) + DSF_{(org)} \Leftrightarrow AgCl.DSF_{(org)} + 2\ Cl^-(aq) \qquad (3)$$

There is also some possibility of having half of a *DSF* molecule "solvating" the silver ion, i.e. 0.5 DSF.AgCl, suggested by the low slope of the straight line obtained from the log D *vs.* log [DSF] plot (Figure 1).

For the case of *DBT*, some basic character is expected, motivated by the electronic density on nitrogens, which is more stereochemically accessible than in *DSF*. This feature, associated with the lack of synergism granted by iron for the extraction of silver from acidic chloride media, and also to the data presented in Figure 1, suggests the occurrence of equilibria (4) and (5).

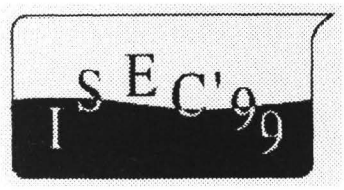
$$2\ DBT_{(org)} + 2\ HCl_{(aq)} \Leftrightarrow 2\ DBTH^+\ Cl^-_{(org)} \qquad (4)$$

$$2\ DBTH^+\ Cl^-_{(org)} + AgCl_3^{2-}(aq) \Leftrightarrow 2\ DBTH^+\ AgCl_3^{2-}(org) + 2\ Cl^-(aq) \qquad (5)$$

These equilibria may be the predominant ones, although there is also the possibility of formation of species of the type AgCl.2DBT in organic phase. Moreover, if a slight acidic aqueous solution is involved (silver is equally well extracted from a 5 mol/dm^3 NaCl solution when *DBT* is used), the "solvation" mechanism must occur, as there is not enough proton concentration to fully guarantee the ion-pair reaction pathway.

REFERENCES

1. Dalton RF, Price R, Henmana E, Hoffmann B, "*Separation Processes in Hydrometallurgy*", Davies GA (Ed.), Ellis-Horwood, Chichester, 466, (1987)
2. Rice NM, Gibson RW, *Proceedings of ISEC'96*, Shallcross DC, Paimin R, Prvcic LM (Eds.), The University of Melbourne, 715, (1996).
3. Rydberg J, Musikas C, Choppin GR (Eds.), *"Principles and Practices of Solvent Extraction"*, Marcel Dekker Inc., New York, 381, (1992).
4. Limpo JL, FigueiredoJM, Amer S, Luís A, *Hydrometallurgy*, **28**, 149, (1992).
5. Fritz JJ, *J. Sol. Chem.*, **14**(12), 865, (1985).
6. Paiva AP, Abrantes LM, *Proceedings of the 5th EPD Congress, 123rd TMS Annual Meeting*, G. W. Warren (Ed.), 243, (1994).
7. Ohto K, Yamaga H, MurakamiE, Inoue K, *Talanta*, **44**(6), 1123, (1997).
8. Paiva AP, Lemaire M, *Sep.Sci.Technol.*, **28**(13-14), 2279, (1993).
9. Sevdic D, Meider H, Pavkovic D, *Solv. Extr. Ion Exch.*, **8**(4-5), 643, (1990).
10. Abrantes LM, Costa MC, Paiva AP, *Proceedings of Hydrometallurgy '94*, Chapman and Hall, 409, (1994).
11. Abrantes LM, Paiva AP, Cote G, *Proceedings of ISEC'96*, Shallcross DC, Paimin R, Prvcic LM (Eds.), The University of Melbourne, 129, (1996).
12. Paiva AP, *Ph.D. Thesis*, University of Lisbon (1995).
13. Rickelton WA, Robertson AJ, *Min. Metallurg. Proc.*, 7-10, (Feb 1987).
14. Dinardo O, Dutrizac JE, *Hydrometallurgy*, **13**, 345, (1985)
15. Kolodziej B, *Hydrometallurgy*, **20**, 219, (1988).



FOAM SEPARATION OF TRIBUTYL PHOSPHATE FROM AQUEOUS SOLUTION BY SODIUM DODECYLSULFATE

Zhidong Chang, Huizhou Liu, Ning Yao and Jiayong Chen
Young Scientist Laboratory of Separation Science & Engineering, Institute of Chemical Metallurgy, Chinese Academy of Sciences, P.O.353, Beijing 100080 China.

ABSTRACT
Tributyl phosphate (TBP) can be recovered from aqueous solution by foam separation, by using sodium dodecylsulfate (SDS) as a surfactant. The highest TBP concentration in the foam overflow from the separation column was almost three times the feed concentration. When the SDS concentration was the lowest, the TBP has the greatest enrichment under the experimental conditions. For higher concentrations, the enrichment decreases. The critical micelle concentration (CMC) is not influenced by the concentration of TBP, when TBP concentration is lower than 0.02% (g/g).

Keywords: tributyl phosphate, foam separation, sodium dodecylsulfate, surfactant

INTRODUCTION

Foam separation techniques have been proven to be extremely effective to remove contaminants from dilute aqueous solutions. Many researchers are working in this field, their investigations include the recovery of proteins, enzymes and cells (or virus) from dilute solutions,[1,2,3] the concentration of metals or other ions in analytical laboratory or industry[4,5] and waste water processing.[6-9]

The fundamental principle of foam separation is that materials that are surface-active tend to adsorb on the gas-liquid interface. If bubbles are passing through the separation column, the surface-active materials can adsorb on the bubbles' surface. While the bubbles have enough stability, they can be separated from the bulk solution, thus the surface-active materials can be recovered and concentrated. If the materials are not surface-active, they can be removed through interaction with surfactants. While surfactants are separated by foam, the target materials are also removed from the bulk solution.

The non-surface-active materials have many ways to interact with surfactants. 1) Ion-ion interaction, this is the main action in the foam separation process. The electrostatic force is great enough to capture any ions. Most of recent researches are focused on this aspect. 2) Ion-dipole force, which is not very effective.[9] 3) Dipole-dipole force or Van de Waals force, which are seldom seen in the literature.

In the last years, concern about the environment has increased. The waste-water from chemical industry should be made clean enough, so that it can be discharged into streams and rivers. This process increases the cost, especially when dealing with water containing dilute solutes using conventional methods. It is necessary to develop a new technique to process such waste-water, which can clean up the water and recover solutes at the same time.

Tributyl phosphate is a neutral donor extractant. Since it has good extraction characteristics such as high boiling point, 289°C (760 mmHg), low solubility, 0.39g/dm^3 (25°C) and it is not flammable,[10] and is widely used in the extraction industry. However, since the water phase of this extraction system contains some TBP, because of large amount of water volume, there are economic and environmental interest in the recovery of this TBP. The traditional methods to recover organics from water are distillation and extraction, but they fail to recover TBP from water because of its high boiling point, low stability at high temperature, low concentration and other economic reasons.

The structure of TBP shows that it cannot be ionised even adding acids or alkalis, so it cannot interact with a surfactant through static electric forces. In this paper, we try to appraise the ion-dipole force in the foam separation of TBP from aqueous solution, using an anionic surfactant sodium dodecylsulfate as surfactant.

© 2000 Society of Chemical Industry

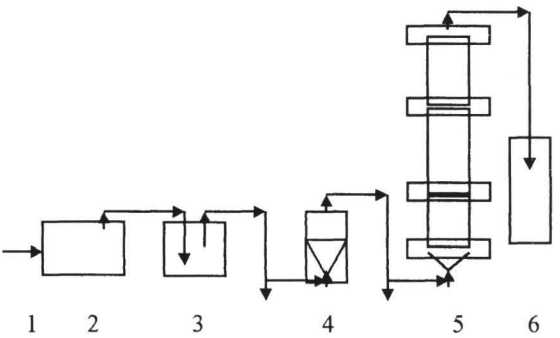
EXPERIMENTAL

Materials

Both tributyl phosphate and sodium dodecylsulfate were analytical grade purity, purchased from Beijing Chemical Import & Export Company. Distilled water was used in all experiments.

Methods

The schematic diagram of the foam separation apparatus is shown in Figure 1. An acrylic glass cylindrical column with 50cm height and 8cm internal diameter was used as the foam separation column. 1dm^3 of premixed liquid containing water, TBP and surfactant was fed into the column. Scrubbed air was introduced into the bottom of the column through a sintered glass disk. A sample port was located 10cm above the bottom and samples of liquid phase were taken at 0 and 8 minutes after bubbling started which represented the initial TBP concentration and residual TBP concentration respectively. All the overflowing foam from the overheads was collected after the experiment started. The foam was broken up for analysis by freezing the foam samples for 30 minutes and then allowing them to melt at ambient temperature. Concentration of TBP was analysed by an HP6890 gas chromatograph equipped with a HP-5 capillary column and a FID detector. Concentration of SDS was analysed using JIS method.[11]



1: air; 2: air compressor; 3: scrubber; 4: flow meter; 5: separation column; 6: container of recovered TBP

Figure 1. Schematic diagram of the experimental apparatus

RESULTS AND DISCUSSION

The effect of surfactant concentration on enrichment

The mean gas flow rate in the experiments was 0.01m^3/hour. Since it is very slow, the adsorption of solute on the surface of the bubble is considered at equilibrium.
The enrichment ratio is defined as:

Enrichment = Concentration of foam that overflow from column / Feed concentration

By fixing the TBP feed concentration at 0.1g/dm^3 while increasing the SDS concentration, it can be seen that the concentration of sodium dodecylsulfate has great effect on the recovery of tributyl phosphate. The results are shown figure 2. When the sodium dodecylsulfate feed concentration is as low as just required for maintaining the lowest foam stability, which is 2.5x10^{-2}g/dm^3, the concentration of the recovery of tributyl phosphate reaches the maximum value. From that value, the recovery of tributyl phosphate went down with the increase of the concentration of SDS. This phenomenon can be explained as follows. There exists a competitive adsorption between TBP and SDS. The equilibrium surface concentration of the solutes in the foam is connected with the feed concentration and increases with the increasing of feed concentration. Therefore, the surface concentration of SDS increases with the increment of the SDS feed concentration. The available adsorption sites on the surface of the foam are limited, so that the surface concentration of TBP decreases. This can be seen from figure 2.b.

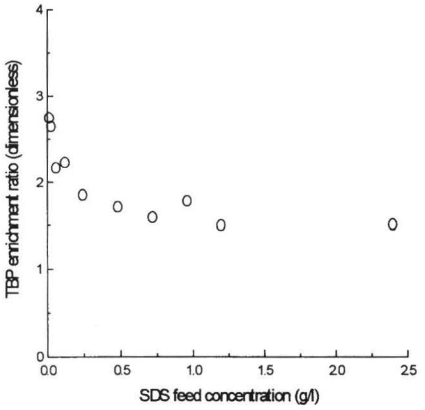


Figure 2.a Effect of the SDS concentration on TBP recovery

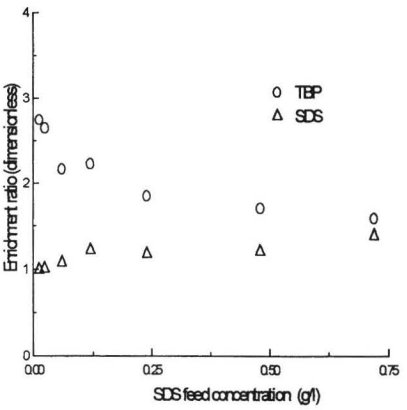


Figure 2.b The contrast of enrichment ratio between SDS and TBP in the foam

The effect of feed concentration of TBP on recovery

The relation between the feed concentration of TBP, C_I, and the concentration of the recovery of TBP, C_R, is shown in figure 3. C_I vs. C_R follows a linear relationship. This is in good agreement with our previous results using Tween series surfactant.[12]

From figure 3 it can be seen that the TBP concentration of recovery increased with the increase of TBP feed concentration when the initial surfactant concentration was constant. When the

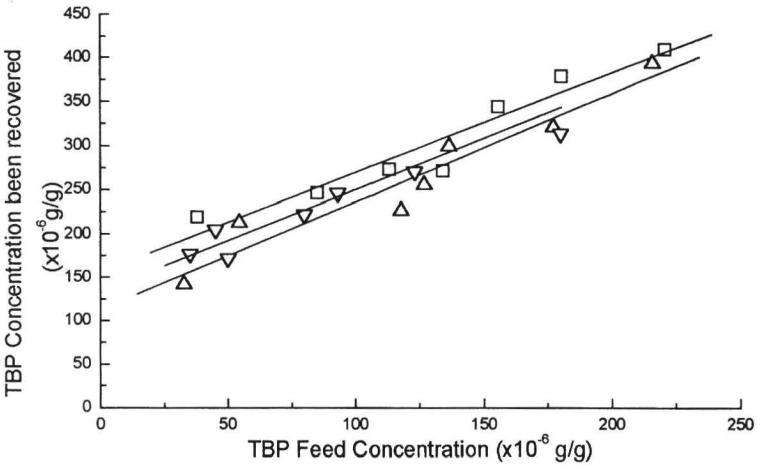


Figure 3 The effect of TBP feed concentration on TBP recovery

initial surfactant concentration increases, the TBP recovery decreases. This also demonstrates that a competition exists between TBP and SDS for the adsorption on the foam surface.

The concentration of recovered SDS vs TBP feed concentration is plotted in figure 4, at

constant surfactant concentration, 10 cm^3/1000 cm^3. The results of electric conductivity of the broken foam solution are also shown in figure 4. It can be seen that the recovered SDS concentration almost keeps the same level considering the experimental error. The electric conductivity of broken foam solution also follows the same trend. Because the structure of TBP is not as effective as that of SDS in occupying the adsorption site, the TBP has little influence on the adsorption of SDS, when the solution concentration was very low. The main role of SDS is only to maintain the stability of foam. If the foam can be formed and blown out, the less SDS usage and the greater the TBP adsorption.

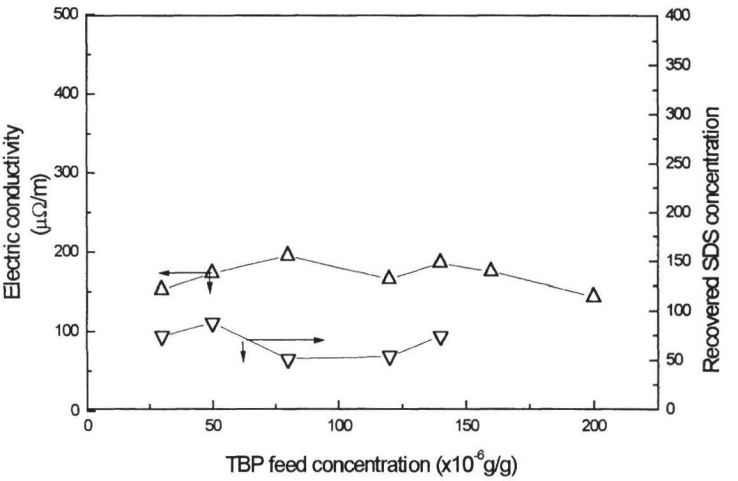


Figure 4 Effect of TBP feed concentration on SDS recovery

The effect of TBP and SDS concentrations on electric conductivity and the critical micelle concentration (CMC)

The effect of different TBP concentrations on the electric conductivity at constant surfactant concentration is shown in figure 5. It can be seen that the TBP concentration has little effect on the electric conductivity of the solution.

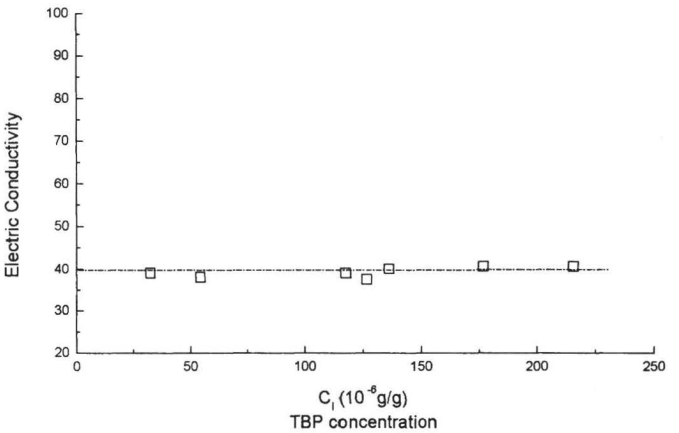


Figure 5 The effect on electric conductivity by different TBP concentration

The effect of SDS concentration on electric conductivity is shown in figure 6, for a 2% TBP fixed concentration. Compared with the electric conductivity of the pure SDS solution, the electric conductivity of the solution of SDS and TBP has the same trend. From figure 6, it can be seen that the addition of TBP has little effect on the critical micelle concentration (CMC) of SDS.

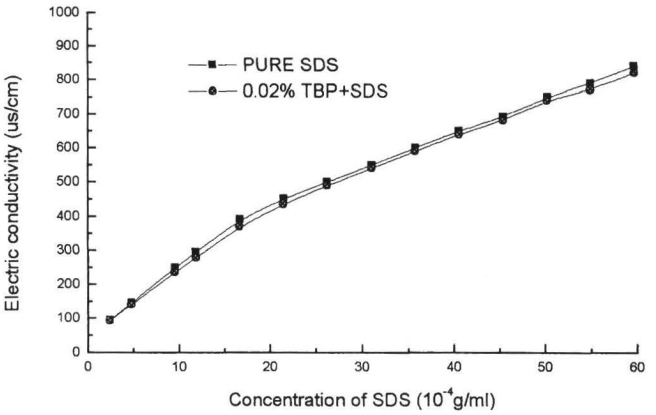


Figure 6 The effect of SDS concentration on the electric conductivity

From figures 5 and 6, it can be seen that some interaction take place between the hydrophilic heads of SDS and TBP, so that the electric conductivity of the SDS solution drops down when TBP is added. This is not observed if the concentration of either TBP or SDS is high enough. The added TBP can interact with the hydrophilic head of the SDS, which is not ionic form and therefore the electric conductivity drops down. However, the added TBP was saturated only part of SDS, so the electric conductivity of SDS decreases only slightly. The trend of the electric conductivity follows the increase in SDS concentration.

The proposed interaction between TBP and SDS is represented in figure 7. The SDS and TBP adsorb on bubble surface respectively. The TBP competes for the bubble surface adsorption site with SDS. But the extend of TBP adsorption depends on SDS concentration. If the SDS concentration is very low, the stability of the bubble is low too. Therefore the foam can not be formed and the separation can not be fulfilled. If the SDS concentration is high, the adsorption of SDS is high, so that the are few available adsorption sites for TBP. That is why in figure 3 the adsorption of TBP decreases with the increase in SDS concentration. However, when the TBP concentration is high enough, the SDS concentration should be increased correspondingly for stabilising the foam. So in figure 3 the TBP adsorption increases after a minimum value.

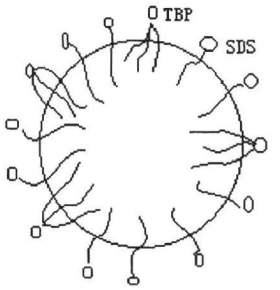


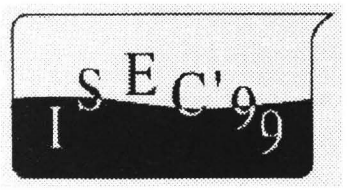
Figure 7 Diagram of TBP and SDS coadsorption on the bubble surface

CONCLUSION

Under the experiment conditions, TBP recovery reaches its maximum when the SDS concentration was the minimum necessary to maintain the stability of the foam. The recovery of both TBP and SDS increases with the increase of feed concentration. The addition of TBP does not change the CMC of SDS.

REFERENCES

1 Gehle RD and Schugerl K. *Applied Microbiology and Biotechnology,* **20**, 133, (1984).
2 Husband DL, Masliyah JH and Gray MR. *Canad J Chem Eng,* **72**, 840, (1994).
3 Phae C-G and Shoda M. *J Ferm Bioeng,* **71**, 118, (1991).
4 Sebba F. *Ion Flotation,* New York: American Elsevier, (1962).
5 Lin J and Huang S-D. *Sci Technol,* **24**, 1377, (1989/90).
6 Tharapiwattananon N, Scamehorn JF, Osunan S, Harwell JH and Haller KJ. *Sep Sci Technol*, **31**, 122, (1996).
7 Chiu H-L and Huang S-D. *Sep Sci Technol,* **26**, 73, (1991).
8 Wungrattanasopon P, Scamehorn JF, Chavedej S, Saiwan C and Harwell JH. *Sep Sci Technol*, **31**, 1523, (1996).
9 Nyssen GA, Lovell GS, Simon AA, Smith JG, Tolar BK and Wilson DJ. *Sep Sci Technol*, **22**, 2127, (1987).
10 Mellan I. *Industrial Solvents*, New York: American Reinhold Publishing Corp. (1977).
11 JIS K 3362, (1978).
12 Chang Z-D, Yao N, Liu H-Z and Chen J-Y. *Chem Metal* (Chinese), accepted.



EXTRACTION EQUILIBRIA OF NICOTINIC ACID USING ALAMINE 300/DILUENT AND CONVENTIONAL SOLVENT SYSTEMS

Aynur Senol
Department of Chemical Engineering, Faculty of Engineering, Istanbul University, 34850 Avcilar, Istanbul, Turkey

ABSTRACT
Distribution of nicotinic acid between water and Alamine 300 (tri-*n*-octylamine) dissolved in various (proton-donating and -accepting, polar and non-polar) diluents, as well as a comparison with the extraction equilibria of pure diluent alone have been studied at 298 K and the phase ratio of 1:1 (v/v). Cyclic alcohol/amine system yields the highest synergistic extraction efficiency. The strength of the complex solvation was found to be reasonably high for halogenated aliphatic hydrocarbons and nitrobenzene, activating mainly the formation of $acid_1$-$amine_1$ structure. The influence of the acid structure over distribution has been evaluated through comparing the extractabilities of three acids containing different functional groups, i.e., nicotinic, benzoic and valeric acids. The results were correlated using various versions of the mass action law, i.e., a modified Langmuir equilibrium model and a chemical modeling (chemodel) approach comprising one or two acid-amine complex formation.

Keywords: nicotinic acid, Alamine 300, modelling

INTRODUCTION

Long-chain, aliphatic tertiary amines (e.g., Alamine 336; 300) dissolved in suitable organic solvents are effective extractants for carboxylic acids.[1-5] Three major factors have been found to influence the equilibrium characteristics of amine extraction of carboxylic acids from aqueous solutions, i.e., the nature of acid, concentrations of acid and amine, and the type of diluent.[1-5] Simultaneously, the effect of additional controlling factors (such as the swing effect of a mixed diluent and the third phase formation) can also modify the reversible complexation stage.[2,5] The spectroscopic studies of Yang *et al.*[3] revealed that Alamine binds the non-dissociated part of acid in the organic phase through reversible complexation. The effect of diluent is mainly focussed on its ability to solvate polar ion-pair species through dipole-dipole interaction or hydrogen bonding, favouring the formation of one or simultaneously at least two acid-amine complexes.[1-5]

In this study, distribution of nicotinic acid (3-pyridinecarboxylic acid) between water and Alamine 300 dissolved in various diluents, as well as a comparison with the extraction capacity of pure diluent alone have been studied at isothermal conditions. Results were correlated in terms of a chemodel approach.

THEORETICAL

Using a chemical modeling approach of Tamada *et al.*,[1] the overall extraction equilibrium of acid/amine/diluent system can be described by the set of reactions (1):

$$pHA + q\overline{NR_3} = \overline{(HA)_p(NR_3)_q} \qquad p = 1, k;\ q = 1, l \tag{1}$$

where HA = the non-dissociated acid in the aqueous phase, $\overline{NR_3}$ = tertiary amine. Overbar denotes species in the organic phase. Supposing the ratio of activity coefficients of species to be constant for a given temperature, it can be incorporated into the "conditioned" extraction constant defined in molarity scale $[(mol/l)^{1-p-q}]$ as:

$$\beta'_{pq} = \overline{C_{pq}} \Big/ \left(C_{HA}^{p} \cdot \overline{C}_{AM}^{q}\right) \qquad p = 1, k;\ q = 1, l \tag{2}$$

© 2000 Society of Chemical Industry

where C_{HA}, $\overline{C_{AM}}$ and $\overline{C_{pq}}$ represent the concentrations of non-dissociated acid in the aqueous phase, free amine and complex (mol/l), respectively. The equilibrium content of complexed acid, $\overline{C_{HA}}$, is the sum of contributions of the individual complexes:

$$\overline{C_{HA}} = \sum_{p=1}^{k} \sum_{q=1}^{l} p\beta'_{pq} C_{HA}^{p} \overline{C}_{AM}^{q} \tag{3}$$

Combining Equation (3) with the overall balance equation for acid, the equilibrium model is derived, $C_{TA}^{\circ} = \overline{C_d} + \overline{C_{HA}} + C_{TA}$, where C_{TA}°, C_{TA} and $\overline{C_d}$ represent the initial and total aqueous phase acid concentrations and concentration related to the acid portion physically extracted by the diluent, respectively. C_{HA} are to be calculated from the dissociation equilibrium in the aqueous phase (pK_a = 4.75).

Poposka *et al.*[5] modified the Langmuir model of Bauer assuming an overall acid-amine complexation with an associated number (z) related to the maximum loading of amine, $z \equiv Z_{max}$, where the undissociated acid molecules are regarded as "adsorbat". The extraction constant (β_z) in $(mol/l)^{-z}$ is attributed to the overall reaction in terms of Equation (4), assuming the formation of only one type aggregated structure.

$$zHA + \overline{NR_3} = \overline{(HA)_z (NR_3)} \tag{4}$$

$$\beta_z = \overline{C_{HA}} / \left(C_{HA}^{\ z} \cdot \overline{C_{AM}} \right) \tag{4a}$$

EXPERIMENTAL

Materials

Alamine 300 (Henkel Co.), is a tertiary amine mixture containing mainly tri-*n*-octylamine (> 93 %). It is a light yellow liquid with an average molecular weight of 354 g/mol and a density of 0.80 g/cm^3. Nicotinic acid (pellagra preventive factor, 99.5 %), as well as the organic solvents of analytical grade (≥ 99.5%, GC) were furnished from Fluka. All the chemicals were used without further purification.

Experiments

The extraction experiments were performed using equilibrium glass cells, each equipped with a magnetic stirrer and thermostatted at (25 ± 0.1)°C. The equal volumes (10 cm^3) of initial aqueous and organic phases were agitated for 2 h and then left to settle and equilibrate for about 18-20 hours at a fixed temperature (25°C) and pressure (101.2 kPa). The effective separation of the phases was ensured by centrifugation. Aqueous-phase pH was measured by Orion 601A pH-meter. Aqueous-phase acid concentration was determined by titration with aqueous NaOH (Titrosol A, Merck) as well as using an UV-spectrophotometer (Waters, LambdaM Model 481, 263 nm). The acid content in the organic phase was determined by mass balance.

Tests covering the influence of diluents and the acid and amine concentrations on acid-amine complexation were performed using cyclopentanol, 1,2-dichloroethane (1,2-DCE), methyl isobutylketone (MIBK) and *n*-heptane diluents in amine mixture. The effect of the acid structure was evaluated for nicotinic, benzoic and valeric acids.

RESULTS AND DISCUSSION

The physical extraction of acid by the diluent alone, as well as the overall distribution in the amine mixture were compared on the basis of Distribution ratio, D (the ratio of total acid (all forms) extracted in organic phase to total acid (all forms) in aqueous phase, $\overline{C_{TA}}/C_{TA}$) and Extraction degree ($E,\% = 100D/(1+D)$).

The overall extraction capacity of amine/diluent system was evaluated with respect to Overall loading of amine (Z_t), i.e., the ratio of total amount of acid extracted to total amount of amine in the organic phase, $\overline{C_{TA}}/\overline{C^{\circ}_{AM}}$. The most probable acid-amine complexation and the strength of the complex solvation were interpreted in terms of the stoichiometric loading factor, Z_s, i.e., the ratio of complexed acid to total amine in the organic phase. This factor includes a correction term for the acid physically extracted by the diluent, $Z_s = \left(\overline{C_{TA}} - \nu \cdot \overline{C^{s}_{TA}}\right)/\overline{C^{\circ}_{AM}}$, where ν = % volume of diluent in mixture, $\overline{C^{s}_{TA}}$ = amount of acid extracted by the diluent alone, mol/l.

Evaluation of results

Study of the extraction system (Table 1) containing 0.102 mol/l aqueous-phase acid solution and 0.0452 mol/l (Alamine 300/diluent) solvent mixture tested for 14 different diluents reveals that the physical solubility of nicotinic acid in pure diluent alone is remarkably small with a distribution ratio of about 1 for cyclopentanol, and less than 1 for others ranging from 0.01 for hydrocarbons to 0.8-0.9 for alcohols, but all not convenient as separation agents. The noticeably low extraction degree of nicotinic acid in polar diluents (e.g.1,2-dichlorobenzene (2.26 D) and nitrobenzene(3.99 D)) may be attributed to the formation of intramolecular hydrogen bonding due to the second proton accepting group in pyridine ring. Conversely, amine/diluent system favours the formation of polar acid-amine complexes (p,q) with different stoichiometry, mainly (1,2) to (1,1). The highest strength of the complex solvation was found for 1,2-DCE, chloroform and nitrobenzene promoting (1,1) complex formation, and some oxygenated aprotic compounds (ketones, benzyl acetate), activating (3,4) and (2,3) acid-amine structures. Referring to Table 1 it can be concluded that the order of increased extraction efficiency of pure diluent alone, as well as the most probable acid-amine complexation (p,q) appear as follows:

kerosene (1,11) ≅ *n*-heptane (1,9) ≅ nitrobenzene (1,1) < cyclohexane (1,9) ≅ 1,2-dichlorobenzene (2,3) < chloroform (1,1) < 1,2-dichloroethane (1,1) < dibenzyl ether (2,3) < benzyl acetate (3,4) < MIBK (2,3) < 1-octanol (1,2) < cyclohexanone (2,3) < benzyl alcohol (1,2) < cyclopentanol (1,2)

No evidence of overloading of amine, i.e. Z_s higher than 1, was observed in any of the systems tested. The highest synergistic extraction efficiency yields amine mixtures of alcohols ($Z_t \approx 1.5$) and cyclohexanone ($Z_t \approx 1.4$), as compared to the hydrocarbons, aromatics, ethers and halogenated hydrocarbons ones varying less than 1 ($Z_t < 1$).

The equilibrium data from Table 1 were interpreted in terms of a modified Langmuir approach using the concepts of Poposka defined by Equations (4) and (4a).

$$Z_t = \frac{\overline{C_d} + \overline{C_{HA}}}{\overline{C^{\circ}_{AM}}} = \frac{\nu D_o C^{\circ}_{TA}}{(1+D_o)\overline{C^{\circ}_{AM}}} + \frac{Z_s \beta_z (C_{HA})^{z_i} \overline{C_{AM}}}{\overline{C^{\circ}_{AM}}} \qquad (5)$$

where D_o, C°_{TA} and $\overline{C^{\circ}_{AM}}$ denote the distribution ratio of acid related to the diluent alone and the initial acid and amine concentrations, respectively. β_z values were correlated by Equation (5)

supposing p/q ratio in Table 1 to represent the associated number of the complex formation related to the maximum loading, i.e., $z = Z_s \approx Z_{s,\max} = p/q$.

Table 1 Summary of extraction equilibrium results for Alamine 300/diluent/nicotinic acid system at 25°C (C°_{TA} = 0.102 mol/l acid; $\overline{C^{\circ}_{AM}}$ = 0.0452 mol/l Alamine)

Solvent	pH	C_{TA} [mol/l]	D	E, %	Z_t	Z_s	$(p,q)^a$ $(\beta_z)^b$
cyclohexane	3.47	0.1005	0.015	1.47			(1,9)
+ Alamine 300	3.49	0.0957	0.066	6.18	0.139	0.107	32.81
n-heptane	3.47	0.1008	0.012	1.18			(1,9)
+ Alamine 300	3.49	0.0960	0.062	5.88	0.133	0.107	31.76
kerosene	3.47	0.1010	0.010	0.98			(1,11)
+ Alamine 300	3.48	0.0972	0.049	4.71	0.106	0.085	16.41
o-dichlorobenzene	3.47	0.1004	0.016	1.57			(2,3)
+ Alamine 300	3.56	0.0728	0.401	28.63	0.646	0.611	66.06
1,2-dichloroethane	3.48	0.0995	0.025	2.45			(1,1)
+ Alamine 300	3.59	0.0632	0.614	38.04	0.858	0.804	69.49
chloroform	3.48	0.1002	0.018	1.76			(1,1)
+ Alamine 300	3.61	0.0602	0.694	40.98	0.925	0.886	138.12
MIBK	3.52	0.0892	0.143	12.55			(2,3)
+ Alamine 300	3.59	0.0635	0.606	37.75	0.852	0.574	40.82
cyclohexanone	3.59	0.0640	0.594	37.25			(2,3)
+ Alamine 300	3.69	0.0382	1.670	62.55	1.412	0.588	69.28
nitrobenzene	3.47	0.1009	0.011	1.08			(1,1)
+ Alamine 300	3.61	0.0596	0.711	41.57	0.938	0.914	191.74
dibenzyl ether	3.48	0.0980	0.041	3.92			(2,3)
+ Alamine 300	3.57	0.0710	0.437	30.39	0.686	0.249	53.98
benzyl acetate	3.50	0.0948	0.076	7.06			(3,4)
+ Alamine 300	3.59	0.0642	0.589	37.06	0.836	0.680	80.31
cyclopentanol	3.63	0.0532	0.917	47.84			(1,2)
+ Alamine 300	3.72	0.0330	2.091	67.65	1.527	0.468	85.60
1-octanol	3.55	0.0758	0.346	25.69			(1,2)
+ Alamine 300	3.63	0.0540	0.889	47.06	1.062	0.494	361.03
benzyl alcohol	3.63	0.0545	0.872	46.57			(1,2)
+ Alamine 300	3.71	0.0345	1.957	66.18	1.493	0.463	71.41

[a] probable acid (p)/amine (q) complex referred to Eq. (4); [b] equilibrium constant in $[(\text{mol/l})^{-z}]$ due to Eq. (5) assuming $z = Z_s = p/q$

It is apparent from Figures 1 and 2 that the longer R-chain of valeric acid (VA) and benzene ring of benzoic acid (BA) make these acids more hydrophobic and thus more easily to extract by a polar diluent alone, yielding D values about 100 times greater, as compared to those of less hydrophobic nicotinic acid capable of intramolecular hydrogen bonding. However, nicotinic acid is more sensitive to ion-pairing complexation with amine through dipole-dipole interaction accompanying the multiple effects at carboxyl group and electronegative (proton accepting) pyridine ring, that is indicative from the reasonably high Z_t values (Fig. 2) in contrast to the rather low D of distribution in polar (1,2-DCE) and protic (cyclopentanol) diluents alone (Figure 1), as compared to the same quantities of valeric and benzoic acids.

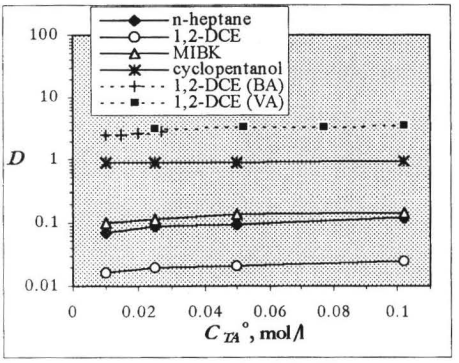


Figure 1. Physical extraction of nicotinic acid by solvents (—). Comparison with valeric (VA) and benzoic (BA) acids (- -).

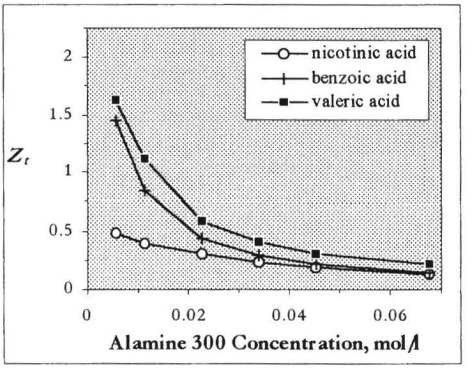


Figure 2. Comparison of overall loading for amine/1,2-DCE system (aqueous-phase acid concentration C_{TA}° = 0.01 mol/l)

Figure 3 illustrates the increased synergistic extraction efficiency of amine mixture with increasing the acid concentration, related to the diluent as: cyclopentanol (1,2) > MIBK (2,3) ≈ 1,2-DCE (1,1) > *n*-heptane (1,4). Since the non-polar Alamine by itself is a relatively poor solvating medium for the polar complexes loading decreases with increasing amine concentration as the active solvent becomes a less favourable solvating agent (Figure 4). For the nonpolar mixture of inert diluent and amine, increasing the amine concentration, however, has little effect upon loading.

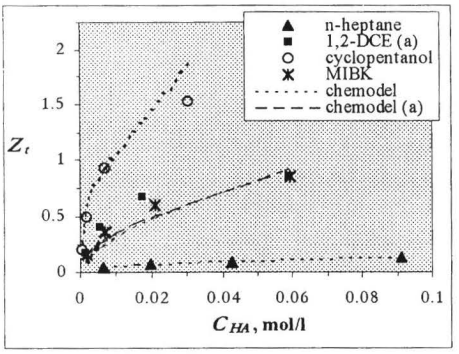


Figure 3 Variation of overall loading with aqueous-phase nicotinic acid concentration ($\overline{C_{AM}^{\circ}}$ = 0.0452 mol/l Alamine 300)

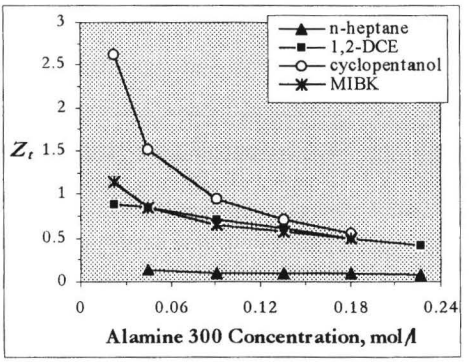


Figure 4 Variation of overall loading with amine concentration (nicotinic acid in aqueous-phase, C_{TA}° = 0.102 mol/l)

The results presented in Figures 1, 3 and 4, were interpreted in terms of a chemodel approach according to Equation (3), using the multivariable procedures of *linpack* for one (S) and two (T) selected complex combinations (Table 2). However, the best fits display the approach comprising the simultaneous formation of two associated complexes (except for 1,2-DCE) depending on the diluent used, i.e., (1,2) and (2,3) for cyclopentanol, (1,1) and (2,3) for MIBK, (1,1) for 1,2-DCE, and (1,2) and (1,9) for *n*-heptane. Table 2 presents a quantitative assessment of the predicted equilibrium constants of individual complexes with respect to the mean relative error ($\bar{e}$,%) and root-mean-square deviation

(σ) of Z_t factor. The model consistency was also studied through a plot of modelled values against observed performance (Figure 3).

Table 2 Extraction constants of Equation (3), root-mean-square deviation (σ) and mean relative error ($\bar{e}$)[a] of chemodel estimates for nicotinic acid-amine complexation

Diluent		$\beta'_{pq};(p,q)$ - comp I	$\beta'_{pq};(p,q)$ - comp II	$\sigma(Z_t)$	$\bar{e},\%$ [a]
n-heptane	T[b]	1.4465×10^{2} (1,2)	2.2182×10^{12} (1,9)	0.004	3.11
	S[b]	1.2045×10^{5} (1,4)		0.008	8.85
1,2-DCE	S	7.4728×10^{1} (1,1)		0.183	26.43
MIBK	T	4.4954×10^{1} (1,1)	1.3609×10^{5} (2,3)	0.084	15.98
	S	1.2021×10^{7} (2,3)		0.220	22.39
cyclopentanol	T	1.2064×10^{4} (1,2)	1.8103×10^{5} (2,3)	0.225	12.32
	S	1.4611×10^{4} (1,2)		0.232	16.68

[a] $\bar{e}=(100/N)\sum_{N=1}^{N}\left|\left(Z_{t,\mathrm{obs}}-Z_{t,\mathrm{cal}}\right)/Z_{t,\mathrm{obs}}\right|$; [b] one (S) or two (T) complex formation (T in fig. 3)

NOMENCLATURE

$\overline{C_{AM}}$	= not complexed concentration of amine in organic phase, [mol/l]
$\overline{C^{\circ}_{AM}}$	= initial concentration of amine in solvent mixture, [mol/l]
$\overline{C_d}$	= concentration of the acid portion extracted by the diluent, [mol/l]
C_{HA}	= concentration of nondissociated acid in the aqueous phase, [mol/l]
$\overline{C_{HA}}$	= concentration of acid complexed with amine, [mol/l]
$C_{TA};\overline{C_{TA}}$	= overall concentrations of acid in aqueous and organic phases, respectively, [mol/l]
C°_{TA}	= initial concentration of acid, [mol/l]
$\overline{C^{s}_{TA}}$	= concentration of acid extracted by the diluent alone, [mol/l]
D_o	= distribution ratio related to the diluent alone
E	= degree of extraction, (extracted acid/initial acid), [%]
HA	= monocarboxylic acid
p	= number of acid molecules involved in complex
q	= number of amine molecules involved in complex
NR_3	= tertiary amine
v	= percentage volume of diluent in the solvent mixture, [%]
z	= associated number
$Z_s;Z_t$	= stoichiometric and overall loading of amine, respectively
$\overline{\text{(overbar)}}$	= related to the species in the organic phase

Greek letters

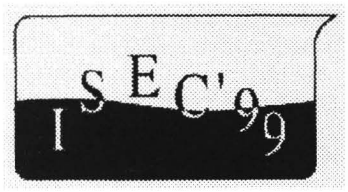
β'_{pq}	= apparent equilibrium extraction constant, Eq. (3), $[(\mathrm{mol/l})^{1-p-d}]$
β_z	= apparent equilibrium extraction constant, Eq. (4a), $[(\mathrm{mol/l})^{-z}]$
σ	= root-mean-square deviation

<Subscripts>

AM	= amine
HA	= nondissociated acid
TA	= total acid

REFERENCES

1. Tamada JA, Kertes AS and King CJ, *Ind. Eng. Chem. Res.*, **29**, 1319 (1990)
2. Tamada JA and King CJ, *Ind. Eng. Chem. Res.*, **29**, 1327 (1990)
3. Yang S-T, White SA and Hsu S-T, *Ind. Eng. Chem. Res.*, **30**, 1335 (1991)
4. Bízek V, Horácek J and Koušová M, *Chem. Eng. Sci.*, **48**, 1447 (1993)
5. Poposka FA, Nikolovski K and Tomovska R, *J. Chem. Eng. Jpn*, **30**, 777 (1997)



SEPARATION OF PHENOL FROM AQUEOUS SOLUTION BY PREDISPERSED SOLVENT EXTRACTION

Yun-Dong Wang, Min Chen, Lilian Xu and You-Yuan Dai
Solvent Extraction Laboratory, The State Key Laboratory of Chemical Engineering, Department of Chemical Engineering, Tsinghua University, Beijing 100084, China

ABSTRACT
Predispersed solvent extraction (PDSE) is a new efficient and prompt method for separating solutes from aqueous solution by solvent extraction and has shown to be promising for extraction from extremely dilute solutions. This technique comprises of the use of colloidal liquid aphrons (CLA) together with colloidal gas aphrons (CGA). The use of colloidal liquid aphrons in predispersed solvent extraction may ameliorate the problems such as emulsion formation, reduction of interfacial mass-transfer and low interfacial mass transfer areas in solvent extraction process. The aim of this work is to experimentally prepare the CLA and CGA and to investigate extraction equilibrium of solutes by PDSE process in semibatch extraction columns. Colloidal liquid aphrons are successfully prepared using kerosene as solvent, tributyl phosphate (TBP) as extractant, sodium dodecylbenzene sulphate (SDBS) as a surfactant in aqueous phase and Tween-20 and polyoxyethylene sorbitane monooleate (Tween-80) in oil phase. Colloidal liquid aphrons are also generated using hexadecyltrimethyl ammonium bromide (HTAB), SDBS and Tween-80 as surfactants. It has been found that the PDSE process is more suitable for extraction of dilute solutions. In addition, PDSE process has a great advantage over traditional single-stage extraction process.

Keyword: predispersed solvent extraction, aphrons, phenol, TBP, surfactant, Tween 80, sodium dodecylbenzene sulphate

INTRODUCTION

Predispersed Solvent Extraction PDSE is a novel technique, which intensifies conventional aqueous two-phase extraction by conversion of dispersed phase (usually the oil phase) into minute droplets called colloidal liquid aphrons. An essential feature of the technique is the buoying of the CLA's to the surface by a flotation process using colloidal gas aphrons (CGA). Two unusual factors that PDSE differs from the conventional solvent extraction are: 1) There is no need for a mixing-settling stage; 2) The ratio of extorting solvent to pregnant solution can be very low, of the order of one to 1 thousand or even lower.[1] The use of CLA's together with CGA's may circumvent the problems such as emulsion formation, reduction of interfacial mass transfer and low interfacial mass transfer areas in separating bioproducts by solvent extraction.[2]

By now, most of the works reported in literatures are in the field of preparing CGA's and CLA's, as well as selection of suitable surfactant, determination of the surfactant concentration and effect of various operation parameters on the CLA's and CGA's sizes and stability.[2-5] Though in an exploiting stage, PDSE is tentatively used widely. Chaphalkar et al[6] and Honeycutt et al[7] used CGA's to harvest bioproducts. Roy et al[8] separated organic dyes from wastewater qualitatively using CGA's. Mention should be made to Save and Pangarkar,[9] who conversed one phase in conventional aqueous two-phase extraction to CGA's to intensify mass transfer. Some other researchers successfully applied CLA's to their separation processes. Lye and Stuckey[10] used CLA's for the extraction and stripping of the antibiotic erythromycin-A. Zhang et al[11,12] studied the preparation, characteristics of colloidal liquid aphrons and colloidal gas aphrons and flotation of a hydrophobic organic dye from wastewater by using PDSE process in semi-batch and continuous countercurrent extraction columns. Limbs and Stuckey[13] used CLA's to immobilise β-galactsidase. Noble and Varley,[14] Jauregi et al[15,16] used CGA's produced from non-ionic surfactants to recover proteins. Noble et al[17] also compared the foam separation to colloidal gas aphrons as potential applications for protein recovery in downstream processing. Recently, Lye and Stuckey[18] investigated the structure and stability of colloidal liquid aphrons using various experimental techniques. Their findings support the structure model proposed by Sebba[1] who suggested that polyaphron (the aggregate of CLA's) phases resemble a biliquid foam while the individual CLA's, when dispersed in a continuous aqueous phase consist of spherical, micro-sized oil droplets surrounded by a thin aqueous "soapy-shell". Hashim et al[19] used CGA's to

© 2000 Society of Chemical Industry

clarify baker's yeast suspension using benzyl dimethyl hexadecyl ammonium chloride as a surfactant. Hashim and SenGupta[20] used CGA's to separate fine fibre from a lean slurry of cellulosic pulp in a flotation column. The pulp fibres were recovered as a foamate from the top. Sodium dodecyl sulphate having a concentration of 2.0 Kg/m^3 was used as a surfactant to generate CGA's in a spinning disc apparatus. The results indicated that up to 70% flotation efficiency could be obtained with a short column height of 0.3~0.35 m. The authors of this paper have performed a substantial research on CLA's and CGA's preparation and characterisation[21,22,24] as well as extractions using CLA's and CGA's.[23,25] The aim of this work is to study the extraction of PDSE process in a semi-batch extraction column and factors affecting the extraction efficiency.

EXPERIMENTAL

Reagents

The solvent used in this work is kerosene (Lanzhou Refinery Plant), the extractant is TBP (tributyl phosphate), and the solute is phenol (AR, Beijing Chemicals Company). The surfactant used were SDBS (sodium dodecyl benzene sulphate, 98.5%), HTAB (hexadecyltrimethyl ammonium bromide, 99%), Tween 80 (polyoxyenthlene sorbitane monooleate).

CLA's and CGA's preparation

To prepare CLA's, the oil phase (50-100 cm^3) containing non-ionic surfactant was gradually added (4 cm^3/min) into a foaming aqueous ionic surfactant solution using a mechanical stirrer at a stirring speed of 700 rpm. The volume ratio of the oil phase to the aqueous phase is defined as the phase volume ratio (PVR). CGA's were generated in an apparatus similar to the one described by Sebba.[26] The generator comprises of a beaker containing 300 cm^3 of aqueous surfactant solution and a stirrer. The solution is stirred at a high speed of 4500 rpm until creamy CGA's were generated. In the PDSE experiments, CGA's were generated *in situ*.

Extraction apparatus and procedure

The extraction equilibrium experiments were performed by contacting aqueous phenol solution with CLA's in a conical flask in a water bath shaker at room temperature (25 ± 0.1°C) for half an hour, keeping a vibration frequency of 200 rpm. After filtration, the phenol concentration in the aqueous phase was measured by UV-visible spectroscopy (HP-8452 UV Spectroscopy). The phenol concentration in the oil phase was then calculated by subtracting the initial phenol concentration with that of the aqueous one at equilibrium. Semi-batch PDSE experiments were carried out in an apparatus described elsewhere.[25] The glass column has a diameter of 5 cm and a height of 150 cm. The initial volume of the phenol solution is 1 dm^3 with concentration ranging from 50 ppm to 2000 ppm. Diluted colloidal liquid aphrons were pumped into the column at a rate of 20 cm^3/min with different CLA's to liquid volume ratio. CGA's, which were 100 to 400 cm^3 at a flow rate between 10 and 30 cm^3/min, were introduced into the column after 5 minutes of completion of CLA's introduction. The thin layer of oil phase containing solute – phenol appeared in the upper part of the column. Samples were collected from the sampling ports at different heights of the column and were analysed after a simple filtration.

RESULTS AND DISCUSSION

When CLA's were prepared, some non-ionic surfactant should be added to the oil phase to maintain the spreading pressure of oil greater than that produced by the surfactant dissolved in water. Figure 1 shows the changes of partitioning coefficients with the surfactant concentrations in oil phase. It has been seen that the partitioning coefficient changes around 10%, which shows that the presence of oil surfactant will not affect the equilibrium of these experiments greatly.

Figure 2 shows the phenol concentration in aqueous phase with extraction time in PDSE process using only CLA's. For two different initial phenol concentrations (100 ppm and 500 ppm), phenol

concentrations drop sharply within 10 minutes of time and then level off for the rest of extraction time, which shows that the majority of the extraction takes place only about 10 minutes.

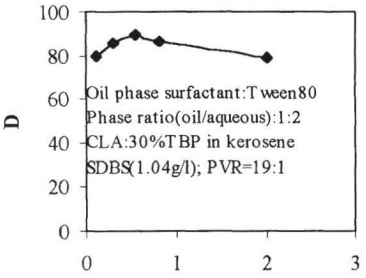


Figure 1 Effect of oil-soluble surfactant concentrations on the extraction equilibrium

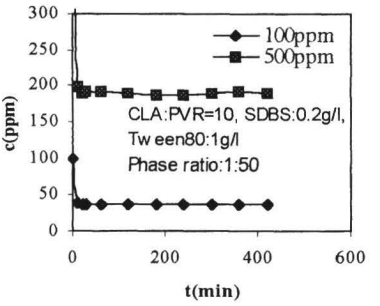


Figure 2 Phenol concentration in aqueous phase versus extraction time

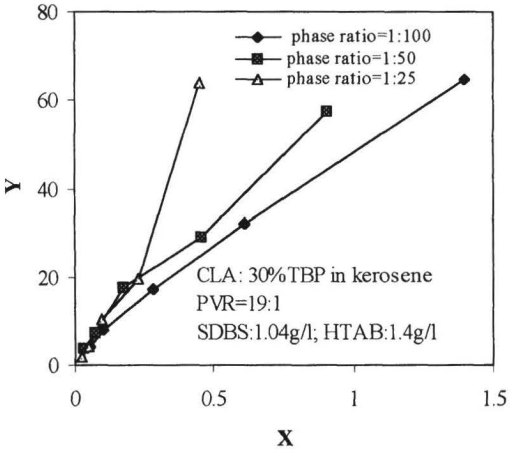


Figure 3 Equilibrium curves at different phase ratios for PDSE process

There exists a linear relationship between phenol concentrations in aqueous phase and in oil phase as shown in Figure 3. High oil to aqueous phase ratio will result in a high partitioning.

Extraction efficiency increases with decrease of initial solute concentration. Higher oil to aqueous phase ratio results in higher extraction efficiency. When oil to aqueous phase ratio changes from 0.005 to 0.04 (Fig. 4), the extraction efficiency increases nearly four times.

The phase volume ratio (PVR) in CLAs preparation also has some effect on extraction but is moderate as compared to the oil to aqueous phase ratio (Figure 5).

Figures 6 and 7 illustrate the effects of the amount of CGA's and its flow rate on the PDSE process efficiency. It was found that the overall percentage of phenol removal increases with increase of CGA's amount, but not quite significantly. When CGA's increase to a certain amount, most of the parts of CLA's are adsorbed by CGA's. The excess CGA's cause the back mixing in the column, which prolongs the residence time of CGA's in the solution and increase the possibility of CGA's breakage, which causes CLA to entry backs to the solution. Therefore, the amount of CGA's added to the solution must be optimised. The flow rate of CGA's is also has an optimised value where the

extraction efficiency reaches its maximum. High flow rate of CGAs may produce a channelling flow in the column which, consequently, results in a poor flotation of CLAs.

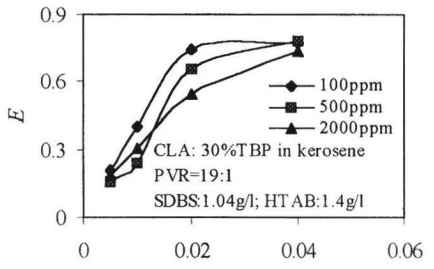


Figure 4 Oil to aqueous phase ratio versus extraction efficiency at different initial phenol concentrations

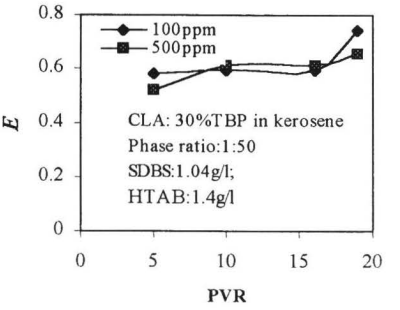


Figure 5 PVR versus extraction efficiency at different initial phenol concentrations

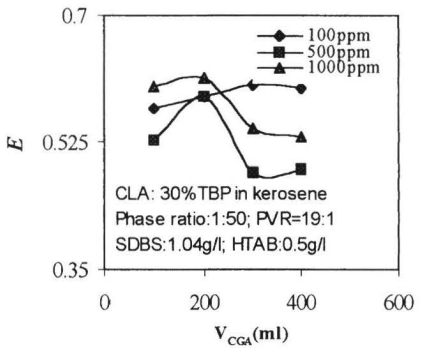


Figure 6 Effect of the CGA volume on the extraction efficiency at various initial phenol concentractions

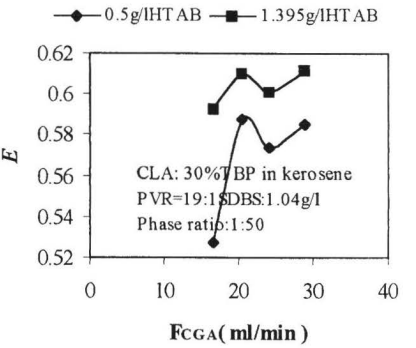


Figure 7 Effect of CGA flow rate on extraction efficiency

CONCLUSIONS

Colloidal liquid aphrons and colloidal gas aphrons have been prepared and used to separate phenol from aqueous solution. Results from semi-batch experiments showed that the initial phase volume ratio in CLA's and oil to aqueous phase ratio affect the separation performance. The PDSE process is also dependent on the amount of CGA's introduced and the flow rate of CGA's and, hence, CGA value and flow rate for the process were optimised.

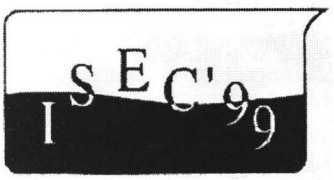
REFERENCES

1 Sebba F. *Chemistry and Industry*, 185, (1987).
2 Stuckey DC. Solvent extraction in Biotechnology, *ISEC'96*, Melbourne, Australia, 25, (1996)..
3 Sebba F. *Chemistry and Industry*, 367, (1984).
4 Matsushita K, Mollah AH, Stuckey DC, del Cerro C and Bailey AI. *Colloids and Surfaces*, **69**, 65, (1992).
5 Amiri MC and Woodburn ET. *Trans IChemE*, **68. Part A**, 154, (1990).
6 Chaphalkar PG, Valsaraj KT and Roy D. *Sep. Sci. Technol.*, **28**, 1287, (1993).

7 Honeycutt SS, Wallis DA and Sebba F. *Biotechnol. and Bioeng. Symp.* **13**, 567, (1983).
8 Roy D, Valsaraj KT and Kottai SA. *Sep. Sci. Technol.*, **27**, 573, (1992).
9 Save SV and Pangarkar VG. *Biotechnol. and Bioeng.*, **41,** 72, (1993).
10 Lye GJ and Stuckey DC. *Proceedings ISEC'96*, Melbourne, Australia, 1399, (1996).
11 Zhang C, Valsaraj KT, Constant WD and Roy D. *Sep Sci Technol*, **31**,1059, (1996).
12 Zhang C, Valsaraj KT, Constant WD and Roy D. *Sep Sci Technol*, **31,**1463, (1996).
13 Lamb SB and Stuckey DC. *IChemE 1997 Jubilee Research Event*, Nottingham, UK, 917, (1997).
14 Noble MJ and Varley J. *IChemE 1997 Jubilee Research Event*, Nottingham, UK, 873, (1997).
15 Jauregi P, Gilmour S and Varley J. *Chem. Eng. J.*, **65,** 1, (1997).
16 Jauregi P and Varley J. *Biotechnol. & Bioeng.*, **59,** 471, (1998).
17 Noble M, Brown A, Jauregi P, Kaul A and Varley J. *J. Chromatography B*, **711,** 31, (1998).
18 Lye GJ and Stuckey DC. *Colloidal and Surfaces A- Physicochemical and Engineering Aspects*, **131,** 119, (1998).
19 Hashim MA, SenGupta B, Kumar SV, Lim R, Lim SE and Tan CC. *J. Chem. Technol. Biotechnol.*, **71,** 335, (1998).
20 Hashim MA and SenGupta B. *Resource Technology*, **64,** 199, (1998).
21 Wang Y, Chen M, Xu L and Dai Y. *2nd China-USA Joint Conference of Chemical Engineering*, May 19-22, Beijing, China, (1997).
22 Wang Y, Chen M, Xu L and Dai Y. *Chem. Ind. Eng. Progr. (China)*, **6,** 1, (1997).
23 Wang Y, Chen M, Xu L and Dai Y. *IChemE 1997 Jubilee Research Event*, Nottingham, UK, 1049, (1997).
24 Wang Y, Chen M, Xu L and Dai Y. *J. of Tsinghua University (Science and Technology)*, **6**, 42, (1998).
25 Wang Y, Chen M, Xu L and Dai Y., submitted to *Separation Science and Technology*, (1998).
26 Sebba F. *Chemistry and Industry*, 91, (1985).



Extraction Equipment and Design



THE AP COLUMN – DEVELOPMENT OF A HIGH CAPACITY EXTRACTION COLUMN

RW Cusack, DJ Glatz, TL Holmes
Koch Process Technologies Inc, 1055 Parsippany Blvd Parsippany, NJ 07054, USA

ABSTRACT
A new agitated liquid-liquid extraction column (AP Column) has been developed, which offers improved efficiency and higher capacity than the rotating disc contactor (RDC) Column. Direct comparison of the AP Column vs. the RDC Column has been demonstrated on a pilot scale for both a standard test system (toluene/acetone/water) and an actual operating plant system (caprolactam process). In addition, scale-up criteria for the AP Column have been developed using 3" diameter and 11½" diameter columns.

Keywords: agitated column, scale-up, column design, toluene/acetone/water system, caprolactam process

INTRODUCTION

Rotating Disc Contactors (RDC) have historically been used for many industrial liquid-liquid extraction (LLE) applications such as lube oil extraction, phenol extraction, and caprolactam production. Originally designed for refinery applications, the RDC offers a simple design with a large amount of free area. This was well suited for these applications which involved viscous and fouling fluids and did not require a large number of theoretical stages. When applied to more conventional aqueous/organic extraction application, however, the RDC suffers from poor efficiency, typically operating at 10 - 15% stage efficiency. This is primarily due to severe axial mixing in the RDC column, especially in large commercial size columns. In addition, the RDC capacity is relatively low, (typically at 20 - 30 m^3/m^2hr), and the column is prone to flooding by emulsification of the phases due to the high sheer action of the rotating discs.

In 1987, the authors presented a paper at the AIChE Summer National Meeting entitled "Performance Characteristics of Packed and Agitated Extraction Columns".[1] At that time, a 3" diameter RDC was compared to both the Scheibel Column (3" diameter with rotating impellers) and Karr Column (2" diameter with reciprocating plates) for the toluene-acetone-water system, and the following conclusions reached:

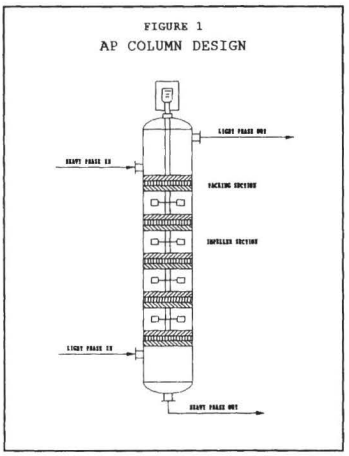
1. the Scheibel Column offers significantly improved efficiency, however it typically operates at lower capacity;
2. the Karr Column offers both improved efficiency and higher capacity.

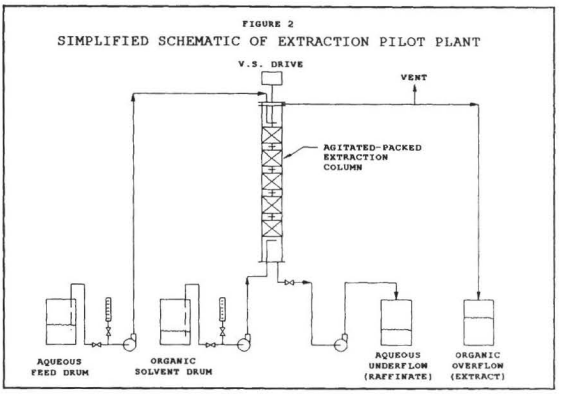
When evaluating existing extraction applications utilizing the RDC column, revamp using either the Scheibel or Karr is generally not practical. The reciprocating action of the Karr Column plate stack requires a true internal surface for the column, and the drive assembly is completely different than the RDC. Generally, plant revamps also require increased capacity, which cannot be achieved with Scheibel internals. For these reasons, the authors began to evaluate alternate internal designs which could be used as a replacement for the RDC internals to achieve both higher efficiency and higher capacity in the same size column

A new agitated extraction column design has been developed and has been named the AP Column. This design features a series of alternating packing and agitated stages, as shown in Figure 1. Extraction performance is maximized by:

1. minimizing axial mixing through the use of the packing stages;
2. maximizing the throughput via the high open flow area of the structured packing;
3. maximizing the mass transfer by supplying agitation to generate fine size dispersed phase drops, thus maximizing the interfacial area.

© 2000 Society of Chemical Industry





EXPERIMENTAL

Preliminary AP Column Testing

Initial pilot plant testing to evaluate the new AP Column was conducted using the standard test mixture (toluene-acetone-water). The pilot column was 3" diameter with a glass shell, and internals consisting of four (4) agitated stages and five (5) packing stages. A simplified schematic of the pilot plant set-up may be seen in Figure 2. The set-up is essentially identical to the set-up utilized earlier for the agitated and packed column comparison studies.

A series of pilot plant test runs generated the data shown Table 1. The optimal results for the 3" diameter AP Column have been plotted on the Stichlmair-Type Plot (Figure 3 for continuous to dispersed phase, c-d, mass transfer), which shows the performance of the pilot scale AP Column compared to the RDC. It shows for example, that at the rate of 20 m^3/m^2hr, the RDC develops 3.5 theoretical stages (TS) per meter while the AP Column develops 6.5 TS per meter. Also, the RDC reaches the flood point at approximately 25 m^3/m^2hr, while the AP Column extends out to 50 m^3/m^2hr.

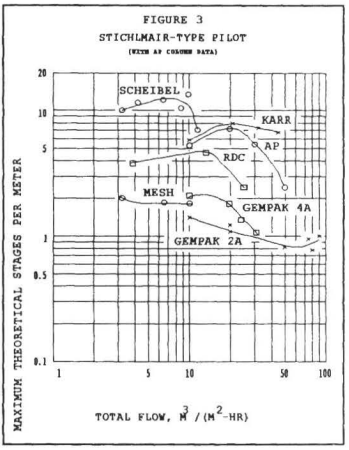


Table 1: Agitated-Packed Extraction Column Test Results Standard test system – toluene/acetone/water

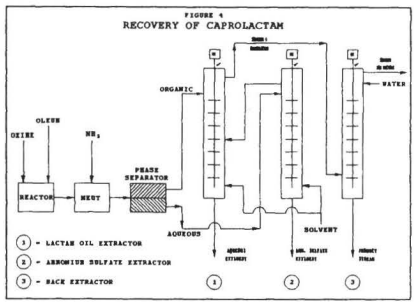
RUN # *	Packing Crimp Height (inch)	Total Flow ($m^3/(m^2h)$)	Agitation (rpm)	Theoretical Stages/meter (m^{-1})	Volumetric Efficiency (h^{-1})
1	0.375	10.00	1000	3.83	38.3
2	0.375	20.00	1000	5.91	118.2
3	0.375	30.00	700	5.43	162.9
4	0.375	40.00	600	4.67	186.8
5	0.375	49.89	300	2.11	105.5
6	0.5	10.58	1200	5.25	55.5
7	0.5	20.48	1500	7.14	146.2
8	0.5	30.73	675	5.09	156.4
9	0.5	41.01	475	2.74	112.4

AP Column For Caprolactam Process

Most caprolactam plants use a three (3) step LLE process for purification and recovery of caprolactam. The schematic for this process is shown in Figure 4. These columns are identified as follows:

- Ammonium Sulfate Extractor:

This column recovers caprolactam from the ammonium sulfate rich phase (approximately 1 - 1.5% leaving the phase separator downstream of the Beckman Rearrangement Reaction Section) by means of counter current extraction with toluene or benzene as the solvent.



- Lactam Oil Extractor:

This column recovers caprolactam from the lactam rich phase (approximately 70% caprolactam leaving the separator downstream of the Beckman Rearrangement) by means of counter current extraction with toluene or benzene

- Backwash Extractor:

This column is used to back extract the caprolactam from the solvent phase into fresh water.

The majority of the caprolactam plants use RDC columns for the each of the extraction steps mentioned above. These plants are essentially carbon copies of original designs developed over 25 years ago, and most have been operating for more than ten (10) years. World demand for caprolactam continues to be on a steady increase, primarily due to Nylon 6 requirements. To meet the increased caprolactam demand, these plants have incrementally increased the throughput in the extraction columns to levels above the design capacity, with a resulting loss in efficiency.

To evaluate the AP Column for the caprolactam process, actual ammonium sulfate and lactam oil feeds, plus solvent (benzene) were obtained from an operating caprolactam plant. Test were conducted over a two (2) month period, using a scale model of the RDC columns (3" diameter), along with a 3" AP column (same height as the RDC) to obtain direct comparison. Results from the test program on the each of the process steps are provided in Tables 2 - 4.

Table 2: AP Column and RDC Pilot Plant Data
Caprolactam Process – Ammonium sulphate column

Run No.	Type of Column	Flow Rate (cc/min) Feed	Solvent	Agitation (rpm)	Wt % caprolactam Feed	Solvent	Extract	Raffinate	caprolactam extracted %
AS-2	57 STG RDC	1090	470	900	1.09	0.13	3.05	0.0199	98.16
AS-4	57 STG RDC	1090	470	1000	1.17	0.13	3.69	0.0302	97.45
AS-7	57 STG RDC	1250	470	950	0.99	0.15	3.41	0.0296	97.15
AS-8	17 STG AP	1090	410	1100	0.92	0.0788	2.84	0.0335	96.3
AS-12	17 STG AP	1090	410	1000	0.8	0.0938	2.98	0.0608	92.04

These test data, and visual observation of the pilot plant column performance, reveal the following:

Ammonium Sulfate Column:

All runs between 100% and 125% of existing operating levels for both the 57 stage RDC and 17 stage AP columns produced similar results. Thus, it appears that this RDC is significantly over-designed for the ammonium sulfate extraction step. Unfortunately, higher rates were not attempted to determine whether or not the AP Column would demonstrate an advantage at rates significantly above design.

Lactam Oil Extractor:

For the 90 stage RDC, optimal performance at the existing operating conditions produced an aqueous raffinate with caprolactam concentration of 1.18%. Operation at 125% of the existing operating conditions resulted in an raffinate concentration of 3.43% caprolactam. The 25 stage AP Column (same height as RDC) generated a raffinate concentration of 0.3% caprolactam at both the existing operating conditions as well at 125%. Thus, the AP Column demonstrated both higher capacity and improved extraction efficiency for the lactam oil extraction step.

Backwash Extractor:

The backwash extraction step showed the highest sensitivity to emulsification and flooding of the three steps studied. The pilot, 90 stage RDC was operated at 75% and 100% of existing operating conditions, giving raffinate (organic) concentrations of 0.15% and 0.6% caprolactam, respectively. Attempts to operate the column at 125% were unsuccessful. Even at very low agitation, emulsification in the bottom section of the column resulted in an inoperable condition. The 25 stage AP Column was operated successfully at 100% and 125% of existing operating conditions, giving raffinate concentrations of 0.006% and 0.04% caprolactam, respectively. Thus, the AP Column is clearly superior to the RDC for the backwash extraction step. Not only does the AP Column provide higher extraction efficiency, it also minimizes the emulsion tendency, allowing trouble free operation.

Table 3: AP Column and RDC Pilot Plant Data

Caprolactam process – Lactam oil extractor

Run No.	Type of Column	Flow Rate (cc/min) Oil Feed	A.S. Benzene Solvent	Extract	Agitation (rpm)	Wt % Caprolactam Oil Feed	A.S. Benzene Extract	Solvent	Raffinate	Extr.	Caprolactam Extracted %
LO-4	90 STG RDC	480	340	1100	1000	84.4	2.62	0.1614	22.36	1.38	99.78
LO-5	90 STG RDC	480	340	1100	1050	76.11	3.61	0.1651	21.99	1.18	99.57
LO-7	90 STG RDC	600	425	1375	800	76.11	3.61	0.0536	19.93	3.43	99.05
LO-10	25 STG AP	480	340	1100	1200	74.43	3.2	0.0662	24.87	0.55	99.83
LO-11	25 STG AP	480	340	1100	1400	74.43	3.2	0.0298	24.81	0.3	99.93
LO-12	25 STG AP	600	425	1375	1200	74.43	3.2	0.0298	23.22	0.3	99.96

Table 4: AP Column and RDC Pilot Plant Data

Caprolactam process – Back extraction column

Run No.	Type of Column	Flow Rate (cc/min) Extr. Feed	Flow Rate (cc/min) ProcessWater	Agitation (rpm)	Wt% Caprolactam Feed	Solvent	Extract	Raffinate	Caprolactam Extracted %
BE-3	25 STG AP	1530	600	1000	22.43	0.0485	41.67	0.0064	99.98
BE-5	16 STG AP	1530	600	1000	22.94	0.0568	26.34	0.0427	99.85
BE-7	90 STG RDC	1150	450	525	20.51	0.0374	28.3	0.145	99.4
BE-8	90 STG RDC	1530	600	300	20.54	0.0374	29.08	0.5536	97.75

* COLUMN ON VERGE OF FLOODING

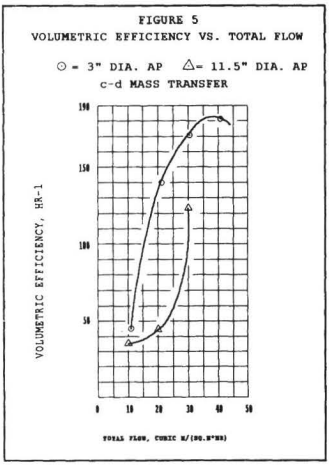
AP Column Scale-Up

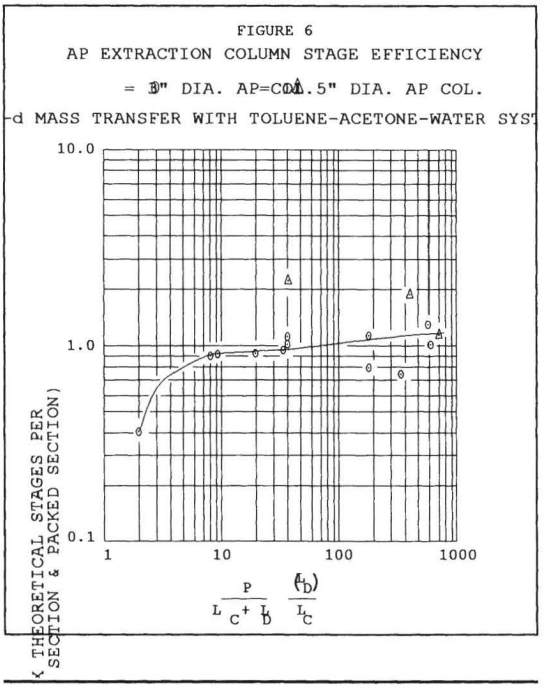
To verify the AP Column scale-up, 3" and 11½" diameter columns with five (5) agitated extraction stages were set up and the standard toluene-acetone-water system tested. Optimal pilot plant test results are shown in Table 5 for c-d mass transfer which was discussed previously for the 3" diameter x 4 stage AP column.

Table 5: Comparison of 3 and 11.5 inch AP Column Performance

Standard Test System – toluene/acetone/water

Run No *	AP Column Diameter (inch)	Total Flow $m^3/(m^2h)$	Agitation rpm	Theo. Stages Per Meter	Stage Efficiency %	Volumetric Efficiency (h^{-1})	$\frac{Pl_c}{L_c(L_c,L_b)}$ lb/fl²	P_T W_T (ft-lb₂)/lbₘ
S1	3	10.24	800	4.36	76.2	44.54	181	10.53
S2	3	20.47	1500	6.85	120	140.22	597	34.71
S3	3	30.72	700	6.33	111	170.52	40.4	2.35
S4	3	40.96	450	5.09	89.2	182.68	8.06	0.468
S5	11.5	10	300	3.56	189.4	35.5	422	24.59
S6	11.5	20	450	2.22	118.4	44.4	713	41.49
S7	11.5	30	200	4.09	217.6	122.7	41.8	2.43



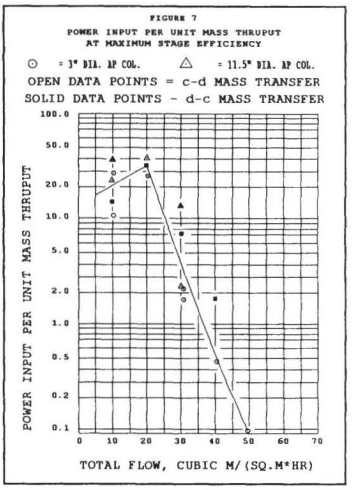


A plot of volumetric efficiency for the 3 and 11.5 inch AP columns may be seen in Figure 5. As discussed previously by Karr,[3] the number of theoretical stages per meter of column height for mechanically agitated column decreases with increasing column diameter.

To characterize AP Column extraction efficiency as a function of agitator power input, the following equation developed by Scheibel[4] for radial turbines was used. A plot of extraction column stage efficiency vs. power input per stage per unit of volumetric throughput may be seen in Figure 6.

$$P = \frac{1.85\, D^5 \alpha\, \rho \iota N^3}{g_c} \equiv \frac{\text{ft-lb}_f}{\text{sec}} \qquad (1)$$

As can be seen from this figure, the stage efficiency of the 11.5 inch diameter AP column is the same as or better than the 3 inch diameter column. Since 5 actual extraction stages were used here, the total power input is 5 times the value calculated from equation 1. A plot of total power per unit of total mass throughout as a function of total volumetric flow (m^3/m^2h) at optimum stage efficiency for both column diameters and both c-d and d-c mass transfer may be seen in Figure 7. For total flows below 20 m^3/m^2h the power input must be reduced to minimize back-mixing. Above $20m^3/m^2h$, the power must be reduced to prevent flooding.



CONCLUSIONS

1. The AP column has been developed from pilot plant tests with the toluene/acetone/water system.
   Increased extractor efficiencies at increased throughput are realized by:
   - minimizing axial mixing through the use of packing stages alternating with agitated stages
   - maximizing the throughput via the high open flow area of the structured packing
   - maximizing mass transfer with radial turbine agitators to generate minimum size dispersed phase drop size while maximizing holdup.
2. The AP column has been applied to the caprolactam recovery process via pilot plant tests with feeds and solvents from an actual operating plant. Test results indicate the following performance advantages as compared to presently used RDC columns:
   - equivalent performance of same sized RDC & AP columns was realized for the ammonium sulfate extractor step
   - same sized AP column provided capacity increases of 25% over RDC design rates for both the lactam oil extractor step and the water backwash step with a caprolactam concentrations in the raffinates well below target specifications
   - the RDC contractor was observed to readily form emulsions in the water backwash step which limited throughput in contrast to the nearly emulsion free AP column operation.
3. Scale-up of the AP column was considered by performing pilot plant tests with 3 and 11.5 inch ID columns using the toluene/acetone/water system. Over the 10-40 m^3/m^2h total flow range considered in this analysis, volumetric efficiency of both columns increased with increasing throughput, while the HETS of the larger column is higher as expected.
   AP extractor agitation power input analysis reveals:
   - at equivalent per stage power input per unit of volumetric throughput, the stage efficiency of the 11.5 inch diameter AP is equal to or greater than that of the 3 inch diameter AP column
   - total power input per unit of total of mass throughput at optimum stage efficiency as a function of total flow (m^3/m^2h) was observed to plot on a single curve for both column diameters and both c-d and d-c mass transfer. The maximum in the specific power input vs. throughput curve occurs at 20 m^3/m^2h. Below 20 m^3/m^2h power input was reduced to prevent backmixing, while above 20 m^3/m^2h power input was reduced to prevent flooding.

REFERENCES

1. Holmes TL, Karr AE, and Cusack RW. "Performance Characteristics of Packed and Agitated Extraction columns". Paper presented at the AIChE Summer National Meeting, Minneapolis, MN (1987).
2. Stichlmair J., *Chemie-Ingenieur-Technik*, **52**, 3 (1980).
3. Karr AE, *AIChE Journal*, **31(4)**, 690 (1985).
4. Scheibel EG, *AIChE Journal* **2(1)**, 74 (1956).

DEVELOPMENT OF A MULTISTAGE MIXER–SETTLER COLUMN WITH A NOVEL IMPELLER

Manabu Yamaguchi, Haruo Yamashita[1], Manpei Kaneda[2] and Hideo Noda[2]

Department of Mechanical Engineering Himeji Institute of Technology Himeji 671-2201, Japan

[1]Osaka University;

[2]Kansai Chemical Engineering Co.Ltd

ABSTRACT

A multi-stage mixer-settler column extractor with novel impellers was developed. The new impeller in the column was developed effectively to provide the functions of disintegrating one liquid and mixing between both phases during contact with the impeller which consists of a disc and static-mixers having a novel structure. The column consists of six stages separated by stator rings equipped with stainless steel mesh coated with Teflon. The effects of the impeller speed, and the flow rates of the continuous and dispersed phases on the hold-up fraction and the flooding flow rate of the dispersed phase were investigated using the system of toluene drops in water phase. The column performance for mass transfer was also investigated using the system of toluene/acetone/water under a variety of operating conditions and was evaluated by the number of theoretical stages per unit column height.

Keywords: mixer-setter column, column hold-up, column flooding, mass transfer, impeller design, toluene/acetone/water

INTRODUCTION

Research strategies of recent extraction equipment are classified into two groups.

1) One is the improvement and new development of the equipment. Some of them are improvement to the internal parts due to imperfect means of conventional contactors; changing the internal residence time required by the process and shortening the time required for separation of both phases.[5,7] The other is the development of novel equipment based on new concepts; application of electric fields to improve the hydrodynamics of the drops involving the breakage/coalescence balance and the interfacial flow of the drops[1, 10] and others.[3, 4]

2) Good understanding of single drop behavior within industrial equipment such as drop breakage, characteristic velocities and mass transfer is required for the more reasonable design of conventional equipment.[2, 9]

The present study is carried out with the objective of improving the contactor in the first group, that is, a novel impeller developed in the present work is devised to allow disintegrating of one liquid and mixing between both phases in the limited space on each stage. The new impeller consists of a special structure of static-mixers fixed on a disc. The dispersed and continuous phases flow through the channels of the static-mixers, and the dispersed phase is disintegrated into the continuous phase by twist shear flow which is produced by the two-phase flow through the static-mixer elements. The present paper presents the experimental results of the hydrodynamics and mass transfer in the vertical multistage mixer-settler column with an impeller.

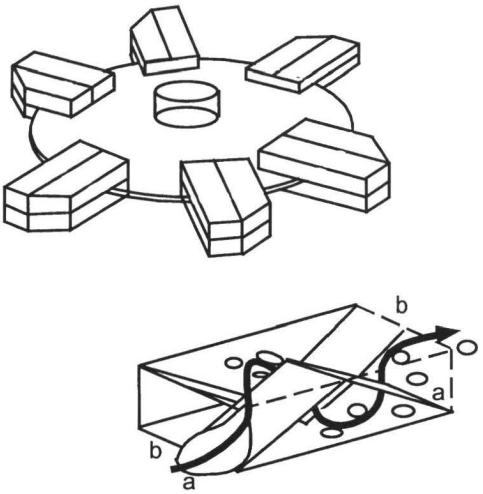


Figure 1 Schematic diagrams of impeller and structure of static mixer

© 2000 Society of Chemical Industry

EXPERIMENTAL STUDIES

Impeller and its construction

A schematic diagram of the impeller and structure of the novel static-mixer used in the present experiment is shown in Figure 1. A typical conventional static-mixer has 180 degrees helical elements with alternating right- and left-hand twists. As the elements are fixed in the tube, they divide the tube into two flow channels. As shown in the figure, the static-mixer element, two plates bent at 140 degrees are fixed side by side in a rectangular channel sized with a 10x10 mm cross section and 28 mm length. The impeller, 110 mm in diameter, is made of stainless steel and consists of a 78 mm diameter disc with 24 pieces of the mixer on the disc. The dispersed and continuous phases sucked by centrifugal force into channel 'a' change the flow direction into the next channel 'b' because of the end of channel 'a', and the change in the flow direction into the original channel 'a' again and then out. Both phases are sucked into channel 'b' flow in a similar manner as the flow pattern in channel 'a'. That is one of both phases flowing through the two channels of the static-mixer is disintegrated into the continuous phase by a twist shear flow which is produced by the static mixer elements at the middle position in the channel. During this flow process, disintegration of the dispersed phase, mixing between both phases and total residence time of both phases are controlled.

Experimental apparatus

The main section of the column consists of a 150 mm diameter, 570 mm high glass column divided into 6 compartments: a phase separation of both phases at the top of the column 100 mm high, 4 stages each 70 mm high, and a phase separation of both phases at the bottom of the column 185 mm high (thereafter called the top stage, 1st stage, 2nd stage, ..., and bottom stage). The diameter of the impellers, located 15 mm above the lower stator ring in each stage, is 110 mm and that of the stator opening is 110 mm. Each stator ring is equipped with a drop coalescer which is made of a stainless steel mesh coated with Teflon and with two downcomers of stainless steel bent into a U shape. Thus, the space in the stage is divided into a mixing zone and a coalescence zone except for the top and bottom of the column. In the experiment, fine droplets formed in the column were carried down with the continuous phase and accumulated at the bottom stage and, in the extreme case, they flowed out with the continuous phase due to entrainment. At the bottom stage, a stainless steel-like sponge layer was placed to prevent such entrainment. Each stage in the column was equipped with probes to sample the liquid phases. The probe was set at a suitable position above the impeller. The structure of the stage is shown in Figure 2.

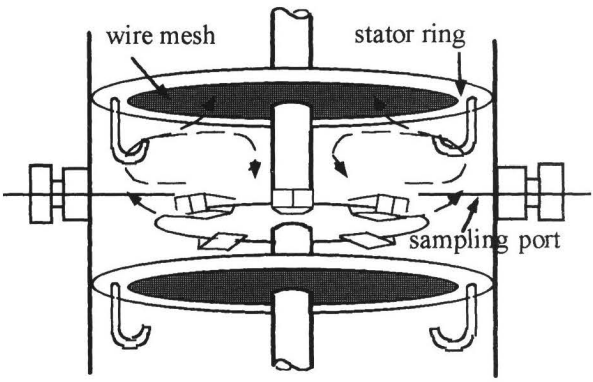


Figure 2 The structure of a stage

A single stage column was separately devised in order to observe the disintegration behavior of one liquid into the continuous phase within the static-mixer channels which is made of a transparent acrylic resin. To clarify the difference between the dispersed and continuous phases within the channels, the dispersed phase was colored and the behavior was observed using a TV system and photographs.

Experimental procedure

Hold-up fraction of dispersed phase:

The column was filled to a given level with water as the continuous phase which was fed at a given flow rate through the flowmeter from the top of the column. The impeller was rotated at a given speed, and the air in the column was exhausted. Toluene as the dispersed phase was fed at a given flow rate through the flowmeter from the bottom of the column. Each of the phases flowed countercurrent under a constant flow rate, and the exhausting rates of both phases, respectively, were controlled in order to keep a constant level of the dispersed phase/continuous phase interface in the top stage of the column. After the steady-state flow of both phases was maintained, the hold-up was measured using the following two methods. For the first method, the liquid phase in each stage was sampled by a syringe from each sampling probe, and the volume of both phases was measured using a volumetric cylinder; the hold-up fraction was defined as the ratio of dispersed phase volume to total volume of both phases. For the second method, after the feeding of both phases were simultaneously stopped, the dispersed phase was collected by intermittently rotating the impeller. A position of dispersed phase/continuous phase interface was measured and the total volume of dispersed phase in each stage was obtained; the ratio of dispersed phase volume to total volume of the 4 stage compartments was determined.

Flooding flow rate of dispersed phase:

When the feeding rate of the dispersed phase attained a critical value under a constant flow rate of the continuous phase and a constant impeller speed, the volume of the uncoalesced drops in the top stage of the column increased and forced the dispersed phase/continuous phase interface down, and finally the interface entered the 1st stage. This behavior made a steady state flow for both phases in the column impossible. Flooding was defined by this behavior.

Mass transfer:

The mass transfer characteristics were investigated using the water/acetone/toluene system which was recommended by EFCE. Mass transfer experiments were carried out under different flow rates for both phases and different revolutions of the impeller. As a part of the experimental conditions, a specific operating condition was chosen to compare the mass transfer performance of the present column with those of conventional contactors in the literature; a constant throughput ratio of 1 to 1.5 (water to toluene phase) was used. The experimental procedures were essentially the same as those in the hold-up experiment except for the liquid-liquid system used. After a steady-state flow for both phases was attained, the liquid phases at each stage were sampled using the probe, and the dispersed and continuous phases at the inlet and the outlet of the column were also sampled. After both the sampled phases were separated into the dispersed and continuous phases, respectively, they were rapidly moved by syringe into the sample bottles with a cover. The acetone concentration in each phase was measured using a gas chromatograph with a packing of polydivinylbenzene.

RESULTS AND DISCUSSION

Hold-up fraction of dispersed phase

A typical result of the experimental hold-up at each stage under constant flow rates of both phases is shown in Figure 3 with revolutions of impeller as a parameter. The hold-up in the 1st stage was the highest irrespective of the impeller speed. This is because the coalesced dispersed phase in the 1st stage was not sucked into the stage due to not having an impeller in the top stage. The hold-up increases with an increase in the impeller speed. This is because an increasing impeller speed caused the decreased drop size and drop rising velocity . The hold-up increased almost linearly with the flow rate of the dispersed phase, but it was the lowest in the 3rd stage. The effect of the continuous phase flow rate on the hold-up was slight. The fixation of the coalescer to disengage drops affected significantly the hold-up behavior. That is, the hold-up of the column equipped with the coalescer was about 50 % higher than that of the column without the coalescer. In addition to the hold-up behavior, the patterns of the drop size distribution in the column were distinctly different from with and without

the coalescer in the low speed region of the impeller, but those in high speed region of the impeller were not very difference. Based on the observations for flow behavior of both phase within the mixer channels, the mechanism of drop formation changed from a single drop formation from the liquid jet at the outlets of the channels, transitional unstable drop formation, to a stable drop formation within the channels depending on the impeller speed. Consequently, the size distribution of the drops changed from a unimodal profile via a bimodal one to a sharp unimodal with an increase in the impeller speed.

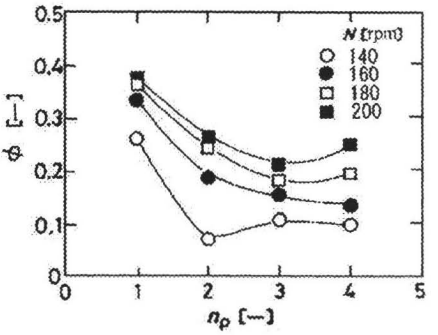


Figure 3 Holdup fraction of dispersed phase on each stage
Q_c=0.00104m^3/(m^{2}s), Q_d=0.00129m^3/(m^{2}s)

Flooding flow rate of dispersed phase

With an increase in the flow rate of the continuous phase, the flooding flow rate of dispersed phase decreased, while the flooding flow rate increased with impeller speed, and decreased through a maximum value at a critical impeller speed.

Mass transfer

The stage efficiency was close to 100% irrespective of the impeller speed and flow rate of both phases. This is because the test liquid used is a relatively easy one with rapid establishment of the phase equilibrium. The column performance was obtained using the Number of Theoretical Stages per Column Height which is often cited in the literature [6,8]; NTS/H [1/m]. Figure 4 shows a typical experimental result between NTS/H and impeller speed under the conditions of with and without the coalescer and constant total flow rate for both phases, 0.002 m^3/(m^{2}s), which maintained a constant throughput ratio of 1 to 1.5 (water to toluene phase).

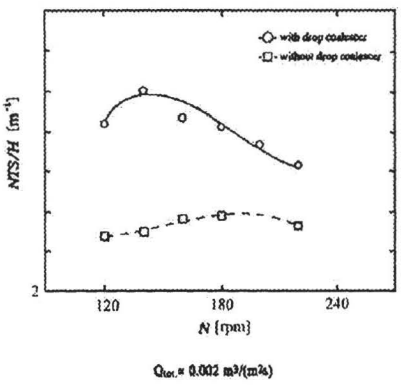


Figure 4 Effect of mass transfer on impeller speed with and without drop coalesce

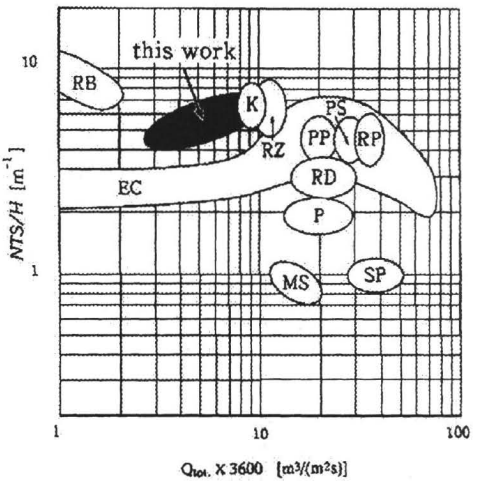


Figure 5 Comparison of mass transfer of different extractor

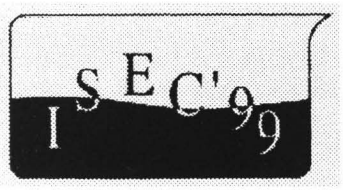
As shown in the figure, the effect of the coalescer on NTS/H is significant and interesting; the influence of impeller speed on NTS/H is reversed with and without the coalescer. The performance of the column equipped with the coalescer strongly depended on the impeller speed and decreased through a maximum value with impeller speed. The efficiency without the coalescer linearly increased with the impeller speed. This may be due to the differences in the dispersion degree and the axial backmixing. Consequently, the column performance with the coalescer will be improved by the position of the impeller because it is proposed that impeller position has a significantly influence the backmixing intensity and the residence time of the dispersed phase. The relation between NTS/H and the total flow rate of both phases is shown in Figure 5 in which the NTS/H of the present column is compared with those reported in the literature.

CONCLUSIONS

A vertical multistage mixer-settler column equipped with novel impellers was developed. The column's hydrodynamic and mass transfer characteristics were investigated using the water/acetone/toluene system. The impeller equipped with novel static-mixers effectively displayed the functions for disintegrating a dispersed phase through the channels of the mixers and mixing between both phases. The coalescers equipped with a stator ring on each stage also satisfactorily worked for disengaging a dispersed phase. The present column ensures performance that compares favorably with conventional extraction equipment.

REFERENCES

1. Bailes PJ and Mani IA, *Proc.ISEC'96*, 1143, (1996).
2. Godfrey JC, Miah A, Mohammed S, Patel R and Slater MJ, *Proc.ISEC'96*, 1203, (1996).
3. He W and Baird MHI, *Chem.Eng.Res.Des.*, **67**, 96, (1989).
4. Lee NN *US Patent 3410794*, (1968).
5. Steiner L, Stofel B, Schopf A and Hartland S *Proc.ISEC'96,* 1173, (1996).
6. Stichlmair J, *Chem.Ing.Tech.*, **52**, 253, (1980).
7. Suzuki J, Nii S and Takahashi K, *Proc.ISEC'96*, 1239, (1996).
8. von Fisher E, Steiner L and Hartland S, *Ger.Chem.Eng.*, **6**, 288, (1983).
9. Wagner G and Blass E, *Proc.ISEC'93*, 415, (1993).
10. Yamaguchi M, *Trans IChemE.*, **75**, Part A, 447, (1997).



DROP SIZE AND PHASE DISTRIBUTION IN EXTRACTION COLUMNS

Jörg Koch and Alfons Vogelpohl
Institut für Thermische Verfahrenstechnik, Technical University of Clausthal, Leibnizstr. 15 D-38678 Clausthal-Zellerfeld, Germany

ABSTRACT
Fundamental investigations of the distribution of the dispersed phase in a column cross section were carried out in a laboratory scale and a technical scale column. For the measurement of the local phase distribution, a new technique was applied. Also a new kind of distributor has been developed, which allows the control of the drop-size distribution generated by pulsing the dispersed phase inside a tubular distributor.

Keywords: column, drop size, phase distribution, distributor design

INTRODUCTION

Several advantages of extraction columns with structured packings have led to an increasing use of this type of packing in solvent extraction. In particular, the structure of the packing allows a high phase throughput in addition to a good separation efficiency due to a reduced backmixing. However, the separation efficiency of this kind of packing depends strongly on the primary distribution and the droplet size of the dispersed phase in the apparatus. The rise of the drops in structured packings follows the channels formed by the packing. Therefore, structured packings have a low capability for the radial distribution of the dispersed phase in the extraction column.[1] So the design of the distributor is one of the most important tasks for a high efficiency and a high phase throughput of a technical scale column.

The importance of an even distribution over a packed column cross-section increases with the diameter of the apparatus. Thus, to examine the efficiency of a distributor, the experiments should be made in a technical scale column, the drop-size distribution and the phase distribution over the column cross-section must be measured in dependence of the phase ratio and the flowrates. The characterisation of the two-dimensional phase-distribution in a column cross-section requires a new method of measurement, which was developed in the laboratory-scale column and applied in the technical-scale column.

The drop-size distribution generated by a distributor normally depends on the fluid velocity in the hole,[2,3] and thus on the flowrate of the dispersed phase. To achieve a drop-size independent of the fluid velocity, a second independent force is required to affect the drop formation. This force can be produced e.g. by the continuous phase as applied in the two phase nozzle.[4] Another approach is the generation of an impulse on the dispersed phase inside the distributor as a second parameter for the control of the drop-size. In this study, electromagnetic pulsation was used to generate the impulse.

EXPERIMENTAL

In all experiments deionised water was used as the continuous phase and Shell KS 111 or ShellSol D70 from the Shell Corporation as the dispersed organic phase. The physical properties are shown in Table 1. The drop-size was measured with the capillary suction method.[5]

Parameter	ShellSol D70	Shell KS 111
density ρ	798 kg m^{-3}	759 kg m^{-3}
viscosity μ	1.68 x 10^{-3} Pa s	1.60 x 10^{-3} Pa s
interfacial tension (water) λ	0.0342 N m^{-1}	0.0337 N m^{-1}

Table 1 Physical properties of the experimental substances

© 2000 Society of Chemical Industry

Laboratory scale setup

The laboratory scale apparatus consists of an extraction column (d_h = 190 mm, h = 800 mm) made from PMMA. The experiments were carried out with the continuous phase at rest. For several distributors, the drop-size and the phase distribution at the top of the column were measured in dependence of the volume flux of the dispersed phase. In addition, the effect of a pulsation of the dispersed phase inside the distributor was investigated.

As distributors, stainless steel tubes with an inner diameter of D = 34 mm and 21 holes with a diameter D_O = 2 mm respectively 19 and 37 holes with a diameter D_O = 3 mm were used. An electromagnetic pulsation device for the generation of the impulse on the dispersed phase is fixed to the distributor.

Technical scale setup

For the technical scale column (d_h = 600 mm, h = 3000 mm) only glass, stainless steel and PTFE were used to avoid corrosion by the experimental substances. A sieve plate ring-distributor with an inner diameter of 390 mm, an outer diameter of 460 mm and 2400 holes with a diameter of 1.5 mm was used for the first experiments. The distributor exists of two chambers. The dispersed phase enters the lower part which is separated from the upper one by a sieve plate with 20 holes with a D_O = 4 mm which causes a high pressure drop to pre-distribute the fluid over the whole distributor cross section. The main formation of the drops takes place in the upper chamber at the 2400 holes with D_O = 1.5 mm. In this way, a decoupling of the distribution of the dispersed phase over the distributor cross section and the formation of the drops is achieved.

In the experiments, the drop-size distribution and the phase distribution were measured at different heights above the distributor and with several phase ratios and flowrates of both the dispersed and the continuous phase.

Phase distribution measurement

The phase distribution over a column cross section is measured by a probe made from stainless steel which could be moved over the whole column cross section. The head of the probe is shown in Fig.1.

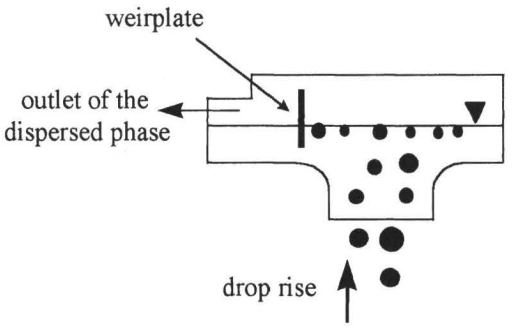


Figure 1. Measurement probe

The drops enter the head through the lower opening and coalesce, the weir plate hinders drops from entering the horizontal outlet so that the dispersed phase leaves the upper section of the outlet tube as a film. The film of the dispersed phase rises in the vertical tube to a separator, in which the fluid level is adjusted at the same level as in the column by an adjustable weir. Two solenoid valves can switch the outflow from the dispersed phase supply to a small vessel where the volume of the dispersed phase is measured. Thus an average value for the local volume flux of the dispersed phase inside the column can be calculated.

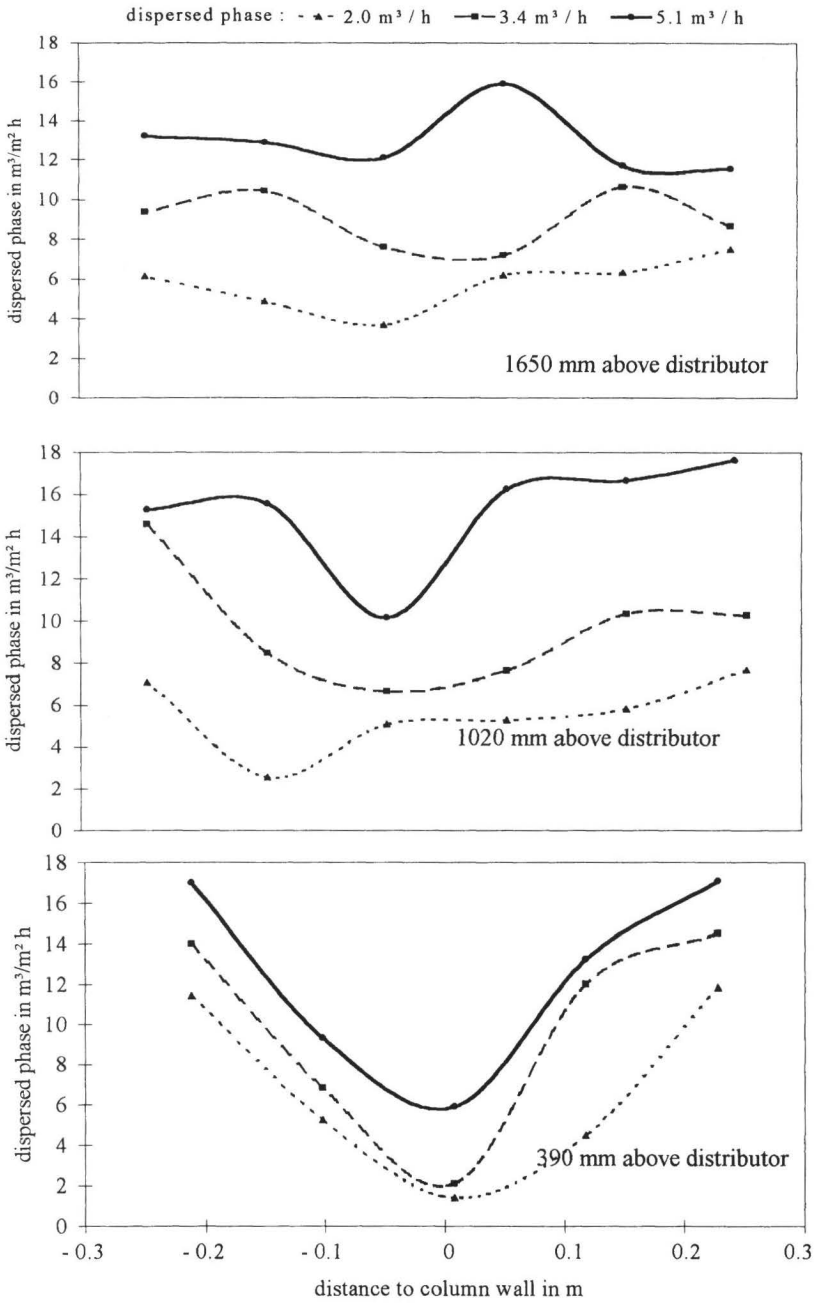


Figure 2. Phase distribution with continuous phase at rest

RESULTS AND DISCUSSION

Phase distribution

Figure 2 shows the local distribution of the dispersed phase at several heights above the distributor without countercurrent flow for three flowrates of the organic phase and without a packing. Because of the shape of the distributor, the distribution at the height of 390 mm is very uneven for all flowrates. With increasing distance from the distributor, the phase distribution becomes more and more even. The self-distribution of the dispersed phase is caused by vortices with a diameter up to the column diameter. At a distance of approximately 2.5 times the column diameter, the dispersed phase is distributed evenly over the cross section.

Figure 3 shows the results of similar experiments with countercurrent flow of the continuous phase. At a short distance above the distributor, the geometric shape of the distributor has the same influence on the phase distribution as discussed above. As distinct from the experiments without Figure 3 shows the results of similar experiments with countercurrent flow of the continuous phase. At a short distance above the distributor, the geometric shape of the distributor has the same influence on the phase distribution as discussed above. As distinct from the experiments without countercurrent flow, the dispersed phase is evenly distributed at a distance of 1.5 times the column diameter. The reduced drop velocity leads to a higher hold-up and, because of the increased drop-drop interaction, the distribution ability of the column increases.

Further experiments will show the influence of the structured packing on the drop-size and the phase distribution.

Pulsed distributor

Figure 4 shows the drop-size distribution generated by a tubular distributor with 21 holes and $D_O = 3$ mm for a Weber number of 9.8. Without pulsation, the drop-size distribution shows two maxima at 3.3 mm and at 4.2 mm. With a pulsation of 35 Hz, up to 80 % of all generated drops have a diameter between 4.6 and 4.8 mm, so the drop size distribution is nearly monodisperse. The pulsation frequency was calculated from the natural frequency of a liquid sphere[6,7]. The strongest effect of the pulsation on the drop formation was found for a pulsation frequency equal to the generation frequency of the drops or its half.

In future experiments, this type of distributor will be applied in the technical scale column and its technical suitability will be investigated.

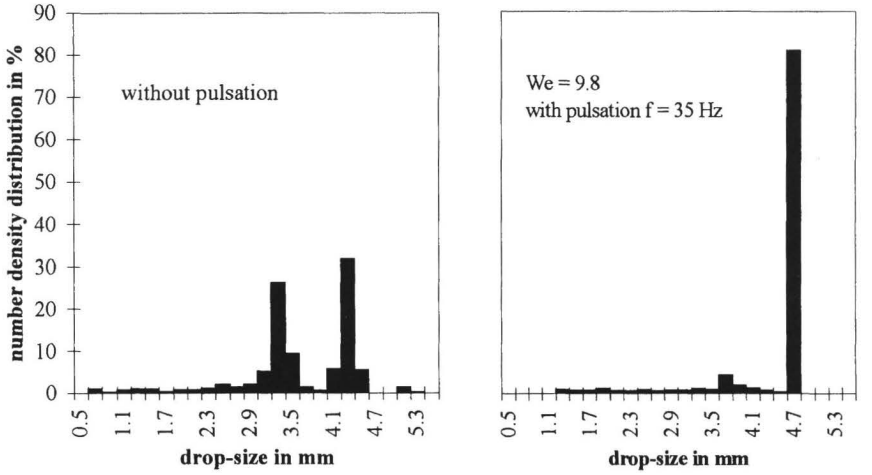


Figure 4. Drop-size distribution of the pulsed and unpulsed distributor

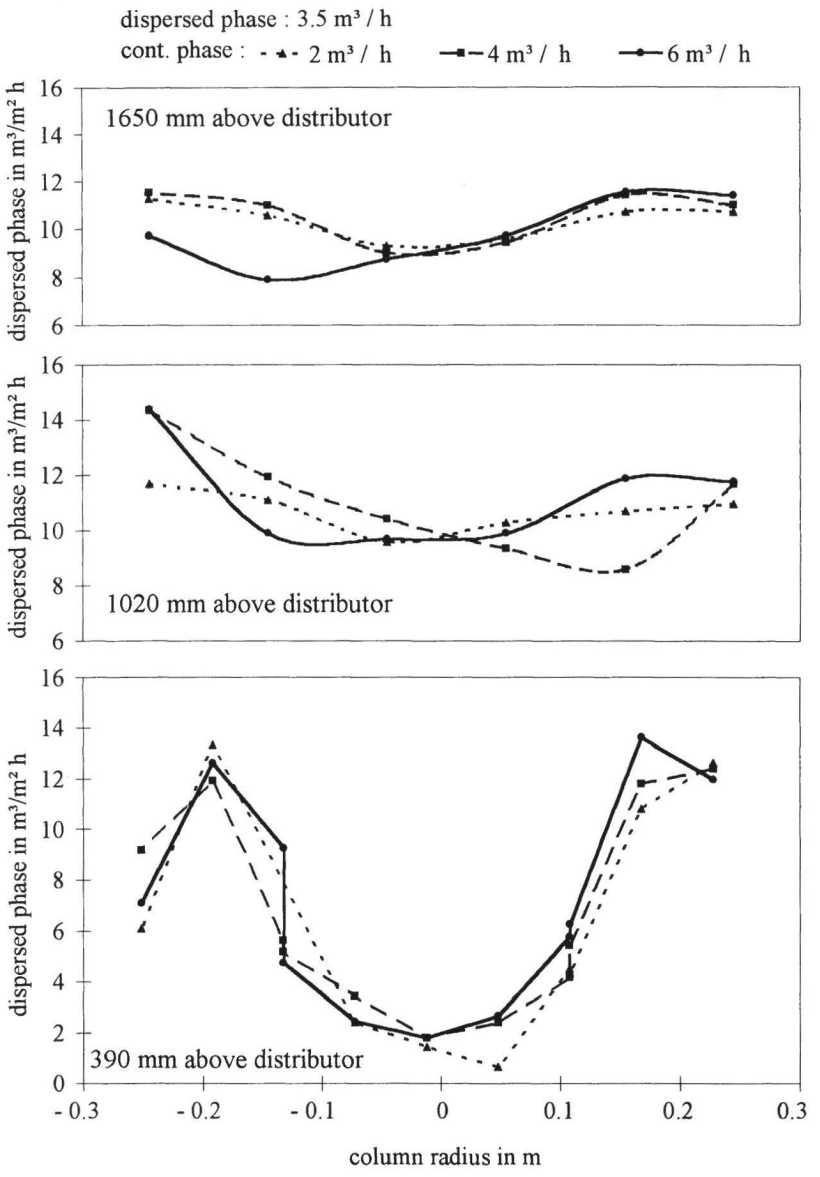


Figure 3. Phase distribution with countercurrent flow

REFERENCES

1. Leu JT, *Dissertation TU Clausthal* (1995)
2. Ruff K, *Chem.-Ing.-Techn.*, **6**, 441, (1978)
3. Dalinaros W, Kumar A and Hartland S, *Chem. Eng. Process*, **20**, 95, (1986)
4. Eckstein A and Vogelpohl A, *Chem.-Ing.-Techn.*, 1998, 12
5. Pillhofer T, *Chem.-Ing.-Techn.*, **46**, 149, (1974)
6. DePaoli DW, Scott TC and Basaran OA, *Sep. Sci. Techn.*, **27**, 2071, (1992)
7. DePaoli DW, Basaran OA, Feng JQ and Scott TC, *Sep. Sci. Techn.*, **23**, 1189, (1995)

THE APPLICATION OF ELECTRICAL CAPACITANCE TOMOGRAPHY TO LIQUID–LIQUID EXTRACTION COLUMNS

GT Bolton[1], WJ Korchinsky[1], RC Waterfall[2] and PD Martin[3]
[1] Department of Chemical Engineering, UMIST, PO Box 88, Manchester, M60 1QD, UK
[2] Department of Electrical Engineering, UMIST, PO Box 88, Manchester, M60 1QD, UK
[3] Separations Processes Service, AEA Technology plc, 404 Harwell, Didcot, Oxfordshire, OX11 0RA, UK

ABSTRACT
Process Tomography uses non-invasive sensors to obtain information on the contents within a process vessel or pipeline. Electrical Capacitance Tomography (ECT) utilises a capacitance measuring system to obtain images of dielectric components in process vessels or pipelines and has previously been used for imaging gas/oil flow in pipelines, flow regimes in pneumatic conveying systems and air bubbles in fluidised beds.
Multiple capacitance electrodes are arranged around the boundary of the region under investigation, resulting in a truly non-invasive and non-intrusive measurement technique. The measured capacitances for all possible combinations of pairs of electrodes give a 'body-scan' of the enclosed volume. An image reconstruction algorithm is used to generate a tomographic image (tomogram) of the dielectric distribution from the capacitance measurements which is converted to a variation in the process vessel's contents.
In this paper the application of this technique to liquid-liquid systems is described. The objective of the work is to apply ECT to the monitoring of dispersed phase distributions in liquid-liquid contactors. Results are very encouraging:
a) a suitable capacitance sensor has been designed.
b) accurate measurements of average dispersed phase volume fractions, or hold-up have been demonstrated.
c) mal-distributions of dispersed phase over a horizontal cross-section of a vessel have been illustrated.

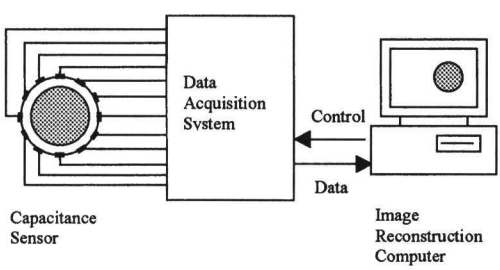
Keywords: tomography, capacitance imaging, dispersion, distribution, extraction columns

INTRODUCTION

Electrical Capacitance Tomography uses tomographic imaging methods to manipulate data obtained from capacitance electrodes to obtain precise quantitative information on processes containing multi-component mixtures. ECT has been successfully applied to a static system containing sand and air representing three common flow regimes: stratified, core and annular[1]. It has been used to obtain real time images of air bubbles within a fluidized bed[2] and it has been used to study the dilute-phase pneumatic conveying of granular solids[3].

A typical ECT system, as shown in Figure 1, consists of a capacitance sensor system to measure capacitance changes in the sensing zone, a data acquisition system to collect the sensor output signals and a computer for image reconstruction.

Figure 1 Electrical Capacitance Tomography System



© 2000 Society of Chemical Industry

The application of ECT to liquid-liquid dispersions could be a valuable tool in measuring dispersed phase hold-up, in identifying poor phase distributions and, in providing an indication of the approach to the column flooding point. An understanding of radial and axial mixing phenomena in extraction columns could follow.

EXPERIMENTAL

Flow Rig

The liquid-liquid contactor test facility (Figure 2) consisted of a 100 mm diameter glass section fitted with a polyethylene distributor with 1 mm diameter holes arranged on a 5 mm triangular pitch. Three different distributors were used in the experimental study. The first had holes perforated throughout its area and hence was expected to produce a uniform distribution of dispersed phase within the sensing zone. The remaining two were expected to produce non-uniform distributions of dispersed phase. One of these had 50% of its area perforated with holes and the remaining 50% had no holes, while the other had 25% of its area perforated with holes and the remaining 75% had no holes. A fixed speed pump was used to pump water from a reservoir through the distributor and column and back to the reservoir. A bypass from the pump back to the reservoir was fitted with a valve to allow control of the water flow rate.

Imaging System

The liquid-liquid contactor imaging system consisted of the three parts shown in Figure 1. A 12-electrode capacitance tomography sensor system was mounted 75 mm below the distributor, as shown in Figure 3. The sensor was fabricated of thin copper strips attached to the outer surface of the glass section. The height of the measuring electrodes was 50 mm, resulting in the image obtained being an average over this 50 mm height of the contactor. Driven-guard electrodes were placed above and below each capacitance electrode. These served to concentrate the electric field between the electrodes. The capacitance electrodes are surrounded (with a clearance of 20 mm) by a section of steel pipe to avoid external electrical interference.

To obtain quantitative images, the tomography system must be calibrated. For this study a new calibration procedure was developed[4]. Calibration was performed by filling the sensing zone consecutively with kerosene, then with acetic acid, in order to set the lower and upper limits of permittivity. When high permittivity material (water) is introduced into a low permittivity background (kerosene) within the sensing zone the capacitance measurements between electrode pairs will increase. An ECT system measures the capacitance changes and reconstructs a cross-sectional image from the capacitance data. It has been shown that the effective permittivity of a mixture of 2 liquids, one dispersed in the other, varies linearly with the volume fraction of the dispersed material for low values of volume fraction. Therefore, the calibration procedure described above produces good quality images for liquid-liquid dispersions containing up to 30 vol. % water in kerosene.

The measured signals from each pair of electrodes were proportional to the permittivity of water droplets in kerosene. Measurements were taken by applying a 15 V electrical potential to the electrodes. Capacitances between any two of the twelve electrodes were measured in all possible combinations, except for adjacent electrodes[4]. For a 12-electrode sensor system there are 54 independent pairs of electrodes (when adjacent pairs of electrodes are ignored). Hence for each image 54 independent measurements were taken. The data capture and image reconstruction time was 20 ms for one image.

An essential requirement of the imaging system is that the capacitance measuring circuit should only measure the capacitance between the selected pair of electrodes. It should be insensitive to stray capacitances between measuring electrodes and earth and due to the cable connecting the electrodes to the circuit itself. This is achieved by the charge/discharge capacitance measuring circuit[5]. The images were reconstructed from these boundary capacitance measurements by a modified linear-back projection algorithm[6]. Each image consisted of 812-pixels.

Figure 2. Flow rig facility

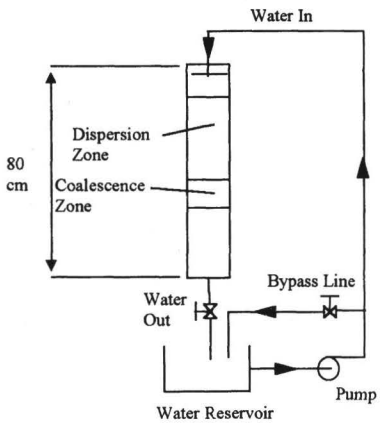
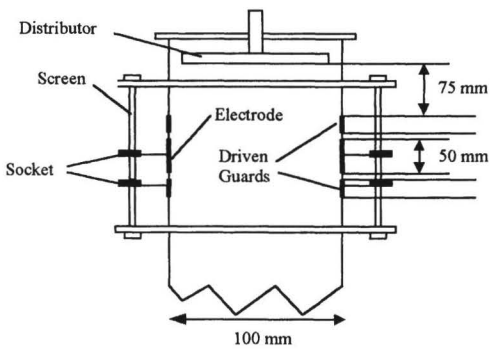


Figure 3. Detailed diagram of the capacitance sensor system



RESULTS AND DISCUSSION

Experiments were conducted for water dispersions in a continuous kerosene phase with no mass transfer. The continuous kerosene phase was stationary. Results are given here for three water superficial velocities (V_d). As previously described, three distributors were used to vary the uniformity of distribution.

Table 1 shows the average dispersed phase hold-up measured by the electrical capacitance tomography system. The figures in brackets are the values obtained in the usual way, from interface levels while the test column was running, and then after the pump had been shut down and the outlet valve closed, allowing the calculation of the volume of accumulated drops at the interface.

Table 1 Average dispersed phase hold-up measured by ECT system

	V_d = 0.44 cm/s	V_d = 0.73 cm/s	V_d = 1.1 cm/s
100% distributor area	0.05 (0.07)	0.11 (0.13)	0.15 (0.14)
50% distributor area	0.05 (0.05)	0.10 (0.10)	0.15 (0.13)
25% distributor area	0.03 (0.06)	0.10 (0.08)	0.13 (0.16)

Previous work[7], which used ECT to measure the average volume fraction of water in water/kerosene mixtures of known composition within a small, agitated vessel, demonstrated that for volume fractions between 0 and 0.3 the ECT measurements were accurate to within ±0.01. In this work it is not possible to accurately obtain a check of ECT results, but the comparisons in Table 1 are very encouraging.

Figures 4, 5 and 6 show three-dimensional surface plots, representing the distribution of dispersed phase hold-up within a cross-sectional plane of the test facility. Figure 4 shows the results for the distributor which had holes throughout its area. Figure 5 shows the results for the distributor which had holes on only 50% of its area (a semicircular distributor) and Figure 6 shows the results for the distributor which had holes on 25% of its area.

Figure 4 100% distributor a) V_d = 0.44cm/s b) V_d = 0.73 cm/s c) V_d = 1.1 cm/s

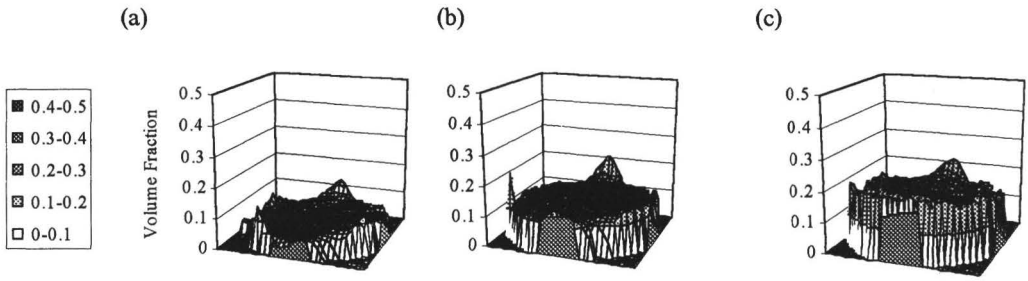


Figure 5 50% distributor free area a) V_d = 0.44 cm/s b) V_d = 0.73 cm/s c) V_d = 1.1 cm/s

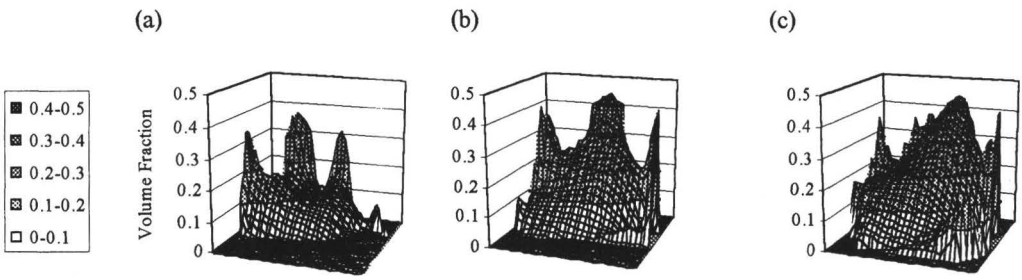
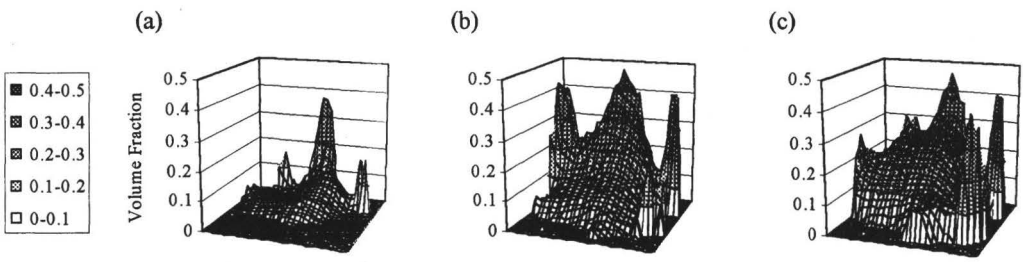


Figure 6 25% distributor free area a) V_d = 0.44 cm/s b) V_d = 0.73 cm/s c) V_d = 1.1 cm/s



It can be seen from Figure 4 that the distribution of dispersed phase is uniform over the measurement plane as expected. Figures 5 and 6 clearly confirm the poor, non-uniform, distributions of dispersed phase, caused by the blanked off distributors. A drawback of the linear-back projection algorithm is that it smears out sharp transitions in relative permittivity[8]. As a result these plots of dispersed phase volume fraction over a slice through the column, near to the distributor, may be blurred between areas of high and low dispersed phase hold-up resulting in these measurements being of a semi-quantitative nature. However, they do still clearly show non-uniform distributions of dispersed phase.

CONCLUSION

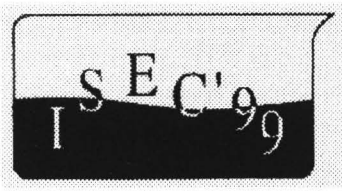
Highly promising results have been obtained for non-invasive measurement of dispersed phase distributions in liquid-liquid systems utilising Electrical Capacitance Tomography.

ACKNOWLEDGEMENTS

The authors acknowledge with thanks the financial support of the UK Engineering and Physical Sciences Research Council (EPSRC) and Separation Processes Service, AEA Technology through a co-operative award in science and engineering (CASE).

REFERENCES

1. Huang SM, Plaskowski AB, Xie CG and Beck MS, *J. Phys. E: Sci. Instrum.*, **22**, 173, (1989)
2. Wang SJ, Dyakowski T, Xie CG, Williams RA and Beck MS, *Chem. Eng. J.*, **56**, 95, (1995)
3. McKee SL, Williams RA, Dyakowski T and Bell TA, *Trans. IChemE, Part A*, **71**, 347, (1993)
4. Bolton GT, Korchinsky WJ and Waterfall RC, *Meas. Sci. Technol.*, **9(11)**, 1797, (1998)
5. Yang WQ, *Meas. Sci. Technol.*, 7(3), 225, (1996)
6. Xie CG, Huang SM, Hoyle BS, Thorn R, Lenn C, Snowden D and Beck MS, *IEE Proceedings-G*, **139(1),** 89, (1992)
7. Bolton GT, *PhD Thesis*, UMIST, 1998 (in preparation)
8. Isaken Ø, *Meas. Sci. Technol.*, 7(3), 325, (1996)



STUDY OF CHARACTERISTICS OF A PULSED PACKED COLUMN USING SUPER-MINI-RING (SMR)

Jie Yu and Weiyang Fei
Department of Chemical Engineering, Tsinghua University, Beijing 100084, China

ABSTRACT
The hydrodynamics and mass transfer of Pulsed Packed Column filled with Super Mini Ring (SMR) and Raschig ring have been studied using 30% TBP-kerosene (d) /acetic acid/water (c) system in a 100mm internal diameter column filled with 1m height packing. The mass transfer and axial mixing parameters were estimated simultaneously from the measured concentration profiles of two phases based on back flow model. It was found from the comparison among packings that SMR has superior characteristics both in terms of capacity and mass transfer efficiency. New empirical equations of characteristic velocity, H_{ox} and H_{oxd} were proposed.

Keywords: pulsed packed column, Super Mini Ring, Raschig ring, hydrodynamics, mass transfer, TBP-kerosene/acetic acid/water

INTRODUCTION

The pulsed packed column (PPC) uses pulsation to enhance its mass transfer. Therefore, it has excellent performance and has successfully applied in the industries.[1~3] Conventional packings such as Raschig rings were usually used for experiments and applications. Though many high efficiency packings have been developed in recent years, there is only a few reports on the characteristics and applications of PPC which use these new packings.[4~6]

The newly developed Super Mini Ring (SMR)[7] has three inner arches and very low high/diameter ratio (about 0.3), which could enhance the "dispersion-coalescence " recycle and control the non-ideal flow of the two phases inside the packing bed. Experiments[8] have shown that the SMR have lower axial mixing and higher mass transfer efficiency compared with many packings used in packed extraction column. The purpose of this paper is, therefore, to study the hydrodynamics and mass transfer of PPC using stainless steel (s.s.)SMR and then compare with those of ceramic and stainless steel (s.s.)Raschig rings.

EXPERIMENTAL

The experimental equipment is shown in Figure 1. The column, which was filled with packing of 1m height, has an internal diameter of 0.1m and was made of flanged glass. Five pairs of elaborate designed samplers were arranged in equal distance along the column, which assured pure samples of each phase could be obtained. Each phase was predistributed by a distributor before entering the packing bed. An air pulsation system was used. The pulsation amplitude was adjusted from $1s^{-1}$ to $2.33s^{-1}$ by pressure modulator and the pulsation frequency could be controlled from 0.005m to 0.0125m by a rotating valve.

Phase	ρ (Kg/m^3)	μ (mPa.s)	γ (mN/m)
Continuous phase	999.0	1.24	9.45
Dispersed phase	853.0	1.97	

Table 1 Physical Properties of Experimental System (15°C)

© 2000 Society of Chemical Industry

Packing	size (mm)	ε	a_p (m^2/m^3)
s.s. SMR	16x5.5x0.4	92.3%	384
ceramic Raschig ring	16×16×4	56.4%	272
s.s. Rachig ring	16×16×0.5	92.0%	350

Table 2 Properties Parameters of Different Packings

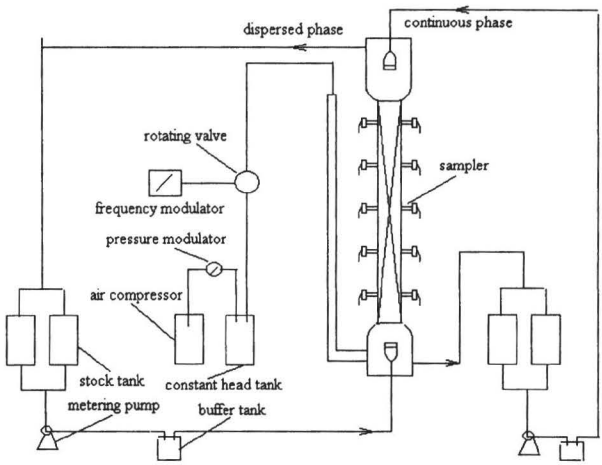


Figure 1. Diagram of experimental equipment

The experimental system was 30%TBP-kerosene/acetic acid/water, its physical properties are shown in Table 1.The equilibrium distribution of the system (15°C) is $y = 0.602x - 0.267x^2$. The properties of the packings used in this paper are shown in Table 2.

The dispersed phase hold-up was measured by the volumetric replacement technique. Flooding velocity was measured by keeping the continuous phase velocity constant and increasing the dispersed phase velocity 0.2mm/s each time until flood occurred.

During mass transfer experiments, the column was first operated into stable state after 5-6 column volume was replaced by streams of two phases. Then seven pairs of samples were collected at the inlets, outlets and along the column in 10 minutes. The samples were analysed by titration.

Data processing

Many kinds of model have been developed recent years since the important impact of axial mixing on the performance of solvent extraction columns. However, none of them is satisfied enough for the scale up of the commercial columns since the complicity of the two phase flow inside the column. Even for the latest developed Population Balance Model "should be considered only as useful guides, helpful for the description and the understanding of the operating conditions of all columns. Although such model clearly indicate a way forward, no confident scaling-up procedures have yet been developed".[9] The back flow model and diffusion model are still the most important and practical approaches for considering the influence of the axial mixing on the column performance. Therefore, they were used in this paper assuming constant flow rates and constant back flow ratios of two phases. The mass transfer and axial mixing parameters were estimated simultaneously from the measured concentration profiles of

two phases based on these models and combined with the maximum likelihood objective function and Marquardt's optimisation procedure.[10]

Packing	C_1	C_2	n
s.s. SMR	7.00	0.70	1.39
ceramic Raschig ring	13.31	0.87	0.64
s.s. Raschig ring	0.37	0.06	0.26

Table 3 Calculated Results of C_1,C_2 and n

RESULTS AND DISCUSSION

Characteristic velocity

The conception of characteristic velocity was proposed[11] to correlate the dispersed phase hold-up and velocity of two phases. It was found that this equation could be only used in the condition of low dispersed phase hold-up and no obvious coalescence. Several modified equations[12,13] which take account of the drop coalescence under high dispersed phase hold-up were developed. Since the pulsed packed column usually operated under high dispersed phase hold-up region, equation of Wang[12] was used in this paper.

$$\frac{U_d}{\varepsilon\phi} + \frac{U_c}{\varepsilon(1-\phi)} = U_0(1-\phi)^n \tag{1}$$

Since characteristic velocity in PPC decrease with the increase of pulsation intensity, an equation was developed to calculate characteristic velocity in PPC:

$$U_0 = 0.683\left(\frac{\varepsilon g}{a_p}\cdot\frac{\Delta\rho}{\rho}\right)^{0.5}\left[(1-C_1(af)^{C_2}\right] \tag{2}$$

where $0.683(\varepsilon g/a_p .\Delta\rho/\rho)$ is used to evaluate characteristic velocity in packed column[14] and C_1, C_2 and n are parameters evaluated from experimental data of pulsed packed extraction columns (see Table 3).

Flooding velocity

Different packings have different interaction with drops because of their difference in voidage, special area and geometry. Therefore, packing type has significant influence on flooding velocity. Figure 2 showed that flooding velocity of PPC filled with s.s. SMR was about 20% higher than that of PPC filled with ceramic Raschig ring. This is mainly because SMR has higher voidage than ceramic Raschig ring. Figure 2 also showed that flooding velocity decreases with the increase of pulsation intensity. Flooding velocity could be evaluated through characteristic as follows .in equations 3-5.

$$U_{df} = \varepsilon\cdot U_0\cdot(n+1)\cdot\phi_f^2\cdot(1-\phi_f)^n \tag{3}$$

$$U_{cf} = \varepsilon\cdot U_0\cdot(1-\phi_f)^{n+1}(1-(n+1)\phi_f) \tag{4}$$

$$\phi_f = 2/\left(n+2+\left(n^2+4(n+1)/L_R\right)^{1/2}\right) \tag{5}$$

Equation 2 was compared with that proposed by Simons.[3] Though Equation 2 is much simple than that of Simons and need not calculate the mean drop size beforehand, both of two equations give reasonable results for ceramic Raschig ring. The standard deviations are 12.2%, 16.8% respectively. However, when s.s. SMR are considered, there are big differences in calculation results (Figure 3). Calculated results by Equation 2 fit experimental data very well, whereas those by Simons' equation[3] are at least two times higher than experimental data. This is mainly because Simons' equation[3] were proposed only

for Raschig ring. It seems that Simons' equation is difficult to use for high voidage, high efficiency packings.

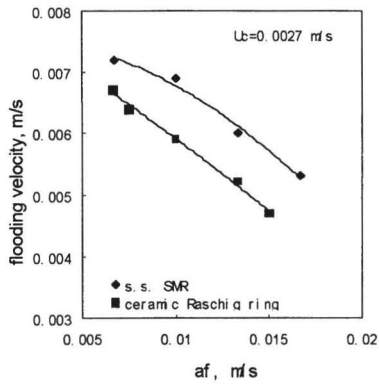


Figure 2. Effect of packing on flooding velocity.

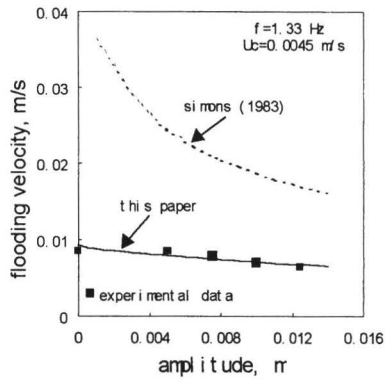


Figure 3. Comparison of flooding velocity between experimental and calculated data

Mass transfer

It is clear from the observation during the experiments that the mean drop size decreases with pulsation. Therefore, the pulsation intensity has great influence on H_{ox} and H_{oxp} (Figure 4).

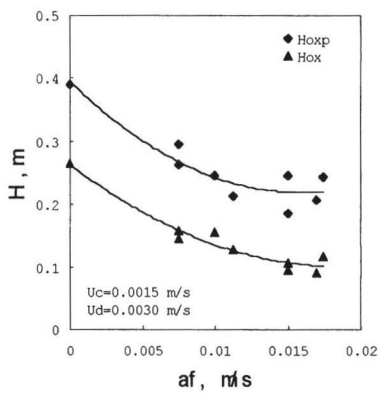


Figure 4, Effect of pulsation intensity on H_{ox} and H_{oxp} (s.s. SMR)

Compared with non-pulsation condition, H_{ox} and H_{oxp} decrease more than 50% under the optimal pulsation condition. Regressed 30 groups of s.s. SMR experimental data by Marquardt's optimisation method, the following equation were developed:

$$H_{ox} = 1.12 * (\frac{af}{U_d})^{-0.65} (L_R)^{-1.62} \quad (6)$$

$$H_{oxd} = 0.093 * (\frac{af}{U_d})^{0.20} (L_R)^{-0.32} \quad (7)$$

Therefore, H_{oxp} could be evaluated by the following equation:

$$H_{oxp} = H_{ox} + H_{oxd} \quad (8)$$

The standard deviations of these equations are 17.5%, 41.2% and 13.7% respectively.

The geometry of SMR can enhance surface renewal and decrease axial dispersion. Therefore, H_{oxp} of PPC filled with s.s. SMR are much lower than that of ceramic and s.s. Raschig ring (Figure 5).

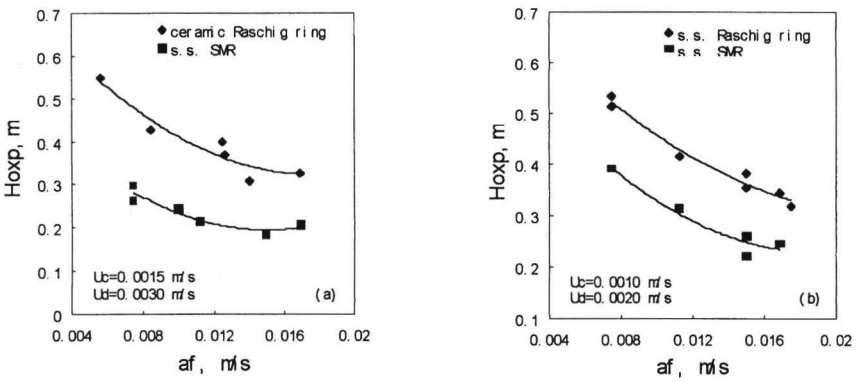


Figure 5. Effect of packing on mass transfer

CONCLUSIONS

1. The mass transfer efficiency increases sharply whereas flooding velocity decrease slowly with increasing of pulsation intensity. Therefore, pulsation has a positive effect on the performance of packed column.
2. PPC filled with the s.s. SMR has much higher mass transfer efficiency than those of ceramic and s.s. Raschig rings.
3. Empirical equations of characteristic velocity, H_{ox} and H_{oxd} were proposed. These equations fit the experimental data reasonably.

ACKNOWLEDGMENT

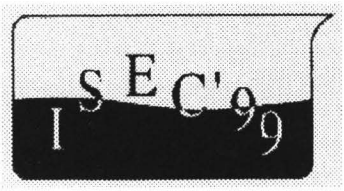
Experiments of this paper were completed at the Solvent Extraction Branch, State Key Laboratory of Chemical Engineering, China. The authors wish to express their appreciation for its supports.

NOMENCLATURE

a	pulsation amplitude, m
a_p	specific interfacial area, m^2/m^3
f	pulsation frequency, s^{-1}
g	acceleration of gravity, m/s^2
H_{ox}	true height of transfer unit, m
H_{oxd}	dispersed height of transfer unit, m
H_{oxp}	apparent height of transfer unit, m
L_R	ratio of phase flow, O/A

REFERENCES

1 Spaay NM, Simons AJF and ten Brink GP, *Proceeding of ISEC'71*, SCI London, 281, (1971)
2 Bender E, Berger R, Leuckel W and Wolf D., *Chem.-Ing.-Tech.*, **51**, 192, (1979)
3 Simons AJF in *"Handbook of Solvent Extraction"*, Lo TC, Baird MHI and Hanson C, Eds., John Wiley & Sons, New York , Chap. 11.1, 343, (1983)
4 Backer W, Schafer JP and Schroter J, *Chem.- Eng.- Tech.*, **63**, 1008, (1991)
5 Hoting B and Vogelpohl A, *Chem.-Ing.-Tech.*, **68**, 105, (1996)
6 Hoting B and Vogelpohl A, *Chem.-Ing.-Tech.*, **68**, 109, (1996)
7 Fei WY, Wen XM, Fang SH and Zhang BQ, *Chinese Patent No.89220935.6*
8 Fei WY et al., *Proceeding of ISEC'93*, 49, (1993)
9 Gourdon C, Casamatta G and Muratet G, in *"Liquid-Liquid extraction equipment"*, Godfrey JG, Slater MJ,eds., John Wiley & Sons, Chichester, Chap. 7, 137, (1994)
10 Rod V, Fei WY and Hanson C, *Chem. Eng. Sci. Res. Des.*, **61**, 290, (1983)
11 Gayler R, Roberts NW and Pratt HRC, *Trans. Inst. Chem. Eng.*, **31**, 57, (1953)
12 Wang JD, Shen ZY and Wang CF, *Huagongxuebao*, **4**, 215, (1965)
13 Misek T and Marek J, *Brit. Chem. Eng.*, **15**, 202, (1970)
14 Degaleesan TE and Laddha GS, *Indian J. Tech.*, **9**, 47, (1967)



IMPACTS OF PACKING ON MASS TRANSFER OF HIGH VISCOSITY SOLVENTS DROP SWARMS

Jie Yu and Weiyang Fei
Department of Chemical Engineering, Tsinghua University, Beijing 100084, China

ABSTRACT
The mass transfer coefficients of drop swarms were measured in a 0.1m diameter glass column equipped with a multichannel precision syringe pump and a computerized video imaging system. The four experimental systems are 30% Cyanex 923S-kerosene/HAc/water, 50% Cyanex 923S-kerosene/HAc/water, 80% Cyanex 923S-kerosene/HAc/water and pure Cyanex 923S/HAc/water. The viscosities of these systems ranged from 3.23 to 53.7 mPa.S. The impact of drop size, viscosity and SMR packing on K_{od} were studied. It is shown from the results that K_{od} decreases sharply with the increase of viscosity, whereas drop size only has a little effect on K_{od}. The SMR packing can enhance K_{od} significantly.

Keywords: high viscosity, droplet swarms, mass transfer, Super-Mini-Ring

INTRODUCTION

Mass transfer coefficient is a key parameter for the scale up of extraction columns. There are many measurements on mass transfer coefficients. However, most of are based on single drop experiments.[1~3] The interaction of drops has not been considered in these cases. Therefore, it is necessary to measure mass transfer coefficient of drop swarms.

Packing can decrease axial dispersion, increase drop breakage probability and enhance surface renewal, which are good for mass transfer. Research on drop behavior with regular packing was done recently.[4] However, there is no information on the hydrodynamic and mass transfer of drop swarms within random packings. Since the Super Mini Ring (SMR) has superior characteristics for liquid-liquid extraction,[5] it is important to study its impact on the mass transfer of drop swarms.

Several new solvents with high viscosity have been developed and applied successfully for hydrometallurgy and petrochemical industries in the recent years. These solvents have favourable thermodynamic properties, however, their mass transfer coefficients are very low. It is evident from the experiments that agitation has only a little influence on the mass transfer coefficients of high viscosity solvent. Therefore, the impact of drop size, viscosity and SMR packing on the mass transfer of drop swarms were studied in this paper.

EXPERIMENTAL

The experimental set-up is shown in Figure 1. The column was made of flanged glass with 100mm i.d. and 600mm working height. Its bottom was made of plexiglass and has ten 3mm pores, which were sealed by vacuum rubber. These pores were arranged to insert needles and their distribution is illustrated in Figure 2.

A multichannel syringe pump (model 74900-10) provided by Cole-Parmer Instrument Company was used to produce drop swarms. The pump could ensure that flow rate of each syringe was all the same. Medical needles of seven different gauges were used in the experiments. Teflon pipe served as a connector between needles and the syringe pump. The flow rate of the pump was controlled so that time of production of each drop was about 2 to 3 seconds. Drop size was calculated according to flow rate of the pump and time used to produce a certain number of drops. Two funnels were arranged 100mm and 500mm away from the bottom to collect samples. The movement of drop swarms was recorded by a computerized video imaging system, which consisted of a PC computer with a capture card, a video camera and a video tape recorder. The image could be recorded on hard discs or record tapes.

© 2000 Society of Chemical Industry

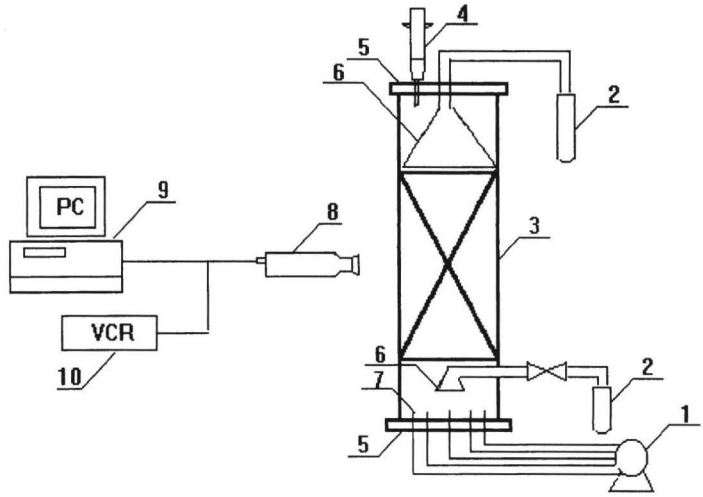


Figure1 Experimental Set-up
1.multichannel syringe pump; 2.sampling tube; 3.extraction column; 4.syringe; 5.flange; 6.funnel; 7.needle; 8.video camera; 9. PC computer; 10.video tape recorder.

When the impact of packing was studied, a tube with 90mm inner diameter was suspended inside the column. The tube was filled with ϕ16 stainless steel SMR of different heights. The surface of SMR was treated by solution of $KMnO_4$ and concentrated sulfuric acid to avoid wetting by dispersed phase.

Deionized water was used as the continuous phase, 30%Cyanex 923S-Kerosene, 50%Cyanex 923S-Kerosene, 80% Cyanex 923S-Kerosene and pure Cyanex 923S were used as dispersed phases. Acetic acid (A.R.) was used as solute to transfer from the continuous phase to the dispersed phase. The concentration of acetic acid was titrated with 0.1M NaOH in presence of thymol blue. The physical properties of experimental systems are listed in table 1.

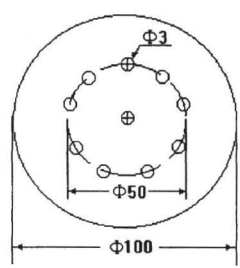


Figure 2 the pore distribution

Since the distribution coefficients of four systems are not very large, the mass transfer resistance in both phases could not be ignored, the drop overall mass transfer coefficient K_{od} was calculated in the experiments. K_{od} was calculated by the following equations:

$$K_{od} = -\frac{d_p}{6t}\ln(1-E) \quad (1)$$

$$E = (y_2 - y_1)/(y^* - y_1) \quad (2)$$

where y_1, y_2 were the concentrations at 100mm and 500mm above the drop formation point respectively and y^* was the equilibrium concentration of the continuous phase.
Diffusion coefficients of experimental systems were calculated by Wilke-Chang equation[6].

Table 1 Physical Properties of Experimental Systems (18°C)

Phases	Density ($Kg \cdot m^{-3}$)	Viscosity ($mPa \cdot S$)	Distribution coefficients
Water/HAc (0.2M) (c)	1001.5	1.066	
30%Cyanex 923 S-Kerosene (d)	789.2	3.23	1.74
50%Cyanex 923 S-Kerosene (d)	816.9	6.36	2.64
80%Cyanex 923 S-Kerosene (d)	854.5	26.58	3.57
Pure Cyanex 923 S (d)	881.7	53.65	4.65

RESULTS AND DISCUSSION

Terminal velocities of different drops under mass transfer condition were measured in the experiments. It is shown from the results that the bigger the drop size, the higher the terminal velocity. There are several equations for evaluating terminal velocity.[7-9] The Klee-Treybal equation[9] is the best one to predict experimental results, but with little higher values than the experimental ones. This is probably because the Klee-Treybal equation was proposed under no mass transfer conditions. The following modified Klee-Treybal equation could fit experimental data very well (Figure 3).

$$U_t = 35.5\rho_c^{-0.45}\Delta\rho^{0.58}\mu_c^{-0.11}d_p^{0.70} \qquad \text{in c.g.s units} \qquad (3)$$

The measured K_{od} of four experimental systems are shown in Figure 4. It is clear from the figure that K_{od} increases with initial drop size, while decreases with increase of solvent viscosity. On the other hand, K_{od} almost keeps constant when the viscosities are large enough (for 80% and pure Cyanex 923 S).

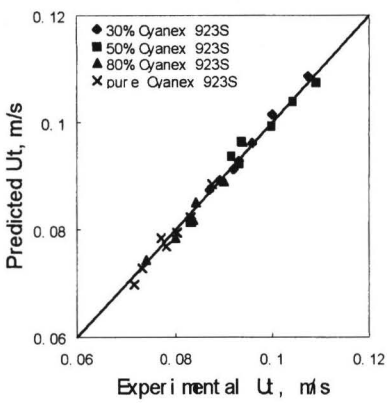


Figure 3 Comparison of U_t between experimental data and calculated one

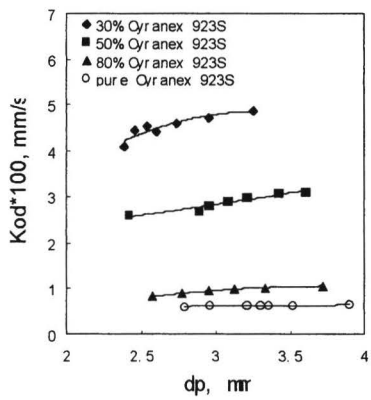


Figure 4 Effect of viscosity on K_{od}

Table 2 Standard Deviations Between Experimental and Calculated Data

Equations for individual mass transfer coefficients	30% Cyanex	50% Cyanex	80% Cyanex	pure Cyanex
Laddha[1] + Laddha[1]	38.4%	48.1%	67.1%	76.3%
Garner-Tayeban[10] + Laddha[1]	57.9%	62.8%	71.4%	28.6%
Laddha[1] + Blass[2]	3.12%	8.25%	35.8%	55.4%
Garner-Suckling[11] + Blass[2]	99.4%	99.6%	94.1%	93.0%
Handlos-Baron[12] + Boussinesq[13]	16.9%	10.2%	6.10%	21.4%

There are many equations used to calculate the inside and outside drop mass transfer coefficients.[10~13] According to two-film theory, K_{od} could be calculated by the following equation:

$$\frac{1}{K_{od}} = \frac{1}{k_d} + \frac{m}{k_c} \tag{4}$$

Several well know equations for calculating k_c and k_d were combined to calculate K_{od} by equation (4), and then calculated results were compared with those of measured. Some of the standard deviations are shown in Table 2. It is clear from the illustrated results that almost all the equations could not evaluate experimental results good enough. Therefore, a new model with an interfacial motion hindrance factor β was proposed to describe the influence of solvent viscosity and surface contaminants.[14] The equations of the model were as follows:

$$Sh_c = 1.13\left[1+\frac{2+3\mu_d/\mu_c+\beta}{1+\sqrt{\rho_d\mu_d/\rho_c\mu_c}}\frac{1.45}{\sqrt{Re}}\right]^{-0.5} Pe^{0.5} \tag{5}$$

$$K_d = -\frac{d_p}{6t}\ln\left[\frac{6}{\pi^2}\sum_{n=1}^{\infty}\frac{1}{n^2}\exp\left(-\frac{4n^2\pi^2 D_{OE}t}{d_p^2}\right)\right] \tag{6}$$

$$D_{OE} = D_d + \frac{d_p U}{2048(1+\mu_d/\mu_c)} \tag{7}$$

where β indicates factors that have influence on interfacial motion. It could be calculated by regressing the experimental data. Its values of four experimental systems are 56, 80, 1027 and 1675 respectively, which indicates that the higher the solvent viscosity, the bigger the resistance in mass transfer. Using this model, the standard deviations of the four systems are 2.31%, 2.54%, 4.14% and 2.73% respectively. Therefore, the new model could evaluate experimental data fairly well.

Packing has complex effects on K_{od}. On the one hand, packing can increase drop breakage probability, enhance surface renewal and inner circulation of drops, which have a positive effects on K_{od}. On the other hand, drop terminal velocity decreases in presence of packing, which has a negative effect on K_{od}. The experimental results showed that K_{od} became bigger in presence of packing, which means that the positive effect of packing was higher than the negative one. Enhancement ratio was defined as ratio between K_{od} with packing and K_{od} without packing.

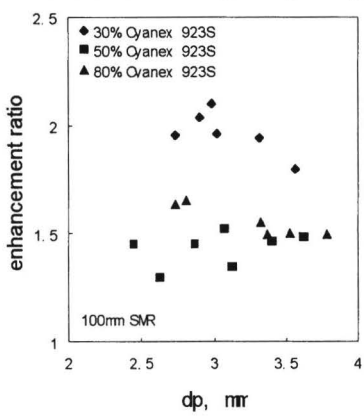


Figure 5 K_{od} enhancement ratio of the SMR

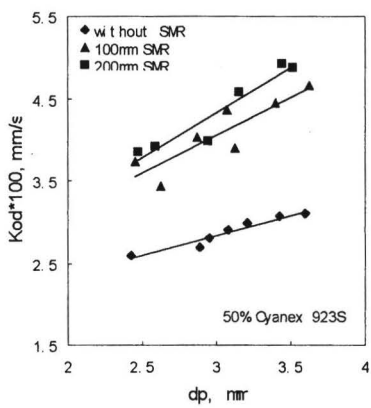


Figure 6 Effect of packing height on K_{od}

Figure 5 showed that enhancement ratio was between 1.3 and 2.1. Since agitation has a little influence on mass transfer of high viscosity solvents, our results provide a way to enhance their mass transfer. The effect of packing height on K_{od} was also investigated, as shown in Figure 6. K_{od} with 200mm packing was a little larger than that with 100mm packing.

CONCLUSIONS

1. The modified Klee-Treybal equation (3) could evaluate the terminal velocity of high viscosity dispersed phases reasonably.
2. The viscosity of solvents has significant impacts on K_{od}, while drop size has only a little effect on it.
3. K_{od} is difficult to estimate by many well known individual mass transfer coefficients equations. A new model considering interfacial motion hindrance factor could fit experimental data fairly well.
4. The SMR Packing can enhance the mass transfer coefficients of high viscosity solvents, the enhancement ratio is about 1.3 to 2.1.

ACKNOWLEDGEMENTS

The authors wish to express their appreciation to the Solvent Extraction Branch, State Key Laboratory of Chemical Engineering, China, for its supports. The authors also wish to express their appreciation to Cytec Industries Inc., Canada for providing Cyanex 923S.

NOMENCLATURE

D	diffusion coefficient
D_{OE}	effective diffusion coefficient
d_p	drop diameter
E	fraction degree of extraction
K_{od}	drop phase overall mass transfer coefficient
m	distribution coefficient
t	time
U_t	terminal velocity

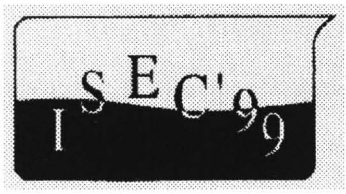
Greek letters

β	interfacial motion hindrance factor
μ	viscosity
ρ	density
$\Delta\rho$	density difference

REFERENCES

1 Laddha GS and Smith JM, Transport Phenomena in Liquid Extraction, New Delhi: Tata McGraw-Hill,
2 Blass E, Goldmann G, Hirschmann K, et .al.,*Ger.Chem.Eng.*, **9**, 222, (1986).
3 Slater MJ, *Liquid-Liquid Extraction Equipment*, Chichester: John Wiley & Sons Ltd., 47, (1994).
4 Mao ZQ, Godfrey JC and Slater MJ, *Chem. Eng. Technol.*, **18**, 33, (1995).
5 Fei WY, Wen XM, Fang SH and Mao H, *Proceedings ISEC'93*, 49, (1993).
6 Wilke CR and Chang P, *AIChE J.*, **1**, 264, (1955).
7 Misek T and Marek J, *British Chem. Eng.*, **15**, 202, (1970).
8 Grace JR, et al., *Trans. Inst. Chem. Eng.*, **54**, 167, (1976).
9 Klee AJ and Treybal RE, *AIChE J.*, **2**, 444, (1956).
10 Garner FH and Tayeban M, *Aun.Fis.Quim.,Series B*, **56**, 479, (1960).
11 Garner FH and Suckling RD, *AIChE J.*, **4**, 114, (1958).
12 Handlos AE and Baron T, *AIChE J.*, **3**, 127, (1957).

13 Boussinesq J, *J. Math.Pure Appl.*, **11**, 285, (1905).
14 Chen DH, *Doctoral Thesis, Tsinghua University*, Beijing, China, (1996).



FLOW STRUCTURE AND TURBULENT FLOW ENERGY IN STAGEWISE EXTRACTION COLUMNS: INFLUENCE OF STAGE CONFIGURATION

G Angelov[1] and C Gourdon

[1]Institute of Chemical Engineering, Bulgarian Academy of Sciences, Sofia, Bulgaria,

Ecole Nationale Supérieure des Ingénieurs de Génie Chimique, Toulouse, France

ABSTRACT

Turbulent operational regimes of extraction equipment are interesting from practical point of view because they ensure favourable conditions for interface contact and mass transfer operations. The structure and energy of the turbulent flow in a pulsed stagewise extraction column is studied. High-energy zones are localised on the stage and their evolution in position, volume, and intensity is registered as depending on stage geometry. A correspondence between these zones and drop-breaking zones is experimentally observed.

Keywords: pulsed columns, turbulent energy, flow phenomena

INTRODUCTION

The flow energy in a solvent extraction device is composed from its own dynamic energy (velocity) and energy induced by external sources (e.g. agitation, pulsations, etc.). External energy is used to create turbulent operating conditions that intensify the mass transfer processes. The flow structure in column apparatuses is strongly influenced by the internals: packing, plates, etc. The concept of optimal internals design needs information how they affect the flow. This paper studies the influence of the stage geometry parameters on flow structure and on turbulent energy distribution in a stagewise extraction column (DRC - Disc and Ring Column) that has revealed itself as a promising contact device tested in various applications of liquid-liquid and solid-liquid extraction.[1-5]

APPARATUS DESCRIPTION

The column is divided into stages by alternating immobile discs and rings (Figure 1). Although the plates are different in configuration, they ensure equal free area e for the flow and are placed equidistantly at distance H. A repeating compartment is formed by two rings and a disc between them. The ring aperture is considered to be the compartment entrance/exit. Its diameter D_r is smaller than the disc diameter D_d in order to close the direct axial way for the flow. Additionally, pulsations are induced to the fluids in the column by means of mechanical or pneumatic devices.

Stage Geometry Parameters

The geometry parameters of the stage are defined by its characteristic dimensions:

The distance between two consecutive plates H and the column diameter D_c define the dimensionless ratio characterising the stage height as a part of column diameter:

$$h = H/D_c$$

Plate free area e is defined as:

$$e = D_r^2/D_c^2 = (D_c^2 - D_d^2)/D_c^2$$

These geometry parameters were varied in reasonable ranges

$$h = 0{,}08 - 0{,}4 \qquad e = 0.2 - 0.5$$

that were chosen by the following practical considerations:

© 2000 Society of Chemical Industry

Small to medium values of h are appropriate. Small values correspond to more compartments in a unit of column height and tolerate the apparatus efficiency. However, too small interplate distance will increase the pressure drop and energy consumption. Too large interplate distance will reduce both the number of plates and overall apparatus efficiency.

In order to avoid a direct axial flow in the column, D_d should be larger than D_r. The case of equal diameters corresponds to e = 0,5. So, values of e over 0,5 are not favourable for the flow structure and apparatus efficiency.

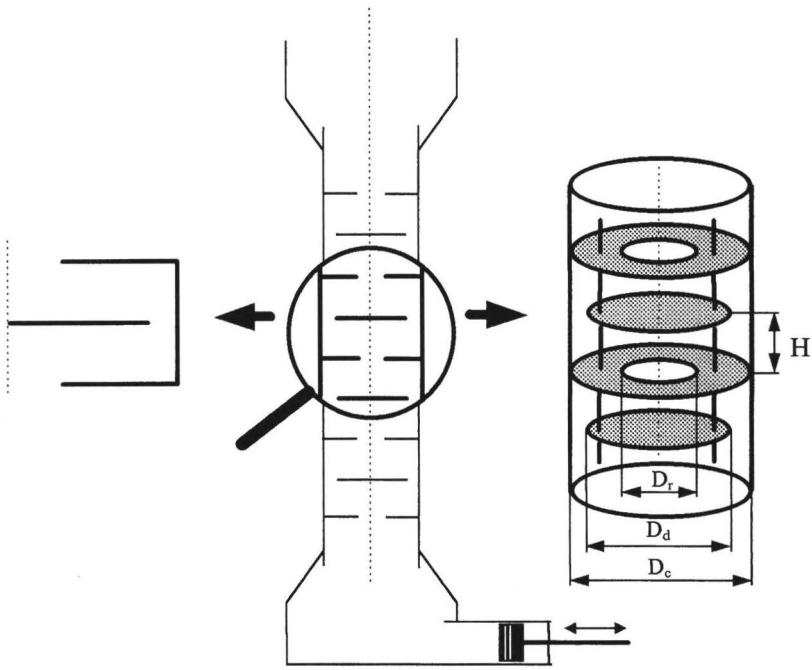


Figure 1. Apparatus scheme

MATHEMATICAL DESCRIPTION

Model and Assumptions

The column is built of identical compartments, the fluid is incompressible Newtonian liquid, the flow is assumed to be axisymmetrical. Simulation of a single compartment should give typical results if flow periodicity exists for each compartments. The latter was proved experimentally in an earlier paper[6] by velocity profile measurements that have also shown the flow symmetry with respect to column axis.

The hydrodynamics of this turbulent pulsed flow was described by Reynolds equations adapted to the specific flow conditions and particular geometry of column compartment. Additional terms were involved to account for the turbulent flow parameters - turbulent kinetic energy k and its dissipation rate ε (k-ε turbulence model).[7]

Boundary Conditions

Symmetry condition was applied on the axis. Logarithmic law was used to specify the boundary conditions (BC) just outside the viscous sublayer along the rigid walls.[7] BC at the compartment open

boundaries were experimentally determined only for the existing pilot column with fixed geometry. For other stage configurations, BC for turbulent quantities were estimated from particular relations for DRC derived earlier:[8]

$$\ln (k/V_s^2) = -5.24 - 4.53 \ln e$$

$$\varepsilon = 2k^{3/2}/(h.D_c)$$

$$Vs = 2\ A_p f$$

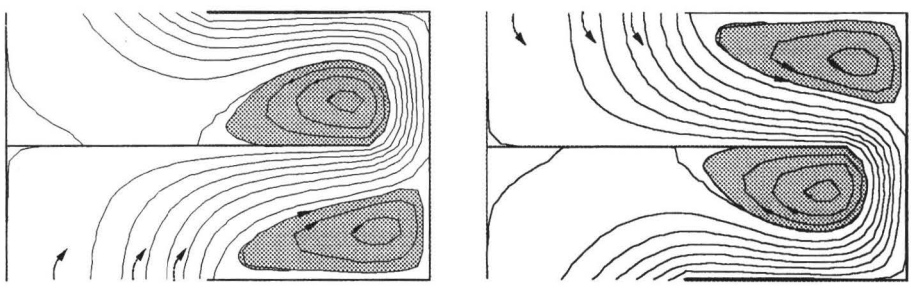
where V_s is the mean superficial velocity during the pulsation cycle,
A_p is peak-to-zero pulsation amplitude,
f is frequency of pulsation.

RESULTS AND DISCUSSION

Simulations of flow hydrodynamics for various geometry of the compartment were made resolving the model equations with particular BC that specify each considered case. The solutions supply results for the flow and turbulent energy parameters that are presented below.

General Flow Structure

A typical flow pattern is illustrated on Figure 2 that represents stream lines in a longitudinal section of the compartment limited by column axis, column wall, and two ring plates. Two large vortices are formed. They change their position corresponding to the ascending and descending phase of the pulsation. Experimental observations on DRC have proved the real existence of these permanent vortices.[1,9,10]

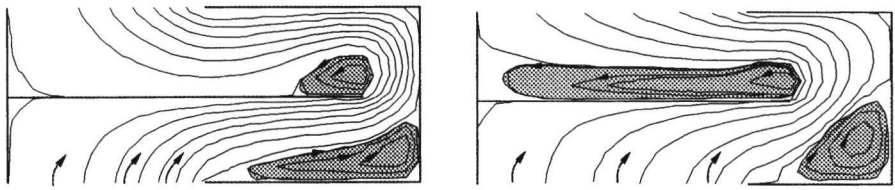


a b

Figure 2. Flow structure in a compartment (h = 0,155; e = 23 %; Re = 15 000)
a) ascending flow b) descending flow

Influence of Plate Free Area

The comparison of Figures 3a and 3b shows that the increased plate free area e changes only the form of lower circulation keeping approximately its volume and position. It becomes more round and is more attached to the column wall.
The upper circulation is very pronouncedly changed. Its volume grows significantly covering nearly completely the disc surface.



a b

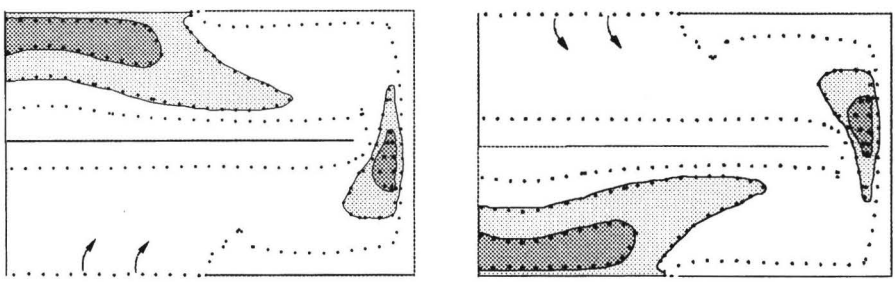
Figure 3. Recirculating zones at various free area (h = 0,086) a) e = 23 % b) e = 40 %

Influence of Interplate Distance

Comparing Figs. 2a and 3a that refer to the same Re number, it is seen that a larger interplate distance increases the volume of circulating zones.

Turbulent Energy Distribution

Higher level of turbulent kinetic energy is found in the annular aperture between the disc edge and column wall and in the median section between the disc and ring in the entrance/exit zones (Figure 4).



a b

Figure 4. Distribution of turbulent kinetic energy in the compartment (h = 0,155; e = 23 %; Re = 15 000) a) ascending phase b) descending phase

$k = 1{,}5.10^{-2}\ m^2/s^2$ $k = 1.10^{-2}\ m^2/s^2$

Influence of Plate Free Area

It is illustrated by Figure 5. In case of smaller free area, higher energy zones are located at their usual places. An increase of plate voidage has the following consequences: the highest energy zone reduces its energy contents and moves over the disc under the ring aperture. The volume of higher energy zone is significantly reduced.

Influence of Interplate Distance

This influence is detected from the comparison of Figures 4a and 5a (the same value of plate free area). The zones with higher energy contents are always placed in the annular aperture and in the median section, but the energy level reduces with the increase of the interplate distance.

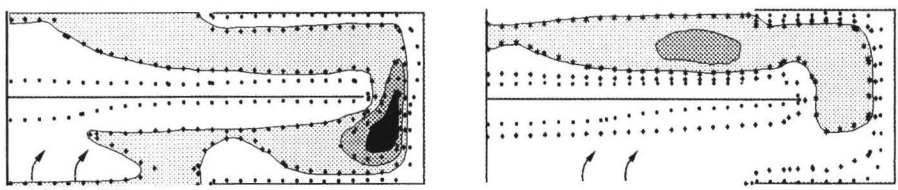
The results of this study also show the relation between the flow structure and turbulent energy contents. Changes in compartment geometry affect both of them. An increase of plate voidage means that plates occupy a lesser part of the column cross-section leaving more space for the flow and reducing its local velocity. An increase of interplate distance means a reduced number of obstacles per unit height. In both cases, the internals generate lesser turbulence. Consequently, the main flow with

lower turbulent energy is not able to sweep the recirculating (dead) zones and conditions for formation of larger circulations are created thus defavouring the mass transfer. The case is illustrated comparing Figures 3b and 5b. Higher energy contents correspond to more homogeneous flow structure with smaller internal circulations (Figures 3a and 5a).

According to these simulation results, higher energy zones in the compartment are :

- annular aperture disc - wall
- median section disc-ring in the zone of ring aperture.

The same zones are experimentally found to be places of intensive break-up processes.[9] It confirms the reliability of the present results because in effect drops are broken in smaller drops in the zones where the level of acting forces is sufficiently high to evoke drop deformation and breakage.



a b

Figure 5. Influence of plate free area on turbulent kinetic energy distribution in the compartment (h = 0,086; Re = 15 000) a) e = 23 % b) e = 40 %

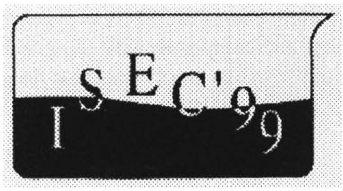
$k = 2.5.10^{-2}\ m^2/s^2$ $k = 2.10^{-2}\ m^2/s^2$ $k = 1.10^{-2}\ m^2/s^2$

ACKNOWLEDGEMENTS

This study is partly supported by the Bulgarian National Fund for Scientific Research and French National Centre for Scientific Research.

REFERENCES

1. Park H, *Ph.D. Thesis, INP-Toulouse*, (1980).
2. Srisuwan G, *Ph.D. Thesis, INP-Toulouse*, (1988).
3. Dimitrova S, Gourdon C and Casamatta G, *Chem. Eng. Sci.*, **44**, 1295, (1989).
4. Milot JF, Duhamed J, Gourdon C and Casamatta G, *Chem. Eng. J.*, **45**, 111, (1990).
5. Haunold C, *Ph.D. Thesis, INP-Toulouse*, (1991).
6. Angelov G and Gourdon C., *Chem. Eng. J*, **45**, 87, (1990).
7. Angelov G and Hung J. Ind. Chem., **25**, 223, (1998).
8. Schistel R, *Modelisation et simulation des ecoulements turbulents*, Hermes, 1993).
9. Laulan A., *Ph.D. Thesis, INP-Toulouse*, (1980).
10. Oh W, *Ph.D. Thesis, INP-Toulouse*, (1984).



HYDRODYNAMIC AND MASS TRANSFER CHARACTERISTICS OF SUPER-MINI-RING (SMR), RASCHIG RING AND PULSED PERFORATED PLATE COLUMN

D Chen[1,2], W Fei[1], HRC Pratt[2] and GW Stevens[2]

[1] Department of Chemical Engineering, Tsinghua University, Beijing, 100084,China

[2] Department of Chemical Engineering, The University of Melbourne, Parkville, VIC 3052, Australia

ABSTRACT

Cyanex 923 has been proposed as an extractant for the removal of sulphuric acid from copper tank house bleed streams. This process requires many of stages and so is ideal for column operation. This paper presents a comparison between three types of columns for this service. The new super-mini-ring (SMR) packing marketed by Glitsch is the first packing developed specifically for liquid-liquid extraction service and is compared with the standard packed column and a pulsed perforated plate column.

Both the hydrodynamic and mass transfer behavior of these columns are presented for the 50% Cyanex 923 in kerosene/ H_2SO_4/water system. The results indicated that this system is unusual in that the HTU values obtained were high. This is ascribed to a slow heterogeneous reaction at the interface, and/or to very slow diffusion in the highly viscous dispersed phase droplets that were observed. The SMR packing was found to give H_{ox} values about 47% below those for Raschig rings.

Keywords: hydrodynamics, mass transfer, Super-Mini-Ring (SMR), Raschig Ring, pulsed perforated plate column, Cyanex 923

INTRODUCTION

In the recovery of copper by leaching and solvent extraction followed by electrowinning, a bleed stream is taken from the electrolyte circuit in order to control the level of impurities in the electrolyte. A typical bleed stream has a flow-rate of 1.0 m^3/hr with a composition of 180 g/L H_2SO_4, 37 g/L Cu plus a number of minor elements. The recovery of sulphuric acid from the waste bleed stream would significantly lower waste production of the electrowinning process and thus reduce the cost of copper production by reducing the amount of acid make-up required.

The recovery of sulphuric acid could be achieved by the selective extraction of sulphuric acid with an organic extractant, a process that would have the ability to produce a concentrated pure product. Cyanex 923, which is a mixture of four trialkylphosphine oxides[1,2], has been proposed as a possible extractant for the recovery of sulphuric acid. It was found that Cyanex 923 displayed a good compromise between its ability to extract sulphuric acid and to be effectively stripped with water. Rickelton also observed that Cyanex 923 has a very high selectivity for acid extraction in preference to both copper and nickel.

These processes require a large number of stages and so are ideal for column operation. Several types of extraction column could be chosen for this service; of these, the pulsed perforated plate column, in which mechanical energy is used to produce the pulsation, provides high turbulence at the interface and a large mass transfer area due to smaller drop sizes. Packed columns are another type of extractor which have also been widely used in the chemical and hydrometallurical industries. In such columns, the packing reduces axial mixing and increases the drop coalescence and breakage rates, thus resulting in increased mass transfer rates. Most packed tower installations use standard manufactured packings, such as Raschig, Lessing or Pall rings, and Berl or Intalox saddles made for gas-liquid contact. But there is evidence that some of these types of packing, which have been found to give high efficiency in distillation service, do not perform well enough for liquid-liquid extraction [3].

The new SMR (Super Mini Ring) marketed by Glitsch is the first packing developed specifically for liquid-liquid extraction service. Thus the structure of the SMR could enhance the dispersion-coalescence cycle and control the non-ideal flow of the two phases in the packed bed and therefore increase its capacity and efficiency [3].

© 2000 Society of Chemical Industry

In the present work the hydrodynamic and mass transfer characteristics of the SMR is studied and compared with the standard Raschig ring packing; these in turn are compared with a pulsed perforated plate column both to obtain comparative information on the performance of such columns, and to study the feasibility of using the SMR packing in the hydrometallurical industry.

EXPERIMENTAL

Equipment

The main section of the packed column was a 1.8 m QVF precision bore glass tube with an internal diameter (i.d) of 0.1 m, packed with 1.32 m of 16 mm ceramic SMR or of 12.5 mm ceramic Raschig rings respectively. The coalescence section comprised of a QVF glass tube of 0.1 m nominal i.d and 0.5 m long. The aqueous phase distributor consisted of a 9.5 mm diameter stainless steel (SS) tube located approximately 50 mm above the top of the packing. The dispersed phase distributor had 19 nozzles each of 2.64 mm, assembled as two circles of six and twelve respectively around a single central nozzle on a plate of diameter 46 mm mounted centrally at the bottom of the column.

The pulsed perforated plate column comprised a 1.0 m precision bore glass tube of 0.0725 m i.d. enclosing a stack of 16 stainless steel (SS) perforated plates, each punched with holes of 3.2 mm diameter on a 6 mm triangular pitch, giving 21% free area; the plate spacing was 50 mm. At the base, a 0.075 to 0.1 m glass converter and a SS conical adapter enclosed a SS dispersed phase distributor. The conical adapter was mounted on a plunger type pulsing unit.

Materials Used

The dispersed phase consisted of 50% Cyanex 923 in Shellsol 2046, which acted as extractant and diluent respectively. The continuous phase was a 2M aqueous solution of H_2SO_4.

Procedure

Hydrodynamic and mass transfer experiments were performed at an organic/aqueous (O/A) ratio of 2.0. For each mass transfer run, the column was filled with the aqueous phase, the dispersed phase flow was then started, and the column allowed to reach steady state operation. Samples of both outlet phases were taken at ten minutes intervals and were later analysed for acid concentration. At the end of each mass transfer run, the dispersed phase holdup was measured by the shutdown technique [4].

RESULTS AND DISCUSSION

Comparison of hydrodynamic characteristics of the three type of columns

Gayler et al.[4] proposed an equation based on the characteristic velocity approach for the prediction of the holdup and flooding point in packed columns, as follows:

$$\frac{V_d}{eX}+\frac{V_c}{e(1-X)} = V_{slip} = V_0(1-X) \qquad (1)$$

Thornton [5] showed that the characteristic velocity concept could be used for the prediction of hold-up in pulsed perforated plate columns. Thus the characteristic velocity, V_0, can be determined from the slope of a plot of the experimental data in the form $V_d + V_c X/(1-X)$ versus eX(1-X), omitting the voidage term e in the case of the pulsed perforated plate column. The resulting value of V_0 is then used to estimate the holdup at any phase flowrate. Typical fits of equation (1) are shown in figures 1 and 2 for the two types of columns.

Thornton [5] also showed that the flooding velocities could be predicted by differentiation of Equation (1) and equating to zero. The flooding velocities attained in this manner are summarized in table 1 and indicate that the SMR and Raschig ring packed columns have similar flooding velocities.

These values are greater than those for the pulsed perforated plate column, so that packed columns give larger throughputs than pulsed perforated plate columns

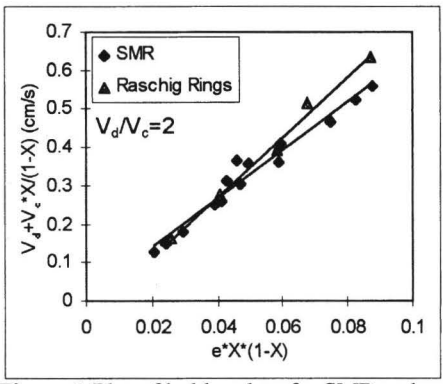


Figure 1 Plot of holdup data for SMR and Raschig Rings packed column

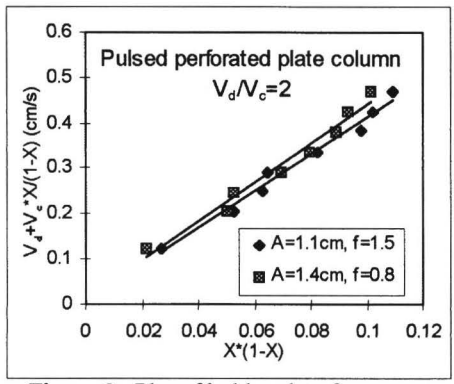


Figure 2 Plot of holdup data for pulsed perforated plate column

Table 1. Predicted Flooding Velocities

Type of Column	V_0 (cm/s)	X_f (%)	V_{cf} (cm/s)	V_{df} (cm/s)
SMR	6.34	38.2	0.571	1.143
Raschig Rings	7.83	38.2	0.706	1.412
Pulsed Perforated Plate Column				
A=1.4cm. f=0.8	4.28	38.2	0.386	0.772
A=1.1cm. f=1.5	4.11	38.2	0.370	0.740

Comparison of mass transfer characteristics of the three type of columns

Axial dispersion must also be considered when assessing the performance of packed columns. Gayler and Pratt[6] showed that backmixing of dispersed phase droplets is relatively small. Wen and Fan [7] recommended the following correlation for E_C, the axial backmixing coefficient for packed columns, based on the original data of Vermeulen et al. [8] and Watson et al. [9].

$$\frac{e\,V_c\,d_p}{E_c} = 7.8\times10^{-3}\left[1.435+\left(\frac{d_p V_c \rho_c}{\psi\mu_c}\right)^{0.1}\left(\frac{V_c}{V}\right)^{0.2}\right]\left(\frac{d_p V_c \rho_c}{\psi\mu_c}\right)^{0.25}\left(\frac{V_c}{V_d}\right)^{0.8} \qquad (2)$$

For the pulsed perforated plate column, it is generally agreed that again the dispersed phase backmixing coefficient, α_d, is small[10], and was therefore assumed to be zero. The continuous backmixing coefficient, α_c, was determined from the dimensionless expression proposed by Prvcic[10] for this contactor.

The "true" height of a transfer unit based on continuous phase, H_{ox}, was determined using a computer program, "coldsn.exe", developed by Pratt[11] at the University of Melbourne. The program is applicable to simple countercurrent extraction in end-fed backmixed columns. The same program was used to determine $(HTU)_x$, assuming zero backmixing in both phases. The comparison of $(HTU)_x$ and the true height of a transfer unit, H_{ox} , between SMR and Raschig rings over a range of holdups is plotted in figures 3 and 4 respectively. These show that both the $(HTU)_x$ and H_{ox} of SMR are

appreciably lower than those for the Raschig rings, indicating that the SMR gives a better mass transfer performance than Raschig rings for this particular system.

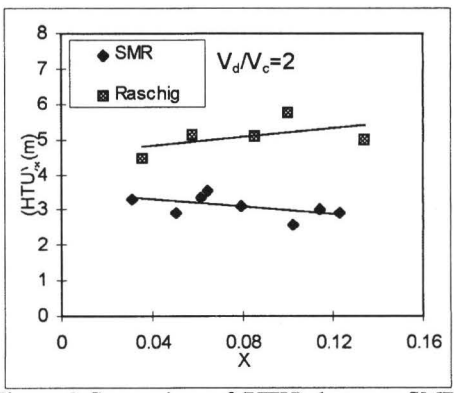


Figure 3 Comparison of $(HTU)_x$ between SMR and Raschig Rings Packed column

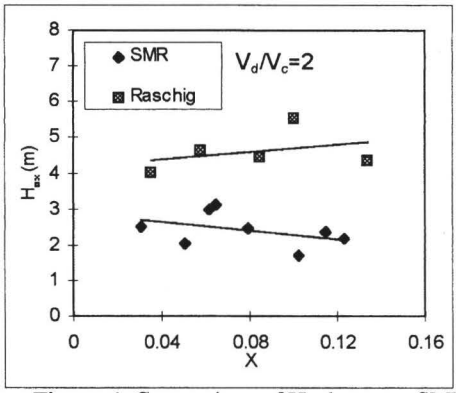


Figure 4 Comparison of H_{ox} between SMR and Raschig Rings Packed column

The $(HTU)_x$ and H_{ox} for the pulsed perforated plate column are showed in figures 5 and 6, which indicate that the mass transfer efficiency of the pulsed perforated plate column increases with increasing pulsation intensity. With low pulsation intensity (f = 0.8Hz), the SMR was more efficient than pulsed perforated plate column. However, at the higher intensity (f = 1.5Hz), the pulsed column was more efficient than the SMR packed column. Thus increase in the energy input into the system can enhance the mass transfer efficiency, although at the expense of a reduced flooding velocity. It can be expected that the mass transfer efficiency of SMR packed columns would also increase with mechanical pulsation.

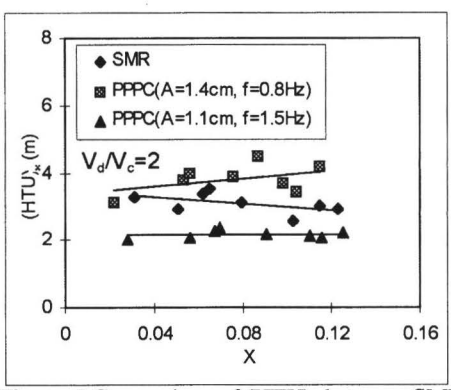


Figure 5 Comparison of $(HTU)_x$ between SMR and pulsed perforated plate column

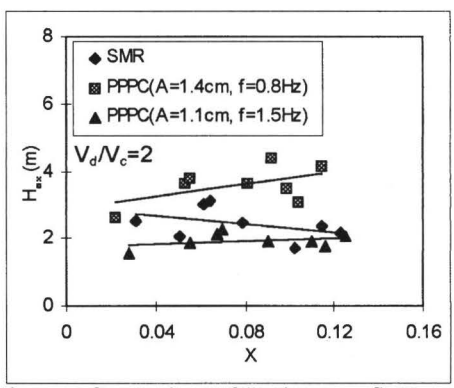


Figure 6 Comparison of H_{ox} between SMR and pulsed perforated plate column

DISCUSSION

A comparison of figures 3 and 4, and of figures 5 and 6, reveals that the $(HTU)_x$ and Hox values are unexpectedly close, with ratios of $H_{ox}/(HTU)_x$ of 0.88 to 0.91 for Raschig rings and 0.73 to 0.82 for SMR packing over the holdup range studied; the differences for the pulsed plate column are also close to unity. It should be noted that the H_{ox} values may be overestimated as the "coldsn.exe" program is subject to increasing error for less than 1 to 2 transfer units in backmixed column.

The reason for these small differences can be identified as due to the unusual properties of the Cyanex 923-H_2SO_4 system used. Thus, it is apparent from the data in figures 3 to 6 that with a packing

height of 1.32 m, or with 0.90 m of perforated plates, the column was equivalent to only about 20-30% of a transfer unit. As a consequence, the concentration change in the continuous phase was very small, and would thus have resulted in a correspondingly small effect of backmixing in that phase.

Two possible reasons for the observed low efficiencies may be considered. Thus, on the one hand the extraction process between the Cyanex 923 reagent dissolved in kerosene and aqueous sulphuric acid may involve a slow heterogeneous reaction at the interface. On the other hand, the transfer of sulphuric acid into the organic phase was observed to result in the formation of viscous drops with very slow diffusional transfer. Further work is therefore required to determine the true mechanism of the process.

In conclusion, it is apparent from the data plotted in figures 3 and 4 that the new SMR packing gives superior performance as compared with Raschig rings for the present unusual system.

ACKNOWLEDGMENTS

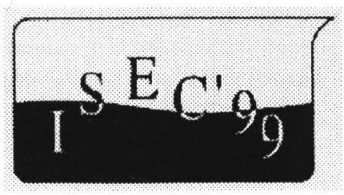
The authors wish to acknowledge Targeted Institutional Links Grant from Australian Government DEETYA, Tsinghua University, Beijing, China and the Advanced Mineral Products Special Research Centre (AMPC) at the University of Melbourne for financial support for this work.

NOMENCLATURE

A	pulsation amplitude, m
H_{ox}	"true" height of a transfer unit, m
$(HTU)_x$	height of transfer unit based on continuous phase, m
X	holdup of dispersed phase
ψ	sphericity of packing

REFERENCES

1 Rickelton WA, *Proc. ISEC'93*, **2**, 731, (1993)
2 Alguacil FJ and Lopez FA, *Hydrometallurgy*, **42**, 245, (1996)
3 Fei WY, Wen XM, Fang SH and Mao H, *Proc. ISEC'93*, **1**, 49, (1993)
4 Gayler R, Roberts NW and Pratt HRC, *Trans.I.Chem.E.*, **31**, 57, (1953)
5 Thornton JD, *Trans.I.Chem.E.*, **35**, 316, (1957)
6 Gayler R and Pratt HRC, *Trans.I.Chem.E.*, **35**, 267, (1957)
7 Wen CY and Fan LT, *"Models for Flow System and Chemical Reactors"*,Marcel Dekker, New York (1975)
8 Vermeulen T, Moon JS, Hennico A and Miyauchi T, *Chem. Eng. Prog.*, **62**, 95, (1966)
9 Watson JS and McNeese LE, *Ind. Eng. Chem.*, **11**, 120, (1972)
10 Prvcic LM, Pratt HRC and Stevens GW, *AIChE J.*, **35**(11), 1845, (1989)
11 Pratt HRC, *Solv. Extr. and Ion Exch.*, **1**(4), 669, (1983)



AXIAL MIXING IN A LARGE-SCALE PACKED EXTRACTOR

O Becker[1], C Lewis[2], R Hardy[3] and F Seibert[2]

[1] Universität Erlangen-Nürnberg, Lehrstuhl für Technische Chemie II, Germany

[2] The University of Texas at Austin, Austin, Texas, USA

[3] Koch-Glitsch, Wichita, Kansas, USA

ABSTRACT

The commercial applications of structured packings in liquid extraction are increasing. Relative to typical tray devices, these packings can provide an increased capacity for retrofitting, improved interface control, and improved mass transfer efficiency. However, these packings were developed for distillation to minimise pressure drop. As a result, structured packings may be subject to axial mixing. In this paper, axial mixing data and models are presented based on four contacting devices: spray, SMV-32, SMVP-32 and SMP-16. The data were obtained from a 42.7 cm diameter (i.d.) column filled with 6-7.5 m of packing. The large-scale column is located at the Separations Research Program (SRP) facilities at The University of Texas. The axial mixing models are applied and compared with mass transfer data obtained from the identical column.

Keywords: axial mixing, packed column, column scale-up

INTRODUCTION

Extraction processes are widely used in the production of chemical, petrochemical and pharmaceutical substances. Beginning in the 1940's and 1950's, extraction equipment was improved continuously to achieve higher separation efficiency at lower cost. Rotating and pulsating agitators combined with properly designed static column internals performed well, as did contactors using centrifugal forces. During this period, the understanding of single drop mass transfer to develop concentration profiles and fluid dynamic calculations grew rapidly. Several authors have developed sophisticated models to describe extraction processes based on laboratory-scale equipment. Unfortunately, the diameter of these columns has seldom exceeded 10 cm because the quantities of liquids required for operation. When scaling up the results from laboratory-scale columns to industrial size columns, differences in performance are often noticed even if the same liquids and packing are used.[1] Visual observations of the phase flows in the SRP small diameter and large-scale columns confirm that there are significant differences in the flow patterns.

During the past 40 years, several authors have worked on the determination and model development of axial mixing in extraction columns. The foundations were laid by publications of Miyauchi et al.[3] and Sleicher in 1959.[4] For both publications, the authors solved the differential equations describing the mass transfer in a countercurrent process under the assumption of eddy diffusional backmixing in each phase. These publications show that the solution of the equations formulated in terms of the continuous mass transfer model is complicated. Concentration profiles can also be calculated iteratively, proceeding on the assumption that the column can be divided into stages with a certain backflow of the respective phase between the compartments.[5,6] Simplified solutions have been provided by Stemerding and Zuiderweg,[7] Richter,[8] Pratt et al.[9,10] and v. Stockar and Lu.[11]

Since the initial articles appeared, much work has been performed to determine eddy diffusion coefficients in various types of columns. The majority of the publications, however, deal with mechanically-agitated columns using rotors or pulsation to enhance the mass transfer. Only a few authors have published results from static spray or packed columns. Furthermore, as knowledge of mixing mechanisms was refined, it became clear that the dispersion model, originally derived for a liquid continuum, should only be used for the dispersed phase at high coalescence and redispersion rates. If the drop identity is maintained for a longer time, convective forward mixing models, as proposed by Rod[12] or Aufderheide et al.,[13] seem to provide improved results.

© Society of Chemical Industry 2000

Axial mixing in small diameter columns filled with laboratory-scale random packings has been studied in some detail. Such studies may be found in the papers of Hennico et al.,[14] Ingham,[15] Vermeulen et al.,[16] Watson and McNeese,[17] Pratt and Anderson,[18] Wen and Fan,[19] and Komasawa and Ingham.[20] Few publications address axial mixing extractors filled with structured packing. Streiff[21] presents data on Sulzer SMV packing installed in a column of 10 cm diameter and 5 m height. In a related publication of Jancic et al.,[22] a plot of Peclet numbers for both the dispersed and the continuous phase is given. It was obtained from experiments in a column of 10 cm diameter and 6 m packed height. Axial mixing in a Sulzer SMV structured packing was also assessed by Rauber[23] in a column of 5 cm inner diameter and 4 m packed height.

EXPERIMENTAL

The computer-controlled extraction system used in the work is described by Seibert et al.[24] in their large-scale mass transfer study. n-Hexane served as the dispersed organic component while city-water was used as the continuous phase. The column has an inner diameter of 42.7 cm and was packed to heights between 6 and 7.5 m. Additional details on the equipment set-up are provided by Becker.[25] Packing geometries are given in Table 1.

Packing	Type	Spec. Surf. Area, cm^2/cm^3	Void Fraction
Koch SMV32	Structured	1.08	0.98
Koch SMVP 32	Structured with intermediate plates (50% open area)	1.08	0.98
Koch SMVP16	Structured with intermediate plates (50% open area)	2.20	0.98

Table 1 Packing Characteristics

To generate a sharp input signal, the continuous water phase in the column was marked with a short impulse of 3.0 mol/dm^3 sodium chloride solution. The tracer was automatically injected into the water inlet pipe through a pneumatic rotary valve for a time of 0.7 seconds at a pressure of 4 bar. Three static mixer elements were inserted into the feed pipe to ensure complete radial distribution of the tracer. The concentration of the tracer was detected with conductivity probes at three locations along the column. The experimental set-up is shown in Figure 1.

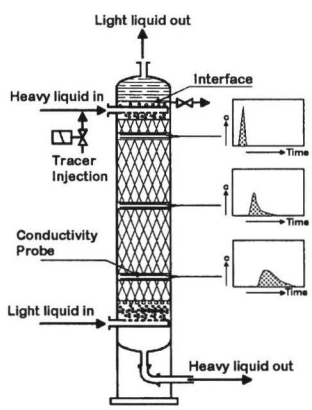


Figure 1. Column setup for tracer injection and detection

The probes were specially constructed to sense the salt concentration over the entire cross-section of the column. A probe occupied only 5.0% of the cross-sectional area for the purpose of not disturbing the flow pattern. The 'time domain fit' was used to evaluate the gathered data. The two-parameter optimisation is necessary because the real velocity of the respective phase is not known and significantly different from the superficial velocity of the continuous phase.

RESULTS AND DISCUSSION

The axial mixing characteristics of each internal are compared in Figure 2. Structured packing with intermediate plates was observed to reduce backmixing relative to structured packing alone. Our data verify that structured packing reduces backmixing relative to the spray column. Nevertheless, it is important to note that structured packings, even with intermediate plates, do not prevent backmixing when operating with low continuous phase velocities (< 0.2 cm/s) suggesting that sieve trays may then be a better selection.

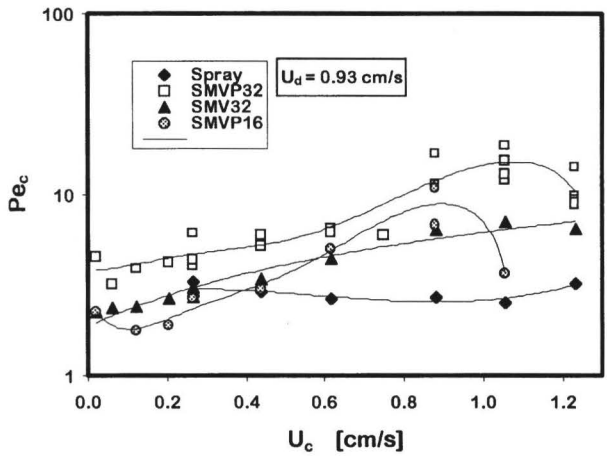


Figure 2. Comparison of Devices

Preliminary models have been developed to predict internal continuous phase velocity ($U_{c,int}$) and the eddy diffusion coefficient. The mechanistic models were develop based on continuous phase velocities ranging from 0.02-1.23 cm/s and dispersed phase velocities ranging from 0.4 -1.34 cm/s. Additional details are described in the report of Becker.[25] The wake-factor (Γ_{mod}) depends on the type of contactor as shown in Table 2. The internal velocities correspond to those evaluated from the tracer experiments. Details regarding the calculation of the internal velocity are given by Becker.[25]

	Γ_o	b
Spray column	1.212	0.516
SMVP-32	0.130	0.229
SMV-32	0.246	1.648
SMVP-16	0.144	0.578

Table 2 Function and parameters for the calculation of the wake-factor $\Gamma_{mod} = \Gamma_0 \cdot e^{-\frac{U_c/U_d}{b}}$ (47)

$$U_{c,\text{int}} = \frac{U_c + \Gamma_{\text{mod}} U_d}{\varepsilon\left(1 - \phi_d\left[1 + \Gamma_{\text{mod}}\right]\right)} \quad \text{(relative error = 14.3\%)} \tag{1}$$

An empirical equation, valid for the spray and packings studied, was established to allow for the calculation of the eddy diffusion coefficient.

$$E_c = 0.583\,\mathrm{Re}_{h,c}^{-0.42}\left(\frac{U_d}{U_c}\right)^{-0.41}\phi_d^{0.44}\Gamma_o^{0.87} \quad \text{(Relative error =23.3\%)} \quad (2)$$

Employing the hydraulic diameter, the respective Reynolds number for the continuous phase can be defined as follows:

$$\mathrm{Re}_{h,c} = \frac{U_{c,\mathrm{int}}\, d_h\, \rho_c}{\mu_c} \quad (3)$$

$$d_h = \frac{4\varepsilon\left[1-\phi_d\left(1+\Gamma_{\mathrm{mod}}\right)\right]}{\left[a_p + a_i\left(1+\Gamma_{\mathrm{mod}}\right)\right]} \quad (4)$$

Mass transfer data have been obtained by Seibert et al.[24] with various packings in the identical column used in the present work. The mass transfer data is based on the system toluene/acetone/water, an extraction factor near unity and acetone transferring from the continuous water to the dispersed toluene phase. The simplified solution proposed by v. Stockar and Lu[11] was used to compare with large-scale mass transfer data. While the design of packed columns is based on the height of a transfer unit (HTU), many industrial designers still prefer to convert the HTU into the height equivalent to a theoretical stage (HETS). The HETS is equivalent to HTU for the case of an extraction factor of one. It should be noted that the dispersed phase Peclet number was assumed to approach plug flow (Pe_E = 10). The model provided reasonable agreement with the experimental data as shown in Figure 3. Further modelling efforts are needed to improve the agreement, particularly for the short packed beds.

$$HTU_{or} = HTU_{or,plug} + \frac{Z}{\left(\frac{\lambda \ln \lambda}{(\lambda-1)}\right) + \frac{1}{\left(\frac{1}{Pe_E} + \frac{1}{\lambda Pe_R}\right)}} \quad (5)$$

Further work is needed with particular emphasis on the development of a physically-derived model that takes the properties of the chemical system into account. Experiments with a second test system (having low interfacial tension) should be carried out to assess the backmixing mechanisms when the drops are small. Since end effects seem to play a significant role in the hydrodynamics of extraction columns, it would also be helpful to use different sets of distributors in order to identify an optimum configuration.

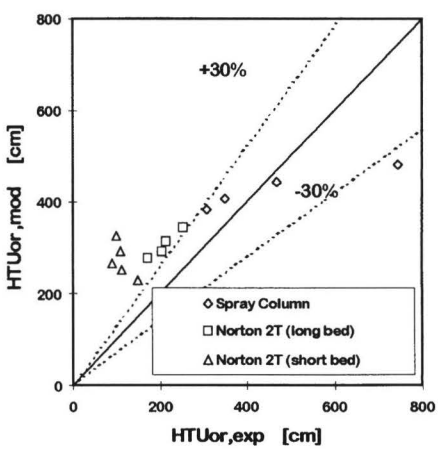


Figure 3. Parity Plot

ACKNOWLEDGEMENT

The authors gratefully acknowledge the financial contributions provided by the DAAD (German academic exchange service), Separations Research Program, and Koch Process Technologies Inc.

NOMENCLATURE

a_i	specific interfacial area ($=6\phi_d\varepsilon/d_{vs}$) , cm^2/cm^3
a_p	specific surface of the column packing, cm^2/cm^3
d_{vs}	Sauter mean drop diameter, cm
d_h	hydraulic diameter (defined in equation 4), cm
E_c	eddy diffusion coefficient, cm^2/s
F	feed rate, g/s
m	equilibrium distribution coefficient, wt./wt.
Pe_i	Peclet number of phase i ($=U_i Z/E_i$)
S	solvent rate, g/s
$U_{c,int}$	calculated internal continuous phase velocity with consideration of the wake factor, cm/s
U_i	superficial velocity of phase I, cm/s
Z	packed height, cm

Greek Symbols

ε	void fraction, cm^3/cm^3
ϕd	fractional dispersed phase holdup, cm^3/cm^3
ρ_c	continuous phase density, g/cm^3
Γ	wake factor (ratio of wake volume to drop volume)
Γ_o	constant in Equation (1)
λ	extraction factor (=Sm/F)
μ_c	continuous phase viscosity, g/cm s

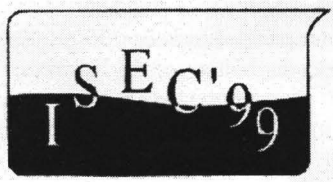
Subscripts

E	extract phase
R	raffinate phase
c	continuous phase
d	dispersed phase

REFERENCES

1 Rosen AM and Krylov VS. *Chem. Eng. J.* **7**, 85, (1974).
2 Pratt HRC in *Handbook of Solvent Extraction*, Eds. Lo TC, Baird MHI and Hanson C. Wiley: New York, (1983).
3 Miyauchi T and Vermeulen T. *Ind. Eng. Chem. Fund.* **2**, 113, (1963).
4 Sleicher CA. *AIChE J.* **5**, 145, (1959).
5 Ricker NL, Nakashio F and King CJ. *AIChE J.* **27**, 277, (1981).
6 Mecklenburgh JC and Hartland S. *The Theory of Backmixing*, Wiley-Interscience, New York (1975).
7 Stemerding S and Zuiderweg FJ. *Chem. Eng.* **5**, 156, (1963).
8 Richter M. *Chem. Techn.*, **30**, 294, (1978).
9 Pratt HRC. *Ind. Eng. Chem. Proc. Des. Dev.* **14**, 74, (1975).
10 Pratt HRC. *Ind. Eng. Chem. Proc. Des. Dev.*, **15**, 34, (1976).
11 Von Stockar U and Lu X. *Ind. Eng. Chem. Res.* **30**, 1248, (1991).
12 Rod V. *Brit. Chem. Eng.* **2**, 483, (1966).

13 Aufderheide E and Vogelpohl A. *Chem. Eng. Sci.* **41**, 1747, (1986).
14 Hennico A, Jaques GL, Moon JS and Vermeulen T. *Univ. of Calif. Rad. Lab.* Rep. No. URCL-10696, (1963).
15 Ingham J. in *Recent Advances in Liquid-liquid Extraction*, Ed. Hanson C. Pergamon Press: Oxford, New York (1971).
16 Vermeulen T, Moon JS, Hennico A and Miyauchi T. *Chem. Eng. Prog.* **62**, 95, (1966).
17 Watson J S, McNeese LE. *Ind. Eng. Proc. Des. Dev.*, **11**, 120, (1972).
18 Pratt HRC and Anderson WS. *Proc. ISEC '77*, **1**, 242, (1977).
19 Wen C-Y and Fan LT. *Models for Flow Systems and Chemical Reactors*, Dekker: New York, (1975).
20 Komasawa I and Ingham J. *Chem. Eng. Sci.* **33,** 479, (1978).
21 Streiff FA. *Chem. Ing. Tech.* **55,** 1102, (1983).
22 Jancic SJ, Zuiderweg FJ and Streiff F. *AIChE Symp. Ser. No. 238*, **80,** 139, (1984).
23 Rauber J. *Dissertation*, University of Erlangen, (1996).
24 Seibert F, Reeves B and Fair J. *Ind. Eng. Chem. Res.*, **29**, 1901, (1990).
25 Becker O. *DAAD Research Report*, October 1998.
26 Steiner L. *Rechnerische Erfassung der Arbeitsweise von Flüssig-Flüssig Extraktionskolonnen, Fortschr.-Ber. VDI Reihe 3 Nr. 154*, VDI-Verlag: Düsseldorf (1988).



PERFORMANCE OF A VIBRATING PERFORATED PLATE EXTRACTOR – HOLDUP AND CHARACTERISTIC VELOCITY

Luiz MN Góis[1], EB Tambourgi[2], JAFR Pereira[2] and JJ Marques[2]

[1]Federal Universty of Bahia, Departament of Chem. Eng. R. Aristides Novais 2 Federação CEP 40.210-630, Salvador, Bahia, Brazil

[2]University of Campinas, DESQ/FEQ CEP 13083-970, Campinas, São Paulo, Brazil

ABSTRACT

The present work refers to dispersed phase holdup in a vibrating perforated plate extractor. Experimental results of holdup are expressed in terms of experimental parameters, in such a way that one can see the isolated influence of each parameter on the holdup. New empirical correlations to characteristic velocity is also presented.

Keywords: holdup, perforated plate pulsed extraction column, characteristic velocity

INTRODUCTION

Liquid-liquid extraction is an established method to promote separation of homogeneous liquid mixtures. It finds wide application in the petroleum refining, petrochemical, nuclear, pharmaceutical, metallurgical and other chemical industries. In most industrial applications, multistage countercurrent contacting is required. The hydrodynamic driving force necessary to promote counter-current flow and subsequent phase separation may be derived from the differential effects of either gravity or centrifugal force on the two immiscible phases.[1]

Due to the great importance of holdup in the project of extraction equipment, some authors have published works with empirical correlations to predict holdup fraction in their apparatus. Thornton,[9] Kumar et al.,[6] Rama Rao et al.,[8] Baird et al.[2] among others appear as the authors of the most important works concerning this issue in the last years.

The objective of the present work is evaluate a reciprocating perforated plate extractor using experimental data of dispersed phase holdup. The effects of frequency and amplitude of pulsation and dispersed phase flow-rate on the behavior of holdup are analyzed for a great number of situations. Furthermore a new correlation for characteristic velocity is also presented.

EXPERIMENTAL

The vibrating perforated plate extractor consisted of a glass tube, 97 cm height and 5.5 cm internal diameter, enclosing a PVC plate arrangement. The plates were attached to a PVC shaft and connected to a pulsation mechanism. The operation ranges are given in Table 1.

Operation Characteristics:	Range of Operation
Number of plates	4 and 7
Percent of Free Area	20% and 38%
Frequency (s^{-1})	0.4; 0.7; 1.2; 1.9
Amplitude (cm)	4.0; 6.0; 8.0
Dispersed Phase Flowrate (cc/sec)	7.3; 8.4; 10.8; 14.2
Continuous Phase Flowrate (cc/sec)	0.83; 3.83; 6.83; 10.00

Table 1 – The Operational Ranges of the equipment

© 2000 Society of Chemical Industry

The continuous phase was water, fed to the top of the column pumped by a centrifugal pump and metered by a rotameter. The dispersed phase was butanol fed to the bottom of the extractor by gravity and metered by another rotameter.

The dispersed phase holdup in steady state operation was measured directly by stopping all flows and then measuring the amounts of each phase present. In the holdup fraction calculation, the known volume of dispersed phase (butanol) in the upper layer was divided by the total volume of the column.

EFFECT OF OPERATING PARAMETERS ON THE HOLDUP

The effect of operating parameters on the holdup are illustrated using graphics and tables where holdup fraction is plotted against the variable analyzed.

Effect of Pulsation Frequency

The effect of pulsation frequency is illustrated by the experimental results shown in the figures 1 and 2. It can be seen the holdup increases with the increase of pulsation frequency values. This fact occurs because the drop breaking is increased at high frequencies. This effect increases the interfacial area and the dispersed phase holdup.

According to the figures, this increase is more effective at higher dispersed phase flowrate.

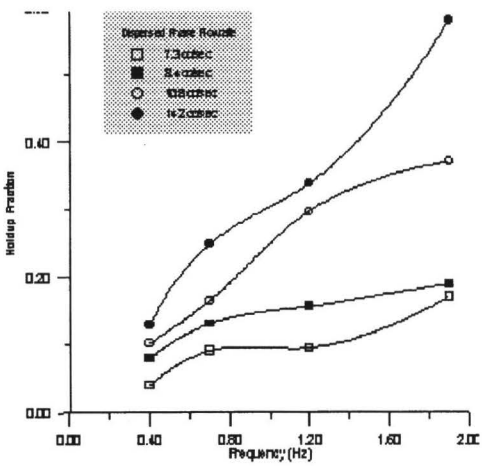


Figure 1 – Holdup fraction against frequency
Free area 20%, 7 plates, A= 4cm,
Q_c = 10.0 cm^3/sec

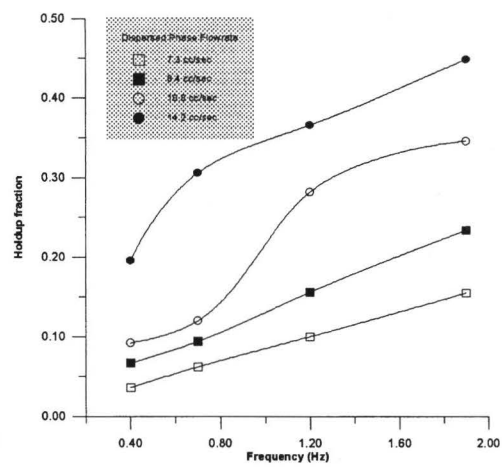


Figure 2 – Holdup fraction against frequency
Free area 20%, 7 plates, A= 4cm,
Q_c = 11.2 cm^3/sec

Effect of Pulsation Amplitude

Figures 3 and 4 are plots of Dispersed Phase Holdup against Pulsation Amplitude. In both cases, most curves show a sharp point corresponding to a relative maximum holdup.

The behavior shown in all the figures can be interpreted through the pulsation energy supplied to the liquid mass. The energy transferred to liquid depends strongly upon amplitude and frequency whose product, *(f.A)*, represents the pulsation velocity. The higher is this velocity the higher will be the energy transferred. However, in the cases studied amplitudes higher than 6.0 cm provided undesirable operating conditions, because the amount of energy reduced the holdup.

Similarly to the frequency effect, the amplitude effect is also based upon on the drop breaking. With the intense break of drops, the contact between the phases is improved. However, for amplitude ranges higher than 6.0 cm, the dispersed phase drops reach small sizes, incurring entrainment and the decrease of the holdup fraction.

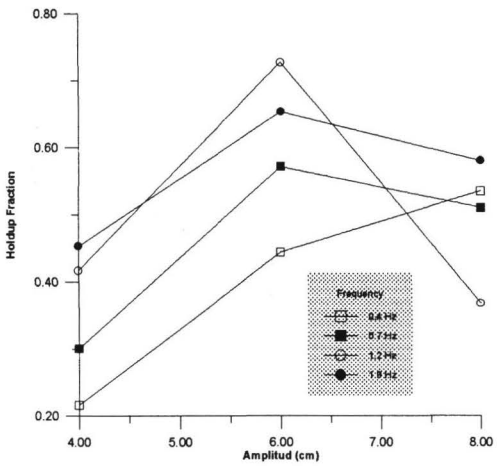


Figure 3 – Holdup fraction against Amplitude
Free area 20%, 7 plates, A= 4cm,
Q_c = 10.0 cm^3/sec

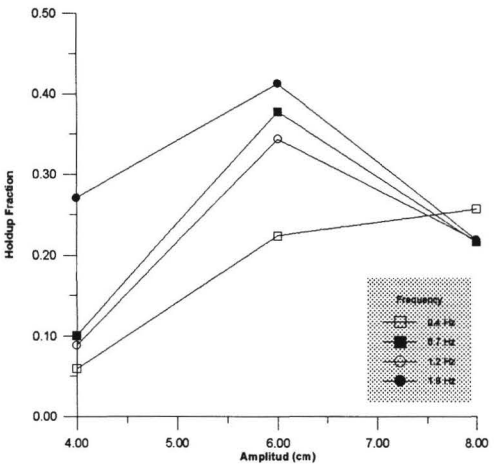


Figure 4 – Holdup fraction against Amplitude
Free area 20%, 7 plates, A= 4cm,
Q_c = 11.2 cm^3/sec

Effect of Dispersed Phase Flowrate

The process of mixing in agitated extractor is enhanced both by agitation energy supplied to liquid and by the countercurrent flow of liquid phases. So it was expected the increase of holdup with the dispersed phase flow.

Observing figures 5 and 6 this expectation can be confirmed. The holdup increases with the dispersed phase flow to different continuous phase flows and internal arrangements. One can expect that in situations where occur flooding phenomena the opposite behavior must occur.

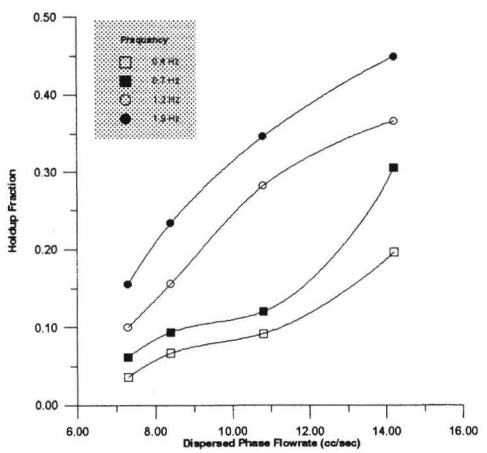


Figure 5 – Holdup fraction against Dispersed Phase Flowrate
Free area 20%, 7 plates, A= 4cm,
Q_c = 11.2 cm^3/sec

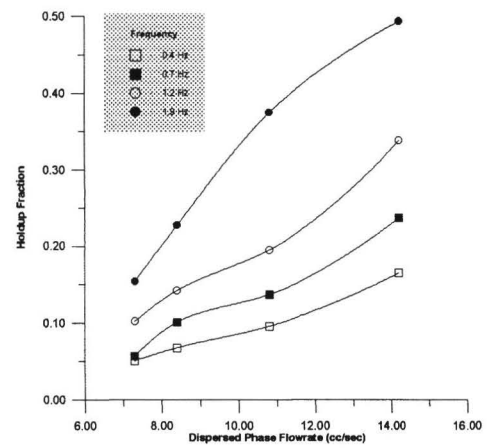


Figure 6 – Holdup fraction against Dispersed Phase Flowrate
Free area 20%, 4 plates, A= 4cm,
Q_c = 10.0 cm^3/sec

CORRELATION FOR CHARACTERISTIC VELOCITY

Analyzing the studies reported on the literature concerning characteristic velocity in agitated mechanical extraction columns, it was concluded that the model proposed by Baird and Shen[2] relating to the concept of relative velocity formerly described by Dell and Pratt,[4] is the most suitable model to correlate experimental data in the present work.

According to Baird and Shen[2] the following equation can be applied to vibrating plate columns:

$$\frac{V_d}{\phi} + \frac{V_c}{1-\phi} = V_0 \frac{(1-\phi)}{\phi^{1/3}} \tag{1}$$

As shown in equation 1 the characteristic velocity can be perfectly obtained by a linearization process. The parameter *Vo* would be the angular coefficient for an *X "versus" Y* plot.

$$X = \frac{1-\phi}{\phi^{1/3}} \quad (2); \qquad Y = \frac{V_d}{\phi} + \frac{V_c}{1-\phi} \tag{3}$$

It was expected that the behavior of the points were conduced to a straight line. However, the figure 7 shows a strong tendency to the behavior of a crescent function. In this case, it was fitted into a third degree polynomial:

$$Y = 0.213X^3 + 0.312X^2 - 0.311X + 1.746 \tag{4}$$

Here, V_0, is interpreted as the angular coefficient of the equation 1. The value of V_0, providing through differentiation of equation 4.

Thus,

$$V_o(X) = 0.639X^2 + 0.624X - 0.311 \tag{5}$$

$$V_0 = 0.639\left[\frac{1-\phi}{\phi^{1/3}}\right]^2 + 0.624\left[\frac{1-\phi}{\phi^{1/3}}\right] - 0.311 \tag{6}$$

This is the equation obtained in the present work to calculate characteristic velocity in function of the holdup fraction.

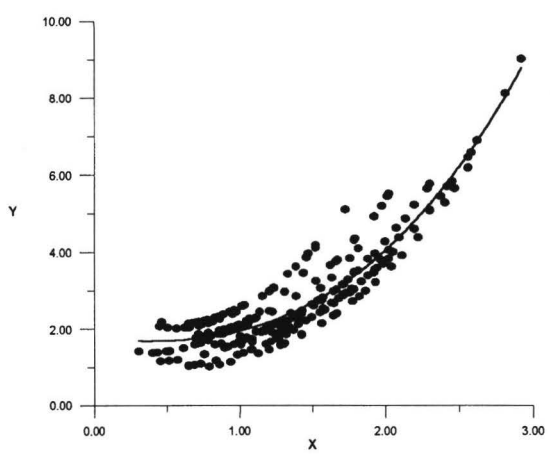


Figure 7 - Linearization Process of the equation 1.

The characteristic velocity is a parameter that depends on drop size and physical proprieties of the liquid system.[2] So, the non-liner behavior presented in the figure 7 is justified due to the dispersed phase entrainment effect that can occur inside the extractor. This effect was reported in the previous items of the present work.

CONCLUSIONS

The experimental results reported in the present work show a good performance of the equipment to provide high values of dispersed phase holdup that is a very important parameter in a mass transfer operation process.

In the studies about the effect of operational parameters, good parameter combinations were obtained like, for example, pulsation frequency of 1.9 s^{-1}; pulsation amplitude of 6.0 cm and dispersed phase flow 14.2 cm^3/sec that provided very satisfactory holdup levels. In the cases studied, the holdup was influenced by the dispersed phase flow.

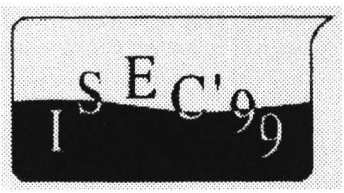
A Velocity Characteristic correlation was obtained with a good adjustment of data. Further, this equation can be tested with other pulsed extractors.

NOMENCLATURE

A - Amplitude (cm)
cm^3/sec - cubic centimeters per second;
f - Frequency (s^{-1})
Q_c - Continuous phase flow (cm^3/sec)
Q_d - Dispersed phase flow (cm^3/sec)
ϕ - Holdup fraction
V_0 - Characteristic velocity (cm/s)
X - Shown by equation 2
Y - Shown by equation 3

REFERENCES

1. Alatiqi G et al, (1995).
2. Baird MHI and Shen ZJ, *Can. J. Chem. Eng.*, **62**, 218, (1984).
3. Chen BH and Liu CH, *Can. J. Chem. Eng.*, **69**, 300, (1991).
4. Dell FR and Pratt HRC, *Trans. Inst. Chem. Eng.*, **29**, 89, (1951).
5. Góis LMNG *Tese de Doutorado*, DESQ/FEQ/UNICAMP, (1995).
6. Kumar A and Hartland S, *Chem. Eng. Res. Des.*, **61**, 248, (1983).
7. Marques JJ *Tese de Mestrado*, DESQ/FEQ/UNICAMP, (1994).
8. Rama Rao NV et al, *Can. J. Chem. Eng.*, **61**, 168, (1983).
9. Thornton J, *Trans. Inst. Chem. Eng.*, **35**, 316, (1957).



THE IMPORTANCE OF DROP COALESCENCE IN A STIRRED LIQUID–LIQUID EXTRACTION (KÜHNI) COLUMN

MLACN Gomes[1], MML Guimarães[1], G Zamponi[2], J Stichlmair[2], PFR Regueiras[3] and JJC Cruz-Pinto[4]

[1] Instituto Superior de Engenharia, Instituto Politécnico do Porto, Portugal

[2]Lehrstuhl A für Verfahrenstechnik, Technische Universität München, Germany

[3] Faculdade de Engenharia, Universidade do Porto, Portugal

[4]Departamento de Química, Universidade de Aveiro, Aveiro, Portugal

ABSTRACT

Experiments performed at low agitation speeds, using the high interfacial tension toluene (dispersed)-water (continuous) system, in a pilot plant Kühni column, show that coalescence events are generally present and cannot be neglected in column-type liquid-liquid contactors, especially when the goal is the accurate modelling of the transient processes for control purposes. In this work, the features of this behaviour and the applicability to this situation of a new, fast and precise, recently developed algorithm,[1] that describes the dynamic behaviour of an agitated column, is illustrated. Experiments were performed at low agitation speeds, using the above high interfacial tension system. The simulations show reasonably good agreement with the experimental results and provide insight on the underlying behaviour mechanisms and important guidelines for the accurate modelling of the dynamics of the column.

Keywords: Kühni column, drop coalescence, drop breakage, column dynamics.

INTRODUCTION

Mechanically agitated devices for liquid-liquid contact in column extraction equipment have acquired great importance, thanks to their ability to create large interfacial areas, which promote mass transfer. The capacity and mass transfer efficiency of these columns have been shown to be greatly influenced by the hydrodynamic and mixing effects caused by drop interactions (breakage and coalescence).

In recent years, many authors have spent great effort in modelling these columns and in the experimental validation of their models. Models such as those of Cruz-Pinto,[2] Casamatta and Vogelpohl,[3] Laso *et al.*,[4] Tsouris *et al.*[5] and, more recently, Gerstlauer *et al.*[6] have been proved able to describe with reasonable accuracy the results of their authors' experiments, but most of them adopted significant simplifications, in order to make calculations feasible in reasonable time. The most important simplification commonly made is to ignore inter-drop coalescence, because the modelling of this effect is responsible for most of the computational effort required for the solutions.

However, even in strongly agitated columns, such as the Kühni type, coalescence is generally present, being responsible for mixing effects that promote higher mass transfer rates. Zamponi *et al.*[7] noted this fact, and explicitly recommended the inclusion of coalescence effects in future modelling efforts. More recently, Kentish *et al.*,[8] although using a simplified model, included coalescence effects to obtain good agreement with experimental data from their Kühni column. In addition, for control purposes, the agitation intensity may be an important manipulating variable and, in order to avoid flooding, its value may be lowered such as to adequately promote drop coalescence.

Recently, a simplified version of an algorithm previously developed by Ribeiro,[9] and further streamlined by Regueiras *et al.*,[10] has been proved able to accurately describe the transient behaviour of a continuous ideally agitated vessel, requiring only modest computer resources and very low computation times. Details of these models and corresponding algorithms are given elsewhere by Ribeiro *et al.*[11] and Regueiras *et al.*[10] A new powerful algorithm that combines the previous ones with a new transport model to describe the hydrodynamics of an agitated column has been developed by

© 2000 Society of Chemical Industry

Regueiras [1] and is used in the present work. Its application yields an encouraging agreement with the experimental results described below, which were obtained in a pilot plant Kühni column (University of Munich).

EXPERIMENTAL

The experimental work was carried out by Gomes[12] in a Kühni pilot plant column (150 mm inside diameter, active height of 2520 mm, divided into 36 stirred compartments). The test system was the equilibrated standard high interfacial tension toluene (dispersed phase)-water (continuous phase) system. Experiments at room temperature, under steady state conditions, were made both at normal and low levels of agitation. For flow capacities (superficial velocities) of about 16 $m^3/(m^2.h)$, for which the normal operating range is within 140-150 rpm for this column, the agitation range was extended down to 100 rpm. Drop size distributions (by a photoelectric technique) and local hold-ups (by an ultrasonic technique) were measured. Due to the low agitation intensity, local hold-ups were much lower than under normal conditions and, consequently, the sampling time needed for sucking in the required 1000 sample drops was much longer than usual.

The local hold-up response to step modifications of the agitation intensity was also measured, by bringing the agitation intensity down to 100 rpm, after steady state was reached at 140 rpm. Local hold-up measurements were also made when the agitation intensity was suddenly increased from 100 to 140 rpm.

THE MODEL

The Kühni column may be adequately described as a sequence of agitated vessels with back- and forward mixing effects on the movement of the dispersed phase along the column, using a population balance formulation, with Coulaloglou and Tavlarides's drop interaction frequencies.[13] The resulting equations were solved for each compartment by the numerical technique developed by Ribeiro[9] and further streamlined by Regueiras *et al.*[10]

A new transport model was developed to describe the drop and continuous phase motions between stages. This transport model is based on the one described by Cruz-Pinto[2] and directly calculates the slip velocities, taking into account the density effects and the drag relationships for the drops, as previously modelled by Barnea and Mizrahi.[14,15]

The backmixing effect was also described and modelled as a random deviation superimposed on the terminal velocities of the drops, taking into account the influence of the agitation intensity, as a function of the rotor peripheral speed. A geometrical constriction factor, C_R, which controls the drop passage between stages, was calculated as a linear function of the fractional free area of the separators, as suggested by Goldmann.[16] The equations for this model are given elsewhere by Regueiras.[1]

RESULTS AND DISCUSSION

Figure 1 shows experimental and simulated local drop size number distributions along the column height, for the indicated continuous (F_C) and dispersed (F_D) phase flows, at moderate (140 rpm) and low (100 rpm) agitation speeds. The values for the parameters of the drop population balance model used (which have not yet been fully optimised) were identical in both simulations and very similar to those used in previous work by Guimarães,[17] concerning agitated vessels, as well as (to within less than 20%) to the ones used by Coulaloglou[12] and Bapat,[18] which have been claimed to be nearly "universal constants" for uniformly agitated contactors.

At the lowest agitation speed, a marked effect of coalescence may be identified, even in the upper stages of the column. The larger drops obtained overall, and the corresponding larger drop diameters at the upper stages, are justified (and can be approximately predicted by the algorithm) by the increased coalescence relative to breakage, combined with the more rapid motion of such large

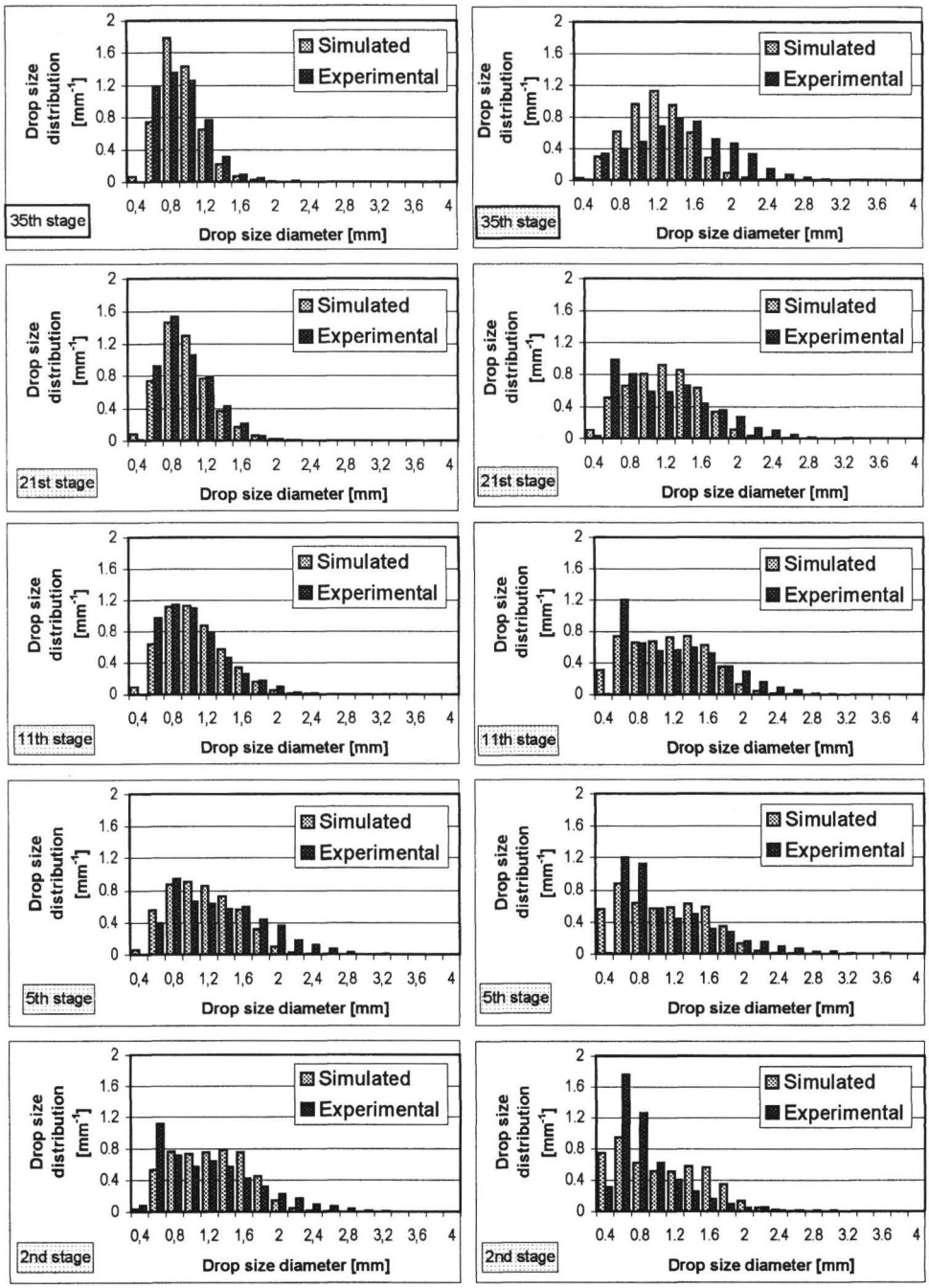


Figure 1. Drop size distributions for the equilibrated toluene-water system: F_C = 125 L.h^{-1}; F_D = 160 L.h^{-1}; left: I = 140 rpm, right: I = 100 rpm.

drops up along the column. The poorest agreement between simulated and experimental drop size distributions was obtained at the lowest instrumented stage (2nd) of the column (also the closest to the inlet dispersed phase distributor, for which experimental drop size data could not be measured, thus having to be grossly estimated).

Additionally, it may be noted that, at 100 rpm, drop coalescence combined with less intensive breakage is responsible for the bimodal shape of the drop size distributions (as also approximately predicted by our model), which dies out only at the highest stages of the column, while the distributions are unimodal at 140 rpm, except at the lowest stages.

It is somewhat intriguing that, at the column's 2nd stage, the experimental drop size distribution is wider and has higher average drop size at 140 rpm than at 100 rpm. At this stage it is also bimodal at 140 rpm, although this feature is quickly lost higher up in the column, whereas such bimodal character appears only at higher stages at 100 rpm, finally to disappear at the highest stages. Here, the average drop size stabilises close to the higher modal size. The same features were found in various other experimental runs at low agitation rates.[12]

These observations, and the way the darker (experimental) size distribution shifts and widens its shape along the column, can only be explained by increased drop coalescence relative to breakage at 100 rpm.

It is also reasonable to presume that, at the indicated flows, the distributor produces static drop size distributions (detectable by photography or any stage sampling method, like the one used) closer to those found at the 2nd stage for the lowest agitation rate. These, for more intensive agitation, given the higher local hold-up, will quickly tend to coalesce, yielding the bimodal distribution found at the bottom stages. Higher up in the column, however, it will quickly become unimodal, with a clearly decreasing average drop size.

Considering that these are as yet non-optimised simulations, the agreement obtained for the local hold-ups may also be considered satisfactory, within the variation range of repeated experimental runs, as indicated in Figure 2.

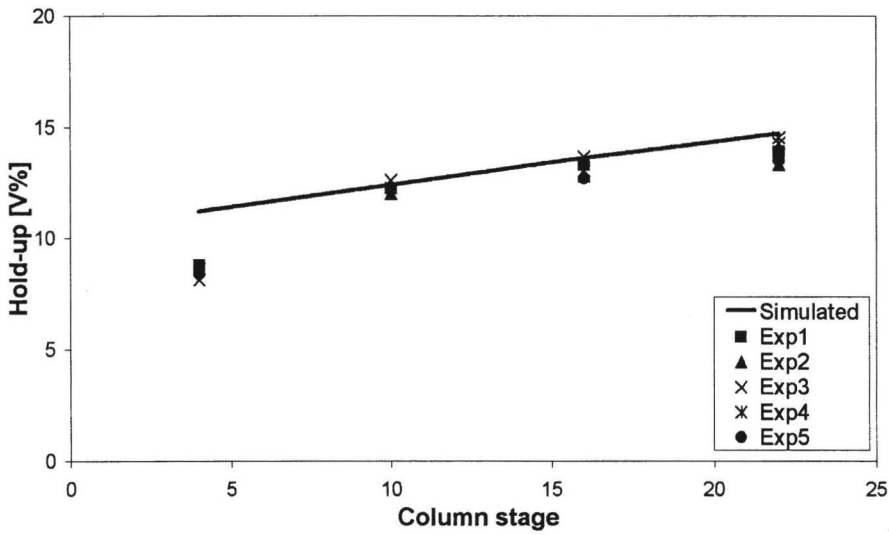


Figure 2. Hold-up profiles at steady-state – F_C = 125 L.h^{-1}, F_D = 160 L.h^{-1}, I = 140 rpm

The same coalescence effect becomes apparent when comparing the local dispersed phase hold-up values experimentally obtained before and after sudden step changes in the agitation rate (Figure 3). In this case, it may be noticed that the dispersed phase hold-up variation between the 16th and the 22nd stages is reversed, after an agitation rate change from 140 to 100 rpm. This may be understood as a

result of increased coalescence/breakage frequency ratios, as the drops are broken down along the column height.

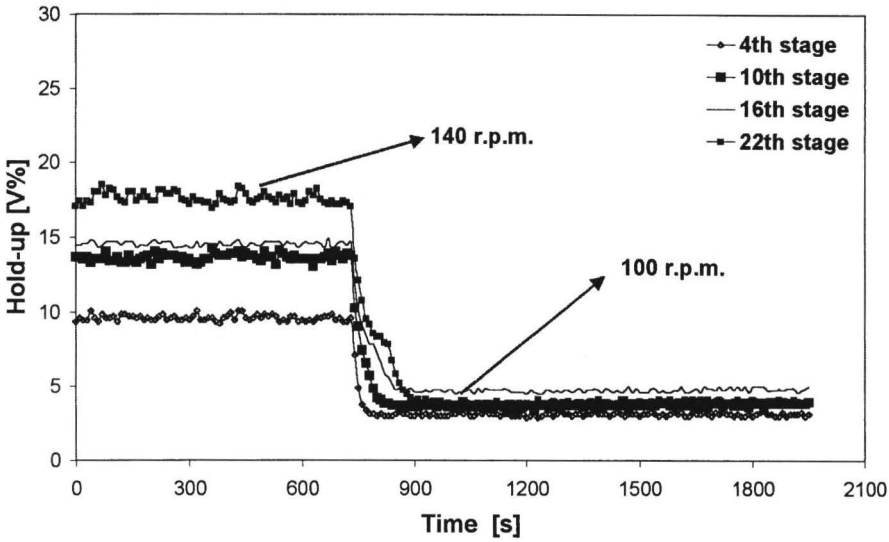


Figure 3. Hold-up profiles before and after sudden step changes in the agitation rate- F_C = 125 $L.h^{-1}$, F_D = 160 $L.h^{-1}$.

CONCLUSIONS

Although the operating range explored in this paper is not representative of normal steady state conditions, inter-drop coalescence cannot be neglected, when predicting (for control purposes) both the steady state and dynamic behaviour of liquid-liquid extraction columns.

A new, powerful, precise and fast algorithm to simulate the hydrodynamic behaviour of a mechanically agitated column (Kühni type) has been developed.

The algorithm is able to predict the local drop size distributions and the local hold-up profiles of a pilot plant Kühni column.

The agreement with the experimental data obtained in the pilot plant suggests that Coulaloglou and Tavlarides' population balance model may be appropriate, as well as, with minor modifications, the values for the breakage and coalescence parameters used by these authors for agitated vessels.

Further optimisation of the interaction constants and transport parameters is possible and is being pursued, along the lines of our previous and current work on mixers, for comprehensive equipment performance predictions.

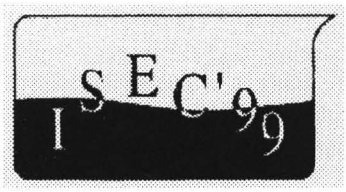
ACKNOWLEDGEMENT

Co-operation is gratefully acknowledged from Professor J. Stichlmair's staff at the Technical University of Munich.

REFERENCES

1. Regueiras PFR, *Ph.D. Thesis*, in preparation.
2. Cruz-Pinto JJC, *Ph.D. Thesis, The Victoria University of Manchester*, (1979).

3. Casamatta G and Vogelpohl A, *Ger. Chem. Eng.*, **8**, 96, (1985).
4. Laso M, Steiner L and Hartland S, *Chem. Eng. Sci.*, **42**, 2429, (1987).
5. Tsouris C, Kirou VI and Tavlarides LL, *AIChE Journal*, **40**, 407, (1994).
6. Gerstlauer A, Mitrovic A, Gilles ED, Zamponi G and Stichlmair J, *Value Adding Through Solvent Extraction, Proc. ISEC'96*, ed.Shallcross DC, Paimin R, Prvcic LM, University of Melbourne, **1**, 1091, (1996).
7. Zamponi G, Stichlmair J, Gerstlauer A and Gilles ED, *Value Adding Through Solvent Extraction, Proc ISEC'96* ed.Shallcross DC, Paimin R, Prvcic LM, University of Melbourne, **1**, 1049, (1996).
8. Kentish SE, Stevens GW and Pratt HC, *Ind. Eng. Chem. Res*, **37**, 1099, (1998).
9. Ribeiro LM, *Ph.D. Thesis, Universidade do Minho, Braga, Portugal*, (1995).
10. Regueiras PFR, Ribeiro LM, Guimarães MML and Cruz-Pinto JJC, *Value Adding Through Solvent Extraction*, Proc ISEC'96 ed.Shallcross DC, Paimin R, Prvcic LM, University of Melbourne, **1**, 1031, (1996).
11. Ribeiro LM, Regueiras PFR, Guimarães MML and Cruz-Pinto JJC *Computing Systems in Engngr.*, **6**, Nl 4/5, 465, (1995).
12. Gomes MLACN, *Ph.D. Thesis*, in preparation.
13. Coulalouglou CA and Tavlarides LL, *Chem. Eng. Sci.*, **32**, 1289, (1977).
14. Barnea E and Mizrahi J, *Ch. Eng. J.*, **5**, 171, (1973).
15. Barnea E and Mizrahi J, *Can. J. Chem. Eng.*, **53**, 461, (1974).
16. Goldman G, *Ph.D. Thesis, Technical University of Munich, Germany*, (1986).
17. Guimarães MML, *Ph.D. Thesis, Universidade do Minho, Braga, Portugal*, (1989).
18. Bapat PM, Ph.D. *Thesis, Illinois Institute of Technology, Chicago, Illinois*, (1982).



STAGE EFFICIENCIES AND MASS TRANSFER COEFFICIENTS IN A MIXER–SETTLER EXTRACTION COLUMN

K Takahashi, T Ban, K Tani, S Nii and F Kawaizumi
Department of Chemical Engineering, Nagoya University, Japan

ABSTRACT
The relationship between the stage efficiency and the volumetric overall mass transfer coefficient in a mixer-settler extraction column has been derived under an assumption of complete mixing within the mixer. Stage efficiencies measured with the extraction of iodine by heptane were in good agreement with the values estimated from the volumetric overall mass transfer coefficient. The latter was calculated with the interfacial area obtained from the drop diameter and the dispersed phase hold-up and the overall mass transfer coefficient determined from the mass transfer coefficients of the dispersed and the continuous phases. This indicates that the stage efficiency can be estimated for the liquid-liquid system where drop coalescence in the mixer play a minor role. The effects of both phase flow rates and the distribution ratio of solute on the stage efficiencies were discussed on the basis of the calculated results.

Keywords: stage efficiency, mixer-settler column, mass transfer

INTRODUCTION

The mixer-settler extraction column (MS column) proposed by Takahashi et.al.[1] has the characteristics that the maximum throughput increases with the agitation speed. At a high agitation speed, the mass transfer efficiency is high because of a large interfacial area due to the small dispersed drops and the large hold-up of the dispersed phase. Therefore, an effective separation with a high mass transfer efficiency and a large throughput can be realized by the MS column. A schematic diagram of one stage (stage number n) in the MS column is shown in figure 1. It consists of the lower mixer part, the upper settler part and the drop coalescer between them. The continuous phase (aqueous phase) flows into the mixer from the upper stage through the downspout, rises into the settler across the drop coalescer with the dispersed phase, and flows into the lower stage through the downspout after separation into two phases. The dispersed phase from the lower stage rises into the mixer through the riser, is dispersed into small drops within the mixer, coalesces within the coalescer and rises into the upper stage after separation from the continuous phase within the settler. The throughput increases with the agitation speed because the suction pressure induced by the lifter-turbine impeller promotes the dispersed phase flow through the riser (50 $m^3/(m^2hr)$) for agitation speed of 10 s^{-1} in a column of 100 mm diameter), and can be determined from a force balance between the pressure drop with the fluid flow and the sum of the suction pressure and the buoyant force of the dispersed phase in the riser.[2] The mass transfer characteristics of the MS column were given by Nii et.al.[3] To determine the practical stage number of the multistage extraction column for a given separation, the stage efficiency is indispensable as well as the theoretical stage number.

In the present study, the relationship between the stage efficiency and the volumetric overall mass transfer coefficient is derived. Stage efficiency calculated from the estimated mass transfer coefficients and the estimated interfacial area is compared with the experimental value measured with a single stage MS column. The effects of the flow rates and the distribution ratio on the stage efficiency are discussed by using the calculated stage efficiencies.

STAGE EFFICIENCY

Assuming that the mass transfer occurs only within the mixer and both phases in the mixer are completely mixed, the mass balance in the n-th stage is given as follows, using the continuous phase concentrations given in figure 1 and the volumetric over-all mass transfer coefficient, $K_{oc}a$, based on the continuous phase concentration:

© 2000 Society of Chemical Industry

$$K_{oc}a\ V_M(C_{c,n} - C_{c,n}^*) = Q_c(C_{c,n-1} - C_{c,n}) \quad (1)$$

where V_M is volume of the mixer, Q_c the flow rate of continuous phase and $C_{c,n}^*$ the continuous phase concentration in equilibrium with the dispersed phase, $C_{c,n}^* = C_{d,n}/m$, where m is the distribution ratio. Drops within the mixer have various concentrations according to the residence time of each drop, and$C_{d,n}$ is an average concentration of dispersed drops leaving the stage. From equation 1, the relationship between the stage efficiency and the volumetric mass transfer coefficient is derived as follows:

$$E_{oc} = (C_{c,n-1} - C_{c,n})/(C_{c,n-1} - C_{c,n}^*) = (K_{oc}a\ V_M/Q_c)/\{1 + (K_{oc}a\ V_M/Q_c)\} \quad (2)$$

In the same way, the stage efficiency, E_{od}, based on the dispersed phase concentration is expressed as:

$$E_{od} = (C_{d,n} - C_{d,n+1})/(C_{d,n}^* - C_{d,n+1}) = (K_{od}a\ V_M/Q_d)/\{1 + (K_{od}a\ V_M/Q_d)\} \quad (3)$$

where $C_{d,n}^*$ is the dispersed phase concentration in equilibrium with $C_{c,n}$, $K_{od}a$ the volumetric over-all mass transfer coefficient based on dispersed phase concentration and Q_d the dispersed phase flow rate. The stage efficiency can be determined by equations 2 or 3 if the volumetric over-all mass transfer coefficient is estimated.

EXPERIMENTAL

The extraction of iodine from I_2-KI aqueous solution into heptane was carried out with a single stage mixer-settler column of 100 mm diameter. When the multistage MS column was used, the outlet concentration was too small to get an accurate result, so the single stage column was used. Iodine concentration in the aqueous phase was determined by titration with a sodium thiosulfate solution and that in the organic phase by a spectrophotometer. The distribution ratio of iodine changes largely with KI concentration, then the ratio was measured for each experimental run. The outlet concentrations normalized with the inlet concentration are shown in figure 2, where $C_{c,in}$, $C_{c,out}$ and $C_{d,out}$ correspond to $C_{c,n-1}$, $C_{c,n}$ and $C_{d,n}$ in figure 1, respectively. When the flow rate of dispersed phase Q_d was larger than that of continuous phase Q_c, almost all solute in the continuous phase was extracted and the change of outlet dispersed phase concentration varied little with the agitation speed N. The stage efficiency is plotted against N in figure 3. The efficiency increases with N until beyond 0.9 for $N > 10\ s^{-1}$. For a given N, E_{oc} was large when the flow ratio Q_d/Q_c was large.

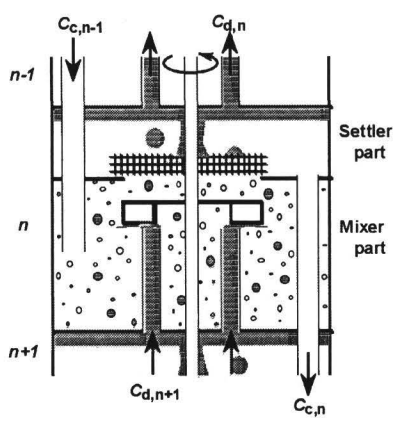


Fig.1 Schematic diagram of one stage in mixer-settler extraction cosumn

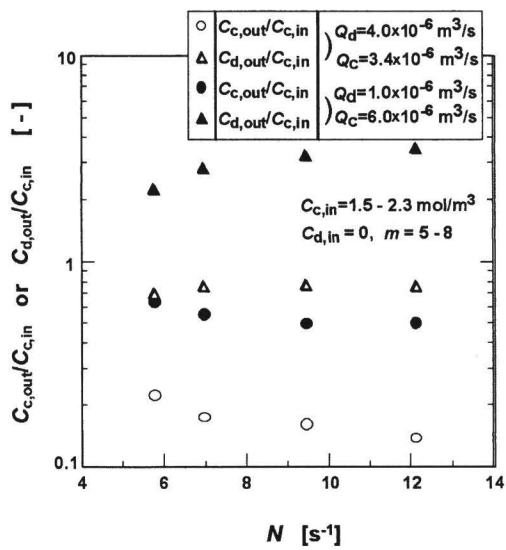


Fig.2 Outlet concentration normalized with inlet concentration

ESTIMATION OF STAGE EFFICIENCY

Interfacial Area

The volumetric over-all mass transfer coefficient is obtained from the specific interfacial area a and the mass transfer coefficients k_d in the dispersed phase and k_c in the continuous phase. The interfacial area is given by:

$$a = 6\phi/d_{32} \tag{4}$$

where ϕ is the dispersed phase hold-up in the mixer and d_{32} Sauter mean diameter of dispersed drops. In the present mixer, the hold-up above the impeller ϕ^U was smaller than that below the impeller ϕ^L, and these hold-ups could be estimated as follows for the mixer-settler extraction column of 100 mm in diameter.[4] The average hold-up in the mixer is given as:

$$\phi = (\phi^U V^U + \phi^L V^L)/V_M \tag{5}$$

where V^U and V^L are volumes above and below the impeller, respectively. Since agitation above the lifter-turbine impeller is mild, ϕ^U can be related with the slip velocity, v_s, between two phases that rise concurrently around the impeller:

$$v_s = (1/A)\{Q_d/\phi^U - Q_c/(1 - \phi^U)\} \tag{6}$$

where A is cross sectional area of flow path around the impeller. This slip velocity could be correlated with the terminal settling velocity v_t as follows[5] for the system in which drops hardly coalesced:

$$v_s = 0.21 v_t \tag{7}$$

From equations 6 and 7, the value of ϕ^U can be calculated for the flow rates Q_c and Q_d. Below the impeller in the mixer, there is a circulating core where the dispersed phase hold-up is expressed by a uniform value of ϕ^L. The dispersed phase comes into the core from the lower stage through the riser, while it may leave the core by two mechanisms: one is transfer by mixing due to the difference in hold-up between above and below the impeller and the other is transfer accompanied by the total flow:

$$Q_d = K_\phi A(\phi^L - \phi^U) + (Q_d + Q_c)\phi^L \tag{8}$$

where K_ϕ [m/s] is the transfer coefficient of dispersed drops and was correlated with N [s] by:

$$K_\phi = 0.0043 + 260\, N^7 \tag{9}$$

The coefficient was independent of Q_d, Q_c, $\Delta\rho$ and interfacial tension γ, and the second term in the right side of equation 9 could be neglected for $N > 7$ s^{-1}. Adding to the above two mechanisms, dispersed phase may leave the circulating core by the slip motion at small N. This makes K_ϕ apparently large, which may appear in the second term of right side in equation 9. The value of ϕ^L is determined from equations 8 and 9 using ϕ^U determined above.

On the other hand, the average diameter of drops was correlated with the Weber number, We (= $N^2 D_i^3 \rho/\gamma$) and the average residence time of dispersed drops, θ_d ($=\phi^L V^L/Q_d$), within the circulating core as follows:[7]

$$d_{32}/D_i = 0.8\ \mathrm{We}^{-0.72}\ \theta_d^{-0.36} \tag{10}$$

where D_i is diameter of the impeller. Dimension of θ_d is [s] and the calculated values of θ_d in the present experiments were 10 - 50 s. Since d_{32} depends on ϕ^L because $\theta_d = f(\phi^L)$ and ϕ^L on d_{32} because $v_t = f(d_{32})$, ϕ^L and d_{32} is determined by a trial and error method using equations 6 -10.

Mass Transfer Coefficients

In the previous paper,[3] it was shown that the mass transfer coefficients in the MS column could be calculated on the basis of mass transfer within and around a rigid sphere, because the diameter of dispersed drops is very small (< 1 mm) for the system of no coalescence in the mixer. The mass balance for the dispersed phase is given as follows with the assumption of the complete mixing within a stage:

$$k_d a V_M(C_{d,n,i} - C_{d,n}) = Q_d(C_{d,n} - C_{d,n+1}) \tag{11}$$

where k_d is the dispersed phase mass transfer coefficient and $C_{d,n,i}$ the interfacial concentration of

dispersed phase. When the dispersed drop is a rigid sphere, the average concentration, $C_{d,n,t}$, of the drop of residence time t within the n-th stage is given as:[5]

$$g(t)=(C_{d,n,t} - C_{d,n+1})/(C_{d,n,i} - C_{d,n+1}) = 1 - (6/\pi^2)\Sigma(1/n^2)\{\exp(-4D_d n^2\pi^2 t)/d^2\} \quad (12)$$

where D_d is the diffusion coefficient in drops, and d the drop diameter. The residence time distribution of drops is expressed for the mixer as:

$$f(t) = (1/\theta_d)\exp(-t/\theta_d) \quad (13)$$

where θ_d is an average residence time (= $\phi V_M/ Q_d$). The outlet dispersed phase concentration, $C_{d,n}$, which is the average concentration of dispersed drops having various residence time, is derived from equations 12 and 13 as follows:

$$X=(C_{d,n} - C_{d,n+1})/(C_{d,n,i} - C_{d,n+1})= \int g(t) f(t) dt \quad (14)$$

From equations 4, 11 and 14, the dispersed phase mass transfer coefficient is described as:

$$k_d = \{d_{32}/(6\theta_d)\}\{X/(1 - X)\} \quad (15)$$

The coefficient can be calculated by use of d_{32} instead of d in equation 12. The values of k_d were measured by the experiments of back extraction of iodine from dispersed phase with aqueous solution of sodium thiosulfate where no mass transfer resistance exists in the aqueous phase (Nii et al., 1997b).[3] Though experimental values of k_d were about 20 % larger than the values calculated with equation 15. Equation 15 can be used to estimate k_d.

When the drop diameter is small as in the MS column, the drops within the mixer is considered to circulate with the continuous phase and the relative velocity between the drop and the continuous phase may be small. The continuous phase mass transfer coefficient, k_c, is determined by the following Ranz-Marshall's correlation:

$$Sh_c = 2.0 + 6.0\ Re^{1/2}\ Sc^{1/3} \quad (16)$$

In the calculation of Re number, the terminal settling velocity of a rigid sphere having the same diameter and density as the dispersed drop is used. The values of a, k_d and k_c calculated for the present experiments are shown in figure 4 for various values of Q_d. The interfacial area increases with the increase in Q_d, and the mass transfer coefficients vary little with the flow rates.

The value of k_d increases with the increase in agitation speed because of the decrease in drop diameter, but k_c varies very little with N. The value of E_{oc} in figure 3 increases with the increase in Q_d, which reflects the variation of a with Q_d. When Q_c is increased, the calculated value of a decreases in contrast to the change with Q_d as shown in figure 5. As a result, E_{oc} in figure 3 decreases with the increase in Q_c.

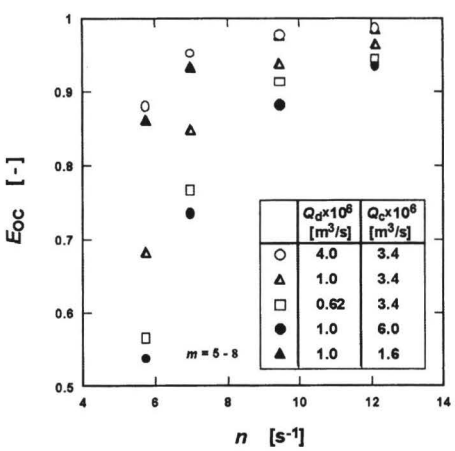


Fig.3 Effects of agitation speed and flow rates on stage efficiency

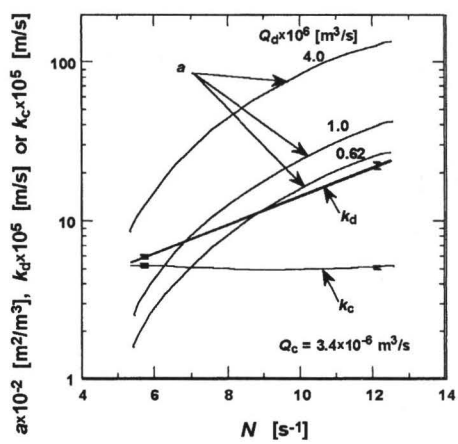


Fig.4 Interfacial area and mass transfer coefficints for various Q_d

The over-all mass transfer coefficients are determined according to the addition rule of mass transfer resistance.

$$1/K_{oc} = 1/k_c + 1/(mk_d) \quad (17)$$

The continuous phase mass transfer resistance is dominant for the present experiments because $m > 1$ and $k_d > k_c$. The over-all volumetric mass transfer coefficients are determined with these over-all mass transfer coefficients as well as the interfacial area described above, and then the stage efficiency is also determined as mentioned above.

The stage efficiencies $E_{oc,cal}$ calculated with the values of a, k_d and k_c estimated for the experimental conditions are compared with the observed values in figure 6. Agreement between the calculated and the observed efficiencies is very well for any flow rates and agitation speed. This indicates that the stage efficiency for the extraction column in which liquid mixing between stages is negligible can be determined if the interfacial area and the mass transfer coefficients are estimated accurately. However, when drop coalescence occurs in the mixer, estimation of the stage efficiency is difficult because the drop diameter and the hold-up of dispersed phase depend on the degree of the coalescence.

ESTIMATION OF FLOW RATES AND DISTRIBUTION RATIO EFFECTS

The stage efficiency E_{oc} in figure 3 varied with the flow rates in both phases. To clarify the effects of flow rates on E_{oc} or E_{od}, the stage efficiencies were calculated for various flow rates by use of the same physical properties and the same column geometry as in the experiment. Figure 7 show the effects of flow rates on E_{oc} or E_{od}. The calculated value of E_{oc} increases with the increase in Q_d, while E_{od} decreases largely with the increase in Q_d. This behavior can be explicable in terms of the change in interfacial area, a, because the mass transfer coefficients of both phases vary little with the change of

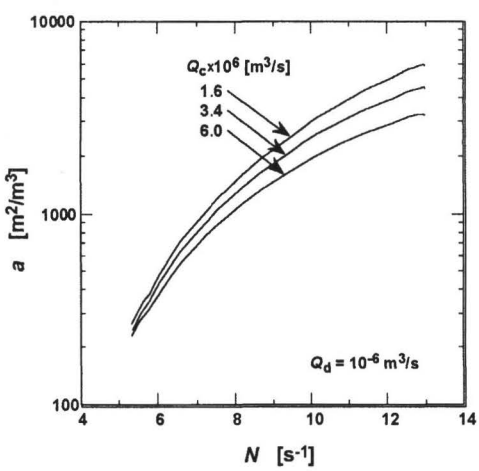


Fig.5 Interfacial area for various Q_c

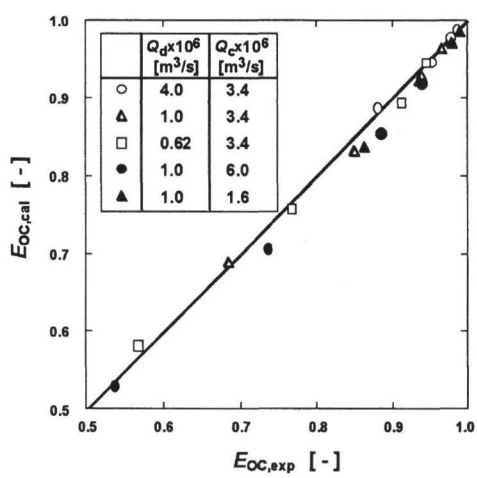


Fig.6 Compaarison between calculated and observed stage efficiencies

flow rate as mentioned above. When the value of Q_d increases at a constant Q_c, the dispersed phase hold-up increases monotonically and the drop diameter also increases due to the decrease in the residence time given by $V^L\phi^L/Q_d$, then the value of a given by $6\phi/d_{32}$ increases for small Q_d and decreases slightly for large Q_d because the drop diameter effect becomes more predominant than the hold-up one. Then the value of E_{oc} increases with Q_d for small Q_d but slightly decreases for large Q_d. On the other hand, $K_{od}aV_M/Q_d$ in Eq.(3) decreases with increase in Q_d, then E_{od} decreases with Q_d as

shown in figure 7. When the continuous phase flow rate increases under constant Q_d, the dispersed phase hold-up decreases and the drop diameter increases, i.e., the value of a decreases with both effects as shown in figure 5. Since the value of $K_{oc}aV_M/Q_c$ in Eq.(2) decreases with increase in Q_c due to both effects of decreasing a and increasing Q_c, the value of E_{oc} decreases rapidly with the increase in Q_c as shown by the broken line in figure 7. The change in E_{od} with the increase in Q_c in figure 7 is moderate because $K_{od}aV_M/Q_d$ in Eq.(3) decreases only by the decrease in a.

Figure 8 shows the effect of the distribution ratio on E_{oc} and E_{od} for constant flow rates of $Q_c = Q_d = 10^{-5}$ m^3/s. The value E_{oc} for a constant agitation speed increases with the increase in m, for $K_{oc}aV_M/Q_c$ in Eq.(2) increases with K_{oc} which increases with the increase in m as given by equation 17. The values of E_{od} decrease with the increase in m, for K_{od} decreases with m. In case of N= 6 s^{-1} where the value of k_c is nearly equal to k_d as shown in figure 4, E_{oc} and E_{od} in figure 8 are symmetric each other. However, in case of N = 12 s^{-1}, variation of E_{oc} is smaller than that of E_{od} because k_d is larger by

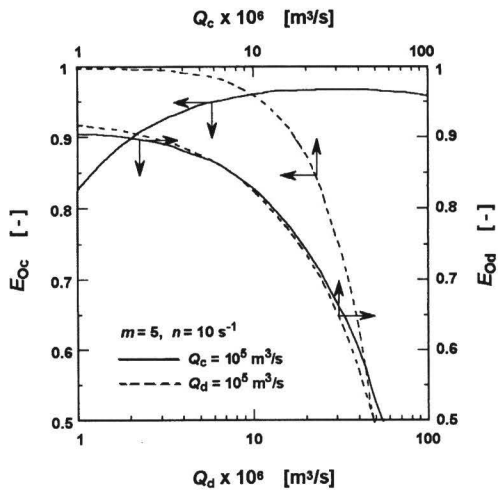


Fig.7 Variation of calculated stage efficiency with flow rates

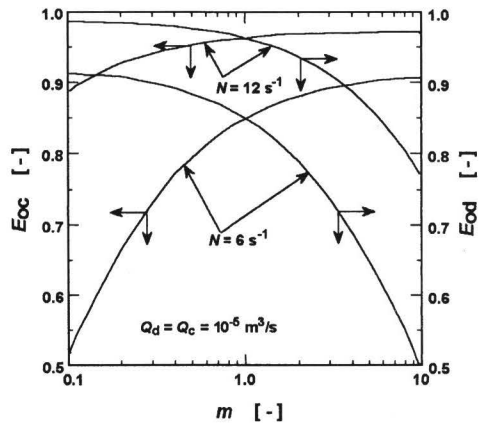


Fig.8 Variation of calculate stage efficiency with distribution ratio

several times than k_c as shown in figure 4.

The stage efficiencies discussed here is used for the extraction systems where extractive reaction rate is large and extraction equilibrium at the interface can be assumed. When the extractive reaction rate is small, the extraction rate is determined with the mass transfer coefficients and the reaction rate ate the interface. Extraction of copper by LIX84I-Shellsol solution with the 5-stage MS column was carried out by Tani et.al.,[5] and the results were explained well with the interfacial area and the mass transfer coefficients described above as well as the reaction rate at the interface.

REFERENCES

1. Takhashi K, Nakashima H and Takeuchi H, *Kagakukogaku Ronbunnshu*, **19**, 440, (1993).
2. Nii S, Suzuki J and Takahashi K, *J. Chem. Eng. Japan*, **30**, 253, (1997).
3. Nii S, Suzuki J, Tani K and Takahashi K, *J. Chem. Eng. Japan*, **30**, 1083, (1997).
4. Takahashi K and Takeuchi H, *J. Chem. Eng. Japan*, **23**, 12, (1990)
5. Tani K, Ohta T, Nii S and Takahashi K, *J. Chem. Eng. Japan*, **31**, 398, (1998)
6. Crank J, *The Mathematics of Diffusion*, Oxford, UK, (1975).
7. Takahashi K and Takeuchi H, *ISEC'90*, 1357, (1992)

EFFECT OF PHASE ENTRAINMENT ON THE PROCESS IN CENTRIFUGAL EXTRACTORS

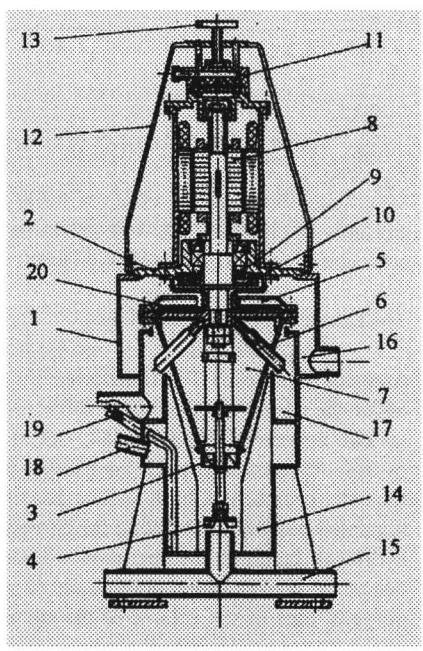
GI Kuznetsov, AV Kosogorov, AA Pushkov and VS Skachkov
Research and Development Institute of Construction Technology (NIKIMT). 43, Altufievskoe Ch., 127410, Moscow, Russia.
International Scientific Technical Center (ISTC). 9, Luganskaya ulitsa, PO Box 25, 11551, Moscow, Russia

ABSTRACT
This paper considers the effect of design and operation features of a single stage centrifugal extractor CENTREK on the value and direction of phase entrainment. At the same time, effect of phase entrainment on extractor capacity, degree of extraction and product decontamination is also considered.

Keywords: centrifugal extractor, entrainment, capacity, efficiency.

INTRODUCTION

Solvent extraction processes are traditionally carried out with minimal phase entrainment. This is justified from the viewpoint of decreasing solvent losses, improvement of ecological criteria and increasing product quality. However, this is not well founded if capacity of extractors is considered. Serious attention should be given to the optimization of the value and direction of the phase entrainment for a given process.
The paper considers the following questions:
- Effect of design and operation features of a single stage centrifugal extractor CENTREK on the value and direction of phase entrainment.
- Effect of phase entrainment on the extractor capacity;
- Effect of phase entrainment on the degree of extraction and product decontamination.



RESULTS AND DISCUSSION

A series of centrifugal extractors (Table 1) has been developed by NIKIMT.[1] Their principal details and units are geometrically similar.
The centrifugal extractor (Figure 1) comprises two principal units: body (1) and rotor-and-drive unit (RDU) (2). Lower part of rotor has a screw conveyor (3) and a stirrer (4). In upper part of rotor there is an hydrolock (5) for the outlet of heavy phase and tubes (6) for the outlet of light phase. The inner space of rotor is supplied with vertical cross-baffles (7), which prevent slippage of the liquids into the rotor. Electric motor (8) is used as a drive. There is a gland (9) and a labyrinth seal (10) which protect the inner cavity of driver from corrosive vapors. The upper part of the rotor has an electro-connector (11), a cramp (12) and a clamp screw (13) that fixes the rotor. The body (1) comprises a mixing chamber (14) with two sleeves (15) for the inlet of feed solution and two annular collectors (one for the heavy phase (16) and for the light phase (17). Overflow sleeve (18) is connected with a collector for control of setup operation. Sleeve (19) is used for emptying the apparatus.

© 2000 Society of Chemical Industry

Parameter	EC100	EC125	EC140	EC160	EC280	EC320
Rotor diameter, mm	100	125	140	160	280	320
Rotating speed, s^{-1}	25	25	25	25	25	25
Capacity,* m^3/h	0.40	0.70	0.9	1.2	4.6	6.3
Volume, l						
Separation chamber	0.35	0.70	1.2	1.5	8.0	12
mixing chamber	0.73	1.1	1.25	1.4	3.2	4.0
Driver power, kWt	0.18	0.37	0.37	0.75	2.2	3.0
Size, mm						
Length	300	260	260	360	550	620
Width	240	270	240	320	530	680
Height	590	590	630	940	1350	1570
Mass, kg	16	20	25	100	480	720

Table 1 Characteristics of centrifugal extractors developed

* - for solutions of 1.1 mol/l of tributylphosphate in kerosene - 2 mol/l of nitric acid with mutual entrainment of phases not over 0.05% (v/v); flow ratio (organic to aqueous solution) equal to 1, and an emulsion of the "oil in water" type used.

The extractor operates as follows.

Feed solutions are fed into the mixing chamber (14) where they are mixed by the stirrer (4). The emulsion thus formed is transferred by the screw conveyor (3) to the rotor (2) where it is separated under the action of centrifugal force. The heavy phase is first directed to the hydrolock (5), then to annular collector (16), and finally out of the extractor. The light phase is withdrawn from the extractor by tube (6), passes through the annular collector (17) and then goes out from the extractor. A length of tube (6) determines the interface position in the separation chamber and allows this position to be regulated without dismantling the extractor.[2] The conical shape of the rotor and fixed activator (20) in hydrolock facilitate the operation with solutions containing some quantities of solids. Recirculation of one of the phases with a multiplicity of up to 100 can be provided in the centrifugal extractors. For this purpose, part of the volume of the annular collector of the recirculating phase is limited by partitions and is joined by pipes to the mixing chamber. The value of the angle θ between the partitions and the multiplicity of recirculation b_r (determined as the ratio of the flow being recirculated to the initial flow) are related by the expression:

$$\theta = 360° * b_r/(1 + b_r).$$

Thus the original design elements are used in a way that allows the control the interface position and the change of the value of the phase entrainment as well as to carry out the directed entrainment into the aqueous or organic phase. In the zone of phase inversion, the emulsion type can be changed by the order of adding the solutions into the mixing chamber (the continuous phase is the one that first enters the mixing chamber). The emulsion type in any flow ratio can be changed by the recirculation of that phase

which is required to be the continuous one. To prevent the contamination of product flow leaving a cascade, the last stages are used as cleaning stages.

The extractor capacity can be considerably increased if one permits operation with increased entrainment or carries out the directed entrainment into heavy or light phases. The dependence of optimized capacity of the centrifugal extractor EC160 (under equal relative entrainment into both phases) on phase entrainment is shown in figure 2. Increasing of the entrainment from 0.1 to 2% allows the capacity to be raised by approximately two times when an "oil in water" emulsion is considered. On the other hand, for a "water in oil" emulsion, the capacity can be raised 1.3 times for the same diapason of entrainment. The dependencies of entrainment corresponding to light and heavy phases on capacity when radial flow of heavy phase (r_h) varies and radial flow of light phase (r_l) is constant, are shown in figure 3 ("oil in water" emulsion) and in figure 4 ("water in oil" emulsion). Changing the value of radius r_h (or r_l) or emulsion type in separating chamber, can affect the value and direction of entrainment. At the same time, the degree of extraction[3] $E = 1 - (\lambda - 1)/(\lambda^{N+1} - 1)$ and decontamination of targeted component should be not lower than desired, where N – number of extraction stages; λ - extraction coefficient under admission that it is constant.

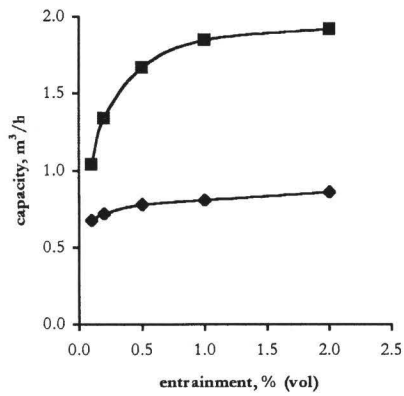


Figure 2. Dependence of capacity on entrainment:
"water in oil" emulsion type
"oil in water" emulsion type

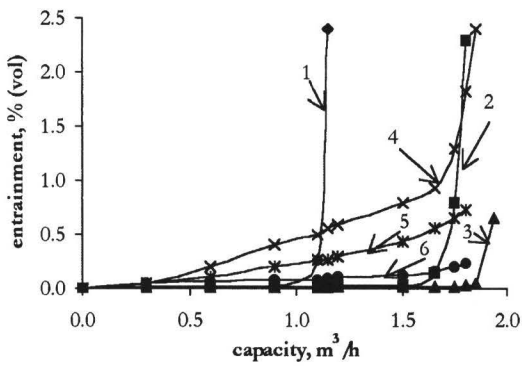


Figure 3. Dependence of entrainments on capacity ("oil in water" emulsion type):
entrainment in light phase — entrainment in heavy phase
1 - r_h = 35 mm — 4 - r_h = 42 mm
2 - r_h = 40 mm — 5 - r_h = 40 mm
3 - r_h = 41 mm — 6 - r_h = 35 mm
r_l is constant

When entrainment is considered,[4]

$$\lambda_e = (mF_s + F_{a/s})/(mF_{s/a} + F_a),$$

where m is distribution coefficient; F_s and F_a are volumetric flows of organic and aqueous phases; $F_{s/a}$ and $F_{a/s}$ are volumetric flows of entrained organic phase into aqueous and aqueous into organic.

The proposed kind of processes conducted with entrainment is illustrated by an example of the calculation of phosphoric acid extraction by tributylphosphate (TBP) and its purification from sulfuric acid for the following initial conditions: concentration ratio of contaminated (C) and target component (T) in feed aqueous solution $x_C/x_T = 0.0857$, $m_T = 0.22$, $m_C = 0.09$, $E_T = 70\%$, decontamination factor of target compound $b_D = 160$ and flow rate ratio of feed aqueous, organic and scrub solutions $F_a : F_s : F_{Sc} = 1 : 7 : 0.56$. The dependence of the total number of extraction stages on the entrainment degree is shown on figure 5. The increasing of entrainment degree from 0.1 to 1% leads to the raising of the capacity of extraction setup (see figure 2). Thus, to keep the same technological performance as without

entrainment, the number of stages needs to be increased only from 25 to 27.

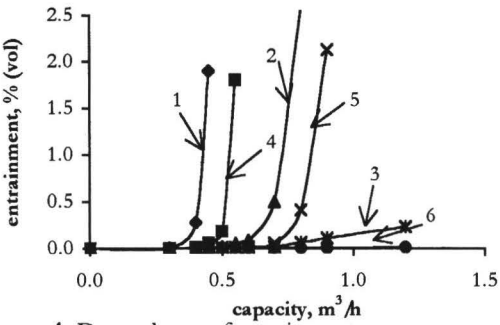


Figure 4. Dependence of entrainment on capacity ("water in oil" emulsion type):

entrainment in light phase — entrainment in heavy phase

1 - r_h = 33 mm — 4 - r_h = 40 mm

2 - r_h = 35 mm — 5 - r_h = 35 mm

3 - r_h = 40 mm — 6 - r_h = 33 mm

r_l is constant

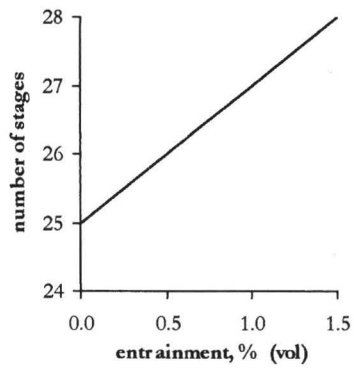


Figure 5. Dependence of total number of extraction stages from entrainments of aqueous phase in organic phase

CONCLUSIONS

The calculation of admissible entrainment degrees, evaluation of their significance for a given process and performance of a process using the optimal entrainment factors allow a considerable increase in capacity without decreasing extraction degree and product decontamination but some increase in the number of stages needed.

The proposed technique for performing extraction process can be used for of any type of apparatus and make it possible to optimize and intensify the extraction process.

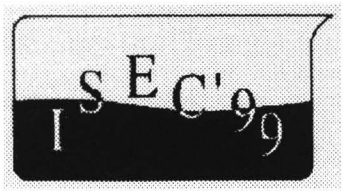
REFERENCES

1 Kuznetsov GI, Pushkov AA, Kosogorov AV and Shklyar LI. *Russian Chem. Ind.*, **2**, 81, (1996).

2 Kuznetsov GI, Shklyar LI, Kosogorov AV et al. *USSR Certificate of Authorship 1031029, Bull. Izobr.* 30, (1988).

3 Alders L. *Liquid - Liquid Extraction*, Elsevier Publishing Company, Amsterdam, (1959).

4 Kuznetsov GI, Pushkov AA, Kosogorov AV and Semenov MI. *Zh. Prikl. Khimii*, **10**, 2258, (1993).



THE EFFECT OF AIR SPARGING ON THE ELECTRICAL RESOLUTION OF A WATER-IN-OIL EMULSION

PJ Bailes[1] and PK Kuipa[2]

[1] Department of Chemical Engineering, University of Bradford, Bradford, West Yorkshire, BD7 1DP, UK

[2] Department of Chemical Engineering, National University of Science and Technology, Bulawayo, Zimbabwe

ABSTRACT

A novel process is described in which the resolution of a 60% v/v water in kerosene emulsion using pulsed electrical fields is augmented by the simultaneous mild bubbling of the emulsion with air. Experiments conducted under continuous flow conditions confirm that electrical resolution of the emulsion with air sparging is superior to that obtained using the electric field on its own. The results obtained with an electrostatic coalescer of innovative design show that it is possible to achieve a 35% enhancement in emulsion resolution. Optimum values of the voltage pulsation frequency at which electrical resolution of the emulsion is best are observed with and without air sparging. The study also shows that emulsion resolution increases with increasing residence time and applied voltage. The addition of charge dispersant to the kerosene gives interesting results which warrant further investigation. The new method is expected to be of benefit to the oil industry and in the processing of liquid membrane emulsions and solvent extraction dispersions that are slow to separate into their constituent phases.

Keywords: emulsion breaking, coalescence, electric field DC, air sparging, electrical resolution

INTRODUCTION

The resolution of water-in-oil emulsions with high intensity alternating current (AC) or direct current (DC) fields is a specific method of emulsion breaking which relies for its effectiveness on the insulating character of the oil continuum, i.e. the need for an intense electric field requires the continuous phase to be insulating so that the field may be maintained. The electric field accelerates the process of phase separation by inducing electrophoretic and dipolar forces between the water droplets resulting in an increased incidence of collision and coalescence between the droplets within the emulsion. These processes cause a shift in the droplet size distribution towards larger droplets, which are inherently quicker to settle to the bulk interface. Resolution of crude oil emulsions by this means is widely practised and recent advances have enabled the treatment of emulsions containing 65% v/v water or more[1]. For such emulsions it has been demonstrated that the deleterious effects of droplet bridging of the electrode pair and the attendant short-circuiting between these electrodes can be circumvented by coating the energized electrode of the pair with a layer of insulating material and applying a pulsed DC field, at a frequency characteristic of the electrode and emulsion system. Excessively strong electric fields will create shearing forces within the emulsion that result in further droplet break-up and stabilization of the water-in-oil emulsion.

It has been shown[2,3] that a significant increase in resolution of a water-in-oil emulsion can be achieved if the emulsion is simultaneously subjected to a pulsed DC field and mild bubbling of the emulsion with air. This finding may be a consequence of closer and more frequent approaches between charged water droplets caused by the agitation associated with air bubbling. Such an explanation is supported by the work of Urdahl et al[4] who found that electrostatic coalescence can be highly effective in an emulsion system undergoing turbulent flow. However, it is also possible that channels created in the viscous emulsion by the passage of the gas bubbles could provide conduits for the coalesced water droplets to fall more rapidly to the bulk interface. Additionally, the coalescence rate is likely to be augmented by the charge accumulation that will occur at the large gas/liquid dielectric interface within the body of the emulsion.

This paper reports the results from a systematic investigation of emulsion breaking with and without air sparging and compares performance over a range of emulsion flow rates, pulsation

© 2000 Society of Chemical Industry

frequency, applied voltage and electrical conductivity of water-in-kerosene emulsions.

EXPERIMENTAL

The Perspex coalescer incorporated zones for introducing and distributing the feed emulsion, a zone for treatment of the emulsion between horizontal electrodes, and a launder for removal of the treated emulsion (figure 1). Its rectangular box-shaped design permitted a treating zone 170 mm in length and 100 mm in breadth, with an electrode spacing of between 35 mm and 45 mm along its length. A corrugated high voltage electrode formed from a rectangular sheet of mild steel (thickness 0.13 mm) laminated with high density polyethylene (thickness 125 μm) was chosen in order to enlarge the energised area. The lower electrode was formed from a brass sheet of thickness 5 mm which was drilled to allow drainage of the coalesced aqueous phase during operation. The air flow into the emulsion was distributed from a central manifold through 6 T-pieces which protruded 15 mm into the treating zone through holes in the earthed electrode.

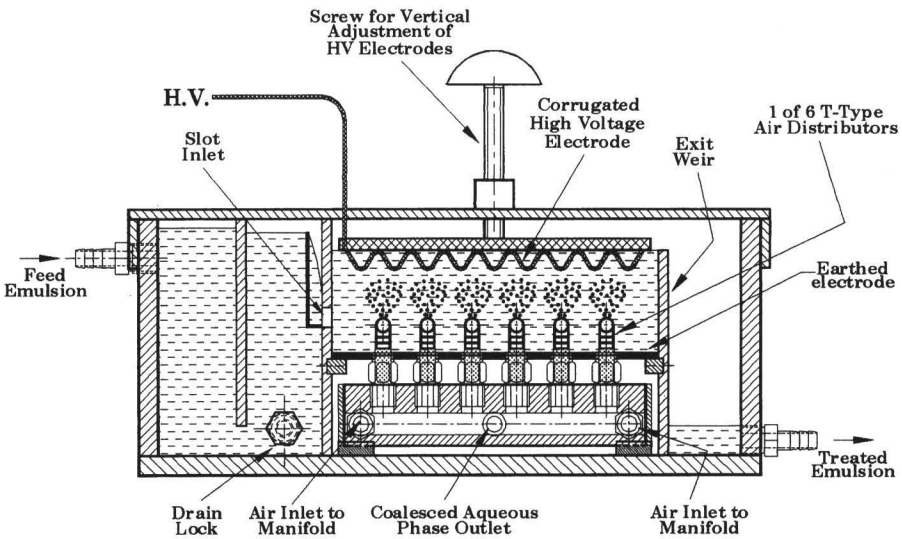


Figure 1 Electrostatic coalescer incorporating air sparging

Operation of the coalescer required an initial charge of distilled water up to the level of the lower electrode. Emulsion was then introduced at the desired flow rate and the high voltage electrode was energised as soon as the emulsion started to trickle over the exit weir. The effective volume of the emulsion treatment zone was 850 mL and the emulsion was fed to the coalescer from an adapted 10L aspirator vessel through a rotameter. Performance comparisons were made for flow rates ranging from 28 mL/min to 116 mL/min, corresponding to emulsion residence times in the coalescer of approximately 30 and 7 minutes, respectively. The water separating from the emulsion during treatment was drained from the coalescer under manual control so that the aqueous bulk interface was maintained at the level of the earthed electrode. Each experiment was allowed to continue for a period equivalent to two emulsion residence times in the coalescer before a sample was collected from the emulsion exit port for analysis of its water content using the Karl Fischer auto-titration method. The results of the analysis

were then used to calculate the percentage change in dispersed phase volume fraction that equates to the percentage resolution of the emulsion.

A high shear Schultshalzer homogeniser was used to prepare small batches of emulsion which were then stirred together and charged to the adapted aspirator vessel. Each batch of emulsion was prepared by adding 196 mL of distilled water in a constant stream to a 130 mL mixture of odorless kerosene and 5% wt/wt Brij 92 in a blending process of 70 seconds total duration. The use of Brij 92 which is a non-ionic surfactant with a hydrophobic-lipophilic balance (HLB) value of 4.9 ensured the formation of a very stable water-in-oil emulsion. When allowed to separate at room temperature under normal gravity conditions, only 2.0% v/v of the water dispersed in the emulsion separated to form a water layer after one month. Only emulsion which was 16 ± 3 hours old was used in this work and experiments were carried out with and without air at a temperature of 25 ± 1°C.

The electrical equipment that was used to supply and monitor the pulsed DC to the coalescer is described elsewhere[5]. Experiments were performed with pulses of nominally square form and a mark/space ratio of unity.

RESULTS AND DISCUSSION

The effect of the frequency of pulsation on the electrical resolution of a flowing emulsion containing 61% v/v water is shown in figure 2. In this case the nominal applied voltage is 20 kV and

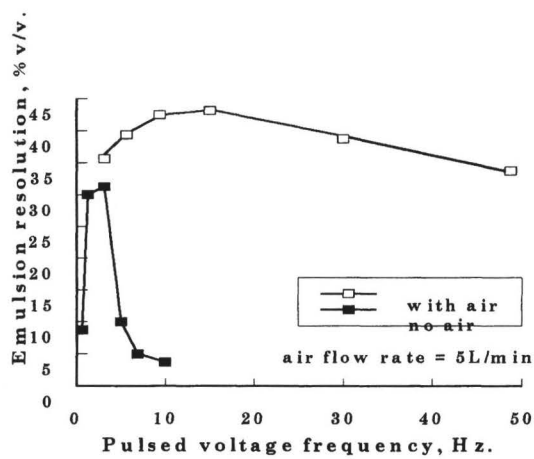


Figure 2 Emulsion resolution in pulsed DC fields, with and without air sparging, as a function of pulsation frequency

the residence time of the emulsion in the treating zone is 17 minutes. There is evidently an optimum pulsation frequency at which resolution is a maximum; furthermore this frequency is increased by the action of the air.

For an emulsion containing 60% v/v water, figure 3 shows a comparison of electrical resolution with and without air sparging made under equally favourable (optimum frequency) conditions. In this case it is seen that regardless of the emulsion residence time in the treating zone the application of air improves emulsion resolution. For the test apparatus an air flow rate of 5 L/min was observed to give the best resolution irrespective of the emulsion flow rate into the coalescer. Variations in the quality of the test emulsions probably account for the discrepancy in the absolute values that are evident from a comparison of figures 2 and 3.

At constant residence time as expected, the emulsion resolution was found to increase with

increases in the applied voltage, performance definitely leveling off at 10 kV for the case with air sparging (figure 4). Air sparging in the absence of an applied voltage had no discernible effect on emulsion resolution.

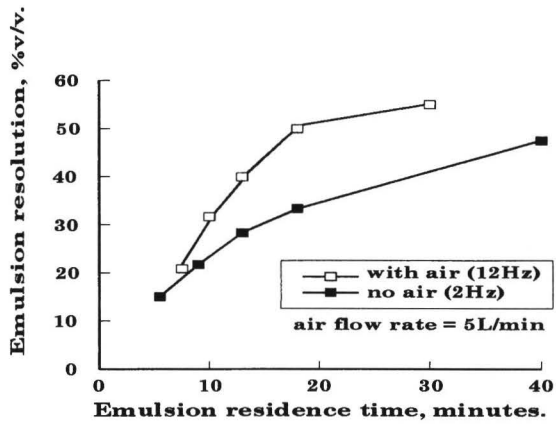


Figure 3 Emulsion resolution in pulsed DC fields, with and without air sparging, as a function of residence time in the treating zone (applied voltage = 20 kV)

Figure 5 shows the result of increasing the conductivity of the organic phase by the addition of the charge dispersant STADIS 450 (supplied by Associated Octel Company Ltd.). The observed decrease in electrical resolution as the charge dispersant concentration is increased can probably be attributed to the increased rate of charge leakage from the water droplets caused by the higher conductivity of the surrounding organic phase. This situation would be expected to reduce the electrophoretic and dipolar forces between droplets and thereby diminish the process of resolution. The upward trend in emulsion resolution that is observed with STADIS concentrations greater than 11 ppm in the absence of air sparging, apparently contradicts this explanation. However, when there is no air sparging, emulsion resolution is very sensitive to pulsation frequency and comparisons made at a fixed frequency of 2 Hz could be misleading, especially if the optimum pulsation frequency is affected by the electrical conductivity of the organic phase. These aspects are currently the subject of further laboratory work.

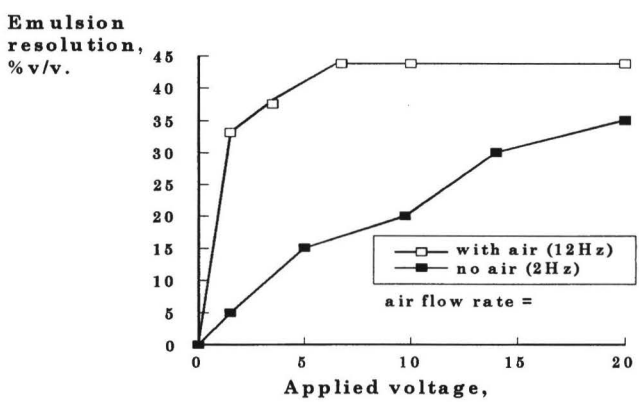


Figure 4 Emulsion resolution in pulsed DC fields, with and without air sparging, as a function of voltage magnitude (emulsion residence time = 17 minutes)

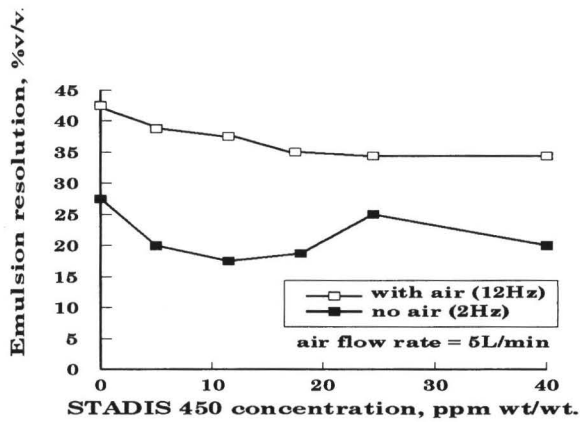


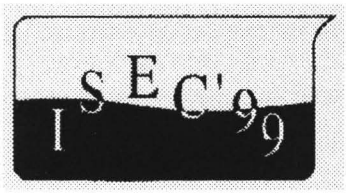
Figure 5 Emulsion resolution in pulsed DC fields, with and without air sparging, as a function of charge dispersant concentration (emulsion residence time = 17 minutes; applied voltage = 20 kV)

ACKNOWLEDGEMENT

The authors wish to thank the Engineering and Physical Sciences Research Council for the financial support that enabled this work to be carried out.

REFERENCES

1. Bailes PJ, Freestone D and Sams GW, *The Chemical Engineer*, **1997**, October, 34-39.
2. Bailes PJ, *European Patent No. 0 632 739 B1*, June 1996.
3. Bailes PJ, *US Patent No. 5,580,464*, December 1996.
4. Urdahl O, Williams TJ Bailey AG and Thew MT, Trans. IChemE., **74(A)**, 158, (1996)
5. Bailes PJ and Larkai SKL, *Trans. IChemE*, **59**, 229, (1981)



THE USE OF VIDEO CAMERA FOR THE DEVELOPMENT, MONITORING AND DOCUMENTATION OF SX PROCESSES

B Grinbaum
IMI(TAMI) Institute for Research and Development, P.O.B. 10140, Haifa Bay 26111, Israel

ABSTRACT
The development of small and cheap camcorders opens new horizons for the use of videotaping in investigation of SX processes. The simple camcorder, operated by an amateur, is usually sophisticated enough to record the interesting phenomena clearly and sharply. It is small enough to be taken into a plant, and gives sharp images even in dim light, so that external illumination is usually unnecessary. Examples of the areas where the technique can be an advantage are discussed.

Keywords: videocamera, flow phenomena,

INTRODUCTION

The visual observation of flow phenomena is of great importance for better analysis and understanding of the hydrodynamics of the solvent extraction process. Several important parameters may be best detected and measured by direct observations: the quality of mixing, the type and shape of a dispersion, the accumulation of crud, the development of flooding, phase inversion, the rate of phase separation etc. The fact that most bench-scale and pilot-plant columns and mixer-settlers are transparent makes the observations easy. The drawback is that observation is always a subjective process, as it depends on the skills of the observer, his impression and interpretation. The use of moving picture photography (video) makes these observations into an objective document, and a hardcopy of the experiment, just like recording of data measured by sensors.

The use of moving pictures for investigation of SX processes has been known for a long time. Its main scientific goal was to follow the changes in the shape of droplets due to mass transfer, or flow patterns during forced motion. Experienced cameramen, using sophisticated and expensive equipment usually did the filming.

The Advantages of the Camcorder Video Movie

The development of small and cheap camcorders opens new horizons for the use of videotaping in investigation of SX processes. The simple camcorder, operated by an amateur, is usually sophisticated enough to record the interesting phenomena clearly and sharply. It is small enough to be taken into a plant, and gives sharp images even in dim light, so that external illumination is usually unnecessary.

The main advantages of the video are:

1. In the investigation of the hydrodynamics of the process, the visual appearance of the dispersion is most important. A video enables one to investigate the characteristics of the flow, i.e. type of dispersion, mixing regime, coalescence and breakage of droplets, degree of foaming, and sometimes helps to estimate the drop size distribution. This analysis, done in the office, on a large monitor, and using the slow motion and still options, is much easier and exact than direct observations.
2. For experiments done in pilot plants at remote sites, e.g. mines and factories, the subjective impression of the expert in site is the only documentation of the phenomena. Videotaping enables the entire team of experts and managers of the research institution as well as the customer to get a direct impression of the work and to analyse the phenomena, without travelling to the site.
3. The phenomena that were observed and videotaped may be used for demonstration of the advantages of the proposed process and/or equipment. Later it may serve for training or educational

© 2000 Society of Chemical Industry

purposes. Especially in columns, it is important to show the operators, who in many cases may not have been present for the pilot experiments, a movie of the glass pilot plant, in order to improve their understanding of the equipment and its behaviour.

EXAMPLES

The following examples describe the situations mentioned above:

1. A Team Can See Better Than a Single Person

Laboratory experiments on mass transfer and phase separation in extraction of Ni-Co were done by a single engineer at a remote site. They consisted on mixing of the organic and aqueous phases in a beaker, under various mixing conditions. The goal of the work was to find the "natural" type of dispersion, the rate of phase separation and the degree of mass transfer as a function of the mixing intensity and the location of the mixer. While the mass transfer and time of phase separation can be determined quantitatively, the type of dispersion was more problematic. In a few cases it was difficult to determine if the dispersion was W/O or O/W. Analysis of the videotape by a team of experts, using VCR in slow motion, enabled determination of the dispersion type by the location of the bubbles in the continuous phase. In a few cases the dispersion was different from what the engineer assumed during the work.

2. Seeing is Believing

The goal of the experiment was to check the feasibility of work with solids in a pulsed column. The test case was stripping of uranium with an ammonia solution. The main question was what happens if, due to an accidental pH rise, some "yellow cake" solids deposit in the column. The team who ran the column found that the solids dissolved quickly after a short distance, without causing any harm, provided that the disturbance was short and occurred above the middle of the column. They then had to convince the customer that this was really the case. Oral presentation left doubts that maybe the interpretation of the results was too optimistic. But after a short movie describing the phenomena was displayed, everyone was convinced of the results. They did not have to simply believe - they saw it themselves, even more clearly than the experimental team.

3. Seeing is Understanding

We teach students, co-workers and operators about various phenomena in solvent extraction. Sometimes it is difficult for them to realise what happens and how it **really looks.** Just a short list of phenomena for which a short movie is better than a long lecture:

a. Generation of O/W or W/O dispersions and the difference between them

This most basic concept in solvent extraction can be easily demonstrated by a video, using either a beaker or any type of column.

b. Flooding

For a person who has never seen an extraction column at work, it is difficult to understand how flooding occurs and what really happens inside the column. A short video clip can clarify it, and show the difference between various types of flooding, i.e. a "cork" of the dispersed phase in the column vs. accumulation of the dispersed phase in its settler.

c. Influence of intensity of mixing on creation of droplets and phase separation

d. Continuous operation of a mixer-settler with a 3-phase dispersion

Many students cannot understand why a 3-phase system is so undesirable and why it should be avoided. A clip that shows the accumulation of the third phase in a settler can clarify this immediately.

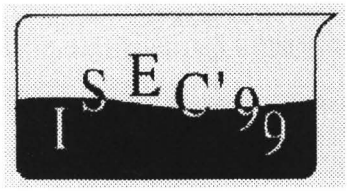
e. Two simultaneous dispersions in one column

In a pulsed column sometimes part of the column works, at steady state, with an O/W dispersion, while the rest of the column works with a W/O dispersion. This phenomenon is usually detected by a sharp

change in the measured hold-ups: aqueous hold-up below 40% indicates a W/O dispersion, while aqueous hold-up above 60% indicates an O/W dispersion. For people who have never seen this, it is rather difficult to believe that it really exists. A video clip can demonstrate it.

CONCLUSION

Possible applications of the video camcorder for demonstration and documentation of solvent extraction phenomena have been described. The list of applications is long. The effort in making the video is relatively small, the costs are negligible, and the impact - impressive.
So, let's use it!



MULTICOMPONENT KINETICS IN LIQUID–LIQUID SYSTEMS: AN EXPERIMENTAL STUDY

Michael J Brodkorb and Michael J Slater
Department of Chemical Engineering, University of Bradford, Bradford, BD7 1DP, UK

ABSTRACT

Experimental mass transfer data have been obtained using a proposed new liquid-liquid extraction test system of toluene – acetone – phenol – water. The system toluene – acetone – water has already been adopted by the European Federation of Chemical Engineering and extension to a quaternary system is felt desirable because the problems of multicomponent mass transfer in liquid systems must be tackled if equipment procedures are to be advanced. The experimental data are being used to evaluate a recently-developed computer program simulating the multi-component mass transfer to single drops in vertical unhindered motion. The model uses Stefan-Maxwell principles to describe solute interactions and employs a drop behaviour model that can describe the effects of interfacial contamination. Combination of these principles with the non-equilibrium idea, considering phase equilibrium only at the interface and a concentration gradient on either side of the interface, results in an advanced mass transfer model. The evaluation of the model with the experimental data introduced here lead to satisfying results.

Keywords: multi-component kinetics, Stefan-Maxwell, drop behaviour, interfacial contamination, test-system, toluene/acetone/phenol/water

INTRODUCTION

Considering the advances in modelling other separation processes during the last few years, mostly a result of the rapid increase in computing power availability, it seems quite odd how far the simulation of liquid-liquid extraction behaviour lags behind. Design procedures still depend on large amounts of experimental data, both bench-scale and pilot plant-scale, which are difficult to obtain and, therefore, expensive. Then, after obtaining these essential data, it is most often proprietary knowledge that allows the scale-up to process-size equipment. This unfortunate situation might result in cases where liquid-liquid extraction could be an economical, as well as an ecological alternative to distillation, but does not find its use because of design difficulties.

It has long been recognised that instead of simulating the mass transfer of the entire extractor content containing two homogeneous phases using transfer heights or stage efficiencies, it seems more promising to model the mass transfer of single drops and to combine the model with one of the hydrodynamic tools such as "drop population balance" or "Monte-Carlo simulation". Several modelling programs have emerged from this concept (e.g. Zimmermann et al.[1] or Ghalehchian[2]). Unfortunately, none of these to our knowledge is in commercial use, as a thorough evaluation of any of the models has not yet been achieved. This is due to the lack of published experimental pilot-plant data and the diversity of the data necessary to validate this type of model, which make it very expensive to obtain a full set, table 1.

If a liquid-liquid extraction column simulation model is to be used in an industrial environment, it has to consider all of the mass transfer influencing conditions. Two major influencing factors are the presence of contamination in industrial systems, and its influence on the hydrodynamics and the mass transfer, and the effects of multiple transferred species, as nearly all industrial systems are multi-component systems.

The study shown here presents the first part of an attempt to provide a complete set of experimental data including the effects of contamination and multiple components. This covers the provision of all necessary physical properties data for one system, single rising drop mass transfer experiments and evaluation of these with a suitable model. The system chosen is a quaternary system, so that multi-component effects can be observed.

The subsequent steps will then be the acquisition of experimental pilot-plant data, and use of the data in validating a column design programme.

© 2000 Society of Chemical Industry

Physical Properties	density, viscosity, interfacial tension, Liquid-liquid equilibrium
Chemical Properties	Reaction?
Single Drop Mass Transfer Data	Mass Transfer = function of concentration, drop size, contamination
Column Type	Geometry, operation limits
Hydrodynamic Data	Break-up behaviour, coalescence behaviour, axial mixing
Pilot Plant Mass Transfer Data	Mass Transfer = function of hold-up, flow ratios, concentration, contamination

Table 1: Experimental data necessary for evaluating pilot plant simulation model

Test System/Physical Properties

The chemical system used for this project is the quaternary system toluene (T) – acetone (A) – phenol (P) - water (W). It is based on the established ternary EFCE test system T-A-W and has been proposed by von Reden and Slater [3]. The system is presented schematically in Figure 1.
As experimental equilibrium data were available only for the ternary sub-system T-A-W [4], quaternary equilibrium data of the complete system (T-A-P-W) have been measured and successfully correlated by the UNIQUAC Gibbs free energy model [5]. The resulting binary interaction parameters and additional experimental density data are presented [6].

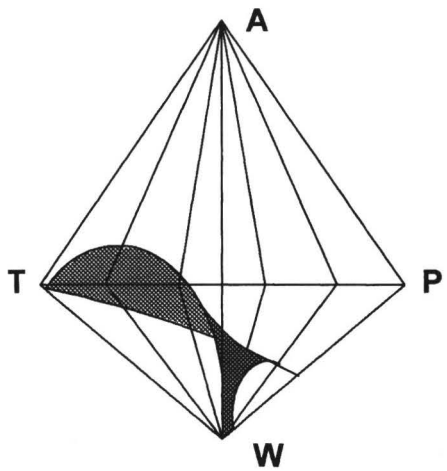


Figure 1: Schematic representation of the liquid-liquid equilibrium of the proposed test system toluene (T) – acetone (A) – phenol (P) - water (W)

Multicomponent Non-Equilibrium Model

A multicomponent non-equilibrium model has been developed by von Reden[7] to describe the mass transfer in single drops. The major characteristics are:

- the effects of multicomponent mass transfer are described by the Stefan-Maxwell equations and application of the linearised theory [8,9];
- equilibrium between the phases is considered only at the interface (rate based approach[10]);
- the effects of contamination are implemented with the contamination factor model given by Slater[11,12].

The model has been improved by including a more sound implementation of the UNIQUAC equilibrium calculations. Through this and the provision of UNIQUAC binary interaction parameters

based on experiments, it was possible to overcome the limitations of the model being valid only for low solute concentrations, as experienced in earlier work[7].

EXPERIMENTAL

The "Single Drop Method" has been established as a simple way of determining the overall mass transfer rate for drops, for example[13]. In this method single drops are released inside a column filled with the continuous phase. The drop rises or falls through the continuous phase and mass transfer between the two phases takes place. The drop composition is determined subsequently to the mass transfer process and the overall mass transfer coefficient can be determined. The advantages of single drop experiments as a crude method of measuring mass transfer is their ease of use. Disadvantages are the limited reproducibility of the acquired data. Every attempt to improve the reproducibility leads consequently to more complex and, therefore, more expensive experiments. Thus a feasible balance has to be found.

In this study a simple apparatus was used. The end effects of drop formation and coalescence are accounted for by the subtraction method[14]. After the mass transfer process, the samples were analysed by gas chromatography. The error in reproducibility of the measured mass transfer was checked by repeating the experiment and was found to be about ± 10%. Thus, the experimental results can be used to give at least qualitative accounts of the influence of the various parameters.

Von Reden[7] compiled an extensive list of single drop experiment data available in the literature. With the exception of the work of Paschke and co-workers[15] there is no published experimental data for the simultaneous mass transfer of multiple components for single drops.

Mass transfer experiments have been carried out for the three different systems T-A-W, T-P-W and T-A-P-W at different concentration levels, different drop sizes and for different levels of contamination.

RESULTS

The comparison of the ternary solute mass transfer with quaternary solute mass transfer under the same conditions for both solutes enables the study of multi-components effects. A good way of presenting mass transfer data is to plot the degree of extraction, which is the ratio of actual mass transfer to maximum possible mass transfer (defined by the equilibrium condition), as a function of exposure time – in this case the rising time.

Phenol and acetone mass transfer data measured at the same experimental conditions are shown in figure 2 and figure 3, respectively. The experimental mass transfer (circles) is compared with the predicted mass transfer at a level of contamination (contamination factor m = 50), which seems reasonable (by experience) for laboratory experiments (solid line). The dotted lines are the prediction of the limiting cases "Potential Flow" (maximum predictable mass transfer) and "Rigid Sphere" (minimum predictable mass transfer).

In the case of the phenol mass transfer, both prediction as well as experiment, show very little influence of the acetone present in the quaternary system. The predicted mass transfer is nearly equal (relative difference < 1%) and the experiments, as well, show no significant difference between quaternary and ternary conditions.

A different picture has been obtained for the mass transfer of acetone. The presence of phenol as the fourth component in the quaternary system reduces the mass transfer rates of acetone relative to those obtained for the ternary system. This effect can also be observed for the mass transfer prediction. A value for the contamination factor of m = 50 has been kept the same for both situations but the value might depend on the solutes and their concentrations.

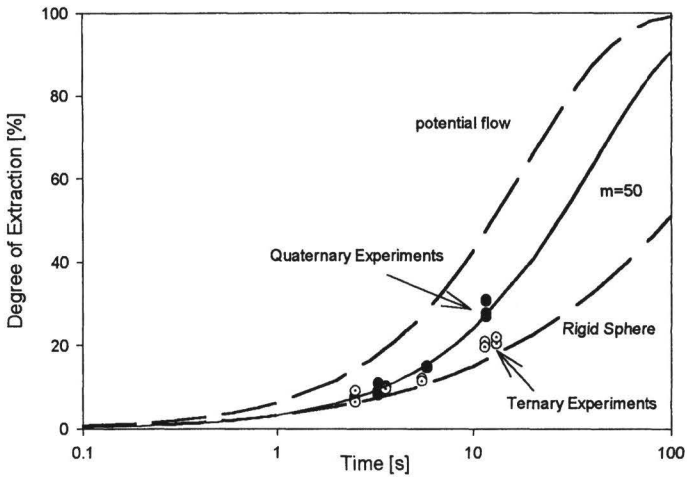


Figure 2 Experiments vs. modelling: Phenol; medium drop size (4 mm) and medium concentration (1 g/L)

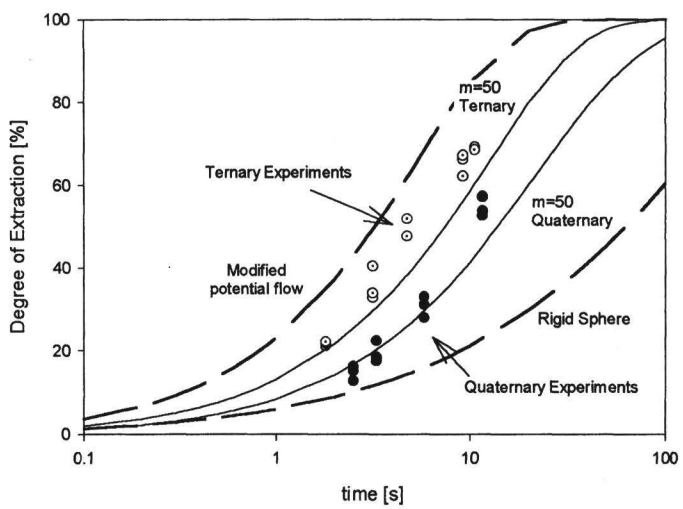


Figure 3 Experiments vs. modelling: Acetone; medium drop size (4 mm) and medium concentration (1 g/L)

CONCLUSIONS

Experimental mass transfer data have been obtained and successfully applied to evaluate a previously proposed multicomponent mass transfer model. The effects of the mass transfer of multiple components have been shown. Thus, it seems necessary to incorporate the modelling of multiple components into liquid-liquid extraction models.

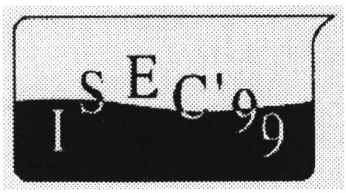
The quaternary system toluene-acetone-phenol-water has been proven to be a useful test system for the investigation of those multicomponent effects in liquid-liquid systems. The introduction as an official EFCE test system is strongly recommended.

ACKNOWLEDGEMENTS

EPSRC have funded current work and we thankfully acknowledge useful discussions with Dr. C. von Reden and Dr. V. Gomis.

REFERENCES

1. Zimmermann A, Joulia X, Gourdon C, and Gorak A *Chem. Eng.* **57**, 229, (1995)
2. Ghalehchian JS *PhD thesis, Department of Chemical Engineering, University of Bradford (UK)*, (1996)
3. von Reden C, Slater MJ, and Gorak A *ISEC96: Value Adding Through Solvent Extraction.* University of Melbourne, Melbourne, 99, (1996)
4. Sørensen JM, and Arlt W *Liquid-Liquid Equilibrium Data Collection;* DECHEMA: Frankfurt, Chem. Data. Ser., 5, (1980).
5. Abrams DS and Prausnitz JM *AIChE J.* **21**, 116, (1975)
6. Brodkorb MJ, Gomis Vand Slater MJ submitted to the Journal of Chemical and Engineering Data 1998
7. von Reden C *PhD thesis, Fakultät Chemietechnik, Universität Dortmund (Germany)* (1998).
8. Toor HL *AIChE J.* **10** (4), 448, (1964)
9. Stewart WE and Prober R *Ind. Eng. Chem. Fundamentals.* **3**, 224, (1964)
10. Krishnamurty R and Taylor R *AIChE J.* **31** (3), 449, (1985).
11. Slater MJ *Can. J.Chem. Eng.* **73**, 462, (1995).
12. Alessi V, Penzo R, Slater MJ and Tessari R. *Chem. Eng. Technol.* **20**, 445, (1997)
13. Bahmanyar H, Chang Kakoti D, Garro L, Liang T and Slater MJ *Chem. Eng. Res. & Design* **68** (1), 74, (1990).
14. Licht W, Pansing WF *Ind. Engng Chem.* **45**, 1885, (1953).
15. Paschke A *Chem. Engng and Process.* **32**, 201, (1993).



IN-LINE MIXERS FOR THE EXTRACTION OF URANIUM BY A TERTIARY AMINE FROM ORE LEACH SULPHURIC ACID SOLUTIONS

Gordon M Ritcey
G.M. Ritcey & Associates Inc. Nepean, Ontario, Canada, K2H 8A9

ABSTRACT
This paper describes the pilot plant investigation of the in-line mixers as a possible replacement for the conventional mixers in the extraction of uranium from sulphuric acid leach solutions. The effect of variables such as flow, phase ratio and number of extraction units on the mass transfer efficiency as well as the effect on the settler requirements were investigated. The pilot plant was on the site of the Ranger uranium mill in Australia that was considering plant expansion.

Keywords: in-line mixers, uranium, tertiary amine, Alamine 336

INTRODUCTION

For many years, uranium solvent extraction plants treating ore leach solutions have used mixer settlers. These are high shear, with the consequence of producing emulsions, and with any solids present, result in crud formation. This means poor utilization of the settler as well as high solvent losses and high maintenance costs.

Because the rate of mass transfer of uranium is rapid, other types of contactors can be considered that could improve on the capital and operating costs. Pulse columns have been proposed for years, and were implemented in France in the late 1970's. More recently, pulse columns have been a success at the Olympic Dam uranium expansion in Australia..

Another type of contactor that could be considered would be the in-line mixer. If mass transfer could be accomplished in such a low shear device, obvious advantages of improved settling could result, with less stable emulsions and cruds being formed. If successful, the in-line mixer could replace the high shear agitators presently in use, where the design is for about 2-minutes mixing.

With that objective, the initial exploratory tests were conducted at the Ranger mill site in Australia during September 1995. Those tests indicated the possible viability of using such mixers, but a more prolonged test program would be required to provide sufficient data such that scale-up and costs could be determined. The subsequent test program was conducted during March-April, 1997.

PLANT PROCESS DESCRIPTION

The ore containing the uranium is leached in sulphuric acid, passed through a CCD thickener circuit, clarified and the clarified pregnant leach solution (PLS) is sent to solvent extraction. The PLS, containing about 1g/L uranium at pH 1.5, is contacted in 3 extraction stages with a tertiary amine in Shellsol 2046 diluent. Following a 2-stage wash of the solvent, the uranium is recovered by stripping with ammonia-ammonium sulphate solution. The solvent is finally contacted with sulphuric acid to protonate it prior to recycle to extraction.

PILOT PLANT DESCRIPTION

The pilot plant was located in the SX plant area, under the mixer settlers. The pilot plant included a long, deep settler which subsequently provided very useful information to relate to the flows through the mixers. The organic and aqueous flows were connected directly to the appropriate plant flows, and valved through flow meters to the pilot plant. Although there are several designs of in-line

© Society of Chemical Industry 2000

mixers, such as the Kenics, Sulzer, Lightning, the Lightning was selected for these trials. Typical plant leach feed solutions, at pH 1.5, contained about 1 g/L uranium. The solvent feed to extraction, in the data presented, contained 0.2- 0.4 g U/L, and the solvent consisted of 2.5% Alamine 336 tertiary amine in Shellsol 2046 diluent. The usual length of each "test run" was 0.5 hour, although some tests ran for 1.5 hours, and a final test went for a duration of about 5 hours to determine consistency. With a retention time in the mixer system of less than 10 seconds, 0.5 hours was considered to be more than ample to attain chemical and physical equilibria.

The specifications of the units are as follows:

In-Line Mixer Units Type: Lightning
Elements: 220 mm length, 25 mm diameter
Glass pipe: 25 mm diameter to accept the mixers
Configuration: horizontal, straight line

Settler
Dimensions: 275 mm wide x 1215 mm long x 650 mm deep
Construction: glass sides, stainless steel ends and reinforced with stainless steel
Picket fences: 2 off-set rows of 25 mm OD poly pipe, extending the depth of the settler;an additional similar stainless steel pipe picket fence was also investigated

In-line mixer dimensions: L 220 mm x D 25 mm
Volume of 1 mixer unit = 0.000107 m^3
Volume of 9 units (9 x 0.107) = 0.00097 m^3
Volume of 6 units (6 x 0.107) = 0.000642 m^3

Time of Contact in Mixers:

At about 85% of flooding flow, of 14.25 L/m, or 855 L/h or 0.885 m^3/h passing through 9 extraction units, then 0.00097/0.855 = 0.0011 h,

or 0.0011 h x 3600 sec = 4.0 sec/9 units; or 2.7 sec/6 mixer elements.

RESULTS

The initial preliminary tests determined the flooding regime for the particular geometry of the equipment. For a 9-unit extraction system, and with the length of settler (1215 mm) being used, the flooding point (for extraction) was indicated as 17.2 L/m of mixed phases at A/O 2/1. Thus, the subsequent tests were run at varying total flows of about 15% less than the flooding point. The results and data achieved from the test program are given below.

Extraction units	Flow	Extraction efficiency (%U)		
Number	L/m	Bench	Plant	Pilot Plant
9	6.95	89.6	90.5	91.9
9	6.95	80.5	82.1	82.3
9	9.75	82.4	81.9	88.9
9	14.65	77.7	80.0	82.9
9	6.95	80.1	95.1	76.3
9	6.95	84.4	81.2	83.1
9	6.95	79.4	80.3	77.9
9	6.95	77.7	80.0	82.4

Table 1: Comparison of Pilot Plant Results with Plant and Bench Shake-Out Tests

Extraction stage

Some of the data are summarised in Figures 1-4, and in Table 1. Observations and conclusions are given in the following:

Figure 1: Extraction vs. Flow Rate
A/O 2/1 9 Extraction Units

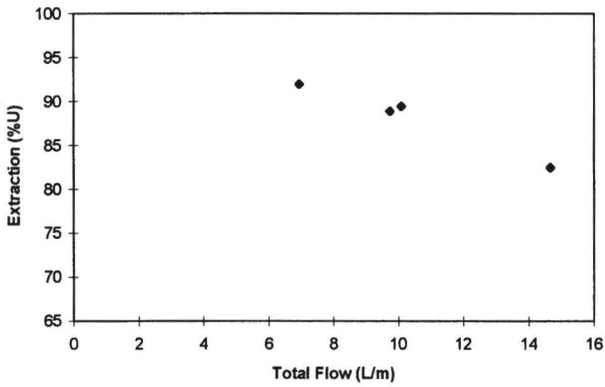


Figure 2: Phase Ratio vs. Extraction
9 Extraction Units

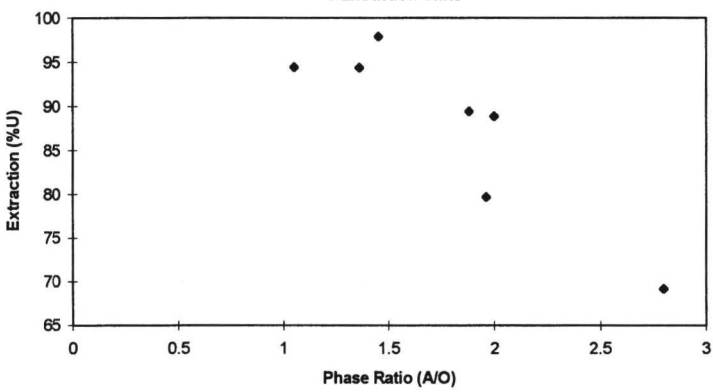


Figure 3: Mixer Units vs. Dispersion Band Length & Extraction

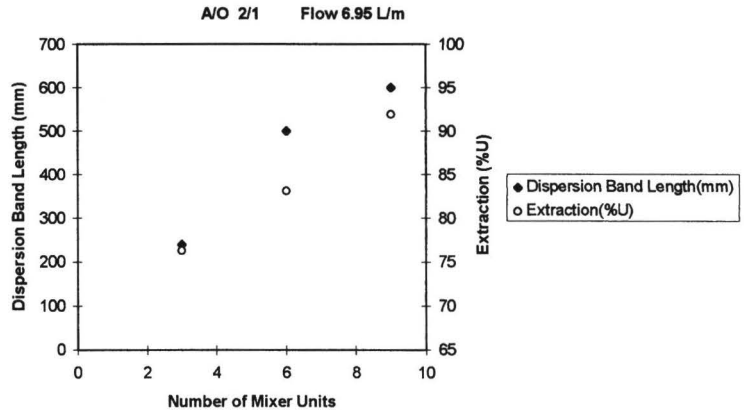
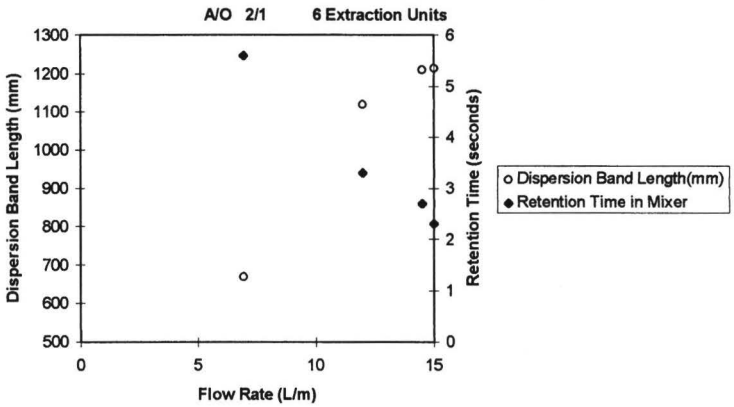


Figure 4: Flow vs. Mixer Time & Dispersion Band Length



Protonation stage

At high O/A ratios normally used, the phases separated in less than 1 minute, and no dispersion band was generated. At the low 10 g/L acid the organic was cloudy, and clarity improved as the acid strength was increased to the higher 40 g/L. The optimum conditions appear to be O/A 4/1 (although probably a higher O/A might be attainable), 3 extraction elements, and protonation with 40 g/L H_2SO_4, at a total flow to these size mixers of about 15 L/m (which is approaching plug flow in this particular size units for this specific system). At optimum conditions, and with recycle of the aqueous over a 6-hour test period, extractions of about 95% U were achieved.

Wash stage

The phase separation was rapid, usually in less than 1 minute. A small settler area would be required because of the lack of a dispersion band. It would appear that the scrub circuit could easily tolerate a high O/A ratio of perhaps 10/1 or higher using the in-line mixers.

CONCLUSIONS

The in-line mixer tests have demonstrated extremely high stage efficiency when evaluated in the uranium solvent extraction process conducted at a uranium mill on process liquors. The following are the indicated advantages:

- no requirement to maintain a specific phase continuity in mixing;
- decreased solvent inventory because of no recycle requirements;
- fine droplets were produced and high mass transfer efficiency resulted without high shear and turbulence;
- no possibility to draw air into mixing which produces serious problems in the conventional high shear pump-mix mixers;
- improved settling rates, and therefore increased settler utilization;
- decreased stable emulsions and crud formation, and therefore decreased solvent losses;
- demonstrated to be viable for extraction, protonation, and washing sections;
- settler area requirements appear to be at least one-half that required as a result of conventional mixing in extraction;
- in both the protonation and wash stages, the dispersion bands were flat, with rapid coalescence; settler area requirements would be minimal;
- settler area requirements are reduced when the mixed flows are organic continuous, that is at high O/A ratios in the mixer units as in protonation and wash sections;
- no tests were performed in the stripping circuit, although the kinetics of stripping may make in-line mixing suitable. Also, if that is possible, then pH control may be greatly facilitated by the introduction of the reagent directly into the pipe.

Thus, the data from these successful continuous pilot tests indicates that the in-line mixer could replace the agitated mixer, which is usually designed for about 2-minutes retention time in mixing in the uranium amine extraction process, and still continue to utilise the present or modified settler design. This alternative to conventional contacting could be particularly attractive for a mill planning an expansion program, as well as in a new plant, where in-line mixers might be considered for incorporation in the solvent extraction plant to reduce mixing shear and thus settler area requirements.

ACKNOWLEDGEMENTS

This project was performed in two stages. I would therefore gratefully acknowledge the assistance of several personnel at the Ranger Mill site who were instrumental in the organising of the facilities, the technical assistance, and in the analyses of the samples: Mike Hoey, Mirek Banaczkowsky, Paul Monaghan, Harry Russell and Bob Sharrock; and to Shell Australia for their contribution and support to the project and providing Peter Shelley in the initial stage of the project and Peter Carlin in the subsequent stages.

FAST PRE-NEUTRALISATION AND EXTRACTION IN A TUBULAR REACTOR USING AN ACIDIC EXTRACTANT

E Jääskeläinen and E Paatero
Lappeenranta University of Technology P.O.Box 20, FIN-53851 Lappeenranta, Finland

ABSTRACT
An agitated tubular reactor was used to study the partial neutralisation of Versatic 10 extractant with aqueous ammonia and the following extraction of nickel with the pre-neutralised extractant. Both reactions are very fast and complete in a few seconds. The fast metal extraction is explained to take place as a pseudo-homogeneous reaction in a micellar media.

Keywords: Versatic acid, pre-neutralisation, nickel, in-line mixer

INTRODUCTION

A notable direction in the technological development at the present time is based on the concept of process intensification in chemical reactor design.[1] In the liquid–liquid extraction of metals with acidic cation exchangers the process can be intensified by neutralising the reagent prior to the contact with the metal bearing aqueous solution instead of controlling the pH during the contact.

In the present work this concept is illustrated using Versatic 10 extractant (Shell Chemicals Co.) which is mixture of highly branched isomers of C_{10} monocarboxylic acids. The ammonium and sodium salts of these types of extractant molecules are amphiphiles, which form microscopic aggregates (micelles and microemulsions) when mixed with water and an organic solvent.[2] In the previous works by the present authors the phase equilibria corresponding to the neutralisation conditions has been reported for Versatic 10 and aqueous ammonia mixtures.[2,3] When the degree of neutralisation is about 50% the system is as a single phase microemulsion. It was also shown that Ni^{2+} could be added into the microemulsion up to 10% of the full nickel load without a break up of the phase into two liquid phases[3] (Figure 1).

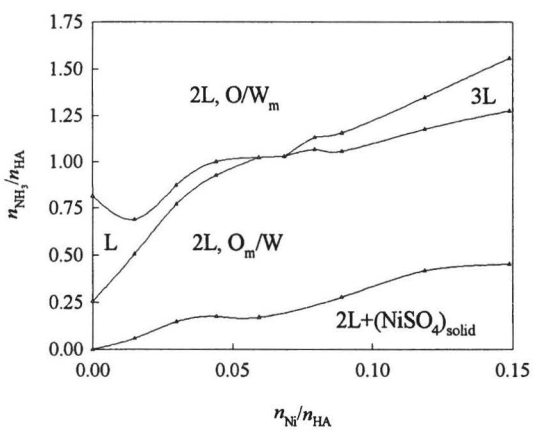


Figure 1. Partial phase diagram for the system water (14M NH_3)/Versatic10/isooctane with increasing amounts of Ni^{2+}.

© 2000 Society of Chemical Industry

The micellar formations are dynamic units that are constantly forming and dissociating on a time-scale in μs to ms range (for review [5]). Furthermore, the microemulsion has an extremely large internal interface. For organic syntheses using microemulsions as medium for interfacial reactions the high solubility of the reactants in the microemulsion and high reaction rates result in excellent space-time yields.[6] It is anticipated that also metal extraction with a microemulsion solution is very fast as the phase diagram in Figure 1 implies that complexation of Ni^{2+} with Versatic is a pseudo-homogeneous reaction at least during the initial moments of the process.

The main aims of the present work were on the other hand to find experimental evidence that the pre-neutralisation step is fast and on the other hand to confirm that metal extraction with the pre-neutralised extractant is pseudo-homogeneous and fast. A special type of experimental tubular reactor with short contact times was constructed for that purpose.

EXPERIMENTAL

All experiments were carried out at 25 °C with 40 wt-% Versatic 10 dissolved in isooctane. The aqueous ammonia was Pro-analysis quality. The ammonia concentration was analysed prior to use by HCl titration. The phase equilibria in test-tubes were determined as described else where.[4]

The phase transition kinetics was studied in a long transparent adiabatic tubular reactor equipped with an equally long stirrer rotating at the speed of 2000 rpm (Figure 2). The aqueous and organic phases at 25 °C were pumped co-currently into the reactor. At the entrance in the reactor the solution mixture was always milky. In case that the system became a microemulsion the solution turned clear and transparent usually at about 10-20 cm from the entrance.

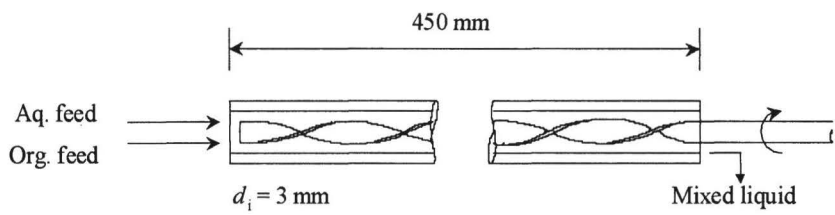


Figure 2. Tubular reactor used for the studies of phase transition kinetics.

RESULTS AND DISCUSSION

Dynamics of pre-neutralisation

The tubular reactor was used to study the phase transition dynamics corresponding to the pre-neutralisation of Versatic 10 with ammonia. Concentrated (13.3 M) aqueous ammonia was fed to the reactor together with the organic phase containing 40 wt-% Versatic in isooctane. The feed ratio was adjusted to keep the degree of neutralisation (N) fixed at 50%.

Pre-neutralisation can be described by the reaction formula:

$$NH_3 + qH_2O + y/2(\overline{HA})_2 \equiv \overline{NH_4A \cdot (y-1)HA \cdot qH_2O} \qquad (1)$$

where $q \approx 3$ for concentrated aqueous ammonia and $y = 2$ when $N = 50\%$.

The total volume flow rate was varied between 13.8 and 70 ml/min corresponding to the residence times of 13.2 and 2.6 s, respectively. In all experiments the mixture turned clear single phase before the outlet which was regarded as an evidence that the pre-neutralisation is fast and only controlled by the mixing characteristics. The pre-neutralised extractant is in form of a hydrotropic

solution ($n_{H_2O}/n_{NH_4A} = 3$) which becomes a microemulsion when diluted with water. This pre-neutralised extractant was used for the metal extraction experiments. Since the neutralisation is exothermic the temperature increased to 37.2 °C due to the reaction. The reaction enthalpy was determined separately using a ChemiSens reaction calorimeter model RM-2 as 83 kJ/mol NH_3. The latter determination was carried out with diluted aqueous ammonia (0.479 and 0.862 M) in a two phase system.

The fast relaxation towards phase equilibrium can be sensitively studied in the tubular reactor by diluting the microemulsion with water and by measuring the solubilized amount of water before the break-up to two phases. The water uptake as a function of the degree of neutralisation is shown in Figure 3. The contact time was 10 s. The maximum of water/ammonia ratio in the system (n_{H_2O}/n_{NH_4A} = 14.2) was recorded when N was equal to 50%. Figure 3 shows also the experimental values obtained in test tubes at fully equilibrium conditions. We can conclude that the equilibria was always reached in the short contact reactor.

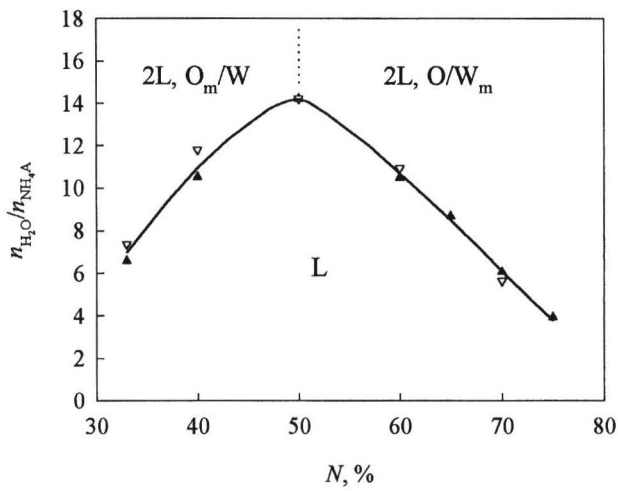


Figure 3. The influence of water addition on the phase equilibria in the system water(NH_3)/Versatic 10/isooctane. The phase boundary between one phase region and two phase region obtained in dynamic studies (∉) and in equilibrium studies (>).

Kinetics of nickel extraction

The pre-neutralised extractant binds Ni^{2+} through a cation exchange reaction: [3]

$$Ni^{2+} + (2+m)/y\overline{NH_4A \cdot (y-1)HA \cdot qH_2O} \equiv 1/x\overline{(NiA_2 \cdot mHA \cdot pH_2O)_x} + (2+m)/yNH_3 + ((2+m)q/y - p)H_2O + 2H^+ \quad (2)$$

The nickel complex may thus remain hydrated in the organic phase.

The effect of nickel was first studied analogously with Figure 3 but adding 0.085 M $NiSO_4$ in the water. The same boundary for the one-phase region was obtained both in the short contact reactor in a few seconds as in test tubes during several hours (see Figure 4). When nickel was present, however, the phase inversion from a O/W_m (=Winsor I) to a W/O_m (=Winsor II) system was not as sharp as with pure water. The error interval for the experimental data at N = 50% was ∀3% for four determinations. The repeatability for all other measurements was better than ∀0.6%. Therefore, the difference between the dynamic conditions and equilibrium conditions is significant

The phase behaviour was further studied in the tubular reactor by increasing the aqueous phase to pre-neutralised organic phase ratio and keeping the aqueous nickel concentration as well as the degree of neutralisation fixed. The A/O-ratio was increased until phase break up was observed. Similar experiments were carried out for different nickel concentrations and for different *N*. The results are plotted in Figures 5a and 5b.

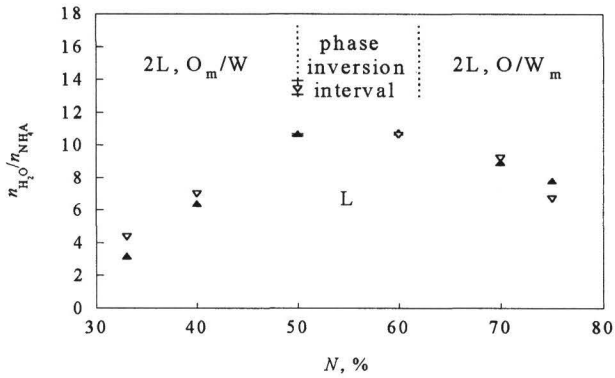


Figure 4. The effect of aqueous Ni^{2+} (0.085 M) on phase equilibria in the system water(NH_3)/Versatic 10/isooctane. The phase boundary between one and two phase regions obtained in dynamic studies (⋐) and in equilibrium studies (>).

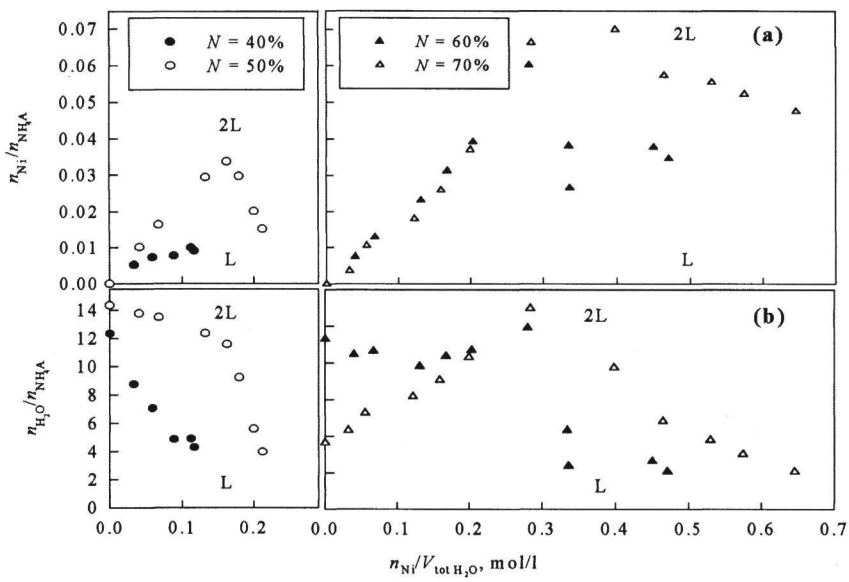


Figure 5. The maximum Ni^{2+}/NH_4^+-ratio **(a)** and the corresponding degree of hydration **(b)** in the microemulsion before break up as a function of Ni^{2+} concentration in the Ni/NH_3/water/Versatic 10/isooctane system.

CONCLUSIONS

1) The neutralisation of Versatic 10 with aqueous ammonia is fast process that can be carried out in tube (e.g., with an in-line mixer) with a short contact of a few seconds.
2) The extraction of nickel with a pre-neutralised Versatic 10 is fast pseudo-homogeneous reaction, which takes place in a microemulsion environment. It can favourably be carried out in a tubular reactor.
3) The degree of neutralisation governs the structure of the phases during nickel extraction. When Ni^{2+} is exchanged to NH_4^+ according to equation (2) the amount of remaining NH_4^+ controls the amount of solubilized water in the organic phase. The maximum amount of water is obtained when the NH_4^+/Versatic ratio is 1:2.

NOMENCLATURE

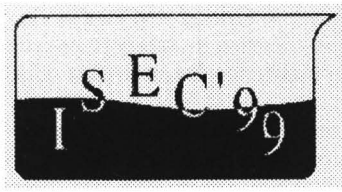
d_i	internal diameter (mm)
m, p, q, x, y	constants used in equations (1) and (2)
n_i	amount of the i species (mol)
N	degree of neutralisation, $= n_{NH_4A}/n_{HA,tot}$
V	volume (l)
HA	monomeric form of carboxylic acid
$\overline{HA}$	monomeric form of carboxylic acid in the organic phase
L, 2L, 3L	regions where one, two, respectively three liquid phases are in equilibrium
O, O_m	normal organic phase, micellar "water-in-oil" phase, respectively
W, W_m	normal aqueous phase, micellar "oil-in-water" phase, respectively

ACKNOWLEDGEMENTS

The authors are grateful to the Outokumpu Research Foundation and Research Foundation of Lappeenranta University of Technology for supporting this work.

REFERENCES

1. Green A, *Chem. Indust.*, **1998**, 2 March, 168.
2. Paatero E and Sjöblom J, *Hydrometallurgy* **25**, 231, (1990).
3. Jääskeläinen E, and Paatero E, in *'Value Adding Through Solvent Extraction'*, (D.C. Shallcross, R. Paimin, L.M. Prvcic (Eds)), The University of Melbourne Press, **1,** 421, (1996).
4. Jääskeläinen E, and Paatero E, *Hydrometallurgy* (in press).
5. Zana R and Lang J, in *'Microemulsions: structure and dynamics'*, (S.E. Friberg and P. Bothorel (Eds)), CRC Press, Boca Raton, Florida, 1987, 156.
6. Tjandra D, Lade M, Wagner O, and Schomäcker R, *Chem. Eng. Technol.* **21(2),** 666, (1998).



COMPARISON BETWEEN DIFFERENT EXTRACTORS FOR A HIGH VISCOSITY EXTRACTION APPLICATION

D Kirschneck[1], H Schmitt[2] and R Marr[1]

[1]Institut für Thermische Verfahrenstechnik und Umwelttechnik, TU Graz, Inffeldgasse 25, A-8010 Graz, Austria

[2]Lucas Meyer, Ausschläger Elbdeich 62, D-20539 Hamburg, Germany

ABSTRACT

Various batch and continuous extraction experiments have been carried out with a high viscous medium used as the delivering phase for the transferring compound. The experiments were performed batch on lab-scale using a stirred tank and a rotor-stator-mixer. On continuous pilot plant scale a stirred column, static mixers and a rotor-stator-extractor were compared. Temperature and phase ratios were varied. It was found that the mass of product in the extract phase is proportional to the Reynolds number and therefore proportional to the power input in the dispersion until Re reaches 10000. Further increase in Re does not change the extraction efficiency. This relationship was found to be nearly independent of the applied extractor type. That means the same extraction yield was reached in different extractors at the same power input. Using adequate definitions of the Reynolds number and taking into account the effective viscosity of the dispersion the extraction performance of different apparatus configurations can be compared in the same diagram. As the dynamic viscosity is indirect proportional to Re energy input increases with higher viscosities, that means only extractors with a high energy input are useful for extractions with the high viscous medium chosen to be the dispersed phase.

Keywords: high viscosity, Reynolds number, extractor comparison

INTRODUCTION

Solvent extraction is a unit operation, which can be used for separation of multicomponent systems. Biological matrices offer a wide range of applications for solvent extraction to reach commercial products by fractionation of compounds having a similar chemical structure. Mass transfer difficulties start when the feed is of high viscosity. As a test system a multicomponent mixture of polar (mostly phospholipids) and non-polar lipids with a viscosity of 1 Pa.s as feed was used. It should be extracted with ethanol (5 mPa.s) as solvent. The aim is to extract one of the phospholipids (phosphatidylcholine). Wagner[1] reviewed extraction equipment for high viscosity applications and came to the conclusion that centrifugal extractors, separators and spray columns were commonly used for high viscosity applications. Stirred and pulsed columns are preferred for medium viscous systems, but the opinion as to which type of equipment should be chosen and how viscosity influences hydrodynamics are different.

Special problems of high viscosity extraction

In an early step of process design it must be decided if the viscous medium should be the continuous or the dispersed phase. If the viscous medium is chosen to be the continuous phase, the force on the drops caused by the density difference shall to be large enough to ensure a reasonable terminal velocity of the drops raising in the continuous phase. Otherwise even in the case of a small energy input intensive drop breakage would cause a lot entrainment. Therefore equipment providing a high effective phase separation (e.g. centrifuge) is needed. If the viscous medium is chosen to be the dispersed phase, a high energy input will be necessary to disperse the viscous fluid. In the present investigation the high viscous raw lecithine is chosen to be the dispersed phase.

High viscous droplets behave like rigid spheres. They have no internal circulation and the diffusion to the surface is limited, since the diffusion coefficient is according to the Stokes-Einstein-Equation proportional to the dynamic viscosity. The diffusion depends linear on the diffusion coefficient. That means only the near-surface-region of the drops can be extracted. The enhancement effect of surface renewal can easily be demonstrated experimentally. In the first experiment the viscous medium is extracted batchwise in a stirred tank. Extraction time is five minutes. Analytical samples of both phases are taken after waiting ten minutes of settling time. In a second experiment

© 2000 Society of Chemical Industry

five dispersion/settling cycles were performed with each dispersion and settling step lasting for one minute. Another five minutes of settling were given afterwards. Note that the overall contact time for dispersing and for settling was the same in both experiments, demonstrating the important effect of surface renewal.

These findings have important implications for the experimental determination of extraction distribution coefficients and on phase equilibrium data in general. To obtain reliable results out of such experiments a sufficient number of settling and redispersing cycles must be performed.

EXPERIMENTAL

In an initial investigation, experiments focused on lowering the viscosity of the viscous phospholipid medium were performed. It was found out that premixing with the solvent can reduce the viscosity. The feed was adjusted to a feed composition corresponding to a state point near the binodeal curve outside the two-phase region. This reduces the viscosity from 1 Pa.s to about 200 mPa.s. Lowering the viscosity by heating the feed was not successful since part of the mixture starts to decompose at temperatures higher than 50°C.

Based on the considerations in Part 2 it was decided to choose a stirrer with a high energy input for lab-scale experiments, to have enough turbulence energy to produce small drops and thereby maximising their interfacial area. 100 g of the lipid mixture was premixed with 19 cm^3 ethanol by means of a stirrer at 500 min^{-1}. The extraction was carried out by means of a rotor-stator-system (Ultraturrax T25 from IKA-Werke/Staufen(Ger) with stirrer unit S25N-18G) by adding 73 cm^3 solvent ethanol and stirring for 5 minutes at speed levels between 8000 and 24000 min^{-1}. The first aim was to maximise the extraction yield to keep the amount of solvent as small as possible.

It was observed that the extraction yield increases by increasing the rotation speed. At certain level no increase of the extraction yield could be observed. The results are further analysed and shown in dimensioness form in figure 1. Settle problems have not been observed even in the cases of high energy input, that cause small drops. Settle problems only occur, if the leaching time of the near-surface-region is too short and phosphatidylcholine acts as a surfactant at the surface of the drop.

Experiments with two different phase ratios and different extractors have been carried out. A conventional stirred tank and two different rotor-stator-systems (Ultraturrax T25/T50) have been used on batch lab-scale. On the pilot plant scale extraction experiments have been carried out continuously by means of either a stirred extraction column or static mixers (plug flow) or of a rotor-stator-system (Ultraturrax T50 carried out as mixed flow vessel). The results are shown in figure 2.

RESULTS AND DISCUSSION

Correlating the energy input to compare different extractors

The aim of the model is it to compare hydrodynamic conditions of different extractors. To do this, physical properties of the two-phase system need to be calculated. The mean density $\bar{\rho}$ of the mixture can be calculated according to Liepe[2]

$$\bar{\rho}=\varphi_S\rho_S+\varphi_F\rho_F \qquad (1)$$

where ρ_F and ρ_S are the densities φ_F and φ_S are the volume fractions of feed and solvent. The effective viscosity $\bar{\eta}$ of the dispersion in the case that the solvent forms the continuous phase can be determined according to Liepe[2]

$$\bar{\eta} = \eta_S \exp\left(\frac{K_1\varphi_F}{1-K_2\varphi_F}\right) \qquad (2)$$

where η_S is the viscosity of the solvent and φ_F is the volume fraction of dispersed feed phase. K_1 and

K_2 are constants. Prikrylova[3] has determined the constants to be K_1=1.7 and K_2=0.5 for different oil-in-water emulsions. For φ_F<0.7 Barnea[4] has found similar effective viscosities.

Mass transfer is strongly influenced by the hydrodynamic conditions in the extraction apparatus. One way to characterise the hydrodynamic conditions is to calculate the Reynolds number. Two different equations have been used to calculate the Reynolds number for the different extractors. The Reynolds number for all stirred extractors (stirred tank with conventional stirrer, stirred tank with Ultraturrax, stirred extraction column) can be calculated by means of equation 3

$$Re_{Stirrer} = \frac{n\, d_R^2\, \bar{\rho}}{\bar{\eta}} \qquad (3)$$

The stirrer or rotor has a diameter of d_R and turns n times per second. The average physical properties can be used as calculated before. For the experiments with static mixers as extractor the Reynolds number is given by the following equation

$$Re_{StaticMixer} = \frac{\bar{\rho}\, v\, d_h}{\varepsilon\, \bar{\eta}} \qquad (4)$$

where v is the superficial velocity. The hydraulic diameter d_h and gap fraction ε are given by the manufacturer.

Comparison between different extractor types

Different extractors are compared by assessing at the extraction yield (in our case the solid content in the extraction phase) in relation to hydrodynamic parameter determining the energy input (in our case the Reynolds number). In figure 1 the solid content of the extracted phase is plotted versus Reynolds number on logarithmic scale for experiments with the same phase ratio.

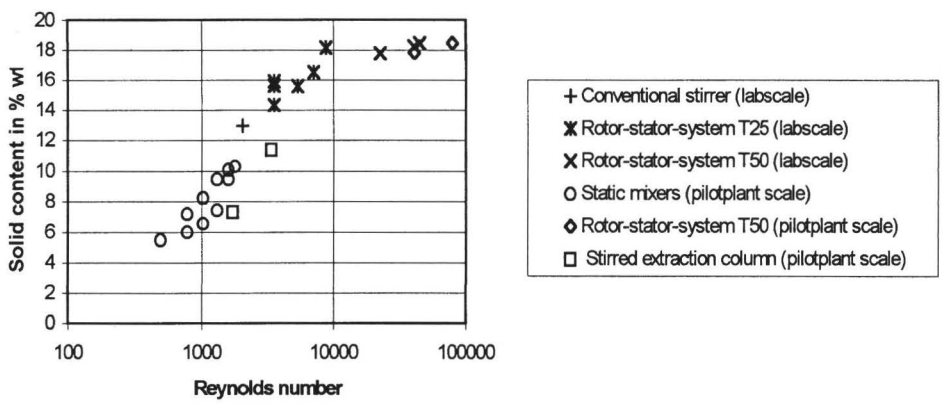


Figure 1: Graph of solid content in the extracted phase versus logarithmic Reynolds number for different extractors

It can be seen from the graph, that the solid content increases linearly until the Reynolds number reaches 10000. After Re = 10000 the solid content is independent of the of the Reynolds number. The important point is that this finding is nearly independent of the extractor type. A window of 2% solid content variance can be seen of experiments done with the same extractor type. Dependent on the type of extractor it maybe shifts parallel to a small extent. All the extraction experiments with the same phase ratio can be summarised in the same diagram.

The graph shifts to smaller solid contents for higher solvent-to-feed ratios. This phenomenon is visualised in figure 2. As in figure 1 the experiments with the high phase ratio are carried out with

different extractors. The overall characteristic of this experimental series is the same with the solid contents just shifted to a lower level.

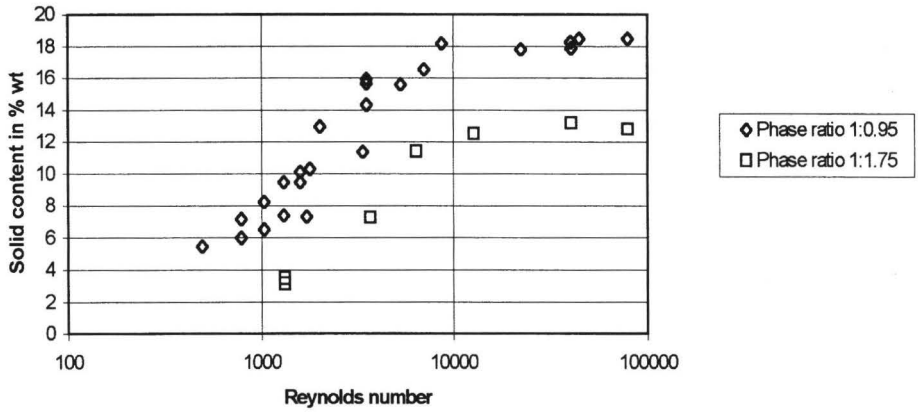


Figure 2: Graph of solid content in the extracted phase versus logarithmic Reynolds number for two different phase ratios

Optimisation on pilot scale

Based on the previous results a pilot plant was designed with a rotor-stator-system as extraction unit and hydrodynamic conditions according to a Reynolds number greater than 10000. The parameters, temperature and phase ratio were varied on two levels. The aim is to maximise the solid content in the extracted phase. The experimental solid content data points were fitted by a surface on the two-dimensional array of the range of the two independent variables temperature and phase ratio. Table 1 summarises the operation conditions of the experiments, the experimental determined values of the solid content as well as the deviation of the data points from the surface fit. The resulting surface is visualised in figure 3.

No.	Temperature [°C]	Phase ratio [kg/l]	Solid content (analysed) [%]	Deviation of the fitted surface [%]
1	44,1	1/0,95	17,9	-0,2
2	39,0	1/0,95	16,9	±0
3	33,7	1/1,8	12,0	+0,2
4	40,8	1/1,4	14,9	±0
5	49,2	1/0,95	18,5	+0,1
6	43,7	1/1,8	12,8	+0,1
7	38,6	1/2,2	10,8	-0,2

Table 1: Dependency of the solid content on the temperature and on the phase ratio

An interesting point experimental results was that the influence of temperature on the solid content is different for two phase ratio levels. While the solid content at high phase ratio is nearly independent of the temperature, a reasonable increase of solid content can be found by increasing the temperature at a low phase ratio level. This demonstrates that the parameters have a strong dependency on each other. Statistical experimental planning can be a useful tool to catch all dependencies of the investigated parameters.

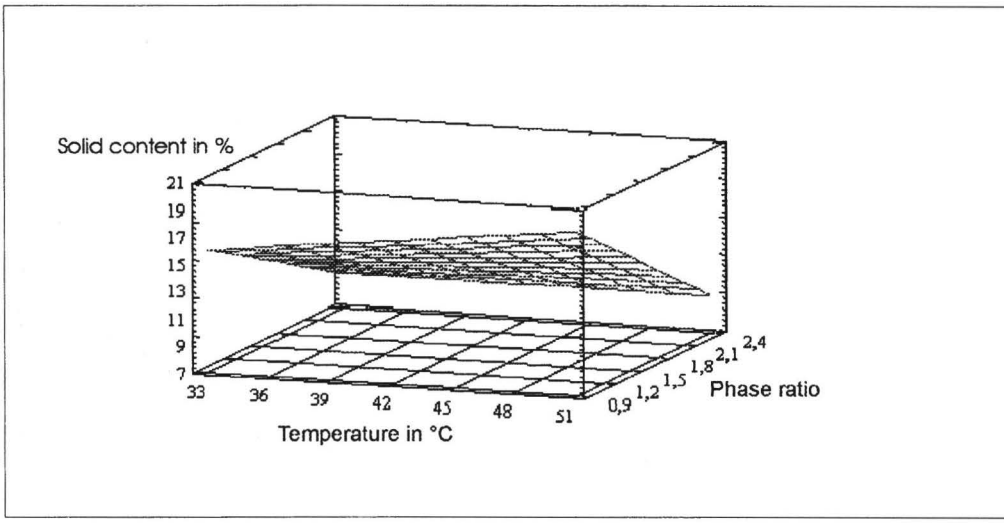


Figure 3: Dependency of the solid content on the temperature and on the phase ratio

CONCLUSIONS

Extractors applying a viscous medium as the continuous phase need an effective separator or a centrifuge to separate the phases and to minimise the entrainment. For extraction with the viscous medium to be the dispersed phase high energy input is necessary to disperse the system sufficiently. The interfacial area and thereby the solid content of extracted phase increases linear with the logarithm of the Reynolds number until Re reaches 10000. After that limit the solid content is independent of the Reynolds number. Different extractors (stirred column, static mixers, conventional stirrer, rotor-stator-systems) show the same characteristic. The extraction yield for the lipid/ethanol system was found to be of similar magnitude in all investigated extractor types. For a given temperature and phase ratio the extraction yield exclusively is a function of energy input.

SYMBOLS

d	diameter	[m]
Re	Reynolds number	[-]
n	rotation per time	[s^{-1}]
K_1, K_2	constants	[-]
v	superficial velocity	[m s^{-1}]
ε	gap fraction	[-]
η	viscosity	[Pa.s]
φ	phase fraction	[-]
ρ	density	[kg m^{-3}]

Subscripts

F	feed phase
h	hydraulic
R	rotor
S	solvent phase
$\bar{x}$	average value

REFERENCES

1. Wagner G, *PhD Thesis, University of Technology Munich,* (1994).
2. Liepe F et al.; *Verfahrenstechnische Berechnungsmethoden-Stoffvereinigung fluider Phasen,* VCH-Verlag, Weinheim, (1988).
3. Prikrylova J and Haman J; *CHISA-Congress* Praha, (1984).
4. Barnea E and Mizrahi J; *Chem. Eng. J.* **5**, 171, (1973),

EXTRACTION BEHAVIOR OF Pd(II) WITH TRI-*n*-OCTYLAMINE IN A VIBRO-MIXER TYPE EXTRACTOR

Y Kawano[1], K Shiomori[1], S Yamada[1], H Yoshizawa[2] and Y Hatate[2]

[1]Dept. of Materials Sci., Miyazaki Univ., Miyazaki, Japan

[2]Dept of Appl. Chem. & Chem. Eng., Kagoshima Univ., Kagoshima, Japan

ABSTRACT

For developing a highly effective extractor, the extraction of Pd(II) in aqueous hydrochloric acid solution by toluene solution of tri-*n*-octylammonium chloride salt was investigated using a vibro-mixer type extractor in the various conditions. The overall extraction rate of Pd(II) were interpreted by (1,1) orders reaction rate of the concentrations of ammonium chloride in toluene and palladium chloride in the aqueous phase. The rate constant increased with vibration frequencies and feed velocities into the extractor. The extraction equilibrium of Pd(II) from hydrochloric acid solutions with tri-n-octylamine in toluene was also investigated.

Keywords: vibro-mixer extractor, extraction kinetics, palladium, tri-*n*-octylamine

INTRODUCTION

Solvent extractions were generally operated by the heterogeneous systems. It is important to increase the contact surface area for achieving high extraction efficiency. Forced mixing type extractor, centrifugal and mixer/settler extractors have been used generally as high efficiency extractors. Vibro-mixer type reactors are able to produce small droplets and to obtain highly surface areas continuously and steadily by vibration of the disks in the extractor[1]. Hence, the vibro-mixer type reactor is suitable for an effective extractor.

Long-chain alkyl amines are one of the most useful extractants of precious metals. We have studied the extraction and the separation processes of precious metals using long chain alkyl amines[2,3]. In this paper, firstly, the extraction equilibrium of palladium(II)[2] from hydrochloric acid solution with tri-n-octylamine (TOA) in toluene was investigated to clarify the complex formed and the equilibrium constants. Furthermore, in order to develop a highly effective extractor, the extraction of palladium from hydrochloric acid solution with TOA in toluene was carried out using the vibro-mixer type extractor. The effects of flow rate of the fluids, frequency of the disks, the concentrations of TOA and palladium on the extraction rates of palladium were examined.

EXPERIMENTAL

Tri-*n*-octylamine (99.7%, TOA) supplied from Koei Chemical Co. was used as an extractant without further purification. TOA was dissolved in toluene at desired concentrations. $PdCl_2$ was dissolved in aqueous hydrochloric acid solutions. The extraction equilibrium was measured by the same method in previous papers.[2,3] In the experiment of the extraction rate, TOA was previously converted to ammonium chloride salt by the equilibrating TOA in toluene with 0.1 M hydrochloric acid in aqueous solution. In this condition, all of TOA is converted to ammonium chloride salt.[4]

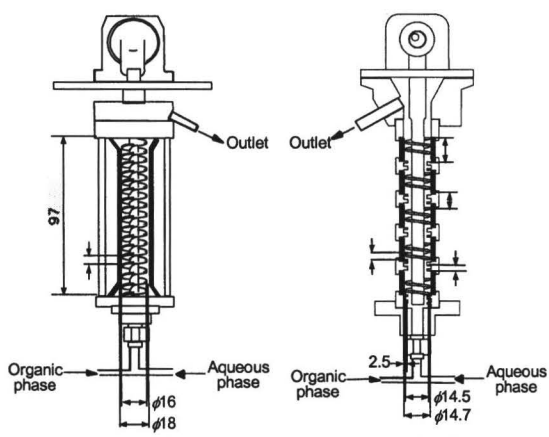


Figure 1 The vibro-mixer type extractor.

© 2000 Society of Chemical Industry

The two types of the vibro-mixer type extractor used in this experiment are shown in figure 1. In the first type of extractor (hereafter called A-type), a set of spiral type vibration disks were put into a cylindrical tube having a net volume of 3.27 x 10^{-5} m^3. In the second type of extractor (B-type), four spiral disks were put into a cylindrical tube with five baffle disks having a net volume of 1.45 x 10^{-5} m^3. The disks were vibrated up and down at 3 mm vibration amplitude. The toluene solution of TOA ammonium chloride salt and the aqueous hydrochloric acid solution of palladium chloride were pumped separately at a fixed flow rate into the bottom of the reactor. The effluent mixed solution from the top of the extractor was settled and was separated quickly into the aqueous and organic phases within one minute. The steady state for the Pd(II) extraction in the extractor was previously found to be achieved after 5 minutes operation time. The concentration of precious metal in the aqueous solution was determined using atomic adsorption spectrometer. The concentration of the metal in the organic phase was calculated from mass balance. The concentration of TOA in toluene was determined by titration with a butanol-methanol mixed solution of hydrochloric acid using bromocresol green as an indicator.

RESULTS AND DISCUSSION

Extraction equilibrium of Pd(II)

The equilibrium concentrations of Pd(II) in the organic phase, $C_{M,org}$, were plotted against the initial concentration of TOA in toluene, $C_{B,0}$, in Figure 2. The values of $C_{M,org}$ increased with an increase in $C_{B,0}$, and with decreasing in C_{HCl}. TOA in toluene reacts with hydrochloric acid in aqueous solution to form the TOA-hydrochloric acid complex as follows;

$$B + HCl \Leftrightarrow BHCl \qquad (1)$$

where B and BHCl indicate TOA and the complex between TOA and hydrochloric acid, respectively. In these experimental conditions, TOA is predominantly existed as the complex and the presence of free TOA is negligibly small[4]. The extraction of Pd(II) with TOA from hydrochloric acid solution is expressed by the following reaction:

$$MCl_Z^{n-} + nBHCl \Leftrightarrow (BH)nMCl_Z + nCl^- \qquad (2)$$

where MCl_Z^{n-} indicate the chloro-complex of the metals. Under the condition of this study, Pd(II) ions exist as the complex of $PdCl_4^{2-}$ [5]. Hence, the values of Z and n are as follows; Z=4 and n=2 for palladium. The equilibrium constant of Eq(2), K_M, is written as:

$$K_M = \frac{[(BH)_nMCl_Z][Cl^-]^n}{[MCl_Z^{n-}][BHCl]^n} \qquad (3)$$

By the consideration of distribution coefficient, $D = (C_{M,org}/C_{M,aq})$, Eq(3) is rewritten as follows;

$$= K_M \frac{[BHCl]^n}{[Cl^-]^n} \qquad (4)$$

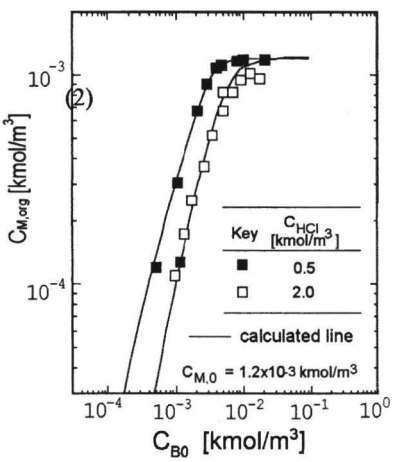


Figure 2 Relationship between $C_{M,org}$ and $C_{B,0}$

The concentration of BHCl, C_B, was evaluated by the initial concentration of TOA, $C_{B,0}$, and equilibrium concentration of the metal in the organic phase, $C_{M,org}$, as follows;

$$C_B = C_{B,0} - nC_{M,org} \quad (5)$$

$[Cl^-]$ is assumed to be the hydrochloric acid concentration in this study. The plot of log$D$ against log{[BHCl]/[HCl]} for Pd(II) is shown in figure 3. The experimental results are plotted on the straight line having a slope of 2.0 for Pd(II), regardless the concentration of hydrochloric acid. The intercept of the straight line gives the equilibrium constant for equation 2. The value of K_M is obtained as $6x10^5$ for Pd(II). The calculated results using K_M shown in figure 2 by solid line are almost agreed with the experimental results.

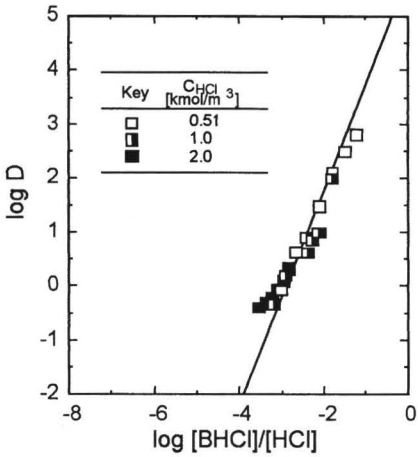


Figure 3 Relationship between log$D$ and log{[BHCl]/[HCl]} for Pd(II)

Extraction Rate in the vibro-mixer extractor.

When the A-type extractor was used, the values of the Pd(II) concentration in the effluent aqueous solution, C_{Pd}, were plotted against the average residence time of the fluid in the extractor, τ, at constant $C_{B,0}$ and $C_{Pd,0}$ for each vibration frequency of the disk, f, in figure 4. In the case of no vibration of the disk, the values of C_{Pd} were not influenced by τ. In the range of f between 50 and 200 spm, C_{Pd} decreased with increasing in τ. The values of C_{Pd} at 300 spm were also not influenced by τ. The values of C_{Pd} were plotted against f in figure 5. C_{Pd} decreased with increasing in f and approached to a constant value dependent on $C_{B,0}$ being calculated by the equilibrium constant for the reaction[2]. Reaction between Pd(II) and ammonium chloride was suggested to affect the extraction rates of Pd(II). As droplets size of the dispersion phase in the extractor decreased with vibration frequency of the disk. In the range of more than 400 spm, the reaction is considered to attain the equilibrium state. The flow velocities of the fluids in the extractor and the vibration frequencies of the disk affect the extraction rates of Pd(II). The mixing of both phases are depend on the fluid dynamic properties in the extractor.

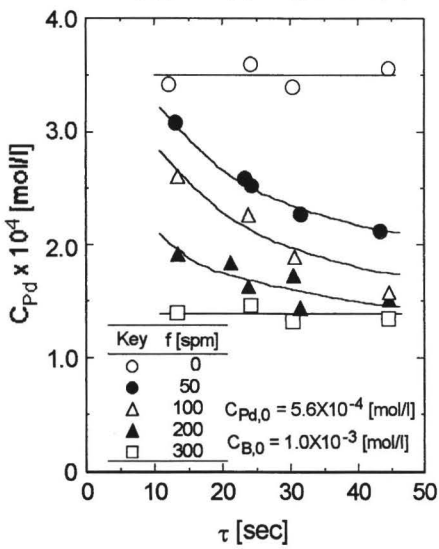


Figure 4 Effect of the mean residence time, τ, on the concentration of Pd(II) in the effluent solution, C_{Pd} in the A-type extractor.

The fraction of extraction of Pd(II), E_A was calculated by the following equation;

$$E_A = (C_{Pd,0} - C_{Pd})/C_{Pd,0} \quad (6)$$

The overall extraction rate, r_{Pd}, was calculated by the following equation;

$$r_{Pd} = (C_{Pd,0} - C_{Pd})/\tau \quad (7)$$

Considering equations 6, equation 7 was transferred as follows;

$$r_{Pd} = C_{Pd,0} \cdot E_A / \tau \quad (8)$$

By considering the reaction between palladium and tri-n-octyl ammonium chloride in equation 2, the overall reaction rate equation was assumed as the first order of Pd(II) and n-th orders of ammonium chloride as follows.

$$r_{Pd} = k_r \cdot C_{Pd} \cdot C_b^n \quad (9)$$

Combining equations 8 and 9 and reforming, the following equation was obtained.

$$\ln\{C_{Pd,0} \cdot E_A/(\tau C_{Pd})\} = \ln k_r + n \cdot \ln C_B \quad (10)$$

The values of ln $\ln\{C_{Pd,0} \cdot E_A/(\tau C_{Pd})\}$ were plotted against $\ln C_B$ for various f in figure 6. The straight lines having a slope of 1.0 were obtained for each f except that of greater than 300 spm. Then the extraction rate of Pd(II) in the extractor was interpreted as the first order for the concentrations of Pd(II) and ammonium chloride respectively.

The following equation was obtained by combining Eqs(6), (8) and (9) at n=1.0.

$$1/E_A = 1/(k_r \cdot \tau C_B) + 1.0 \quad (11)$$

The values $1/E_A$ were plotted against $1/(\tau C_B)$ for each f in figure 7. The values of $1/E_A$ were plotted on the straight lines having a slope dependent on f. The slopes of the straight lines in Fig.7 show the values of $(1/k_r)$ for each f. The values of k_r calculated from the slopes of the straight lines were plotted against f in figure 8. The overall reaction rate constant, k_r, increased with an increase in the frequency of the disk in the extractor.

In case of the B-type extractor was used, the values of E_A at τ = 24 sec. were plotted against f in figure 9. E_A attained the equilibrium values at 200 spm. As shown in the previous analysis, $1/E_A$ was plotted against $1/(\tau C_B)$ for τ = 24 sec. in figure 10. The results were plotted on the straight lines having a slope dependent on f. The result was similar to that shown in figure 7 for the results in the A-type extractor. The values of k_r calculated from the slopes of these straight lines in the B-type extractor were plotted in figure 8 together with the results in the A-type extractor. The values of k_r increased with increasing in f. As decreasing in τ, the linear velocity of the fluids in the extractor increase. The fluids mixing in the extractor become vigorous. Overall extraction rate constant increased with increasing in the fluid velocity in the extractor. The values of k_r in the B-type extractor at τ = 24 sec. was equal to that in the A-type extractor. The mixing of the fluids was not affected by setting of baffle plates installed in the extractor.

By using the vibro-mixer type extractor in the extraction of Pd(II) in the aqueous solution with tri-n-octylamine of toluene solution, 0.1×10^{-5} m^3 of the liquid containing Pd(II) was found to be treated in only 13 sec. to the equilibrium state of the system at 400 spm of vibration.

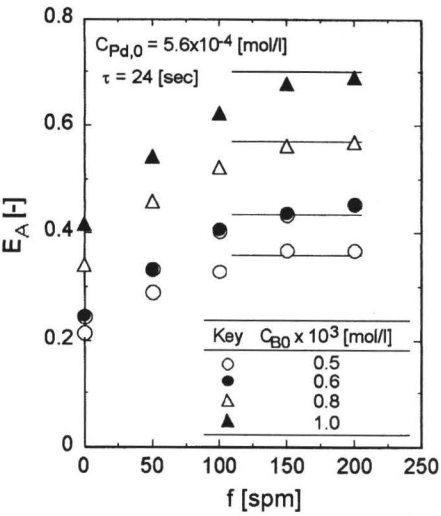


Figure 5 Effect of the vibration frequency, f, on the concentration of Pd(II) in the effluent *solution*, C_{Pd}, in the A-type extractor.

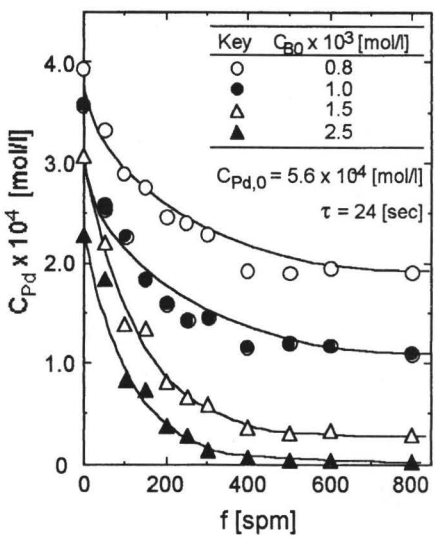


Figure 6 Relationship between $\ln\{C_{Pd,0} \cdot E_A/(\tau \cdot C_{Pd})$ and $\ln C_B$ in the A-type extractor.

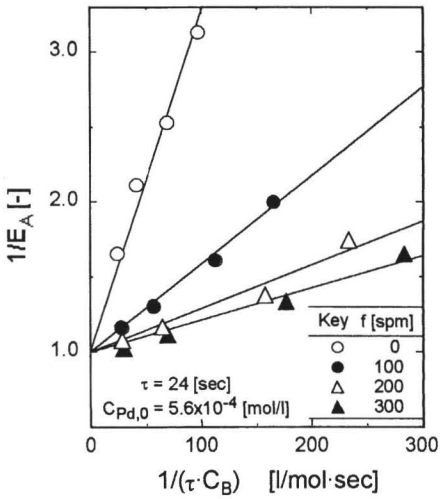


Figure 7 Relationship between $1/E_A$ were and $1/(k_r \cdot \tau C_B)$ in the A-type extractor.

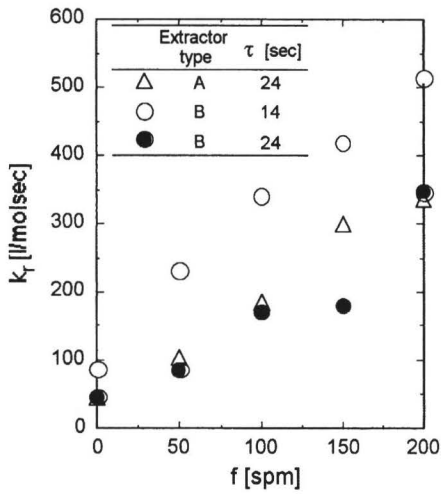


Figure 8 Effect of the vibration frequency of the disks, f, on the overall rate constant, k_r.

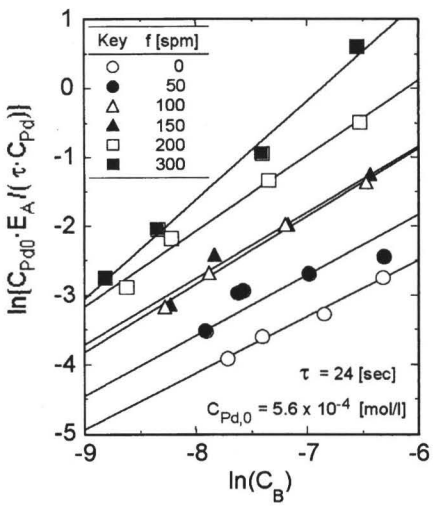


Figure 9 Effect of the vibration frequency of the disks, f, on the fraction of the extraction, E_A in the B-type extractor

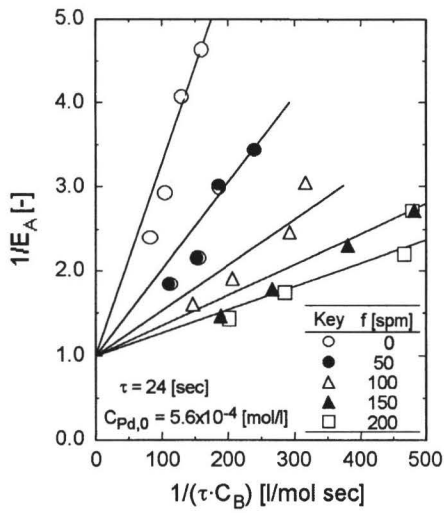


Figure 10 Effect of the vibration frequency of the disks, f, on the fraction of the extraction, E_A, in the B-type extractor

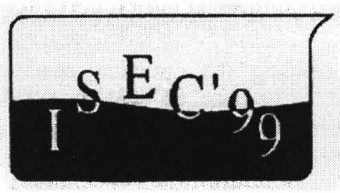
NOMENCLATURE

C = concentration [mol/l]
E_A = fraction of extraction [–]
f = vibration frequency of the disk [spm]
K_M = equilibrium constant [–]

k_r = overall extraction rate constant [l·min/mol]
r_{Pd} = overall extraction rate [mol/(l·min)]
τ = mean residence time [min.]
<subscript>
M = precious metal
org = organic phase
0 = initial state

REFERENCES

1. Kawano Y, Kiyoyama S, Shiomori K, Baba Y and HanoT, *J. Ferment. Bioeng.*, **78**, 293, (1994).
2. Kawano Y, Osada S, Shiomori K, Baba Y, Kondo K, Yoshizawa H, and Hatate Y, *J. Chem. Eng., Japan*, **28**, 227, (1995).
3. Yoshizawa H, Shiomori K, Yamada S, Baba Y, Kawano Y, Kondo K, Ijichi K and Hatate Y, *Solv. Extr. Res. Develop. Japan*, **4**, 157, (1997).
4. Kawano Y, Matsui T, Kondo K and Nakashio F, *J. Chem. Eng., Japan*, **22**, 443, (1989).
5. Hoh YC, Chuang WS and Yueh PS, *J. Chem. Tech. Biotechnol.*, **34A**, 97, (1984).



COMPARISON OF MEMBRANE-ASSISTED SOLVENT EXTRACTION TECHNOLOGIES FOR THE SEPARATION OF Cd–Ni MIXTURES

I Ortiz, F San Román, B Galán and AM Urtiaga
Departamento de Química. E.T.S.I.I. y T. Universidad de Cantabria. Avda. de Los Castros s/n. 39005. Spain

ABSTRACT
Having established the mathematical model and parameters that describe the separation of cadmium and nickel from highly concentrated aqueous solutions, using hollow fibre modules as contactors and D2EHPA as a selective extractant, in this work the analysis of the influence of the operation variables has been performed to find the optimum conditions for the separation. The variables analysed were the organic cadmium concentration and the volume of the organic solution. Finally, the kinetic results obtained with the Non-Dispersive Solvent Extraction (NDSX) configuration, working under optimum conditions were compared to the kinetic results obtained with a supported liquid membrane configuration.

Keywords: nickel-cadmium batteries, cadmium, nickel, non-dispersive solvent extraction, supported liquid membrane

INTRODUCTION

Separation of nickel and cadmium from highly concentrated aqueous solutions has become a subject of interest, mainly due to the necessary treatment of wastes generated during the manufacture of nickel-cadmium rechargeable batteries and in the recycling of battery scrap. In previous works,[1,2] the viability of the separation of both metals from highly concentrated aqueous solutions that simulated acidic leaching solutions by means of the non-dispersive solvent extraction technology was reported. D2EHPA was used as selective extractant and a high acidic solution for the back-extraction, BEX, step. Details of the membrane are shown in Table 1.

Characteristic of the Modules	Values
fibre	X-30/polypropylene
Internal diameter	240 μm
wall thickness	30 μm
Number of fibres	10200
Nominal porosity	40%
Shell material	Polypropylene
Potting material	Epoxy resin
shell inner diameter	63 mm
Shell length	203 mm
effective mass-transfer length	150 mm
effective mass-transfer area	1.4 m^2

Table 1 Hollow-fibre membrane module characteristics.

Working in the concentration range of 0.2 - 0.4 mol/dm^3 of cadmium and nickel in the feed solution it was demonstrated that both metals could be efficiently separated if the pH was kept equal to 3.5. Under these conditions, the nickel remained in the feed whereas the cadmium was transferred to the BEX phase, where it can be concentrated to high values making easy the final management of this solution. Thus the separation-concentration process was governed by the kinetics of cadmium transport between the two aqueous phases, and therefore the optimisation of the operation variables is necessary.

Two variables exert major influence on the process kinetics: i) the initial concentration of cadmium in the organic phase, and ii) the volume of the organic phase. The NDSX technology requires the use of two hollow fibre modules in order to perform the extraction and the back-extraction

© 2000 Society of Chemical Industry

steps, processes that are coupled through the organic solution and that are influenced by the conditions of the intermediate phase.

After having analysed the influence these variables defining the optimum operation conditions, in this work the comparison the kinetic results that would be obtained working under a different configuration, i.e., supported liquid membranes, has been also made. Supported liquid membranes imply the use of only one contactor reducing considerably the volume of the organic phase.

RESULTS

As already mentioned the separation of cadmium and nickel mixtures can be achieved working with pH values in the feed solution of 3.5. Figures 1a and 1b, show representative results of the separation-concentration process. It is observed that while the cadmium in the feed was almost depleted, the nickel concentration remained practically unchanged (<6%). Therefore the kinetics of the separation process would be determine by the kinetics of Cd removal and concentration in the stripping phase.

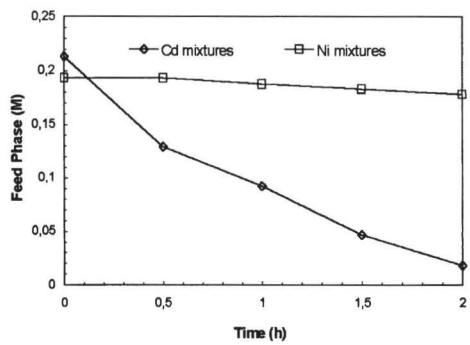


Figure 1a. Cadmium and nickel concentrations in the extraction process.

A kinetic model for the description of the mass transport rate of cadmium from the feed to the BEX solution has been developed based on the mass balances to the cadmium in the three fluid phases flowing through the two hollow fibre contactors and tree stirred tanks. The system used in this work is the same procedure described in other works.[3,4,5]

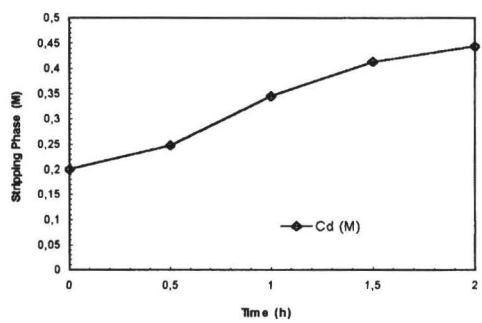


Figure 1b. Cadmium concentration the stripping process.

Extraction module

Aqueous Solution

$$-\frac{V_{me}^{E}}{F_e L^{E}}\frac{\partial C_e^{E}}{\partial t}=\frac{\partial C_e^{E}}{\partial z^{E}}+\frac{A^{E}}{F_e L^{E}}Km^{E}(C_{oi}^{E}-C_o^{E}) \quad (1)$$

$$t=0,\ C_e^{E}=C_{e,in}^{E}\ ;\ z^{E}=0,\ C_e^{E}=C_{e,in}^{E}$$

Organic Solution

$$\frac{V_{mo}^{E}}{F_o L^{E}}\frac{\partial C_o^{E}}{\partial t}=-\frac{\partial C_o^{E}}{\partial z^{E}}+\frac{A^{E}}{F_o L^{E}}Km^{E}(C_{oi}^{E}-C_o^{E}) \quad (2)$$

$$t=0,\ C_o^{E}=C_{o,initial}\ ;\ z^{E}=0,\ C_o^{E}=C_o^{T}$$

Back-extraction module

Aqueous Solution

$$-\frac{V_{ms}^{S}}{F_s L^{S}}\frac{\partial C_s^{S}}{\partial t}=\frac{\partial C_s^{S}}{\partial z^{S}}+\frac{A^{S}}{F_s L^{S}}Km^{S}(-C_o^{S}) \quad (3)$$

$$t=0,\ C_s^{S}=C_{s,initial}\ ;\ z^{S}=0,\ C_s^{S}=C_s^{T}$$

Organic Solution

$$\frac{V_{mo}^{S}}{F_o L^{S}}\frac{\partial C_o^{S}}{\partial t}=-\frac{\partial C_o^{S}}{\partial z^{S}}+\frac{A^{S}}{F_o L^{S}}Km^{S}(-C_o^{S}) \quad (4)$$

$$t=0,\ C_o^{S}=C_{o,initial};\ z^{S}=0,\ C_o^{S}=C_o^{E}\ (z^{E}=L^{E})$$

The mathematical equations for the three tanks, considered as ideal stirred vessels are as follows:

$$\frac{dC_o^{T}}{dt}=\frac{F_o}{V_o}\left(C_{o,in}^{T}-C_o^{T}\right) \quad (5);\qquad \frac{dC_s^{T}}{dt}=\frac{F_s}{V_s}\left(C_{s,in}^{T}-C_s^{T}\right) \quad (6);\qquad \frac{dC_E^{T}}{dt}=\frac{F_E}{V_E}\left(C_{E,in}^{T}-C_E^{T}\right) \quad (7)$$

$t=0,\ C_o^{T}=C_{o,\ initial}$ $\qquad$ $t=0,\ C_s^{T}=C_{s,\ initial}$ $\qquad$ $t=0,\ C_E^{T}=C_{E,\ initial}$

Integration of the system of differential equations and comparison of the theoretical results with the experimental data allowed the determination of the design parameters: membrane mass transport coefficient, km = 0.158 μm/s and equilibrium parameter of the extraction reaction of cadmium with D2EHPA, ke =177. Simulated results are also included in figures 1a and 1b (solid line) showing a good agreement with the experimental results.

Next, with the obtained parameters the analysis was performed of the influence of the main operation variables having influence on the kinetics of the separation process, i.e., 1) the cadmium loading in the organic phase and 2) the total volume of the organic phase. Figures 2a and 2b show the influence of the initial concentration of cadmium in the organic phase in the kinetics of the extraction and back-extraction. An opposite influence is observed, that is the higher the initial organic cadmium concentration the lower the extraction rate but the higher the rate of the BEX step, concluding that the time of the back-extraction would determine the initial value of the organic cadmium concentration.

Next the influence of the organic phase volume on the kinetics of the extraction and stripping processes has been analysed. Figures 3, 4 and 5 show representative simulated results considering different concentration of the organic phase. At low concentrations of organic cadmium, Co < 0.1 mol/dm^3 an increase in the organic phase volume represents a slight increase in the extraction rate and a slight decrease in the BEX rate. Whereas for high organic concentrations, Co > 0.2 mol/dm^3, the influence in the extraction rate remains the same but in the BEX phase a favourable influence is observed when the volume is increased from 1 L to 5 L. Obviously the increase of the organic volume would lead to an increase in the process costs, it being desirable to work with the minimum possible volume.

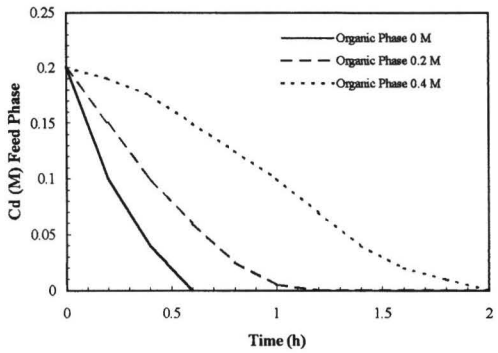


Figure 2a. Evolution of cadmium concentration in the extraction phase.

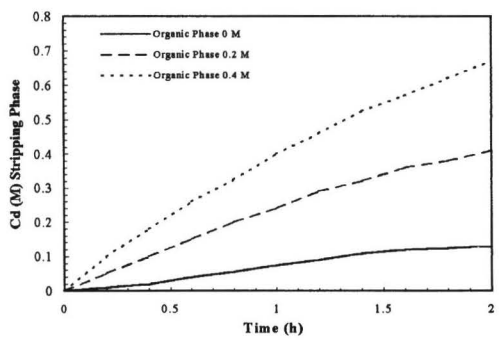


Figure 2b. Evolution of the cadmium concentration in the stripping.

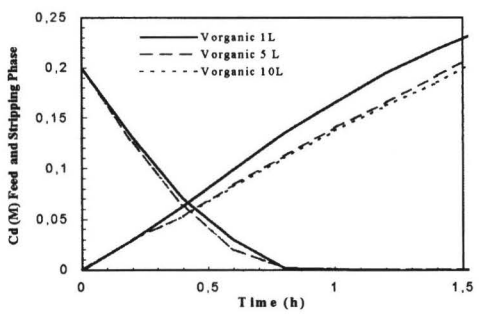


Figure 3. Influence of the organic phase volume. Initial concentration of organic cadmium equal to 0.1 mol/dm^3. Volume of extraction phase 1 L.

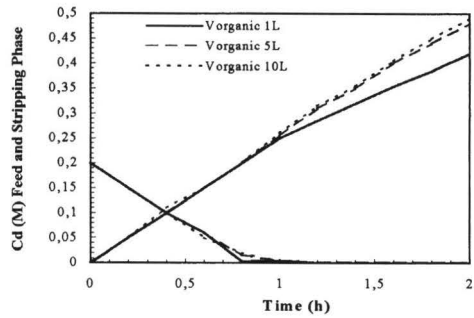


Figure 4. Influence of the organic phase volume. Initial concentration of organic cadmium equal to 0.2 mol/dm^3. Volume of extraction phase 1 L.

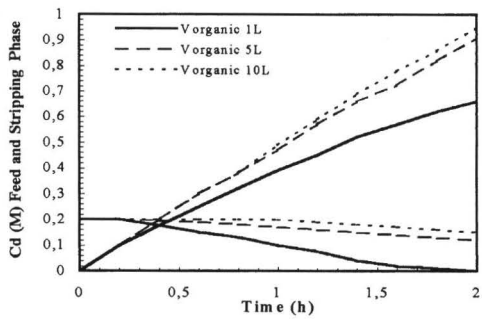


Figure 5. Influence of the organic phase volume. Initial organic cadmium concentration equal to 0.4 mol/dm^3. Volume of extraction phase 1 L.

After these results the analysis of the process kinetics has been performed working with the same hollow-fibre contactor but under the performance of a supported liquid membrane. In the supported liquid membrane that the two aqueous phases flow through the same module the organic phase impregnating the pores of the hollow fibres. With the same assumptions made in the mathematical modelling of the NDSX process, the mass balance differential equations able to describe the process are given by the following equations[6,7,8]

Feed Solution

$$-\frac{V_{me}}{F_e L}\frac{\partial C_e}{\partial t} = \frac{\partial C_e}{\partial z} + \frac{A}{V_{me}} KmC_{oi}^{E} \qquad (8)$$

$$t = 0,\ C_e = C_{e,initial}\ ;\ z = 0,\ C_e = C_{e,initial}$$

Stripping Solution

$$-\frac{V_{ms}}{F_s L}\frac{\partial C_s}{\partial t} = \frac{\partial C_s}{\partial z} - \frac{A}{V_{ms}} KmC_{oi}^{E} \qquad (9)$$

$$t = 0,\ C_s = C_{s,initial}\ ;\ z = 0,\ C_s = C_s^T$$

Feed Tank $\frac{dC_E^T}{dt} = \frac{F_E}{V_E}\left(C_{E,in}^T - C_E^T\right)$ (10) Stripping Tank $\frac{dC_s^T}{dt} = \frac{F_s}{V_s}\left(C_{s,in}^T - C_s^T\right)$ (11)

$t=0,\ C_E^T = C_{E,\ initial}$ $t=0,\ C_s^T = C_{s,\ initial}$

Using the design parameters previously determined for the NDSX configuration, km=0.158 μm/s and ke=177 in order to simulate the kinetic results corresponding to the separation-concentration process of an aqueous solution containing initially cadmium and nickel in a concentration of 0.2M, a similar organic phase to that previously described and an acidic solution, pH=0.5 as the BEX phase, the

curves represented in Figure 6 were obtained; this figure shows also the comparison with the results obtained under the NDSX configuration.

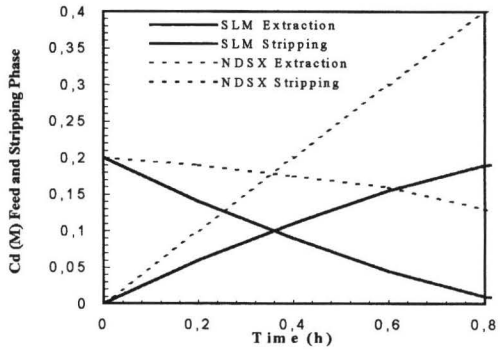
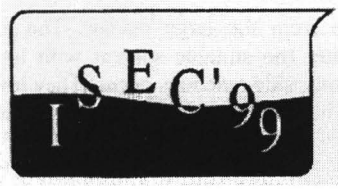


Figure 6. Evolution of the extraction and stripping for process NDSX and SLM

It is possible to find conditions for the NDSX configuration that allows higher concentrations in the BEX solution that those obtained with the SLM technology.

REFERENCES

1. Soler J, Urtiaga AM, Irabien A and Ortiz I, *Proceedings of ISEC'96*, **2**, 851-856, (1996).
2. Galán B, San Román F, Irabien A and Ortiz I, *Chem. Eng. J.*, In press.
3. Ortiz I; Galan B and Irabien A, *J. Membr. Sci.*, **31**, 46, (1996).
4. Alonso AI; Urtiaga AM; Zamacona S; Irabien A and Ortiz I, *J. Membr. Sci.*, 130, 193, (1997).
5. Alonso, Galán B and González M, *Ind. Eng. Chem Res.*, In press.
6. Urtiaga AM, Ortiz MI, Salazar E and Irabien A, *Ind. Eng. Chem Res.*, **31**, 877-866, (1992).
7. Urtiaga AM, Ortiz MI, Salazar E and Irabien A, *Ind. Eng. Chem Res.*, **31**, 1745-1753 (1992).
8. Urtiaga AM, Irabien A and Stroeve P, *Ind. Eng. Chem Res.*, **31**, 1362-1366 (1992).



REACTIVE EXTRACTION USING A KARR COLUMN FOR THE PRODUCTION OF DIOXOLANE FROM AN ALDEHYDE

B Grinbaum, M Adda and Ch Eidelman
IMI (TAMI) Institute for Research and Development, P.O.B. 10140, Haifa Bay 10140, Israel

ABSTRACT
The process of production of an aromatic dioxolane from the corresponding aldehyde is carried out by a reaction with ethylene glycol, in a two phase system: The water produced must be eliminated, in order to obtain quantitative conversion of the aldehyde. Continuous reactive extraction, instead of the batch reaction in mixed vessel, was tested: the glycol was fed in excess to the bottom of the extraction column: while the aldehyde was fed to the top. The glycol acts as a reactant and as an extractant for the water removal. The continuous process was carried out successfully, with results superior to those obtained in the mixed vessel.

Keywords: reactive extraction, Karr column, dioxalane

INTRODUCTION

The production of an aromatic dioxolane from the corresponding aldehyde is carried out by a reaction with ethylene glycol, according to the general equation:

$$RCO + CH_2OH\text{-}CH_2OH \rightarrow \text{Dioxolane} + H_2O$$

where R stands for the aromatic group.
The water produced must be eliminated, to obtain quantitative conversion of the aldehyde. The process is carried out in a two phase system: the heavy organic phase contains the aldehyde and the dioxolane, while the lighter polar phase contains the glycol and the water.

This behaviour gave rise to the idea of using reactive extraction instead of the mixed vessel: the glycol is fed in excess to the bottom of the extraction column: while the aldehyde is fed to the top. The glycol acts as a reactant and as an extractant for the water removal. The wet glycol is then dried in a separate distillation column, and recycled to the bottom of the extraction column. The entire process - extraction and distillation - was carried out continuously, with the dried glycol fed to the extraction column, and the wet one - to the distillation.
The final conversion, in a column with an equivalent of 3.5 theoretical stages, residence time of 7.5 min. and temperature of 90°C in the column, was 98% wt.

For comparison, in a mixed vessel, a similar conversion was achieved with a residence time of 20 hr, and at 120°C, but with lower product quality, due to creation of heavy decomposition products.

In most of the chemical processes, there is interaction between reaction and mass transfer. In many cases, the reaction rate is or even the ability to quantitatively perform the reaction is controlled by the transport phenomenon and not by the chemical kinetic.

Typical reactions of this type are esterifications, or more generally reactions in which water is formed and should be removed, in order to shift the equilibrium and enhance the reaction.
These reactions follow the general formula:

$$A + B \Leftrightarrow C + H_2O$$

Typically, there is the main (i.e. most expensive) raw material A, which is reacted with B to produce C. In order to obtain maximal conversion on A, the process should be operated with large excess of B and with continuous removal of the water formed, by distillation for example.
In the dioxolane process, the raw material A is an aldehyde, which reacts with ethylene glycol (EG) to yield dioxolane and water. In the original industrial process, the batch reaction is carried out with a 100% molar excess of ethylene glycol, and the water is removed by an azeotropic distillation with a suitable solvent. The duration of the batch, in a 20 m^3 reactor, is 20 hour, at a temperature of 120°C.

© 2000 Society of Chemical Industry

This long residence time is determined by the distillation rate from the large reactor. The high temperature is required for the azeotropic distillation of the water (no suitable solvent with lower boiling point of the azeotrop could be found). Under these conditions, side reactions occur. They lower the purity of the product and cause a stable emulsion between the product and the excess ethylene glycol.

PROPOSED PROCESS

The proposed alternative is to perform the reaction in an extraction column. The ethylene glycol (EG) forms a separate phase which is more polar and which extracts the water, which is formed by the reaction. The process may be schematised as by the following model:

The raw material (A), which is essentially in the apolar phase, passes to the polar one, in which it reacts with ethylene glycol (B) to give the product (C) and water. The water remains in the polar phase and C passes to the apolar one. In the proposed process, the reaction occurs in a liquid/liquid multistage extraction column. The ethylene glycol (EG) is fed, countercurrently to A, in stoichiometrical excess, and acts both as reactant and as extractant of the water which are formed in the reaction. The model of this process is shown in figure 1:

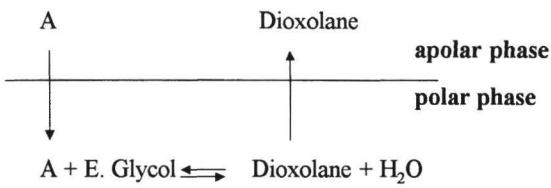


Figure 1: Model of the reactive distillation process

EXPERIMENTAL

The reaction is carried out in a 1" diameter, 1.5 m length Karr type reciprocating extraction column. A is fed at the top of the column, and EG at the bottom. Under optimal conditions, a conversion of 98% is obtained.

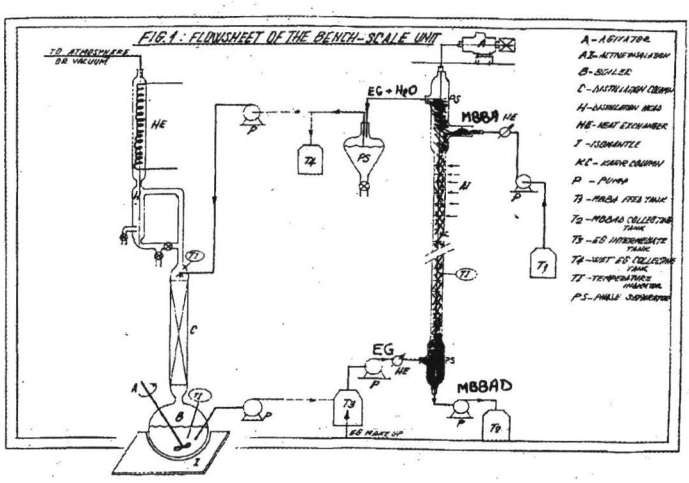


Figure 2: Scheme of bench scale unit

The dry EG absorbs water in the column, and exits with 5 to 10% of water. The EG is dried by fractional distillation, and recycled to the extraction. Scheme of the experimental unit is shown in figure 2.

The temperature is the column is between 70°C to 90°C. At such a temperature, practically no by-products are formed. The distillation of water from the EG is performed at 120°C. The EG after the distillation contains 0.25% H2O, which is adequate for the process. We therefore separate between the reaction, which should be performed at moderate temperature for high selectivity, and the distillation at high temperature, which is performed in a mixture free of product. The solvent is present all the time in the apolar phase.

RESULTS

The results of the experiments are summarised in Table 1.

EG:A Molar Ratio	3	3	6	6	6
Temperature (□C)	70	70	70	70	90
Flowrate of A (l/hr)	0.75	1.5	1.0	2.0	2.0
Residence time (min)	30	15	15	7.5	7.5
$\%H_2O$ in EG feed	0.75	0.25	0.25	0.25	0.25
Agitation Frequency (pulse/min)	90	90	90	67	53
Conversion (%wt.)	92	73	98	93	98

Table 1 Effect of operating conditions on the yield of the process

All the experiments were carried out at amplitude of 40 mm. No problems of phase separation or entrainment were observed.

DISCUSSION

The proposed process enables us to obtained the desired conversion of 98% A in 7.5 minutes at 90°C, compared with a contact time of 20 hours at 120°C in the batch process. The product from the extraction process is superior, due to lack of side reactions. The molar ratio of EG:A should be 6:1. Temperature has strong effect on the desired contact time: for a contact time of 7.5 min., increasing the temperature from 70°C to 90°C, increased the conversion from 93% and 98%. The strong effect of the temperature indicates that we achieve the conditions of kinetic limitation. This is the opposite of the batch process, which was totally diffusion limited.

Higher molar ratio of EG:A improves the conversion and decreases the desired contact time, due to better extraction of the water into the apolar phase. At an EG:A molar ratio of 3, the conversion was 73% and 92% for a contact time of 15 and 30 minutes respectively. Increasing the molar ratio to 6, increased the conversion to 93% and 98% for a residence time of 7.5 and 15 minutes respectively.

The reaction of formation of the dioxolane is reversible and the final conversion is related to the concentration of the water in the EG. This conversion was found experimentally to fit the linear equation:

$$\text{Conversion} = 100 - 3^* c_{H2O} \qquad (1)$$

where both the conversion and the concentration of water are in %weight.
A maximal concentration of 0.5% water is allowed to obtain the required conversion of 97 - 98%. Up to an initial concentration of 1.5% water in the EG, the conversion achieved from the extraction

column was near to the theoretical value, according to the equilibrium data. At an initial concentration of 5%, the conversion obtained in the column is lower than expected. The model provided at the beginning may explain this phenomenon. The reaction takes place in the EG phase; the solubility of A in EG is reduced in presence of water; therefore the water slows down the reaction rate and does not permit full conversion to be achieved in a reasonable time.

Evaluation of the number of plates

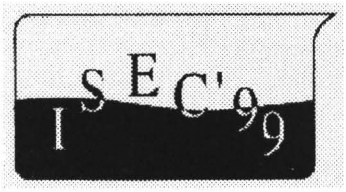
For molar phase ratio of 6, and 0.25% H_2O in the dried EG, the humidity of the wet EG in the raffinate is 6.7% (from total mass balance, assuming 98% conversion).
A simple calculation shows that a total of 3.5 theoretical plates are required to obtain a conversion of 98%.

CONCLUSIONS

In the proposed process the water formed in the reaction is removed by extraction instead of distillation. That permits a drastic reduction of the time of reaction and of the temperature with a consecutive increase of the selectivity. Use of such a methodology may also be applied in process using phase transfer catalyst.



Fundamental Studies



STUDIES OF THE EXTRACTION THERMODYNAMICS OF f-ELEMENTS

Kenneth L Nash
Chemistry Division, Argonne National Laboratory, 9700 S. Cass Ave. Argonne, IL 60439-4831, U.S.A

ABSTRACT
Though they were discovered in the 18th century, practical applications of individual lanthanides were not possible until the development of first ion exchange and later solvent extraction techniques. Today, solvent extraction using lipophilic organophosphorus complexants is the principal separation technique applied for lanthanide production by hydrometallurgy. Separation chemistry (co-precipitation, ion exchange, and solvent extraction) also was central to both the discovery of the individual actinides and to the preparation of samples of sufficient purity to allow elucidation of their chemical/physical properties. Solvent extraction, in the form of the PUREX process, has become the single most important separations process in actinide technology. In this report, the basic thermodynamics of extraction of actinide and lanthanide metal ions is discussed.

Keywords: thermodynamics, lanthanide, actinide

INTRODUCTION

Solvent extraction separations of f-elements are central to the technological development of both material science utilizing the lanthanides and to nuclear waste processing for isolation and production of actinides. For the lanthanides, acidic organophosphorus extraction reagents are most commonly used, as their extraction characteristics are suitable for both isolation of the group from many mineral matrix cations and of individual members of the series. As the extractant in the PUREX process, tributyl phosphate (TBP) is the most important reagent in actinide processing.

The transfer of a metal ion from an acidic medium to an organic extractant solution and back is governed by the relative positions of several overlapping and competing equilibrium processes. In the aqueous phase, hydration and protonation equilibria of metal cations, chelating agents, and metal complexes, and the complexation equilibria of metal ions and ligands control the relative extractability of metal ions. In the organic phase, metal-ligand bonding, non-specific and specific solvation of complexes, and ligand-ligand interactions are the most important thermodynamic processes. Most often, solvent extraction reactions are characterized by reversible equilibria, though kinetically inert processes can contribute to apparent irreversible reactions.

In this report, the thermodynamics of extraction of lanthanide and actinide ions by different types of solvent extraction reagents will be discussed, emphasizing the general characteristics of different systems. The concept of enthalpy-entropy compensation in extraction equilibria will be examined to provide additional insights into the different separations processes.

EXPERIMENTAL

Most investigations of the thermodynamics of f-element solvent extraction thermodynamics have been performed relying on the change in the extraction equilibrium constant (Kex) as a function of temperature and the Van't Hoff relationship ($d(\ln Kex)/d(1/T) = -\Delta H/R$). Second order thermodynamic effects from changes in ΔCp do not often complicate the application of this technique, as the temperature range is generally restricted by solubility and volatility considerations. There have been several reports of enthalpies measured calorimetrically in synergistic systems. In these experiments, measured enthalpies describe the addition of a co-extractant to the primary chelate complex of the extracted metal ion in a homogeneous organic phase. The experimental results described below are

© 2000 Society of Chemical Industry

derived from a variety of literature reports. The reader is referred to the original references for details of the experimental procedures.

RESULTS AND DISCUSSION

Acidic Extractants

For extraction of polyvalent metal ions by acidic extractants, the phase transfer equilibrium reaction is:

$$M_{m+aq} + m\,HL \underset{}{\overset{K1}{=}} \overline{ML_m} + m\,H^+ \qquad (1)$$

where species in the organic phase are indicated by the bar above the symbol. Measured heats for metal ion extraction by this reaction include contributions from (partial or complete) dehydration of the aquo-metal ion; the solvation of the 'm'H^+ ions released by the extractant; deprotonation of the extractant; degrees of freedom lost by the free ligands upon complexation; bond energies from ligand coordination of the metal ion; and readjustment of the organic solvent from solvation of 'm' protonated ligand species to solvation of one complex.

Perhaps the most extensively investigated reactions in f-element solvent extraction are the trivalent lanthanide-thenoyltrifluoroacetone (TTA) systems. Partly because of the consistent stoichiometry of the system (M:L = 1:3), the $Ln(TTA)_3$ complex is the preferred platform for studies of synergism. Dukov et al [1] report that the ΔH for extraction of Pr^{3+}, Gd^{3+}, and Yb^{3+} from 1 M Na/HCl is endothermic (+43.0 to +45.4 kJ/mol) and independent of the organic diluent (C_6H_6, $CHCl_3$, CCl_4). Differences in the free energy of extraction between the metal ions and/or the diluents are therefore derived primarily from changes in entropy, which ranges between -43 and +24 J/mol-K. These general characteristics have been confirmed by other authors who have investigated the Ln-TTA system [2,3]. Extraction by acidic pyrazolone ligands display similar enthalpies while the extraction entropies are more positive than for TTA[4]. The favorable ΔS accounts for the generally stronger extraction of lanthanides and actinides by pyrazolones than by β-diketones.

Sulfonic acid extractants like dinonylnaphthalenesulfonic acid (HDNNS) are highly aggregated in organic solvents, even at very low concentrations. Micellar extractants generally exhibit little sensitivity to the size of the cation being extracted, extracting classes of metal ions (like the lanthanides) approximately equally. Otu and Westland [5] have reported that the extraction of La^{3+}, Nd^{3+}, Gd^{3+}, and Er^{3+} is characterized by ΔH = 7.3 to 10.2 kJ/mol and ΔS = +69 to +80 J/mol-K. The narrow range of thermodynamic parameters is consistent with the low selectivity of the extraction system for individual members of the series.

Monoacidic organophosphorus extractants also aggregate in lipophilic solutions, typically existing as hydrogen bonded dimers. For some extractants, the dimer arrangement is maintained in the metal complexes, for others the ligands monomerize on complexation. Westland and Otu[6] observe that increasingly exothermic ΔH values (-19.9 to -32.5 kJ/mol) across the series Nd^{3+}, Gd^{3+}, Dy^{3+}, Er^{3+} accounts for the increasing extraction strength by 2-ethylhexyl-p-phenylphosphonic acid (H(EHFP)) in the same order.

The greater affinity of actinides for donor atoms softer than oxygen is at the heart of all successful separations of the trivalent ions of the transplutonium elements from the lanthanides[7]. This difference in interaction strength has been attributed to a greater tendency for the actinides towards covalency in their bonding, which should, in principle, be manifested thermodynamically by exothermic complexation heats.

Dithiophosphinic acid extractants (e.g. Cyanex 301) have been shown to exhibit separation factors of greater than 103 for trivalent actinide ions over lanthanides of comparable size. Zhu et al [8] have reported enthalpy for the extraction of Am^{3+} and Eu^{3+} from 1.0 M Na/HNO_3 by purified Cyanex 301 as ΔH_{Am} = +18.1 kJ/mol, ΔH_{Eu} = +43.6 kJ/mol with corresponding entropies of ΔS_{Am} = -87 J/mol-K, ΔS_{Eu} = -66 J/mol-K. The enthalpy difference is the principal source of the greater selectivity

of Cyanex 301 for Am^{3+} ($\Delta(\Delta H)$ = -25.5 kJ/mol, $\Delta(-T\Delta S)$ = +6.3 kJ/mol) which is consistent with increased strength of the Am-S bonding relative to that of Eu-S.

Neutral Extractants

Neutral extraction reagents accomplish phase transfer of the metal ion by solvating electroneutral complexes of the metal ions. The generic extraction equilibrium reaction is:

$$M^{m+} + m\,X^- + y\,S \underset{}{\overset{K2}{=}} \overline{MX_mS_y} \qquad (2)$$

The most common neutral extractants for f-elements are trialkyl phosphates, phosphonates, phosphinates, and phosphine oxides. As equilibrium 2 requires the organization of 1+m+y species into one product species, one might predict that the net extraction entropy for such reactions should be consistently negative. In fact, for extraction of trivalent lanthanides, actinides, Th^{4+}, and UO_2^{2+} by simple monodentate or complex bidentate organophosphorus extractants (which represent the bulk of such neutral extractant systems) the extraction entropies range between -40 and -150 J/mol-K independent of the nature of the counter ion Y^-. Extraction enthalpies are exothermic and in the range of -30 kJ/mol to -90 kJ/mol.

The relative extraction of trivalent lanthanides and actinides in neutral systems has been examined comparing the relative extraction of Am^{3+} and Eu^{3+} by octyl(phenyl)carbamoyl-methyphosphine oxide (CMPO)[9], dihexyldiethylcarbamoylmethylphosphonate (DHDECMP)[10] from nitrate and thiocyanate media. The thiocyanate systems demonstrate a greater selectivity for Am equivalent to about $\Delta(\Delta G)$ = 4-5 kJ/mol (a separation factor of 5-7). Substantially more exothermic extraction enthalpies are observed in both the Eu^{3+} and Am^{3+} thiocyanate systems than in the corresponding nitrate reactions. This difference has been attributed to the energy required to transfer three SCN^- ions from the aqueous to the organic phase [9]. Differences in the enthalpy of extraction of Am relative to Eu are not substantial enough to attribute the enhanced extraction of the actinide to a soft donor effect.

Synergistic Extraction Systems

Synergistic extraction systems combine thermodynamic features of both acidic extractants and neutral extractants according to the extraction equilibrium expression:

$$M^{m+} + m\,\overline{HL} + y\,S \underset{}{\overset{K3}{=}} \overline{ML_mS_y} + m\,H^+ \qquad (3)$$

In most cases, the stoichiometry of the extracted complex with respect to the primary extractant (L) does not differ from that obtaining in the synergist-free system (equation 1). The net reaction for addition of the synergist to the extracted complex in the organic phase can be obtained as:

$$\overline{ML_m} + y\,S \underset{}{\overset{\beta}{=}} \overline{ML_{my}} \qquad (4)$$

by subtracting the appropriate equilibrium for equation 1 from equation 3. The constant β is K3/K1. Because the adduct formation reaction can be formulated to occur completely in the organic phase, the heats of reaction are amenable to direct determination by titration calorimetry.

The most thoroughly investigated synergistic extraction systems involving f-elements are those in which HTTA is the primary extractant. The thermochemistry of neutral organophosphorus compounds, aliphatic amines, crown ethers, bipyridyl and phenanthroline, and aliphatic sulfoxide

extractants have all been investigated as synergistic reagents for lanthanide and actinide extraction by TTA. Most of the thermodynamic data were determined using the temperature variation method, some were investigated by calorimetry, and some systems have been studied using both techniques. Adduct formation reactions are generally exothermic (ΔH between -20 and -70 kJ/mol) while the entropies cover a wide range of both favorable and unfavorable contributions to the net equilibrium, dependent primarily on the nature of the synergist. The tris-TTA complex of the lanthanides is a di- or tri-hydrate in most organic diluents, thus the adduct entropy partly reflects the ability of the synergist to displace this residual hydration. Caceci et al.[11] studied using calorimetry the addition of both TBP and trioctylphosphine oxide (TOPO) to the neutral TTA complexes of UO_2^{2+}, Nd^{3+}, and Th^{4+} in benzene. The enthalpies of adduct formation were 10-20 kJ/mol more exothermic in the dry solvent than the water-saturated equivalent. The Δ(ΔS) values changed to almost fully compensate for the Δ(ΔH) and maintain ΔG constant. Crown ether adducts on the corresponding TTA complexes[12] were characterized by entropy neutral contributions in the trivalent lanthanide adduct, but moderately unfavorable entropies for the UO_2^{2+} and Th^{4+} complexes.

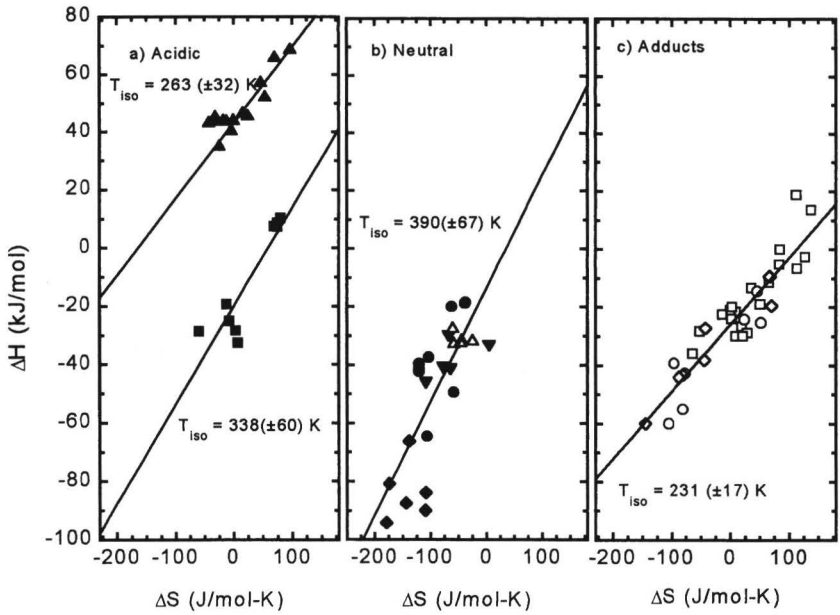
Addition of pyridine-based donors like bipyridyl to lanthanide TTA complexes or dipivaloylmethane (also a β-diketone) is characterized by a strongly exothermic enthalpy (-40 to -70 kJ/mol) partially compensated by an unfavorable entropy [13-15]. The synergistic extraction of lanthanides by mixtures of TTA and trialkylamines exhibits no temperature dependence implying that the addition of the adduct to $Ln(TTA)_3$ is characterized by an enthalpy of the same magnitude but opposite in sign to that of the extraction of the lanthanide by TTA alone. This curious observation has been made for the combination of tertiary amines and pyrazolone extractants as well.

Linear Free Energy Relationships and Enthalpy-Entropy Compensation

In equilibrium thermodynamics, changes in the enthalpy are often compensated by entropy changes to keep the net free energy of a series of related reactions nearly constant. Because there are so many processes contributing to metal ion solvent extraction processes, whether enthalpy and entropy changes compensate in comparing a series of reactions is a complex question. In figure 1, a linear free energy plot is shown for extraction of trivalent lanthanides, thorium, and uranium(VI) by acidic extractants, by the neutral extractant systems, and for adduct addition in synergistic systems as discussed above. If enthalpy-entropy compensation is complete, the slope of the plot of ΔS vs ΔH should be linear with a slope equal to the average temperature of the reaction. In figure 1a, the separate slopes for lanthanide extraction by TTA in benzene (several authors) and by H(EHFP) or HDNNS in petroleum ether have slopes within one standard deviation of 298 K. For extraction of lanthanides, Th^{4+}, and UO_2^{2+} by neutral extractants from nitrate and thiocyanate solutions (figure 1b), the slope (temperature) exceeds 298 K (though it overlaps at ñ□2 s) while the process of adduct formation in synergistic extraction systems (figure 1c) is substantially lower than the mean experimental temperature of 298 K. If we assume that the measured ΔH values are representative of the bonding changes in the respective systems, it appears that the neutral extractant systems are more ordered than expected, while adduct formation produces excess entropy relative to the net bond strength increase.

These results are generally consistent with the nature of the reactions as written in equations 1, 2, and 4. For interactions with acidic extractants, a straight-forward replacement of water molecules by chelating extractant molecules leads to extraction, and so enthalpy-entropy compensation is reasonable.

For extraction by neutral ligands, several species must join to form the extracted complex and the system clearly becomes substantially more ordered. The overcompensation of ΔS (excess entropy) in adduct formation is consistent with equation 4 if the predominant mechanism for adduct formation involves displacement of residual waters of hydration from the extracted chelate complex. Several literature reports indicate that this is the most common mechanism for synergism.

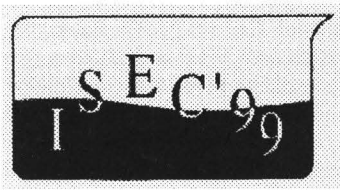


ACKNOWLEDGMENT:

Work performed under the auspices of the U.S. Department of Energy, Office of Basic Energy Sciences, Division of Chemical Sciences under contract number W-31-109-ENG-38

REFERENCES

1 Dukov IL, Al-Nimri AF and Kassabov GI, *Monatsch. Chem.* **116**, 737 (1985).
2. Kandil AT and Farah K, *J. Inorg. Nucl. Chem.* **42**, 1491 (1980).
3. Bhatti MS, *J. Radioanalyt. Chem.* **57**, 69 (1980).
4. Dukov IL, *Hydrometallurgy* **44**, 21 (1997).
5. Otu EO and Westland AD, *Solv. Extr. Ion Exch.* **8**, 827 (1990).
6. Westland AD and Otu EO, *Solv. Extr. Ion Exch.* **9**, 607 (1991).
7. Nash KL, *Solv. Extr. Ion Exch.* **11**, 729 (1993).
8. Zhu Y, Chen J and Jiao R, *Solv. Extr. Ion Exch.* **14**, 61 (1996).
9. Mathur JN and Nash KL, *Solv. Extr. Ion Exch.* **16**, 1341 (1998).
10. Muscatello AC, Horwitz EP, Kalina DG and Kaplan L, *Sep. Sci. Technol.* **17**, 859 (1982).
11. Caceci M, Choppin GR and Liu Q, *Solv. Extr. Ion Exch.* **3**, 605 (1985).
12. Mathur JN and Choppin GR, *Solv. Extr. Ion Exch.* **11**, 1 (1993).
13. Kassierer EF and Kertes AS, *J. Inorg. Nucl. Chem.* **34**, 3221 (1972).
14. Kertes AS and Kassierer EF, *Inorg. Chem.* **11**, 2108 (1972).
15. Dakternieks DR, *J. Inorg. Nucl. Chem.* **38**, 141 (1976).



SYNERGISTIC SOLVENT EXTRACTION OF ALUMINIUM(III), GALLIUM(III), AND INDIUM(III) WITH 2-THENOYLTRIFLUOROACETONE AND TOPO

Junji Noro[1], Aliko Hokura[2], Ichiro Tanaka[2], Meri Yamada[2] and Tatsuya Sekine[2]

[1]Research Department, Nissan ARC, Ltd., Natsushima-cho, Yokosuka-shi, Kanagawa 2370061, Japan

[2]Department of Chemistry, Science University of Tokyo, Kagurazaka, Shinjuku-ku, Tokyo 1628601, Japan

ABSTRACT

Solvent extraction of aluminium (III), gallium (III), and indium (III) with 2-thenoyltrifluoroacetone (Htta) into non-polar solvents was studied in the absence and presence of trioctylphosphine oxide (TOPO). The extraction of gallium (III) and indium (III) with Htta was enhanced by an addition of TOPO and a marked extraction of aluminium (III) which was essentially not extracted with only Htta when the two-phase agitation was continued for a short time was also found in the presence of TOPO. Furthermore, the rate of solvent extraction of both aluminium (III) and gallium (III) with Htta was found to be increased by the addition of TOPO. The distribution ratio of metal ions was determined as a function of the concentration of Htta and TOPO but the results were complicated and the chemical form of the extracted species could not always be identified.

Keywords: aluminium(III), gallium(III), indium(III), 2-thenoyltrifluoroacetone, trioctylphosphine oxide

INTRODUCTION

The synergistic enhancement of solvent extraction of metal ions with a chelating extractant and a solvating type extractant is usually explained in terms of extraction of adduct complexes with both of the extractants. It is known that a marked synergistic effect is caused by the combination of a β-diketone such as 2-thenoyltrifluoroacetone (Htta) and a solvating type extractant such as tributylphosphate (TBP) or trioctyl-phosphine oxide (TOPO). However, it is supposed that such a synergistic effect should not be found when all of the coordination sites of the extracted metal chelate complex in the organic phase are already occupied with the bidentate chelating ligands and therefore no vacant sites are left that are available for further coordination with the solvating ligand. A good example for the lack of synergistic effect by the occupation of all of the coordination sites of a metal ion with a chelating ligand is that the solvent extraction of indium (III) with Htta into carbon tetrachloride was not enhanced by an addition of TBP. Furthermore, an impairment of the extraction (antagonistic effect) was found when the concentration of TBP was higher than 0.1 mol dm^{-3}, whereas the solvent extraction of several other trivalent metal ions, lanthanum (III), europium (III), lutetium (III), and scandium (III) with Htta was very much enhanced by an addition of 0.1 mol dm^{-3} TBP.[1]

In the present study, the solvent extraction of aluminium (III), gallium (III), and indium (III) from aqueous solutions with Htta into non-polar solvents and the effect of addition of the solvating extractant, TOPO, both on the degree of extraction and on the rate of extraction was studied. The extraction equilibrium of these metal ions in the liquid-liquid systems was measured as a function of the concentration of Htta and TOPO in the organic phase and pH in the aqueous phase. The rate of extraction of metal ions was also measured as a function of these in the system.

EXPERIMENTAL

All the reagents were of reagent grade. Solvent extraction was carried out in a thermostated room at 298K. Since Htta and TOPO partially associate in the organic phase and the association decreases the concentration of these reagents and since the rate of association is not high,[2] the organic solvent and aqueous solutions were prepared as follows. A portion of 0.1 mol dm^{-3} sodium nitrate or sodium perchlorate solution containing acetate buffer, nitric acid, or perchloric acid was placed in a

© 2000 Society of Chemical Industry

stoppered glass tube (capacity $50cm^3$) and a 10 cm^3 portion of carbon tetrachloride or toluene containing $2x10^{-3}$ to 0.1 mol dm^{-3} of Htta and none or $1x10^{-3}$ to 0.1 mol dm^{-3} of TOPO was added. The two phases were agitated for two hours to equilibrate the association and partition of the reagents in the liquid-liquid system and then a portion of stock solution of one of the metal ions was added. The initial concentration of metal ions was $1x10^{-5}$ to $1x10^{-4}$ mol dm^{-3}. Then the two phases were agitated vigorously for a certain time and centrifuged. For the extraction of indium (III), the extracted metal ions in the organic phase were stripped by 1 mol dm^{-3} nitric acid. Since the back-extraction of gallium (III) from the organic phase was very slow, it was carried out as follows. A portion of the organic phase which extracted the metal complex was transferred into another tube and the same volume of 4-methyl-2-pentanone (MIBK) containing 0.2 mol dm^{-3} TOPO was added, and it was agitated with 1 mol dm^{-3} perchloric acid for one hour.[3] The stripping of extracted aluminium (III) with Htta was much slower than gallium (III). Thus no stripping of extracted aluminium (III) with Htta was made. The metal content in an aqueous solution and that in a stripped solution was determined by inductively coupled plasma atomic emission spectrometry or atomic absorption spectrometry. The concentration of hydrogen ion in the aqueous phase was measured by potentiometry.

RESULTS AND DISCUSSION

In the present paper, chemical species in the organic phase are denoted by the subscript "org" while those in the aqueous phase are denoted by lack of subscript. The volumes of two liquid phases were always assumed to be the same. The metal ion is represented by M^{3+}. The solvent extraction equilibrium of M^{3+} can be written as:

$$M^{3+} + 3Htta_{(org)} = M(tta)_{3(org)} + 3H^+ \ ;$$

$$K_{ex3,0}^* = [M(tta)_3]_{org}[H^+]^3 / [M^{3+}]\,[Htta]_{org}^3 \qquad (1)$$

It can also be written as:

$$M^{3+} + 3tta^- = M(tta)_{3(org)} \ ; \ K_{ex3,0} = [M(tta)_3]_{org} / [M^{3+}][tta^-]^3 \qquad (2)$$

When the formation of metal complexes with Htta in the aqueous phase is negligible, the distribution ratio of metal ion, $D = [M(III)]_{org,total} / [M(III)]_{aq,total}$, can be written as:

$$D = [M(tta)_3]_{org} / [M^{3+}] = K_{ex3,0}^*[Htta]_{org}^3 / [H^+]^3 = K_{ex3,0}[tta^-]^3 \qquad (3)$$

The formation of adduct complexes of $M(tta)_3$ with TOPO in the organic phase can be written as:

$$M(tta)_{3(org)} + nTOPO_{(org)} = M(tta)_3(TOPO)_{n(org)} \ ;$$

$$K_{(org)n} = [M(tta)_3(TOPO)_n]_{org} / [M(tta)_3]_{org}[TOPO]_{org}^n \qquad (4)$$

The distribution ratio can be written as:

$$D = ([M(tta)_3]_{org} + [M(tta)_3TOPO]_{org} + [M(tta)_3(TOPO)_2]_{org} + ...) / [M^{3+}]$$

$$= K_{ex3,0}^*[Htta]_{org}^3 (1 + K_{(org)1}[TOPO]_{org} + K_{(org)2}[TOPO]_{org}^2 + ...) / [H^+]^3$$

$$= K_{ex3,0}[tta^-]^3 (1 + K_{(org)1}[TOPO]_{org} + K_{(org)2}[TOPO]_{org}^2 + ...) \qquad (5)$$

A part of Htta in the organic phase associates with TOPO and the equilibrium can be written as:[4]

$$Htta_{(org)} + TOPO_{(org)} = Htta\,TOPO_{(org)}$$

$$K_{ass} = [Htta\,TOPO]_{org} / [Htta]_{org}[TOPO]_{org} \qquad (6)$$

The rate of extraction of the metal ions in the absence of TOPO may be written as:

$$v = -d[M^{3+}] / dt = k_0[M^{3+}][Htta]_{org}^a[H^+]^b ..... \qquad (7)$$

$$\log ([M^{3+}] / [M(III)]_{initial}) = -(k_{obsd} / 2.303)t \qquad (8)$$

Here k_0 is the rate constant and k_{obsd} is the observed rate constant, $k_{obsd} = k_0[Htta]_{org}^a[H^+]^b .....$ When TOPO is added, the rate of extraction of the metal ions may be written as:

$$v = -d[M^{3+}] / dt = k_0\,[M^{3+}][Htta]_{org}^a[H^+]^b \times (1 + f_1[TOPO]_{org} + f_2[TOPO]_{org}^2 + ...) \qquad (9)$$

The extraction equilibrium of indium (III) was reached by the two-phase agitation for a short time

such as within 3 minutes or even less. However gallium (III) was found to reach equilibrium by two-phase agitation for a long time; agitation for one day to one week was necessary. The rate of solvent extraction of aluminium (III) with Htta was even lower than that of gallium (III). The extraction equilibrium did not be achieved by the two-phase agitation for one week and no extraction equilibrium was determined with aluminium (III).

The quantitative stripping of the extracted indium (III) was achieved by an agitation of the organic phase with 1 mol dm^{-3} nitric acid for three minutes. The stripping of gallium (III) was slow but it was accelerated by an addition of MIBK and TOPO into the organic phase, as was found with the stripping of beryllium (II) extracted with benzoylacetone into a non-polar organic solvent.[3] Thus the extracted gallium (III) chelate was stripped by 1 mol dm^{-3} perchloric acid after the organic phase was added the same volume of MIBK containing 0.2 mol dm^{-3} TOPO and the two phases were agitated for 30 minutes. The stripping of extracted aluminium (III) chelate was extremely slow and the amount of aluminium (III) extracted was estimated from the difference of the concentration in the aqueous phase between the initial feed and that after the extraction.

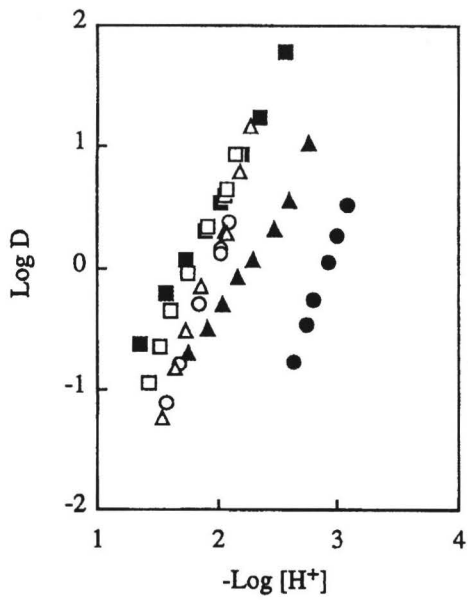


Fig.1 Distribution ratio as a function of concentration of hydrogen ion in the aqueous phase. Open symbols: Metal ion is gallium(III). Closed symbols: Metal ion is indium(III) The concentrations of TOPO are 0 (○,●), 0.01 (△,▲) , and 0.03 (□,■) mol dm^{-3}.

Figure 1 gives the distribution ratio of gallium (III) and indium (III) extracted with Htta in the absence and presence of TOPO as a function of hydrogen ion concentration. As is seen from figure 1, the distribution ratio of gallium (III) and indium (III) in the absence of TOPO is inverse third order of the hydrogen ion concentration. Furthermore, the distribution ratio of gallium (III) and indium (III) determined as a function of the Htta concentration in the organic phase at a certain given hydrogen ion concentration in another series of experiments was found to be the third order dependent to the Htta concentration. Thus the solvent extraction equilibrium of the metal ions with Htta in the absence of TOPO is represented by equations 1- 3. The value of extraction constant $K_{ex3,0}$* in equation 1 and $K_{ex3,0}$ in equation 2 are given in table 1.

	Log $K_{ex,3,0}$	Log $K_{ex,3,0}$*
Gallium (III)	24.3	0.12
Indium (III)	20.4	-2.55

Table 1 Summary of equilibrium constants

Since the rate of extraction of aluminium (III) was very low, the extraction equilibrium could not be determined. As is seen from figure 1, the extraction of indium (III) and gallium (III) is enhanced when TOPO is added to the organic phase containing Htta. It was also found that the extraction from the aqueous phase, 0.1 mol dm^{-3} sodium nitrate solutions for indium (III) or 0.1 mol dm^{-3} sodium perchlorate solutions for gallium (III), was negligible with TOPO only. This suggests that the extracted species contained both Htta, which is most probably in the anionic form tta^-, and TOPO. This was further studied by measuring the dependence of distribution ratio on the concentration of Htta, TOPO, and hydrogen ions. By analyzing the extraction data thus obtained on the basis of equation 5, it was concluded that the dominant extracted species was $M(tta)_3(TOPO)_2$ when both Htta and TOPO were present and when the TOPO concentration was not low. The extraction data of indium (III) in the presence of both Htta and TOPO could not be well explained on the basis of equation 5. As can be seen from figure 1, the distribution ratio of indium (III) in the presence of TOPO is not inverse third order of the hydrogen-ion concentration as is given by equation 5. The extraction of aluminium (III) with Htta only was poor. However, when TOPO was added, the extraction was enhanced even when the conditions were otherwise identical. For example, the log D was 0.11 when the two phases were agitated for 16 hours and when the initial Htta concentration in carbon tetrachloride was 0.1 mol dm^{-3} and the pH was 2.3. However, if 0.1 mol dm^{-3} of TOPO was added to the organic phase of this solvent extraction system and the two phases were agitated for the same time, the log D was found to be 0.62.

The extraction of aluminium (III) and gallium (III) was accelerated when TOPO was added. The rate of extraction should be dependent on the concentration of Htta, hydrogen ions, and also on the TOPO. It was found that the rate of extraction is inverse second order with respect to the hydrogen ion concentration. As was pointed out, Htta and TOPO associate with each other and the concentration of both of the reagents decreased and the association should cause an effect not only the degree of the extraction but also the rate of extraction.

The rate of extraction of aluminium (III) and gallium(III) with Htta was enhanced by addition of TOPO. Figure 2 gives the dependence of the observed rate constant, k_{obsd}, on the initial TOPO concentration when the initial Htta concentration was the same and the pH was kept constant.

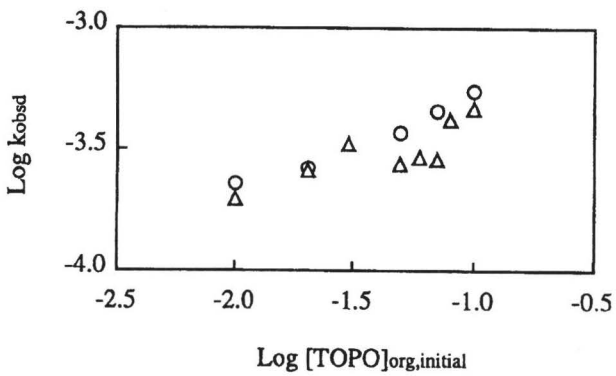


Fig.2 Depenndence of the obsereved rate constant of extraction of aluminum(III) (○) and gallium(III) (△) on the initial concentration of TOPO.

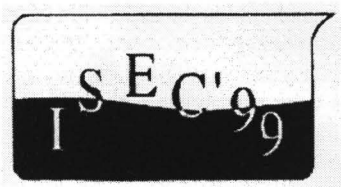
As is seen from figure 2, the apparent slope of log k_{obsd} vs. log $[TOPO]_{org,initial}$ is not large. However, when the decrease of the both Htta and TOPO concentration due to the association of these reagents is corrected on the basis of equation 6, it was concluded that $k_{obsd}/[Htta]_{org}^2$ was proportional to $[TOPO]_{org}$, when the pH is constant, that is, the rate is second order dependent on Htta and first order dependent on TOPO.

The rate of solvent extraction of gallium (III) with Htta is rather complicated as was reported.[5] The mechanism of solvent extraction may be changed by the addition of TOPO. This should cause the enhancement of the rate of extraction. The mechanism of extraction of aluminium (III) with Htta in the presence of TOPO may be similar to that of gallium (III).

It is known that the maximum coordination number of these three metal ions, aluminium (III), gallium (III), and indium (III) is usually six. Thus when these metal ions are combined with three tta^- ions that are bidentate chelating ligands, no vacant coordination sites should be left. From this, it is assumed that when the tris-tta complexes of these metal ions accept one or more than one TOPO on the coordination sites, the tta^- ions can not be a bidentate ligand. However, the details of such changes in the structure of the complex cannot be estimated only from the extraction data

REFERENCES

1. Sekine T and Dyrssen D, *J. Inorg. Nucl. Chem.*, **29**, 1481, (1967).
2. Hokura A and Sekine T, *Anal. Sci.*, **13**, 19, (1997).
3. Sekine T and Kurihara T, *Anal. Sci.*, **2**, 137, (1986).
4. Sekine T, Saito T, and Iga H, *Bull. Chem. Soc. Jpn.*, **56**, 700, (1983).
5. Sekine T, Kometsu Y, and Yumikura J, *J. Inorg. Nucl. Chem.*, **35**, 3891, (1973).



THE INFLUENCE OF 1-OCTANOL ON METAL EXTRACTION BY DI-2-ETHYLHEXYL-PHOSPHORIC ACID

OA Sinegribova, V Kim, NV Bukar, OV Sviridenkova and OO Olenicheva

D. Mendeleyev University of Chemical Technology of Russia, Moscow, Russia

ABSTRACT

The dependence of distribution coefficient on the molar ratio between the concentrations of octanol-1 and di-2-ethylhexylphosphoric acid (HDEHP) for aqueous solutions containing alkaline-earth metals, (Ca, Sr, Ba nitrates), rare-earth metals, (La, Pr, Ce nitrates), and zirconium sulphate extraction by HDEHP solutions in inert diluent containing of 1-octanol has a maximum for all investigated metals. The location of the maximum value of the distribution coefficient depends on the nature of extracted metal and pH. The study of physical properties of lanthanum extracts indicated that in the organic phase the association and the formation of colloidal aggregates of metal dialkylphosphates takes place in the presence of 1-octanol. These aggregates can interact and be forced to structural transitions depending on aliphatic alcohol content in the organic phase. Using lanthanum extraction as a model system it was found that in the presence of different aliphatic alcohols or such surfactants as TBP, TOPO and CH_3COOH the interrelation between metal distribution coefficient and molar ratio of the concentration of added surfactant and HDEHP has a maximum too.

Keywords: 1-octanol, di-2-ethylhexylphosphoric acid, colloidal aggregates, alkaline earths, lanthanides, zirconium

INTRODUCTION

The micellar mechanism of extraction is one of intensively developing concepts in the theory of solvent extraction. The formation of colloidal particles, their composition and type, ion parameters of their interaction and structure of the mesomorphic phases formed can affect the kinetic and thermodynamic features of metal extraction.[1-3]

It is known that the metal extraction by di(2-ethylhexyl)phosphoric acid (HDEHP) is a result of cation exchange combined sometimes with additional solvation. But under certain conditions the formation of the micellar species, for example, by salts of HDEHP and Fe,[1] Na,[4,5] Ni and Co,[6] takes place in the organic phase. The formation of the reversed emulsion in the aqueous/organic systems, containing sodium di-2-ethylhexylphosphate, in the presence of long chain alcohols[7,8] was found. However, the effect of alcohol on the metal extraction by HDEHP has not been studied in detail.

In the present work the influence of 1-octanol on the extractability of alkaline-earth metals, rare-earth metals and zirconium in HDEHP solutions in octane, decane and toluene has been investgated. The main attention was given to the establishment of the relationship between the parameters of extractability and the type of structural organisation of the extract in organic phase for lanthanum extraction. The effect of other co-surfactants: aliphatic alcohol (1-butanol; isopentanol; 1-hexanol; 1-decanol), TBP (tri-n-butylphosphate $(C_4H_9O)_3PO$), TOPO (tri-n-octylphosphine oxide $(C_8H_{17})_3PO$), CH_3COOH has been studied also for lanthanum extraction.

EXPERIMENTAL

In the present work the following substances have been used: HDEHP, TOPO, TBP, acetic acid, octane, decane, toluene, aliphatic alcohols, alkaline and rare earth metals nitrates and zirconium sulphate with the content of main material not less than 98 %.

The experimental procedure of solvent extraction was carried out as follows. Equal volumes of aqueous and organic phases (10 cm^3) were mixed for 20 minutes. After phase separation the concentrations of metals in aqueous and organic phases were determined by complexometric titration with EDTA and murexide (for alkaline earth metals), xylenol orange (for rare earth metals and zirconium) as indicators.

© 2000 Society of Chemical Industry

To study the association and aggregation equilibrium in the organic phase the techniques of low frequency dielectrometry, conductometry, photon-correlation spectrometry were used. Dielectric measurements were performed by the resonance method in the frequency range 50-500 kHz, using Q-meter "Tesla BM 560". Conductivity investigations of the solutions were carried out with the help of automatic device "Tesla BM- 484" at an operation frequency of 1592 Hz using platinum electrodes in the measurement cell. Viscosity measurements of solutions were performed using a capillary cell (cell constant equal to 0.56). All investigations of organic phase properties were conducted at a temperature of 293 ± 0.1 K.

Photon-correlation spectrometer included He-Ne laser with the operation wavelength of 632,8 nm, photometer F-221 and correlator "Unicor SP" with 128 high-speed signal processors. The computing program allowed the calculation of the correlation function in the real-time mode, using cumulant method.

RESULTS AND DISCUSSION

The influence of 1-octanol on the distribution coefficient (D) for alkaline-earth metals, lanthanides and zirconium extracted into HDEHP is shown in figures 1-3. In all cases the dependence of distribution coefficient on the molar ratio between the concentrations of 1-octanol and HDEHP U=[1-octanol]/[HDEHP] has a maximum. The value Ucrit corresponding to the maximum value of the distribution coefficient and depends on the nature of extracted metal and pH.

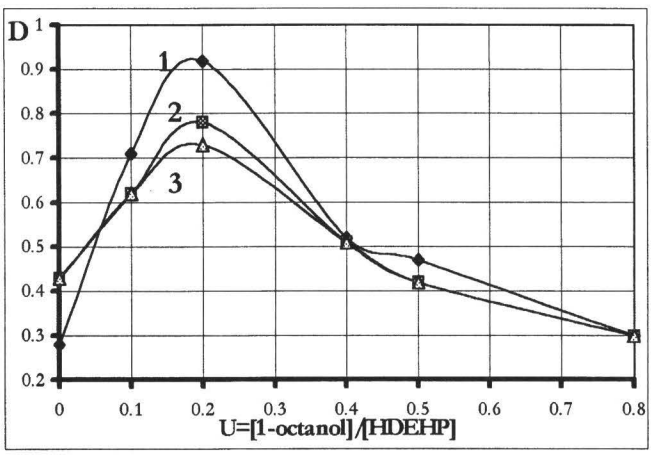


Figure 1. The influence of 1-octanol on the extraction of alkaline-earth metals in HDEHP.
1[$Ca(NO_3)_2$]=0.55mol/dm^3, pH=1.8;
2-[$Ba(NO_3)_2$]=0.40mol/dm^3, pH=2.0;
3-[$Sr(NO_3)_2$]=0.26mol/dm^3, pH=2.0.
[HDEHP]=0.8 mol/dm^3

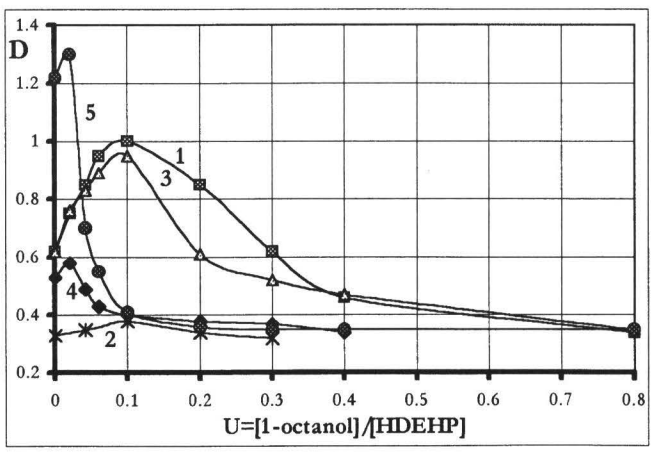


Figure 2. The influence of 1-octanol on the extraction of rare-earth metals in HDEHP.
1.[$La(NO_3)_3$]=0.33mol/dm^3, pH=1.7;
2.[$La(NO_3)_3$]=0.57mol/dm^3, pH=2;
3.[$Ce(NO_3)_3$]=0.3mol/dm^3, pH=1.8;
4.[$Ce(NO_3)_3$]=0.3mol/dm^3, pH=1.3;
5.[$Pr(NO_3)_3$]=0.13mol/dm^3, pH=1.3.
[HDEHP]=0.7mol/dm^3 in octane (1,3-5) and 2 mol/dm^3 in toluene(2).

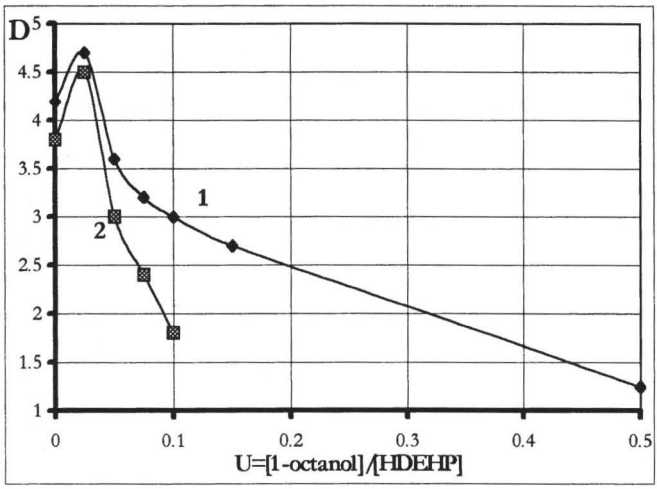


Figure 3. The influence of 1-octanol on the extraction of zirconium in HDEHP. 1.$[Zr(SO_4)_2]$=0.05 mol/dm^3, pH=0.95, [HDEHP]=0.7 mol/dm^3 in octane; 2.$[Zr(SO_4)_2]$=0.57 mol/dm^3, pH=2.0, [HDEHP]=2 mol/dm^3 in toluene.

The experimental data for lanthanum extraction in the presence of different aliphatic alcohols indicate the maximum of the dependence D on U to remove to lower values with increasing molecular mass of alcohol (figure 4).

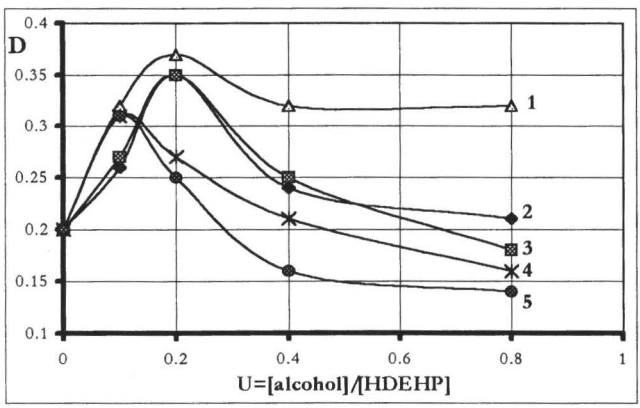


Figure 4. Dependence of the lanthanum distribution coefficient on the molar ratio alcohol/ HDEHP in the presence of aliphatic alcohols. 1. 1-butanol; 2. isopentanol; 3. 1-hexanol; 4. 1-octanol; 5. 1-decanol $[La(NO_3)_3]$=0.33mol/dm^3, pH=1.7; [HDEHP]=0.25mol/dm^3 in toluene.

To reveal peculiarities of processes, occurring in the organic phase in the presence of alcohols, a complex study of lanthanum di-2-ethylhexylphosphate – toluene - 1-octanol system has been carried out. Conductivity (figure 5, curve 1), determination of hydrodynamic radius of particles (figure 5, curve 2) and dielectric permeability increments ($\Delta\varepsilon=\varepsilon_0-\varepsilon$, where ε_0 and ε- dielectric permeability solvent and solution, respectively, figure 6, curve 1) as well as viscosity measurements (figure 6, curve 2) at different amounts of octanol-1 have been performed. In all cases the presence of bend point at mole ratio U=Ucrit was found. Analysis of the data allows the proposal that at small amounts of alcohol in the organic phase the association of lanthanum di-2-ethylhexylphosphate molecules in the form of chain structures takes place, as has been described.[10] Increasing the number of links in the chain structure leads to a rise in conductivity.[11] However, at U=Ucrit, the conductivity of organic phase abruptly falls (figure 5, curve 1), which could be explained by structural transition of the chains to more complex associates, for instance, micellar or vesicular structures.[12] It should be noted that in the micellar

(microemulsion) systems the conductivity must increase,[13] because of the dynamic nature of particles, both in kinetic behaviour, and also in the aspect of aggregation stability. Consequently, a decrease of conductivity as well as simultaneous rise of hydrodynamic radius of particles above Ucrit (figure 5, curve 2) indicates the formation of vesicles, which have a rigid structure and therefore inflexible phase boundaries.[14] Substitution of a molecular (with certain part "relay race") mechanism of conductivity on interparticle causes a decrease in conductivity. Dielectric measurements confirm this proposition. Dielectric permeability correlates to increase of dipole moment and molecular (particles) polarizability in the liquid medium.[15] At the reorganisation of chain associates to vesicular structures with spherical symmetry, the dipole moment decreases due to the mutual influence of molecules that leads to the reduction $\Delta\varepsilon$ (figure 6, curve 1). At U>Ucrit, processes of vesicle aggregation (dimerisation) as well as their transition to elliptical forms bring about the growing polarizability of particle and $\Delta\varepsilon$, accordingly. In particular, dynamic light scattering (figure 5, curve 2) showed that change of U from 0.1 up to 0.15 resulted in a increase of the hydrodynamic radius of particles from 20 to 60-70 nm. The structural transition process in the organic phase is also confirmed by viscosity studies (figure 6, curve 2).

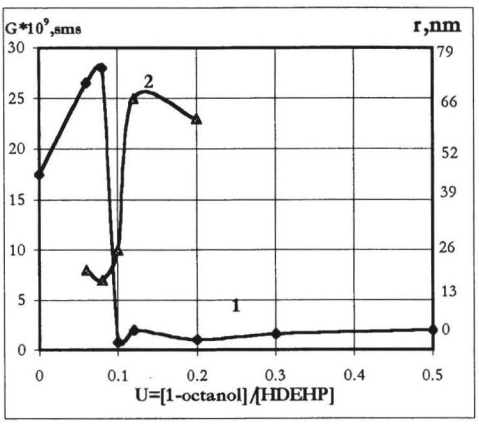


Figure 5. Dependence of conductivity (1) and of particle radius (2) on 1-octanol content in the system $La(NO_3)_{3(aq)}$/ HDEHP/ 1-octanol /toluene.
$[La(NO_3)_3]$=0.57 mol/dm^3, pH=2;
[HDEHP]=2 mol/dm^3 in toluene.

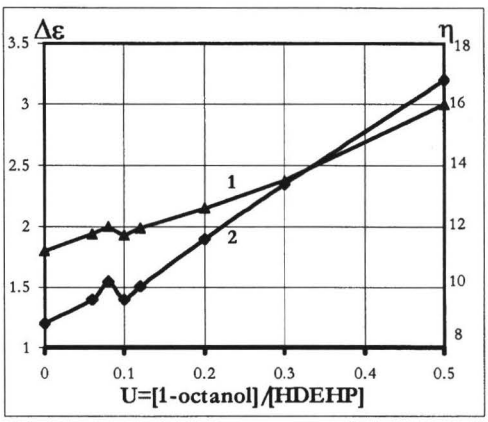


Figure 6. Dependence of dielectric permeability increment (1) and of viscosity (2) on the 1-octanol content in the system $La(NO_3)_{3(aq)}$/ HDEHP/ 1-octanol /toluene.
$La(NO_3)_3$=0.57 mol/dm^3, pH=2;
[HDEHP]=2 mol/dm^3 in toluene.

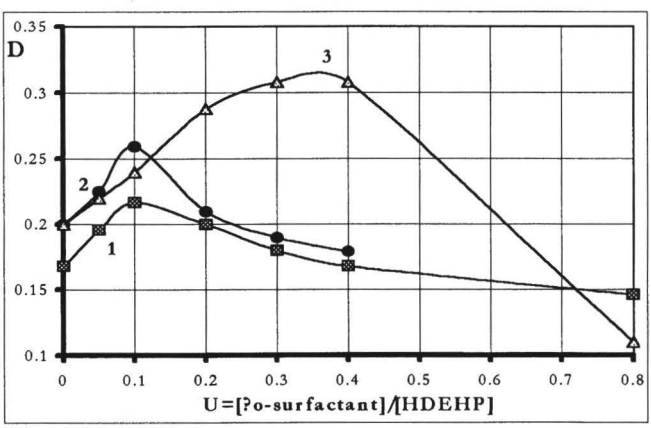


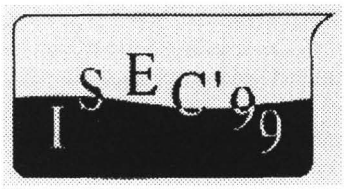
Figure 7. The influence of co-surfactant on the extraction of lanthanum in HDEHP.
1-TBP;
2-TOPO;
3-CH_3COOH
$[La(NO_3)_3]$=0.33mol/dm^3, pH=1.7;
[HDEHP]=0.2mol/dm^3 (1) and 0.25 mol/dm^3 (2,3) in toluene.

So, small additions of alcohol lead to the formation of the chain associates, whose presence promotes the metal mass transfer into organic phase. However at higher concentrations of alcohol in the extraction system the formation of other structural species (vesicles) is preferred. This structure contains the extracted salt, extractant and the aliphatic alcohol. It leads to a decrease of the extractant activity in the organic phase, which results in a decrease of the metal distribution coefficients. Since the increase of alcohol hydrocarbon chain length (as well as their molecular weight) stimulates the formation of lyophilic particles,[14] it can lead to a change of extraction parameters.

The influence of TBP (curve 1), TOPO (curve 2) and CH_3COOH (curve 3) on the lanthanum extractability is shown in figure 7. The presence of maximum at the certain value U was characteristic. It was established, that there is no actual thermodynamic extraction equilibrium between the lanthanum extract and aqueous (pH=2) phase. We supposed that it is dealing with the presence of vesicles in the organic phase. It was known that the vesicles are not really lyophilic particle.[14]
For complete lanthanum back extraction the extract was needed to strip by strong acid solution (5 mol/dm^3 HCl).

REFERENCES

1. Dias Lay ML, Perez de Ortiz ES and Cruertges K, *Proc.Int. Solv. Conf. ISEC'96,* **1**, 409, (1996).
2. Paatero E and Sjoblom J, *Hydrometallurgy*, **25**, 231, (1990).
3. Nitsch W and Plucinski P, *J. Phys. Chem.*, **97**, 8983, (1994).
4. Faure A, Tistchenko AM, Zemb T and Chachaty C, *J. Phys. Chem.*, **89**, 3373, (1985).
5 Yurtov EV and Murashova NM, *Proc. of XI Russian Conference in Solvent Extraction (Russ)*, Moscow, 159, (1998).
6 Neuman RD, Yu ZJ and Ibrahim T, *Proc.Int. Solv. Conf. ISEC'96*, **1**, 135, (1996).
7 Chekmarev AM, Sinegribova OA, Kim V et al., *Colloidal Journal* (Russ), **59**, 399, (1997).
8 Bukar NV, Kim V, Chekmarev AM et al., *Colloidal Journal* (Russ), **58**, 441, (1996).
9 Fourche G, Bellocq M and Brunetti S, *J. Colloid Interface Sci.*, **88**, 302, (1982).
10 Osseo-Asare K, *Sep. Sci. Technol.*, **23**, 1269, (1988).
11 Dvalaitzky M, Laguës M, LePesant JP et al., *J.Phys. Chem.*, **84**, 1532, (1980).
12 .Chen SY, Evans DF and Ninham BW, *J. Phys. Chem.*, **88**, 1631, (1984).
13 *Interfacial Phenomena in ApolarMedia* eds. Eicke HF, Parfitt GD, Dekker NY, (1987).
14 Fendler JH *Membrane Mimetic Chemistry*. Wiley-Interscience, (1982).
15 Eicke HF, Geiger S, Sauer FA, Thomas H and Bunsenges B. *Phys. Chem.*, **90**, 872, (1986).



EXTRACTING EMULSIONS – THEORETICAL REVIEW AND PRACTICAL USAGE

EV Yurtov and M Yu Koroleva
Mendeleev University of Chemical Technology, Moscow, Russia

ABSTRACT
The extracting emulsions - liquid heterogeneous systems, which can extract substances from different mediums, were observed. The properties of extracting emulsions such as viscosity, stability to sedimentation and to coalescence were investigated. Different methods of liquid membrane structuring and the creation of highly concentrated extracting emulsions are discussed.

Keywords: emulsion liquid membrane, surfactant,

INTRODUCTION

Extracting emulsions are emulsions, which can extract substances from different media. They are often high dispersed and concentrated liquid heterogeneous systems that can be used in different fields: chemical industry; environmental protection; medicine; etc.[1]
Along with the traditional method of liquid membrane extraction, i.e. extraction in a multiple emulsion, such systems can be used without dispersing the emulsion in a feed solution. Thus they can be applied in the form of a thin layer in a special apparatus or on the cleaning surface, for example as protective creams for human skin in industry and as curing creams in medicine or cosmetics.

In considering the possible fields of application, extracting emulsions should possess different properties (Table 1). For the concentration of substances into the internal phase the capacity of extracting emulsions should be large and can be varied by the nature of the extracting substance. For the simplest form, i.e. non-polymeric anions or cations the capacity of the extracting emulsion is selected by the internal phase composition. For the recovery of substances with surface-active properties the extracting emulsions should have a very high value of the interfacial area.

Properties	Industry	Medicine	
	Recovery and concentration of substances from industrial and waste solutions	Recovery of harmful substances from human blood	Skin protection
Capacity	High	Average	Average
Stability	Average	High	High

Table 1 Requirements of Extracting Emulsions in Different Fields of Application

The stability of such extracting emulsions may be different in various applications. Thus if it is necessary to carry out a rapid and low-energy separation of internal phase components, the stability of the extracting emulsion need not be very high.

The application of extracting emulsions in medicine and pharmacology demands very stable dispersed systems to prevent the penetration of the liquid membrane and internal water phase components into biological fluids. The problem of the capacity can be solved in many cases by the using of additional amounts of extracting emulsion.

The capacity of extracting emulsions depends on the amount of the active components in the internal water phase, and consequently it depends on the internal phase concentration in the emulsion (ϕ).

© 2000 Society of Chemical Industry

Extracting emulsions are the most often reversed (W/O) dispersed systems. These systems are thermodynamically unstable and phase separation takes place over time. The stability of the extracting emulsions should be divided in the aggregative (water phase separation) and sedimentation stability (oil phase separation).

Aggregative stability of W/O emulsions depends on the structure and properties of the adsorption layer at the interface: its viscosity; flexibility; the presence of a structural-mechanical barrier of nanodispersion which prevents coalescence of the internal phase droplets; composition of internal phase and liquid membrane; etc. The loss of aggregative stability leads to coalescence of internal water phase droplets in the extracting emulsion.

The stability to sedimentation depends on the internal water phase concentration in emulsion, the structure of the oil phase – liquid membrane, etc.

So the problem of the possible use of extracting emulsions can be divided in two parts. The first is the creation of a highly concentrated emulsion with internal phase concentration $\phi > 0.74$ which are stable to sedimentation, and does not often required high stability to coalescence. The second one is the use of an extracting emulsion with $\phi = 0.60\text{-}0.7$, but with modification of the oil phase and the addition of special structure forming additives which greatly increase their stability to sedimentation.

Extracting emulsions stabilized by: a) a monomeric surfactant, sorbitanmonooleate, and b) a polymeric surfactant, an ester of polyglycerol and oleic acid (molecular mass ~3000) have been studied. For the investigations of the influence of the internal water phase concentration on the stability to coalescence and sedimentation extracting emulsions with a surfactant concentration corresponding to the complete adsorption at the interface were used.[2]

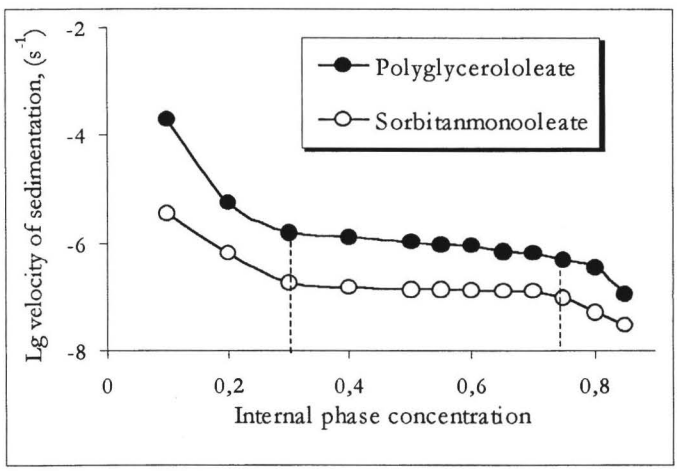


Figure 1. The influence of the internal water phase concentration on the sedimentation stability of extracting emulsions

Internal water phase concentration and the creation of highly concentrated extracting emulsions

The velocity of sedimentation was calculated as the gradient of the oil phase separation on the time limiting to zero (Figure 1). Its value is very high in emulsions with $\phi < 0.30$. In the more concentrated extracting emulsions the velocity of the oil phase separation decreases gently with the growth of ϕ. In the highly concentrated extracting emulsions with $\phi > 0.74$ the liquid membrane is very stable, and at $\phi > 0.90$ oil phase separation is not observed at all.

Liquid membranes in such systems are thin layers, in which the role of interfacial phenomena is great and influences to a large extent the kinetics of the extracting processes.

The stability of extracting emulsions to coalescence also depends of the internal phase concentration. There is a maximum on the curves of half-separation period of the water phase (Figure 2)

at ϕ=0.65 in the case of the polymeric surfactant, ester of polyglycerol and oleic acid, or the monomeric surfactant, sorbitanmono-oleate.

Apparently, this is connected with the formation of periodic structures of water droplets, corresponding to the fixing in the first minimum on the curves of attraction-repulsion energy. At the higher concentrations of the internal phase the deformation of water droplets takes place, and extracting emulsion stability towards coalescence decreases.

At the low concentration of the internal water phase half-separation period of water phase in emulsions with polyglyceroloIeate has the second maximum at ϕ=0.30.

The stability of emulsions with Span 80 increases with the decrease of the internal water phase concentration at $\phi < 0.40$ and at ϕ=0.10 emulsion stability to coalescence is as high as at ϕ=0.65. This phenomenon is related with the formation of special structured systems during the water droplet sedimentation. But such dispersed systems cannot be used for extracting process because of its low capacity.

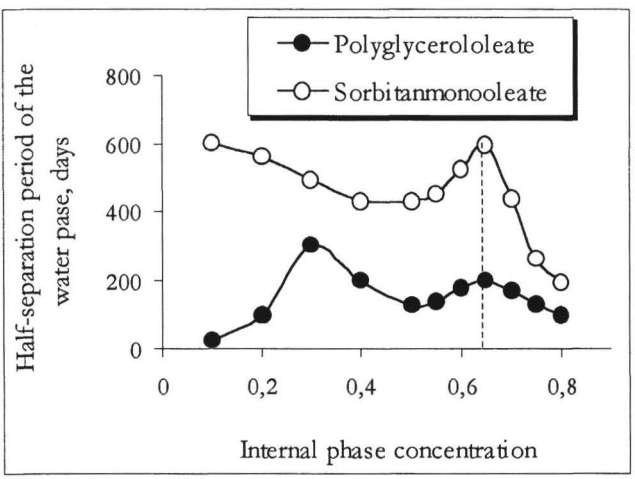


Figure 2. The half-separation period of the water phase versus the internal phase concentration in extracting emulsions

Thus extracting emulsions with the high internal phase concentration are very stable to sedimentation. Their stability to coalescence is not the greatest, but they are stable over several weeks, and can be used in industry.

So the region of existence of stable highly concentrated W/O emulsions ($\phi > 0.74$), and their physical-chemical properties were investigated. There are several methods for preparations of highly concentrated gel-emulsions with $\phi > 0.99$.[3,4] But such dispersed systems are very viscous so their use in stirring extraction systems is difficult. Such emulsions can be used as a thin layer on the cleaning surfaces, but they have a low stability to heterocoagulation. For this reason only highly concentrated emulsions were investigated, which could be prepared by stirring in a special apparatus, as in system more similar to extracting one.

Figure 3 illustrates the area of stable W/O emulsion existence in relation to the surfactant concentration. The highest concentration of the water phase in extracting emulsions, which can be obtained by this method of dispersing, is 0.90. The half-separation period of water phase in such emulsions decreases in spite of increasing of surfactant concentration due to the large extent of droplet deformation, but the stability to coalescence is large enough for the use of such dispersed systems for extraction.

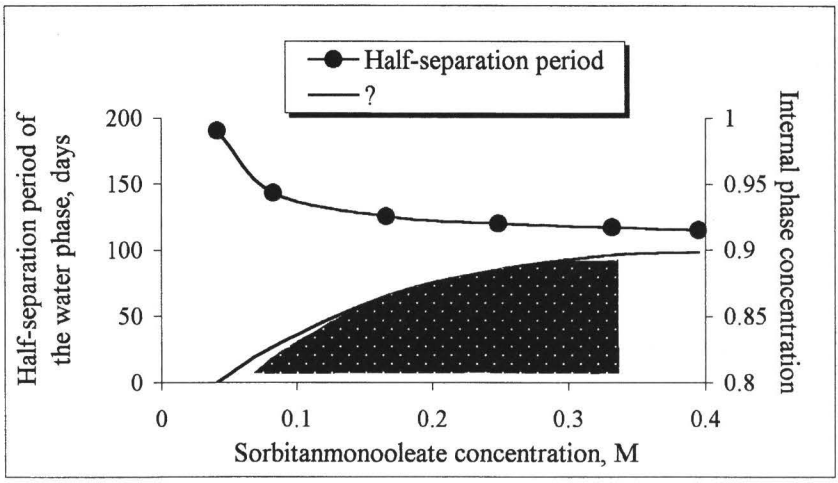


Figure 3. Maximum available concentration of the dispersed phase and the half-separation period of water phase in such emulsions versus surfactant concentration. The hatched area corresponds to the existence of stable W/O emulsions

Liquid membrane structure and stability to sedimentation of the extracting emulsions

As mentioned above extracting emulsions with internal phase concentration $\phi = 0.65$ are very stable to coalescence, but oil phase separation takes place. Sedimentation stability can be improved by the creation of different structures in the liquid membrane (Figure 4). For the creation of solid particle dispersion in the oil phase paraffin and cetyl alcohol were used. Organogels were formed by surfactant molecules, emulsifier T-2 (the mixture of polyglycerol dialkanates with M=2000), or by the polymeric apolar compounds, polyethylene and polypropylene.

Sorbitanmono-oleate was used for the stabilization of extracting emulsions, except those of emulsions with emulsifier T-2 as this possesses surface-active properties, and so other surfactants are not necessary.

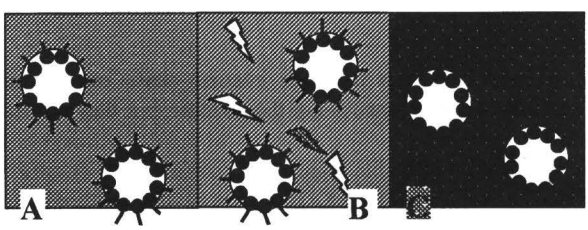


Figure 4. The scheme of extracting emulsion: A - unstructured type, B - with dispersion of solid particles, C - with organogel

Figure 5 illustrates the influence of the structure-forming additive concentration on the velocity of the oil phase separation in the extracting emulsions. The dispersion of solid particles or formation of organogel in the liquid membrane leads to the increase of emulsion stability to sedimentation. The most stable systems were with the organogel in the disperse phase. Low concentrations of polyethylene or polypropylene in the liquid membrane of the extracting emulsions results in a sharp decrease of sedimentation velocity. It was not possible to prepare emulsions with a higher concentration of these

substances and with an internal water phase concentration ϕ=0.65 because of the dramatic increase of emulsion viscosity.

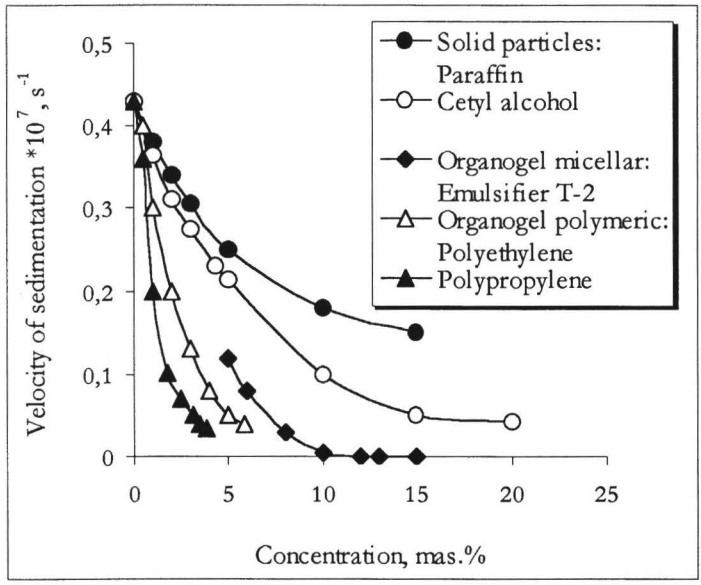


Figure 5. Velocity of oil phase separation versus concentration of structure-forming additive in the liquid membrane of extracting emulsions. The internal phase concentration - 0.65.

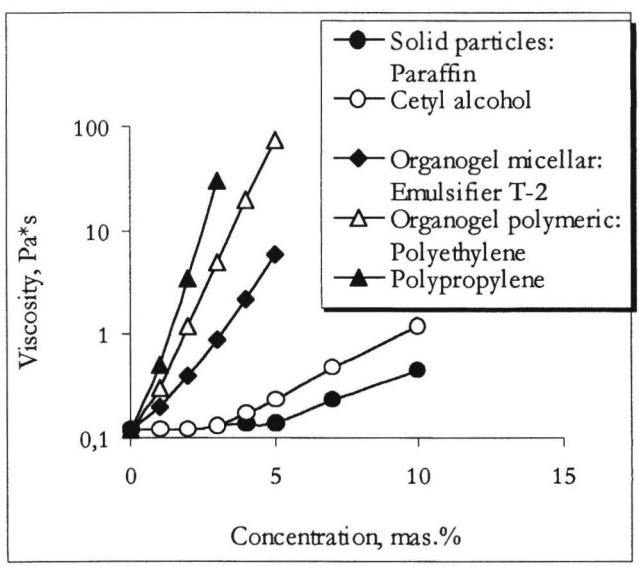


Figure 6. Viscosity of the liquid membranes in the extracting emulsions with structure forming additives.

It follows from the data in figure 5 that oil phase separation does not take place in the extracting emulsions with emulsifier T-2 concentration above 10 mas.%. It should be mentioned that such emulsions are also very stable to coalescence. During two years of investigations no visual amounts of water separated from these extracting emulsions.

Figure 6 illustrates the viscosity of the structured liquid membranes. The formation of organogel (micellar or polymeric) results in the sharp rise of viscosity. This effect is the greatest in the case of polypropylene.

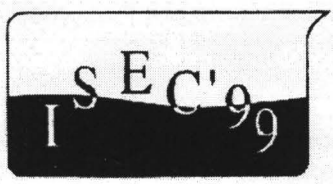
So extracting emulsions very stable to sedimentation can be obtained. It is necessary to take into account that any structure-forming of the liquid membranes leads to the increase of its viscosity. This fact is detrimental to the kinetics of the diffusion processes in liquid membrane.

ACKNOWLEDGMENTS

This work was supported in part by the Ministry of Education of the Russian Federation - the Grant "Fundamental Natural History" and Russian Foundation of Fundamental Researches - Grant ? 98-03-32564.

REFERENCES

1. *Chemical Separations with Liquid Membranes* ACS Symposium Series, **642**, Washington, DC, 422 , (1996).
2. Yurtov EV and Koroleva M Yu, *Chemical Separations with Liquid Membranes,* ACS Symposium Series, **642**, Washington, DC, 89, (1996).
3. Pons R, Carrera I, Erra P, Kunieda H and Solans C, *Colloid and Surfaces*, **91**, 259, (1994).
4. Williams JM, *Langmuir,* 7, 1370, (1991).



GEL-LIKE DEHPA SALT SYSTEMS IN ORGANIC SOLUTIONS AND ON THE INTERFACE

EV Yurtov and NM Murashova
Mendeleev University of Chemical Technology, Moscow, Russia

ABSTRACT
Gelation in DEHPA/NaOH/decane/water system has been investigated. Transparent, viscous and thixotropic gel forms are formed in the system with excess of NaOH when a determined amount of water is added. The structure of the gel is probably formed by long cylindrical swollen reverse micelles. Such gel films may arise on the interface in extraction systems, containing DEHPA. The breakage of the gel film can cause interfacial instability and interfacial convection. The DEHPNa gel can be destroyed by increasing temperature or by addition of aliphatic alcohol.

Keywords: DEHPA, gelation, micelle, interfacial convection, kinetics

INTRODUCTION

Aggregation processes in extraction systems using di(2-ethylhexyl)phosphoric acid (DEHPA) solutions often influence equilibrium and kinetics of the system. In general, they also complicate equipment performance and technological processes. One of the mechanisms for such phenomena could be gelation of DEHPA salts in the organic solutions and at the oil-water interface. The gelation of DEHPA salts in the interfacial area can cause the formation of a structural-mechanical barrier, which influences extraction process and phase separation.

DEHPA salts in apolar organic solvents can form reverse micelles of different size and structure including giant cylinders.[1,2] It is interesting that the structure of the DEHPA molecule is similar to lecithin molecule, which can form giant cylindrical micelles and organogels in organic solutions.[3] The mechanism of lecithin gelation was investigated in detail by Luisi et al.[4] and it helped to understand better the mechanism of gelation in the DEHPA salt solutions.

In this work the formation of gel-like DEHPA salts, their compositions, properties and stability have been studied. Methods of gel breakage, which could be important for practical applications have also been investigated.

EXPERIMENTAL

DEHPA, technical grade (DEHPA content 63.5 %) was used without further purification. DEHPA of such low purity was used to reproduce the conditions of real extraction processes. All the samples investigated were prepared by mixing required amounts of DEHPA, NaOH, water and decane at room temperature. For the rheological measurements a rotation viscometer with coaxial cylinders "Rheotest 2" was used. The measurements were carried out at shear rates of 3-1312 s^{-1} (cylinder N) and the temperature was controlled with an accuracy of 0.25 °C. Before any measurement was carried out, the sample was left to attain the required temperature for 40 minutes.

RESULTS AND DISCUSSION

Conditions of gelation in DEHPA/NaOH/decane/water system at high concentrations (0.1-1 mol/dm^3) of DEHPA and NaOH and at comparatively low (1-5 % mass) water concentrations were investigated. To reproduce conditions used in industrial extraction processes, DEHPA of technical grade was used. Introduction of NaOH in the system, which results in DEHPNa formation, was chosen due to both the comparatively good knowledge of the aggregation processes in the DEHPNa/organic solvent/water system and to the presence of sodium in some extraction systems.

© 2000 Society of Chemical Industry

The influence of each component concentration (separately or together) on the viscosity of DEHPA/NaOH/decane/water system was investigated.

Influence of water concentration.

The investigation of the influence of water concentration on the viscosity of the DEHPNa/decane/water system without excess NaOH (i.e.only containing the neutral sodium salt) showed not very significant variation (Figure 1a). The maximum value of viscosity was reached at the molar concentrations of water to DEHPNa equal to 3. On further increase of water content, the viscosity sharply decreased and then, at values of W = [H2O]/[DEHPA] greater than 4, slow and linear growth of the viscosity was observed. The system having DEHPNa concentration of 1 mol/dm^3 was able to solubilize more than 20 mol of water per 1 mol of the salt and remained transparent and of low viscosity. Probably, in this case microemulsion formation was observed at W>4 that is in good agreement with the data for DEHPNa/heptane/water system studied by Yu et al. [5]

Influence of DEHPNa concentration.

DEHPNa concentration without excess NaOH and at a fixed W value does not strongly influence the viscosity of the system in the concentration range 0.1-1 mol/dm^3. Considerable increase in viscosity was observed only at very high concentrations (more than 50 % mass) of the salt (Figure 1b). It is very unlikely that such high concentrations of salts would be encountered in real extraction systems.

Influence of excess of NaOH.

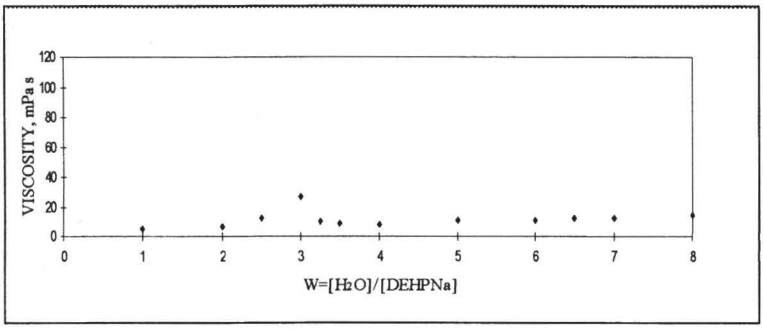
It was found that the addition of NaOH in the system at fixed values of DEHPA, decane and water concentrations does not cause considerable growth of viscosity. The maximum value of viscosity took place at an acid-base ratio equal to approximately to 2:3 (Figure 1c). Viscosity decrease and sediment formation was observed on further addition of NaOH.

Gelation under the combined influence of water and excess of NaOH.

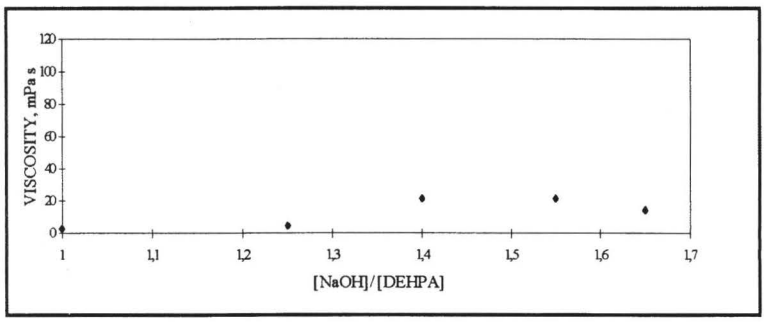
Investigation of the combined addition of water and sodium hydroxide in the system afforded an interesting result, only in this case strong growth of viscosity took place. The greatest viscosity change was observed when the ratio acid : base : water molar concentrations was equal to 2:3:9 (Figure 1d). At the component concentration ratio close to that mentioned above, viscous and transparent gels were formed. These gels flow as non-Newtonian liquids with an exponent value in the Ostwald-Veil equation less than one (i.e. viscosity decreases with the increase of shear rate). Small hysteresis was observed on the rheological curves of the gels, thus gels have weakly expressed thixotropic properties. Such rheological behaviour is similar to the behaviour of the other well-studied system - lecithin gels in hydrocarbon oil.[3,6]

Phase behaviour of DEHPA/NaOH/decane/water system.

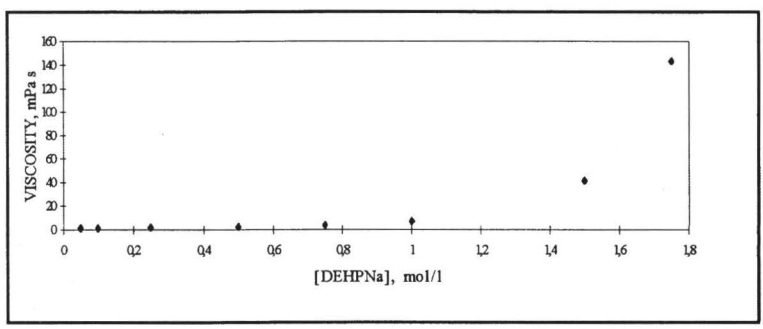
Phase transitions of DEHPA/NaOH/decane/water systems and lecithin/ hydrocarbon oil/water are very similar. The examples of the viscosity changes and the phase transitions caused by the addition of water in these systems are shown in Figures 2 (DEHPA/NaOH/decane/water at the excess of NaOH) and 3 (lecithin/vaseline oil/water). In both cases, sharp viscosity growth (gelation) began at a determined W value. When further water was added, the viscosity change was not considerable. Again, when water concentration exceeded a critical value, viscosity decreased and clouding of the systems was observed and the gels were found to separate into two phases - a non-viscous upper one and the viscous bottom phase. In both cases, the upper phase was enriched with the organic solvent and the lower phase was enriched by the gelling substances - DEHPA, NaOH and water in the first case and lecithin and water in the second case.



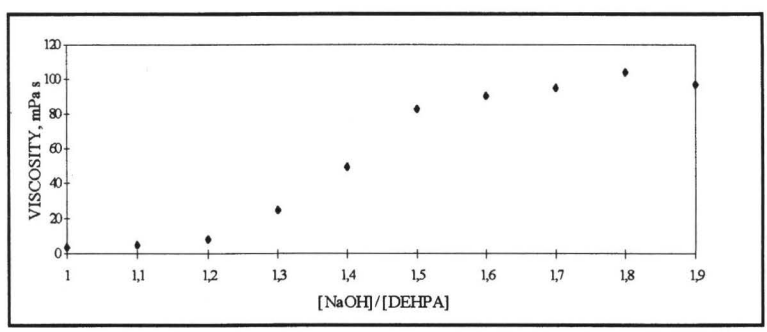
a) Viscosity as a function of water concentration [DEHPNa]=1 mol/dm^3



b) Viscosity as a function of NaOH concentration [DEHPA]=0.635 mol/dm^3



c) Viscosity as a function of DEHPNa concentration W=3.0



d) Viscosity as a function of NaOH and water concentrations [H2O]/[NaOH]=3 [DEHPA]=0.635 mol/dm^3

Figure 1. Influence of the component concentrations on the viscosity of the system DEHPA/NaOH/decane/water. Shear rate 1312 s^{-1}, T=20 C

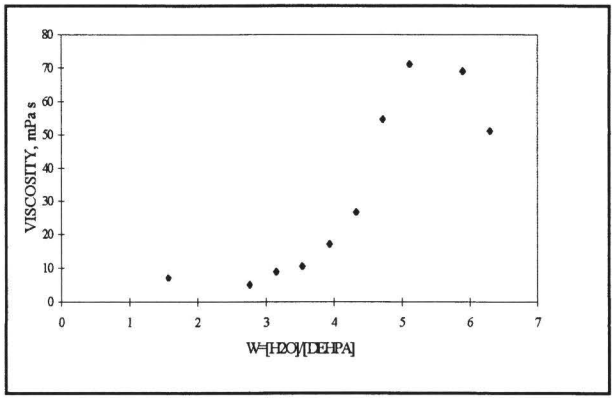


Figure 2. Gelation and the gel destruction in the system DEHPA/NaOH/decane/water. [DEHPA] = 0.635 mol/dm^3 [NaOH]=1 mol/dm^3, T=20 C, shear rate 1312 s^{-1}

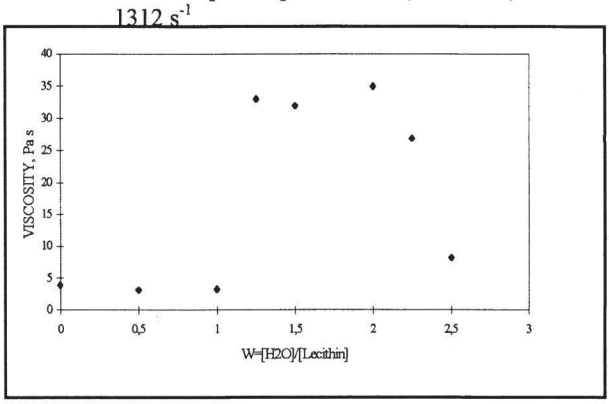


Figure 3. Gelation and the gel destruction in the system lecithin/vaseline oil/water. Lecithin concentration 20 g/dm^3, T=20 C, shear rate 3.0 s^{-1}

The DEHPA salt gel structure.

Based on the similarity of the phase transitions and the rheological behaviour of the DEHPA/NaOH/ decane/water and lecithin/ hydrocarbon oil/water systems and on the similarity of the DEHPA and lecithin molecules, similar structures of the gels formed in these systems can be proposed. It is known that lecithin gel structure is built up by the entangled transient network of long cylindrical reverse lecithin micelles, and water is solubilized in the micelles. Gelation results from the gradual transformation of small spherical micelles into long and flexible cylindrical ones and addition of water induces this transformation. The molecule of water forms hydrogen bonds with P=O and P-OH groups of two phosphatidylcholin molecules that play the role of a bridge [4,7]. The gels obtained in the system DEHPA/ NaOH/decane/water also may be formed by the network of giant cylindrical swollen reverse micelles. The existence of giant cylindrical reverse micelles in the heptane solutions of DEHPNa [1,2] can be considered as an argument for this proposition.

Gelation on the interface.

The following mechanism of the interfacial phenomena in some extraction systems with DEHPA can be proposed. The gel built up by the network of the giant cylindrical swollen reverse micelles may arise at the interface between the DEHPA solution in an apolar organic solvent and water solution of NaOH and metal salts. These conditions take place in the real extraction systems at the interface: the high concentration of DEHPA and its salts resulting from the adsorption, the water concentration, which is high in comparison with that in the organic phase, and low, in comparison with that in the water phase. The gel film formed at the interface can exist and grow and then destroy. The gel film destruction may be accompanied by intensive fluxes of substances and cause interfacial instability and results in the spontaneous interfacial convection (Figure 4). Sometimes nanodispersion droplets may result from the interfacial instability like nanodispersion formation described earlier.[7] Thus the gelation phenomenon starts decreasing which results in increase of the extraction rate, depending on the formation or the breakage of the gel structure. This is in agreement with the fact that sometimes, in extraction systems, interfacial film formation and spontaneous interfacial convection were observed during an extraction process under suitable conditions.

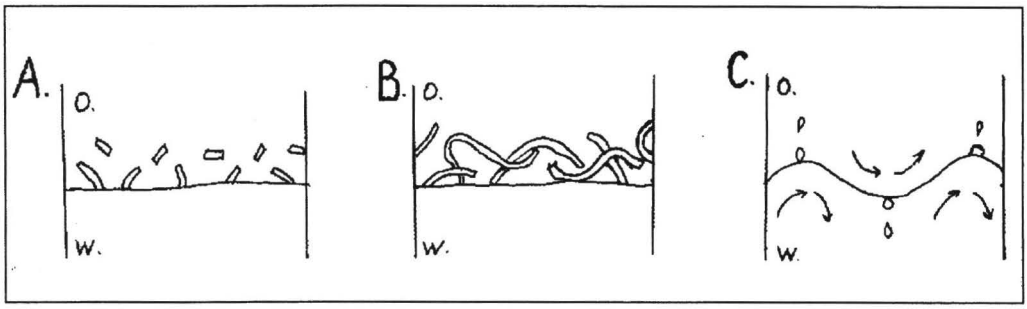


Figure 4. Scheme of the structures formation and breakage on the interface (O - organic phase, W - water phase)
A. short and rigid cylindrical reverse micelles;
B. gel-like structure formed by long and flexible cylindrical reverse micelles;
C. destruction of the gel film and interfacial instability appearance. Sometimes it may cause nanodispersion formation

Similar interfacial phenomena were described in the system lecithin solution in decane - water. When water contacts with the lecithin solution the gel film forms on the interface. The film is stable for some time and then the gel destruction takes place resulting in the further appearance of substance flux.[8]

Gel breakage.

It is interesting to investigate not only the process of the gel formation but also ways in which gel destruction occurs in the DEHPA/NaOH/decane/water system and to compare the data obtained with those of the interfacial film destruction and mass transfer intensification in the industrial extraction processes. The action of two factors - temperature increase and addition of small amounts of aliphatic alcohol with different hydrocarbon chain length on the gels were investigated. The increase of temperature in the range 20-35°C causes the decrease of the gel viscosity from 54.7 mPa s at 20°C to 18.2 mPa s at 35°C. It is found that viscosity dependence is linear in the Arrhenius coordinates and it gives a value of the viscous flow activation energy approximately equal to 55 kJ/mol.

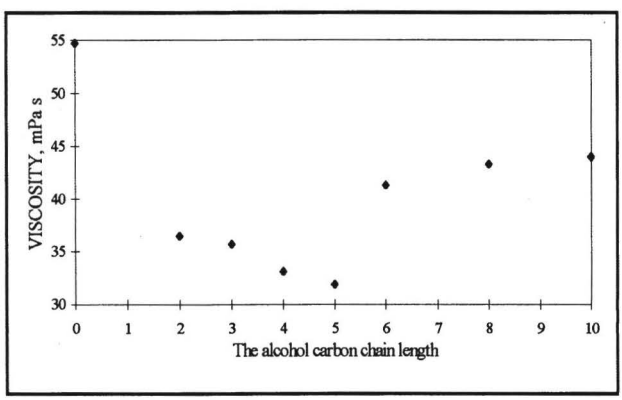


Figure 5. Influence of aliphatic alcohol addition on the gel viscosity in DEHPA/NaOH/decane/water system. [DEHPA] = 0.635 mol/dm^3, [NaOH] = 1 mol/dm^3, W = 3.0, T = 20 C , shear rate 1312 s^{-1}

Addition of a small concentration 0.5% of an aliphatic alcohol results in considerable reduction of viscosity of the gels in DEHPA/NaOH/decane/water system. The most effective action is observed in the case of butanol and pentanol (Figure 5). Viscosity reduction caused by the addition of alcohol was observed also with the lecithin gels. This phenomenon may be explained by the influence of the alcohol on the micelle shape - in the presence of the alcohol spherical, but not cylindrical swollen reverse micelles that form in the system.

CONCLUSIONS

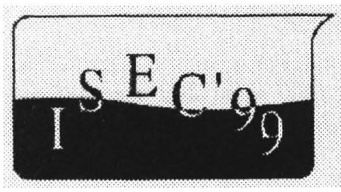
Gelation in the DEHPA/NaOH/decane/water system was investigated in similar conditions to those arising at the interface during extraction processes. A transparent, viscous and thixotropic gel forms when excess of NaOH in the system was obtained by maintaining a determined amount of water. The rheological behaviour and phase transitions in such systems are quite similar to lecithin gels, thus, suggesting the resemblance of the structures of these gels as a transient network of long cylindrical swollen reverse micelles. The gel film of such structure may arise at the interface in extraction systems, containing DEHPA. The destruction of such a gel film can cause interfacial instability and interfacial convection. DEHPNa gel destruction was investigated where it was found that increase of temperature and addition of aliphatic alcohols cause considerable viscosity reduction in the DEHPA/NaOH/ decane/water system, which is in agreement with the practical methods of the interfacial film destruction. Currently gelation of some transition and DEHPA-rare metal salts is under investigation.

ACKNOWLEDGEMENTS

This work was partly supported by the Russian Foundation of Fundamental Research (grant N 98-03-32564) and the Ministry of Education of Russian Federation (grant "Fundamental Natural History").

REFERENCES

1 Yu Z-J and Neuman RD. *Langmuir*, **10**, 2553, (1994).
2 Faure A, Ahlnas T, Tistchenko AM and Chachaty C. *J. Phys. Chem.* **91**, 1827, (1987).
3 Yurtov EV and Murashova NM. *CHISA'98 Congress Summaries*, Praha, Czech Republic, (1998).
4 Luisi PL, Scartazzini R, Haering G and Schurtenberger P. *Colloid & Polymer Sci.* **268**, 356, (1990).
5 Yu Z-J and Neuman RD. *Langmuir*, **11**, 1081, (1995).
6 Yurtov EV and Murashova NM, *International Conference on Colloid Chemistry and Physical-Chemical Mechanics Abstracts*, Moscow, Russia (1998).
7 Yurtov EV, Koroleva MY and Golubkov AM. *Dokl. Akad. Nauk SSSR*, **302**, 1164, (1998).
8 Shchipunov YA and Schmiedel P. *Langmuir*, **12**, 6443, (1996).



EXTRACTION BEHAVIOUR OF ALKALI METALS UNDER THE CONTROL OF pH IN CROWN ETHER–β-DIKETONE EXTRACTION AND CROWN ETHER–SUBSTITUTED PHENOL EXTRACTION SYSTEMS

T Shimosato, N Hirayama and T Honjo
Department of Chemistry, Faculty of Science, Kanazawa University, Kakuma-machi, Kanazawa, Ishikawa, 920-1192, Japan

ABSTRACT
The extractability of alkali metals increased as follows; Na, Li, Cs<Rb<K, with 12C4, B12C4, 15C5 <18C6<DB18C6<DC18C6, along with DBM, DPM<NTA<BFA<TTA, in chloroform<benzene, 1,2-dichloroethane<monochloro-, o-dichloro- benzene<o-, p-, m-xylene<toluene<nitrobenzene, and Li<Na<Rb<K<Cs with 12C4, B12C4<DB18C6<15C5<18C6<DC18C6, along with p-nitrophenol <2,4-dinitrophenol<picric acid<2,4-dinitro-1-naphthol(DNN), in benzene, toluene<1,2-dichloroethane <nitrobenzene . The selectivity (separation factor, α=D,j/D,l) was 140 for K/Na, 170 for K/Li, 7.4 for K/Rb and 73 for K/Cs, and %E was 88.4 for K, 5.2 for Na, 4.3 for Li, 50.6 for Rb and 9.5 for Cs, without extraction plateau, at pH7.9 in 0.01mol/l DB18C6-0.1mol/dm^3 TTA-toluene extraction system. However, the selectivity was 100 for K/Na, 360 for K/Li, 3.4 for K/Rb and 0.69 for K/Cs, and %E was 86.3 for K, 6.2 for Na, 1.7 for Li, 65.1 for Rb and 90.1 for Cs, with extraction plateau, at pH 7.6 in 0.01mol/dm^3 DB18C6-0.002mol/l DNN- 1,2-dichloroethane extraction system. The selectivity of K with DB18C6 for Na and/or Li, and the high hydrophobicity of DNN having suitable pK_a may contribute to the good separation of K from Na and/or Li. The extracted species was estimated to be the type of K:TTA:DB18C6 and K:DNN:DB18C6 in the ratio of 1:1:1. The recovery of K in initial amount was also found to be 98% within 5 minutes by established methods.

Keywords: synergism, alkali metal, crown ether, β·diketone, phenol derivative

INTRODUCTION

The extraction of alkali metals is generally known to be difficult because of their formation of aqueous stable complexes. The synergistic extraction of alkali metals was investigated with thenoyltrifluoroacetone (TTA) in the presence of some neutral ligands such as trioctylphosphineoxide (TOPO) and tributylphosphate (TBP).[1,2] Several ion pair extractions of alkali metals were also studied with crown ethers using picrate as counter anion,(R). However, the extractability of alkali metals described above is often less than 80%.

One of the present authors has reported that the synergistic extraction of lithium is possible with TTA in the presence of TBP in benzene, (Q) or 12-crown-4 (12C4) in o-dichlorobenzene. T was his applied to the separation and determination of a trace amount of lithium in ppb to ppm level in water, (S). In the present work, the extraction behaviour of alkali metals (Li, Na, K, Rb and Cs) with crown ethers (12C4, B12C4, 15C5, 18C6, DC18C6 and DB18C) along with β·diketones (TTA, BFA, NTA, TAA, DBM and DPM) and substituted phenols (p-nitrophenol, 2,4-dinitrophenol, picric acid and 2,4-dinitro-1-naphthol (DNN)) in organic solvents (benzene, toluene, xylene, chlorobenzene, nitrobenzene, chloroform and 1,2-dichloroethane) has been investigated in detail, and the optimum separation condition of alkali metals has also been ascertained by using crown ethers under the control of pK_a and hydrophobicity of ion-pair reagents such as β·diketones and phenol derivatives.

EXPERIMANTAL

Apparatus

A Hitachi model Z-6100 polarized Zeeman atomic absorption/flame emission spectrophotometer, a Shimadzu model UV-160 spectrophotometer, a Taiyo model SR-II Recipro shaker, a Tomy Seiko model CD-50R swing type centrifuge, and a Hitachi-Horiba model F-12 pH meter, were used.

© 2000 Society of Chemical Industry

Materials

Standard solutions of alkali metals (Li:10μg/ml, Na:10μg/ml, K:5μg/ml, Rb:10μg/ml, and Cs:10μg/ml) were prepared by diluting each of a certified solution of 1000 μg/ml alkali metals (Kanto Chemical Industries Ltd.) with distilled-deionized water prepared by the Nanopure system (Barnstead, Ltd.).

Buffer solutions (0.01mol/dm^3 Bis-Tris and 0.5mol/mol/dm^3 Tris) were prepared by diluting bis(2-hydroxyethyl)aminomethane (Bis-Tris, Wako Pure Chemical Industries, Ltd.) and tris(hydroxymethyl)aminomethane (Tris, Nakarai Chemical Industries, Ltd.) with distilled-deionized water, respectively. Hydrochloric acid was used for a suitable pH adjustment. β-diketones e.g. thenoyltrifluoroacetone (TTA), benzoyltrifluoroacetone (BFA), trifluoroacetylacetone (TFA) and dipivaloylmethane (DPM) (Dojindo Chemicals Ltd.), naphthoyltrifluoroacetone (NTA)(Aldrich), dibenzoylmetane (DBM) (Tokyo Kasei Ltd.), and substituted phenols e.g. p-nitrophenol and 2,4-dinitrophenol (Wako Pure Chemical Industries, Ltd.), picric acid (Kanto Chemical Industries Ltd.), 2,4-dinitro-1-naphthol (Schmid), were purchased. Crown ethers e.g. 12-crown-4 (12C4), 15-crown-5 (15C5), 18-crown-6 (18C6), dibenzo-18-crown-6 (DB18C), and dicyclohexyl-18-crown-6 (DC18C) (Merck), and benzo-12-crown-4 (B12C) (Tokyo Kasei Ltd.), were purchased. All other chemicals were guaranteed grade materials and were used without further purification.

Extraction and back extraction

A solution containing a metal(Li:1μg/ml, Na:10μg/ml, K:1μg/ml, Rb:2μg/ml, and Cs:1μg/ml) was adjusted to a desired pH using the buffer solutions of Bis-Tris (0.1mol/mol/dm^3) and Tris (0.5mol/mol/dm^3) with hydrochloric acid(0.1mol/mol/dm^3).

A 5 cm^3 of an aqueous solution and the same volume of organic solvent containing an ion-pair reagent and/or a crown ether were placed into a 10 cm^3 glass-stoppered centrifuge tube, and were agitated on a shaker for 5 minutes. The two phases were separated by centrifugation at 2500 rpm for 5 minutes. The pH of aqueous phases was determined after the extraction, and the value was used as the pH at extraction equilibrium. In the back extraction, the organic phase (4 cm^3) extracted was shaken with 0.1mol/mol/dm^3 hydrochloric acid for 5 minutes. The two phases were separated by centrifugation. The amount of metals stripped from the organic phases was determined by flame photometry at 670.8 nm for Li, 589.0 nm for sodium, 766.5 nm for potassium, 780.0 nm for rubidium, and 852.1 nm for caesium, respectively, and their extractability (%E) was calculated by using the results obtained.

RESULTS AND DISCUSSION

Effect of solvent

The effect of organic solvent on the extractability of the potassium TTA chelate with or without DB18C6 was investigated by varying organic solvents such as benzene, nitrobenzene, toluene, o-xylene, m-xylene, p-xylene, monochlorobenzene, o-dichlorobenzene, chloroform, and 1,2-dichloroethane. The %E of potassium increased as follows: chloroform<benzene, 1,2-dichloroethane <monochloro-, o-dichloro-benzene<o-, p-, m-xylene<toluene<nitrobenzene. It was found that the quantitative extraction of potassium was achieved by using nitrobenzene and toluene. Figure 1 shows the difference between the extractability of potassium and that of sodium in nitrobenzene and toluene. Taking into account the low solubility of the organic solvent in water and its high separability for potassium, toluene was selected as the extracting solvent. The effect of organic solvent on the extractability of the potassium DNN complex with or without DB18C6 was also investigated by varying organic solvents such as benzene, nitrobenzene, toluene, and 1,2-dichloroethane. The %E of potassium increased as follows: benzene, toluene<1,2-dichloroethane<nitrobenzene. It was found that the higher extractability of potassium was achieved by using nitrobenzene and 1,2-dichloroethane. Figure 2 shows the difference between the extractability of potassium and that of sodium in nitrobenzene and 1,2-dichloroethane. The %E of sodium in 1,2-dichloroetanne was lower than that in

nitrobenzene. Then, 1,2-dichloroethane having high separability for potassium was selected as the extracting solvent.

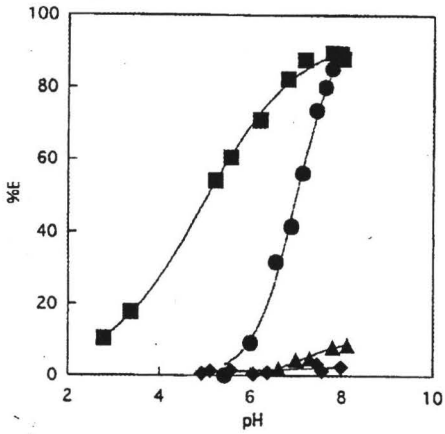


Fig.1. Effect of solvent on the extractability of K and Na with TTA and DB18C6. TTA: 0.1mo/l, DB18C6: 0.01mol/l, Shaking time: 10 min
■: K-nitrobenzene, ●: K-toluene, ▲: Na-nitrobenzene, ◆: Na-toluene

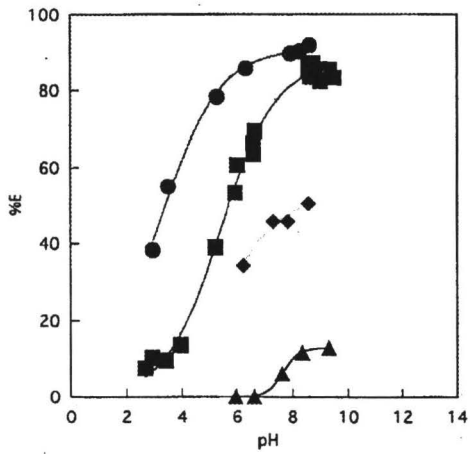


Fig.2. Effect of solvent on the extractability of K and Na with DNN and DB18C6. DNN: 0.002mol/l, DB18C6: 0.01mol/l Shaking time: 30min
■: K-1,2 -dichloroethane, ●: K-nitrobenzene, ▲: Na-1,2-dichloroethane, ◆: Na-nitrobenzene

Effect of shaking time

To ascertain the appropriate shaking time to equilibrate the extraction of alkali metals, the %E of potassium with DB18C6 and TTA in toluene was determined at various shaking times (0-10 minutes) at several fixed pH values (6.6 and 7.5). It was found that the quantitative extraction of potassium with DB18C6 and TTA in toluene was achieved within 5 minutes. The %E of potassium with DB18C6 and DNN in 1,2-dichloroethane was also determined at various shaking times (0-15 minutes) at several fixed pH values(4.8 and 6.5). It was found that the quantitative extraction of potassium with DB18C6 and DNN in 1,2-dichloroethane was also achieved within 5 minutes.

Effect of β·diketone and substituted phenol

The extractability of potassium with some β·diketones along with DB18C6 in toluene was determined to ascertain the most suitable β·diketone among TTA, BFA, TFA, NTA, DBM, and DPM.

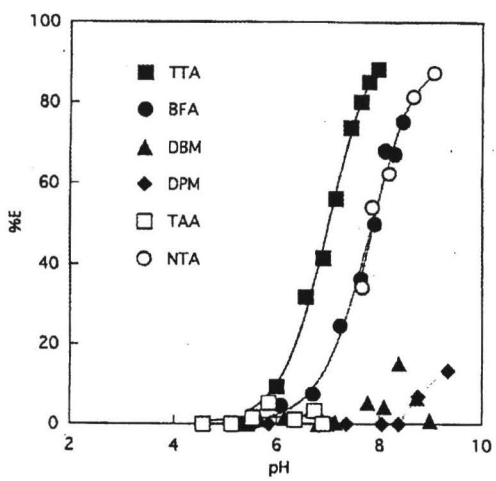


Fig.3. Effect of β ·diketones on the extractability of K with DB18C6 in toluene.
β ·diketones: 0.1mol/l, DB18C6: 0.01mol/l, Shaking time: 5 min

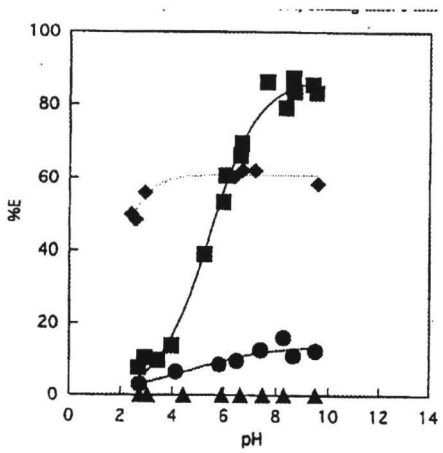


Fig.4. Effect of substituted phenols on the extractability of K with DB18C6 in 1,2-dichloroethane.
Substituted phenols: 0.002mol/l, DB18C6: 0.01mol/l, Shaking time: 5min
▲: p-Nitrophenol, ●: 2,4-Dinitrophenol, ■: DNN, ◆: Picric acid

As shown in figure 3, it is evident that TTA ($logK_{D,TTA}$ = 1.73, pKa = 6.18) is the most suitable reagent, because it gives high extractability. The extractability of potassium with some substituted phenols along with DB18C6 in 1,2-dichloroethane was also determined to ascertain the most suitable substituted phenol among p-nitrophenol, 2,4-dinitrophenol, picric acid and DNN. As shown in figure 4, it is evident that DNN ($log_{KD,DNN}$ = 1.23, pKa = 5.92) is the most suitable reagent, because it has hydrophobic naphthalene ring, and gives high extractability of potassium under the controllable range of pH.

Effect of crown ether

The extractability of potassium with TTA along with various crown ethers in toluene was studied. The %E of potassium increased as follows; being in 12C4, B12C4, 15C5 <18C6<DB18C6<DC18C6, as shown in figure 5. Figure 6 shows the difference between the extractability of potassium and that of sodium with TTA in the presence of DB18C6 and DC18C6 in toluene. The %E of sodium with DB18C6 was lower than that with DC18C6. Then, DB18C6 having high separability for potassium was selected as the crown ether. The extractability of potassium with DNN along with various crown ethers in 1,2-dichloroethane was also studied. The %E of potassium increased as follows; being in 12C4, B12C4<DB18C6<15C5<18C6<DC18C6, as shown in figures 7 and 8. These figures show the difference between the extractability of potassium and that of sodium with DC18C6, 18C6, 15C5, and DB18C6. The %E of sodium with DB18C6 was lower than that with other crown ethers. Then, DB18C6 having high separability for potassium was selected as crown ether.

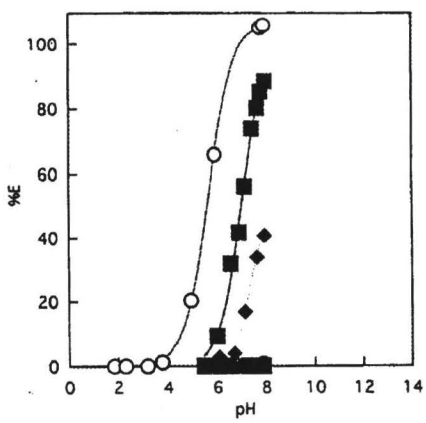


Fig.5. Effect of crown ethers on the extractability of K with TTA in toluene.
TTA: 0.1mol/l, Crown ethers: 0.01mol/l, Shaking time: 5min
□: 12C4, ●: B12C4, ▲: 15C5, ◆: 18C6, ■: DB18C6, ○: DC18C6

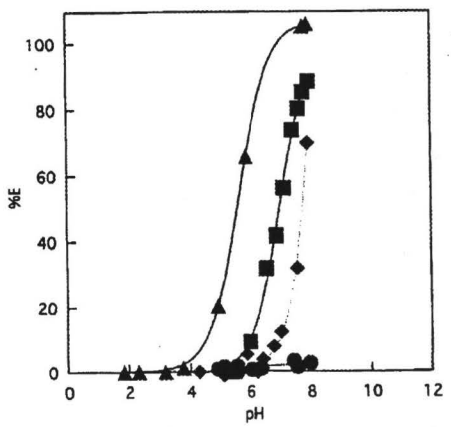


Fig.6. Effect of DB18C6 and DC18C6 on the extractability of K and Na with TTA in toluene.
TTA: 0.1mol/l, Crown ethers: 0.01mol/l, Shaking time: 5min
■: K-DB18C6, ●: Na-DB18C6, ▲: K-DC18C6, ◆: Na-DC18C6

Selectivity of DB18C6

The selectivity of alkali metals was ascertained by using TTA along with DB18C6 in toluene, and the results are shown in figure 9. The extractability of alkali metals increased as follows: Na, Li, Cs<Rb<K . This result depends on the ionic radius of alkali metals, namely on their fitness for DB18C6,R. The selectivity of alkali metals was also ascertained by using DNN along with DB18C6 in 1,2-dichloroethane, and the results are shown in figure 10. The extractability of alkali metals increased as follows: Li<Na<Rb<K<Cs. The selectivity, (separation factor, α=D,j/D,l, the ratio of distribution ratios between K and other alkali metals), was 140 for K/Na, 170 for K/Li, 7.4 for K/Rb and 73 for K/Cs, and the %E was 88.4 for K, 5.2 for Na, 4.3 for Li, 50.6 for Rb and 9.5 for Cs, without extraction plateau, at pH7.9 in 0.01mol/l DB18C6-0.1mol/dm^3 TTA-toluene extraction system.

However, the selectivity was 100 for K/Na, 360 for K/Li, 3.4 for K/Rb and 0.69 for K/Cs, and %E was 86.3% for K, 6.2 for Na, 1.7 for Li, 65.1 for Rb and 90.1 for Cs, with extraction plateau, at pH 7.6 in 0.01mol/dm^3 DB18C6-0.002mol/dm^3 DNN- 1,2-dichloroethane extraction system.

The selectivity of DB18C6 for K, Na and Li, and the high hydrophobicity of DNN having suitable pKa may contribute to the good separation of K from Na and Li by forming ion-pair complex.

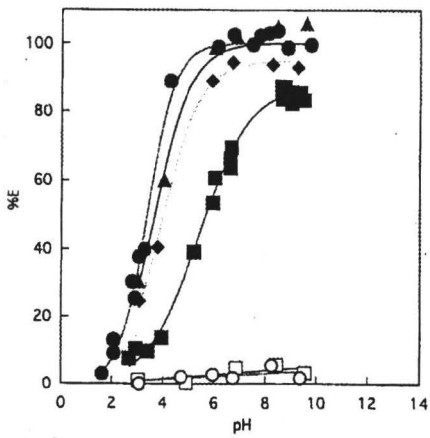


Fig.7. Effect of crown ethers on the extractability of K with DNN in 1,2-dichloroethane.
DNN: 0.002mol/l, Crown ethers: 0.01mol/l, Shaking time: 5min
○: 12C4, □: B12C4, ◆: 15C5, ▲: 18C6, ●: DC18C6, ■: DB18C6

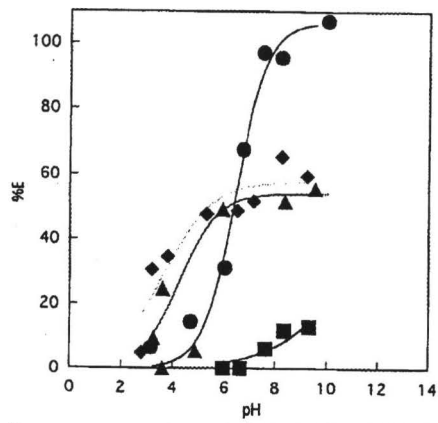


Fig.8. Effect of crown ethers on the extractability of Na with DNN in 1,2-dichloroethane.
DNN: 0.002mol/l, Crown ethers: 0.01mol/l, Shaking time: 5min
◆: 15C5, ▲: 18C6, ●: DC18C6, ■: DB18C6

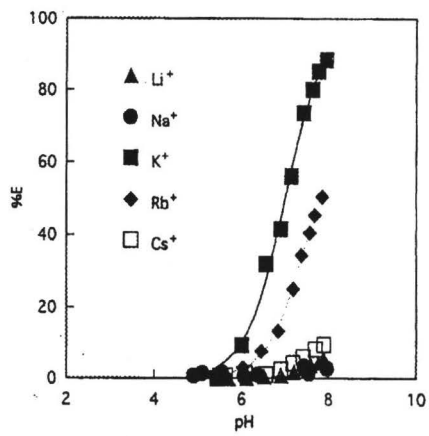


Fig.9. Effect of pH on the extractability of alkali metals with TTA and DB18C6 in toluene.
TTA: 0.1mol/l, DB18C6: 0.01mol/l, Shaking time: 5 min
▲: Li, ●: Na, ■: K, ◆: Rb, □: Cs

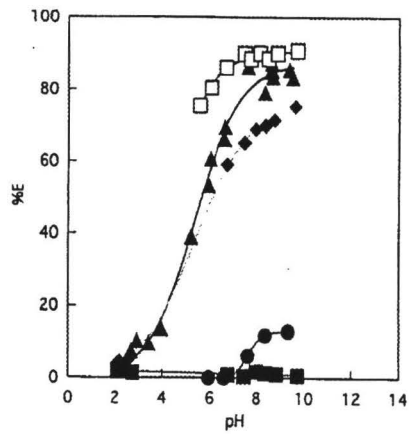


Fig.10. Effect of pH on the extractability of alkali metals with DNN and DB18C6 in 1,2-dichloroethane.
DNN: 0.002mol/l, DB18C6: 0.01mol/l, Shaking time: 5min
■: Li, ●: Na, ▲: K, ◆: Rb, □: Cs

Composition of extracted species

The composition of the extracted species on the extraction of potassium with TTA (0.001~0.1mol/dm^3) along with DB18C6 (0.005~0.01mol/dm^3) in toluene was ascertained by plotting log D vs. log $[TTA]_o$ and/or log $[DB18C6]_o$ at pH7.6. Each plot gave the straight line with a slope of unity, and the extracted species was estimated to be the type of K:TTA:DB18C6 = 1:1:1; the logarithmic extraction constant being -3.80. The extraction of potassium with DNN (0.0001~0.01mol/dm^3) along with DB18C6 (0.005~0.01mol/dm^3) in 1,2-dichloroethane was also

ascertained by plotting log D vs. log $[DNN]_o$ and/or log $[DB18C6]_o$ at pH 6.7. Each plot gave the straight line with a slope slightly less than unity, in which the extracted species should be dissociated partially in 1,2-dichloroethane; its composition being expected to be the type of K:DNN:DB18C6 = 1:1:1.

Recovery of potassium

The established methods were used to ascertain the recovery of 1μg/cm^3 potassium in water. When the volume of the organic phase of 0.002mol/dm^3 DNN along with 0.01mol/dm^3 DB18C6 in 1,2-dichloroethane was varied from 10 to 50cm^3, and when that of the aqueous phase was kept at 10cm^3, the extractability of potassium at pH 8.8 increased from 86 to 98%. When the extraction in the same volume (10cm^3) of both phases was repeated three times under the conditions described above, the extractability of potassium at pH 8.8 also increased from 86 to 98%.

CONCLUSION

The high extractability of K having an extraction curve in plateau with DB18C6 and DNN in 1,2-dichloroethane, the high selectivity of K with DB18C6 for Na and/or Li, and the high hydrophobicity of DNN having suitable pK_a may contribute to the good separation of K from Na and/or Li.

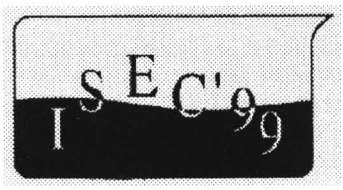
When K or Na is determined, much attention should be paid, because they are so easily contaminated elements, and only a trace amount of Na interferes for the determination of K by flame photometry.

The extracted species was estimated to be the type of K:DNN:DB18C6 in the ratio of 1:1:1.

The recovery of K in initial amount was also found to be 98% within 5 minutes by the established methods.

REFERENCES

1. Healy TV, *J.Inorg.Nuc.Chem.*, **30**, 1025, (1968).
2. Ooka N, Honjo T and Terada K, *Process Metallurgy*, **7A**, 457, (1992).
3. Honjo T, *Bunseki*, 127, (1997).
4. Itho T, Billah M, Honjo T and Terada K, *Anal.Sci.*, 7(supplement), 47, (1991).



A MECHANISTIC STUDY ON ION ASSOCIATION EXTRACTION WITH QUATERNARY AMMONIUM IONS

Shoji Motomizu, Toshio Takayanagi and Eiko Wada
Department of Chemistry, Faculty of Science, Okayama University, Tsushimanaka, Okayama 700-8530 Japan

ABSTRACT
The mechanism of liquid-liquid extraction of ion associates formed between anions and quaternary ammonium ions was studied. Monovalent organic and inorganic anions were extracted into chloroform as ion associates with the cations, and the extraction constants, K_{ex}, were determined. In this work, the ion association constants in the aqueous solution, K_{ass}, were determined on the basis of ionic mobility measurement, which was carried out by high-performance capillary electrophoresis. Distribution coefficients of the formed ion associates, K_D, were also determined by using the extraction constants (K_{ex}) and the ion association constants (K_{ass}) obtained in this work. From the results obtained, the contribution of an alkyl group of the quaternary ammonium ions to ion association and ion extractability was found to increase regularly with an increase in the number of methylene groups. The contribution of the ion association reaction in an aqueous phase, as well as the distribution coefficient, to the extraction constants was also clarified by considering each pair of the constants.

Keywords: ion-pair extraction, quaternary ammonium ion, mechanism of extraction, capillary electrophoresis

INTRODUCTION

Ion association reaction is widely used for the separation and determination of ionic substances. In liquid–liquid distribution, more bulky or less charged ions, such as monovalent hydrophobic organic ions, are found to be more extractable into the organic phase.[1] The separability and/or extractability have been estimated from the extraction constants give in equation 1, related to its extraction reaction.

$$Q^+ + A^- \overset{K_{ex}}{\leftrightarrow} (Q^+ \bullet A^-)_o$$

$$K_{ex} = [Q^+ \bullet A^-]_o / [Q^+]\,[A^-] \qquad (1)$$

where Q^+, A^- and $(Q^+ \bullet A^-)$ are respectively a quaternary ammonium ion, its pairing anion and an ion associate formed, and the subscript (o) denotes the species in the organic phase. The extraction reaction consists of two processes; the ion association reaction in an aqueous phase and its distribution between an aqueous phase and an organic phase. These equilibria are written as in the following equations 2 and 3.

$$Q^+ + A^- \overset{K_{ass}}{\leftrightarrow} (Q^+ \bullet A^-) \qquad (2)$$

$$K_{ass} = [Q^+ \bullet A^-] / [Q^+]\,[A^-]$$

$$(Q+\bullet A-) \overset{K_D}{\leftrightarrow} (Q+\bullet A-)o \qquad (3)$$

$K_D = [Q^+ \bullet A^-]_o / [Q^+ \bullet A^-]$The extraction constant can be represented by using an ion association constant (K_{ass}) in an aqueous phase and a distribution coefficient of the ion associate (K_D) between the organic and the aqueous phase, as in equation 4.

$$K_{ex} = K_{ass} \times K_D \qquad (4)$$

Ion association reactions in an aqueous solution have often been studied by conductometric measurements. However, measurements in aqueous solution has been limited for inorganic ion

© 2000 Society of Chemical Industry

associate, because of low solubility of organic ion associates, and therefore direct measurements for organic ion associates have been hardly studied.

In this study, the authors propose a novel method for the analysis of ion association reaction in aqueous solution by using the mobility change in capillary zone electrophoresis (CZE). In this method, relatively large amounts of pairing cation are present in migrating solutions, and small amounts of pairing anions in the sample solution are injected into a capillary. As the amount of formed ion associate is dominated by the amount of the pairing anion, the formation of the precipitates does not occur.

The tendency to ion association of a series of quaternary ammonium ions with some aromatic anions was investigated, and the contribution of methylene groups to this parameter was clarified. By using the ion association constants in an aqueous solution, the distribution coefficient of some ion associates was successfully estimated.

EXPERIMENTAL

Apparatus

An Applied Biosystems Model 270A-HT capillary electrophoresis system with an UV detector was used. A fused silica capillary (50 μm i.d.) was purchased from GL Sciences, and was cut to the required length; the size of the capillary was of 72 cm total length and 50 cm effective length to the UV detector.

Reagents

Migrating solutions were prepared with phosphate buffer, borate buffer or NaOH. Quaternary ammonium salts ($Q^+ \cdot Br^-$), such as tetramethylammonium bromide ($TMA^+ \cdot Br^-$), tetraethylammonium bromide ($TEA^+ \cdot Br^-$), tetrapropylammonium bromide ($TPA^+ \cdot Br^-$), tetrabutylammonium bromide ($TBA^+ \cdot Br^-$), and tetraamylammonium bromide ($TAA^+ \cdot Br^-$), were purchased from Tokyo Kasei Kogyo and added in the migrating solutions. Some aromatic anions were used as analyte ions.

Mobility measurement in capillary zone electrophoresis

The migrating buffer was transferred into a cathodic and an anodic reservoir, and then filled into a capillary tube before each measurement with a vacuum system. Sample solution was introduced into the capillary from the anodic end with the vacuum system for 3 seconds (injection volume about 9 nl). A voltage was then applied, and electrophoresis was started. The capillary was held in a thermostated compartment at 35°C throughout the experiment. The analyte anions were detected photometrically at a defined wavelength; 230 nm for the detection of naphthalene compounds and 210 nm for the detection of benzene compounds. Electroosmotic flow (EOF) was monitored by adding about 3 (v/v)% of ethanol to the sample solution.

The apparent electrophoretic mobility of an analyte, $-\mu_{ep}'$, and the electroosmotic flow, μ_{EOF}, were calculated in the usual manner.[2] Three or more measurements were carried out to obtain the mean electrophoretic mobility in each instance.

RESULTS AND DISCUSSION

Comparison of electrophoretic method and conductometric method

The conductometric method is well known for the analysis of ion-ion interactions in solutions. Along with the increase in the concentration of single-component salt, the molar conductivity of the salt in the solution decreases. The decrease in molar conductivity is compared with the theoretical value, and the ion association constant can be determined. On the other hand, the electrophoretic method proposed here can treat several ion associates in a time, because the method includes "separation."

Capillary electrophoretic method has another merit that the concentration of sample ion is at sufficiently low concentrations, which eliminates the possible precipitates of ion associate.

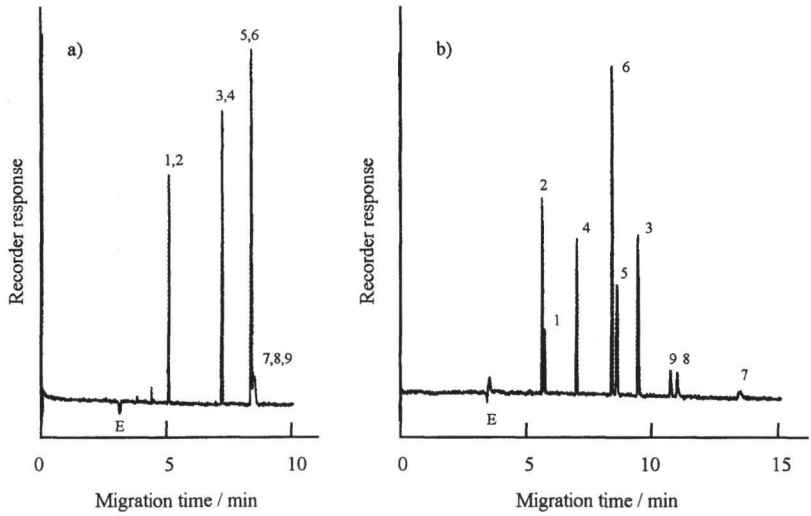


Figure 1 Typical electropherograms for aromatic anions. Migrating buffer: a), 10mM borax; b), 10 mM borax + 20mM $TBA^+ \cdot Br^-$. Sample: $1x10^{-5}$ M anions. CE conditions: voltage, 20 kV; detection wavelength, 200nm; injection period, 3 s; capillary temperature, 35 °C. Signal identifications: 1, naphthalene-1-sulfonate; 2, naphthalene-2-sulfonate; 3, naphthalene-2,3-dicarboxylate; 4, naphthalene-2,6-dicarboxylate; 5, naphthalene-1,5-disulfonate; 6, naphthalene-2,6-disulfonate; 7, phthalate; 8, *iso*-phthalate; 9, *tere*-phthalate. E, EOF (ethanol).

Capillary electrophoretic separation of isomers by ion association in aqueous solution

To investigate the ion association properties by the electrophoretic method, 10 mM borax (pH 9.2) or 5 mM NaOH (pH 11.7) was used as a migrating buffer, because the carboxylic and phenolic analyte anions can exist as anions at such pH conditions. On the other hand, sulfonate compounds exist as anions over wide pH ranges in aqueous solutions. The CZE separation of nine kinds of analyte anions was performed: the electropherograms are shown in figure 1. In the absence of an ion association reagent, separation of positional isomers is not sufficient (fig. 1a). This is because each anion exists as its anionic form and their mobility is almost the same. However, the isomers can be well separated by the addition of ion association reagent, TBA^+, in the migrating solution (fig.1b). In the case of TAA^+ used as a pairing ion, the baseline got noisy when TAA^+ was present at higher concentrations above 5 mM. It should be attributed to the formation of precipitates.

Change in electrophoretic mobility by the addition of quaternary ammonium ions

Changes in apparent electro-phoretic mobility, $-\mu_{ep}$', on addition of TBA^+ are shown in figure 2. For each analyte anion, $-\mu_{ep}$' values decreased more significantly when the concentration and the bulkiness of Q^+ increased. When TMA^+ was used as an ion association reagent, the decreases were less than those obtained with TBA^+ and TAA^+. Separation of isomers was not sufficient in TMA^+, compared with TBA

Determination of ion association constants

Ion association constants, K_{ass}, between quaternary ammonium ions and aromatic anions were

determined by measuring the change in electrophoretic mobility with the change in the concentrations of pairing ion. Four analysis methods, including three linear methods[3-5] and one non-linear least-squares method,[6] were performed to determine ion association constants most precisely.

The apparent electrophoretic mobility, $-\mu_{ep}'$, can be written as:

$$-\mu_{ep}' = \frac{1}{1 + K_{ass}[C^+]}(-\mu_{ep}) + \frac{K_{ass}[C^+]}{1 + K_{ass}[C^+]}(-\mu_{epIA}) \quad (5)$$

where $-\mu_{ep}$ and $-\mu_{epIA}$ are the electrophoretic mobility of a certain analyte anion and its ion associate, respectively. In the equation, a series of C^+ concentrations and corresponding $-\mu_{ep}'$ values were input in a laboratory-written program in BASIC, and the values of $-\mu_{ep}$, $-\mu_{epIA}$, and K_{ass} were optimized.

When an ion associate consists of an equally charged cation and anion, such as $(C^+ \cdot A^-)$ and $(C^{2+} \cdot A^{2-})$, it should be an electrically neutral ion associate. Therefore, the value of $-\mu_{epIA}$ can be assumed to be zero in the equation, when applied to such ion associates. The assumption was proved to be valid for ion associates with various kinds of pairing cations; optimized $-\mu_{epIA}$ values for such ion associate without neglecting the value were almost zero.

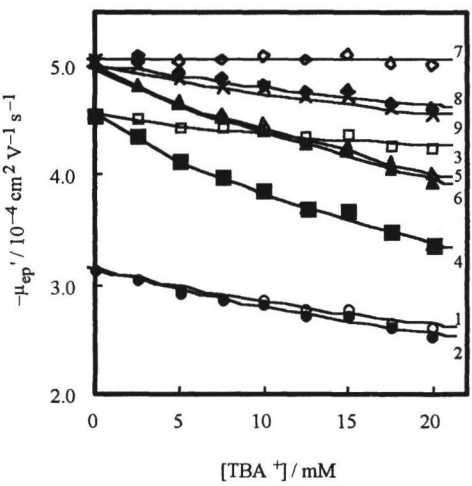


Figure 2 Change in electrophoretic mobility of anions by increasing the concentration of TBA^+ in the migrating solution. 1, naphthalene-1-sulfonate; 2, naphthalene-2-sulfonate; 3, naphthalene-2,3-dicarboxylate; 4, naphthalene-2,6-dicarboxylate; 5, naphtha-lene-1,5-disulfonate; 6, naphthalene-2,6-disulfonate; 7, phthalate; 8, *iso*-phthalate; 9, *tere*-phthalate.

Factors contributing to ion associability in an aqueous solution

The capillary electrophoretic method has some advantages; for example, ion association constants are determined very precisely and simultaneous measurement is possible owing to the electrophoretic separation. Therefore, the ion association constants are easily determined. The present authors investigated some factors contributing to ion associability. The ion associability increases by utilizing hydrophobicity,[6] the size of ionic charge,[6,7] basisity,[8] multipoint interaction,[7] and stacking of aromatic moieties.[9]

Contribution of methylene group to ion associability in an aqueous solution

The ion association constants of some aromatic anions were plotted against the number of methylene group on the quaternary ammonium ions (figure 3). The slopes were about 0.06 in logarithmic value, and the value, 0.06, is attributed to the contribution of methylene group to ion associability in an aqueous solution. The value is about 1/10 of the contribution in the extraction constant ($\log K_{ex}$) in the liquid–liquid distribution of ion associates.

Ion associability and extractability of aromatic anions

The extraction constants of some aromatic anions with tetrabutylammonium ion were determined by the solvent extraction method, and the values are summarized in table 1.

Ion association constants in an aqueous solution were determined by the proposed CZE method, and the values obtained are also summarized in Table 1. Distribution coefficients of the ion associates are calculated by using Eq. (4), and summarized in Table 1.The ion association constants

(K_{ass}) obtained were almost identical even when nitro groups are introduced to the phenolate anion. On the other hand, the extraction constants increased significantly by the introduction of nitro groups. The increases are very significant when the number of nitro group is large.

Nitro groups can withdraw electron and disperse anionic charges. Therefore, the basisity around anionic oxygen is decreased, which can decrease the electrostatic interaction between pairing ions and would not enhance the ion associability so much. From the comparison K_D values, it is concluded that larger extraction constant of nitro-substituted anions is attributed to the larger K_D values. The reason should be explained by the dispersion of anionic charge and increased molecular size.

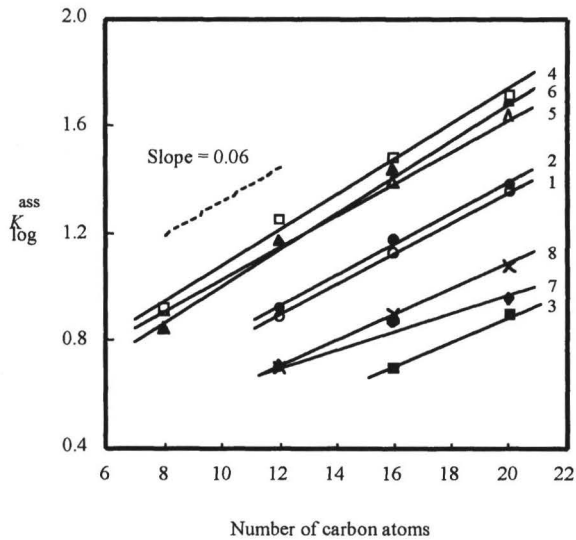


Figure 3 Relationships between log K_{ass} values and the number of carbon atoms on quaternary ammonium ion. 1, naphthalene-1-sulfonate; 2, naphthalene-2-sulfonate; 3, naphthalene-2,3-dicarboxylate; 4, naphthalene-2,6-dicarboxylate; 5, naphthalene-1,5-disulfonate; 6, naphthalene-2,6-disulfonate; 7, *iso*-phthalate; 8, *tere*-phthalate.

Anion	log K_{ass}	log K_D**	log K_{ex}
Phenolate	0.40	-0.70	-0.30
o-Nitrophenolate	0.64	1.53	2.17
m-Nitrophenolate	0.60	1.09	1.69
p-Nitrophenolate	0.80	1.72	2.52
2,4-Dinitrophenolate	0.80	3.21	4.01
2,6-Dinitrophenolate	0.68	3.30	3.98
2,4,6-Trinitrophenolate	0.67	4.86	5.53
Benzoate	0.62	0.06	0.68
p-Nitrobenzoate	0.55	1.12	1.67
Benzenesulfonate	0.61	1.11	1.72
p-Nitrobenzenesulfonate	0.64	2.38	3.02

*Tetrabutylammonium ion was used as a pairing cation. ** The values are obtained using the ion association constants and the extraction constants.

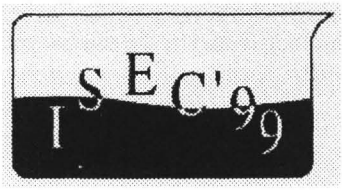
Table 1 Equilibrium constants of liquid-liquid distribution of ion associates between an aqueous and a chloroform phase*

CONCLUSIONS

The tendency to ion association of organic ion associates in an aqueous solution was successfully analyzed by the proposed method using the change in electrophoretic mobility in capillary zone electrophoresis. Contribution of the stepwise reactions on ion association extraction was clarified by the ion association constants determined. Investigation of the tendency to ion association in an aqueous solution will extend the research field related to ion association extraction.

REFERENCES

1. Motomizu S, *Bunseki Kagaku*, **38**, 147 (1989).
2. *"Handbook of Capillary Electrophoresis,"* ed by Landers JP, CRC Press 614, (1993).
3. Rundlett KL and Armstrong DW, *J. Chromatogr. A*, **721**, 173 (1996).
4. Honda S, Taga A, Suzuki K and Kakehi K, *J. Chromatogr.*, **597**, 377 (1992).
5. Shimura K and Karger BL, *Anal. Chem.*, **66**, 9 (1994).
6. Takayanagi T, Wada E and Motomizu S, *Analyst*, **122**, 57 (1997).
7. Takayanagi T, Wada E and Motomizu S, *Analyst*, **122**, 1387 (1997).
8. Takayanagi T, Wada E and Motomizu S, *Bunseki Kagaku*, **46**, 467 (1997).
9. Wada E, Takayanagi T and Motomizu S, *Analyst*, **123**, 493 (1998).



pH DEPENDENCE OF DICARBOXYLIC ACID EXTRACTION BY A STRONG AMINE BASED EXTRACTANT

Riki Canari and Aharon M Eyal
Casali Institute of Applied Chemistry, The Hebrew University of Jerusalem, 91904 Jerusalem, Israel

ABSTRACT
The mechanisms for extracting dicarboxylic acids by a strong amine-based extractant were determined by the loading curve dependence on the pH and confirmed by IR and NMR spectra. Three main acid species are involved, the dominant one being determined by the pH. Extraction of undissociated acid takes place at above-stoichiometric ratios and strongly drops at a pH around the pK_{a1} of the acid. A monovalent ion-pair is the dominant species at stoichiometric extraction and divalent ion-pair when the concentration of the acid in the organic phase is half that of the amine. The reaction of two monovalent ion-pairs to form a divalent ion-pair is analysed as a neutralisation reaction of the second carboxylic acid by the amine. Therefore, this reaction takes place when the amine is a stronger base than the second anion of the dicarboxylic acid, $pK_{a2}<pK_{aB}$, and the pH range is close to the second dissociation constant of the acid, pK_{a2}.

Keywords: dicarboxylic acid, amine, NMR

INTRODUCTION

Recently great effort is being made to produce commercial products using renewable resources (mainly cereals) as raw material. Therefore, fermentation processes for producing carboxylic acids are of great interest. Unfortunately most of the suitable microorganisms are sensitive to low pH. Separation science is, therefore, faced with the need to create methods for separating carboxylic acids from fermentation liquors of relatively high pH.

Only a few publications deal with the pH effect on extraction of acids[1,2,3] and the understanding of this area is limited. In a previous article[4] we analysed the effect of the pH on the extraction of mono-carboxylic acids by means of amine-based extractants. The extraction mechanisms were divided into two main categories: H-bonding and Solvation, on one hand, and Ion-pair formation on the other. For relatively weak bases, extraction is controlled by H-bonding or solvation and mainly determined by the concentration of the undissociated acid. The extraction is strongly dependent on the pK_a of the acid. The ion-pair formation is the dominating mechanism when the amine extractant is more basic than the anion of the extracted acid ($pK_{aB}>pK_a$) (where pK_{aB} is the half neutralisation pH as determined by Grinstead's method[5]). In these cases the extraction strongly depends on the pK_a of the extractant.

More complicated is the pH effect on the extraction of dicarboxylic acids. Where the main species in the organic phase are the undissociated acid, HAH, monovalent ion-pair, BH^+AH^- and divalent ion-pair, $BH^+A^{=}{}^+HB$ (where B stands for the amine and A is the anion of the acid).

Gusakova et.al.[6] concluded from IR spectra that malonic acid formed divalent ion-pair when extracted by dibutylamine in various diluents or by triethylamine in methanol. That was not the case on extraction by a mixture of triethylamine and dioxane, acetonitrile or chloroform. They concluded that the alcohol hydroxyl group interferes with the intramolecular hydrogen bond of the dicarboxylic acid, allowing divalent ion-pair formation. Tamada et.al.[7] analysed the formation of divalent ion-pair ("(1,2) complex") by mass action law analysis and confirmed it by means of IR spectra. They concluded that succinic acid does form divalent ion-pair on extraction by Alamine-336 (tertiary amine) in octanol, but not by Alamine-336 in methylene chloride, chloroform, nitrobenzene or methylisobuthylketone (MIBK). Fumaric acid forms divalent ion-pair when extracted by Alamine-336 in chloroform or in MIBK, and no evidence for divalent ion-pair formation was found for maleic acid extraction by Alamine-336 in chloroform. Tamada's main conclusion was that the dicarboxylic acids that form intramolecular hydrogen bonds, like maleic acid, are inhibited from forming divalent ion-pair.

© 2000 Society of Chemical Industry

In summary, although there is some evidence for divalent ion-pair formation in the literature, there is not enough knowledge of the mechanism, the parameters controlling it, and its dependence on pH.

EXPERIMENTAL

Materials

Primene JMT- a primary amine of C18-C22 (Rohm & Haas), maleic acid (HOOC-CH=CH-COOH(cis)) with pK_{a1}=1.8 and pK_{a2}=6.1(BDH 99.5-105%), glutaric acid (HOOC-$(CH_2)_3$-COOH), pK_{a1}=4.4 and pK_{a2}=5.4 (Fluka 98.5%), DL maleic acid (HOOC-CH_2CH(OH)-COOH), pK_{a1}=3.4 and pK_{a2}=5.1 (BDH 99%) and *n*-octanol (Merck, 99%).

Experimental methods

Extractants composed of Primene JMT in octanol were loaded with maleic, glutaric or maleic acid at molar ratios of 2:1, 1.2:1 and 1.2:1 respectively. Samples of the loaded extractants were equilibrated with increasing amounts of NaOH solutions. At equilibrium the pH of the aqueous phase and the acid content of the organic phase were determined by NaOH titration. In the case of maleic acid, IR spectra of the organic phases were obtained on Nicolet (510) FT-IR spectrometer, and ^{1}H NMR spectra of therse phases were recorded on a Bruker AMX-400 and 300 MHz spectrometer of the. (More details are presented in reference(4))

RESULTS AND DISCUSSION

Figure 1 shows the pH dependence of maleic, glutaric and maleic acid extraction by an extractant composed of 0.5 mol/kg JMT in octanol. The extraction curves of maleic and glutaric acids show two plateaus and two drops: a plateau in the stoichiometric extraction range (at a loading of ~0.5mol acid/kg) followed by a drop at around pH~4 for maleic acid and around pH~5 for glutaric acid, then a plateau at a loading of ~0.26mol acid/kg and a second drop around pH~7.

The following analysis is suggested. A monovalent ion-pair formation is the dominating mechanism at stoichiomentric extraction, forming BH^+ AH^-. On raising the pH, two monovalent ion-pairs react to form a divalent ion-pair and an acid molecule leaves the organic phase as follows:

$$2OH + 2BH^+ AH^-_{(org)} \leftrightarrow BH^+ A^{=} {}^+HB_{(org)} + A^{=}_{(aq)} + 2H_2O_{(aq)} \quad (1)$$

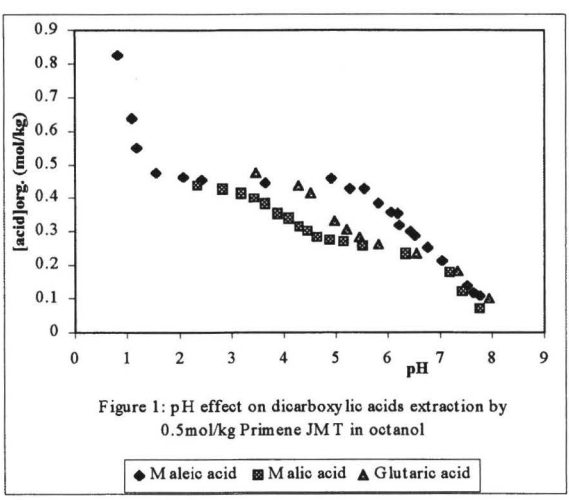


Figure 1: pH effect on dicarboxylic acids extraction by 0.5mol/kg Primene JMT in octanol

In this reaction the second carboxylic group is neutralised in the organic phase by the amine. Therefore, it takes place when the amine is a stronger base than the second anion of the dicarboxylic acid, $pK_{a2}<pK_{aB}$, and the concentration of the amine is higher than that of the acid in the organic phase $[HAH]_{org}<[B]_{org}$. Moreover, the pH range for the first drop in these extraction curves is close to the second dissociation constant value of the acid, pK_{a2}. A second plateau is found with amine to acid molar ratio of 1:2, indicating that the divalent ion-pair is the dominant specie. Starting at this point, the system shows a second sensitivity of extraction at pH around 7, which refers to the dissociation constant of the

protonated amine, pK_{aB}, to form free amine in the organic phase according to equation (2):

$$2OH_{(aq)} + \mathbf{BH^+ A^-}\ {}^+\mathbf{HB}_{(org)} \leftrightarrow \mathbf{B}_{(org)} + 2H2O_{(aq)} + A^-_{(aq)} \quad (2)$$

This analysis explains Tamada et. al.'s results. The tertiary amines they were using are relatively weak bases. The pK_{aB} for tertiary amine in an alkanol diluent is above 5 and in a non-protic diluent around 4[4] (the pK_{aB} value of the tertiary amines depends strongly on the ability of the diluent to stabilise ion-pairs and also on the extracted acid properties). Therefore, succinic acid with a pK_{a2}=5.5 can form a divalent ion-pair with the tertiary amine diluted in octanol (pK_{aB} above 5), but not diluted by a non-protic diluent (pK_{aB} around 4). Fumaric acid forms a divalent ion-pair upon extraction with tertiary amine in almost all of the diluents, due to its relatively low pK_{a2} value (pK_{a2}=4.4). But, divalent ion-pair formation is not expected when extracting maleic acid due to its high pK_{a2} of 6.07 compared to that of the extractant (the amine with the diluent). Therefore, by comparing the pK_{a2} of the extracted acid to the pK_{aB} of the extractant one can predict the ability of forming a divalent ion-pair.

Focusing on the maleic acid extraction curve (figure 1), the initial total maleic acid to amine molar ratio was 2:1. The extraction shows high dependence on pH at two pH ranges, around pH=1.1 and around pH of 6-8. At the lower pH range, undissociated maleic acid is extracted through H-bond to the monovalent ion-pair to form: $BH^+\ AH^-\ldots\mathbf{HAH}$ or through solvation mechanism. The above-stoichiometric extraction strongly drops at a pH around the pK_{a1} of the acid, to reach the stoichiometric level of a monovalent ion-pair, according to equation (3):

$$OH_{(aq)} + BH^+\ AH^-\ldots\mathbf{HAH}_{(org)} \leftrightarrow BH^+\ AH^-_{(org)} + H2O_{(aq)} + \mathbf{HA}^-_{(aq)} \quad (3)$$

Starting at this point, the system shows only a single drop, a large one, in the pH range of 6-8, compared with the two drops observed for the extraction of glutaric and maleic acids.

The pK_{a2} of maleic acid is 6.07 and the pK_{aB} of JMT in octanol is about 7. According to the suggested mechanism the formation of the divalent ion-pair species would be expected in this pH range. One suggestion is that the large drop in the pH range of pH~6-8 is actually a combination of two drops representing the first reaction (at a pH of about pK_{a2} of maleic, 6.07), and the second reaction (at a pH of about the pK_a of the protonated amine, 7), respectively. Alternative suggestion is that the large drop is only a single drop indicating no divalent ion-pair formation. IR and NMR spectra were taken in order to clarify the picture.

Figure 2 presents the IR spectra of 0.5 mol/kg JMT in octanol with various concentrations of maleic acid. The area of interest is around 1630-1720 cm^{-1}, with the peak of dissociated carboxylic acid at the lower end and that of undissociated acid at the higher end.

The spectra of the above-stoichiometrically loaded organic phase (0.83, 0.64, 0.55mol/kg) shows a peak at 1712cm^{-1}, which diminishing as the concentration of the acid decrease. This peak belongs to the acid molecules, H-bonded to the monovalent ion-pair $BH^+\ AH^-\ldots\mathbf{HAH}$. It almost disappears in the spectrum of the 0.465 mol/kg loaded organic phase, for which the two main peaks are at 1630 and 1680cm^{-1}. These peaks refer to the two carboxylic groups in the monovalent ion-pair $BH^+\ AH^-$, the dissociated and undissociated ones, respectively. One of the explanations suggested above for the single drop was that the monovalent ion-pair is neutralised by the base with no formation of the divalent ion-pair. In that case one would expect a decrease of these two peaks on pH elevation with no formation of another carboxylic acid-related peak. The spectra, however, show that, while these two peaks disappear, a new peak at 1650cm^{-1} forms (0.25, 0.14 mol/kg). We presume that this peak belongs to the two carboxylic groups in their undissociated form. This observation indicates that divalent ion-pair specie does form and that what seems to be a single drop (in figure 1) is a combination of two reactions (according to equations 1 and 2) taking place at similar pH.

L. Meyer[8] developed a new, NMR-based, method for analysing the mechanism of acid extraction. We used this method to study maleic acid extraction by JMT in octanol. The NMR spectra of the maleic acid loaded extractant show four groups of peaks (figure 3).

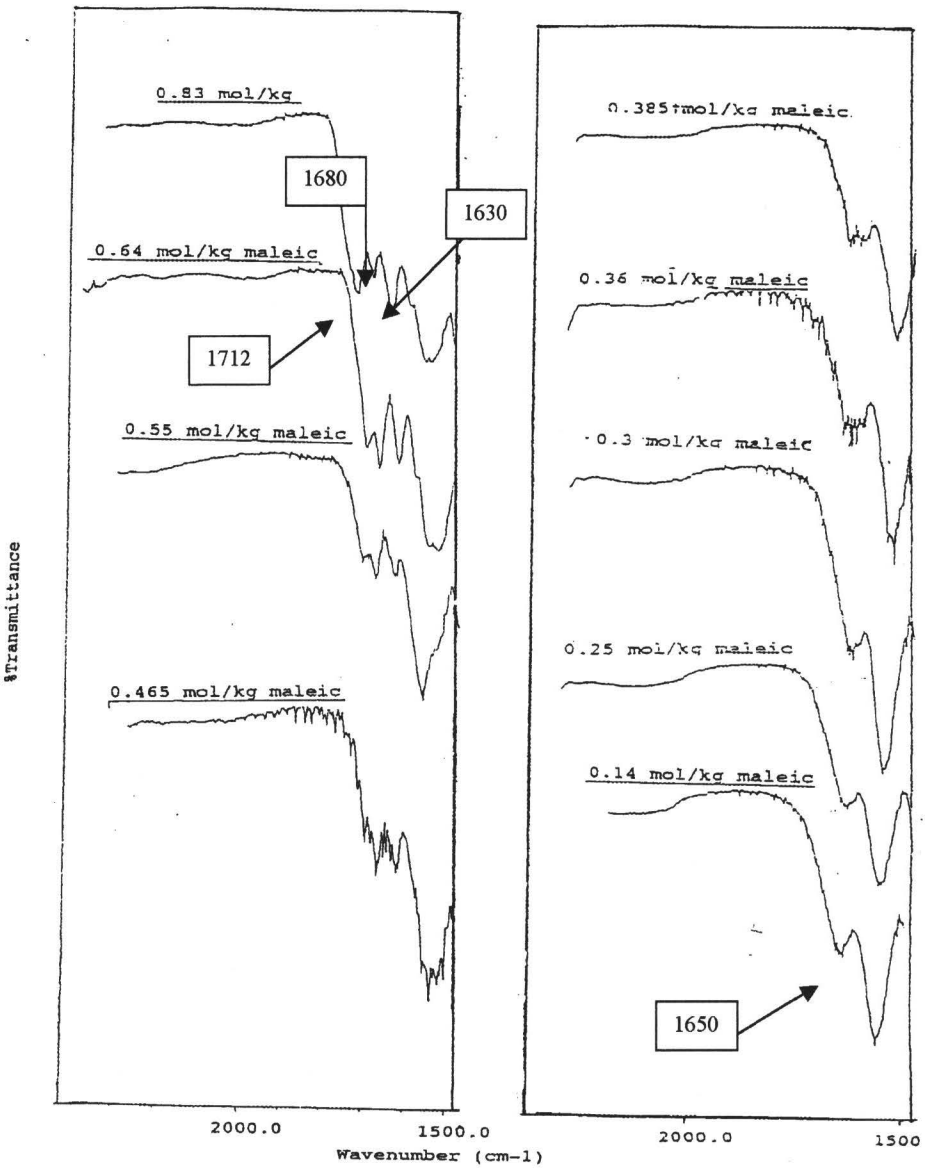


Figure 2: IR spectra of 0.5mol/kg JMT in octanol loaded with maleic acid

A large group of peaks is observed upfield (1.1-1.9 ppm) and related to the alkyl chains of the amine and of the octanol molecules (CH3(CH2)CH2-OH). A triplet is found further downfield (3.9-3.8ppm), relating to the methyl hydrogens in the α-position to the hydroxyl group of the octanol molecules (CH3(CH2)CH2-OH). A broad peak in the 5.7-6.2 ppm range is related to the hydrogen of the alcoholic group of the octanol molecules(CH3(CH2)CH2-OH), to the proton bound to the amine ($R3NH^+$) and to the hydrogens of the water molecules in the organic phase. The last peak is a singlet at ~6.2 ppm related to the vinylic hydrogens of maleic acid (HOOC-CH=CH-COOH). Two interesting phenomena occur as a result of raising the pH. First, the peak in the range of 5.7-6.2 ppm becomes

sharper. Secondly, there is an upfield shift of the singlet peak, which refers to the vinylic hydrogens of the acid. This upfield shift indicates that the hydrogens are in a more negative charged surrounding.

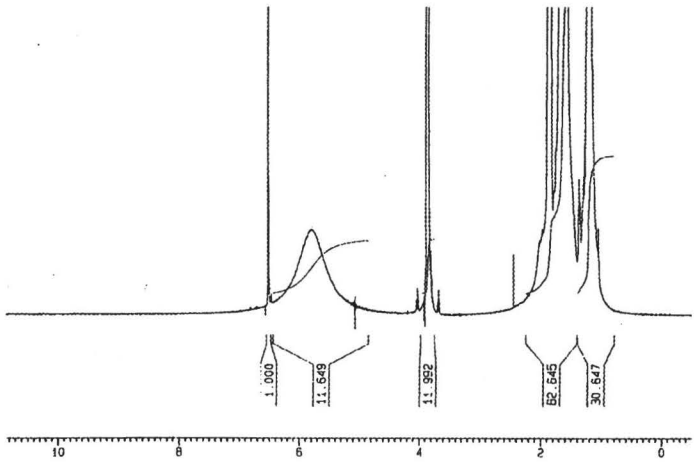


Figure 3: NMR spectrum of 0.5mol/kg JMT in octanol loaded with maleic acid

Figure 4 presents an analysis for these NMR spectra along with those of maleic acid extraction by 0.5 mol/kg TOA (trioctyl amine) in kerosene + 20% octanol. The X axis refers to the maleic acid concentration in the organic phase and the Y axis to the peak location of the vinylic hydrogen atoms. This figure presents the sharp upfield shift of this peak in the JMT case, starting at a pH of about 6.2, which is close to the pK_{a2} of the acid. At this pH the acid to amine molar ratio is 0.33/0.5(=2/3), indicating similar concentrations of monovalent ion-pairs, $\mathbf{BH^+\ AH^-}$, and divalent ion-pairs, $\mathbf{BH^+\ A^{=}\ ^+HB}$. In contrast, the location of this peak does not change in the case of extracting the acid by a tertiary amine extractant.

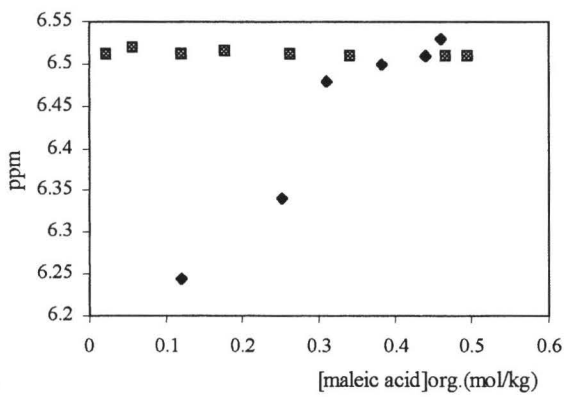


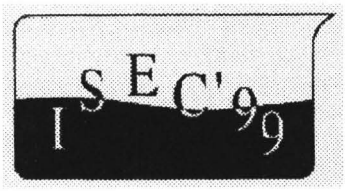
Figure 4: The NMR peak location(ppm) of the vinylic hydrogens of the maleic acid in the organic acid

As explained above, the second carboxylic anion is a stronger base than the tertiary amine extractant, but weaker compared with the primary amine. Therefore, neutralising the second acidic group by the

amine (and forming the divalent ion-pair) is energetically favourable in the case of extraction by the primary amine, but not for tertiary amine.

REFERENCES

1 Yang S-T, Whitte SA and Hsu ST. *Ind. Eng. Chem. Res.* **30**, 1335, (1991).
2 Tung LA and King CJ. *Ind. Eng .Chem. Res.* **33**, 3217, (1994).
3 Reisinger H and King C. J.; *Ing. Eng. Chem. Res.* **34**, 845, (1995).
4 Eyal AM and Canari R. *Ind. Eng. Chem. Res.* **34**, 1789, (1995).
5 Grinstead RR. *Proc Inter Conf Solv Extn. ISEC*, **2**, 723, (1967).
6 Gusakova GV, Denisov GS and Smolyanskii AL. *J. Gen. Chem. USSR* (Engl. Transl), **56**, 531, (1989).
7 Tamada JA and King CJ. *Ind.Eng.Chem.Res.* **29**, 1327, (1990).
8 Meyer L and Eyal AM. *Proc. ISEC'99*, 595, (2000)



A SPECTRAL STUDY OF THE RELATIVE BASICITY OF LONG CHAIN WATER-IMMISCIBLE ORGANIC AMINES

Lily Poulad-Meyer and Aharon M Eyal
Casali Institute of Applied Chemistry, School of Applied Science and Technology, The Hebrew University of Jerusalem, Jerusalem, 91904 Israel

ABSTRACT
A spectroscopic method is described for solving the problems related to determining the relative basicity of water immiscible amines. A correlation was found between said basicity and the NMR peak of the α-methylene protons of the amine - the stronger the base, the more upfield shifted are those protons. This correlation was explained, verified and used for determining the effect of various parameters on the basicity of amines used in industrial extraction of acids. The basicity sequence for long chain water immiscible amines, as derived from the spectral method, follows the sequence tertiary > secondary > primary, similar to that determined for short chain water-miscible amines by the gas phase basicity method. The spectral method exhibits a slight increase in basicity on going from methyl to ethyl and propyl amine. However, only negligible increase in basicity was observed on further increasing the chain length. In addition, the chemical shift of the α–methylene protons indicate that substitution of a hydrogen atom on a carbon atom, which is close to the amine nitrogen, increases the basicity through the inductive effect.

Keywords: NMR, organic amines.

INTRODUCTION

Solid anion exchangers and some of the most important industrial extractants use amines as active groups. While in a salt form, they bind anions mainly through ion exchange. The present article deals primarily with the case in which the amine is used in a free base form. The main focus is on solvent extraction process using amine-based extractants.

An increasing fraction of the biotechnologically manufactured carboxylic acids are separated from fermentation liquors by such extractants. In most cases, the separated acid needs to be recovered in its acid form, rather than as the salt, meaning that stripping the acid out of the loaded extractant is important. Hence, optimization of extractant composition requires, in addition to selectivity, a combination of efficient extraction and reversibility. Better understanding the extraction mechanism and the role of the amine are therefore essential tools for developing solvent extraction processes using amine-based extractants.

Previous studies pointed out two main mechanisms. If the amine is a significantly stronger base than the anion of the extracted acid, an acid-base interaction takes place forming an ion pair in the organic phase. That is the case for the extraction of most mineral acids with extractants containing aliphatic amines. Going to the other extreme, if the pK_a of the acid is significantly greater than that of the amine, the latter is not protonated and the extraction follows hydrogen bond or solvating mechanisms. Above-stoichiometric extraction is usually due to binding a second acid molecule to an ion-pair.

Knowing the basicity of the amine in the extractant is therefore very important. That basicity is determined by a number of parameters including: the number of substituents on the nitrogen atom, whether they are aliphatic or aromatic, the chain length and degree of branching, the nature of the solvent(s) of the amine, the concentration of the latter, temperature, etc.

Grinstead and co-workers[1] used pH half neutralization, pHhn, as a method for determining the apparent basicity of water immiscible amines. Grinstead's method is suitable for comparing the apparent basicities of water insoluble amines. As a means of determining the actual basicity of water insoluble amines, pH of half neutralization has many drawbacks, one of which is the assumption that the pH in the equilibrium aqueous phase is equal to that in the organic phase. The main problem by that method is, however, in the determination of the apparent basicity rather than the actual one. The result is therefore dependent on several parameters, which are not related to the amine itself. Eyal and

© 2000 Society of Chemical Industry

Canari[2] showed that the apparent basicity is determined by the properties of the amine the diluent and the anion of the extracted acid.

No method has been found in the literature for direct determination of the basicity of long chain amines in the organic solution. However, many authors in the past have used NMR analysis for the study of various aspects such as: comparison of the base strength of three amines in DMSO,[3] proton transfer and titration curves,[4,5] gas phase basicities,[6] acid base equilibria,[7] and ionization constants.[8] The present work suggests the use of NMR analysis towards the study of basicity of long chain amines and compares the results to previously available data.

EXPERIMENTAL

Materials

Primary, secondary and tertiary amines, with linear and branched chains were used: Primene-JMT, R_3CNH_2 (a mixture of isomeric amines in the range of C_{16-22}, produced by Rohm & Haas, technical grade), n-octyl amine, n-OA, (Sigma, pure 99%), di-2-ethylhexyl amine, DEHA, (Hoechst, technical grade) and di-isononyl amine, DINA (Hoechst, technical grade); tri-n-octyl amine, TOA, (Aldrich, 98%), tri-iso-nonylamine, TINA, (Hoechst technical grade), tris-2-ethylhexyl amine, TEHA, (Hoechst, technical grade). An industrial kerosene, Isopar K (Exxon), was used as a diluent.

Technical grade amines were used without further purification, in order to study the industrial amines as sold.

Methods

The molecular weights of the amines were determined by titration with HCl.

The organic solutions were prepared by diluting the amine of interest with IsoparK to the desired concentration.

pH_{hn} measurements were determined in the method as described by Grinstead[1].

^1H NMR spectra of the organic phases were recorded on a Bruker AMX-400 and a 300 MHz spectrometer. 5-mm o.d. NMR tubes were used. A sealed capillary containing benzene-D_6 was inserted into the NMR tube and used as an external ^2H lock and reference.

RESULTS AND DISCUSSION

Principle of NMR Analysis

In general, the chemical shift of a proton is approximately proportional to the electron density around it, and hence, to the electronegativity of the atom or group to which it is attached. The greater the electronegativity of that atom, the lower the electron density around the attached proton is and the further downfield the chemical shift.

The electron withdrawal by the nitrogen atom of the amines lowers the electron density in the vicinity of the α-methylene protons, thus causing their de-shielding. The more electronegative the nitrogen atom is, the lower is that density. A more electronegative nitrogen would have lower tendency to share its non-bonding electron with a proton and would thus be less basic. Thus, higher chemical shift of the α-methylene protons is expected to be correlated with weaker basicity.

The validity of the spectroscopic method

The approach suggested in section above was first tested by comparing amines with alkanols. Amines are more basic since the nitrogen is less electronegative than oxygen, and can better accommodate the positive charge of the ion. Based on this analysis, the chemical shift for amines should be smaller than that of alkanol of a similar chain. The data shown in table 1 confirms this expectation.

For short chain water-miscible alkyl-amines, the basicity sequence measured by potentiometric titration in water and in some organic solvents is: $NH_3<RNH_2<R_2NH>R_3N$[10,11,12,13]. Because the ion of the secondary amine carries one more hydrogen atom than that of the tertiary amine, the ion of the secondary amine has greater capacity for forming hydrogen bonds, and consequently will be stabilized more[14].

Base	δ(α-methylene protons)ppm[a]
n-hexanol	3.63
n-hexylamine	2.69
n-heptanol	3.60
n-heptylamine	2.65

a) Chemical shift, δppm, values are from Pouchert[9].

Table 1: Chemical shift of alkanols and amines with similar chain

As alkyl groups are electron-donating, one would expect that in the gas phase, where, solvation effects do not exist, the basicity order of amine towards the proton should be tertiary > secondary > primary > ammonia. This was indeed confirmed.[11,13-17]

Thus, two effects act in opposite directions; the field effect increases the basicity as the number of the methyl groups increases, and the hydration effect decreases it.

The NMR data and gas phase basicity values suggest the following sequence of basicity for water miscible amines: primary amines < secondary amines < tertiary amines. pH half neutralization data for amines show an opposite sequence.

As explained in the introduction, there is no way to compare the NMR data to pH based pK_a determination for water immiscible amines, but it can be done for water miscible ones. In Table 2 pKa values of various amines in aqueous solutions, taken from Hall[10], are compared with gas phase basicities, taken from Aue[13] and with chemical shifts of α–methylene protons taken from Pouchert.[9]

Amine	pKa[a]	GB KJ/mol[b]	$\delta_{(\alpha\text{–methylene protons})}$ppm[c]
ammonia	9.26	821.7	-
methylamine	10.64	860.6	1.95[d]
dimethylamine	10.61	888.3	1.87[d]
ethylamine	10.75	873.2	2.65
diethylamine	11.00	907.5	2.59
triethylamine	10.74	934.7	2.47
n-propylamine	10.59	879.1	2.67
di-n-propylamine	10.91	917.1	2.60
tri-n-propylamine	10.70	943.9	2.39
n-butylamine	10.61	881.2	2.69
di-n-butylamine	11.31	921.3	2.60
tri-n-butylamine	10.89	949.8	2.37

a) pKa values in aqueous solutions at 25°C, from Hall[10], (0.01mol lit^{-1} aqueous solutions of amines).
b) Gas phase basicities measured relative to ammonia (821.7 KJ mol^{-1}), from Table 1 in Aue[13].
c) Chemical shift, δppm, from Pouchert[9].
d) These amines are measured in a 40% aqueous solution.

Table 2: Comparison of the pKa values in aqueous solutions, gas phase basicities and chemical shift of the α-methylene protons in water miscible short chain amines

The apparent pK_a values of the water immiscible amines in table 3 range over nearly nine orders of magnitude compared with 0.5 orders of magnitude for those in table 2. There is no clear correlation between the pK_a values for the latter and NMR data. A reason for that could be the effect of the

diluent, water. Therefore, the chemical shift of the α–methylene protons have been compared with the gas phase basicities.

A rather good correlation was found, as shown in figure 1. This correlation provides another confirmation for the spectroscopic method of amine basicity determination suggested here.

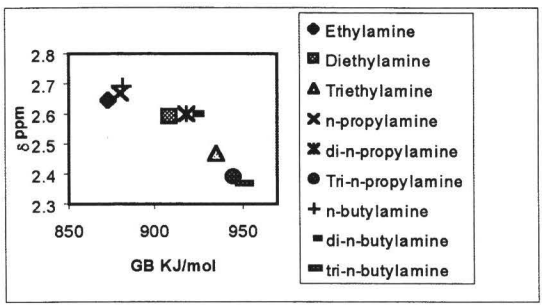


Figure 1: Gas phase basicity values, GB, of amines compared with their α–methylene chemical shifts, δppm.

The effect of the degree of substitution on the nitrogen atom

Table 3 summarizes the chemical shifts of the α-methylene protons for the non-diluted long chain amines and compares them to the pHhn values measured.

The NMR data in table 3 suggests the following sequence of amine basicity: primary <secondary<tertiary. pH half neutralization data for those amines show an opposite sequence. The explanation for this follows.

AMINE	δ(α-methylene protons)ppm[a]	pHhn[b]
n-OA	2.98	9.21
JMT	-[c]	7.64
DINA	2.82	-[d]
DEHA	2.72	2.71
TOA	2.62	-[e]
TINA	2.55	1.64
TEHA	2.23	0.89

a) NMR analysis of the non-diluted amine.
b) pHhn values of 0.5mol/kg solutions of the amine in an inert solvent, Isopar K.
c) JMT does not contain an α-methylene proton, the α-carbon is a tertiary carbon.
d) Gel formation upon contact with the aqueous phase, and therefore the pH could not be measured.
e) Third phase formation occurred upon contact the aqueous phase, thus, a deviation in the pHhn value.

Table 3: The chemical shift of the α-methylene protons of the non-diluted amines and their measured pH_{hn} values.

The conflict between the data for water immiscible amines and those of the pH half neutralization, as shown in the opposite sequences in table 3, should therefore be explained by the effect of the method of determination. As explained in the introduction, pH half neutralization determines the apparent basicity and is therefore dependent on the extraction mechanism and on the parameters affecting it.

According to Grinstead, the increasing steric hindrance due to the bulk of the alkyl groups renders solvation of the ammonium cation or the ion pair more difficult and reduces the stability of the salt relative to the free amine. This tends to reduce the basicity of the more highly alkylated amines.

The spectroscopic method, on the other hand, studies the amine itself (rather than its extraction capacity) and therefore is independent of solvation effects.

Effect of chain length.

Table 4 summarizes pK_a data in aqueous phase, gas phase basicity and spectroscopic data for primary amines with a number of carbon atoms increasing from 1 - 8. The gas phase data show some increase in basicity on going from methyl amine to ethyl amine and propyl amine, but very little effect on further increase in number of carbon atoms. The implication for the amines of interest to us is that for water immiscible amines the chain length would not have significant effects on amine basicity.

Amine	pKa	GB KJ mol^{-1}[a]	δ(αmethylene protons) ppm[b]
methylamine	10.64[c]	860.6	-
ethylamine	10.67[d]	873.2	2.65
n-propylamine	10.69[d]	879.1	2.67
n-butylamine	10.61[e]	881.2	2.69
n-pentylamine	10.63[e]	883.7	2.69
n-hexylamine	10.64[e]	885.8	2.75
n-heptylamine	10.66[e]	-	2.70
n-octylamine	10.65[e]	887.0	2.65[f]

a) Gas phase basicities measured relative to ammonia (821.7 KJ mol^{-1}) taken from Aue[13] in table 1.
b) Chemical shift, δ ppm, values are from Pouchert[9].
c) pKa values in aqueous solutions at 25°C, Hall[10].
d) pKa values in aqueous solutions at 25°C, ref. 22 in Smith[12].
e) pKa values in aqueous solutions at 25°C, ref. 29 in Smith[12].
f) The cause for the observed difference in chemical shift of the n-octylamine protons, (ours vs. literature), is explained by the calibration method used. A capillary containing benzene D_6 was inserted into each nmr tube for calibration, and thus shifts the peaks by 0.33ppm, relative to external TMS.

Table 4: pK_a values, gas phase basicities and chemical shifts of the α-methylene protons for primary amines with increasing chain length.

Effect of branching.

The chemical shift data in table 5 indicate that branching increases the basicity of the amine. The pH half neutralization based pK_a data showed an opposite trend. Data for amines in gas phase could help in clarifying this apparent conflict.

An agreement was found for these amines between the chemical shift data and those of gas phase basicities. Both showed that branching increases the basicity as found for water-immiscible amines. (The α position showed a deviation in their analysis. This result was interesting, however, at this point in our research we do not have a clear explanation. The explanation will be given in a future article.) As in previous cases, the conflict between the spectroscopic data and those of pH half neutralization might be due to the difference between independent and apparent basicity determination.

Branching on a carbon atom, which is close to the amine nitrogen, increases the basicity through the inductive effect as indicated by the chemical shift of the α–methylene protons. Yet, on extraction of acids to form ion-pairs, it increases the steric hindrance for stabilization through aggregation and decreases thereby the apparent basicity. Thus, as in the case of the degree of substitution on the N atom, the chemical shift teaches about the basicity of the amine as such, while apparent basicity is strongly affected by steric and medium effects.

Amine	GB KJ mol^{-1} [a]	δ(α-methylene protons) ppm[b]
$CH_3CH_2CH_2NH_2$	879.1	2.67
(α) $CH_3CH_2(CH_3)CHNH_2$	887.4	2.75
(β) $(CH_3)_2CHCH_2NH_2$	883.2	2.50
(β, β) $(CH_3)_3CCH_2NH_2$	886.2	2.40
(γ) $CH_3CH_2CH_2CH_2NH_2$	881.2	2.69
(γ,γ) $(CH_3)_2CHCH_2CH_2NH_2$		2.70
$(CH_3CH_2CH_2)_2NH$	917.1	2.60
(β) $[(CH_3)_2CHCH_2]_2NH$	922.2	2.40
$CH_3CH_2CH_2CH_2NH_2$	881.2	2.69
(α) $CH_3CH_2CH_2(CH_3)CHNH_2$		2.85
(β) $CH_3CH_2(CH_3)CHCH_2NH_2$		2.60
(γ) $(CH_3)_2CH_2CH_2CH_2NH_2$		2.70
(δ) $CH_3CH_2CH_2CH_2CH_2NH_2$	883.7	2.69

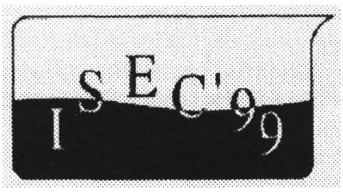
a) Gas phase basicities measured relative to ammonia (821.7 KJ mol^{-1}) taken from Aue (1979).

b) Chemical shift, δ ppm, values are from Pouchert (1983).

Table 5: Gas phase basicities and chemical shifts of the α-methylene protons in water-miscible short chain amines – the effect of branching

REFERENCES

1. Grinstead RR. *Proc.ISEC*, 426, (1967).
2. Eyal AM and Canari R, *Ind. Eng. Chem. Res.*, **34**, 1789, (1995).
3. Reyes A and Scott RM, *J. Phys. Chem.*, **84**, 3600, (1980).
4. Matthies M and Sapper H, *Chem. Phys. Lett.*, **68** (1), 61, (1979).
5. Perrin CL and Fabian MA, *Anal. Chem.*, **68**, 2127, (1996).
6. Chauvel JP, Folkendt MM and True NS, *Mag. Res. Chem.*, **25**, 101, (1987).
7. Grunwald E, Loewenstein A and Meiboom S, *J. Chem. Phys.*, **27** (3), 641, (1957).
8. Loewenstein A and Roberts JD, *Org. Biol. Chem.*, **82**, 2705, (1960).
9. Pouchert CJ, *"The Aldrich Library of NMR Spectra"* ed. II, vol. I and II, Aldrich Chemical Company Inc., Milwaukee, Wisconsin, (1983).
10. Hall HK Jr, *J. Phys. Chem.*, **60**, 63, (1956).
11. March J, *"Advanced Organic Chemistry"* third edition, Ch. 8, Interscience, New York, (1985).
12. Smith JW in Patai S, *"The Chemistry of the Amino Group"* 161, Interscience, New York, (1968).
13. Aue DH and Bowers MT, in Bowers MT *"Gas Phase Ion Chemistry"*, Academic Press, New York, **2**, (1979).
14. Trotman-Dickenson AF, *J. Chem. Soc.*, 1293, (1949).
15. Bohme DK in Patai S, *"The Chemistry of Functional Groups, Supplement F,"* pt. 2, Wiley, New York, 731 (1982).
16. Brauman JI, Blair LK, *J. Am. Chem. Soc.*, **90**, 5636, (1968).
17. Wolf JF, Staley RH, Koppel I, Taagepera M, McIver RT Jr, Beauchamp JL, and Taft, RW, *J. Am. Chem. Soc.*, **99** (16), 5417, (1977).



A STUDY OF THE MOTION OF A SINGLE DROP UNDER THE INFLUENCE OF A PULSED DC ELECTRIC FIELD

PJ Bailes[1], JGM Lee [2] and AR Parsons[1]

[1] Department of Chemical Engineering, University of Bradford, Bradford, BD71DP, UK

[2]Department of Chemical Engineering, University of Newcastle, Newcastle, UK

ABSTRACT

The application of a pulsed DC electric field has been shown to be effective in improving the separation of liquid-liquid dispersions when an aqueous phase is dispersed in an organic phase. The improvement in the rate of separation has been attributed to the formation of dipoles in the aqueous drops caused by the action of the electric field. However, improved separation could also be due to the drops acquiring a charge from the continuous phase. The experimental system consisted of a de-ionised water drop falling vertically through n-dodecane between a pair of parallel plate electrodes, the positive electrode being insulated. A pulsed DC voltage was applied to the electrodes and the drop motion was recorded using a high-speed video camera at 60 frames per second. The voltage was recorded simultaneously with the images so that any correlation between the drop motion and the applied voltage could be observed. Image analysis of a sequence of images yielded the x, y co-ordinates of the drop centre, allowing the drop trajectory to be obtained. Experiments were carried out to investigate the effect of varying the continuous phase conductivity and it was found that an increase in conductivity produced a decrease in the amplitude of the drop motion.

Keywords: electric field (pulsed DC), drop behaviour,

INTRODUCTION

The efficient separation of liquid-liquid dispersions is a necessary feature of solvent extraction operations and in processes such as crude oil dehydration. One way of accelerating the rate of phase disengagement of water-in-oil emulsions using AC fields was first demonstrated in 1911.[1] Since then there have been many advances in the technology including the comparatively recent finding[2] that pulsed DC fields using an insulation coated, high voltage electrode allow higher water fractions to be treated than is the case with other electrical arrangements.

The enhanced separation rate arises from the increased coalescence between drops, which is caused by the applied electric field. The interaction between the applied field and the charge on the drops is complex and poorly understood. One mechanism that is certainly evident is the formation of dipoles within the drop which leads to subsequent attraction and coalescence within the drop population due to dipole polarisation.[3] Alternatively, drops can become charged by contact with separated charges that may be present in the continuous phase. In such circumstances, drops of opposite charge attract each other and coalesce. This mechanism is believed to occur when pulsed DC fields are used with an insulation coated electrode since this promotes charge separation. Experimental work with different pulsation frequencies has shown here that maximum available charge density correlates with optimum liquid phase separation.[4]

From the foregoing it is apparent that enhanced drop coalescence can be the result of drops carrying a net charge migrating towards each other under the influence of an applied field. However, the enhanced coalescence can also be caused by an interaction between induced dipoles on drops that do not carry a net charge. In the latter case the drops would not be expected to migrate in a parallel field. The existence of a net charge can therefore be deduced if the drop is observed to migrate when under the influence of the field. In order to better understand this situation it is helpful to study a single drop as it falls through an insulating liquid to which an electric field is applied.

The work presented below covers experiments carried out using single water drops in a continuous dodecane phase. The aim of these experiments was to investigate the effect of conductivity, applied voltage and pulse frequency on the motion of a single drop.

© 2000 Society of Chemical Industry

EXPERIMENTAL

Experiments were carried out using pure n-dodecane (supplied by Avocado) as the continuous phase; the conductivity was altered by adding Stadis 425 (an antistatic additive supplied by Associated Octel Company Ltd). De-ionised water was used to form the drops.

The apparatus is illustrated in figure 1. The experimental cell consists of 2 parallel electrodes. The positive electrode is a mercury filled, cuboid hollow, insulated by a 3.1mm layer of Perspex. The negative electrode is a brass plate. The temperature of the dodecane is controlled between 25 and 27°C by circulating water through an external jacket.

The drop is formed from a brass monofilament (diameter = 0.06mm) and positioned across the width of the cell (horizontal position) by means of 2 concentric, brass, cylinders. The monofilament, attached to the inner cylinder, is first dipped in water and then in the dodecane, as it is removed a drop is released into the dodecane. The outer cylinder keeps the monofilament in position. Using this method, drops of between 150 and 500mm diameter can be formed and positioned within a range of 1mm across the width of the cell. The drop positioning apparatus is earthed to prevent the drop becoming charged as it is formed.

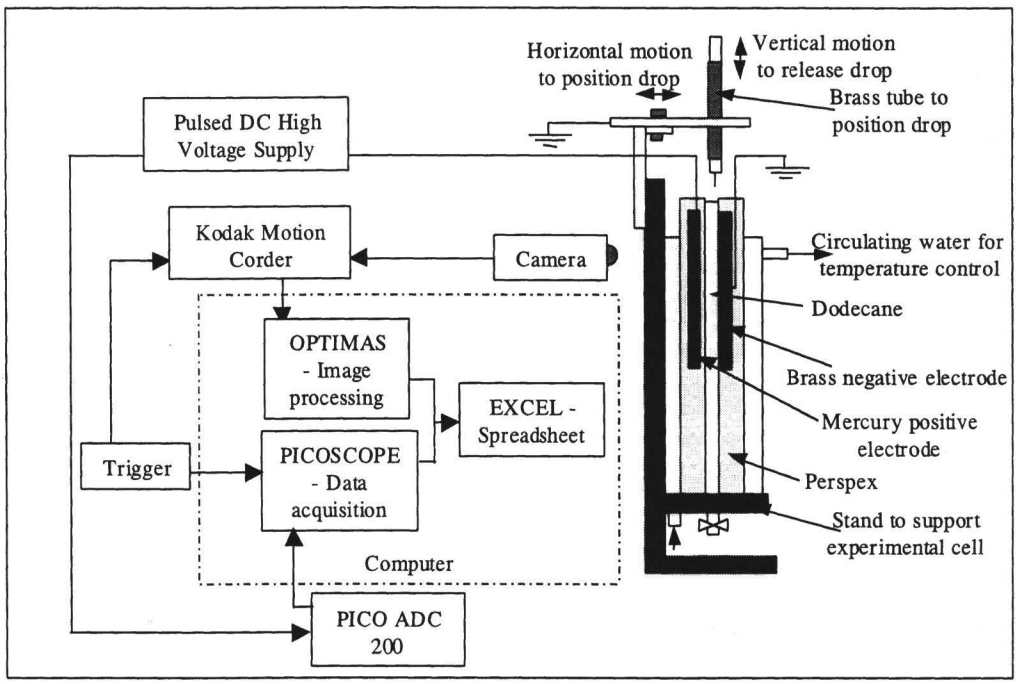


Figure 1. Apparatus for single drop experiments

The drop falls under gravity and its motion was filmed for a portion of its fall using a video camera. For the work reported here, a 50mm focal length lens combined with a 25mm extension tube was used to give a calibrated frame width of 11mm. The camera is connected to a Kodak Motion Corder Analyzer (Model 1000B) which has a 1086 frame memory, a resolution of 640 by 480 pixels and a trigger facility. A film rate of 60 f.p.s. was used. The cell was backlit using a Teflon filter and a 75 Watt halogen light to obtain the best possible image contrast.

The sequence of images stored on the Motion Corder was transferred to OPTIMAS, an image analysis package. The images were calibrated by means of a clear plastic ruler positioned in the same plane as the drop positioning apparatus at the start of each set of experiments. After enhancing each image, a circle was fitted to the drop and the required information (namely the drop centre x, y co-ordinates and diameter) was collected and exported to an EXCEL spreadsheet. The time of each frame

was noted and added to the spreadsheet. Typically a drop motion sequence would consist of 25 to 35 images and last for 1 to 2 seconds. The initial position of the drop for each set of experiments was found by recording the trajectory of 10 drops with no field applied and taking the average x co-ordinate of the drop centres.

The sequence of images stored on the Motion Corder was transferred to OPTIMAS, an image analysis package. The images were calibrated by means of a clear plastic ruler positioned in the same plane as the drop positioning apparatus at the start of each set of experiments. After enhancing each image, a circle was fitted to the drop and the required information (namely the drop centre x, y co-ordinates and diameter) was collected and exported to an EXCEL spreadsheet. The time of each frame was noted and added to the spreadsheet. Typically a drop motion sequence would consist of 25 to 35 images and last for 1 to 2 seconds. The initial position of the drop for each set of experiments was found by recording the trajectory of 10 drops with no field applied and taking the average x co-ordinate of the drop centres.

The voltage circuit used to produce the pulsed DC field is described by Bailes and Larkai.[2] A square waveform was used with a mark/space ratio of one. An ADC 200 analogue to digital converter with PICOSCOPE software (supplied by Pico Technology Ltd) was used to record the voltage over a set time period and allowed the data (time and voltage) to be exported to an EXCEL spreadsheet. PICOSCOPE has a BNC trigger facility that was connected to the Motion Corder trigger to allow both instruments to begin recording simultaneously; the drop motion could then be compared with the action of the pulsed field.

RESULTS AND DISCUSSION

Figure 2 is a plot of the drop position against time. The edge of the Perspex which insulates the positive electrode lies along the y = 0mm line and the earth electrode lies on the y = 10.6mm line. Superimposed over the drop position data is the voltage applied across the cell. It can be clearly seen from Figure 2 that the drop moves as the voltage is pulsed on and off, demonstrating that the drop has a net charge. The amplitude of the motion during the 'off' period of the voltage pulse is greater than that during the 'on' period causing the drops to move towards the earth electrode. At present we cannot say which mechanism is responsible for the drop becoming charged. The possible mechanisms include drop charging during formation, stripping away of the electrical double layer surrounding the drop as it falls,[5] or contact charging with space charges in the dodecane.

The next comparison, shown in figure 3, is for drops of approximately the same size, moving through the cell under the same applied electric field conditions, with only the conductivity of the dodecane being changed by adding varying amounts of an antistatic additive. It can be seen that as the conductivity of the dodecane increases, the amplitude of the motion of the drops decreases.
The explanation for this relies on the model developed by Bailes[4] to explain the existence of an optimum pulsation frequency for separating water in oil dispersions using a pulsed DC coalescer. The model assumes that the electrical behaviour of the dispersion layer and the layer of Perspex insulating the positive electrode is analogous with the behaviour of two sets of a large resistor and capacitor in parallel, connected in series. If pure dodecane is used as the continuous phase then the conductivity of the dodecane is less than the conductivity of the Perspex layer. When applying a steady voltage across the cell, the majority of the voltage drop occurs across the dodecane creating a strong electric field. If the conductivity of the dodecane is increased so that it is greater than that of the Perspex, then under a constant voltage the stronger electric field will be in the Perspex.

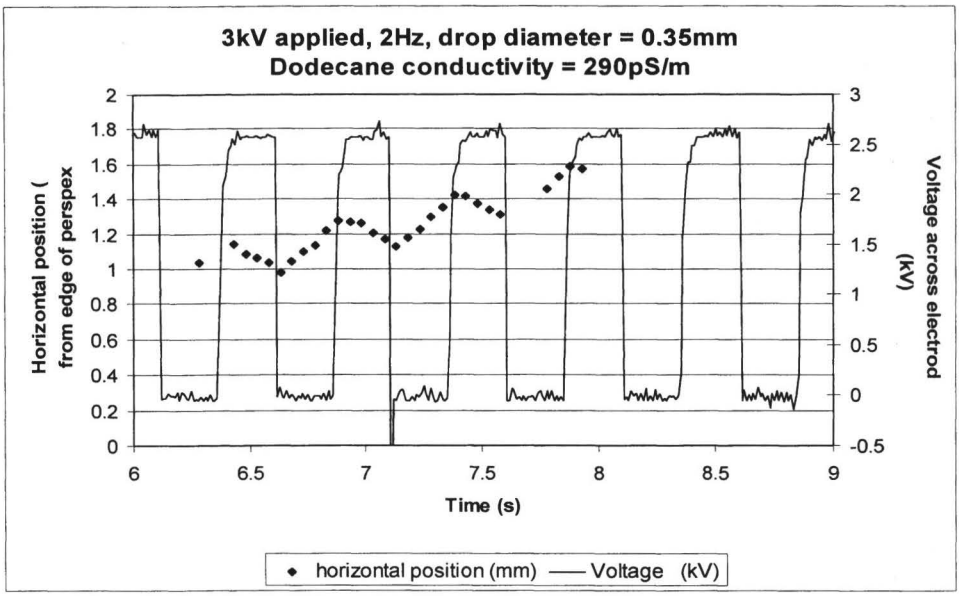


Figure 2 Drop position and applied voltage as a function of time

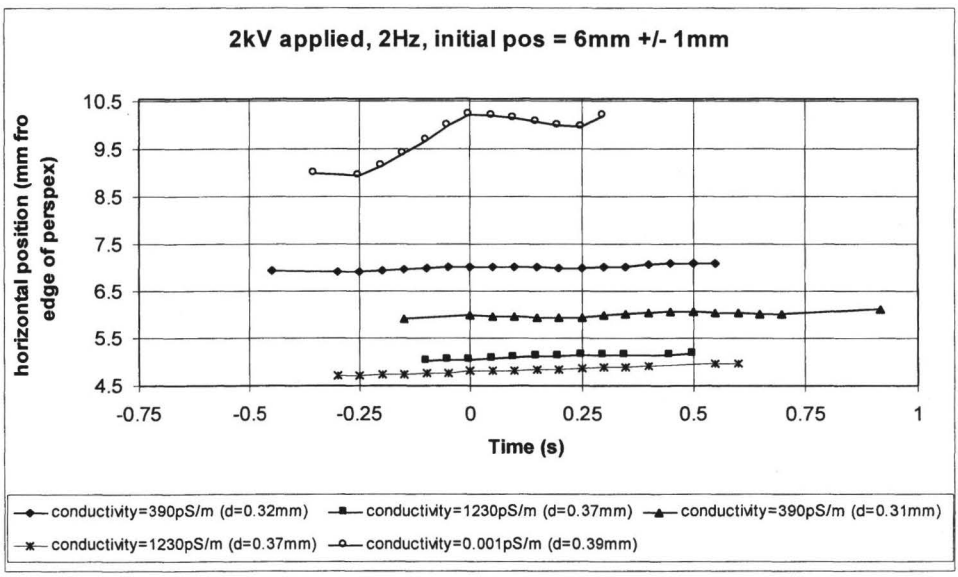


Figure 3 Effect of continuous phase conductivity on drop motion

Drop motion is caused by an electrostatic force acting on the drop, the magnitude of this force is equal to the charge on the drop multiplied by the electric field strength. Figure 4(a) is a comparison of the drop motion when there is no applied field and when there is a constant applied field for pure dodecane. In comparison figure 4(b) shows the drop motion with no field and a constant field for

dodecane whose conductivity is greater than that of the Perspex. It is clear that in the pure dodecane case, the magnitude of the electrostatic force is greater as the drop moves further, indicating that the electric field is stronger for the pure dodecane under a constant applied field.

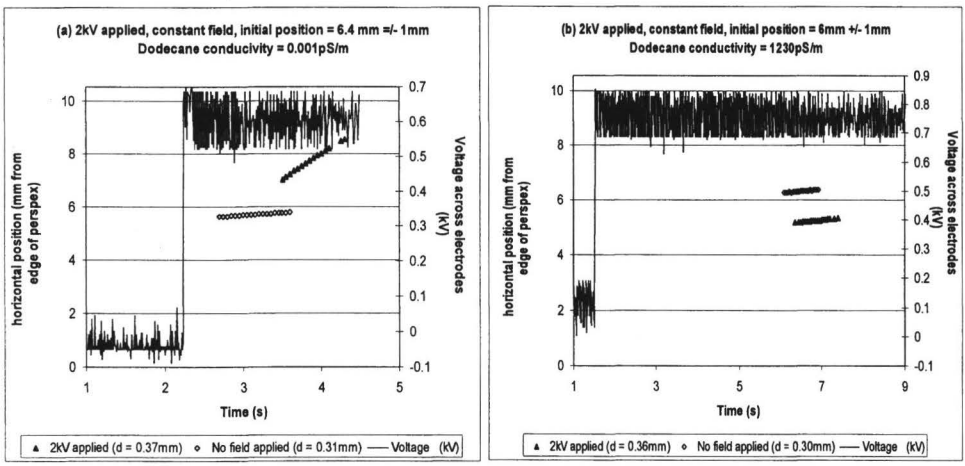


Figure 4 Drop motion in a constant field

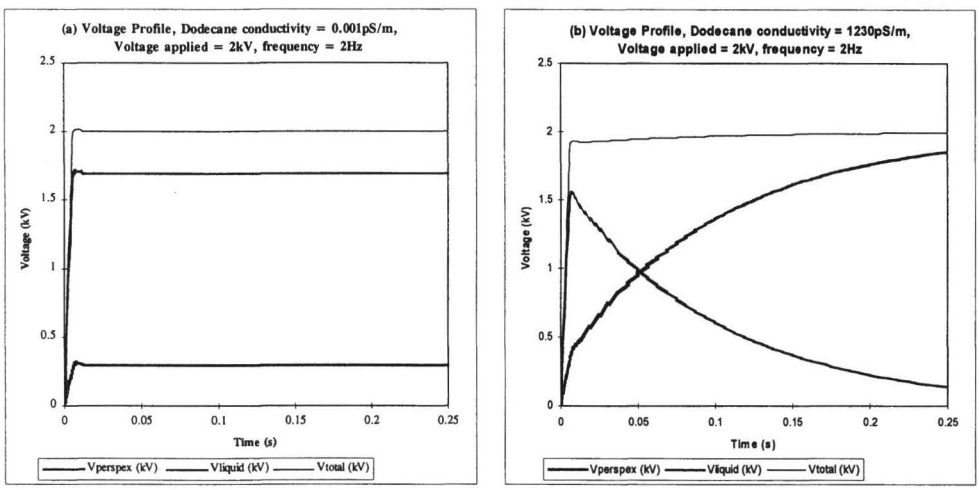


Figure 5 Voltage profile across experimental cell during 'on' period

When the voltage is pulsed on and off the situation changes. Figure 5(a) shows the voltage drop across the liquid and Perspex layers for pure dodecane during the 'on' period of the pulse. It shows that soon after the voltage is switched on, a large voltage drop across the pure dodecane is established implying that there is a strong electric field in the liquid layer. Figure 5(b) shows the 'on' pulse when the liquid layer conductivity is greater than that of the Perspex. In this case the voltage drop across the liquid layer is initially large, but decays with time towards its constant field value.

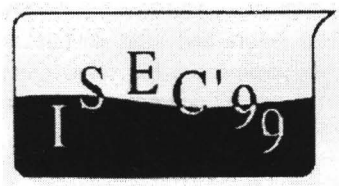
This explains why the drops in the pure dodecane move more when the voltage is pulsed, as the magnitude of the electrostatic force will be greater due to the stronger field that prevails over the 'on' pulse. For the case where the dodecane conductivity is greater than the Perspex conductivity, the field strength in the liquid is only high at the start of the pulse so the drop motion is consequently less as shown in figure 3.

ACKNOWLEDGEMENTS

The authors wish to thank the Engineering and Physical Sciences Research Council for their financial support and Amerada Hess Ltd, BP Exploration, NATCO London Inc, Shell Internationale and Texaco Britain Ltd for their financial support and guidance during the course of this work.

REFERENCES

1. Cottrell FG and Speed JB, *US Patent 987115*, (1911)
2. Bailes PJ and Larkai SKL, Trans IChemE, **59(4)**, 229, (1981)
3. Taylor SE, Trans IChemE, **74**, Part A, July 1996
4. Bailes PJ, Trans IChemE, **73**, Part A, July 1995
5. Klinkenberg A and van der Minne JL, *"Electrostatics in the Petroleum Industry"*, Elsevier Publishing Company, Part II, Chapter VI, 64, (1958)



SINGLE DROP COALESCENCE – EXPERIMENT AND SIMULATION

A Eckstein and A Vogelpohl
Institut für Thermische Verfahrenstechnik, Technical University Clausthal, Leibnizstraße 15 38678 Clausthal-Zellerfeld, Germany

ABSTRACT
The complex behaviour of drop swarms in liquid-liquid extraction columns can be described with a simplified drop population balance model. The required parameters for the characterisation of drop velocity, mass transfer, break-up and coalescence have to be obtained from single drop experiments in laboratory scale apparatus. These single drop parameters are determined in dependence of the drop size, pulsation energy input and the column equipment, e.g. sieve-plates or structured packings.

Keywords: droplet breakage, droplet coalescence, droplet swarms, mass transfer, column

INTRODUCTION

Until now the safe construction of an extraction column requires extensive pilot-scale experiments that are quite costly. To minimise these costs, experiments may be carried out on a lab-scale or pilot-scale. For this purpose several "standard apparatus" were developed at the Institut für Thermische Verfahrenstechnik, e.g. for the determination of single drop velocity,[1,2] drop break-up[2,3] and mass transfer.[4] The single drop parameters were implemented successfully in a simplified drop population balance model for coalescence inhibited liquid systems.[3,4] These "standard apparatus" have now been supplemented by an apparatus for determining coalescence parameters.

Drop Coalescence

Two parameters exist to describe the coalescence process: the coalescence time and the coalescence probability. The coalescence time is the time from drop collision till drop fusion. The number of drop fusions out of the number of drop collisions is the coalescence probability. Several experimental set-ups have been implemented to study the coalescence of drops.

For the measurement of coalescence time the problem is often reduced to the collision of one drop with a plane interface.[5,6,7] The disturbance caused by the drop on the interface due to collision is detected and its duration is defined as coalescence time. The measurement of coalescence probability is investigated in pilot-scale extraction columns by addition of a tracer into a fraction of drops entering the column.[8,9] The drop size and tracer distributions are measured at column entrance and exit. From this the coalescence parameters can be calculated with the knowledge of single drop break-up parameters. But this method uses a tracer that can influence the interface activities concerning the coalescence behaviour and the pilot-scale experiments are costly.

To develop a measurement cell for the coalescence of single drops it is necessary to know where the coalescence takes places in an extraction column. Investigations of sieve-plate extraction columns have shown that coalescence takes place in the drop accumulation zone directly underneath the sieve-plates.[3] The place of coalescence in structured packings was not detectable in observations of a glass packing with a high speed video camera.[2]

EXPERIMENTAL

The experimental set up to determine the coalescence probability is shown in figure 1. The apparatus consists mainly of a cone where a swarm of drops with the same diameter d_S and the number n is held in place by a counter-current flow of continuous phase. The drops are produced with a precise dosing system. A single drop with the diameter d_E rises into and through the drop swarm

© 2000 Society of Chemical Industry

because of its higher rising velocity v_T ($d_E > d_S$). The size of the single drop after contact with the swarm d_C is measured with a photoelectric suction probe[10]. The drop sizes before and after contact are compared. If $d_C \neq d_E$, coalescence has taken place, if $d_C = d_E$, no coalescence has taken place. Observation of 50 single drops gives a coalescence probability $K_c = f(d_E, d_S, n)$, dependent on the size of the single drop and the swarm drop and the number of drops in the swarm.

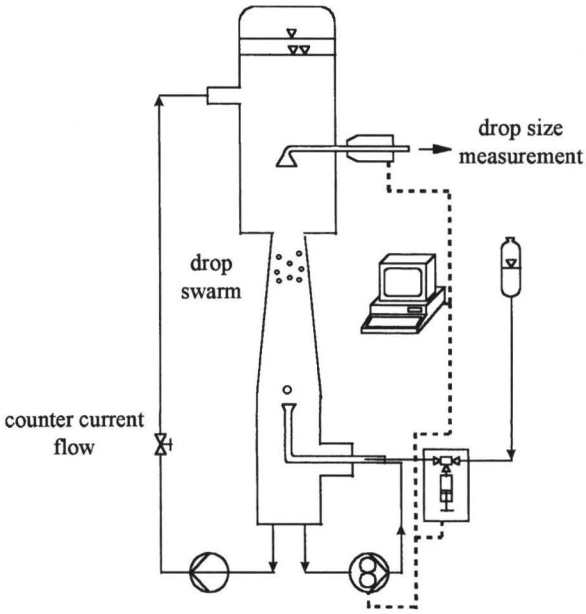


Figure 1. Experimental set up for the determination of the coalescence probability

The experiments were carried out with the liquid system n-butylacetate (dispersed) / water. The number of drops in the swarm was varied from 20 up to 40. The number is limited by coalescence events of the swarm drops among one another.

RESULTS AND DISCUSSION

Figure 2 shows the coalescence probability dependent on the number of drops in the swarm for a single drop diameter of $d_E = 3{,}5$ mm and a drop swarm diameter of $d_S = 3{,}0$ mm.

In general one expects an increasing coalescence probability with increasing number of drops in the swarm. This is confirmed for 20 and 30 drops. At higher numbers the drops start to influence one another in the swarm. The swarm extends over a larger part of the cone, so the drop density becomes lower with a higher number of drops.

An equivalent hold-up of dispersed phase can be calculated with the measurement of the volume taken by the drop swarm and the number of drops. Figure 3 shows the coalescence probability dependent on the hold-up for a single drop diameter of $d_E = 3{,}5$ mm.

The trend of increasing coalescence probability with increasing hold-up is confirmed.
The number of data is still to small to present correlations for $K_c = f(d_E, d_S, n)$ and implement them into the drop population model. But the first experiments show the this measurement cell is suited for the observation of coalescence of single drops within a drop swarm.

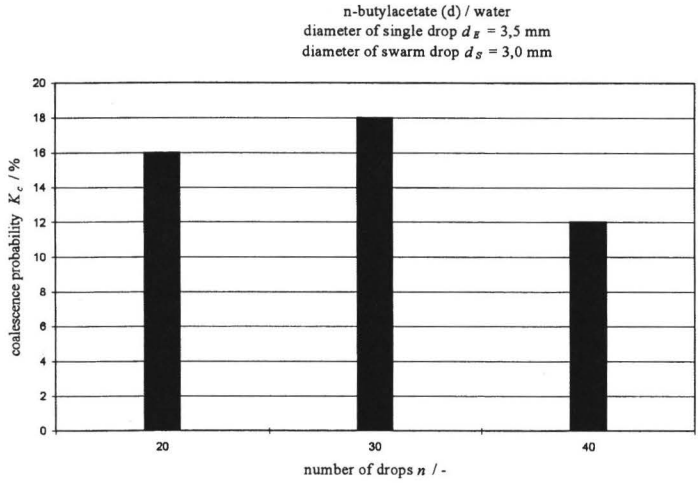


Figure 2. Coalescence probability vs. the number of drops in the swarm

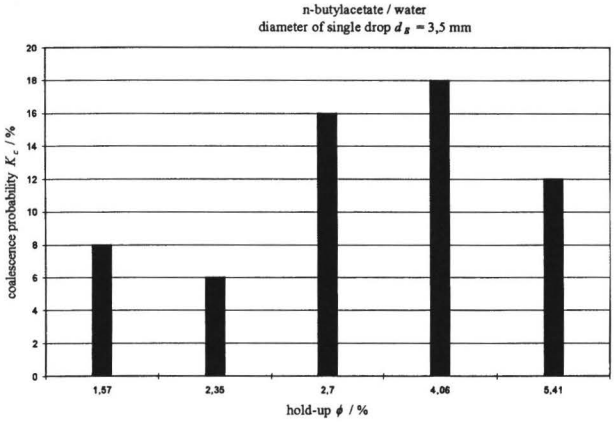


Figure 3. Coalescence probability vs. hold-up

Besides the experimental investigation of the coalescence probability a simulation with the simplified drop population model was done.[11] The model was extended by the coalescence parameters. They were changed until the best fit was achieved with the data from two pilot-scale pulsed sieve-plate extraction columns. Figure 4 shows measured and calculated drop size distributions as a function of the column height for the two columns and the liquid system n-butylacetate / water.

The results of the simulation are:

the coalescence probability increases with increasing pulsation intensity for the column with the smaller diameter, the column with the larger diameter shows no dependency on the pulsation intensity;

the coalescence probability in the column with the smaller diameter is higher compared to the column with the larger diameter;

the coalescence probability decreases with increasing drop diameter.

These results will be checked with the newly developed coalescence cell.

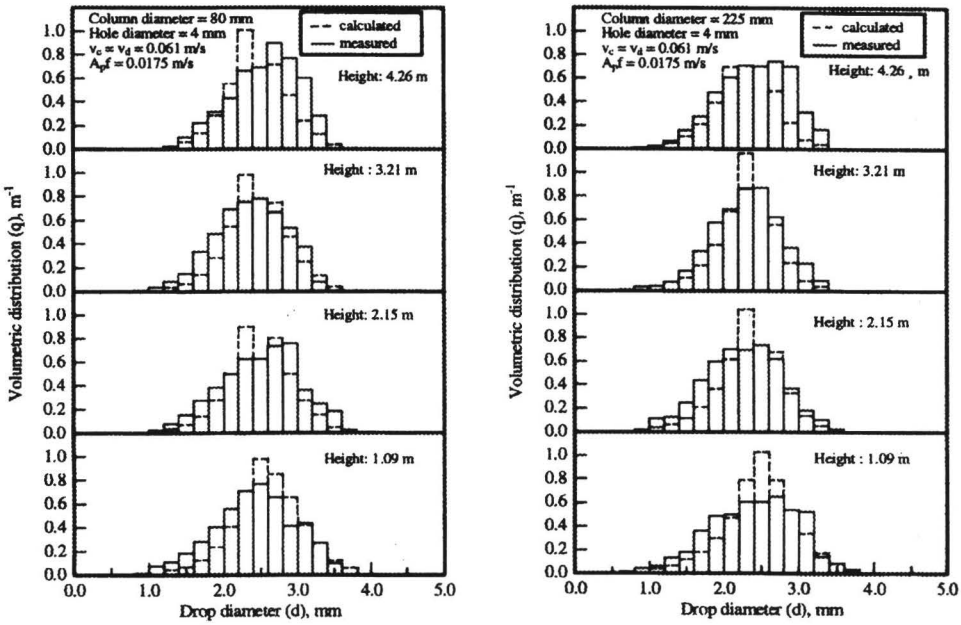


Figure 4. Measured and calculated drop size distributions vs. column height for two pulsed sieve-plate extraction columns with different column diameter

CONCLUSIONS

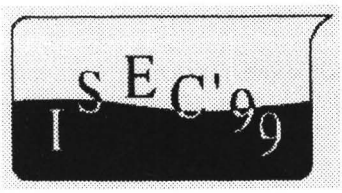
As the results show it is possible to measure the phenomena of single drop coalescence with the developed coalescence cell. More experimental data is needed to implement it into the drop population model. With this further single drop set up the aim, to simulate a whole extraction column with laboratory-scale experiments, becomes closer.

NON-STANDARD NOMENCLATURE

d_C size of single drop after contact with the drop swarm; d_E size of single drop
d_S size of drops in the swarm; K_c coalescence probability

REFERENCES

1. Hussain AA, Liang T-B and Slater MJ, *Chem. Eng. Res.*, 66, (1988)
2. Leu JT, *Dissertation*, Technical University of Clausthal, (1995)
3. Haverland H, *Dissertation*, Technical University of Clausthal, (1988)
4. Hoting B, *Dissertation*, Technical University of Clausthal, (1996)
5. Gourdon C and Casamatta G, *Chem. Eng. Sci.*, **46**, 11, (1991)
6. Aderangi N and Wasan DT, *Chem. Eng. Comm.*, 132, (1995)
7. Dähler A, Term Paper, Technical Univ. of Clausthal in co-operation with Melbourne University (1996)
8. Hamilton JA and Pratt HRC, *AIChE J.*, **30**, 3, (1984)
9. Weiss C, Köhler V and Marr R, *AIChE J.*, **43**, 5, (1997)
10. Pilhofer T and Miller H-D, *Chem.-Ing.-Tech.*, **44**, 5, (1972)
11. Mohanty S and Vogelpohl A, *Chem. Eng. Proc.*, 36, (1997)



DIFFUSIVITIES FOR MULTICOMPONENT MASS TRANSFER CALCULATIONS

AR Uribe-Ramírez[1] and WJ Korchinsky[2]

[1]Facultad de Química, Universidad de Guanajuato, Col. Noria Alta s/n, 36050 Guanajuato, Gto., México.

[2]Department of Chemical Engineering, UMIST, PO Box 88, Manchester M60 1QD, UK.

ABSTRACT

In previous works[1,2] the authors presented an alternative solution to the problem of mass transfer in single drops for single-component and multi-component systems for the intermediate Reynolds number range ($10 \leq Re \leq 250$). In this work, the problem of calculating the diffusivity matrix using the Maxwell-Stefan approach and the Modified UNIFAC Activity Coefficient Model to calculate the thermodynamic factors is addressed.

Keywords: Maxwell-Stefan, multicomponent mass transfer, diffusivity, UNIFAC model.

INTRODUCTION

The problem of multi-component mass transfer in liquid drops is of interest from the theoretical and the practical point of view. Many attempts have been made using both approaches, but so far the success has been restricted to some simplified situations. On one hand, the theoretical models resulting from mass balances in the drop are very complicated due to the fact that diffusive, convective and transient terms appear in the variation equation of mass transfer. Adding to this difficulty, the presence of more than one solute being transferred between the phases result in coupled systems of partial differential equations, which are possible to solve only when the matrix of diffusivities is constant. Uribe-Ramirez[3] and Uribe-Ramírez and Korchinsky[2] presented one possible solution. They obtained a solution using the property of a constant, square matrix, which can be diagonalized using the so-called linearisation theory proposed by Toor[4], and Stewart and Prober.[5] An alternative solution was presented by Von Reden.[6] which uses the mass transfer model proposed by Slater,[7] generalised to multi-component systems. In all the previous works, the authors claim that their models closely fit the experimental data. However, there is still much work to be done in order validate these models.

The exact solution of the multi-component problem in liquid systems cannot be obtained by analytical methods, due to the concentration dependence of the diffusivity matrices, which result in non-linear, coupled partial differential equations. In this case, a numerical method of solution can be tried. However, a first look into the solution can be obtained by considering that the diffusivity matrices for the liquid systems are constant, which is approximately true for small concentration changes.[8]

To calculate the matrix of diffusivities using the Maxwell-Stefan approach, the thermodynamic factors have to be calculated using an activity coefficient model. Taylor and Krishna[8] carried out the calculation of these factors using some activity coefficient models: UNIQUAC, Wilson, NRTL. However, these models require experimental parameters, which are not always available, particularly for multi-component systems. In this case, a predictive model can be used instead, such as the Modified UNIFAC Activity Coefficient Model,[9] which is the one used in this work.

© 2000 Society of Chemical Industry

THEORY

The generalised Fick's Law for multi-component mass transfer can be written in matrix form as

$$\mathbf{J} = -\mathbf{D} \cdot \nabla \mathbf{c} \tag{1}$$

where **J** is the vector of diffusive fluxes, **D** is the matrix of multi-component diffusivities and $\nabla \mathbf{c}$ is the vector of concentration gradients. The matrix of multi-component Fick diffusivities can be written as

$$\mathbf{D} = \mathbf{B}^{-1}\,\Gamma \tag{2}$$

The matrix Γ is the matrix of thermodynamic factors, **B** is the matrix of Maxwell-Stefan diffusivities, whose elements are given by

$$B_{i,i} = \frac{x_i}{\mathcal{D}_{i,n}} + \sum_{\substack{k=1 \\ i \neq k}}^{n} \frac{x_k}{\mathcal{D}_{i,k}} \quad \text{and} \quad B_{i,j} = -x_i\left(\frac{1}{\mathcal{D}_{i,j}} - \frac{1}{\mathcal{D}_{i,n}}\right) \tag{3}$$

x_i is the mole fraction of species i and $\mathcal{D}_{i,j}$ is the Maxwell-Stefan diffusion coefficient of the binary pair i, j. The calculation of the thermodynamic factors is a cumbersome step, because the derivatives of the activity coefficients are required. The Modified UNIFAC Model, Dortmund Version,[9] is written as

$$\ln\gamma_i = \ln\gamma_i^{\,C} + \ln\gamma_i^{\,R} \tag{4}$$

$$\ln\gamma_i^{\,C} = 1 - V'_i + \ln V'_i - 5q_i\left(1 - \frac{V_i}{F_i} + \ln\left(\frac{V_i}{F_i}\right)\right) \tag{5}$$

$$\ln\gamma_i^{\,R} = \sum_k \nu_k^{(i)}\left(\ln\alpha_k - \ln\alpha_k^{(i)}\right) \tag{6}$$

$$V'_i = \frac{r_i^{3/4}}{\sum_k x_k r_k^{3/4}} \qquad V_i = \frac{r_i}{\sum_k x_k r_k} \qquad F_i = \frac{q_i}{\sum_k x_k q_k}$$

and the parameters r_i and q_i are defined in the original reference,[9] $\nu_k^{(i)}$ is the number of groups of type k in the molecule i. α_k is the activity coefficient of group k in the actual mixture and $\alpha_k^{(i)}$ is the activity coefficient of group k in a pure liquid formed with only molecules of type i. They are given by the expressions

$$\ln\alpha_k = Q_k\left[1 - \ln\left(\sum_m \theta_m \Psi_{m,k}\right) - \sum_m \frac{\theta_m \Psi_{k,m}}{\sum_n \theta_n \Psi_{n,m}}\right] \qquad \theta_m = \frac{Q_m X_m}{\sum_n Q_n X_n}$$

$$X_m = \frac{\sum_n \nu_m^{(n)} x_n}{\sum_n \sum_o \nu_o^{(n)} x_n} \qquad \Psi_{n,m} = \exp\left(-\frac{a_{n,m} + b_{n,m}T + c_{n,m}T^2}{T}\right)$$

The thermodynamic factors are given by the following expression,[8]

$$\Gamma_{ij} = \delta_{ij} + x_i \left.\frac{\partial \ln\gamma_i}{\partial x_j}\right|_{T,P,\Sigma} \tag{7}$$

where $\delta_{i,j} = \begin{cases} 1 \text{ if } i = j \\ 0 \text{ if } i \neq j \end{cases}$ and $\left.\frac{\partial \ln\gamma_i}{\partial x_j}\right|_{\Sigma} = \left.\frac{\partial \ln\gamma_i}{\partial x_j}\right|_{\Sigma} - \left.\frac{\partial \ln\gamma_i}{\partial x_n}\right|_{\Sigma}$ (8)

The symbol Σ is used to indicate that the differentiation of $\ln\gamma_i$ with respect to the mole fraction x_j is to be carried out while keeping constant the mole fractions of all other species, except the n^{th}. The symbol Σ is shorthand notation to emphasise that the mole fractions of all species, except the j^{th}, are kept constant while performing the differentiation. This differentiation will be performed at constant

temperature (T) and pressure (P); therefore, these subscripts will be omitted for the sake of simplicity in the subsequent calculations.

For the Modified UNIFAC (Dortmund) Model,[9] the partial derivatives in Equation (8) can be written, using Equation (4), as

$$\left.\frac{\partial \ln \gamma_i}{\partial x_j}\right|_{\Sigma} = \left.\frac{\partial \ln \gamma_i^{C}}{\partial x_j}\right|_{\Sigma} + \left.\frac{\partial \ln \gamma_i^{R}}{\partial x_j}\right|_{\Sigma} \tag{9}$$

The first term on the right hand side of Equation (9) can be obtained from Equation (5) as

$$\left.\frac{\partial \ln \gamma_i^{C}}{\partial x_j}\right|_{\Sigma} = V'_j\left(V'_i - 1\right) + 5q_i\left(V_j - F_j\right)\left(1 - \frac{V_i}{F_i}\right) \tag{10}$$

The second term requires more manipulation. From Equation (6), it becomes

$$\left.\frac{\partial \ln \gamma_i^{R}}{\partial x_j}\right|_{\Sigma} = \frac{\partial}{\partial x_j}\left(\sum_k \nu_k^{(i)} \ln \alpha_k\right)_{\Sigma} - \frac{\partial}{\partial x_j}\left(\sum_k \nu_k^{(i)} \ln \alpha_k^{(i)}\right)_{\Sigma} \tag{11}$$

therefore

$$\left.\frac{\partial \ln \gamma_i^{R}}{\partial x_j}\right|_{\Sigma} = -\sum_k \nu_k^{(i)} Q_k \left[\frac{P_{kj}}{P_k} + \sum_m \Psi_{km}\frac{\theta_m}{P_m}\left(\frac{\theta_{mj}}{\theta_m} - \frac{P_{mj}}{P_m}\right)\right] \tag{12}$$

where the following parameters are defined as

$$P_k = \sum_m \theta_m \Psi_{mk} \qquad \theta_{mj} = \frac{\partial \theta_m}{\partial x_j} = \theta_m\left(\frac{X_{mj}}{X_m} - \frac{\sum_n Q_n X_{nj}}{\sum_n Q_n X_n}\right)$$

$$X_{mj} = \frac{\partial X_m}{\partial x_j} = X_m\left(\frac{\nu_m^{(j)}}{\sum_n \nu_m^{(n)} x_n} - \frac{\sum_o \nu_o^{(j)}}{\sum_n \sum_o \nu_o^{(n)} x_n}\right) \qquad P_{kj} = \frac{\partial P_k}{\partial x_j} = \sum_m \theta_{mj} \Psi_{mk}$$

Finally, substitution of Equations (10) and (12) into (9) yields

$$\left.\frac{\partial \ln \gamma_i}{\partial x_j}\right|_{\Sigma} = V'_j\left(V'_i - 1\right) + 5q_i\left(V_j - F_j\right)\left(1 - \frac{V_i}{F_i}\right) - \sum_k \nu_k^{(i)} Q_k \left[\frac{P_{kj}}{P_k} + \sum_m \Psi_{km}\frac{\theta_m}{P_m}\left(\frac{\theta_{mj}}{\theta_m} - \frac{P_{mj}}{P_m}\right)\right] \tag{13}$$

The thermodynamic factors are given by substitution of Equation (13) into Equation (8) and this into Equation (7). It should be noted that the matrix in Equation (7) has $(n\text{-}1) \times (n\text{-}1)$ elements.

SAMPLE CALCULATIONS

One proposed liquid system for mass transfer studies is the quaternary system acetone-phenol-water-toluene. This system was recommended by von Reden, et al.[10] Uribe-Ramirez and Korchinsky[2] performed multicomponent mass transfer calculations using this system. The initial, equilibrium and average concentrations at 293.15 K are given in Table 1.

The mass fractions in the continuous phase are assumed to remain constant. The mass fractions of the solutes in the dispersed phase are assumed to reach equilibrium with those in the continuous phase at the end of the mass transfer process. When the binary Maxwell-Stefan diffusivities are not available from experimental data, they must be predicted. Taylor and Krishna[8] recommended the prediction, firstly, of these diffusivities at infinite dilution of the solute by using a

suitable mathematical model. One of the best models for the prediction of the diffusivities in most liquid systems is the well-known equation of Wilke and Chan,[11] given as

$$Đ^{\infty}_{i,j} = 7.4 \times 10^{-8} \frac{T\sqrt{\phi_j M_j}}{\mu_j \tilde{V}_i^{0.6}} \tag{14}$$

where $Đ^{\infty}_{i,j}$ is the infinite-dilution diffusion coefficient of the solute i into the solvent j in cm^2/s, T is the temperature in K, M_j is the mole weight of j, μ_j is the viscosity of j in cP, $\tilde{V}_i$ is the molar volume of i in cm^3/mole, and ϕ_j is an association factor for the solvent j, which can be found in the original reference.[11]

Substance	Dispersed phase mass fractions			Continuous phase mass fractions
	Initial	Equilibrium	Average	
Acetone	0	0.02449	0.012245	0.023
Phenol	0	0.01751	0.008755	0.008
Water	0	0	0	0.969
Toluene	1	0.958	0.979	0

Table 1 Mass fractions of the chemical species used for the calculations

At higher concentrations, the Maxwell-Stefan diffusivities can be calculated by the following interpolating formula[8]

$$Đ_{i,j} = (Đ^{\infty}_{i,j})^{(1+x_j-x_i)/2} (Đ^{\infty}_{j,i})^{(1+x_i-x_j)/2} \tag{15}$$

The matrix **B** can be calculated from Equation (3). The mass distribution coefficients for the solutes acetone and phenol are 1.06 and 2.19, respectively.

The matrices of thermodynamic factors and diffusion coefficients are assumed constant over the diffusion path; therefore, it is convenient to calculate these matrices at the average concentrations. The average concentrations are given in Table 1. The matrices of thermodynamic factors are calculated from Equation (7) as

$$\Gamma_1 = \begin{bmatrix} 0.99029 & -0.215571 \\ -0.096553 & 0.945302 \end{bmatrix} \text{ and } \Gamma_2 = \begin{bmatrix} 0.956567 & -0.220592 \\ -0.04763 & 0.95242 \end{bmatrix}$$

The diffusivity coefficients at infinite dilution, calculated from Equation (14) are

$$Đ_1^{\infty} = \begin{bmatrix} 0 & 0.177 & 2.62 \\ 3.544 & 0 & 2.381 \\ 3.142 & 0.142 & 0 \end{bmatrix} \times 10^{-9} \frac{m^2}{s} \text{ and } Đ_2^{\infty} = \begin{bmatrix} 0 & 0.177 & 1.066 \\ 3.544 & 0 & 0.969 \\ 9.099 & 0.412 & 0 \end{bmatrix} \times 10^{-9} \frac{m^2}{s}$$

Using Equation (15), the matrices of Maxwell-Stefan diffusion coefficients for concentrated mixtures at the average compositions, given in Table 1, are

$$Đ_1 = \begin{bmatrix} 0 & 0.804 & 2.631 \\ 0.804 & 0 & 2.262 \\ 2.631 & 2.262 & 0 \end{bmatrix} \times 10^{-9} \frac{m^2}{s} \text{ and } Đ_2 = \begin{bmatrix} 0 & 0.798 & 1.085 \\ 0.798 & 0 & 0.965 \\ 1.085 & 0.965 & 0 \end{bmatrix} \times 10^{-9} \frac{m^2}{s}$$

The B-matrices, calculated from Equation (3) are

$$B_1 = \begin{bmatrix} 3.875 & -0.167 \\ -0.068 & 4.575 \end{bmatrix} \times 10^{8} \frac{s}{m^2} \text{ and } B_2 = \begin{bmatrix} 9.224 & -0.024 \\ -0.0034 & 10.382 \end{bmatrix} \times 10^{8} \frac{s}{m^2}$$

Using Equation (2) the matrices of multicomponent diffusion coefficients in the molar reference frame are given by

$$Dn_1 = \begin{bmatrix} 2.548 & -0.468 \\ -0.173 & 2.059 \end{bmatrix} \times 10^{-9} \frac{m^2}{s} \quad \text{and} \quad Dn_2 = \begin{bmatrix} 1.037 & -0.237 \\ -0.046 & 0.917 \end{bmatrix} \times 10^{-9} \frac{m^2}{s}$$

Finally, the matrices of multicomponent diffusivities in the mass average reference frame are given by

$$D_1 = \begin{bmatrix} 2.55 & -0.291 \\ -0.276 & 2.058 \end{bmatrix} \times 10^{-9} \frac{m^2}{s} \quad \text{and} \quad D_2 = \begin{bmatrix} 1.038 & -0.142 \\ -0.075 & 0.917 \end{bmatrix} \times 10^{-9} \frac{m^2}{s}$$

These matrices can be used for multicomponent mass transfer calculations in liquid-liquid systems. Some results for two different systems using the method of calculation reported in this work are presented in Table 2. In this Table, the theoretical results are compared with the experimental results reported in two different works.[13,14]

The results presented in Table 2 show the discrepancies between the predicted and the experimental results. Larger errors are found in the system acetone-benzene-methanol. However, the benzene-methanol and acetone-methanol systems are associated binaries; the method does not perform well for such systems.[12] The errors are slightly lower than those calculated using the NRTL activity coefficient model, presented by Kooijman and Taylor.[12] However, the UNIFAC model does not need experimental values of the parameters, which is an advantage over other activity coefficient models. For this system, the maximum overall error is 27% with a maximum diagonal error of 50.6%. For the system acetone-benzene-carbon tetrachloride the maximum overall error is 8.7% with a maximum diagonal error of 10.5%. The direction of the off-diagonal coefficients is well predicted in all cases, except in one of them, for the system acetone-benzene-carbon tetrachloride at x_1=0.1497 and x_2=0.6984, where $D_{1,2}$ experimental is 0.0137 and $D_{1,2}$ predicted is –0.128.

x_1	x_2	x_3	$D_{1,1}$	$D_{1,2}$	$D_{2,1}$	$D_{2,2}$
Acetone (1) – Benzene (2) – Methanol (3)						
0.3500	0.3020	0.3480	2.8790*	-0.4300*	-1.0260*	1.2530*
			3.6499†	-0.0693†	-0.3022†	2.3021†
0.4000	0.5000	0.1000	3.6950*	0.8890*	-1.1510*	1.1050*
			3.8649†	0.8928†	-0.3052†	2.2371†
0.7660	0.1140	0.1200	3.9780*	0.3470*	-0.4580*	2.4550*
			3.9119†	0.3259†	-0.5119†	3.1681†
Acetone (1) – Benzene (2) – Carbon Tetrachloride (3)						
0.2989	0.3490	0.3521	1.8490*	-0.3180*	-0.0910*	2.2440*
			1.8690‡	-0.2129‡	-0.0043‡	2.2730‡
0.1497	0.6984	0.1519	2.2020*	-0.1280*	-0.2480*	2.1270*
			1.9652‡	0.0137‡	-0.1522‡	1.9248‡
0.6999	0.1497	0.1504	2.3030*	-0.2850*	0.0630*	2.7420*
			2.3041‡	-0.4019‡	0.1848‡	2.9969‡

* Data from this work
† Data from Alimadadian and Colver[13] and cited by Kooijman and Taylor[12]
‡ Data from Cullinan and Toor[14] and cited by Kooijman and Taylor[12]

Table 2 Comparison of the Diffusion Coefficients in the molar average velocity reference frame for two different systems at 25°C (all values of diffusion coefficients are expressed in $m^2/s \times 10^9$).

CONCLUSIONS

In this work, a calculation procedure for the determination of the matrices of multi-component Fick diffusivities using the Modified UNIFAC Activity Coefficient Model, Dortmund Version,[9] is described. This method is simple and straightforward to use once the partial derivatives of the natural logarithm of the activity coefficients are found. The results from the theoretical calculations are compared to the results reported in different works.[13,14] From the comparison, it was found that for the

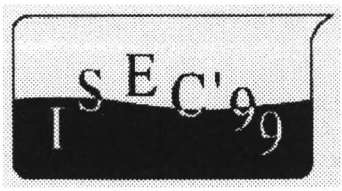
system acetone-benzene-methanol the maximum average error is 27%, whereas for the system acetone-benzene-carbon tetrachloride the maximum average error is 8.7%. Further work to improve the accuracy of the predictions is recommended.

ACKNOWLEDGEMENTS

This work was supported by the *Universidad de Guanajuato, México* and the *Consejo Nacional de Ciencia y Tecnología* (CONACYT).

REFERENCES

1. Uribe-Ramírez R and Korchinsky WJ, *Proc. ISEC 96*, **1**, 111, (1996).
2. Uribe-Ramírez R and Korchinsky WJ, *Proc. 1997 Jubilee Research Event*, Nottingham, UK, **2**, 1109, (1997).
3. Uribe-Ramírez R, *PhD Thesis*, UMIST, Manchester, UK, (1997).
4. Toor HL, *AIChE J.*, **10**, 448, (1964).
5. Stewart WE and Prober R, *Ind. Eng. Chem. Fund.*, **3**, 224, (1964).
6. von Reden C, *PhD Diss.*, Univ. Dortmund, Ger, (1998).
7. Slater MJ, *Can. J. Chem. Eng.*, **73**, 462, (1995).
8. Taylor R and Krishna R, *'Multicomponent Mass Transfer'*, John Wiley & Sons, USA, (1993).
9. Weidlich U and Gmehling J, *Ind. Eng. Chem. Res.*, **26**, 1372, (1987).
10. von Reden C, Slater MJ and Gorak A, *Proc. ISEC 96*, **1**, 99, (1996).
11. Wilke CR and Chang P, *AIChE J.*, **1**, 264, (1955).
12. Kooijman HA and Taylor R, *Ind. Eng. Chem. Res.*, **30**, 1217, (1991).
13. Alimadadian A and Colver CP, *Can. J. Chem. Eng.*, **54**, 208, (1976).
14. Cullinan HT and Toor HL, *J. Phys. Chem.*, **69**, 3941, (1965).



CHARACTERIZATION OF POLYMERIC REVERSED MICELLES

Yun-Dong Wang, Zhengmin Li, Hansong Huang and You-Yuan Dai

Solvent Extraction Laboratory, The State Key Laboratory of Chemical Engineering, Department of Chemical Engineering, Tsinghua University, Beijing 100084, China

ABSTRACT

Block copolymers of poly(ethylene oxide) (PEO) and poly(propylene oxide) (PPO) are macromolecular surfactants. Variations of the molecular characteristics (PPO/PEO ratio, molecular weight) of the copolymer during synthesis allows the production of molecules with optimum properties that meets the specific requirements in different areas. Polymeric reversed micelle extraction using amphiphilic block copolymers in organic solutions is a new extraction technique, which is proposed by the State Key Laboratory of Chemical Engineering, China. In this paper, polymeric reversed micelle formation and water solubilisation by PPO-PEO-PPO triblock copolymers have been systematically investigated. The effect of poly(ethylene oxide) (PEO) and poly(propylene oxide) (PPO) ratio on micellisation of block copolymers in various organic solvents such as n-hexane, n-heptane, benzene, xylene, etc. has been studied. The results show that GP330 with PPO content of 100% can dissolve in any proportion with organic solvents. However, the L series of copolymers (L61, L62 and L64) only has small solubility in organic phase. Water solubilisation studies indicate that polymeric reversed micelle solutions prepared by aromatic hydrocarbons can solubilise more water than those of straight chain alkyl hydrocarbons.

Keywords: reversed micelles, water solubilisation, polyethylene oxides

INTRODUCTION

Surfactants have long been playing an important role in a wide variety of industries as a product performance aid. They are amphiphilic molecules containing a non-polar hydrophobic tail, usually a straight or branched hydrocarbon chain at one end, and a polar hydrophilic group which can be either non-ionic, zwitterionic or ionic at the another end. As a result of the solvophobic association, these molecules are capable of forming a rich variety of structurally organized assemblies such as micelles and reversed micelles. Reversed micelle solutions consist of aggregates that are formed spontaneously by self-aggregation of surfactant molecules in organic solutions.[1]

Water-soluble block copolymers of poly(ethylene oxide) (PEO) and poly(propylene oxide) (PPO) are macromolecular surfactants. Variations of the molecular characteristics (PPO/PEO ratio, molecular weight) of the copolymer during synthesis allows the production of molecules with optimum properties that meets the specific requirements in different areas. It is well established by now that block copolymers consisting of a hydrophobic PPO block with hydrophilic PEO blocks on each side can form micelles in aqueous solutions if the PPO block is large enough and the concentration is high enough.[2] An interesting property of aqueous polymeric micelle systems is their ability to enhance the solubility in water of otherwise sparsely water-soluble hydrophobic compounds for the core of the micelles provides a hydrophobic micro environment, suitable for solubilising such molecules.[3] Promising applications are in separations. Hydrophobic pollutants, such as polycyclic aromatic hydrocarbons (PAHs), can be selectively solubilised in aqueous solutions of block copolymer micelles.[4] However, polymeric micelle extraction has many limitations. Extraction can only be achieved by a membrane process, in other words, the two phases of micelle and aqueous solutions cannot be easily separated if they are brought into contact directly. Polymeric micelle extraction is very efficient for extracting non-polar hydrocarbons, but less efficient for polar or water-soluble solutes.

Recent study by Alexandridis and Andersson[5] has shown that polyoxyalkylene block copolymers can form reversed micelles in organic phase. The solubilisation of water by these polymeric reversed micelles has been investigated. Wu, Zhou and Chu.[6] Wu and Chu,[7] have also reported the water-induced micelle formation of a PEO-PPO-PEO copolymer in o-xylene. However, the solubilization of water-soluble solute in the polymeric reversed micelle solution has received scant attention in the literature. The extraction of phenol by polymeric reversed micelles has been

© 2000 Society of Chemical Industry

extensively investigated by the State Key Laboratory of Chemical Engineering.[7-11] A preliminary experimental study on the preparation and characterisation of polymeric reversed micelles was carried out in the Solvent Extraction Laboratory.[12]

In this paper, the possibility of block copolymer reversed micelle formation and micellisation thermodynamics have been experimentally investigated. The specific objective of this paper is to explore the potential for using PEO-PPO-PEO block copolymer reversed micelles in the solubilisation of water or a dye for the determination of the solution cmc as well as w_0 (water solubilisation) values. The latter is defined as the molar ratio of water solubilised in polymeric reversed micelle solution to molar surfactant. The fact that reversed micelles can solubilise relatively large amount of water can be used to determine the onset of polymeric reversed micelle formation. Preliminary results have shown that the solubility of water in various copolymer/solvent solutions increases in order of magnitude.

EXPERIMENTAL

The polymers used in this study were L61, L62, L64 and GP330 (Jiangsu Petrochemicals Plant, P. R. China). Their formula, PPO content and total molecular weights are listed in table 1. Solvents used are n-hexane, n-heptane, n-octane, benzene and xylene. The water solubilisation equilibrium experiments were performed by contacting equal volumes of polymeric reversed micelle solution with water in a conical flask in a water bath shaker at room temperature (25±0.1°C) for one hour, at a vibration frequency of 200 rpm, then centrifuged for phase separation. After centrifugation, both phases were transparent with a distinct phase boundary. The amount of water solubilised in the organic phase was measured by Karl-Fischer titration system.

Name	Formula	PPO/(PEO) content(%)	M.W. of PPO	Total M.W.
L61	$H(C_2H_4O)_{n1}$-$(C_3H_6O)_{n2}$-$(C_2H_4O)_{n3}$ -OH	90(10)	1750	1944
L62	$H(C_2H_4O)_{n1}$-$(C_3H_6O)_{n2}$-$(C_2H_4O)_{n3}$-OH	80(20)	1750	2188
L64	$H(C_2H_4O)_{n1}$-$(C_3H_6O)_{n2}$-$(C_2H_4O)_{n3}$-OH	60(40)	1750	2917
GP330	H_2C-O-$(C_3H_6O)_{n1}$-OH | HC-O-$(C_3H_6O)_{n2}$-OH | H_2C-O-$(C_3H_6O)_{n3}$-OH	100(0)	3000	3000

Table 1 Physicochemical properties of copolymers

RESULTS AND DISCUSSION

Water solubilisation by triblock copolymers in organic solvents is used as an indication of polymeric reversed micelle formation and determination of critical micellisation concentration (cmc). The amount of water solubilised in copolymer-alkyl hydrocarbon solutions over a wide range of GP330 concentrations is shown in figure 1. There is a GP330 concentration after which the solubility of water in GP330- alkyl hydrocarbon solutions has a dramatic increase. The GP330 concentrations are 3%, 4% and 8%, respectively for GP330-n-octane, GP330-n- heptane and GP330-n-hexane. As the carbon number in an alkyl hydrocarbon increases, the GP330 concentration at which water solubility increases dramatically is decreasing. A sharp increase in the water solubilisation capacity is an indicative of the polymeric reversed micelle formation.

The solubilisation of water can thus be used to determine the cmc of amphiphilic block copolymers in organic solvents. This is similar to the use of the solubilisation of organic compounds for detecting micelle formation in aqueous solutions. The cmc for polymeric reversed micelles is then determined from the copolymer concentration at which the water solubilisation capacity starts to increase sharply as shown in Figure 1. Water solubilisation in polymeric reversed micelle solutions formed with

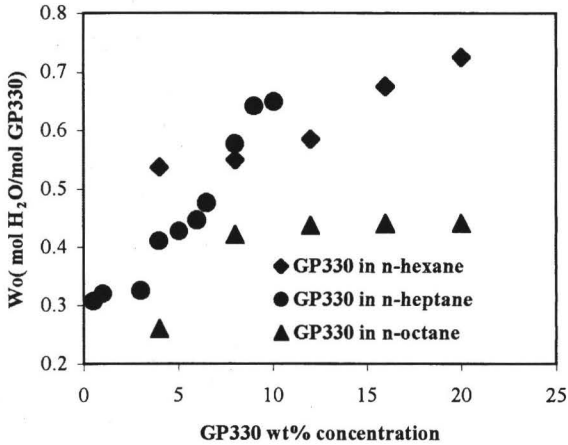


Figure 1 Water solubilisation in GP330 in different organic solvents

different types of hydrocarbons is illustrated in Figure 2. It has been noted that the water solubilisation capacity of polymeric reversed micelle solutions with aromatic hydrocarbons is much higher than that with straight chain alkyl hydrocarbons.

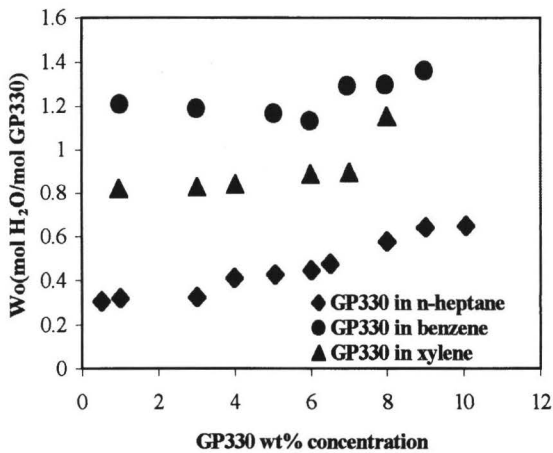


Figure 2 Comparison of water solubilisation in GP330 in different organic solutions

The amount of water solubilised in copolymer-organic solutions over a wide range of copolymer concentrations is shown in Figure 3 to Figure 5 for different poly-oxyalkylene copolymers of L61, L62 and L64, respectively. They reflect the effect of the copolymer hydrophilic PEO block size on water solubilisation and polymeric reversed micelle formation by these triblock copolymers in organic solvents. The water solubilisation capacity with L62 (PEO content of 20%) in xylene is much higher compared to that with L61 which has the PEO content of 10%. The cmc of L61 and L62 has merely a slight difference as they are expressed in molar concentration. The water solubilisation capacity increases with the increase of PEO content.

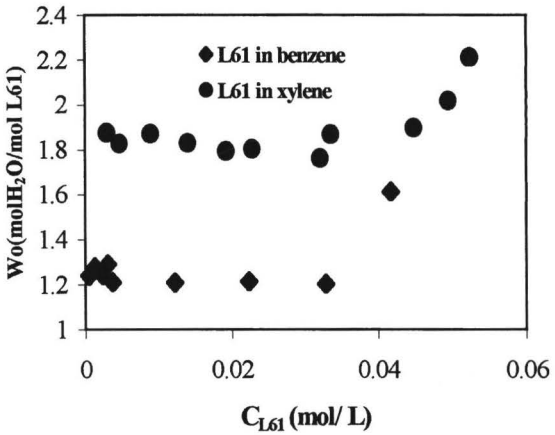


Figure 3 Water solubilisation in L61 in organic solutions

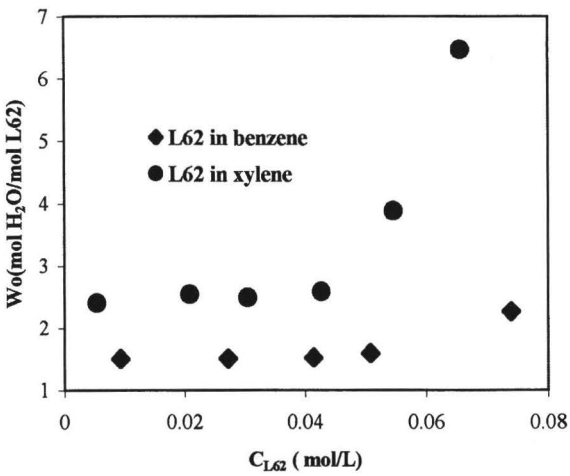


Figure 4 Water solubilisation in L62 in organic solutions

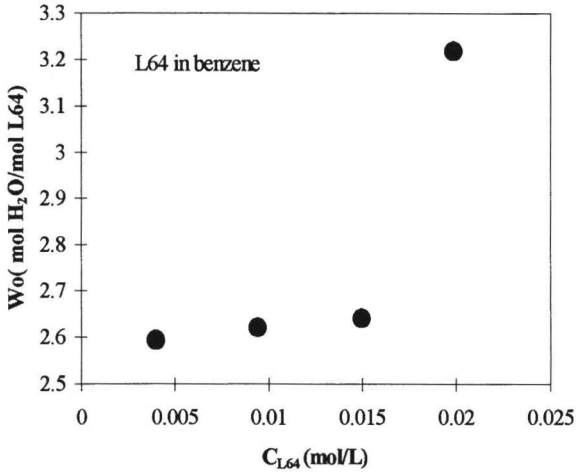


Figure 5 Water solubilisation in L64 in benzene solutions

CONCLUSIONS

The polymeric reversed micelle formation by poly(propylene oxide)/poly(ethylene oxide)/ poly(propylene oxide) triblock copolymers in various organic solvents and the water solubilisation in these systems are presented. The ability of the polymeric reversed micelles to solubilise water has been used to detect the formation of the polymeric reversed micelles and determine the copolymer cmc in organic solvent, just as solubilisation of organic compounds is employed for detecting micellisation in aqueous solutions. Water solubilisation in polymeric reversed micelle solutions varies with different types of hydrocarbons. Water solubilisation in polymeric reversed micelles is much higher with aromatic hydrocarbons that that with straight chain alkyl hydrocarbons. The polymeric reverse cmc values were in the range of 0.01-0.04 mol/dm^3. The investigation of the polymeric reversed micelle formation is useful for the study of polymeric reversed micelle extraction process.

ACKNOWLEDGEMENT

Project (No 29836130) supported by The National Natural Science Foundation of China.

REFERENCES

1. Eicke HF, *Top. Curr. Chem.* **87**, 85, (1980).
2. Wanka G, Hoffmann H and Ulbricht W, *Colloid Polym. Sci.*, **268**, 101, (1990).
3. Hurter PN and Hatton TA, in *Solubilization in Surfactant Aggregates*; Christian SD and .Scamehorn JF, Eds., Marcel Dekker Inc., New York, (1995).
4. Nagarajan R and Ruckenstein E, *Langmuir*, **2(2)**, 210, (1986).
5. Alexandridis P and Andersson K, *J. Phys. Chem. B*, **101**, 8103, (1997).
6. Wu G, Zhou Z and Chu B, *Macromolecules*, **26**, 2117, (1993).
7. Wu G and Chu B, *Macromolecules*, **27**, 1766, (1994).
8. Yang S, *MSc Thesis*, Tsinghua University, Beijing, (1996).
9. Yang S, Wang Y, Yang Y and Dai Y, *In Proceedings of the 8th National Conference on Chemical Engineering*, Oct. 21~24, 1996, Tianjin, P. R. China.
10. Yang S, Wang Y, Yang Y and Dai Y, *ibid.*
11. Yang S, Wang Y and Dai Y, *2nd China/USA Joint Conference of Chemical Engineering*, May 19~22, 1997, Beijing, P. R. China.
12. Huang Y, *BSc Dissertation*, Tsinghua University, Beijing, (1998).

MEMBRANE COALESCENCE AS A NOVEL PHASE SEPARATION STAGE FOR EXTRACTION PROCESSES

Sandra Hoffmann and Walter Nitsch
Technical University of Munich. Institute of Technical Chemistry.
D - 85748 Garching, Germany

ABSTRACT
This paper will propose membrane coalescence as an innovative and efficient process for phase separation of stable oil-in-water-emulsions. It has shown to be capable to separate oil droplets even when strongly stabilized by surfactants and thus only of micrometer size, whereby high efficiency of separation (up to > 95 %) and huge flow rates [< 680 $m^3/(m^2h)$] are reached. Fundamental studies[1,2,3] on coalescence behavior concentrated on a substance selection known from research on extraction topics (additive of DEPA, an interfacially active complexing agent).
The method is based on the phenomena, that two-phase flow of the emulsion through a hydrophobic, microporous membrane leads to coalescence of dispersed organic phase. Oily domains, as enlarged to millimeter size (i.e. unstable aggregates of organic phase containing few aqueous phase), will instantaneously float to the surface and separate in a settler. Results concerning effect of technically relevant parameters on separation efficiency will be presented and discussed with respect to the mechanistic course.

Keywords: coalescence, phase separation, microporous membrane, emulsion surfactant membrane, entrainment

INTRODUCTION

Regarding the unit operation extraction holistically, one will find technical problems not only in the context of mass transfer and concentration. Occurring entrainment, i.e. oily phase dispersed in the effuent, has to be removed in a subsequent phase separation stage. In case of emulsion stabilization by interracially active substances, the applicable range of mechanical separation methods is reduced to ultrafiltration and coalescing by fibre beds.[4] The aim of this study was to investigate membrane coalescence as a new method in regard to the operational range of separation performance as well as to the physical mechanism.

EXPERIMENTAL

The principle of process is operated in three functional groups of the pilot plant (figure 1):

I. preparation of o/w-emulsion feed by either one of two dispersing tools;
II. membrane coalescence;
III. phase separation and volumetric measurement of its efficiency.

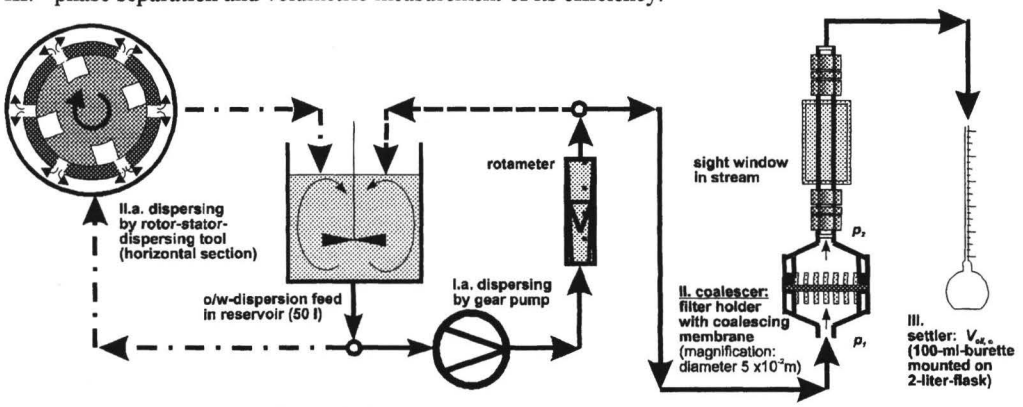


Figure 1: Scheme of Experimental Plant

© 2000 Society of Chemical Industry

Preparation of Emulsion

First, a 50 dm^3 batch of a stable emulsion with a standard o/w-concentration of c_0 = 3,3 vol.-% was prepared by recirculating for several hours (> 4 hours), by connecting different tools:

Ia. Dispersion by gear pump, due to shear forces occurring at the gear rim: A circuit flow (150 dm^3/h) passing a gear pump ('M 838', Schwinherr) was installed in most cases.

Ib. Dispersion according to the rotor-stator-method: In the case of high viscosity oil phases, for emulsion preparation the in-line-dispersing tool 'IKA-Super-Dispax SD 41' was used.

Plant Unit of Membrane Coalescence

The central unit is the coalescer through which the prepared stable o/w-testemulsion was transferred by a gear pump (flow up to 190 dm^3/h). This was a hydrophobic, microporous membrane (table 1) held in place by polypropylene frits of a polycarbonate filter holder ('SM 165 08 B', Sartorius). Then, the coalesced phases pass through a sight window for observation purposes, to enable a direct view onto the membrane itself while functioning. A special clamping device combining sight flow cell and filter holder was developed.[3].

material	diameter ∅	d_{pore}	$h_{membrane}$	porosity ε
PTFE	50 mm	5 µm	110 µm	69 %

Table 1: Geometric Features of Membrane ('Sartorius 11842') in Standard Case

Determination of Phase Separation Efficiency

After two-phase flow through the coalescer, liquid phases will be led into scaled settling flasks (see figure 1) which serves for volumetric determination of phase separation efficiency η commonly defined by:

$$\eta = \frac{V_{org,\omega}}{V_{org,\alpha}} * 100\%$$

Since the strong narrowing geometry of the settling flask shows a significant wall effect usually separated $V_{org,\omega}$ is measured after 100 minutes; yet, it must be mentioned that in a normal scale settler sedimentation of coalescescing oil domains is spontaneous in all cases.

Droplet Size Analysis by Measurement of Diffraction Light

Experiments were accompanied by droplet size analysis ('LS 230', Coulter Electronics), i.e. laser diffraction spectrometry as well as 'Polarization Intensity Differential Scattering' for the submicron particle range. Results will be presented as volume percentage curves.

Experimental Determination of Organic Load $V_{org,m}$ inside Membrane Pores

After all the contents of membrane pore volume had been extracted by iso-propanol (HPLC grade), the volumetric fraction of organic load inside the membrane could be detected by uv/vis-spectrometry ('Cary 4'; λ = 262 nm), after a small portion (13 vol-%) of toluene had been first added to the aliphatic main phase, due to its distinct extinction coefficient.

Substance Selections and their Characterization

Process development was mainly carried out with iso-dodecane / water as a model effluent, always with 0.1-mol/dm^3 additive of DEPA [bis(2-ethylhexyl)-phosphate] as an inter-facially active complexing agent exclusively soluble in the oily phase. Therefore interfacial tension was halved to

λ = 20,0 e-3 N/m (measured by ring method,[5] tensiometer 'K10'-Kruess). Deionized water served as continuous phase. Effect of dispersed phase kinematic viscosity ν = 1.5-127 e-6 m^2/s ('mgw lauda' capillary viscosimeter) was investigated with aliphatic technical grade components (paraffins / 0.1 mol/dm^3 DEPA).

RESULTS AND DISCUSSION

Droplet Sizes of O/W-Emulsions

Figure 2 shows droplet size distributions d_3 of two tested emulsions.
All o/w-emulsions with iso-dodecane / DEPA as comparably liquid organic phase can be dispersed by gear pump (see 'I.a'), the batch being recirculated (> 18 times).
Independent from o/w-concentration (0.1 - 7 vol.-%), dispersing equally resulted in droplet size distributions d_3 as shown for the standard case (3.3 vol.-%) in Figure 2.
Also, for higher viscosity oil emulsions, comparable droplet diameters (Figure 2, viscous paraffin) can be reached by plant connection with rotor-stator-dispersing-tool ('I.b',Figure 1).

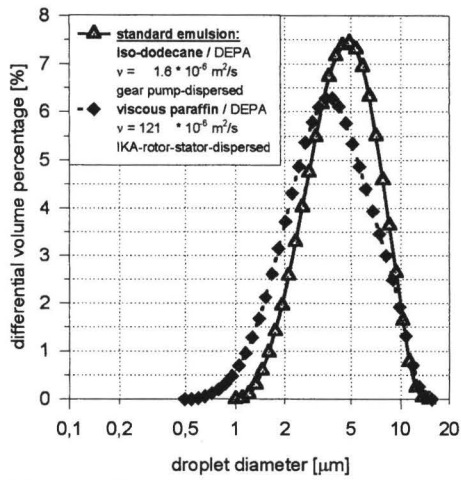


Figure 2: Droplet Size Distributions d_3

The Phenomenon of Formation of W/O-Domains

Apparently membrane coalescence cannot be treated as mere droplet enlargement from micro- to millimeter size, but as formation of unstable 'liquid/liquid-foam'. This resulted from photographs[3] showing the fluid phases passing the sight window at the membrane outlet. Observations, at various flow velocities, led to the conclusion that oil domains built continually from coalescing droplets will be displaced from the membrane, carrying with them enclosed fractions of water. In the standard case of emulsion, the foamy w/o-domains are so unstable that their instantaneous breakdown forms oil droplets of millimeter size.

Effect of Flow Rate, O/W-Concentration and Oil Viscosity on Separation Efficiency

Typically the curve (Figure 3) is characterized by a steep increase of separation efficiency η in the range of low superficial velocities w up to a required value of $w_{min} = 1*10^{-2}$ m^3/m^2s where a separation plateau of ca. 95 % is reached. As a remarkable fact, residence times inside the thin membrane (Table 1) can be calculated as of milliseconds for this technically interesting operational range; that, in the context of necessary hydrophobicity of membrane, hints at the important role of wetting. Transmembrane pressure drops show to be very low [e.g. ΔP = 0.3 bar at a flow rate J = 100 $m^3/(m^2h)$, standard emulsion].

Membrane coalescence does not much depend on o/w-concentration of emulsion c_0. This is correct to say for emulsions prepared with c_0 = 0.3 - 7 vol.-% oil-in-water, for the curve shown for the standard experiment (see Figure 3, c_0 = 3.3 vol.-%) did not change. Only an organic fraction as low as c_0 = 0.1 vol.-% seems to mark the beginning of a performance limit since the plateau of separation efficiency will be decreased to less than 80 %.

From Figure 4 showing the dependencies $\eta(w)$ of three emulsions with increasing kinematic oil viscosity ν it can be seen that the separation plateau breaks off at successively declining

superficial velocities w_{max}, though its value remains on high level (for maximum phase separation efficiencies see Figure 6). Therefore, oil viscosity shows an effect as the technically interesting flux range shortens with distinct vicousness of the dispersed phase.

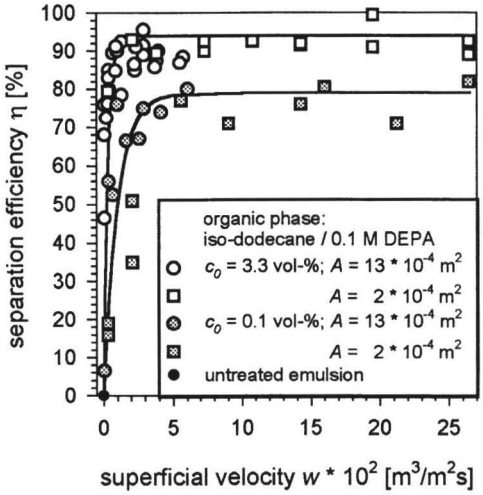


Figure 3: Effect of Superficial Velocity w and of O/W-Concentration c_0

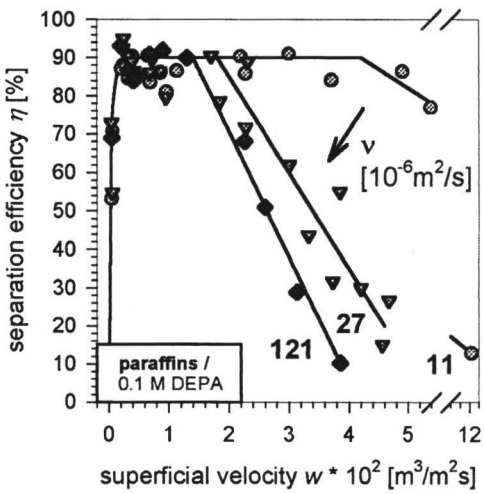


Figure 4: Effect of Oil Viscosity on Separation Efficiency $\eta(w)$

Oil/Water Ratio inside Membrane Pores

Resulting from further experiments concerning the ratio of organic versus aqueous phase inside the membrane pores (Figure 5), it can be concluded that efficient coalescence always correlates to a significant accumulation of oil inside the membrane; this result indicates an important role of wetting. In spite of steady state organic load inside the membrane to be expected at rather low oily volume percentage c_0 = 0.1 - 7 vol.-% of biphasic affluent as well as effluent flux, up to more than half of free pore volume can be measured filled with oil ($v_{org,\,m}$ < 70-vol. %).

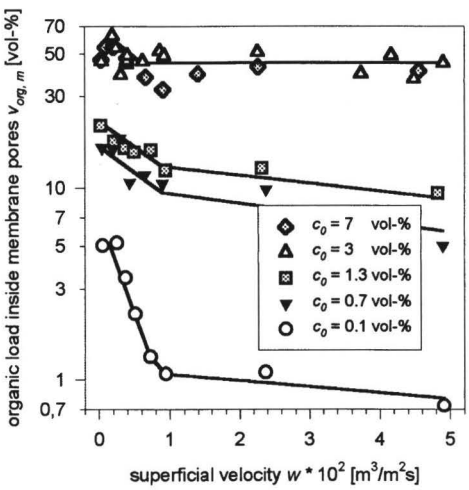


Figure 5: Effect of Superficial Velocity w on Organic Load $v_{org,\,m}$ for Various O/W-Concentrations c_0

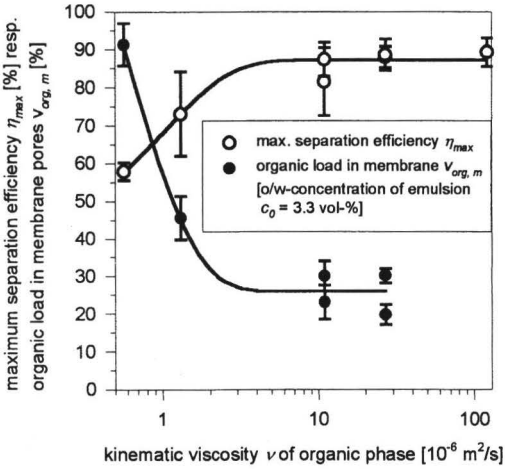


Figure 6: Effect of Oil Viscosity ν on Organic Load $v_{org,m}$ (O/W-Concentration c_0 = 3 %)

From the fact of different oily loads measurable for various o/w-concentrations no value of maximum hold-up, but a ratio of equivalence can be inferred. Furthermore it must be hinted at the point of steep decrease of oily load $v_{org,m}$ with superficial velocity, up to reaching w_{min}, characterizing also beginning of phase separation plateau. Further experiments show accumulation of organic phase still being high for extremely viscous oils also ($v_{org,m} \approx 25$ vol-%, see Figure 6).

Model Scheme of Membrane Coalescence According to Steps I to IV

Processes inside the membrane leading to coalescence and aggregation can be understood with the model scheme according to Figure 7 as a description for a single membrane pore.

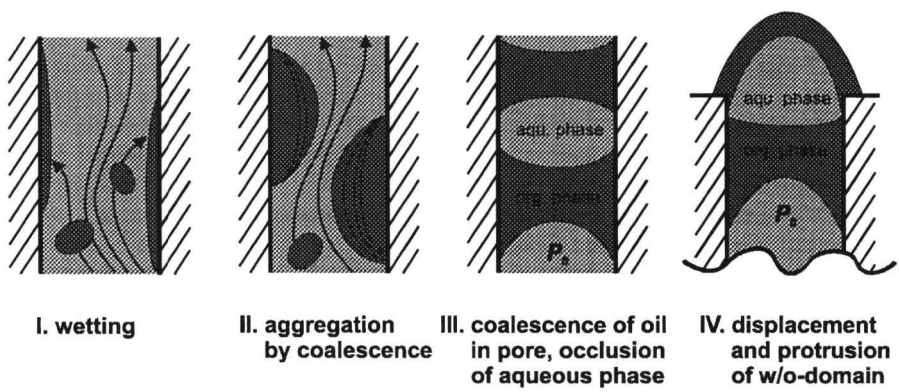


Figure 7: Model Scheme of Coalescence Process inside a Single Membrane Pore

I. Wetting of inner surfaces of hydrophobic membrane by striking oil droplets.
II. Aggregation of oil wetted regions due to further droplet coalescence.
III. Coalescence in pore to oily domains thus occluding aqueous phase.
IV. Displacement from pore and protrusion of w/o-domain.

The most decisive evidence of easily coalescing huge w/o-domains is borne by mentioned photographs showing the membrane effluent stream [3]. Their existence can be understood as formation of aggregates inside the membrane and at its outlet, induced by coalescence and flow

through numerous, sponge-like connected pores. A 'tri'-phasic situation (conti-nuous aqueous phase, oil domains occluding aqueous droplets) must be favored by obser-ved strong accumulation of oil, filling up to more than half of the membrane pore volume.

CONCLUSIONS

Table 2 gives a survey into both membrane and fibre bed as coalescing methods by two-phase flow of emulsion through porous media. Comparison suggests a special capability of the membrane to coalesce tiniest oil droplets, even in the presence of interfacially active substances as DEPA. While fibre beds separate best with droplet sizes close to 100 µm, the lower limit for easy gravity settling of primary emulsions, membrane coalescence might fill the technical gap in the range of micrometer size oil droplets. With usage of nonionic surfactants good separability of the oil phase could also be adjusted [3]. Also, applying the membrane, highly efficient phase separation takes place in a broad range of flow rates up to over ten times higher. Yet, due to absence of turbulence ($Re \leq 1$, also see [8]), possible redispersing eventually causing diminution of separation efficiency can be excluded.

	membrane coalescer [3]		fibre bed coalescer [6]	[7]
organic phase	iso-dodecane + DEPA, paraffin + DEPA; nonionic surfactants (Brij 52, 56, 58)		butyl benzoate, gas., kerosene (Tergitol TMN, Sarkosyl O)	toluene, octanol, butyl acetate
o/w-concentration [vol.-%]		0.1 - 7	2 - 5	0.1 - 0.2
inlet droplet diameter [10^{-6} m]		1 - 10	< 100	10 - 100
flow rate J [10^{-2} m^3/m^2s]		0.1 - 19	0.07 - 1.8	0.2 - 1.3
separation efficiency [%]		ca. 80 - 98	complete or partial	50 - 98

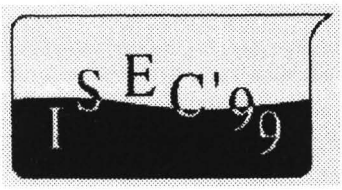
Table 2: Technical Survey on Novel Membrane Coalescer and State-of-the-Art Fibre Bed

NOMENCLATURE

c_0	oil-in-water-concentration of emulsion	vol-%
J	flow rate	m^3/m^2h
$v_{org,m}$	organic load inside membrane pore volume	vol-%
w	superficial velocity (flow rate per free pore cross-sectional area)	m^3/m^2s
ν	kinematic viscosity of organic dirpersed phase	m^2/s

REFERENCES

1. Daiminger U et al., *J. Membr. Sc.*, 99, 197, (1995).
2. Hoffmann S et al., *Proc. ISEC'96*, Melbourne, Australia, **2,** 863, (1996).
3. Hoffmann S, *Doctoral Thesis*, University of Munich, (1999).
4. Menon VB and Wasan DT, Demulsification, in Becher P (Ed.), *'Encyclopedia of Emulsion Technology'*, Marcel Dekker, N.Y., **2,** (1985).
5. de Noüy, *J. Gen. Physiol.*, **1**, 521, (1919).
6. Langdon WM and Wasan DT, *CRC Press*, West Palm Beach, USA, **5**, 159, (1979).
7. Magiera R and Blass E, *Elsevier Applied Science*, London, **1**, 134, (1993).
8. Bernsdorf J et al., *Int.J.Numer.Met.Fluids*, in press, (1999).



THIRD PHASE FORMATION: A NEW PREDICTIVE APPROACH

Lydie Lefrancois[1], Frédéric Belnet[2], Didier Noel[2] and Christian Tondre[1]

[1]Laboratoire de Chimie Physique Organique et Colloïdale, Unité Mixte de Recherche CNRS-UHP (UMR 7565), Université Henri Poincaré-Nancy I, B.P. 239, 54506 Nancy-Vandoeuvre Cedex, France

[2]EDF, Centre de Recherche des Renardières, Section Chimie et Corrosion, B.P. n° 1, Ecuelles, 77250 Moret-sur-Loing, France

ABSTRACT

Third phase formation is a common phenomenon in solvent extraction. It has been experimentally well documented, especially in relation with the separation of actinides in nitric acid solutions, but the phenomenon also exists in the absence of metal ions. Its relation with the existence of molecular aggregates in the organic phase seems to be now established. The Flory-Huggins theory of polymer solutions has been successfully applied to predict the demixing behaviour in the quaternary system dimethyldibutyltetradecylmalonamide (DMDBTDMA)/n-dodecane/water/nitric acid. The experimental observations concerning the effects of solvent, temperature and acid counter-ion on the critical aqueous phase acidity are presented and can be taken into account by this predictive approach.

Keywords: third phase, Flory-Huggins theory, solubility parameter, malonamides, nitric acid

INTRODUCTION

It has often been reported, in solvent extraction, that the organic phase can split into two layers in certain loading conditions of the aqueous phase. This phenomenon especially occurs when the latter is highly concentrated in acids. It has been commonly observed in the separation of actinides[1-3] and it constitutes a major drawback for the industrial development of such extraction processes. To avoid as far as possible the problem caused by the phase separation a better understanding of the mechanisms involved appears necessary. Several reviews[2-4] have analysed the influence of various parameters to try to clarify the origin of third phase formation. The aggregation of the extractant molecules has been recognised as one of the possible explanations, since aggregation and third phase formation are both favoured by high acidities.[4] Up to now the approach of this problem had remained essentially qualitative. It is only recently that different efforts have been made to gain some insight into the chemical origin of this process at the molecular level and to predict the phenomenon of third phase formation on theoretical grounds. In a first approach, which concerned the extraction system consisting of dimethyldibutyltetradecylmalonamide (DMDBTDMA)/n-dodecane/water/nitric acid, Erlinger et al[5] have considered the role of the interactions between the aggregates formed by the extractant molecules in the organic phase. A Baxter type potential (hard sphere sticky potential) was used to describe the behaviour of this complex fluid. This model was further developed to predict the demixing curves when different diluents were considered,[6] showing a satisfactory agreement with the experimental results. A completely different predictive approach based on thermodynamic considerations has been attempted by Lefrançois et al. who have made use of the Flory-Huggins theory of polymer solutions. A preliminary report[7] of this work has demonstrated very encouraging results. We will recall here the principles that are behind this new approach; we will report some new experimental data concerning the above mentioned extraction system and we will compare them with the theoretical prediction from the model used.

© 2000 Society of Chemical Industry

EXPERIMENTAL

The extractant dimethyldibutyltetradecylmalonamide (DMDBTDMA) 99 % pure was obtained from PANCHIM (France) and used as received; n-dodecane (purum), n-hexane (puriss) and nitric acid (65 %) were from Fluka; n-hexadecane (pro synthesis) from Merck; HCl (37%) from SDS; H_2SO_4 (95-98%) from ACROS; HCl (70-72%, normapur) from Prolabo. For details concerning the preparation of the diphasic or triphasic systems and for the analysis of their composition the reader is referred to previous publications.[5,7] A digital densimeter (Anton Paar, Austria) was used to perform the density measurements (calculation of the apparent molal volumes).

THEORY

The Flory-Huggins theory of polymer solutions[8] was applied before to the case of aqueous solutions of non-ionic surfactants to predict the demixing behaviour associated with the so-called clouding phenomenon.[9] We found that there was some analogy between this phenomenon and the splitting of the organic phase observed in liquid-liquid extraction. In both cases the part played by the inter-aggregate interactions have been stressed. We have previously discussed the limitations of this approach and the approximations that are involved[7]. To treat the problem of third phase formation, the existence of the aqueous phase is ignored, and is only considered for the acidity it brings to the system, and we analyse the splitting of the organic phase. For this we calculate an "interaction parameter" χ_{12} between the extractant aggregates and the organic diluent. This interaction parameter has been shown correlate with the acidity of the aqueous phase.[7] Phase splitting occurs when this parameter reaches a critical value. In addition a relationship exists between χ_{12} and the "solubility parameter" δ_2 of the extractant aggregates; the latter should be considered as an apparent parameter since it depends on the acid loading.

The system is described by the following equations (application of the equilibrium condition to the chemical potentials of the solvent (subscript 1) and of the solute (subscript 2) in each organic phase) :

$$\mathrm{Ln}v_1' - (1-\frac{1}{x})v_2' + \chi_{12}v_2'^2 = \mathrm{Ln}v_1'' - (1-\frac{1}{x})v_{21}'' + \chi_{12}v_2''^2 \qquad [1]$$

$$\frac{1}{x}\mathrm{Ln}v_2' - (1-\frac{1}{x})v_1' + \chi_{12}v_1'^2 = \frac{1}{x}\mathrm{Ln}v_2'' - (1-\frac{1}{x})v_1'' + \chi_{12}v_1''^2 \qquad [2]$$

where v_i' are the volume fractions in the less concentrated phase and v_i'' in the more concentrated one.

$$v_1' = 1 - v_2' \qquad [3]$$

$$v_1'' = 1 - v_2'' \qquad [4]$$

$$x = \frac{nV_2}{V_1} \qquad [5]$$

where n is the number of extractant molecules in the aggregates (aggregation number) and V_i the molar volumes of the solvent or of the solute molecules (molar volume of a monomeric unit in the aggregates). For the calculations the V_2/V_1 ratio will be approximated by the ratio of the molecular weights M_2/M_1. These equations have to be solved for given values of x in order to obtain v_2', v_2'' and χ_{12} (see references[7, 10] for more details).

The experimental values of v_2' and v_2'' were calculated from the following equations applied to both phases :

$$v_2 = C\varphi_2 / 1000 \qquad [6]$$

$$\varphi_2 = \frac{M_2}{d_0} - 10^3\frac{d-d_0}{d_0 C} \qquad [7]$$

where C is the extractant concentration, d the density of the phase, d_0 that of the diluent and M_2 the molecular weight of a monomeric unit in the aggregates. For reasons discussed before[7] these monomeric units, *near the critical acidity*, were assumed to consist of the association of one extractant molecule with one molecule of nitric acid (DMDBTDMA: HNO_3).

Each experimental couple of values of (v_2', v_2'') can be associated with a value of χ_{12} (and thus with the corresponding HNO_3 concentration), the value of x being fixed. The best agreement between the experimental data and the theoretical prediction is found by adjusting the value of x.
The apparent solubility parameter of the extractant aggregates δ_2 for a fixed aqueous phase acidity is related to χ_{12} by the following expression[11]:

$$\chi_{12} = \frac{V_1}{RT}(\delta_1 - \delta_2)^2 \qquad [8]$$

RESULTS AND DISCUSSION

The conditions of third phase formation were investigated varying the nature of the solvent, the temperature and the nature of the aqueous acid solution.

Solvent effect

Although the qualitative behaviour was already known for the three solvents n-hexane, n-dodecane and n-hexadecane[7], no quantitative comparison between experiment and theory had been possible so far because the volume fractions v_2' and v_2'' were not determined for n-hexane and n-hexadecane. This has now been done and we compare in Figures 1 and 2 the experimental results with the best fits obtained from the Flory-Huggins approach.

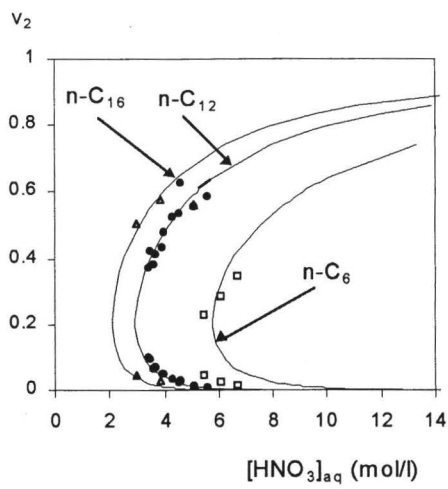


Figure 1. Solvent effect: experimental results and theoretical curves (x=14). T=25°C

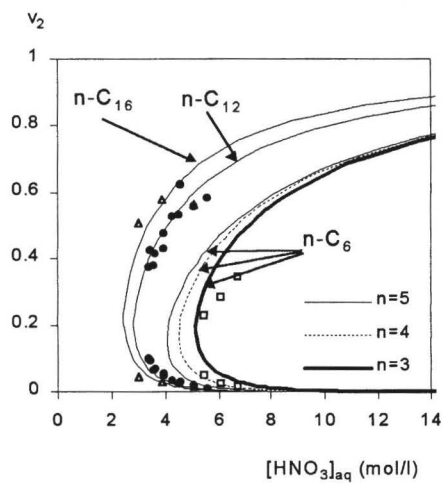


Figure 2. Solvent effect: experimental results and theoretical curves (variable x; n as indicated). T=25°C

The theoretical demixing curve drawn for n-dodecane corresponds to the minimised sum of squared deviations, obtained for x=14, which gives an aggregation number of about 5. The relationship between χ_{12} and the HNO_3 concentration could then be established and from equation [8] we can associate an apparent value of δ_2 to each value of χ_{12} after introducing in the equation the molecular parameters of n-

dodecane (V_1=228.6 $cm^3 \cdot mole^{-1}$ and δ_1=7.8)[12]. For the two other solvents χ_{12} was recalculated using now the proper parameters of the solvent considered (131.6 $cm^3 \cdot mole^{-1}$, 7.3 and 294.1 $cm^3 \cdot mole^{-1}$, 8.0 for n-hexane and n-hexadecane, respectively)[12], leading to new relationships between χ_{12} and acidity. The results are represented in Figure 1. The theoretical prediction is quite food for n-hexadecane and n-dodecane but it could be better for n-hexane. It should be emphasised that x being fixed (x=14), equation [5] implies that the aggregation number will change depending on the solvent considered (here we would obtain an aggregation number of about 2 in n-hexane and 6 in n-hexadecane). In Figure 2, we have kept the relationships between χ_{12} and acidity as established before, but we have i) fixed the value of the aggregation number to n=5 in all the solvents (the value of x is no longer fixed), and ii) varied this value for n-hexane. The results show that the model correctly predicts the shift of the critical acidity, although there is some uncertainty on the actual aggregation number, which may slightly change from one solvent to another.

Temperature effect

The critical aqueous phase acid concentration above which a third phase starts forming has been determined at different temperatures. The results obtained when a 0.3 M solution of DMDBTDMA in n-dodecane is equilibrated with different aqueous solutions of HNO_3, are represented in Figure 3. In first approximation we expect a variation of χ_{12} inversely proportional to the temperature as indicated by equation [8]. The variations of V_1 and δ_i with temperature have been neglected, but they should obviously be taken into account in a further refinement of this approach. Within the previous approximation, we can associate with each acidity and each temperature a value of the interaction parameter. For each temperature the demixing is assumed to occur when χ_{12} attains the critical value χ_{12}=0.81 which was previously obtained in n-dodecane with x=14. The corresponding critical acidity have been represented in Figure 3. There is a slight and almost constant shift between the experimental data and the theoretical prediction, but the trends are very similar. Data previously reported in the literature by Smith et al[3] show the same trends in the case of 0.5 M DMDBTDMA in TPH, but the critical acidities are shifted towards higher values, branched solvent being known to reduce third phase formation.

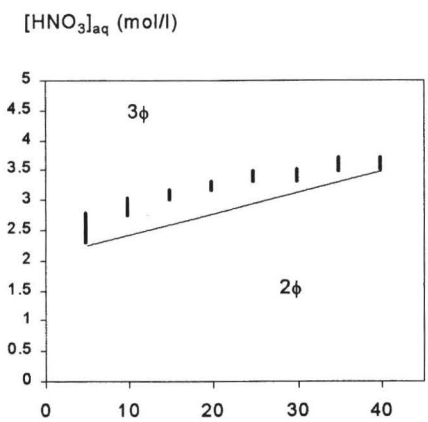


Figure 3. Temperature effect: limit of the 2 phase- 3 phase transition (experiments (|); theory (continuous line))

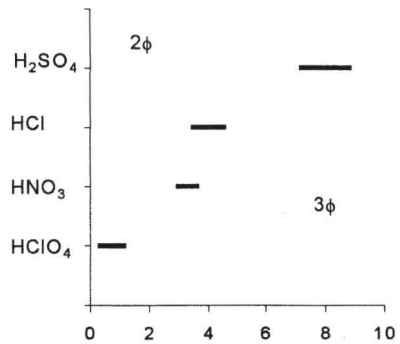


Figure 4. Domain of 2 phase- 3 phase transition for different acids. Organic phase: 0.3M DMDBTDMA in n-dodecane. T=25°C

Effect of the nature of the aqueous acid solution

For the experiments reported in Figure 4, we have fixed the initial concentration of DMDBTDMA in n-dodecane at 0.3 M, and this solution was equilibrated with an aqueous solution containing increasing concentrations of acids, to determine the critical concentrations (or at least the concentration domain) at

which third phase formation occurs. This was done for four different acids, for which the critical concentrations were found in the order:

$$HClO_4 < HNO_3 < HCl < H_2SO_4$$

This order follows the Hofmeister ion series (or "lyotropic" ion series), which is known to express the effect of these anions on the water structure[13]. The large ClO_4^- ion, at one end of the series, has been qualified as a "water structure breaker" and its transfer in an organic phase is much easier than for the SO_4^{2-} ion, at the other end of the series, known as a "water structure maker"[13,14]. By comparison with our previous results obtained with HNO_3 (taken here as a reference) we can thus assume that the critical value of the interaction parameter χ_{12} will be attained with either a lower (case of $HClO_4$) or a larger (cases of HCl and H_2SO_4) acid loading of the aqueous phase. This means that for a same acid concentration in the external phase the apparent solubility parameter δ_2 will vary with the nature of the acid. For instance at 3 M of acid, where the theory predicts an apparent δ_2 of 10.75 for HNO_3[7], we expect that the corresponding values for $HClO_4$ and H_2SO_4 will be respectively larger and lower than 10.75. We cannot say more at this stage of this work and a quantitative estimate of the δ_2 values will require additional experiments.

CONCLUSIONS

We have shown here that the influence of many parameters known to affect the conditions of formation of a third phase in solvent extraction can be predicted within the framework of the theory of Flory-Huggins. The concept of the interaction parameter χ_{12} predicting the stability of polymer solutions was extended to the case of the extractant aggregates existing in solvent extraction. The demixing is governed by the value of the apparent solubility parameter of these aggregates associated with the critical value of χ_{12}.

ACKNOWLEDGEMENTS

We are indebted to Drs C. Madic, M.C. Charbonnel and C. Nicol (CEA, Marcoule) for providing us with the DMDBTDMA extractant and for fruitful discussions. We thank GDR P.R.A.C.T.I.S. for initiating this work.

REFERENCES

1. Nigond L, Condamines N, Cordier PY, Livet J, Madic C, Cuillerdier C, Musikas C and Hudson MJ *Sep. Sci. Technol.* **30**, 2075 (1995)
2. Rao PRV and Kolarik Z *Solv. Extr. Ion Exch.* **14**, 955 (1996)
3. Smith BF, Wilson KV, Gibson RR, Jones MM and Jarvinen GD *Sep. Sci. Technol.* **32**, 149 (1997)
4. Osseo-Asare K *Adv. Colloid Interface Sci.* **37**, 123 (1991)
5. Erlinger C, Gazeau D, Zemb T, Madic C, Lefrancois L, Hebrant M and Tondre C *Solv. Extr. Ion Exch.* **16**, 707 (1998)
6. Erlinger C, Madic C and Zemb T, Communication at *Journées P.R.A.C.T.I.S. 1997*, Villeneuve-les-Avignon (January 15th, 1998)
7. Lefrancois L, Belnet F, Noel D and Tondre C, *Sep. Sci. Technol.*, in press
8. *Chimie Macromoléculaire;* ed Champetier G; Hermann, Paris **II**, 13, (1972)
9. Weckstrom K and Zulauf M, *J. Chem. Soc. Faraday Trans 1* **81**, 2947 (1985)
10. Flory PJ, *J. Chem. Phys.* **12**, 425 (1944)
11. *Regular and Related Solutions;* ed Hildebrand JH, Prausnitz JM and Scott RL, Van Nostrand Reinhold Company, New York , p. 189, (1970)
12. Beerbower A and Hill MW *McCutcheon's Detergents and Emulsifiers Manual,* Allured Publ. Co., Ridgewood NJ 07450, p. 223, (1971)
13. Firman P, Haase D, Jen J, Kahlweit M and Strey R *Langmuir* **1**, 718 (1985); Luck WAP *Top. Curr. Chem.* **64**, 113, (1976)
14. Tondre C and Derouiche A, *J. Phys. Chem.* **94**, 1624 (1990)

SALT EFFECT IN THE QUATERNARY SYSTEM WATER + ETHANOL + 1-PENTANOL + SODIUM CHLORIDE AT 25°C

MM Olaya, A Botella and A Marcilla
Chemical Engineering Department. University of Alicante. Apdo. 99. Alicante, Spain

ABSTRACT
The liquid-liquid-solid equilibria in the two-liquid and two-liquid + one-solid quaternary regions for the quaternary system water + ethanol + 1-pentanol + sodium chloride at 25 °C have been determined. Tie lines and tie-triangles data were measured after separating the conjugated phases. Distribution and selectivity curves are represented to analyse the sodium chloride salt effect and to compare these results with those obtained for the water + ethanol + 1-butanol + sodium chloride water + ethanol + 1-butanol + potassium chloride and water + ethanol + acetone + sodium chloride. A modification of the Eisen-Joffe equation has been used to correlate the tie-line and tie-triangle data yielding good results

Keywords: phase equilibria, salting-out, salt effect.

INTRODUCTION

The addition of a salt to a liquid-liquid ternary system modifies the solubility of the solute and its distribution between two liquid phases (salt effect). This effect can be used to improve the conditions of extraction of some solutes. This paper is part of a series of studies involving quaternary systems including an inorganic salt. In all these systems the solute is ethanol and we study its distribution between organic and aqueous phases and the selectivity of the solvent for the ethanol extraction using different salts and solvents (water is present in all the systems studied). To obtain this information in a systematic and useful way it is necessary to determine the equilibrium data (tie-lines, tie-triangles and solubility surface of the salt) in all the equilibrium regions of the systems (two liquids, one liquid + one solid and two liquids + one solid regions). The systems previously studied at 25°C are the following:

Water + Ethanol + 1-Butanol + Sodium Chloride[1]
Water + Ethanol + 1-Butanol + Potassium Chloride[2]
Water + Ethanol + Acetone + Sodium Chloride[3]

The objective of the present work is to study the system Water + Ethanol + 1-Pentanol + Sodium Chloride and compare the salt effect with the previous systems considered.

EXPERIMENTAL

Chemicals

Water used was bidistilled, and ethanol, 1-pentanol and 1-propanol (used as internal standard in the chromatographic analysis) were analytical reagent grade (Merck). The contents of possible volatile impurities were examined by gas-liquid chromatography. The purity of all compounds determined by chromatography was minimum 99.5% (mass). Sodium chloride (Merck) was anhydrous and of reagent grade, and was dried before used.

Analytical Methods

Equilibrium measurements were made by preparing mixtures of known overall composition, stirring intermittently for 48 hours and allowing the mixtures to settle for 24 hours at a constant temperature of 25±0.1°C. At the end of each experiment, samples were taken from the liquid phases and analysed. Water, ethanol and 1-pentanol were determined by gas chromatography using a Shimadzu gas chromatograph GC-14A with an AOC-14 Auto Injector and an electronic integrator C-R64 Chromatopac. The column used was a 2m x 1/8" Porapack Q 80/100 and the column temperature was 180 °C. The helium flow rate was 30 cm^3min^{-1}. The internal standard method was applied for the

© 2000 Society of Chemical Industry

quantitative analysis, using 1-propanol as the standard. For the analysis of water, ethanol and 1-pentanol in the organic phases a thermal conductivity detector (TCD) was used. Nevertheless, when 1-propanol was added to the aqueous phases, sodium chloride precipitated. Consequently, these samples were diluted with water until transparency, ethanol and 1-pentanol contents were determined using a flame ionization detector (FID) and water was calculated by mass balance.

Sodium chloride was determined by two different methods depending on its concentration. In samples with concentrations higher than 0.5% (mass) it was gravimetrically determined by evaporating the solution at 105°C, until constant mass. Samples with lower concentrations were titrated with $AgNO_3$. At low salt concentrations the error involved with the gravimetrical method is large.

Duplicates of each heterogeneus mixture were prepared and analysed. The relative accuracy of the mass fraction measurements of each of the components was approximately 1%.

Experimental Methodology

The methodology used to study the water-solute-solvent-inorganic salt systems has not always been adequate nor systematic, and it could lead to doubtful conclusions.[4] In a previous paper[1] a methodology for the determination of the equilibrium data of quaternary systems including an inorganic salt was suggested. This methodology is applied in the present paper to the quaternary system Water (A) + Ethanol (B) + 1-Pentanol (C) + Sodium Chloride (D) at 25°C.

Figure 1(a) shows a qualitative representation of this or similar systems (systems with only one partially miscible liquid pair and the two other liquid pairs being totally miscible and the salt does not form hydrates). In these systems the following equilibrium regions can be distinguished:

The two liquids region (2L)
The one liquid + one solid region (1L+1S)
The two liquids + one solid region (2L+1S)
The one liquid region (1L)

To discuss the salt effect of the salt for the solute extraction it is necessary to determine the equilibrium data in the system without salt and in the 2L and 2L+1S quaternary equilibrium regions.

Figure 1(b) shows a schematic representation of the methodology used, where the initial mixtures (a, d and h) and the compositions of the equilibrium phases (b-c, e-f-g, and i-g) have been indicated.

In the 2L zone, an initial mixture represented by point a, splits into two liquid phases (b and c).

In the 2L+1S zone, an initial mixture, represented by point d, splits into two liquid phases (e and f) and one solid phase (g).

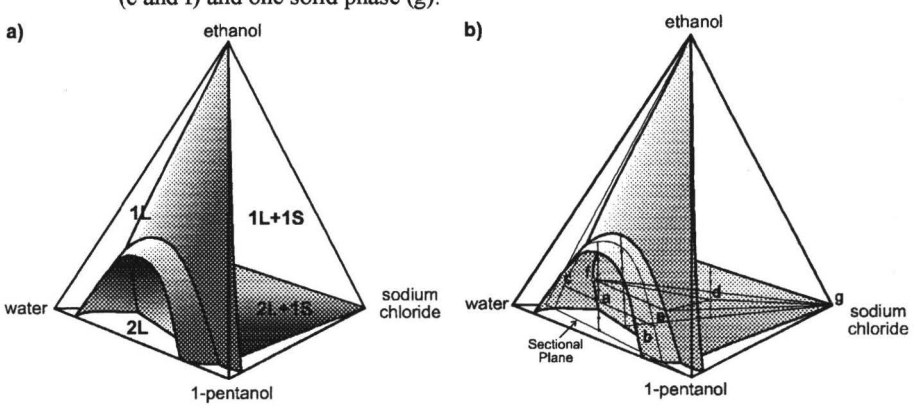


Figure 1. a) Qualitative representation of the liquid-liquid-solid equilibrium in water + ethanol + 1- pentanol + sodium chloride system at 25 °C.
b) Representation of the initial mixture network to determine the quaternary regions.

Then, preparing initial mixtures as a and d and analysing the compositions of the b, c, e and f phases (g is in all cases the salt) the equilibrium data can be determined. The initial mixture points (as a in Figure 1(b)) to obtain the tie-lines in the 2L region have been prepared in sectional planes. These mixture points, in different sectional planes, form a network in the 2L region.

RESULTS

Ternary systems

Two of the four ternary systems including in the quaternary system reported in this paper have been published in previous papers: water + ethanol + 1-pentanol [5], water + ethanol + sodium chloride.[1] The ternary system water + 1-pentanol + sodium chloride has been submitted for publication.[6] The ternary system ethanol + 1-pentanol + sodium chloride shows a solubility curve of the sodium chloride. The ternary system ethanol + 1-pentanol + sodium chloride has been determined by titration with $AgNO_3$. The values of solubility of the sodium chloride in ethanol and 1-pentanol are very low (0.068 and 0.012 %mass, respectively).

Quaternary system

Two sectional planes (SP1 and SP2) were selected to study the 2L region:

SP1: (92.1%A + 7.90%D) + 100%B + (9.50%A + 90.5%C)

SP2: (84.0%A + 16.0%D) + 100%B + (8.00%A + 92.0%C)

Table 1 and table 2 show the tie-lines obtained in the sectional planes SP1 and SP2, respectively. Table 3 shows the equilibrium data (tie-triangles) in the 2L+1S region.

Aqueous phase				Organic phase			
100 w(A)	100 w(B)	100 w(C)	100 w(D)	100 w(A)	100 w(B)	100 w(C)	100 w(D)
91.8	0	0.958	7.23	8.41	0	91.5	0.039
86.8	4.52	1.06	7.57	10.1	7.19	82.7	0.040
82.7	8.56	1.14	7.58	12.6	14.9	72.4	0.120
79.0	12.1	1.23	7.67	15.7	21.9	62.2	0.159
75.4	15.0	1.60	7. 97	20.0	28.2	51.2	0.597
71.6	17.6	2.50	8.33	25.9	32.9	39.9	1.29

Table 1. Tie-lines obtained (preparing initial mixtures in SP1) in the two-liquids quaternary region for the water(A) + ethanol (B) + 1-pentanol (C) + sodium chloride (D) system at 25°C.

Aqueous phase				Organic phase			
100 w(A)	100 w(B)	100 w(C)	100 w(D)	100 w(A)	100 w(B)	100 w(C)	100 w(D)
83.8	0	0.379	15.9	6.70	0	93.3	0
80.6	3.45	0.429	15.6	8.63	9.13	82.1	0.119
77.2	7.00	0.477	15.4	11.1	18.5	70.1	0.197
74.1	10.0	0.576	15.3	14.0	27.0	58.5	0.478
71.1	12.6	0.739	15.5	17.8	34.3	46.8	1.07
67.9	15.2	1.11	15.9	22.4	39.4	36.2	1.95
64.0	17.9	1.90	16.1	26.7	41.7	27.9	3.67

Table 2. Tie-lines obtained (preparing initial mixtures in SP2) in the two-liquids quaternary region for the water(A) + ethanol (B) + 1-pentanol (C) + sodium chloride (D) system at 25°C.

Aqueous phase				Organic phase			
100 w(A)	100 w(B)	100 w(C)	100 w(D)	100 w(A)	100 w(B)	100 w(C)	100 w(D)
73.6	0	0.121	26.3	4.74	0	95.2	0.039
72.4	2.40	0.155	25.0	6.10	10.3	83.5	0.080
71.5	4.57	0.208	23.7	8.57	21.4	69.7	0.316
70.4	6.82	0.273	22.5	10.6	28.7	60.1	0.598
69.1	9.53	0.376	21.0	13.9	34.3	50.6	1.20
67.0	12.3	0.624	20.1	18.9	41.9	37.1	2.11
64.5	15.8	1.44	18.2	25.4	44.2	26.4	3.87

Table 3. Tie-triangles obtained in the two-liquids + one-solid quaternary region for the water(A) + ethanol (B) + 1-pentanol (C) + sodium chloride (D) system at 25°C.

DISCUSSION

To analyse the salt effect, the distribution curves of ethanol between water and 1-pentanol (Figure 2(a)) and the selectivity curves of 1-pentanol for the ethanol extraction (Figure 2(b)) have been presented. The distribution (K_d) and the selectivity (m) coefficients are defined as

$$K_{d_i} = \frac{(w_i)_{or}}{(w_i)_{aq}} \qquad (1)$$

$$m_i = \frac{\left(\frac{w_i}{(w_i + w_{water})}\right)_{or}}{\left(\frac{w_i}{(w_i + w_{water})}\right)_{aq}} \qquad (2)$$

where $(w_i)_p$ is the mass fraction of component i (ethanol in this case) in phase p (or=organic phase and aq=aqueous phase).

In these figures, points corresponding to the tie-triangles, the tie-lines of SP1 and SP2 for the quaternary system water + ethanol + 1-pentanol + sodium chloride and the tie-lines of the ternary system water + ethanol + 1-pentanol have been plotted. As can be observed, the distribution of ethanol in the organic phase and the selectivity of 1-pentanol for the ethanol extraction follow the sequence: three-phase region > SP2 > SP1 > no-salt ternary. Consequently, these coefficients are favoured by increasing the amount of salt in the system.

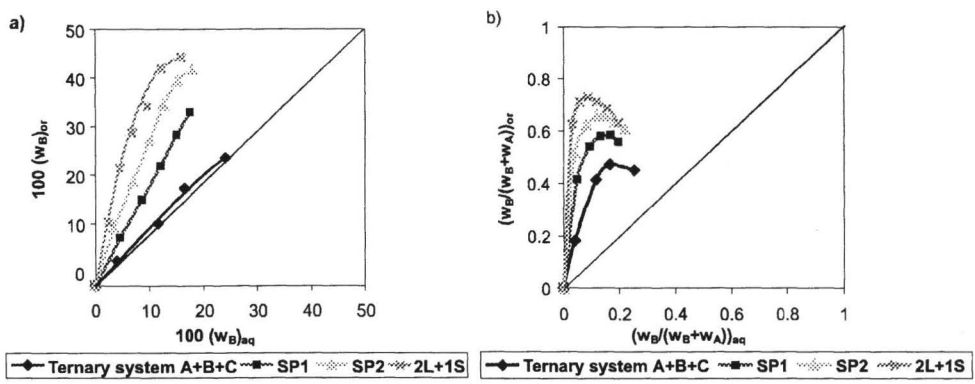


Figure 2(a) Distribution curves of ethanol. (b) Selectivity curves of 1-pentanol for ehanol extraction, obtained in the different regions studied for the quaternary system water + ethanol + 1-pentanol + sodium chloride at 25°.

In figures 3 and 4 the distribution curves of ethanol and selectivity curves of the solvent for the ethanol extraction, respectively, for different ternary (without salt) and quaternary (saturated with

salt) systems have been represented to compare the magnitude of the salt effect with different salts and solvents.

It can be deduced that the highest values of ethanol concentration in the organic phase (approx. 45 % mass) are achieved using 1-pentanol and sodium chloride (figure 3). With 1-butanol and sodium chloride the maximum is approx. 40 % and with 1-butanol and potassium chloride less than 35 %. With acetone and sodium chloride the concentrations of ethanol in organic phases are very low (less than 10 %), but we have to consider that in the ternary system without salt (water + ethanol + acetone) all binary pairs are totally miscible. If the extraction with 1-butanol and 1-pentanol are considered without salt, only less than 15 % and 25 % of ethanol can be obtained, respectively.

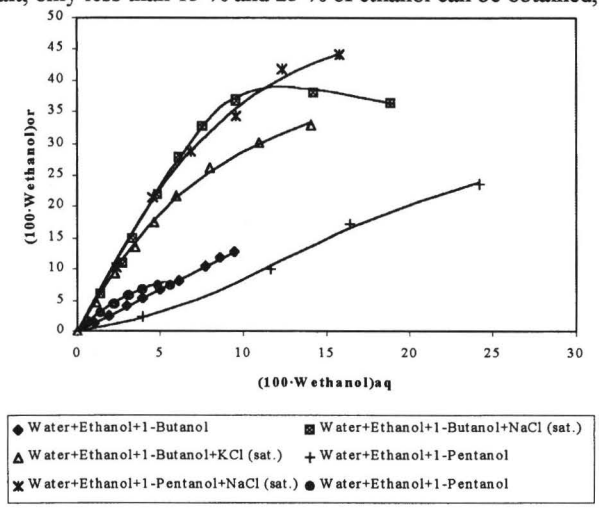


Figure 3. Distribution curves of the ethanol for different quaternary and ternary systems to compare the salt effect.

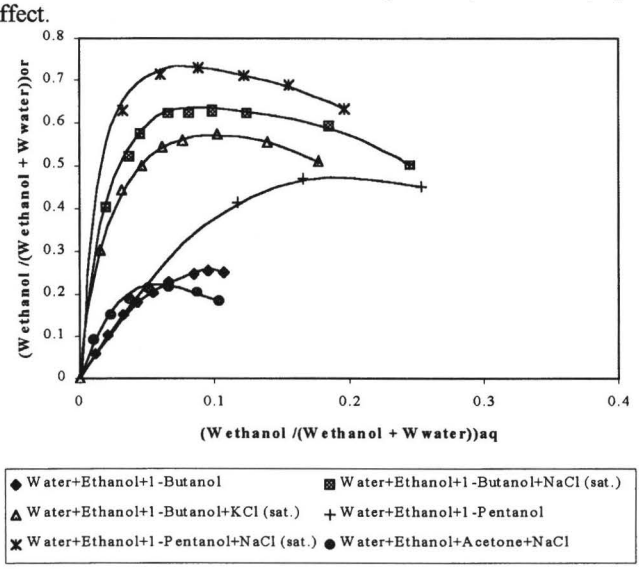


Figure 4. Selectivity curves of the ethanol for different quaternary and ternary systems to compare the salt effect.

If the selectivity of the different solvents (1-butanol, 1-pentanol and acetone) for the ethanol extraction is considered both with and without salt (figure 4), it can be seen that the highest selectivity is achieved using 1-pentanol and sodium chloride. But if we compare the results obtained for the same

system with and without salt the highest salt effect is produced in the ternary system water + ethanol + 1-butanol, when sodium chloride is added to saturation.

The methods for correlating the equilibrium data can be classified into two broad general groups. The first group could include models with a physical background, which use equations like NRTL, UNIQUAC,... to represent the interactions between the binary pairs. These models must be combined with any of the existing theories to represent the activity coefficient of the ionic species, such as those by Debye-Hückel, Pitzer,[7,8]. Nevertheless, this approach is out of the scope of the present paper and has not been considered. The second broad group corresponds to merely empirical models suitable for representing the behaviour observed. The Eisen-Joffe equation[9] and the modified Eisen-Joffe equation,[1] which is the model attempted in this paper, belong to this latter group. This modified Eisen-Joffe equation can be written as

$$\log\left(\frac{w_i}{w_j}\right)_{or} = \left(\alpha + \beta \cdot 100\,(w_{salt})_{aq}\right) + \left(\gamma + \delta \cdot 100\,(w_{salt})_{aq}\right) \cdot \log\left(\frac{w_{solute}}{w_{water}}\right)_{aq} + \left(\lambda + \eta \cdot 100\,(w_{salt})_{aq}\right) \cdot \left(\log\left(\frac{w_{solute}}{w_{water}}\right)_{aq}\right)^2 \quad (3)$$

and it was applied to the systems: water + ethanol + 1-butanol + sodium chloride, water + ethanol + acetone + sodium chloride and water + ethanol + 1-butanol + potassium chloride. Very good agreement between experimental and calculated data were obtained where $(w_{solute}/w_{water})_{aq}$ was the ratio $(w_{ethanol}/w_{water})$ in the aqueous phase and the ratios (w_i/w_j) or selected were $(w_{ethanol}/w_{water})$, $(w_{ethanol}/w_{solvent})$ and $(w_{salt}/w_{solvent})$, in the organic phase.

In order to determine the organic phase in equilibrium with a given composition of the aqueous phase, three equations of this type are needed. The three equations used to correlate the equilibrium quaternary data of the system water + ethanol + 1-pentanol + sodium chloride have been:

$$\log\left(\frac{w_B}{w_A}\right)_{or} = \left(\alpha + \beta \cdot 100 (w_D)_{aq}\right) + \left(\gamma + \delta \cdot 100 (w_D)_{aq}\right) \cdot \log\left(\frac{w_B}{w_A}\right)_{aq} + + \left(\lambda + \eta \cdot 100 (w_D)_{aq}\right) \cdot \left(\log\left(\frac{w_B}{w_A}\right)_{aq}\right)^2 \quad (4)$$

$$\log\left(\frac{w_B}{w_C}\right)_{or} = \left(\alpha' + \beta' \cdot 100 (w_D)_{aq}\right) + \left(\gamma' + \delta' \cdot 100 (w_D)_{aq}\right) \cdot \log\left(\frac{w_B}{w_A}\right)_{aq} + + \left(\lambda' + \eta' \cdot 100 (w_D)_{aq}\right) \cdot \left(\log\left(\frac{w_B}{w_A}\right)_{aq}\right)^2 \quad (5)$$

$$\log\left(\frac{w_D}{w_B}\right)_{or} = \left(\alpha'' + \beta'' \cdot 100 (w_D)_{aq}\right) + \left(\gamma'' + \delta'' \cdot 100 (w_D)_{aq}\right) \cdot \log\left(\frac{w_B}{w_A}\right)_{aq} + \left(\lambda'' + \eta'' \cdot 100 (w_D)_{aq}\right) \cdot \left(\log\left(\frac{w_B}{w_A}\right)_{aq}\right)^2 \quad (6)$$

where $(w_i)_p$are the mass fraction of component i (A=water, B=ethanol, C=1-pentanol and D=sodium chloride) in phase p (or = organic phase and aq = aqueous phase) and α, β, γ, δ, λ and η are empirical parameters to be optimized. The tie-triangle and tie-line data were correlated together.

The simplex flexible method [10] has been used as the optimization method to determine the parameters of the correlation. The objective function and the standard deviation used have been calculated using the equations 7 and 8, respectively,

$$O.F. = \sum_{k=1}^{n}\left[\left(\log\left(\frac{w_i}{w_j}\right)_{k,or}\right)_{exp} - \left(\log\left(\frac{w_i}{w_j}\right)_{k,or}\right)_{cal}\right]^2 \quad (7)$$

$$\sigma = \sqrt{\frac{\sum_{k=1}^{n}\left((w_i)_{k,exp} - (w_i)_{k,cal}\right)^2}{4 \cdot n}} \quad (8)$$

where i,j = water, ethanol, 1-pentanol, sodium chloride, $i \neq j$, exp = experimental, cal = calculated and n = number of tie-lines and tie-triangles.

Table 4 shows the results of the correlation (parameters calculated and objective function and standard deviations values). Figure 5 shows the representation of experimental and calculated data for the three correlations carried out. A very good agreement can be observed for all the data.

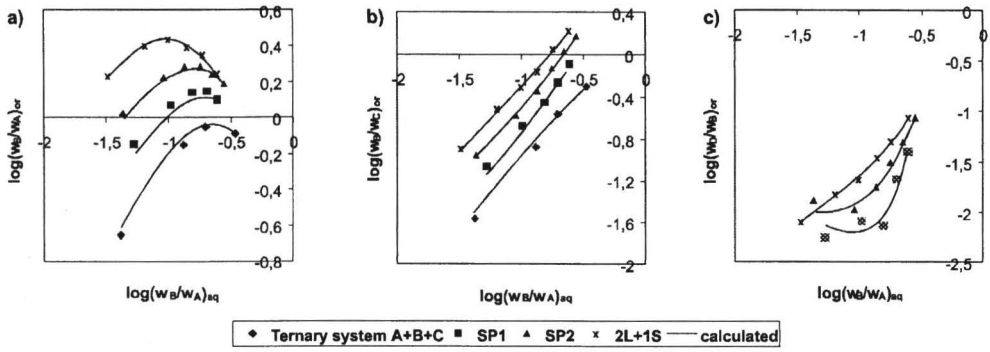


Figure 5. Correlation of results, using a modification of the Eisen-Joffe equation, for the water + ethanol + 1-pentanol + sodium chloride system at 25°C. Calculated data using a) eq 4, b) eq 5, and c) eq 6.

Equation (4)		Equation (5)		Equation (6)	
α	-0.55374363	α'	0.2587267	α''	2.4250426
β	0.00248787	β'	0.05508861	β''	-0.07641547
γ	-1.54290825	γ'	1.07981596	γ''	9.61849893
δ	-0.0208272	δ'	0.04363218	δ''	-0.27970938
λ	-1.15049718	λ'	-0.14505601	λ''	4.64264389
η	0.00362459	η'	0.01877037	η''	-0.16216138
O.F.	0.01445775	O.F.	0.03695552	O.F.	0.07395524
σ			0.94337		

Table 6. Correlation results.

CONCLUSIONS

The two-liquid, two liquid + one-solid and one-liquid + one-solid regions of the system water + ethanol + 1-pentanol + sodium chloride have been systematically studied at 25°C.

The addition of sodium chloride improves ethanol extraction by 1-pentanol. This improvement results from the salt effect that modifies the phase equilibria, increasing the distribution coefficient for ethanol and the selectivity of 1-pentanol as the mass of salt increases.

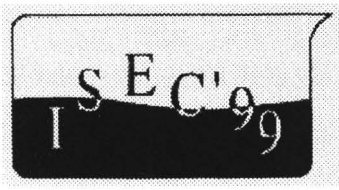
The distribution of ethanol and the selectivity for the ethanol extraction are more favourable using 1-pentanol and sodium chloride than using the following combinations: 1-butanol + sodium chloride, 1-butanol + potassium chloride and acetone + sodium chloride.

A modification of the Eisen-Joffe equation has been used to correlate the tie-line and tie-triangle data for the 2L and 2L + 1S regions, yielding good results.

REFERENCES

1. Marcilla A, Ruiz F and Olaya MM, *Fluid Phase Equilibria*, **105**, 71, (1995).
2. Olaya MM, Conesa JA and Marcilla A, *J. Chem Eng.*, **42**, 858, (1997).
3. Marcilla A, Ruiz F and García AN, *Fluid Phase Equilib.*, **112**, 273, (1995).
4. Ruiz Bevia F and Marcilla Gomis AJ, *Fluid Phase Equilib.*, **89**, 387, (1993).
5. Othmer DF, White RE and Trueger E, *Ind. Eng. Chem.*, **33,** 1240, (1941).

6. Gomis V, Ruiz F, Boluda N and Saquete MD, *J. Chem. Eng.* (1998) (submitted).
7. Annesini M, Gironi F and Marrelli L, *J. Chem. Eng.*, **39**, 502, (1994).
8. Chen C-C., Britt HI, Boston JF and Evans LB, *AIChE Journal*, **28**, 588, (1982).
9. Eisen EO and Joffe J, *Journal of Chemical and Engineering*, **11**, 4, (1966).
10. Himmelblau DM, Ed. John Willey & Sons, (1968), New York.



STUDY OF INCLUSION COMPLEX FORMATION OF SUBSTITUTED CYCLODEXTRINS WITH XYLENE ISOMERS

I Uemasu
National Institute for Resources and Environment, 16-3 Onogawa, Tsukuba, Ibaraki 305-8569, Japan

ABSTRACT
6-O-α-D-glucosyl-α-cyclodextrin (CD) showed high selectivity in forming an inclusion complex with p-xylene. On the other hand, 2,6-di-O-methyl-α-CD and 6-O-maltosyl-β-CD did not show such selectivity. It corresponded to the values of the formation constants of inclusion complexes determined on the basis of fluorescence measurements. 6-O-α-D-glucosyl-α-CD was supposed to form mainly the 2:1(CD: p-xylene) inclusion complex, while the latter CDs form the 1:1 inclusion complex. The value of the formation constant of 6-O-α-D-glucosyl-α-CD-p-xylene complex was greater than those of the CD-other xylene isomer complexes. The values of the formation constants of 2,6-di-O-methyl-α-CD-p-xylene complex and 6-O-maltosyl-β-CD-p-xylene complex were not very large compared to those of the CD-other xylene isomer complexes. The high selectivity in the inclusion of p-xylene by 6-O-α-D-glucosyl-α-CD seems to be attributable to the formation of the 2:1 inclusion complex.

Keywords: cyclodextrins, xylene, inclusion complex

INTRODUCTION

Cyclodextrins(CDs) have the structure of a doughnut-shaped ring composed of six or more α-1,4-linked D(+)-glucopyranoses. They can accommodate various kinds of organic compounds in their apolar cavities to form inclusion complexes. The selectivity in the complex formation chiefly depends on the size and shape of guest species.[1] It was previously demonstrated that selective liquid-liquid extraction of xylene isomers is possible by the use of aqueous solutions of branched cyclodextrins.[2,3] In particular, branched α-cyclodextrins show high-selectivity in forming inclusion complex with p-xylene and extracting it from a xylene mixture. The great advantage is that it can avoid the formation of solid inclusion complexes that are extremely fine and sticky. In this study the inclusion complex formation of three kinds of substituted cyclodextrins (see figure 1) with xylene isomers were examined in aqueous solution systems. To clarify the property of inclusion selectivity, the complex formation constants in the aqueous solution systems of the substituted cyclodextrins and xylene isomers were determined measuring the fluorescence intensity change and were compared.

EXPERIMENTAL

Materials

6-O-α-D-glucosyl-α-CD (G-α-CD) and 6-O-maltosyl-β-CD (M-β-CD) were supplied by Ensuiko Sugar Refining Co., Ltd. (Japan). These branched CDs contain less than 1.5% impurities. 2,6-Di-O-methyl-α-CD (D-α-CD), o-xylene, m-xylene, p-xylene, xylene mixture and diethyl ether were purchased from Wako Pure Chemical Industries, Ltd. (Japan). Ethylbenzene were obtained from Tokyo Kasei Kogyo Co., Ltd.(Japan). All were guaranteed reagents. Distilled and deionized water was used.

Inclusion Extraction

0.10 mol/dm^3 aqueous solutions of substituted CDs, i.e. G-α-CD, D-α-CD and M-β-CD, were prepared. 1 cm^3 of xylene mixture was added to 10 cm^3 of a CD solution and stirred in a thermostatic bath at 25°C for 15 minutes. No solids deposited. The reaction mixture was left undisturbed for a few minutes. Then it separated into two layers: the upper was the organic phase of xylene isomers and the lower was the CD aqueous solution in which guest species were extracted by inclusion complex formation. The CD aqueous solution was centrifuged at 3,000 rpm for 15 minutes to remove the

© 2000 Society of Chemical Industry

dispersed organic components in it. Then 5 cm^3 of the CD solution was taken into a separatory funnel, diluted with water and shaken with diethyl ether. Then the inclusion complex was dissociated and the aqueous layer became a transparent solution of a substituted CD. The guest species were extracted into the ether layer. The ether solution was subjected to chromatographic analysis.

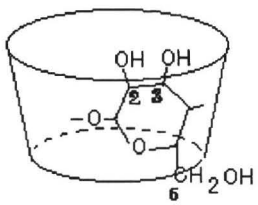


Figure 1. Scheme of Cyclodextrin

A glucopyranose unit is shown. α-CD is composed of six units. G-α-CD has one glucosyl group replacing the H atom of the OH group at the 6-position carbon. D-α-CD has twelve methyl groups replacing the H atoms of the OH groups at the 2- and 6-position carbons. M-β-CD is composed of seven glucopyranose units and has one maltosyl group replacing the H atom of the OH group at the 6-position carbon.

GC Analysis of Xylene Isomers.

Xylene isomers were analysed with a GC-14B gas chromatograph (Shimadzu Corporation, Japan) mounted with a fused silica megabore column with DB-WAX as the stationary phase (30 m x 0.72 mm o.d , film thickness 1.0 μm, J & W Scientific, USA). The measurement conditions were as follows: carrier gas, He; pressure 0.3 kg/cm^2; injection port temperature 300°C; sample size, 1.0 μl; splitting ratio, 1:50; flame ionisation detector; column temperature: isothermal at 50°C. Under these conditions, the retention times were 11.8 minutes for ethylbenzene, 12.4 minutes for p-xylene, 12.9 minutes for m-xylene and 16.9 minutes for o-xylene, respectively.

UV and Fluorescence Measurements.

UV absorption spectra and fluorescence spectra of xylene isomers were measured in the absence or presence of substituted CDs at room temperature. Although xylene isomers are said to be practically insoluble in water, we prepared the aqueous solutions as follows: 3.0 μl of a xylene isomer was added to 100 cm^3 of water. It was shaken vigorously for a few minutes. 10 cm^3 of the solution was taken and diluted with water or CD aqueous solution to 25 cm^3. Thus we prepared six kinds of solutions of a xylene isomer: one did not contain CD and the other five contained CD from 0.0015 - 0.005 mol/dm^3. UV absorption spectra were measured using these samples. However, no isosbestic point was found. The wavelength at which UV absorption for each solution was close was chosen as the excitation wavelength to measure the fluorescence spectra. These measurements were carried out with a U-3410 spectrophotometer (Hitachi, Ltd., Japan) and an FP-777 spectrofluorometer (JASCO Corporation, Japan).

RESULTS AND DISCUSSION

Inclusion Selectivity

As can be seen from table 1, G-α-CD showed high selectivity in the extraction of p-xylene from a xylene mixture. On the other hand, D-α-CD and M-β-CD did not show such selectivity. D-α-CD seems to form the complex more favorably with ethylbenzene rather than the other isomers. M-β-CD showed the selectivity of including o-xylene more than the other isomers.

	Starting Sample Oil	G-α-CD	D-α-CD	M-β-CD
o-Xylene	20.8%	3.6%	10.6%	42.5%
m-Xylene	43.8%	19.1%	43.0%	29.5%
p-Xylene	20.1%	57.7%	17.1%	17.0%
Ethylbenzene	15.3%	19.6%	29.3%	11.0%

Table 1 Changes in Composition of Oils Extracted by Cyclodextrins

	Starting Sample Oil	G-α-CD	D-α-CD	M-β-CD
m-Xylene	50.0%	14.5%	52.6%	43.2%
p-Xylene	50.0%	85.5%	47.4%	56.8%

Table 2 Changes in Composition of Oils Extracted by Cyclodextrins

To confirm the inclusion selectivity to m-xylene and p-xylene, inclusion extraction was carried out using an equimolar mixture of m- and p-xylenes. The results are listed in table 2. It is remarkable that D-α-CD did not include p-xylene more than m-xylene because unsubsituted α-CD and its derivatives usually make inclusion complexes more favourably with p-xylene than m-xylene.

Formation Constants of Inclusion Complexes.

Fluorescence spectra were measured to obtain formation constants of CD–xylene isomer complexes. In all the systems, fluorescence enhancement was observed with increasing the concentrations of cyclodextrins, which indicates that xylene isomers were included in the apolar cavities of CDs. By making the Benesi-Hildebrand plot, the complex formation constant can be calculated. Except the case of G-α-CD–p-xylene, the plots of ΔI^{-1} vs. $[CD]^{-1}$ showed a linear relationship in all of the other cases. This indicates that 1:1 complexes are formed between the CDs and xylene isomers.

Fluorescence spectra of G-α-CD–p-xylene system are shown in figure 2 and the Benesi-Hildebrand plot is shown in figure 3. When a linear line fitting was applied, the plot gave a negative value of formation constant. Then the plot was analysed supposing that both 2:1 complex of CD and p-xylene and 1:1 complex are present.[4] The formation of 2:1 complex of α-CD and p-xylene has been already reported.[5] Simplex method was employed for the non-linear least squares fit.[6] Then the formation constant of 1:1 complex (K_1) and that of 2:1 complex (K_2) were obtained.

$$\text{G-α-CD} + \text{p-Xylene} \rightarrow \text{G-α-CD–p-Xylene} \quad \ldots\ K_1$$

$$\text{G-α-CD} + \text{G-α-CD–p-Xylene} \rightarrow (\text{G-α-CD})_2 - \text{p-Xylene} \quad \ldots\ K_2$$

Formation constants of inclusion complexes calculated on the basis of changes in fluorescence intensity are listed in table 3. The formation constant of G-α-CD–p-xylene complex is greater than those of the other G-α-CD–xylene isomer complexes. It corresponds to the high inclusion selectivity of the CD to p-xylene. On the other hand, D-α-CD forms the 1:1 complex with p-xylene but does not form the 2:1 complex. The complex formation constant is smaller than that of D-α-CD–m-xylene complex. This is in agreement with the results of inclusion extraction.

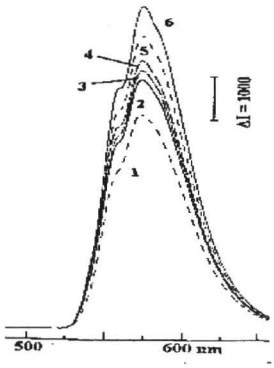


Figure 2. Fluorescence Spectra of p-Xylene in Aqueous Solutions. [p-Xylene]=$1x10^{-4}$ M; 1:[Gd-α-CD]=0 M, 2: [Gd-α-CD]=0.00141 M, 3: [Gd-α-CD]=0.00169 M, 4: [Gd-α-CD]=0.00218 M, 5:[Gd-α-CD]=0.00286 M, 6:[Gd-α-CD]=0.00421 M, λ_{ex}:272.5 nm

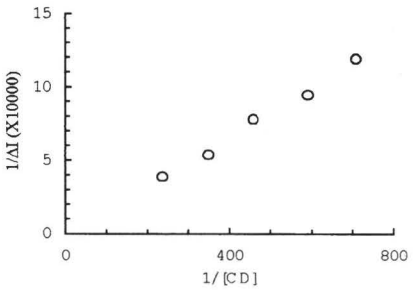


Figure 3. Benesi-Hildebrand Plot for Changes in Fluorescence Intensity at 570nm for p-Xylene Solutions with Different Concentrations of G-α-CD.

	G-α-CD	D-α-CD	M-β-CD
o-Xylene	100	61	18
m-Xylene	125	210	76
p-Xylene	38(K_1), 81(K_2)	140	220
Ethylbenzene	130	260	220

Table 3 Formation Constants of Inclusion Complexes of Cyclodextrins with Xylene Isomers (mol/dm^3)

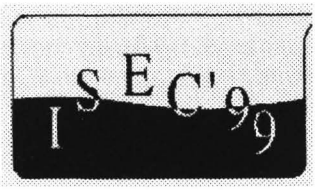
Comparison between G-α-CD and D-α-CD.

The cavity of unsubstituted α-CD can accommodate one molecule of benzene. A p-xylene molecule can be included by an α-CD molecule or two α-CD molecules. It is supposed that a p-xylene molecule is included very stable in the apolar cavity of a dimer formed by two α-CD molecules facing head-to-head. In the case of o- and m-xylenes, although one methyl group of xylene enters in the cavity of α-CD, the other methyl group causes steric hindrance so that a more stable inclusion complex cannot be formed. Such steric hindrance does not occur in the case of β-CD since the cavity of β-CD is wider by ca. 0.2 nm than that of α-CD.

As can be seen from figure 1, the broader rim of G-□-CD undergoes no modification. Thus G-□-CD can form a head-to-head dimmer like unsubstituted □-CD. The hydrogen bonding by the OH groups of the broader rim is supposed to contribute the formation of dimmer. A p-xylene molecule is included stable in the apolar cavity of the dimmer, to which the high inclusion selectivity of G-□-CD to p-xylene seems to be attributable. In the case of D-□-CD, the formation of such a dimmer should be difficult because of the presence of the methoxyl groups at the 2-position.

REFERENCES

1. Szejtli J, *'Cyclodextrin Technology'* Kluwer Academic Publishers, Dordrecht, (1988).
2. Uemasu I, *J. Incl. Phenom*, **13**, 1, (1992).
3. Uemasu I and Takahashi H, *Sekiyu Gakkaishi*, **36**, 210, (1993).
4. Ricci RW, *Carbohydr. Res.*, **129**, 278, (1984).
5. Sanemasa and Akamine Y, *Bull. Chem. Soc. Japan*, **60**, 2059, (1987).
6. Yamaoka K, Tanigawa Y, Nakagawa T and Uno T, *J. Pharmacobio-Dyn.*, **4**, 879, (1981).



MODELLING TBP/DILUENT MIXTURES AND WATER EXTRACTION BY THESE MIXTURES USING THE UNIQUAC EQUATION AND TAKING ACCOUNT OF COMPLEX FORMATION

Béatrice Rat[1], Binh Dinh[1] and Claude Poitrenaud[2]

[1] CEA - VALRHO (Marcoule), BP 171 - 30207 Bagnols-sur-Cèze Cedex, France

[2] CEA-SACLAY/INSTN, 91191 Gif-sur-Yvette Cedex, France

ABSTRACT

The possibility of using UNIQUAC and UNIFAC equations to correlate thermodynamic properties of organic phase in metal solvent extraction is considered. UNIQUAC interaction parameters, regressed on TBP/diluent (alkane, CCl_4, $HCCl_3$) mixtures, permitted the calculation of both activity coefficients and enthalpies of mixing. UNIFAC, using group contribution, permitted the representation of different TBP/n-alkane mixtures with only two interaction parameters, but made no distinction between branched alkanes. The interaction parameters regressed on binary system TBP/diluent and TBP/H_2O were used to estimate the solubility of water in TBP/diluent mixtures as a function of water activity and TBP percentage. For a correct description of TBP/diluent/H_2O/LiCl system, it was necessary, except in case of alkane, to supplement UNIFAC equation by explicitly taking into account formation of complexes (Chem-UNIFAC).

Keywords: modelling, UNIQUAC, UNIFAC, Chem-UNIFAC, TBP/diluent/H_2O/LiCl

INTRODUCTION

The main advantages of UNIQUAC and UNIFAC equations in estimating thermodynamic properties of organic phase in metal solvent extraction, are to take into account extractant percentage and diluent influence, and to use only binary parameters to describe multi-component systems. The advantage of UNIFAC equation lies in group contribution which give it a predictive power. These advantages led to the use of UNIQUAC and UNIFAC equations to estimate deviations from ideality of organic phases in nuclear fuel reprocessing.

UNIQUAC and UNIFAC models

For a multicomponent system, the UNIQUAC equation for the molar excess Gibbs energy is composed of two parts:[1,2] the combinatorial part, essentially due to differences in size and shape of the molecules, and a residual contribution, essentially due to energetic interactions.

$$\frac{g^E}{RT} = \begin{cases} \dfrac{g^E_{combinatorial}}{RT} = \sum_i x_i \ln\dfrac{\phi_i}{x_i} + \dfrac{z}{2}\sum_i q_i x_i \ln\dfrac{\theta_i}{\phi_i} \\ + \\ \dfrac{g^E_{residual}}{RT} = -\sum_i q_i x_i \ln\left(\sum_i \theta_i \exp\left(-\dfrac{a_{ji}}{T}\right)\right) \end{cases}$$

q_i is the area parameter of component i
ϕ_i and θ_i are the volume and area fractions of component i
a_{ji} is the interaction parameter between molecule i and j

UNIFAC model adopts the same formalism as UNIQUAC model but introduces the group contribution concept, i.e. molecules are considered as structural group assemblies. The UNIFAC method being based on the group contribution concept has the advantage that it can be used in the calculation of multi-component system with a small number of parameters.

Some authors[3,4,5,6] were already interested in UNIQUAC and UNIFAC models to evaluate non-ideality of such organic phases. In the present work, a progressive procedure was followed to fit interaction parameters, using experimental data of Rozen et al.[6] and Li et al.[3,4,5] and carrying out additional acquisitions. Firstly, the ability of UNIQUAC to represent thermodynamic properties of TBP/diluent mixtures with diluents (alkane, CCl_4, $HCCl_3$) which exhibit interactions with TBP differing by their

© 2000 Society of Chemical Industry

nature and their strength was investigated. Then group contribution possibilities were tested, applying UNIFAC equation to TBP/*n*-C_8H_{18}, TBP/*iso*-C_8H_{18} and T*i*BP/*n*-C_8H_{18} mixtures. Finally, we tried to apply interaction parameters regressed on binary systems to predict thermodynamic properties of the TBP/diluent/H_2O ternary systems.

RESULTS AND DISCUSSION

TBP/diluent mixtures

Experimental data on liquid-vapour equilibria were used to estimate activity coefficients in liquid binary solutions. Rozen et al.[6] measured the vapour pressure of volatile solvents (*n*-C_6H_{14}, CCl_4 and $HCCl_3$) with TBP. In the present work, a FTIR spectrophotometer equipped with a gas cell, was used for measurements of volatile solvent concentration in the vapour phase equilibrated with the liquid sample. TBP/*n*-C_8H_{18}, TBP/*iso*-C_8H_{18} and T*i*BP/*n*-C_8H_{18} mixtures were studied.

UNIQUAC model

UNIQUAC interaction parameters between TBP and diluent were regressed from experimental activity, and then, were used to predict enthalpy of mixing. Figures 1 and 2 compare experimental values of activity coefficients of Rozen et al.[6] and enthalpies of mixing of Pyartman [7] with calculated curves.

Calculated and experimental results are in agreement. Parameters were also regressed from activity coefficient in TBP/$HCCl_3$ mixture, predicted enthalpy of mixing was not so good, due to large deviation from ideality.

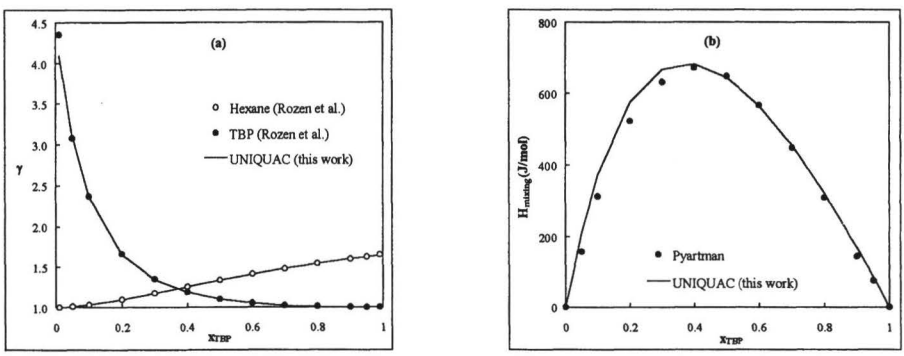


Figure 1 : Activity coefficients (a) and enthalpy of mixing (b) in TBP/hexane at 25°C

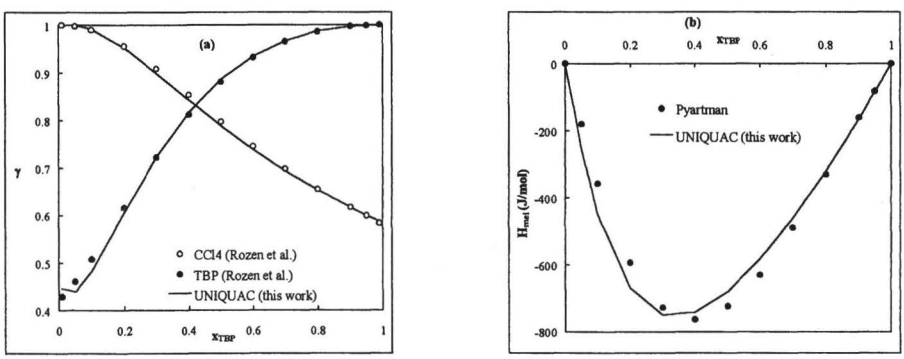


Figure 2 : Activity coefficients (a) and enthalpy of mixing (b) in TBP/CCl_4 at 25°C

UNIFAC model

To apply UNIFAC equation to correlate TBP/alkane experimental data, we defined structural group "CH_2" and $(CH_2O)_3PO$. CH_3, CH_2, CH, C are subgroups of the "CH_2" principal group, they only differ in size and shape but have the same interaction parameters with the other groups. Interaction parameters between "CH_2" and $(CH_2O)_3PO$ were regressed on TBP/hexane experimental data and were applied to all the studied TBP/alkane systems.

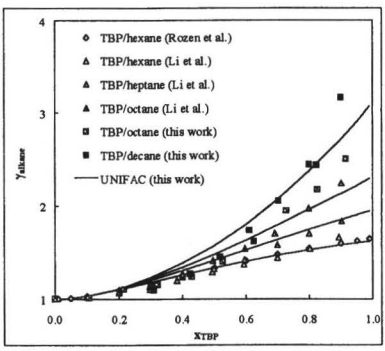


Figure 3: Activity coefficients in TBP/ n-alkane systems at 25°C

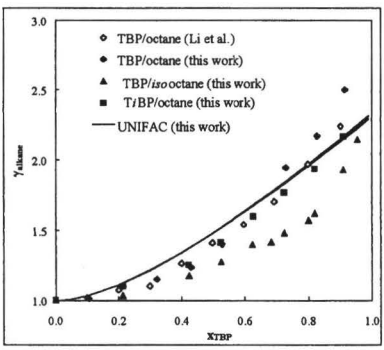


Figure 4: Activity coefficients in TBP/alkane systems at 25°C

As seen in 3, experimental data exhibit an increase of activity coefficients in TBP/n-alkane mixtures with the lengthening of the alkane chain. TBP/alkane exhibit positive deviation from ideality. This deviation increases as the area of alkane increases, i.e. as the length of alkane increases. UNIFAC equation, with two interaction parameters, reproduces this increase of activity coefficients.

The effect of branching is shown on 4. The experimental activity coefficients decrease when the alkane chain is branched. The effect is less pronounced when the extractant chain is branched. The reason is the same as previoulsly : a branched alkane has a smaller area than a straight-chain alkane. So the TBP/branched alkane mixtures are more favoured than TBP/n-alkane mixtures. UNIFAC made no distinction beween a straight-chain alkane and a branched alkane wih the same carbon atom number. A corrected area of *iso*-octane did not improve activity coefficient calculation. It seems that the combinatorial term of UNIFAC equation did not permit the isomers to be distinguished.

TBP/diluent/H_2O/LiCl

Experimental

For ternary systems, measurements were carried out on water extraction by TBP/diluent (*n*-C_6H_{14}, CCl_4 and $HCCl_3$) mixtures (Figure 5). The salting-out agent LiCl was used to fix water activity in the TBP/diluent/H_2O/LiCl system.

As seen in Figure 5, the solubility of water in TBP/diluent mixtures decreases in the order TBP/*n*-C_6H_{14} > TBP/CCl_4 > TBP/$HCCl_3$ at moderate and high TBP percentage. At low TBP percentage, CCl_4 and $HCCl_3$ are inverted. We expected the TBP/$HCCl_3$ mixture to extract more water than TBP/CCl_4 and TBP/hexane, considering the better affinity of $HCCl_3$ with TBP and H_2O. This point of view did not consider that TBP, which interacts strongly with $HCCl_3$, is less available to extract H_2O. These experimental results made us wonder if UNIQUAC equation with only binary parameters can calculate solubility of water in these TBP/diluent mixtures.

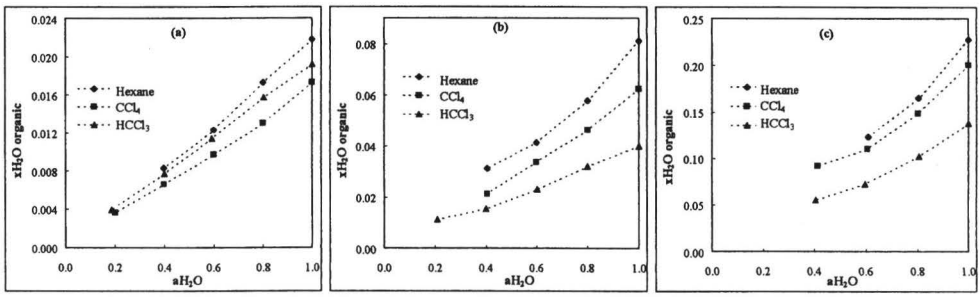


Figure 5: Experimental extraction isotherms of water by TBP as a function of water activity - extraction system H_2O/LiCl/TBP((a) 8.5, (b) 20.5, (c) 45.5 mol%)/diluent

UNIQUAC Model

UNIQUAC interaction parameters between TBP and H_2O were regressed on experimental solubility of water in undiluted TBP. Interaction parameters between diluent and H_2O were either regressed (hexane) or found in literature[8,9] (CCl_4). These parameters and those between TBP and diluent, previously regressed, were used to predict water solubility in TBP/diluent mixtures as a function of water activity and TBP percentage.

Predicted solubilities of water were in good agreement with experimental data for hexane but were overestimated for CCl_4 (Figure 6) and $HCCl_3$. Thus, UNIQUAC with only binary interaction parameters do not take into account diluent and water competition with TBP.

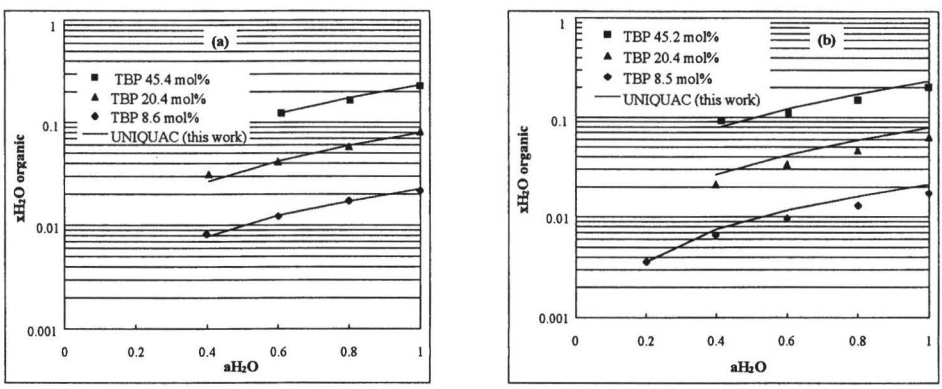


Figure 6: Extraction isotherms of water - H_2O/LiCl/TBP/diluent ((a) hexane, (b) CCl_4)

Chem-UNIFAC Model

The application of UNIQUAC to predict water solubility in different TBP/diluent mixture, showed clearly that UNIQUAC method, in which chemical interactions are not allowed for explicitly, failed to describe mixtures where hydrogen bonding or other strong interactions are appreciable. The non-ideality of such solutions must be interpreted in terms of chemical interactions, taken account by an equilibrium constant for complex formation, and physical forces between all molecules represented by UNIQUAC or UNIFAC equation. Rozen et al.[6] called this model Chem-UNIFAC. We used this model, but unlike Rozen et al.,[6] we did not apply group contribution to describe TBP or diluent as group assemblies but to describe complexes. The AB complex, for example, was considered as formed with one group A and one group B. So, the interaction parameters number was minimised, an A/B mixture, where AB formed, is modelled with only 2 interaction parameters and 1 equilibrium constant.

Modelling of the two binary systems TBP/CCl_4 and TBP/H_2O was carried out by taking account of TBP.CCl_4 and TBP.H_2O formation, i.e. new interaction parameters and equilibrium constants were

regressed. These parameters and literature H_2O-CCl_4 parameters (Table 1) were used to predict water solubility in TBP/CCl_4 mixture (Figure 7).

Good agreement was obtained between predicted and experimental solubilities. For TBP/hexane/H_2O/LiCl system the results obtained with Chem-UNIFAC were the same as UNIQUAC model.

a_{nm}	H_2O	CCl_4	TBP
H_2O	0	497	84
CCl_4	1201	0	92
TBP	242	-58.5	0

Table 1 :UNIFAC interaction parameters for TBP/CCl_4/H_2O mixture

$$TBP + CCl_4 \Leftrightarrow TBP.CCl_4 \quad K_{T_{TBP.CCl_4}} = 0.44$$

$$TBP + H_2O \Leftrightarrow TBP.H_2O \quad K_{T_{TBP.H_2O}} = 0.1$$

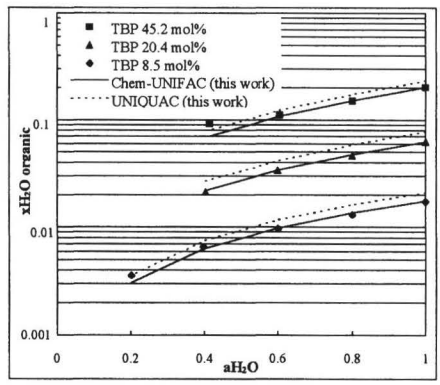


Figure 7 : Extraction isotherms of water TBP/CCl_4/H_2O/LiCl

CONCLUSIONS

UNIQUAC permits the representation of TBP/diluent binary mixtures with diluents which exhibit of a very different nature and strength interactions with TBP. UNIFAC (UNIQUAC plus group contribution concept) permits the reproduction of TBP/n-alkane behaviour for different chain lengths with only two interaction parameters but not the difference between branched alkanes. UNIQUAC can correctly predict water solubility in TBP/diluent mixture, as a function of water activity and TBP percentage, when the diluent is an alkane but overestimates water solubility when TBP and diluent interact strongly. To obtain a good agreement with experimental data, Chem-UNIFAC, which takes into account complex formation, must be applied. We are looking forward to applying of Chem-UNIFAC to nitric acid and metallic nitrate extraction.

NOMENCLATURE

a_{ji}	interaction parameter between molecules i and j in the UNIQUAC equation
H_{mixing}	enthalpy of mixing
q_i	area parameter of component i
x_i	mole fraction of component i in the mixture
γ_i	activity coefficient of component i in the mixture (rational scale)
ϕ_i	volume fraction of component i in the mixture
θ_i	area fraction of component i in the mixture

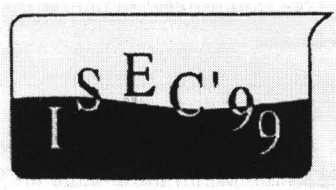
REFERENCES

1. Prausnitz JM, Lichtenthaler RN and d.Azevedo EG, *'Molecular Thermodynamics of Fluid Phase Equilibria'*, Englewood Cliffs ed., Prentice-Hall, NJ (1986).
2. Fredenslund A,Gmehling J and Rasmussen P, *Vapor-Liquid Equilibria using UNIFAC, a Group Contribution Method*, Elsevier Scientific Publishing Company (1977).
3. Li Z, Chen J, Bao T, Shang Y and Li Y, *Thermochim Acta*, **169**, 287, (1990)
4. Li J, Li Y, Chen J, Lu J and Teng T, *Fluid Phase Equilibria*, **58**, 307, (1990)

5. Chen J, Li Z, Lu J and Li Y, *Fluid Phase Equilibria*, **81**, 1, (1992)
6. Rozen AM, Yurkin VG, Konovalov YV, Shapovalov MP and Krupnov BV, *Russ. J. Phys.Chem*, **69(2)**, 225, (1995)
7. Pyartman AK and Kopyrin AA, *Radiochemistry*, **38(2)**, 154, (1996)
8. Skold-Jørgensen S, Kolbe B, Gmehling J and Rasmussen P, *Ind. Eng Chem. Proc.Des.Dev.*, **18(4)**, 714, (1979)
9 Gmehling J, Rasmussen P and Fredenslund A, *Ind. Eng. Chem. Proc. Des.Dev.*, **21**, 118, (1982)



Guest-Host Binding



A NOVEL STRATEGY FOR THE DESIGN OF ORGANIC LIGANDS OF HIGH SELECTIVITY

Shigeo Umetani [1] and Quyen TH Le [2]

[1] Institute for Chemical Research, Kyoto University, Uji, Kyoto 611-0011, Japan

[2] Los Alamos National Laboratory, Los Alamos, NM 87545, U.S.A.

ABSTRACT

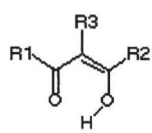
It has been shown that highly selective ligands for metal ions could be successfully designed taking into consideration the bite size (O-O distance in the ligand or chelate ring) and the interligand contact in the complex. The distance between the two donating oxygen atoms in the ßdiketone type of ligands can be readily controlled by appropriate structural modifications. The complexation of Al^{3+} was found to be greatly influenced by the effect of the interligand contact and that of In^{3+} the bite size. The appropriate substituents were introduced to the ß-diketone type ligands to control the bite size and the volume of the ligand.

Keywords: acylpyrazolone, molecular recognition, substituent effect, bite size, interligand contact.

INTRODUCTION

Studies on the solvent extraction of metal ions with acylpyrazolones[1,2] and acylisoxazolones,[3] which are structurally analogous to β-diketones derived from 5-membered heterocyclic compounds, revealed that the improved extraction with strongly acidic extractants is usually accompanied by poor selectivity. These ligands were found to have longer distances between the two donating oxygen atoms as compared to the conventional β-diketones according to estimation by molecular orbital calculations. These facts prompted the consideration that the O-O distance plays an important role in complexing metal ions. Recently, on studying the extraction of lanthanides using 2-trifluoroacetylcyclo-alkanones[4] and acylpyrazolones having bulky substituents at the 4-position,[5] it has been found that the separability of lanthanides was clearly improved with those ligands having the shorter O-O distance. It could be concluded that the O-O distance is one of the most significant factors that govern selectivity in the complexation of β-diketones with lanthanides. If the structure of β-diketone could be suitably modified introducing bulky groups at suitable positions for creating a steric effect, the O-O distance could be intentionally controlled, and, consequently, the extractability and/or the separability could be improved. Following the work on lanthanide ions, with ionic radii very similar to each other, this research has now been expanded to ions of the metals of group 13, which have large differences in ionic radii, in an attempt to investigate how the O-O distance and other factors in the structure of β-diketones would affect their complexation reactions.

In this paper, the selectivity of modified β-diketones for Al^{3+} (r = 0.53 Å for coordination number 6), Ga^{3+} (r = 0.62 Å) and In^{3+} (r = 0.80 Å) have been examined via solvent extraction, and the stability of Al^{3+}, Ga^{3+} and In^{3+} β-diketonates has been discussed based on the structures of the ligands and their metal complexes.



R1	R2	R3	
$-CH_3$	$-CH_3$	-H	AA
$-CH_3$	$-CH_3$	-Ph	PhAA
$-CH_3$	-Ph	-H	BA
$-CH_3$	-Ph	-Ph	PhBA

© 2000 Society of Chemical Industry

EXPERIMENTAL

Chemicals

α-Phenylbenzoylacetone (PhBA) was synthesized according to the literature.[6] Acylpyrazolones were synthesized according to the method of Jensen.[7] α-Phenylacetylacetone (PhAA) and benzoylacetone (BA) were purchased from Dojindo and used without further purification. Aqueous solutions of Al^{3+}, Ga^{3+} and In^{3+} were prepared from standard solutions by Wako Chemicals and stocked in 0.02 mol dm^{-3} hydrochloric acid solution. Other chemicals were of analytical reagent grade. Water was demineralized and distilled.

Apparatus

Metal ion concentrations were measured with a Japan Jarrell Ash Model ICAP-500 inductively coupled argon plasma atomic emission spectrophotometer. pH measurements were made with a Hitachi-Horiba F-8L pH meter equipped with a Horiba 6028 glass combination pH electrode. ^{1}H-NMR spectra were measured with a Varian VXR-200 spectrometer (200 MHz) at 25 °C in $CDCl_3$.

Semi-empirical MNDO/H calculation was performed on fully optimized molecular geometries on a Cray Y-MP2E/264 using MNDO93 (Cray Research Inc.).

Solvent Extraction Procedure

A 10 cm^3 aliquot of an aqueous phase containing $1x10^{-4}$ mol dm^{-3} of metal ion, 0.1 mol dm^{-3} sodium perchlorate and 0.01 mol dm^{-3} sodium acetate as a buffering component was adjusted to the desired pH with hydrochloric acid or sodium hydroxide solution. The aqueous phase was shaken with an equal volume of benzene containing the required amount of ligand in a 30 cm^3 centrifuge tube at 25 °C until the reaction reached to the equilibrium. After centrifugation, the pH of the aqueous phase was measured and taken as the equilibrium value. The metal concentration in the aqueous phase was determined by ICP-AES and that in the organic phase was measured in the same way after back-extraction by stripping with hydrochloric acid solution. The sum of the metal concentrations in the two phases agreed well with the initial concentration.

RESULTS AND DISCUSSION

Molecular Orbital Calculations

The distances between the two donating oxygens were estimated by semi-empirical MNDO/H calculation, which is the MNDO calculation that takes the hydrogen bond into consideration. The O-O distances obtained by MNDO/H for various β-diketones are shown in table 1. The distances between the two donating oxygens of acetylacetone (AA) and BA are 2.50 and 2.51Å, respectively, whereas those for PhAA and PhBA are reduced to 2.44 Å. A shortening of this distance was made by introducing a phenyl group to the α-position of AA and BA. The steric repulsion raised between the phenyl group and the two terminal groups in the structure of AA and BA brings a narrowing of this distance. This structural change is also supported by ^{1}H-NMR data. The very broad peaks assigned to the enolic proton (-OH) for AA and BA appear at 1.44 and 16.15 ppm, respectively, while those for PhAA and PhBA are very sharp and shift downfield to 16.77 and 17.39 ppm, respectively. The sharp and downfield shift of the enolic proton signal is caused by the strong intramolecular hydrogen bonding arising from the narrow O-O separation. The intramolecular hydrogen bond energy (EOH) can be estimated as the energy difference between the hydrogen-bonded structure and the open structure in which the O-H is rotated by 180° to minimize the hydrogen bond energy; these values are shown in table 1.

In addition, the facts that the enolic proton signals correspond to one proton and there were observed no methyne protons for PhAA and PhBA indicate that both PhAA and PhBA exist quantitatively in the enol form in $CDCl_3$. It has been reported that the presence of an α-substituent usually favors the keto tautomer,[8] and previous results[9] are in agreement with this tendency. The

results obtained here agree with reports[10,11] demonstrating that the α-aryl group markedly increases the enol content unlike other α-substituents, such as the methyl or bromo groups.

	AA	PhAA	BA	PhBA
O-O distance (Å)[a]				
HA	2.50	2.44	2.51	2.44
A^- [b]	3.09	2.83	3.10	2.84
EOH (kJ/mol) [a]	65.56	77.53	63.51	75.69
^{1}H-NMR (-OH, ppm)	15.44	16.67	16.15	17.39
pK_a [c]	12.65	12.85	12.66	12.90

[a] MNDO/H. [b] fixed at planar.
[c] measured in 1,4-dioxane/H2O (75:25 v/v). $[(CH_3)_4NClO_4] = 0.1$ mol dm^{-3}.

Table 1 Comparison of properties of AA, PhAA, BA and PhBA

Equilibrium Analysis

The complexation of the two extractants PhAA and PhBA with Al^{3+} and In^{3+}, compared to that of AA and BA, has been investigated using solvent extraction. The extraction behaviour significantly changed following the introduction of a phenyl group to the α-position. Almost 100% of Al^{3+} is extracted around pH 4.6 with PhAA, while In^{3+} is totally unextracted below pH 5. A similar result was also obtained for PhBA.

The extraction equilibrium can be expressed as follows:

$$Al^{3+} + 3HAo == AlA_{3,o} + 3H^+ \qquad (1)$$

The extraction constant, K_{ex}, is defined in equation (2).

$$K_{ex} = [AlA_3]_o [H^+]^3 / [Al^{3+}] [HA]^3_o = D[H^+]^3 / [HA]^3_o \qquad (2)$$

The log K_{ex} values were obtained by substituting the $pH_{1/2}$ values, the pH read from log D vs pH plots at which half of the metal ion is extracted (log D = 0), in equation (2) and are summarized in table 2.

As previously mentioned, Al^{3+} and In^{3+} are extracted with AA and BA with similar extraction constants. On the contrary, In^{3+} is not extracted at all with PhAA and PhBA, while Al^{3+} is extracted with the smaller extraction constants compared to those for AA and BA. Considering that the substituents at the α-position of the β-diketones should be essentially independent of their complexation with the metal ions, the present results are surprising.

	$pH_{1/2}$ [a]		log K_{ex}	
	Al	In	Al	In
AA	3.30	3.95	-6.90	-8.85
PhAA	4.01	—	-9.03	—
BA	3.20	3.39	-6.60	-7.17
PhBA	4.24	—	-9.72	—

[a] $[HA]_o = 0.1$ mol dm^{-3} in benzene. $[NaClO_4] = 0.1$ mol dm^{-3}.

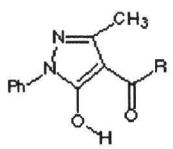
Table 2 Extraction data for Al and In

An X-ray crystallographic study of Al and In β-diketonates was made to confirm the role of the substituent at the α-position. The O-O distances of the β-diketones in $Al(AA)_3$,[12] $In(AA)_3$,[13] and

$In(TTA)_3$[14] were reported to be 2.726, 2.905 and 2.905 Å, respectively. A survey of X-ray data of Al and In β-diketonates shows that the O-O distances in Al β-diketonates are among the shortest ones, while those in In ß-diketonates are among the longest ones. According to MNDO/H calculations seen in table 1, the O-O distances in the anionic form of PhAA and PhBA are 2.83 and 2.84 Å, while those for AA and BA are 3.09 and 3.10 Å. The non-extractability of In^{3+} with PhAA and PhBA could be ascribed to the phenyl group at the α-position which prevents the O-O separation of the anionic form from broadening to fit to the desired configuration in the In complex owing to the between the α-phenyl group and the terminal groups.

Interligand Contact in Al and In β-diketonates

The intracomplex interligand contacts should have great influence on the stability of Al β-diketonates, which could be deduced from the extraction order of Al^{3+} and In^{3+} with β-diketones. In general, the organic ligands including β-diketones form more stable complexes with metal ions having smaller ionic radii when their valency is the same. Consequently, the extraction constants for the smaller metal ions are usually higher than those for the larger ones. However, in the extraction of Al^{3+} and In^{3+}, the reverse in the extraction order is frequently seen depending on the bulkiness of the ligands. Al^{3+} is extracted better than In^{3+} with AA and BA. In the case of bulky β-diketones, such as dibenzoylmethane (DBM) and TTA, the steric crowding of the ligands around Al^{3+} greatly destabilizes complexation because of its very small ionic radius, while this is not so serious in the case of In^{3+}. As a result, In^{3+} is better extracted than Al^{3+} with these bulky β-diketones. It should be noted here that the O-O distances of AA, BA, TTA and DBM are similar to each other according to the molecular orbital calculations.



		R
HPMAP	(G)	$-CH_3$
HPMBP	(E)	-Ph
HPM1NP	(S)	-1-Naph
HPM2NP	(C)	-2-Naph
HPMPiP		$-C(CH_3)_3$

Extraction with Acylpyrazolones

Five acylpyrazolone derivatives have been prepared as seen in the scheme. They are 1-phenyl-3-methyl-4-acetyl (HPMAP), -benzoyl (HPMBP), -(1-naphthoyl) (HPM1NP), -(2-naphthoyl) (HPM2NP), and -pivaloyl (HPMPiP) -pyrazolones. The O-O distances were estimated by the MNDO/H calculation and seen in table 3. The O-O distances of the acylpyrazolones except for HPMPiP are 2.60 - 2.65 Å, while that of HPMPiP is 2.46 Å.

	HPMAP	HPMBP	HPM1NP	HPM2NP	HPMPiP
O-O distance (Å)[a]					
HA	2.60	2.65	2.64	2.65	2.46
A^- [b]	3.04	3.06	3.06	3.06	2.84
E_{OH} (kcal/mol)[a]	13.74	12.43	12.64	12.40	18.38
^{1}H-NMR (-OH, ppm)	—	—	—	—	14.9
pK_a	3.94	3.92	—	4.13	4.26

[a] MNDO/H. [b] fixed at planar.

Table 3 Comparison of Acylpyrazolones

The ^{1}H-NMR spectra show the evidence for the hydrogen bond strength. The signal assigned to the hydroxyl proton of HPMPiP appeared at 14.9 ppm; whereas those for the other acylpyrazolones are too broad at 10-20 ppm to be observed .

The extractions of Al^{3+}, In^{3+} and Ga^{3+} into benzene are shown in figure 1 plotting the logarithmic value of the distribution ratio of metal ions (D) against pH. The results are summarized in table 4. Being derived from the five membered heterocyclic 4-pyrazolone, the O-O distances of the present acylpyrazolone derivatives except for HPMPiP are longer than those of the conventional β-diketones. Owing to their long O-O distances, the extraction of In^{3+} was not disturbed and was made at pH 1-2. The extraction of Al^{3+} was seen in the higher pH region, although the ionic radius of Al^{3+} is much smaller than that of In^{3+}.

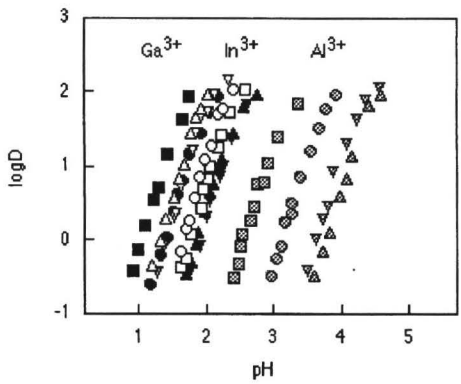


Figure 1 Extraction of Al^{3+} (gray symbol), Ga^{3+} (solid symbol) and In^{3+} (blank symbol) into benzene with acylpyrazolones.
[acylpyrazolone]o = 5 x 10^{-3} mol dm^{-3} [$NaClO_4$] = 0.1 mol dm^{-3}.

	Al^{3+}		Ga^{3+}		In^{3+}	
	$pH_{1/2}$	log K_{ex}	$pH_{1/2}$	log K_{ex}	$pH_{1/2}$	log K_{ex}
HPMBP	3.12	-2.47	1.39	2.74	1.65	1.96
HPMAP	2.56	-0.78	1.04	3.78	1.75	1.64
HPM1NP	3.78	-4.45	1.86	1.32	1.31	2.96
HPM2NP	3.63	-4.00	1.91	1.18	1.41	2.68
HPMPiP	4.30	-6.01	2.43	-0.39	4.04	-5.21

$[HA]_o$ = 5x10^{-3} mol dm^{-3} in benzene, [$NaClO_4$] = 0.1 mol dm^{-3}.

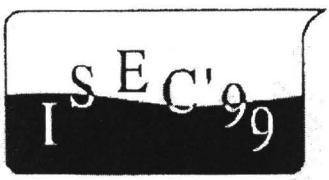
Table 4 Extraction constants for group 13 metal ions

Considering that the acylpyrazolones themselves are bulky ligands and their acidities are quite similar, it is clear that the extraction of Al^{3+} is under the effect of the interligand contact. It was found that the extraction reduces, as the substituent at the 4-position becomes bulkier. The quantitative separation of Al^{3+} from In^{3+} can be readily achieved with the naphthoylpyrazolones. The extraction of In^{3+} does not depend on the size of the substituents. The effect of the interligand contact is also seen in the extraction of Ga^{3+}. While the ionic radius of Ga^{3+} is smaller than that of In^{3+}, their extractions were similar. In addition, the extractability decreases as the substituents becomes bulkier, like the case of Al^{3+}. All of the acylpyrazolones examined are available to quantitatively separate Al^{3+} and Ga^{3+}. Owing to the steric repulsion between the 4-pivaloyl and 3-methyl groups, the O-O distance of HPMPiP is narrowed and the extraction of In^{3+} came close to that of Al^{3+} resulting in a quantitative

separation of Ga^{3+} from Al^{3+} and In^{3+}. From results so far, there are two factors governing the complexation of group 13 metal ions with β-diketones: the distance between the two donating oxygens and the interligand interaction. The balance between the two should decide the stability of each complex, that is, the extraction order, as well as the separation of Al^{3+} and In^{3+}. This observation may contribute to the basic knowledge on organic ligands, especially on the concepts of their complexation with metal ions, and confirms the suggestion for a perspective strategy for designing novel ligands of high selectivity from well-known typical ones.

REFERENCES

1. Roy A and Nag K, *J. Inorg. Nucl. Chem.*, **40**, 331, (1978).
2. Umetani S and Freiser H, *Inorg. Chem.*, **26**, 3179, (1987).
3. Le QTH, Umetani S, Takahara H and Matsui M, *Anal. Chim. Acta*, **272**, 293, (1993).
4. Umetani S, Kawase Y, Takahara H, Le QTH and Matsui M, *J. Chem. Soc., Chem. Commun.*, 78, (1993).
5. Umetani S, Kawase Y, Le THQ and Matsui M, to be published.
6. Hauser CR, Swamer FW and Adams JT, *Organic Reactions*, 59, (1954).
7. Jensen BS, *Acta Chem. Scand.*, **13**, 1668, (1959).
8. Emsley J, *Struct. Bonding* (Berlin), **57**, 147, (1984).
9. Le THQ, Umetani S, Suzuki M and Matsui M, *J. Chem. Soc., Dalton Trans.*, 643, (1997).
10. Emsley J and Ma YYL, *J. Mol. Struct.*, **178**, 297, (1988).
11. Emsley J, Freeman JN, Bates AP and Hursthouse BM, *J. Chem. Soc., Perkin Trans. I*, 297, (1988).
12. Hon PK and Pfluger CE, *J. Coord. Chem.*, **3**, 67, (1973).
13. Palenik GJ and Dymock KR, *Acta Cryst.*, **B36**, 2059, (1980).
14. Soling H, *Acta Chem. Scand.*, **A30**, 163, (1976).



LIGAND-THICKNESS EFFECT LEADS TO ENHANCED PREFERENCE FOR LARGE ANIONS IN ALKALI METAL EXTRACTION BY CROWN–ETHERS

Bruce A Moyer, Tamara J Haverlock and Richard A Sachleben
Chemical and Analytical Sciences Division, Bldg. 4500S, MS-6119, Oak Ridge National Laboratory, P.O. Box 2008, Oak Ridge, TN 37831-6119, U.S.A.

ABSTRACT
Jean-Marie Lehn (Nobel laureate, 1987) suggested *ligand thickness* to be an important consideration in the design of host molecules for cation recognition. We have recently expanded the role of this simple ligand property by demonstrating a case in which ligand thickness contributes significantly to anion discrimination. It was found that in the extraction of sodium nitrate and perchlorate by a simple crown ether, bis(*t*-octylbenzo)-14-crown-4 (BOB14C4), the normal preference for perchlorate is almost completely lost when the complex cation has the "open-face sandwich" vs. the "sandwich" structure.

Keywords: crown-ether, anion effect, equilibrium modeling, sodium perchlorate, sodium nitrate

INTRODUCTION

In this paper the fundamental question dealing with whether the structure of a crown-ether and its complexes may influence the preference for a given co-anion in the extraction of salts of alkali metals is addressed. The converse question, namely whether the anion influences the preference of a crown ether for a given alkali metal cation, has been addressed by previous authors and answered in the affirmative.[1] One would thus expect that the properties of the crown-metal complex would have an effect on anion preference.

We were led to investigate this issue in the course of developing a process for the extraction of the pertechnetate anion, TcO_4^-, from alkaline waste solutions by use of crown- ethers.[2] The process, known as SRTALK (strontium and technetium extraction from alkaline solution), is depicted by the cycle shown in figure 1. As shown, the function of the crown- ether involves complexation of the abundant Na^+ or K^+ cations in the waste, facilitating the transfer of the cation to the organic phase. Although any of the anions present in the waste represent potential co-anions in the net extraction process, the thermodynamically preferred co-anions are those having large radii and correspondingly low (more negative) Gibbs energies of hydration or, more exactly, low Gibbs energies of partitioning to organic solvents.[3] Even in the presence of an abundance of nitrate, nitrite, hydroxide, carbonate, aluminate, and other anions in the waste, the large, poorly hydrated pertechnetate anion at trace concentrations can be efficiently extracted.

From the practical issue of selecting an appropriate crown ether for the SRTALK process arises the fundamental issue of how the crown ether structure can be tailored for the purpose of controlling anion selectivity. Although one may envisage many types of structural modifications to crown ethers that might influence anion interactions, one of the simplest properties of a crown ether in this regard relates to the degree to which it envelops the metal cation and prevents close contact between the cation and anion. In 1973, Jean-Marie Lehn examined the question of ligand thickness in connection with the selectivity of a host ligand for a given cation.[4] Here, we examine this same property of ligand thickness, but in connection with co-anion selectivity. The example chosen for study is a simple system involving the small-cavity crown-ether bis(*t*-octylbenzo)-14-crown-4 (BOB14C4) as an extractant for sodium nitrate and perchlorate salts into 1,2-dichloroethane (1,2-DCE). Perchlorate was chosen, as a model anion for the experiments, since the high anion concentrations required would have made radioactive pertechnetate difficult to use. As will be discussed below, this particular system allows a direct assessment of the ligand-thickness effect by virtue of the formation of both 1:1 and 1:2 metal:crown complexes.

© 2000 Society of Chemical Industry

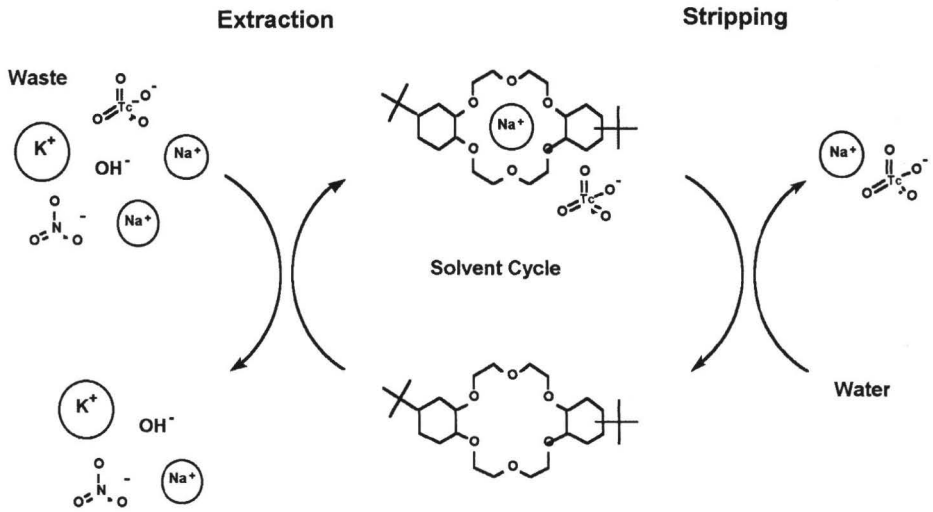


Figure 1. SRTALK process for separating pertechnetate from alkaline nitrate wastes.

THEORY

Consider the extraction of a cation M^+ by a crown ether CE to form an ion pair consisting of the complex cation $M(CE)^+$ or $M(CE)_2^+$ and co-anion X^- (overbars indicate organic-phase species):

$$\textit{Net reaction:} \quad M^+ + X^- + n\overline{CE} \overset{\Delta G^\circ_{ex}}{\rightleftharpoons} \overline{M(CE)_n{}^+X^-} \qquad (1)$$

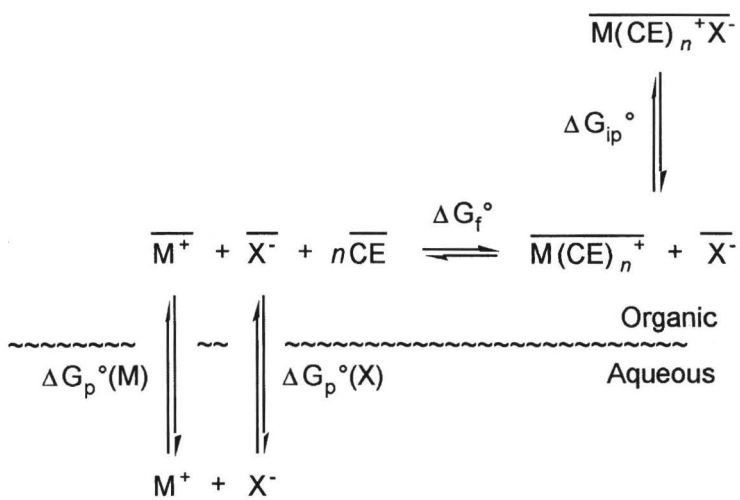


Figure 2. Component equilibria in the extraction of an alkali metal salt by a crown ether.

Component equilibria are defined in figure 2. These consist of partitioning of the free ions M^+ and X^- to the organic phase, formation of the complex in the organic phase, and ion pairing of the complex cation with the co-anion.[5,6] The corresponding standard Gibbs energy changes comprise the net

standard Gibbs energy change for the extraction process, and it may be seen that the ion-pairing term is the only term in which the crown structure and anion both have an effect:

$$\Delta G°_{ex} = \Delta G_p°(M) + \Delta G_p°(X) + \Delta G_f° + \Delta G_{ip}°$$

Dependent on anion

Dependent on crown structure

(2)

For extraction of sodium nitrate and perchlorate, the reactions may be written specifically:

$$Na^+ + NO_3^- + n\overline{CE} \overset{\Delta G°_{ex}(NO_3^-)}{\rightleftharpoons} \overline{Na(CE)_n^+NO_3^-} \quad (3)$$

$$Na^+ + ClO_4^- + n\overline{CE} \overset{\Delta G°_{ex}(ClO_4^-)}{\rightleftharpoons} \overline{Na(CE)_n^+ClO_4^-} \quad (4)$$

If nitrate and perchlorate are considered to be in competition, selectivity may be viewed in terms of anion exchange, obtained by subtraction of equation 3 from equation 4:

$$ClO_4^- + \overline{Na(CE)_n^+NO_3^-} \overset{\Delta G°_{exch}}{\rightleftharpoons} NO_3^- + \overline{Na(CE)_n^+ClO_4^-} \quad (5)$$

The value of $\Delta\Delta G_{exch}°$ follows by analogous subtraction of eq.uation. 2 written for NO_3^- from equation 2 written for ClO_4^- to give four difference terms: $\Delta\Delta G_p°(Na) = 0$, $\Delta\Delta G_p°(X) = \Delta G_p°(ClO_4^-) - \Delta G_p°(NO_3^-)$, $\Delta\Delta G_f° = 0$, and $\Delta\Delta G_{ip}° = \Delta G_{ip}°(ClO_4^-) - \Delta G_{ip}°(NO_3^-)$. It may be seen that the ligand contributes to only the ion pairing term $\Delta\Delta G_{ip}°$:

$$\Delta\Delta G°_{exch} = \Delta\Delta G_p°(X) + \Delta\Delta G_{ip}°$$

Dependent on anion

Dependent on crown structure

(6)

Equation 6 is the same expression used to evaluate the selectivity of anion exchange generally.[3] Various levels of electrostatic theory may be used to estimate both $\Delta\Delta G_p°(X)$ and $\Delta\Delta G_{ip}°$ to the typical effect for the univalent case that for a large anion replacing a small anion, $\Delta\Delta G_p°(X)$ is negative and dominant and $\Delta\Delta G_{ip}°$ is a positive counter-effect. Because of the behavior of the first term, then, the larger the thermochemical radius of an anion is, the greater will be its tendency to exchange with another anion. At the same time, the ion-pairing term $\Delta\Delta G_{ip}°$ becomes more positive, but since the first term dominates, the net effect still is higher selectivity toward the larger anion. However, as the cation radius becomes larger, the ion-pairing term for a given pair of anions becomes smaller and ultimately approaches zero. That is, for sufficiently large cationic radius, the contribution of ion pairing to selectivity becomes negligible, and selectivity toward the larger anion is maximized. Hence, the larger the radius of the cation is, the greater will be the selectivity toward the larger of a pair of anions up to a maximum plateau value. If the cation is a complex of a metal cation and one or more ligands, the thickness of the ligands determines the overall cationic radius and the corresponding selectivity in anion exchange. Ligands with greater thickness force the anion to lie at larger distance from the cationic charge, bringing about greater preference for larger anions.

EXPERIMENTAL

Solutions of BOB14C4 in 1,2-DCE were contacted with equal volumes of aqueous solutions of either $NaNO_3$ or $NaClO_4$ for 2 h at 25 ± 1 °C by end-over-end rotation. Aqueous phases also contained ^{22}Na radiotracer, and distribution ratios were determined by gamma counting using a NaI detector. The following data sets were collected:

M $NaNO_3$	M BOB14C4	M $NaClO_4$	M BOB14C4
0.05 - 2.5	0.1	0.0001 - 5	0.1
0.5	0.005 - 0.2	0.001 - 2.5	0.01
2.5	0.005 - 0.2	0.1	0.0001 - 0.1
		0.005	0.00025 - 0.1

A total of 50 data points were subjected to equilibrium modeling using the program SXLSQI. As described elsewhere,[6,7,8] the program employs Pitzer parameters and Hildebrand-Scott solubility parameters to respectively estimate the aqueous- and organic-phase activity coefficients. Values of log K corresponding to postulated equilibria thus refer to the condition of infinite dilution.

RESULTS AND DISCUSSION

Extraction experiments consisted of varying the concentration of either $NaNO_3$ or $NaClO_4$ while holding the concentration of BOB14C4 constant in 1,2-DCE, or holding the concentration of either $NaNO_3$ or $NaClO_4$ constant while varying the concentration of BOB14C4. By use of the program SXLSQI, the observed behavior was found to be consistent with the equilibrium scheme in figure 2, assuming the following set of species:

$$Na(CE)X \quad Na(CE)^+ \quad Na(CE)_2X \quad Na(CE)_2^+ \quad X^-$$

It was found possible to simultaneously fit the nitrate and perchlorate data sets in a single model based on the six sodium species $Na(CE)NO_3$, $Na(CE)ClO_4$, $Na(CE)^+$, $Na(CE)_2NO_3$, $Na(CE)_2ClO_4$, and $Na(CE)_2^+$. The nitrate and perchlorate data could be fit separately, but the two cationic complexes are common to both systems, making it preferable to fit all of the data together. Consistent with the somewhat polar nature of 1,2-DCE, it was necessary to assume the partial dissociation of the anion from the cationic complexes. The observation that two crown ether molecules could accommodate the metal cation follows reasonably from the small cavity size of the crown ether and the common tendency of the Na^+ cation to take on a coordination number of 8. In fact, it was possible to obtain crystals with the stoichiometries $Na(DB14C4)ClO_4$ and $[Na(DB14C4)_2]ClO_4{\cdot}CHCl_3$ (DB14C4 = dibenzo-14-crown-4). The structures of these complexes as determined by X-ray crystallography[9] entail an "open-face sandwich" structure with coordination to the metal by bidentate perchlorate in the first case and a "sandwich" structure with perchlorate unable to coordinate to the metal in the second case.

The preliminary log K values obtained from fitting revealed a dramatic effect of sandwich formation on anion selectivity in this system. Results are summarized in part in figure 3. Since the fitting gave -20.6 kJ/mol as an estimate for $\Delta\Delta G_p^\circ$, equation 6 becomes $\Delta\Delta G_{exch}^\circ = -20.6 + \Delta\Delta G_{ip}^\circ$, and $\Delta\Delta G_{ip}^\circ$ may be estimated to be 18.3 and 1.2 kJ/mol for the open-face sandwich and sandwich complexes, respectively. It may be seen that the close approach of the anion to the Na^+ cation in the open-face sandwich complex yields ion pairs that are more stable by 18.3 kJ/mol more for nitrate than perchlorate. When the anion is forced away by sandwich formation, nitrate ion pairs are only slightly more stable (1.2 kJ/mol), and the overall selectivity toward perchlorate increases three orders of magnitude. The example illustrates how the thickness of the ligand plays a key role in ion-pair extraction.

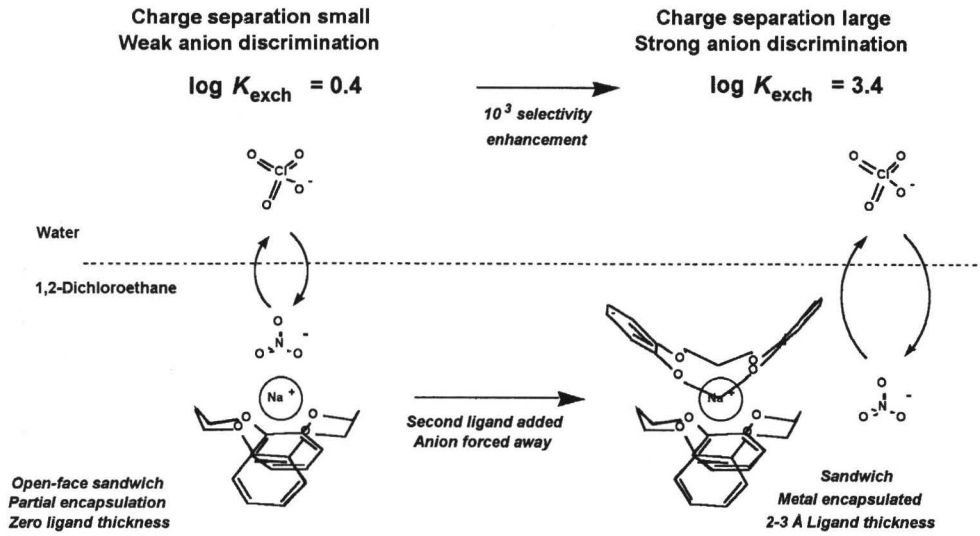


Figure 3. Scheme showing the effect of sandwich formation on anion selectivity, the extent of nitrate being displaced by the larger perchlorate.

ACKNOWLEDGMENTS

This research was sponsored by the Division of Chemical Sciences, Office of Basic Energy Sciences, U. S. Department of Energy, under contract number DE-AC05-96OR22464 with Oak Ridge National Laboratory, managed by Lockheed Martin Energy Research Corp. LHD thanks the ORNL Postdoctoral Research Associates Program administered by ORNL and the Oak Ridge Institute for Science and Education.

REFERENCES

1. (a) Jawaid M and Ingman F, *Talanta*, **25**, 91, (1978). (b) Yakshin VV, Abashkin VM, and Laskorin BN, *Dokl. Akad. Nauk SSSR*, , **252**, 373, (1980). (c) Olsher U, Hankins MG, Kim YD, and Bartsch RA, *J. Am. Chem. Soc.* **115**, 3370, (1993).
2. (a) Bonnesen PV, Moyer BA, Haverlock TJ, Armstrong VS, and Sachleben RA, in *'Emerging Technologies in Hazardous Waste Management VI'*, Tedder DW and Pohland FG, Eds., American Academy of Environmental Engineers, Annapolis, MD, 245, (1996). (b) Bonnesen PV, Moyer BA, Presley DJ, Armstrong VS, Haverlock TJ, Counce RM, and Sachleben RA, *'Alkaline-Side Extraction of Technetium from Tank Waste Using Crown Ethers and Other Extractants'*, Report ORNL/TM-13241, Oak Ridge National Laboratory, Oak Ridge, TN, U.S.A., June, 1996. (c) Leonard RA, Conner C, Liberatore MW, Bonnesen PV, Presley DJ, Moyer BA, and Lumetta GJ, *Sep. Sci. Technol.* (In press).
3. Moyer BA and Bonnesen PV, in *'Supramolecular Chemistry of Anions'*, Bianchi A, Bowman-James K, and Garcia-Espana E, Eds., Wiley-VCH, New York, 1, (1997).
4. Lehn J-M, *Structure and Bonding*, **16**, 1, (1973).
5. Moyer BA, in *'Comprehensive Supramolecular Chemistry'*, Atwood JL, Davies JED, MacNicol DD, Vögtle F, and Lehn J-M, Eds., Pergamon, Elsevier, Oxford, **1**, 377, (1996).
6. Deng Y, Sachleben RA, and Moyer BA, *J. Chem. Soc., Faraday Trans.*, **23**, 4215, (1995).
7. Baes, Jr. CF, 'SXLSQI, *A Program for Modelling Solvent Extraction Systems*', Report ORNL/TM-13604, Oak Ridge National Laboratory, Oak Ridge, TN, 1998.
8. Baes, Jr. CF, Moyer BA, Case GN, and Case FI, *Sep. Sci. Technol.*, **25**, 1675, (1990).
9. Bryan JC, Haverlock TJ, Sachleben RA, and Moyer BA, Oak Ridge National Laboratory, manuscript in preparation.

LIQUID–LIQUID EXTRACTION OF METAL IONS WITH A MONOAZATETRATHIACROWN ETHER AND ITS ACYCLIC ANALOGUES

Kenji Chayama[1], Chieko Kurihara[1], Haruo Tsuji[1] and Eiichi Sekido[2]

[1] Department of Chemistry, Faculty of Science, Konan University, Kobe, Japan

[2]Department of Chemistry, Faculty of Science, Kobe University, Kobe, Japan

ABSTRACT

Cyclic and acyclic reagents containing 4 sulfur atoms and a nitrogen atom were successfully synthesized. A cyclic monoazatetrathiacrown ether, 1-aza-4,7,11,14-tetrathiacyclohexadecane (ATCH) and acyclic monoazatetrathioether 9-aza-3,6,12,15-tetrathiaheptadecane (ATH) were synthesized by the reaction between appropriate dithiols and alkyl halides. Liquid-liquid extraction of metal ions was performed. Soft metal ions such as Ag(I), Cu(I) and Hg(II) ions which are classified as class *b* metal ions were selectively extracted. On the other hand, hard (class *a*) and intermediate (class *ab*) metal ions such as Mg(II), Mn(II), Zn(II), Co(II) and Ni(II) were not extracted at all. The extraction behavior of silver(I) and copper(I) ions with ATCH and ATH was examined in detail.

*Keywords:*silver, copper(I), monoazathiacrown ether.

INTRODUCTION

Chemistry of thiacrown-ethers has been widely studied in these three decades as well as the chemistry of crown ethers. It has been shown that thiacrown-ethers have an excellent selectivity for class *b* metal ions.[1-3] These compounds are suitable for the solvent extraction of class *b* metal ions, because of their hydrophobic character and the solubility in the organic solvents such as 1,2-dichloroethane and chloroform. However, the acyclic analogues of the cyclic compounds have not been widely studied.[3-8] Cyclic and acyclic polythioethers have both been synthesized and the selectivity and the extraction efficiency for the metal ions studied.[3] Furthermore, some new derivatives of cyclic and acyclic tetrathioethers containing a nitrogen atom in the molecule have also been synthesized. In this study, the extraction behavior of metal ions with a cyclic and an acyclic monoaza-tetrathioether derivatives are examined .

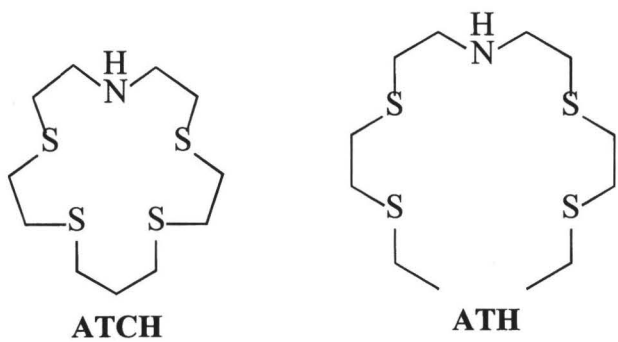


Figure 1 Structures of ATCH and ATH.

© 2000 Society of Chemical Industry

EXPERIMENTAL

Synthesis of the reagents

A cyclic monoaza-tetrathiacrown-ether, 1-aza-4,7,11,14-tetrathiacyclohexadecane (ATCH) was synthesized by the cyclization reaction between 1,4,8,11-tetrathiaundecane and bis(2-chroloethyl)amine.[9] Acyclic monoazatetrathioether 9-aza-3,6,12,15 tetrathiaheptadecane (ATH) was synthesized by the 2:1 reaction between 1,4-dithiahexane and bis(2-chloroethyl)amine.[10] The HCl-salt of the products was recrystallized twice with chloroform-benzene.

Other reagents and Apparatus

Reagents used for liquid-liquid extraction were of reagent grade except 1,2-dichloroethane. The extraction solvent 1,2-dichloroethane, was shaken three times with 2 mol/dm^3 potassium hydroxide solution followed by shaking three times with water, dried over calcium chloride, and distilled. Extraction was carried out in a Taiyo M incubator. A Hitachi Z-8000 atomic absorption spectrophotometer was used to determine the concentration of metal ions in the aqueous solutions. The pH of the aqueous solutions was measured with a Hitachi-Horiba M-7 pH meter.

Liquid-liquid extraction of the metal ions

An aliquot (10 cm^3) of aqueous solution containing the metal ion (5 x 10^{-5} mol/dm^3), picrate ion (1 x 10^{-3} mol/dm^3) and acetate buffer (1 x 10^{-2}mol/dm^3) was adjusted to an ionic strength of 0.1 with sodium sulfate. This solution and 10 cm^3 of the reagent solution in 1,2-dichloroethane in a stoppered cylindrical tube were shaken (180 strokes min^{-1}) for 30min at 25 ± 0.1°C. The mixture was then centrifuged for 5 minutes at 2000 rpm. After the two phases were separated, the pH of the aqueous phase was measured and the concentration of the metal ion in the aqueous phase and in the organic phase was determined by atomic absorption spectrometry.

RESULTS AND DISCUSSION

Liquid-liquid distribution of reagents

The cyclic and acyclic polythioethers are insoluble in water, however the monoaza-polythioethers are soluble in acidic aqueous solution. The distribution behavior of ATCH and ATH between 1,2-dichloroethane and water was different from that of polythioethers that do not contain any nitrogen atoms. Protonated ATCH and ATH distributed to aqueous phase from 1,2-dichloroethane phase at pH values less than 3-4. As the pH in aqueous phase increases, ATCH and ATH were transferred to the organic phase. More than 99% reagent distributed to an organic phase at pH over 6.0. In this study, picrate ion was used as the counter anion to form the ion pair with the metal complex cation. However the protonated reagent forms the ion pair with picrate ion, even in the case of the absence of the metal ion. This causes the reduction of picrate ion concentration in the aqueous phase, and results in a decrease of metal extraction. Then, the extraction behavior of picrate ion with ATCH and ATH was examined. It is concluded that the picrate ion formed the ion pair with ATCH and distributes to the organic phase below pH 4.0. On the other hand, the ion pair of ATH with picrate ion distributes to the organic phase below pH 2.0.

Liquid-liquid extraction of metals

Liquid-liquid extraction of the metals Mg(II), Mn(II), Zn(II), Co(II), Ni(II), Cu(II), Cd(II), Ag(I), Cu(I) and Hg(II) was performed. As shown in table 1 with a softness parameter α[11], soft metal ions such as Ag(I), Cu(I), and Hg(II) ions which are classified as class *b* metal ions were selectively extracted. On the other hand, hard (class *a*) and intermediate (class *ab*) metal ions such as Mg(II) , Mn(II), Zn(II) Co(II) and Ni(II) were not extracted at all. Although Cu(II) ion belonging to class ab was slightly extracted, Cd(II) ion belonging to class *b* was not extracted at all. Copper(II) was

extracted 15% with ATCH at pH5.6. However, ATH did not extract Cu(II) at all. On the other hand, the extraction efficiency of Hg(II) with acyclic ATH is much higher than that with ATCH. As Ag(I) and Cu(I) were extracted perfectly, the extraction behavior of Ag(I) and Cu(I) with ATCH and ATH was examined.

Metals	Class	fi	ATCH		ATH	
			pH	%E	pH	%E
Mg(II)	a	0	5.6	0	4.8	0
Mn(II)	ab	1.04	5.0	0	5.3	0
Zn(II)	ab	1.25	5.3	0	5.3	0
Co(II)	ab	1.39	5.0	0	5.3	0
Ni(II)	ab	1.41	4.9	0	5.6	0
Cu(II)	ab	1.64	5.6	15.4	5.0	0
Cd(II)	b	1.65	5.6	0	5.0	0
Ag(I)	b	3.60	5.5	99.8	5.0	100
Cu(I)	b	3.92	5.6	99.4	5.0	95
Hg(II)	b	5.83	5.0	37.2	4.8	71

Table 1 Data on the extraction of various metal ions with ATCH and ATH

Liquid-liquid extraction of silver (I) ion

Liquid-liquid extraction of silver (I) ion was examined. Extraction was greater than 99% with ATCH above pH 3.0, and with ATH at pH above 2.0. Molar ratio methods were performed to clarify the composition of the extracted species. Figure 1 shows the plots of the percentage extraction of the silver ion vs. molar ratio of ATCH in the organic phase and silver (I) ion in the aqueous phase. The plots indicate that the molar ratio of the silver(I) ion to ATCH is 1:1. The plots of the logarithmic distribution ratio of the silver (I) ion vs. the logarithmic concentration of picrate ion are shown in figure 2. The relationship between the extraction constant Kex and the distribution ratio $D_{M(I)}$ is expressed as follows:

$$M^+ + mL + nPic^- \Leftrightarrow ML_mPic_n \qquad (1)$$

$$\text{Log } D_{M(I)} = \log K_{ex} + m\log[L] + n\log[Pic] \qquad (2)$$

The plots in figure 2 gave a straight line with slope 1, suggesting that n = 1 in equations 1 and 2. These results suggest that the composition of the extracted species with ATCH is Ag(I): L : Pic^- = 1:1:1. For ATCH, the extraction constant was evaluated as log K_{ex} = 9.8 ± 0.3 by the plots of log$D_{Ag(I)}$ vs. log[Pic] and equation 2.

Figures 3 and 4 show the results of the molar ratio method for Ag(I)-ATH-Picrate system. The results indicate that the molar ratio of the extracted species should be Ag(I):ATH:Pic^- = 1:1:1. In this case, the plots of the logarithmic distribution ratio of the silver (I) ion vs. the logarithmic concentration of free picrate ion did not give a straight line with slope 1, because silver ion was extracted perfectly with ATH even in the low concentration of picrate ion. This means that the K_{ex} with ATH might be higher than that with ATCH.

Liquid-liquid extraction of copper (I) ion

Liquid-liquid extraction of copper (I) with ATCH and ATH was performed. Figure 5 shows the plots of the %E of the copper (I) ion vs. the molar ratio of ATCH in the organic phase and copper (I) ion in the aqueous phase. The result of molar ratio method indicates the molar ratio of the copper (I) ion to ATCH in the extracted species is 1:1. The plots of log $D_{cu(I)}$ vs. the log[Pic] are shown in figure 6 and the straight line with slope 1, suggesting again that n=1 in equations 1 and 2 and that the composition of the extracted species with ATCH is Cu(I): L : Pic^- = 1:1:1. The value of the K_{ex} For ATCH was evaluated as logKex = 8.9 ± 0.1.

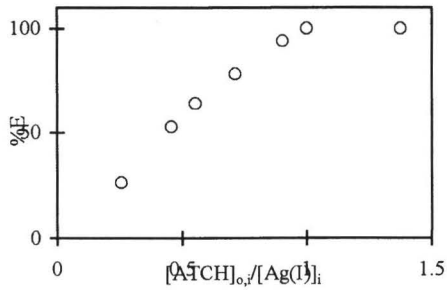


Fig.1 Molar ratio method of Ag(I) complexes
Initial concentration ; Silver(I) : 5×10^{-5}M
Picrate ion : 1×10^{-3}M pH 5

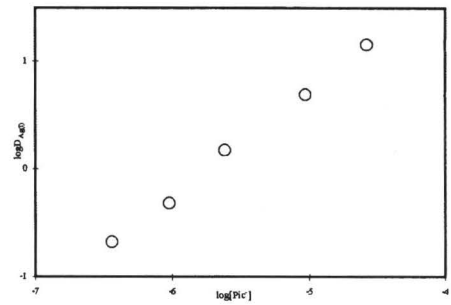


Fig.2 Plots of $\log D_{Ag(I)}$ vs. $\log[Pic^-]$
Initial concentration ; Silver(I) : 5×10^{-5}M
ATCH : 1×10^{-3}M pH 5

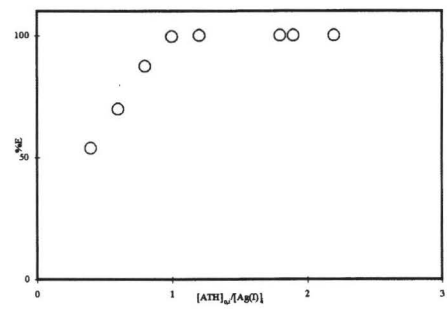


Fig.3 Molar ratio method of Ag(I) complexes
Initial concentration ; Silver(I) : 5×10^{-5}M
Picrate ion : 1×10^{-3}M pH 5

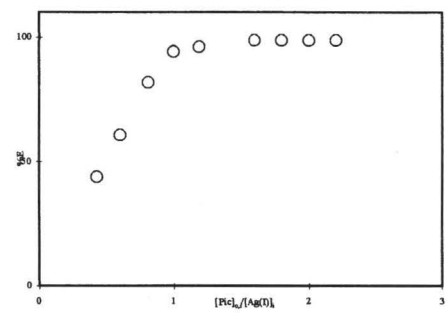


Fig.4 Molar ratio method of Ag(I) complexes
Initial concentration ; Silver(I) : 5×10^{-5}M
ATH : 1×10^{-3}M pH 5

Figures 7 and 8 show the results of the molar ratio method for Cu(I)-ATH-Picrate system. The results indicate the composition of the extracted species is Cu(I):ATH:Pic^- = 1:1:1. It is thought that both the silver (I) and copper (I) atoms take a tetrahedral configuration. Like the silver (I) system, slope analysis could not be performed, because of the percentage extraction was greater than 99% for copper (I), even at low concentrations of picrate ion. It means that acyclic ATH has a higher extraction efficiency for copper (I) than cyclic ATCH as with silver(I). It is thought that the flexibility of the acyclic ligand contributes either for the metal complex formation reaction or for the distribution of ion pair complex in the extraction system.

CONCLUSION

Cyclic and acyclic monoazatetrathioether, ATCH and ATH were synthesized. Liquid-liquid extraction of several metal ions was examined. Selectivity of these reagents was similar to that of thiacrown-ethers. The extraction behaviour of silver (I) and copper (I) ions were examined. The results show that the composition of extracted species was 1:1:1 for metal:ligand:picrate. The comparison of the two ligands for the extraction of silver (I) and copper (I) demonstrates the benefit of acyclic ligand to extract the monovalent soft metal ions effectively. It is very important to note that the selectivity of the monoazatetrathioether for the soft metal ions is almost same as that of the tetrathioethers.[9,10] There are some possibility for these ligands containing a nitrogen atom that a functional groups might be introduced to a imino group in the molecule. The attempt to synthesize such new ligands which has high selectivity for some soft metal ions would be important for the development of the separation science and for the analytical chemistry.

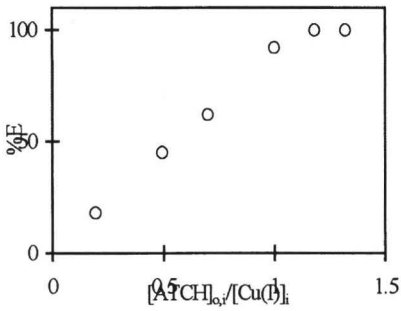


Fig.5 Molar ratio method of Cu(I) complexes
Initial concentration ; Copper(I) : 5×10^{-5}M
Picrate ion : 1×10^{-3}M pH 5

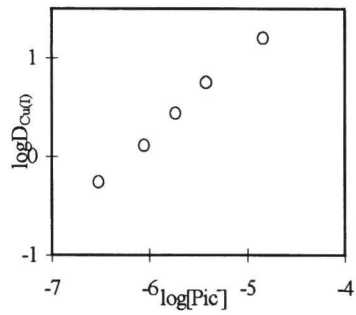


Fig.6 Plots of $\log D_{Cu(I)}$ vs. log[Pic$^-$]
Initial concentration ; Copper(I) : 5×10^{-5}M
ATCH : 1×10^{-3}M pH 5

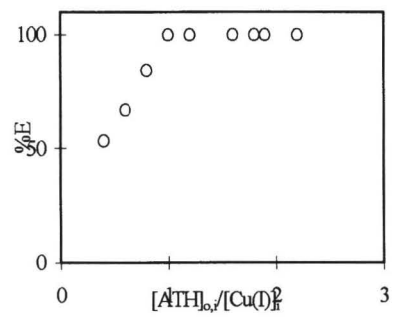


Fig.7 Molar ratio method of Cu(I) complexes
Initial concentration ; Copper(I) : 5×10^{-5}M
Picrate ion : 1×10^{-3}M pH 5

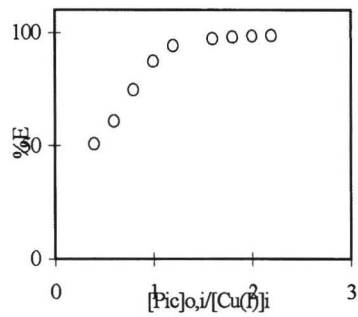


Fig.8 Molar ratio method of Cu(I) complexes
Initial concentration ; Copper(I) : 5×10^{-5}M
ATH : 1×10^{-3}M pH 5

REFERENCES

1. Sekido E, Chayama K and Muroi M, *Talanta*, **32**, 797, (1985).
2. Sekido E, Chayama K and Iwamoto H, *Analytical Sciences*, **4**, 511, (1988).
3. Chayama K and Sekido E, *Analytical Sciences*, **3**, 535, (1986).
4. Chayama K and Sekido E, *Bull. Chem. Soc. Jpn.*, **63**, 2420, (1990).
5. Chayama K and Sekido E, *Analytical Sciences*, **6**, 883, (1990).
6. Chayama K and Sekido E, *Anal. Chim. Acta*, **248**, 511, (1991).
7. Chayama K, Hara K, Tamari Y, Tsuji H, Kusaka Y, Sekido E and Mori Y, *Proc Int Solv. Ext. Conf., ISEC'93* ,York 585, (1993).
8. Chayama K, Koyama N, Tamari Y, Tsuji H and Sekido E, *Proc. Int. Solv. Ext.Conf, ISEC'96.*, Melbourne, 641, (1996).
9. Chayama K, Awano N, Tamari Y, Tsuji H and Sekido E, *Bunseki Kagaku* (in Japanese), **42**, 687, (1993).
10. Chayama K, Kurihara C, Tsuji H and Sekido E, *Bunseki Kagaku*, **47**, 1077, (1998).
11. Ahrland S, Chatt J and Davis NR, *Quart. Rev.*, **12**, 265, (1958)

SOLVENT EXTRACTION OF RARE EARTH NITRATES BY PHOSPHORYLATED CALIX[4]ARENES

M Burgard[1], B Ernst[1], MR Yaftian[2], CB Dieleman[3], C Wieser-Jeunesse[3] and D Matt[3]

[1]Ecole Européenne de Chimie, Polymères et Matériaux, C.N.R.S.-UMR 7512, F-67008 Strasbourg, France.

[2]Department of Chemistry, Zandjan University, PO BOX 313, 45195 Zandjan, Iran.

[3]Groupe de Chimie Inorganique Moléculaire, C.N.R.S.-UMR 7513, F-67008 Strasbourg, France.

ABSTRACT

The solvent extraction properties of neutral, phosphorylated calix[4]arenes towards rare earth ions are presented. The extraction selectivity is discussed in terms of chemical, conformational and structural effects. The extraction properties are compared to related standard extractants (TOPO, carbamoylmethylphosphonates).

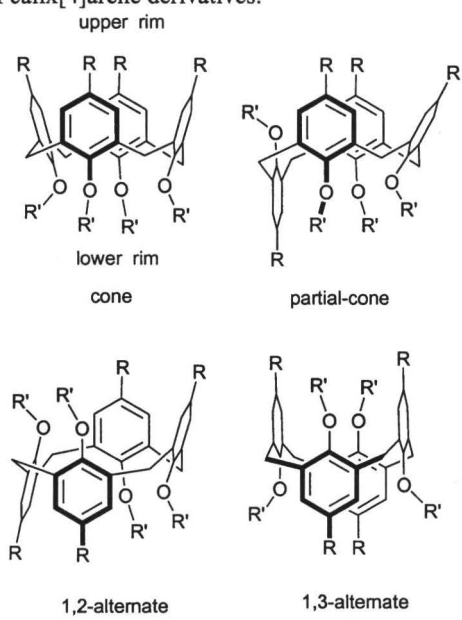
Keywords : rare earths, phosphorylated calix[4]arene, nitrate

INTRODUCTION

There is currently a growing need to discover new selective and effective extractants for metal ions. Research in this area is mainly motivated by major environmental and economic considerations.

It is well known that phosphoryl groups are suitable for complexation and extraction of rare-earth (RE) ions. Recent investigations carried out by Harrowfield *et al.*[1] have shown that calix[4]arene multiphosphate ligands provide interesting possibilities for the extraction of the RE-elements. Our approach for the selective extraction of rare earth metal ions is based on the use calix[4]arene-derived phosphine oxides where the phosphoryl-containing groups are anchored either at the lower or the upper rim.

Figure 1. Conformations of calix[4]arene derivatives.



© 2000 Society of Chemical Industry

The calix[4]arene matrix is a particularly attractive building block since it possesses at both rims four circularly-arranged anchoring points where suitable binding functions can be tethered. The calixarene backbone itself may exist in four different conformations so as to provide access to a wide variety of receptors of well-defined shape and size (Figure 1), thus allowing its effective use in a number of separation problems.[2-7]

The present study focusses on the selectivity changes obtained in the competitive extraction of 11 rare earth metal ions (RE^{3+}) (RE = La, Pr, Nd, Sm, Eu, Gd, Dy, Ho, Er, Yb and Y) originated by chemical and structural modifications within a series of neutral calix[4]arenes involving the phosphoryl function (Figure 2).

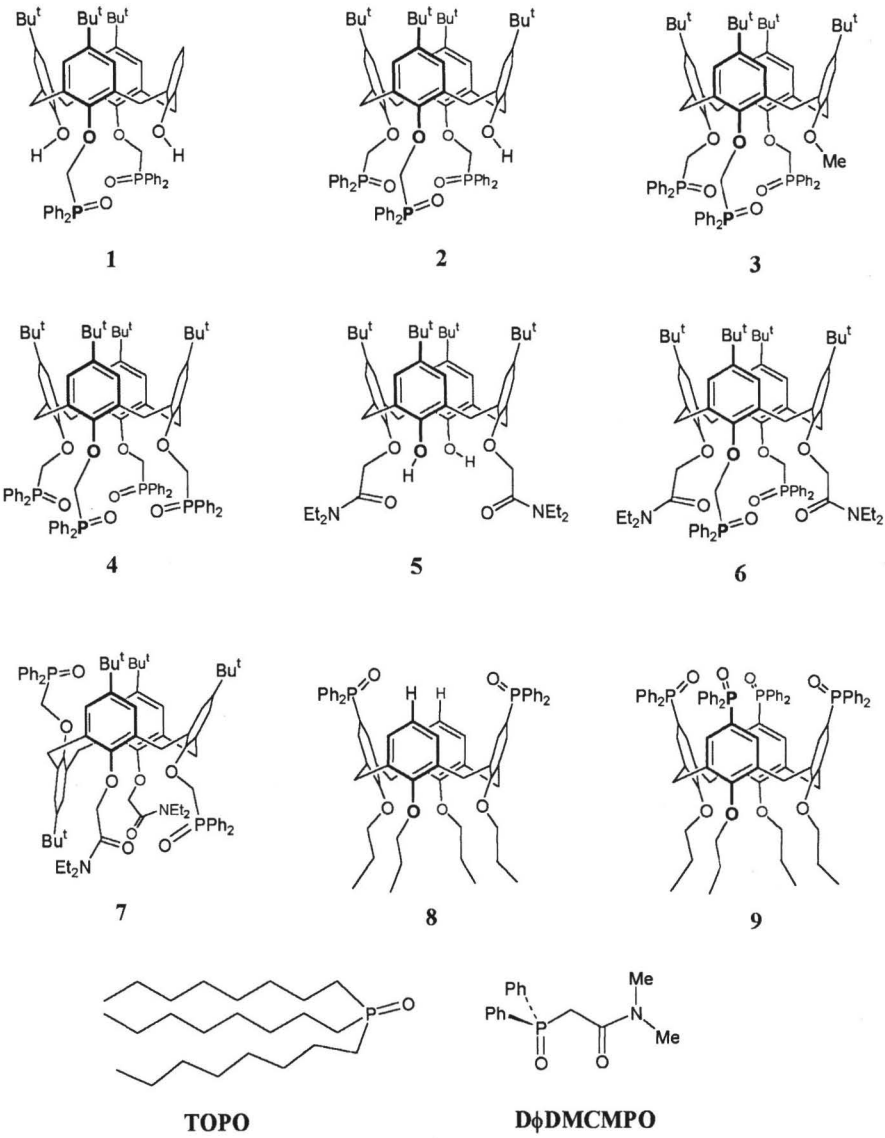


Figure 2. Chemical structure of the studied extractants.

RESULTS AND DISCUSSION

Calixarenes in the *cone* conformation substituted at the lower rim by phosphoryl groups.

Comparison with tri octyl phosphine oxide (TOPO)

Competitive extraction studies of calix[4]arenes[5,6] bearing two (**1**), three (**2, 3**) and four (**4**) phosphoryl groups show that the extraction efficiency increases as the number of PO groups increases (Figure 3). *Cone*-shaped tetra-PO-calix[4]arene **4** exhibits a significant selectivity for light rare earths. Particularly interesting is the observed peak selectivity which favours the extraction of praseodymium and neodymium. Although weakened, similar trends are observed with the di-PO derivative **1** (peak selectivity for samarium). Comparison with a dicarbamoyl analog (**5**) (Figure 4) suggests that the peak selectivity is a specific feature of the di-phosphoryl derivative.

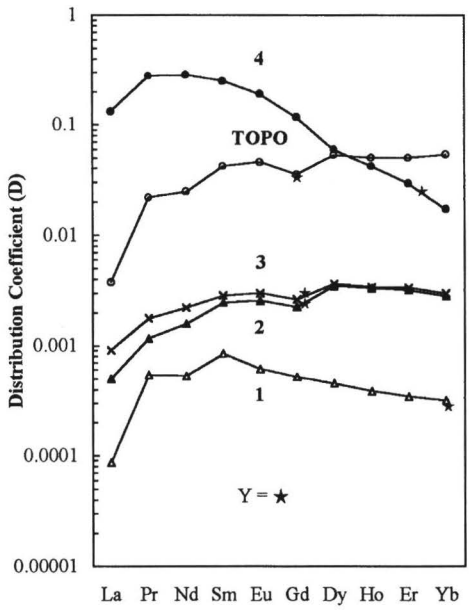


Figure 3. Competitive extraction for 11 rare-earth metal ions by **1**, **2**, **3**, **4** ($[L]_0$ = 0.002 M) and TOPO ($[L]_0$ = 0.008 M) in the presence of aluminium nitrate (0.9 M).
Organic diluent : 1,2-dichloroethane. T = 25°C.

The tri-PO compounds **2** and **3** exhibit very similar selectivity orders indicating that there is no significant influence of the fourth O-substituent group (Me or H). Note, the selectivity compares well with that of trioctylphosphine oxide (**TOPO**). This suggests that there is no particular cavity effect in the RE complexation with the considered tri-PO-calix[4]arenes.

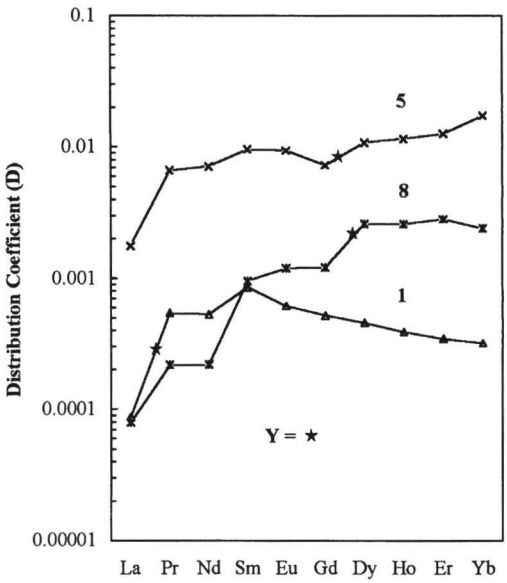


Figure 4. Competitive extraction for 11 rare-earth metal ions by **1**, **5** and **8** ($[L]_0 = 0.002$ M) in the presence of aluminium nitrate (0.9 M). Organic diluent : 1,2-dichloroethane. T = 25°C.

Calixarenes in the *cone* conformation substituted at the lower rim by phosphoryl and carbamoyl groups.

Comparison with conventional carbamoylmethylphosphine oxides (CMPO's)

Substitution of one couple of distal pendant groups of **4** by two $-CH_2C(O)NEt_2$ arms results in an important modification of the selectivity and an apparent loss of the particular effects observed for the tetra and diphosphoryl derivatives.

Furthermore, it was shown that the carbamoylmethylphosphine oxide ligand DΦDMCMPO extracts RE nitrates by forming 1:2 metal-ligand complexes while the di carbamoyl - di-PO-calix[4]arene **6** forms a 1:1 complex with the RE[6]. Our findings (Figure 5) clearly show that the selectivity generated by two chelating CMPO groups cannot be correlated with that of the four pendant functions of the *cone*-shaped ligand **6**, suggesting that different structural arrangements of two phosphoryl and two carbamoyl functions are conceivable around a rare earth metal centre.

Conformational effects

Changing the calixarene conformation may affect (Figure 5) significantly the extraction efficiency. Thus, it was found that the extraction is lower for the *partial-cone* conformer **7**. The same trend holds for the selectivity.

Comparison of upper rim *vs* lower rim functionalized *cone* conformers

It is shown (Figure 4) that the behavior of the upper rim functionalized derivative **8** is markedly different from that of the lower rim analog **1**, but is similar to that of TOPO (Figure 3).

A remarkable feature was observed for the upper rim phosphorylated compound **9**, for which a peak selectivity was observed within the light RE series (La-Gd) as already observed for **4**. For the heavy RE earth elements, the selectivity order is similar to that of conventional phosphine oxides, thus contrasting with the behaviour of **4**.

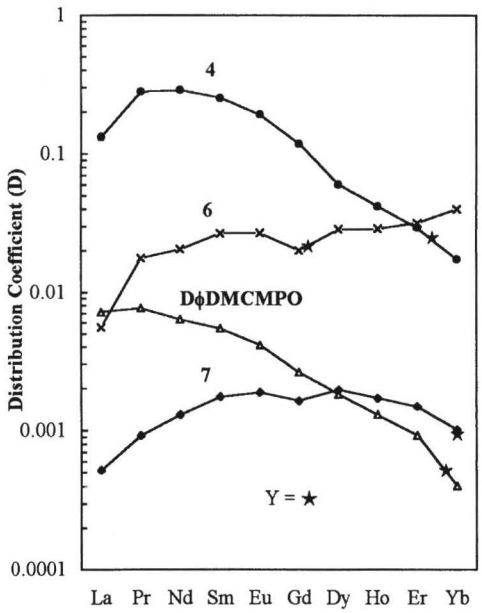


Figure 5. Competitive extraction for 11 rare-earth metal ions by **4**, **6** and **7** ($[L]_0$ = 0.002 M) and DΦDMCMPO ($[L]_0$ = 0.004 M) in the presence of aluminium nitrate (0.9 M). Organic diluent : 1,2-dichloroethane. T = 25°C.

CONCLUSION

Within the extraction systems investigated, two types can be distinguished :

1. The "TOPO like" systems which are characterized by an overall increase of extraction efficiency as the atomic number increases and a poor selectivity within the heavy RE series. In this category, one can include the tri-PO lower rim derivatives (**2**, **3**), the mixed di-PO-di carbamoyl lower rim derivatives **5** and **6** and the di-PO upper rim derivative **8**. The overall increase of extraction efficiency can be rationalised in terms of increasing acidity with the atomic number.
2. The second type of systems is characterized by a higher extraction efficiency for light RE ions except for La accompanied by a significant peak selectivity in the praseodymium-samarium sequence. Both tetraphosphorylated compounds **4** (lower rim) and **9** (upper rim), the upper rim diphosphorylated extractant **8**, and the carbamoylmethylphosphine oxide DΦDMCMPO belong to this group.

For a complete understanding of the various chemical and conformational factors which influence the extraction efficiency as well as the selectivity, further experimental and theoretical investigations are needed.

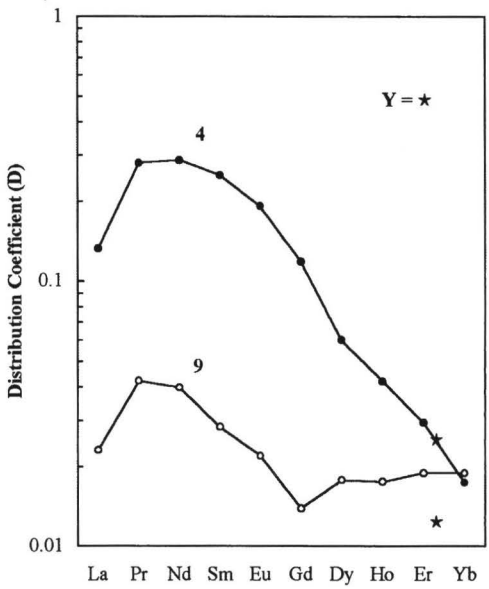
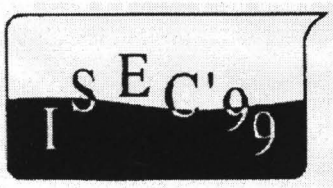


Figure 6. Competitive extraction for 11 rare-earth metal ions by **4** and **9** ($[L]_0 = 0.002$ M) in the presence of aluminium nitrate (0.9 M). Organic diluent : 1,2-dichloroethane. T = 25°C.

REFERENCES

1. Harrowfield JM, Morcino M, Peachy BJ, Skelton BW and White AH, *J.Chem.Soc.Dalton Trans.*, **1995**, 1687.
2. Wieser-Jeunesse C, Matt D, Yaftian MR, Burgard M and Harrowfield J, *CR.Acad.Sci. 1*, Série IIC, **1998**, 479.
3. Yaftian MR, Burgard M, Matt D, Wieser C and Dieleman C, *J. Incl. Phen. and Mol. Recogn. Chem.*, **27**, 127, (1997).
4. Yaftian MR, Burgard M, El Bachiri A, Matt D, Wieser C and Dieleman C, *J. Incl. Phen. and Mol. Recogn. Chem.*, **29**, 137, (1997).
5. Yaftian MR, Burgard M, Matt D, Dieleman CB and Rastegar F, *Solv. Extr. Ion Exch*, 1997, **15**, 975, (1997).
6. Yaftian MR, Burgard M, Wieser-Jeunesse C, Dieleman CB and Matt D, *Solv. Extr. Ion Exch.*, **16**, 1131, (1998).
7. Yaftian MR, Burgard M, Matt D and Dieleman C, *J. Membr. Sci.*,**144**, 57, (1998).



QSPR OF EXTRACTABILITY TRENDS OF THE LANTHANOID SERIES USING NOVEL MOLECULAR MECHANICS CALCULATIONS

Kazuharu Yoshizuka, Katsutoshi Inoue, Keisuke Ohto, Karsten Gloe[1], Holger Stephan[1], Torsten Rambusch[1] and Peter Comba[2]
Department of Applied Chemistry, Saga University, Honjyo 1, Saga 840-8502, Japan.
[1]Dresden Institute of Technology, Mommsenstrasse 6, D-01062 Dresden, Germany.
[2]Inorganic Chemistry Institute, University of Heidelberg, Im Neuenheimer Feld 270, D-69120 Heidelberg, Germany.

ABSTRACT
A novel molecular mechanics force field for lanthanoid complexes coordinated to organophosphate, calixarene and aqua type ligands is presented. The ligand-metal-ligand (L-M-L) bending interaction is modeled with 1,3-non-bonded interactions (point on a sphere approach) and a harmonic M-L stretching potential is used for the stretching modes. A quantitative structure property relationship (QSPR) can be obtained, which relates the complexation strain energy difference between the lanthanoid cations and La(III) with their relative extractability. We provide that the molecular mechanics is an efficient tool for the design of new extractants of bisalkyl hydrogenphosphates and calixarene carboxylates having the specific lanthanoid(III) extractability properties.

Keywords: QSPR, molecular mechanics calculation, lanthanoid, calixarene carboxylate, bisalkyl hydrogenphosphate,

INTRODUCTION

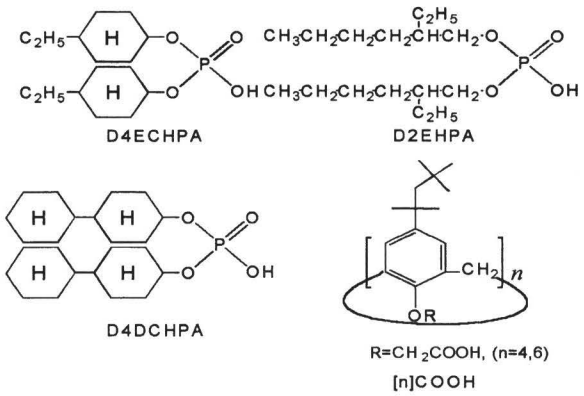
Molecular mechanics is a routine tool in organic chemistry,[1] and the development of novel approaches to optimize transition metal ion coordination geometries[2] and of extensive parameterization schemes has lead to a situation, where many problems involving inorganic compounds may now be solved satisfactorily with the support of force field calculations.[3] The design of metal ion selective ligands seemed to be an ideal task for molecular modeling but there are a number of inherent problems that limit its applicability. A few published reports of successful applications to predict selective metal ion complexation demonstrate the possibilities and limits of force field calculations in this area.[4]

Force fields for several lanthanoid complexes have been reported by Cundari *et al.*[5] and Hay,[6] although no systematic study throughout the lanthanoid series has been carried out so far. Since the majority of commercial separation and refining of lanthanoids has been carried out by the solvent extraction with organophosphorus extractants,[7] force field for lanthanoid complexes having O donor atoms connected with P atom becomes one of the most helpful tools, in order to develop the novel organophosphorus extractants having high selectivity among adjacent lanthanoids.

In this study, we present force field parameters for lanthanoid complexes with O donor atoms connected to phosphoryl P atom, carbonyl C atom and in aqua. Moreover, we perform the quantitative structure property relationship (QSPR) between total strain energy of complexes and extractability trends of lanthanoids(III) with some bisalkyl hydrogenphosphates and calixarene carboxylates described in previous papers,[8,9] *i.e.* bis(4-ethylcyclohexyl) hydrogen-phosphate (D4ECHPA), bis(4-cyclohexylcyclohexyl) hydrogenphosphate (D4DCHPA), bis(2-ethylhexyl) hydrogen-phosphate (D2EHPA), and calix[4]- and calix[6]arene carboxylates ([4]COOH and [6]COOH) (Figure 1). The force field presented here is, we believe, it represents the first attempt to model to high coordinate class of lanthanoid complexes as well as QSPR study using the molecular mechanics calculations.

© 2000 Society of Chemical Industry

Figure 1. Chemical Structures of D4ECHPA, D4DCHPA, D2EHPA, [4]COOH and [6]COOH



EXPERIMENTAL

The calculations were performed with the strain minimization program MOMEC97.[10] Within the molecular mechanics frame work, the structure of a molecule is modified in order to minimize its total strain energy consisting of bond length deformation, valence angle deformation, torsion angle deformation and nonbonded interaction. Though other terms may be included to account for out-of-plane deformation, electrostatic interactions and hydrogen bonding, we have not attempted to simply model these effects.

No symmetry restrictions were imposed on the local coordination sphere, and nonbonded interactions involving the metal center were neglected. This approach has also been taken by others in earlier force field calculations of transition metal complexes,[2,11] and some lanthanide complexes.[5,6]

Input coordinates were obtained from X-ray crystal structure data in literatures or produced with the graphics package HyperChem™ Release 5 (Hypercube, Inc., Canada). The strain-free bond length and force constant for each type of bond were adjusted until an optimal agreement between calculated and observed structures was obtained throughout the entire range of available structures. For each metal–O atom (M-O) bond, the discrepancies between the calculated and observed bond lengths were also examined in all complexes which contained that bond type and parameters were adjusted in such a way as to minimize those discrepancies.

RESULTS AND DISCUSSION

Force Field Parameters of Lanthanoid Complexes.

The parameters necessary to describe metal complexes can be conceptually divided into two types: metal-independent and metal-dependent. A common simplification is to assume that metal-independent parameters, derived for metal-free ligands, are transferable to coordinated ligands. This assumption of transferability seems particularly reasonable in light of the ionicity of M-L bonding.[2,6]

The metal-independent and metal-dependent force field parameters for calculating the structures in our work have been given in a previous work.[12] No constraints were placed on the O-M-O angles instead, the 1,3-non-bonded repulsions of the donor atoms accounted for the geometry of the coordination sphere. This approach has the advantage to another are the strain-free M-L bond length (r_0) and force constants (k_r) appropriate for the metal ion in question.

Figure 2 shows RMS overlays of the calculated lowest energy structures of all the extractants, calculated by MOMEC97 with those by the PM3 type semi-empirical orbital method (MOPAC93). The RMS value of residual distances in Ångstroms denotes as a common measure of the similarity of the structures. Since both calculated structures are in good agreement with corresponding, we consider

that these force field parameters are also adaptable in order to obtain the calculated lowest energy structures of these extractants alone.

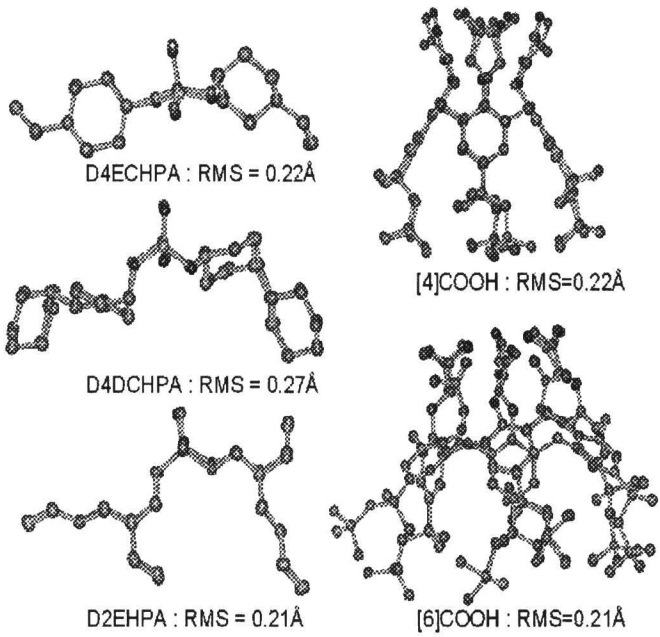


Figure 2. RMS overlay of computed MOMEC and PM3 structures of metal-free ligands (hydrogen atoms omitted for clarity).

Some lanthanoid(III) complexes available in literature,[13,14] mostly exhibit octa- to deca-coordinate. In particular, nona-coordinate complexes form regular or distorted tricapped trigonal prismatic (TCTP) geometry around metal centers. The bond lengths in these complexes were averaged and resulting bond lengths ($r_{M\text{-}O}$) are shown in figure 3, together with r_0 values parameterized in our work and van der Waals diameters ($2r_{vdW}$).[15] All the parameterized r_0 values are about 8% smaller than $r_{M\text{-}O}$. Moreover, it is interesting that r_0 values are in good agreement with $2r_{vdW}$.

QSPR of Extractability Trends of Lanthanoids

In previous papers,[8,9] we proposed the structures of lanthanoid complexes with D4ECHPA, D4DCHPA, D2EHPA, [4]COOH and [6]COOH from the stoichiometry of extracted species in organic phase.

Hancock *et al.* firstly proposed QSPR theory for estimating the strain energy contribution to thermodynamics of complex formation on the system of transition metal complexes with polyamines.[4,16] Under this theory and arrangement to our system, relation between the total strain energy and complex formation can be expressed by following equations.

For the extraction with bisalkyl hydrogenphosphates:

$$\underset{U_M}{M(H_2O)_9^{3+}} + \underset{6U_{HR}}{6HR} \rightleftharpoons \underset{U_{Mcom}}{M(HR_2)_3{\cdot}3H_2O} + \underset{3U_H}{3H^+} + \underset{6U_{aq}}{6H_2O} \qquad (1)$$

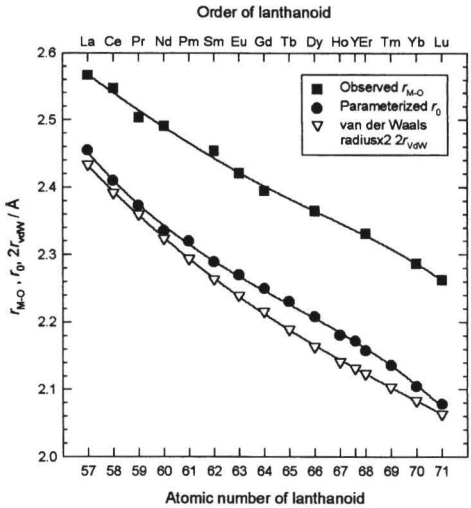


Figure 3. Plot of $r_{M\text{-}O}$, r_0 and $2r_{vdW}$ vs. the atomic number of lanthanoids.

For the extraction with calix[4]arene carboxylate:

$$\underset{U_M}{M(H_2O)_9^{3+}} + \underset{2U_{H4R}}{2H_4R} \rightleftharpoons \underset{U_{Mcom}}{M{\cdot}H_3R{\cdot}H_2R{\cdot}3H_2O} + \underset{2U_H}{2H^+} + \underset{6U_{aq}}{6H_2O} \qquad (2)$$

For the extraction with calix[6]arene carboxylate:

$$\underset{U_M}{M(H_2O)_9^{3+}} + \underset{U_{H6R}}{H_6R} \rightleftharpoons \underset{U_{Mcom}}{M{\cdot}H_3R{\cdot}3H_2O} + \underset{2U_H}{2H^+} + \underset{6U_{aq}}{6H_2O} \qquad (3)$$

where U_i (i = M, HR, H_4R, H_6R, Mcom, H and aq) is the energy of respective molecule.

Increase in the energy on complex formation and relation for relatively comparing mutual lanthanoid complex against La(III) complex are expressed by following equations:

$$\Delta U_M = U_{Mcom} + 3U_H + 6U_{aq} - U_M - 6U_{HR} \qquad (4)$$

$$\Delta U_M = U_{Mcom} + 2U_H + 6U_{aq} - U_M - nU_X \qquad (5)$$

(n=2 at X=H_4R; n=1 at X=H_6R)

$$\Delta U_M - \Delta U_{La} = (U_{Mcom} - U_{Lacom}) - (U_M - U_{La}) \qquad (6)$$

From the extraction equilibrium constant ($K_{ex,M}$), the following free energy relationship is obtained:

$$\Delta G_M = -RT \ln K_{ex,M} \qquad (7)$$

From Eqs.(6) and (7), the following equation can be finally derived:

$$\Delta U_M - \Delta U_{La} = \alpha \cdot \log (K_{ex,M} / K_{ex,La}) \qquad (8)$$

where α is the apparent QSPR constant of above relationship.

Plot of ΔU_M - ΔU_{La} vs. log ($K_{ex,\,M}$ / $K_{ex,\,La}$) for bisalkyl hydrogenphosphates and calixarene carboxylates shown in Figures 4(a) and (b) revealed good linear relationship with a slope (α) of 1.26 for all extractants in our work. We consider that this calculations can successfully expressed the complex formation behavior by strain energy terms around metal center.

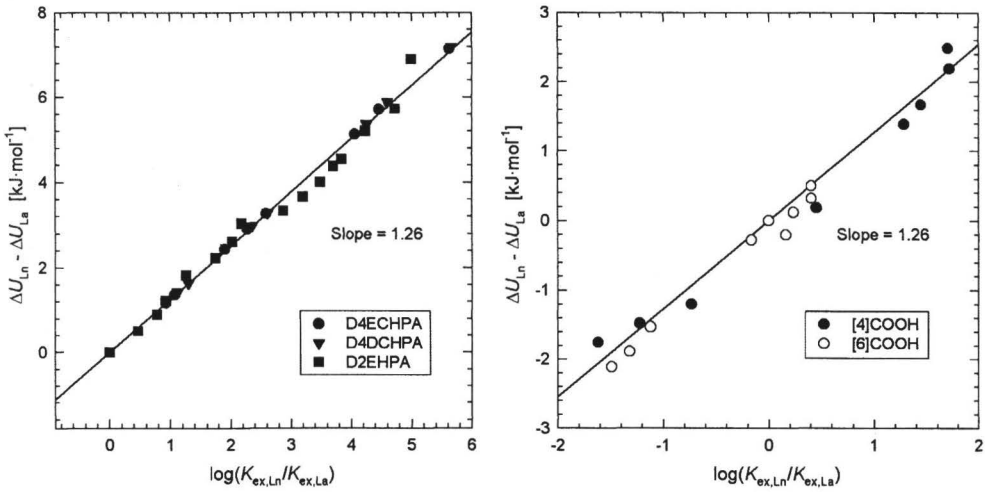


Figure 4. Plot of ΔU_M - ΔU_{La} vs. log($K_{ex,\,M}$ / $K_{ex,\,La}$) for bisalkyl hydrogenphosphates (a, left) and for calixarene carboxylates (b, right).

CONCLUSION

This work shows how molecular mechanics methodology can be successfully applied to the calculation of structure in lanthanoid complexes. A simple method based on 1,3-nonbonded interactions of L-M-L and the use of harmonic M-L stretching potential yields very reasonable geometric results.

We evaluated that QSPR between extractability trends of lanthanoid series with three bisalkyl hydrogenphosphates and two calixarene carboxylates can be obtained a good linear relationship for all the extractants. The QSPR study can be provide the possibility of application for predicting the selectivity of mutual lanthanoid(III) with fanciful extractants.

Although this work has focused on modeling geometries found in lanthanoid complexes, the methodology is not limited to the *f*-block metals. Force field based on 1,3-nonbonded interactions between ligand donor atoms are suitable models for many of the more common geometries in coordination chemistry.

ACKNOWLEDGMENTS

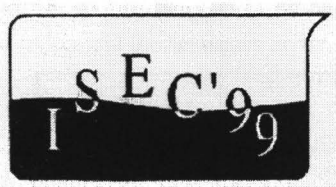
K. Y. gratefully acknowledges the financial support for a visit for foreign academic personnel to Germany from the DAAD to the Dresden University of Technology and the University of Heidelberg. P.C. and K.G. are grateful for financial support by the Deutsche Forschungs-gemeinschaft. K.I. acknowledges financial support by a Grant-in-Aid for Scientific Research from the Ministry of Education, Science, Sports and Culture of Japan.

NOMENCLATURE

ΔG_M	=	free energy difference in complex formation [kJ·mol^{-1}]
$K_{ex,M}$	=	extraction equilibrium constant [-]
k_r	=	force constant for bond length deformation [mdyn·Å^{-1}]
R	=	gas constant [kJ·mol^{-1}·K^{-1}]
$r_{M\text{-}O}$	=	observed bond length of M-O [Å]
r_0	=	strain-free bond length [Å]
r_{vdW}	=	van der Waals radius [Å]
U_i	=	strain energy of species i [kJ·mol^{-1}]
ΔU_M	=	energy difference in complex formation [kJ·mol^{-1}]
α	=	apparent QSPR constant [-]

REFERENCES

1. Allinger NL, *Adv. Phys. Org. Chem.*, **13**, 1 (1976).
2. Bernhardt PV and Comba P, *Inorg. Chem.*, **31**, 2638 (1992).
3. Hancock RD and Martell AE, *Chem. Rev.*, **89**, 1875 (1989).
4. Hancock RD, Ngwenya PW, Evers A, Wade PW and Boeyens JCA, *Inorg. Chem.*, **29**, 264 (1990).
5. Cundari TR, Moody EW and Sommerer SO, *Inorg. Chem.*, **34**, 5989 (1995).
6. Hay BP, *Inorg. Chem.*, **30**, 2876 (1991).
7. Coleman CF and Roddy JW, *Solvent Extr. Rev.*, **1**, 63 (1971).
8. Yoshizuka K, Kosaka H, Shinohara T, Ohto K and Inoue K, *Bull. Chem. Soc. Jpn.*, **69**, 589 (1996).
9. Ohto K, Yano M, Inoue K, Yamamoto TM, Goto M, Nakashio F, Shinkai S, and Nagasaki T, *Anal. Sci.*, **11**, 893 (1995).
10. Comba P, Hambley TW and Okon N, "MOMEC97, a molecular mechanics package for transition metal complexes", University of Heidelberg, Heidelberg, Germany (1997).
11. Hambley TW, Hawkins CJ, Palmer JA and Snow MR, *Aust. J. Chem.*, **34**, 45 (1981).
12. Comba P, Gloe K, Inoue K, Krüger T, Stephan H, and Hoshizuka KY, *Inorg. Chem.*, **37**, 3310 (1998).
13. Kulpe S, Seidel I, Szulzewsky K and Kretschmer G, *Acta Crystallogr.*, **B38**, 2813 (1983).
14. Kapoor PN, Saraswati R and Mcmahon IJ, *Inorg. Chim. Acta*, **110**, 63 (1985).
15. Shannon RD, *Acta Crystallogr.* **A32**, 751 (1976).
16. Hancock RD, McDougall GJ and Marsicano F, *Inorg. Chem.*, **18**, 2847 (1979).



EXTRACTION BEHAVIOR FOR TRIVALENT LANTHANIDES WITH AMIDES AND EXAFS STUDY OF THEIR COMPLEXES

H Narita, T Yaita and S Tachimori

Separation Chemistry Laboratory, Department of Materials Science, Japan Atomic Energy Research Institute, Tokai-mura, Naka-gun, Ibaraki, 319-1195 Japan

ABSTRACT

Solvent extraction of trivalent lanthanide (Ln(III)) ions with *N,N'*-dimethyl-*N,N'*-diphenyl-malonamide (DMDPhMA) and –diglycolamide (DMDPhDGA) and structural studies of their complexes in solution system by extended X-ray fine structure (EXAFS) spectroscopy were carried out. The distribution ratios (*D*'s) of Ln(III) in the DMDPhDGA system were much higher than those in the DMDPhMA system. In the DMDPhGA-HNO_3 system, the *D*'s increased with an increase in the atomic number, while the *D*'s decreased in the DMDPhDGA-HCl and DMDPhMA-HCl / –HNO_3 systems. The EXAFS data shows that the DMDPhMA directly coordinates to Er(III) ion with a bidentate mode, while the DMDPhDGA with a tridentate mode. The counter ion of the Er(III) ion, NO_3^-, Cl^-, did not exist in the first coordination sphere of the Er(III) ion in the DMDPhDGA complex, indicating that the local structure around Er(III) in the DMDPhDGA-$Er(NO_3)_3$ complex is identical with that in the DMDPhDGA-$ErCl_3$ complex.

Keywords: diamide, malonamides, glycolamides, lanthanide, EXAFS

INTRODUCTION

Amide compounds have recently become attractive as useful extractants in the nuclear waste reprocessing.[1] Unlike organophosphorus compounds, they are completely incinerateable, because of consisting of carbon, hydrogen, nitrogen and oxygen. Therefore, they do not generate additional waste. Among these compounds, the malonamides ($(R^1R^2NCO)_2CHR^3$), bifunctional amides, have been widely investigated by Musikas et al. and showed the good extractabilities of trivalent f-block elements.[2] The diglycolamides (3-oxapentanediamides) ($(R^1R^2NCOCH_2)_2O$), tri-functional amides, showed extremely high extractabilities for a few Ln(III) and Am(III) ions[3]. However, a systematic extraction for all Ln(III) ions using these diamides has been limited. An understanding of the extraction properties of Ln(III) with diamide compounds requires the knowledge of the structure and composition of the coordination sphere of Ln(III) ion. Extended X-ray absorption fine structure (EXAFS) spectroscopy can determine a local structure around a specific metal of interest. The EXAFS, therefore, is one of the most powerful methods for the structural studies of organic ligand – metal complexes in solution. The EXAFS study of the organophosphorus compounds - holmium chloride complexes in ethanol solution showed that the diphosphine dioxides (DPDO) coordinates directly to holmium with symmetric bidentate mode, while the carbamoyl phosphin oxides (CMPO) with asymmetric bidentate mode.[4] The detailed coordination properties of diamide–Ln(III) complexes in solution system are not clarified yet. In this study, we report the extraction behavior of all Ln(III) (except Pm) ions from nitric acid and hydrochloric acid solutions with *N,N'*-dimethyl-*N,N'*-diphenyl-malonamide (DMDPhMA) and *N,N'*-dimethyl-*N,N'*-diphenyl-diglycolamide (DMDPhDGA) (Figure 1), and the local structure of DMDPhMA and DMDPhDGA–erbium nitrate and erbium chloride complexes in solution.

EXPERIMENTAL

Reagent

DMDPhMA and DMDPhDGA were synthesized by a method similar to that described in the reference.[5] (DMDPhMA Found: C, 72.3; H, 6.4; N, 9.8. $C_{17}H_{18}N_2O_2$ requires C, 72.3; H, 6.4; N, 9.9. DMDPhGA, Found: C, 69.1; H, 6.5; N, 8.8. $C_{18}H_{20}N_2O_3$ requires C, 69.2; H, 6.4; N, 9.0) The purity

© 2000 Society of Chemical Industry

was more than 99% on the basis of ^{1}H-NMR and IR spectroscopy and liquid chromatography. All the other reagents were of reagent grade.

Extraction

The organic solution (diluent: chloroform) was pre-equilibrated with the same volume of the HNO_3 or HCl solution in the absence of Ln(III) ions. An aliquot of the pre-equilibrated organic phase and the same volume of the HNO_3 or HCl solution containing 10^{-6} M of 14 Ln(III) ions (La-Nd, Sm-Lu) were shaken for 20 min in a glass tube and were then centrifuged. A portion of the organic phase was transferred to another glass tube, and a specific volume of water was added. The mixture was shaken for 20 min and the Ln(III) ions in the organic phase were back-extracted into water. The recovery of the Ln(III) ions was very nearly 100%. The back-extraction was duplicated. The concentrations of the Ln(III) ions were measured by ICP-MS (Fisons, VG-PQ Ω) as described in the previous paper.[6] The distribution ratio was defined as the concentration of the Ln(III) ions in the organic phase divided by the concentration of the Ln(III) ions in the aqueous phase. All the extractions were performed at 23±1°C.

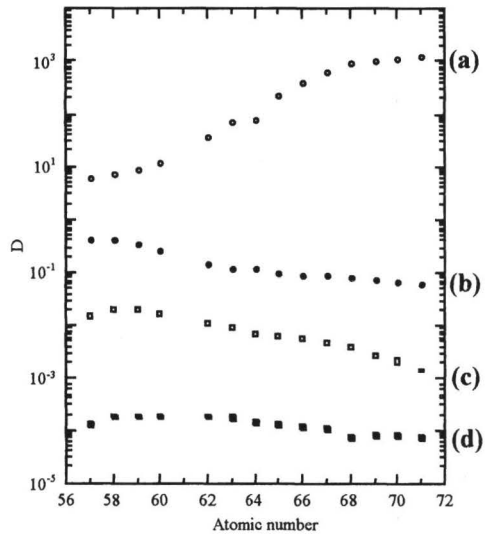


Figure 2. The relation between the D's of Ln(III) and the atomic number in the (a)DMDPhDGA-HNO_3,(b)DMDPhDGA-HCl, (c)DMDPhMA-HNO_3 and (d)DMDPhMA-HCl systems. [diamide]:0.2M; [HNO_3]:4M; [HCl]:9M

EXAFS measurements

The EXAFS samples were prepared by dissolving hydrated erbium chloride salt or hydrated erbium nitrate salt into ethanol solution containing the diamides. The concentration of the diamides (0.8M) was four times of erbium (0.2M). EXAFS spectra at Er L_{III}-edge of the samples were measured in transmission mode at the BL27B station of the Photon Factory in the High Energy Accelerator Organization (KEK). Synchrotron radiation from a storage ring operated at 2.5 GeV with a beam current of 100-250 mA was monochromatized with a Si (111) double crystal monochromator. The EXAFS data was reduced as the previous paper.[4]

RESULTS AND DISCUSSION

Extraction of Ln(III) ions

Figure 2 shows the distribution ratios (D's) versus the atomic number (lanthanide pattern for the D's) in (a) the DMDPhDGA-HNO_3 system, (b) the DMDPhDGA-HCl system, (c) the DMDPhMA-HNO_3 system and (d) the DMDPhMA-HCl system ([DMDPhMA], [DMDPhDGA]:0.5M; [HNO_3]:4M; [HCl]:9M). These lanthanide patterns are typical in each system, before the D's reach maximum. The D's from both the HNO_3 and the HCl solution in the DMDPhDGA system are much higher than those in the DMDPhMA system. The D's in the DMDPhDGA-HNO_3 system increase with an increase in the atomic number. The D of Lu(III), thus, is 10 times higher than that of La(III). In contrast, the D's in the other systems decrease with an increase in the atomic number. The number of DMDPhDGA molecules in the extracted species obtained from slope analysis in 4M HNO_3 increased with an increase in the atomic number.[7] Therefore, the hydrophobicity of the extracted species for heavier Ln(III) ions can be larger than that for lighter Ln(III) ions. This may result in the increasing D's with an increase in the atomic

number. On the other hand, in the other systems, the number of the extractants in the extracted species is constant in the lanthanide series.

EXAFS studies

The radial structural function (RSF) obtained by the absolute values Fourier transforms of k^3-weighted EXAFS for $ErCl_3$-DMDPhMA and –DMDPhDGA complexes in ethanol are shown in Figure 3.

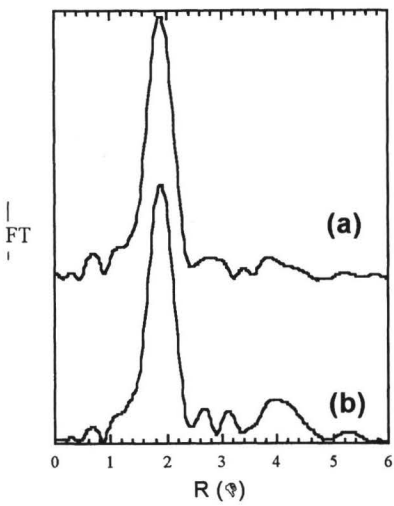


Figure 3. Radial structural function for (a)DMDPhMA-$ErCl_3$ complex and (b)DMDPhDGA-$ErCl_3$ complex in ethanol

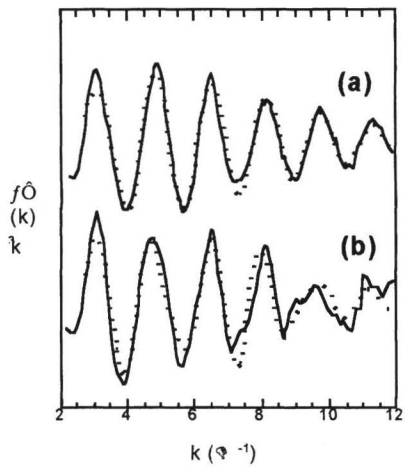


Figure 4. Raw Er L_{III}-edge k^3-weighted EXAFS data for (a) the DMDPhMA-$ErCl_3$ complex and (b) DMDPhDGA-$ErCl_3$ complex. The solid lines are the experimental data and the dotted lines are the theoretical fits of data

The RSF phase shifts associated with the absorber-scatter interaction were not corrected. The first peak around 2.0Δ arises from the oxygen of the coordinated water and the ligand. Figure 4 shows that the Fourier filtered EXAFS spectrum of the first peak weighted with k^3 and the fitting results for these two complexes in ethanol solution. The fitting results are shown in Table 1. The interatomic distances of Er-O(carbonyl) in the DMDPhMA and DMDPhDGA complexes are 2.32Δ and 2.33Δ, respectively. For the DMDPhDGA, Er-O(ether) is 2.47Δ, indicating that the DMDPhDGA coordinated to Er(III) ion in a tridentate mode.

	Er-O(C=O)			Er-O(H_2O)			Er-O(C-O-C)		
	r(Δ)	N[1)]	σ^2	r(Δ)[2)]	N[1)]	σ^2	r(Δ)	N[1)]	σ^2
DMDPhMA	2.32	4	0.006	2.34	4	0.01	-	-	-
DMDPhDGA	2.33	4	0.004	2.34	2	0.009	2.47	2	0.003

r: Bond distance, N: Coordination number, σ: Debye-Waller factor.
[1)] All the coordination number held constant during fit. [2)] r=2.34Δ held constant during fit.

Table 1 EXAFS structural parameters for diamide- $ErCl_3$ complexes in ethanol

Figure 5 shows the comparison of the RSF between erbium nitrate ion system and the erbium chloride system: (a) erbium ion in the absence of the diamide, (b) DMDPhMA-erbium ion system and (c) DMDPhDGA-erbium ion system (The RSF phase shifts were not corrected.) The RSF for erbium nitrate in Figure 5a apparently consists of 2 peaks. The second peak around 3.7Δ is attributed to non-

coordinated oxygen of nitrate ion. For DMDPhMA-Er$(NO_3)_3$ complex, the second peak around 3.7Δ is also observed. Accordingly, nitrate ion coordinates directly to erbium ion, but chloride ion does not in Fig.ures 5a,b. This result indicates that no nitrate ion exists in the inner-sphere of Er(III) ion and the local structure around Er(III) ion (–5Δ) in the DMDPhDGA-Er$(NO_3)_3$ is identical with that in the DMDPhDGA-ErCl_3.

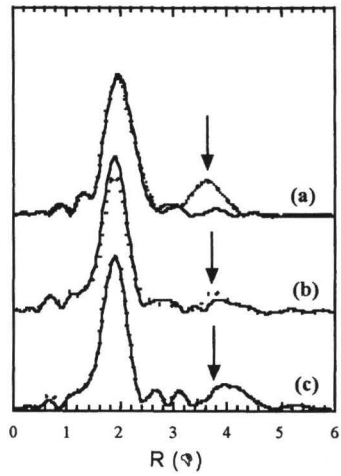


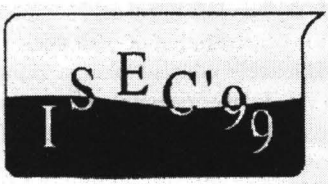
Figure 5. Radial structural function for
(a)the erbium ion in the absence of the diamide
(b)the DMDPhMA-Er complex and
(c)the DMDPhDGA-Er complex in ethanol.
The solid lines are the nitrate ion system and the dotted lines are the chloride ion system.

CONCLUSION

The distribution ratios of Ln(III) in the DMDPhDGA system were much higher than those in the DMDPhMA system. The EXAFS data showed the DMDPhMA coordinated to Er ion with two carbonyl oxygen atoms and the DMDPhDGA with an ether oxygen atom and two carbonyl oxygen atoms. The tridentate coordination of the DMDPhDGA may reflect the high extractability. The extraction behavior of Ln(III) with the DMDPhDGA exhibited a large difference between the HNO_3 and HCl system. However, the local structures of the DMDPhDGA-Er$(NO_3)_3$ complex and DMDPhDGA-ErCl_3 complex were very similar. This result suggests that the outer-sphere structure of complexes would play an important role for lanthanide extraction.

REFERENCES

1 Gasparini GM and Grossi G, *Sep. Sci. Technol*, **15**, 825, (1980); Musikas C, *Sep. Sci. Technol*, **23**, 1211, (1988)
2 Musikas C and Musikas H, *Solvent Extr. Ion Exch.* **5**, 877, (1987); Cuillerdier C, Musikas C, Hoel P, Nigond L and Vitart X, *Sep. Sci. Technol.*, **26**, 1229, (1991)
3 Stephan H, Gloe K, Beger J and Müel P, *Solv, Extr. Ion. Exch*, **9**, 459, (1991)
4 Yaita T, Narita H, Suzuki S, Tachimori S, Shiwaku H and Motohashi H, *J. Alloy Compd*, **271**, 184, (1998)
5 Thiollet G and Musikas C, *Solvent Extr. Ion Exch*, **7**, 813, (1989); Yao J, Wharf RM and Choppin GR, *'Separation of f elements'*, Plenum Press, New York, (1977)
6 Yaita T and Tachimori S, *Radiochim. Acta*, **73**, 27, (1996)
7 Narita H, Yaita T, Tamura K and Tachimori S, *Radiochim. Acta*, in press



EXTRACTION OF URANIUM(VI) AND PLUTONIUM(IV) FROM NITRIC ACID SOLUTIONS BY SUBSTITUTED CYCLIC AMIDES

Shinichi Suzuki[1], Kazunari Tamura[1], Shoichi Tachimori[1] and Yoshiharu Usui[2]

[1]Department of Material Science, Japan Atomic Energy Research Institute, Naka-gun, Ibaraki 319-1195, Japan

[2]The Graduate School of Science and Engineering, Ibaraki University, Mito 310-8512, Japan

ABSTRACT

In this study, seven substituted cyclic amides have been synthesized and the extraction of U(VI) and Pu(IV) by the amides was investigated under various conditions. From the results of distribution ratio(D_M) as functions of nitric acid and cyclic amide concentrations, we discussed the effects of the amides structure, i.e., the branched alkyl group attached nitrogen atom and position of substituted octyl group on the extraction behavior of U(VI) and Pu(IV). D_U and D_{Pu} by OCLA is larger to small extant than that by EHCLA. OCLA and EHCLA respective concentration of 1 M in dodecane have produced the third phase. By introducing an octyl group to ring part, the third phase disappeared due to the increase of hydrophobicity of cyclic amides. D_U and D_{Pu} with 2OEHCLA were lower than that with the mixture of 3OEHCLA and 5OEHCLA. Steric hindrance caused by n-octyl group neighboring C=O to the extraction of Pu(IV) is larger than that of U(VI). In this paper, the relationship between the D_M and ring structure, especially steric effect around oxygen donor atom of the amides.

Keywords: cyclic amide, uranium, plutonium, spent fuel reprocessing

INTRODUCTION

N,N-dialkylamides[1~7] have been studied extensively as possible alternative extractants to tributylphosphate (TBP) for actinide separation in spent fuel reprocessing. As cyclic amides[8~14] are also useful for extraction of actinides, extraction behavior of U(VI) and Th(IV) by N-alkyl-caprolactam have been reported so far. In this study, solvent extraction of U(VI) and Pu(IV) with substituted cyclic amide was studied under various conditions. Cyclic amides, 2OEHCLA and 3O,5OEHCLA, have been synthesized in order to increase the lipophilicity of EHCLA. Compound 3O,5OEHCLA and 3O,5OOCLA are a mixture of 3OEHCLA and 5OEHCLA and that of 3OOCLA and 5OOCLA. The present study clarified the effects of amides structure, i.e., the branched alkyl group attached to nitogen atom and the position of substituted octyl group on the extraction of U(VI) and Pu(IV) by cyclic amide.

EXPERIMENTAL

Reagents

Cyclic amides, i.e. N-(2-ethyl)hexylcaprolactam (EHCLA), N-octylcaprolactam (OCLA), 2-octyl-N-(2-ethyl)hexylcaprolactam (2OEHCLA), a mixture of 3-octyl-N-(2-ethyl)hexylcaprolactam and 5-octyl-N-(2-ethyl)hexylcaprolactam (3O,5OEHCLA) and that of 3-octyl-N-octylcaprolactam and 5-octyl-N-octylcaprolactam (3O,5OOCLA) were synthesized in our laboratory. The cyclic amides prepared were characterized by gas-chromatography, IR and NMR spectrometry. N-dodecane (Wako Pure Chemical Industries,. Ltd.) as a diluent was of reagent grade and used as received.

Distribution experiment

Equal volumes of the aqueous of the required acidity containing U and Pu and pre-equilibrated organic phase by required concentration of HNO_3 were shaken for 10 minute. After the equilibration,

© 2000 Society of Chemical Industry

the system was centrifuged for 5 minutes. Distribution coefficient of U: D_U between nitric acid solution and cyclic amides in dodecane was determined from measurement U(VI) concentration of both phases. U(VI) concentration was measured after dilution with HNO_3 by inductively coupled plasma mass spectrometry (ICP-MS : Fisons, PQΩ). The concentration of U(VI) in the organic phase was determined by ICP-MS after stripping in twice with 0.2 mol/dm^3 oxalic acid. Distribution coefficient of Pu: D_{Pu} between nitric acid solution and cyclic amides in dodecane was determined from measurement of Pu(IV) activity by using liquid scintillation counter(Packard, 2700TR/AB).

RESULTS AND DISCUSSION

Nitrogen alkyl branching effect on D_M (M:U, Pu)

Previous researcher reported slightly higher D_U and D_{Th} by N-n-octylcaprolactam than those by EHCLA. D_U and D_{Pu} by OCLA is larger to small extant than that by EHCLA. Figure 1 shows that nitric acid concentration dependency of D_U by 1 M OCLA and EHCLA in dodecane. D_U increased with an increase in acid concentration and the third phase has been appeared in aqueous conditions of 1.0 M

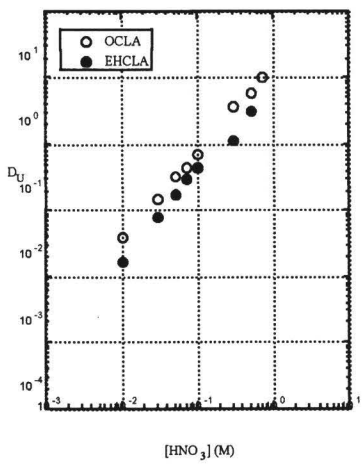


Figure 1 Nirtic acid denendency of D_U by 1 M cyclic amides

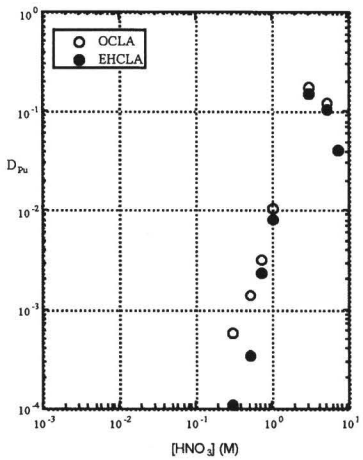


Figure 2 Nirtic acid denendency of D_{Pu} by 0.1 M cyclic amide

HNO_3 for OCLA and 0.7 M HNO_3 for EHCLA.

This effect is caused by difference in solubility of these amides, the third phase formation must be caused by distinction of physical property of cyclic amides which is due to carbon chain length of alkyl group attaching nitrogen atom, therefore the third phase formation order is EHCLA > OCLA. Figure 2 shows cyclic amide concentration dependency on D_U. The slopes of each line are 2.0 for OCLA, 2.3 for EHCLA, respectively, which indicated that approximately 2 cyclic amides molecule concerned in U extraction system.

Figure 3 shows that nitric acid concentration dependency of D_{Pu} also for two cyclic amides. D_{Pu} had maximum in aqueous conditions of 3.0 M HNO_3 for OCLA, and 3.0 M HNO_3 for EHCLA, in which D_{Pu} is 0.26 for EHVLA and 0.15 for EHCLA at 25 °C, respectively. The order of magnitude of D_{Pu} is also OCLA > EHCLA in nitric acid concentration lower than 1.0 mol/dm^3, compared with U extraction result by same cyclic amides. Figure 4 shows cyclic amide concentration dependency on D_{Pu}. The slopes of each line are 4.2 for OCLA, 3.9 for EHCLA, respectively, which indicated that approximately 4 cyclic amides molecule concerned in U extraction system.

In order to promote lipophilicity of EHCLA, n-octyl group attached to carbon atom of EHCLA. Then D_U by 3O,5OOCLA and 3O,5OEHCLA were compared and shown in figure 5. The D_U by

3O,5OOCLA showed a slightly higher value over the whole concentration of HNO_3. This weak deleterious effect seen by 3O,5OEHCLA is also the steric one caused by branching. Figure 6 shows nitric acid concentration dependency of D_{Pu} by 3O,5OOCLA and 3O,5OEHCLA. The D_{Pu} by 3O,5OOCLA showed almost same. Maximum D_{Pu} was obtained is 45.4 for 3O,5OEHCLA and 41.2

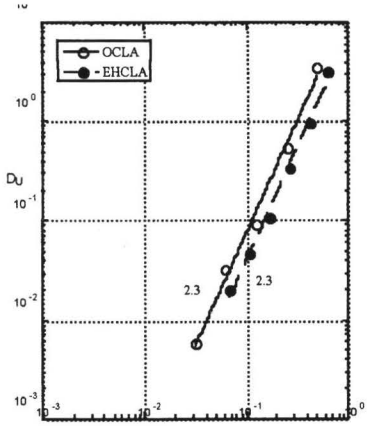


Figure 3 D_U as a function of cyclic amide concentration

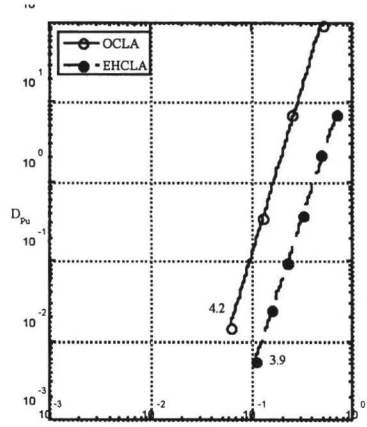


Figure 4 D_{Pu} as a function of cyclic amide concentration

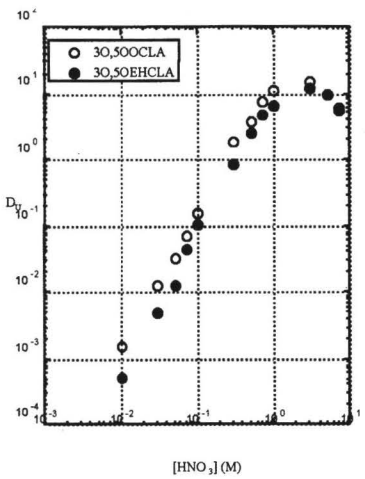


Figure 5 Nirtic acid denendency of D_U by 1 M cyclic amides

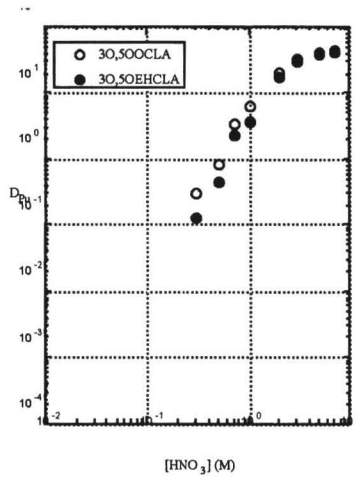


Figure 6 Nirtic acid denendency of D_{Pu} by 1 M cyclic amides

for 3O,5OEHCLA. D_{Pu} by 3O,5OOCLA is larger than D_U by one. From the result of U and Pu extraction by 3O,5OOCLA and 3O,5OEHCLA, nitrogen alkyl branching effect on D_U and D_{Pu} is slightly small.

Cyclic amide concentration dependencies of D_U and D_{Pu} by 3O,5OOCLA and 3O,5OEHCLA are shown in Figure 7 and Figure 8 respectively. Slopes of D_U of each line are 2.0 for 3O,5OOCLA and 2.0 for 3O,5OEHCLA and that of D_{Pu} are 2.9 for 3O,5OOCLA and 2.9 for 3O,5OEHCLA respectively. From the report of C.Musikus, D_{Pu} by N,N-dialkylmonoamide which has nitrogen alkyl branch drastic decrease due to steric hindrance but D_{Pu} by cyclic amide could not seen the effect of nitrogen alkyl branching. In this respect, it is considered that rotation of amide bonding around C-N bond is restricted in cyclic amides.

Effect of appending n-octyl group to the cyclic amide ring on D_M (M:U, Pu)

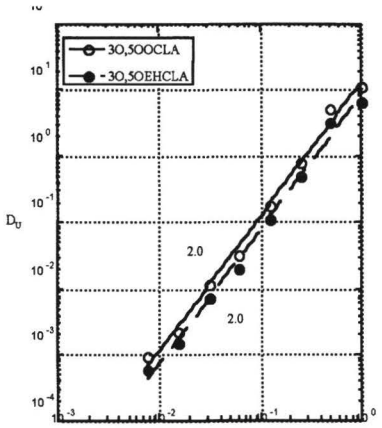


Figure 7 D_U as a function of cyclic amide concentration

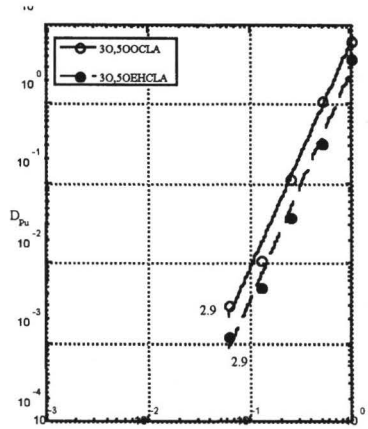


Figure 8 D_{Pu} as a function of cyclic amide concentration

In order to increase the solubility of the U(VI)-cyclic amide complex in the nonpolar diluent and avoid third phase formation, the introduction of n-octyl group to the cyclic amide frame of EHCLA was tried, to improve the lipophilicity of the cyclic amide molecule. Two derivatives of EHCLA, 2OEHCLA and 3O,5OEHCLA, were synthesized to verify the behavior in the U and Pu extraction. The resulting D_U was shown in figure 9 comparing with D_U by EHCLA. The 1 M EHCLA in n-dodecane formed the third phase at the acidity higher than 1 M as seen in figure 1 and figure 9. Whereas both 2OEHCLA and 3O,5OEHCLA produced no third phase even at high acidity and the acid dependency of D_U is larger with 3O,5OEHCLA than that with EHCLA. A drastic decrease of D_U with 2OEHCLA, caused by n-octyl group which appended to the carbon atom nearest to the functional C=O group, seems awing to the steric hindrance around oxygen donor atom.

Figure 10 shows that cyclic amide concentration dependency of D_U in acid condition 1.0 M HNO_3. The slopes of each lines are 2.3 for EHCLA, 1.9 for 2OEHCLA and 2.0 for 3O,5OEHCLA. It

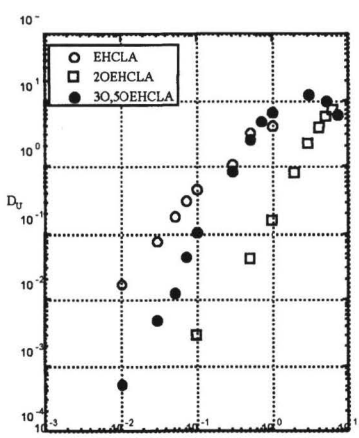


Figure 9 Nirtic acid denendency of D_U by 1 M cyclic amides

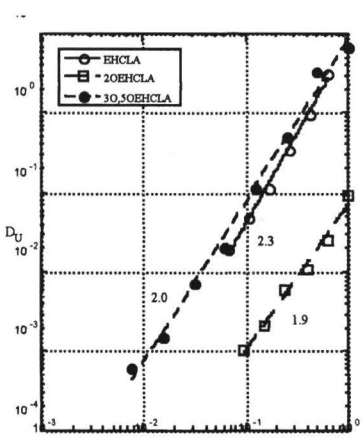


Figure 10 D_U as a function of cyclic amide concentration

is indicated that about two cyclic amide attributed to extraction of U.

The acid dependency of D_{Pu} by both 2OEHCLA and 3O,5OEHCLA was smaller than that by EHCLA in acidity less than 1M(figure 11). But maximum D_{Pu} obtained is 41.2 for 3O,5OEHCLA. In the case of 2OEHCLA, third phase did not appear even high nitric acid concentration area, however, D_{Pu} is still several orders of magnitude below the values obtained by use of 3O,5OEHCLA. This D_{Pu} reduction was mentioned above is attributed to increasing of steric hindrance around oxygen atom to introducing n-octyl group to nearest C=O carbon atom. The reduction of D_{Pu} 2OEHCLA is remarkably

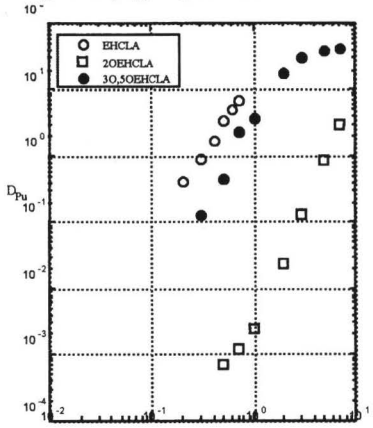


Figure 11 Nirtic acid denendency of D_{Pu} by 1 M cyclic amide

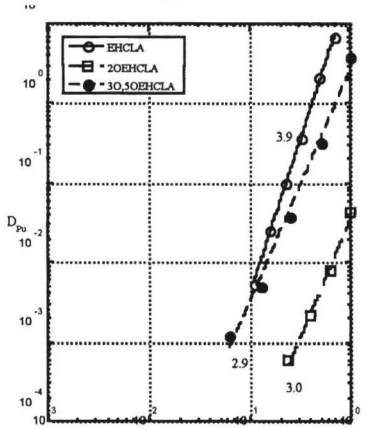


Figure 12 D_{Pu} as a function of cyclic amide concentration

low, comparison with that of D_U. This result means that Pu is more sensitivity for steric effect of extractant than U on the extraction by cyclic amide. Comparison of D_{Pu} between EHCLA and 3O,5OEHCLA, D_{Pu} by 3O,5OEHCLA is slightly smaller than that by EHCLA. It is indicated that a little steric hindrance presence on Pu extraction by 3O,5OEHCLA, comparing eith U extraction by 3O,5OEHCLA.

Figure 12 shows that cyclic amide concentration dependency of D_{Pu} in acid condition 1.0 M HNO_3. The slope of each lines is 3.9 for EHCLA, 3.0 for 2OEHCLA and 2.9 for 3O,5OEHCLA. Solvation number of 2OEHCLA and 3O,5OEHCLA which appended n-octyl group to the EHCLA were reduced due to steric hindrance.

CONCLUSION

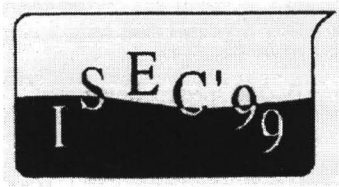
It could be concluded, from all above results, that a proposing amide, whose extraction behavior is most appropriate as an alternative to TBP, is the 3O,5OOCLA which possesses the highest extractability and enough solubility among the extractants evaluated. Comparison of D_M with N,N-dialkylamide which is the most possible to replace TBP as extractant in spent fuel reprocessing process, D_{Pu} obtained by 3O,5OOCLA is enable us to considered to adjust to process. However separation factor of between U and Pu by 3O,5OOCLA is small which is a subject in near future.

ACKNOWLEDGMENT

This work carried out under the entrustment of the Science and Technology Agency of Japan. The authors gratefully acknowledge the permission to publish this work.

REFERENCES

1. Siddal TH III, *J.Phys.Chem.*,**64**, 1863, (1960)
2. Siddal TH III, *DP-541* (1961)
3. Gasparini GM and Grossi G, *Sep.Sci.Technol.*,**15**, 825, (1980).
4. Gasparini GM and Grossi G, *Solv.Extr.Ion Exch.*,**4**, 1233, (1986).
5. Musikas C, *Sep.Sci.Technol.*,**23**, 1211, (1988).
6. Musikas C, Condamine N and Cuillerdier C, *Anal.Sci.*,**7**, 11, (1991).
7. Condamine C and Musikas C, *Solv.Extr.Ion Exch.*,**10,** 69, (1992).
8. Shen C, Bao B, Wang G, Qian J, Bao Y and Cao Z, *J.Radioanal.Nucl.Chem.,Art.*,**162** 207, (1992)
9. Bao B, Shen C, Wang G and Qian J, *Solvent Extraction in the Process Industries, Proc. ISEC'93*,Eds.,D.H.Logsdail and M.J.Slater, Elsevier **3**, 1821, (1993).
10. Yang L, Akita S and Takeuchi H, *Value Adding Through Solvent Extraction, Proc.ISEC'96*, Eds. D.C.Shallcross, R.Paimin and L.M.Prvcic, The University of Melbourne **2**, 1321, (1996).
11. Yang L and Takeuchi H, *Solv.Extr.Res.Dezp.Jpn.*,**3,** 124, (1996)
12. Yang L and Takeuchi H, *Solv.Extr.Ion Exch.*,**15**(2), 189, (1997)



OXIDATION OF CYANEX 302 AND CYANEX 301 BY FT-RAMAN AND UV-V SPECTROSCOPY

A Almela, B Menoyo, MP Elizalde and F Mijangos[1]
Departamentos de Química Analítica e Ingenieria Química[1]
Universidad del País Vasco, Aptdo. 644, 48080 Bilbao. Spain

ABSTRACT
The effect that exposure to nitric acid has on the extractants Cyanex 302 and Cyanex 301 has been studied by FT-Raman spectroscopy. It has been observed that an oxidation process in several steps takes place, leading to the formation of intermediate compounds which finally give rise to the formation of their oxy-acid analogues as well as other organophosphorus compounds. A kinetic study of the deactivation process that Cyanex 302 suffers on contact with HNO_3 by UV-V spectroscopy is also presented.

Keywords: Cyanex 302, Cyanex 301, Cyanex 272, nitric acid, FT-Raman spectroscopy, UV-V spectroscopy.

INTRODUCTION

The organothiophosphinic acids Cyanex 302 and Cyanex 301 whose major components are bis(2,4,4-trimethylpentyl)thiophosphinic acid and bis(2,4,4-trimethylpentyl)dithiophosphinic acid respectively have proved to be valuable solvent-extraction reagents as they are able to extract metal ions at very low pH values. However, one of the drawbacks of sulphur-containing extractants is that they are susceptible to oxidation and decomposition in the presence of mineral acids. Their stability in sulphuric and nitric acids has been studied by using IR spectroscopy,[1] and a severe oxidative decomposition as well as damages in the alkylchain has been reported after prolonged periods of exposure to nitric acid concentrations greater than 2.0 M. Moreover, for Cyanex 301, the formation of S-O linkages has also been proposed. On the other hand, the radiolytical stability of commercial and purified Cyanex 301 has been studied by IR and P-NMR[2,3] and the formation of the monothiophosphinic and phosphinic acid homologues as well as other organic phosphorus compound species was proposed.

The possibility of the formation of S-S and S-O linkages is also suggested by Sole et al.[4] in the study of the solvent extraction of copper by these reagents. Previous works [5] on the oxidation of short-chain dithiophosphinic acids have reported evidence of the formation of sulphanes ot the type $R_2P(S)\text{-}S_n\text{-}(S)PR_2$ (n=1, 2, 3).

In this work, FT-Raman spectroscopy has been applied to the study of the inactivation process of Cyanex 301 and Cyanex 302 in the presence of nitric acid. A kinetic study of the oxidation of Cyanex 302 solutions with nitric acid in a biphasic system has also been carried out by means of UV-V spectroscopy.

EXPERIMENTAL

Cyanex 272, Cyanex 302 and Cyanex 301 were kindly supplied by Cytec. Canada Inc. and were used without further purification. The rough extractants were used for the Raman and Infrared measurements while for the UV-V experiments organic solutions of Cyanex 302 in n-heptane (Merck p.a.), were prepared at a concentration of 0.1%.
Solutions of mineral acids were prepared from HCl, H_2SO_4 and HNO_3 (Merck p.a.).

The Raman measurements were accomplished using a Nicolet 950 FT-RAMAN spectrometer equipped with an InGaAs detector. Excitation at 1064 was provided by a Nd:YAG laser operating at 1000 mW. Data were collected at a spectral resolution of 8 cm^{-1} and 100 scans were acumulated. Infrared spectra were recorded using a Perkin Elmer R-1430.

© 2000 Society of Chemical Industry

Several confirmative assays were made by gas chromatography using a HP5890 gas chromatograph equipped with a GC-MS detector. A HP-5 columm 12.5 m x 0.25 mm x 0.25 μm film thickness was used.
Absorbance measurements were carried out using a UV-V Shimazu UV-260 spectrophotometer.

RESULTS AND DISCUSION

FT-Raman spectroscopy

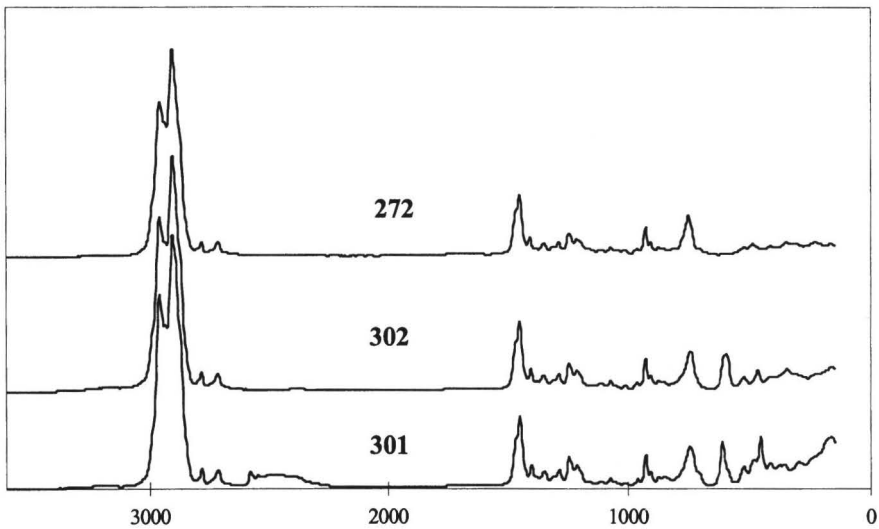


Figure 1. Raman spectra of Cyanex 272, Cyanex 302 and Cyanex 301.

In the Raman spectra of the three extractants the majority of the bands observed correspond to vibrations of the alkyl chain of the organophosphorus molecule (bis(2,4,4-trimethylpentyl) radical): 2954, 2904, $\nu(CH_3)$ as; 1450, $\delta(CH_3)$ as; 1407, 1351, $\delta(CH_3)$ sym of the tert-butyl group; 1246, 1212, ν(C-C) of the tert-butyl group; 955, 929, 908, bands characteristic of the branched chain; 750, ν(sketetal) sym of the tert-butyl group as well as ν(P-C). On the other hand, the vibrational band at approximately 610 cm^{-1} corresponding to P=S can be observed in both Cyanex 302 and Cyanex 301. The bands at 522 cm^{-1} and 480 cm^{-1} that appear in the spectrum of Cyanex 301 can be assigned to the PS(SH) stretch, the former also corresponding to the tert-butyl group. Cyanex 301 also exhibits a band at 454 cm^{-1} corresponding to P-S (this band is weak in Cyanex 302 due to the tautomeric form), and a signal in the region of 2500 cm^{-1} due to the vibration of S-H. In the Raman spectra of these extractants the bands corresponding to the bonds P-O-H and P=O are very weak and are masked by the bands of the alkyl chain.

Additionally, in the infrared spectra of these extractants, Cyanex 272 shows a strong band at 950 cm^{-1} due to P-O-H, this band having medium intensity in the case of Cyanex 302 and being negligible in the case of Cyanex 301. On the other hand, the band appearing at 1175 cm^{-1} in Cyanex 272 can be attributed to the P=O stretch, this signal being very weak in both Cyanex 301 and Cyanex 302 spectra (indicating the predominance of the thiono form of the monothiophosphinic acid).

The three rough extractants Cyanex 272, Cyanex 302 and Cyanex 301 were treated with the mineral acids most frequently used as stripping agents: hydrochloric, sulphuric and nitric acids. No effect with the hydrochloric and sulphuric acids was observed whereas nitric acid (5.0 M) caused degradation of Cyanex 302 and Cyanex 301.

The stability of Cyanex 301 and Cyanex 302 that had previously been on contact with 5.0 M nitric acid for a short period of time was studied by carrying out two kind of experiments. In this sense, after mechanical agitation for 15 minutes, part of the organic phase was removed and kept in a tube while the rest remained on contact with nitric acid. The aim of the experiment was to find out whether the degradation process occurred even in the absence of prolonged contact with nitric acid. The results of the experiment showed that the degradation takes place only when the rough extractants are on contact with 5.0 M nitric acid for a long time.

Figure 2 shows the variation of Raman spectra with time in the range of interest 1400-150 cm^{-1}. Concerning Cyanex 301, the degradation process becomes to be important after three days, when the organic phase is completely yellow, and a yellow solid appears to be formed at the interface. Raman spectrum of this solid confirmed that sulphur was being formed which means that cleavages of the sulphur containing bonds are taking place. This fact is confirmed by the progressive decrease in the intensity of the bands at 2500 cm^{-1} (S-H), 610 cm^{-1} (P=S), 522 cm^{-1} (PS(SH)) and 454 cm^{-1} (P-S). On the other hand, new bands at 474 $cm^{-1}$and 812 cm^{-1}appear, as well as a peak at 218 cm^{-1}. The degradation process seems to be practically completed in eight days as the bands corresponding to the P=S and P-S bonds have disappeared. The spectrum finally obtained practically matches the spectrum of Cyanex 272, suggesting the oxidation of the extractant from the thiophosphinic acid to the phosphinic acid. However, it must be taken into consideration that after three days a new band around 474 cm^{-1} appears, this band overlaps the band at 454 cm^{-1} and increases, finally decreasing. This may indicate the formation of S-S linkages for a short period of time.

Concerning Cyanex 302, Figure 2 shows that the degradation process takes less time to be completed. Thus, after being on contact with nitric acid for a few hours, the organic phase is yellow and there is again a yellow solid at the interface, which was confirmed to be sulphur. The Raman spectra shows that the bands at 602 cm^{-1} (P=S) and 466 cm^{-1} (P-S) experiment a decrease with time and in seven days they have disappeared, while new bands at 819 cm^{-1}, 476 cm^{-1} and 218 cm^{-1} are being formed. The spectrum finally obtained shows its similarity to that of Cyanex 272 and also to the spectrum of Cyanex 301 after nitric acid treatment.

Examination of the spectra of these nitric acid treated extractants shows the developing of new absorption bands at around 474 cm^{-1} and 218 cm^{-1} which seem to suggest that a new compound could be formed as well as the phosphinic acid. These findings are consistent with the results obtained by using gas chromatography where the comparison of the gas chromatograms obtained before and after contact of the organic phases diluted in toluene with 5.0 M nitric acid revealed that the monothiophosphinic acid is almost completely oxidized to the corresponding alkylphosphinic acid, whereas the dithiophosphinic acid is partially oxidized to both the monothio and to the phosphinic analogues. The chromatograms also show the formation of other organophosphorus compounds. Moreover, additional extraction experiments have confirmed that the organic solutions of Cyanex 302 after nitric acid treatment are able to extract the metal ions, but at higher pH values, as corresponds to the Cyanex 272 analogue, thus agreeing with Modolo et al [3].

Finally, it has to be pointed out that additional experiments carried out with H_2O_2 instead of nitric acid gave rise to similar results, although this time the degree of the degradation process seemed to be less severe.

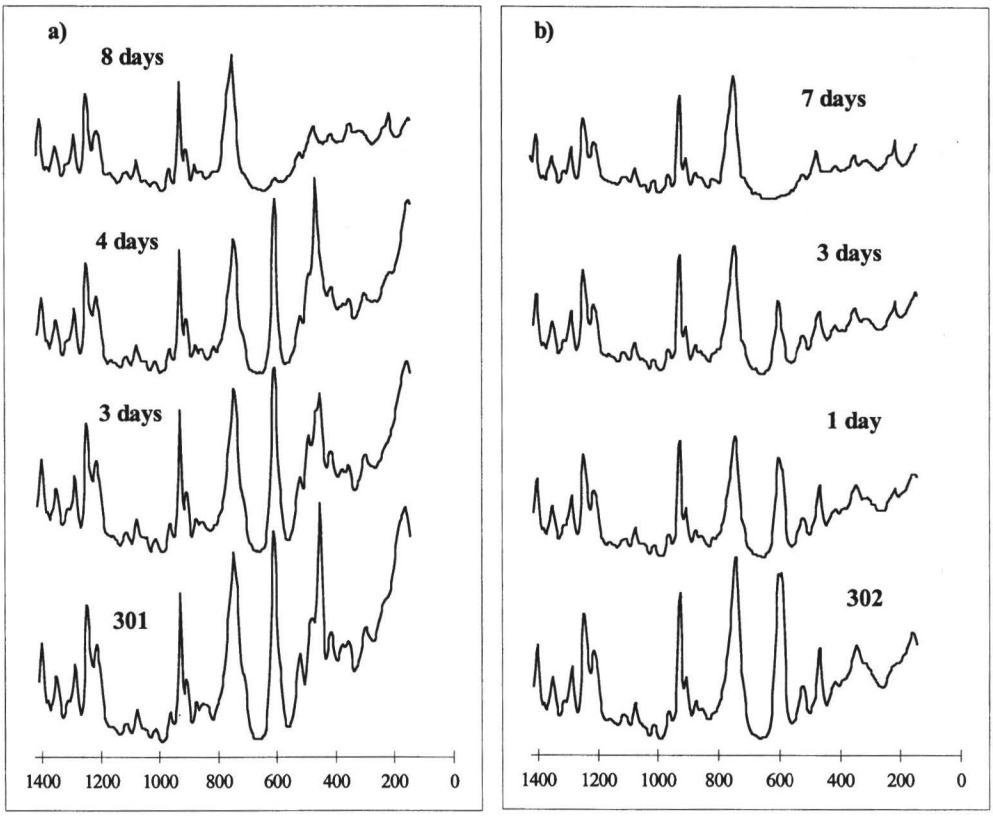


Figure 2. Raman spectra of the organic solutions of (a) Cyanex 301 and (b) Cyanex 302 before and after prolonged contact with 5.0 M nitric acid.

Ultraviolet - Visible Spectroscopy

Preliminary experiments using UV-V spectroscopy showed that organic solutions of Cyanex 302 on contact with nitric acid solutions developed a peak around 275 nm which increased gradually with time, reached a maximum and then decreased. These results indicated that the oxidation process could be studied from a kinetic point of view. Similar results were obtained with H_2O_2 aqueous solutions, although in this case only the increasing of the absorbance of the organic solutions was observed.

Thus, the experiments were performed in a spectrophotometer cell (1 cm path), containing 0.5 ml of nitric acid solutions and 2 ml of 0.1% Cyanex 302 in n-heptane. The measuring distance was 10.5 mm above the interface. No shaking was allowed in the experiments, trying to avoid any source of turbulence. Following this procedure, six series of experimental data were collected in the form A = f(time). Each series corresponded to a nitric acid concentration in the aqueous solution: 2.9, 4.0, 5.0, 7.2, 9.2, and 14.4 M. Figure 3 shows the representation of the experimental data at the different nitric acid concentrations.

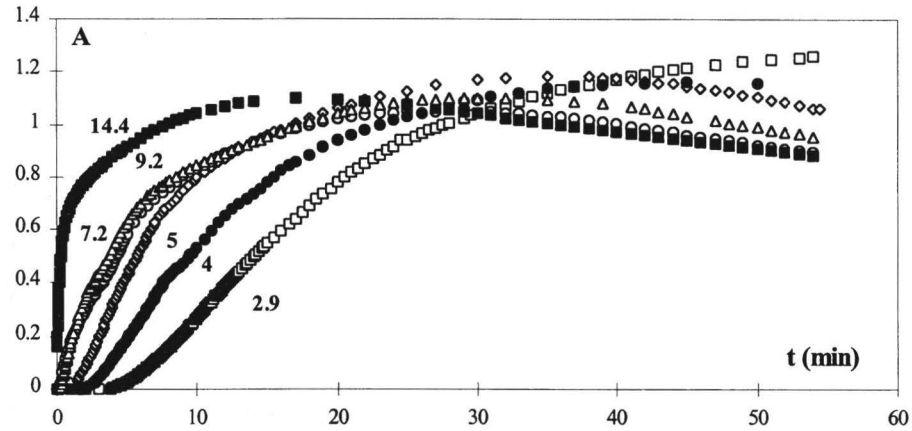


Figure 3. Variation of the absorbance (275 nm) of organic solutions of Cyanex 302 with time at different total nitric acid concentrations (M) in the aqueous phase.

Data treatment was carried out taking into account the following assumptions:

a.- The process occurs in two main steps: diffusion step and chemical reaction.
In the diffusion step HNO_3 diffuses to the interface and reacts with the active component of the extractant giving rise to the oxidized intermediate that diffuses through the organic phase to the measuring zone. The chemical reaction assumes the degradation of the intermediate species to final products.

b.- Only intermediate species are measured at 275 nm.

c.- There are no volume changes in both phases.

d.- It is an isothermal system. No heat dissipation occurs.

As a first approach, only the diffusion process was considered. Under these assumptions, this system can be treated as that described by Crank,[6] and the solution of the continuity equation, taking into account the Lambert - Beer law, has the expression: $A/A_{inf} = \text{erfc}\ [\delta / (D_{II}\ t)^{0.5}]$ where A represents the measured absorbance and A_{inf} a parameter corresponding to the absorbance that would be obtained if only a diffusion process took place. δ is the fixed measured distance (10.5 mm), and D_{II} represents the diffusion coefficient of the species measured in the organic phase.

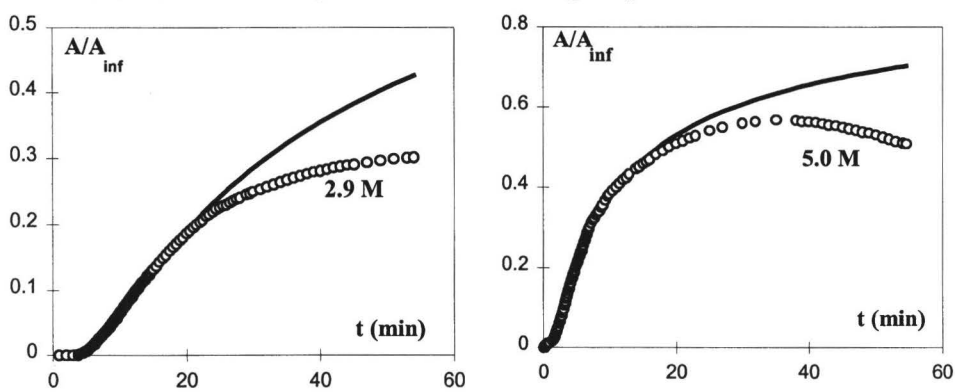


Figure 4.- Comparison of some of the experimental data with the theoretical curves (continuous lines) assuming a diffusion kinetic model.

The function represented by the above equation was theoretically calculated using A_{inf} and D_{II} as fitted parameters. Numerical calculations were carried out minimizing the error square sum by means of the Solvent option of the Excel program[7]. The estimated diffusion coefficient ranged from $0.27 \cdot 10^{-7}$ to $5.79 \cdot 10^{-7}$ m^2/s, depending on the nitric acid concentration in the aqueous phase.

As an example, Figure 4 shows the comparison between the experimental and theoretical functions for the experiments carried out at 2.9 and 5.0 M nitric acid concentrations. As it can be seen, both functions show a good agreement in the first part of the curves (short periods of time) whereas for prolonged periods of exposure strong deviations due to chemical reactions following the diffusion step can be appreciated.

The results obtained in this kinetic study agree with those obtained previously by Raman spectroscopy in the sense that the interaction between the alkylthiophosphinic acids and nitric acid gives rise to oxidation processes in which the initial oxidized form of the extractants, which probably are related to disulphide dimers of the acids, degradates to yield finally, as well as other compounds, the alkylphosphinic acid.

ACKNOWLEDGEMENTS

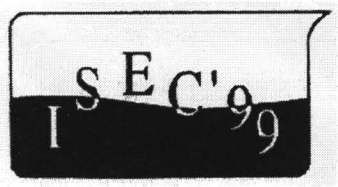
The authors thank the University of the Basque Country as well as The Ministery of Education for the financial support.

REFERENCES

1. Sole KC, Hiskey JB and Ferguson TL, *Solv. Extr. Ion Exch.*, **11**(5), 783, (1993).
2. Chen J, Jiao R and Zhu Y,. *Solv. Extr. Ion Exch* **14**(4), 555, (1996).
3. G. Modolo and R. Odoj, *J. Radioanal.Nucl. Chem.*, **1-2**, 83, (1998).
4. Sole KC and Hiskey JB, *Hydrometallurgy*, **37**, 129, (1995).
5. Kuchen W and Hertel H, *Angew. Chem. Int. Ed. Engl.*, **8**, 89, (1969).
6. Crank J, *The Mathematics of Diffusion*, Clarendon, Oxford, (1975).
7. Microsoft, EXCEL 5.0.



Hydrometallurgy



INDIUM RECOVERY FROM INDUSTRIAL ZINC RESIDUES

JS Benedetto[1], EB Tambourgi[2] and RM Mingote[1]

[1] Centro de Desenvolvimento da Tecnologia Nuclear CDTN /CNEN, R.Prof. Mário Werneck s/n, Cidade Universitária, Pampulha, CEP 30.123-970, Belo Horizonte, Minas Gerais, Brazil.

[2] Universidade Estadual de Campinas UNICAMP, Faculdade de Eng. Química, Depto de Eng. de Sistemas, Campinas – São Paulo, Brazil.

ABSTRACT

This work presents a study of indium recovery from sulphuric liquor generated during the hydrometallurgical processing of zinc. The investigation aims at defining a process to obtain a purified solution of the metal fitting industrial requirements for further use. The main steps of the process were studied. Indium was initially precipitated with a small amount of iron to generate a solution with a lower Fe/In ratio. Following that, the solution was fed into the solvent extraction experimental unit for the recovery of indium, which was subsequently purified.

A study of the main parameters of the process was conducted for the steps: iron reduction, indium precipitation, precipitate solubilization, solvent extraction and stripping of indium.

The experimental results indicated that it was possible to obtain aqueous indium solutions with a high grade of purity. The recovery was practically complete: over 98%.

Keywords: indium, iron reduction, D2EHPA, zinc residues

INTRODUCTION

Indium is a strategically important element. To date, most of the world's supply of indium has been recovered from the dusts and residues generated during the processing of Zn, Zn-Pb and Zn-Cu sulphate concentrates. It is known that most of indium in the feed to the jarosite circuit collects in the jarosite residue. In^{3+} replaces Fe^{3+} in the jarosite structure to form a nearly ideal solid solution series. The consequence is that it is virtually impossible to avoid indium losses in jarosite, while at the same time it is difficult to concentrate indium in the jarosite precipitate.[1]

In common with many of the rarer metals, indium becomes concentrated in the by-products of the recovery of other metals, especially lead and zinc. Indium is most frequently associated with zinc and, as a result, is commercially recovered from zinc residues and smelter slags. At the present time these by-products constitute the only commercial sources of indium.[2]

The industrial solution is a sulphuric liquor with 80 $\mu g/cm^3$ of indium and other metal ions such as iron, zinc, and copper. Iron is present in significant amounts (25.7 g/dm^3) and its removal and disposal constitutes a major operational problem. Presently iron removal is accomplished by precipitation techniques as used in the zinc industry. These, despite their effectiveness, are associated with high consumption of neutralising agents, causing the accumulation of complex iron residues that might lead to environmental problems.[3]

Since the leach solutions are extremely complex and exhibit low concentrations of scarce metals, the method ultimately employed should be extremely selective and active, and the accomplished upgrade in concentration should be very high to obtain the proper liquors and eventually produce the metals. Most desirable would be a solvent extraction process for direct recovery of the metals from sulphuric acid liquors.[4]

The indium and iron Eh-pH diagrams are very useful in indicating the best conditions to attain an indium rich precipitate. This precipitate after solubilization can be fed in a solvent extraction process to obtain the purified metal. Indium is quantitatively extracted under adequate conditions but a competitive extraction of Fe^{3+} and Zn^{2+} ions also occurs at this stage. To minimise the extraction of iron, Fe^{3+} has been reduced to Fe^{2+}, since the ferrous ion has a higher pH range of extraction.[5]

© 2000 Society of Chemical Industry

EXPERIMENTAL

The route of the process includes four main steps. These are:

Iron reduction

Preliminary batch tests were carried out to investigate the parameters that most affect the process.[6] Two reduction agents were tested: zinc sulphite (ZnS), and zinc powder (Zn). In this step the temperature and the time of reaction were investigated.

Indium Precipitation

The purpose of these experiments was to obtain maximum precipitation of indium with minimum iron contamination. Recovery of high purity indium would be reached on the next step by solvent extraction. The effect of the parameters that influence indium and iron separation was studied. These parameters are pH, temperature and sedimentation time,

Precipitate Solubilization

The indium concentrate was dissolved in sulphuric acid, and the acidity adjusted for the conditions required by the subsequent experiments.

Solvent Extraction and Stripping of Indium

This process provides a highly selective indium separation. Di-2-ethylhexylphosphoric acid (D2EHPA) diluted in isoparaffin has been used as the extractant for the recovery of indium. Previous batch tests with a synthetic solution indicated the range of the main parameters.[6] Subsequently a few tests were run with the real solution to achieve the optimum conditions for this process.

Sample characterisation

The sample used in this investigation was collected from the sulphuric liquor flowing from the acid leach step of the industrial zinc process. The concentrations of the main elements present in the sulphuric liquor are shown in table 1:

Species	Concentration
In	80 $\mu g/cm^3$
Ga	20 $\mu g/cm^3$
Fe	25.7 g/dm^3
Zn	95.0 g/dm^3
Cu	4.30 g/dm^3
Acidity	0.76 mol/dm^3

Table 1 Characterisation of the Main Species in the Feed

Theoretical Basis

The Eh-pH diagrams for indium and iron are shown in figures 1 and 2. The most effective separation of both elements occurs at a negative potential and at pH nearly 4. In these conditions indium should precipitate whereas iron would remain in solution as Fe^{2+}.

The main reactions at the indium precipitation step are:

$$Fe(OH)_2 = Fe^{2+} + 2OH^- \quad Kps = 8.0 \times 10^{-16}$$
$$Fe(OH)_3 = Fe^{3+} + 3OH^- \quad Kps = 4.0 \times 10^{-38}$$
$$In(OH)_3 = In^{3+} + 3OH^- \quad Kps = 6.3 \times 10^{-34}$$

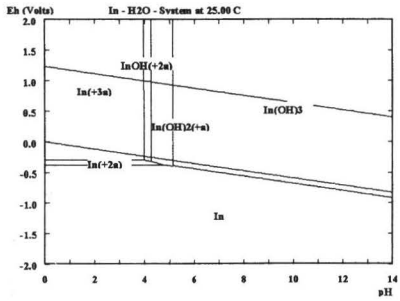


Figure 1 – Indium Eh-pH diagram

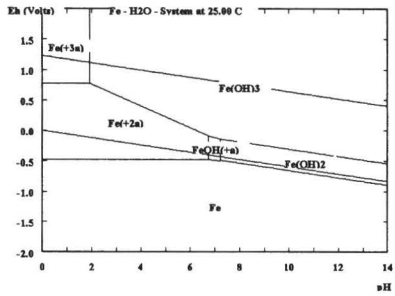


Figure 2 – Iron Eh-pH diagram

Taking into account that the concentrations of iron and indium in the solution are 25.7g/dm^3 (0.4602 mol/dm^3) and 80 μg/ml (0.697x 10^{-4} mol/dm^3) respectively, the pH values at which metal precipitation begins are:

Fe^{2+}: $[OH^-] = \sqrt{\frac{8\times10^{-16}}{0{,}4602}}$ $\Rightarrow$ [OH$^-$] = 4.17 x 10^{-8}

pOH = - log[OH] = 7.4, $\Rightarrow$ pH = 6,6

Fe^{3+}: $[OH^-] = \sqrt[3]{\frac{4\times10^{-38}}{0{,}4602}}$ $\Rightarrow$ [OH-] = 4.42 x 10-13,

pOH = -log[OH] = 12.3, $\Rightarrow$ pH = 1,6

In^{3+}: $[OH^-] = \sqrt[3]{\frac{6{,}3\times10^{-34}}{0{,}697\times10^{-4}}}$ $\Rightarrow$ [OH-] = 2.08x 10-10

pOH = -log[OH] = 9.7 $\Rightarrow$ pH = 4,3

With the above specified concentrations the onset of indium hydroxide precipitation is at pH 4.3. Taking into account the acidity, all the Fe^{2+} remains in the solution; however if ferric ions are present in the solution, they will precipitate together with indium hydroxide.

RESULTS AND DISCUSSIONS

Iron Reduction

Figure 3 shows the influence of the temperature on the yield of iron reduction for both reducing agents tested, zinc sulphide and zinc powder. The amounts of ZnS and Zn used were 10% and 50% above their respective stoichiometric ratio to iron. Under such conditions the best yields for iron reduction were achieved with ZnS at temperatures over 50°C. The zinc powder is an effective reducing agent even at ambient temperature.

Zinc powder is not recommended for this application as its recycle in the process cannot become economically viable. The following experiments were conducted with a ZnS reagent that may be substituted for the natural ore at the leaching step.

Figure 4 shows the iron reduction as a function of time at two temperatures, 70°C and 90°C . Two hours are sufficient to reach the optimum reaction yield. After two hours the yield of the process is practically the same at both temperatures.

Indium Precipitation

Figure 5 shows the influence of the equilibrium pH on the precipitation of indium and iron. It can be seen that the recovery of indium increases with decreasing acidity. The best condition was reached at pH 4, where all indium was precipitated and iron contamination was nearly 7.0 % that of the feed.

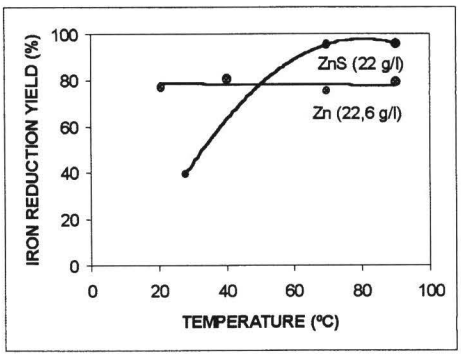


Figure 3 – Influence of temperature on iron reduction yield. Time of reaction = 2h

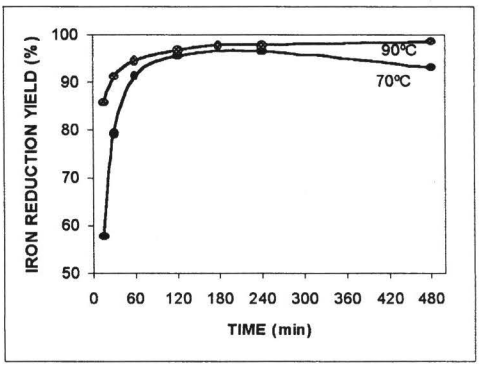


Figure 4 - – Influence of time on iron reduction yield

Figure 6 shows the effect of temperature on the precipitation of impurities. The recovery of indium is nearly 100%. The grade of indium in the precipitate however decreases with increasing temperature due to the co-precipitation of impurities such as copper, iron and zinc.

The effect of sedimentation time on the precipitation of impurities was also investigated. It has been observed that higher sedimentation times lead to an increased co-precipitation of copper, zinc and iron. Indium recovery reaches the maximum, nearly 100%, after the pH adjustment; thus it is not recommended to wait a long time for sedimentation.

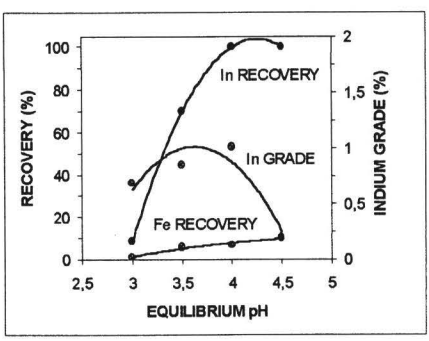


Figure 5 – Influence of pH on Indium recovery. T° amb., time of sedimentation = 30 min.

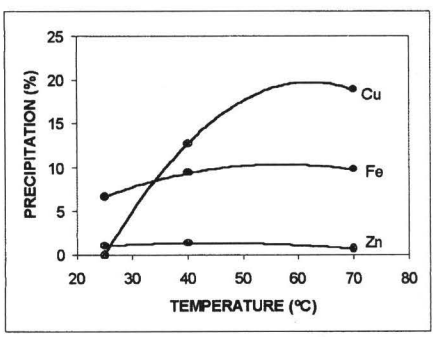


Figure 6-Influence of temperature on Indium recovery. pH= 4, time of sedimentation = 30 min

Precipitate Solubilization

After solubilization of the precipitate with sulphuric acid the resulting solution presented an indium / iron ratio almost 100 times higher than in the initial solution, whose composition is shown in table 2.

Solvent extraction and stripping of indium

Previous tests with a synthetic solution of indium and iron indicated the use a diluted concentration of the D2EHPA extractant, around 2.0%, for the selective separation of indium. Figure 7 shows the comparison of indium and iron extraction from the process solution using this extractant at different concentrations ranging from 1.0% to 5.0%. The recovery of indium reaches 99% and the iron extraction was lower than 15.3%.

Species	Concentration	
In	683	$\mu g/cm^3$
Fe	2.48	g/dm^3
Ga	124	$\mu g/cm^3$
Zn	9.1	g/dm^3
Cu	0.25	g/dm^3
H^+	0.3	mol/dm^3
SO_4^{2-}	68.0	g/dm^3

Table 2 Characterisation of the solvent extraction feed solution

Figure 8 shows the influence of the sulphuric acid concentration on the indium and iron extraction, also using D2EHPA . The recovery of indium decreases with increasing acidity, whereas that of iron is not sensitive to variations over the range of acid tested.

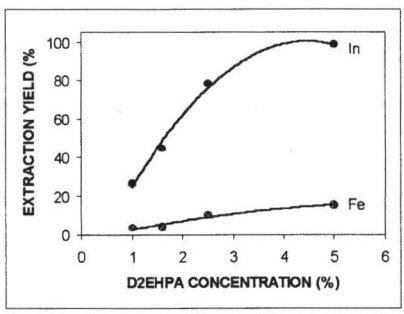


Figure 7 –Influence of D2EHPA concentration on indium and iron extraction. Acidity $[H^+]$ = 0.3M,contact time = 5.0 minutes at A/O = 1

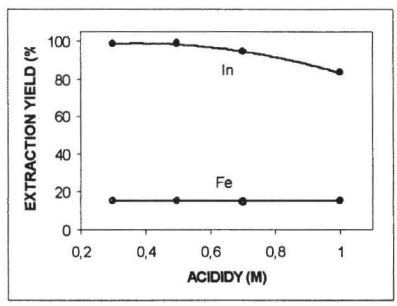


Figure 8 - Influence of acidity on indium and iron extraction. D2EHPA concentration = 5%, contact time = 5.0 minutes at A/O = 1

The kinetics of indium and iron extraction using D2EHPA was investigated. Indium is extracted very quickly, requiring near one minute to reach equilibrium and the iron extraction is slow. Long times of phases contact are therefore not recommended because iron substitutes part of the indium that has already been complexed with the extractant.

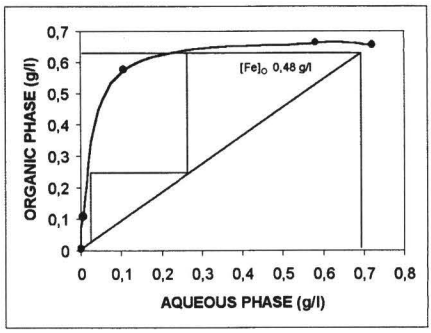


Figure 9- Equilibrium isotherm for indium extraction with D2EHPA 2.5%. Acidity $[H^+]$ = 0.3M

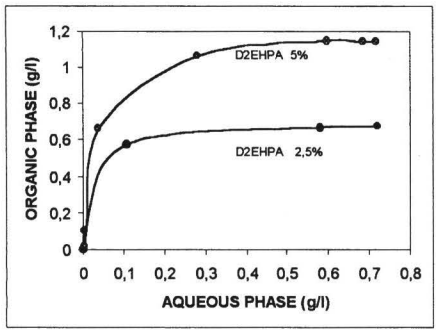


Figure 10- Equilibrium isotherms for indium extraction with D2EHPA. Acidity $[H^+]$ = 0.3M.

Figures 9 and 10 show the extraction isotherms for indium with 2.5% and 5.0% of D2EHPA. Two stages are sufficient for complete extraction of this metal at the conditions of the study. In the first case the iron in the saturated organic is around 0.5g/dm^3 and it can be separated in the next step of stripping. This iron contamination can be reduced using shorter contact times between the phases.

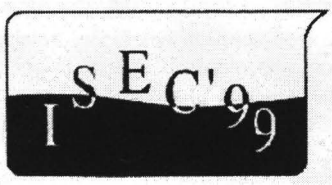
The stripping of indium was tested with sulphuric and hydrochloric acids. Iron and indium were stripped in the same proportion by the sulphuric acid. Hydrochloric acid displayed high selectivity in the separation of these metals. Indium was extracted preferentially even with reduced acidity of this medium.

CONCLUSIONS

The results show that it is possible to obtain a precipitate with the Fe/In ratio reduced almost a hundred times lower then that of the feed. The recovery of indium in the product was almost 100%. After solubilization this product allowed a better separation of the metals in the solvent extraction process, using D2EHPA as the extracting reagent and hydrochloric acid in the stripping step . The results demonstrated that indium can be selectively separated.

REFERENCES

1 Dutrizac JE and Mingmin D. *International Symposium-World Zinc '93*, (1993).
2 Mills JR, King RA and White CET. *Indium. Rare Metals Handbook*, 220, (1990).
3 Demopoulos GP. *Hydrometallurgy*. **12** (1984).
4 Zhou T, Zhong X, and. Zheng L. *JOM*, (1989).
5 Bonora R, Zoner D. *ECCE-1*. Florence, Italy, (1997).
6 Fortes MCB and Benedetto JS. *Minerals Engineering*, **11**, 447, (1998).



INDIUM RECOVERY BY SOLVENT EXTRACTION WITH D2EHPA USING A STATISTICAL APPROACH TO THE EXPERIMENTAL DESIGN

MCB Fortes,[1] AH Martins[2] and JS Benedetto[1]

[1]Centro de Desenvolvimento da Tecnologia Nuclear - CDTN/CNEN Rua Prof. Mário Werneck, S/No - C. P. 941 - CEP 30123-970 Cid. Universitária, Pampulha. Belo Horizonte. Minas Gerais, Brazil

[2] Universidade Federal de Minas Gerais – UFMG, Departamento de Engenharia Metalúrgica e de Materiais, Rua Espírito Santo no. 35 sala 206 - CEP 30160 – 030 Centro. Belo Horizonte. Minas Gerais, Brazil

ABSTRACT

Several new industrial applications of indium have been discovered, particularly in the highly competitive field of microelectronics. However, these applications require high purity grade indium and its inorganic compounds. Indium has been recovered as a byproduct from residues generated from the sulfuric acid leaching circuits in mineral plants for zinc recovery. Indium is associated in trace amounts to other metals in zinc ores, especially iron found in high concentrations in the leach liquor. This work presents the results for determination of the best experimental conditions to obtain a high indium concentration solution and minimum iron poisoning by solvent extraction with di(2-ethylhexyl)-phosphoric acid (D2EHPA) solubilized in isoparaffin. The variables studied were extractant concentration in the organic phase, acidity of the aqueous phase and contact time between the phases. The optimization procedure adopted was the Ascending Path Statistical Method which used the numeric values determined in the Yates Algorithm of the Full Factorial Design approach also applied in this work. The optimum experimental conditions led to a 99% indium solution with less than 1% iron as impurity, suitable for some industrial applications.

Keywords: indium, iron, factorial design, D2EHPA

INTRODUCTION

Indium tends to be associated with other metals of similar chemical properties such as zinc, lead, copper and tin. It does not occur naturally in concentrations that are high enough for mining purposes. The treatment of indium is a particular challenge for the extractive metallurgist because it exhibits a considerable chemical affinity for other elements making its separation difficult. The main hydrometallurgical techniques used for indium extraction and refining include solvent extraction, cementation and electrorefining.

Most of the hydrometallurgical research work for indium recovery and refining involves solvent extraction. Hoffmann[1] described the process developed by Cerro de Pasco, Peru using the sulfuric acid leach liquor from the zinc process for indium recovery. This solution was contacted with D2EHPA, 20 % v/v diluted in kerosene, as the organic phase. Stripping was accomplished with hydrochloric acid. Iron was maintained in the divalent state (Fe^{2+}) to prevent co-extraction. The indium concentration of the final aqueous phase was six times the initial concentration. Indium was recovered from the solution by cementation with aluminum sheets.[1]

Bonora and Zoner[2] studied indium separation from a liquid industrial effluent containing 0.46% indium by solvent extraction. The extractant used was D2EHPA, 20 % v/v in xylene. Attention was paid to iron and zinc that co-extracted under similar conditions to indium. Fe^{3+} was reduced to Fe^{2+}, while for zinc removal a stripping stage with sulfuric acid was inserted, a fourteen-fold increase was observed.[2]

Fortes and Benedetto[3] investigated the separation of indium and iron by solvent extraction using a replicated Full Factorial Design Method for three variables at two levels. The experimental work was carried out using synthetic solutions with iron and indium in sulfuric acid media and D2EHPA diluted in isoparaffin. The main solvent extraction variables studied were extractant concentration in the organic phase, acidity of the aqueous phase and contact time between the organic

© 2000 Society of Chemical Industry

and aqueous phases. The statistical evaluation showed that D2EHPA was effective for this indium and iron separation. The most significant results were obtained using a feed solution where the trivalent iron was first reduced to the divalent state. Satisfactory separation was obtained at low levels of D2EHPA concentration (0.025 mol/dm^3) with 0.2 N acidity in the aqueous phase and 1.0 minute contact time between the phases. Under these conditions, indium extraction was nearly 90 % while iron impurity was around 3 %.[3]

This paper concerns the statistical optimization of the Fortes and Benedetto[3] experimental results aiming at determining the best experimental conditions for the main variables for the solvent extraction with D2EHPA in isoparaffin which led to highly concentrated indium solution with minimum iron poisoning. The main variables studied were extractant concentration in the organic phase, acidity of the aqueous phase and contact time between the phases. The optimization procedure adopted was the Ascending Path Statistical Method [4] which used the numeric values determined in the Yates Algorithm of the replicated Full Factorial Design approach also applied in this work. The extraction isotherms for indium, under the optimum experimental conditions determined by the statistical approach and confirmed in bench-scale tests, were also constructed allowing the prediction of the theoretical number of countercurrent stages for indium extraction using the McCabe-Thiele diagram [5].

EXPERIMENTAL PROCEDURE

The aqueous feed solutions were prepared from indium oxide (99.9 % In_2O_3, Aldrich Chemical Co.), and iron sulfate (21-23 % $Fe_2(SO_4).xH_2O$, Hoechst Brazil) in sulfuric acid solution (95-97 % H_2SO_4 PA Vertec). The hydrogen ion concentration of the solution was adjusted according to the selected experimental levels and the optimum conditions determined by the statistical approach. The iron and indium concentrations in the aqueous feed solution were 2.5 g/dm^3 and 0.5 g/dm^3 respectively. The metal concentrations were chosen based on the leach liquor composition generated by the sulfuric acid leaching of a zinc ore after a previous mineral concentration. Analytical grade reagents and distilled water were used throughout the experiments.

The organic phases were prepared with D2EHPA, (Daihachi Chemical Industry Co. Ltd, Japan) diluted in isoparaffin (Unipar Química, Brazil). Tests were carried out in 100 cm^3 open vessels with mechanical stirring at 27±1° C and using 1:1 organic/aqueous (O/A) phase ratio.

The ascending path method is a statistical procedure for moving the numeric values of the variables under study towards the direction of maximum increase in the experimental response. The validity of the statistical approach adopted in this experimental work was checked by the Fisher test.[4]

The full factorial design method of three variables at two experimental levels for replicated responses was used. The main variables studied were organic extractant concentration in the organic phase, D2EHPA; acidity of the aqueous phase, $[H^+]_a$ and contact time between organic and aqueous phases, t. The upper and lower levels were, D2EHPA, 0.05-0.025 mol/dm^3; $[H^+]_a$, 0.8-0.2 N; and t, 10-1 min respectively.

A sample of the aqueous phase after each test was collected for determination of iron and indium concentration in the solution by atomic absorption spectrophotometry (computerized model 932 AA GBC Scientific Equipment, Australia). The iron (Fe^{2+}) concentration was titrated with potassium dicromate.[6]

Extraction isotherms were constructed using the optimum experimental conditions determined by the statistical approach. Successive contacts between the phases were made using open vessels with mechanical stirring at room temperature and 1:1 O/A phase ratio. Figure 1 shows a schematic diagram of the experimental setup used to obtain the numeric values to build the extraction isotherms for indium. Four contacts between both organic loading and exhausting stages were made. The number of theoretical countercurrent stages required for indium extraction was determined using the McCabe-Thiele diagram. Batch stripping tests were carried out using sulfuric acid at different concentrations for indium recovery.

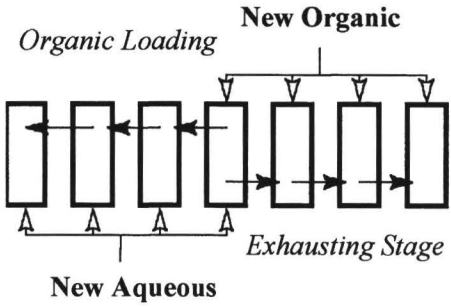


Figure 1 Schematic diagram of procedure used to determine the extraction isotherms for indium

RESULTS AND DISCUSSION

The influence of some main variables on the indium and iron extraction by solvent extraction with D2EHPA was studied using a statistical approach. Table 1 shows the design matrix block for replicated experiments and the numerical values assumed for each variable using the replicated full factorial design method for three variables at two experimental levels. The negative sign represents the lower experimental level of the respective variable and the positive sign its upper level. The experimental responses were the percentage extraction of indium (In) and iron (Fe).

Experiments	Variables			Replicated Experimental Results			
	A	B	C	In (%)	In (%)	Fe (%)	Fe (%)
1	-	-	-	95	88	5	0
2	+	-	-	96	96	11	10
3	-	+	-	20	10	1	1
4	+	+	-	73	81	1	4
5	-	-	+	81	85	14	11
6	+	-	+	95	96	29	26
7	-	+	+	35	40	6	3
8	+	+	+	87	81	9	12

Table 1 Matrix for replicated experiments for indium and iron extraction

The Yates Algorithm [3,4] was used to calculate effects of the variables and their interactions from the experimental results of indium and iron extraction. The Yates calculations showed that all parameters studied had significant statistical effects but with different intensities. The acidity of the aqueous phase exhibited the greatest influence on the experimental response of indium extraction. As expected on a system using an acidic organic extractant, the lower the acidity of the aqueous phase, the higher the indium extraction. This can be explained through an equilibrium equation of metal extraction by a cation-exchange system since its extraction is highly pH dependent.[5]

The ascending path method was adopted to determine the optimum experimental conditions to reach maximum indium extraction using the acidity of the aqueous phase as a parameter. So, the optimum experimental conditions for maximum indium extraction were: concentration of D2EHPA = 0.05 mol/dm^3; acidity of the aqueous phase, $[H^+]_a$ = 0.25 N; and contact time between the phases, t = 6 minutes.

According to the statistical methods used the predicted response for indium extraction was 99.4%. Table 2 presents the results of the experimental tests using the optimum conditions of maximum indium extraction. These tests were carried out to check the results obtained by the statistical model adopted in this work. The validity of the statistical model was confirmed using the

Fisher Test where the confidence level was higher than 95% and the experimental error was lower than 5%. It can be seen that the predicted value is very close to the experimental one for indium extraction with D2EHPA diluted in isoparaffin.

Results	In extraction %	Fe extraction %
Predicted	99.4	—
Experimental	99.8	1.6

Table 2 Experimental results for indium and iron extraction under the optimum conditions for maximum indium extraction

From the statistical model fitted to reach maximum indium extraction, it as not able to predict the iron extraction. From the experimental results it was observed that a good separation of the two metals can be reached under these conditions.

To obtain indium aqueous solutions with satisfactory purity, the experimental conditions for minimum iron extraction must be used. Following the same procedure used for indium statistical analysis, it was noted that the time of contact between the phases had the greatest influence on the iron extraction. Therefore, the time of contact between the phases should not permit oxidation of iron (II). Such oxidation could permit competition between iron (III) and indium (III) due to their similar solvent extraction properties resulting in the replacement of In^{3+} in the organic phase by Fe^{3+} ions.[2,7]

The ascending path statistical method permitted the optimum conditions for minimum iron extraction to be determined at a 95% statistical confidence. The best conditions were: concentration of D2EHPA = 0.03 mol/dm^3; acidity of the aqueous phase, $[H^+]_a$ = 0.70 N, and contact time between the phases, t = 2 minutes. These experimental conditions predicted the iron extraction at nearly 0.3%. Table 3 shows the predicted and experimental results.

Results	In extraction %	Fe extraction %
Predicted	—	0.3
Experimental	59.0	Not detected

Table 3 Experimental results for indium and iron extraction under the optimum conditions for minimum iron extraction

These tests were carried out to check the values obtained by the statistical model adopted for minimum iron extraction conditions. The validity of the statistical model was confirmed using the Fisher Test where the confidence level was higher than 95% and the experimental error was lower than 5%.

It was observed that iron was not detected in the raffinate (atomic absorption detection limit lower than 0.05 mg/dm^3). Therefore, the predicted response of iron extraction was reached in the experimental tests. Although the statistical calculations for iron extraction could not predict the values for indium extraction, it presented good experimental result in just one contact stage between the phases.

The isotherm extraction curves were constructed to determine the number of theoretical countercurrent stages required for indium extraction. Figures 2a and 2b present the isotherms of indium extraction for the optimum conditions of maximum indium extraction and minimum iron extraction. A 4% level of iron extraction was found for the isotherm construction using the maximum indium extraction conditions. This value was constant during all experiments for the isotherm construction. For the isotherm curve constructed using the minimum iron extraction conditions, iron was not detected in the organic phase.

The McCabe-Thiele Diagram (Figures 2a and 2b) shows that two theoretical countercurrent stages are required for full indium recovery. However, at least three stages are required for the indium extraction with minimum iron extraction.

A preliminary stripping study from loaded D2EHPA for indium recovery showed that sulfuric acid solutions were effective to recover indium, using the maximum indium extraction experimental conditions. Moreover, it could separate indium and iron. However the sulfuric acid solution did not show satisfactory results using the minimum iron extraction conditions.

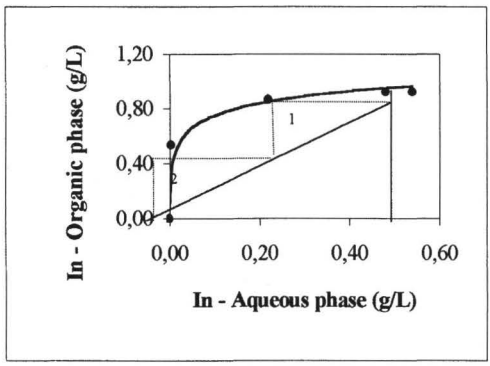


Figure 2a Indium extraction isotherm for maximum indium extraction conditions

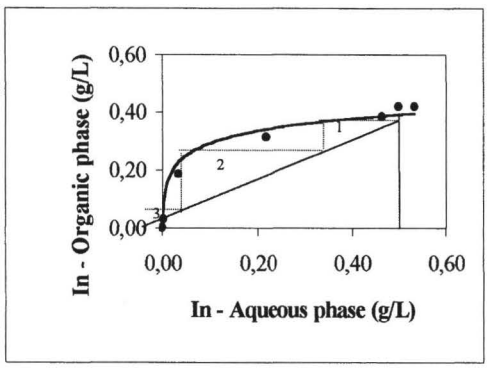


Figure 2b Indium extraction isotherm for minimum iron extraction conditions

CONCLUSION

Two experimental conditions for indium recovery were determined, one to obtain maximum indium extraction using 0.05 mol/dm^3 D2EHPA concentration in the organic phase; aqueous solution 0.25 N acidity, and 6 minutes of contact time. The other experimental conditions for minimum iron extraction were 0.03 mol/dm^3 D2EHPA concentration in the organic phase; 0.70 N aqueous solution acidity, and 2 minutes of contact time.

These optimum conditions at a 95% statistical confidence, led to a solution with high indium concentration with minimum iron poisoning. The indium recovery reached values greater than 99 % with iron below 1 %.

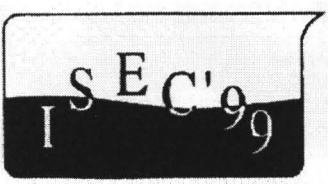
For complete indium recovering, two countercurrent stages were necessary using the optimum conditions for maximum indium extraction. However, at least three stages are required for indium extraction keeping the optimum conditions for minimum iron extraction.

ACKNOWLEDGMENTS

The authors are thankful to the Comissão Nacional de Energia Nuclear - CNEN/Brazil and PRONEX/MCT-Brazil for the financial support to conclude this work.

REFERENCES

1. Hoffmann, JH *JOM*, **43**(4), 18, (1991).
2. Bonora, R and Zoner, D *Proc. First European Congress on Chemical Engineering, Florence.*, 3019, (1997).
3. Fortes, MCB and Benedetto, JS *Minerals Engineering*, **11**(5), 447, (1998).
4. Duckworth, WE *Statistical Techniques in Technological Research. 1st ed.* Methuen Co. Ltd. London, 303, (1968).
5. Ritcey, GM and Ashbrook, AW *Solvent Extraction: Principles and Applications to Process Metalurgy. Part I.* Elsevier, New York 361, (1984).
6. Ohlweiler, OA *Quantitative Analytical Chemistry. vol 2.* Livros Técnicos e Científicos, . 432, (1981) (in Portuguese).
7. Dutrizac, JE and Mingmin, D *Proc. International SymposiumWorld Zinc'93, Hobart.* Aust. Inst. Min. Metall., 365, (1993).



A SEPARATION AND RECOVERY PROCESS OF GALLIUM AND INDIUM FROM ZINC REFINERY RESIDUE

Syouhei Nishihama, Takayuki Hirai and Isao Komasawa
Department of Chemical Science and Engineering, Graduate School of Engineering Science, Osaka University, Toyonaka, Osaka 560-8531, Japan

ABSTRACT
The separation and recovery process of Ga and In from zinc refinery residue by liquid-liquid extraction with organophosphorus compounds, such as bis(2-ethylhexyl)phosphoric acid (D2EHPA), 2-ethylhexyl phosphonic acid mono-2-ethylhexyl ester (EHPNA) and bis(2-ethylhexyl)phosphinic acid (PIA-226), was investigated. The extraction equilibrium formulations for Ga, In and Zn were established up to high loadings of the extractant. D2EHPA is the most suitable extractants for separation of Ga/In. The simulation for the separation and recovery process of Ga and In from zinc refinery residue was carried out based on the equilibrium studies, and showed that effective separation and recovery of Ga and In was carried out with high purity.

Keywords: gallium, indium, bis(2-ethylhexyl)phosphoric acid, 2-ethylhexyl phosphonic acid mono-2-ethylhexyl ester, bis(2-ethylhexyl)phosphinic acid, tri-*n*-butylphosphate, counter-current cascade, zinc residues

INTRODUCTION

Ga and In have become very important in advanced electronic industries in recent years. One source for two metals is zinc refinery residue, since both metals are contained as minor components in Japan.[1] There are some reports for the extractive separation of Ga/In with several types of the extractants.[2, 3]

In the present work, the separation and recovery process of Ga and In from zinc refinery residue with organophosphorus compounds is investigated. Firstly, the removal of major metal components other than Zn with TBP is investigated. Secondly, the extraction equilibrium formulations of Ga, In and Zn in the aqueous chloride media is investigated up to the high loading ratios in the single, binary and ternary systems. The separation of Ga/In with the three extractants was also investigated.[4] Finally, the separation and recovery of Ga and In from zinc refinery residue is shown to be practicable by simulations based on the equilibrium studies.

EXPERIMENTAL

Reagents

The extractants, tri-*n*-butyl phosphate (TBP), bis(2-ethylhexyl)phosphoric acid (D2EHPA), 2-ethylhexyl phosphonic acid mono-2-ethylhexyl ester (EHPNA) were supplied by Daihachi Chemical Ind. Co., Ltd., Osaka, Japan. Bis(2-ethylhexyl)phosphinic acid (PIA-226) was synthesised as reported in the previous papers.[5, 6] TBP was used without dilution. D2EHPA, EHPNA and PIA-226 were diluted in kerosene. The aqueous feed solution was prepared by dissolving metal chlorides into water.

Procedure

For the extraction with TBP, the aqueous and organic solutions were shaken for 6 hours at 298 K. The concentration of each metal was analysed by using an inductively coupled argon plasma emission spectrophotometer (ICP-AES). The corresponding organic phase concentrations were determined by mass balance. For extraction with D2EHPA, EHPNA and PIA-226, the aqueous and organic solutions having an O/A volume ratio of 1 were shaken for 2 hours at 298K. The metal-loaded organic solutions were stripped using 6 mol/dm^3 HCl for the case of D2EHPA, 3mol/dm^3 HCl for the case of EHPNA and PIA-226. The chloride ion concentration in the organic phase was measured by a potentiometric titration method with $AgNO_3$ after stripping with H_2SO_4. Infrared

© 2000 Society of Chemical Industry

spectra of metal-loaded organic solution were recorded on a FT-IR infrared spectrometer in an IR cell with TlBr/TlI windows. The loading ratio was defined as $[\overline{M}]/[\overline{(RH)_2}]_{feed}$.

RESULTS AND DISCUSSION

Removal of major components

A typical composition of the liquor from zinc refinery residue available for liquid-liquid extraction is reported to be (3.0 - 4.3) x 10^{-3} mol/dm^3 Ga, (9.0 - 9.6) x 10^{-3} mol/dm^3 In, (2.3 - 4.6) x 10^{-1} mol/dm^3 Zn, (3.7 - 5.6) x 10^{-1} mol/dm^3 Al and (1.8 - 3.6) x 10^{-1} mol/dm^3 Fe.[1] The aqueous solution containing these metals was extracted with TBP. Al was not extracted with TBP at all. The extractability of Fe(II) was extremely low in the low range of HCl concentration. Thus, Fe(II) and Al were removed easily by TBP at low concentrations of HCl. Thus, Zn was considered to be the only major impurity in the succeeding operations.

Extraction equilibrium formulations of Ga, In and Zn

Ga and In in single metal system

The effect of equilibrium pH on the distribution ratio was investigated. In D2EHPA and EHPNA systems, straight lines with slope of 3 were obtained, and a slope of 2 in the PIA-226 system. In the PIA-226 system, another anion was co-extracted with the metals. In this system, the ratio of chloride to metal in the organic phase is rather high in the low loading region, indicating that the chloride ion was co-extracted into organic phase to compensate the positive charge of the metals.

For the determination of extraction equilibrium formulations of Ga and In up to high loading ratios, the analytical composition of extract species at the high loading ratios was investigated. The loading ratios approached about 1.0 for all extractant systems, suggesting that a complex containing the dimeric extractant and the metal with the mole ratio of 1:1 was possibly formed at the extreme conditions of maximum loading ratios. For chloride ion, the ratios of chloride to metal approach around 0.25 for Ga species and 0.5 for In species. Moreover, the loaded organic solutions were studied by the IR spectrometry. The M-OH stretching sharp band appeared at 3700 - 3500 cm^{-1} in the high loading region, indicating that the hydroxyl ion is involved in the extract species.[7] These ions may compensate the positive charge of metals. Considering the results obtained, the extraction equilibrium formulations were determined (table 1), and extraction constants were calculated by the non-linear least squares method based on the mass balance equations and the formation of metal-chloro complexes.[8]

Ga/In in binary system

Figure 1 shows the effect of equilibrium pH value on the distribution ratios in the Ga/In binary system. In binary systems with EHPNA and PIA-226, the mixed complex containing Ga and In with mole ratio of 1:1 was formed at high loading ratios for the EHPNA system and whole range of loading ratios for the PIA-226 system. The extraction equilibrium formulations and constants of EHPNA and PIA-226 systems were determined taking the mole ratio of mixed complexes into consideration, and these can express the extraction behaviour up to high loading ratios. The calculated distribution ratio are shown by solid lines in figure 1, together with the calculated separation factor, defined as D_{In} / D_{Ga}. D2EHPA is the most suitable extractant for the separation of Ga/In because of no interaction between the two metals. Thus, D2EHPA was employed for the recovery process of the two metals from zinc refinery residue.

Zn with D2EHPA

Slope analysis and the investigation of the analytical composition of the extracted species indicate the extraction equilibrium formulation of Zn as shown in table 1.

Extractant	metal	extraction equilibrium formulation
D2EHPA	Ga	$Ga^{3+} + 2\overline{(RH)_2} \leftrightarrow \overline{GaR_3(RH)} + 3H^+$
EHPNA		$Ga^{3+} + GaCl^{2+} + 3OH^- + 2\overline{GaR_3(RH)} \leftrightarrow \overline{Ga_4R_8Cl(OH)_3} + 2H^+$
	In	$In^{3+} + 2\overline{(RH)_2} \leftrightarrow \overline{InR_3(RH)} + 3H^+$
		$InCl^{2+} + OH^- + \overline{InR_3(RH)} \leftrightarrow \overline{In_2R_4Cl(OH)} + H^+$
PIA-226	Ga	$GaCl^{2+} + 2\overline{(RH)_2} \leftrightarrow \overline{GaR_2Cl(RH)_2} + 2H^+$
		$3Ga^{3+} + 3OH^- + \overline{GaR_2Cl(RH)_2} + 2\overline{(RH)_2} \leftrightarrow \overline{Ga_4R_8Cl(OH)_3} + 6H^+$
	In	$InCl^{2+} + 2\overline{(RH)_2} \leftrightarrow \overline{InR_2Cl(RH)_2} + 2H^+$
		$In^{3+} + OH^- + \overline{InR_2Cl(RH)_2} \leftrightarrow \overline{In_2R_4Cl(OH)}$
D2EHPA	Zn	$Zn^{2+} + 2\overline{(RH)_2} \leftrightarrow \overline{ZnR_2(RH)_2} + 2H^+$
		$Zn^{2+} + \overline{ZnR_2(RH)_2} \leftrightarrow \overline{Zn_2R_4} + 2H^+$
D2EHPA	In/Zn	$InCl^{2+} + \overline{ZnR_2(RH)_2} \leftrightarrow \overline{InZnR_4Cl} + 2H^+$

Table 1 Extraction equilibrium formulations

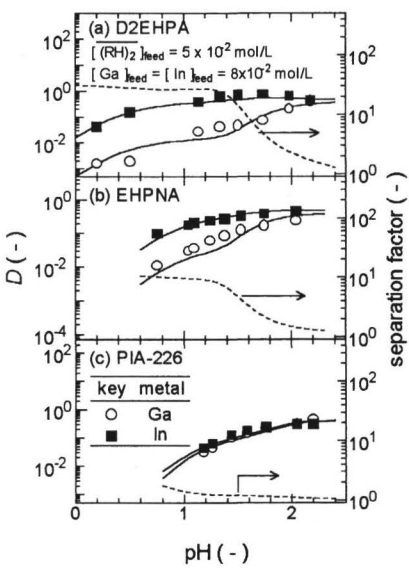


Figure 1 Effect of equilibrium pH on the distribution ratio and calculated separation factor in Ga/In binary system. Comparison of observed data with predictions shown by solid lines

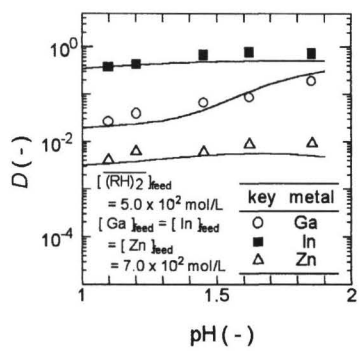


Figure 2 Effect of equilibrium pH on the distribution ratio in Ga/In/Zn ternary system. Comparison of observed data with predictions shown by solid

Ga/Zn binary system

In Ga/Zn binary system, the extraction behaviour can be expressed up to high loading ratios by the extraction equilibrium formulations obtained with single metal systems.

In/Zn binary system

In In/Zn binary system, the mixed complex containing both metals with a mole ratio of 1 : 1 was formed, as shown in Table 1.

Ga/In/Zn ternary system

Figure 2 shows the effect of the equilibrium pH on distribution ratios in ternary system with D2EHPA. The prediction lines are calculated by the extraction scheme for binary systems on the assumption of no interaction among the three metals. The proposed scheme is found to be applicable to ternary system.

Figure 3 shows the experimental loading ratios of the three metals after scrubbing with (a) metal-free and (b) metal-containing aqueous solutions. Solid lines show comparative values according to the proposed extraction scheme. The results show that with metal-free solution both Ga and Zn are scrubbed into the aqueous phase, with most of In remaining in the organic phase. With metal-containing solution, the metal exchange reaction between Ga and Zn in the organic phase and In in the aqueous phase is shown very well by comparison with the concentration of the three metals in the organic feed solution. The extraction of the more extractable In reduces the concentration of the free extractant, thus causing a decrease in the extraction of the less extractable Ga and Zn. This effect is, thus, notable at high loading region for the extractant. The experimental data are seen to cluster on the prediction lines, indicating that the proposed extraction scheme is equally applicable to the scrubbing treatment.

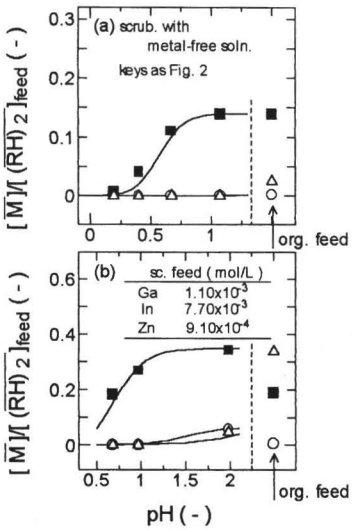


Figure 3 Effect of scrubbing. Comparison of observed data with predictions shown by solid lines

Simulation for the separation and recovery process of Ga and In from zinc refinery residue

A simulation of the separation and recovery of Ga and In from zinc refinery residue was carried out based on the equilibrium studies with D2EHPA. A schematic flowsheet for a counter-current mixer-settler cascade is shown in Figure 4. The calculation was carried out by using equilibrium relationship in each extraction stage and mass balances for each metal, chloride ion, and hydrogen ion in each stage and in the cascade.

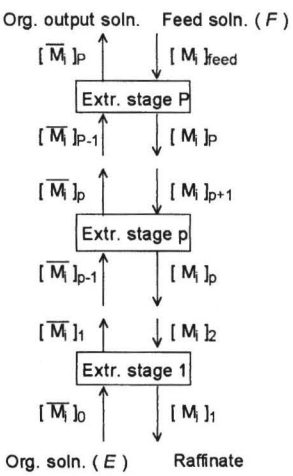


Figure 4 Schematic flowsheet for counter-current mixer-settler cascade

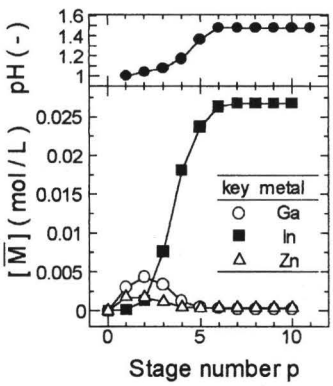


Figure 5 Simulation of In recovery by counter-current cascade of 10 extraction stages

Zn reduction section

The calculated results of the extraction with D2EHPA based on the feed concentration of 3.0 x 10^{-3} mol/dm^3 Ga, 9.0 x 10^{-3} mol/dm^3 In and 2.3 x 10^{-1} mol/dm^3 Zn are listed in table 2 as Ex. #1. The effective recovery of Ga and In was carried out, while leaving most of Zn in the raffinate solution. For stripping of metal-loaded organic solution, the use of low concentrations of hydrochloric acid is preferable, since the separation of Ga/In is affected by chloride ion concentration, as shown in the extraction equilibrium formulations. A high ratio of organic solution to stripping solution is also preferable, since the metal concentrations are increased in the stripping stage. Effective stripping can be carried out with 3.98 x 10^{-1} mol/dm^3 of hydrochloric acid, a flow ratio of F/E = 1/3, and a counter-current cascade of 2 stages. The results are summarised in Table 2 as St. #1.

Section		Stage number	$[\overline{(RH)_2}]_{feed}$ (mol/L)	pH	[Ga] (mol/L)	[In] (mol/L)	[Zn] (mol/L)	$[\overline{Ga}]$ (mol/L)	$[\overline{In}]$ (mol/L)	$[\overline{Zn}]$ (mol/L)
Zinc reduction										
Ex. #1	input	1	5.0×10^{-1}		3.00×10^{-3}	9.00×10^{-3}	2.30×10^{-1}	0	0	0
	output			2.20	2.78×10^{-4}	6.20×10^{-5}	2.11×10^{-1}	2.72×10^{-3}	8.94×10^{-3}	1.93×10^{-2}
St. #1	input	2	5.0×10^{-1}	0.401	0	0	0	2.72×10^{-3}	8.94×10^{-3}	1.93×10^{-2}
	output			0.400	8.16×10^{-3}	2.67×10^{-2}	5.79×10^{-2}	1.56×10^{-6}	5.67×10^{-5}	1.49×10^{-6}
Indium recovery										
Ex. #2	input	10	5.0×10^{-1}	1.48	8.16×10^{-3}	2.67×10^{-2}	5.79×10^{-2}	0	0	0
	output			1.00	7.92×10^{-3}	1.84×10^{-5}	5.75×10^{-2}	2.39×10^{-4}	2.67×10^{-2}	3.79×10^{-4}
Sc. #1	input	1	5.0×10^{-1}	1.91	0	0	0	2.39×10^{-4}	2.67×10^{-2}	3.79×10^{-4}
	output			1.10	2.36×10^{-4}	3.87×10^{-3}	3.78×10^{-4}	2.92×10^{-6}	2.28×10^{-2}	1.26×10^{-6}
Gallium recovery										
Ex. #3	input	10	1.0×10^{-1}	1.99	7.92×10^{-3}		5.75×10^{-2}	0		0
	output			1.77	1.89×10^{-5}		5.75×10^{-2}	7.91×10^{-3}		7.58×10^{-5}

Table 2 Simulated Ga, In and Zn concentrations

In recovery section

The recovery of In from the resulting solution following the Zn reduction operation was also investigated. Figure 5 shows the organic phase concentration profiles obtained for each metal based on the counter-current cascade. The results are summarised in table 2 as Ex. #2. Ga and Zn extracted at stages 1 to 3 into the organic phase are returned back into the aqueous phase at higher stage numbers of the cascade. This is because the decreased concentration of free D2EHPA caused by the extraction of In acts to reduce the extraction of Ga and Zn. This exchange reaction is in accordance with the results shown in figure 3(b). The scrubbing effect using dilute acid solution was also investigated. The simulation shows that Ga and Zn in the organic phase are effectively scrubbed, such that In with a purity, $[\overline{In}]/([\overline{Ga}]+[\overline{In}]+[\overline{Zn}])$, of 1.00 is obtained. The results are shown in table 2, as Sc. #1.

Ga recovery section

The separation of Ga from Zn by the counter-current cascade with 10 stages and 1.0 x 10^{-1} mol/dm^3 D2EHPA was investigated. In this case, a lower concentration of extractant is preferable. The extracted Zn is excluded to the aqueous phase by the progressive extraction of Ga. An effective recovery of Ga was carried out with a purity of 9.91 x 10^{-1}. The results obtained are summarised in table 2 as Ex. #3.

CONCLUSIONS

The separation and recovery process for Ga and In from zinc refinery residue using liquid-liquid extraction has been investigated, with the following results.

Extraction equilibrium formulations for the single metal and binary system containing Ga

and In are well established taking co-extraction of chloride and hydroxyl ion into consideration, when employing D2EHPA, EHPNA and PIA-226 as extractants. In Ga/In binary system with EHPNA and PIA-226, the mixed complexes containing both metals with the mole ratio of 1:1 are formed. D2EHPA is the most suitable extractant for the separation of Ga/In.

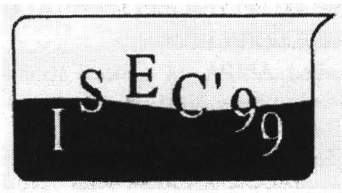
Extraction equilibrium formulations for the ternary system containing Ga, In and Zn are well established, when employing D2EHPA as extractant.

The scrubbing effect of metal-loaded organic solutions with metal-free or metal-containing solution was investigated. Ga and Zn in the organic phase are effectively scrubbed into the aqueous phase with both types of scrubbing solution. The scrubbing effect can also be expressed by proposed extraction scheme.

The separation and recovery process of Ga and In from zinc refinery residue with D2EHPA has been evaluated by simulation work based on the equilibrium studies. The process consists of three sections, (i) zinc reduction, (ii) indium recovery and (iii) gallium recovery. Gallium and indium are capable of effective recovery with purity of 9.91×10^{-1} and 1.00, respectively.

REFERENCES

1 Abe H, *J. Min. Inst. Jpn.*, **98**, 561, (1982).
2 Kikuchi S and Kamagami S, *Nippon Kogyo Kai-shi*, **104,** 601, (1988).
3 Inoue K, *Shigen-to-Sozai*, **105**, 751, (1989).
4 Nishihama S, Hino A, Hirai T and Komasawa I. *J. Chem. Eng. Jpn.*, **31**, 818, (1998).
5 Hino A, Hirai T and Komasawa I, *J. Chem. Eng. Jpn.*, **29**, 1041, (1996).
6 Hino A, Nishihama S, Hirai T and Komasawa I, *J. Chem. Eng. Jpn.*, **30**, 1040, (1997).
7 Nakamoto K. *Infrared and Raman Spectra of Inorganic and Coordination Compounds*, John Wiley & Sons, New York, (1973).
8 Hogfeldt E. *Stability Constants of Metal Ion, part A*, Pergamon Press, UK, (1982).



A HIGHLY EFFICIENT PROCESS TO STRIP IRON FROM A NEW ORGANOPHOSPHORUS EXTRACTANT

F Delmas and CA Nogueira
INETI, Instituto Nacional de Engenharia e Tecnologia Industrial
Est. Paço do Lumiar, 1699 Lisboa Codex, Portugal

ABSTRACT
Aminomethylenephosphonic acid derivatives (AMPA), formulae $R_2NCH_2PO(OH)_2$, have been recently proposed for metals extraction from acidic aqueous chloride and sulphate solutions. It is already known that this type of extractants exhibits a higher loading capacity for iron and a much better kinetic behaviour than the traditional organophosphorus acids like D2EHPA. Nevertheless the usual difficulties on iron stripping were also found in AMPA extractants, even using extremely acidic strip solutions. This paper reports a new extraction-stripping process developed by INETI, which combines iron extraction with AMPA with a new reductive stripping method. Using this new approach the selective removal of 73% of the iron (III) contained in a zinc-like process solution with 80 g/l zinc, 14 g/l iron (III) and 40 g/l free sulphuric acid was achieved without pH control in the minimal configuration of 1 stage of extraction and 1 stage of stripping. An overall removal yield of about 99% is predictable for a 2+2 stages configuration.

Keywords: iron, reductive stripping, aminomethylenephosphonic acid, D2EHPA

INTRODUCTION

Iron is present as contaminant in practically all the hydrometallurgical process streams and effluents. Iron removal is generally made by means of precipitation methods, which originates thousands of tones of solid wastes without any application. These unfriendly materials contain large amounts of accompanying hazardous metals and highly pollutant anions. Up to now they are being stored by industry in private overloaded lagoons. No consistent application or treatment of this kind of residue has been made so far.

Solvent extraction has been long suggested as the alternative to solve that problem. Through it iron could be recovered selectively in marketable forms. Organophosphorus solvents have been considered as the most selective and practicable extractants for iron as they can extract selectively Fe(III) from very acidic solutions. As is well known, acidic stripping of iron from organophosphorus acids is a very difficult task to carry out in the same way that extraction is easy to fulfil. The stripping reaction is very slow, not complete and impracticable even when made using very concentrated and active acids like HCl and HF.

Several non-classical stripping techniques has been proposed to back-extract iron from acidic extractants but without remarkable success, namely hydrolytic stripping from Versatic acid developed by Monhemius and Thorsen[1] and reductive stripping with hydrogen under pressure to produce metals directly from loaded solvents proposed by Burkin[2]. More recently B. Belew et al.[3] and Chi-Ming-Chang et al.[4] at Missouri-Rola University used a so-called galvanic stripping with zinc metal and zinc alloys to strip Fe(III) co-extracted by D2EHPA from pregnant zinc solutions. Their results seem to be non-conclusive and the process does not seem to solve the problem of iron recovery in pure forms from pregnant hydrometallurgical solutions and effluents.

A new process for iron extraction and stripping combining an aminomethylene-phosphonic acid derivative (AMPA) with a new reductive stripping method developed in INETI is proposed in this paper. The AMPA extractant used had been already synthesised and proposed by Y. Baba et al.[5] for palladium and platinum recovery and by BASF[6] for iron recovery from zinc process solutions and used within the European RTD IRONEX Project.[7,8]

© 2000 Society of Chemical Industry

MATERIALS AND METHODS

An aminomethylenephosphonic acid derivative further called AMPA, of general formula $R_2NCH_2PO(OH)_2$ synthesised and made available by BASF, was used in the extraction and stripping testwork. Di-(2 ethylhexyl) phosphoric acid (D2EHPA) was used for comparative purposes.

The aqueous feed solution assaying 25 g/L Fe(III), 80 g/L Zn and 40 g/L H_2SO_4 was prepared with reagent-grade chemicals. Iron turnings of carbon-steel with about 0.5% of carbon were used as reductive agent under inert atmosphere. The organic phases AMPA (10 or 15%), isodecanol (10 or 15%) and D2EHPA (10 or 15%), Isodecanol (10 or 15%) was equilibrated with the feed solution for 30 minutes in separatory funnels at several O/A ratios to load organics with 8 to 14 g/L Fe(III). Discontinuous stripping tests were made in closed glass cylindrical reactors at 50 °C for 30 minutes. The stripping solution was 2M H_2SO_4 and the stirring speed 500 rpm.

The concentration of iron in the aqueous phases was determined by Atomic Absorption Spectrometry and in organic phases directly by quantitative EDXRF or by difference.

The continuous extraction-stripping testwork with AMPA was carried-out in a thermostatised cascade of close glass 0.5 litre mixers -1 litre settlers.

RESULTS AND DISCUSSION

Comparative behaviour of AMPA and D2EHPA was already accessed in previous research work.[7,8] In fact, although the higher effectiveness of AMPA in Fe(III) extraction from very acidic solutions and its higher loading capacity, iron stripping from AMPA with 2M H_2SO_4 alone was even more inefficient than from D2EHPA. Fortunately AMPA shows a very unusual and favourable kinetic behaviour either in extraction or in stripping. The authors believed that this could be the potential key to open a way for a successful iron stripping process. Really, for the first time an acidic extractant for iron could achieve the equilibrium values within practicable residence times (one minute in extraction and less than five minutes in stripping). It will be surely interesting to exploit such behaviour in reductive stripping. The idea put in practice was to test the iron (Fe^0) itself as reductive agent to reduce Fe(III) to Fe(II) as it transfers to the aqueous phase by the reaction (1) below, so favouring the displacement of the equilibrium to the side of the stripping reaction(left side) and obtaining a pure iron (II) product.

$$3\ R_2NCH_2PO(OH)_2 + 2\ Fe^{3+} \rightleftarrows (R_2NCH_2POO_2)_3Fe_2 + 6\ H^+ \qquad (1)$$

Discontinuous Testwork

The results and conditions of comparative stripping testwork using D2EHPA and AMPA are shown in Figures 1 and 2. The influence of the stripping conditions and agents in stripping efficiency are demonstrated.

It can be seen from the Figures above that reductive stripping is not effective with D2EHPA. Acidic stripping alone and reductive stripping with zinc metal confirmed the poor results expected. On the contrary, reductive stripping with iron turnings under an inert environment was a successful operation, attaining more than 98% efficiency in a single contact. The very good results obtained in reductive stipping of AMPA can be attributed to the very fast stripping of Fe (III) in simultaneous with the regeneration of AMPA to its acidic form through the reaction (1) and to the fast reduction of Fe (III) by Fe^0 as far it attains the aqueous phase, so favouring the reaction in the sense of the stripping. Reductive reaction surely prevails over the attack of the metallic iron by the free acid contained in the stripping solution. In fact the great liberation of H_2 and the high consumption of iron observed in the tests with D2EHPA seems to confirm the above suppositions.

The overall redox reaction (2) below is spontaneous (ΔE^o positive, so ΔG^o negative),

$$Fe^o + 2\ Fe^{3+} \rightleftarrows 3\ Fe^{2+} \qquad (\Delta E^o = +1.21V) \qquad (2)$$

and the overall reductive stripping reaction with Fe^o can be written as follows :

$$(R_2NCH_2POO_2)_3Fe_2 + 6\,H^+ + Fe^o \rightleftarrows 3\,R_2NCH_2PO(OH)_2 + 3\,Fe^{2+} \quad (3)$$

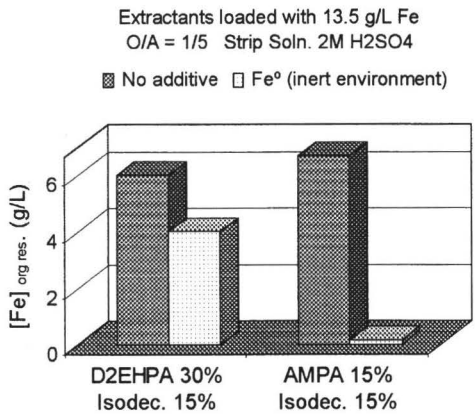


Figure 1 – Comparative stripping tests.

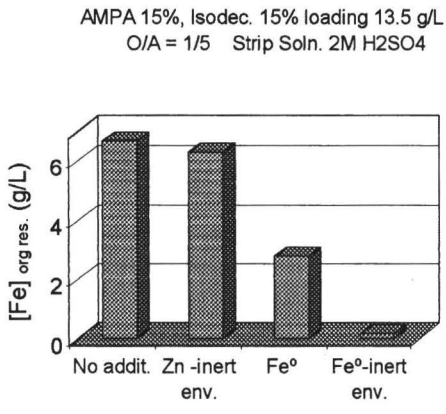


Figure 2 – Reductive stripping of AMPA.

Stripping Isotherms

A reductive stripping isotherm for AMPA 15%, Isodecanol 15% in kerosene, loaded with 12.4 g/l Fe is shown in Figure 3. Stripping with 2M H_2SO_4, Fe^o and inert atmosphere. The slope of the AMPA reductive stripping isotherm is very favourable to back-extract practically all the iron and to produce a strip liquor highly concentrated in Fe^{2+}.

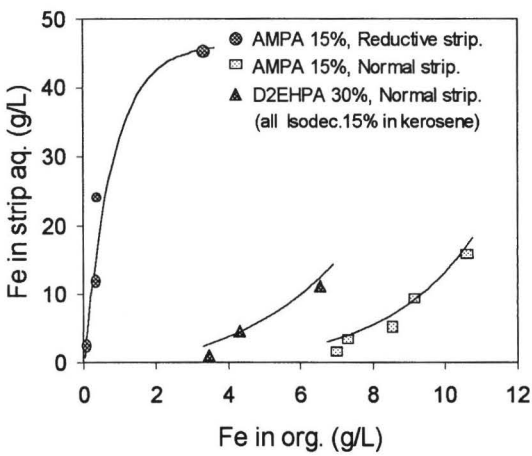


Figure 3 – Comparison of stripping isotherms.

Continuous reductive stripping

The continuous test for a preliminary evaluation of the process was carried-out using the minimal configuration. The conditions of the test were selected by a trial and error method based on a worksheet. The results of the simulation are represented in Figure 4.

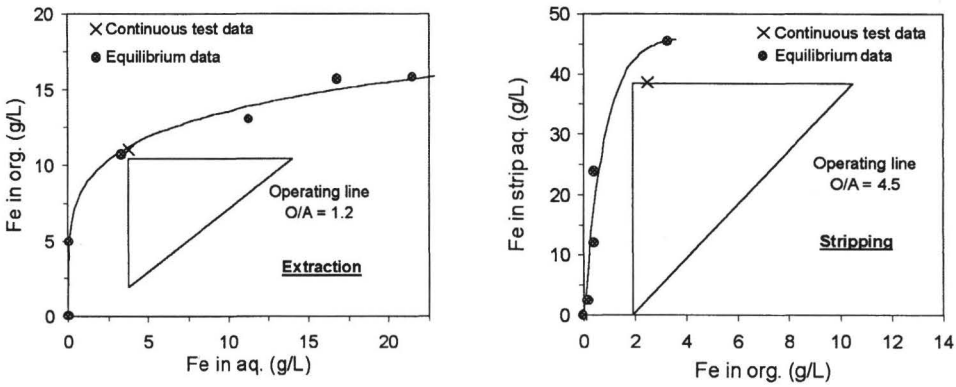


Figure 4 – Simulation for the continuous reductive stripping test (1+1 stages). Extractant: AMPA 15%, Isodecanol 15% in kerosene; stripping with 2M H_2SO_4 and Fe^o under inert environment.

The goals of the test were to decrease the Fe(III) in the solvent from 14 g/L to 4 g/L (Δ=10 g/L) and to produce a strip liquor over 50g Fe(II)/L. Stage efficiencies of 95% in extraction and stripping were considered. The flow-rates of the iron pregnant feed solution, solvent and stripping solution were derived from the simulation.

The operative conditions established for the continuous test were: residence time 8 min in mixers and 16 min in settlers; configuration: 1 extraction stage and 1 stripping stage (2 mixer-settlers); flow-rates: QA=0.75 l/h QO=0.90 l/h QS=0.20 l/h; flow-ratios: (O/A)ext = 1.2 (O/A)strip = 4.5; temperature = 50°C and reductive agent in the mixer: iron turnings. The results obtained in the continuous test are presented in Table 1 and Figure 5.

Working Time (h)	Fe concentration (g/l)			Average Fe^o consumption	
	Feed	Raffinate	Strip liquor	g/h	g/g Fe extracted
6	14	4.6	59.8	4.40	0.62
14		3.1	60.6	3.85	0.46
21		4.1	58.1	3.81	0.51
28		3.8	57.9	4.09	0.53

Table 1 Continuous extraction and reductive stripping of iron (III) with AMPA 15%, Isodecanol 15% in kerosene.

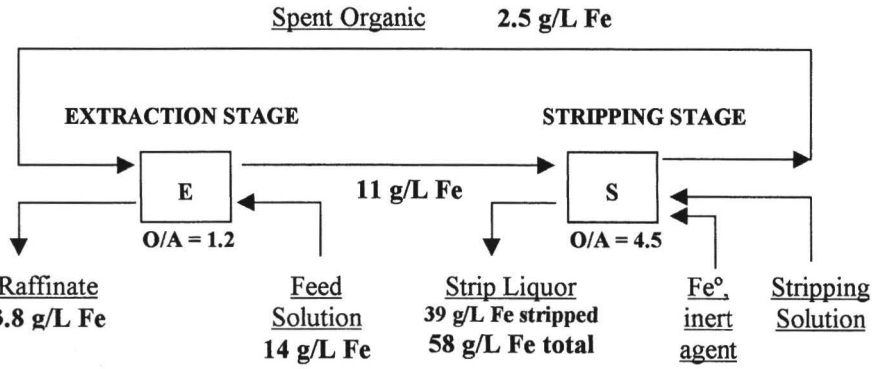


Figure 5 – Results and flow diagram of the bench-scale continuous test.

From the figure it can be concluded that after 6 hours the system reached stationary values. During the remaining 22 hours the system stabilised giving more or less constant values for the raffinate and strip liquor concentrations. The Fe^{o} consumption was around 4 g/l, correspondent to 0.5 gram per gram of extracted iron which is the stoichiometric quantity of iron metal used to reduce the stripped iron from its ferric to its ferrous state by the global redox reaction (2). This indicates that the proposed stripping mechanism is correct and that Fe(III) reduction takes place in the aqueous phase or in the interface organic-aqueous and Fe^{3+} is stripped by the reaction inverse of the extraction reaction (1). It confirms also that the reactions inside the stripping reactor are adequately represented by the global equation (3). A further simulation was carried-out, showing that is possible to attain 99% of selective iron removal in a 2+2 stage configuration.

It must be stressed out that the efficiency of reductive stripping of D2EHPA with Fe^{o} or other metal can not be comparable with the efficiency found when iron metal is used to strip iron from AMPA. And this is due to the unfavourable kinetics of D2EHPA reactions, which is the controlling factor of stripping operation.

CONCLUSIONS

The already known ability of aminomethylenephosphonic acid derivatives to extract efficiently and selectively iron from acidic solutions,[6-8] conjugated with a new reductive stripping method developed in INETI (Portugal), resulted in a new promising process for iron removal from acidic solutions. Continuous testwork shown that is possible by tis new concept to recover selectively about 99% of the iron contained in acidic process solutions in a 2+2 cascade configuration.

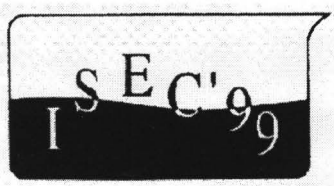
ACKNOWLEDGEMENTS

The authors which to thank to all people involved in the E.C. Environment project EV5V-CT94-0568 (IRONEX), particularly to Dr. M. Ehle from BASF, for its kind cooperation, and to E.C. for its financial support.

REFERENCES

1. Monhemius AJ and Teixeira LA, *Hydromet. Proc. Fundamentals*, Plenum Press, 647, (1984)
2. Burkin AR and Burgess JE, 1st Ann. Meeting of Can. Hydrometallurgists, 51, (1971).
3. Belew B, Harlamovs JR, O'Keefe T and Watson JL, *Hydrometallurgy Fundamentals, Technology and Innovation*, Edited by the S.M.M.E, Inc, AIME,USA, 817, (1983)

4. Chang C, Gu H and O'Keefe TJ, Iron Control and Disposal, *Proc. of the Second Int. Symp. Iron Control in Hydrometallurgy*, Ottawa, Canada, 417-428, (1996).
5. Baba Y and Shimizu Y, *Proceedings of ISEC'93*, 565-561, (1993).
6. BASF *International Patent No.WO 96/00309.*
7. Delmas F, Ehle M, Koch R, Nogueira C, Oppenländer K, Plazanet C, Ujma K and Weigel V, *Proceedings of ISEC '96*, Melbourne , Australia, 133, (1996).
8. Delmas F, Nogueira CA, Ehle M, Oppenlander K, Koch RO, Lemmert F, Plazanet C, Weigel V, Ujma KH and Ketels E, Iron Control and Disposal, *Proc. of the Second Int. Symp. Iron Control in Hydrometallurgy*, Ottawa, Canada, 1381-1393, (1996).



SOLVENT EXTRACTION STUDIES FOR COBALT AND NICKEL SEPARATION FROM THE PROCESSING OF AMMONIUM CARBONATE MIXED SULFIDES

E García Liranza, AM Moreno Daudinot, R Viera Martínez and B Rosales Bárzaga

Solvent Extraction Department, Research Center for Laterite Minerals, Moa, Cuba

ABSTRACT

The conventional separation of cobalt and nickel has usually been from acidic solutions derived from sulfides treatment. The Cuban Nickel Industry has two plants based on Caron process, which produce mixed cobalt-nickel sulfides as a final product. This paper describes the results obtained in studies carried out at laboratory and miniplant scale, using solvent extraction to separate cobalt and nickel from liquors obtained from the acid leaching of Ni + Co mixed sulfides produced at Punta Gorda Plant, Cuba in the Ammonium Carbonate leaching technology (Caron process). A comparison of the several extractants: phosphoric (DP 8R), phosphonic (PC88 A, P507), and phosphinic (Cyanex 272, Cyanex 302) acids was made to determine the best overall performance as regards cobalt selectivity over nickel and impurities, scrubbing and stripping efficiency and phase separation. Miniplant continuous circuits were run on two extractants to verify the above and to provide some data on relative product purity. The key to ultimate product purity would not only be the selectivity in extraction but also the relative ease in scrubbing for purity enhancement.

Keywords: cobalt, phosphoric acid extractant (DP 8R), phosphonic acid extractant (PC88 A, P507), phosphinic acid extractant (Cyanex 272, Cyanex 302), ammonium carbonate liquors, Caron process, cobalt-nickel mixed sulfides

INTRODUCTION

The Cuban Nickel Industry, with more than fifty years of operation of the first of its production plants, is located in the eastern region of the country. It has a capacity of 50,000 t/year of nickel which is exported as a concentrate of Ni + Co sulphides, Ni oxide and Ni sinter.

The systematic development of this industry is necessary to increase nickel and cobalt product diversity. Cobalt-nickel selective separation has been studied intensely in the last fifteen years, evaluating the use of different organic reagents: phosphoric, phosphonic, phosphinic acids, which increase their Co/Ni selectivity in this order.[1]

Several authors have studied the extraction properties of the different representatives of these groups. A comparative study of the extractants D2EHPA, PC-88A and Cyanex 272 in sulphate solution,[2] details the optimum conditions of Co-Ni separation, showing extraction isotherms and determination of process theoretical stages.

A detailed study at laboratory and bench scale has been carried out with Cyanex 272,[3,4] and a comparative study of the extractants Cyanex 302 and Cyanex 272 from sulphate solution has been published.[5] Different methods have been studied for Co-Ni separation from sulphate and chloride solutions: precipitation methods and recently, solvent extraction. Results from pilot scale using PC-88A and tertiary amines to remove cobalt from sulphate solutions have been analysed and discussed.[6] An extensive study of the theory and practice solvent extraction in nickel and cobalt hydrometallurgy is also available.[7]

EXPERIMENTAL

Laboratory scale

Materials and methods

Co-Ni sulphate solution from mixed sulphides dissolution was partially purified, with (g/dm^3) 32.28 Ni, 10.14 Co, 0.019 Zn, 0.48 Ca, 0.88 Mg and 0.19 Mn. Extractants DP 8R, PC 88A, P 507,

© 2000 Society of Chemical Industry

Cyanex 272 and Cyanex 302 were dissolved in kerosene (20 % by volume). NH_4OH (25 %) was used as neutraliser and loaded organic phases were stripped into dilute sulfuric acid. The metal ions were analysed by atomic absorption spectroscopy.

RESULTS AND DISCUSSION

The organic phase neutralisation was studied, with the conclusion that concentration and the nature and addition of the neutralising agent is very important in the extraction process. The optimum concentration of the neutralising agent was determined to reach the pH equilibrium where a high percentage of cobalt extraction would be achieved. The kinetics were studied at times from 30 to 420 seconds. The extraction reaction was rapidly in all cases.

The cobalt extraction isotherm for DP-8R, PC-88A, and P-507, was performed by repeated contact of the organic phase with fresh aqueous phase until the equilibrium was obtained, figures 1, 2 and 3. The cobalt extraction isotherm for Cyanex-272 and Cyanex-302 was carried out varying the aqueous and organic phase ratio figures 4 and 5.

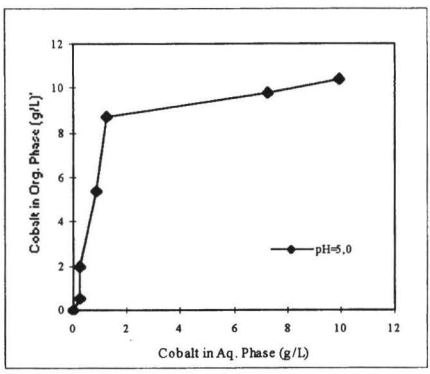


Figure 1. Cobalt Extraction Isotherm by DP 8R. Initial Co=10.14

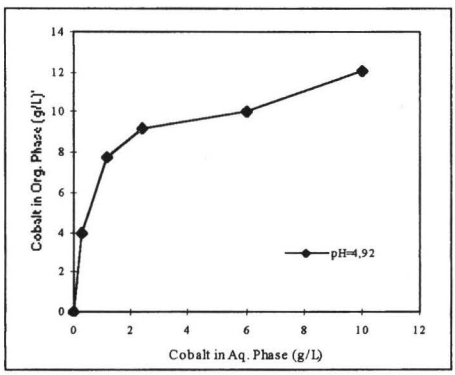


Figure 2. Cobalt Extraction Isotherm by PC 88A. Initial Co=10.14

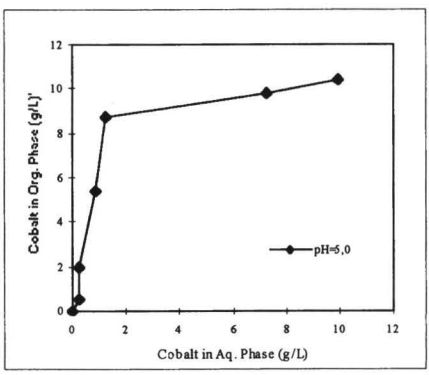


Figure 3. Cobalt Extraction Isotherm by P507. Initial Co=10.14

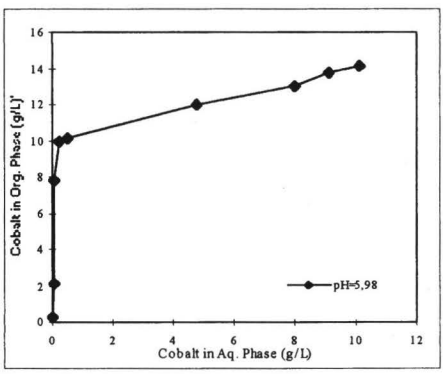


Figure 4. Cobalt Extraction Isotherm by CYANEX 272. Initial Co=10.14

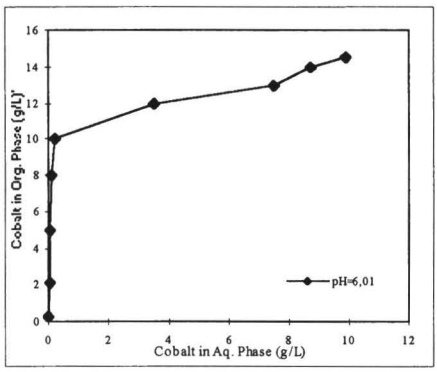


Figure 5. Cobalt Extraction Isotherm by CYANEX 302. Initial Co=10.14

To decrease the content of co-extracted nickel scrubbing of the loaded organic phase was studied using scrub solutions containing nickel and cobalt at different levels, nickel (1-10 g/dm^3) and cobalt (14-32 g/dm^3). The volume ratio of the organic and the aqueous phase was 1:1; the pH values of the aqueous phase 3.5, 4.5, 5, 5.5 and 6.5. The phases were equilibrated for 5 minutes at room temperature (25 - 27°C). Scrubbing is more effective if nickel concentration in aqueous phase is maintained at the lower level and the cobalt concentration at the higher level, as in this case effective elimination of nickel from the organic phase results. The optimum pH of the scrubbing solution was 5.0.

Stripping solutions included sulfuric acid in a range of 100 to 160 g/L. The volume ratio of the two phases was 1:1.Tables 1, 2 and 3 summarize the conditions in each experiment, Co/Me separation factor and the extraction percent.

Extractants	DP 8R	PC 88A	P 507	Cyanex 272	Cyanex 302
Extraction time (s)	120	90	90	60	60
Neutralising concentration (cm^3 NH_4OH/cm^3 Organic Phase)	0.030	0.036	0.034	0.043	0.056
Equilibrium pH	4.5-5.1	4.8-5.3	4.8-5.3	5.5-6.2	5.5-6.2

Table 1 Specific Experimental Conditions.

Extractants	Distribution Coefficient (D)				Separation Factor (SF)		
	Ni	Co	Ca	Mg	Co/Ni	Co/Ca	Co/Mg
DP 8R	0.085	2.794	5.41	1.23	33	0.516	2.270
PC 88 A	0.013	13.39	3.71	1.06	1030	3.609	12.57
P 507	0.015	10.34	6.35	1.25	689	1.628	8.280
Cyanex 272	0.028	51.49	0.18	0.77	1839	292	66.27
Cyanex 302	0.042	78.19	0.09	0.31	1862	806	250.0

Table 2 D and SF values for various extractants

Extractants	Extracted Metal Percent (%)						
	Co	Ni	Zn	Ca	Mg	Mn	pH
DP 8R	73.64	7.83	100	84.4	55.1	95.7	5.08
PC 88 A	93.05	1.28	100	78.7	51.6	100	5.03
P 507	91.18	1.48	100	86.4	55.5	100	5.10
Cyanex 272	98.09	2.72	100	14.9	43.7	100	5.78
Cyanex 302	98.74	4.03	100	8.80	23.8	97.3	5.81

Table 3 Extraction Percentages with difference extractants

Miniplant scale.

The materials used are similar to the ones used in the laboratory scale test. Ten mixer-settlers of transparent acrylic form the continuous circuit. Each mixer-settler unit has mixing and settling volumes of 2.736 and 9.360 dm^3 respectively.

The mixing all units was performed using variable speed mechanic stirrers, and the flow controlled by means of rotameters and manual valves. Peristaltic pumps were used to feed the mixer-settlers.

The circuit consisted of three extraction stages, one scrubbing stage with H_2O at pH 4.5, two scrubbing stages with $CoSO_4$ solution, two cobalt-stripping stages and one zinc-stripping stage.

Experimental test runs were performed in a continuous way over fifty hours with, for PC 88A extraction phase ratio of O/A = 1.18 (15 and 13.2 dm^3/h respectively) and for Cyanex 272 flows were increased to 19.8 and 11.4 dm^3/h (O/A = 1.74).

RESULTS AND DISCUSSION

Extraction

The average chemical composition of the initial solutions and raffinates during test runs are shown in the table 4.

Extractant	Concentrations (g/dm^3)						
	Elements	Ni	Co	Zn	Mg	Mn	Ca
PC 88 A	Feed Solution	29.40	13.12	0.007	0.55	0.15	0.62
	Raffinate	27.71	0.95	0.000	0.32	0.00	0.10
Cyanex 272	Feed Solution	25.93	14.82	0.008	0.47	0.14	0.53
	Raffinate	23.82	0.02	0.000	0.07	0.00	0.35

Table 4 Feed Solution and Raffinate for Acid Extractants.

PC 88A, with an equilibrium pH 5.00 extracted 96 % cobalt and a raffinate was obtained with 25:1 Ni:Co ratio and 97% purity. Certain quantities of impurities such as Zn, Mn, Ca and Ni were co-extracted with cobalt during the extraction. Ni extraction percentage was low at 0.29 %. Zn and Mn were totally extracted together with 14% Mg and 96 % Ca. According to these results the extractant

selectivity was in the following order: Zn>Mn>Ca>Co>Mg>Ni with a Co:Ni ratio in the organic phase of 155:1.

When working at larger phases ratios and equilibrium pH 6.0 - 6.3 , Cyanex 272 reached 99.8% Co extraction and a raffinate containing a Ni:Co ratio 2240:1 and a purity of 98%. Nickel co-extraction was low (0,3 %), and Ca did not exceed 5% extraction, demonstrating the capacity of this extractant to reject this element. Zn and Mn were totally extracted, while Mg extraction reached 64 %. According to these tests, Cyanex 272 order of selectivity was Zn>Mn>Co>Mg>Ca>Ni with a ratio of Co:Ni in the organic phase of 145:1.

Scrubbing

The scrubbing solution was prepared from the $CoSO_4$ product liquor of the bench initial run test, (g/dm^3): 21.55 Co, 0.69 Ni, 0.02 Zn, 0.37 Mg, 0.03 Mn and 0.24 Ca.

Due to the impurities presence in this liquor, Zn, Mn and Mg concentrations in loaded organic phase increased during the first run tests hours, afterwards there was a decrease in nine hours. Scrubbing was effective, decreasing the Ni content to 2 ppm. The Co:Ni ratio in scrubbed organic phase was 2 586:1 for PC 88A and 4 269:1 for CYANEX 272. In the table 5 a resume of these results is shown. < Here Table 5 >

Extractants	Composition (g/dm^3)							
	Loaded Organic Phase				Scrubbed Organic Phase			
	Co	Ni	Zn	Mn	Co	Ni	Zn	Mn
PC 88 A	9.55	0.03	0.001	0.134	9.270	0.003	0.017	0.390
Cyanex 272	9.21	0.09	0.005	0.082	10.35	0.003	0.007	0.110

Table 5 Scrubbing results for acid extractants.

Stripping

Stripping was performed with H_2SO_4 liquor at pH 0.7 for both extractants. With PC 88A the O/A ratio used was 1:1, for this reason the acid solution was recycled the entire test run time, controlling the initial pH.

The chemical composition of the stripped product solution obtained (in g/dm^3) was 0.006 Ni, 70.57 Co, 0.051 Zn, 0.048 Mg, 1.102 Mn and 0.69 Ca. This liquor purity is 97.4 %, with a Co:Ni ratio of 11,762:1. The impurity content is due, mainly, to the high selectivity of this solvent towards these elements. Co stripping was 99.5%. In this section calcium was the most damaging element for circuit operation (it extracts more than 90%), due to calcium sulphate (gypsum) precipitation in the stripping stages, causing obstructions in the settlers.

In the run test carried out with Cyanex 272, inner re-circulation in the stripping stages was implemented to operate with high O/A ratios of 11:1. The chemical composition of the cobalt product (in g/dm3) was 66.96 Co, 0.018 Ni, 0.007 Mg, 0.42 Mn and 0.01 Ca. The stripped product solution was obtained with 99.2 % purity and low impurity content. The Co/Ni ratio was 4 082. There were no difficulties with precipitation as the calcium content was low.

Zn stripping was performed in a later stage, with H_2SO_4 at 150 g/dm^3 concentration at an O/A = 1:1. Zinc content decreased to 1 ppm, obtaining by-product liquor with 0.083 g/dm^3 of this metal.

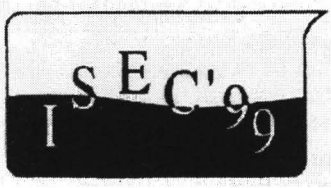
CONCLUSIONS

The extractants studied can be used for separation of Co-Ni sulphate solutions from the Ni+Co mixed sulphides dissolution, because they offer an efficient cobalt extraction at room temperature without requiring many stages, only DP 8R extraction cannot achieve in these conditions.

It advantageous to use the phosphinic acid extractant to separate Co-Ni from this solution, as gypsum precipitation is avoided because these reagents have little selectivity for calcium.

REFERENCES

1. Flett DS, Warren Spring Laboratory, Stevenage, pp 85-95.
2. Preston JS, *J S. Afr.Inst.Min.Metal.* June (1983).
3. Rickelton WA, Flett DS and West DW, *Int.Solv.Extr.Conf.(ISEC'83)*, Denver, (1983).
4. Xun F, Golding JA, *Solvent Extraction and Ion Exchange*, **5**(2), 205, (1987).
5. Tait BK, *Proc. Int. Solv.Extr.Conf.(ISEC'93)* York,, 1303, (1993).
6. Coussement MA, De Schepper and Standaert R: Metalurgic Hoboken Overpelt (MHO) Belgium.
7. Ritcey GM, Ashbrook AW, Part II, Elsevier (1979)



APPLICATION OF SOLVENT EXTRACTION IN METAL RECOVERY FROM SPENT NICKEL-METAL HYDRIDE BATTERIES

Pingwei Zhang[1], Toshiro Yokoyama[2], Osamu Itabashi[2], Yoshito Wakui[2], Toshishige M Suzuki[2] and Katsutoshi Inoue[3]

[1]Japan Science and Technology Corporation, Sendai 983-8551, Japan

[2]Tohoku National Industrial Research Institute, Sendai 983-8551, Japan

[3]Department of Applied Chemistry, Saga University, Saga 840-8502, Japan

ABSTRACT

Sulphuric acid leaching of spent nickel-metal hydride secondary batteries yields an acidic solution containing high levels of metal values such as nickel, cobalt and rare earths, together with an appreciable amount of metal impurities such as iron, aluminium, zinc and manganese. In the present work, solvent extraction has been used for separation and recovery of nickel, cobalt and rare earths from this leach liquor. A mixed rare earth oxide of over 99.8% purity was obtained by the use of an extraction circuit with 25 vol.% bis(2-ethylhexyl) phosphoric acid in kerosene, followed by precipitation with oxalic acid, and calcination of the precipitate. The total yield of rare earths approached 93.6%. The cobalt and nickel in the raffinate are separated efficiently by selective extraction of cobalt with 20 vol.% bis-(2,4,4-tri-methylpentyl)phosphinic acid in kerosene. Subsequently the cobalt and nickel are recovered as oxalates by the addition of oxalic acid. The purities of cobalt and nickel oxalates were close to 99.6% and 99.8%, respectively. The overall recoveries were found to be over 96% for both cobalt and nickel.

Keywords: nickel-metal hydride batteries, cobalt, nickel, rare earths, sulphuric acid, Cyanex 272, D2EHPA.

INTRODUCTION

Over the past decades, solvent extraction has been successfully applied on a commercial scale for the extraction of metals from primary metal resources, such as recovery of cobalt and nickel, copper, niobium and tantalum, rare earth elements, as well as platinum group metals and nuclear fuels like thorium and uranium, zirconium and hafnium. Solvent extraction also plays an important role in hydrometallurgical recovery of valuable metals from secondary raw materials as given in table 1. In our earlier works,[7-9] solvent-extraction processes were developed for the recovery of molybdenum, vanadium, cobalt and nickel from spent hydrodesulfurization catalysts which are generated from the petroleum industry. In a recent publication a hydrometallurgical process was described for the recovery of cobalt and lithium from spent lithium-ion secondary batteries.[10] This paper presents the results on the separation and recovery of cobalt, nickel and rare earths from spent nickel-metal hydride (Ni-MH) secondary batteries using solvent extraction.

Ni-MH batteries were developed in 1989 and commercialized in 1990 in Japan. In recent years, these batteries have been used extensively in portable electronic applications including personal computer, video-recorder and telephone, etc. It can be seen from table 2 that the Ni-MH batteries are being produced at an extremely high rate in Japan. Additionally, because of their high energy density and design flexibility, the Ni-MH batteries are particularly well suited for battery powered electric vehicles (EV) and other mobile applications. Consequently, an appreciable amount of spent Ni-MH batteries will be generated in the near future. The expected tonnages of both primary and secondary scrap are potentially very large. Recycling of metal values from the scraps has thus become an important issue from the point of view of the economic incentive, since the Ni-MH batteries contain nickel, cobalt and rare earths, etc. The aim of this work was to develop an effective hydrometallurgical process for the recovery of metal values such as nickel, cobalt and rare earths from spent Ni-MH batteries.

© 2000 Society of Chemical Industry

Processes	Secondary materials	Objectives	Leaching	Extractants	Ref
Metallurgie Hoboken (Belgium)	Ni-Co alloy scrap	Co, Ni	$HCl + Cl_2$	Alamine 336	1
Valberg (Sweden)	waste soln. from rayon	Zn	waste soln. from rayon	D2EHPA	2
International Nickel (Canada)	anode slime	Au	aqua regia	dibutylcarbitol	3
Zincex (Spain)	pyrite cinder	Zn	chloridizing-roasting	D2EHPA	4
Calsinter (USA)	fly ash	Al	sulfatizing-roasting H_2SO_4 leaching	Primene JMT	5
MECER (Sweden)	etching soln.	Cu	ammonia leaching	LIX 54	6

Table 1 Application of Solvent Extraction in the Recovery of Metal Values from Secondary Raw Materials

Year	1994	1995	1996	1997
Output of Ni-MH batteries (units)	2.05×10^8	3.06×10^8	3.56×10^8	5.8×10^8

Table 2 Production of Nickel-Hydride Secondary Batteries in Japan[11]

EXPERIMENTAL

Materials

The Ni-MH batteries used in this work were cylindrical batteries (TOSHIBA TH-3A type). The cells weighed an average of 24.8 g each and contained an AB_5-type (rare earth metal system) negative electrode. The positive electrode of the batteries was composed mainly of 88% Ni, 6% Co and 5.6% Zn. The major components of the negative electrode are Ni (48%), RE (15.4% La, 1.0% Ce, 3.0% Pr, 9.7% Nd and 0.3% Sm), Fe (13%) and Co (3.5%). The other metals (Zn, Al and Mn) accounted for less than 6.4%. The commercial extractants employed, bis(2-ethylhexyl)phosphoric acid (D2EHPA) was donated by Daihachi Chemical Industry Co. Ltd. and, Cyanex 272, the active component of which is bis(2,4,4-tri-methylpentylphosphinic acid was purchased from Cyanamid Canada Inc. These reagents were utilized as supplied. The diluent used was kerosene. Other reagents were of analytical reagent grade.

Procedures

Leaching

The Ni-MH batteries were cut in half longitudinally to separate the metallic cases from the internal battery rolls. The battery roll (~17.8 g) was leached in 350 cm^3 of 2 mol/dm^3 H_2SO_4 solution, under agitation for 4 hours at 95°C. After leaching, the insoluble residue was filtered off and washed with water. The final pregnant liquor contained: (g/dm^3) 10.6 Ni, 0.85 Co, 1.70 Fe, 0.36 Zn, 0.21 Al, 0.54 Mn, 1.73 La, 0.10 Ce, 0.33 Pr, 1.10 Nd and 0.032 Sm (Total RE 3.29). The pH of the solution was about 0.4. The leach efficiencies of cobalt, nickel and rare earths were 100%, 97% and 96%, respectively.

Solvent extraction

The extraction equilibrium data were obtained by contacting suitable volumes of the organic and aqueous solutions in 50 cm^3 centrifuge tubes. The batch counter-current extraction processes were carried out by mechanically shaking separatory funnels of suitable sizes. All experiments were done at a temperature of 25°C. The pH adjustment was performed by the addition of a concentrated NaOH solution.

Precipitation of rare earths, cobalt and nickel

The mixed rare earths were precipitated by addition of concentrated ammonia solution until a pH 2-3 was reached, followed by an excess of saturated oxalic acid solution. The oxalate was calcined in a muffle furnace at 850-900°C to convert it to a mixed rare earth oxide product. Precipitation of cobalt and nickel was performed by a similar technique to that described above.

Analysis

The concentrations of metals in aqueous solutions were determined by ICP-AES. Those in the organic phase were calculated in the light of mass balance, unless otherwise specified. The total concentration of rare earths, which is represented by [RE] in the text, is the summation of the concentrations of individual rare earth elements in the solution. The pH value was measured with a pH meter.

RESULTS AND DISCUSSION

Recovery of Rare Earth Elements

Preliminary extraction tests on the actual leach solution at different pH values by 25 vol.% D2EHPA in kerosene at an equal phase ratio showed that at pH close to 2.5, complete rare earths and iron as well as most of aluminium and zinc could be extracted, whereas the extraction of cobalt was negligible and no nickel extraction took place. But, the extraction of manganese was insufficient under the conditions to remove manganese entirely from the solution. Thus it is necessary to increase organic-to-aqueous phase ratio and use a multi-stage counter-current operation. For this purpose the distribution isotherm for extraction of manganese were determined by contacting the two phases at different phase ratios at pH around 2.6. The equilibrium data are presented in figure 1.

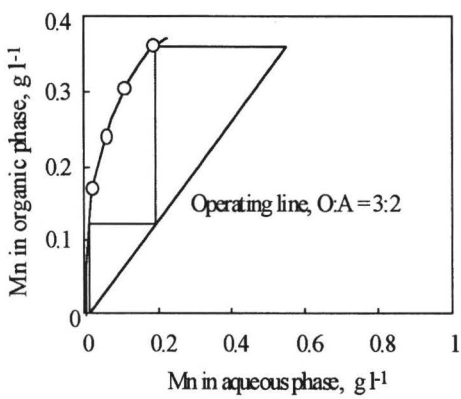


Figure 1. McCabe-Thiele equilibrium isotherm for the extraction of manganese from the leach liquor at pH 2.6 by 25 vol.% D2EHPA in kerosene.

McCabe-Thiele construction shows that essentially complete extraction of manganese is attainable in 2 counter-current stages at an O:A ratio of 3:2 and an equilibrium pH 2.6. Therefore, the

aqueous feed liquor was processed in a 2-stage batch counter-current test, using 120 cm^3 of organic phase and 80 cm^3 aqueous phase for each contact. The equilibrium pH values for each contact were controlled at 2.56-2.60. After six cycles, the concentration of manganese in the raffinate was found to be 0.010 g/dm^3. Those of aluminium and zinc were 0.002 g/dm^3 and 0.042 g/dm^3 respectively. As expected iron and rare earths were never detected. The incomplete extraction of zinc is probably attributed to complexation of zinc ion with sulfate ion in the leach liquor.[12] The extraction of cobalt was less than 4.7% and that of nickel 0.8%.

Small amounts of cobalt and nickel co-extracted to the organic phase was removed easily by scrubbing with 0.15 mol/dm^3 H_2SO_4 solution at an O:A ratio of 25:1 in a single stage. The scrub solution contained (g/dm^3), 0.63 Co, 1.38 Ni, 1.21 Mn, 0.027 Zn, 0.019 Al and 0.045 La. No iron and none of the other rare earths were detected in the scrub solution. In practical applications, this solution can be returned to be mixed with the leach liquor.

The rare earths in the scrubbed organic phase were stripped quantitatively by 1 mol/dm^3 H_2SO_4 solution in a single contact at an O:A ratio of 20:3, thereby giving rise to a strip liquor containing, (g/dm^3), 14.4 RE, 0.78 Al, 1.34 Zn, 2.02 Mn, 0.013 Co and 0.001 Fe. The stripping of iron by sulfuric acid was inefficient. However, investigations showed that the iron stripping was considerably improved by using hydrochloric acid. Nearly complete removal of iron from the organic phase is theoretically possible using 6 mol/dm^3 HCl solution in four counter-current stages at an O:A ratio of 5:1.

Separation of rare earths from metal impurities in the strip liquor was achieved by selective precipitation of rare earths with oxalic acid. Calcination of the oxalate gave a mixed rare earth oxide product containing 52.9% La_2O_3, 3.3% CeO_2, 10.3% Pr_6O_{11}, 32.5% Nd_2O_3 and 0.9% Sm_2O_3. With respect to impurities other than rare earths, analyses for three samples showed them to contain 0.007% CoO, 0.034% MnO, 0.052% ZnO, 0.006% Fe_2O_3 and 0.10% Al_2O_3. The loss of rare earths was approximately 1.2%.

Recovery of Cobalt and Nickel

Following removal of rare earths and impurities from the leach liquor by extraction with D2EHPA, Cyanex 272 was used to selectively extract cobalt away from nickel in the raffinate. Figure 2 gives the distribution isotherm for extraction of cobalt from the raffinate by 20 vol.% Cyanex 272 in kerosene at pH around 4.8. The McCable-Thiele construction demonstrates that it should be possible to achieve nearly total extraction of cobalt from a solution initially containing 0.80 g/dm^3 of cobalt in two counter-current stages at an O:A ratio of 1:1.2.

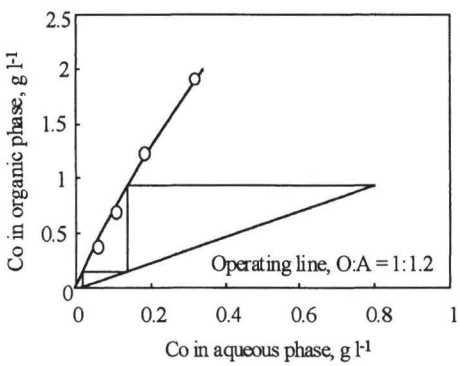


Figure 2. McCabe-Thiele equilibrium isotherm for the extraction of cobalt from the raffinate at pH 4.75-4.80 by 20 vol.% Cyanex 272 in kerosene. The raffinate contained, in g l^{-1}, 0.80 Co, 9.93 Ni, 0.042 Zn; 0.010 Mn, 0.002 Al, pH = 2.60.

To confirm this, a 2-stage counter-current batch simulation was carried out. After six cycles the representative raffinate was found to contain 0.015 g/dm^3 of cobalt corresponding to an extraction yield of > 98%. The concentrations of other metals in the loaded organic phase were (g/dm^3): 0.065 Ni, 0.012 Mn and 0.002 Al.

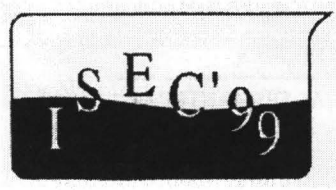
Trace levels of nickel co-extracted in the loaded organic phase could be removed by contacting it with a scrub feed (19.2 g/dm^3 Co as sulfate, initial pH 3.65) at an O:A ratio of 25:1 in a single stage. The concentration of cobalt in the scrubbed solvent was 1.01 g/dm^3 and the Co/Ni ratio was found to be 1530, indicating that nearly full elimination of nickel has been achieved under these conditions. The scrub solution contained (g/dm^3): 17.5 Co, 1.63 Ni and 0.065 Mn. In commercial operation, this contaminated solution can be fed back to the extraction stage.

The cobalt in the scrubbed organic phase was stripped readily and completely by 0.5 mol/dm^3 solution initially containing 0.80 g/dm^3 of cobalt in two counter-current stages at an O:A ratio of 1:1.2 H_2SO_4 solution at an O:A ratio of 20:1.1 in one contact. This final strip liquor contained (g/dm^3): 18.4 Co, 0.012 Ni, 0.18 Mn, 0.002 Al and 0.005 Zn. The cobalt was further recovered as a cobalt oxalate precipitate by addition of oxalic acid. Analyses for the products showed them to contain 0.025% Ni, 0.01% Zn, 0.38% Mn and 0.004% Al. The percentage precipitation of cobalt was up to 98%.

The nickel in the final raffinate was recovered directly as nickel oxalate by precipitation with oxalic acid. The contents of cobalt and zinc in the products were determined to be 0.058% and 0.15%, respectively. No other metal impurities were detected by ICP-AES. The precipitation yield of nickel was about 99%.

REFERENCES

1. Fletcher AW, *Chem. Ind.*, 414, (1973).
2. Reinhardt H, *Chem. Ind.*, 210, (1975).
3. Ritcey GM and Ashbrook AW, *Solvent Extraction. Principles and Applications to Process Metallurgy*. Elsevier (Amsterdam), Part II, 737, (1979).
4. Nogueira ED, Regife JM and Blythe PM, *Chem. Ind.*, 63, (1980).
5. Egan BZ, Seeley FG and Kelmers AD, *Process and Fundamental Considerations of Selected Hydrometallurgical System*, Kuhn, M. (ed.), SME/AIME (New York), 169, (1981).
6. Andersson SOS and Reinhardt H, *Handbook of Solvent Extraction*, Lo, T.C., Baird MHI and Hanson C (eds.), John Wiley & Sons (New York), 751, (1983).
7. Zhang P, Inoue K and Tsuyama H, *Energy & Fuels*, **9**, 231, (1995).
8. Zhang P, Inoue K, Yoshizuka K and Tsuyama H, *Hydrometallurgy*, **41**, 45, (1996).
9. Zhang P, Inoue K, Yoshizuka K and Tsuyama H, *Kagaku Kogaku Ronbunshu*, **23**, 1, (1997), (in Japanese).
10. Zhang P, Yokoyama T, Itabashi O, Suzuki TM, Inoue K, *Hydrometallurgy*, **47**, 259, (1998).
11. Industrial Rare Metals, No. 114 (Annual Review '98/'99), Arumu Press, 8, (1998), (in Japanese).
12. Smith RM and Martell AE, *"Critical Stability Constants"*, Vol 4: Inorganic Complexes, Plenum Press, New York,.84, (1981).



A HYDROMETALLURGICAL PROCESS FOR Ni AND Cd RECOVERY FROM BATTERIES: PRELIMINARY DATA

Loris Pietrelli, Gianni Ponzo and Laura Ranieri
ENEA, CR Casaccia, Environmental Dpt. Via Anguillarese, 301 – 00100 Rome, Italy

ABSTRACT
Technological change is now generally regarded as essential in achieving the major advances in pollution reduction and the main reason to develop battery recycling processes is to avoid the waste of natural resources, in fact batteries cannot be dumped directly in common landfill because the raw material will be lost and therefore new material must be imported. The exhausted batteries management consists, generally, of thermal processes and in particular cadmium is usually recovered by pyrometallurgical processes. At present some hydrometallurgical processes have been developed to treat battery waste. In this paper a hydrometallurgical process for the recovery and recycling of metals from Nickel-Cadmium exhausted batteries is presented and discussed. The process is based on leaching of batteries by H_2SO_4 followed by metals recovery and separation by using a macroporous ion exchanger with aminomethylphosphonic acid group. Leaching of electrodes have been studied at different acid concentration and temperature. Adsorption isotherms have been assessed to predict resin loading, kinetics, pH effect on the adsorption and the separation coefficients were investigated in batch tests with synthetic metal solution. Breakthrough and metal elution curves are reported for synthetic solution. The use of selective exchangers under optimised conditions allows quantitative separation of these metals and production of pure highly concentrated solution. The versatile process also allows the treatment of other similar wastes such as catalysts or liquid waste coming from metal finishing industry.

Keywords: Ni-Cd Batteries, ion exchange, aminophosphonic acid, sulphuric acid

INTRODUCTION

In the late seventies or early eighties the industrialised countries tackled the problem of "batteries", at first not in general but only the special case of "mercury content batteries" was considered: it was the beginning of a discussion about the environmental and health impact assessment. The environmental risk associated with uncontrolled disposal of exhausted batteries was increasing, therefore in 1991 the EC adopted a Directive (91/57) on batteries and accumulators containing dangerous compounds. In addition to the Directive some other regulations have to be taken into consideration such as reducing the content of dangerous substances to a minimum and promotion of research on recycling processes.

At present technological change is generally regarded as essential in achieving the major advances in pollution reduction and to avoid landfilling of materials from our limited natural resources, and from this point of view "separation processes" seem to be suitable to reach this goal.

Recycling plants operating with economical benefits cannot be effectively realised but strongly depends on the quality (purity) of the recovered products and on the flexibility of the process (how many materials can be treated). From this point of view, the treatment of metal solutions using hydrometallurgical techniques is a well-known and efficient method to recover metals from the original sources and from wastes, moreover it can reduce specific energy demand while improving energy efficiency.

At present some hydrometallurgical processes have been developed to treat battery waste but only one has an application on a large scale and for different types of primary and secondary batteries (maximum capacity of 7500 tons/y).[1]

Portable energy has many forms and within these Nickel-Cadmium batteries are widely used in many applications such as electronic communications, railways, emergency power supplies and domestic items. It seems that for many years Ni-Cd batteries will have no competitors in particular in some areas (emergency tools or mobile communications) mainly because Ni-MH and Lithium ion batteries are more expensive than Ni-Cd ones. As Cd would not be banned by authorities for use in batteries, Ni-Cd types probably will keep an important market segment. Therefore Ni-Cd batteries could be considered as recyclable material due to their high metal content. Industrial application of Ni-

© 2000 Society of Chemical Industry

Cd battery recycling is known in Sweden, France, Korea, Japan and USA. In these plants cadmium is usually recovered by pyrometallurgical processes transforming it into oxide or metallic form.
In this paper the preliminary results concerning a hydrometallurgical process for the recovery and recycling of metals from Ni-Cd exhausted batteries are presented.

EXPERIMENTAL

The general layout of the preliminary process includes the steps shown in Figure 1. The flow sheet is mainly based on mechanical dismantling, leaching and metal separation by ion exchange.
Preliminary tests were performed to select a suitable exchanger among commercial materials.[2] We selected an exchanger (20-50 mesh, bulk density 0.546 g/ml) with aminomethylphosphonic acid functional groups as the sodium form,obtained by treatment with NaOH . Adequate contact time between metal solution and exchanger is essential to allow equilibrium, therefore kinetics of adsorption were studied in batch tests. During these experiments known weights of exchanger were contacted, at constant shaking velocity at 20°C, with known amounts of metal solution for three hours. After 20 minutes of contact time about 100% equilibrium was obtained. The metal concentration in aqueous phase was determined by atomic absorption spectrochemical analysis using a Perkin-Elmer 5000 spectrophotometer. The ion exchangers were characterised by using synthetic leaching metal solutions made from analytical grade chemicals.

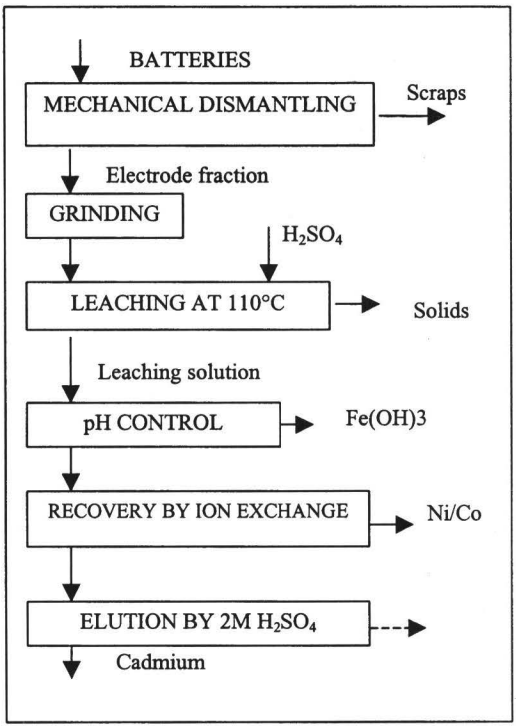


Fig. 1 Preliminary flow sheet of the process

The leached samples were prepared by separating and desegregating the electrodes (58.8 % of the total weight) without grinding. For the small sized (cylindrical batteries) the electrodes are each a single rolled sheet.

RESULTS AND DISCUSSION

Leaching of batteries

The electrodes are composed of the active materials containing Cd, Ni, Co and Fe. Nickel is the main component of the cathodes while Cd is the main component of the anodes. However a

Metal	Electrodes	Anode	Cathode
Nickel	28.9%	21.8%	26.4%
Cadmium	30.7%	51.9%	19.8%
Cobalt	0.081%	0	0.02%
Iron	0.69%	0.02%	0.005%
Graphite	21.6%	10.1%	34.0%
Stainless steel	18.1%	16.2%	19.8%

Table 1 Composition of electrodes from small size Ni-Cd batteries (Panasonic KXA36A 300mAh)

significant amount of Ni (21.8 %) can be found in the anodic materials (Table 1). Nickel seems to be present in two different forms: metallic and small amounts of $Ni(OH)_2$.[3]

Leaching studies of electrodes were performed by using H_2SO_4 as leaching agent mainly due to its low cost and less corrosive action on iron from battery components contained in the electrodes. Tests have been carried out at different temperature (25°C and 110°C) and H_2SO_4 concentration (0.6M and 1.8M). In Figure 2 the yield leaching profiles for electrodes at 110°C are illustrated.

From the data it can be seen that leaching with 1.8M sulphuric acid is easy and quick particularly for the anodes, mainly containing cadmium. At 25°C long contact time (about 6 hours) was needed to reach about 60% of leaching for cathodes and 97% for anodes.

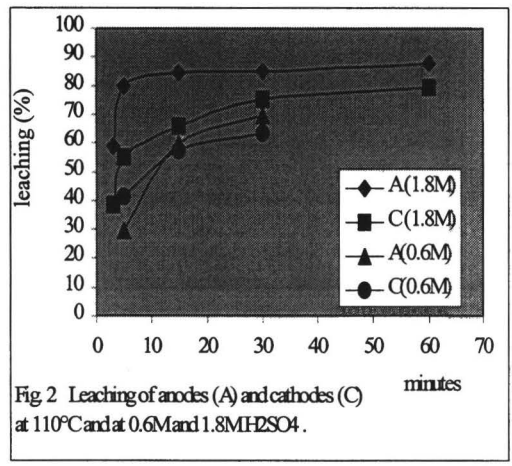


Fig.2 Leaching of anodes (A) and cathodes (C) at 110°C and at 0.6M and 1.8M H_2SO_4.

Equilibrium rates and sorption capacities

The sample solution and the exchanger were placed in a 10ml beaker and equilibrated by mechanical shaking for a time sufficient to establish equilibrium condition at 20°C. The distribution coefficients (Kd) were calculated by measuring the concentration of metal in aqueous phase before and after equilibrium with sorbent, according to:

$$Kd=[M]_{ex}/[M]_{sol}=(M_i-M_{eq})V/W \times 1/Meq$$

where M_i and M_{eq} are, respectively, the initial and final metal concentration, V is the volume of sample (ml) and W is the weight of the exchanger.

The Kd value obtained by using a batch method can be useful to predict the elution behaviour of the metals on the packed ion-exchange column. Therefore the effects of the pH on the rate of loading capacity for metals from sulphuric acid solution on the resin is shown in Figure 3. These Kd values indicate that Cadmium could be separated from Nickel at pH 3-4, where the separation factor [α= Kd(Cd)/ Kd(Ni)] for Cd from Ni is sufficiently high (α>10).

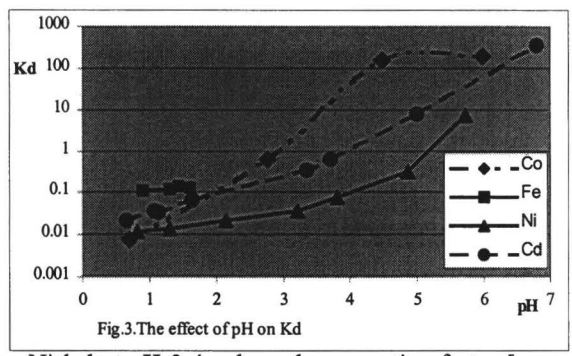


Fig.3.The effect of pH on Kd

Sorption isotherms were evaluated in aqueous medium and two models were used to quantify sorption relationship at equilibrium on a logarithmic diagram:

1) the Freundlich equation, $a= K_f Ceq^{1/n}$

where "a" is the amount of metal sorbed on the solid phase, Ceq is the equilibrium concentration of the element in the liquid phase, Kf and 1/n are empirical constants;

2) the Langmuir model, $a= Q° bC_{eq}/(1+bC_{eq})$

where Q° and b correspond, respectively, to complete the coverage of available sites (monolayer) or limiting adsorption capacity and to an empirical coefficient related to the enthalpy.

Table 2 and Figure 4 show the values of the isotherm parameters and the comparison between theoretical and experimental data. The preliminary data obtained for Cd and Ni are generally best described by the Langmuir equation.

Parameter	Cd	Ni	Parameter	Cd	Ni
1/n	0.2149	0.1174	Q°	82.64	37.45
Kf	16.03	12.43	b	0.0147	0.007

Table 2 Isotherm model parameters from Langmuir and Freundlich equations for Ni and Cd.

Figure 5 shows experimental break-trough and elution curves for Ni and Cd recovery at pH=2.2. The initial concentrations of Ni and Cd were 790 ppm and 900 ppm respectively. A 91.1% of yield for nickel was obtained from about 25 bed volumes of feed solution and at that time the experiment was concluded. The Ni breakthrough curve rises rapidly to a value greater than the feed concentration indicating that Cd displaces nickel from resin. If the absorption process had been continued until the resin was nearly saturated with Cd practically no nickel would have remained on the resin.

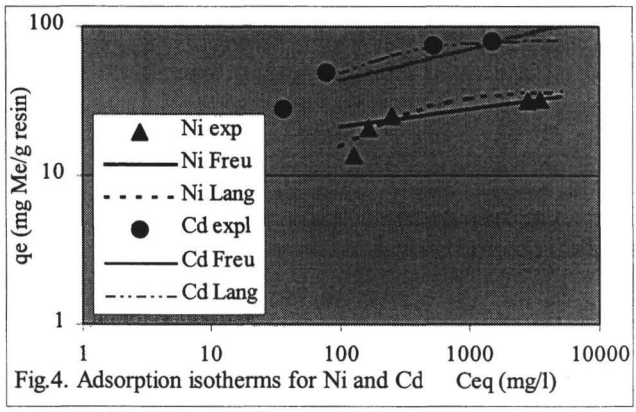


Fig.4. Adsorption isotherms for Ni and Cd

Cadmium was eluted with about 5 bed volumes of 2M H_2SO_4 and 89.3% of yield of pure metal was obtained. A small amount of Ni was eluted at the beginning mainly due to the incomplete saturation of the resin by cadmium. Based on the elution assays, the resin loading was 42.2 mg/g for Cd.

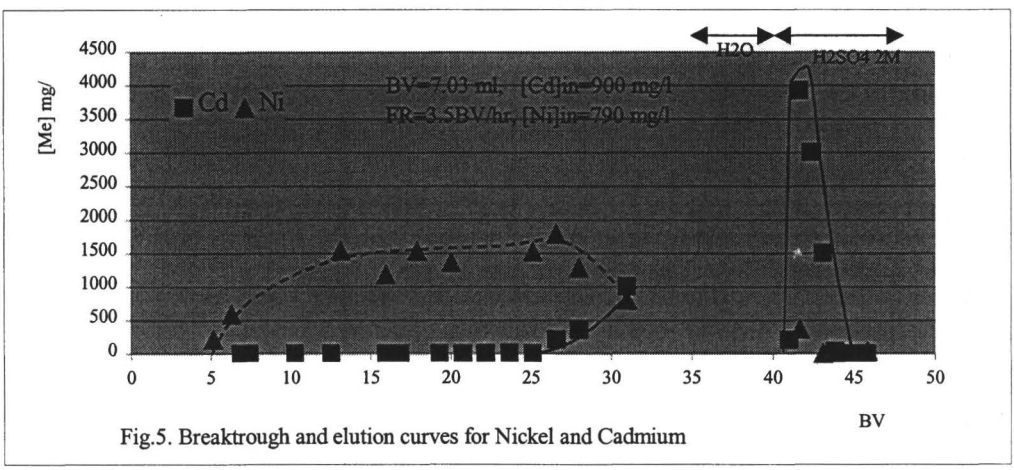


Fig.5. Breaktrough and elution curves for Nickel and Cadmium

CONCLUSIONS

Hydrometallurgy is a well-established process for separation and recovery of metal ions and the process under development shows the possibility of treat spent Ni-Cd batteries.

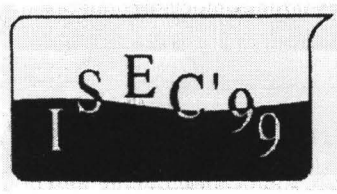
The new approach to minimise and reuse battery waste consists of an integrated process scheme to allow the treatment of dry batteries such as other products coming from different sources. The benefits are: complete recovery of metals at high purity; low energy requirement; minimisation of

wastewater; final waste of the process cannot be considered a hazardous waste so it could be reused as construction material or disposed in a common landfill to avoid air emissions.

The process for Ni-Cd recovery is now undergoing experimentation on the bench scale. In this context particular attention will be devoted to the influence of competition by other metals in particular cobalt, considering that at pH=4 iron should be recovered by precipitation, as well as to the resin retention kinetics themselves. Considering that the chosen resin exhibits a good affinity for Cd ions, the next experiments will be done by using real solutions coming from electrode leaching.

REFERENCES

1 Frohilich S and Sewing D. *J. Power Sources*, **57**, 27, (1995).
2 Pietrelli L, Ponzo G and Ranieri L. *Conferenza Nazionale Chimica ambientale*, Mantova June 1998, p 166.
3 Pons C et al. *ASM International Conference on the Recycling of Metals*, Barcelona, June 1997, p 489.



CATION SEPARATION IN SULPHATE MEDIUM USING SOLVENT EXTRACTION

Aurora María Moreno Daudinot and Elízabeth García Liranza
Solvent Extraction Department, Research Center for Laterite Minerals. Moa, Cuba.

ABSTRACT
Cobalt – nickel mixed sulphide is obtained as a product of a laterite acid leaching. Several acidic extractants were evaluated with the liquor obtained from sulphide leaching. The extractants PC 88A or DP 8R removed Zn, Mn and Ca from sulphate liquor in the first circuit, obtaining zinc sulphate as product and a cobalt and nickel raffinate. These elements are separated with Cyanex 272 in the second circuit using pH 6.0 and stripped by acid treatment, obtaining as product cobalt sulphate while nickel remains in the liquor.

Keywords: cobalt-nickel mixed sulphide, nickel laterite, Cyanex 272, Cyanex 302, PC 88A, DP 8R.

INTRODUCTION

Separation of nickel and cobalt is quite difficult because of the similarities of their physical and chemical properties. It iss more than 30 years since Ritcey and Ashbrook[1] proved the technical feasibility of solvent extraction to separate cobalt and nickel and obtain acceptable products.[2,3]

There are several reagents that can extract cobalt without extracting nickel. First phosphoric acid (DEHPA, P204), then phosphonic acid (PC 88A, P507, Ionquest 801) and later phosphinic acid (Cyanex 272, Cyanex 301, Cyanex 302) derivatives have been used and the selectivity increases in the same order. These extractants work in a pH range of 2.0 to 6.0.[4]

Nickel and cobalt mixed sulphide is produced in the processing plants of nickeliferous laterites that use the CARON process. Nicaro and Punta Gorda in Cuba obtain this mixed sulphide and a Ni-Co mixed sulphide is also obtained through the laterite pressure acid leaching of the Moa Plant. Sumitomo Metal Mining Co., Ltd. and Nippon Mining Co., Ltd. carry out sulphide refining by solvent extraction. These sulphides come from plants that process laterites with ammonia carbonate. Both companies produce Ni and Co cathodes, the first one in chloride medium and the second one in sulphate medium.[5,6,7,8] The Ni/Co ratio in sulphides obtained by ammonia carbonate leaching of laterites range between 2.5:1 and 3:1. This differs from the mixed sulphide obtained in the process of laterite pressure acid leaching that have a 10:1 Ni-Co ratio. They differ also in the content of elements present as impurities in both sulphides.

This paper explains the evaluation of different acidic extractants at laboratory scale with a liquor obtained by dissolution of Ni and Co mixed sulphides. It has the aim of definign the pattern to follow to remove impurities and to separate cobalt from nickel in this liquor.

EXPERIMENTAL

Aqueous Phases.

Experiments were made with liquor obtained by leaching in the sulphide autoclave. This sulphide is the product of the process of laterite pressure acid leaching. It was re-pulped at up to 80°C with mechanical and pneumatic agitation and feed to the autoclave where it was leached at 140°C and 7 atm oxygen pressure for 8 hours. This liquor was partially purified with coral to remove iron, aluminium, chromium and some copper impurities This liquor then had pH 4.5 and an average chemical composition in g/dm^3 as follows:

Ni	Co	Zn	Mn	Mg	Ca
96.43	9.72	2.01	0.032	0.364	0.611

The pH variation and solvent neutralization were made with 32% NaOH.

© 2000 Society of Chemical Industry

Sulphuric acid solutions were prepared with 96% commercial reagent and industrial water contained 0.015 g/dm^3 magnesium and 0.008 g/dm^3 calcium.

Organic Phases

The extractants studied were DP 8R, PC 88A, Cyanex 272 and Cyanex 302.
JET A-1 was the diluent used to prepare organic solvents with a density 0.791 g/cm^3. Solvents were scrubbed with 200 g/dm^3 sulphuric acid over 30 minutes to use them for further studies.

Analytical

Chemical analyses were made by atomic adsorption and visible ultraviolet spectrophotometry.

Experimental Procedure

Studies were carried out in the conventional way according to the methodology used by Gordon Ritcey. The pre-neutralization of the organic solution was made with caustic soda. Later the mixing of aqueous and organic phases was carried out in beakers with mechanical agitation for the time set in the conditions for each experiment. Once this was completed, both phases were separated in separating funnels and the loaded organic phase was stripped twice with sulphuric acid. All solutions were filtered prior to their analysis.

Then the extraction optimum pH of elements for each solvent, the number of extraction and stripping stages were determined.

The objective of the work and its experimental results marked the route to follow, defining the specific conditions under which each experiment was to be carried out .

Counter-current run tests at a laboratory scale were made with extractant PC 88A. This experiment consisted in simulating the continuous process with the number of stages determined by the McCabe-Thiele diagram. The number of starting cycles required to reach representative results depends on the number of stages in the process. This kind of experiment allows the confirmation that the number of stages theoretically determined is enough to reach the expected results. The counter-current extraction experiment of Zn, Mn and Ca were carried out using PC 88A in three stages.

RESULTS AND DISCUSSION

Zinc and manganese were extracted before cobalt by the extractants DP8R, PC88A, Cyanex 272 and Cyanex 302, figures 1,2,6 and 9.

DP 8R is a commercially used extractant. It is suitable to remove impurities because of their high extraction and the low coextraction of cobalt at a pH that requires a low consumption of alkali. This solvent extracts more than 95% zinc, 50% manganese, 67% calcium, 5% magnesium and only 1.4% cobalt at pH 2.0 in only one contact stage, figure 1.

The commercially extractant PC 88A at pH 3.0 gives a low extraction of Ni and Co but extraction of zinc, manganese and calcium were higher. For extraction at a phase ratio of 1:1in a single contact stage the results were as follows: 6% Co, 99% Zn, 60% Mn, 40% Ca. Theoretically from the McCabe-Thiele diagram only one extraction stage is required to extract 99% Zn, two stages for manganese and three for calcium . The extracted zinc can be stripped in two stages, figures 2,3,4 and 5, and tables 1and 2.

Cyanex 272, also a commercially used reagent, rejects calcium and nickel at pH 6.0 where the extraction of cobalt, zinc and manganese is higher. This extractant only required preliminary zinc and manganese separation from the Ni-Co sulphate liquor to obtain a cobalt product of high purity. Three stages are necessary for cobalt extraction with an organic/aqueous phase ratio of 1 in 180 seconds, figures 6,7 and 8. A cobalt sulphate product can be obtained by stripping the cobalt loaded solvent by an acid solution in two stages, in 300 seconds and at a phase ratio > 10.

Cyanex 302 is not used commercially. It extracts 93% Zn at pH 2.0 with minimum extraction of the other elements. It has the inconvenience that manganese has to be removed before solvent

extraction. This reagent also extracts 99% Co at pH 6 with a phase ratio of 1, but at this pH zinc and manganese extraction is also higher.

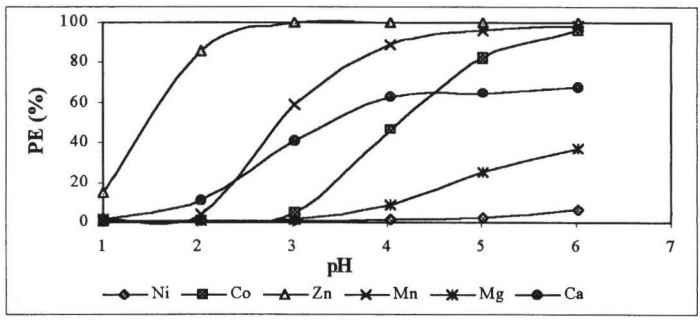


Figure 1. Effect of pH change on DP 8R extraction. O:A = 1. Time: 5 min.

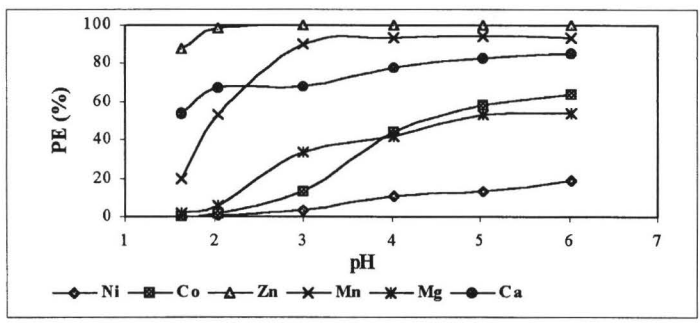


Figure 2. Effect of pH change on PC 88A extraction. O:A = 1. Contact Time: 5 min.

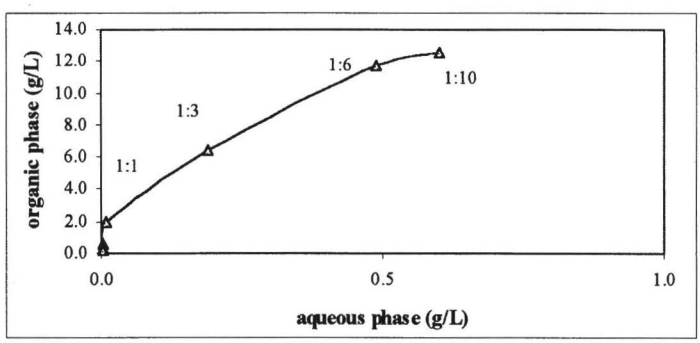


Figure 3. Zinc Extraction Isotherm. PC 88A. pH: 3.0. Contact Time: 5 min. T=30°C.

According to the results obtained in the experiments carried out at laboratory scale, the following scheme was chosen for the purification of the liquor and Co-Ni separation. Extraction of Zn (99%) and Mn (91%) with PC 88A at pH 3.0 from the liquor purified from iron, aluminium and chromium; scrubbing with zinc sulphate and acid stripping to give a zinc product. To the raffinate obtained from this circuit Co is extracted with Cyanex 272; the Co extract is scrubbed with Co sulphate and later Co is obtained in the sulphate form as product from stripping. Nickel remains in the raffinate. The results are summarised in tables 1 and 2.

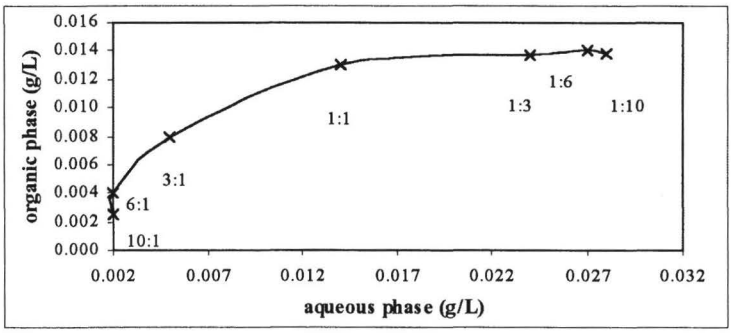


Figure 4. Manganese Extraction Isotherm. PC 88A. pH: 3.0. Time: 5 min. T=30°C.

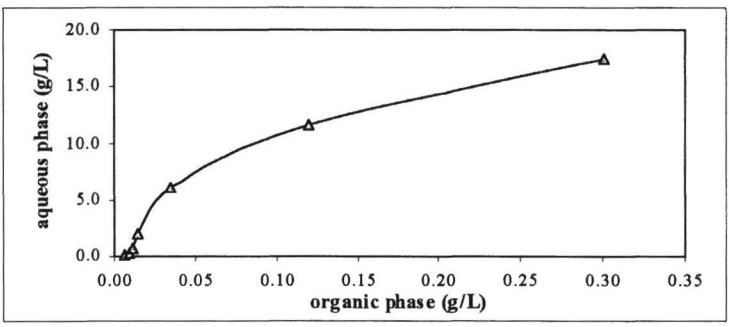


Figure 5. Zinc Stripping Isotherm.PC 88A. Time: 10 min. T=30°C. H_2SO_4 150 g/dm^3.

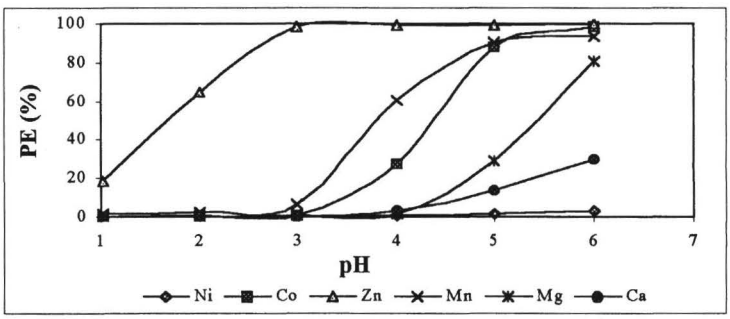


Figure 6. Effect of pH change on CNX 272 extraction. O:A = 1. Time: 5 min.

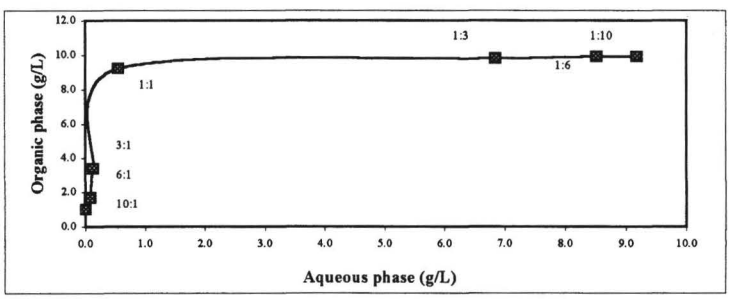


Figure 7. Cobalt Extraction Isotherm. CNX 272. pH: 6.0. Contact Time: 5 min. T=30°C

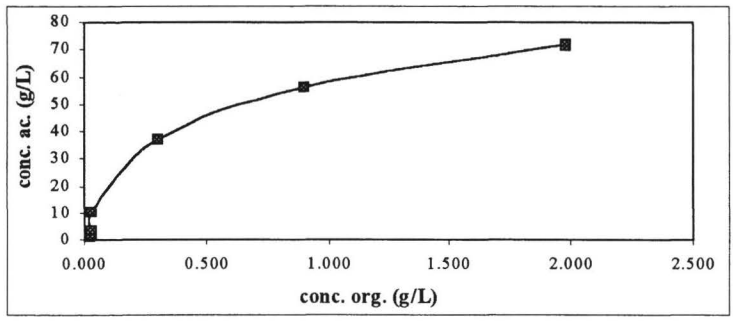


Figure 8. Cobalt Stripping Isotherm CNX 272. Time: 10 min. T=30°C. H_2SO_4 150 g/dm^3

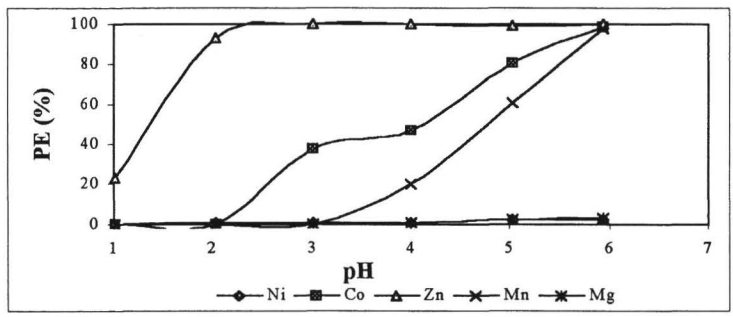


Figure 9. Effect of pH change on CNX 302 extraction. O:A = 1. Time: 5 min.

Parameters (g/dm^3)	Ni	Co	Zn	Mn	Co/Zn Ratio	Co/Mn Ratio
Feed Solution	97.52	10.14	2.03	0.036	5.0	281.7
Raffinate	94.56	8.45	0.000	0.002	84500	3841

Table 1 Principal Analytical Results of PC 88A Counter – Currents Test

	Extraction Coefficient				Separation Factor	
Stages	Ni	Co	Zn	Mn	Zn/Co	Mn/Co
First	0.008	0.04	6733	1.64	158854	38.73
Second	0.003	0.08	-	1.22	-	15.05
Third	0.003	0.08	-	1.09	-	14.14

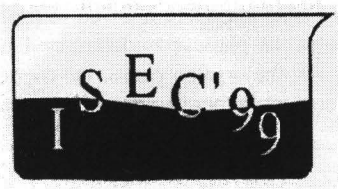
Table 2 General Results of PC 88A Counter –current tests

CONCLUSIONS

Manganese reaches its maximum extraction after zinc and before cobalt with all evaluated extractants. To obtain high pure cobalt it is necessary to include a solvent extraction circuit to remove zinc, manganese and calcium from sulphate liquors with the extractants PC 88A or DP 8R and another circuit to separate Co-Ni with Cyanex 272. Three products are obtained: zinc sulphate, cobalt sulphate and nickel sulphate.

REFERENCES

1 Ritcey GM. US Patent No. 3 399 055, (1968).
2 Ritcey GM and Ashbrook AW. *Process Metallurgy 1*. Elsevier, (1984).
3 Ritcey GM and Taylor A. *Ni/Co SX/EW Seminar*. Melbourne, Australia, (1996).
4 Ritcey GM. *SITLA '91*, Moa, Cuba, (1991).
5 Sumitomo, article from Research and Development. Okochi Memorial Prize, Japan, (1980).
6 Kasai T et al. *Fourth Joint Meeting MMIJ – AIME*, Tokyo, Japan, (1980).
7 Tyroler GP and Landolt CA. *117th TMS Annual Meeting,* Phoenix, Arizona, (1988).
8 Preston JS. *J. S.Afric.Inst.Min.Metal.*, (1983).



EXTRACTION OF COPPER CONTAINED IN AMMONIA SOLUTIONS FROM THE ELECTRONICS INDUSTRY WITH LIX84

JM Chimenos, MA Fernández, M Segarra, AI Fernández, A Esparducer and F Espiell

Department of Chemical Engineering and Metallurgy, University of Barcelona, Martí i Franquès, 1, 08028 - Barcelona, Spain.

ABSTRACT

A batch process is described for extracting copper from ammonia solutions, which are a by-product in the manufacture of integrated circuits, by the electronics industry. These solutions contain copper (150 g/l), ammonia and ammonium chloride (150 g/l NH_4^+) as the main constituents. A commercial solvent is used for laboratory study of the influence of different parameters on the yield of extraction. Thus, with one extraction, 96% of the initial copper can be extracted by using 40% LIX® 84 in kerosene, with an organic/aqueous ratio of 6 and a temperature below 40°C for 30 minutes.

The copper re-extraction from the organic phase was tested with hydrochloric and sulphuric acid. The results showed that re-extraction with HCl led to a low copper concentration in the organic phase with no addition of foreign ions (as is the case of sulphate).

A possible scheme for treating these ammonia solutions without by-products being generated is proposed (extraction - washing - re-extraction - washing) with re-circulation and re-utilisation of washing waters, to obtain an ammonia solution with 1-2 ppm copper and a hydrochloric solution with 20g/l copper.

Keywords: copper, LIX 84, ammoniacal etching solution.

INTRODUCTION

One of the most widely used etchants for the recovery of copper in printed circuit board (PCB) manufacturing is the ammoniacal etchant.[1] When the copper concentration in the etchant reaches about 140 g/l, the rate of etching decreases and a part of it has to be replaced. The replaced spent etchant is discharged as waste. To treat these spent ammoniacal solutions for regeneration and reuse, a number of methods have been proposed: electrolysis,[2] ion exchange[3] and solvent exchange methods.[4-7] This last method is most commonly used. In most solvent extraction (SX) methods, copper is removed from the etchant by extracting it with an organic solvent which is then stripped with an aqueous acidic solution. The copper contained in these acidic solutions can be further recovered as copper salts.

LIX® 84 (2-hydroxy-5-nonylacetophenone oxime, Henkel Corp.) is used as selective extractant of copper from ammoniacal solutions that also contains zinc.[8] Although β-diketones have been used for the extraction of copper from ammoniacal liquors,[9] this paper shows the possibilities of the recovery of copper from these solutions by this organic solvent dissolved in kerosene, followed by the stripping from the organic phase with an aqueous mineral acid solution. The application of SX circuits to copper extraction at an industrial scale has been discussed by other authors.[7,10,11] This paper proposes a batch SX circuit for treating these copper alkaline etching solutions.

EXPERIMENTAL PROCEDURE AND RESULTS

LIX 84 is a solvent extraction reagent that forms insoluble complexes with various metallic cations in a manner similar to the copper as is described in the following equation:

$$2RH_{org} + Cu^{2+}_{aq} \Leftrightarrow R_2Cu_{org} + 2H^+$$

Batch equilibration experiments were carried out in separatory funnels at room temperature. The organic solvent was supplied by Henkel, the diluent used was commercial kerosene and the aqueous solutions were spent etchants supplied by a leading local PCB manufacturing company. The aqueous

© 2000 Society of Chemical Industry

solution and the organic solvent were shaken for different lengths of time and were allowed to settle before sampling for analysis. The concentration of copper in the aqueous phase was determined by Atomic Absorption Spectrophotometry (AAS) after proper dilution. For the organic phase, the copper was stripped with aqueous solutions of H_2SO_4 and HCl. The copper content in these aqueous phase was determined by AAS.

Determination of optimum parameters

LIX 84 concentration in kerosene and org/aq phase ratio

Optimal LIX 84 concentration in kerosene was determined by mixing a known volume of ammoniacal copper solution of 130g/l in copper with variable LIX 84 concentrations in kerosene for 24 hours. Organic/aqueous phase ratio was studied following the same procedure: mixing the same volume of ammoniacal copper solution with different volumes of LIX 84 dissolved in a known volume of kerosene. As the LIX 84 concentration in kerosene increases and/or the phase ratio increases, the copper in the aqueous ammoniacal solution decreases. Both variables are co-operative, as is shown in Figure 1.

Figure 1

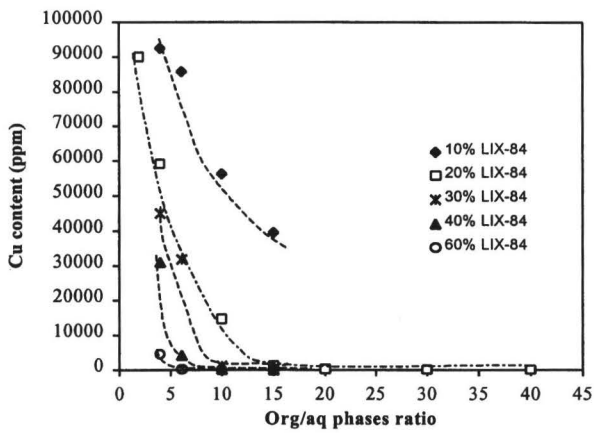


Figure 1. Copper content in the alkaline etching solution, after extraction with the organic solvent at different LIX 84 concentrations, vs. organic/aqueous phase ratio.

Extraction time

The variation of the final copper concentration in the aqueous ammoniacal etching solution with the mixing time was studied, for an organic/aqueous phase ratio of 6 and different LIX 84 concentrations, (Figure 2). In the primary stages, copper concentration decreases with the increasing time, achieving a constant and minimum value for each organic phase composition. In all the cases studied, this minimum value was achieved after 30 minutes mixing time, and the phase separation was completed after 5 minutes.

Temperature effect

Table I compares the different copper concentrations in the ammoniacal solution and the amounts of copper extracted when the reaction was carried out at 25° and 40°C. At 40°C, the copper concentration in the ammoniacal solution was half of that obtained at 25°C.

Temperature (°C)	[Cu] in ammoniacal solution (ppm)	Extracted Cu (%)
25	6770	94.80
40	3125	97.60

Table I. Copper concentrations in the ammoniacal solution and amount of extracted copper achieved after 30 min extraction in org/aq ratio of 6 and 40%v/v of LIX 84

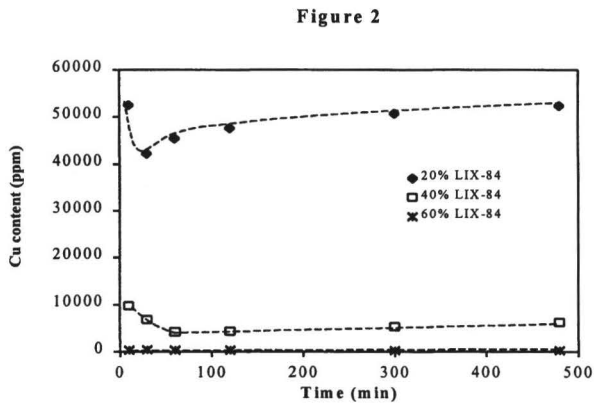


Figure 2. Copper content in the alkaline etching solution, after extraction with the organic solvent at different LIX 84 concentrations, vs. mixing time of extraction.

Stripping with mineral acid: effect of the acid concentration.

The effect on the copper stripping of the concentration of HCl and H_2SO_4 in the stripping aqueous solution was studied. For an initial copper concentration of 19.37g/l, an organic/aqueous phase ratio of 1 and mixing time of 30 minutes, the results obtained for H_2SO_4 are depicted in Table II, which also details the copper concentration in the aqueous acid solution after stripping. The amount of stripped copper increased with the concentration of both acids, achieving its maximum value for 6M H_2SO_4 and for HCl between 4 and 5M. It was observed that this reaction, for the maximum acid concentration studied, was exothermic enough to achieve the temperature of 40°C. Otherwise, at higher acid concentrations, the organic solvent degrades and the separation of the phases were more difficult. The summary of the optimized conditions at laboratory scale are detailed in Table III.

H_2SO_4 concentration (M)	[Cu] in stripping solution (ppm)	Stripped Cu (%)
2	13750	70.99
4	15000	77.44
6	19200	99.12

Table II. Copper concentration in stripping solution and amount of stripped copper for different H_2SO_4 concentrations.

LIX 84 (%) in kerosene	40
Org/aq ratio	6
Time (min)	30
Temperature (K)	40
Aq/org ratio in stripping reaction	1
[H_2SO_4] in strip solution (M)	6

Table III. Summary of the optimized parameters for the extraction and stripping .

Batch Process Design

On the basis of the above results, a batch process, consisting in two stages of extraction, was designed. The organic solvent was re-circulated from the second to the first extraction stage, which was followed by two stages of stripping with clean 6M H_2SO_4. The regenerated organic solvent re-entered the circuit at the second extraction stage, but had high sulfate and ammonia concentrations. To solve this problem, a washing step was introduced after and before each stripping operation. Table IV shows the nomenclature of the SX circuit.

LIX-84	LIX 84 solved in kerosene at 40%
AES	Alkaline etching solution
OS	Organic solvent
BW	Alkaline washing waters
AW	Acid washing waters
SW	Organic solvent recirculated
Product	Recovered copper in aqueous solution

Table IV. Nomenclature employed for the flows of the different batch processes employed.

To minimize water consumption, the possibilities of re-circulation of the acid and alkaline cleaning waters were studied. The acid waters from the washing steps after stripping, were re-circulated to the entry of new acid. This circuit also introduced sulfates as impurities in the recovered ammoniacal aqueous solution. To eliminate them, 4-5M HCl aqueous solution, starting from commercial HCl (10-11M), was used as stripping agent.

The alkaline waters, from the cleaning of the organic solvent after extraction, are re-circulated to the first extraction stage. The optimized batch process, with the intermediate washing operations, stripping with HCl and re-circulation of washing waters, is depicted in Figure 3.

The effect of the number of cycles made by the organic solvent was determined by measuring the copper concentration of the different currents involved, after each cycle. Thus, after 6 cycles, copper concentration in the cleaned ammoniacal aqueous etching solution (AES2) was 1.4mg/l, while the copper content in the acid aqueous solution from the re-extraction was 18.1g/l. The amount of NH_3/NH_4^+ in the recovered ammoniacal aqueous solutions was also established. This was performed by addition of an excess of NaOH and then distillation. The distillate was then collected on standarized HCl aqueous solution. Thus, the measured loss of NH_3/NH_4^+ was 36% v/v. These losses can be attributed to the use of an hydroxyoxime reagent that extracts ammonia,[9] and/or the evaporation due to the increase of temperature at the stripping stage.

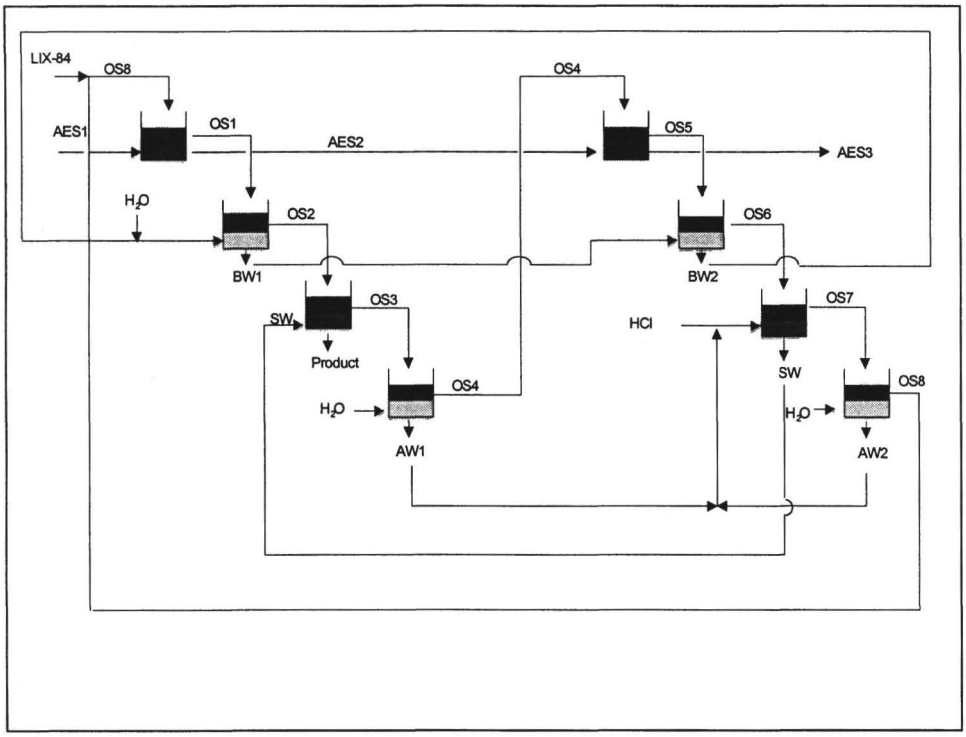


Figure 3. Batch process circuit with HCl 4-5M as stripping agent, which includes the recirculations of the washing waters.

CONCLUSIONS

Solvent extraction of copper from aqueous alkaline etching solutions from the printed circuit industry is feasible with LIX 84 dissolved in kerosene as extractant by a batch process. With prior optimization of the extraction-stripping parameters, 99.9% of the copper was recovered in one step.

After three cycles, copper concentration in the ammoniacal copper solution fell from 130g/l to 3.99mg/l with H_2SO_4 as stripping agent, under the optimized conditions and with recirculation of the acid washing waters. However, this stripping agent introduced sulfate ions into the organic solvent and the recovered ammoniacal alkaline solution.

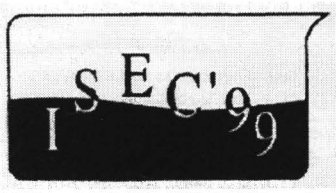
A batch process design, using HCl as stripping agent, which also introduced recirculation of the alkaline washing waters, achieved similar results to H_2SO_4, but foreign ions did not enter the process, and a final concentration of copper in the ammoniacal alkaline aqueous solution of 2mg/l was obtained after two cycles. Recovered ammoniacal alkaline aqueous etching solution lost a 36% v/v NH_3/NH_4^{+}.

ACKNOWLEDGEMENTS

The authors would like to thank the company Industria Químicas del Vallès for financing and supporting this investigation. We also grateful to the Fundació Bosch i Gimpera as well as Mr Robin Rycroft for his linguistic and stylistic advice.

REFERENCES

1 Peter Sze Y and Ching Wong J *Environ. Tech.*, **15**, 785
2 Hillis MR *Trans. Inst. Metal Finish.*, **62**, 21
3 Dejak M. *Plat. and Surf. Fin.*, **75**, 35
4 Hamby WD and Slade MD *U.S.Patent, 4,083,758*
5 Andersson SOS and Reinhart H *U.S.Patent 4,350,667*
6 Law HH and Tierney V *Plat. and Surf. Fin.*, **74**, 74
7 Andersson SOS and Reinhardt H *Handbook of Solvent Extraction* (eds. Lo, Baird and Hanson) Krieger Pub. Co, (1991).
8 Fucheng H. *Value Adding Solvent Extr., [Proc.ISEC'96],* **1**, 727, (1996)
9 Flett DS *Handbook of Solvent Extraction* (ed. Lo, Baird and Hanson) Krieger Pub Co, (1991)
10 Velea T, Segarceanu T, Vasiliu C and Motoiu, S. *Value Adding Solvent Extr.*, [Proc.ISEC'96], **1**, 757, (1996)
11 Jiaoyong Y. *Value Adding Solvent Extr., [Proc.ISEC'96*], **1**, 807-812, (1996).



RECOVERY PROCESS OF Ni WITH EHO FROM A WASTE ETCHING SOLUTION OF LEAD FRAME MATERIAL

J Shibata, S Matsumoto, M Sano and S Nishimura
Faculty of Engineering, Kansai University
Suita, Osaka 564-8680, Japan

ABSTRACT
Fe-Ni alloy, namely 42 alloy, has a wide use for lead frame of chip package in electronic industries. Usually acidic ferric chloride solutions are used as an etching solution. As dissolution of the material procedes, the etching efficiency deteriorates as Ni or Fe ions accumulate in the etching solution. To keep the etching efficiency at a certain level, a part of the waste solution is replaced with a fresh etching solution. It is known that EHO (2-ethylhexanal oxime) an extractant which can extract Ni prior to Fe. EHO can extract Ni(II) and Cu(II) from chloride ion concentration, 2-8 mol/dm^3, while other metal ions except Fe(III) do not transfer sufficiently to the EHO organic phase. The Fe(II) is extracted with EHO in small amounts. The recovery of concentrated Ni from the waste etching solution with solvent extraction was examined to establish the new process to recycle the etching solution.

Keywords: Fe-Ni alloy etch solution, Ni, 2-ethylhexanal oxime

INTRODUCTION

One of the traditional ways of using Fe-Ni alloy is for lead frame material in electronic industries. In the processessing of the lead frame, acidic concentrated ferric chloride solution is used as an etch solution. As the dissolution of lead frame material procedes, the etching efficiency decreases because Ni accumulates in the etching solution. Consequently, some amounts of the contaminated etching solution are replaced with the fresh solution to maintain the efficiency. The waste etching solution in this process contains highly concentrated Ni(II), Fe(II) and Fe(III). Table 1 shows the typical composition of this waste etching solution. The Ni concentration in the waste solution is no less than 10-30g/dm^3. The current treatment process of the waste solution is based on precipitation or cementation methods.[1] There are some reports that the extractant, 2-ethylhexanal oxime (EHO) has a significant ability to extract Ni prior to Fe.[1-4] Still now there is no extractant which can extract Ni selectively when Ni and Fe ions coexist in chloride solutions. Therefore, it can be a great development to apply EHO to this separation. It was the objective of this work to recover high purity Ni from the waste etching solution by solvent extraction and to establish a new process of recycling of the solution.[5]

EXPERIMENTAL

As the organic phase, certain concentrations of EHO diluted in Solvesso 150 were prepared. The aqueous phases for Fe(III), Ni(II) and other metal ions were prepared by dissolving the corresponding metal chlorides in distilled water. Purified water was used as a stripping agent.

The extraction experiments were carried out as follows; solutions of the same volume(15cm^3) of the aqueous and organic phases were shaken in a 50cm^3 centrifuge tube at 298K and 300spm. After shaking, the two phases were separated each other and then analyzed. The metal concentration in the aqueous phase was measured with an atomic absorption spectrophotometer, and the difference between the initial and equilibrium metal concentrations in the aqueous phase determined the metal concentration in the organic phase. The concentrations of acid and chloride ion were determined by titration with sodium hydroxide solution and silver nitrate solution, respectively. The Fe(II) concentration in the aqueous phase was obtained by oxidation-reduction titration with 0.01mol/dm^3 of Ce(IV) standard solution.

© 2000 Society of Chemical Industry

$FeCl_3$	214 – 230 g/dm^3	Fe (III)	74 – 80 g/dm^3
$FeCl_2$	137 – 412 g/dm^3	Fe (II)	60 – 180 g/dm^3
$NiCl_2$	22 –65 g/dm^3	Ni (II)	10 – 30 g/dm^3
HCl	65- 73 g/dm^3	HCl	1.8 – 2.0 mol/dm^3

Table 1 Composition of typical waste etching solutions

RESULTS AND DISCUSSION

Extraction characteristics of metal ions with EHO

The extraction experiments of some metal ions with 0.1mol/dm^3 EHO from the aqueous solution containing various concentrations of HCl were carried out to clarify the extraction property of common metal ions with EHO. The selected metal ions were Ni(II), Cu(II), Fe(III), Co(II), Zn(II), Ca(II), Mn(II), Fe(II) and Na(I), and their concentrations were 0.01mol/dm^3. Figure 1 shows the extraction of metal ions as a function of initial HCl concentration. In the HCl concentration range of 1-9mol/dm^3, Ni (II), Cu(II), Fe(III), Co(II) and Zn(II) are obviously extracted, though other metal ions do not have good extractability. Especially, both Ni(II) and Cu(II) are significantly extracted over a wide range of HCl concentration. When HCl concentration is nearly 5.0mol/dm^3, the maximum extraction of Cu(II), about 90%, is obtained, while at HCl concentration more than 5.0mol/dm^3, the amount of extracted Cu(II) decreases significantly.

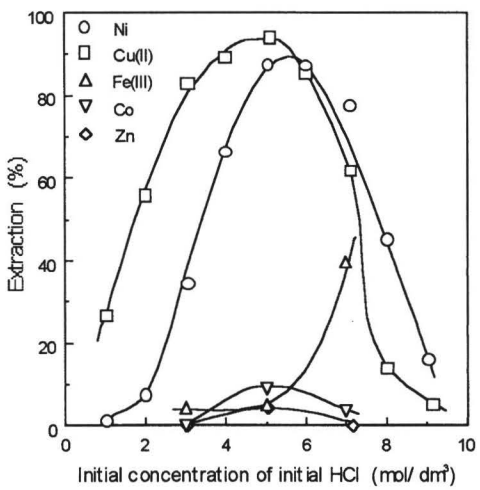


Figure 1 Extraction of various metals with EHO from hydrochloric acid solution

The Ni(II) extraction behaviour is similar to that of Cu(II). There has already been reported that Cu(II) is extracted with EHO by the solvation reaction and the extracted species is considered to be $CuCl_2 \cdot 2EHO$.[1] The authors explain that the formation of $CuCl_3^-$ and $CuCl_4^{2-}$, which cannot be extracted, causes the decrease in Cu(II) extraction at high HCl concentration. The results of Cu(II) extraction with EHO obtained in this study supports the extraction mechanism which Inoue et al.[1] suggested.

Figure 2 shows Ni(II) extraction isotherm with 0.3, 0.5 and 0.7mol/dm^3 EHO. The extraction isotherm of Ni(II) demonstrates that the maximum loadings of Ni(II) are 4.4, 7.4 and 10.4g/dm^3 for the organic phase containing 0.3, 0.5 and 0.7mol/dm^3 EHO, respectively. The ratio of the stoichiometric combination of EHO and Ni(II) in the organic phase can be obtained from the maximum loading. When using 0.3, 0.5 and 0.7mol/dm^3 EHO, the combination ratios of $[EHO]_{org}/[Ni]_{org}$ are 4.00, 3.97 and 3.95, respectively. It is clear that 4 molecules of EHO are required to extract 1 atom of Ni(II). Nickel(II) does not easily form chloro-complexes, but we can assume $NiCl_2 \cdot 4EHO$ as an extracted species of Ni(II).

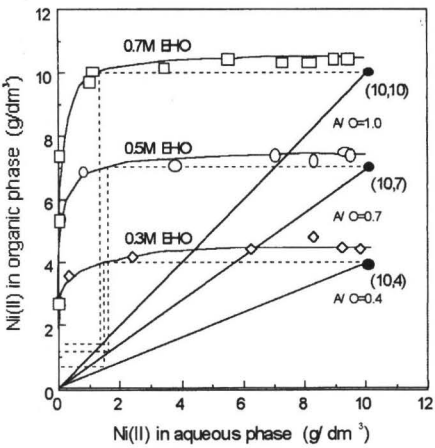


Figure 2 Extraction isotherm of Ni(II)

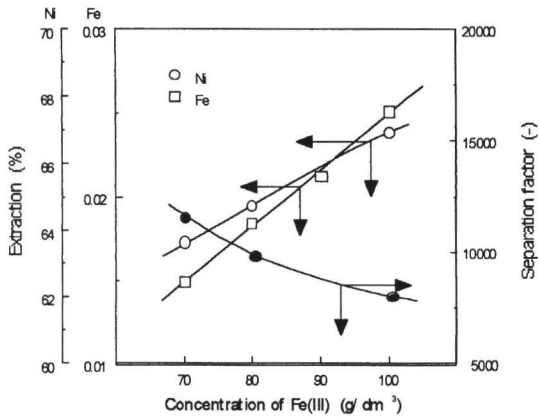


Figure 3 Effect of ferric chloride concentration on extraction (0.5mol/ dm^3 EHO diluted in Solvesso150,10.0g/ dm^3 Ni(II) dissolved in 1.5mol/ dm^3 HCl)

Effect of ferrous and ferric chloride concentrations on Ni(II) extraction

In the practical etching process, the amounts and the ratios of dissolved Fe(II) and Fe(III) fluctuate according to the operation conditions, so the effect of Fe(II) and Fe(III) concentrations on Ni(II) extraction was investigated in this section. The extraction of Ni(II) was carried out in the presence of 70-100g/dm^3 Fe(III), when the concentrations of Ni(II) and HCl were 10g/dm^3 and 1.5mol/dm^3, respectively. The effect of ferric chloride concentration on Ni(II) extraction is shown in figure 3. The Ni(II) extraction increases from 63.5% to 66.5% with increasing Fe(II) concentration, whereas the Fe(II) extraction increases by a small amount. As the result, the separation factor of Ni(II) over Fe(II) is reduced, but we can completely separate them because the separation factor is more than 6500. The Ni(II) extraction was examined in order to clarify the effect of the ratio of dissolved Fe(II) and Fe(III) on the extraction of Ni(II), when the concentration of Fe, Ni(II) and HCl were 105g/dm^3, 10g/dm^3 and 1.5mol/dm^3, respectively. The Ni(II) extraction increases from 63% to 67% with increasing the Fe(III) concentration, while the extracted Fe(III) is small amount. The separation factor decreases from 15000 to 7000, but it is sufficiently large to separate them completely. Ferrous ion is never extracted with EHO from the mixed solution at any ratio. It is considered that the increase in Ni(II) extraction is caused with the increase in the chloride ions in the ferric chloride solutions.

Extraction and stripping isotherm of Ni(II)

When the Ni(II) concentration in the wasted etching solution is 10g/dm^3 and the stripping is perfectly carried out, we can make the operating lines in the extraction isotherm as shown in figure 2. The Ni(II) in the recovered organic phase changes with EHO concentration: when EHO concentrations are 0.3, 0.5 and 0.7mol/dm^3, the Ni(II) in the recovered organic phase are 4, 7 and 10g/dm^3, respectively. The almost perfect recovery of Ni(II) from the waste etching solution can be accomplished with 2 stage counter-current extraction at any EHO concentration.[6]

The stripping isotherm of Ni(II) with water was obtained at 298K for three EHO

concentrations. The stripping isotherm gave the capability of Ni(II) concentration up to 20g/dm^3 in the stripped aqueous solution, but so many stripping stages are required to reduce Ni(II) concentration in the outlet organic phase. As the recovery methods for Ni(II) from the stripped Ni(II) aqueous solution, electro-winning and crystallization are suggested. When electro-winning is applied to reduce Ni(II) to metal Ni, the appropriate Ni(II) concentration should be controlled in the stripping process. In one of the practical electro-winning processes for Ni(II) from chloride solutions, Ni(II) concentrations in the aqueous solution are up to 20-23g/dm^3. [7]

The effect of temperature on extraction and stripping of Ni(II) was examined. Extraction decreases when the temperature goes up, while the stripping is promoted with an increase in temperature. From the van't Hoff formula the heat of extraction is calculated to be 35.1kJ/mol (ΔH=-35.1kJ/mol) and the heat of stripping as 23.7kJ/mol (ΔH=23.7kJ/mol). Since stripping is endothermic, then stripping at high temperature was investigated as one of the improved stripping methods. Figure 4 shows Ni(II) stripping isotherm from 0.5mol/dm^3 EHO at 298K and 333K. The stripping isotherm at 333K is shifted considerably towards the left compared with that at 298K, which improves the stripping process.

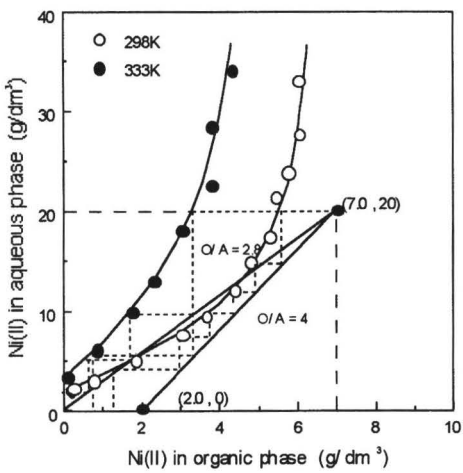


Figure 4 Effect of temperature on the stripping isotherm of Ni(II) from 0.5M EHO

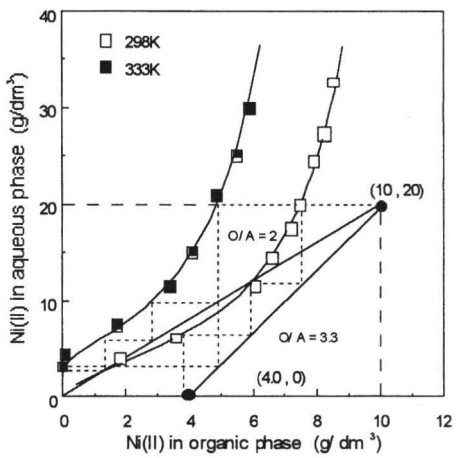


Figure 5 Effect of temperature on the stripping isotherm of Ni(II) from 0.7M EHO

When multistage counter-current stripping is applied, the coordinates (7.0, 20), which are the Ni(II) in the inlet organic phase and the Ni(II) in the outlet aqueous phase respectively, and the coordinates (2.0, 0), which correspond to the Ni(II) in the outlet organic phase and the Ni(II) in the initial strip solution are placed in figure 4. When applying McCabe-Thiele analysis with the operating line tied between the two coordinates, it becomes clear that the stripping operation at 298K could be the one with the phase ratio (A/O) = 4 and 6 stripping stages. If the stripping temperature is 333K and the operation conditions are the same as mentioned above, the theoretical stripping stages might be 2. When the phase ratio (A/O) = 2.8 and theoretical stripping stages of 4-5 are adopted at 333K, there might not be any Ni(II) in the outlet organic phase.

The stripping isotherms of Ni(II) from 0.7mol/dm^3 EHO at 298K and 333K are shown in figure 5. As previously stated, the operating conditions of O/A = 3.3 and 4 theoretical stripping stages at 298K and the condition of 0/A=2 and 4 theoretical stripping stages at 333K are obtained from each isotherm. Still more, if the stripping is operated at 333K, a solution containing more than 20g/dm^3 Ni(II) can be recovered. With the results obtained in this study, the epoch making process is finally established as shown in figure 6. In the solvent extraction step, Ni(II) is separated from Fe contained in the waste etching solution. The Ni extracted with EHO is stripped with the spent electrolyte and then Ni(II) is electrically reduced to Ni in the electro-winning step. Ferrous ion in the raffinate becomes Fe(III) in the chlorine oxidation step.

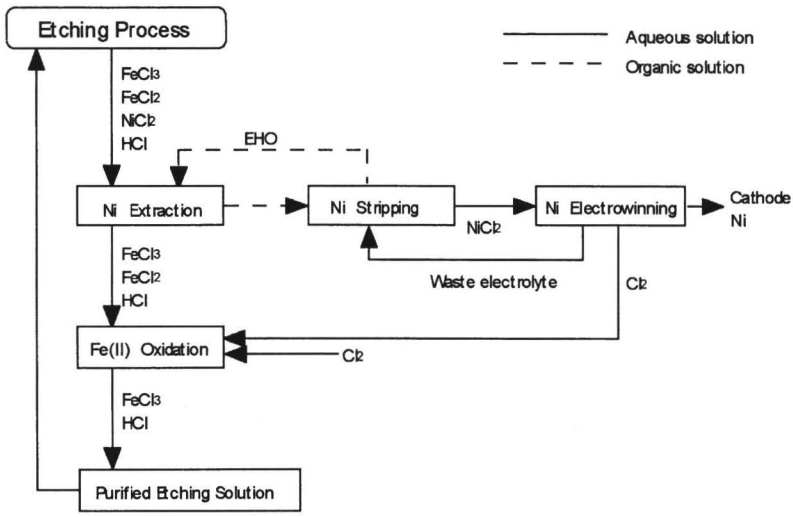


Figure 6 Flowsheet of Ni recovery and recycling of etching liquor

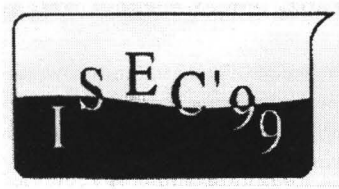
It is known that the decomposition of aldoxime like EHO into aldehyde and hydroxyl amine occurs by the contact with mineral acid shown in the following equation:

$$RHC{=}N\text{-}OH_{org} + H_2O + HCl \leftrightarrow RHC{=}O_{org} + NH_2OH{\cdot}HCl$$

Though the degradation of EHO has been investigated in detail in this study, the results are briefly introduced here. The degree of the degradation depends on the EHO concentration, mineral acid concentration, temperature and contact time, when the organic phase containing EHO and the aqueous phase containing mineral acid are mixed in the mixing chamber. For example, when the 1.0mol/dm^3 EHO diluted in toluene and the aqueous solution of 1.0mol/dm^3 HCl are contacted at phase ratio 1/1 for 100 hours at 298K, about 8% of EHO would be decomposed. In the case of contact with 5mol/dm^3 HCl under the same conditions, the decomposition reaches to about 30%. The decomposition never takes place if there is the contact between EHO and water even for 100 hours at 333K. It was confirmed that regeneration can easily be accomplished by mixing partly degraded EHO in the organic phase with an aqueous solution containing hydroxyl amine and NaOH. These organic compounds were analyzed by the gas chromatograph with capillary columns (Shimadzu, GC-17A).

REFERENCES

1. Inoue K and Baba Y, *Solv.Extr.Ion Exch.*, **4**(2), 237, (1986).
2. Preston JS, *Hydrometallurgy*, **11**, 105, (1983).
3. Preston JS, *Hydrometallurgy*, **10**, 187, (1983).
4. Rice NM and Smith DC, *Proc ISEC '86*, **2**, 633, (1986)
5. Ono N, *Journal of the Mining and Materials Processing Institute of Japan*, **95**, 441, (1979).
6. Shibata J and Otomo S, *Kagaku Kogaku Ronbunshu*, **19**(2), 214, (1993).
7. Ishikawa Y, Fukui I and Tsuchida N, *Metall. ReviewMMIJ*, **9**(2), 126, (1992)



STRATEGIES FOR PLATINUM GROUP METAL (PGM) SEPARATION USING IMPREGNATED RESINS

M Rovira, JL Cortina and AM Sastre
Department of Chemical Engineering, ETSEIB, Universitat Politècnica de Catalunya, Diagonal 647, E-08028, Barcelona, Spain

ABSTRACT
Platinum Group Metals (PGM) Separation from hydrochloric solutions by means of impregnated resins is reported in this work. Two different impregnated resins were prepared using a dry impregnation method and adsorbing the extractants di-(2-ethylhexyl)-thiophosphoric acid (DEHTPA) and Alamine 336 onto macroporous polymeric supports (Amberlite XAD2). On the basis of the experimental results obtained, a flowsheet is proposed for the separation of Pd(II), Pt(IV) and Rh(III).

Keywords: impregnated resins, di-(2-ethylhexyl)thiophosphoric acid, Alamine 336, XAD2, platinum group metals (PGM), Pd, Pt, Rh

INTRODUCTION

Catalytic converters, which allow the purification of automotive exhaust emissions, contain significant amounts of platinum group metals (PGM), specifically: palladium (Pd), platinum (Pt) and rhodium (Rh). This resource is particularly significant because the PGM concentrations in catalysts are, in general, higher than those of the richest ore bodies. Since a substantial share of the world demand for PGM is used for autocatalyst production, the quest for new processes focused on the recovery of these metals to be re-used in the production of new catalysts is required.[1,2] When the PGM are recovered by means of hydrometallurgical schemes, the ceramic matrix containing the metals is leached in acidic media, and subsequently Pd, Pt and Rh would be separated using conventional techniques such as solvent extraction and ion-exchange. Although processes based on ion exchange and solvent extraction have been published or patented, the research for specific strategies for separation and recovery of PGM based in these technologies is required.[3]

In recent years, the development of impregnated resins considered, as a link between solvent extraction and ion exchange technologies has been an important field of development in separation science. These materials are prepared by immobilisation of selective metal reagents used in solvent extraction onto high surface polymeric macroporous supports.[4] Our research group has been conducting intensive research dealing with PGM recovery and separation using impregnated resins.[5-9] The main objective of the work presented in this article was try to devise and develop straightforward PGM separation patterns in acidic media using impregnated resins prepared by adsorption onto Amberlite XAD2 of two different organic extractants: Alamine 336 and di-(2-ethylhexyl)thiophosphoric acid (DEHTPA).

EXPERIMENTAL

Reagents and Solutions.

Alamine 336 was kindly supplied by Henkel and used as extractant without further purification. Its purity was found to be 92.2%.[6] Alamine 336 is a mixture of saturated and straight chain trialkylamines with carbon chains C_8 and C_{10}, with the carbon chain C_8 predominating by about 2 to 1. Di-(2-ethylhexyl)thiophosphoric acid (DEHTPA or HL) was kindly supplied by Bayer and was purified obtaining a product with a purity of 96.15%.[5] Stock metal solutions were prepared by dissolving an appropriate amount of $PdCl_2$, $PtCl_4$ or $RhCl_3.3H_2O$ (Johnson Matthey) in

© 2000 Society of Chemical Industry

hydrochloric acid medium, and were used to prepare the mixed-metal solutions employed in the extraction experiments.

Amberlite XAD2 (Rohm and Hass) with particle diameter between 0.3 and 0.9 mm, was used as a macroporous polymer adsorbent. Impregnated resins were prepared by using a dry impregnation method,[4] mixing an appropriate amount of Alamine 336 or DEHTPA dissolved in ethanol or acetone respectively with dry XAD2, until total evaporation of the diluent was reached.

Metal Extraction and Stripping.

The metal extraction experiments were carried out in batch experiments at room temperature. Samples of 0.1 g of impregnated resin, unless otherwise stated, were shaken vigorously with 20 ml of metal aqueous phase until equilibrium was achieved. Metal stripping tests were performed in batch experiments at room temperature and using single-metal solutions. After the metal extraction step, 10 ml of stripping reagent were added to the loaded resin and were shaken vigorously for 24 hours. The metal concentrations after the extraction and stripping steps in the aqueous phases were determined by Inductively Coupled Plasma Atomic Emission Spectrophotometry ICP-AES (Spectroflame, Spectro Analytical Instruments).

RESULTS AND DISCUSSIONS

PGM extraction using XAD2/DEHTPA resins.

The metal extraction percentages of the different metals were calculated as follows:

$$E(\%) = 100\frac{[M]_i - [M]_e}{[M]_i} \quad (1)$$

where $[M]_i$ and $[M]_e$ are the initial and the equilibrium concentration of metal in the aqueous phase respectively.

Figure 1 shows the percentage extraction of Pd(II), Pt(IV) and Rh(III) by XAD2/DEHTPA resins as a function of aqueous HCl concentration.

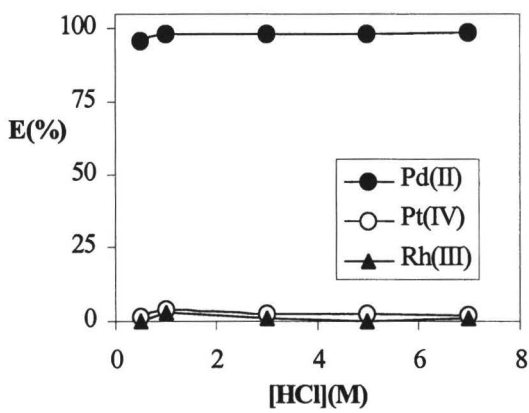


Figure 1. Pd(II), Pt(II), Rh(III) extraction from hydrochloric solutions. [PGM] 4.7 x 10^{-4} M Pd, Pt, Rh and phase ratio (V/m)=200.

Pd(II) was completely extracted from the multi-metal solution, whereas Pt(IV) and Rh(III) in practice exhibited no sorption. Such a difference between Pd(II) and the other metals is mainly as a result of the soft Lewis acid character of Pd(II); studies have unambiguously established that extractants

containing sulphur as DEHTPA, soft Lewis bases, are highly effective and selective for soft Lewis acids.[10,11]

From Pd(II) distribution data at different DEHTPA concentrations on the resin reported in a previous work [5] it was found that the extraction of Pd(II) from HCl solutions with XAD2/DEHTPA was described by the following reaction:

$$PdCl_4^{-2}{}_{aq} + 4HL_{org} \Leftrightarrow PdL_2(HL)_{2\,org} + 4Cl^-{}_{aq} + 2H^+{}_{aq} \qquad (2)$$

The stripping of the Pd(II) sorbed on the resin was studied using thiourea (Tu) in 1M HCl media as eluant. Table 1 shows the effect of the aqueous concentration of Tu on the extent of Pd(II) stripping from the sorbent. In all the cases complete recovery of the metal was obtained. This can be justified as Tu, which is a soft ligand, can re-extract the Pd(II) from the resin phase as a water soluble complex. On the other hand when HCl was employed as stripping agent varying the acid concentration from 0.5 to 10.2 M, zero stripping was found in all cases.

Tu(M) in 1M HCl	0.05	0.11	0.18
S(%)-Pd	100.0	85.3	90.8

Table 1 Stripping of Pd(II) loaded with XAD2/DEHTPA.Org. phase: 0.1 g of 0.35 mol Pd/kg impregnated resin. Aq. phase: 10 ml Tu in 1 M HCl. Shaking time: 24 h

PGM extraction using XAD2/Alamine 336 resins

The extraction percentages for Pd(II), Pt(II) and Rh(III) at different HCl concentrations using XAD2/Alamine 336 are illustrated in Figure 2.

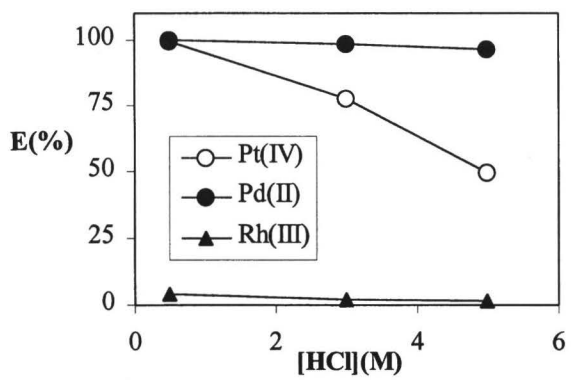


Figure 2. Effect of HCl concentration on metal percentage extraction of PGM. Org. Phase ratio (V/m)=200; 0.94 mol/kg XAD2 resin and 4.7×10^{-4} M Pd, Pt, Rh. Shaking time: 4 h

Almost complete extraction of Pd(II) is attained in the HCl concentration range studied. Pt(IV) extraction is complete at 0.5 M HCl but decreases by increasing HCl concentration. In contrast to Pd(II) and Pt(IV) Rh(III) is not extracted independently of the acid concentration.

The sorption of Pd(II) and Pt(IV) on the impregnated sorbent can be expressed according the following reaction[6]:

$$2\,R_3NH^+Cl^-{}_{org} + MCl_n^{-2}{}_{aq} \Leftrightarrow (R_3NH^+)_2MCl_n^{-2}{}_{org} + 2Cl^-{}_{aq} \qquad (3)$$

with n=4 for Pd(II) and n=6 for Pt(IV).

HCl, $HClO_4$ and Tu in HCl were tested for stripping of Pd(II) and Pt(IV) and the results are summarised in Table 2.

Tu(M) in 1M HCl	0.05 M	0.1 M	0.21 M
S(%)-Pd	100.0	93.0	85.3
S(%)-Pt	92.8	90.5	89.6
$HClO_4$(M)	0.5 M	1.0 M	3.0 M
S(%)-Pd	92.9	100.0	92.2
S(%)-Pt	86.0	91.4	87.0
HCl(M)	1.0 M	7.1 M	10.2 M
S(%)-Pd	1.8	59.3	95.8
S(%)-Pt	0.8	12.5	43.3

Table 2 Stripping (S%) of Pd(II) and Pt(IV) loaded with XAD2/Alamine 336. Org. phase: 0.1g - 0.18 mol metal/kg impregnated resin. Aq. phase: 10 ml – Tu in 1 M HCl. Shaking time: 24 h

Either $HClO_4$ or Tu are able to effectively re-extract Pd(II) and Pt(IV). $HClO_4$ acts through an anion exchange mechanism, and Tu is effective since Pt(II) (Tu having previously reduced Pt(IV) to Pt(II)) and Pd(II) form very stable complexes with compounds containing sulphur as stated previously. Concerning HCl stripping ability, it was found that increasing HCl concentration, metal stripping increases and for instance concentrated HCl can strip quantitatively Pd(II), nevertheless only partial elution of Pt(IV) was found over all the HCl range investigated.

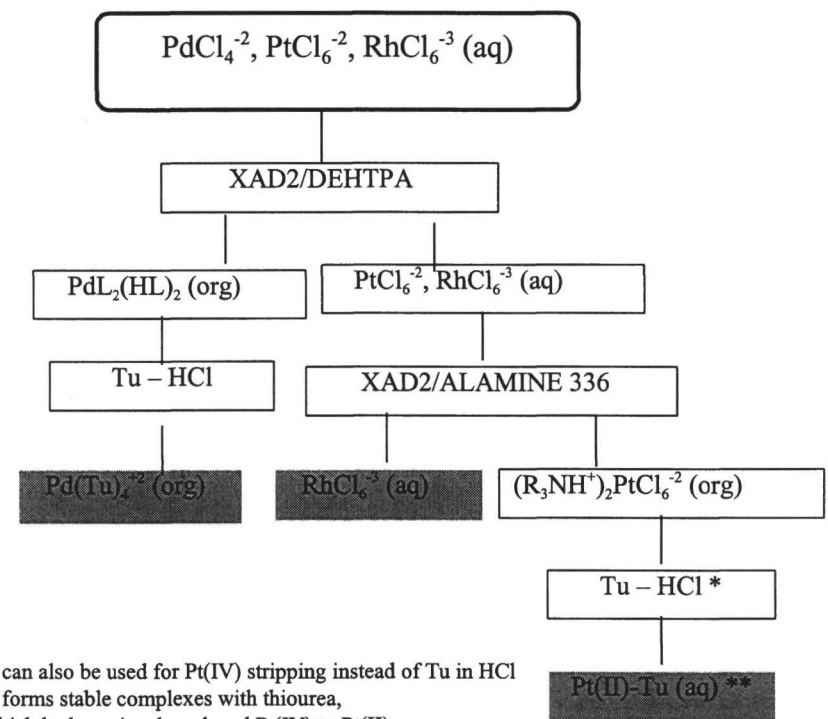


Figure 3. Pd(II)-Pt(IV)-Rh(III) separation from HCl media

Pd(II), Pt(IV) and Rh(III) separation

Following the results presented in this work, a flowsheet for the separation of Pd(II), Pt(IV) as well as Rh(III) from HCl solutions using impregnated resins is envisaged and presented in Figure 3.

A PGM solution containing Pd(II), Pt(IV) and Rh(III) in 1 M HCl is brought in contact with XAD2/DEHTPA impregnated resins and selective Pd(II) extraction takes place, thus the Pd(II) in the organic resin may be stripped with Tu in HCl and therefore separated from the other metals. Recovery of Pt(IV) can be accomplished by contacting the aqueous solution obtained in the previous step; rich in Pt(IV) and Rh(III); with XAD2/Alamine 336 resin, which will selectively extract Pt(IV) while Rh(III) will remain in the aqueous solution. Finally Pt stripping may be conducted with either Tu or $HClO_4$.

CONCLUSIONS

This work has shown that an alternative process for selective extraction and separation of Pd(II), Pt(IV) and Rh(III) from HCl solutions on the basis of impregnated resins is feasible.

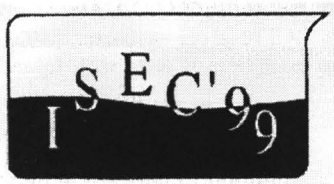
Impregnated resins maintain the advantages of ion exchange technology over conventional processes, such as the use of simple equipment and easy phase separation, therefore it is easily anticipated that the development of improved extractants and resins may be readily adopted by the refineries.

ACKNOWLEDGEMENTS

This work was supported by CICYT Project QUI 96-1025-CO3 (Ministry of Science and Culture of Spain) and 96SGR 00101 (Autonomous Government of Catalonia). We are grateful to Bayer AG Hispania and Henkel for kindly donating DEHTPA and Alamine336 respectively.

REFERENCES

1. Hoffmann JE, *J. Met*, June (1988) 40.
2. Hagelüken C, Recycling of Automotive Catalytic Converters - *2nd. European Precious Metals Conference*, Lisbon, (1995).
3. Mishra RK in '*Precious Metals'89'*, M. C. Jha and S. D. Hill, Eds. The Minerals, Metals & Materials Society, 483, (1988).
4. Cortina JL and Warshawsky A, in *"Ion Exchange and Solvent Extraction"*, J. A. Marinsky and Y. Marcus, Eds. Marcel Dekker, New York, **13**, 195, (1997).
5. Rovira M, Hurtado L, Cortina JL, Arnaldos J and Sastre AM, *Solv. Extr. Ion Exch.***16**, 545, (1998)
6. Rovira M, Cortina JL, Arnaldos J and Sastre AM, *Solv Extr. Ion Exch.*, **16**, 1279, (1998)
7. Rovira M, Hurtado L, Cortina JL, Arnaldos J and Sastre AM, *Reactive and Functional Polymers* , in press, (1998).
8. Rovira M, Cortina JL, Arnaldos J and Sastre AM, *Solv. Extr. Ion Exch.*, in press (1998)
9. Rovira M, Hurtado L, Cortina JL, Arnaldos J and Sastre AM in *"Second European Meeting on Chemical Industry and Environment"*, N. Piccinini and R. Delorenzo. Eds., Politecnico di Torino, **2**, 469, (1996)
10. Handley T, *Anal. Chem.*, **35**, 991, (1963)
11. Cote G and Bauer D, *Rev. Inorg. Chem.*, **10**, 121, (1989).



SOLVENT EXTRACTION OF GOLD FROM CHLORIDE COPPER ANODE SLIME LIQUORS

K Soldenhoff and D Wilkins
Australian Nuclear Science & Technology Organisation (ANSTO) New Illawara road, Lucas Heights, NSW, Australia

ABSTRACT
A phosphine sulphide and two phosphine oxide type reagents were tested for the recovery of gold from liquors derived by the oxidative chloride leaching of copper anode slimes. The phosphine sulphide reagent Cyanex 471X was found to be very selective for gold with respect to impurities such as Se, Te, Bi, Pb and Cu. Using this reagent, an upgrading of Au concentration from 7% in the feed liquor to 99.9% in the loaded solvent was achieved.

Keywords: gold, copper anode slimes, Cyanex 471X, Cyanex 923, Cyanex 925

INTRODUCTION

Anode slimes derived from the electrorefining of anode copper contain significant amounts of gold and silver. The processing of the slimes is complicated by the impurities present such as Te, Se, Pb, As and Bi.[1,2] The flowsheets adopted in commercial operations depend largely on the individual feed compositions, but generally involve leaching to remove copper and tellurium. Roasting and/or smelting are commonly used to control lead and selenium. Silver is then recovered by electrolysis and gold is recovered last by electrorefining.

Oxidative chlorination of decopperised anode slimes is an attractive processing alternative, in that it offers the opportunity of separating silver and gold early in the processing, leading to decreased Au lock-up time and potentially to a simpler totally hydrometallurgical flowsheet. The oxidative chloride leach rejects most of the silver to the residue and produces a solution from which Au can be recovered by solvent extraction. This approach has been used in both the Kennecott chloride process[3] and the Minataur™ process.[4,5] In the Kennecott process, chlorination is applied to the decopperised slimes, and gold is extracted from solution by dibutyl carbitol, a solvent which suffers from some serious drawbacks, one of which is its high solubility in the aqueous phase. The Minataur™ Process has been applied to the gold mud, but has not been tested in solutions with the higher levels of impurities generated by direct treatment of decopperised slimes.

There is therefore some incentive to develop a solvent extraction process for the extraction of gold from chloride liquors derived from leaching of decopperised anode slimes. In this paper, we present results on the extraction of Au from such liquors, and compare the selectivity of some commercially available reagents with respect to major impurities present in the liquor.

EXPERIMENTAL

A chloride liquor was produced by leaching decopperised anode slimes with concentrated hydrochloric acid under reflux at 96°C, with addition of hydrogen peroxide as an oxidant. The leaching time was 4 hours and the slurry density 62%.

For the solvent extraction tests, equal volumes of diluted leach liquor and organic phase were contacted in separating funnels, and mechanically agitated for 1 hour at room temperature. Except where otherwise stated, an extractant concentration of 0.5 M was used, and this was at least in ten fold excess to the total aqueous metal concentration. After equilibration, the two phases were allowed to settle. The percentage extraction of Au, Ag, Cu, Pb, Bi, Se, Te and As was calculated by the difference in the initial and final aqueous concentrations as determined by either ICP-OES or ICP-MS. Dibutyl carbitol (DBC) and methyl iso-butyl ketone (MIBK) were AR grade reagents purchased from Merck. Cyanex 471X or tri-isobutylphosphine sulphide, Cyanex 923, a mixture of phosphine oxides

© 2000 Society of Chemical Industry

with n-octyl and n-hexyl groups and Cyanex 925, a mixture of phosphine oxides with n-octyl and 2,4,4-trimethylpentyl groups, were kindly supplied by Cytec, Canada. All reagents were used without further purification. The diluent used was Shellsol 2046, with the exception of tests with Cyanex 471X, which was mixed with toluene.

RESULTS AND DISCUSSION

A solvent extraction process for gold recovery from anode slimes chloride leach liquors needs to be able to fulfill certain criteria. Primarily, gold has to be extracted selectively from fairly concentrated hydrochloric acid solutions. The major elements that are of concern are Se, Te, Bi and some base metals. Silver is effectively separated during the oxidative chloride leaching process.[3,6] Selectivity of the solvent for Au with respect to Pd and Pt is also important but this issue is not addressed in the present paper, as these two elements were not present in the feed material used for these tests.

Copper anode slimes feed liquor

The first step in most processes for copper anode slime treatment is decopperising. This usually involves a sulphuric acid leach and the copper is returned to the process.[7] We therefore used decopperised anode slime material to produce the liquors required for the solvent extraction testwork. The anode slimes, containing 1.7% Au, were leached in hydrochloric acid as described in the experimental section. Greater than 98% Au dissolution was achieved, with 99.9% of the Ag reporting to the leach residue. The solution produced contained 10 g L^{-1} Au. The main impurities present in the leach liquor were Se, Te, Bi, Cu and Pb. The gold constituted 7% by weight of the metals dissolved.

Extraction of gold from hydrochloric acid solution with dibutyl carbitol and methyl iso-butyl ketone

Gold recovery from chloride solutions by solvent extraction has been practiced commercially by platinum group metal refiners. Dibutyl carbitol (DBC), has been used at INCO [8] and is also the solvent of choice in the Kennecott process.[3] As a basis for comparison with other reagents, we tested the extraction of Au and other impurities with DBC as a function of hydrochloric acid concentration. Results are shown in Figure 1.

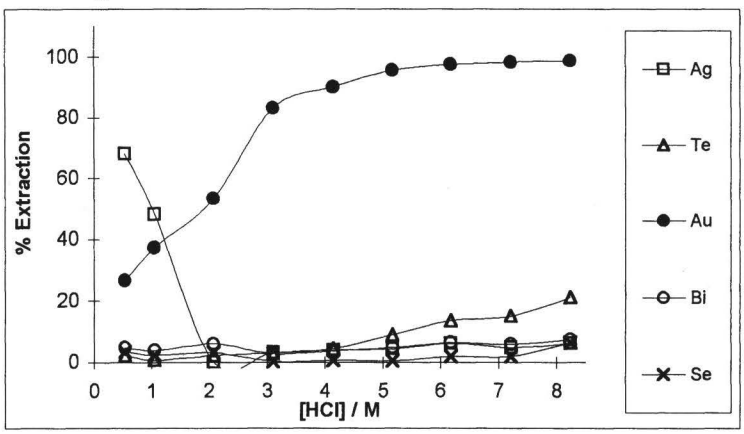


Figure 1 Extraction with 50 vol.% (2 M) dibutyl carbitol

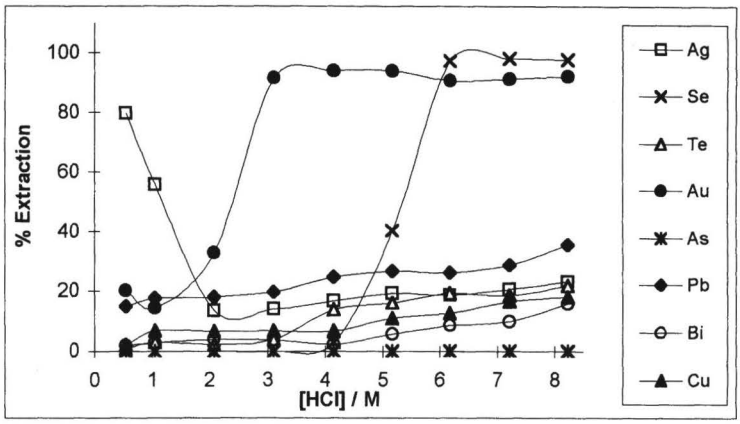


Figure 2 Extraction with 40 vol.% (3.2 M) MIBK

The data indicate that above 3 M hydrochloric acid, the single-stage extraction of gold with 50 vol.% DBC is greater than 80% and there is good rejection of all the impurities. In terms of its selectivity, DBC is an excellent reagent for gold extraction from decopperised anode slimes leach liquors. There are, however, serious process related disadvantages reported for the use of this reagent.[3,8] These include high aqueous solubility, a requirement for batch operation in scrub circuits due to slow phase separation, and the need for reductive stripping to elemental gold, with the product having to be separated from the stripped solvent by filtration.

Another solvent that has been used for gold extraction on a commercial scale by Mattey Rustenburg Refiners,[9] is methyl isobutyl ketone (MIBK). Our results, shown in Figure 2, for the extraction of various elements with 3.2 M MIBK, indicate that between 3-4 M HCl concentration, gold extraction can be fairly selective. We also tested the stripping of 3.2 M MIBK, loaded with 3 g L^{-1} gold, with water, 0.5 M HCl and 0.1 M oxalic acid. We found that precipitation occurred in all instances. Reductive stripping with oxalic acid was the most effective with 87% stripping achieved in a single stage contact. It would seem therefore, that back extraction of gold in a process using MIBK requires separation of precipitated Au from the solvent, which is a disadvantage from a practical processing point of view.

Extraction of Au from hydrochloric acid solution with Cyanex 923, Cyanex 925 and Cyanex 471X

As part of the screening exercise for suitable extractants for gold, two phosphine oxide type reagents and a phosphine sulphide were tested. The reagents were Cyanex 923, Cyanex 925 and Cyanex 471X. The percent extractions of gold and other impurities are shown in Figures 3-5. High extractions were registered for gold under all conditions. Cyanex 923 and 925 showed no selectivity for Au over Ag and Bi and limited selectivity over Te, Cu and Pb. These reagents are therefore considered to be unsuitable for the intended purpose. It is of interest to note however, that there is some improvement in the selectivity of Cyanex 925, relative to Cyanex 923. This is manifested by a shift in the Te and Cu extraction curves to higher acidities, and a decrease in the extraction of Pb and As. We suggest that this effect is due to the increased branching in the alkyl groups of Cyanex 925, as opposed to Cyanex 923, which contains only straight carbon chains.

Compared to the phosphine oxides, the gold selectivity of the phosphine sulphide reagent is much improved. Tellurium, Cu and Se only extract significantly at hydrochloric acid concentrations greater than 4 M. Lead, Bi and As are not well extracted. To test the loading capacity of this reagent, a 0.26 M Cyanex 471x solution of toluene was contacted at various phase ratios with leach liquor containing 10 g L^{-1} Au. The equilibrium acidity used was 4.4 M HCl. A maximum capacity of 26.7 g

L^{-1} Au was achieved which is close to a molar ratio of L:Au of 2:1 (L= Cyanex 471x), and would suggest the presence of an extracted complex with a stoichiometry of $HAuCl_4L_2$. Martinez et al.[10] also measured equilibrium loading isotherms of gold with Cyanex 471x and reported L:Au ratios of 1.5. Their tests, however, were performed at much lower extractant and gold concentrations with a maximum gold loading of only 0.2 g L^{-1}. They defined the solvent species as a mixture of $HAuCl_4L_2$ and $HAuCl_4L$.

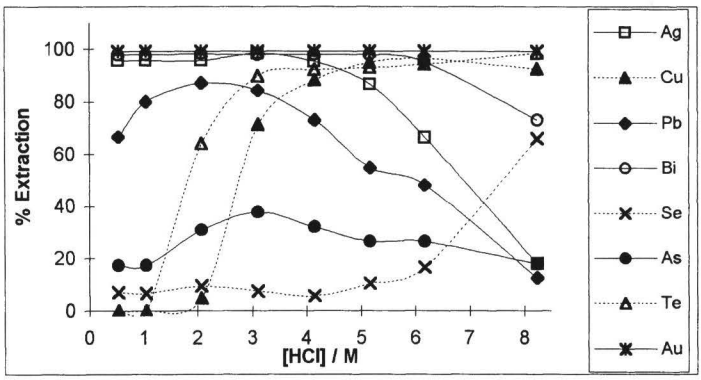


Figure 3 Extraction with 0.5 M Cyanex 923

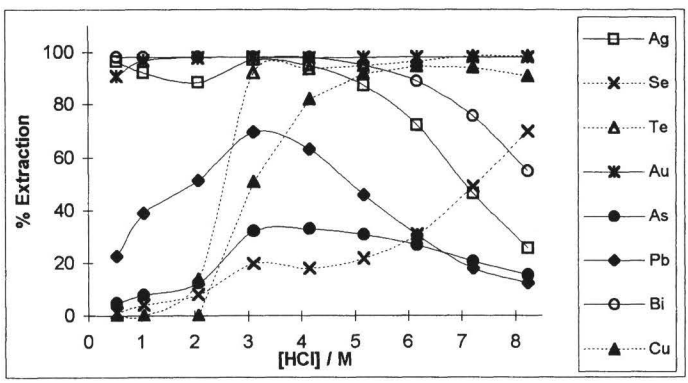


Figure 4 Extraction with 0.5 M Cyanex 925

The concentrations of the major impurities at maximum loading are shown in Table 1, together with the predicted levels in a resultant gold product. The results indicate that an upgrade from 7% Au in the feed solution to 99.9% in the loaded organic is feasible with the use of the Cyanex 471X reagent. Improvements on this figure can be expected with counter-current operation and the introduction of a scrub circuit. Preliminary results on the back-extraction of Au, indicate that stripping of Au into an aqueous phase is easily achieved with sodium thiosulphate. In a single contact of 0.1 M $Na_2S_2O_3$ with 0.26 M Cyanex 471X loaded with 2.6 g L^{-1} Au, 96% stripping was achieved. From a processing point of view, this is an advantage compared to reductive stripping to elemental gold, since the back extraction and gold recovery step can be separated. It is therefore considered that Au

recovery from copper anode slime leach liquors with Cyanex 471X is possible and other aspects of processing are currently being investigated.

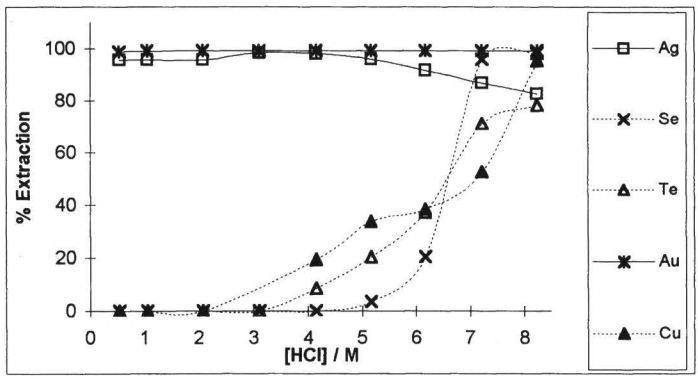


Figure 5 Extraction with 0.5 M Cyanex 471X

Element	Concentration in Solvent (mg L^{-1})	Calculated Au product purity (ppm)
Au	26690	99.9 %
Ag	0.55	20.6
Cu	0.09	3.4
Pb	0.03	1.1
Bi	0.09	3.4
Se	8.5	318
Te	9.4	353
As	0.02	0.8

Table 1 Level of major impurities in Cyanex 471X loaded with Au

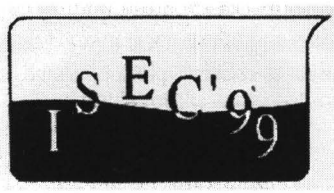
CONCLUSION

This work has demonstrated that solvent extraction of Au with Cyanex 471X can be applied to liquors derived by oxidative chloride leaching of copper anode slimes. This reagent has been shown to be selective over impurities such as Se, Te, Bi, Pb and Cu. Using a 0.26 M Cyanex 471X solution in toluene, Au was concentrated from 10 g L^{-1} in the feed liquor to 26 g L^{-1} in solvent with a corresponding increase in percent purity from 7% to 99.9% Au. Two other reagents, namely, Cyanex 923 and Cyanex 925 were also tested but were found not to be sufficiently selective for Au.

REFERENCES

1 Morrison BH, *Extraction Metallurgy '85*, IMM Symposium, London, pp 249, (1985).
2 Zarate G and Gonzalez F, in "*Copper 87, Hydrometallurgy and Electrometallurgy of Copper*", vol. 3, Ed. W.C. Cooper, G.E. Lagos and G. Ugarte, pp 499, (1987).

3 Hoffmann JE, Sutliff KE, Wells BA and George BD in *Proceedings of COPPER 95* International Conference, Ed. W.C. Cooper, J.E. Dutrizac, H. Hein, G. Ugarte, The Metallurgical Society of CIM, vol III, pp 42 (1995).
4 Feather A, Sole KC and Bryson LJ, *The Journal of the South African Institute of Mining and Metallurgy*, July/August 1997, pp 169.
5 Feather A, Sole KC and Bryson LJ, *Randol Gold Forum '97*, Monterey, California, USA, (1997).
6 Bilodeau A, Harris GB, Hooper K, MacDonald CA and Stanley RW, in *The Electrorefining and Winning of Copper*, Ed. J.E. Hoffmann, R.G. Bautista, V.A. Ettel, V. Kudryk and R.J. Wesely, TMS 116th Annual Meeting, Denver, Colorado, pp 527 (1987).
7 Segawa C and Kusakabe T, *1996 EPD Congress*, Ed. G.W. Warren, The Minerals, Metals & Materials Society, pp 43 (1995).
8 Thomas JA and Farias A, in *Proceedings to The First International Symposium on Precious Metals Recovery*, Nevada, USA, XXVIII, 112 (1984).
9 Fuwa A, *Metallurgical Review of MMIJ*, **4**(1), 98, (1987)
10 Martinez S, Navarro P, Sastre A and Alguacil FJ, *Hydrometallurgy*, 43, (1996)



STUDY OF A MICROEMULSION SYSTEM FOR APPLICATION IN THE EXTRACTION OF GOLD

Tereza Neuma de C Dantas, Afonso A Dantas Neto and Wendell F de La Salles
Universidade Federal do Rio Grande do Norte, UFRN/ PPGEQ-Campus Universitário, 59.072-970 - Natal/RN, Brazil

ABSTRACT
A microemulsion system has been studied for the extraction of gold from chloride media. The components of the system were: surfactant, saponified coconut oil; co-surfactant, n-butanol; kerosene, aqueous sodium chloride solution and either a standard aqueous solution of gold or a gold leachate. The effect of pH, salinity and concentration of active matter on the formation of the microemulsion have been studied. It was found that the best extraction was obtained with the gold leachate at a pH of 10.5 which gave a percentage extraction of about 68%. The gold could be re-extracted by solutions of hydrochloric acid, the optimum concentration being 8 mol/dm^3 when 99% of gold was recovered. The extraction parameters could be satifactorily correlated using the Scheffe Net model due to the multilinear behavior that these parameters have shown within the studied domain.

Keywords: microemulsion extraction, saponified coconut oil, gold, chloride,

INTRODUCTION

Gold is an exception in the economic crisis that the Brazilian's mineral and metallurgical industries are going through. Until some time ago, deposits that presented low gold concentrations were considered uneconomical for exploitation. Today, with the development and improvement of new hydrometallurgical extractive technologies special attention is being given to this particular area of study. In this work the main parameters that influence in the Winsor's phases were studied and the favorable conditions for the extraction of gold established starting from the aqueous solutions and leach, using microemulsions systems, already tested with success, for other metallic cations.

EXPERIMENTAL METHODOLOGY

The reagents used in the study were the following: n-butanol P.A.; Kerosene (Petrobrás); sodium chloride (NaCl) P.A.; sodium carbonate (Na_2CO_3) P.A.; OCS (saponified coconut oil - synthesized); standard solution of gold 1010 (g Au/cm^3 in 5% of HCl – SIGMA), leach of gold (8.24 ppm).

The system used in this study was as follows: Surfactant: OCS; Co-surfactant: n-butanol; Kerosene; NaCl and the aqueous solution of gold. This choice was based on the proven efficiency of this system in the extraction of other metallic cations.

Some parameters were studied that influence the microemulsion, such as: pH, salinity and C/T ratio. For the study of the pH aqueous solutions of gold were used with pH 0.31; 2; 4; 5; 7; 9; 10 and 11, obtained by the addition of a solution of Na_2CO_3, 0.5mol/dm^3, to an aqueous solution of gold 10.1 ppm (pH = 0.31).

After the pH study, the next step was to choose the best salinity and concentration of active matter (C/T ratio) that favoured all the Winsor's phases. The study was accomplished with the salinity varying from 0 - 6% of NaCl, for the ratios C/T = 1 and C/T = 2.

The extraction was carried out using as an experimental methodology, the Scheffe net. Points, distributed in Winsor's II phase, were prepared which were analysed with the objective of evaluating the behaviour of some important parameters in the study of the extraction.

The analysis of gold concentration in the aqueous phase was made by atomic absorption spectroscopy (λ = 242.8 nm, slit width = 1.0 nm).

© 2000 Society of Chemical Industry

The study of the re-extraction was carried out at the point where the best extraction results were obtained . The following reagents were tested for the re-extraction of the gold: Na_2CO_3 (3%); NaOH (6M), HCl (9.5mol/dm^3) and concentrated H_2SO_4. In all the cases a relative phase volume of microemulsion and solution of re-extraction used was 1:1.

RESULTS AND DISCUSSIONS

The results of the study of the pH, salinity and C/T ratio were appraised through the graphs presented in the figure 1:

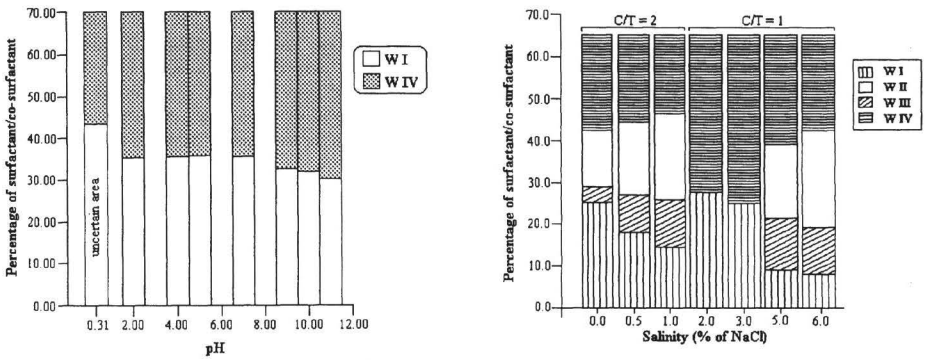


Figure 1 - Influence of the pH, C/T ratio and salinity on the Winsor's phases.

In the study of the pH it was observed that starting from the pH = 2, very defined areas were obtained that practically did not vary until pH = 7, with the increase of the pH the reduction was observed in Winsor I area. For continuation of the work pH = 10 was adopted, because it is the pH at which the gold is leached and that will be used later for extraction.

In the study of the salinity it was observed that for the ratio C/T = 1, only the Winsor II area was obtained for a very high salinity (above 5%).

For the ratio C/T = 2, the Winsor II area was obtained without the need of adding NaCl, this is due to the fact of the presence of other salts in the aqueous solution.

The best results were obtained to the ratio C/T = 2 and salinity above 1% of NaCl.

With the objective of verifying in a quantitative way the influence of the salinity in the Winsor's phases, diagrams of microemulsions were constructed for the systems 1 and 2, varying the salinity of NaCl percentage in aqueous solution, using the following compositions:

System 1: Surfactant: OCS; Co-surfactant: n-butanol; Kerosene; C/T = 2 ratio; Aqueous solution of gold, pH 10; 1% of NaCl.

System 2: Surfactant: OCS; Co-surfactant: n-butanol; Kerosene; C/T = 2 ratio; Aqueous solution of gold, pH 10; 2% of NaCl.

The result of this study is presented in figure 2 in which can be observed all the Winsor systems, as well as an increase of the area of WII when going from 1% for 2% NaCl.

A diagram was also constructed using a gold leachate as the aqueous phase, System 3 described below and shown in figure 3.

System 3: Surfactant: OCS; Co-surfactant: n-butanol; Kerosene; ratio C/T = 4; leachate of gold, pH 10.5; 2% of NaCl.

Initially this diagram was constructed for a ratio C/T = 2, even so the area of Winsor II obtained was very small, so the diagram was repeated with the ratio C/T = 4 with the objective of providing a more appropriate area to the study of the extraction.

In both studies (aqueous gold solution and leachate) it was observed that the area of WII is favourable for the extraction system.

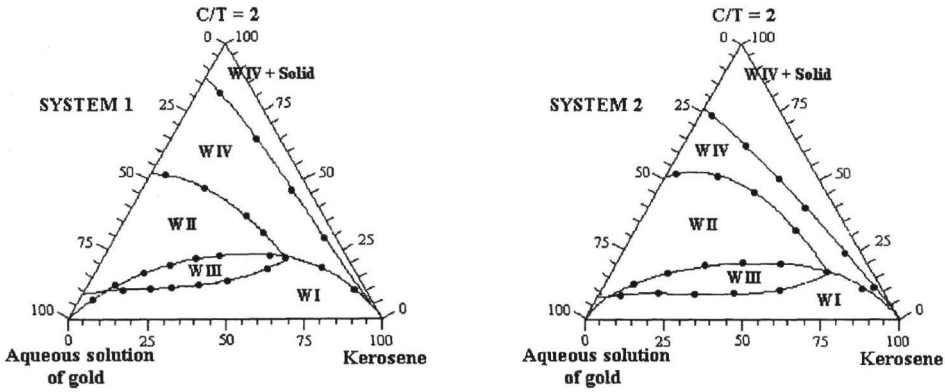


Figure 2 - Diagram of microemulsion for the aqueous solution of gold

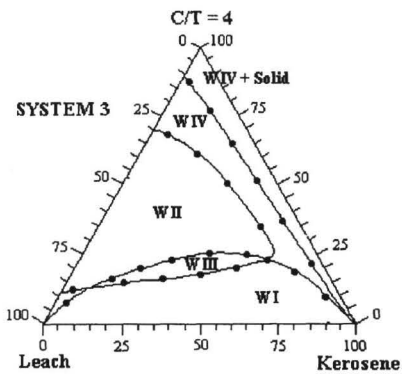


Figure 3 - Diagram of microemulsion for the leach of gold.

Extraction

The extraction was carried out on the three systems previously described, and figure 4 presents the points used for this study.

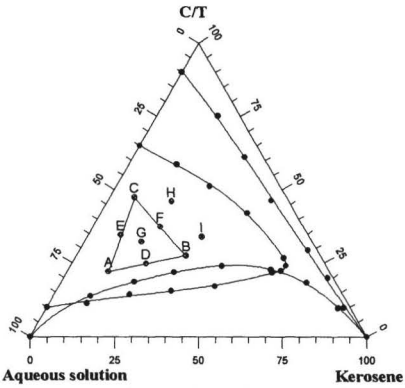


Figure 4 - Points used for the study of the extraction (Scheffe net)

Table I presents the results obtained in the analysis of the extraction, for the three systems studied .

				System 1		System 2		System 3	
Point	$X_{C/T}$	X_A	X_O	% E	Vr	% E	Vr	% E	Vr
A	21.99	65.80	12.21	38.91	1.34	11.31	1.18	32.52	0.99
B	27.40	40.10	32.50	57.97	5.36	31.13	4.09	50.18	3.17
C	47.36	45.29	7.350	80.40	15.3	61.21	7.27	89.41	4.75
D	24.75	53.25	22.00	41.65	2.60	16.60	1.99	46.68	1.85
E	34.60	55.77	9.630	53.88	3.56	48.85	2.67	68.62	1.93
F	37.28	42.72	20.00	57.18	6.84	40.31	4.82	75.66	3.93
G	32.20	50.81	16.99			18.60	2.73	64.54	2.40
H	46.00	35.00	19.00			10.46	1.57	88.82	7.69
I	33.99	32.02	33.99			46.01	7.48	68,00	6.60

Table I Composition of the points, extraction percentage and relative volume of the aqueous phases and microemulsion phase for the studied systems

The analysis of the results shows that the system 3 is the most favorable to the extraction of the gold by microemulsions, due to the fact that the extraction percentage extends up to 89.41%. Even so, the best extraction result occurred at the point "E" (system 3) where its composition is Xa = 0.5577; Xc/t = 0.346; Xo = 0.0963, for a relative volume of the aqueous phase and microemulsion phase approximately equal to 1.93:1.

In spite of the extraction percentage in the point "E" being only 68.62%, it is considered better than the points "C" and "H", due to its smaller value of Vr.

Model of the extraction system:

A model was made for the system which gave the best results for extraction (system 3), including the domain that presents the best perspectives of results for the evaluated parameters. The system was solved by using Math Cad software. The equations obtained by solving these systems was evaluated using an error analysis calculated for each parameter. The equation is acceptable for representing the parameter if it is in the range of error limits. The equations for the percentage extraction (%E) and relative volume of the phases (Vr), and the correlation curves (figure 5) for the calculated data and the experimental data are the following:

$$\%E = -1.033007X_{C/T} - 1.500587X_A - 4.948747X_O + 0.08806X_{C/T}X_A + 0.182054X_{C/T}X_O + 0.11349.X_AX_O - 0.003005X_{C/T}X_AX_O \quad (1)$$

$$Vr = 0.355971X_{C/T} + 0.03888X_A - 0.04144X_O - 0.006221X_{C/T}X_A + 3.17091x10^{-4}X_{C/T}X_O + 9.240073x10^{-4}X_AX_O - 4.051934x10^{-5}X_{C/T}X_AX_O \quad (2)$$

Equations 1 and 2 show that both parameters, extraction percentage (%E) and relative volume of the phases (Vr), were best adjusted by a reduced cubic equation, for a validity limit within 2% and 3.5%, respectively.

Re-extraction

In the re-extraction stage a new solution promotes the exchange of the gold in the complex, allowing the recovery of the metal in a new aqueous phase at a higher concentration. The results show that the solution of HCl is the best re-extraction agent. Because, H_2SO_4 reacted with the microemulsion (detected by the presence of a red coloration) harming the analysis of the results.

With the aim of determining the concentration of HCl where the best percentage re-extraction of gold is obtained, reextraction was carried out with different concentration of HCl (4, 6, 8 and 9.5 mol/dm^3). The best result was obtained for the concentration of 8 mol/dm^3 (1:1), where the percentage re-extraction was practically constant (around 99%).

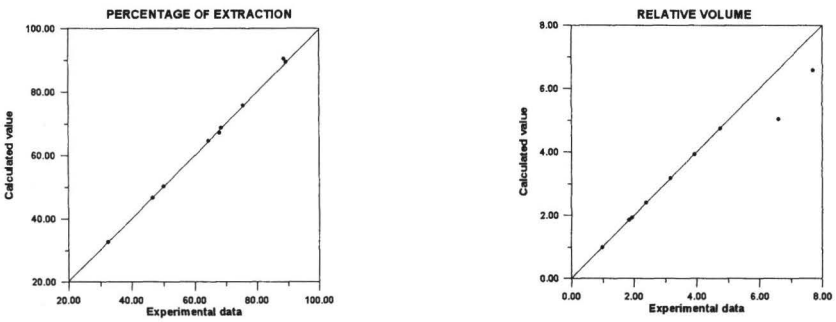


Figure 5 - Correlation Curves for Experimental and Calculated Data

Figure 6 presents the results obtained in the study of the best condition for re-extraction, including the re-extraction agent and the concentration of the HCl solution.

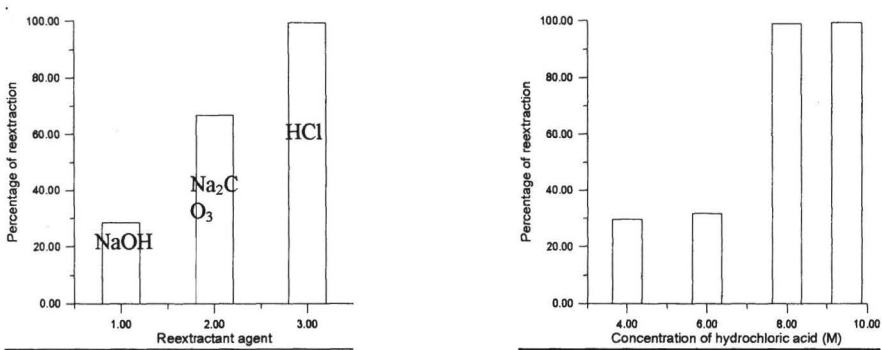


Figure 6 - Study of Re-extraction

CONCLUSIONS

The system which gave the highest percentage of gold extraction was: Surfactant: OCS; Co-surfactant: n-butanol; Kerosene and gold leachate, 2% NaCl, C/T=4, pH=10.5. The best

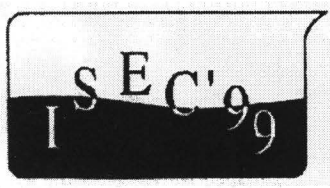
result of the extraction was obtained in the point "E" (system 3) where the composition of this point is: X_A = 0.5577; $X_{C/T}$= 0.346; X_O = 0.0963, for a phase relative volume (microemulsion and aqueous phases) approximately 1.93:1. The extraction percentage in this point was 68.62%.
The re-extraction process shows the best result using as stripping agent a solution of HCl (8 mol/dm^3) and a relative phase volume of 1:1 which gave a percentage reextraction of 99%.
The Scheffe Net model is a good tool for correlating parameters in extraction by microemulsions, due to the multilinear behavior that these parameters have shown within the studied domain.

NOMENCLATURE

OCS	saponified coconut oil.
W I,W II,W III,W IV	Winsor's phases.
$X_{C/T}$	mass fraction of co-surfactant/surfactant.
X_A	mass fraction of aqueous solution/leach.
X_O	mass fraction of kerosene.
%E	extraction percentage.
Vr	phase relative volume (ml).
(λ)	wavelength (nm)

REFERENCES

Barros EL. *Extração de Cobre Utilizando Microemulsões: Otimização e Modelagem, Master of Science Thesis*, UFRN-PPGEQ, Natal, (1996).
Cornell, JA. *Experiments With Mixtures: Designs, Models, and the Analysis of Mixture Data.* 2nd ed., Flórida, (1990).
Forestier JP, Puech E andTichadou J. *Int. J. of Cosmetic Science 7*, 233, 219, (1985).
Leite RHL. *Extração de Cromo de Efluentes de Curtumes Utilizando Microemulsões, Master of Science Thesis*, UFRN-PPGEQ, Natal, (1994).
Ramos AC. *Extração de Tungstênio Utilizando Microemulsões, Master of Science Thesis*, UFRN-PPGEQ, Natal, (1996).



PRODUCTION OF HIGH PURITY TANTALUM OXIDE BY SOLVENT EXTRACTION

Angus Feather[1], Paul Clark[2] and Gert Boshoff[3]
[1] Mintek, Randburg, South Africa
[2] SCMB Asset Management, Johannesburg, South Africa
[3] Usutu Pulp, Mbabane, Kingdom of Swaziland

ABSTRACT
A solvent-extraction process using a tertiary amine extractant to produce high-purity tantalum hydroxide powder has been evaluated on a pilot-plant scale. Tantalum, derived from the treatment of a Southern African-sourced tin slag, was selectively extracted from niobium and impurities in a fluoride medium. The tantalum hydroxide was calcined to produce tantalum oxide powder that exceeded 99.99% purity. Capital and operating cost estimates of the process are presented.

Keywords: Alamine 336, Aliquat 336, niobium, tantalum, fluoride medium

INTRODUCTION

Tantalum is extensively used in the electronics industry for the dielectric oxide coatings on capacitors. Other uses include tantalum carbide working surfaces on cutting tools, corrosion-resistant applications, and as alloying additives to high-temperature superalloys. Tantalum and niobium (columbium) commonly occur together, and their similar chemistry makes their separation difficult. A few suppliers have firm control of the supply of high-purity tantalum oxide products and the details of the refining technologies to produce them are tightly held.

The feed solution to the solvent-extraction (SX) process was derived from the leaching of an upgraded tantalum-containing tin slag. Tantalum was selectively extracted from niobium and other impurities using a tertiary amine extractant. The loaded organic phase was scrubbed to remove co-extracted impurities before tantalum was stripped from the organic phase and precipitated as the hydroxide in a single step using ammonium hydroxide. The tantalum hydroxide powder was filtered off, dried and then calcined to produce an oxide with a purity exceeding 99.99%.

Although the recovery of niobium hydroxide is beyond the scope of this study, it was envisaged that it would be recovered in a second SX step.

LABORATORY TESTWORK

Feed solution preparation

The feed solution to the SX circuit was prepared by leaching a tantalum-niobium intermediate concentrate in 25% (m/m) hydrofluoric acid at ambient temperature. The leach liquor produced contained 62 g/L tantalum and 93 g/L niobium.

Solvent system selection

Tantalum and niobium can be extracted from fluoride solutions using tri-*n*-butyl phosphate and methyl isobutyl ketone.[1,2] Both of these systems extract tantalum and niobium together, with the separation being achieved by the selective stripping of niobium. The extraction of tantalum using tertiary amines has also been reported.[3,4] In this study, the tertiary amine, Alamine 336 (trioctyl amine), and the quaternary amine, Aliquat 336 (tricaprylylmethyl ammonium hydroxide), were tested.

Because the phase disengagement characteristics of the system were relatively poor, various phase modifiers were tested. Diluents with varying extents of aromaticity were tested for their effect on both loading capacity and phase-separation characteristics. The optimised organic-phase composition consisted of 16 vol.% Alamine 336 and 4 vol.% isodecanol in the aromatic diluent Shellsol AB. The extraction isotherms measured under these conditions are shown in Figure 1.

© 2000 Society of Chemical Industry

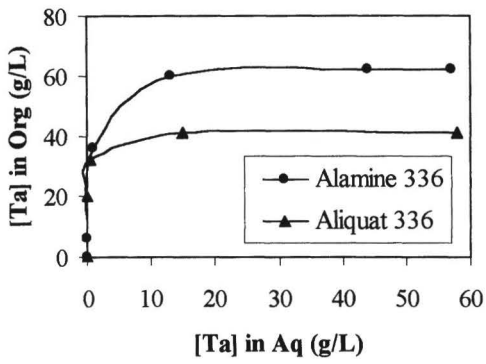


Figure 1. Tantalum extraction isotherms.

Although tantalum is preferentially extracted over niobium by the chosen solvent system, some niobium is co-extracted. Most of this co-extracted niobium can be squeezed off the loaded organic phase by carefully controlling the phase ratio in the extraction circuit. Any remaining niobium and other impurities that are less favourably extracted can be scrubbed off using 0.8 *M* nitric acid at an appropriate phase ratio.

A variety of stripping agents failed to adequately strip tantalum into an aqueous phase from either extractant. For this reason, ammonium hydroxide was chosen, which stripped the tantalum from the scrubbed organic phase by deprotonation of the amine and precipitated it as the hydroxide.

PILOT-PLANT TESTWORK

The process was tested on a pilot scale to generate mass balance data for a full-scale design. In addition, practical aspects such as phase separation and filtration were tested. At the same time, sufficient quantities of high-purity tantalum oxide were produced to supply to end-users for market evaluation.

Equipment

Ten conventional box-type mixer settlers were used for the extraction and scrubbing sections. Each mixer settler had a mixer volume of 500 mL and a settling area of 256 cm^2. Peristaltic pumps with appropriate tubing were used to feed aqueous solutions into the plant. A centrifugal pump and steady-head tank system with a control valve was used to regulate the organic flowrate. Interstage solution transfer was effected using pumping impellers in the mixer-settler units. The scrubbed organic phase was stripped in a 5 L mechanically stirred tank on a batch basis. Tantalum hydroxide was filtered from the stripped organic by vacuum filtration. All equipment was constructed of polypropylene or Teflon® and the plant was placed under a fume extraction hood for adequate ventilation. The flowsheet of the pilot plant is shown in Figure 2.

The plant was operated for two shifts per day (16 h) for twelve days. Each process stream was sampled at the end of each shift for analysis of major elements by inductively coupled plasma emission spectroscopy. The tantalum oxide powders were analysed by mass spectrometry.

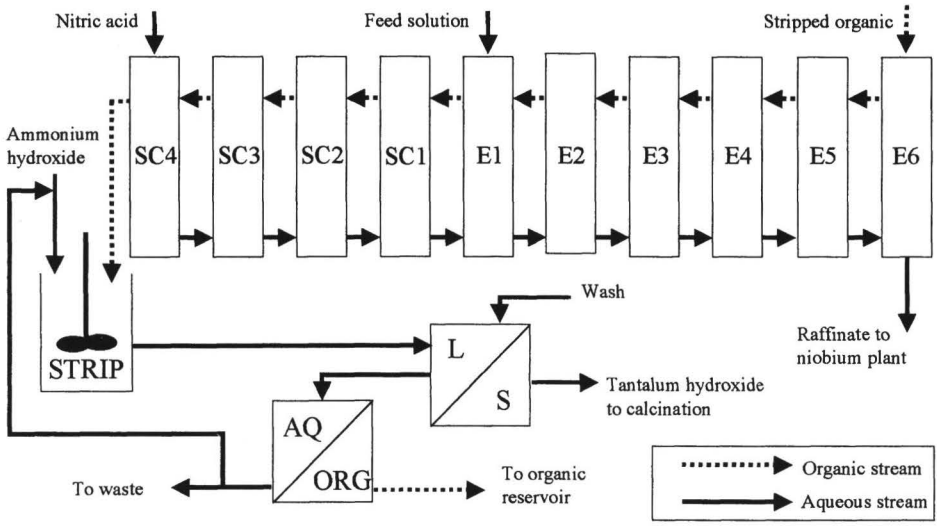


Figure 2. Pilot-plant flowsheet.

Extraction

During the pilot-plant campaign, batches of leach liquor containing between 15 and 35 g/L tantalum were processed. A typical leach liquor composition is shown in Table 1. The tantalum and niobium concentrations were lower than those in the solution used for the laboratory work.

Component	Concentration (g/L)	Component	Concentration (g/L)
Ta	18.1	Ca	0.2
Nb	32.8	Mg	0.03
Si	6.8	Sn	4.2
Fe	1.03	Mn	0.07
Ti	9.58	HF	50

Table 1 Pilot-plant feed solution

Operating the extraction section at a phase ratio (O:A) of 0.45, tantalum extraction efficiencies of 96 to 97% were achieved. At the same time, approximately 16% of the niobium and 2% of the calcium were co-extracted into the organic phase. The concentrations of tantalum, niobium, and calcium in the extraction section are shown in Table 2.

Element	Feed solution (g/L)	Raffinate (g/L)	Extraction efficiency (%)
Ta	18.1	0.63	96.5
Nb	32.8	27.6	15.8
Ca	0.200	0.195	2.5

Table 2 Tantalum and niobium in the extraction section

During the pilot-plant campaign, formation of a third phase was noticed. This was eliminated by increasing the isodecanol concentration in the organic phase from 4 to 10 vol. %. No significant phase-separation problems were noted. The small scale of operation caused the specific power input into the mixers to be high. This increased the entrainment of organic in the aqueous phase and was largely responsible for the measured settling duty requirement of approximately 1 $m^3/m^2/h$. The relatively poor phase separation of the system would not be a high economic burden due to the small size of a full-scale operation and the low cost of the organic reagents.

Scrubbing

The loaded organic phase was scrubbed with 0.8 *M* nitric acid at an O:A of 5.9. Niobium and calcium organic-phase concentrations were monitored to control the efficiency of the scrubbing section. These were reduced to acceptable levels in four stages. All other co-extracted impurities, with the exception of a small amount of manganese, were removed to less than 0.002 g/L in the scrubbing section. Table 3 shows the concentrations of tantalum and other impurities in the scrubbing section.

Element	Loaded organic (g/L)	Scrubbed organic (g/L)	Scrubbing efficiency (%)
Ta	38.8	34.7	10.6
Nb	11.5	< 0.002	> 99.9
Ca	0.12	< 0.002	> 99.9
Mn	0.009	0.002	77.8

Table 3 Tantalum and impurities in the scrubbing section

The spent scrub liquor was routed to the first extraction stage for the recovery of the tantalum scrubbed from the organic phase with the niobium. Approximately 10% of the tantalum on the loaded organic phase was recycled in this manner. The addition of a small amount of nitric acid to the extraction section did not adversely influence the process.

Stripping and calcination

Tantalum was stripped and precipitated from the scrubbed organic phase using ammonium hydroxide. Initially, this operation was carried out in a continuous mixer settler which had been designed to separate three phases. This proved impractical, and the stripping was subsequently carried out on a batch basis by mixing the scrubbed organic with a small volume of distilled water, and adding 8 *M* NH_4OH solution until an equilibrium pH of 7.5 to 7.8 was reached.

The tantalum hydroxide precipitate was filtered, washed with distilled water, and then washed with high-purity ethanol to remove traces of the organic phase. After drying, the precipitate was calcined at 950 °C to produce tantalum oxide. Table 4 compares the analysis of the tantalum oxide product from the pilot-plant campaign with that of one of the commercially produced tantalum oxide products (Cabot Corporation). Both oxides were analysed for all impurities detected and then the purity was calculated by difference.

CAPITAL AND OPERATING COST ESTIMATES

The capital and operating costs of a plant to produce approximately 9000 kg per year of high-purity tantalum oxide are summarised in Table 5. The plant costing does not include any crushing, grinding or pre-concentration that may be required to upgrade the tantalum-containing feed material. The leaching of the concentrate in hydrofluoric acid has been included.

The capital has been estimated by using the cost of the equipment from vendors. An installation factor was applied to the vendor cost of each item of equipment to arrive at an installed capital cost for the process.

Site preparation, engineering, and safety equipment costs were included in the estimate.

This estimate assumes that an existing building with utilities, management, analytical and technical support is available. Amortisation of capital, purchase of the tantalum concentrate, plant maintenance and insurance have been excluded from the operating cost. Effluents are discharged at defined battery limits and their disposal is not included in the operating cost estimate.

Element (mg/kg)	Pilot-plant product	Commercial product
Ta_2O_5 (%)	> 99.995	> 99.993
Nb	< 5	13
Mn	9	6
Sn	< 5	7
W	< 5	5
Mg	< 3	3
Si	< 3	10
Fe	< 3	10
Ca	5	3
Ti	< 3	6
Ag	3	3
Al	1	< 1

Table 4 Analysis of high-purity tantalum oxide

Cost item	Cost * (US$)
Installed capital	505 000
Operating (per annum)	
Fixed	55 000
Variable	155 000
Cost (per kg Ta_2O_5)	23.33
Cost (per lb Ta_2O_5)	10.61

* Costing is based on South African conditions and currency, and converted to US$. An exchange rate of R 5.80 = US$ 1.00 was used.

Table 5 Capital and annual operating cost estimate

CONCLUSIONS

A simple, relatively inexpensive solvent-extraction route for the production of tantalum oxide has been tested on a pilot-plant scale. Concentrates with a wide range of tantalum concentrations can be processed, although some of these concentrates may require pre-concentration or impurity removal.

The purity of the tantalum oxide product from the process is comparable with that of other commercially available oxides. The product from the pilot-plant campaign consistently exceeded 99.99% purity.

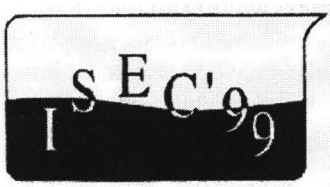
After removing tantalum from the raffinate, a similar circuit could be used to produce a niobium oxide powder. It is unlikely that the niobium would require the same degree of purification as the tantalum, as its main market use is as a steel additive.

ACKNOWLEDGEMENTS

This paper is published by permission of Mintek. The amine extractants and the phase modifier were kindly supplied by Henkel. The authors would like to thank the staff of Mintek's Analytical Science Division for their efforts during the pilot-plant campaign.

REFERENCES

1. Soisson DJ *et al.*, *Ind. Eng. Chem.*, November 1961, 99.
2. Iorio G and Tyler MS, *Mintek Report, No. M292*, (1987).
3. Mizza M *et al.*, *Analyt. Chim. Acta.*, , **37**, 402, (1967).
4. Markland SA, *Proc ISEC '74,* Society of Chemical Industry, London, **3**, 2185, (1974).



RECOVERY AND PURIFICATION OF CERIUM(IV) AND THORIUM(IV) FROM BASTNASITE ORE

Jun Lu, Deqian Li, Jide Tang and Tingming Zheng
Laboratory of Rare Earth Chemistry and Physics, Changchun Institute of Applied Chemistry, Chinese Academy of Sciences, Changchun, 130022, China

ABSTRACT
A simple method has been developed for separating cerium and thorium from bastnasite ore in Sichuan province. The bastnasite was leached with H_2SO_4 after being calcinated and the addition of boric acid. The effects of the amount of H_2SO_4 on the cerium recovery were investigated. The leaching solution was then diluted with 1mol/dm^3 H_2SO_4 and extracted by primary amine N1923. The addition of boric acid does not affect the extraction of Ce(IV) by N1923. Having been scrubbed with H_2SO_4 the loading organic phase was stripped with a solution containing different mineral acids and H_2O_2. The dependence of Ce(IV) percentage stripping on the acidity of H_2SO_4 and HNO_3 is investigated. The stripping of cerium from the loaded organic phase by H_2SO_4 and H_2O_2 has a low efficiency but high recovery of cerium can be obtained by stripping with HNO_3 and H_2O_2. Cruds, emulsions and precipitates did not appear in the presence of addition of boric acid, which was the vital factor for extraction of cerium from bastnasite.

Keywords: cerium(IV), thorium(IV), bastnasite ore, primary amine N1923, boric acid

INTRODUCTION

The method of precipitating trivalent rare earths as double sulphate salts with sodium sulphate is usually employed to recover trivalent rare earths and cerium dioxide from bastnasite and monazite. However, the percentage recovery of trivalent rare earths and cerium dioxide is low, only 60-70% rare earths and cerium dioxide being obtained in production and the highest purity of cerium dioxide obtained by this method is always 99% which cannot meet the trend in commercial usage of rare earths for 'high technology' applications. Furthermore this method yields some radioactive waste solids and waste water containing Th(IV). Thus the method of solvent extraction which could be used to recover Ce(IV) and Th(IV) from the bastnasite leaching solution becomes more attractive.[1,2]

The extraction of Ce(IV) and Th(IV) by Primary amine N1923 has been studied.[3,4] This extractant has also been employed to extract Th(IV) from the sulphuric acid liquor of bastnasite in the absence of fluoride ion. It is showed that N1923 can extract Th(IV) from trivalent rare earths selectively and effectively. It also demonstrated that fluoride ion which is one of the main elements in bastnasite would interfere in the extraction of Th(IV) by N1923. Furthermore, cruds, emulsions and precipitates may occur in the extraction of Ce(IV) from bastnasite by N1923 which could block the extraction. In this paper boric acid was added to prevent the appearance of precipitates and to investigate the possibility of recovery of Ce(IV) and Th (IV) from bastnasite.

EXPERIMENTAL

Reagent

Primary amine N1923 ($R_1R_2NH_2$) with a total number of carbon atoms of 19~23, was supplied by Shanghai Institute of Organic Chemistry, Chinese Academy of Sciences, and was diluted directly with kerosene without any purification.

Leaching studies

The bastnasite concentrate was calcined in air at about 500°C in a rotary kiln. A batch of the calcine was made into a sludge by adding boric acid and water and then the sludge was leached with concentrated sulphuric acid, preliminary tests showed that leaching by the method could produce the same recovery as leaching by diluted H_2SO_4 and the leaching reaction is quick so that the cerium

© 2000 Society of Chemical Industry

recovery is independent on the leaching time over the range of 1 to 24 hours. The leaching tests were usually carried out with only occasional manual stirring. The sludge was filtered to obtain a leach liquor containing RE(III), Th(IV) and Ce(IV) and was washed with 0.5mol/dm^3 H_2SO_4 to recover the residual rare earths.

Solvent extraction studies

Both extraction and stripping experiments were carried out using the following procedure: certain volumes of organic and aqueous solutions were placed in separatory funnels and shaken for 30 minutes at room temperature after which time the phases were separated by centrifugation.

Analytical methods

The concentrations of Th(IV) was determined spectrophotometrically by the Arsenazo III method after extraction by PMBP. The absorption of Th(IV) was measured at 660nm. The concentration of Ce(IV) in aqueous phase was determined by titration with standard $(NH_4)_2Fe(SO_4)_2$ using o-phenanthroline as indicator.[5,6] The solution containing Ce(IV) and Ce(III) was oxidized by $(NH_4)S_2O_8$-$AgNO_3$ solution, then the concentration of Ce_{total} was determined by the same procedure as for the Ce(IV) determination. The concentration of metal ions in the organic phase was determined by difference. The sulfuric acid concentrations of the aqueous and organic phases were obtained by titrating with standard NaOH solution, using phenolphthalein as an indicator.

RESULTS AND DISCUSSION

Selection of leaching acid medium

The leaching of bastnasite with sulphuric acid was more effective than with nitric acid under comparable conditions. As shown in table 1 the cerium recovery increases with the increase in the ratio of acidity to bastnasite and the maximum recovery of cerium could be reached at the ratio of 0.9:1 for

Sulphuric acid medium				Nitric acid medium		
Ratio of acid to bastnasite (g/g)	H_3BO_3 /bastnasite (g/g)	percentage of Ce(IV) in total cerium(%)	cerium recovery (%)	Ratio of acid to mine (g/g)	percentage of Ce(IV) in total cerium(%)	cerium recovery (%)
0.7:1	0	94.2	86.8	0.70:1	78.0	67.1
0.9:1	0	93.7	88.4	1.08:1	89.3	85.3
1.1:1	0	93.8	89.0	1.43:1	90.3	90.1
1.3:1	0	93.9	88.9	1.80:1	85.4	91.4
1.4:1	0	93.9	90.6	2.6:1	80.4	68.0
0.7:1	0.05	95.1	89.3	3.8:1	83.3	89.1
0.9:1	0.05	95.0	89.5	5.0:1	84.2	92.4
1.1:1	0.05	94.8	89.7	6.2:1	84.3	89.0
1.3:1	0.05	95.5	89.2	5.8:1	79.2	85.5
1.4:1	0.05	95.2	90.2			

Table 1 The effect of ratio of mineral acid to bastnasite on the leaching

the leaching with sulphuric acid and at the ratio of 1.08:1 for the leaching with nitric acid. The percentage of cerium(IV) in the total cerium in the nitric acid leaching solution is so low that the leach liquor cannot be used as the feed of extraction of Ce(IV) directly. So sulphuric acid was chosen as the leaching acid for further studies. It can also be seen in table 1 that nearly 10% of cerium was left in

residue which should be leached more than once to get a high recovery. The residue was leached again and a high recovery of 98% was obtained.

Effect of addition of boric acid on leaching process

Fluoride exited in the leach liquor as a complex with cerium(IV). Preliminary tests showed that little fluoride was extracted by N1923 into the organic phase. After the extraction of Ce(IV), a large number of fluorides will be released and these fluorides could precipitate with trivalent rare earths. So it is necessary to add appropriate amounts of substances to the leach solution to diminish the free fluoride concentration by the formation of stable complexes (Al^{3+}, Fe^{3+} etc.). In this paper boric acid was chosen as the additive and a higher efficiency of reduction of free fluorides can be achieved by adding boric acid before leaching than after leaching. The effect of the amount of boric acid added in the leach solution on the leach process is shown in tables 1 and 2 in terms of the percentage recovery of cerium into the leach liquor. It can be seen that addition of boric acid is almost without effect on the first leaching efficiency.

ratio of boric acid to bastnasite	cerium (g/L)	percentage of Ce(IV) in total cerium, %	cerium recovery, %
0	22.4	94.3	87.0
0.01:1	22.7	94.2	88.0
0.03:1	22.7	94.4	87.9
0.05:1	22.5	94.7	87.3
0.1:1	22.3	94.3	86.4

Table 2 The effect of the ratio of boric acid to bastnasite on the first leaching

Studies on the Ce(IV) extraction by N1923

It has been reported that Ce(IV) and Th(IV) can be extracted from sulphuric acid solution with high efficiency by the primary amine N1923. Standard Ce(IV) can be separated from trivalent rare earth elements with a high separation factor. The extraction mechanism of Ce(IV) is shown:[3]

at low aqueous acidity:

$$Ce^{4+} + 2SO_4^{2-} + 2(RNH_3)_2SO_4 \rightleftharpoons (RNH_3)_4Ce(SO_4)_4$$

and at high aqueous acidity:

$$Ce^{4+} + 2SO_4^{2-} + 4RNH_3HSO_4 \rightleftharpoons (RNH_3)_4Ce(SO_4)_4 + 2H_2SO_4$$

Th(IV) can be recovered efficiently by extraction with 1%N1923-1%ROH-98% kerosene, washing with 0.06-0.08 mol/dm^3 HNO_3, stripped with 0.4-0.6mol/dm^3 HNO_3. The percentage recovery of Th(IV) is above 99% with a high purity of 99%. Little literature reports the extraction of cerium by N1923 in sulphuric acid solution containing fluoride, especially with the addition of boric acid.

ratio of boric acid to bastnasite	extraction percentage of Ce(IV)	saturation capacity of N1923(g/dm^3)
0	94.6%	16.4
0.040	94.5%	16.3
0.050	94.4%	16.7
0.060	95.1%	16.4
0.080	94.9%	16.8

Organic phase :15% N1923 - 6% ROH- 79% kerosene,
Aqueous phase: Ce(IV) 23.4g/dm^3, H_2SO_4 1.58 mol/dm^3, O/A: 2:1

Table 3 The effect of addition of boric acid on the Ce(IV) extraction by N1923

The boric acid had little effect on the extraction behavior of Ce(IV), as shown in table 3, The extraction percentage of Ce(IV) by the organic phase containing 15% N1923 - 6% ROH- 79% kerosene and the capacity of this organic phase for Ce(IV) were independent on the addition of boric acid.

The extraction of Ce(IV) by N1923 is very effective and almost 94% Ce(IV) can be extracted into organic phase by one stage and the capacity of this organic phase is 16.4 g/dm^3, no precipitation occurred during the extraction process.

Studies on the stripping

The stripping of Ce(IV) from the loading organic phase with sulphuric acid was determined by the formation of the loading organic phase. Figure 1 shows the stripping of loading Ce(IV) organic phase by the solution containing sulphuric acid and H_2O_2. When the loading organic phase was obtained from the extraction of standard cerium bisulfate solution, a high recovery of cerium by stripping with sulphuric acid and H_2O_2 can be obtained(♦). However when the loading organic phase was formed from the leach liquor, the recovery is poor, no more than 10% of cerium in the loading organic was stripped(●), just same as the result of washing with sulphuric acid(□).

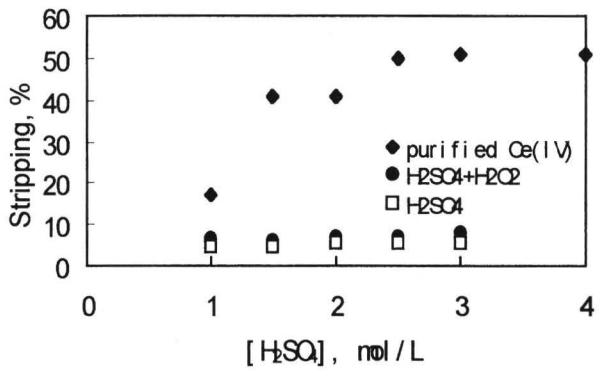


Figure 1 Effect of sulphuric acid concentration on Ce(IV) stripping
loaded organic phase obtained from purified $Ce(SO_4)_2$ solution(♦):
Ce(IV) 16.4 g/dm^3, 15% N1923-6% ROH-79% kerosene
loaded organic phase obtained from leach solution(●,□):
Ce(IV) 16.4 g/dm^3, 15% N1923-6% ROH-79% kerosene
aqueous phase : H_2SO_4 + 3% H_2O_2(v/v)(♦), H_2SO_4 + 3% H_2O_2(v/v)(●),
H_2SO_4 (□)

The effect of nitric acid concentration on the stripping was also investigated, a high recovery of cerium from the loading Ce(IV) phase was obtained by extraction of leach solution with N1923 as shown in figure 2. The recovery of cerium increases with the increase in the acidity and the stripping efficiency reached a plateau in the region of 0.5 mol/dm^3 HNO_3. The addition of boric acid showed little effect on the stripping.

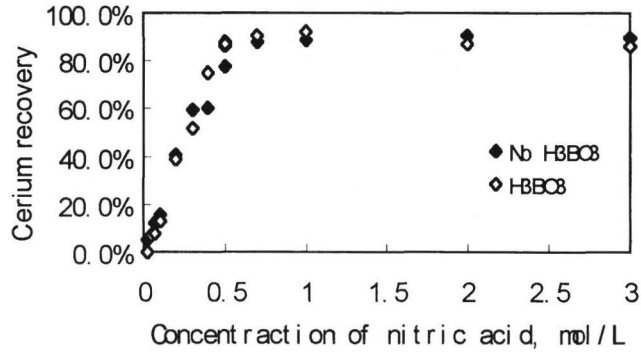


Figure. 2 Effect of nitric acid concentration on Ce(IV) stripping
Organic phase: Ce(IV) 16.4 g/dm^3, 15% N1923-6% ROH-79% kerosene
Aqueous Phase : HNO_3 + 3% H_2O_2(V/V)

A flowsheet for recovery Ce(IV) and Th(IV)

Cerium can be recovered by stripping with nitric acid effectively, however as previously shown[4] Th(IV) was also completely stripped into aqueous phase.

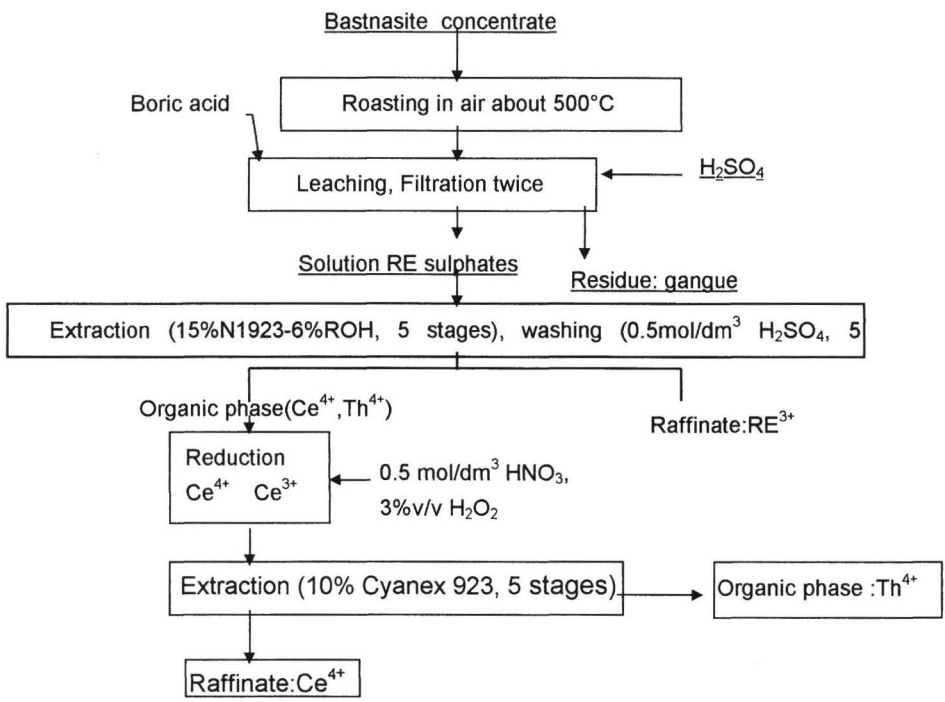


Figure 3 Flowsheet for recovery of cerium and thorium from bastnasite

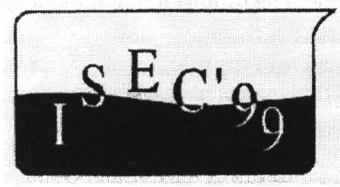
Another excellent extractant Cyanex 923 which can extract Th(IV) from trivalent rare earths with high efficiency[7,8] could be used to recover Th(IV) from the stripped solution. Based on these thoughts a flowsheet to recover Ce(IV) and Th(IV) was proposed for further continuous tests.

ACKNOWLEDGEMENT

This project was supported by the National Program entitled "Basic Research of Rare Earths" and National Natural Science Foundation of China.

REFERENCES

1. Li DQ, Wang ZH, Zeng GF and Xue ZY, *J. Chinese Rare Earth Society*, **2**, 9, (1984).
2. Huang XW and Zhang GC, *Chinese Patent, CN-1133346.*
3. Li DQ, Wang ZH and Zeng GF, *Nucl. Chem. & Radio. Chem.*, **6**, 153, (1984).
4. ChangChun Institute of Applied Chemistry, *Collecting on Rare Earth Extraction*, 125, (1976).
5. Busev AI, Tiptsova VG and Ivanov VM, *Analytical Chemistry of Rare Elements* (English translation), Mir publishers Moscow(1981).
6. Zhen-zhou Y, *Chemical Analysis of Th(IV) and U(IV) from Rock and Ore*, Atomic Energy Press, (1980). (in Chinese)
7. Lu J, Li DQ, Wei ZG and Jiang ZC, *Acta Metallurgica Sinica.*(in press)
8. Lu J, Wei ZG, Li DQ, Ma GX, Jiang ZC, *Hydrometallurgy* (in press)



PRECIPITATION STRIPPING OF SAMARIUM HYDROXIDE FROM TRI-*n*-BUTYL PHOSPHATE WITH AQUEOUS NaOH SOLUTIONS

K Koyama and M Tanaka

Materials Processing Department, National Institute for Resources and Environment, MITI, 16-3 Onogawa, Tsukuba, Ibaraki 305-8569, Japan

ABSTRACT

In this study, a method of precipitation stripping from organic solution consisting of tri-n-butyl phosphate (TBP) loaded with samarium by reaction with aqueous NaOH solution at room temperature was investigated to increase the use of solvent extraction. The precipitation rate with NaOH solution is fast and precipitation of more than 99% is obtained within 60 seconds. These precipitates were identified as $Sm(OH)_3$ from X-ray diffraction analysis. When a more dilute NaOH solution is used, precipitates cannot be found though samarium is completely stripped. This result is attributed to the decrease of the OH^- ions which react with nitric acid simultaneously extracted with samarium by TBP. An aqueous NaOH solution whose concentration is higher than that of nitric acid extracted by TBP in an extraction stage is found to be necessary for the precipitation stripping.

Keywords: precipitation stripping, TBP, samarium, rare earth metals

INTRODUCTION

Solvent extraction is now widely used in the recovery of certain base metals and rare earth metals. A conventional solvent extraction circuit is associated with a step of electrowinning or precipitation using gas or precipitant. In order to develop a new recovery method of metals from aqueous solutions and enlarge the use of solvent extraction, a single-stage precipitation stripping method in which metal ions are stripped from an organic phase and simultaneously precipitated have been proposed.[1,2]

Some studies on the precipitation stripping methods using carboxylic acid as extractant have been reported.[3,4] However, few studies on this method with other extractants, such as tri-n-butyl phosphate (TBP) or tri-octylamine (TOA), have been reported.

Trivalent rare-earth metals are moderately well extracted by TBP. In this paper, precipitation stripping of samarium hydroxide from an organic solution containing TBP was examined.

EXPERIMENTAL

The extractant used was TBP, and it was diluted in kerosene without further purification. Concentrations of TBP used were 20-100 vol%. Aqueous solutions of samarium were prepared by dissolving pure samarium oxide in nitric acid. Samarium-loaded TBP solutions were prepared by solvent extraction from aqueous solutions into TBP-kerosene solution. Organic solutions containing samarium were used without being passed through a phase-separation paper in order to remove entrained water. The initial concentration of samarium in the organic phase was varied from 0.01-0.3 kmol m^{-3}. An aqueous sodium hydroxide solution was used as stripping agent. The aqueous solution was prepared with deionized water having a specific resistivity of 5×10^6 Ω cm.

A 50 cm^3 volume of samarium-loaded organic solution was shaken vigorously with an equal volume of stripping agent for 15 minutes. In order to study the stripping rate of samarium, organic solution was mixed with aqueous stripping solution using an impeller. The experimental temperature was 298K.

Samarium concentration was measured by the titration with EDTA. The precipitates were characterized by X-ray diffraction analysis (XRD).

© 2000 Society of Chemical Industry

RESULTS and DISCUSSION

Stripping experiments were conducted using deionized water and aqueous solution of 1 kmol/m^3 NaOH as stripping agent. Figure 1 shows the time variation of the stripping percentages of samarium. In this experiment, samarium-loaded TBP solution and the aqueous solution were agitated at 3.3 s^{-1} using an impeller. Stripping rate was fast and more than 99% was stripped within 60 seconds. In addition, the equilibrium value was obtained within 2 minutes under any condition. Initial strippng rate with 1 kmol/m^3 NaOH solution was lower than that with deionized water, due to the difference in the dispersion of the organic solution. Precipitates were obtained using 1 kmol/m^3 NaOH solution. An emulsion phase cannot be observed between the organic and aqueous phases after settling. Precipitates were easily settled at the bottom of an aqueous phase.

The precipitates were filtered, washed with deionized water and acetone, and dried at room temperature. For comparison of precipitate characteristics, samarium hydroxide was prepared by the following procedure. Aqueous NaOH solution of 1 kmol/m^3 was added to a nitric acid solution containing samarium of 0.001 kmol/m^3. XRD patterns were observed for the precipitates by the two different methods. It was found that these precipitates were samarium hydroxide, $Sm(OH)_3$, and there was no difference in crystallinity between these samples.

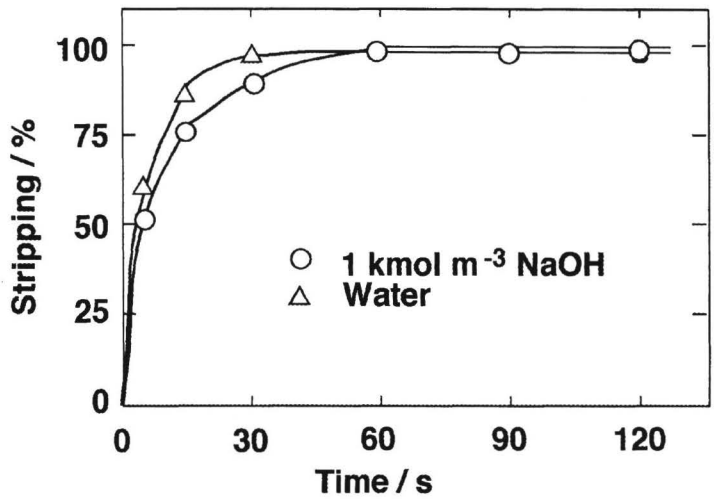


Figure 1 Time variation of percentage stripping.
(Initial soln. Sm^{3+} 0.21 kmol/m^3, HNO_3 2.0 kmol/m^3,Org. soln 50 vol% TBP in kerosene)

The concentrations of NaOH in the stripping solution were varied to examine the effect of NaOH concentration on the stripping precipitation. Figure 2 shows the percentages of samarium in aqueous stripping solution and pH values of the aqueous solution after stripping. When the NaOH concentration was less than 0.46 kmol/m^3, samarium in the organic solution was completely stripped into the aqueous solution but was not precipitated as samarium hydroxide. On the other hand, when the NaOH concentration was more than 0.46 kmol/m^3, the concentration of samarium in the aqueous solution was less than 0.0001 kmol/m^3. However, precipitates of samarium hydroxide were obtained. From an E-pH diagram,[5] samarium hydroxide is found to be formed at pH>7.2 in an aqueous solution containing samarium of 0.01 kmol/m^3. In this experiment, the pH value of the aqueous solution after stripping gradually increased with NaOH concentration and greatly increased at NaOH concentration of

about 0.46 kmol/m^3. TBP extracts nitric acid as well as samarium. Nitric acid concentration extracted into the organic solution was measured by stripping with deionized water. In this extracting condition, a 0.44 kmol/m^3 nitric acid was extracted. This value corresponded with the NaOH concentration where stripping percentage of samarium changed greatly. When NaOH concentration was more than 0.46 kmol/m^3, an amount of OH^- ions was larger than that of H^+ ions extracted into the organic solution. As a result the aqueous solution after stripping became alkaline, and samarium hydroxide was precipitated.

Some experiments were conducted to examine the effect of the concentration of HNO_3 in the aqueous solution used for the preparation of samarium-loaded TBP solutions. The concentrations of HNO_3 considered were 0.8, 2.0 and 10.0 kmol/m^3. Figure 3 depicts the relationship among the pH value of the aqueous solution after stripping, the concentration of NaOH in the stripping solution, and the concentration of HNO_3. NaOH concentration where the pH values changed greatly were 0.060, 0.46 and 1.78 kmol/m^3, respectively. Each value corresponded with the concentration of H^+ extracted into the organic solution.

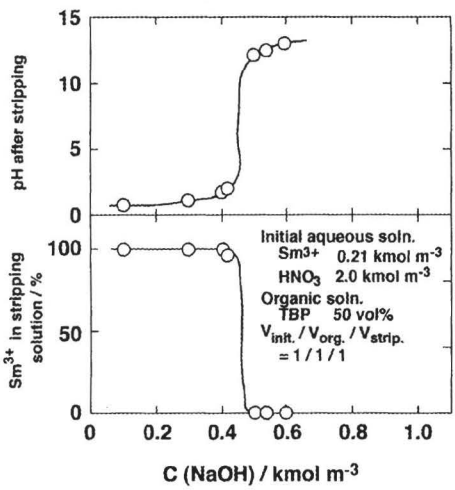


Figure 2 Effect of NaOH concentration on stripping percentage of Sm^{3+} and pH value after stripping.

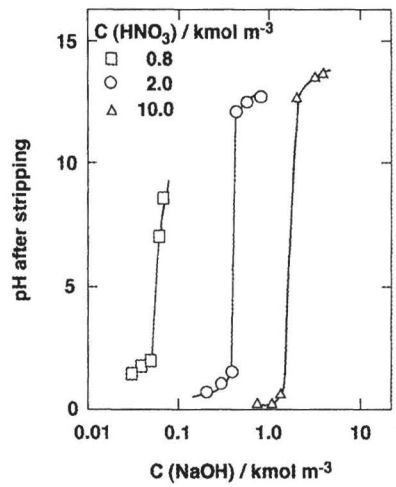


Figure 3 Effect of HNO_3 concentration on the pH value after stripping.

The purity of the precipitates from the stripping precipitation method was examined. Carbon concentrations are listed in Table 1. Precipitates after washing with both deionized water and acetone contained 1.2 wt% carbon which was due to mechanical entrainment of the extractant and the organic solvent. However, the carbon concentration of precipitates after roasting at 1000K became less than 0.01wt%.

Washed with water and acetone	1.2 wt%
Roasting at 1000 K	<0.01 wt%

Table 1 Carbon concentrations in precipitates

CONCLUSIONS

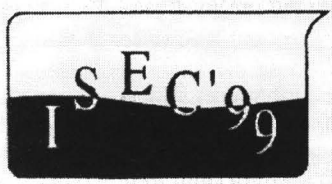
A precipitation stripping method from an organic solution of TBP loaded with samarium by the reaction with aqueous NaOH solution at room temperature was studied to develop a new recovery method for rare metals from aqueous solutions and enlarge the use of solvent extraction.

The precipitation rate with NaOH solution was fast and more than 99% precipitation was obtained within 60 seconds. An aqueous NaOH solution whose concentration was higher than that of nitric acid extracted by TBP in an extraction stage was found to be necessary for the precipitation stripping.

When the aqueous NaOH solution of 1.0 kmol/m^3 was used as stripping agent, precipitates were obtained and confirmed to be $Sm(OH)_3$ from XRD analysis. Carbon concentration of these precipitates was 1.2% due to the contamination by the extractant and/or organic solvent and can be reduced to less than 0.01% by roasting at 1000K.

REFERENCES

1. Monhemius AJ and Thorsen G *ISEC'80, Proc. Int. Solvent Extraction Conf.*(Liege, Belgium). **3**, 80, (1980).
2. Doyle FM and Monhemius AJ, *Hydrometallurgy*, **35**, 251, (1994).
3. Konishi Y, Asai S and Murai T, *Ind. Eng. Chem. Res.*, **32**, 937, (1993).
4. Shibata J, Okuda A, Sano M and Nishimura S, *J. Min. Metal. Inst. Japan*, **104**, 97, (1988).
5. Pourbaix M, *Atlas of Electrochemical Equilibria in Aqueous Solutions*, Pergamon Press, Oxford, (1966).



NEW EXTRACTION TECHNOLOGIES FOR THE TREATMENT OF RARE METAL RAW MATERIALS USING MECHANOCHEMICAL METHODS

SV Chizhevskaya, AM Chekmarev, MV Povetkina, VL Shafirov and M Cox[1]

D. Mendeleev University of Chemical Technology of Russia, Moscow, Russia

[1]University of Hertfordshire, Hatfield, UK

ABSTRACT

Eudialyte is a complex raw material with high silicon content that is an important source of a number of rare metals. This mineral, which is easily decomposed using mineral acids, is used to discuss the application of new extraction technologies. These combine leaching and liquid-liquid extraction for the concentration and separation of zirconium and rare earths using TBP saturated with nitric acid, with mechanoactivation of the mineral to increase the overall efficiency of the process. Two alternative strategies are discussed, the first of which involves mechanoactivation in the presence of the organic leaching/ extraction reagent, and the second a pre-activation of the ore before contact with the organic phase. Results indicate that the second process gives excellent recovery of zirconium and yttrium following a brief period of mechanoactivation. In all cases an easily filterable pulp was obtained with no problems resulting from the high silica content of the ore.

Keywords: silicic acid, interfacial cruds, stable emulsions, mechanochemical assisted extraction, TBP.

INTRODUCTION

The commercial use of relatively low-grade sources of metals is becoming increasingly more important to meet the needs of industry for mineral raw materials, among which are the rare metals. This leads to a sharp rise in the cost of production and hence the price of the metals to the consumer. Such increases can be offset by solving the following problems: the use of complex ores and introduction of new technological tools and schemes in extractive metallurgy.[1]

The main world industrial source of zirconium, one of the important rare metals used extensively not only in the nuclear industry but also in advanced ceramics, refractory materials, glazes, etc. is still zircon $ZrSiO_4$ (ZrO_2 - 67%, SiO_2 -33%) which however is also one of the most resistant minerals to decomposition. Also the high silica content in the resulting feed solution posed a major problem for many plants using TBP solvent extraction for the extraction of zirconium and separation from hafnium.[2-6] Therefore many technological flowsheets for zircon processing are based on the removal of most of the silica before acid leaching.

A potential industrial source of zirconium and rare earths is eudialyte, a complex zirconosilicate (ZrO_2 - 10-15%, $SiO_2 \geq 50\%$). Examination of the crystal structure indicates that the mineral can be represented by the formula: $Na_{12}Ca_6Fe_3Zr_3[Si_3O_9]_2[Si_9O_{24}(OH)_3]_2$.[7] Along with zirconium and rare earths, the mineral also contains niobium, tantalum, titanium and some other elements. Weak chemical bonds between separate fragments of the mineral allow easy decomposition by mineral acids. However, during leaching the large amount of silica in the concentrate leads to the formation of difficulty filterable pulps and a low concentration of the desired elements. Therefore most of known processes for the decomposition of eudialyte concentrates are based on the application of sulfuric acid with results in the formation of silica in easily filterable form.

In practice it is impossible to decrease significantly the content of silica in concentrate before leaching. At best it is only possible to remove the silica from the admixture minerals contained within the composition of the concentrate.[8] To obtain easily filterable pulps from the leaching of eudialyte concentrates by nitric or hydrochloric acids special techniques are necessary, which lead to prolongation of the process, increase of costs, etc.

The problems of hydrometallurgical processing of raw materials with high silica content result from the behaviour of the silica that dissolves during leaching with mineral acids. This soluble silica readily undergoes polymerization and condensation in solution forming polynuclear silicic acid species with various compositions and structures, finally resulting in stable gels. These polymeric species impede filtration, reduce the extraction of desired components and inhibit subsequent solvent

© 2000 Society of Chemical Industry

extraction by forming interfacial films, cruds, and stable emulsions.[2-6, 8-12] Various techniques have been used which largely overcome such difficulties,[10] particularly to carry out high removal of silica from the feed solution.[13]

In recent years mechanochemical methods have become one of the most effective advanced methods to be introduced for the treatment of raw materials.[14-16] Preliminary mechanical activation of raw materials allows significantly increased recovery of desired components, decrease in reagent consumption, and the number and duration of stages of treatment.

In earlier publications[17,18] it was shown that by using short-term mechanoactivation of eudialyte concentrate with the high energy devices described here it was possible to intensify the acid leaching of eudialyte concentrate to provide a high degree of dispersion and preservation of the general framework of the crystal structure. We have established that preliminary short-term (30 seconds) mechanical treatment of eudialyte concentrate in the high energy activator D1 or in the planetary activator AGO-2 increased the recovery of the desired elements (zirconium, rare earths) in the subsequent acid decomposition, whereas the filtration rate of the pulp was not affected. Increasing the activation time to 1 minute decreased the recovery of desired components but accelerated the pulp separation (average particle size < 6 μm). Eudialyte concentrate treated in the activator D1 for 5 minutes transforms the mineral into an X-ray amorphous state resistant to acid leaching (average particle size < 5 μm).

Preliminary mechanical treatment of eudialyte concentrate in presence of small amounts of nitric acid decreases the consumption of the leaching agent more than two fold (from 800 to 350% of stoichiometric amount), also decreases the leaching time by more than three times (from 3 to 1 hour) and reduces the amount of solution retained by the silica cake significantly.

The combination of mechanical activation, leaching and liquid extraction of desired components of eudialyte concentrate (zirconium, rare earths) by 100% TBP saturated with concentrated nitric acid in a specially designed extractor,[8,19] seems to be very efficient. Under optimal conditions both zirconium and rare earths are almost completely extracted into the organic phase within 3 minutes and the phase separation time is less than 2 minutes.

The aim of the present work is to study the influence of preliminary mechanical activation of eudialyte concentrate on subsequent extractive leaching of zirconium and rare earths.

EXPERIMENTAL

The feed material used in this study was 75% eudialyte flotation concentrate with an average particle size about 100μm (90% <190μm). Main admixture minerals in the feed were aegirite, nepheline and feldspar. Percentage composition of concentrate: ZrO_2 8.3; Y_2O_3 0.36; Ce_2O_3 0.49; Nb_2O_5 0.57; Ta_2O_5 0.056; Fe_2O_3 4.4; Al_2O_3 5.4; TiO_2 0.78; MnO_2 1.9; Na_2O 12; CaO 6.3; SiO_2 52%. The concentration of silica was determined by spectro-photometry and the other elements by atomic emission spectrometry.

Mechanical activation was carried out using planetary ball-mills "Pulverizette-5", (FRITSCH GmBH). Particle size analysis was carried out using a Laser Particle Sizer "Analyzette-22" (FRISCH GmBH). X-ray powder diffraction analysis (XRD) was performed using DRON-3 diffractometer with Cu K_α radiation.

The extraction of the desired components (Zr, rare earths) from preliminary mechanical activated eudialyte concentrate was carried out in an agitated thermostatically controlled cell (T= 20-70°C) using 100% TBP saturated with HNO_3 at a phase ratio liquid:solid from 10:1 - 20:1.

RESULTS AND DISCUSSION

Experiments on the optimization of the decomposition process using nitric acid (8 mol dm^{-3}, L:S > 10:1) showed that it is only possible to attain a satisfactory rate of pulp filtration at a rather high acid consumption when using a regime of slow charging of the concentrate at 100°C. Nevertheless, even under such conditions, the maximum recovery of zirconium did not exceed 65-67% and considerable losses of the solution within the filter cake occurred.

One of the process modifications which significantly decreased the length of processing the eudialyte concentrate, reduced the retention of nitric acid in the silica filter cake, and solved the problem of stable emulsion or crud formation was the combination of mechanoactivation and extractive leaching in a device which simultaneously subjected the concentrate to effects arising from: acoustic, magnetostriction, magnetic and electrical processes. The presence of a large number of hydrodynamic vortices within the system causes the autogenous comminution of eudialyte concentrate. Such intensive mixing of the suspension increases mass transfer between the solid and liquid phases such that after 10 minutes of leaching by 100% TBP saturated with 3.5 mol dm^{-3} nitric acid, is possible to completely recover cerium and yttrium and 50% of zirconium is also leached (figure1).

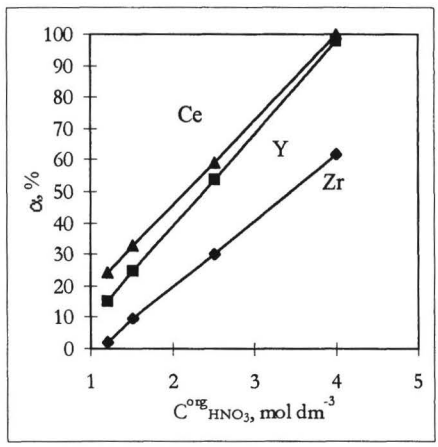


Figure 1. Effect of nitric acid concentration in organic phase on the extent of extraction of desired components of eudialyte concentrate during extraction leaching with 100% TBP combined with mechanical treatment (L:S = 1:20, t = 10 min).

In the absence of a water phase the silica from the concentrate does not form silicic acid and so precipitates as a easily filterable residue. Separation of the leachate from the residue is practically instantaneous. Another advantage of this technique is that the retention of the organic phase by the solid phase is very low (1-2%) giving a higher recovery of the metal values.

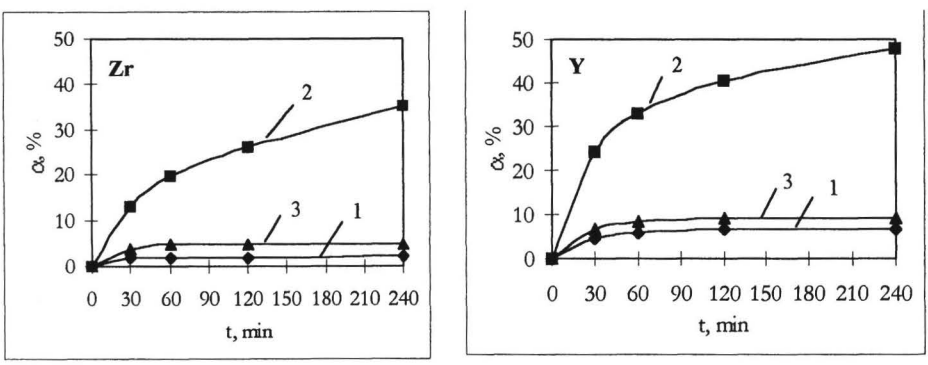


Figure 2. Kinetics of extraction of zirconium and rare earths from untreated (1) and mechanically activated (2,3) eudialyte concentrate (L:S = 20:1; C^{org}_{HNO3} = 3.6 mol/dm^3). Time of mechanical treatment, (2) 1 minute; (3) 3 minutes.

A modification of this process of leaching eudialyte with nitric acid saturated TBP is based on the preliminary mechanical activation of the concentrate followed by extraction leaching in an agitated contactor. Results of the leaching of zirconium and rare earths from the untreated feed and mechanically activated concentrate are shown in figure 2. In this case the leaching of zirconium and rare earths both from the untreated eudialyte concentrate as well as a sample mechanically activated for 3 minutes was poor. However preliminary short-term mechanical treatment of concentrate for 1 minute in the planetary ball-mill "Pulverisette-5" significantly increases the extent of extraction of zirconium and yttrium from 2.4 to 35% and 6.7 to 48% respectively.

It is worth mentioning that increasing the duration of mechanical treatment from 1 to 3 minutes was accompanied by a decrease of extraction of both zirconium and yttrium although the particle size of concentrate, from particle size data, significantly decreases, i.e. the specific surface area increases (figure 3). XRD data indicates an increasing amount of amortization of eudialyte and admixture minerals with longer mechanical treatment times. Similar behavior has been observed by us earlier with another grinding device.[17]

Finally it was noted that an increase of the temperature of the process was accompanied by a decrease of extent of extraction of both zirconium and rare earths.

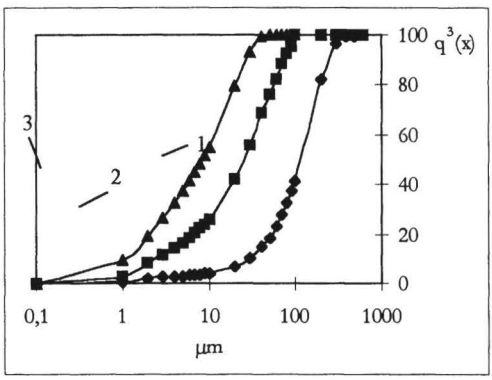


Figure. 3. Integral particle size distribution of untreated eudialyte concentrate (1) and samples mechanically activated in "Pulverizette-5" for 1 minute (2) and 3 minutes (3).

As has been demonstrated above, substitution of an aqueous acid solution by TBP saturated by nitric acid, allows a significant increase in the extent of extraction of rare metals from the mineral and also, as a result of the absence of hydration, prevents the dissolution of a large amount of silica. Currently traditional hydrometallurgical, and sometimes pyrometallurgical, processes are fairly often carried out using non-aqueous and aqueous - non-aqueous reagents. It is natural to suppose that following the creation of necessary theoretical principles and accumulation of the available experimental data it is possible to speak about the formation of a new branch of extractive metallurgy, which logically can be called solvometallurgy[1]

REFERENCES

1. Chekmarev AM, Buchikchin EP, Chizhevskaya SV, et al. *Proc. of Intern. Sci. Conf. "Metallurgy of the XXIst Century: a Step into the Future".* Krasnoyarsk, Russia, 22, (1998).
2. Hudswell F and Hutcheon. *Chemistry of Nuclear Fuel,* 533, (1956).
3. Solovkin AS and Yagodin GA, *Itogi Nauki. Neorg. Khim. VINITI.* (Rus.) Moscow, 46, (1970).
4. Ritcey GM, *Canad. Metall.* Quart., **25**(1). 31, (1986).
5. Ritcey GM, *Proc. ISEC'96,* ed Shallcross DC, Paimin R and Prvcic LM, Melbourne Australia, **1**, 17, (1996).
6. Golyshev VM, Simonov VI and Belov NV, *Crystallographia.*, **17**(6), 1119, (1972).
7. Chizhevskaya SV, Chekmarev AM, Klimenko OM et al. *Proc. Hydrometallurgy'94.* Chapman and Hall, 219, (1994).

8. Chizhevskaya SV, Sinegribova OA, Chekmarev AM and Cox M, *Proc. ISEC'96,* ed Shallcross DC, Paimin R and Prvcic LM, Melbourne Australia, **1**, 683, (1996).
9. Sinegribova OA, Chizhevskaya SV, Bobirenko AYu, et al. *Proc. ICHM'88*, China, 259, (1988).
10. Sinegribova OA, Chizhevskaya SV and Kotenko AA, *Radiochimia*, **31**(6), 87, (1989).
11. Sinegribova OA, Chizhevskaya SV, Klimenko OM, et. al, *J. Neorgan. Chimii*, **41**(11),1898, (1996).
12. Chekmarev AM, Chizhevskaya SV, Sinegribova OA et. al, *Russian Patent 2034797*, (1991).
13. Avvakumov EG, *Mechanical Activation of Chemical Processes*. Novosibirsk: Nauka, 301, (1986)
14. Kulebyakin VG, *Application of Mechanochemistry in Hydrometallurgical Processes.* Novosibirsk: Nauka, 272, (1988)
15. Molchanov VI, Selezneva OG, Jirnov EN, *Activation of Minerals in the Course of Grinding*. Moscow: Nedra, 208, (1988).
16. Chizhevskaya SV, Povetkina MV, Chekmarev AM, et. al, *Chemistry for sustainable development*, **6**, 199, (1988).
17. Chizhevskaya SV, Chekmarev AM, Povetkina MV, et al, *Proc. of the IV Inter. Conf. on Clean Technologies for the Mining Industry.* Chile, **2**, 523, (1998).
18. Chizhevskaya SV, Povetkina MV, Chekmarev AM and Cox M,. *Proc. of ARS Separatoria.* Poland, 69, (1996).

AUTHOR INDEX

Abu-Shady AI 1325
Adachi M 107
Adda M 549
Afonin MA 1371
Aguilar JC 1013
Aguilar M 1127 1267 1555 1561
Ahuis F 239
Akiba K 1103
Akita S 363 387
Al-Mudhaf HF 1325
Alessi V 1567
Alguacil FJ 381 1155
Almela A 703
Alonso E 167
Alonso JJ 167
Aly HF 347 1351 1387
Amer SA 1325
Angelov G 463
Anticó E 1115
Arnaldos J 1285
Asakura T 1469
Asano T 829
Avila-Rodríguez M 1209

Babain VA 1345
Bailador H 161
Bailes PJ 503 609
Bakastova NV 971
Ban T 493
Bandekar SV 71
Bandyopadhyay M 921
Bao B-R 353 1357 1361
Baranov SM 1381
Barron Zambrano JA 1209
Bart H-J 125 835 847 927 939 959 1573
Becker O 475
Belnet F 637
Beltran JL 1555
Belova VV 1139
Benedetto JS 189 711 717
Benjamin I 3
Benzal G 1529
Berrama T 983
Berthon C 1333
Biddlestone AJ 1639
Birkett JE 1463
Blanco MA 1607 1629
Bogacki MB 1193
Böhmer V 1095
Bolton GT 445
Boluda N 161
Bond AH 299
Bonnesen PV 1365
Borowiak-Resterna A 359 1197
Boshoff G 789
Botella A 643
Bothwell P 1463
Boubals N 317
Bourget CC 1187
Bouvier C 871
Brajenovic N 1167
Brewer KN 1345
Brodkorb MJ 513
Buchalier EM 1455
Bukar NV 567
Burgard M 681

Canari R 597
Canselier JP 171
Cara G 1023
Carvalho JMR 915 959 977
Castillo E 47
Cattrall RW 1053
Chang Z 405
Charbonnel MC 1333
Chartroux C 239
Chayama K 675
Chekmarev AM 805 1161 1493
Chen D 469
Chen J 405
Chen M 419
Chen S-J 259
Chen W-J 259
Chiarizia R 53 299
Chimenos JM 759
Chizhevskaya SV 805
Chowdhury DA 393
Chu D 1109
Cichy W 1065
Ciminelli VST 953
Cinti M 1623
Clark P 789
Cocero MJ 167
Cohn-Syzov N 131
Cole PM 1437
Comba P 687
Conner C 1365
Cordier PY 317 323
Correia PFMM 977
Cortina JL 47 771 1127 1267 1285 1555 1561
Costa MC 271
Costic S 1403
Cote G 871 1197
Cox M 805 1187
Cruz-Pinto JJC 487
Cusack RW 427
Czapla C 835

Da Silva CE 189
Da Silva GL 953
Dai YY 177 183 419 625
Daldon M 1333
Dannus P 25
Dantas Neto AA 195 783

Dantas TN de C 195 783
Daoud JA 1351
Datta S 921
Davies BM 1437
de Barros Neto EL 171
de Gyves J 1013 1019
de Haan AB 1543
De Ketelaere RF 947 995
de La Salles WF 783
de Lucas A 1607
Del Re G 1623
Delgado A 1611
Deljouie P 813
Delmas F 729
Delmau LH 1365
Delshams A 1529
Denniss IS 1381 1463
Dhadke PM 71 245
Di Giacomo G 1619 1623
Diaz G 201 1449
Dieleman CB 681
Dietz ML 53 299
Ding S-D 259
Dinh B 655
Dozol JF 1095
Drake A 1417
Dreisinger DB 1443
Drew MGB 281
Druzhinina IA 1475
du Preez AC 305 311
Dunga NTK 249
Dunowicz R 369
Durand G 965 983 1071 1143
Dzygiel P 1035

Eckstein A 615
Eidelman Ch 549
El Gharbi M 1561
El-Afifi S 347
El-Hefny N 1387
Elizalde MP 703 1227
Enachescu F 1403
Enarsson Å 323
Ennassef K 1071
Ernst B 681
Escalante H 1499
Esimantovskiy V 1345
Esparducer A 759
Espiell F 759
Eyal AM 131 369 597 603

Falgueras J 201
Fan Z-P 353
Feather A 789 1443
Fedorov A 1523
Fei W 451 457 469 1543 1579
Fernandes CE 271
Fernández AI 759
Fernández MA 759
Flett DS 1187
Fogassy E 1601
Fontàs C 1029
Fortes MCB 717
Foulon C 1143
Fox RV 1657
François N 317
Franzoni A 1567
Frías C 1449
Fujinaga K 341
Fujine S 1469
Fukunaga S 393
Furusaki S 83 1297

Galán B 543
Gallego Lizon T 1511
García MA 201
García-Carrera A 1095
García Liranza E 735 753
Gautam PK 1001 1375
Gega J 1007
Geist A 1517
Giganov GP 1493
Giganov VG 1493
Glatz DJ 427
Glazkov IN 1645
Gloe K 239 687
Góis LMN 481
Gomes MLACN 487
Gomis V 161
Gonzalo A 1273
Gordillo MD 1675
Goto M 83 865 1297 1469 1669
Gourdon C 171 463
Gracia I 1607
Gradella C 1567
Granados M 47
Grieser F 813
Grinbaum B 509 549 1455
Grishchenko AB 893
Guimarães MML 487

Haddad R 1155
Hall S 1455
Hampe MJ 329
Hano T 219 989 1297
Harada M 107
Hardy R 475
Hatate Y 537
Hatton TA 83
Haverlock TJ 669 1365
Hay BP 299
Hebrant M 207
Hegazi MF 1325
Helal A-A A 213
Hendrawan H 877
Herbst RS 1345
Herlinger AW 299
Herranz J 1285
Hidalgo M 1029 1121

Hill NJ 1339
Hirai T 723 1397
Hirata A 137 143 149
Hirata M 219 989
Hirayama N 585
Hirose T 1669
Ho JMY 231
Hoffmann A 947
Hoffmann S 631
Hokura A 561
Holmes TL 427
Honbu T 95
Honjo T 585 1149
Horwitz EP 53
Hossain KZ 1149
Hotoku S 1469
Hotta M 1173
Huang H 625
Huang Z 259
Huber VJ 299
Hudson MJ 271 281 317 323
Hutahaean LS 1585
Hyodo N 363 387

Ibach S 239
Iberhan L 1261
Iglesias M 1115
Inoue K 255 687 741
Irabien A 1499
Ishibashi H 255
Ishikawa I 1215
Ismael C 915
Itabashi O 741
Ito M 59 1173
Iveson PB 271 281 323

Jääskeläinen E 525
Jakovljevic B 1133
Jakubiak A 1203
Jarudilokkul S 101 113
Jensen MP 1089
Jerabek K 1267
Jiang WB 183
Jidkova TI 1139
Jing Y-D 259

Kafarski P 1035
Källvenius G 323
Kamata S 393
Kamei K 1469
Kaneda M 433
Kanel JS 1585
Kanki T 829
Kanno A 1423
Kaplan P 965
Kato D 859
Kato T 1423
Katoh S 107
Kaunisto J 1595
Kawaizumi F 493
Kawakita H 137
Kawano Y 95 537 1181
Kelly N 1417
Kemény S 1601
Keszei S 1601
Kholkin AI 1139
Khopkar SM 245
Kihara T 1469
Kim H 829
Kim JI 335 1517
Kim V 567
Kimura S 1469
King MB 1639
Kinugasa T 89
Kirschling P 1411
Kirschneck D 531
Kleinberger R 1455
Kobayashi N 363 387
Koch J 439
Kocherginsky NM 893
Kodama A 1669
Kojima D 865
Kojima I 59
Koltunov VS 1381
Komasawa I 95 723 1397
Kokubu S 219
Kolev SD 1053
Komatsu Y 265 1249
Kondo K 899
Korchinsky WJ 445 619
Korda TM 1475
Koroleva MYu 573 971
Kosogorov AV 499
Koyama K 801 1549
Kozlowski C 1007
Krzyanowska E 287 293
Kuboi R 95
Kubota F 1297
Kuipa PK 503
Kumar A 47 1001 1155
1303 1375 1529
Kunogi K 249
Kurihara C 675
Kusakabe S 1309
Kuwata S 255
Kuznetsov GI 499
Kyuchoukov G 1193 1203

Laitinen A 1595
Lam CSW 231
Law JD 1345
Le QTH 663
Le S 911
Lee J-D 65
Lee JGM 609
Lefrancois L 637
Lenhard Z 1177
Leonard RA 1365
Lewis C 475

Li D 795 889 905 911 1081 1109 1233 1239
Li HB 1579
Li SS 277
Li Z 625
Liljenzin JO 281 317 323
Liu H 405
Liu Z-Q 259
Lo J-M 65
Lo TC 1503
Long WK 231
Lu J 795 905
Lu T 1639
Lu YC 183
Ludwig R 249
Lumetta GJ 1365
Luo GS 183 1579

Ma G 905 1109
Ma HL 277
Ma L 353 1357
Macanas J 1047
Mack C 329
McMurtrey RD 1657
Madic C 281 317 323 1333
Maiboroda AB 1161
Maljkovic Da 1177
Maljkovic Du 1177
Malkhede DD 245
Malve SP 77
Mansur MB 953
Mantell C 1615
Marchenko VI 1381
Marcilla A 643
Marques JJ 481
Marr R 531
Marták J 1041
Martín D 201 1449
Martin PD 445
Martínez de la Ossa E 1607 1611 1615 1619 1629 1633 1675
Martins AH 717
Masson IO 1127
Masutani M 1279
Matsumoto M 219 899
Matsumoto S 765
Matsumoto Y 1423
Matsunaga H 1313
Matt D 681
Mattison P 375
May I 1339 1381 146
McMurtrey RD 1657
Mendes-Tatsis MA 155
Menoyo B 703 1227
Mewes D 841
Mezhov EA 1381
Mickler W 225
Miesiac I 1411
Mijangos F 703
Millies M 841
Mineo H 1469
Mingote RM 711
Miralles N 1285
Miranda TLS 953
Mizrahi J 1481
Mizuno T 59
Modes G 1573
Molero A 1611 1629 1633 1675
Moreno Daudinot AM 735 753
Moriya Y 819
Mörters M 847
Motomizu S 591
Moulin C 1333
Moura MCPA 195
Movsowitz RL 1455
Moyer BA 669 1365
Muhammed M 9
Muñoz M 1023 1047
Murakami Y 137 143 149 1423
Murashova NM 579
Muraviev D 1273 1291

Nagao S 865
Nagayoshi K 1181
Nagel VM 1437
Nakahara Y 989
Nakamura K 859
Nakano Y 1469
Nakashio F 865 933 1297
Nanoti A 927
Narita H 693
Nash KL 555 1089
Navarro Mendoza R 1209
Navratil JD 1657
Niemann SH 1537
Nieuwoudt I 1319
Nii S 363 387 493 1059 1279
Nishihama S 723
Nishiki T 859
Nishimura S 765
Nitsch W 631 853 1517 1523
Noda H 433
Noel D 637
Noguchi Y 1245
Nogueira CA 729
Noro J 561
Nucciarone D 1133

Oda T 143
Ogawa N 819
Ohto K 255 687
Okubo T 899
Okumura M 341
Olaya MM 643
Oleinikova M 1047
Olenicheva OO 567
Olszanowski A 287 293

Onoe Y 883
Oprea F 1403
Ortiz I 1487
Osipov AN 893
Otu EO 1663

Paatero E 525
Pagnucco CD 1133
Paimin R 1053
Paiva AP 399
Palet C 1029
Pareau D 965 983 1071
Pareau S 1143
Parsons AR 609
Pastuschak VG 1381
Penzo R 1567
Pereira JAFR 481
Perera JM 813
Pereyra C 1619
Pérez O 1449
Pérez de Ortiz ES 1511
Pietrelli L 747
Phillips C 1431
Plucinski P 335 1517 1523
Poitrenaud C 655
Ponzo G 747
Poppenborg LH 101 113
Poulad-Meyer L 603
Povetkina MV 805
Prat MD 47
Pratt HRC 469
Prechl A 1601
Presson MT 1333
Preston JS 305 311
Pursell MR 155
Pushkov AA 499

Qin W 119

Rambocus S 1417
Rambusch T 239 687
Ranieri L 747
Rat B 655
Regueiras PFR 487
Reich A 225
Reis MTA 959
Reitmeir J 335
Renard EV 1475
Reuben BG 1417
Revelsky IA 1645
Rice NM 1255
Rickelton WA 1133
Rincón J 1607
Ritcey GM 37 519
Rodríguez M 1615
Rodríguez de San Miguel E 1013 1019
Romanovski VV 1371
Romanovskiy VN 1345
Roos M 939
Rosales Bárazaga B 735
Rosinda M 915
Rouquette H 1095
Rovira M 771 1285
Ruiz F 161
Russell ML 323

Sabolová E 1041
Sachleben RA 669 1365
Sakoguchi A 933
Salum A 953
Salvadó V 1029 1115 1121
San Román F 543
Sana T 1181
Sanagi K 89
Sánchez JM 1121
Sano M 765
Sano N 829
Santos R 1639
Sanyal SK 921
Sastre AM 47 381 771 1001 1095 1155 1209 1285 1303 1375 1529
Sato K 1215 1221 1245
Sato T 1173 1215 1221 1245
Saucedo Medina TI 1209
Savilova OA 1381
Sawinsky J 1601
Schaefer DM 1585
Schlosser S 1023 1041 1065
Schmitt H 531
Schöneberger A 927
Schöner P 1523
Segarra M 759
Seibert F 475
Seike Y 341
Sekido E 675
Sekine T 561
Senol A 411
Shafirov VL 805
Shehata FA 347 1387
Shibata J 765 1549
Shimosato T 585
Shioi A 107
Shiomori K 95 537 1181
Shiraishi Y 1397
Shukla JP 1001 1375
Simándi B 1601
Simonin JP 877
Sinegribova OA 567 825
Singh RK 1001 1375
Skachkov VS 499
Slater MJ 513 1567
Smirnov IV 1345
Soares PSM 1127
Soldenhoff K 777
Sole KC 1443
Spjuth L 281 323
Stambouli M 965 983 1143
Stefanska A 1639
Stepanov SI 1493

Stephan H 687
Stevens GW 469 813
Stichlmair J 487
Stuckey DC 101 113 155
Su G 1543
Sun D 911
Suzuki S 697
Suzuki TM 741
Svirdenkova OV 567 825
Szczepaska I 359
Sze YKP 231
Székely E 1601
Szymanowski J 19 1065 1193 1197 1203 1261 1411

Tachimori S 693 697
Tahiani F 1221
Takada T 219
Takahashi K 363 387 493 1059
Takanashi H 219 989
Takayanagi T 591
Takehara A 143
Takeuchi H 89 363 387 1279
Tambourgi EB 189 481 711
Tamhina B 1167
Tamura K 697
Tanaka I 561
Tanaka M 801 1549
Tang J 795
Tani K 493
Tarasov VV 825
Tatarchuk VV 1475
Tauler R 1561
Tavlarides LL 1651
Taylor RJ 1339 1381 1463
Todd TA 1345 1371
Tokarz A 841
Tomita A 829
Tomlinson MA 1255
Tondre C 207 637
Torgov VG 1475
Torrado A 1291
Traving M 125
Troshkina ID 1161
Tseng C-M 65
Tsuchiya M 1423
Tsuji H 675
Tsurubou S 265 1249
Tsuzaki K 1423

Uchiyama G 1469
Uemasu I 651
Ueoka R 933 1423
Uhlemann E 225
Umetani S 265 663 1249
Uribe-Ramírez AR 619
Urtiaga AM 1487
Usui Y 697

Valiente M 1023 1047 1121 1273
Van Brunt V 1291 1585
Van der Linden J 995
Varadarajan A 77
Varga V 1601
Venter DL 1319
Verhaege M 947
Viera Martínez R 735
Virnig M 375
Vogelpohl A 439 615
Vögtle F 239
Vojkovic V 1167

Wada E 591
Wakui Y 741 1103
Walford T 1639
Walkowiak W 1007
Wallwork AL 1463
Wang C 1233 1239
Wang JD 1579
Wang L 1053
Wang T-J 1361
Wang Yujie 889
Wang Yujun 177
Wang Y-D 419 625
Warshawsky A 1267
Watanabe K 89
Watanabe M 1469
Watarai H 819 883
Waterfall RC 445
Wei Z 1233
Weigl M 853
Weill J 877
Wen X 1543
Wieczorek P 1035
Wieser-Jeunesse C 681
Wildberger A 927
Wilkins D 777
Wiœniewski M 359
Wisniewski M 1261
Wood DJ 1345 1371

Xia C 259
Xu L 419

Yaftian MR 681
Yaita T 693
Yamada M 561
Yamada S 537
Yamaguchi M 433 865
Yamashita H 433
Yang ST 119
Yang Y-Z 353
Yano K 899
Yao N 405
Yokosawa R 1059
Yokoyama T 741 1103
Yoshizawa H 537
Yoshizuka K 687 933 1297
Yu J 451 457

Yu S-N 353 1357
Yuan CY 277
Yuan SG 277
Yurtov EV 573 579 971

Zagorodni AA 9
Zaitsev B 1345
Zamacona S 1487
Zamponi G 487
Zeid MM 1351
Zhang P 741
Zheng T 795
Zheng Z 905
Zhou W 1651
Zhu L 259
Zhu S 177
Zhuravleva GI 1381
Zolotov Yu A 1645
Zushi E 933

KEYWORD INDEX

ANALYSIS

analysis 47 65 71 77 83 245
ATR spectroscopy 813
capillary electrophoresis 591
external reflection spectra 819
EXAFS 693
FAB-MS spectra 1233 1239
flame A A S 59
fluorescence tracers 847
FT-Raman spectroscopy 703
ICP-AES 1149
NMR spectroscopy 597 603 1333
optosensor 47
organic pollutants 1651
preconcentration 53
radiochemical-spectrophotometry 83
Time-Resolved Laser-Induced Fluorescence (TRLIF) 1333
UV-Visible spectroscopy 703 1167 1333
voltammetry 65

BIOTECHNOLOGY

antigen-antibody interaction 107
bioaffinity separation 107
enzymatic hydrolysis 149
extractive fermentation 119
fermentation broth 131 155 167
non-aqueous enzymology 137
surfactant-coated enzyme 137

EXTRACTANTS 277 341
bite size 663
easily solidifying 341
in situ formation 341
interligand contact 663
molecular recognition 663
substituent effect 663
Acorga CLX-50 871
alcohols: 1221
butanol 183
1-decanol 155
diol derivatives 219
1-dodecanol 161
2-ethylhexanol 219
fatty alcohols 161
glycols 1319
1-octanol 567
amides:
cyclic amide 697
diamide 259 693
glycolamides 693
malonamides 271 281 637 693 1333
nicotinamide derivatives 359
amines; 95 101 519 597 603 1161 1537
Alamine 304-1 1417
Alamine 336 231 411 519 771 789 1417 1455 1499
Amberlite LA-2 1065
di-n-octylamine 971 1161
dodecylamine 1161
Hostarex A327 977
primary amine N1923 795 889
Primene JMT 915
tertiary amines 1417
sec-tridecylamine 1411
tri-dodecylamine 983
tri-n-octylamine 537 835 971 1007 1041 1065 1161 1245 1279 1411
quaternary ions
Aliquat 336 231 789 905 1001 1029 1053 1143 1375 1417 1487
amines 375 591 1417 1537
alkylammonium alkylbenzenesulphonates 1139
alkylammonium carbonates 1493
cetylpyridinium ion 1167
cetyltrimethylammonium ion 1167
tetrabutylammonium chloride 1417
tetrabutylphosphonium chloride 1417
tetraoctylammonium chloride 1417
trioctylmethylammonium chloride 1155 1245
tetraphenylarsonium 1167
tetraphenylphosphonium 1167
benzene 1543
bis(ethanedithioamido)-2,4-dioxo-3-oxymino pentane 77
butyraldehyde 1469
carboxylic acid: 311 317
2-bromodecanoic acid 323
humic acid 213 335
oleic acid 971
sodium oleate 971
Versatic acid 525 1437
chloroform 177
β-diketone 265 585
acylpyrazolone 225 663
LIX54 225 1193
thenoyltrifluoroacetone 561 1249 1387
dimyristoyl-phosphatidylcholine 1423
diphenylsemicarbazide 47
dithiocarbamic acids: 341
pyrrolidinedithiocarbamic acid 341
tetramethylene dithiocarbamate 65

© 2000 Society of Chemical Industry

dithizone 853
EDTA-DOA 865
guanidine:
LIX79 1303
hydroxamic acid: 347 1339
neo-decanohydroxamic acid 1261
acetohydroxamic acid 1463
8-hydroxyquinoline compounds
5-chloro-8-hydroxy-quinoline 899
Kelex 100 207 813 871 1013 1203 1221
isopropylmyristate 877
macrocyclic compounds 239 265
cage compounds 239
calixarene: 245 249 1095 1365
calixarene (resorcarene) 965
calixarene carboxylate 255 687
phosphorylated calix[4]arene 681
cobalt dicarbollide 1345 1371
crown ether 299 585 669 1149 1365 1371 1387
stereoisomers 299
monoazathiacrown ether 675
cryptand derivatives 265
nitriles: 1319
acetonitrile 1397
nitrogen bases 1319
nitrogen disulphides 399
oximes: 293 1555
degradation 287 293
isomerisation 293
Acorga M5640 995
2-ethylhexanal oxime 765
2-hydroxyoxime 883
2-hydroxy-5-nonylacetophenone 287
2-hydroxy-5-nonylbenzaldehyde 287
2-hydroxy-5-t-octylbenzaldehyde 293
2-hydroxy-5-t-octylbenzophenone 293
2-hydroxy-5-t-octylacetophenone 293
LIX63 1143 1173
LIX84 759 1193 1285
LIX84I 1279
LIX 860 995 1181 1487
M5640 1487
P5100 287
SME529 287
phenolic derivatives 585
4-n-dodecyl-6-(2-thiazolylazo) resorcinol 1313
nonyl phenol 375
phospholenes: 381
1-(dodecyloxy)-3-methyl-oxo-Δ^3-phospholene 1209
1-(2,6-dimethylhept-4-yloxy)-3-methyl-1-oxo-Δ^3-phospholene 1209
phosphorus acids: 225 299 305
phosphinic acids
1,3-benzenedimethylbis(phenyl-phosphinic acid) 1103
bis(2-ethylhexyl)phosphinic acid 723
PIA-8 1187
PIA-226 723
bis(2,4,4-trimethylpentyl) phosphinic acid 1239
Cyanex 272 703 735 741 753 953 1019 1079 1081 1133 1187 1239 1303 1443 1487 1561
bis(2,4,4-trimethylpentyl))dithio-phosphinic acid
Cyanex 301 703 947 1001 1081 1155 1227 1375 1517
bis(2,4,4-trimethylpentyl)mono-thiophosphinic acid 1233
Cyanex 302 703 735 753 1081 1155 1227 1233 1375 1511
di-2-ethylhexylmonothiophosphoric acid 225
di-2-ethylhexyldithiophosphoric acid 1291
DP 8R 735 753
diphosphinic acid 53
P507 735
phosphonic acids
aminomethylenephosphonic acid 729
2-ethylhexylphosphonic acid mono-2-ethylhexyl ester 71 723 899 905 1125 1133 1177
Ionquest 801 1127 1187
PC-88A 71 735 753 1187 1297
mono-octyloctanphosphonate (MOOP) 1177
N-piperidinomethane-1,1-diphosphonic acid 1089
phosphonic acid esters 305 1035
chiral 1035
diphosphonate derivatives 305
bis(dialkylphosphonates) 393
phosphoric acids
bisalkyl hydrogenphosphate 687
di(2-ethylhexyl)phosphoric acid D2EHPA 189 201 225 329 543 567 579 711 717 723 729 741 825 829 847 865 877 915 927 947 971 989 1023 1089 1113 1115 1121 1181 1185 1273

D2EHPA cont 1291 1351 1437 1443 1481 1517 1523
salts 1255
di(2-ethylhexyl)thiophosphoric acid 771 959 1047
phosphoric acid esters 1035
chiral 1035
di(1-methylheptyl)methyl phosphate 911
octylphenyl acid phosphate 1351
tri-n-butylphosphate, TBP 189 265 419 655 723 801 805 921 1161 1209 1585 1669
N-piperidinomethane-1,1-diphosphonic acid 1089
phosphorus oxides: 265 381 1133
acetoamidophosphine oxide groups (CMPO) 1095
Cyanex 921 381 1007 1133
Cyanex 923 381 469 777 1065 1081 1109 1261
Cyanex 925 381 777 1155 1261
trioctylphosphine oxide 561 1309 1325 1357 1417
polyethylene oxides 625
polyoxyethylene nonyl phenyl ether 363 387
polyoxyethylene-10-dodecyl ether 1423
poly-siloxane
aminopoly-siloxane 927
pyrazolone derivatives 225
pyrazole-thione 1357 1361
4-benzoyl-2,4-dihydro-5-methyl-2-phenyl-3H-pyrazol-3-thione 1357 1361
pyridine derivatives: 311 1437
pyridine carboxylate ester 1437
pyridine-3,5-dicarboxamides 1197
pyridylazo 883
oligopyridines 323
terpyridine 317
N-8-quinolylsulfonamide 933
saponified coconut oil 195 783
silver nitrate 1059
sulfolane 1549
sulfoxide derivatives: 353
dihexylsulphoxide 1215
sulphide derivatives 1475
3,6-dithiaoctane 59
phosphorus sulphides:
Cyanex 471X 777 1071
surfactants: 83 155 335 405 419 573 853
AOT 83 95 101 853 859
dodecyltrimethylammonium bromide 853
ECA 4360 953 977 983 1071
ECA 11522 959
nonionic surfactant 107 171 363 387
Parabar 9220 965
Parabar 9551 947
sodium dodecylbenzene sulfate 419
sodium dodecylsulfate 405
Softanol 30 155
Softanol 120 155
Span 80 947 983 989 1071
Triton X-100 207
Tween 80 419 971
thiourea derivatives 399
toluene 1573
triazines 317 323

EXTRACTION EQUIPMENT

air sparging 503
capacitance imaging 445
capacity 499
centrifugal contactors 499 1345 1365 1381 1463
coalescence 487 503 615 631
co-current mixers 1573
scale-up 1573
columns: 439 445 615
agitated column 427 1601
axial mixing 475 915 1585
column design 427 1503
column dynamics 487
column flooding 433 1591
column hold-up 433
column scale-up 427 1503
column stirred 959
distributor design 439
fluidised bed column design 1285
Karr column 549
Kuhni column 487
mixer-settler column 493
Oldshue-Rushton column 1601
packed column 475 915 1591
packings 1591
Raschig ring 451 469
Super-mini-ring 451 457 469
pulsed column 463 965 1455
packed column 451
perforated plate 469
sieve-plate column 469 1585
Rotating Disc Contactor 1579 1601
Scheibel column 1503
spray column 1403
stirred column 959
transfer units 1585

vibrating perforated plate column 481
dispersion 445
distribution 445
drop behaviour 513 609
drop coalescence 615
drop size 439
droplet breakage 487 1579
droplet swarm 457 615 847
efficiency 493 499
electric field (DC) 503 609
electrical resolution 503
emulsion breaking 503
emulsion formation 101
emulsion swelling 971
entrainment 499 631
extractor comparison 531
flow phenomena 463 509
fluid dynamics 1579
horizontal rotating cell 825
Graesser contactor 101
high viscosity 457 531
hydrodynamics 451 469
in-line mixers 519 525 531
impeller design 433
membrane extraction:
activated composite membranes 1047
bulk liquid membrane 1041 1059 1065
emulsion/surfactant liquid membrane 503 573 631
947 953 959
965 971 977
983 989 1071
1511
hollow fibre membrane 183 889 893
1029
impregnated Langmuir-Blodgett membrane 1313
liposomes 1423
microporous membrane 631
polymer inclusion membranes 1007 1053
porous membrane 1053
rotating membrane cell 877
supported liquid membrane 47 543 995
1001 1007 1013
1019 1023 1029
1035 1155 1297
1529
water diffusion 971
mixer-settler 1455
Morris extractor 195
phase distribution 439
phase equilibria 643
phase separation 631
pilot plant 1443
Reynolds number 531
stirred cell 847 853
tomography 445
turbulent energy 463
Vibro-mix extractor 537
videocamera 503

EXTRACTION TECHNIQUES
aphrons 419
applied voltage 865
aqueous/organic biphasic system 137 155 143
aqueous two-phase system 149
binary extractants 1001 1139 1155
1375
biphasic reactions 369
coalescence 487 503 615
631
colloidal aggregates 567
concentrated solutions 25
counter-current cascade 723 1555
diffusion coefficient 841
diffusivity 619
diluent effect 1121 1387
dispersion model 131
electrolytes 25
electrophoretic mobility 835
extraction
acid base couple extraction 131
aqueous two-phase system 149
cloud point extraction 19 171 363
co-current extraction 1573
coextraction 255
electro-extraction 183
exchange extraction 1255
extraction chromatography 53 125 927
1267
extractive reaction 143
ion-pair extraction 59 131 271
591
mechanism of extraction 95 387 591
899 921 1109
1333
reactive extraction 549 939 1523
foam separation 405
gelation 579
ion-size selective masking reagents 265
impregnated resins 8 771 1115
1267 1273 1285
impregnated polymers 927
Amberlite resins 131
Amberlite XAD-2 771 1115 1273
1285
Amberlite XAD-4 125 927 1273
Amberlite XAD-7 1313 1273
Amberlite XAD-16 125 927
aqua impregnated resins 1291
continuous fluidized bed 1285
encapsulated resins 1279
new supports 1267
inclusion complex 651
interfacial effects:
interfacial adsorption 3 939
interfacial behaviour 579 933
interfacial complexation 883

interfacial contamination 503
interfacial convection 155 579
interfacial covering 835
interfacial cruds 805
interfacial films 825
interfacial kinetics 813 853 893 905 911 1143
new methods of study 883
interfacial reaction 829 847 859
interfacial resistance 893
interfacial tension 829
liquid-liquid interface 819 841
ion exchange:
aminomethylphosphonic acid 747
dihydrogen tetratitanate hydrate 1249
double and triple phase separation (IX-SX) 1249
resins:
carboxylic acid 1291
iminodiacetic acid 1291
phosphoric acid 1291
ion hydration 1309
ion solvation 1309
kinetics 95 101 329 537 579 871 877 883 889 893 899 927 933 1333 1381
Lewis cell 101 155 865 871 905 911 921 1333
mass transfer 433 451 457 469 493 615 825 829 835 841 847 921 1511 1517 1537 1573 1673
multicomponent kinetics 513 619 847
medium effects 871
reaction kinetics 939
salt effects 643 877
solvent effects 329
'test system' 513
two-film theory 893
mechanochemical assisted extraction 805
micellar extraction: 207
micellar enhanced ultrafiltration 19
reversed micellar extraction 859
reverse micelle 83 89 95 101 107 113 119 335 579 625
microemulsion extraction 195 783
non-dispersive solvent extraction 543 1303 1487 1499 1517 1523 1537
hollow fibre module 1041 1297 1411 1499 1517 1523 1537
pertraction 1023 1041 1065
phase equilibria 643
predispersed solvent extraction 419
preneutralisation 525
reactive sorption 125 927
reducing agents:
hydroxylamine derivatives 1381
salting out 643 1325
separation 53
enantiomeric separation 1607
solubility parameters 637
solvation 3 271
stable emulsions 805
stripping
precipitation stripping 9 801
synergism 277 299 305 311 317 323 329 561 585 899 1357 1371 1437
supercritical extraction 167 1601 1607 1613 1617 1621 1625 1629 1635 1639 1645 1651 1657 1663 1669 1673 1679
carbon dioxide 167 1601 1607 1613 1617 1621 1625 1629 1635 1639 1645 1651 1657 1663 1669 1673 1679
nitrous oxide 1651
ethanol co-solvent 1645
methanol co-solvent 1621 1657
ligand-assisted 1663
thermodynamics 555 841 1109 1143
third phase 637 1177
water content of extracted complexes 1187
water solubilisation 625

FEEDS

activated carbon 1669
alkaline high-level nuclear wastes 1365
alkaline solution 375 1221
ammoniacal solution 1193
ammonium carbonate liquors 735
ammoniacal etching solution 759
ARSEP process 1449
bastnasite ore 795
batteries 201
nickel-cadmium 537 747
nickel-metal hydride 741
borage leaves 1617
brine 1255
Caron process 735
C_3-C_4 fraction 1403
cobalt-nickel mixed sulphide 735 753

contaminated sediments 1657
copper anode slimes 777
CUPREX process 1449
β–cyclodextrin-cholesterol complex 1629
dyestuffs 183
electroplating wastewater 231
enzyme condensation reaction 369
Fe-Ni alloy etch solution 765
fermentation broth 125 1645
fission products 1475
geological standard rocks 59
grape pomace 1621
irradiated fuel 1431
Kakanda tailings 1443
landfill leachate 225
light oil 1397
desulfurisation 1397
MERCUREX process 1449
neutral oils 1319
nickel laterite 753
nuclear reprocessing 697 1469
olive leaves 1613
olive mill waste-water 977
PARC process 1469
phosphate rock 1481
phosphoric acid 1227 1351 1487 1511
pickling liquor 189 197
Purex process 1339 1381 1431 1463 1469 1475
silvered copper wires 1071
spent fuel reprocessing 697
TALSPEAK 1089
tannery effluent 195
Thorp process 1431
tri-n-butyl phosphate (TBP) 409
waste-water 195 219 225 231
wheat germ 1635
ZINCEX process 201 1449
ZINCLOR process 1449
zinc residues 711

MEDIA/ANIONS

ammonium sulphate 1543
anion effect 669
boric acid 795
carbonate 1493
chloride: 359 381 399 783 1197 1203 1245 1255
hydrochloric acid 271 387 393 1173 1215 1481
cyanide 375 1669
fluoride 789
hydrogen phthalate 1417
hydrogen sulphide removal 1403
hydroxide 1221 1403
nitrate 669 681 1387
nitric acid 259 637 703 1585
nitroxide radicals 893
perchlorate 669 1309
phosphoric acid 1227 1481
silicic acid: 805
silicates 989
sodium nitrate 669
sodium perchlorate 669
sulphate 1233 1239
sulphuric acid 741 747 915
thiocyanate 1167

METALS

acid 189 1209
actinides: 249 317 555 1089 1095 1333 1339 1345
americium 259 281 323 1371 1517
neptunium 1381 1469
rejection 1463
plutonium 697 1381 1431
alkali metals: 265 585 1249 1309
caesium 965 1345 1365 1371
potassium 1255
sodium 255 1255 1371
alkaline earth metals: 265 299 567 825 1249 1309
calcium 305 989 1047 1255 1437
magnesium 1047 1255
aluminium 561 1047
anion extraction (cyanides) 375
antimony 71
arsenic 65 1261
bismuth 71 245
boron 219
cadmium 543 747 1013 1053 1215 1303 1487 1511 1517
cerium(IV) 795 889
chromium: 47 195
chromium (III) 245 329 1007
chromium (VI) 231 1007
cobalt 311 347 735 741 753 933 953 1177 1313 1443
copper:
copper(I) 59 675
copper (II) 759 813 871 933 995 1047 1053 1071 1193 1197 1203 1273 1285 1279 1291 1303 1313 1487

copper (cont.) 1517 1555 1567
gallium 363 387 561
723 899
germanium 871
gold 381 393 777
783 1155 1303
1669
indium 561 711 717
723 1019 1047
iron: 271 711 717
729 829 915
1019 1173 1481
reduction 711
reductive stripping 729
***lanthanoid** (rare earth):* 249 317 335
555 567 681
687 693 741
801 825 865
889 911 1023
1081 1089 1095
1103 1109 1309
1333
stripping 1133
erbium (III) 905 1127
europium 259 323 1371
1387 1517
gadolinium 1297
holmium 1023
lanthanum 1103
lutetium 1103
neodymium 1023 1121
samarium 801 1297
thulium 1387
yttrium 1109 1115
lead 245 1013 1221
1227
manganese 245 1047 1443
molybdenum 1493
nickel 207 311 525
543 735 741
753 747 765
877 883 947
953 1177 1181
1187 1313 1437
1517
niobium 789
platinum group metals: 771 1139
osmium 1161
palladium 71 359 537
771 883 1143
1475
platinum 71 771 1143
rhodium 71 771 1029
ruthenium 1167
radionuclide 53 1663
selenium(IV) 77 921
scandium 1233 1239
silver 239 399 675
1001 1071 1375
strontium 1345 1371
tantalum 789
technetium 1365 1431 1469
tellurium (IV) 921
thallium 71
thorium(IV) 213 245 353
795 1357 1361
tin 71 1047 1245
transition metals 1309
tungsten 1493
uranium 347 353 519
697 1351 1357
1361 1431 1455
yttrium 1109 1115
zinc 201 847 853
877 927 933
959 1047 1203
1209 1215 1221
1273 1279 1291
1303 1517 1523
zirconium 567 825

MODELLING

3 25 411
655 921 1127
1511 1517 1523
1529 1537 1543
1549 1555 1561
1591 1673 1679
ab initio calculations 281
alternative least squares 1567
articial neural networks 1549
bite size 663
computational chemistry 277
computer simulation 933 1555 1561
concentrated solutions 25
curve resolution 1567
dispersion model 125
electrolytes 25
equations of state 1679
equilibrium modeling 669 1561
factorial design 717
Flory-Huggins theory 637
HSAB principle 277
interligand contact 663
molecular dynamics 3
molecular modeling 239
molecular dynamics simulations 883 933
molecular mechanics calculation 277 687
molecular recognition 663
numerical simulation 959
277
quantitative structure property relationship, QSPR 687
semi-empirical molecular orbital method 933
simultaneous mass transfer 939
steady-state local linearisation 1555
Stefan-Maxwell principles 503 619

UNIFAC model 619 655
Chem-UNIFAC 655
UNIQUAC 655

ORGANIC COMPOUNDS

ACE inhibitory peptides 149
acetone 1573
amine 1035
aromatics: 1549
aromatics/phenol/water 1573
polyaromatic hydrocarbons 1651
acids: 1041
acetic acid 835 877 1325 1625
amino acid: 131 1035 1537
glycylphenylalanine 143
phenylalanine 859 1499
carboxylic acid 119 1041 1537
chiral separation 1035
citric acid 125 1411
dicarboxylic acid 597
lactic acid 983
linoleic acid 1639
γ–linolenic acid 1617
nicotinic acid 411
permetric acid 1607
phthalic acid 1417
phthalates 1651
propionic acid 1325
tartaric acid 125
unsaturated fatty acid 1059
anthocyanin 1621
biologically active peptides 149
chlorinated biphenyls 1651 1657
chlorinated pesticides 1651
caprolactam 427 1543 1573
β–cyclodextrin 1629
cyclodextrin 651
desulfurization 1397
enzyme 89
erythromycin 155
essential oil 1673
ethanol 161 1601
organic compounds/water 1591
pancreatin 107
phenol: 171 419 1065 1319 1573
phenol cleavage stream/ acetone-carboxylic acid salts/water 1573
hydroxybenzoic acid 977
β–phenylethylamine 1035
pleuromutilin 1645
porphyrin 819
protein extraction 83 89 95 119
selectivity 101 113
TBP-kerosene/acetic acid/water 451
TBP-diluent/H_2O/LiCl 655
tetramisole 1607
tocophenol 1613 1635
toluene/acetone/water 427 433
toluene/acetone/phenol/water 503
toluene/cyclohexanone oxime/water 1573
trypsin 107
volatile organic compound (VOC) 177
wheat germ oil 1639
xylene 651
zein 149
zwitterion 131

PRODUCTS

alkylglucoside 369
antitumour effect 1423
apoptosis 1423
dioxalane 549
enzymatic hydrolysis 149
enzymatic peptide synthesis 137 143
kyotorphin synthesis 143
thermolysin catalysed hydrolysis 149
thermolysin catalysed synthesis 143
silicate microballoons 989
synthesis of materials 8
templating 8



ISBN 0 901001 83 X (volume one)
available as a two volume set only
ISBN 0 901001 84 8 (volume two)